Jasvir S. Khurana *Editor*

Bone Pathology

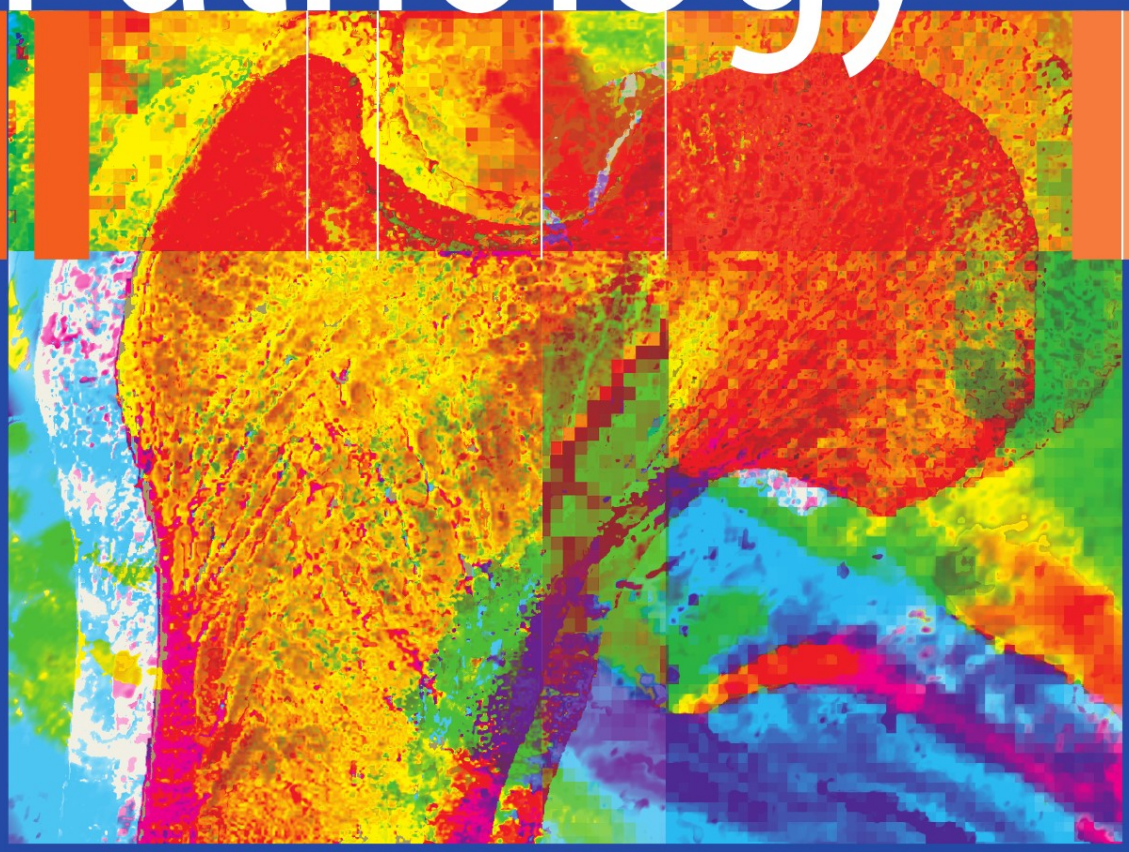

Second Edition

Humana Press

Bone Pathology

Jasvir S. Khurana
Editor

Bone Pathology

Second Edition

Humana Press

Editor
Jasvir S. Khurana
Temple University Hospital
3401 North Broad Street
Philadelphia PA 19140
USA
jkhurana@temple.edu

ISBN: 978-1-58829-766-2 e-ISBN: 978-1-59745-347-9
DOI: 10.1007/978-1-59745-347-9
Springer Dordrecht Heidelberg London New York

Library of Congress Control Number: 2008939906

Printed on acid-free paper

Springer is part of Springer Science+Business Media (www.springer.com)

Preface

This is the second edition of the book *A Compendium of Skeletal Pathology* published 8 years ago. Similar to the prior edition, the goal of this book is to form a blend between new information and serve as a bench-side companion to the surgical pathologist. In this book, established and tested information is emphasized over the new but untried. In the same spirit, and in order to promote brevity, referencing has been kept to a minimum or eliminated altogether in many chapters. Some chapters however, where there is considerable new information (such as anatomy and molecular biology), are more completely referenced. In this context, I am reminded of Sir Hutchinson's book of clinical signs and symptoms, which begins "Before handing the cup of knowledge to the youth, wait for the froth to settle."

There are several changes to this edition. Since there have been several new advances in our understanding of the molecular biology of bone, the first chapter has been extensively rewritten. A new section on the molecular diagnosis of soft-tissue sarcomas and a new section on biomechanics have been included in this edition. An entirely new chapter on soft-tissue tumors has been added, since there is a close relationship between the soft tissue and bone pathology; and because pathologists, surgeons, and radiologists with an interest in bone often have to deal with soft-tissue tumors as well. The chapter on skeletal dysplasia is updated, but being current on the genetic advances in skeletal dysplasia is almost impossible because of the tremendous speed at which knowledge is accumulating. The interested reader is therefore advised to use the website on *Mendelian Inheritance* by the National Center for Biotechnology Information. The authors have somewhat reluctantly agreed to concede to the recent trend of doing away with the apostrophe s in eponyms. The reader will therefore, for example, find Paget disease or Ewing sarcoma instead of the more familiar Paget's disease or Ewing's sarcoma. We will however continue to miss the apostrophe s for some time to come.

Once again, this edition is a combined effort from authors of different specialties including surgeons, pathologists, radiologists, and basic scientists all of whom have in common an interest in bone diseases. Although the book is aimed at the surgical pathology resident, it is hoped that it will be of value to the practicing pathologist, the graduate student, the academic orthopedic surgeon, and the skeletal radiologist.

Philadelphia — Jasvir S. Khurana

Acknowledgements

Acknowledgments are due to my family, Divya, Saranya and Kiran, and my mentors. They are especially due to Dr. Krishnan Unni of the Elmbrook Memorial Hospital, Brookfield, Wisconsin. They are also due to Drs. Rosenthal and Rosenberg of the Massachusetts General Hospital, Boston; to the late Dr. Wolfe of the New England Medical Center, Boston; to Drs. Wold, Nascimento, and Inwards of the Mayo Clinic, Rochester, Minnesota; to Dr. Malawer, Washington Hospital Center, Washington, DC; and to Drs Dave, Kotwal, Jayaswal and Verma of All India Institute of Medical Sciences, New Delhi, India.

A very special acknowledgement to Drs. Gill and Ashok-Raj, New Delhi, and to Dr. Alman of the Hospital for Sick Children, Toronto, Canada – they helped write and edit the first edition.

Acknowledgements are also due, to Drs. Shore and Kaplan for the sections on Fibrodysplasia ossificans progressive and Progressive osseous heteroplasia in chapter 14. They are also due to Dr. Hurford for the section on hematopoetic tumors in Chapter 18. Andrea Edmonds helped tremendously to the editing and finalizing of Chapter 8. Our aknowledgements and sincere thanks to her for spending so much time with the chapter.

I also thank Peter and Greta Beigton in *The Man Behind the Syndrome* (Springer Verlag, Berlin, 1986) for the use of their wonderful book for historical details that appear in several chapters. Our historical details of various people draw extensively from their delightful book.

May 2008 Jasvir S. Khurana
Philadelphia

Contents

Preface v

Acknowledgements vii

Contributors xi

1 Bone Structure, Development and Bone Biology 1
Fayez F. Safadi, Mary F. Barbe, Samir M. Abdelmagid, Mario C. Rico, Rulla A. Aswad, Judith Litvin, and Steven N. Popoff

2 Structure and Function of Joints 51
Mary F. Barbe, Jeff Driban, Ann E. Barr, Steven N. Popoff, and Fayez F. Safadi

3 Biomechanics – Part I 61
Sudheer Reddy, Michele Dischino, and Louis J. Soslowsky

4 Biomechanics – Part II 69
Solomon Praveen Samuel, George R. Baran, Yen Wei, and Brian L. Davis

5 The Laboratory in Orthopedic Practice 79
Vivian Arguello-Guerra and Jasvir S. Khurana

6 Genetics and Molecular Biology of Bone and Soft Tissue Tumors 91
Dolores López-Terrada and John M. Hicks

7 Grossing of Bone and Soft Tissue (Common Specimens and Procedures) 125
Jasvir S. Khurana and Vivian Arguello-Guerra

8 Bone Histomorphometry and Undecalcified Sections 129
Mei-Shu Shih

9 Radiology of the Musculoskeletal System 139
William R. Reinus, Susan V. Kattapuram, and Jasvir S. Khurana

10 Skeletal Trauma and Common Orthopedic Problems 159
Harish S. Hosalkar, Jesse T. Torbert, Jennifer Goebel, and Jasvir S. Khurana

11 The Surgical Pathology of Bone Infections 179
Jasvir S. Khurana

12 Arthropathies 187
William R. Reinus, Mary F. Barbe, Steven Berney, and Jasvir S. Khurana

13 The Surgical Pathology of Prosthetic Materials..... 209
Jasvir S. Khurana and Vivian Arguello-Guerra

14 Osteoporosis and Metabolic Bone Disease..... 217
Jasvir S. Khurana and Lorraine A. Fitzpatrick

15 Inherited and Dysplastic Conditions of the Skeleton..... 239
Vivian Arguello-Guerra, Eileen M. Shore, Fredrick S. Kaplan, and Jasvir S. Khurana

16 Musculoskeletal Neoplasms: An Introduction 249
Harish S. Hosalkar, Jennifer Goebel, Jasvir S. Khurana, and Richard D. Lackman

17 The Medical Management of Sarcomas..... 267
Richard B. Womer

18 Radiation Therapy for Sarcomas 277
Amit Maity

19 The Surgical Pathology of Bone Tumors and Tumor-Like Lesions..... 285
Jasvir S. Khurana

20 Tumors of Soft Tissue 347
Paul J. Zhang

Index..... 407

Contributors

Samir M. Abdelmagid
Department of Plastic and Reconstructive Surgery, Children Hospital of Philadelphia, University of Pennsylvania, Philadelphia, PA 19104

Vivian Arguello-Guerra
Department of Pathology, Pennsylvania Hospital, University of Pennsylvania Health System, Philadelphia, PA 19140

Rulla A. Aswad
Department of Periodontology and Oral Implantology, Kronberg School of Dentistry, Temple University, Philadelphia, PA 19140

George R. Baran
Center for Bioengineering and Biomaterials, Temple University, Philadelphia, PA 19122

Mary F. Barbe
Department of Physical Therapy, College of Health Professions; Department of Anatomy and Cell Biology, Temple University School of Medicine, Philadelphia, PA 19140

Ann E. Barr
Department of Physical Therapy, College Health Professions, Jefferson University, Philadelphia, PA 19107

Steven Berney
Section of Rheumatology, Temple University Hospital, Philadelphia, PA 19140

Brian L. Davis
Department of Biomedical Engineering/ND-20, Lerner Research Institute, Cleveland, OH 44195

Jeff Driban
Department of Kinesiology, College Health Professions, Temple University, Philadelphia, PA 19140

Michele Dischino
Department of Technology and Engineering Education (K-12), Central Connecticut State University, New Britain, CT

Lorraine A. Fitzpatrick
Group Director, Musculoskeletal Diseases and Women's Health Clinical Development, GlaxoSmithKline RN 420 2301 Renaissance Blvd King of Prussia, PA 19406

Jennifer Goebel
Department of Orthopaedics, Children's Hospital of Philadelphia, Philadelphia, PA

Harish S. Hosalkar
Department of Orthopedic Surgery, Rady Children's Hospital, School of Medicine, University of San Diego, California

John M. Hicks
Department of Pathology, Baylor College of Medicine and Texas Children's Hospital, Houston, TX 77030

Fredrick S. Kaplan
Department of Orthopedic Surgery, Hospital of the University of Pennsylvania, Philadelphia, PA 19104

Susan V. Kattapuram
Department of Radiology, Massachusetts General Hospital, Harvard Medical School, Boston, MA 02114

Jasvir S. Khurana
Department of Pathology, Temple Univesity School of Medicine, Philadelphia, PA 19140

Richard D. Lackman
Department of Orthopaedic Surgery, University of Pennsylvania School of Medicine, Philadelphia, PA

Judith Litvin
Department of Anatomy and Cell Biology, Temple University School of Medicine, Philadelphia, PA 19140

Dolores Lopez-Terrada
Department of Pathology, Baylor College of Medicine and Texas Children's Hospital, Houston, TX 77030

Amit Maity
Department of Radiation Science, University of Pennsylvania, School of Medicine, Philadelphia, PA 19140

Steven N. Popoff
Department of Anatomy and Cell Biology, Temple University School of Medicine, Philadelphia, PA 19140

Sudheer Reddy
McKay Orthopaedic Research Laboratory and Department of Orthopaedic Surgery, Hospital of University of Pennsylvania, Philadelphia, PA 19104

William R. Reinus
Department of Radiology, Planning, and Development; Musculoskeletal and Trauma Radiology, Temple University Hospital, Philadelphia, PA 19140

Mario C. Rico
Department of Physiology, Temple University School of Medicine, Philadelphia, PA 19140

Fayez F. Safadi
Department of Anatomy and Cell Biology, Temple University School of Medicine, Philadelphia, PA 19140

Solomon Praveen Samuel
Department of Orthopedics, Albert Einstein Medical Center, Philadelphia, PA 19141

Mei-Shu Shih
Pharma Legacy Laboratories (Shanghai), Co., Ltd. Building 7, Lane 388, Galileo Road Zhangjiang High-Tech Park Pudong, Shanghai 201203 China

Eileen M. Shore
Department of Orthopedics, University of Pennsylvania, School of Medicine, Philadelphia, PA 19104

Louis J. Soslowsky
Department of Orthopaedic Surgery and Bioengineering; Penn Center for Musculoskeletal Disorders; McKay Orthopaedic Research Laboratory, University of Pennsylvania, Philadelphia, PA 19104

Jesse T. Torbert
Department of Orthopedics, Hospital of the University of Pennsylvnia, Philadelphia, PA 19104

Yen Wei
The Center for Advanced Polymers and Materials Chemistry, Department of Chemistry, Drexel University, Philadelphia, PA 19104

Richard B. Womer
Division of Oncology, The Children's Hospital of Philadelphia, Philadelphia, PA 19104

Paul J. Zhang
Department of Pathology and Laboratory Medicine, Hospital of the University of Pennsylvania, Philadelphia, PA

Chapter 1
Bone Structure, Development and Bone Biology

Fayez F. Safadi, Mary F. Barbe, Samir M. Abdelmagid, Mario C. Rico, Rulla A. Aswad, Judith Litvin, and Steven N. Popoff

Keywords Runx-2 (runt-related transcription factor 2) • cbfa-1 (core binding factor alpha1) • Pebp2aA (Polyoma enhancer binding protein 2aA) • Osterix • cleidocranial dysplasia • osteopontin • Leptin • osteoblast specific factor-1, N-syndecan • osteoblast/osteocyte factor-45 (OF45) • dentin matrix protein 1 • fibroblast growth factor 23 • sclerostin • Sclerosteosis • SOST gene • osteocyte • osteoclastogenesis • parathyroid hormone • 1, 25 dihydroxyvitamin D_3 • transforming growth factor alpha • epidermal growth factor • tartrate resistant acid phosphatase • osteoprotegerin • integrins • integral membrane proteins • fibronectin • collagen type I • bone sialoprotein II • osteopontin • suppressor of cytokine signaling-1 • osteoclast-associated receptor • apposition • growth plate • drosophila • sarcolemma • myofilaments • motor end plate • somites • skeletogenesis • osteoactivin • biglycan • decorin • calcitonin • calcitriol • bone morphogenetic proteins • connective tissue growth factor

Introduction

The skeleton serves as an internal structural support system for vertebrates. It has mechanisms to grow and change in shape and size to suit varying stressors including the ability to resist the mechanical forces. In addition, bone is a major source of inorganic ions, and actively participates in the body's calcium/phosphate balance.

Bone tissue is continuously formed and remodeled throughout life. Initially, the bone achieves its increase in size and shape through *growth* (increase in size) and a complicated process known as *skeletal modeling*. In late childhood and adulthood there is continuous renewal of the skeleton via a process termed *remodeling.* Both modeling and remodeling *require* two separate processes namely bone resorption and bone formation to *occur simultaneously* to be effective. This requirement is known as "coupling".

Overview Bone forms the skeletal framework of all vertebrates. It is a composite tissue consisting of organic matrix, inorganic minerals, cells, and water. Bone is formed by the hardening of this matrix entrapping osteoblasts which then become osteocytes.

The inorganic portion of bone matrix is composed mainly of crystalline calcium phosphate salts, present in the form of hydroxylapatite. This allows bone to serve as a reservoir of calcium and phosphate that can be stored or mobilized in a controlled fashion. Bone also contains carbonate, fluoride, acid phosphate, magnesium, and citrate. Hydroxyapatite crystals also form in tissues that are not normally calcified, including in atherosclerotic plaque, in soft tissues of some patients with abnormally high circulating calcium or phosphate, and in articular cartilage of some patients with degenerative joint diseases. Crystals in these situations are often distinctly larger.

The organic component of bone matrix comprises 40% of the dry weight of bone. Most of the organic component is Type I collagen, which is synthesized intracellularly as tropocollagen and then exported as collagen fibrils. Pathological disorders of the bone matrix exist, such as *osteogenesis imperfecta*, a disorder caused by a defect in Type I collagen. This defect results in less organized bone with loss of normal osteon structure. With loss of normal osteons, which function to withstand deformation, the bone fails (fractures) with only minimal amounts of force. In addition to collagen, bone matrix is composed of proteoglycans, glycoproteins, phosopholipids and phosphoproteins, as well as various growth factors including osteocalcin, osteonectin, and bone sialoprotein.

Bones are fashioned in the form of a hollow tube or a bilaminar plate of bone, each commonly termed *compact bone*. Additionally, the architecture is strengthened by internal "struts" of *trabecular bone* that follow the lines of stress. Trabecular or cancellous bone is a metabolically active component of bone and has about nine times greater turnover than the outer compact bone. This kind of design is known in engineering terms as "composite" and allows bone to take

J.S. Khurana (ed.), *Bone Pathology*, DOI 10.1007/978-1-59745-347-9_1,

advantage of the strength of components. This type of design also allows bone to resist mechanical compression and able to deform significantly before failing (i.e. breaking).

Part 1 Bone Structure

Macroscopic Features of Bone

At the gross level, bone can be broadly categorized into five types: long bones (femur, tibia, ulna and radius), short bones (carpal bones of the hand), flat bones (skull, sternum and scapula), irregular shaped bones (vertebra and ethmoid), and sesamoid bones (bones embedded in tendons). These bones form through different mechanisms during embryonic development. The long bones form by endochondral mechanisms, while the flat bones form by intramembranous mechanisms. These processes are discussed later in this chapter. Both long and flat bones are organized with a hard, but relatively thin, outer region composed of dense, *compact* bone called the *cortex or cortical bone*. Inside the cortex is the marrow cavity containing hematopoietic elements, fat and spicules of bone. The bone spicules are also referred to as *trabecular, spongy*, or *cancellous* bone (Fig. 1).

Types of Bones

Long-bones: Macroscopic examination of long bone shows two extremities (*epiphysis*) and a cylindrical tube in the middle (*diaphysis*) and a transitional zone between them (*metaphysis*) (Fig. 2). In growing long bone, the epiphysis and the diaphysis originate from independent ossification centers and are separated by a layer of cartilage, termed the *epiphyseal* or *growth plate* (see more details later in this chapter).

Short bones: Carpal and tarsal bones of the hand and foot, respectively, are examples of short bones. These bones are typically cube-shaped, and have only a thin layer of compact bone surrounding a spongy (trabecular bone) interior.

Flat-bones: Excellent examples are the bones of the skull, which consist of inner and outer tables of compact bone with spongy (trabecular) bone (diploe) between them.

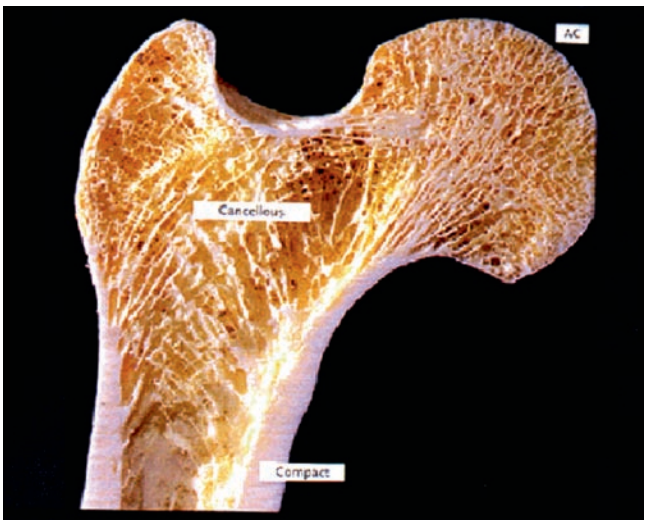

Fig. 1 Adult long bone. Sagittal section through long bone showing the internal structure of the bone. Note the outer dense compact bone (also called cortical bone) and the inner cancellous bone filled with spicules (trabeculae), these latter small bundles of bone traverse the inner substances of bone and are usually interconnected with one another.

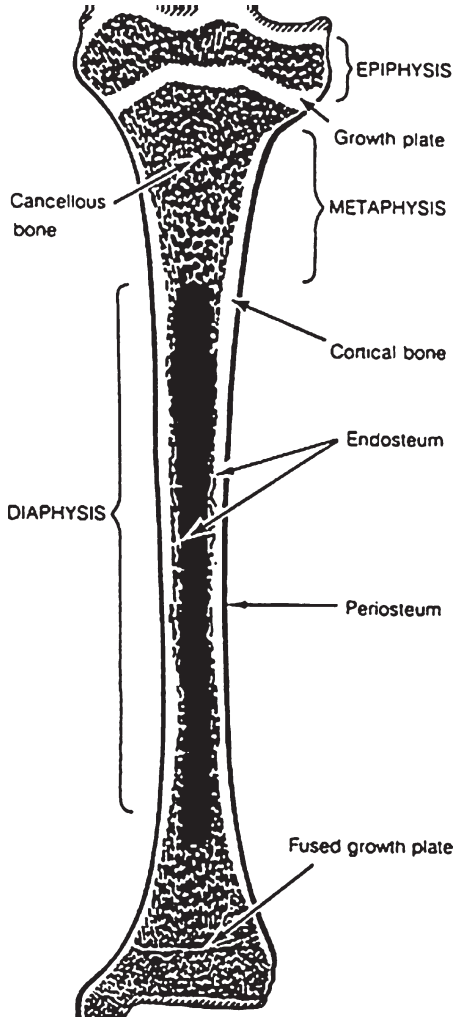

Fig. 2 Schematic diagram of a tibia. The interior of a typical long bone showing middle diaphysis, a growing proximal end (epiphysis) with a still active epiphyseal growth plate and a distal end with the epiphysis fused to the metaphysis. The diaphysis (shaft) of a long bone contains a large marrow cavity surrounded by thick-walled tube of compact bone. A small amount of spongy bone lines the inner surface of the compact bone. The proximal and distal ends, or epiphyses, of the long bone consist of spongy bone with a thin outer shell of compact bone. The outer surface of the bone is covered by a fibrous layer of connective tissue called the periosteum.

Irregular bones consist of an outer thin layer of compact bone covering an inner region of spongy bone. The scapula is an example of an irregular bone.

Sesamoid bones: These bones are a subtype of short bones that are embedded in tendons. The patella and pisiform are examples of sesamoid bones.

Individual Bone Structure

Cortical (compact) bone refers to the dense hard, calcified bone that forms the hard outer "shell" of bone that surrounds the marrow cavity (Figs. 1, 2). This type of bone has few gaps or spaces. In the adult, cortical bone (or the cortex) is composed of dense aggregations of lamellar type bone (see below). Compact bone also contains within it Haversian (2) and Volkmann canal systems for vascular supply (Fig. 3). Cortical bone is surrounded externally and internally by a *periosteum* and *endosteum*, respectively.

Epiphysis: This term refers to the end of a tubular bone, lying between the epiphyseal (growth) plate (in developing bone) and the articular cartilage (Fig. 2). In adults, the growth plate is absent. The place it is thought to have occupied is arbitrarily selected to define the portion referred to as the epiphysis. The epiphyses consist mostly of spongy bone inside a thin sheet of dense bone.

Physis or Epiphyseal Plate: This term refers to the growth plate in children (before cessation of growth). Injuries or other disruptions such as infections can seriously affect the subsequent size and shape of the bone. For example, increased vascularity around the epiphysis, occurring during the repair process after a fracture at this site, can cause elongation of the limb. Inflammatory destruction of the physis may cause shortening while its partial destruction may cause an angular deformity. Fractures of the physeal plate have been classified based on the amount and kind of disruption caused. This is the basis for the Salter-Harris classification *(3)*.

Metaphysis: This refers to the widened portion of bone occupying the area between the cylindrical diaphysis and the physis/epiphysis (Fig. 2). Remodeling and modeling defects in this region are frequent in conditions such as multiple osteochondromatosis. Several tumors have an epicenter in the metaphysis.

Diaphysis (shaft): This refers to the middle, cylindrical portion of a tubular bone (Fig. 2). There is a thick cortex surrounding a marrow space.

Bone Marrow: The medullary cavity is filled with varying proportions of hematopoietic marrow, fat and trabecular bone. The marrow is most prevalent in younger age groups and in the metaphyseal region of long bones. The diaphysis contains mainly fat in adults. In comparison to the appendicular (limb) skeleton, the axial skeleton has a greater proportion of bone marrow.

Periosteum: The periosteum is a thick fibrous membrane that covers the entire surface of a bone, with the exception of the articular cartilage. It is composed of an *outer fibrous* layer and an *inner cambium* (cellular) layer. The outer layer is a connective tissue layer containing fibroblasts as well as nerves and blood vessels supplying the underlying bone. The inner cambium layer contains osteoprogenitor cells capable of forming new bone, and is thus an osteogenic layer. When tendons insert into bone, the collagen fibers (*Sharpey's fibers*) pass through the periosteum and then into the bone lamellae. The Sharpey's fibers contribute to the appositional growth of bone (see intramembranous bone formation).

Endosteum: The endosteum is composed of a resting layer of marrow at its interface with bone. This is not a morphologically recognizable layer of tissue at the light or electron microscopic level. However, it is a convenient concept which exists to explain the functional changes seen in physiologic and pathologic alterations in bone.

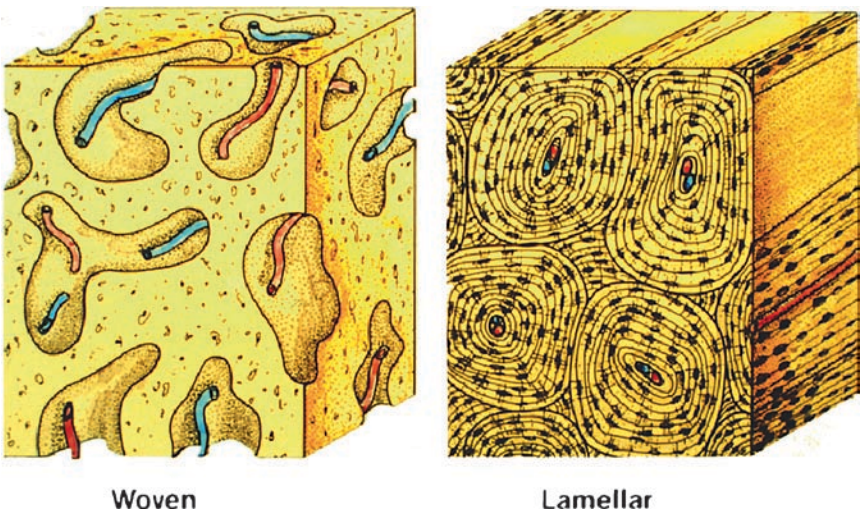

Fig. 3 Diagram of immature and mature bone. Immature (woven) bone displays a disorganized lamellar appearance because of the interlacing arrangement of collagen fibers. The cells (osteoblasts and osteocytes) tend to be randomly arranged, whereas the cells in the mature bone are organized in circular fashion that reflects the lamellar structure of the Haversian system. Resorption canals in mature bone have their long axes in the same direction as the Haversian canals.

Trabecular bone, also called *spongy* or *cancellous* bone, consists of slender spicules and trabeculae of bone that are separated by marrow spaces. Trabecular bone fills the interior of long bones, the metaphyseal region of long bones, and epiphyseal ends of bones. Trabeculae form a network of rod- and plate-like elements that act as scaffolding for the marrow cavity, lighten bone, and allowing room for blood vessels and marrow. The spicules of trabeculae usually consist of several lamellae of bone tissue.

Microscopic Features of Bone

Bone tissue can be classified based on collagen fiber arrangements into two different types: woven bone and lamellar bone. To repeat from above, bone is also classified into compact bone and trabecular bone.

Woven Bone: This form of bone consists of randomly oriented collagen fibers, with large numbers of osteoblasts and osteoprogenitor cells alongside (Fig. 3). Under polarized light, it has a haphazard structure which is in great contrast to lamellar bone (see below). Woven bone contains relatively more cells per unit area than mature bone. Although woven bone is the major bone type in the developing fetus, and lamellar (mature) bone is the major bone type in the adult, areas of immature bone are also present in adults, especially where bone is being remodeled. Areas of woven bone are also seen regularly in the alveolar socket of the adult oral cavity and where tendons insert into bones. Except for the above examples, woven bone is generally considered pathologic if seen in adults. It occurs in regions of rapid growth, such as in the growing skeleton especially in the embryo, fracture callus, fibrous dysplasia, areas of remodeling osteosarcoma, and several other tumors. The molecular signals that are required to trigger woven bone synthesis are thought to include platelet derived growth factor (PDGF A and B), insulin like growth factor (IGF I and II) and perhaps others. It is likely that a combination of growth factors may be required (for more details see growth factors in this chapter).

Lamellar bone: Lamellar bone is the mature form of adult bone. It is readily identified on polarized light microscopy as parallel lines of deposited bone (Fig.3). Studies have shown that lamellar bone has a well-organized arrangement of collagen fibers. Lamellar bone is formed when the rate of deposition is slow. In general, it is formed only on pre-existing bone, either woven or lamellar. The control mechanisms involved in the formation of lamellar bone are still under investigation.

Secondary organization is a hallmark of lamellar bone. In the cortex, the lamellae are arranged in *circumferential* as well as tubular arrangements (Figs. 3, 4). The tubular arrangement is called an *osteon* (Fig. 4). Under the microscope, these tubes can look like circles or parallel sheets depending on how they are sectioned during histologic preparation. The central part of the tube is the Haversian canal (Figs. 4, 5), which contains blood and lymphatic vessels and nerves. The osteons play an important role in the mechanical properties of cortical bone, since the long axis of an osteon is parallel to the long axis of a long bone. Each osteon acts as a fiber that resists failure (fracture) with deformation (stretch).

Types of Lamellae:Outer circumferential lamellae are several lamellae that lie next to the periosteum and are oriented parallel to it. *Inner circumferential lamellae* lie next to the endosteum (Fig. 5). The circumferential lamellar bone resists compressive forces. The *interstitial lamellae* are remnants of previous concentric lamellae (Fig. 5).

Haversian systems (osteons) and Volkmann's canals: These are cylindrical units of 5 to 15 concentric lamellae, which surround a central *Haversian canal*. Each lamella is several microns in thickness and its fibers run in a spiral fashion around the canal. The Haversian canal contains capillaries, venules, lymphatic vessels, and a loose connective tissue containing osteoprogenitor cells. Since the Haversian systems are arranged around branching blood vessels, it is easy to see how the Haversian systems comprise a *branching system* of cylinders that are oriented in the long axis of the bone. *Volkmann's canals* are vascular channels that connect Haversian canals to each other as well as connect the Haversian system with the blood vessels in the periosteum. Canaliculi containing the processes of osteocytes (see below) are largely arranged in a radial pattern with respect to the canal. The system of canaliculi that opens to the Haversian canal also serves for the passage of substances between the osteocytes and blood vessels.

Compact versus Trabecular Bone

Compact bone: To summarize from above, compact bone usually consists of *concentric lamellae* arranged into Haversian systems (osteons), *interstitial lamellae* between the Haversian systems, and *inner and outer circumferential lamellae* (Figs 4 and 5). Located in spaces between these lamellar are bone cells called *osteocytes* (see below and Fig. 5). Because of this organization, compact mature bone is also called lamellar bone.

*Trabecular bone:*This type of bone refers to the spongy spicules of bone found within the marrow space and is also called spongy, cancellous or medullary bone (Fig. 1 and 6). Each spicule of trabecular bone is composed of several lamellae and is usually not more than 0.2-0.4 mm in thickness to allow for diffusion of nutrients to the osteons. If they were thicker, they would need osteonts in order to insure adequate vascular perfusion (Fig. 6). In trabecular bone the lamellae are normally arranged in a longitudinal fashion, and osteons are usually not formed.

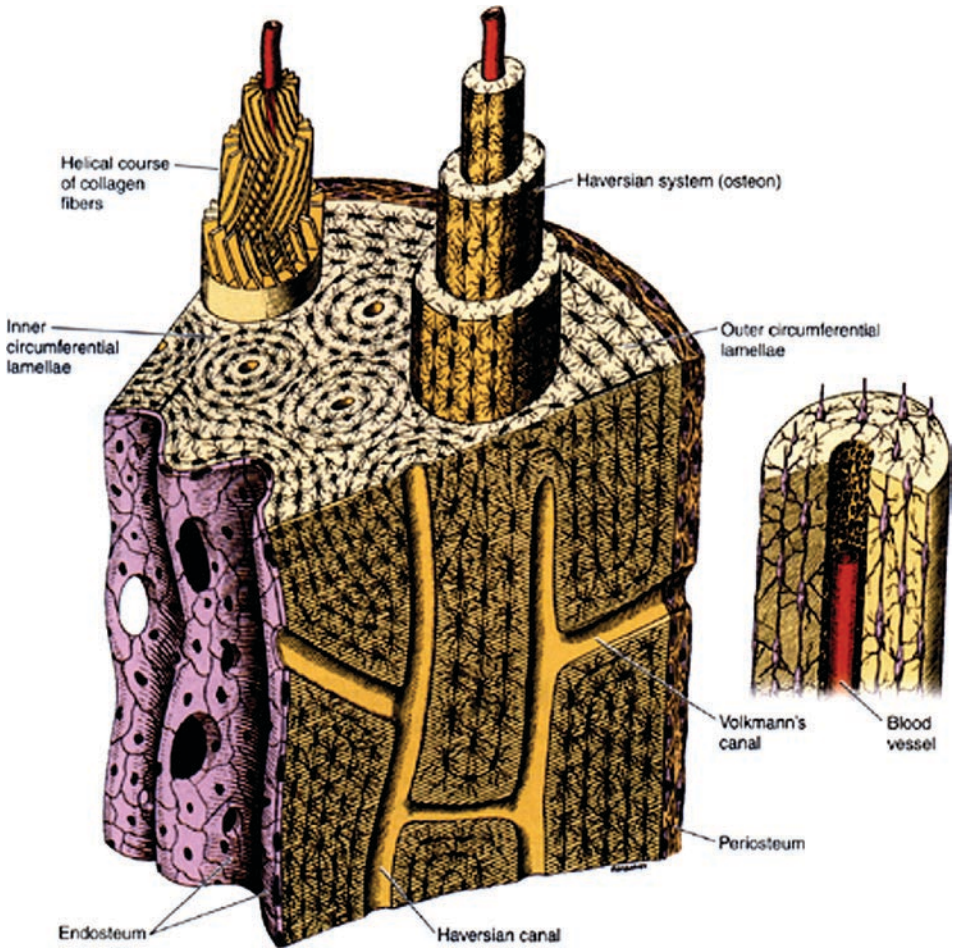

Fig. 4 Schematic drawing of the cortical bone. Sectioned cortical bone showing the tubular and circumferential arrangement of osteon. In the center of each osteon is a canal, called the Haversian canal. Each Haversian canal contains blood vessels, nerve endings and lymphatic vessels.

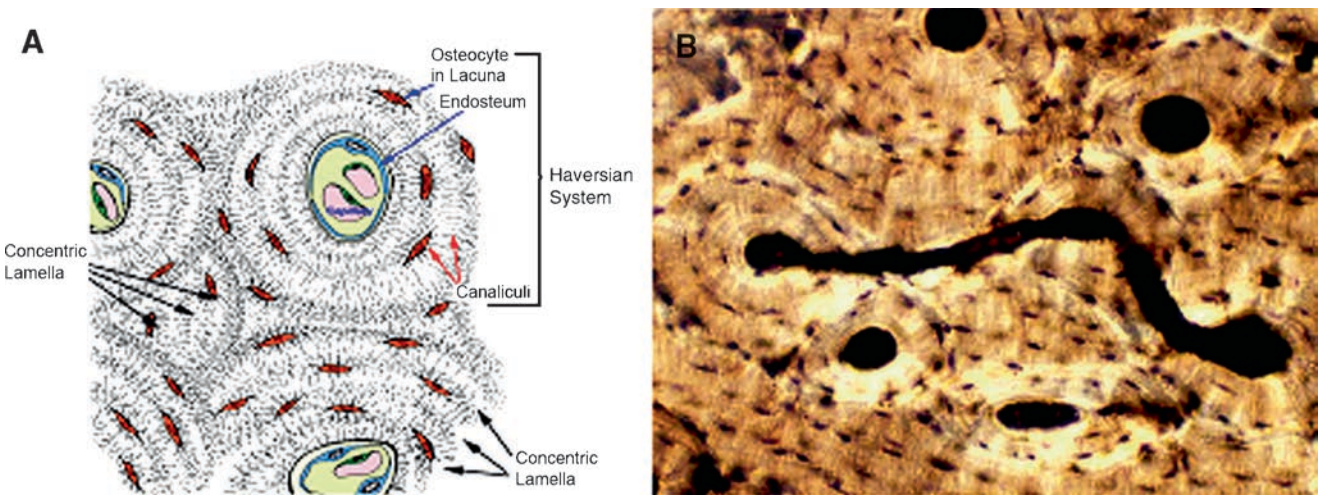

Fig. 5 Cartoon and a microscopic photograph depicting the lammelar organization of bone. **A**. Cartoon representing a Haversian system (osteon) with interstitial lamellae, osteocytes and canaliculi (cellular processes). **B**. Histological representation of Volkmann's canal connecting Haversian canals of adjacent osteons.

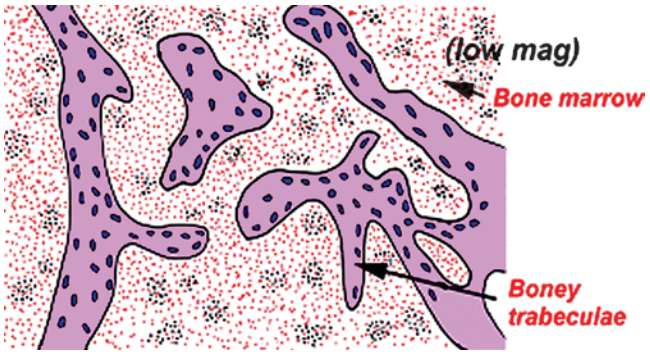

Fig. 6 Cartoon of spongy bone. Spongy bone (also called trabecular bone) is composed of trabeculae surrounded by bone marrow. Each trabecula consists of lamellar bone, osteocytes and mineralized matrix. Bone marrow fills the space between trabeculae.

Separating the trabeculae from the marrow is an endosteum. Under electron microscopy, the endosteal layer has a rich supply of osteoclasts and osteoblasts. Trabecular bone is more metabolically active than compact bone. Consequently, metabolic bone studies are best carried out on this component of bone. Radiologic studies (such as dual and single energy computerized tomography (CT) scan methods as well as micro-CT developed for the study of osteoporosis) have devised methods to exclusively study the trabecular component and to exclude the cortex. Some amount of success has been achieved using these approaches with the ability of obtaining a "region of interest" by modern computer software. Microscopically this is done using bone histomorphometry with image analysis software such as Bioquant Osteo (www.bioquant.com), Osteomeasure (www.osteometrics.com), and SkyScan CTAn (www.skyscan.be).

Bone Matrix

The organic component of bone makes up 40% of the dry weight and is composed of collagen, proteoglycans, glycoproteins, phosopholipids and phosphoproteins. The inorganic component makes up the remaining 60% of the dry weight of bone and is composed primarily of calcium hydroxyapatite $Ca_{10}(PO_4)_6(OH)_2$. At an ultrastructural level, bone is organized to maximally resist applied mechanical forces. Calcium hydroxyapatite crystals are arranged parallel to collagen fibers (59). This orientation maximizes the collagen's resistance to tensile (stretch) forces and the calcium hydroxyapatites resistance to compressive forces. Diseases characterized by abnormal bone collagen content result in weak bone matrix and lowered abilityof the bone to resist mechanical forces. A more detailed discussion on the bone matrix is given below in Part III, the section on Bone Biology.

Blood Supply of Bone

Bone has a rich vascular supply. It receives 10-20% of the cardiac output. Blood supply varies with different types of bones. Blood vessels are especially rich in areas containing red bone marrow. The extent to which the periosteal and endosteal vascular supplies meet the metabolic needs of bone is controversial. Some authors feel that the periosteal and endosteal supplies are able to meet the needs of the outer and inner halves of the cortex. Others contend that the periosteal supply is able to meet only the ends of the outer third of the cortex. The question however is an important one, especially in situations of operative fracture repair and in the surgical technique of bone elongation called distraction osteogenesis.

Vasculature and Nerve Supply in Long Bones

The diaphyseal nutrient artery is the most important supply of arterial blood to a long bone. One or two principal diaphyseal nutrient arteries first pass through the cortical bone obliquely. These arteries then divide into ascending and descending branches and supply the inner two thirds of the cortex and medullary cavity. There are also numerous metaphyseal and epiphyseal arteries supplying the ends of bones. They arise mainly from the arteries that supply the adjacent joints. They anastomose with the diaphyseal capillaries and terminate in bone marrow, cortical bone, trabecular bone, and articular cartilage. In growing bones, these arteries are separated by the epiphyseal cartilaginous plates. Finally, periosteal arterioles are vessels that supply the outer layer of cortical bone.

Arterial Supply of Large Irregular Bones, Short Bones, and Flat Bones

These bones receive a superficial blood supply from the periosteum and frequently from large nutrient arteries that penetrate directly into the medullary bone. These two arterial systems anastomose freely.

Venous and Lymphatic Drainage of Bone

Blood is drained from bone through veins that accompany the arteries and frequently leave through foramina near the articular ends of the bones. Lymph vessels are abundant in the periosteum.

Nerve Supply of Bones

Nerves are most rich in the articular extremities of the long bones, vertebrae, and larger flat bones. Many nerve fibers accompany the nutrient blood vessels to the interior of the bones and to the perivascular spaces of the Haversian canals. Accompanying the arteries inside the bones are vasomotor nerves, which control vascular constriction and dilation. The periosteal nerves are sensory nerves, some of which are pain (nociceptive) fibers. Therefore, the periosteum is especially sensitive to tearing or tension. Nerve endings have also been demonstrated adjacent to bone trabeculae and in proximity to bone cells.

Bones are also innervated by sympathetic fibers. In the upper limb, the sympathetic fibers destined for bone originate from the sympathetic ganglion. In the lower limb, selective peripheral neuroctomy studies revealed that the sympathetic nerves, with reference to the tibia, descend in the sciatic nerve, and thereafter principally in the medial popliteal nerve, and enter bone alongside the nutrient vessels (4).

Neurotransmitters and Bone

Neurotransmitters released by these nerve endings within bone are the subject of increasing interest in the field of bone biology since they appear to have a role in bone formation and remodeling. For example, mice homozygous for deletion of the dopamine transporter gene DAT (-/-) demonstrated reduced bone mass and strength. Cancellous bone volume in DAT (-/-) proximal tibial metaphysis was significantly decreased with reduced trabecular thickness. The ultimate bending load (femoral strength) for the DAT (-/-) mice was 30% lower than the wild-type mice. Thus, deletion of the DAT gene resulted in deficiencies in skeletal structure and integrity (5).

Cannabinoids and Bone

Recent studies have shown that the endogenous cannabinoid system plays a role in regulating bone remodeling. The endogenous cannabinoids bind to and activate two G protein-coupled receptors, the predominantly central cannabinoid receptor type 1 (CB1) and peripheral cannabinoid receptor type 2 (CB2). Whereas CB1 mediates cannabinoid psychotropic and analgesic effects, CB2 has been implicated recently in the regulation of liver fibrosis and atherosclerosis. Genetically engineered mice null for CB2 receptors showed accelerated age-related trabecular bone loss and cortical expansion, although cortical thickness remains unaltered. These changes are reminiscent of human osteoporosis and may result from differential regulation of trabecular and cortical bone remodeling. The CB2 null mouse phenotype is also characterized by increased activity of trabecular osteoblasts (bone forming cells), increased osteoclast (bone resorbing cell) number, and a markedly decreased number of diaphyseal osteoblast precursors. CB2 is expressed in osteoblasts, osteocytes, and osteoclasts (6). A CB2-specific agonist enhances endocortical osteoblast number and activity and restrains trabecular osteoclastogenesis, apparently by inhibiting proliferation of osteoclast precursors and receptor activator of NFκB ligand expression in bone marrow-derived osteoblasts/stromal cells. This same agonist attenuates ovariectomy-induced bone loss in animals and markedly stimulates cortical thickness through the respective suppression of osteoclast number and stimulation of endocortical bone formation. These results demonstrate that the endocannabinoid system is essential for the maintenance of normal bone mass by osteoblastic and osteoclastic CB2 signaling. Hence, CB2 offers a molecular target for the diagnosis and treatment of osteoporosis, and other bone-loss associated diseases (6,7).

Bone Cells

The cells important in bone biology are osteoblasts, osteocytes and osteoclasts. Osteoblasts are the primary cells responsible for bone formation (osteogenesis) and mineralization, while osteoclasts are primarily responsible for bone resorption. Osteoblasts and osteocytes are derived from mesenchymal stem cells, while osteoclasts are derived from hematopoeitic stem cells and are related to monocyte/macrophages.

Osteoblasts

Osteoblasts originate from mesenchymal stem cells that have the potential to proliferate and the capacity to differentiate into several connective tissue cell types. These pluripotent mesenchymal cells can differentiate into osteoblasts, chondroblasts, bone marrow stromal cells, fibroblasts, muscle cells or adipocytes depending on the nature of the stimulus within their local microenvironment. Given the appropriate stimuli to differentiate into osteoblasts, they will first give rise to osteoprogenitor cells, cells still capable of proliferating yet committed to the osteoblast lineage. Osteoprogenitor cells can be found in the inner layer of the periosteum, the endosteum lining marrow cavities, osteonal (Haversian) canals, perforating (Volkmann's) canals, and in perivascular tissue adjacent to bone. Osteoprogenitor cells can also be found in

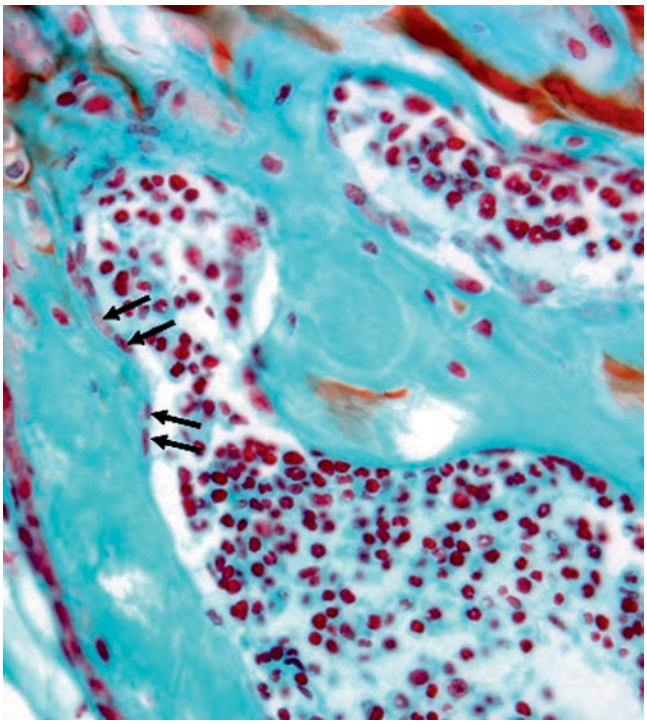

Fig. 7 Bone lining cells. Histological microphotographs of femurs stained with Saffranin-O and counter stained with Goldner stain showing metaphyseal bone with bone lining cells (black arrows). These cells are inactive but can redifferentiate into active, bone forming osteoblasts in response to the appropriate stimuli.

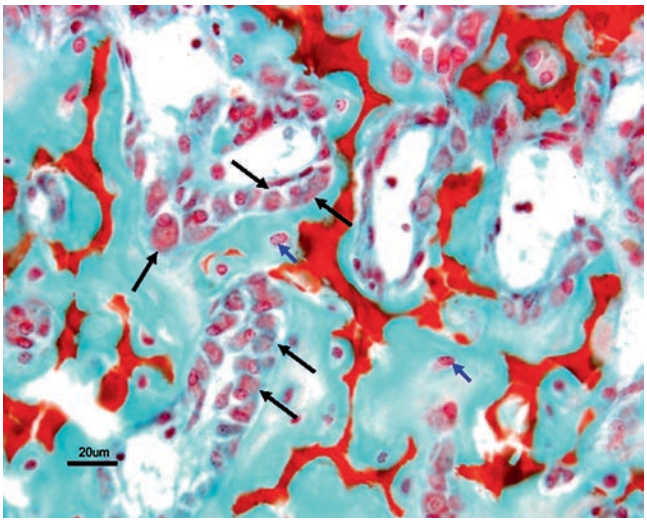

Fig. 8 Osteoblasts lining trabecular bone surface. Photomicrographs of metaphyseal trabecular bone, showing active cuboidal osteoblasts lining the trabecular bone surfaces (black arrows). Note also some osteocytes encased within the bone matrix (blue arrows).

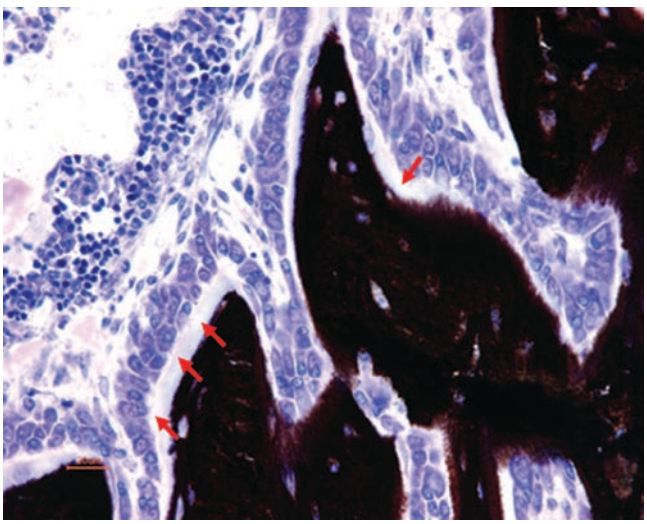

Fig. 9 Osteoid synthesis by active osteoblasts. Photomicrographs of undecalcified metaphyseal trabecular bone stained with von Kossa (for mineral, black stain) and toluidine blue. Note the osteoid, unmineralized bone matrix (red arrows), compared to the mineralized matrix (black).

the bone marrow where they are indistinguishable from marrow stromal cells to which they are related.

Osteoblasts are generally cuboidal or columnar in shape, and are found lining bone surfaces at sites of active bone formation such as during bone development (see below) or fracture repair (Fig. 8). Osteoblasts are responsible for the production of type I collagen and the proteoglycans (glycosoaminoglycans) that largely comprise the organic component of bone matrix, also known as osteoid. Osteoid can be visualized using specific stains as shown in Fig. 9. Osteoblasts are also involved in the subsequent mineralization of osteoid via the liberation of matrix vesicles and the deposition of calcium and phosphate (8,9). Osteoblasts are joined by adherens type junctions, including desmosomes and tight junctions. Cadherins are transmembrane proteins that are integral to these adherens junctions and function to join cells through their cytoskeleton.

The phenotypic characteristics of osteoblasts depend on their stage of differentiation. Ultrastructurally, osteoblasts are typical protein producing cells with an extensive amount of rough endoplasmic reticulum, a large Golgi apparatus and numerous mitochondria. Alkaline phosphatase enzyme activity is one of the earliest markers of the osteoblast phenotype. In addition to the production of type I collagen and proteoglycans, osteoblasts also produce a variey of other non-collagenous proteins including osteocalcin, osteopontin, bone sialoprotein and osteonectin (see below). These proteins are also markers of the osteoblast phenotype and each has a unique temporal pattern of expression during osteoblast differentiation. Osteoblasts secrete a variety of cytokines and colony stimulating factors (CSF), such as interleukin-6, interleukin-11, granulocyte-macrophage colony stimulating factor (GM-CSF) and macrophage colony stimulating factor (M-CSF), and

thus play a role in myelopoesis. Osteoblasts also secrete numerous growth factors including transforming growth factor-beta (TGFβ), bone morphogenetic proteins (BMPs), platelet derived growth factors (PDGFs), and insulin-like growth factors (IGFs). Mature osteoblasts possess receptors for parathyroid hormone (PTH) and 1,25-dihydroxyvitamin D, two hormones that play important roles in regulating bone metabolism and mineral homeostasis (see below). Osteoblasts also secrete receptor activator of nuclear factor kappa B (RANK) ligand, a protein that plays an essential role in the differentiation of osteoclasts (see below).

Constant mechanical stress is essential for the maintenance of bone mass and strength, which is achieved through the cooperative functions of osteoblasts, osteocytes and osteoclasts. Osteoblasts respond to mechanical stimuli to mediate changes in bone size and shape. This effect may be modulated by a piezo-electric effect of the calcium hydroxyapatite crystals (see section on mechanosensory systems and stretch studies).

Bone lining cells are flattened, squamous cells found lining bone surfaces in areas where there is no active bone formation. They are particularly prevalent in adult and aging bone where many of the bone surfaces are inactive. These cells can be thought of as quiescent osteoblasts and are similar to osteoprogenitor cells in that they can be reactivated to become functional osteoblasts under conditions that warrant active bone formation such as during remodeling, fracture repair and in certain types of bone pathology (Fig. 7).

Regulation of Bone Formation and Osteoblast Differentiation

Osteoblast differentiation is regulated by numerous secreted growth factors including transforming growth factor-β (TGFβ), bone morphogenetic proteins (BMPs), fibroblast growth factors (FGFs), and others (see matrix proteins of bone below) (10,11). Furthermore, various transcription factors also play important roles in osteoblast differentiation. Runx-2 (runt-related transcription factor 2)/cbfa-1 (core binding factor alpha 1) and osterix are essential transcription factors for osteoblast differentiation (12,14). Experimental animal models with targeted deletion of the Runx-2 gene demonstrated that mice develop to term but have a skeleton consisting exclusively of cartilage that does not ossify. There is no evidence of osteoblast differentiation or bone formation in these mice. In addition, Runx-2 null mice lack osteoclasts (see regulation of osteoclast differentiation). Although null mutations for Runx-2 have not been identified in humans, mutations in the Runx-2 gene cause a disease known as cleidocranial dysplasia (CCD) (12,14). CCD is characterized by hypoplastic clavicles and delayed ossification of cranial sutures. Runx-2 target genes include osteocalcin, bone sialoprotein, osteopontin and collagen α1 (15,16). Osterix is another transcription factor that was more recently shown to play a role in osteoblast differentiation presumably by acting downstream of Runx-2 (13).

Leptin is a peptide synthesized by adipocytes with binding affinity to its receptor in the hypothalamus. This protein regulates bone formation via a central mechanism. Mice deficient for leptin or its receptor have considerably higher bone mass than normal wild-type mice. It has been shown that patients with generalized lipodystophy (absence of adipocytes and white fat) exhibit osteosclerosis and accelerated bone growth (17). Although details of the leptin-hypothalamic control mechanism are not fully understood, additional experimentation on the role of the central nervous system and the regulation peripheral leptin production will enhance our understanding of how the leptin-hypothalmic axis regulates bone metabolism.

Other transcription factors, secreted proteins and receptors have been reported to have significant effects on osteoblast differentiation and bone formation. Many of these effects were identified or confirmed in studies involving genetically modified animals (for list of these animal models refer to Table 1).

Due largely to the mineralized matrix of bone, it has proven difficult to study osteoblasts experimentally in vivo. Many studies of osteoblast differentiation and function utilize organ or cell culture systems. Some studies employ primary osteoblast cultures in which osteoblasts are enzymatically digested from the endocranial surface of neonatal rodent (rat and mouse) calvaria. Primary cultures of human osteoblasts are generally established by enzymatic digestion of osteoblasts from the surfaces of cancellous bone samples. When cultured under conditions that favor the osteogenic lineage (i.e. ascorbic acid and β-glycerophosphate supplemented media), many of the cells in these primary cultures differentiate into mature osteoblasts capable of producing a mineralized bone matrix. One major drawback to these cultures is the heterogeneity of cells that can be isolated from calvaria or cancellous bone resulting in significant contamination of non-osteogenic cells as well as heterogeneity in the stage of differentiation of the osteogenic cells. To eliminate the potential heterogeneity of cell types inherent in primary culture systems, some investigators have utilized osteosarcoma cell lines. However, transformed cells may not behave the same as non-neoplastic cells prompting questions about the physiological relevance of data generated using transformed osteoblast cell lines. Another approach has been to establish permanent cell lines from primary osteoblast cultures such as the widely used MC3T3-E1 cell line derived from mouse calvaria. There have also been many studies of osteogenic differentiation from less differentiated (osteoprogenitor) stromal or

Table 1 Skeletal phenotype of selected genetically engineered mice

Gene Name	Skeletal phenotypes of the null, mutant and transgenic animals
Runt-Related Transcription Factor 2; Runx2, Cbfa1	**Null mice:** Complete lack of ossification of the skeleton. Mice died just after birth (14) and showed marked changes in tooth morphogenesis (312). Transgenic mice: Normal skeleton at birth but developed an osteopenic phenotype thereafter (313).
Secreted Phosphoprotein 1; Spp1, Osteopontin	**Null mice:** Normal and viable with altered wound healing (314). These animals also showed resistance to ovariectomy-induced bone resorption (315). These knockout animals demonstrated an increase in ectopic calcification especially in the medial layer of the arteries (316).
Gamma-Carboxyglutamic Acid Protein, Bone; Osteocalcin	**Null mice:** Develop higher bone mass and bones of improved functional quality. Histomorphometric studies showed an increase in bone formation without impairing bone resorption (317).
Secreted Protein, Acidic, Cysteine-Rich; Osteonectin	**Null mice:** After six months of age, the animals developed severe osteopenia, cataracts, rupture of the lens capsule and accelerated closure of dermal wounds (318). These animals also have greater deposits of subcutaneous adipose tissue (319).
Connective Tissue Growth Factor; CTGF	**Transgenic mice:** Just a few months after birth the animals showed dwarfism, decreased bone density, alterations in endochondral ossification and affected fertility (202).
	Null Mice: CTGF deficiency leads to skeletal dysmorphisms as a result of impaired chondrocyte proliferation and extracellular matrix composition within the hypertrophic zone (204).
Thrombospondin I; Tsp1	**Null mice:** Abnormal curvature of the spine, lung abnormalities and increase in the number of circulating leukocytes (320).
Thrombospondin II; Tsp2	**Null mice:** Increase cortical bone thickness and density and abnormal long bleeding times (321).
Thrombospondin III; Tsp3	**Null mice:** Young adult TSP3-null mice are heavier than controls, and analyses of the geometric and biomechanical properties of long bones show increases in the moments of inertia, endocortical and periosteal radii, and failure load (322).
Transcription Factor Sp7; Osterix	**Null mice:** Absent bone formation and no deposition of bone matrix in these animals (13).
Parathyroid Hormone; PTH	**Null mice:** These animals showed reduced cartilage matrix mineralization and decreased metaphyseal osteoblasts and trabecular bone (323).
Parathyroid Hormone-Like Hormone; PTHrP	**Trangenic mice:** Chondrocyte-specific overexpression of PTHrP causes a profound delay in the developmental program of chondrocyte differentiation and endochondral ossification (324).
Sry-Box 9; Sox9	**Tissue specific null mice:** Inactivation of Sox9 in limb buds before mesenchymal condensations resulted in a complete absence of both cartilage and bone, but markers for the different axes of limb development showed a normal pattern of expression (325).
Vitamin D Receptor; VDR	**Null mice:** After weaning, animals showed severe impairment of bone formation such as the phenotype observed in vitamin D-dependent rickets type II. Animals also exhibit alopecia, hypocalcemia and infertility. Animals died within 15 weeks after birth (326).
Peroxisome Proliferator-Activated Receptor-Gamma; PPARg	**Heterozygous mice:** PPARgamma-deficient mice exhibited high bone mass with increased osteoblastogenesis, but normal osteoblast and osteoclast functions. The osteogenic effect of PPARgamma haploinsufficiency became prominent with aging but was not changed upon ovariectomy (327).
V-Src Avian Sarcoma (Schmidt-Ruppin A-2) Viral Oncogene; Src	**Null mice:** These animals demonstrated severe osteoclast dysfunction resulting in osteopetrosis. Animals survived for only a few weeks (328)
Serum Response Factor; Srf, c-Fos	**Null mice:** Embryos failed to gastrulate and died due to cardiac insufficiency during chamber maturation (329). Mice lacking Fos (encoding c-Fos) develop osteopetrosis due to an early differentiation block in the osteoclast lineage (330).
Spleen Focus Forming Virus Proviral Integration Oncogene; Spi1, PU.1	**Null mice:** Exhibit the classic hallmarks of osteopetrosis, a family of sclerotic bone diseases. Animals were rescued by marrow transplantation, with complete restoration of osteoclast and macrophage differentiation, verifying that the PU.1 is intrinsic to haematopoietic cells (331).
Dickkopf; Dkk1	**Heterogygous mice:** Progressive Dkk1 reduction increases trabecular and cortical bone mass and even a 25% reduction in Dkk1 expression could produce significant increases in trabecular bone volume fraction. Thus Dkk1 is a negative regulator of normal bone formation in vivo (332).

mesenchymal cells (isolation of primary cells and established cell lines have been employed for these types of cultures). These types of cultures have been particularly useful to study osteogenic commitment and early differentiation.

As opposed to cell culture studies, bone organ cultures utilizing whole calvaria obtained from fetal rats or mice have been used to study bone responses to exogenous factors such as vitamin D and cortisol. These organ cultures allow one to examine the effects of systemic (hormones) and locally-produced factors on the multitude of cell types within the context of their normal microenvironment. However, the major drawback is that it is often not possible to attribute primary versus secondary effects due to the different cell types that coexist in these organ cultures. From this description of cell/organ culture systems employed to study osteoblast differentiation and bone formation, it is

clear that each particular culture model has certain advantages as well as limitations compared to the others. It is particularly important to be aware of the limitations when choosing a culture model for an experimental approach, and also when interpreting and extrapolating data generated using these culture models.

The osteoblast cell culture systems are widely used to study the effects of growth factors, secreted proteins, extracellular matrix components and transcription factors on differentiation and function (reviewed in Aubin and Triffit, 2002 (18) (Fig. 10). Many of the osteoblast culture models have been well characterized identifying the temporal sequence of gene/protein expression associated with osteoblast differentiation. In general, after the cells are plated in osteogenic medium, there are three stages of differentiation; proliferation, matrix production/maturation, and mineralization. The proliferative phase involves the expression of cell cycle and histone genes. This is followed by expression of genes associated with the formation of bone matrix such as type I collagen and alkaline phosphatase. In the final stage, genes associated with mineralization, such as osteocalcin and bone sialoprotein, are expressed at the highest levels.

Osteocytes

In contrast to surface cells, such as osteoblasts, osteocytes are bone cells that live within the substance of bone. These cells comprise 90%–95% of all bone cells. They are derived from osteoblasts (Fig. 10) that became trapped and surrounded by bone matrix which they themselves produced.

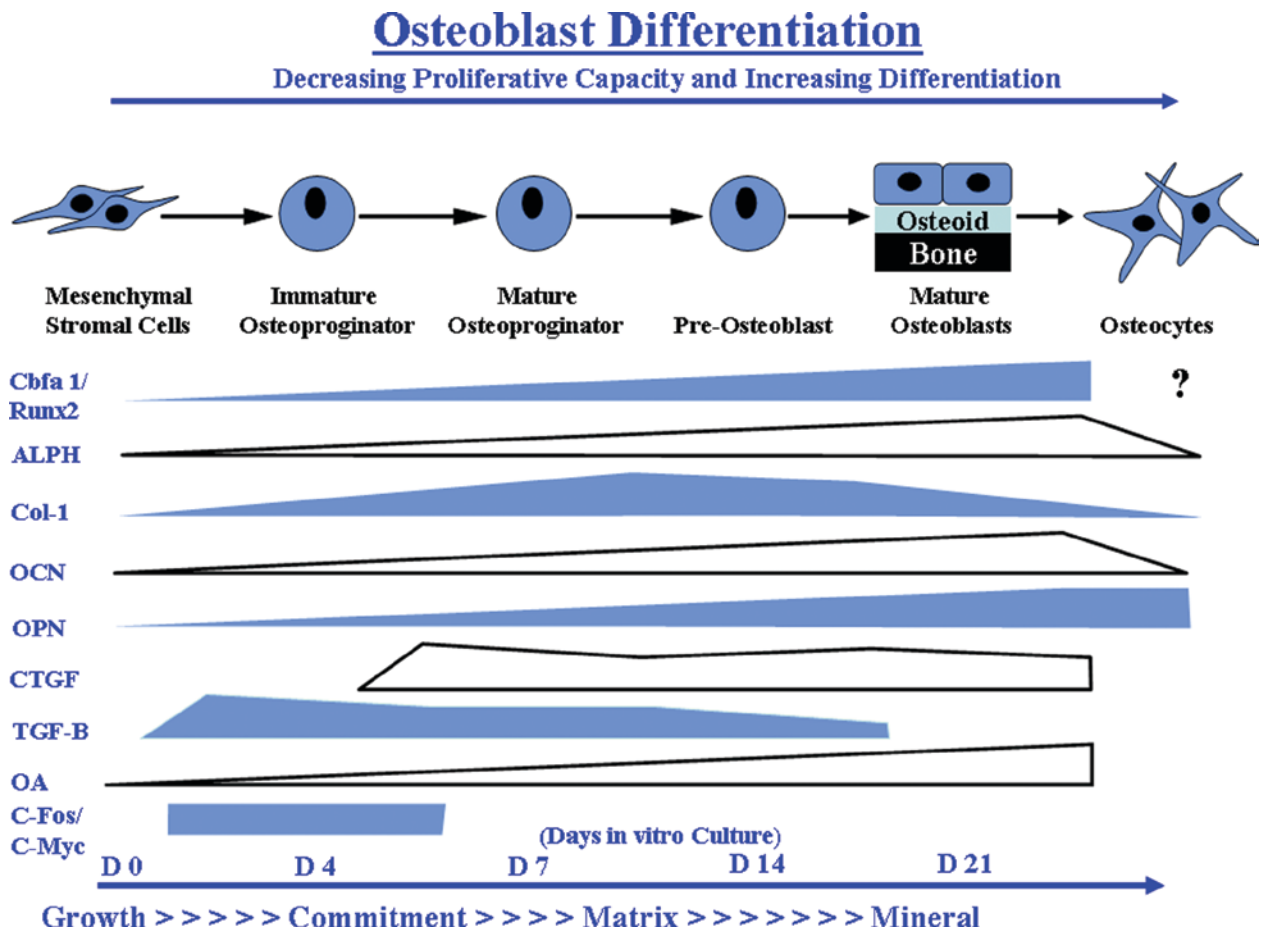

Fig. 10 Temporal pattern of expression of markers during osteoblast differentiation in culture. As osteoblasts proliferate and differentiate from mesenchymal stem cells they express/produce various proteins including growth factors, transcription factors and extracellular matrix (ECM) proteins, each of which has a distinct temporal pattern of expression. Runx2 (Cbfa1), c-fos and c-myc are transcription factors; ALPH, alkaline phosphatase; Col-1, Collagen type I; OCN, osteocalcin; OPN, osteopontin; CTGF, connective tissue growth factor; OA, Osteoactivin; TGF-β, transforming growth factor-β.

The spaces which they occupy are known as lacunae. They are said to be involved in cell signaling and maintaining the viability of bone matrix. The processes of osteocytes communicate with each other and with osteoblasts through a network of canaliculi. The processes of adjacent osteocytes are joined together by gap junctions thereby allowing this vast network of cells within the bone matrix to communicate with one another and with cells outside of the bone matrix. It is also believed that osteocytes are important in the translation of mechanical loads to cellular events such as bone formation and remodeling.

Osteocytes have the ability to stimulate osteoblasts and the accompanying matrix by expressing osteoblast specific factor-1 (OSF-1) (19). OSF-1 accumulates on bone surfaces near the osteocytes and binds to its receptor, N-syndecan (20) located on osteoblast progenitor cells. Dentin matrix protein 1 (termed *DMP1*) is highly expressed in osteocytes and, when deleted in mice, results in a hypomineralized bone phenotype. A recent study investigated the potential role of this gene to direct skeletal mineralization as well as to regulate phosphate (P_i) homeostasis. Both *Dmp1*-null mice and individuals with a newly identified disorder, autosomal recessive hypophosphatemic rickets, manifest rickets and osteomalacia with isolated renal phosphate-wasting associated with elevated fibroblast growth factor 23 (FGF23) levels and normocalciuria (21,22). Mutational analyses revealed that an autosomal recessive hypophosphatemic rickets family carried a mutation affecting the *DMP1* start codon, while a second family carried a 7-base pair deletion disrupting the highly conserved C terminus of DMP1. Studies using the *Dmp1*-null mice demonstrated that the absence of DMP1 resulted in defective osteocyte maturation and increased fibroblast growth factor 23 (FGF23) expression, leading to pathological changes in bone mineralization. These findings suggest a bone-renal axis that is central to guiding proper bone mineral metabolism (21,22).

Osteocyte-derived signals have remained largely enigmatic, but it was recently reported that human osteocytes secrete sclerostin, an inhibitor of bone formation. Sclerosteosis, a skeletal disorder characterized by high bone mass due to increased osteoblast activity, is caused by a loss of the SOST gene product, sclerostin (23). Osteocytes possess receptors for parathyroid hormone (PTH), a known regulator of mineral ion homeostasis (24). Osteocytes also express molecules typically associated with nerve cells, such as NMDA receptors, which are involved with glutamate neurotransmission.

Finally, osteocytes act as mechanosensory cells. Their cell body and processes are surrounded by a thin layer of unmineralized matrix, which allows a loading-derived flow of interstitial fluid over the osteocyte surface. Their mechanosensory receptor ability has been demonstrated in studies examining loading-facilitation of macromolecule diffusion (25).

Osteoclasts

Osteoclasts are multinucleated cells generally containing 3-25 nuclei per cell. Osteoclasts are related to the monocyte/macrophage lineage, with both cell types being derived from hematopoietic progenitor cells. Although the lineages of osteoclasts and osteoblasts are independent of one another, the genesis of osteoclasts requires the presence of osteoblasts along with a variety of hematopoetic cytokines, such as interleukins 1, 3, 6, and 11, tumor necrosis factor (TNF), colony stimulating factors (CSF), stem cell factor and others (26).

Colony stimulating factors are required for the proliferation and differentiation of osteoclast progenitor cells. After the osteoclast is formed, other cytokines are required for their activation and bone resorption. Parathyroid hormone (PTH), 1,25 dihydroxyvitamin D_3, transforming growth factor alpha (TGFα), and epidermal growth factor (EGF) act to stimulate osteoclastogenesis, whereas calcitonin inhibits the formation of osteoclasts (26).

Osteoclasts are the primary bone resorbing cells. Osteoclasts are found at sites where resorption is taking place, or if active resorption has already occurred, within "eaten out" pits or cavities known as **Howship's lacunae** (Fig. 11). Osteoclasts can also tunnel through cortical bone creating channels. Osteoclasts are highly polarized cells and the nuclei congregate away from the resorbing bone surface. The cell surface in direct apposition to the bone has an extensive infolding of the plasma membrane called the ruffled border. When the cell is in the resting state or in certain pathological conditions in which the osteoclast is dysfunctional, the ruffled border disappears or is absent (28). There is a three dimensional ring-like area of the cell membrane around the perimeter of the ruffled border called the clear zone or sealing zone. This zone contains abundant microfilaments (actin filaments) but lacks other organelles. It is here in the clear

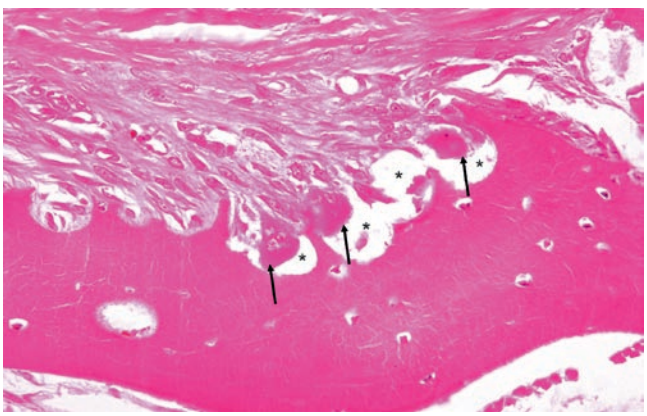

Fig. 11 Osteoclasts in actively growing bone. Osteoclasts are multinucleated cells (arrows) associated with a shallow pits or concavities (Howship's lacunae, *) along the bone surface.

zone that the osteoclasts attach to the bone matrix, a process involving the participation of actin filaments and the $\alpha_v\beta_3$ integrin. The actin reorganization or actin ring within the clear zone can be visualized microscopically by staining for actin filaments (28,29). The area of cytoplasm between the nuclei and the ruffled border is rich in carbonic anhydrase and in tartrate resistant acid phosphatase (TRAP) (27). By electron microscopy, there is also an abundance of mitochondria, lysosomes, vesicles and free ribosomes in the cytoplasm.

Molecular Mechanism of Osteoclast-mediated Bone Resorption

The mechanism of bone resorption is complex and involves an initial trigger by osteoblasts (see below). Once osteoclasts have been formed, bone resorption requires the secretion of hydrogen ions by an ATP driven proton pump in the ruffled border. This results in acidification of the extracellular space between the bone surface and the ruffled border which is sealed off from the general extracellular compartment by the clear zone forming a tight seal around the perimeter of the ruffled border region. The enzyme carbonic anhydrase II is essential in the generation of hydrogen ions. Simultaneously, acid hydrolases are released from lysosomes into the acidified extracellular space thus creating an extracellular lysosome. Osteoclasts can move over the bone surface, creating many resorption pits in their path. These pits are easily visualized by scanning electron microscopy, and correspond to the Howship's lacunae in routine sections. It is believed that osteoclasts must be stationary for resorption to occur, and therefore they do not resorb bone during the motile phase. Instead they cycle between motility and resorption, moving about, attaching to and resorbing bone, then releasing and moving to another region for resorption.

A combination of the acid created by the hydrogen ions and the proteolytic enzymes released from the lysosomes provide optimal conditions for the resorption of bone and degradation of collagen. This environment also results in the release and activation of certain growth factors and cytokines such as TNF-α and TGF-β. It is possible that oxygen-derived free radicals are also important in this process.

Osteoclastic stimulation may also be influenced by interactions of the integral membrane proteins (integrins) present on the osteoclast cell membrane and proteins in the bone matrix that contain the amino acids RGD (arganine-glycine-aspargine). These bone matrix proteins include fibronectin, collagen type I, bone sialoprotein II and osteopontin, all of which bind integrins and initiate out-side-in signaling pathways that can regulate the bone resorption process. Much of the data regarding factors that are important for the development, differentiation and function of osteoclasts have come from genetically modified animal models (see Table 1.1).

Osteoclasts have calcitonin, but not PTH or Vitamin D receptors. They are stimulated by IL-6 (perhaps in combination with IL-1, IL-3 and IL-11) and RANK-ligand. These cytokines are produced locally by cells of the osteoblast lineage under the influence of PTH, Vitamin D_3, TGF-β, IL-1 and TNF-α. It is interesting to note, that giant cell tumor (osteoclastoma) cells respond to IL-6 (30, 31). Anti IL-6 antibodies have been shown to inhibit osteoclastic activity in these cells. However, in the physiologic state, the evidence for the action of IL-6 in osteoclastogensis is lacking. Perhaps threshold levels or additional cytokines play a role (32, also reviewed in 26).

Regulation of Osteoclast Differentiation

Macrophage colony-stimulating factor (M-CSF) is a secreted protein that is produced by osteoblasts and bone marrow stromal cells. M-CSF is required for the proliferation and survival of osteoclast precursors, cells of the monocyte-macrophage lineage (Fig. 12). Both osteoblasts and stromal cells produce RANK-ligand that has a high affinity for binding to the RANK receptor on osteoclast precursors. Treatment of osteoblasts or stromal cells with PTH, vitamin D, PGE2, or IL-11 stimulates the expression of RANK-ligand mRNA (Fig. 12)(33).

The interaction between RANK (on osteoclast precursors) and RANK-ligand (on osteoblasts and stromal cells) requires cell-cell contact for further maturation of osteoclast precursors (34–36). Osteoblasts also secrete osteoprotegerin (OPG), a member of the TNF-α receptor superfamily (37). This protein lacks the transmembrane domain and is presented as a secreted form. OPG is a soluble protein and acts as a decoy receptor that binds RANK-ligand and prevents RANK/RANK-ligand interaction. Through this mechanism, OPG can modulate the process of osteoclastogenesis. Macrophage-colony stimulating factor (M-CSF) is also essential for osteoclastogenesis. M-CSF induces cells of the monoctye/macrophage lineage to proliferate and become osteoclast precursors. RANK-ligand stimulates M-CSF-induced cells to differentiate into functional osteoclasts. Animal models of genetically modified RANK, RANK-ligand and OPG have been generated to understand the role of these proteins in osteoblast biology (see below). Mouse knockouts for RANK and RANK-ligand share similar phenotypes (38–40). Both models develop severe osteopetrosis, a disease associated with the absence of osteoclasts and failure of tooth eruption. Transgenic mice that over-express OPG in the liver also resulted in severe osteopetrosis. Therefore, the RANK/RANK-ligand/OPG axis appears to play a key physiological role in osteoclast differentiation and function. Clinically,

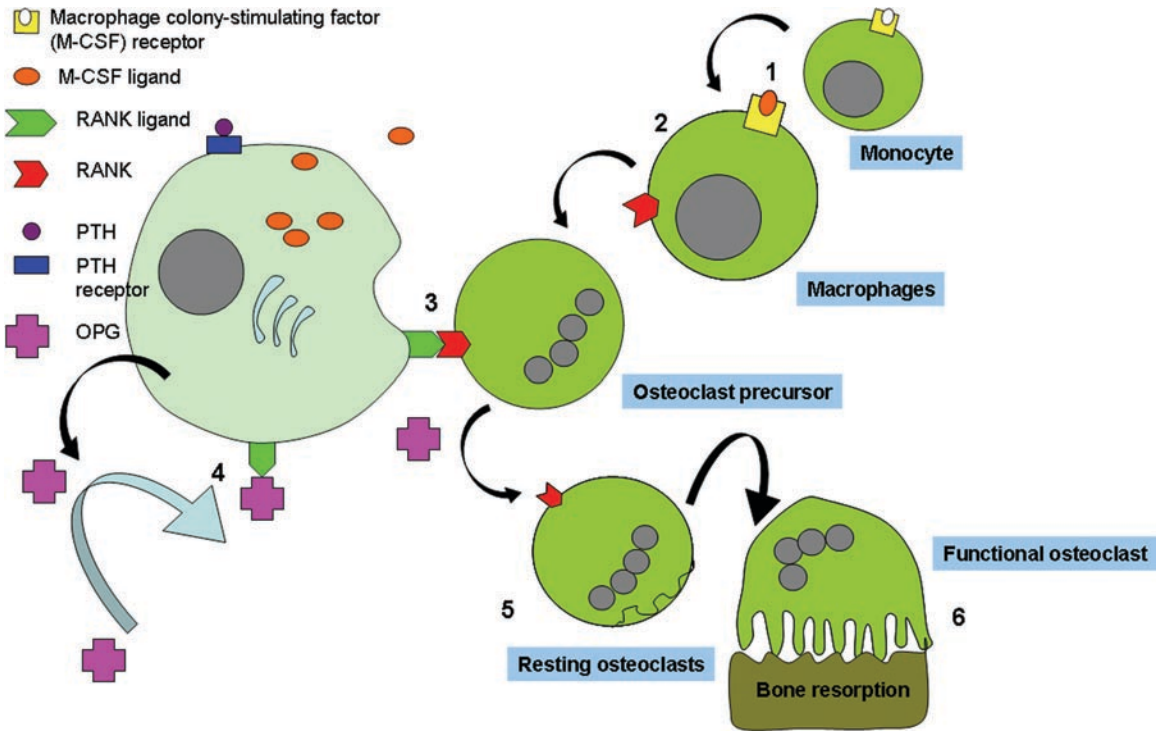

Fig. 12 Regulation of osteoclast differentiation. 1. Monocytes derived from vessels in the bone marrow, reach an area of bone formation or remodeling. Monocytes express M-CSF receptor on their cell surface. 2. Monocytes differentiate into macrophages. M-CSF binds to M-CSF receptor and induces the expression of RANK. 3. RANK ligand (RANKL) is produced by stromal cells/osteoblasts and binds to the receptor, RANK, on mononuclear osteoclast progenitors (bone marrow macrophages). 4. OPG, a decoy receptor that binds to RANKL and inhibits osteoclast differentiation. 5. Following the interaction between RANK and RANKL, mononuclear osteoclast progenitors fuse to form a resting (non functional) multinucleated osteoclast that uncouples from the osteoblast. 6. Multiple factors including transcription factors, hormones, locally produced cytokines/growth factors and matrix proteins, mediate the activation (bone resorption) of osteoclasts.

it has been reported that two mutations of heterozygous insertion were detected in the first exon of RANK in families with familial expansile osteolysis or familial Paget's disease of bone (41).

Signaling Pathway of RANK

The cytoplasmic tail of RANK interacts with TNF receptor-associated factor (TRAF) TRAF family members. TRAF2-mediated signals appear important for inducing osteoclast differentiation, and TRAF6-mediated signals are indispensable for osteoclast activation. Activation of NF-κB, JNK and ERK pathways, all induced by RANK–ligand in osteoclast precursors and mature osteoclasts, appear to be involved in the differentiation and function of these cells (42,43). OPG strongly blocks osteoclastic bone resorption *in vivo*, suggesting that inhibiting the RANK-ligand/RANK interaction or RANK-mediated signals are promising targets to prevent increased bone resorption in metabolic bone diseases such as rheumatoid arthritis, periodontitis and osteoporosis. Studies have also shown that TNF-α and IL-1 can substitute for RANK-ligand in inducing osteoclastogenesis *in vitro*. These studies suggest that signals other than these induced by RANK may also play important roles in osteoclastic bone resorption under pathological conditions.

Positive Regulation of Osteoclastogenesis

Suppressor of cytokine signaling-1 (SOCS-1) is an inhibitor of cytokine signaling and may play a positive role in the regulation of T-cell-mediated osteoclastogenesis by counteracting inhibitory cytokines such as interferon-gamma (IFN- γ) (44). It has been reported that (SOCS)-1-deficient osteoclast precursor cells are more susceptible to the inhibitory effects of IFN-γ on osteoclastogenesis when compared to wild-type cells (44). SOCS-1 has been shown to be induced by RANK-ligand stimulation during osteoclastogenesis (45), indicating that these precursor cells are resistant to IFN-γ-mediated inhibition if they are first stimulated by RANK-ligand. It is likely that the fate of osteoclast precursor cells is determined not only by the balance of cytokines, including IFN-γ and RANKL (46), but also by the cytokine first encountered (47).

Negative Regulation of Osteoclastogenesis by Interferon-β

Using a genomewide screening of RANK-ligand-inducible genes, several interferon (IFN)-α/β-inducible genes were identified in RANKL-stimulated osteoclast precursor cells. The bone phenotype of mice deficient in a subunit of the interferon- α/β receptor, IFN- α receptor type I (IFN-α-R1), was analyzed (48). These mice exhibited marked osteopenia accompanied by enhanced osteoclastogenesis in vivo. Detailed molecular analyses showed that RANK-ligand induces interferon-β in osteoclast precursor cells, and IFN-β inhibits the expression of c-Fos, an essential transcription factor for osteoclastogenesis. RANK-ligand-mediated induction of interferon- β is dependent on c-Fos, constituting a negative feedback loop in which RANK-ligand-induced c-Fos induces its own inhibitor. Thus, although type I interferons were originally characterized as critical antiviral factors, these studies situate the interferon system in a novel context and provide a compelling example of osteoimmunologic regulation (49).

Transcriptional Regulation of Osteoclastogenesis

Genomewide screening of RANK-ligand-inducible genes identified NFATc1 (nuclear factor of activated T-cells) to be the most highly induced transcription factor in osteoclast precursor cells. NFATc1 binds to the Nfatc1 promoter and induces itself (50). This strategy is often observed in hematologic cells that undergo irreversible differentiation (51). Nfatc1$^{-/-}$ embryonic stem cells cannot differentiate into osteoclasts in vitro and overexpression of NFATc1 induces osteoclastogenesis. These results suggest that NFATc1 is an essential regulator of osteoclastogenesis (52), but it has proven difficult to show that this transcription factor is indispensable for osteoclast differentiation in vivo due to the embryonic lethality of Nfatc1$^{-/-}$ mice.

Immunoreceptors in Osteoclastogenesis

The close relationship between bone and immune system extends beyond the cytokines and transcription factors they share. Activation and nuclear localization of NFAT are dependent on its dephosphorylation by the phosphatase calcineurin, which is activated by calcium (Ca^{2+}) signaling. Ca^{2+} oscillation is observed during osteoclastogenesis, and the calcineurin inhibitors cyclosporine A and FK506 strongly inhibit osteoclastogenesis (52). It is not clear, though, how Ca^{2+} signaling is activated during osteoclastogenesis. DNAX-activating protein 12 (DAP12) is an adaptor molecule that associates with immunoglobulin-like receptors and harbors an immunoreceptor tyrosine-based activation motif (ITAM), which is known to be crucial for the activation of Ca^{2+} signaling in the immune cells. The osteopetrotic phenotype in DAP12-deficient mice made evident the importance of ITAM for osteoclastogenesis (53). Mice deficient in both DAP12 and the Fc receptor common γ subunit (FcRγ) have been shown to exhibit severe osteopetrosis, indicating that immunoglobulin-like receptors also provide important signals for osteoclastogenesis in addition to the RANK and M-CSF receptors (54,55). However, immunoreceptor signaling alone cannot induce osteoclastogenesis, suggesting that these receptors provide co-stimulatory signals for RANKL. FcRγ-associating receptors include osteoclast-associated receptor (OSCAR) and paired immunoglobulin-like receptor-A, while DAP12-associating receptors include triggering receptor expressed on myeloid cells (TREM-2) and signal-regulatory protein (SIRP-β) (54). The ligands for these immunoreceptors on osteoclasts are yet to be identified. OSCAR expression is upregulated significantly during osteoclast differentiation and its induction is mediated by NFATc1 (56, 57). Thus, OSCAR-NFATc1 constitutes a positive feedback loop in osteoclast precursor cells.

Physiological versus Pathological Bone Resorption

Under physiological conditions, osteoclast formation requires cell-to-cell contact with osteoclast/stromal cells which express RANK-ligand as a membrane-bound factor in response to a number of factors that have been shown to stimulate bone resorption. In contrast, under pathological conditions that stimulate bone resorption, such as in rheumatoid arthritis, macrophages and/or T cells secret inflammatory cytokines such as TNF-α and IL-1. These cytokines act directly on osteoclast progenitors and mature osteoclasts without cell-to-cell contact. This paradigm is characterized by the uncoupling of bone resorption and bone formation.

Model Systems Used to Study Osteoclasts

Given the technological challenges associated with isolating sufficient numbers purified osteoclasts, it has been difficult to study these cells experimentally. The models developed to study osteoclasts in culture are more cumbersome than those for osteoblasts. The recent discovery of the role for RANK-ligand and M-CSF in osteoclastogenesis has allowed investigators to differentiate large numbers of osteoclasts from bone marrow progenitors or splenic macrophages (58) in the presence of recombinant forms of these essential factors. Large numbers of osteoclasts can also be generated from the

RAW cell line, a macrophage cell line that has the ability to differentiate into osteoclasts when treated with RANK-ligand and M-CSF. Another alternative is the osteoclast-osteoblast co-culture system in which primary osteoblasts are cultured with bone marrow hematopoietic cells containing osteoclast progenitors (monocytes/macrophages). This culture system requires both vitamin D and PGE_2(26).

Osteopetrosis (see section on metabolic bone disease) in humans and animals has been useful in providing models to study osteoclast development and function. One form of the disease is associated with carbonic anhydrase II deficiency. Osteoclasts are present but functionally incompetent in CAII deficiency, and children afflicted with this disease also suffer from renal tubular acidosis. In the *op/op* osteopetrotic mouse and the *tl/tl* toothless rat models, there are abnormalities in the coding region of the CSF-1 gene resulting in the production of trauncated and functionally incompetent CSF-1 protein. In these forms of osteopetrosis, osteoclasts are absent or greatly reduced in number, and treatment with exogenous CSF-1 results in normal osteoclastogenesis and correction of the disease. There are other mouse models in which targeted disruption of certain proto-oncogenes, such as src and fos, causes osteopetrosis (for a more comprehensive list, see Table 1).

Part 2 Bone Development

The bones of the axial and appendicular skeleton are formed by one of two processes, intramembranous or endochondral bone formation. The primary difference between these two processes is the absence or presence of a cartilaginous intermediary. In intramembranous bone formation, bone is formed in the absence of a cartilage model while in endochondral bone formation, a cartilage model is first formed and then replaced by bone tissue.

Intramembranous Bone Formation (Membranous)

The flat bones of the skull and face are formed by intramembranous ossification (Fig. 13). Osteoprogenitor cells (which will give rise to osteoblasts and osteocytes) are present within the mesenchyme. These cells aggregate at the sites where new bone is to be formed and differentiate into osteoblasts that actively synthesize new bone matrix. Growth of intramembranous bones occurs by *apposition* (deposition upon prior bone) of osteoblasts lining the surfaces of the growing bones. Ossification centers develop within the bone and enhance the rates of mineralization. As the growth rate slows down, the bones take on a *lamellar* character. In the adult, Haversian remodeling occurs.

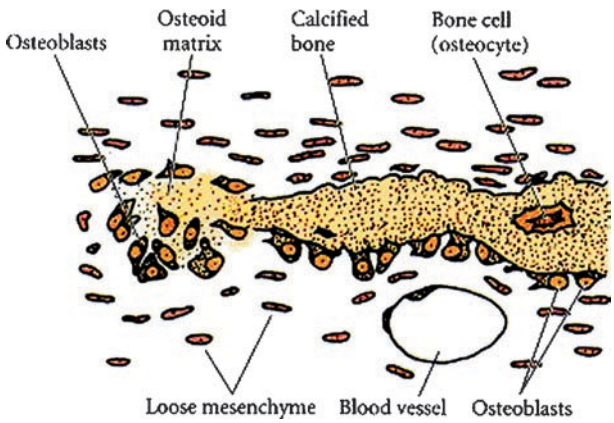

Fig. 13 Intramembranous Ossification. Mesenchymal stem cells condense to produce osteoblasts, which deposit osteoid and mineralize the bone matrix. These osteoblasts line the surfaces of the developing bone and continue to produce bone matrix by apposition. Osteoblasts that become trapped within the bone matrix become osteocytes. There is no cartilage that precedes the formation of bone in this type of bone formation. Permission granted from Sinauer Associates (Gilbert, 6th edition, 1997).

Chondroid bone has also been described within the skull, occurring in association with suture closure. This type of bone has a histological intermediate between cartilage and bone, containing both types I and II collagen. Chondroid bone forms a scaffold upon which lamellar bone is deposited. It is not replaced by bone as occurs in the endochondral model (see below).

There are many factors that play potential roles regulating bone formation, and their functions and interactions are complex. For instance, core binding factor-alpha1 (cbfa-1) is responsible for osteoblast differentiation, and binds the osteocalcin promoter, resulting in osteocalcin expression. Mutation of cbfa-1 causes cleidocranial dysplasia, a disorder in which there is delayed ossification of cranial sutures.

Endochondral Bone Formation (Cartilage Model)

Endochondral ossification involves the formation of cartilage tissue from aggregated mesenchymal cells and the subsequent replacement of this cartilage tissue by bone tissue (60). All of the skeletal components of the vertebral column, the pelvis, and the appendicular skeleton (limbs) develop via endochondoral ossification. The process of endochondral ossification is divided into five stages (Fig. 14). ***First***, the mesenchymal stem cells are committed to become cartilage cells through expression of two transcription factors,

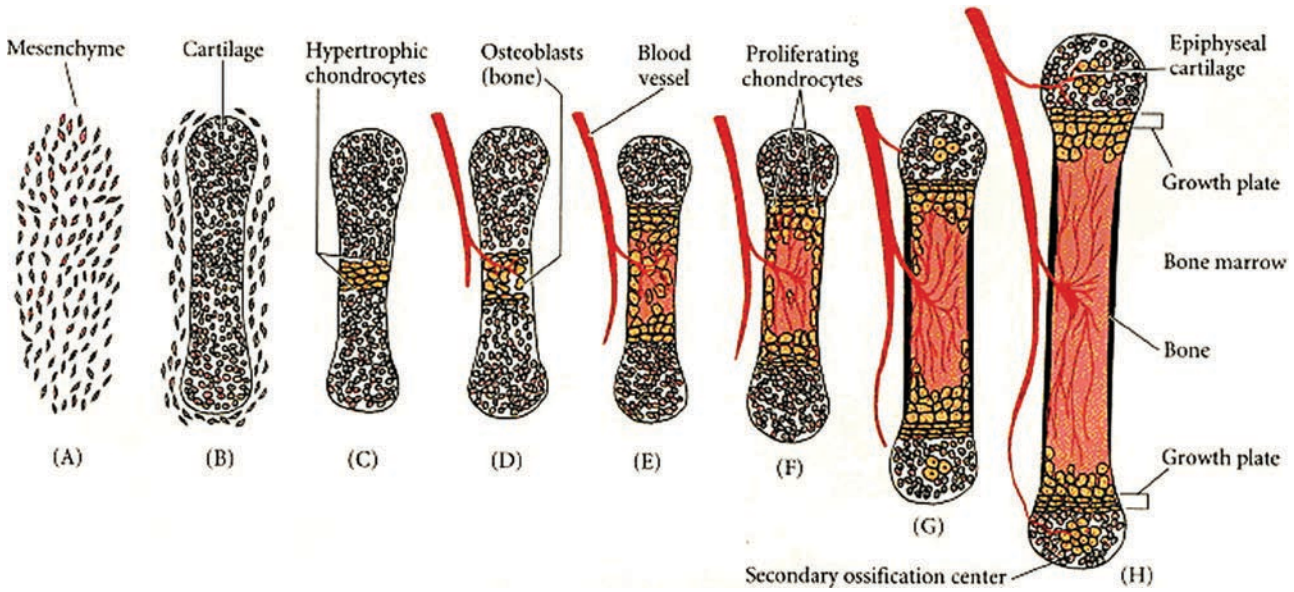

Fig. 14 Endochondral Ossification. (A, B) Long bones such as humerus, femur and tibiae develop through endochondral ossification where the mesenchymal stem cells condense and differentiate into chondrocytes to form the cartilaginous model of the bone. (C) Chondrocytes in the center of the shaft undergo hypertrophy and apoptosis and their death allows blood vessels to enter that region (primary ossification center). (D, E) Blood vessels bring in osteoblasts, which lay down new bone matrix on the remants of the calcified cartilage (scaffold). (F-H) Secondary ossification centers also form as blood vessels enter near the ends of the bone. Bone formation and growth in length continue at the growth (epiphyseal) plates with ordered arrays of resting, proliferating, hypertrophic (mineralizing) chondrocytes. Permission granted from Sinauer Associates (Gilbert, 6th edition, 1997).

Pax1 and Scleraxis. These factors are thought to activate cartilage-specific genes (61–63). During the ***second*** phase of endochondral ossification, the committed mesenchymal stem cells condense into compact nodules and differentiate into chondrocytes. N-cadherin appears to be crucial for the initiation and maintenance of these condensations (64,65). In humans, the SOX9 gene (sex reversal Y-related high-mobility group box protein) and chondrocyte commitment, that encodes a DNA-binding protein, is expressed in the precartilaginous condensations. Mutation of the SOX9 gene alters skeletal development and results in deformities of most of bones of the body. Infants with specific mutations of the SOX9 gene die from respiratory failure due to poorly formed tracheal and rib cartilages (66). During the ***third*** phase of endochondral ossification, chondrocytes proliferate rapidly to form the cartilage model that will eventually be replaced by bone tissue. As they divide, chondrocytes secrete a cartilage-specific extracellular matrix. In the ***fourth*** phase, the chondrocytes stop dividing and become hypertrophic. Hypertrophic chondrocytes have increased production of collagen type X and fibronectin, thus altering the remaining cartilage matrix so that it can be mineralized by calcium carbonate. Finally, in the ***fifth*** phase, blood vessels begin the invasion of the cartilage model. The hypertrophic chondrocytes undergo apoptosis and the spaces are invaded by ingrowing blood vessels. As the cartilage cells die, osteoprogenitor cells differentiate into osteoblasts and begin to lay down bone matrix on the partially-degraded, mineralized cartilage remnants (67,68). The site at the center of the cartilaginous model where ossification first occurs is known as the ***primary center of ossification*** (the eventual diaphysis of the long bone). Eventually, all the cartilage is replaced by bone so the cartilage tissue serves as an intervening model for the bone that will eventually replace it. In experimental models, the precise sequence of events has been worked out reasonably well (for a detailed review see 85).

In the long bones of mammals, this process of endochondral ossification spreads along the vertical axis of the developing bone in both directions from the primary ossification center (Fig. 14). As the bones grow in length, **secondary centers of ossification** form at the ends of each bone. Once these secondary ossification centers form, there remains an area of cartilage between the primary and secondary ossification centers. The secondary ossification center becomes the epiphysis and the primary center becomes the diaphysis. The intervening cartilage is the epiphyseal growth plate and it is here that continued growth in length occurs at both ends of the developing bone. The epiphyseal plates contain three regions: a region of chondrocyte proliferation, a region of chondrocyte maturation, and a region of hypertrophic chondrocytes (reviewed in 69). A complex series of events occur in the growth plate as the resting chondrocytes

proliferate, mature and become oriented in columns. As the cells hypertrophy at the expense of the intervening cartilaginous matrix, the cartilage matrix becomes calcified. It is these calcified cartilage remnants that then serve as a scaffold for the deposition of bone matrix by osteoblasts. The spaces left behind by the apopototic hypertrophic chondrocytes are invaded by blood vessels, a critical event in the formation of new bone tissue. Abnormalities in chondrocyte function can disrupt this sequence and produce abnormally short and misshapen bones. One illustration of this is achondroplasia, a condition causing short stature and thought to be caused by a mutation in fibroblast growth factor (FGF). Without the normal cellular processing of the signal from the fibroblast growth factor, the chondrocytes do not proliferate normally (70). This results in a disorganized and malfunctioning growth plate.

Molecular Regulation of Growth Plate (Chondrocytes)

Chondrocytes of the growth plate behave very differently than chondrocytes of articular cartilage. Chondrocytes within different parts of the growth plate are markedly different from each other. Investigators have been studying the factors that are important in each region. Indian hedgehog, is a factor that plays a role in the normal differentiation of growth plate chondrocytes. The study of factors that activate Indian hedgehog (Ihh) and other associated factors are advancing our understanding of the molecular biology of the growth plate and its disorders (69).

There are systemic and local mediators that regulate growth plate chondrocyte proliferation and differentiation. Systemic factors include insulin growth factor-1 (IGF-1) (71), growth hormone (72), thyroid hormone (73), estrogens (74), vitamin D (75) and glucocorticoids (76). All of these factors have been reported to have an effect on the linear growth of bone both prenatally and postnatally. Other factors act locally to regulate growth plate chondrocytes, include TGF-β, PTHrP (78), Ihh (79) and FGF-receptor type 3 (FGFR3) (80,81). It has been reported that TGF-β has the ability to inhibit chondrocyte proliferation, hypertrophic differentiation and matrix mineralization (82).

Control of the growth plate is also an area of intense research. Indian hedgehog (Ihh), a protein of the same family as sonic hedgehog, regulates the rate of hypertrophic chondrocyte differentiation. It is produced by the pre-hypertrophic chondrocytes and induces the expression of parathyroid hormone related protein (PTHrP) in the perichondrium, which blocks chondrocyte differentiation. The Ihh/PTHrP axis acts as a negative feedback loop modulating chondrocyte differentiation. One can imagine that abnormalities in this control loop can alter growth plate function or lead to inhibition of chondrocyte proliferation (83).

The overlapping expression of FGFR3 and PTH-receptor-1 (PTHR1) in the growth plate suggested that these signaling pathways interact. Genetic inactivation of either PTHrP or the PTHR1 in mice resulted in a marked decrease in the size of the proliferative zone of the growth plate, a phenotype that is seen with the constitutive activation of the FGFR3 signaling. Other *in vivo* studies have shown that FGFR3 signaling can repress Ihh and PTHR1 expression in the growth plate (84). These studies suggest a link between Ihh/PTHrP signaling and the FGFR3 pathway in the growth plate.

Limb Development

The development of the human limb begins at day 24 of gestation and is orchestrated by the expression of a sequence of genes expressed in specific regions of the developing limb. Three zones typify the growing limb bud: a thickened ectoderm located distally at the periphery, called the apical ectodermal ridge (AER), proliferating mesoderm just deep to the AER called the progress zone (PZ); and a zone of polarizing activity (ZPA) located posterior to the PZ (86).

The AER is responsible for general limb and bone development. Grafting the AER from one animal to the PZ of another, patterns the growing limb after the donor AER. In contrasts, the ZPA orients the limb in an anterior-posterior direction. Grafting the ZPA to the anterior border of a developing limb, results in a duplicated limb in opposite orientation. The AER maintains continuous limb bud outgrowth along the proximal-distal (P-D) axis (shoulders to digits). Concomitant to its elongation along the P-D axis, the limb becomes flattened along the dorso-ventral (D-V) axis (back of hand to palm) and is asymmetric along the antero-posterior (A-P) axis (thumb to little finger). Differentiation of mesenchymal stem cells becomes morphologically apparent as these cells condense to form the primordia of individual skeletal elements. The most proximal elements (stylopod) begin to differentiate first, followed by the progressive differentiation of more distal structures (zeugopod and autopod) (87, 88).

Limb patterning also plays a role in how bones develop (89). Genes such as sonic hedgehog, and the homeobox genes, organize segmentation, anterior-posterior, medial, lateral and longitudional limb patterning during fetal development. Abnormalities in patterning genes may lead to extra or deficient digits, short or long limbs, or congenital amputations. The growth plate is altered in many of these malformations, and thus, the patterning genes likely modify factors involved in chondrocyte function and differentiation in the growth plate.

Molecular Biology of Limb Formation

As the limb bud grows, the proximal-distal, dorso-ventral and antero-posterior axes are apparent and development is mediated by multiple signaling molecules. Members of the fibroblast growth factor (FGF) family produced by AER cells are required for P-D outgrowth. FGF signals are responsible for keeping the underlying undifferentiated mesenchymal cells in the progress zone, in an undifferentiated, rapidly proliferating stage. At least five FGFs (FGF 2, FGF 4, FGF 8-10) and two FGF-receptors (FGFR1 and FGFR2) are expressed during limb bud initiation. FGF 2, 4, 8, 9 and FGFR 2 are found in the ectoderm and AER while FGF 10 and FGFR 1 are present in the underlying mesenchyme (90,91). Sonic hedgehog (Shh) is an important molecule in the ZPA, and is responsible for duplication of limb structures as demonstrated in grafting experiments. FGF maintains *Shh* expression in the ZPA and FGF 4 is largely responsible for maintenance of its expression as the limb elongates (92). Select FGFs in conjunction with *Shh* regulates expression of the bone morphogenetic (BMP2 and 7) and Hox genes, mostly Hoxd-12 and Hoxd-13. These genes are members of the *Hoxd* complex and are expressed in the distal wrist (Hoxd 12), within the hand and fingers (Hoxd 12 and 13). These genes regulate proximal-distal differentiation of limb segments and mutation of Hoxd-13 in the human transforms metacarpals to carpals and metatarsals to tarsals. On other hand, overexpression of Hoxd13 in chick limb bud in vivo resulted in the transcriptional repression in the proximal part of the limb of *Meis*, the vertebrate ortholog of an homeo-box containing gene in *drosophila* called *homothorax* (hth) that is required for proximal leg development (92).

Wnt proteins regulate many events in limb development, from patterning to controlling cell proliferation, differentiation and survival. The Wnt family signals through ten different transmembrane frizzled receptors. These receptors also function together with the LDL-related protein receptor (LRP). Two LRP receptors bind Wnt, LRP 5 and 6.

Wnt signals through three pathways, the β-catenin pathway, the JNK (planer polarity) pathway and the Wnt/Ca^{+} pathway (93). The β-catenin pathway is also called the canonical Wnt signaling pathway and is well characterized (94,95). Wnt signaling is antagonized by different factors, such as members of the TGFβ and FGF families, frizzled related proteins (Sfprs), cerberus, dickkopfs (DDKs) and members of the CCN family of proteins (93). Wnt proteins are expressed in the AER which controls limb outgrowth (97) and the dorsal ectoderm which controls dorso-ventral patterning. Wnts are also expressed in the AER and in lateral plate mesoderm where their overexpression leads to ectopic limb formation (96). Mutation in Wnt proteins and their downstream signaling molecules has been linked to human limb malformations. Wnt3a and 7a regulate the expression of Csa1, mutated in human pre-axial polydactyly (98). Spontaneous, naturally occurring mutations in Wnt7a has also been associated with postaxial hemimelia characterized by duplication of the sesamoid bones and foot pads (93). It is evident that Wnt and associated signaling pathways play a major role in limb development and pathogenesis of limb deformities and our knowledge of the Wnt signaling pathways and their role in limb development will enhance our understanding of the genetic basis of limb deformities.

Skeletal Muscle

Type(s) of Muscle

Muscle is characterized as either striated or non-striated. The term striated originated from the appearance of the ordered structure of this muscle type under the microscope. As opposed to this, non-striated muscle does not show the same regimented pattern of order. Striated muscle includes two types of muscle: skeletal and cardiac. Smooth muscle is classified as non-striated. Here we will focus on only one type of striated muscle: skeletal muscle. In longitudinal section, these cells appear tubular with multiple nuclei/cell located at the periphery of cells. In cross-section the cells are polygonal with the nuceli located at the periphery. They are characterized as striated, voluntary muscles with the ability to undergo strong; quick contractions.

Organization of Skeletal Muscle at the Light and Electron Microscope Level

A muscle cell or fiber is surrounded by a plasma membrane referred to as the sarcolemma. In normal muscle, an important component of the sarcolemma is dystrophin, where it forms a complex with the sarcolemmal cytoskeletal network. Dystrophin is absent in patients with muscular dystrophy. Muscular dystrophy is a general term used to describe a group of inherited myogenic disorders. The cytoplasm is referred to as the sarcoplasm. The sarcoplasm is filled with filamentous myofibrils which run parallel to the long axis of the cell. The myofibrils are composed of myofilaments which are made up of polymers of primarily myosin and actin, proteins responsible for contraction. A view of a myofilament shows thick filaments made up of myosin and thin filaments of actin. The filaments interdigitate and have the appearance of light and dark bands. The light bands are comprised of actin and are termed the I band (isotropic). The dark bands are made up of myosin and the overlapping region of actin and are called A bands (anisotropic). These alternating light

and dark bands give skeletal (and cardiac) muscle their striated appearance. The actin filaments are attached to Z lines. The actin filaments extend on either side of the Z line (disc) to interdigitate with the myosin molecules. The Z disc is composed of a variety of proteins which anchor the actin filaments to the Z line and which extend from one myofibril to another in cross-section. Alpha-actinin is one of those proteins involved in anchoring actin to the Z disc. Another more recently identified giant (300kD) protein 'titin' spans the distance between the Z disc and the M line of the sarcomere. It is involved in providing elasticity to the sarcomere and a main contributor to 'passive tension' (passive or resting tension is that which is present in a muscle even before contraction is initiated and is a result of the elastic forces in the muscle). Although not discussed here many other proteins are part of the contractile apparatus including C protein, Myomesin, and Nebulin. The region between Z lines is called a sarcomere, a unit repeated throughout the structure of the myofibril. The A band is bissected by the M line. This is the region where lateral connections are made between the thick filaments. The main component of the M line is creatine kinase, an enzyme that catalyzes the transfer of a phosphate group from phospho-creatine (storage form of high energy phosphate) to ADP. This provides the energy in the form of ATP necessary for muscle contraction.

Characteristics of the Contractile Filaments

The myosin thick filament is made up of many myosin molecules. The tail region is made up of two polymers of myosin heavy chain molecules twisted together as a double helix forming the body of the thick filament. At the end of the tail is found two pairs (four) of myosin light chain molecules which form the head region of the myosin polymer. The head region has an ATPase, an enzyme essential to the production of energy for contraction. The head region and a portion of the helix of the myosin molecule (which makes up the arm: can move away or towards the helix) extends outward to form cross bridges that make contact with the thin actin filaments as described in the "sliding filament theory". These cross bridges that extend outward can bend and have hinges at two points: one, where the head attaches to the arm and the second, where the arm attached to the axial body of the myosin molecule. These hinges facilitate movement. Cross bridges project around the entire thick.

The actin filament is a double stranded helix of F-actin protein. Polymerized G- actin molecules make up the F-actin filament. Each G-actin molecule has a myosin head binding site. The thin actin filament also contains two strands of the tropomyosin molecule which cover the myosin interactive sites on actin, preventing interaction of actin and myosin. Also, along the tropomyosin molecules is found the globular troponin complex. Troponin I has a strong affinity for actin, Troponin T for tropomyosin and Troponin C for calcium ions.

Innervation of Muscle

Myelinated motor nerves which originate from spinal cord neurons give rise to several terminal branches which make contact with multiple individual muscle cells. At the site of innervation the nerve terminal sits in a trough *(motor end plate)* at the surface of the muscle cell. The space between the axon and the muscle is the *synaptic cleft.* An action potential at the neuromuscular junction (or motor end plate) causes the release of acetylcholine from the axon which binds to receptors on the highly folded sarcolemma *(junctional folds).* In patients with myasthenia gravis, acetylcholine receptors on the sarcolemma are blocked by antibodies generated as an autoimmune response. The muscle cell cannot respond to the nerve stimulus resulting in muscle weakness. After acetylcholine binds to its receptor, the sarcolemma becomes permeable to sodium ions resulting in membrane depolarization. Depolarization is propagated along the muscle cell into the cell via the *transverse tubule system.* This is a network of tubules arising as invaginations of the sarcolemma and surrounds the A-I interface of each sarcomere in each myofibril. These tubules associate with two *terminal cisternae* (expanded regions of the SR) of the sarcoplasmic reticulum and together are known as *triads.* At the triad the depolarization signal is transmitted to the SR resulting in the release of stored calcium ions and initiating contraction. Calcium is released near the thick and thin filaments. When depolarization ends; calcium reenters the SR and contraction ceases.

Mechanism of Contraction

The actin filament is inhibited from interacting with the myosin cross bridges by the troponin-tropomyosin complex. Before contraction can take place this inhibitory interaction must be removed. It is the introduction of large amounts of calcium ions that changes this inhibitory effect. Calcium ions released from the sarcoplasmic reticulum combine with troponin C which changes the configuration of the troponin complex and moves the tropomyosin molecules further into the grooves between the actin filaments. This makes the active sites on the actin filament available for interaction with the cross bridges of myosin and is the binding step in the contraction process. Once the cross bridges are attracted

to the active site on actin the process of contraction begins. The hypothesized mechanism is referred to as the "walk-along" theory of contraction.

Remember that the head of the myosin molecule binds ATP. ATPase activity in the head cleaves the ATP but the ADP remains attached. In this conformation the head is extended towards the actin filament. When the inhibitory effect of the tropomyosin-troponin complex is lifted, the myosin head binds to the actin molecule. This causes a conformational change in the myosin head causing it to tilt towards the arm and this process causes a power stroke. The energy for this is already stored in the head from the cleavage of ATP. ADP and Pi is released allowing for a new ATP to bind to its site on the myosin head. This binding causes the myosin to detach from the actin and return to its original perpendicular position, the new ATP is cleaved and the myosin forms a new bond further down the actin filament to again perform a power stroke and consequently move another step. These steps occur again and again as the actin filament pulls the Z disc towards the ends of the myosin filament. Remember that contraction is not a result of shortening of individual filaments but an increase in overlap between the actin and myosin filaments. Therefore, as sarcomere length decreases, tension in the muscle and strength of contraction increase.

The Neuromuscular Spindle

The sensors that keep the central nervous system informed of the state of contraction and position of voluntary muscle are referred to as neuromuscular spindles (NMS). This structure consists of modified muscle fibers encased in a fluid filled sheath of connective tissue. The fibers comprising the neuromuscular spindle are referred to as intrafusal fibers. The fibers we have discussed earlier (making up the bulk of skeletal muscle) are extrafusal fibers. Intrafusal fibers come in two varieties: nuclear bag fibers (nuclei accumulated in the midregion) and nuclear chain fibers (nuclei arranged in a central chain). Nuclear bag fibers extend beyond the confines of the connective tissue sheath and are attached to the extrafusal fibers (i.e. skeletal muscle proper)

Innervation is a very complex subject. Anterior horn cells may be either large alpha motor neurons that give rise to motor nerve fibers that innervate extrafusal fibers or even smaller gamma motor neurons that give rise to fibers that innervate the small intrafusal fibers. Afferent sensory fibers transmit information from the NMS to cell bodies in the sensory posterior horn of the spinal cord. Therefore, these encapsulated proprioceptors are a mechanism by which the CNS remains informed as to the state of your muscles allowing the CNS to better coordinate the function of voluntary muscle.

Repair of Skeletal Muscle

Satellite cells are stem cells found between the plasma membrane and the basal lamina of muscle fibers. These cells can differentiate to form myotubes. If damage includes disruption of the basal lamina satellite cells are not responsible for the repair that results. Instead fibroblast repair results in scar tissue.

The Origins of Skeletal Muscle

The development and maturation of skeletal muscle has been studied since the early 1900's and much is know compared to either cardiac or smooth muscle. It is fashioned during embryogenesis from the mesoderm which is generated after the process of gastrulation. On either side of the neural tube, that lies dorsal to the notochord, extends a band of mesoderm called the paraxial mesoderm (Fig. 15). This band of mesoderm separates into blocks referred to as somites. This separation and the subsequent development of somites proceeds in a rostral to caudal direction, with the rostral somites budding off and developing before those located caudal. The number of somites is often used as an indicator of the stage of embryonic development, i.e. how far development has progressed. For example, a chicken embryo is defined as being at stage 11 (40–45 hours of incubation after laying) by the presence of thirteen pairs of somites (99,100).

Somites are transient structures that supply cells which populate the vertebrae and ribs, the dermis of the dorsal skin, the skeletal muscles of the back, body wall and limbs (101,102). They form as mesenchymal structures but convert to an epithelial block with tall columnar cells arranged

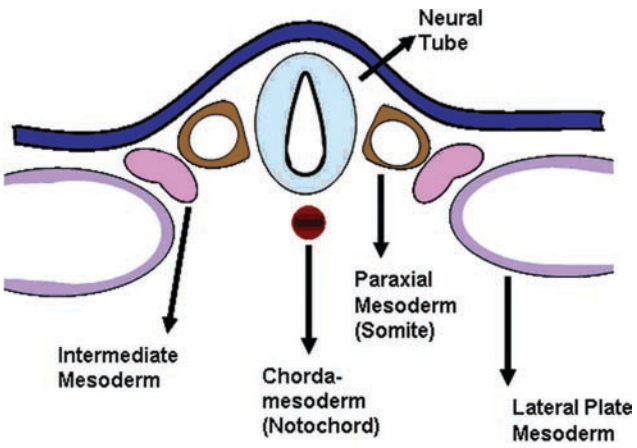

Fig. 15 Diagram of cross-sectional area of a vertebrate embryo that shows organization of mesoderm tissue. Somites which comprise the paraxial mesoderm generate skeletal muscle, the focus of this section in the chapter. Drawing by James O.H. Montgomery

around a central cavity, a process referred to as epithelialization. This process is accompanied by changes in cell-cell and cell-matrix interactions and the signals regulating the segmentation and epithelialization of somites has been studied extensively (103–105). Although all somites look very much alike they form different structures along the anterior-posterior axis and this specification is dictated by the expression of Hox genes (106,107).

Somites contribute cells to different structures and the commitment of cells to their ultimate fate takes place during the early stages of somite development. As the somite matures its various regions become destined (committed) to form certain cell types. Cells in the ventral/medial region, those which are furthest from the back and closest to the neural tube change their shape, become mesenchymal and migrate away to form the sclerotome. These cells ultimately form the chondrocytes of the vertebrae and the ribs. The remaining epithelial somite becomes organized into three regions. The region closest to, and furthest from, the neural tube (epaxial and hypaxial myotome, respectively) is the myotome. The cells in the myotome proliferate and delaminate to produce a lower layer of myoblasts, precursor cells committed to the skeletal muscle lineage. This double layered structure is referred to as the dermamyotome. Myoblasts formed from the region of the dermamyotome closest to the neural tubed will form the muscles of the back (epaxial muscles), whereas the myoblasts in the region farthest from the neural tube will form the muscles of the body wall, limbs and tongue (hypaxial muscles). The dermatome located in the central region of the dermamyotome will form the dermis of the skin of the back (Fig. 16). Signals that direct the formation of the sclerotome, dermatome and myotome are well understood. Briefly, formation of the sclerotome from the ventral-medial cells of the somite is directed by Sonic Hedgehog secreted from the notochord and the floor plate of the neural tube. The sclerotomal cells which become chondrocytes of the vertebrae and ribs themselves express Pax 1, a transcription factor necessary for the formation of cartilage (108,111). The dermatome forms under the direction of two factors secreted by the neural tube: Neurotropin 3 and Wnt 1 (112,113). The epaxial portion of the myotome is induced by factors from the neural tube (Wnt 1 & 3a and Sonic hedgehog) whereas the hypaxial portion is specified by proteins from the epidermis (Wnt) and from the lateral plate mesoderm (bone morphogenetic protein 4). It should be noted that in this brief discussion of muscle, the inhibitory or negative signals are not discussed. Nonetheless their role is vital to normal somite development (114,116). After formation of the double layered dermamyotme, a subset of cells located in the central region of the dermamyotome, identified as being Pax 3 and 7 positive, were found to proliferate and give rise to skeletal muscle cells upon activation of muscle specific transcription factors. Later in development, these cells make

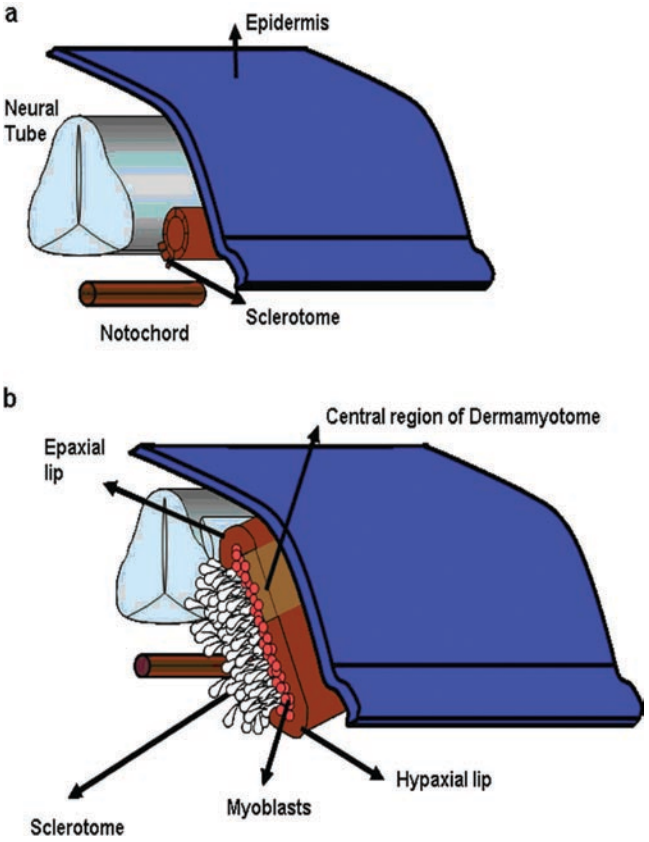

Fig. 16 Maturation of the somite in vertebrate embryos. (**a**) In the 3 day old chicken embryo cells detach from the ventral-lateral somite and begin to migrate away to form the sclerotome. (**b**) In the late 4 day old chicken embryo a layer of myoblasts (muscle precursor cells) are formed beneath the overlying dermatome. Drawing by James O.H. Montgomery. Adapted after Developmental Biology, 7th, edition, Scott F. Gilbert

a major contribution to the embryonic and fetal muscle mass. These cells also give rise to dermal cells. In addition, the dermamyotome gives rise to endothelial and smooth muscle cells of the dorsal aorta.

Techniques used to Study Skeletal Muscle Development

The development and maturation of skeletal muscle is most often studied in vertebrate animals: amphibians, chicken, quail and mice, but the avian model system is most commonly used. This is attributed to the ease with which avian embryos can be manipulated and dissected, cultured either in vitro or *in ovo* during embryonic development observed under a dissecting scope or sectioned and then analyzed. Chicken-quail chimeras have been used to trace the origin of muscles from specific somites. A natural marker that differentiates quail nucleoli from chicken is used to identify tissues

of chicken versus quail origin. Consequently, when quail somites are transplanted into recipient chicken embryos and the embryos studied after a period of incubation, the muscles derived from the quail somite can be easily identified and studied. This same model has been used to study Notch signaling and somite formation (101,117). Genetic manipulations to determine the function of a protein by knock-out or transgenic methods are most often performed in mice (118,119).

Development of Skeletal Muscle

Signals that induce the formation of muscle differ from the epaxial and hypaxial regions of the dermamyotome. In the hypaxial portion, factors from surrounding tissues induce expression of the transcription factor Pax 3, which in turn induces the expression of MyoD. However, in the epaxial portion MyoD is induced by the Myf5 protein. Both MyoD and Myf5 are basic helix-loop-helix (bHLH) transcription factors that belong to the myogenic bHLH family of myogenic regulatory factors (MRFs). These transcription factors bind to similar sites (-CANNTG-) to turn on transcription of muscle-specific genes.

Cells in the epaxial and hypaxial regions of the dermamyotome that produce MyoD and Myf5 are myoblasts, cells committed to the myogenic lineage. How these cells progress from stellate-appearing single cells to tube-like myofibers in mature skeletal muscle has been studied in culture as well as in chimeric mice. Myoblasts proliferate when cultured in media containing serum. As serum is withdrawn the cells withdraw from the cell cycle and fuse to ultimately form multinucleated myofibers or mature skeletal muscle cells. Once growth factors, specifically fibroblast growth factor, are withdrawn from the culture media (by lowering the serum concentration) the myoblasts begin to produce fibronectin and interact with this extracellular matrix protein through the integrin receptor $\alpha_5\beta_1$. The myoblasts then line up, a process mediated by plasma membrane proteins such as CAMs and cadherins and the cells fuse. Fusion of myoblasts to form myotubes also referred to as myofibers is calcium mediated process and appears to require metalloproteinases, enzymes involved in remodeling of the extracellular matrix. Just prior to fusion the cells expresses another MRF, myogenin. Myogenin mediates differentiation of these cells. Differentiation is the process whereby cells become specialized; in this case they express muscle-specific contractile proteins and acquire the ability to contract. In vivo, the force of contraction of skeletal muscle is transmitted via tendons to bones, allowing these structures to move. During adult muscle regeneration, satellite cells (adult skeletal muscle stem cells) that are present under the basal lamina become activated, proliferate to generate additional satellite cells and differentiate into muscle fibers. As during embryonic development, both Pax and MRFs are involved in this process (109,111,116).

Part 3 Bone Biology

The structure and function of bone can best be understood with an insight into the composition of the bone matrix, its mineral, its cells, the mechanism of turnover and remodeling and the unique responses that the mechanical environment evokes in bone. These studies are forming the basis of a rapidly evolving field of bone biology.

Collagen

Classification of Collagens

Connective tissues contain varying amounts of collagen, elastin (a related fibrous protein), glycosaminoglycans and proteoglycans. Of these, collagen is the most abundant. The details of collagen synthesis and function have been extensively reviewed in several specialized texts, and only some of the relevant aspects will be discussed.

Collagens are a class of proteins with common features such as a unique triple helix composed of three component polypeptide alpha chains. However, there are several subtypes (types I to XIII) . Each of these are a product of a different gene and differ from each other in their biochemical structure. Several different types of *fibrillar, basement membrane-associated, fiber-associated, and short chain* collagens are recognized. Type I collagen is the most abundant type of collagen in most connective tissues.

Type I Collagen, The Primary Component of Bone

Type I collagen is a fibrillar type collagen and is found in bone, skin, meniscus, tendon, ligaments, annulus fibrosis and joint capsules. About 90% of bone matrix is composed of type I collagen. There are several subtypes of type I collagens. The bone type I collagen appears to have predominantly galactosyl-hydroxylysine as opposed to glucosyl-galactosyl-hydroxylysine, the predominant amino-acid configuration found in the skin. Hydroxylation and glycosylation are post-translational modifications of collagen and are specific to bone. These modifications, partially explain why mineralization only occurs in bone and not in other sites (120).

The basic structure of type I collagen is composed of a repeating tripeptide sequence that form a left handed helix.

Type I collagen is a hetero-trimer of two pro-αI and one pro-α2 chains. The helix (the α chain) is highly coiled. The α chain corresponds to the basic chemical structure of Gly-X-Y where X and Y represent various amino acids; in practice however, X and Y are rich in proline and hydroxyproline and to a lesser extent, lysine and hydroxylysine. The helix is supertwisted, which provides enormous strength. Collagen fibers can support 10,000 times their own weight and are said to have greater tensile strength than steel wire of equivalent cross section.

Other Collagen Types

Types II, III, V and XI are also fibrillar type collagens. Type II collagen is located mainly in articular cartilage, fibrocartilage, the vitreous humor of the eye and the nucleus pulposus of the intervertebral disk. The other fibrillar collagens are the "minor" collagens. Type III is present in large blood vessels (30%), and in other tissues in association with Type I. Type III collagen is also present in tissues undergoing repair. Type V collagen is present in large blood vessels (5%), cornea, bone, and a few other connective tisues, while Type XI is present only in articular cartilage, comprising 5-20% of articular cartilage.

Basement membrane-associated and fiber-associated type collagens include Types IV, VII, IX and XII. Type IV collagen is the prototype and major component of the *basement membrane* (95%). Type VII forms the anchoring filament in epithelial basement membranes, while Type IX comprises 5-20% of cartilage. Small amounts of Type XII collagen are associated with Type I. The least understood class of collagens is the *short chain* collagens and are comprised of the Types VI, VIII and X. Short chain collagens may function in association with other collagens and have a role in cartilage physiology.

Collagen Synthesis and Cross-linking

Collagen synthesis is under the control of over 20 genes (120). The biosynthesis of collagen, its secretion and aggregation is a complicated process, and has been the subject of several reviews (121,122). Aspects directly applicable to musculoskeletal pathology will be mentioned in other chapters of this book.

The promoters for synthesis of many of the collagen chains have been identified. Many growth factors and hormones also exert their effect on collagen synthesis at the transcriptional level. Collagen mRNAs usually contain a large number of introns. Once the precursor mRNA is transcribed, the introns are removed and the mRNA is transported from the nucleus to the cytoplasm for translation. At this point, additional translational control can be exercised. The N and C propeptidases (see later) are thought to act at this level. Like many other proteins, a precursor form (procollagen) is first synthesized, with peptide extensions at each end. It is at this point that the α chain of collagen is formed and is transfered into the endoplasmic reticulum. At this stage of synthesis, several amino acids are modified posttranslationally (such as hydroxylation of proline residues and lysine residues, forming hydroxyproline and hydroxylysine, respectively), the addition of sugars (such as glucose and galactose to the hydroxylysines), and the formation of hydroxylysine and lysine aldehydes. Co-factors for these processes include atmospheric oxygen, ascorbic acid, ferrous ion and several required enzymes. Once the translation is complete, the triple helix forms, from the C terminal end, and intra- and inter- molecular disulfide bonds are formed. The completed procollagen is then secreted via vesicles into the extracellular space. Glycosylation may be important to facilitate this final step.

As stated earlier, the fundamental units of collagen fibrils are three polypetide chains arranged in a helical fashion. The polypeptide chains aggregate in units of threes to form *tropocollagen*. The tropocollagen, in turn, aggregates in a staggered fashion in a collagen microfibril. Collagen fibers are made up of several of these microfibrils. The process of collagen fibril formation is not fully understood. Removal of the N and C propeptides may be important. After their removal, the molecules aggregate in a head-to-tail fashion with a characteristic stagger, resulting in a 64 nm banding pattern seen under the electron microscope. The ultrastructurally dark area between two tropocollagen molecules is termed a "hole". It measures about 41 nm and is the site where mineralization is thought to first occur (121).

The collagenous scaffolding is stabilized by cross linking and perhaps by interaction with proteoglycans. The process of cross-linking is important for stabilization and structural integrity. The first step is the enzymatic production of aldehydes by the removal of terminal amino groups of lysyl or hydroxylysyl groups of tropocollagen (123). These then can either condense with a lysyl or hydroxyl group to form a cross link and produce a Schiff base, or condense with a similar aldehyde in an aldol reaction (a stronger bond). The amino-oxidase enzyme that catalyzes the aldehyde formation is susceptible to blockage by nitriles. Nitriles are alkyl cyanide substances involved in the disorder called Lathyrism. Lathyrism is characterized by spinal deformities, demineralized bone, dislocations, aortic aneurysm, and various nervous system manifestations.

Cross-linking of collagen occurs in the extra-cellular space. Collagen molecules are cleaved in this space at both the N- and the C- terminal ends by specific peptidases. Cross-linking then occurs and the collagens are packed into a one-quarter stagger array. Specific interactions also occur among collagen and other extracellular macromolecules such as fibronectin, osteonectin and the proteoglycans.

Extensive "cross-linking" between α component chains results in a rigid, brittle character to the connective tissue. This type of cross-linking is found in aging individuals. Defects in the process of forming cross links can render the collagen susceptible to collagenases (discussed more below). Penicillamine prevents collagen cross-linking; and is administered to patients with scleroderma, a disorder of excessive collagen deposition. Genetic defects in collagen can also result in several lethal and non-lethal conditions. Examples include Ehlers-Danlos syndrome (loose joints, characterized by a Gly to Serine change) or Osteogenesis imperfecta (brittle bones, characterized by a Gly to Cystine change). Osteogenesis imperfecta (see section on metabolic diseases) is a heritable disorder of Type I collagen. It is due to a variety of point mutations in either the pro-α1 or pro-α2 collagen chains. Over 100 point mutations have been found in probands with osteogenesis imperfecta. In a few cases, the mutations cause a decrease in the synthesis of pro-α1 and pro-α2 chains. In the majority of cases, however, there is a production of structurally abnormal collagen chains (124). A mouse model has also been developed which demonstrates the relationship between abnormal collagen genes and osteoporosis in heterozygous animals. In homozygous animals, osteogenesis imperfecta develops (125,126).

Collagenases are enzymes that catalyze the hydrolysis of collagen. Several collagenases have been isolated, purified and synthesized. Collagenase levels are increased in rheumatoid arthritis nodules and in synovial fluid from patients with rheumatoid and septic arthritis. Colchicine and heparin increase collagenase synthesis. Collagenases and several other enzymes, such as cathepsin B, are capable of degrading collagen and have been implicated in the pathogenesis of collagen-vascular diseases.

Urinary excretion of hydroxyproline (found exclusively in collagen) and other products of collagen degradation (cross-linked products such as pyridinoline and deoxypyridinoline), act as markers of collagen breakdown. The level of collagen degradation byproducts in urine or serum reflect the amounts of bone turnover (see section on the laboratory in orthopaedic practice).

Non Collagenous Matrix Proteins

Calcium Binding Proteins (The Glyco- and Phosphoproteins)

This is not an easily classified group, since some glycoproteins are also phosphorylated. In the former class are three "sialoproteins" (bone sialoprotein or BSP), including BSP I or osteopontin, BSP II, and bone acidic glycoprotein-75 or BAG-75. There is also a dentin sialoprotein which is found in the jaw. These compounds play a role in the control of extracellular calcium, regulation of crystal growth and shape, and cell adhesion to bone surfaces. Another important phosphorylated glycoprotein is osteonectin.

Osteopontin

The amino acid sequence has been determined, and its gene localized to chromosome 4. Osteopontin is a sialated and highly phosphorylated phosphoprotein, which exists in multiple forms, due to both alternate splicing as well as post-translational variations in the degree of phosphorylation. This protein is transcriptionally regulated by substances such as 1,25 dihydroxyvitamin D, TGF-β, dexamethasone and parathyroid hormone, at least in experimental models.

Osteopontin contains a GRGDS cell attachment sequence similar to binding proteins such as fibronectin (see below). Osteopontin in particular is important in that it has been shown to bind to the integrin receptor on osteoclasts. This binding leads to the activation of the phospholipase C pathway in osteoclasts, and a resultant increase in intracellular calcium. This process may involve the src tyrosine kinase.

Immunolocalization of osteopontin reveals high amounts in the extracellular matrix of developing intramembranous and endochondral bones. Its localization within cells reveals a broad pattern, including osteoblasts, osteocytes, osteoclasts, precursor cells, chondrocytes and fibroblasts. In situ hybridization studies have also shown the presence of mRNA in mononuclear marrow cells, proximal convoluted tubules of the kidney, neuronal cells within the brain and inner ear as well as (murine) placenta (127,128).

Bone Sialoprotein-II (BSP II)

The gene for this sialoprotein has been localized to chromosome 4. Northern blot studies have suggested that BSP II is fairly bone specific. Fetal bone studies have indicated that the initial translation product may differ significantly from the mature form. Like BSP I, this protein has cell attachment properties due to its RGD sequence. However, osteopontin is more active than BSP II in this regard, and maintains cell attachment for more prolonged periods (129).

Bone Acidic Glycoprotein (BAG -75)

This protein binds to the small bone proteoglycans. There is cross-reaction of antibodies with osteopontin in some species; however there are significant differences between this protein and BSP I at the N-terminal end. Complete characterization of this protein is not clearly understood (130,131).

Phosphoproteins (Example: Osteonectin, SPARC or BM-40)

These proteins have a role in regulating the extracellular calcium hydroxyapatite formation and mineralization. Examples include phosphorylated glycoproteins like *osteonectin*. This protein also called secreted protein, acidic, rich in cysteine (SPARC), culture shock protein or basement membrane-40 (BM-40). Osteonectin binds to Ca^{2+}, collagen type I, hydroxyapatite and thrombospondin. It promotes and initiates crystal growth. The gene for osteonectin has been localized to chromosome 5. Several tissues express osteonectin, however, its concentration is extremely high in bone (up to 10,000 times that of other connective tissues). In fact, in bone it may be the most abundant non-collagenous protein. The concentration of osteonectin in bone increases with maturity. Other tissues /cells having osteonectin include skin fibroblasts, tendon cells (but not tendon matrix) and odontoblasts. Interestingly, when osteonectin was activated by the use of blocking antibodies during tadpole development, there was a disruption of somite formation and malformation in the head and trunk (132). Mice lacking osteonectin develop severe cataracts (133) and low turnover osteopenia. *In vitro* studies of osteonectin-null osteoblastic cells showed that osteonectin supports osteoblast formation, maturation and survival (134). Osteonectin also plays role in cell attachment, migration, proliferation and differentiation.

Mineralization Proteins: Gamma-carboxyglutamic acid proteins ("Gla" proteins)

Osteocalcin (also called bone Gla protein) is an example of this group. Osteocalcin contains three γ-carboxyglutamic acid (Gla) residues. It comprises about 20% of the non collagenous proteins in human bone. There is also a matrix Gla protein found in bone, cartilage, lung, heart and kidney (135).

Osteocalcin is made by osteoblasts and odontoblasts in response to 1,25 dihydroxyvitamin D_3. It is secreted into the osteoid after the initiation of mineralization. The bone localization of osteocalcin has been confirmed by several different methods including Northern blotting, immunohistochemistry and electron microscopy. It therefore serves as marker for mineralized tissue. In fact, both osteocalcin and alkaline phosphatase are valuable markers in the repertoire of the surgical and clinical pathologist. Osteocalcin serves as a marker of increased bone turnover, in particular of enhanced osteoblastic activity. Serum osteocalcin levels do not always correspond well with the levels of serum alkaline phosphatase, suggesting that these two markers may be synthesized by osteoblasts at different stages of development. These substances can be used for following the progress of patients with osteosarcoma and may be can be used as a marker for recurrences or metastases in this situation (135).

The role of osteocalcin in the body is unclear, but it may function in regulating mineralization and remodeling. It may also act as a chemoattractant for osteoclast progenitors (also see section on mineralization). Its secretion is under the control of many factors including Vitamin D, TGF-β, PTH and others. Serum levels reflect bone turnover. Osteocalcin has an affinity for Ca^{2+} that is dependent on the presence of Gla residues and an intact disulfide bond. It therefore may have a role in the regulation of crystal growth and recruitment of osteoclasts. Developmentally, low levels are found in the early stages of bone development while maximal levels are reached at maturity. The entire primary structure of osteocalcin has been determined (amino acid sequencing, cDNA clone sequencing, etc.) and the gene is localized to chromosome 1 in humans. The promoter region has a TATA box and a CCAAT sequence. There is a NF1 site, and a binding site for two other nuclear factors AP1 and AP2. There is a cAMP responsive region as well as a 1,25-dihydroxyvitamin D_3 enhancer element. Genetic studies showed that osteocalcin acts as an inhibitor of osteoblast function. Osteocalcin knockout mice were reported to have increased bone mineral density compared to normal controls, but the changes in mineral properties that occur with age were not observed in osteocalcin deficient mice compared to age-matched normal control mice (136,137). Collectively, the published literature provides evidence that osteocalcin is required to stimulate bone mineral maturation.

Adhesion Proteins (Osteopontin, Fibronectin, Sialoproteins and Thrombospondin)

These proteins contain an arginine-glycine-aspartic acid (RGD) amino acid sequence in their composition. This sequence mediates the attachment to certain integral membrane proteins or integrins, which are located on cell surfaces.

Osteopontin: Discussed earlier (see section on Calcium binding proteins)

Fibronectin (FN)

FN is a multifunctional glycoprotein present in the extracellular matrix as an insoluble component or in circulating plasma as a soluble protein. FN mediates the adhesion, migration, differentiation, and proliferation of cells and has been implicated in wound healing and embryonic development

(138). FN is one of the most prevalent and versatile of the extracellular matrix proteins. Disruption of the FN gene in mice results in an embryonic lethality, confirming the importance of FN in embryonic development (139,140). The molecule is a dimer, its subunits being held together by two disulfide bonds. The subunits contain binding domains for fibrin, heparin, bacteria, gelatin, collagen, other extacellular matrix proteins, DNA and cell surfaces. The primary sequence of fibronectin has been determined, and the gene localized to chromosome 7. Fibronectin is characterized by several repeat sequences, for fibrin, collagen and integrin receptor binding. The latter is composed of the Gly-Arg-Gly-Asp-Ser cell attachment consensus sequence known as the GRGDS sequence.

There is heterogeneity associated with fibronectin mRNA, both dependent on origin (plasma versus tissue) and on stage of development (fetal versus adult). This results from alternative splicing of the primary transcript. This may allow the cell to utilize the form more suited to its needs. FNs exhibit molecular heterogeneity arising from alternative splicing of the primary transcript at three distinct regions termed EDA, EDB, and IIICS (141–144). Alternative splicing at the EDA and EDB regions is regulated in a tissue specific and developmental stage-dependent manner. Despite accumulating evidence for the regulated expression of EDA- and/or EDB-containing FNs *in vivo*, the biological functions of these isoforms are poorly understood. Recent studies have shown that the EDA segment regulates the binding affinity of FNs for integrin $\alpha5\beta1$ and thereby stimulates integrin-mediated signal transduction and subsequent cell cycle progression. Unlike the EDA segment, the EDB segment does not enhance FN binding to integrin $\alpha5\beta1$ (145,146).

Fibronectin is synthesized during bone development. During embryonic development, fibronectin is present at high levels during mesenchymal condensations and plays a crucial role in the overt differentiation of these cells into chondrocytes (65). It is also present around osteoblasts during osteogenesis. Osteoblasts can utilize fibronectin as a cell attachment protein. The synthesis of fibronectin from osteoblasts is probably under the control of TGF-β.

Mice deficient for the EDB domain of FN were apparently normal and fertile, although the fibroblasts obtained from the homozygous mice exhibited reduced potential for cell growth and FN matrix assembly *in vitro* (147). Skeletal characterization of EDB null mice revealed no changes in any cartilage elements of skeletal development when compared to the wild type mice.

Thrombospondin (TSP)

This is a 450 kilo Dalton trimeric glycoprotein. It is composed of identical subunits that are disulfide-bonded to each other. It is the predominant protein of the α granules of platelets, but is synthesized in several connective tissues. Like fibronectin, there are "domains" for binding to a host of connective tissues and serum proteins. The molecule also binds Ca^{2+} to hydroxyapatite and to osteonectin. Thrombospondin and osteonectin co-localize in the α granules of platelets, where they bind to one another.

The structure of thrombospondin reveals a homology to fibrinogen with binding sites to collagen, thrombin, fibrinogen, laminin, plasminogen activator and plasminogen. There are areas with homology to α (1) chains of types I and III collagen, von Willebrand factor and epidermal growth factor. There is a region for activating platelet aggregation, as well as sequences with homology to calmodulin and paralbumin. In addition there is an RGD sequence in the middle of a Ca^{2+} binding region. Thrombospondin is distributed in a variety of tissues, including the dermo-epidermal junction of skin, in small blood vessels, surrounding skeletal muscle and beneath glandular epithelium.

Temporally, there is an orderly increase in amounts during organogenesis, followed by a reduction as differentiation proceeds. There is evidence to suggest that TGF-β may be involved in the modulation of thrombospondin biosynthesis. The proposed functions of this molecule include mediation of platelet aggregation, organization of the extracellular matrix (by its multiple binding sites) and action as an autocrine growth factor (148).

TSP is expressed by bone cells such as osteoblasts as well as chondrocytes and this protein is usually deposited into the matrix and regulates other extracellular matrix proteins. There are different types of TSP including TSP1, 2, 3 and 4, some of which have common physiological roles while others do not. Genetically targeted mouse models have been used to define the physiological role of TSPs in bone and other tissues (149). Mice lacking TSP1 exhibit curvature of the spine and minor abnormalities in trabecular bone (150). TSP2-null mice display increased endocortical, but not periosteal, bone formation rates, compared to wild-type, normal mice, as a result of a larger pool of marrow osteoprogenitor cells (151). From the above information it is evident that the role of TSPs in bone is varied and is largely context-dependent.

Other Proteins, Cytokines and Growth Factors

Osteoblast cell culture studies have revealed the presence of several bio-products. Plasminogen activator and its inhibitor have been identified. Collagenase and tissue inhibitor of metalloproteinase (TIMP) have been isolated from such experiments. The extrapolation of these results across species and to *in vivo* situations should be treated with caution. Several plasma products including albumin and α 2 HS-glycoprotein

can bind to bone. There is evidence in the literature suggesting a role for plasminogen activators in bone remodeling. Plasminogen activators tPA and uPA are involved in tissue remodeling and bone metabolism. Mice lacking tPA and uPA show increased bone formation and bone mass associated with increase osteoblast function and delay in extracellular matrix degradation (152).

Connective Tissue Growth Factor

Connective Tissue Growth Factor (CTGF) is a cysteine-rich protein first discovered by Bradham and colleagues (153) while screening a human umbilical vein endothelial cell cDNA expression library using a polyclonal anti-PDGF antibody. At about the same time, two independent groups isolated mouse CTGF (Fisp 12/βIG-M2) from serum-stimulated NIH-3T3 cells and TGF-β -stimulated mouse AKR-2B cells using differential cloning techniques (154,155). Since that time CTGF has been isolated, cloned and sequenced in other species including the cow, pig (156), frog (157), and most recently in the rat (158). The CTGF gene belongs to a larger CCN gene family that also includes Cyr61/CEF10 and *nov.* Cyr61 and CEF10 were isolated by differential cloning techniques from mouse and avian fibroblasts, respectively, and *nov* was identified from myeloblastosis-associated virus-induced avian nephroblastomas (159). More recent additions to this protein family include ELM-1 (WISP-1) (160,161), WISP-3 (161) and COP-1 (WISP-2) (161), bringing the total to six distinct members. With the exception of *nov*, CTGF family members are immediate early growth-responsive genes that regulate the proliferation and differentiation of various connective tissue cell types (159,162). Most of the functional information on CCN proteins has emerged within the last 5 years, including the identification of receptors (i.e. integrins) and the elucidation of potential mechanisms of action, the field is poised for major advances in understanding the activities and functions of these proteins. For reviews of CTGF and the CCN family see 163–166.

All members of the CTGF gene family share 30-50% amino acid sequence identity overall, possess a secretory signal peptide at the N terminus, and contain 38 cysteine residues that are largely conserved (165,166). The CCN proteins are organized into four discrete and conserved structural domains, each encoded by a separate exon. Domain I shares significant sequence homology with the N-terminal region of the insulin-like growth factor binding proteins (IGFBPs) (167), although only low levels of IGF binding activity have been demonstrated for CTGF (168). Since the affinity of CTGF for IGF is much lower than that of the IGFBPs, the physiological significance of this binding is unclear. Domain II includes a von Willebrand factor type C repeat followed by a variable region that is highly charged and devoid of cysteine residues. This variable region may serve as a hinge connecting the N- and C-terminal halves of the protein. The central hinge region located between domains II and III of CTGF and other CCN family members is highly susceptible to enzymatic cleavage with additional sites of proteolysis between other domains (169). Domain III contains a region that is homologous to the thrombospondin type I repeat and may be involved in binding to the extracellular matrix via sulfated glycoconjugates (170). Domain IV is the C-terminal (CT) module resembling the CT domains of several other extracellular proteins believed to mediate protein-protein interaction or dimerization (171). Within this domain are six cysteines forming a motif called a cysteine knot. Cysteine knots are also found in other growth factors (TGF-β, PDGF and NGF) and are involved in their dimerization.

CTGF Effects on Cellular Functions and Role in Biological and Pathological Processes

In general, CTGF (as with most other members of the CCN family) is a secreted, extracellular matrix-associated protein that regulates a diversity of cellular functions including adhesion, proliferation, migration, differentiation, matrix production, and survival. *In vivo*, CTGF mRNA is expressed in many tissues with highest levels in the kidney and brain (155,165). In bone, CTGF has been reported to be expressed in normal rat bone and overexpressed in osteopetrotic bone (158). To date, CTGF mRNA expression and protein production has been demonstrated in endothelial cells, fibroblasts (169,172) and chondrocytes (173). It is believed that CTGF acts as an autocrine or paracrine regulator of various cellular processes with its specific effects being target cell-dependent (169). Although CTGF is mitogenic for various cell types, it also promotes the differentiation of fibroblasts and chondrocytes in culture (173–175). CTGF has been shown to up-regulate the expression and production of extracellular matrix (ECM) proteins, such as type I collagen and fibronectin in fibroblasts (174–175) and osteoblasts (176), and collagen types II and X and aggrecan in chondrocytes (177) Since secreted CTGF is an ECM-associated heparin-binding protein, it is able to mediate cell-matrix interactions (178). CTGF also stimulates the migration/chemotaxis of fibroblasts, mesenchymal stem cells, endothelial cells and vascular smooth muscle cells (179,180). CTGF has also been shown to enhance cell survival or block apoptosis under conditions where cell adhesion is prevented (179,181) but induces apoptosis in vascular smooth muscle cells (182,183).

In addition to the cellular activities discussed above, CTGF has been implicated in more complex biological processes including embryonic development, angiogenesis,

endochondral ossification and wound healing. Based on the angiogenic activity of CTGF, it has been proposed that CTGF is involved in neovascularization of the mineralized hypertrophic cartilage during endochondral ossification (184,186) CTGF expression is induced during cutaneous wound healing. Its effects on fibroblast chemotaxis, extracellular matrix production and angiogenesis suggest that it contributes to wound repair (174,185,187). It has been postulated that CTGF family members play a role in various pathological processes including tumorigenesis such as in cartilaginous tumors (188), atherosclerosis, and various fibrotic diseases (189). It is interesting to note that several different mutations of WISP3, another CCN family member, have been associated with the autosomal recessive disorder progressive pseudorheumatoid dysplasia in which patients experience continued cartilage loss and destructive bone changes around synovial joints (190). This is the first study establishing a definitive link between a CCN family member and the pathogenesis of a disorder affecting bone and cartilage.

CTGF and Skeletogenesis–CTGF and MSC Condensation

During embryonic development there two types of mesenchymal skeletal condensations, pre-cartilaginous condensations that develop into primary cartilage (endochondral ossification during limb development), and pre-osseous condensations that develop into membranous bones (65, 191, 192). During endochondral ossification, mesenchymal stem cells (MSC) aggregate and undergo condensation and subsequent chondrogenic differentiation to form a cartilaginous core (193). This cartilaginous core is then shaped to become the cartilaginous anlage of the future skeleton (192). The cellular condensation process is dependent on signals initiated by cell-matrix and cell-cell adhesion, and these signals are modified by a cell's response to growth and differentiation factors in the extracellular milieu. The hallmarks of cellular condensation include changes in cell adhesion and cytoskeletal architecture (194). The roles of adhesion molecules including N-cadherin, neural cell adhesion molecule (N-CAM), syndecans, and ECM proteins (fibronectin), and other signaling molecules, such as focal adhesion kinase (FAK), paxillin and Wnt have been reported in mesenchymal condensations (65,195). Perturbation of the functions of these molecules leads to disruption in MSC condensation and inhibition of normal cartilage formation (194). It has been reported that CTGF mRNA expression in the newly forming cartilage is high during the initial stage of condensation (193), and deceases as the chondrocytes mature (193,196) Studies by others has shown that CTGF mRNA is expressed strongly in mesenchymal condensations during Meckel's cartilage development, decreases in newly differentiated chondrocytes, and surges again in hypertrophic chondrocytes (193,197). In mice at embryonic stage E10.5, the CTGF protein is highly expressed in mesenchymal condensations of the developing vertebral column and is associated with strong expression of the condensation-matrix protein, fibronectin. In a model of fracture repair, CTGF mRNA and protein are expressed early in the developing fracture callus suggesting that CTGF plays a role in tissue repair. Primary high-density chick and murine limb bud micromass cultures are ideal methods of analyzing *in vitro* the process of mesenchymal condensation (198). Micromass cultures of the mouse cell line, C3H10T1/2, treated with TGF-β results in the formation of a three-dimensional spheroid structure (mesenchymal condensation) (191) Another study showed that Cyr-61, a closely related member of the CCN family, is expressed during mesenchymal condensation *in vivo*. Treatment of mesenchymal cells with recombinant Cyr-61 (199) or rCTGF induced mesenchymal condensation. CTGF is highly expressed during *in vitro* mesenchymal condensation, and that its expression is associated with the expression of condensation-related ECM proteins including fibronectin and N-cadherin. Together, these data suggest that CTGF plays an important role in mesenchymal condensation.

CTGF and Chondrogenesis

During development and in newly formed cartilage, CTGF expression is localized in mesenchymal condensation and disappears in mature cartilage. This coincides with the strong proliferative effects of CTGF on chondrocytes (193) and the down regulation of the expression of this factor during chondrocyte re-differentiation (200) Whole mount *in situ* hybridization of CTGF mRNA in E17 mouse embryos showed that CTGF is selectively expressed in the hypertrophic, but not, proliferative chondrocytes, and in cells of the zone of calcifying cartilage (193) which correspond to the region of chondrocyte cell death. CTGF has been shown to induce apoptosis in a number of cell types including smooth muscle cells, mesangial cells and mammary cells (193). CTGF has also been shown to stimulate chondrocyte proliferation, and and late differentiation associated with increased expression of type X collagen (201). Important functional insights may also be gained from developmental approaches such as targeted gene disruption or cell/tissue-specific overexpression. Transgenic mice that over-expressed CTGF under the control of type XI collagen promoter were generated and their embryonic and neonatal growth was normal (202,203). However, they showed dwarfism within a few months of birth associated with decreased bone mineral density. These results suggest that CTGF over-expression in the growth plate can affect the process of endochondral ossification. The CTGF null mouse has provided great insight into the role of CTGF during chondrogenesis and

osteogenesis (204). These mice have an obvious skeletal phenotype involving both cartilage and bone. CTGF -/- mice die shortly after birth due to respiratory distress and cyanosis caused by severe malformation of the rib cage. CTGF deficiency resulted in impairment of chondrocyte proliferation and ECM composition within the hypertrophic zone, including aggrecan and link protein, suggesting a role of CTGF in acquisition of tensile strength in cartilage (204). It has been shown that there is an inverse relationship between CTGF and Sox-9 expression in MSC. TGF-β treatment inhibits Sox-9 expression, but this effect is completely abolished when the cells are transfected with CTGF siRNA. High levels of CTGF correlate with low levels of Sox-9 and vice versa, suggesting that CTGF is a negative regulator of early chondrocyte commitment/differentiation from MSC.

CTGF and Osteogenesis

Using the *osteopetrotic* (*op*) rat as a model to examine differential gene expression in bone from normal and osteopetrotic rats, CTGF mRNA and protein expression was discovered in bone (158). *In situ* hybridization and immunohistochemical analyses demonstrated that CTGF mRNA and protein are localized in osteoblasts lining metaphyseal trabeculae. Examination of CTGF expression in the fracture callus of a fracture repair model demonstrated that CTGF was primarily localized mesenchymal cells and in osteoblasts lining active, osteogenic surfaces. In primary osteoblast cultures, CTGF mRNA levels demonstrated a bimodal pattern of expression, being high during the peak of the proliferative period, abating as the cells became confluent, and increasing to peak levels and remaining high during mineralization (205). This pattern suggests that CTGF may play a role in osteoblast proliferation and differentiation. Treatment of primary osteoblast cultures with anti-CTGF neutralizing antibody caused a dose-dependent inhibition of nodule formation and mineralization. Treatment of primary osteoblast cultures with rCTGF caused an increase in cell proliferation, alkaline phosphatase activity and calcium deposition, thereby establishing a functional connection between CTGF and osteoblast differentiation (205). *In vivo* delivery of rCTGF into the femoral marrow cavity induced osteogenesis that was associated with increased angiogenesis. These studies clearly showed that CTGF is important for osteoblast development and function *in vitro* and *in vivo*. Studies of CTGF null mice showed an impairment of endochondral ossification associated with decreased vascular endothelial growth factor (VGEF) in the ossification zone of the growth plates. CTGF null mice have decreased bone mineral density and osteopenia (204). Another group of investigators identified and cloned a CTGF-like cDNA from human osteoblasts encoding a protein of 250 amino acids (26 kDa) and sharing approximately 60% homology with other members of the CCN protein family (206). This CTGF-like protein is secreted in primary human osteoblast cultures and it promotes osteoblast adhesion. It was recently shown that CYR61, another member of the CCN family that is closely related to CTGF, is produced and secreted in cultures of human osteoblasts, suggesting that it may also function as an extracellular signaling molecule in bone (207). Furthermore, CYR61 has been shown to be up-regulated during fracture repair particularly in proliferating chondrocytes and osteoprogenitor cells suggesting that it may serve as an important regulator of fracture healing (208).

Mechanisms of Action of CTGF in Skeletogenesis

The mechanisms of action of CTGF involved in mesenchymal stem cells, chondrocytes, osteoblast differentiation and bone formation are not well understood. One recent study reported synergistic or antagonistic roles for CTGF with TGF-β1 or BMP-4, respectively (209). In this study, CTGF enhanced TGF-β1 signaling through receptor and cell-surface binding, Smad-2 phosphorylation, activation of gene expression and cell differentiation. Since TGF-β1 has been shown to have a proliferative effect on osteoblasts (210) and to stimulate CTGF gene expression, it is possible that CTGF may mediate some of TGF-β1 effects on osteoblasts. This same study also demonstrated that CTGF binds directly to BMP-4 through its chordin-like domain, and that CTGF inhibited alkaline phosphatase activity induced by BMP-4 in C3H10T1/2 mesenchymal cells and Smad1 phosphorylation in human 293T cells. Another study showed that CTGF inhibits Wnt-3a and BMP-9-induced osteogenic differentiation of MSC, suggesting that CTGF may act as a negative regulator of early osteogenic differentiation of MSC (211). The inhibitory effect of CTGF in osteogenic differentiation of MSC is interesting.

In chondrocytes, another group has shown that CTGF mediates its effect on chondrocyte proliferation via the ERK pathway and on chondrocyte maturation via the p38 MAK kinase pathway (201) In separate studies by Nishida and colleagues (212,213), they identified a 280-kDa binding protein complex for CTGF on chondrocytic and osteoblastic cells lines, but the nature of the protein(s) contained in this binding complex has not been determined. CTGF has also been shown to bind low-density lipoprotein receptor-related protein (Lrp), such as Lrp5 and 6 and antagonizes Wnt signaling (214). However, the downstream signal transduction pathways in response to this interaction are not fully understood. Clearly, the association between CTGF and MSC is an interesting one that requires further investigation. For other cytokines and growth factors please see section on Regulation of Bone and Cartilage.

Osteoactivin

Identification and Characterization of Osteoactivin (OA) in Bone

The initial identification of OA came from studies using an animal model of osteopetrosis (*op*) in rats. This model was used to examine the differential gene expression in bone from normal rats and *op* mutant osteopetrotic rats. Osteopetrosis is a sclerosing bone disease characterized by generalized increase in the bone mass and has severe skeletal phenotype resulting from abnormalities during development (215). Using the technique of mRNA differential display, a novel cDNA that is highly up-regulated in *op* compared to normal bone was identified.

The over-expression of osteoactivin in *op* mutant bone compared to normal one was confirmed by Northern blot analysis and found to be increased 4 fold in *op* versus normal long bones and calvaria (216). Subsequent cloning and sequencing of the full-length OA cDNA revealed sequence homology with the previously reported human NMB (217), DC-HIL (dendritic cell heparan sulfate proteoglycan integrin dependent ligand) (218), HGFIN (hematopoietic growth factor inducible neurokinin) (219) and PMEL17 (melanocyte specific gene) (220).

Osteoactivin has an open reading frame of 1716 bp with a short 5'- untranslated region, encoding a protein sequence of 572 amino acids (a.a.) with a native M.W of 65 kDa. The first 22 a.a. represent a potential signal peptide, so OA is potentially a secreted protein (216). Bioinformatic analysis of the full length OA a.a. sequence revealed a potential polycystic kidney domain and an RGD integrin recognition site at position 556 that constitutes a potential site for cell attachment. OA protein sequence analysis revealed 11 N-linked and 19 O-linked potential glycosylation sites suggesting that OA is a highly glycosylated protein. A potential transmembrane hydrophobic sequence has been identified in OA protein sequence from a.a. 499 to a.a. 522 suggesting that OA may have a transmembrane isoform.

Characterization of OA Expression in Primary Osteoblast Cultures

OA expression in primary osteoblast cultures showed that the level of OA increased markedly as the cells differentiate with maximal expression during matrix maturation and mineralization as correlated with the early differentiation marker, alkaline phosphatase and the late differentiation markers, osteopontin and osteocalcin (216). By RT-PCR analysis, OA showed the highest level in normal bone (long bones and calveria) and primary osteoblast cell cultures compared to much lower expression levels in brain, heart and skeletal muscles (216). The high level of OA expression during osteoblast terminal differentiation in culture and the preferential expression in bones compared to other tissues are consistent with a gene that has a functional role in osteoblast cell biology.

OA is highly expressed in various malignant tumors such as in glioma (221) and hepatocellular carcinoma (222). It has been shown that over-expression of OA in glioma cell lines (223), as well as in hepatoma cell lines (222), permits tumor invasiveness. OA also has been found to function as an activator of fibroblasts infiltrated into denervated skeletal muscles (224). Treating mouse NIH-3T3 fibroblast cell cultures with recombinant mouse osteoactivin increased the amounts of fibroblast markers, MMP-3 and MMP-9, suggesting that OA has a pathophysiological role in skeletal muscles atrophied by degeneration (224).

Enzyme: Alkaline Phosphatase

Although not generally thought of as a matrix component, this enzyme is an osteoblast product (such as osteocalcin and osteonectin) and would best be discussed here. There are three related isozymes that are tissue related and are associated with three separate genes (reviewed in 225). These are the placental, intestinal and tissue nonspecific forms. The last is seen at high levels in a variety of tissues such as bone, liver, kidney and skin. All three isozymes require Zn^{2+} and Mg^{2+} and catalyze the hydrolysis of monoester phosphates (such as pyridoxal-5'-phosphate) at a pH between 8 and 10 (alkaline pH). The isozyme important in bone is the tissue non-specific form.

Although the tissue non-specific isozyme is associated with a single gene (on chromosome 1), there are electrophoretic and other subtle differences with the other isozymes from different tissues. These differences are probably due to altered glycosylation. The enzyme is attached to the cell membrane via phosphotidyl inositol and can be removed from the cell surface by phospholipase C. This may be a mechanism whereby it enters the serum. The enzyme can be demonstrated by a variety of histochemical and immunohistochemical methods. It has been seen that the bone form of the enzyme can be localized to osteoblasts and young osteocytes, but mature osteocytes are consistently negative for its presence. Vitamin D and thyroxin increase the biosynthesis of alkaline phosphatase. Glucocorticoids and parathyroid hormone inhibit it. The expression of alkaline phosphatase is cell cycle dependent with its activity increasing through the G_1 and S phases, and decreasing in G_2 and M phases.

The role on alkaline phosphatase in biomineralization is still speculative. It has been found in matrix vesicles, but its exact role is unclear. Serum alkaline phosphatase activity is increased in growing children, pregnancy, healing fractures, Paget's disease, rickets, osteomalacia, hyperparathyroidism, bone-forming tumors and certain skeletal metastases. It is reduced in hypophosphatasia.

The Hydrated (Muco)Polysaccharide Gels

The functional units of bone extracellular matrix "gels" are the Glycosaminoglycans (GAGs). Of the several GAGs, four main groups are present. Hyaluronic acid, chondroitin and dermatan sulfates, heparan sulfate and heparin, and keratan sulfate. The majority are aggregated to a protein core to form a proteoglycan. Prior to release from the synthesizing cell, GAGs (except hyaluronic acid) are sulfated. This step imparts a net negative charge on these molecules. In turn, this charge serves two functions. First, it keeps the molecules extended, increasing the volume to weight ratio. Second, by attracting osmotically charged cations, it attracts water. This mechanism creates a gel with very high swelling pressures and tremendous resistance to compression.

The highly viscous hyaluronic acid is a major constituent of synovial fluid, where it helps in lubrication. Additionally, it may impede bacteria, by its physical and chemical properties. Its synthesis is thought to involve a pathway located in the cell membrane, thus hyaluronic acid is not sulfated. The remaining GAGs (mentioned above) are synthesized within the Golgi.

The kind of GAG present within bone is different than those in cartilage. Bone has longer chains, and is rich in chondroitin-4-sulfate. Cartilage on the other hand contains chondroitin-6-sulfate. Developing bone has been shown to contain a large chondroitin sulfate proteoglycan and a small chondroitin sulfate proteoglycan.

Further characterization of the small proteoglycan in turn reveals two proteoglycans (PG I or biglycan and PG II or decorin). Biglycan is rich in Leu, whereas Decorin is rich in Glu/Gln. Each is demonstrable by non-cross reacting antibodies. In bone, both biglycan and decorin can be immunolocalized within the matrix and cells of new bone formation. In mature bone, biglycan (but not decorin) is detected in lacunae and canaliculi.

Both biglycan and decorin have central proteins of 45 kilo Daltons. Biglycan contains two chondroitin sulfates, whereas decorin contins a single chondroitin sulfate which occurs in a periodic manner within collagen fibrils. In fact decorin was so named because of its peculiar localization around collagen ("decoration" of collagen fibers). For more details on biglycan and decorin refer to Table 2.

Biglycan	Decorin
The gene for biglycan is located on chromosome X, the mRNA contains sites of homology to two morphogenic proteins (Toll and Chaoptin) as well as von Willebrand factor.	The mRNA for decorin contains a sequence of epidermal growth factor.
Rate of synthesis is faster, but reduced by vitamin D	Slow synthesis
Rate of degradation slows with age	Remains the same with age
Mouse null for biglycan has increased osteoclast differentiation due to defective osteoblasts (225) and hypomineralization of dentin (227).	Mouse null for decorin has hypomineralization of dentin (227).

The rates of synthesis as well as degradation are faster for biglycan as compared to decorin. The rates for degradation of biglycan however, significantly slow down with advancing age. This leads to a relative accumulation of biglycan. Whether this reflects an added need for biglycan is speculative. Additionally, the rate of synthesis of biglycan is significantly reduced by 1,25 dihydroxyvitamin D, whereas for decorin it is unaffected.

The role of compressive forces and its role in proteoglycan removal prior to mineralization are controversial. Similarly, their role in mineralization and in the developing bone is unclear. There is a probable role in "space capture", hydroxyapatite precipitation and the development of collagen scaffolding.

Mineralization

Calcium hydroxyapatite is the main form of mineral in the human. In invertebrates the mineral most prevalent is calcium carbonate, whereas in plants it is the oxalate. The body's "biologic" hydroxyapatite crystal however differs from the form found in igneous rocks in its crystallographic structure and its size.

Calcification in the body occurs in several different situations. Firstly, there is the physiologic process of cartilage and osteoid mineralization. Secondly, there is the pathologic extracellular or intracellular "dystrophic" calcification, which occurs in association with tissue damage. Thirdly, there is a "metastatic" calcification, which occurs in association with altered serum levels of calcium and phosphate, and finally, there are the diseases of abnormal crystal deposition.

Most cases of calcium deposition within the soft tissues are caused by calcium hydroxyapatite - trauma, fat necrosis, scleroderma, hyperparathryroidism, familial hyperphosphatemia, sarcoidosis, myeloma, metastases, and others. These encompass both dystrophic and metastatic calcification. Punctate or linear calcification seen radiographically along

menisci, articular cartilage or intervertebral disks is generally due to calcium pyrophosphate deposition (CPPD disease). This deposition is rarely massive and simulates tophaceous deposits. In such cases the term tophaceous pseudogout may be appropriate (228). In the latter, tissue processing may remove the crystals making the diagnosis difficult. Additionally, areas of chondroid metaplasia and chondrocyte cellular atypia may raise the possibility of chondrosarcoma. The identification of areas of granulomatous inflammation may be the only clue to the real nature of the process.

Calcification of osteoid (bone mineralization) differs from soft-tissue calcification in being an orderly process. It is distributed within the hole-zones of collagen molecules. This method does not disrupt the spatial organization of collagen. The process is tightly regulated, but poorly understood. The mineral is initially deposited as amorphous calcium phosphate. The initial solid phase is formed at neutral pH. This phase is randomly and poorly oriented. Subsequently a series of solid phase transformations occur that lead to crystalline hydroxyapatite as the final stable solid phase. The initiation of mineralization is probably caused by heterogeneous nucleation, the active binding of calcium, phosphate and calcium phosphate complexes at the nucleation site in the matrix rather than by simple precipitation. In mature bone, it is possible that crystalline calcium carbonate containing hydroxyapatite is deposited rather than an amorphous calcium phosphate or hydroxyapatite.

The Process of Mineralization

The process of mineralization is complicated and has not been satisfactorily elucidated. It is probably under genetic control, and since the physiologic state of extracellular fluids is supersaturated with respect to octacalcium phosphate, there are probably crystal inhibitors present. These include substances such as pyrophosphate and serum proteins. A local increase in concentration far beyond supersaturation is required to overcome the energy of the reaction of crystal formation. Additionally a local environment containing phosphatases and proteases to remove the inhibitors is essential.

A candidate for such a local environment is the "matrix vesicle". These are membrane bound cell free structures derived from chondrocytes and osteoblasts. Matrix vesicles are eccentrically placed within these cells. They are likely to be important in calcified cartilage and woven bone, but less so in mature lamellar bone. Extrusion of the matrix vesicle occurs at cell surfaces, next to mineralizing bone. These structures are rich in alkaline phosphatases and in ATPases. They presumably function by concentrating calcium and phosphate, and also by removing the inhibitors of calcification.

It must be emphasized that mineralization is also under hormonal control. Vitamin D plays an important role. Other exogenous factors that affect mineralization include aluminum intoxication, fluoride intoxication (osteofluorosis), and phosphate deficiency. The mechanisms of action of aluminum and fluoride are unclear. Mineralization is thus more than just a straight-forward physico-chemical process.

Hydroxyapatite crystal formation follows two phases: nucleation and propagation (multiplicative proliferation). The mechanisms operative to achieve this are thought to include: *matrix vesicle mediated* and *collagen mediated* hydroxyapatite precipitation. There are at least two hypotheses for mineralization. The first (229,230) gives primacy to matrix vesicles. The second (231) gives primacy to factors within the matrix. Each has been under investigation since the 1960s.

Hypothesized Mechanisms of Mineralization in Tissues

Mineralization in Cartilage

Mineralization occurs within "matrix vesicles" derived from chondrocytes. These are structures 2-4 μm in size, where hydroxyapatite is deposited. They are derived from the plasma membrane of cells. The membrane retains its phosphatases, which serves to raise the phosphate level. The lipid component of the membrane helps to concentrate calcium. This leads to intravesicular crystal formation. Subsequently, part of or the whole crystal is extruded. This leads to crystal propagation. This phase of crystal growth is physico-chemical and matrix factors play an important part. These matrix factors include collagen, carboxyglutamate proteins (Gla proteins), phosphoproteins, glycoproteins such as chondrocalcin, calcium-acidic phopholipid-phosphate complexes and proteolipids. Inhibitors of calcification include proteoglycans, magnesium, pyrophosphate, ATP, ADP and several synthetic compounds such as diphosphonates.

Mineralization in Woven bone

It occurs both within matrix vesicles and within the "holes" of the fibers of Type I collagen. Rapid mineralization occurs since the matrix vesicles act as a nidus for the larger deposits in the collagen fibers. This works well for the bone to act as repair or reactive bone, but the organizational architecture is haphazard. The bone has a lower strength and is less rigid. It is likely that a phosphoprotein is involved in modulating this process. The rapid mineralization is reflected on the presence of only a thin zone of osteoid separating the osteoblast from

the mineralization front. Mineralization is seen to occur within 24–72 hours of matrix deposition.

Mineralization in Lamellar bone

Mineral is deposited in a regular fashion within the collagen fibers, initiating from the "hole" region (see section on collagen structure). It takes up to 10 days for this slow mineralization to occur, consequently the osteoid zone separating the osteoblast and the mineralization front is wider in lamellar bone. This collagen mediated mineralization is thought to be a "heterogeneous" nucleation - and non-collagenus proteins may play a role in mediating the process.

Surgical Pathology of Mineralization

It is difficult to visualize the site of mineralization in routine decalcified sections. Increased basophilia in the cartilage or woven bone lends suspicion for its location. However, it is reasonably straight forward to be able to do so in undecalcified sections. This is especially true in the case of lamellar bone mineralization. Fluorescent microscopy following a flurochrome (such as a tetracycline) administered 48 hours prior to the study aids the delineation. Osteoid mineralization commences 7-9 days following a resorptive front, and takes up to 200 days to complete.

Mineral Deposits

Pathologic mineralization can be of several different types (dystrophic, metastatic or crystal deposition). Metastatic calcification (associated with increased serum calcium) is often intracellular. The increased Ca^{2+} of the tissue fluid is initially taken up by mitochondria in the cytosol in an attempt to preserve the cytoplasmic homeostasis. When the mechanism is "overwhelmed" the calcium precipitates within the cell. With intra-cellular dystrophic calcification the process may be similar. The plasma membrane associated Ca^{2+} pump is thought to be destroyed as a result of tissue damage. In this situation, there are increased cytosolic levels of calcium and a similar process follows. Extracellular dystrophic calcification is associated with a different mechanism. It is postulated, in this situation, that tissue damage leads to extrusion of matrix vesicles, which then cause calcium precipitation outside the cell. Crystal deposition disease (chondrocalcinosis or pseudogout) is the most difficult to explain. The role of matrix vesicles is un-established. An imbalance between the production of intrasynovial inorganic pyrophosphate and its removal by joint phosphatases may be more important.

Recent studies by Xiao et al. using proteomic analysis of matrix vesicles of mineralizing osteoblasts showed these vesicles produce different proteins. Some of these are previously known proteins such as annexins and peptidases, while others are novel proteins including a variety of enzymes, osteoblast-specific factors, ion channels, and signal transduction molecules, such as 14-3-3 family members and Rab-related proteins. These studies suggest that these proteins play a role in osteoblast matrix mineralization (232).

Factors Important in Mineralization

Collagen	Collagen provides oriented support for the newly formed crystals. The post-translational changes in collagen type I make it possible for diffusion of large hydrated ions such as calcium phosphate into the fibril. Collagen also has sites that may initiate crystal precipitation. Also, there are high energy phosphate bonds (obtained from molecules such as ATP) which facilitate the formation of solid phase from solution. Collagen however is unable to initiate mineralization.
Calcium binding proteins	Phosphoproteins and sialoproteins in the bone matrix may bind calcium to promote crystal deposition and growth, thus acting as nucleators. Crystal growth could then depend upon the conformational change in these proteins after deposition. The initiation of mineralization is coincident with the deploymerization of proteoglycan molecules. Proteoglycans may inhibit calcification by a number of mechanisms including shielding of collagen, chemical interaction with collagen side chains, sequestering calcium or phosphate ions or occupying critical space in the molecule. Different phosphoproteins have varying importance in mineralization.
Pyrophosphate	This is a naturally occurring inhibitor of calcification. It has a short half-life due to its rapid degradation by pyrophosphatases. Pyrophosphates are present in body fluids and increase the stability of the solution phase of calcium phosphate. Diphosphonates are pyrophosphate analogs, and are powerful inhibitors of calcification in large doses.
Bone Gla proteins	Osteocalcin is a highly conserved protein which is abundant in the bone matrix. Because of the Gla residues, it is able to bind calcium. Its role in mineralization is controversial and there is debate over whether it promotes or inhibits mineralization (233). Depletion of osteocalcin from newly formed bone by warfarin treatment results in no impairment of mineralization (234). (see also osteocalcin described above).
Lipids and proteolipids	Within bone there are acid phospholipids that form complexes with calcium phosphate and could thereby influence mineralization. These substances have the capacity to bind to calcium.

Factors Important in Mineralization

Alkaline phosphatase	This is an ectoenzyme produced by osteoblasts and is likely to be involved with the mineralization process. Patients with decreased amounts of enzyme (hypophosphatasia) have impaired mineralization (see rachitic syndromes in metabolic bone disease). Bone alkaline phosphatase is present in high concentrations in matrix vesicles, but its precise role in mineralization is unclear. Alkaline phosphatase may be involved in the degradation of inorganic pyrophosphate, thus providing a sufficient level of organic phosphate for mineralization to proceed.

Remodeling of Bone

Bone undergoes remodeling throughout life. This involves the coupling of resorption of existing bone and the formation of new bone. Thus the entire bony skeleton is "renewed" on a continuous basis. This mechanism is important, because of the cyclical loading and torsional stresses that the skeleton undergoes. In the absence of renewal, bone would exceed its tolerance limits within a short period of time.

Bone turnover or remodeling is thought to occur in discrete foci or packets scattered throughout the skeleton. Each packet takes 3-4 months to complete. Such foci have been termed bone remodeling units or BRUs by Frost, who described the process in 1964. About 25 percent of the metabolically active trabecular bone and about 3 percent of the cortical bone completely renews itself each year (32,235). The amount of bone added in each remodeling cycle, however, reduces slightly with age. This is probably due to a decreased number of osteoblasts. This has been suggested as a possible mechanism for age related (but not post-menopausal) osteoporosis.

In the adult bone, remodeling involves activation, resorption and formation at endosteal and periosteal surfaces and within Haversian systems. Remodeling at the endosteal and periosteal surfaces would result in alterations in the thickness and width of tubular bones. Conditions such as acromegaly, osteopetrosis and hypo- or hyperthyroidism alter trabecular and cortical bone mass.

Bone formation during a remodeling process requires a prior resorption. Resorption takes approximately 10 days. The resorption is carried out by a "cutting cone" of osteoclasts. The trigger for resorption includes the stimulatory cytokines IL-1 and IL-6 produced by osteoblasts, as well as the modulation of the integrin-RGD sequence interaction and other factors such as transcription factors and membrane proteins.

The defect created after resorption, is filled in by fibrovascular tissue. The vessel component is especially important. The formation of the Haversian and the Volkmann systems are thought to be created by these mechanisms. In addition, the fibrovascular core contains pericytes, loose connective tissue, macrophages, mesenchymal stem cells and undifferentiated osteoprogenitor cells. The outer edge of the osteon (where resorption ends and bone formation first starts) is marked by an intensely basophilic line - the "cement" or the "reversal" line. This area is poor in collagen and mineral, and has a high content of sulfur.

Bone formation is carried out by osteoblasts. The process takes approximately 3 months. As the remaining bone and its osteocytes (old, partially resorbed osteons) gets cut off by newly forming osteons, they remain as "interstitial" lamellae. Osteoblastogenesis has identifiable processes of chemotaxis, proliferation and differentiation of osteoblasts. This is then followed by mineralization and the cessation of osteoblast activity.

Mediators of osteoblastic activity and bone formation include transforming growth factor-beta (TGF-β), bone Gla protein fragments, platelet derived growth factors A and B (PDGF A and B), all of which are chemotactic for osteoblasts. The second event, proliferation of osteoblasts, is thought to be mediated by TGF-β, PDGF, IGF I and II, and fibroblast growth factors (FGFs). Cytokines that may play a role in the differentiation of osteoblasts and the production of alkaline phosphatase activity within these cells include IGF-I and bone morphogenetic protein-2 (BMP-2).

The linking or "coupling" of bone resorption and bone formation is complex and difficult to explain. There is emerging evidence however to suggest that "osteoclastogenic" cytokines such as IL-6, IL-1 and IL-11 as well as "osteoblastogenic" cytokines such as leukemia inhibitory factor may be stimulated together by the same signal transduction pathway. Glycoprotein 130 is a molecule present in this pathway, and is involved in the transduction of the signal delivered by each of these cytokines. Sex steroids inhibit, whereas parathyroid hormone and vitamin D increase glycoprotein 130 in experimental models (32,235). This type of model would conveniently explain bone formation-resorption coupling as well as the various acknowledged effects of these hormones on bone turnover.

Another mechanism that may help explain coupling, is the release of osteoblast stimulating factors such as IGF I and II and TGF-β during the osteoclastic process. Another possible mechanism to explain coupling is the RANK/RANKL interaction in which osteoblasts regulate the development and function of osteoclasts (please refer to regulation of osteoclastogenesis). Coupling is the rationale for the counterintuitive, but clinically validated method of treating osteoporosis by giving intermittent parathyroid hormone therapy.

Several diseases of bone are superimposed on this normal cellular remodeling sequence. In diseases such as primary hyperparathyroidism, hyperthyroidism and Paget's disease, there is osteoclast activation. However, there is also a

compensatory and relatively balanced increase in bone formation, due to the coupling of these events.

Other diseases of bone are the result of abnormal coupling. One example is the decreased bone formation after extensive resorption in the osteolytic lesions of myeloma, where there may be a defect in osteoblast maturation. In solid tumors and in elderly patients with age-related osteoporosis there may be similar mechanisms operating, increased bone resorption and decreased bone formation. Osteoblastic activity in the absence of prior osteoclastic activation is thought to occur in some special situations such as osteoblastic metastases and in the response of bone to fluoride therapy.

Regulation of Bone by Endocrine and Paracrine Factors

Endocrine Control

Endocrine control of the bony skeleton is multifarious and includes the need to maintain a balance between bone formation and loss, maintenance of homeostasis in calcium and phosphate levels in the body, and maintenance of a reservoir of phosphate required for generating energy. The major players in the endocrine system that participate in this regulation include parathyroid hormone, PTH-related peptide, calcitonin, vitamins A and D, estrogens, androgens and growth hormone.

Parathyroid Hormone

Parathyroid hormone (PTH) viewed as catabolic for bone is synthesized in the parathyroid gland from a biosynthetic precursor pro-PTH. PTH, a single chain polypeptide (84 amino acids referred to as PTH 1-84) impacts bone, intestine and kidney function. PTH mediates bone loss in older animals in its role to maintain calcium homeostasis and is required in fetal and neonatal animals for normal trabecular bone formation. In response to a decrease in serum calcium, PTH is released from the parathyroid gland. It targets the kidney to reduce calcium excretion, inhibits phosphate resorption and stimulates 1, 25 - dihydroxy vitamin D production which in turn targets the gastrointestinal tract to increase dietary absorption of calcium resulting in suppression of PTH. In addition, both PTH and 1, 25 $(OH)_2$-vitamin D are able to bind to osteoblasts and through RANK and RANKL increase osteoclastic activity which results in calcium and phosphate release from the bony skeleton returning serum calcium levels to normal by an increase in bone resorption. Receptors for PTH are found on pre-osteoblasts, osteoblasts and chondrocytes. They are not, however present on osteoclasts supporting the notion that the action of PTH on osteoclasts is osteoblast-dependent and mediated via substances such as IL-1, IL-6 and prostaglandins of the E series. The net result is osteoclast activation and initiation of bone resorption leading to calcium release from bone.

Evidence suggests that in certain situations PTH stimulates bone formation. When administered continuously, it increases osteoclastic resorption and suppresses bone formation. When administered in low doses, intermittently, it stimulates bone formation without resorption. This anabolic effect, like the resorptive effect is probably indirect, and mediated via IGF-1, TGFβ, etc. High serum PTH levels, maintained for even a few hours, initiates osteoclast formation resulting in bone resorption that overrides the effects of activating genes that direct bone formation. Identification of PTH-related protein (PTHrP) expression early in the osteoblast progenitor cells, its action through the PTH 1 receptor (PTH1R) on mature osteoblasts, and the observation that PTHrP+/- mice are osteoporotic, raise the possibility that PTHrP is a crucial paracrine regulator of bone formation.

Calcitonin

Calcitonin is a peptide hormone synthesized and secreted by thyroid parafollicular C cells, is regulated by extracellular calcium levels, and gastrointestinal hormones such as gastrin. It is encoded by a gene that undergoes alternate splicing to generate several other peptides including calcitonin gene related peptide. Calcitonin receptors are present on osteoclasts, preosteoclasts, monocytes and certain tumor cells and increased levels result in a short lived fall in plasma calcium. In bone, calcitonin blocks bone resorption probably via mature osteoclasts, by enhancement of adenylate cyclase and cAMP or as a mitogen acting on bone cells. It promotes renal calcium excretion possibly to maintain normocalcemia after a large calcium containing meal.

The physiological role of calcitonin remains controversial. Calcitonin and alpha-calcitonin gene-related peptide (alphaCGRP)-deficient mice exhibit high bone mass mediated by increased bone formation with normal bone resorption. The absence of significant changes in bone mineral density caused by a decline or overproduction of calcitonin in humans questions the physiological relevance of calcitonin as an inhibitor of bone resorption. A recent study on the age-dependent bone phenotype in two mouse models, one lacking calcitonin and alphaCGRP (Calca-/-), the other lacking alphaCGRP (alphaCGRP-/-) reported osteopenia at all ages in AlphaCGRP-/- mice. However, the Calca-/- -mice displayed increased bone turnover with age and at 12 months of age a

significant increase in bone formation and resorption. These data suggest that calcitonin may have dual actions, in bone formation and resorption, which may explain, at least in part, why alterations of calcitonin serum levels in humans do not result in major changes in bone mineral density (236). In addition, calcitonin has a role in the therapy of hypercalcemia of malignancy, in Paget's disease and in osteoporosis. Osteoclasts from Paget's patients are hyper-responsive to calcitonin, for longer periods of time than control cells although the molecular mechanism(s) for this hyper-responsivity is unknown (233).

Vitamin D

Ergosterol and 7-dehydrocholesterol are the precursors for vitamin D, best labeled as a hormone and vitamin. These compounds are stored in the skin, transported in the body via an alpha-globulin binding protein/vitamin D binding protein (DBP) and become activated by ultraviolet light. Findings procured from gene targeting experiments in mice suggest that DBP possibly maintains stable serum stores of vitamin D metabolites and modulates the rate of its bioavailability, activation, and end-organ responsiveness. These properties may have evolved to stabilize and maintain serum levels of vitamin D in environments with variable vitamin D availability (238).

Activation of ergosterol and 7-dehydrocholesterol in turn generates calciferol and cholecalciferol. These substances are hydroxylated in the liver to yield 25-hydroxy-vitamin D in the presence of magnesium, and then are converted in the proximal tubule of the kidney to generate metabolites of 25-hydroxy-vitamin D. The most active form of vitamin D is 1,25-dihydroxyvitamin D. This hormone is key to the control of calcium metabolism in the gut, proximal tubule in the kidney and bone. 1,25-dihydroxyvitamin D production is regulated by calcium and PTH . It stimulates calcium binding protein, affects osteocalcin production, osteoclastic resorption, monocytic maturation, myelocytic differentiation, skin growth and insulin secretion. Lack of vitamin D results in impaired mineralization of newly formed bone which results in rickets in children, and osteomalacia in adults. These conditions are typified by an increase in proteinaceous bone matrix which does not mineralize. An excess of vitamin D leads to an increase in bone resorption and hypercalcemia.

Vitamin D acts via vitamin D receptors, and receptor sites of 1,25-dihydroxyvitamin D have been identified on several cell types. The vitamin D receptor is a transcription factor which forms homo- or heterodimers with members of the steroid hormone receptor superfamily (most notably the retinoic acid receptor RXR). Errors in genes that code for these nuclear receptors are reported in several forms of rickets. It is also suggested that postmenopausal osteoporosis may be genetically predetermined by polymorphisms present on the vitamin D receptor gene (237).

The vitamin D receptor type II (VDR-II) null mouse suggests a role for vitamin D in bone metabolism. These mice are phenotypically normal at birth, survive to 6 months of age, develop hypocalcemia at 21 days of age, at which time their parathyroid hormone (PTH) levels begin to rise. They also develop hyperparathyroidism accompanied by an increase in the size of the parathyroid gland with a concomitant increase in PTH mRNA levels. This phenotype is also associated with rickets and osteomalacia as early as day 15, and there is an expansion in the zone of hypertrophic chondrocytes in the growth plate. Interestingly the VDR-II knockout mouse also develops progressive alopecia at 4 weeks of age (239). Studies using primary calvarial cultures revealed that ablation of VDR-enhanced osteoblast differentiation was associated with an increase in alkaline phosphatase activity, as well as an early sustained increase in formation of mineralized matrix. The expression of bone sialoprotein, a marker for mineralization, was also increased in VDR null osteoblasts. These studies demonstrate that VDR attenuates osteoblast differentiation in vitro, and that other endocrine and paracrine factors may modulate the effect of VDR on osteoblast differentiation in vivo (240).

Evidence suggests that marrow mononuclear cells and monocytes fuse to form osteoclasts on exposure to vitamin D (233). Vitamin D receptors are not present on mature osteoclasts, thus osteoblasts are needed to mediate the effects of vitamin D to induce bone resorption and PTH may act synergistically with vitamin D to mediate this activity. In addition, it is likely that IL-1 and IL-2 play an intermediary role in bone resorption mediated by vitamin D.

Calcitriol and Osteogenesis

Calcitriol (1α, $25(OH)_2 D_3$), the active form of vitamin D3, is synthesized from 25-hydroxyvitamin D_3 by the action of 1α hydroxylase which is present predominantly in the kidney (247). Mutations in the human1α hydroxylase gene cause pseudo-vitamin D deficiency rickets (248). Targeted ablation of the 1α hydroxylase gene in a mouse model leads to development of retarded growth, and skeletal abnormalities characteristic of rickets (249). Calcitriol resorbs bone by stimulating the formation of osteoclasts. Receptors for 1α, $25(OH)_2 D_3$ are found on osteoblasts and osteoprogenitor cells but not osteoclasts (241). Stimulation of osteoclast formation requires cell-cell contact between osteoblasts and osteoclast precursor cells, and involves the upregulation of the osteoclast-differentiating factor, RANK ligand in

osteoblasts, and downregulatation of OPG expression, an osteoclastogenesis inhibitory factor that works as a decoy receptor for RANK (242). Through stimulation of osteoclast formation, 1α, $25(OH)_2$ D_3 is believed to mediate bone resorption and remodeling. In addition, 1α, $25(OH)_2$ D_3 has been shown to inhibit osteoblast proliferation and stimulate apoptosis through induction of tumor necrosis factor alpha (243).

I*n vitro* studies demonstrate that vitamin D_3 stimulates osteoblast differentiation through induction of osteocalcin and alkaline phosphatase expression (both markers of mature osteoblasts) (244). These findings are supported by studies showing that the Ca^{+2} binding proteins osteocalcin and osteopontin secreted by osteoblasts during differentiation, are upregulated by 1α, $25(OH)_2$ D_3 through its response element on the osteocalcin and osteopontin promoter (245). Moreover, 1α, $25(OH)_2$ D_3 stimulates osteoblast differentiation by the release of alkaline phosphatase (ALP) through the ERK-MAPK signaling pathway. Treatment of primary osteoblast cultures with an ERK inhibitor resulted in reduced 1α, $25(OH)_2$ D_3 induction of ALP, which confirms that 1α, $25(OH)_2$ D_3 stimulates ERK expression in primary human osteoblasts (246).

Vitamin A

Retinoids, in excess, decrease the formation of bone and cartilage matrix, whereas a deficiency has the opposite effect. Several years ago, it was discovered that an imbalance of vitamin A during embryonic development had dramatic teratogenic effects. These effects have since been attributed to vitamin A's most active metabolite, retinoic acid (RA), which itself profoundly influences the development of multiple organs including the skeleton. After decades of study, researchers are still uncovering the molecular basis whereby retinoids regulate skeletal development. Retinoid signaling involves several components, from the enzymes that control the synthesis and degradation of RA, to the cytoplasmic RA-binding proteins, and the nuclear receptors that modulate gene transcription. As new functions for each component continue to be discovered, their developmental roles appear increasingly complex and each has been implicated in skeletal development. Moreover, retinoid signaling comes into play at distinct stages throughout the developmental sequence of skeletogenesis, highlighting a fundamental role for this pathway in forming the adult skeleton. Consistent with these roles, manipulation of the retinoid signaling pathway significantly affects the expression of the skeletogenic master regulatory factors, Sox9 and Cbfa1. In addition to the fact that we now have a greater understanding of the retinoid signaling pathway on a molecular level, we are able to place retinoid signaling within the context of other factors that regulate skeletogenesis. Here we review these recent advances and describe our current understanding of how retinoid signaling functions to coordinate skeletal development. We also discuss future directions and clinical implications in this field.

Retinoic acid (RA) is an endogenous metabolite of vitamin A that acts as potent regulator of osteoblast growth and differentiation of (250). The actions of RA are mediated by nuclear receptors that belong to the steroid hormone receptor superfamily (251). Changes in levels of RA during skeletal development result in severe abnormalities in the appendicular and craniofacial skeleton (252–254). Several studies have investigated the effects of RA on osteoblasts *in vitro*. Low doses of RA (0.01 μM) resulted in a increased levels of osteopontin and osteocalcin mRNA in fetal rat calvarial osteoblasts (255). Similarly, treatment of clonal pre-osteoblasts with pharmacologic doses (1 μM) of RA have shown an increase in osteopontin transcript levels and enhancement in nuclear processing of primary mRNA transcripts (256). While these reports suggest a direct relationship between RA level and osteoblast differentiation, other studies have demonstrated a decrease in alkaline phosphatase activity with both low and high-doses of RA, and decreases in osteocalcin transcription at higher doses (255,257). Thus, the actual effect that RA has on osteoblast differentiation and matrix mineralization remains to be determined.

An extensive literature on the role of steroid hormones (estrogens and androgens), and growth hormone reviews their impact on musculoskeletal development and disease and is not covered in the introductory chapter. In brief, in experimental situations, reduced estrogen leads to bone loss. This may be a direct effect on osteoblasts and possibly osteoclasts, and may be mediated via PTH and calcitonin. Androgens are reported to maintain bone mass via receptors on osteoblasts and the effect of growth hormone on bone is primarily mediated via insulin-like-growth factor (IGF). There may however also be a direct effect through growth hormone receptors on osteoblasts and chondrocytes.

Growth Factors

Transforming Growth Factor-Beta

Initially isolated from "transformed" neoplastic cells in tissue culture studies. Two "factors" were isolated and named TGFα and-β. TGFα is not found in bone and is now called epidermal growth factor. A number of similar compounds also exist (the TGFβ supergene family) including bone morphogenetic proteins (BMP). There are four known receptors for TGFβ. Additionally, there are cross effects from the stimulation of similar receptors. The net effect is to increase DNA

at low concentrations, enhance the synthesis of type I collagen and non collagenous proteins (fibronectin, proteoglycans etc.), and reduce the activity of alkaline phosphatase. There is less information on the effect on osteoclasts. There may be stimulation at low and inhibition at high concentrations. The latter effect is in association with the production of prostaglandins. TGFβ is said to have a prominent role in soft tissue healing, in a cascade fashion. It is released from the degranulation of platelets as well as from macrophages. It may help in the deactivation of the production of hydrogen peroxide, inhibit proteolytic enzymes and upregulate the integrin receptors for extracellular matrix proteins allowing the production of abundant granulation tissue (258,259). The current hypothesis is that TGFβ induces bone formation during remodeling. Additionally, high amounts are seen in tissues undergoing endochondral ossification. Experimental evidence suggests that TGFβ plays a positive role in intramembranous and endochondral bone formation as well as fracture and wound healing in experimental animals (258,259). The action of TGFβ in bone induction may however be only in conjunction with other factors such as the BMPs.

Role of TGFβ-1 in Osteoblast Development *in Vitro*

It is well established that the members of the TGFβ superfamily play a crucial role in bone development, remodeling, and disease. However, the various TGFβ members have contradictory functions that have been documented *in vitro* and *in vivo* models. For example, knockout of TGFβ-2 has been shown to result in bone defects, indicating a positive role for these molecules in bone development (260). However, transgenic mice over-expressing TGFβ-2 under the control of an osteocalcin promoter displayed an osteoporosis-like phenotype (261). On the other hand, TGFβ-1 has been demonstrated to either stimulate or inhibit bone formation *in vivo*, and to differentially modulate distinct osteoblast markers *in vitro*. It has been suggested that TGFβ-1 enhances the proliferation and early differentiation of osteoblasts *in vitro*, which is characterized by a high rate of collagen synthesis, but impairs their terminal differentiation based on osteocalcin production (a differentiation marker) and mineralization of culture matrix (262). The TGFβ-1 signaling pathway begins by the binding of TGFβ to TGFβ specific type I and type II receptors leading to the phosphorylation of Smads 2 and 3, complex formation with Smad 4, translocation of Smad 2/3/4 to the nucleus, and transcriptional activation of specific target genes (263).

TGFβ-1 enhances intracellular Ca^{+2} transport. This is crucial for osteoblast adhesion and early development in culture, since Ca^{+2} enhances expression of α5 integrin, which is important in the formation of focal contact adhesions and cytoskeletal reorganization. These early events are necessary for osteoblast adhesion. Thus, they determine the fate of the osteoblast cell and ultimately affect bone function (264).

TGFβ-1 abrogates the steady-state levels of mRNA for lysyl hydroxylase in human osteoblast-like cells *in vitro* thus inhibiting the matrix maturation by affecting the degree of lysyl hydroxylation in newly synthesized collagen. The mRNA for lysyl hydroxylase was reduced by one-third under the influence of TGFβ-1. However, the mRNAs for both procollagen I alpha-chains were stimulated by TGFβ-1. Thus, TGFβ-1 increases collagen production and decreases its maturation (265). TGFβ-1 also stimulates osteoblast proliferation indirectly through inhibition of p57 cyclin-dependent kinase inhibitory protein (CKIs), a negative regulator of the cell cycle acting through the ubiquitin-proteasome pathway in newly proliferating osteoblast cells (266).

Nishimori and his colleagues, (267) found when the constitutively active form of the TGFβ-1 type I receptor was ectopically expressed in osteoblast cells, the p57 that had been accumulated by serum starvation and causing the cell-cycle arrest was rapidly degraded in a manner analogous to TGF-β1 stimulation. Moreover, Smad2 or Smad3 binding to Smad4 enhanced the proteolytic pathway of p57. All of the pathways mediated by TGFβ-1 growth factor suggest its important role in osteoblast proliferation but not terminal differentiation.

Studies on TGFβ-1 null mice have shown that growth plates, alkaline phosphatase (ALP) activity and collagen maturity were reduced in the tibiae at all ages compared to age-matched wild-type (WT) control animals using Fourier transform-infrared imaging (FTIRI) and immunohistochemistry (268). Also analysis of proximal tibial metaphyses showed significant decreases in the bone mineral content of the TGFβ-1 null mice compared to TGFβ-1 wild-type (WT) control animals. However, no significant differences were observed in bone mineral density (BMD) between the groups of mice. Histomorphometry revealed that the width of the tibial growth plate and the longitudinal growth rate were significantly decreased in the TGFβ-1 null mice, resulting in shorter tibia (269).

Bone Morphogenetic Proteins (BMP)

A bone inducing principal was first postulated in 1952 by Marshall Urist et al. (270) Since then, at least ten proteins with this property have been extracted from *demineralized bone*, the amino acid sequence has been characterized and synthesized by recombinant DNA technology (271–276). These have been named bone morphogenetic proteins 1-10. BMP 3 is also called osteogenin, BMP 4 is also called BMP 2B, BMP 6 is also Vgr-1 and BMP 7 is known as osteogenic protein-1. This clash of terminology is due to the reclassification after characterization. These BMPs can be thought of as three separate families. One consisting of BMP 2 and 4,

the other of BMPs 5, 6 and 7 and the last consisting of BMP 3. These divisions are on basis of homology of structures. The issue has become complicated by the finding that these proteins (mostly members of the TGFβ super gene family) are found in several tissue types other than bone (277). In fact, the developing embryo has areas such as the apical epidermal ridge, which exhibit this property of bone induction, possibly due to such factors being elaborated.

Urist's work had suggested that demineralized bone matrix contains biologic signals to induce endochondral bone formation when implanted in soft tissues (osteoinduction). The relative osteoinductive contribution of bone cells as opposed to matrix in demineralized bone is debated. In the 1970's Japanese workers identified bone inducing activity in certain osteosarcoma cell lines. The molecule involved in this bone induction was later characterized as BMP 4. Certain human osteosarcoma cell lines such as the Saos-2 have also shown to produce several BMPs and TGFβ. Current recombinant technology however, has allowed the synthesis of these proteins from cDNA, obviating the need of large amounts of demineralized bone or neoplastic cell lines. Most of the BMPs (except for BMP 1) are basic proteins of 15 kDa, existing as dimers and belonging to the TGFβ superfamily. Disulfide bonds link these dimers. BMP-1 has recently been shown to be a protease with procollagen as its substrate (275–276). The synthesis of most BMPs has been performed by Wozney et al. at the Genetics Institute (Cambridge, Massachusetts). Their approach has been to isolate and sequence the cDNA for each BMP using a cDNA library obtained from the U-20S human osteosarcoma line. Following cloning, functional regions of the BMP sequences were transfected into a second mammalian line (Chinese hamster ovary) for expression and secretion of the mature BMP molecules. These were then isolated and purified by a chromatographic method developed by the Genetics Institute and Genentech (Cambridge, Massachusetts). Osteoinductive activity was tested using a bioassay employing rats.

Purified BMPs have been used to promote bone repair. Several trials have shown their efficacy in experimental models (278–280). Mixtures of BMPs have also been used, and shown to be more effective than comparable doses of single homodimeric BMP (281).

Bone Morphogenetic Proteins and Osteogenesis

Bone morphogenetic proteins (BMPs) are osteotrophic factors as well as members of the TGFβ superfamily. The activity of BMPs was first identified in the 1960s (282), but the proteins responsible for bone induction remained unknown until the purification and sequence of bovine BMP-3 (osteogenin) and cloning of human BMP-2 and BMP-4 in the late 1980s (274,283,284).

BMP-2 induces gene expression and synthesis of osteoblast differentiation markers, alkaline phosphatase and osteocalcin, in pluripotent and preosteoblast cells. BMP-2 exposure for a short duration is sufficient to induce cell differentiation (285). Functions of bone morphogenetic proteins, such as BMP-2, are initiated by signaling through specific type I and type II serine/ threonine kinase receptors. It was previously reported that BMP receptor type IB (BMPR-IB) plays an essential and specific role in osteoblast commitment and differentiation (285). Smad1, 5, and 8 are substrates for BMP receptor I (BMPR-I) and mediators of the BMP signals that inhibit myogenic differentiation and induce osteoblast differentiation, in the mesenchymal C2C12 cell line (286). Studies from transgenic and knockout mice and from animals and humans with naturally occurring mutations in BMPs and related genes have shown that BMP signaling plays critical roles in heart, neural and cartilage development. BMPs also play an important role in postnatal bone formation (287).

BMP-2 is known to induce osteoblast differentiation by inducing Runx2. a global regulator for osteogenesis. Runx2 co-operates with BMP-2-induced Smad proteins to stimulate osteoblast differentiation (288). BMP-2 receptor activated Smad proteins induce Runx2; however, Smad does not directly induce Runx2 expression. The mitogen-activated protein kinase/p38 (MAPK/p38) cascade is also involved in the induction of Runx2 by BMP-2 (289). In addition, BMP-2 induces osteoblast differentiation through activation of an endogenous β-catenin signaling pathway thus implicating β-catenin in early steps of BMP-2 mediated osteoblast differentiation (290). In support, ectopic expression of stabilized β-catenin in the murine embryonic mesenchymal C3H10T1/2 cell line or activation of endogenous β-catenin signaling with lithium chloride induced expression of alkaline phosphatase mRNA and protein (an early osteoblast differentiation marker). However, unlike BMP-2 protein, stabilized β-catenin does not induce osteocalcin gene expression (a late osteoblast differentiation marker) (291).

Insulin like Growth Factors: IGF I and II

Insulin-like growth factors are produced by many cell types including osteoblasts and chondrocytes. They act via receptors to promote proliferation, differentiation and matrix production of bone and cartilage. The action of growth hormone is closely linked with the IGFs. It is thought that growth hormone binding with specific receptors in target tissues stimulates the production of IGF-1. This, in turn, may have endocrine, paracrine and autocrine effects. IGF-1 is transported via carrier proteins, such as IGF-binding proteins and IGFBPs of which, IGFBP-3 is the most important. Deficiency of IGF or IGFBP-3 may be responsible for certain kinds of dwarfism, such as Laron type dwarfism.

Other Growth Factors

Growth factors discussed earlier include Epithelial Growth Factor, Acid and Basic Fibroblast Growth Factors and Platelet Derived Growth Factors A and B (PDGFA and PDGFB). PDGFs, in particular, are potent mitogens of osteoblasts in vitro and have a chemotaxic effect on them. PDGFs are thought to be particularly important in bone remodeling. They are heterodimers of A and B chains, and function via specific receptors. Mutations in fibroblast growth factors are thought to play a role in certain kinds of skeletal deformities, including achondroplasia, Apert's syndrome, Cruzon syndrome, Pfeiffer syndrome, and Jackson-Weiss syndrome.

Cytokines: Prostaglandins and Interleukins

Prostaglandins: Prostaglandins have multiple effects on bone cells, and sometimes opposite effects in different species. Their role is therefore difficult to discern. They are powerful bone resorbers in certain culture studies, yet they are potent anabolic (bone forming) agents when administered in vivo. (especially true of the E series). Prostaglandins are produced by monocytes under appropriate stimuli. It is possible that some effects of interleukins are mediated by prostaglandins.

Interleukin 6 (IL-6): This cytokine is produced by many cell types, including osteoblasts and bone marrow stromal cells. Bone cells produce IL-6 in response to PTH, Vitamin D_3, TGFβ, IL-1 and TNFα, to name a few. Human osteoclastoma cells respond to this cytokine; however, it is still unclear whether normal mature osteoclasts respond to IL-6. It is known though that IL-6 has a pathogenetic role in diseases such as multiple myeloma, Paget's disease, rheumatoid arthritis and Gorham's disease (vanishing bone disease). Experimentally, estrogens and androgens inhibit the production of IL-6 by osteoblasts. Additionally, there is evidence to suggest that osteoclastic activity may be inhibited by anti-IL-6 antibodies (32).

Mechanosensory Systems and Stretch Studies (Wolff's Law)

Wolff's Law - Every change in *form and function* of bones, is followed by changes in *the internal architecture and external conformation,* in strict accordance with mathematical laws (Julius Wolff, 1882).

Wolff's law has been confirmed by experimental studies. However, only recently have studies been performed to investigate the basis of this law at *a molecular level*. It is clear that mechanical forces effect skeleton morphology. For example, individuals who lift weights tend to develop bigger and stronger bones. If use of a limb is stopped, it undergoes "disuse" osteoporosis. Children with malunited limb fractures frequently remodel into almost normal appearing bones. If, though, they are unable to bear weight or use the limb (such as with poliomyelitis), then the limbs stay malunited. Paraplegics or quadriplegics with a spastic form of paresis often have exuberant callus formation. In contrast, patients with flaccid paresis fail to develop such an exaggerated response. Weightlessness in space causes rapid decrease in bone mass reflecting the need for constant force in maintaining skeletal bone.

All these examples illustrate the close link of mechanical forces with skeletal response and bone formation. What is still under investigation, however, is how these mechanical forces are translated into cellular events. It is likely, that signaling mechanisms, such as electricity or chemical messengers, such as certain cytokines, mediate these responses.

Computer controlled membranes holding tissue cultures of osteoblasts and fibroblasts have been used to alter the amounts of "stretch" provided to the cells. These studies have suggested that there is an altered metabolism and DNA synthesis under conditions of load. It has been suggested (292–294) that there may be two components to this system:

The Cell Network: This consists of osteocytes and their processes in communication with surface cells. Stretch sensitive ion channels are thought to exist on osteoblasts and fibroblasts.

The Mineralized Matrix: Stream generated potentials are created when fluid flowing through the matrix carries along a species of ion (in the presence of another species attached to the matrix).

These two mechanisms may be responsible for the signal for altered cellular metabolism observed. A "piezo-electric" effect as a result of compression of the hydroxyapatite crystal is also theoretically possible, but unlikely to be responsible for the coupling of mechanical-electric phenomena in bone.

The mechanism by which strain induces osteoblast proliferation in strain studies has thought to be mediated by the inositol 1,4,5 triphosphate system (295–296). Inhibition of phospholipase C (by neomycin) blocks inositol triphosphate production and subsequent proliferation. Additional signaling pathways (such as by cyclic AMP) may co-exist.

There is a hypothesis that cells maintain a basal equilibrium stress state that is a function of the number and quality of focal adhesions, the polymerization of the cytoskeleton and the amount of extrinsic applied mechanical deformation (297). A load stimulus detected by a mechano-electrochemical sensory system (including stretch sensitive ion-channels, integrin cytoskeletal machinery, and load-conformational sensitive receptor tyrosine kinase) activates G proteins, induces second messengers, and activates another kinase cascade to allow a respose.

It is also possible that integrins serve as important components of the mechanical sensory system. The RGD sequence of matrix proteins undergoes conformational changes with tension. This allows matrix tension to be "communicated" to bone cells. Signaling molecules such as nitric oxide (NO) have also been postulated in this process (298). Some studies have suggested that molecules such as osteopontin might be intermediary in this signalling process. For example, the binding of the $\alpha_v\beta_3$integrin with the RGD sequence of osteopontin might trigger osteoclastic resorption (299).

References

1. Cowin SC. Tissue growth and remodeling. Annu Rev Biomed Eng 2004;6:77–107.
2. Havers. http://www.biology-online.org/dictionary/Haversian_system. 1691.
3. Brown JH, DeLuca SA. Growth plate injuries: Salter-Harris classification. Am Fam Physician 1992;46(4):1180–4.
4. Duncan CP, Shim SSJ. Edouard Samson Address. The autonomic nerve supply of bone. An experimental study of the intraosseous adrenergic nervi vasorum in the rabbit. J Bone Joint Surg Br 1977;59(3):323–30.
5. Bliziotes M, Gunness M, Eshleman A, Wiren K. The role of dopamine and serotonin in regulating bone mass and strength: studies on dopamine and serotonin transporter null mice. J Musculoskelet Neuronal Interact 2002;2(3):291–5.
6. Tam J, Ofek O, Fride E, et al. Involvement of neuronal cannabinoid receptor CB1 in regulation of bone mass and bone remodeling. Mol Pharmacol 2006;70(3):786–92.
7. Idris AI, van't Hof RJ, Greig IR, et al. Regulation of bone mass, bone loss and osteoclast activity by cannabinoid receptors. Nat Med 2005;11(7):774–9.
8. Landis WJ, Song MJ, Leith A, McEwen L, McEwen BF. Mineral and organic matrix interaction in normally calcifying tendon visualized in three dimensions by high-voltage electron microscopic tomography and graphic image reconstruction. J Struct Biol 1993;110(1):39–54.
9. Hohling HJ, Barckhaus RH, Drefting ER, Quint P, Athoff J. Quantitative electron microscopy of the early stages of cartilage mineralization. Metab Bone Dis Res 1978;1:109–14.
10. Khan SN, Bostrom MP, Lane JM. Bone growth factors. Orthop Clin North Am 2000;31(3):375–88.
11. Rodan GA. Control of bone formation and resorption: biological and clinical perspective. J Cell Biochem Suppl 1998;30/31:55–61.
12. Otto F, Thornell AP, Crompton T, et al. Cbfa1, a candidate gene for cleidocranial dysplasia syndrome, is essential for osteoblast differentiation and bone development. Cell 1997;89(5):765–71.
13. Nakashima K, Zhou X, Kunkel G, et al. The novel zinc finger-containing transcription factor osterix is required for osteoblast differentiation and bone formation. Cell 2002;108(1):17–29.
14. Komori T, Yagi H, Nomura S, et al. Targeted disruption of Cbfa1 results in a complete lack of bone formation owing to maturational arrest of osteoblasts. Cell 1997;89(5):755–64.
15. Ducy P. Cbfa1: a molecular switch in osteoblast biology. Dev Dyn 2000;219(4):461–71.
16. Ducy P, Karsenty G. The family of bone morphogenetic proteins. Kidney Int 2000;57(6):2207–14.
17. Ducy P, Amling M, Takeda S, et al. Leptin inhibits bone formation through a hypothalamic relay: a central control of bone mass. Cell 2000;100(2):197–207.
18. Aubin JE, Triffit JT. Mesenchymal Stem Cells and Osteoblast Differentiation In: J. P. Bilezikian, L. G. Raisz, G. A. Rodan, Eds. Principles of Bone Biology. 2nd ed. San Diego: Academic Press; 2002:59–81.
19. Tezuka K, Takeshita S, Hakeda Y, Kumegawa M, Kikuno R, Hashimoto-Gotoh T. Isolation of mouse and human cDNA clones encoding a protein expressed specifically in osteoblasts and brain tissues. Biochem Biophys Res Commun 1990;173(1):246–51.
20. Raulo E, Chernousov MA, Carey DJ, Nolo R, Rauvala H. Isolation of a neuronal cell surface receptor of heparin binding growth-associated molecule (HB-GAM). Identification as N-syndecan (syndecan-3). J Biol Chem 1994;269(17):12999–3004.
21. Lorenz-Depiereux B, Bastepe M, Benet-Pages A, et al. DMP1 mutations in autosomal recessive hypophosphatemia implicate a bone matrix protein in the regulation of phosphate homeostasis. Nat Genet 2006;38(11):1248–50.
22. Lorenz-Depiereux B, Benet-Pages A, Eckstein G, et al. Hereditary hypophosphatemic rickets with hypercalciuria is caused by mutations in the sodium-phosphate cotransporter Gene SLC34A3. Am J Hum Genet 2006;78(2):193–201.
23. Poole KE, van Bezooijen RL, Loveridge N, et al. Sclerostin is a delayed secreted product of osteocytes that inhibits bone formation. FASEB J 2005;19(13):1842–4.
24. Poole KE, Reeve J. Parathyroid hormone – a bone anabolic and catabolic agent. Curr Opin Pharmacol 2005;5(6):612–7.
25. Oster G. Cell Motility and Tissue Morphogenesis. In: W. D. Stien andF. Bronner, Eds. Cell Shape: Determinants, Regulation and Regulatory Role. San Diego: Academic Press; 1989:33–61.
26. Takahashi N, Udagawa N, Takami M, Suda T. Cells of Bone, Osteoclast Generation. In: J. P. Bilezikian, L. G. Raisz, G. A. Rodan, Eds. Principles of Bone Biology 2nd ed. 2002:109-26.
27. Watanabe H, Yanagisawa T, Sasaki J. Cytoskeletal architecture of rat calvarial osteoclasts: microfilaments, and intermediate filaments, and nuclear matrix as demonstrated by detergent perfusion. Anat Rec 1995;243(2):165–74.
28. Horne WC. Toward a more complete molecular description of the osteoclast. Bone 1995;17(2):107–9.
29. Sakai D, Tong HS, Minkin C. Osteoclast molecular phenotyping by random cDNA sequencing. Bone 1995;17(2):111–9.
30. Roodman GD, Kurihara N, Ohsaki Y, et al Interleukin 6. A potential autocrine/paracrine factor in Paget's disease of bone. J Clin Investig 1992;89(1):46–52.
31. Ohsaki Y, Takahashi S, Scarcez T, et al. Evidence for an autocrine/paracrine role for interleukin-6 in bone resorption by giant cells from giant cell tumors of bone. Endocrinology 1992;131(5):2229–34.
32. Manolagas SC, Jilka RL. Bone marrow, cytokines, and bone remodeling. Emerging insights into the pathophysiology of osteoporosis. N Engl J Med 1995;332(5):305–11.
33. Wong BR, Rho J, Arron J, et al. TRANCE is a novel ligand of the tumor necrosis factor receptor family that activates c-Jun N-terminal kinase in T cells. J Biol Chem 1997;272(40):25190–4.
34. Yasuda H, Shima N, Nakagawa N, et al. Identity of osteoclastogenesis inhibitory factor (OCIF) and osteoprotegerin (OPG): a mechanism by which OPG/OCIF inhibits osteoclastogenesis in vitro. Endocrinology 1998;139(3):1329–37.
35. Yasuda H, Shima N, Nakagawa N, et al. Osteoclast differentiation factor is a ligand for osteoprotegerin/osteoclastogenesis-inhibitory factor and is identical to TRANCE/RANKL. Proc Natl Acad Sci USA 1998;95(7):3597–602.
36. Lacey DL, Timms E, Tan HL, et al. Osteoprotegerin ligand is a cytokine that regulates osteoclast differentiation and activation. Cell 1998;93(2):165–76.
37. Bucay N, Sarosi I, Dunstan CR, et al. Osteoprotegerin-deficient mice develop early onset osteoporosis and arterial calcification. Genes Dev 1998;12(9):1260–8.

38. Kong YY, Feige U, Sarosi I, et al. Activated T cells regulate bone loss and joint destruction in adjuvant arthritis through osteoprotegerin ligand. Nature 1999;402(6759):304–9.
39. Kong YY, Yoshida H, Sarosi I, et al. OPGL is a key regulator of osteoclastogenesis, lymphocyte development and lymph-node organogenesis. Nature 1999;397(6717):315–23.
40. Dougall WC, Glaccum M, Charrier K, et al. RANK is essential for osteoclast and lymph node development. Genes Dev 1999;13(18):2412–24.
41. Hughes AE, Ralston SH, Marken J, et al. Mutations in TNFRSF11A, affecting the signal peptide of RANK, cause familial expansile osteolysis. Nat Genet 2000;24(1):45–8.
42. Galibert L, Tometsko ME, Anderson DM, Cosman D, Dougall WC. The involvement of multiple tumor necrosis factor receptor (TNFR)-associated factors in the signaling mechanisms of receptor activator of NF-kappaB, a member of the TNFR superfamily. J Biol Chem 1998;273(51):34120–7.
43. Darnay BG, Haridas V, Ni J, Moore PA, Aggarwal BB. Characterization of the intracellular domain of receptor activator of NF-kappaB (RANK). Interaction with tumor necrosis factor receptor-associated factors and activation of NF-kappab and c-Jun N-terminal kinase. J Biol Chem 1998;273(32):20551–5.
44. Ohishi M, Matsumura Y, Aki D, et al. Suppressors of cytokine signaling-1 and -3 regulate osteoclastogenesis in the presence of inflammatory cytokines. J Immunol 2005;174(5):3024–31.
45. Hayashi T, Kaneda T, Toyama Y, Kumegawa M, Hakeda Y. Regulation of receptor activator of NF-kappa B ligand-induced osteoclastogenesis by endogenous interferon-beta (INF-beta) and suppressors of cytokine signaling (SOCS). The possible counteracting role of SOCSs- in IFN-beta-inhibited osteoclast formation. J Biol Chem 2002;277(31):27880–6.
46. Takayanagi H, Ogasawara K, Hida S, et al. T-cell-mediated regulation of osteoclastogenesis by signalling cross-talk between RANKL and IFN-gamma. Nature 2000;408(6812):600–5.
47. Huang W, O'Keefe RJ, Schwarz EM. Exposure to receptor-activator of NFkappaB ligand renders pre-osteoclasts resistant to IFN-gamma by inducing terminal differentiation. Arthritis Res Ther 2003;5(1):R49–R59.
48. Takayanagi H, Kim S, Matsuo K, et al. RANKL maintains bone homeostasis through c-Fos-dependent induction of interferon-beta. Nature 2002;416(6882):744–9.
49. Takayanagi H, Sato K, Takaoka A, Taniguchi T. Interplay between interferon and other cytokine systems in bone metabolism. Immunol Rev 2005;208:181–93.
50. Asagiri M, Sato K, Usami T, et al. Autoamplification of NFATc1 expression determines its essential role in bone homeostasis. J Exp Med 2005;202(9):1261–9.
51. Ouyang W, Lohning M, Gao Z, et al. Stat6-independent GATA-3 autoactivation directs IL-4-independent Th2 development and commitment. Immunity 2000;12(1):27–37.
52. Takayanagi H, Kim S, Koga T, et al. Induction and activation of the transcription factor NFATc1 (NFAT2) integrate RANKL signaling in terminal differentiation of osteoclasts. Dev Cell 2002;3(6):889–901.
53. Kaifu T, Nakahara J, Inui M, et al. Osteopetrosis and thalamic hypomyelinosis with synaptic degeneration in DAP12-deficient mice. J Clin Investig 2003;111(3):323–32.
54. Koga T, Inui M, Inoue K, et al. Costimulatory signals mediated by the ITAM motif cooperate with RANKL for bone homeostasis. Nature 2004;428(6984):758–63.
55. Mocsai A, Humphrey MB, Van Ziffle JA, et al. The immunomodulatory adapter proteins DAP12 and Fc receptor gamma-chain (FcRgamma) regulate development of functional osteoclasts through the Syk tyrosine kinase. Proc Natl Acad Sci USA 2004;101(16):6158–63.
56. Kim Y, Sato K, Asagiri M, Morita I, Soma K, Takayanagi H. Contribution of nuclear factor of activated T cells c1 to the transcriptional control of immunoreceptor osteoclast-associated receptor but not triggering receptor expressed by myeloid cells-2 during osteoclastogenesis. J Biol Chem 2005;280(38):32905–13.
57. Kim K, Kim JH, Lee J, et al. Nuclear factor of activated T cells c1 induces osteoclast-associated receptor gene expression during tumor necrosis factor-related activation-induced cytokine-mediated osteoclastogenesis. J Biol Chem 2005;280(42):35209–16.
58. Ono K, Kaneko H, Choudhary S, et al. Biphasic effect of prostaglandin E2 on osteoclast formation in spleen cell cultures: role of the EP2 receptor. J Bone Miner Res 2005;20(1):23–9.
59. Sela J, Amir D, Schwartz Z, Weinberg H. Ultrastructural tissue morphometry of the distribution of extracellular matrix vesicles in remodeling rat tibial bone six days after injury. Acta Anat 1987;128(4):295–300.
60. Horton WA. Biology of bone growth. Growth Genet Horm 1990;6(2):1–5.
61. Cserjesi P, Brown D, Lyons GE, Olson EN. Expression of the novel basic helix-loop-helix gene eHAND in neural crest derivatives and extraembryonic membranes during mouse development. Dev Biol 1995;170(2):664–78.
62. LeClair EE, Bonfiglio L, Tuan RS. Expression of the paired-box genes Pax-1 and Pax-9 in limb skeleton development. Dev Dyn 1999;214(2):101–15.
63. Cserjesi P, Brown D, Ligon KL, et al. Scleraxis: a basic helix-loop-helix protein that prefigures skeletal formation during mouse embryogenesis. Development 1995;121(4):1099–110.
64. Oberlender SA, Tuan RS. Spatiotemporal profile of N-cadherin expression in the developing limb mesenchyme. Cell Adhes Commun 1994;2(6):521–37.
65. Hall BK, Miyake T. Divide, accumulate, differentiate: cell condensation in skeletal development revisited. Int J Dev Biol 1995;39(6):881–93.
66. Wright E, Hargrave MR, Christiansen J, et al. The Sry-related gene Sox9 is expressed during chondrogenesis in mouse embryos. Nat Genet 1995;9(1):15–20.
67. Bruder SP, Caplan AI. Discrete stages within the osteogenic lineage are revealed by alterations in the cell surface architecture of embryonic bone cells. Connect Tissue Res 1989;20(1–4):73–9.
68. Hatori M, Klatte KJ, Teixeira CC, Shapiro IM. End labeling studies of fragmented DNA in the avian growth plate: evidence of apoptosis in terminally differentiated chondrocytes. J Bone Miner Res 1995;10(12):1960–8.
69. Kobayashi T, Kronenberg H. Minireview: transcriptional regulation in development of bone. Endocrinology 2005;146(3):1012–7.
70. Praul CA, Ford BC, Leach RM. Effect of fibroblast growth factors 1, 2, 4, 5, 6, 7, 8, 9, and 10 on avian chondrocyte proliferation. J Cell Biochem 2002;84(2):359–66.
71. Yakar S, Liu JL, Stannard B, et al. Normal growth and development in the absence of hepatic insulin-like growth factor I. Proc Natl Acad Sci USA 1999;96(13):7324–9.
72. Ohlsson C, Bengtsson BA, Isaksson OG, Andreassen TT, Slootweg MC. Growth hormone and bone. Endocr Rev 1998;19(1):55–79.
73. Weiss RE, Refetoff S. Effect of thyroid hormone on growth. Lessons from the syndrome of resistance to thyroid hormone. Endocrinol Metab Clin North Am 1996;25(3):719–30.
74. Faustini-Fustini M, Rochira V, Carani C. Oestrogen deficiency in men: where are we today?Eur J Endocrinol/Eur Feder Endocr Soc 1999;140(2):111–29.
75. Boyan BD, Schwartz Z, Swain LD, Bonewald LF, Khare A. Regulation of matrix vesicle metabolism by vitamin D metabolites. Connect Tissue Res 1989;22(1–4):3–16; discussion 53–61.
76. Canalis E. Clinical review 83: mechanisms of glucocorticoid action in bone: implications to glucocorticoid-induced osteoporosis. J Clin Endocrinol Metab 1996;81(10):3441–7.
77. Millan FA, Denhez F, Kondaiah P, Akhurst RJ. Embryonic gene expression patterns of TGF beta 1, beta 2 and beta 3 suggest different developmental functions in vivo. Development 1991;111(1):131–43.

78. Philbrick WM, Wysolmerski JJ, Galbraith S, et al. Defining the roles of parathyroid hormone-related protein in normal physiology. Physiol Rev 1996;76(1):127–73.
79. Vortkamp A, Lee K, Lanske B, Segre GV, Kronenberg HM, Tabin CJ. Regulation of rate of cartilage differentiation by Indian hedgehog and PTH-related protein. Science 1996;273(5275):613–22.
80. Bellus GA, Hefferon TW, Ortiz de Luna RI, et al. Achondroplasia is defined by recurrent G380R mutations of FGFR3. Am J Hum Genet 1995;56(2):368–73.
81. Bellus GA, McIntosh I, Smith EA, et al. A recurrent mutation in the tyrosine kinase domain of fibroblast growth factor receptor 3 causes hypochondroplasia. Nat Genet 1995;10(3):357–9.
82. Serra R, Karaplis A, Sohn P. Parathyroid hormone-related peptide (PTHrP)-dependent and -independent effects of transforming growth factor beta (TGF-beta) on endochondral bone formation. J Cell Biol 1999;145(4):783–94.
83. St-Jacques B, Hammerschmidt M, McMahon AP. Indian hedgehog signaling regulates proliferation and differentiation of chondrocytes and is essential for bone formation. Genes Dev 1999;13(16):2072–86.
84. Chen L, Li C, Qiao W, Xu X, Deng C. A Ser(365)–Cys mutation of fibroblast growth factor receptor 3 in mouse downregulates Ihh/PTHrP signals and causes severe achondroplasia. Hum Mol Genet 2001;10(5):457–65.
85. Caplan AI. Bone development. Ciba Found Symp 1988;136:3–21.
86. Larsen WJ. Human Embryology. Churchil Livingstone Inc; 1997.
87. Erlebacher A, Filvaroff EH, Gitelman SE, Derynck R. Toward a molecular understanding of skeletal development. Cell 1995;80(3):371–8.
88. Johnson RL, Tabin CJ. Molecular models for vertebrate limb development. Cell 1997;90(6):979–90.
89. Schwabe JW, Rodriguez-Esteban C, Izpisua Belmonte JC. Limbs are moving: where are they going? Trends Genet 1998; 14(6):229–35.
90. Martin GR. The roles of FGFs in the early development of vertebrate limbs. Genes Dev 1998;12(11):1571–86.
91. Xu X, Weinstein M, Li C, Deng C. Fibroblast growth factor receptors (FGFRs) and their roles in limb development. Cell Tissue Res 1999;296(1):33–43.
92. Krumlauf R. Hox genes in vertebrate development. Cell 1994;78(2):191–201.
93. Church VL, Francis-West P. Wnt signalling during limb development. Int J Dev Biol 2002;46(7):927–36.
94. McEwen DG, Peifer M. Wnt signaling: Moving in a new direction. Curr Biol 2000;10(15):R562–R564.
95. Boutros M, Paricio N, Strutt DI, Mlodzik M. Dishevelled activates JNK and discriminates between JNK pathways in planar polarity and wingless signaling. Cell 1998;94(1):109–18.
96. Kengaku M, Capdevila J, Rodriguez-Esteban C, et al. Distinct WNT pathways regulating AER formation and dorsoventral polarity in the chick limb bud. Science 1998;280(5367):1274–7.
97. Yamaguchi TP, Bradley A, McMahon AP, Jones S. A Wnt5a pathway underlies outgrowth of multiple structures in the vertebrate embryo. Development 1999;126(6):1211–23.
98. Farrell ER, Munsterberg AE. csal1 is controlled by a combination of FGF and Wnt signals in developing limb buds. Dev Biol 2000;225(2):447–58.
99. Hamburger V, Hamilton HL. A series of normal stages in the development of the chick embryo. 1951. Dev Dyn 1992; 195(4):231–72.
100. Bellairs R, Osmond M. The Atlas of Chick Development. San Diego, California.: Academic Press; 1998.
101. Konigsberg IR. The Embryonic Origin of Muscle. In: A. G. Engel, B. Q. Banker, Eds. In: Myology. USA: McGraw-Hill Book Company; 1986.
102. Gilbert SF. Paraxial and Intermediate mesoderm. In: Developmental Biology. Sunderland, Massachusetts.: Sinauer Associates, Inc., Publishers; 2003.
103. Hatta K, Takagi S, Fujisawa H, Takeichi M. Spatial and temporal expression pattern of N-cadherin cell adhesion molecules correlated with morphogenetic processes of chicken embryos. Dev Biol 1987;120(1):215–27.
104. Tajbakhsh S, Sporle R. Somite development: constructing the vertebrate body. Cell 1998;92(1):9–16.
105. Nakaya Y, Kuroda S, Katagiri YT, Kaibuchi K, Takahashi Y. Mesenchymal-epithelial transition during somitic segmentation is regulated by differential roles of Cdc42 and Rac1. Dev Cell 2004;7(3):425–38.
106. Nowicki JL, Burke AC. Hox genes and morphological identity: axial versus lateral patterning in the vertebrate mesoderm. Development (Cambridge, England) 2000;127(19):4265–75.
107. Nowicki JL, Takimoto R, Burke AC. The lateral somitic frontier: dorso-ventral aspects of anterio-posterior regionalization in avian embryos. Mech Dev 2003;120(2):227–40.
108. Buckingham M, Bajard L, Daubas P, et al. Myogenic progenitor cells in the mouse embryo are marked by the expression of Pax3/7 genes that regulate their survival and myogenic potential. Anat Embryol 2006;211(Suppl 1):51–6.
109. Buckingham M. Myogenic progenitor cells and skeletal myogenesis in vertebrates. Curr Opin Genet Dev 2006;16(5):525–32.
110. Smith CA, Tuan RS. Functional involvement of Pax-1 in somite development: somite dysmorphogenesis in chick embryos treated with Pax-1 paired-box antisense oligodeoxynucleotide. Teratology 1995;52(6):333–45.
111. Pownall ME, Gustafsson MK, Emerson CP, Jr. Myogenic regulatory factors and the specification of muscle progenitors in vertebrate embryos. Annu Rev Cell Dev Biol 2002;18:747–83.
112. Brill G, Kahane N, Carmeli C, von Schack D, Barde YA, Kalcheim C. Epithelial-mesenchymal conversion of dermatome progenitors requires neural tube-derived signals: characterization of the role of neurotrophin-3. Development (Cambridge, England) 1995;121(8):2583–94.
113. Ikeya M, Takada S. Wnt signaling from the dorsal neural tube is required for the formation of the medial dermomyotome. Development (Cambridge, England) 1998;125(24):4969–76.
114. Dietrich S, Schubert FR, Healy C, Sharpe PT, Lumsden A. Specification of the hypaxial musculature. Development (Cambridge, England) 1998;125(12):2235–49.
115. Marcelle C, Stark MR, Bronner-Fraser M. Coordinate actions of BMPs, Wnts, Shh and noggin mediate patterning of the dorsal somite. Development (Cambridge, England) 1997;124(20): 3955–63.
116. Brent AE, Tabin CJ. Developmental regulation of somite derivatives: muscle, cartilage and tendon. Curr Opin Genet Dev 2002;12(5):548–57.
117. Sato Y, Yasuda K, Takahashi Y. Morphological boundary forms by a novel inductive event mediated by Lunatic fringe and Notch during somitic segmentation. Development (Cambridge, England) 2002;129(15):3633–44.
118. Morimoto M, Sasaki N, Oginuma M, et al. The negative regulation of Mesp2 by mouse Ripply2 is required to establish the rostro-caudal patterning within a somite. Development (Cambridge, England) 2007;134(8):1561–9.
119. Grifone R, Demignon J, Giordani J, et al. Eya1 and Eya2 proteins are required for hypaxial somitic myogenesis in the mouse embryo. Dev Biol 2007;302(2):602–16.
120. Ressoret J, De Crombrugghe B. Type I Collagen. In: J. P. Bilezikian, L. G. Raisz, G. A. Rodan, Eds. Principles of Bone Biology. 2nd ed. San Diego: Academic Press; 2002:189–210.
121. Robins SP, Brady JD. Collagen Cross-Linking and Metabolism In: J. P. Bilezikian, L. G. Raisz, G. A. Rodan, Eds. Principles of Bone Biology. 2nd ed. San Diego: Academic Press; 2002:211–23.

122. Buckwalter JA, Pita JC, Muller FJ, Nessler J. Structural differences between two populations of articular cartilage proteoglycan aggregates. J Orthop Res 1994;12(1):144–8.
123. Royce PM, Barnes MJ. Failure of highly purified lysyl hydroxylase to hydroxylate lysyl residues in the non-helical regions of collagen. Biochem J 1985;230(2):475–80.
124. Kobayashi Y, Takahashi N. [The pathophysiology of osteoporosis/osteopenia in gene mutant mice]. Clin Calcium 2006;16(2):311–18.
125. Bonadio J, Ramirez F, Barr M. An intron mutation in the human alpha 1(I) collagen gene alters the efficiency of pre-mRNA splicing and is associated with osteogenesis imperfecta type II. J Biol Chem 1990;265(4):2262–8.
126. Bonadio J, Saunders TL, Tsai E, et al. Transgenic mouse model of the mild dominant form of osteogenesis imperfecta. Proc Natl Acad Sci USA 1990;87(18):7145–9.
127. Sodek J, Ganss B, McKee MD. Osteopontin. Crit Rev Oral Biol Med 2000;11(3):279–303.
128. Denhardt DT, Noda M. Osteopontin expression and function: role in bone remodeling. J Cell Biochem Suppl 1998;30/31:92–102.
129. Fisher LW, McBride OW, Termine JD, Young MF. Human bone sialoprotein. Deduced protein sequence and chromosomal localization. J Biol Chem 1990;265(4):2347–51.
130. Gorski JP, Wang A, Lovitch D, Law D, Powell K, Midura RJ. Extracellular bone acidic glycoprotein-75 defines condensed mesenchyme regions to be mineralized and localizes with bone sialoprotein during intramembranous bone formation. J Biol Chem 2004;279(24):25455–63.
131. Midura RJ, Wang A, Lovitch D, Law D, Powell K, Gorski JP. Bone acidic glycoprotein-75 delineates the extracellular sites of future bone sialoprotein accumulation and apatite nucleation in osteoblastic cultures. J Biol Chem 2004;279(24):25464–73.
132. Purcell L, Gruia-Gray J, Scanga S, Ringuette M. Developmental anomalies of Xenopus embryos following microinjection of SPARC antibodies. J Exp Zool 1993;265(2):153–64.
133. Bassuk JA, Birkebak T, Rothmier JD, et al. Disruption of the Sparc locus in mice alters the differentiation of lenticular epithelial cells and leads to cataract formation. Exp Eye Res 1999;68(3):321–31.
134. Delany AM, Amling M, Priemel M, Howe C, Baron R, Canalis E. Osteopenia and decreased bone formation in osteonectin-deficient mice. J Clin Investig 2000;105(7):915–23.
135. Gokhale JP, Robey PG, Boskey AL. The Biochemistry of Bone. In: Osteoporosis. San Diego: Academic Press; 2001.
136. Boskey AL. Noncollagenous matrix proteins and their role in mineralization. Bone Miner 1989;6(2):111–23.
137. Boskey AL. What's in a name? The function of the mineralized tissue matrix proteins. J Dent Res 1989;68(2):159.
138. Hynes RO. Fibronectin. New York: Springer-Verlag; 1990.
139. George EL, Georges-Labouesse EN, Patel-King RS, Rayburn H, Hynes RO. Defects in mesoderm, neural tube and vascular development in mouse embryos lacking fibronectin. Development 1993;119(4):1079–91.
140. Georges-Labouesse EN, George EL, Rayburn H, Hynes RO. Mesodermal development in mouse embryos mutant for fibronectin. Dev Dyn 1996;207(2):145–56.
141. Schwarzbauer JE, Tamkun JW, Lemischka IR, Hynes RO. Three different fibronectin mRNAs arise by alternative splicing within the coding region. Cell 1983;35(2 Pt 1):421–31.
142. Kornblihtt AR, Vibe-Pedersen K, Baralle FE. Human fibronectin: cell specific alternative mRNA splicing generates polypeptide chains differing in the number of internal repeats. Nucleic Acids Res 1984;12(14):5853–68.
143. Zardi L, Carnemolla B, Siri A, et al. Transformed human cells produce a new fibronectin isoform by preferential alternative splicing of a previously unobserved exon. EMBO J 1987;6(8):2337–42.
144. Schwarzbauer JE, Patel RS, Fonda D, Hynes RO. Multiple sites of alternative splicing of the rat fibronectin gene transcript. EMBO J 1987;6(9):2573–80.
145. Manabe R, Ohe N, Maeda T, Fukuda T, Sekiguchi K. Modulation of cell-adhesive activity of fibronectin by the alternatively spliced EDA segment. J Cell Biol 1997;139(1):295–307.
146. Manabe R, Oh-e N, Sekiguchi K. Alternatively spliced EDA segment regulates fibronectin-dependent cell cycle progression and mitogenic signal transduction. J Biol Chem 1999;274(9):5919–24.
147. Fukuda T, Yoshida N, Kataoka Y, et al. Mice lacking the EDB segment of fibronectin develop normally but exhibit reduced cell growth and fibronectin matrix assembly in vitro. Cancer Res 2002;62(19):5603–10.
148. Chen H, Herndon ME, Lawler J. The cell biology of thrombospondin-1. Matrix Biol 2000;19(7):597–614.
149. Alford AI, Hankenson KD. Matricellular proteins: extracellular modulators of bone development, remodeling, and regeneration. Bone 2006;38(6):749–57.
150. Bornstein P, Sage EH. Matricellular proteins: extracellular modulators of cell function. Curr Opin Cell Biol 2002;14(5):608–16.
151. Hankenson KD, Bain SD, Kyriakides TR, Smith EA, Goldstein SA, Bornstein P. Increased marrow-derived osteoprogenitor cells and endosteal bone formation in mice lacking thrombospondin 2. J Bone Miner Res 2000;15(5):851–62.
152. Daci E, Everts V, Torrekens S, et al. Increased bone formation in mice lacking plasminogen activators. J Bone Miner Res 2003;18(7):1167–76.
153. Bradham WG, Lewis JV, Sewell DH, Garrett A. Bullet embolus to the ascending aorta following a gunshot wound to the chest. J Tenn Med Assoc 1991;84(12):592–3.
154. Brunner A, Chinn J, Neubauer M, Purchio AF. Identification of a gene family regulated by transforming growth factor-beta. DNA Cell Biol 1991;10(4):293–300.
155. Ryseck RP, Macdonald-Bravo H, Mattei MG, Bravo R. Structure, mapping, and expression of fisp-12, a growth factor-inducible gene encoding a secreted cysteine-rich protein. Cell Growth Differ 1991;2(5):225–33.
156. Brigstock DR, Steffen CL, Kim GY, Vegunta RK, Diehl JR, Harding PA. Purification and characterization of novel heparin-binding growth factors in uterine secretory fluids. Identification as heparin-regulated Mr 10,000 forms of connective tissue growth factor. J Biol Chem 1997;272(32):20275–82.
157. Ying Z, King ML. Isolation and characterization of xnov, a Xenopus laevis ortholog of the chicken nov gene. Gene 1996;171(2):243–8.
158. Xu J, Smock SL, Safadi FF, et al. Cloning the full-length cDNA for rat connective tissue growth factor: implications for skeletal development. J Cell Biochem 2000;77(1):103–15.
159. Joliot V, Martinerie C, Dambrine G, et al. Proviral rearrangements and overexpression of a new cellular gene (nov) in myeloblastosis-associated virus type 1-induced nephroblastomas. Mol Cell Biol 1992;12(1):10–21.
160. Hashimoto Y, Shindo-Okada N, Tani M, et al. Expression of the Elm1 gene, a novel gene of the CCN (connective tissue growth factor, Cyr61/Cef10, and neuroblastoma overexpressed gene) family, suppresses in vivo tumor growth and metastasis of K-1735 murine melanoma cells. J Exp Med 1998;187(3):289–96.
161. Pennica D, Swanson TA, Welsh JW, et al. WISP genes are members of the connective tissue growth factor family that are up-regulated in wnt-1-transformed cells and aberrantly expressed in human colon tumors. Proc Natl Acad Sci USA 1998;95(25):14717–22.
162. Kothapalli D, Grotendorst GR. CTGF modulates cell cycle progression in cAMP-arrested NRK fibroblasts. J Cell Physiol 2000;182(1):119–26.
163. Brigstock DR. The connective tissue growth factor/cysteine-rich 61/nephroblastoma overexpressed (CCN) family. Endocr Rev 1999;20:189–206.
164. Moussad EE, Brigstock DR. Connective tissue growth factor: what's in a name?. Mol Genet Metab 2000;71(1–2):276–92.

165. Oemar BS, Luscher TF. Connective tissue growth factor. Friend or foe? Arterioscler Thromb Vasc Biol 1997;17(8):1483–9.
166. Sabe H, Hata A, Okada M, Nakagawa H, Hanafusa H. Analysis of the binding of the Src homology 2 domain of Csk to tyrosine-phosphorylated proteins in the suppression and mitotic activation of c-Src. Proc Natl Acad Sci USA 1994;91(9):3984–8.
167. O'Brien TP, Yang GP, Sanders L, Lau LF. Expression of cyr61, a growth factor-inducible immediate-early gene. Mol Cell Biol 1990;10(7):3569–77.
168. Kim HS, Nagalla SR, Oh Y, Wilson E, Roberts CT, Jr., Rosenfeld RG. Identification of a family of low-affinity insulin-like growth factor binding proteins (IGFBPs): characterization of connective tissue growth factor as a member of the IGFBP superfamily. Proc Natl Acad Sci USA 1997;94(24):12981–6.
169. Kireeva ML, Latinkic BV, Kolesnikova TV, et al. Cyr61 and Fisp12 are both ECM-associated signaling molecules: activities, metabolism, and localization during development. Exp Cell Res 1997;233(1):63–77.
170. Holt GD, Pangburn MK, Ginsburg V. Properdin binds to sulfatide [Gal(3-SO4)beta 1–1 Cer] and has a sequence homology with other proteins that bind sulfated glycoconjugates. J Biol Chem 1990;265(5):2852–5.
171. Bork P. The modular architecture of a new family of growth regulators related to connective tissue growth factor. FEBS Lett 1993;327(2):125–30.
172. Dammeier J, Brauchle M, Falk W, Grotendorst GR, Werner S. Connective tissue growth factor: a novel regulator of mucosal repair and fibrosis in inflammatory bowel disease? Int J Biochem Cell Biol 1998;30(8):909–22.
173. Nakanishi T, Kimura Y, Tamura T, et al. Cloning of a mRNA preferentially expressed in chondrocytes by differential display-PCR from a human chondrocytic cell line that is identical with connective tissue growth factor (CTGF) mRNA. Biochem Biophys Res Commun 1997;234(1):206–10.
174. Duncan MR, Frazier KS, Abramson S, et al. Connective tissue growth factor mediates transforming growth factor beta-induced collagen synthesis: down-regulation by cAMP. FASEB J 1999;13(13):1774–86.
175. Frazier KS, Grotendorst GR. Expression of connective tissue growth factor mRNA in the fibrous stroma of mammary tumors. Int J Biochem Cell Biol 1997;29(1):153–61.
176. Arnott JA, Nuglozeh E, Rico MC, et al. Connective tissue growth factor (CTGF/CCN2) is a downstream mediator for TGF-beta1-induced extracellular matrix production in osteoblasts. J Cell Physiol 2007;210(3):843–52.
177. Nakanishi T, Nishida T, Shimo T, et al. Effects of CTGF/Hcs24, a product of a hypertrophic chondrocyte-specific gene, on the proliferation and differentiation of chondrocytes in culture. Endocrinology 2000;141(1):264–73.
178. Chen CC, Chen N, Lau LF. The angiogenic factors Cyr61 and connective tissue growth factor induce adhesive signaling in primary human skin fibroblasts. J Biol Chem 2001;276(13): 10443–52.
179. Babic AM, Kireeva ML, Kolesnikova TV, Lau LF. CYR61, a product of a growth factor-inducible immediate early gene, promotes angiogenesis and tumor growth. Proc Natl Acad Sci USA 1998;95(11):6355–60.
180. Bradham DM, Igarashi A, Potter RL, Grotendorst GR. Connective tissue growth factor: a cysteine-rich mitogen secreted by human vascular endothelial cells is related to the SRC-induced immediate early gene product CEF-10. J Cell Biol 1991;114(6):1285–94.
181. Kothapalli D, Frazier KS, Welply A, Segarini PR, Grotendorst GR. Transforming growth factor beta induces anchorage-independent growth of NRK fibroblasts via a connective tissue growth factor-dependent signaling pathway. Cell Growth Differ 1997;8(1):61–8.
182. Hishikawa K, Nakaki T, Fujii T. Connective tissue growth factor induces apoptosis via caspase 3 in cultured human aortic smooth muscle cells. Eur J Pharmacol 2000;392(1–2):19–22.
183. Hishikawa K, Oemar BS, Tanner FC, Nakaki T, Fujii T, Luscher TF. Overexpression of connective tissue growth factor gene induces apoptosis in human aortic smooth muscle cells. Circulation 1999;100(20):2108–12.
184. Babic AM, Chen CC, Lau LF. Fisp12/mouse connective tissue growth factor mediates endothelial cell adhesion and migration through integrin alphavbeta3, promotes endothelial cell survival, and induces angiogenesis in vivo. Mol Cell Biol 1999; 19(4):2958–66.
185. Grotendorst GR. Connective tissue growth factor: a mediator of TGF-beta action on fibroblasts. Cytokine Growth Factor Rev 1997;8(3):171–9.
186. Igarashi A, Okochi H, Bradham DM, Grotendorst GR. Regulation of connective tissue growth factor gene expression in human skin fibroblasts and during wound repair. Mol Biol Cell 1993;4(6):637–45.
187. Morin PJ. Beta-catenin signaling and cancer. Bioessays 1999;21(12):1021–30.
188. Shakunaga T, Ozaki T, Ohara N, et al. Expression of connective tissue growth factor in cartilaginous tumors. Cancer 2000;89(7): 1466–73.
189. Yu C, Le AT, Yeger H, Perbal B, Alman BA. NOV (CCN3) regulation in the growth plate and CCN family member expression in cartilage neoplasia. J Pathol 2003;201(4):609–15.
190. Hurvitz JR, Suwairi WM, Van Hul W, et al. Mutations in the CCN gene family member WISP3 cause progressive pseudorheumatoid dysplasia. Nat Genet 1999;23(1):94–8.
191. Dunlop LL, Hall BK. Relationships between cellular condensation, preosteoblast formation and epithelial-mesenchymal interactions in initiation of osteogenesis. Int J Dev Biol 1995;39(2):357–71.
192. Hall BK, Miyake T. The membranous skeleton: the role of cell condensations in vertebrate skeletogenesis. Anat Embryol (Berl) 1992;186(2):107–24.
193. Friedrichsen S, Heuer H, Christ S, et al. CTGF expression during mouse embryonic development. Cell Tissue Res 2003;312(2):175–88.
194. Haider AS, Grabarek J, Eng B, et al. In vitro model of "wound healing" analyzed by laser scanning cytometry: accelerated healing of epithelial cell monolayers in the presence of hyaluronate. Cytometry A 2003;53(1):1–8.
195. Hall B, Miyake T. All for one and one for all: condensation and the initiation of skeletal development. Bioessays 2000;2:138–47.
196. Kadota H, Nakanishi T, Asaumi K, et al. Expression of connective tissue growth factor/hypertrophic chondrocyte-specific gene product 24 (CTGF/Hcs24/CCN2) during distraction osteogenesis. J Bone Miner Metab 2004;22(4):293–302.
197. Shimo T, Kanyama M, Wu C, et al. Expression and roles of connective tissue growth factor in Meckel's cartilage development. Dev Dyn 2004;231(1):136–47.
198. Zhang X, Ziran N, Goater JJ, et al. Primary murine limb bud mesenchymal cells in long-term culture complete chondrocyte differentiation: TGF-beta delays hypertrophy and PGE2 inhibits terminal differentiation. Bone 2004;34(5):809–17.
199. Wong M, Kireeva ML, Kolesnikova TV, Lau LF. Cyr61, product of a growth factor-inducible immediate-early gene, regulates chondrogenesis in mouse limb bud mesenchymal cells. Dev Biol 1997;192(2):492–508.
200. Imabayashi H, Mori T, Gojo S, et al. Redifferentiation of dedifferentiated chondrocytes and chondrogenesis of human bone marrow stromal cells via chondrosphere formation with expression profiling by large-scale cDNA analysis. Exp Cell Res 2003;288(1):35–50.
201. Yosimichi G, Nakanishi T, Nishida T, Hattori T, Takano-Yamamoto T, Takigawa M. CTGF/Hcs24 induces chondrocyte differentiation through a p38 mitogen-activated protein kinase (p38MAPK),

and proliferation through a p44/42 MAPK/extracellular-signal regulated kinase (ERK). Eur J Biochem/FEBS 2001; 268(23):6058–65.
202. Nakanishi T, Yamaai T, Asano M, et al. Overexpression of connective tissue growth factor/hypertrophic chondrocyte-specific gene product 24 decreases bone density in adult mice and induces dwarfism. Biochem Biophys Res Commun 2001;281(3): 678–81.
203. Takigawa M, Nakanishi T, Kubota S, Nishida T. Role of CTGF/HCS24/ecogenin in skeletal growth control. J Cell Physiol 2003;194(3):256–66.
204. Ivkovic S, Yoon BS, Popoff SN, et al. Connective tissue growth factor coordinates chondrogenesis and angiogenesis during skeletal development. Development (Cambridge, England) 2003; 130(12):2779–91.
205. Safadi FF, Xu J, Smock SL, et al. Expression of connective tissue growth factor in bone: its role in osteoblast proliferation and differentiation in vitro and bone formation in vivo. J Cell Physiol 2003;196(1):51–62.
206. Kumar S, Hand AT, Connor JR, et al. Identification and cloning of a connective tissue growth factor-like cDNA from human osteoblasts encoding a novel regulator of osteoblast functions. J Biol Chem 1999;274(24):17123–31.
207. Lechner A, Schutze N, Siggelkow H, Seufert J, Jakob F. The immediate early gene product hCYR61 localizes to the secretory pathway in human osteoblasts. Bone 2000;27(1):53–60.
208. Hadjiargyrou M, Ahrens W, Rubin CT. Temporal expression of the chondrogenic and angiogenic growth factor CYR61 during fracture repair. J Bone Miner Res 2000;15(6):1014–23.
209. Abreu JG, Ketpura NI, Reversade B, De Robertis EM. Connective-tissue growth factor (CTGF) modulates cell signalling by BMP and TGF-beta. Nat Cell Biol 2002;4(8):599–604.
210. Allison TM, Derynck R. Transforming Growth Factor Beta in Skeletal Development and Maintenance. Philadelphia: Lippincott, Williams and Wilkins; 2000.
211. Luo Q, Kang Q, Si W, et al. Connective tissue growth factor (CTGF) is regulated by Wnt and bone morphogenetic proteins signaling in osteoblast differentiation of mesenchymal stem cells. J Biol Chem 2004;279(53):55958–68.
212. Nishida T, Nakanishi T, Asano M, Shimo T, Takigawa M. Effects of CTGF/Hcs24, a hypertrophic chondrocyte-specific gene product, on the proliferation and differentiation of osteoblastic cells in vitro. J Cell Physiol 2000;184(2):197–206.
213. Nishida T, Nakanishi T, Shimo T, et al. Demonstration of receptors specific for connective tissue growth factor on a human chondrocytic cell line (HCS-2/8). Biochem Biophys Res Commun 1998;247(3):905–9.
214. Mercurio S, Latinkic B, Itasaki N, Krumlauf R, Smith JC. Connective-tissue growth factor modulates WNT signalling and interacts with the WNT receptor complex. Development (Cambridge, England) 2004;131(9):2137–47.
215. Stoker DJ. Osteopetrosis. Semin Musculoskelet Radiol 2002;6(4):299–305.
216. Safadi FF, Xu J, Smock SL, Rico MC, Owen TA, Popoff SN. Cloning and characterization of osteoactivin, a novel cDNA expressed in osteoblasts. J Cell Biochem 2001;84(1):12–26.
217. Weterman MA, Ajubi N, van Dinter IM, et al. nmb, a novel gene, is expressed in low-metastatic human melanoma cell lines and xenografts. Int J Cancer 1995;60(1):73–81.
218. Shikano S, Bonkobara M, Zukas PK, Ariizumi K. Molecular cloning of a dendritic cell-associated transmembrane protein, DC-HIL, that promotes RGD-dependent adhesion of endothelial cells through recognition of heparan sulfate proteoglycans. J Biol Chem 2001;276(11):8125–34.
219. Bandari PS, Qian J, Yehia G, et al. Hematopoietic growth factor inducible neurokinin-1 type: a transmembrane protein that is similar to neurokinin 1 interacts with substance P. Regul Pept 2003;111(1–3):169–78.
220. Berson JF, Harper DC, Tenza D, Raposo G, Marks MS. Pmel17 initiates premelanosome morphogenesis within multivesicular bodies. Mol Biol Cell 2001;12(11):3451–64.
221. Loging WT, Lal A, Siu IM, et al. Identifying potential tumor markers and antigens by database mining and rapid expression screening. Genome Res 2000;10(9):1393–402.
222. Onaga M, Ido A, Hasuike S, et al. Osteoactivin expressed during cirrhosis development in rats fed a choline-deficient, L-amino acid-defined diet, accelerates motility of hepatoma cells. J Hepatol 2003;39(5):779–85.
223. Rich JN, Shi Q, Hjelmeland M, et al. Bone-related genes expressed in advanced malignancies induce invasion and metastasis in a genetically defined human cancer model. J Biol Chem 2003;278(18):15951–7.
224. Ogawa T, Nikawa T, Furochi H, et al. Osteoactivin upregulates expression of MMP-3 and MMP-9 in fibroblasts infiltrated into denervated skeletal muscle in mice. Am J Physiol Cell Physiol 2005;289(3):C697–C707.
225. Seibel MJ, Eastall R, Gundberg CM, Hannon R, Pols HAP. Biochemical Markers of Bone Metabolism. In: J. P. Bilezikian, L. G. Raisz, G. A. Rodan, Eds. Principles of Bone Biology. 2nd ed. San Diego: Academic Press; 2002:1543–71.
226. Bi Y, Nielsen KL, Kilts TM, et al. Biglycan deficiency increases osteoclast differentiation and activity due to defective osteoblasts. Bone 2006;38(6):778–86.
227. Goldberg M, Septier D, Rapoport O, Iozzo RV, Young MF, Ameye LG. Targeted disruption of two small leucine-rich proteoglycans, biglycan and decorin, excerpts divergent effects on enamel and dentin formation. Calcif Tissue Int 2005;77(5):297–310.
228. Ishida T, Machinami R. Reactive bone and cartilage forming processes of the hands and feet. Pathol Int 1995;45(12):975–6.
229. Buchanan M, Sandhu HS, Anderson C. Changes in bone mineralization pattern: a response to local stimulus in maxilla and mandible of dogs. Histol Histopathol 1988;3(4):331–6.
230. Reinholt FP, Wernerson A. Septal distribution and the relationship of matrix vesicle size to cartilage mineralization. Bone Miner 1988;4(1):63–71.
231. Glimcher MJ. Mechanism of calcification: role of collagen fibrils and collagen-phosphoprotein complexes in vitro and in vivo. Anat Rec 1989;224(2):139–53.
232. Xiao Z, Camalier CE, Nagashima K, et al. Analysis of the extracellular matrix vesicle proteome in mineralizing osteoblasts. J Cell Physiol 2007;210(2):325–35.
233. Mundy GR, Boyce B, Hughes D, et al The effects of cytokines and growth factors on osteoblastic cells. Bone 1995;17(2 Suppl):71S–5S.
234. Price PA, Fraser JD, Metz-Virca G. Molecular cloning of matrix Gla protein: implications for substrate recognition by the vitamin K-dependent gamma-carboxylase. Proc Natl Acad Sci USA 1987;84(23):8335–9.
235. Manolagas SC, Bellido T, Jilka RL. New insights into the cellular, biochemical, and molecular basis of postmenopausal and senile osteoporosis: roles of IL-6 and gp130. Int J Immunopharmacol 1995;17(2):109–16.
236. Huebner AK, Schinke T, Priemel M, et al. Calcitonin deficiency in mice progressively results in high bone turnover. J Bone Miner Res 2006;21(12):1924–34.
237. Morrison NA, Qi JC, Tokita A, et al. Prediction of bone density from vitamin D receptor alleles. Nature 1994;367(6460):284–7.
238. Safadi FF, Hermey DC, Popoff SN, Seifert MF. Skeletal resistance to 1,25-dihydroxyvitamin D3 in osteopetrotic rats. Endocrine 1999;11(3):309–19.
239. Li YC, Pirro AE, Amling M, et al. Targeted ablation of the vitamin D receptor: an animal model of vitamin D-dependent rickets

type II with alopecia. Proc Natl Acad Sci USA 1997;94(18): 9831–5.
240. Sooy K, Sabbagh Y, Demay MB. Osteoblasts lacking the vitamin D receptor display enhanced osteogenic potential in vitro. J Cell Biochem 2005;94(1):81–7.
241. Takeda S, Yoshizawa T, Nagai Y, et al. Stimulation of osteoclast formation by 1,25-dihydroxyvitamin D requires its binding to vitamin D receptor (VDR) in osteoblastic cells: studies using VDR knockout mice. Endocrinology 1999;140(2):1005–8.
242. Lee SK, Kalinowski J, Jastrzebski S, Lorenzo JA. 1,25(OH)2 vitamin D3-stimulated osteoclast formation in spleen-osteoblast cocultures is mediated in part by enhanced IL-1 alpha and receptor activator of NF-kappa B ligand production in osteoblasts. J Immunol 2002;169(5):2374–80.
243. Pascher E, Perniok A, Becker A, Feldkamp J. Effect of 1alpha,25(OH)2-vitamin D3 on TNF alpha-mediated apoptosis of human primary osteoblast-like cells in vitro. Horm Metab Res 1999;31(12):653–6.
244. Gurlek A, Kumar R. Regulation of osteoblast growth by interactions between transforming growth factor-beta and 1alpha,25-dihydroxyvitamin D3. Crit Rev Eukaryot Gene Expr 2001;11(4):299–317.
245. Sneddon WB, Demay MB. Characterization of an enhancer required for 1,25-dihydroxyvitamin D3-dependent transactivation of the rat osteocalcin gene. J Cell Biochem 1999;73(3):400–7.
246. Chae HJ, Jeong BJ, Ha MS, et al. ERK MAP kinase is required in 1,25(OH)2D3-induced differentiation in human osteoblasts. Immunopharmacol Immunotoxicol 2002;24(1):31–41.
247. Hewison M, Zehnder D, Bland R, Stewart PM. 1alpha-hydroxylase and the action of vitamin D. J Mol Endocrinol 2000;25(2): 141–8.
248. St-Arnaud R, Dardenne O, Prud'homme J, Hacking SA, Glorieux FH. Conventional and tissue-specific inactivation of the 25-hydroxyvitamin D-1alpha-hydroxylase (CYP27B1). J Cell Biochem 2003;88(2):245–51.
249. Panda DK, Miao D, Tremblay ML, et al. Targeted ablation of the 25-hydroxyvitamin D 1alpha-hydroxylase enzyme: evidence for skeletal, reproductive, and immune dysfunction. Proc Natl Acad Sci USA 2001;98(13):7498–503.
250. Song HM, Nacamuli RP, Xia W, et al. High-dose retinoic acid modulates rat calvarial osteoblast biology. J Cell Physiol 2005;202(1):255–62.
251. Chambon P. A decade of molecular biology of retinoic acid receptors. FASEB J 1996;10(9):940–54.
252. Collins MD, Mao GE. Teratology of retinoids. Annu Rev Pharmacol Toxicol 1999;39:399–430.
253. Means AL, Gudas LJ. The roles of retinoids in vertebrate development. Annu Rev Biochem 1995;64:201–33.
254. Schneider RA, Hu D, Rubenstein JL, Maden M, Helms JA. Local retinoid signaling coordinates forebrain and facial morphogenesis by maintaining FGF8 and SHH. Development 2001;128(14): 2755–67.
255. Ohishi K, Nishikawa S, Nagata T, et al. Physiological concentrations of retinoic acid suppress the osteoblastic differentiation of fetal rat calvaria cells in vitro. Eur J Endocrinol 1995;133(3):335–41.
256. Manji SS, Ng KW, Martin TJ, Zhou H. Transcriptional and post-transcriptional regulation of osteopontin gene expression in preosteoblasts by retinoic acid. J Cell Physiol 1998;176(1):1–9.
257. Ahmed N, Sammons J, Khokher MA, Hassan HT. Retinoic acid suppresses interleukin 6 production in normal human osteoblasts. Cytokine 2000;12(3):289–93.
258. Einhorn TA. Enhancement of fracture-healing. J Bone Joint Surg 1995;77(6):940–56.
259. Einhorn TA, Majeska RJ, Rush EB, Levine PM, Horowitz MC. The expression of cytokine activity by fracture callus. J Bone Miner Res 1995;10(8):1272–81.
260. Sanford LP, Ormsby I, Gittenberger-de Groot AC, et al. TGFbeta2 knockout mice have multiple developmental defects that are non-overlapping with other TGFbeta knockout phenotypes. Development 1997;124(13):2659–70.
261. Erlebacher A, Filvaroff EH, Ye JQ, Derynck R. Osteoblastic responses to TGF-beta during bone remodeling. Mol Biol Cell 1998;9(7):1903–18.
262. Kassem M, Kveiborg M, Eriksen EF. Production and action of transforming growth factor-beta in human osteoblast cultures: dependence on cell differentiation and modulation by calcitriol. Eur J Clin Investig 2000;30(5):429–37.
263. Sakou T, Onishi T, Yamamoto T, Nagamine T, Sampath T, Ten Dijke P. Localization of Smads, the TGF-beta family intracellular signaling components during endochondral ossification. J Bone Miner Res 1999;14(7):1145–52.
264. Nesti LJ, Caterson EJ, Wang M, et al. TGF-beta1 calcium signaling increases alpha5 integrin expression in osteoblasts. J Orthop Res 2002;20(5):1042–9.
265. Seitzer U, Batge B, Acil Y, Muller PK. Transforming growth factor beta 1 influences lysyl hydroxylation of collagen I and reduces steady-state levels of lysyl hydroxylase mRNA in human osteoblast-like cells. Eur J Clin Investig 1995;25(12): 959–66.
266. Urano T, Yashiroda H, Muraoka M, et al. p57(Kip2) is degraded through the proteasome in osteoblasts stimulated to proliferation by transforming growth factor beta1. J Biol Chem 1999;274(18): 12197–200.
267. Nishimori S, Tanaka Y, Chiba T, et al. Smad-mediated transcription is required for transforming growth factor-beta 1-induced p57(Kip2) proteolysis in osteoblastic cells. J Biol Chem 2001;276(14):10700–5.
268. Atti E, Gomez S, Wahl SM, Mendelsohn R, Paschalis E, Boskey AL. Effects of transforming growth factor-beta deficiency on bone development: a Fourier transform-infrared imaging analysis. Bone 2002;31(6):675–84.
269. Geiser AG, Zeng QQ, Sato M, Helvering LM, Hirano T, Turner CH. Decreased bone mass and bone elasticity in mice lacking the transforming growth factor-beta1 gene. Bone 1998;23(2): 87–93.
270. Urist MR, Mc LF. Osteogenetic potency and new-bone formation by induction in transplants to the anterior chamber of the eye. J Bone Joint Surg 1952;34-A(2):443–76.
271. Urist MR, Wallace TH, Adams T. The function of fibrocartilaginous fracture callus. Observations on transplants labelled with tritiated thymidine. J Bone Joint Surg Br 1965;47:304–18.
272. Urist MR, DeLange RJ, Finerman GA. Bone cell differentiation and growth factors. Science (New York, NY) 1983;220(4598): 680–6.
273. Urist MR, Sato K, Brownell AG, et al. Human bone morphogenetic protein (hBMP). Proc Soc Exp Biol Med Soc Exp Biol Med (New York, NY) 1983;173(2):194–9.
274. Wozney JM, Rosen V, Celeste AJ, et al. Novel regulators of bone formation: molecular clones and activities. Science 1988;242(4885):1528–34.
275. Kessler E, Takahara K, Biniaminov L, Brusel M, Greenspan DS. Bone morphogenetic protein-1: the type I procollagen C-proteinase. Science (New York, NY) 1996;271(5247):360–2.
276. Reddi AH. BMP-1: resurrection as procollagen C-proteinase. Science (New York, NY) 1996;271(5248):463.
277. Alman BA, Greel DA, Wolfe HJ. Activating mutations of Gs protein in monostotic fibrous lesions of bone. J Orthop Res 1996;14(2):311–5.

278. Cook SD, Salkeld SL, Rueger DC. Evaluation of recombinant human osteogenic protein-1 (rhOP-1) placed with dental implants in fresh extraction sites. J Oral Implantol 1995;21(4):281–9.
279. Cook SD, Wolfe MW, Salkeld SL, Rueger DC. Effect of recombinant human osteogenic protein-1 on healing of segmental defects in non-human primates. J Bone Joint Surg 1995;77(5):734–50.
280. Shimizu K, Yoshikawa H, Takaoka K. Local effects of bone morphogenetic protein-4 on skeletal tissues. Clin Orthop Relat Res 1995(318):243–50.
281. Bentz H, Thompson AY, Armstrong R, Chang RJ, Piez KA, Rosen DM. Transforming growth factor-beta 2 enhances the osteoinductive activity of a bovine bone-derived fraction containing bone morphogenetic protein-2 and 3. Matrix (Stuttgart, Germany) 1991;11(4):269–75.
282. Urist MR. Bone: formation by autoinduction. Science 1965;150(698):893–9.
283. Luyten FP, Cunningham NS, Ma S, et al. Purification and partial amino acid sequence of osteogenin, a protein initiating bone differentiation. J Biol Chem 1989;264(23):13377–80.
284. Wozney JM. The bone morphogenetic protein family and osteogenesis. Mol Reprod Dev 1992;32(2):160–7.
285. Zhao M, Harris SE, Horn D, et al. Bone morphogenetic protein receptor signaling is necessary for normal murine postnatal bone formation. J Cell Biol 2002;157(6):1049–60.
286. Yamamoto N, Akiyama S, Katagiri T, Namiki M, Kurokawa T, Suda T. Smad1 and smad5 act downstream of intracellular signalings of BMP-2 that inhibits myogenic differentiation and induces osteoblast differentiation in C2C12 myoblasts. Biochem Biophys Res Commun 1997;238(2):574–80.
287. Chen D, Zhao M, Mundy GR. Bone morphogenetic proteins. Growth Factors 2004;22(4):233–41.
288. Bae SC, Lee KS, Zhang YW, Ito Y. Intimate relationship between TGF-beta/BMP signaling and runt domain transcription factor, PEBP2/CBF. J Bone Joint Surg Am 2001;83-A Suppl 1(Pt 1): S48–S55.
289. Lee KS, Hong SH, Bae SC. Both the Smad and p38 MAPK pathways play a crucial role in Runx2 expression following induction by transforming growth factor-beta and bone morphogenetic protein. Oncogene 2002;21(47):7156–63.
290. Mbalaviele G, Sheikh S, Stains JP, et al. Beta-catenin and BMP-2 synergize to promote osteoblast differentiation and new bone formation. J Cell Biochem 2005;94(2):403–18.
291. Bain G, Muller T, Wang X, Papkoff J. Activated beta-catenin induces osteoblast differentiation of C3H10T1/2 cells and participates in BMP2 mediated signal transduction. Biochem Biophys Res Commun 2003;301(1):84–91.
292. Cowin SC, Moss-Salentijn L, Moss ML. Candidates for the mechanosensory system in bone. J Biomech Eng 1991;113(2):191–7.
293. Cowin SC, Sadegh AM. Non-interacting modes for stress, strain and energy in anisotropic hard tissue. J Biomech 1991;24(9): 859–67.
294. Cowin SC, Sadegh AM, Luo GM. Correction formulae for the misalignment of axes in the measurement of the orthotropic elastic constants. J Biomech 1991;24(7):637–41.
295. Brighton CT, Sennett BJ, Farmer JC, et al. The inositol phosphate pathway as a mediator in the proliferative response of rat calvarial bone cells to cyclical biaxial mechanical strain. J Orthop Res 1992;10(3):385–93.
296. Brighton CT, Strafford B, Gross SB, Leatherwood DF, Williams JL, Pollack SR. The proliferative and synthetic response of isolated calvarial bone cells of rats to cyclic biaxial mechanical strain. J Bone Joint Surg 1991;73(3):320–31.
297. Banes AJ, Tsuzaki M, Yamamoto J, et al. Mechanoreception at the cellular level: the detection, interpretation, and diversity of responses to mechanical signals. Biochem Cell Biol = Biochim Biol Cell 1995;73(7–8):349–65.
298. Pitsillides AA, Rawlinson SC, Suswillo RF, Bourrin S, Zaman G, Lanyon LE. Mechanical strain-induced NO production by bone cells: a possible role in adaptive bone (re)modeling? FASEB J 1995;9(15):1614–22.
299. Terai K, Takano-Yamamoto T, Ohba Y, et al. Role of osteopontin in bone remodeling caused by mechanical stress. J Bone Miner Res 1999;14(6):839–49.
300. Frost HM. Perspectives: a proposed general model of the "mechanostat" (suggestions from a new skeletal-biologic paradigm). Anat Rec 1996;244(2):139–47.
301. D'Souza RN, Aberg T, Gaikwad J, et al. Cbfa1 is required for epithelial-mesenchymal interactions regulating tooth development in mice. Development (Cambridge, England) 1999;126(13):2911–20.
302. Ducy P, Starbuck M, Priemel M, et al. A Cbfa1-dependent genetic pathway controls bone formation beyond embryonic development. Genes Dev 1999;13(8):1025–36.
303. Liaw L, Birk DE, Ballas CB, Whitsitt JS, Davidson JM, Hogan BL. Altered wound healing in mice lacking a functional osteopontin gene (spp1). J Clin Investig 1998;101(7):1468–78.
304. Yoshitake H, Rittling SR, Denhardt DT, Noda M. Osteopontin-deficient mice are resistant to ovariectomy-induced bone resorption. Proc Natl Acad Sci USA 1999;96(14):8156–60.
305. Speer MY, McKee MD, Guldberg RE, et al. Inactivation of the osteopontin gene enhances vascular calcification of matrix Gla protein-deficient mice: evidence for osteopontin as an inducible inhibitor of vascular calcification in vivo. J Exp Med 2002;196(8):1047–55.
306. Ducy P, Desbois C, Boyce B, et al. Increased bone formation in osteocalcin-deficient mice. Nature 1996;382(6590):448–52.
307. Gilmour DT, Lyon GJ, Carlton MB, et al. Mice deficient for the secreted glycoprotein SPARC/osteonectin/BM40 develop normally but show severe age-onset cataract formation and disruption of the lens. EMBO J 1998;17(7):1860–70.
308. Bradshaw AD, Graves DC, Motamed K, Sage EH. SPARC-null mice exhibit increased adiposity without significant differences in overall body weight. Proc Natl Acad Sci USA 2003;100(10): 6045–50.
309. Lawler J, Sunday M, Thibert V, et al. Thrombospondin-1 is required for normal murine pulmonary homeostasis and its absence causes pneumonia. J Clin Investig 1998;101(5):982–92.
310. Kyriakides TR, Zhu YH, Smith LT, et al. Mice that lack thrombospondin 2 display connective tissue abnormalities that are associated with disordered collagen fibrillogenesis, an increased vascular density, and a bleeding diathesis. J Cell Biol 1998;140(2):419–30.
311. Hankenson KD, Hormuzdi SG, Meganck JA, Bornstein P. Mice with a disruption of the thrombospondin 3 gene differ in geometric and biomechanical properties of bone and have accelerated development of the femoral head. Mol Cell Biol 2005;25(13):5599–606.
312. Miao D, He B, Karaplis AC, Goltzman D. Parathyroid hormone is essential for normal fetal bone formation. J Clin Investig 2002;109(9):1173–82.
313. Weir EC, Philbrick WM, Amling M, Neff LA, Baron R, Broadus AE. Targeted overexpression of parathyroid hormone-related peptide in chondrocytes causes chondrodysplasia and delayed endochondral bone formation. Proc Natl Acad Sci USA 1996;93(19):10240–5.
314. Akiyama H, Chaboissier MC, Martin JF, Schedl A, de Crombrugghe B. The transcription factor Sox9 has essential roles in successive steps of the chondrocyte differentiation pathway

and is required for expression of Sox5 and Sox6. Genes Dev 2002;16(21):2813–28.
315. Yoshizawa T, Handa Y, Uematsu Y, et al. Mice lacking the vitamin D receptor exhibit impaired bone formation, uterine hypoplasia and growth retardation after weaning. Nat Genet 1997;16(4):391–6.
316. Akune T, Ohba S, Kamekura S, et al. PPARgamma insufficiency enhances osteogenesis through osteoblast formation from bone marrow progenitors. J Clin Investig 2004;113(6):846–55.
317. Soriano P, Montgomery C, Geske R, Bradley A. Targeted disruption of the c-src proto-oncogene leads to osteopetrosis in mice. Cell 1991;64(4):693–702.
318. Niu Z, Yu W, Zhang SX, et al. Conditional mutagenesis of the murine serum response factor gene blocks cardiogenesis and the

Chapter 2
Structure and Function of Joints

Mary F. Barbe, Jeff Driban, Ann E. Barr, Steven N. Popoff, and Fayez F. Safadi

Abstract This chapter covers many aspects of joint anatomy, histology, and cell biology. First, joint types and movements allowed are covered, followed by a brief review of joint embryology. Next, a review of joint anatomy and histology is given covering innervations, synovial membrane histology, as well as synoviocytes and synovial fluid characteristics. Various aspects of articular cartilage histology and cell biology are discussed in this chapter as well as aspects adaptive remodeling of cartilage after joint loading. A discussion of joint pathology completes the chapter.

Keywords Joint anatomy • Joint histology • Joint pathology • Rheumatoid arthritis • Osteoarthritis • Cytokines • Growth factors

Introduction

Segmentation of the skeleton allows for movement and segmental growth. A joint is the articulation or union between two or more bones or parts of bones. Joints are most commonly classified according to the material by which the articulating bones are united. Thus, there are synarthroses (that include syndesmoses that have intervening fibrous tissue, synchondroses, that have intervening cartilage synostoses, that have intervening bone and symphyses that have intervening fibrocartilage) and synovial joints (also called diarthrodial joints) (Table 1). Syndesmoses, eventually convert to synostosis after the fibrous tissues joining the bones ossify. The *diarthroses* are designed for movement and include all synovial joints. As is the case with all aspects of the musculoskeletal system, the structure of a joint, in this case concerning the manner in which the joints are held together, determines its function. As described further below, some of these joint types allow no movement; others allow only slight movement, while others are free movable.

Joint Classification

(1) *Syndesmoses* (fibrous joints) are defined as joints in which the adjoining bones are bound together by a thin sheet of fibrous tissue, either a ligament or a fibrous membrane. Since the fibrous tissue is flexible, these joints allow partial movement. The amount of movement allowed depends on the length of the fibers uniting the bones. Examples of syndesmoses are the suture joints of the skull and the union of the radius and ulna in the forearm by the interosseous membrane. A gomphosis or dentoalveolar syndesmosis (the bonds between the roots of teeth and the jaw bones) is also included in this category. (2) *Synchrondroses* are joints joined together by cartilage and permit slight bending in early life. A key example of this type of cartilaginous joint is the joining of the epiphysis of a long bone with the metaphysis by a cartilaginous epiphyseal plate, a region also known as the growth plate (Fig. 1a and 1b). This is a temporary synchondrosis since the epiphyseal plate eventually ossifies in the mature adult. (3) *Symphyses* are joints joined by fibrocartilage and in which the two opposing surfaces are covered by hyaline articular cartilage. Symphyses are also considered cartilaginous joints. The strength of the fibrocartilage allows for only a little movement but much stability, while the hyaline cartilage on the articulating surfaces allows for shock absorption. The pubic symphyses and intervertebral joints are examples of symphyses. The intervertebral disc is the binding fibrocartilage joining two vertebrae. (4) *Synostoses* are temporary joints that eventually close by bony union. With aging, many syndesmoses and all synchondroses ossify. Once ossified, these joints allow no movement. (5) *Synovial joints* are the most common types of joints and are defined as two or more bones whose ends are covered by hyaline cartilage, united by a fibrous tissue capsule that encloses the joint, and separated by a joint cavity (Fig. 1c). The cavity is filled with synovial fluid produced by a synovial membrane lining the interior of the fibrous capsule. The synovial fluid is a lubricant providing a smooth, nearly frictionless, gliding motion of the opposing joint surfaces.

J.S. Khurana (ed.), *Bone Pathology*, DOI 10.1007/978-1-59745-347-9_2,

Table 1 Classification of joints by type of union.

Syndesmosis – fibrous material joins the bones; fibrous joint
Synchondrosis – cartilage joins the bones; cartilaginous joint
Synostosis – fibers/cartilage ossify, totally closing joint; bony union
Symphysis – fibrocartilage joins the bones; cartilaginous joint
Synovial – a loose fibrous capsule joins the bones separated by a joint cavity

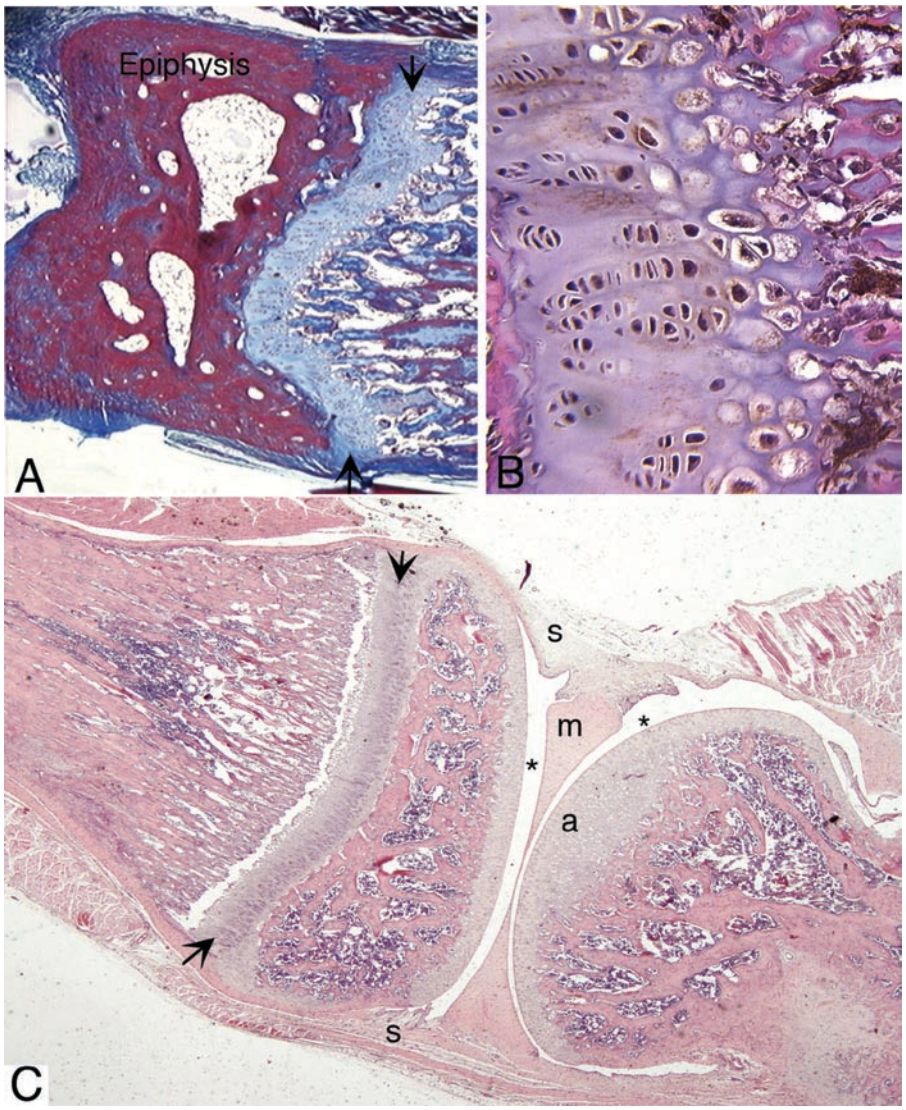

Fig. 1 Photomicrographs showing examples of joints classified by type of union. **A** A synchondrosis in a rat radial bone. The epiphyseal plate (indicated by black arrows) located below the epiphysis of a long bone of a young mammal is an example of a cartilaginous type of bony union. This type of union eventually ossifies. Masson trichrome stain. **B** Higher power of the syndesmosis showing rows of chondrocytes stained positive for the cytokine, interleukin 6. **C** A synovial joint, the knee joint, in a rat. Synovial joints are defined as two or more bones whose ends are covered by hyaline articular cartilage (a), and possessing a joint cavity (*) lined with a synovial membrane (s). The knee joint also contains medial and lateral menisci (m) for additional cushioning and congruence between the bones. The arrows indicate the epiphyseal plate in the femur of this young rat. Figure (**C**) is stained with hematoxylin and eosin (H&E)

This type of joint allows more movement at the cost of reduced stability. As a consequence, synovial joints are usually reinforced by extrinsic ligaments or strategic thickenings of the joint capsule (intrinsic ligaments). Some synovial joints also have other distinguishing features such as menisci (Fig. 1c), labrums, or fibrocartilage articular discs that allow for shock absorption and/or additional stability. Nearly all of the joints of the limbs are synovial.

Movements Allowed by Different Types of Joints

Osteokinematics describes the relative movement between two bones on either side of a joint. Although all bony segments on either side of a joint are theoretically capable of three rotations about three axes of motion and three translations in three planes of motion, otherwise known as the six degrees of freedom of movement in three-dimensional space, soft tissue constraints along with bony shape frequently constrain osteokinematics to fewer axes and planes of motion. Arthrokinematics describes the movements occurring between the joint surfaces, such as rolling, spinning, and gliding of joint surfaces. *Plane joints* are characterized by opposing bony surfaces that are flat, or nearly so (Fig. 2a). The arthrokinematics of a plane joint include gliding and spinning, or a combination thereof. Gliding refers to a translation of one surface with respect to another, whereas spinning refers to a clockwise or counterclockwise rotation of one surface with respect to another. Depending on the precise curvature of the surfaces of a plane joint, their orientation and their constraints by soft tissue structures, the osteokinematics of plane joint movement ranges from uniaxial to triaxial. Examples of plane joints include the acromioclavicular joint, which is triaxial, and the vertebral zygopophyseal (facet) joints, which are uniaxial. The osteokinematics of *hinge joints* are constrained to movement in one plane, usually sagittal, about one axis of rotation, usually mediolateral. The elbow joint is one example of a hinge joint. *Saddle (sellar) joints* are characterized by opposing surfaces that are concave and convex, but along opposite planes so that they are contoured to fit together (Fig. 3). The osteokinematics of saddle joints are inconsistently described as either biaxial (motion about two primary axes in two planes) or triaxial. This inconsistency can be explained by the fact that the majority of motion typically occurs in two planes (usually flexion–extension and abduction–adduction), while there is a small amount of internal–external rotation. The carpometacarpal joint of the thumb is an example of a saddle joint in which flexion–adduction–internal rotation combine to produce the action of opposition. *Condyloid joints* are composed of a nearly spherical convex surface opposing a shallow, nearly flat concave surface. The osteokinematics of these joints are considered biaxial owing to the predominance of movement about two axes and in two planes. The arthrokinematics during movement of condyloid joints are described by the "concave–convex rule," which specifies that to maintain congruence of joint surfaces during bone movement, the convex condyloid component must roll in the direction of bony movement and glide in the opposite direction with respect to the concave component (Fig. 4). Examples of condyloid joints include the metacarpophalangeal joints of the fingers, in which the condyloid distal portion of the metacarpal joint forms the knuckle of the finger ray; the knee joint, in which the distal femoral condyles articulate with the shallow, concave tibial plateaus; and the atlanto-occipital joint between the occipital condyles and the atlas (C1). *Ball and socket joints* are distinguished by one bone with an ovoid or spherical convex surface that moves within a relatively deep concave surface (Fig. 2b). Ball and socket joints allow movement about all three axes and in all three planes of motion, flexion–extension, abduction–adduction, and internal–external rotation. The coxofemoral (hip) and glenohumeral (shoulder) joints are examples of ball and socket joints. *Pivot joints* are characterized by one

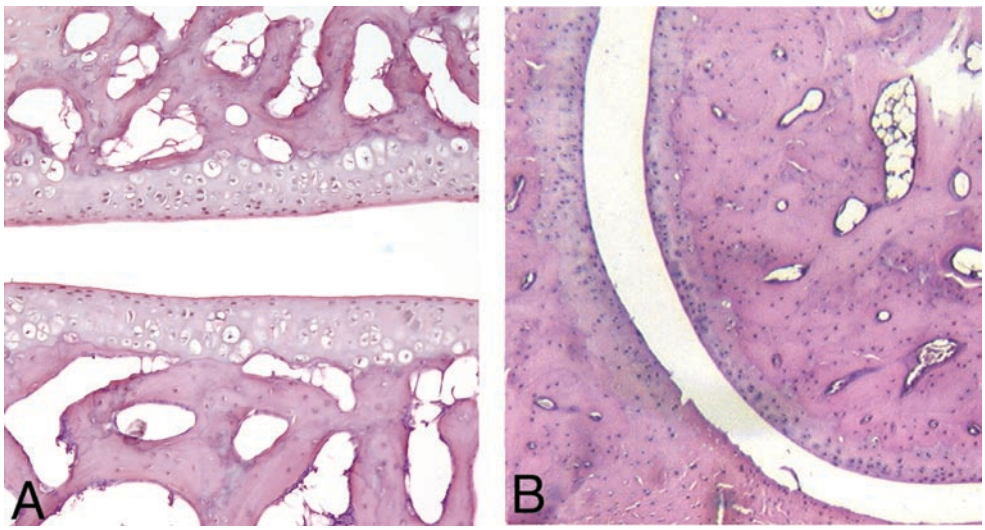

Fig. 2 Photomicrographs showing **A** a plane joint and **B** a ball-and-socket joint. H&E staining

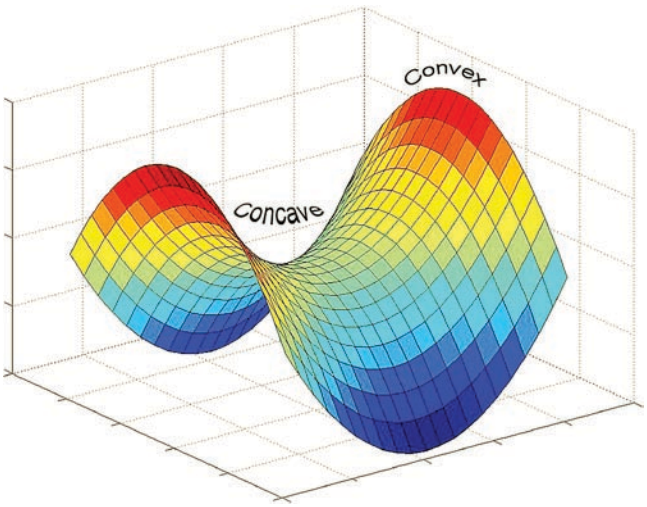

Fig. 3 Mesh grid representation of a saddle-shaped (sellar) joint showing that the joint surface is concave along one axis and convex along the axis perpendicular to the first. In a saddle joint, the opposing joint surface would have concavity and convexity rotated 90° so that the two surfaces would be maximally congruent. While the majority of motion occurs along the axis defined by the concavity and convexity, depending on the leverage of muscles acting on the joint, a small amount of rotation (spinning) is also permitted, as with the carpometacarpal joint of the thumb during opposition

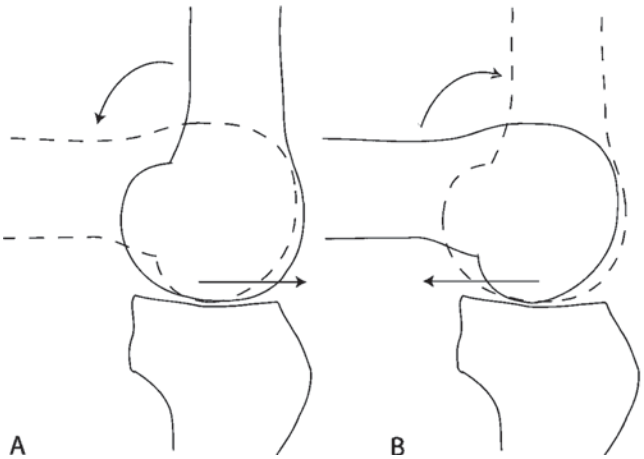

Fig. 4 The arthrokinematics of the condyloid knee joint during the motions of flexion and extension and an example of the concave–convex rule. **A** During flexion of the femur on a fixed tibia, the convex femoral condyles roll posteriorly and glide anteriorly. **B** During extension of the femur on a fixed tibia, the convex femoral condyles roll anteriorly and glide posteriorly. These complimentary arthrokinematics maintain joint congruence. Modified from Oatis (1, Figure 7.4, p. 101). Cartoon Compliments of Susan Fecho

bone with a rounded process that moves within a sleeve or ring formed by the opposing bone. They permit rotation about a single axis, and are therefore uniaxial joints. Examples include the proximal radioulnar and atlantoaxial joints.

Joint Embryology and Ossification

Embryology of Synovial Joints

The development of joint tissue begins shortly after the emergence of the primitive limb buds (days 26–28 of gestation). The limb bud initially contains a central continuous condensation of mesenchymal cells, which will develop into a cartilage model of the bones and their joints (see Chap. 1). Constrictions appear in the limbs, dividing them into recognizable segments by week 6 of embryological development. While the external shape of the limb is being defined, a hyaline cartilage model is formed during the same week (week 6). An articular disc of mesenchyme, the primitive joint plate, appears within the condensing mesenchymal cells at the site of future synovial joints. These cells of the primitive joint plate organize into a trilayer structure composed of two chondrogenic regions and a central layer of mesenchymal material. The outer chondrogenic region surrounds the primitive joint plate and is the forerunner of the joint capsule. By the seventh or eighth week of embryonic life, the central layer undergoes cavitation along planes destined to become the articular surfaces of the joints. Spaces filled with tissue fluid appear in the primitive joint plate. These spaces gradually coalesce to form a single joint cavity. The outer chondrogenic region of the joint capsule condenses and differentiates into fibrous tissue, while the inner chondrogenic region differentiates into the synovial membrane. Hartmann and Tabin (2) have shown that Wnt-14 is expressed in primitive joint plate regions prior to segmentation of the cartilage model, and plays a central role in initiating synovial joint formation in the chick limb. It is known that intrauterine movements of the limbs begin in the third month of fetal life and are essential for normal embryonic development of synovial joints.

Embryology of Intervertebral Discs

The vertebra and intervertebral discs are axial skeletal elements that arise from the sclerotome portion of segmental somites arranged on each side of the notochord. During week 4 of embryonic life, cells of the sclerotome shift in position to surround the spinal cord and notochord. The caudal portion of each sclerotomal segment proliferates extensively, condenses, and then moves into the subjacent intersegmental tissue. This proliferation is so strong that the caudal half of one sclerotome segment binds to the cephalic half of the subjacent sclerotome. Some of the densely packed sclerotomal cells move cranially and form the intervertebral disc, while the remainder forms the centrum of the vertebral body.

In this manner, vertebral bodies become intersegmental and come to lie beside intersegmental arteries located on each side of the vertebral bodies. The notochord later degenerates and forms the gelatinous nucleus pulposus of the intervertebral disc, which is later surrounded by the harder, circular fibers of the annulus fibrosis. Chondrification of the vertebral body begins in embryonic week 6. Extensions form dorsally and laterally from the chondrification centers in the vertebral arch and begin the formation of the neural arch and costal processes. Chondrification spreads until a cartilage model of the vertebrae is formed. The conversion of the cartilage model into bone (*ossification*) begins in embryonic week 9 and continues until year 25 of life.

Joint Ossification

Ossification of the limb bones via the mechanisms of endochondral ossification begins by the end of the embryonic period of development (week 12). Primary ossification centers are present in the diaphysis of long bones by the 12th week of embryonic life, while the epiphyses remain cartilaginous until birth. After birth, ossification centers (secondary ossification centers) appear on each end of long bones, a region known as the epiphyses. At that point of joint development, the synchondrosis type joint (described earlier) appears, joining the epiphyseal ossifying ends with the rest of the ossified long bone. The cartilage plate of this joint, the epiphyseal plate, allows for growth of the long bone on both sides of that plate. When the bone has reached full length, these epiphyseal plates ossify as well, merging the ossified end of the long bones with their ossified shafts (diaphysis).

Dynamic axial loading can suppress longitudinal bone growth by acting directly on the growth plate (3). High axial compressive loads (17N) on the ulna for 10 min/day for 8 days, followed by a 7-day waiting period prior to tissue collection and examination, results in complete suppression of longitudinal mineralization rate at the distal growth plate. Longitudinal growth recovers within 1 week after lower compressive loads (4N and 8.5N). Several morphological changes are observed in the growth plate after 17N loading including trauma-induced cracks in the growth plate, increased vascular endothelial growth factor (VEGF; a coordinator of chondrogenesis and angiogenesis), suppression of cartilage mineralization, and capillary invasion beneath the growth plate. The authors of this study postulate that there is a correlation between loading force magnitude and the period for recovery of growth suppression, and that if they had allowed the rats to recover for a longer period (e.g., 1 month) that endochondral ossification growth rates might have returned (3).

Synovial Joint Anatomy and Histology

The basic overall structure of a synovial joint consists of a fibrous capsule joining and surrounding the adjoining bony surfaces. The capsule is often reinforced by localized thickenings of collagen fibers (intrinsic ligaments) as well as additional ligaments outside the capsule (extrinsic ligaments). The joint capsule is lined by a synovial membrane, which is divided into inner and outer parts (see below for more details). The two bones are separated by a joint cavity filled with synovial fluid, and the articulating bony ends are covered by articular cartilage (see below for more details).

Joint Capsule Anatomy, Vasculature, and Innervation

The joint capsule is composed of two layers of connective tissue. The outer layer is the fibrous membrane and consists of collagenous fibers. This layer surrounds the entire joint and attaches firmly to the periosteum of the adjoining bones. Although it is poorly vascularized, the joint capsule is highly innervated by a variety of somatic sensory fibers mediating sensations of pain, proprioception, pressure, and vibration. Most joint blood vessels, normally from periarticular anastomotic plexes, penetrate the capsule to pass to the synovial membrane and the epiphyses.

The inner layer of the joint capsule is the synovial membrane (Fig. 1). It is highly vascularized, but poorly innervated. The articular cartilage also lacks innervation. Thus, the synovial membrane and the articular cartilage are insensitive to pain. However, joint ligaments and the periosteum associated with the adjoining bones are highly innervated, as are adjacent attaching tendons and the outer layer of the joint capsule. Any swelling within a joint from disease or trauma stimulates nociceptors (pain endings) in joint structures, giving rise to the sensation of pain in or near a joint.

Joint pain, such as that associated with osteoarthritis, is the result of underlying acute or chronic joint inflammation or injury. Increased response to painful stimuli at the site of injury or inflammation is termed *hyperalgesia*. Animal models have been developed to study joint hyperalgesia and the control of this type of pain. In one such well-characterized model, kaolin and carrageenan is injected into the knee joint to produce an initial inflammatory response that coverts in about 1 week to chronic inflammation (4). The inflammation is associated with decreased latency to paw withdrawal in response to heat (hyperalgesia), increased withdrawal after compression of the inflamed knee, and increased response to mechanical stimuli of the paw (mechanical allodynia). The hyperalgesia and mechanical allodynia are a result of

increased sensitization of joint nociceptors, increased nociceptor spontaneous activity, and increased response of previously silent neurons (5). The kaolin and carrageenan model of joint inflammation has been used to assess the effectiveness of various treatments of arthritic pain. For example, high and low frequency transcutaneous electrical nerve stimulation (TENS) has been used successfully to reverse the hyperalgesia induced by carrageenan injections (6).

In addition to nociceptors, there are other types of nerves innervating joint structures. The joint capsule contains Ruffini-type endings and paciniform corpuscles (small, elongated pacinian corpuscles). These receptors respond to the bending of joints (proprioception), as do some of the free nerve endings in the joint capsule. These two types of joint capsule receptors play a protective function against the extremes of hyperextension and hyperflexion (7–9). However, the receptors just named are not the only nerves involved in joint proprioception. Apparently, pressure receptors and free nerve endings localized in skin surrounding the joint also serve this same function, since patients with anesthetized or removed joint capsules experience no loss of joint position sense (7–9). The Ruffini endings (also referred to as Ruffini corpuscles, flower spray organs, and SAII axons) also function as slow adapting mechanoreceptors that fire with changes in joint angle and motion (10). Finally, Golgi tendon organs can be found in the fibrous ends of tendons that attach on or immediately adjacent to a joint capsule. These afferents detect both muscle and capsule tension. They terminate in and among collagen fibers, so that when the collagen fibers are stretched by muscle contractions or joint capsule movements, the terminals of the Golgi tendon organs are compressed and discharge (9). In summary, joint structures are innervated by a variety of sensory nerve endings that detect motion, compression, tension, proprioception, and pain.

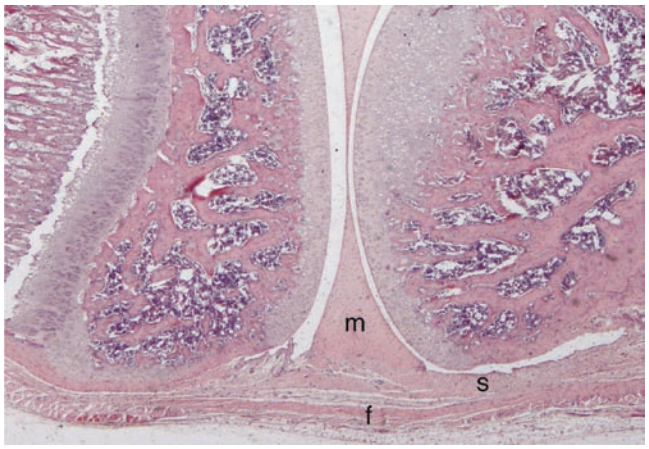

Fig. 5 Photomicrograph showing the inner synovial membrane (s) and the outer fibrous capsule (f) surrounding a synovial joint. Note the articular cartilage (a) on the articulating bone surfaces. H&E staining

Synovial Membranes

Synovial membranes and the fluid that they produce are components of synovial joints only. These membranes have the ability to absorb as well as secrete. They consist of cuboidal cells or *synoviocytes* that are arranged one to four cell layers deep along the inner surface of the fibrous capsule surrounding the joint (Fig. 5). The synovial membrane lines the entire joint cavity except for on the articular cartilage surface. The outer fibrous capsule is composed of irregularly arranged connective tissue. There are three key types of variations of synovial membranes: fibrous, areolar, and adipose. The fibrous type, which is located over tendons, consists of a thin cellular layer resting on connective tissue fibers that merge with the outer fibrous capsule. The areolar type allows movement of the membrane over the fibrous capsule, while the adipose type is found over intraarticular fat pads, such as those found in the knee joint. The inner layer of the areolar type of synovial membrane is thicker than the other two types and consists of fibroblasts and synovial cells. The outer layer of this type of synovial membrane consists of fibroblasts, mast cells, macrophages, as well as collagen and elastic fibers. The synovial cells and macrophages of synovial membranes are key producers of inflammatory cytokines associated with arthritic degenerative joint diseases to be discussed in another chapter.

During joint movement, synovial tissues and cells contribute to bearing mechanical loads (11). The synovial membrane is the initial target of rheumatoid arthritis, and becomes a primary source of matrix metalloproteinases (MMPs) and cytokines in the synovium and synovial fluid (11, 12). Affected chondrocytes also contribute MMPs to synovial fluid.

Synoviocytes

Traditionally, the synoviocytes are separated into type A cells (macrophage-like), which are phagocytic and synthesize hyaluronic acid, and type B cells (fibroblast-like) which produce various proteins. It is possible that these cells belong to one cell population, but have altered phenotypes. Synoviocytes secrete collagen and proteoglycan and have a highly characteristic phenotype that includes the strong expression of vascular cell adhesion molecule-1 (VCAM-1). Synoviocytes are also immunoreactive for vimentin, an interfilament molecule, but not for epithelial markers.

Synovial cells are flexible in order to line fibrous capsules and cover exposed osseous surfaces and intracapsular ligaments during joint movements (11). In rheumatoid arthritis, a chronic autoimmune disease, the fibroblast-like synoviocytes

proliferate aggressively and invade adjacent cartilage and bone (*pannus*) (12, 13). The hyperplastic synovial cell activity eventually destroys both the cartilage and the underlying bone (14).

Synovial Fluid

Synovial fluid from a normal joint is clear or pale-yellow in color, viscous, and consists of hyaluronic acid and lubricin, a glycoprotein that reduces friction (15). The hyaluronic acid provides viscosity, reduces friction between joint surfaces, and provides nutrients to chondrocytes in the articular cartilage. The hyaluronic acid is also known as hyaluronate and is a large, highly polymerized mucopolysaccharide (glycosaminoglycan). The synovial fluid is a plasma dialysate with many electrolytes present at levels comparable to that of blood. However, it lacks most proteins, particularly those with high molecular weights, under normal conditions. Also, synovial fluid is acellular under normal conditions. However, under arthritic and other inflammatory conditions, synovial fluid contains infiltrating immune cells (monocytes/macrophages and T cells) and inflammatory mediators such as cytokines.

It has long been known that the long-term integrity of a joint and its articular cartilage is dependent upon synovial fluid nourishment and protection from friction-induced wear. Lubricin, a key component of synovial fluid, as mentioned above, is a secreted glycoprotein encoded by the gene PRG4 (16). An autosomal recessive disorder in humans called camptodactyly-arthropathy-coxa vara-pericarditis syndrome (CACP), associated with a loss of lubrican function leading to precocious joint failure (16), has been studied for the expression of PRG4 mRNA during mouse joint development, and created a lubricin-mutant mice strain. It was found that as the mice aged, abnormal protein deposits appeared on the articular cartilage surface and the chondrocytes of the underlying superficial zone disappeared. Also, synovial cells became hyperplastic, further contributing to joint destruction. Addition of purified or recombinant lubricin inhibited the synoviocytes proliferation in vitro, suggesting that lubrican functions to protect articulating surfaces and control of synovial cell growth (16).

Effects of Mechanical Stress of Synovial Cavities and Membranes

Under both normal and pathological conditions, the synovial cavity is exposed to a high degree of mechanical stress (13). Mechanical stress from the load of body weight is present, as are shearing forces during movement. The motion of synovial fluid during exercise is one of the primary sources of shear forces on the synovial cavity (17, 18). Shear forces by fluids have been shown to activate the mitogen-activated protein kinase (MAPK) pathways, which then results in c-jun and c-fos transcription factor activation leading to cell growth and proliferation (19, 20). Such changes allow the tissues to adapt to many stressful conditions. Besides MAPKs, mechanical shear forces can influence other signaling pathways, such as those inducing the production of heat shock proteins (hsps) 60 and 70. Hsps when induced protect the stressed and/or injured cells against apoptotic death (21, 22). Given that the rate of cell death from apoptosis is low in synovial membrane, cells are obviously able to adapt to a variety of mechanical stresses successfully, unless additional joint pathologies are present such as rheumatoid arthritis or osteoarthritis.

> A study of normal tidemark histology is pertinent to pathologists since early osteoarthritic changes occur in the deep layer of cartilage near the tidemark. The tidemark is an important clue to the surgical pathologist, as a marker of articular cartilage. This is because cartilage injury at the histological level of the tidemark (stained with hematoxylin and eosin) precedes any visible denudation of articular cartilage. Surgical specimens are often fragmented, and architectural clues are lost – the presence of a tidemark may help establish the origin of submitted fragments from the articular region, implying that accidental breach may have occurred.

Articular Cartilage

Articular cartilage covers the end of long bones and is usually hyaline cartilage in composition. It varies in thickness from 2 to 4 mm and is thickest at the periphery of concave surfaces and in the central portions of convex surfaces. This type of cartilage is usually the remains of the original hyaline cartilage model from which the bones and joints derived. No perichondrium covers the bone at this point. Instead, the bony ends within a joint are covered with a sparse number of cartilage cells embedded in a hyaline cartilage matrix. The cartilage cells are arranged in rows parallel to the surface in distinct zones. There is a superficial tangential zone (STZ) of elongated chondrocytes with their long axes arranged tangentially to the articular surface. The STZ contributes to the maintenance of joint lubrication through fluid film and boundary

lubrication mechanisms (23). Chondrocytes in the STZ have higher elastic moduli (i.e., are stiffer) and have higher apparent viscosities compared to those in deeper zones (24, 25). In addition, the STZ contributes to both lateral and deep load transmission under compressive loading conditions (26). The STZ is adjacent to a transitional or intermediate zone where the chondrocytes are oriented more randomly in small groups. Subjacent to this, and comprising the majority of the cartilage, there is a deep radial zone where chondrocytes are oriented perpendicular to the surface. This deep radial zone undergoes substantial loss in height and increase in stiffness under compressive loads (26). A thin zone of calcified cartilage lies between the deep radial zone and the subchondral bone. The deepest layer of articular cartilage, a thin zone, is firmly apposed to bone and is calcified. This calcified zone contains a sinuous hematoxyphilic line called the "tidemark," which separates the uncalcified articular cartilage from the underlying subchondral bone (Fig. 6).

The articular cartilage matrix is highly hydrophilic, but fluid moves freely between the matrix of the cartilage and the intracapsular joint space under conditions of intermittent loading. The thickness of cartilage varies from one joint to another, from one area of a joint to another, and across the course of a day (due to cumulative pressure on the cartilage throughout the day). Articular cartilage is also thinner in aged joints, partially due to the reduced ability of aged cartilage to hold water. The volume of articular cartilage in patients can be quantified using a volummetric, fat-suppressed spoiled gradient-recalled signal acquisition in the steady-state (SPGR) magnetic resonance (MR) sequence (for further information, see Dupuy et al. (27)).

Articular cartilage chondrocytes, although sparse in number, are metabolically active and capable of cell division under pathologic stimuli and these chondrocytes show all the ultrastructural features of a dividing cell. Chondrocyte division (also termed chondrocyte cloning) can be seen in a number of situations such as osteoarthritis, and is not necessarily an indication of malignancy. The articular cartilage is avascular and the cells receive sustenance by absorption of nutrients from the synovial fluid. The basal chondrocytes may also get some nutrition from the vasculature at the cartilage bone interface.

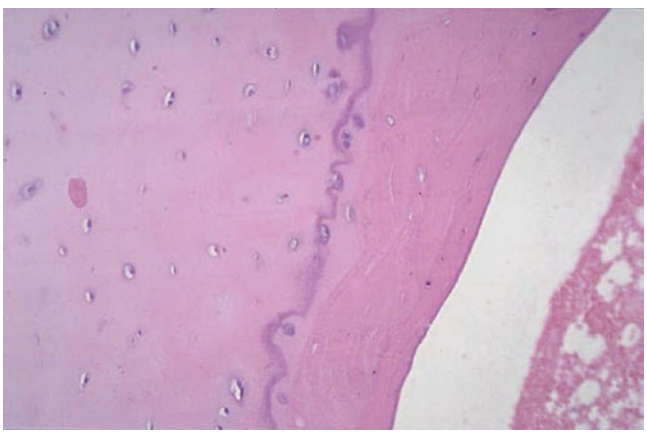

Fig. 6 Photomicrograph showing hyaline articular cartilage. The cartilage cells in the superficial zone are flattened, while those in the middle zone are rounded. The deep layer is separated from the subchondral bone by a tidemark (*arrow*). H&E staining

Hyaline Articular Cartilage

Hyaline articular cartilage is a specialized type of joint cartilage that has the consistency of firm, resilient rubber. It was termed hyaline cartilage originally due to its pearly, translucent, glass-like quality. This type of cartilage is composed of chondrocytes (less than 2% of its weight) embedded in an extensive extracellular matrix (ground substance) consisting of water (70–80% of the weight of the cartilage), a dense network of collagen (10–15%) and elastin fibers, and proteoglycan molecules (10–15%) cross-linked into an integrated network with hyaluronic acid (also known as hyaluronate) (28, 29). Most of the collagen in hyaline cartilage is type II. Cartilage also contains a number of noncollagenous proteins, such as cartilage oligomeric matrix protein (COMP), which is structurally related to the thrombospondins (30). Studies have shown that the proteoglycan aggregate of hyaline cartilage is composed of a central core of hyaluronic acid, link proteins, and bristle-like rods of three glycosaminoglycans: chondrotin-4-sulfate, chondroitin-6-sulfate, and keratan sulfate (31–33).

Hyaline articular cartilage is arranged into three zones. The superficial zone (horizontal zone) is characterized by collagen fibers and small oval cells that are arranged parallel to the surface. This zone is also called the limiting membrane or lamina splendans. The middle zone (vertical zone) contains younger, more active chondrocytes. As a consequence, mitotic figures may be present in this zone. In the deep zone, bundles of collagen fibers can be seen that ascend vertically from their deep attachment to the subchondral bone in the surface of the cartilage. These collagen bundles become more apparent after articular cartilage fracture and other injuries. Such bundles have been called *Benninghoff's arcades*. These collagen bundles are visible as darker pink streaks in hyaline articular cartilage after staining with hematoxylin and eosin (Fig. 6).

Fibrous Articular Cartilage

At some articulations, such as the acromioclavicular and sternoclavicular joints, the bony ends are covered with *fibrous-type articular cartilage* rather than hyaline articular cartilage. Fibrous cartilage is a combination of collagen fibers and chondrocytes, the latter in lacunae lying within hyaline cartilage surrounds. In contrast to hyaline cartilage, most of the collagen in fibrous articular cartilage is type I.

Intervertebral discs are thick fibrocartilaginous discs located between two opposing vertebral bodies. An outer region, termed the annulus fibrosis, consists of many layers of fibrous tissue in a matrix of cartilage that are strongly attached to the ends of the vertebral bodies and thus serves to bind them together. An interior soft center, called the nucleus pulposus, is a semigelatinous material containing 70–80% water molecules. Together, the annulus fibrosis and the nucleus pulposus serve as shock absorbers for the vertebral bodies. Because of the high water content of the intervertebral discs, they are prone to dehydration. Also, compressive forces on the discs during standing and moving cause water to be squeezed out of the discs into the bloodstream. Adaptive remodeling of this type of cartilage to loading is discussed further below.

Articular Cartilage Vascularization and Innervation

Articular cartilage lacks blood supply, lymph channels, and innervation (as mentioned earlier). Metabolic exchange is made by diffusion through the cartilage matrix to and from synovial fluid, capillaries in nearby periosteum, and vessels in the underlying bone. Exchange of nutrients chiefly comes via diffusion from synovial fluid. This lack of blood supply hinders repair and regeneration of the injured or torn cartilage. However, the mixture of elastic solid and viscous liquid (the hyaluronate) in cartilage gives it strong biomechanical resilience, allowing the cartilage to distribute joint loads over a wide joint surface and decrease the stress of compression on the subchondral bone. The hyaluronate, also called mucin, in cartilage and synovial fluid is a "weeping" type of lubrication that allows easy movement of opposing joint surfaces with limited wear.

Menisci-Cartilaginous Joint Modifications

The menisci of the knee (medial and lateral) are cartilaginous modifications that serve to reduce loading damage to subchondral bone and improve joint stability by providing a more congruous articular surface between the femur and the tibia (Figs. 1 and 5). Collagen type I is the key component of meniscal cartilage matrix (28). Surgical removal of menisci typically leads eventually to secondary degenerative arthritis and joint destruction.

Adaptive Remodeling of Joint Cartilage to Loading

Water, proteoglycans, and collagen are the main components of the extracellular matrices of articular cartilage, the fibrocartilage of intervertebral discs, and ligaments. Type I collagen is the key component present in connective tissues subjected to loading forces and tension and adds tensile strength to these tissues. A dynamic balance of synthesis and degradation of collagen is needed for adequate health and maintenance of connective tissues (34, 35). Adaptive remodeling such as increasing the synthesis of collagen occurs with increasing mechanical loading, strengthening the tissue and its ability to withstand higher forces in the future (36). Unfortunately, a greater amount of collagen in the matrix reduces the water binding properties of connective tissue and may impair other aspects of tissue integrity such as viscoelastic deformation. In humans, greater levels of physical loading leads to spinal shrinkage (height loss of spinal segments and cross-sectional areas of intervertebral discs) and to increasing levels of serum biomarkers of collagen type I synthesis (35). These biomarkers, the carboxyterminal propeptide of type I collagen, and the carboxyterminal telopeptide region of type I collagen, may be predictive for degenerative changes in the spine and are under further exploration.

The Importance of Knowing Typical Joint Anatomy and Development During Radiological Diagnoses of Joint Pathologies

Many joint pathologies, as well as a few others, can be evaluated radiographically. In fact, the radiograph is the primary tool for evaluating osteoarthritis as well as other types of arthritis (37). Joint narrowing in arthritic conditions is due to articular cartilage destruction (Table 2). One should also be aware that the epiphyses of a growing synchondrosis-type joint can be displaced and separated from the surrounding bone, and may be interpreted as a fracture. Thus, knowing the patient's age and the location of epiphyses is necessary for appropriate interpretation of radiological images. The key differences between fractures and epiphyseal displacements are that bone fractures leave a sharp and usually uneven edge of bone, while the edges of the epiphysis and diaphysis are smooth and curved in the region of the growth plate.

Table 2 Typical radiographic findings in arthritis that alter joint structure

Osteoarthritis	Rheumatoid arthritis	Gout arthritis
Irregular joint narrowing	Symmetric joint narrowing	Osteoporosis is absent
Cysts or pseudocysts	Periarticular soft tissue thickening (earliest finding)	Sharply marginated articular and juxtaarticular erosions
Osteophytes form on joint margins	Bony ankylosis of joint (a late finding)	Tissue nodules

References

1. Oatis CA. Kinesiology. Philadelphia, Lippincott, Williams and Wilkins, 2004
2. Hartmann C, Tabin CJ. Wnt-14 plays a pivotal role in inducing synovial joint formation in the developing appendicular skeleton. Cell. 2001; 104(3):341–351.
3. Ohashi N, Robling AG, Burr DB, Turner CH. The effects of dynamic axial loading on the rat growth plate. J Bone Miner Res. 2002; 17(2):284–292.
4. Radhakrishnan R, Sluka KA. Spinal muscarinic receptors are activated during low or high frequency TENS-induced antihyperalgesia in rats. Neuropharmacology. 2003; 45(8):1111–1119.
5. Schaible H-G, Schmidt RF. Effects of an experimental arthritis on the sensory properties of fine articular afferent units. J Neurophysiol. 1985; 54:1109–1122.
6. Vance CG, Radhakrishnan R, Skyba DA, Sluka KA. Transcutaneous electrical nerve stimulation at both high and low frequencies reduces primary hyperalgesia in rats with joint inflammation in a time-dependent manner. Phys Ther. 2007; 87(1):44–51.
7. Clark FJ, Horch KW. Kinesthesia. In: Handbook of Perception and Human Performance: Sensory Processes and Perception. Editors: Boff KR, Kaufman L, Thomas JP. New York, Wiley, 1986; 1–62.
8. McCloskey DI. Kinesthetic sensibility. Physiol Rev. 1978; 58:763–820.
9. Hendry SHC, Hsiao SS, Bushnell MC. Somatic sensation. In: Fundamental Neuroscience. 1st ed. Editors: Zigmond MJ, Bloom FE, Landis SC, Roberts JL, Squire LR. San Diego, California, Academic Press, 1999; 761–798.
10. Torebjork HE, Vallbo AB, Ochoa JL. Intracranial microstimulation in man: its relation to specificity of tactile sensations. Brain. 1987; 110:1509–1529.
11. Sun HB, Yokota H. Reduction of cytokine-induced expression and activity of MMP-1 and MMP-13 by mechanical strain in MH7A rheumatoid synovial cells. Matrix Biol. 2002; 21(3):263–270.
12. Firestein GS. Invasive fibroblast-like synoviocytes in rheumatoid arthritis. Passive responders or transformed aggressors? Arthritis Rheum. 1996; 39(11):1781–1790.
13. Schett G, Tohidast-Akrad T, Steiner G, Smolen J. The stressed synovium. Arthritis Res. 2001; 3:80–86.
14. Niki Y, Yamada H, Kikuchi T, Toyama Y, Matsumoto H, Fujikawa K, Tada N. Membrane-associated IL-1 contributes to chronic synovitis and cartilage destruction in human IL-1 alpha transgenic mice. J Immunol. 2004; 172(1):577–584.
15. Jagmin, MG. Structure and function of the musculoskeletal system. In: Pathophysiology: Biological and Behavioral Perspectives. 2nd ed. Philadelphia, Saunders, 2000; 1126–1145.
16. Rhee DK, Marcelino J, Baker M, Gong Y, Smits P, Lefebvre V, Jay GD, Stewart M, Wang H, Warman ML, Carpten J. The secreted glycoprotein lubricin protects cartilage surfaces and inhibits synovial cell overgrowth. J Clin Investig. 2005; 115(3):622–631.
17. Hlavacek M. The role of synovial fluid filtration by cartilage in lubrication of synovial joints. IV. Squeeze-film lubrication: the central film thickness for normal and inflammatory synovial fluids for axial symmetry under high loading conditions. J Biomech. 1995; 28:1199–1205.
18. Gomez JE, Thurston GB. Comparison of the oscillatory shear viscoelasticity and composition of pathological synovial fluids. Biorheology. 1993; 30:409–427.
19. Shay AK, Bliven ML, Sampoli DN, Otterness IG, Milici AJ. Effects of exercise on synovium and cartilage from normal and inflamed joints. Rheumatol Int. 1995; 14:183–189.
20. Hu Y, Cheng L, Hockleitner BW, Xu Q. Activation of mitogen-activated protein kinases (ERK/JNK) and AP-1 transcription factor in carotid arteries after balloon injury. Arterioscler Thromb. 1997; 17(11):2808–2816.
21. Hiskikawa K, Oemar BS, Yang Z, Luscher TF. Pulsatile stretch stimulates superoxide production and activates nuclear factor-kß in human coronary smooth muscle. Circ Res. 1997; 81:797–803.
22. Hochleitner BW, Hochleitner EO, Obrist P, Eberl T, Amberger A, Xu Q, Margreiter R, Wick G. Fluid shear stress induces heat shock protein 60 expression in endothelial cells in vitro and in vivo. Arterioscler Thromb. 1998; 20:617–623.
23. Kumar P, Oca M, Toguchida J, Kobayashi M, Uchida E, Nakamura T, Tanaka K. Role of uppermost superficial layer of articular cartilage in the lubrication mechanism of joints. J Anat. 2001; 199:241–250.
24. Darling EM, Zauscher S, Guilak F. Viscoelastic properties of zonal articular chondrocytes measured by atomic force microscopy. Osteoarthritis Cartilage. 2006; 14:571–579.
25. Shieh AC, Athanasiou KA. Biomechanics of single zonal chondrocytes. J Biomech. 2006; 39:1595–1602.
26. Glaser C, Putz R. Functional anatomy of articular cartilage under compressive loading: quantitative aspects of global, local and zonal reactions of the collagenous network with respect to the surface integrity. Osteoarthritis Cartilage. 2002; 10:83–99.
27. Dupuy DE, Spillane RM, Rosol MS, Rosenthal DI, Palmer WE, Burke DW, Rosenberg AE. Quantification of articular cartilage in the knee with three-dimensional MR imaging. Acad Radiol. 1996; 3(11):919–924.
28. Salter RB. Textbook of Disorders and Injuries of the Musculoskeletal System. 3rd ed. Baltimore, Williams and Wilkins, 1998.
29. Moskowitz RW, Kelly MA, Lewallen DG. Understanding osteoarthritis of the knee-causes and effects. Am J Orthop. 2004; 33(S2):5–9.
30. Rosenberg K, Olsson H, Morgelin M, Heinegard D. Cartilage oligomeric matrix protein shows high affinity zinc-dependent interaction with triple helical collagen. J Biol Chem. 1998; 273(32):20397–20403.
31. Zhu W, Mow VC, Rosenberg LC, Tang LH. Determination of kinetic changes of aggrecan-hyaluronan interactions in solution from its rheological properties. J Biomech. 1994; 27(5):571–579.
32. Buckwalter JA, Smith KC, Kazarien LE, Rosenberg LC, Ungar R. Articular cartilage and intervertebral disc proteoglycans differ in structure: an electron microscopic study. J Orthop Res. 1989; 7(1):146–151.
33. Neame PJ, Choi HU, Rosenberg LC. The primary structure of the core protein of the small, leucine-rich proteoglycan (PG I) from bovine articular cartilage. J Biol Chem. 1989; 264(15):8653–8661.
34. Hascall V, Glant T. Proteoglycan epitopes as potential markers of normal and pathologic cartilage metabolism. Arthritis Rheum. 1987; 30:586–588.
35. Kuiper JI, van Dieen JH, Verbeek JHAM, Frings-Dresen MHW. Association between serum markers of collagen metabolism and spinal shrinkage. Clin Biomech. 2004; 19:209–212.
36. Hutton WC, Toribatake Y, Elmer WA, Ganey TM, Tomita K, Whitesides TE. The effect of compressive force applied to the intervertebral disc in vivo. A study of proteoglycans and collagen. Spine. 1998; 23(23):2524–2537.
37. Erkonen WE, Smith WL. Radiology 101: The Basics and Fundamentals of Imaging. 2nd ed. Philadelphia, Lippincott, Williams and Wilkins, 2004.

Chapter 3
Biomechanics – Part I

Sudheer Reddy, Michele Dischino, and Louis J. Soslowsky

Abstract Biomechanics is the science of the action of forces, internal or external, on the living body. It includes the fields of statics, dynamics, and kinetics. This section will discuss some basic terminology used in biomechanics and also discuss the mechanical properties of some tissues and biomaterials that are important in orthopedic practice.

Keywords Stress–Strain curve • Newton's law • Young's modulus of elasticity • Hooke's law • Wolff's law

Definitions

Biomechanics is the science of the action of forces, internal or external, on the living body. Statics is the study of the action of forces on bodies at rest (in equilibrium).

Dynamics is the study of bodies in motion and the forces related to producing motion. The field of *kinetics* relates the effects of forces to the motion of bodies, while *kinematics* is the study of motion (displacement, velocity, and acceleration) without reference to the forces causing the motion.

Newton's Laws (Brief Summary)

Central to understanding the principles of biomechanics and how they affect the skeletal system are Newton's three laws governing forces. The first law, the law of inertia, is simply stated as follows: if the net external force acting on a body is zero, the body will remain at rest or move uniformly (zero acceleration). This allows for static analysis of the forces acting upon a body via the equation $\Sigma F = 0$. The second law, the law of acceleration, is the principle that the net force acting on an object is the product of the object's mass and its acceleration. Newton's third law, the law of reactions, states that there is an equal and opposite reaction. An understanding of these forces allows one to analyze the action of forces on bodies (free body analysis). Free body analyses are useful for understanding stresses in bone and bone remodeling in response to these stresses. They are useful in that they allow one to analyze what forces are acting upon a bone or joint. An example would be lifting a weight with your arm such that the weight would exert a downward force on the hand and forearm while the biceps would be exerting an upwards force from its insertion on the radius.

Joint Biomechanics

Definitions

Degrees of Freedom: Joint motion is described as rotations and translations occurring in the x, y, and z planes, requiring six parameters or degrees of motion (freedom to function). It is important to note that not all joints exhibit 6 degrees of freedom (abduction, adduction, flexion, extension, internal rotation, and external rotation) due to anatomic constraints to motion.

Hip: The hip is a joint that does exhibit 6 degrees of freedom and is termed a ball and socket joint. The stability of the joint is largely based upon the ball and socket design. The bone of the hip is also designed to withstand the significant stress that is placed upon it during daily activities. The reactive force of the hip can reach three to six times body weight, primarily due to the contraction of muscles that cross the hip joint. These muscles, primarily the abductor group (the gluteus medius and minimus) confer stability to the hip and are important in stabilizing the pelvis during gait. Table 1 shows the range of motion that the hip joint is capable of producing.

Knee: In contrast to the hip, the knee exhibits only 4 degrees of freedom: internal/external rotation, flexion, and extension. The knee is a hinge joint and stability is conferred upon it by the ligamentous structures that surround it. For example, the collateral and cruciate ligaments confer coronal plane stability with the knee in extension. While there is purely rotational movement about the hip, the knee does allow for translational motion during flexion and extension and is rather a complex series of rotations and translations about an instantaneous center of rotation. While understanding this complex series of motions of the knee is beyond the scope of this text, it is important to note that the knee does undergo additional motions besides flexion and extension and that the functional range of

J.S. Khurana (ed.), *Bone Pathology*, DOI 10.1007/978-1-59745-347-9_3,

Table 1 Range of motion of hip joint (Source: Ref. 1)

Motion	Average range (°)	Functional range (°)
Flexion	115	90 (120 to squat)
Extension	30	Not required
Abduction	50	20
Adduction	30	Not required
Internal rotation	45	0
External rotation	45	20

Table 2 Range of motion of knee joint

Motion	Average range (°)	Functional range (°)
Extension	–10 (hyperextension)	0
Flexion	130	90[a]
Internal rotation (at 90° of flexion)[b]	30	Not required[c]
External rotation (at 90° of flexion)[b]	45	Not required[c]

[a]117° required for squatting and lifting; 110° of flexion required to arise from a chair following a total knee arthroplasty.
[b]True rotation of the knee varies with degree of flexion.
[c]During the last 15° of extension, the femur internally rotates on the tibia, allowing full extension. This is called the "screw home" mechanism. (*Source*: Ref. 1).

motion is different than the total range of motion that the knee is able to undergo. Table 2 shows the actual and functional range of motion of the knee.

Joint reaction force: Forces are generated within a joint in response to forces acting on the joint (both intrinsic and extrinsic). Muscle contractions about a joint are the major contributory factor to the joint reaction force. As an example, the gluteus medius and minimus attach to the greater trochanter of the proximal femur and create an abductor moment on the hip. When they contract pulling the femur proximally, the force of contraction creates a joint reactive force against the acetabular wall by the femoral head.

Instant center of rotation: This is the point about which a joint rotates. For some joints, the instantaneous axis of rotation (IAR) is static and for others it is dynamic (changes during the arc of motion, such as in the knee and unconstrained total disc replacement). It is helpful in understanding the types of motion that various joints undergo.

Rolling/sliding motion: Most joints exhibit simultaneous rolling and sliding motion, such as the knee. Pure rolling occurs when the instant center of rotation is at the rolling surfaces and the contacting points have zero relative velocity. Pure sliding occurs with pure translation or rotation about a stationary axis; there is no angular change in position and no instant center of rotation.

Friction/lubrication: The predominant mechanism of lubrication during dynamic joint function is *elastohydrodynamic, which means that during joint loading there is cartilage deformation leading to an efflux of fluid into the joint.* With joint function and loading, there is deformation of the articular cartilage (hyaline cartilage). This leads to an efflux of fluid from the cartilage, contributing to the lubrication of the joint (which has a thin film of joint lubricant separating the surfaces) and reduces the coefficient of friction between the articular surfaces. The coefficient of friction (a specific measure of the degree of friction between two surfaces) in joints is a function of synovial fluid, an ultrafiltrate of blood plasma produced by the synovial membrane.

Tissue Biomechanics

Definitions

Load refers to the force(s) acting on a body, and can be applied in compression, tension, shear or torsion, or some combination of these. Deformation is the change in shape produced in a body as a result of an applied load. This alteration can be temporary (elastic) or permanent (plastic). Stiffness describes the resistance of a body to deformation. Each of these properties is dependent upon the geometry of a specimen and is therefore considered a *structural property.* Properties that are independent of geometry are termed *material properties* and include stress and strain, which are discussed below. Stress is defined as force per unit area and can be normal (perpendicular) to a surface or act in shear (parallel to the surface). It is typically reported in Newtons per square meter (N/m^2) (also called pascals). Strain can also be normal or shear and is defined as the change in length/original length of a specimen. As strain is a proportion, it is unitless.

Modulus (Young's modulus of elasticity) is the measure of the ability of a material to resist deformation and is equal to stress/strain, it has no units.

The Stress–Strain Curve

A stress–strain curve plots stress versus strain for a specimen under uniaxial load (Fig. 1). As illustrated in the figure, a specimen will typically exhibit linearly elastic behavior up to a limit, which is referred to as the proportional limit, or *yield point*. In this region, the material obeys *Hooke's law*, which states that stress is proportional to strain or $F/A = E(\Delta l/l_0)$, where F is the force (or load) applied to the specimen, A is its cross-sectional area, and $\Delta l/l_0$ is the resultant strain. The proportionality constant, E, is referred to as *Young's modulus*, and is an important property of the material as it measures its resistance to deformation. This property is independent of specimen geometry.

Beyond the yield point, stress is no longer proportional to strain and deformation is no longer fully recoverable because of damage to the internal microstructure of the specimen. Other

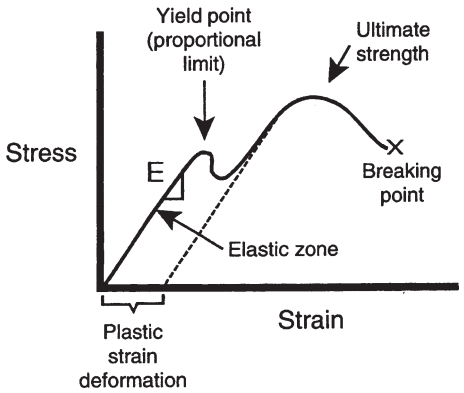

Fig. 1 Stress–strain curve

important features of the stress–strain curve are the *ultimate strength* (the maximum stress value attained by the specimen), the *breaking point* (the point at which the specimen fails, and the *plastic deformation* (the change in length after removing the load in the plastic range, before the breaking point).

In addition to this information, the stress–strain curve can also be used to calculate *strain energy*, or *toughness*, which is the energy required to bring the specimen to failure and is represented by the area under the curve (i.e., the stress–strain curve). Strain energy is a useful measure because injuries transfer energy to a body, which results in deformation and possibly fracture. By determining how much energy can be absorbed by a material before failure, it may be possible to enhance fracture prevention. Strain energy may also be useful in determining possible causes of existing fractures.

On the basis of the concepts outlined above, several categories exist that describe material characteristics and behavior:

Brittle	Exhibit a linear stress–strain curve to failure and elastic deformation only. An example of a brittle material encountered in orthopedics is polymethylmethacrylate (PMMA).
Ductile	Undergo a large amount of plastic deformation before reaching failure, such as metals.
Elastic	Stress is directly proportional to strain for elastic materials and deformation is fully recovered when a load is removed. The properties of elastic materials are insensitive to the rate of loading.
Viscoelastic	The stress–strain behavior of viscoelastic materials depends on time and rate of loading. Viscoelasticity is a function of internal friction in the material. For such materials, a constant force will produce *creep*, that is, the deformation will increase with time as long as the force is maintained on the material, until equilibrium is reached. Conversely, a constantly held deformation will cause *stress relaxation* to occur, that is, the force required to maintain the deformation will diminish with time until equilibrium in reached. Articular cartilage, intervertebral disk, ligament, tendon, and bone exhibit pronounced viscoelastic behavior.
Isotropic	Have the same mechanical properties in all directions.
Anisotropic	Mechanical properties vary with the direction of applied load in these materials. Biologic tissues are anisotropic in nature.

Mechanical Properties of Bone

Bone is a composite material, consisting of minerals, proteins, water, cells, and other macromolecules. Its composition varies with anatomic site, age, diet, and the presence of disease. In general, however, ~90% of the organic matrix of bone is collagen and the main constituent of its mineral phase is hydroxyapatite. Collagen has a low modulus, good tensile strength, and poor compressive strength. Hydroxyapatite is a stiff, brittle material with good compressive strength. This combination yields an anisotropic material that is strongest in compression, weakest in shear, and intermediate in tension.

The mineral content is the main determinant of the elastic modulus of cortical bone. Cortical bone is excellent in resisting torque, while trabecular bone is good in resisting compression and shear. Trabecular bone is 25% as dense, 10% as stiff, and 500% as ductile as cortical bone. Trabecular bone density varies significantly with anatomic location and age, and such variations directly impact the mechanical properties of the tissue. For example, trabecular bone properties within the proximal tibia can vary by up to 2 orders of magnitude because of changes in density alone. To further complicate matters, the mechanical properties of trabecular bone also depend on architecture, which, like density, depends on anatomic site and age. Cortical bone is a low porosity solid. Trabecular bone is an open-celled porous foam, composed of a series of thin and thick interconnecting trabeculae. Depending on the type and orientation of these basic structures, the mechanical properties can vary by at least an order of magnitude.

Bone is a dynamic material, capable of self-repair and adaptation. Prolonged immobilization induces bone weakness. Exercise increases bone strength. With aging, the mechanical properties of cortical bone progressively deteriorate. This has been demonstrated in cortical bone samples taken from the femoral mid-diaphysis (Fig. 2), which showed a decrease in elastic modulus and ultimate strength of ~2%

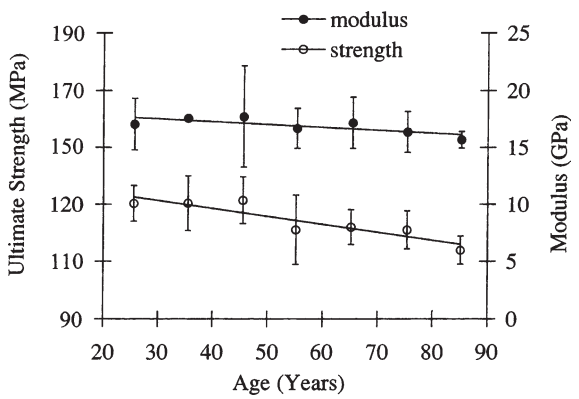

Fig. 2 Age-related effects on longitudinal modulus and ultimate tensile strength of human femoral cortical bone (8)

per decade after 20 years of age. Probably the most significant change in terms of fracture risk, however, is the ~7% reduction in energy absorption that occurs with aging. Taken together, these data indicate that cortical bone becomes less stiff, weaker, and more brittle with aging. To offset age-related loss in mechanical properties, bone remodels its geometry to increase the inner and outer cortical diameters, thus minimizing bending stresses. The bending rigidity of a cylinder is proportional to r^4.

Wolff's law states that bone structure adapts to changing loads. As an example, the trabecular patterns in the femoral head and neck (Fig. 3) are distributed in a pattern to allow the proximal femur to withstand the typical forces experienced by the hip in daily activities. Both the primary and secondary compression groups of trabecular lines are centered on the proximal, medial cortex (calcar) allowing it to withstand the compressive forces that are placed upon it during gait. These stress patterns develop as a person first learns to walk. In certain diseases, Wolff's Law may no longer hold true as bone loses its ability to remodel to stress. This increases the propensity of abnormal bone to fail under normal loading conditions, leading to a pathologic fracture (Fig. 4).

Fractures and mechanism of injury

- *Stress fractures* can occur as a result of fatigue damage. In fatigue fractures, there are three characteristic stages: crack initiation, crack growth, and final fracture. In cortical bone, Haversian canals and lacunae serve as crack initiators since they represent discontinuities in the cortical bone microstructure. The most important factor in fatigue damage is the second stage of crack propagation, as microcracks join together once they have progressed beyond the initiation stage. The final stage of fracture is reached when these cracks coalesce and become large enough to overcome the absorptive properties (ability of bone to absorb energy and resist crack propagation) of the Haversian system.

Tension fractures occur by muscle pull with the bone failing in tension. The fracture line is transverse, perpendicular to the load and axis of the bone (Fig. 5).

Compression fractures occur by axial loading of bone, with cancellous-type bone failing typically. It results in a crush type of fracture, such as a buckle fracture in a child.

Shear fractures occur with a load that is parallel to the bone surface, with the resultant fracture parallel to the direction of loading. Pure shear fractures are rare; however, it is a component in spiral fracture patterns.

Fractures that are produced as a result of a bending force produce a characteristic called a *butterfly fragment* that is indicative of this fracture pattern. The fracture starts on the tension side of the bone and continues transversely (or obliquely) to the compression side of the bone. The bone bifurcates producing a butterfly fragment.

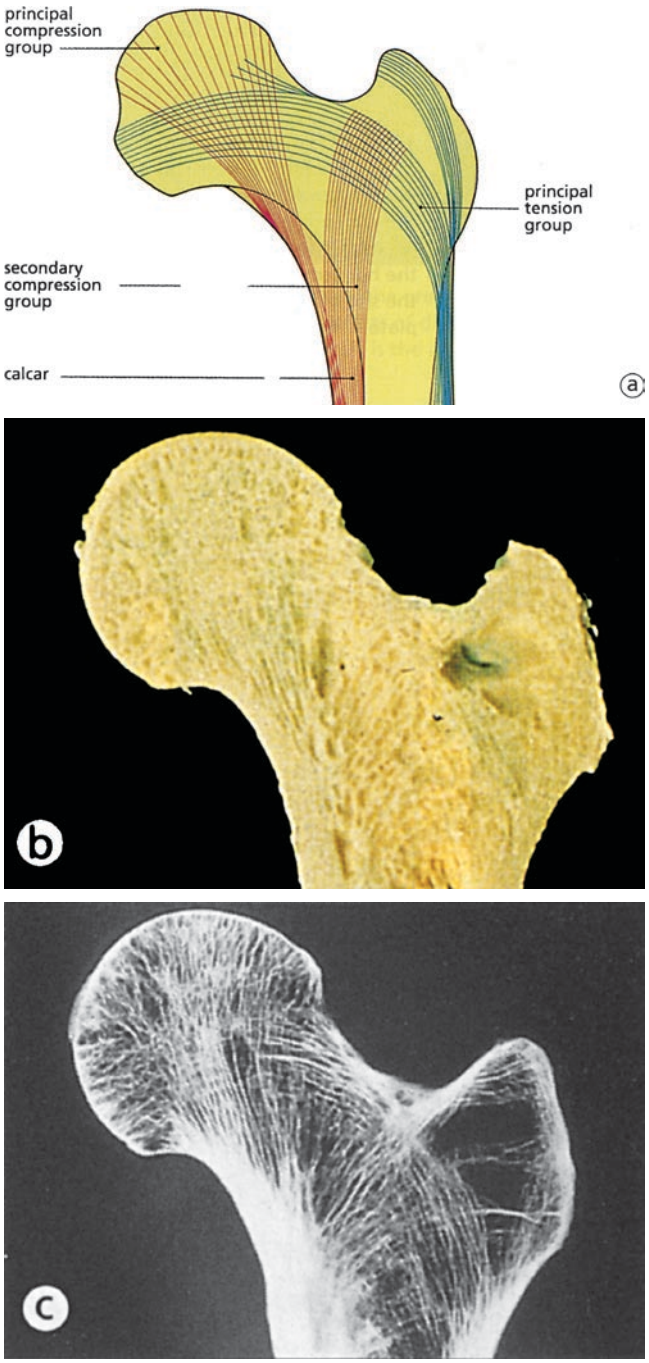

Fig. 3 **a** Wolff's law is well demonstrated in the head and neck of the femur. In this area, the bone trabeculae radiate from the articular surface down onto the medial cortex of the femoral neck (the calcar), which is much thicker than the cortex on the lateral side of the femoral neck. **b** In this slice through the upper end of the femur, the marrow fat has been washed out of the specimen to demonstrate the distribution of the cancellous bone. **c** The best way to demonstrate clearly the arrangement of the bone trabeculae is by radiography of the specimen

Spiral fractures are a result of tensile and shear forces. In a long bone that undergoes torsion, the greatest stress on the bone is experienced on the periosteal (outer) surface, as opposed to the endosteal surface (Fig. 6).

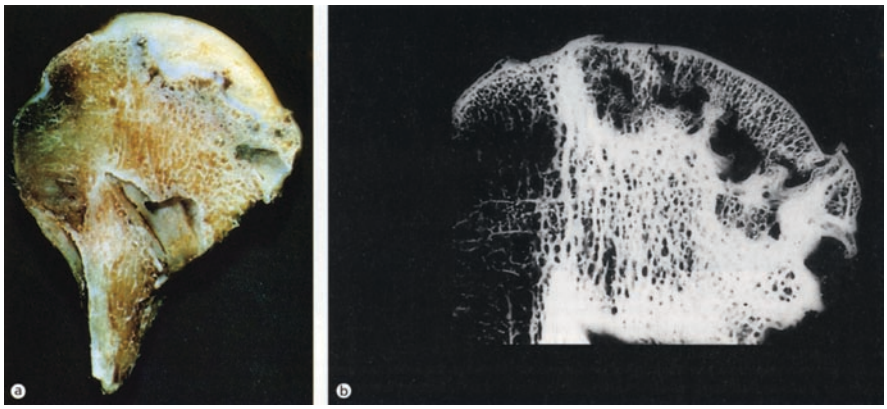

Fig. 4 **a** Photograph of a slice through a femoral head showing an area of infarction seen as a triangular opaque yellow area lying immediately beneath the articular surface. Also seen in this photograph is the track of the nail that was used for fixation of the subcapital fracture that preceded the necrosis. **b** Radiograph of the specimen shown in (**a**). Note the unaltered trabecular pattern of the infarcted bone. In contrast, the viable bone at the base of the infarct is dense, resulting from the formation of new bone in this area by the process of creeping substitution. The lucent area at the base of the infarction results from fibrous granulation tissue eroding the necrotic bone. The collapse of the necrotic segment is well demonstrated by the fracture through the subchondral plate, which is seen at both edges of the infarct

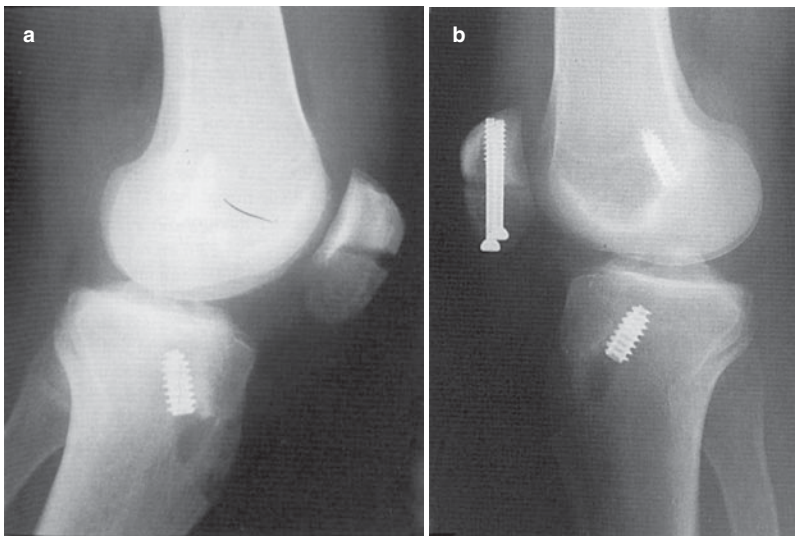

Fig. 5 **a** Transverse patella fracture following central third patellar tendon autograft harvest. **b** Open reduction and internal fixation of an inferomedial quadrant fracture following central third patellar tendon autograft harvest with dual compression screws

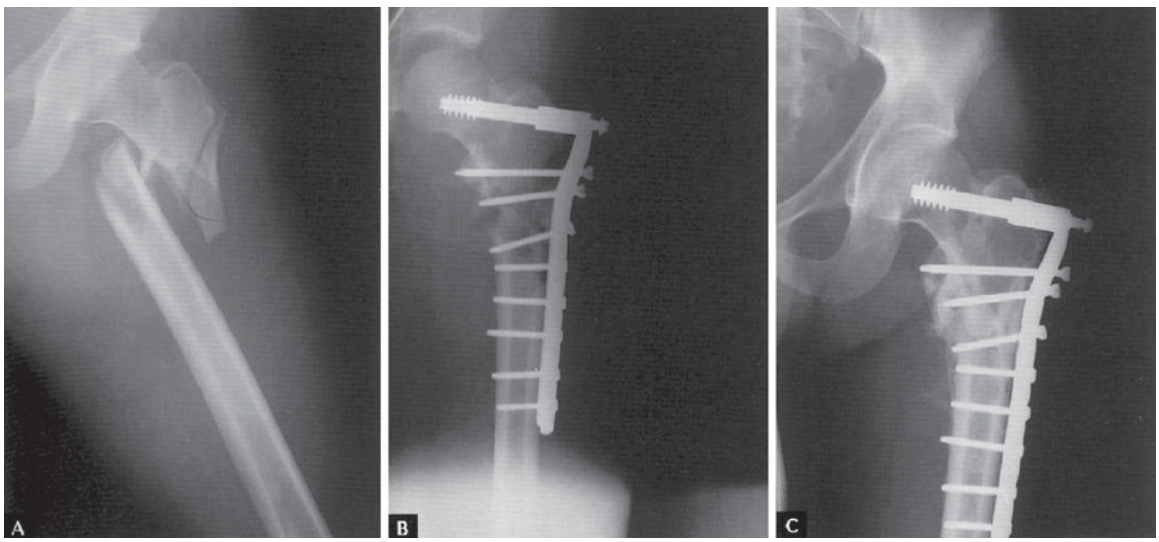

Fig. 6 **a** Radiograph of a subtrochanteric femur fracture. **b** Stable limb alignment and length are achieved with open reduction and internal fixation. **c** The fracture has consolidated in acceptable alignment after 8 months

Comminuted fractures result from high-energy injuries without a specific force or force pattern creating the fracture. It is a function of the amount of energy transmitted to the bone, resulting in comminution. Furthermore, with high-energy injuries (such as those from a motorcycle), the energy can be dissipated to the surrounding soft tissues resulting in soft-tissue damage (muscle, vascular, and skin damage) (Fig. 7).

Mechanical Properties of Tendon and Ligament

Tendons and ligaments are anisotropic and viscoelastic, and can sustain 5–10% tensile strain before failure (vs. 1–4% in bone). A typical stress–strain curve for these tissues (Fig. 8) can be divided into a low modulus (toe) region, followed by a linear region with higher modulus. The toe region has been attributed to the straightening of the crimped fibrils and to nonuniform recruitment of individual fibers. Tendon, which has one of highest tensile strengths of any soft tissue in the body, consists almost exclusively of fibers oriented along a single direction of force. Ligament, however, has a broader distribution of fiber directions due to more varied loading conditions in vivo.

Mechanical Properties of Intervertebral Disk

Intervertebral disks are anisotropic and viscoelastic, and also exhibit toe and linear regions in tensile extension, as illustrated in Fig. 8. The anulus fibrosus exhibits high values for Young's modulus, stiffness, and failure stress, all of which indicate that this tissue is well equipped to sustain the large tensile stresses that it endures in situ. In particular, the outer

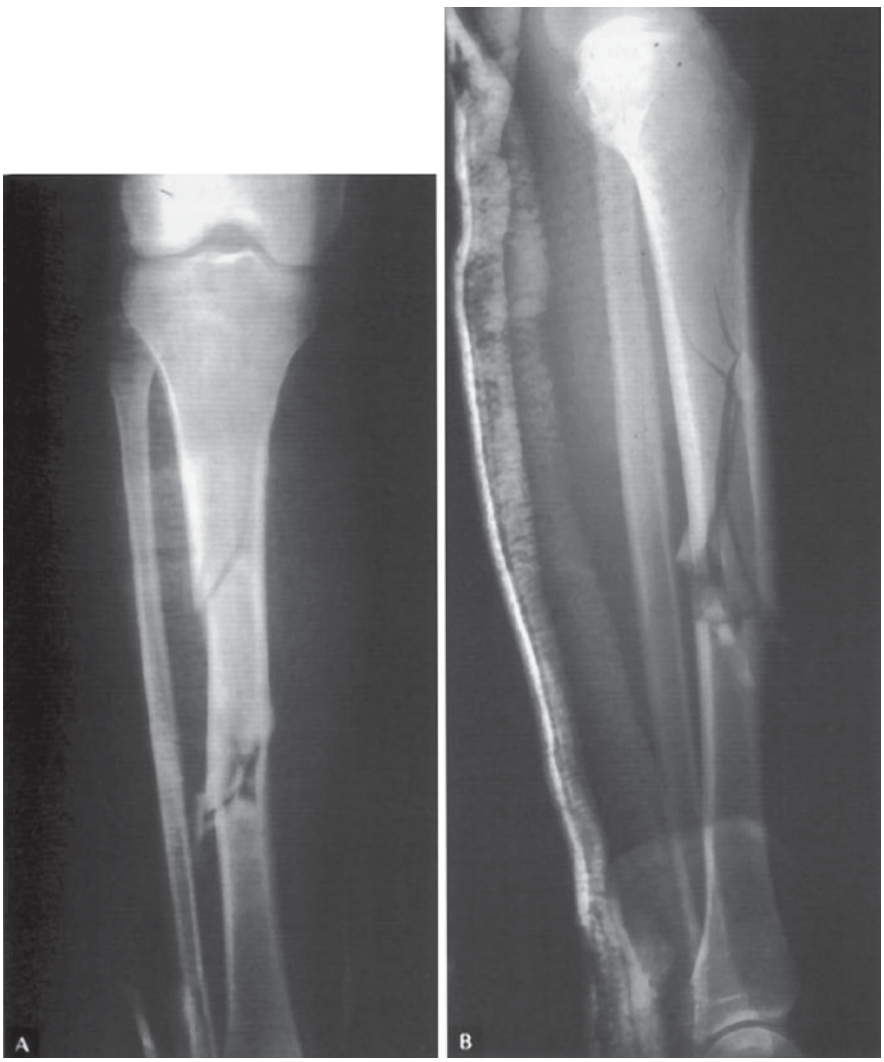

Fig. 7 Closed segmental tibia fracture from motor vehicle trauma. **a** Anteroposterior radiograph. **b** Lateral radiograph

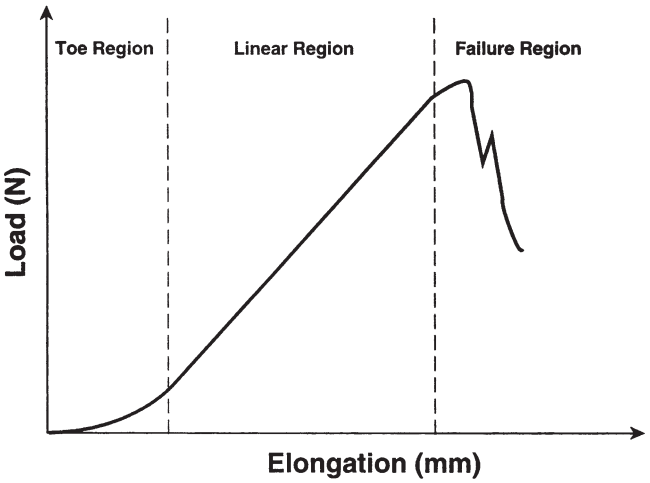

Fig. 8 A schematic load–elongation curve for tendon, indicating three distinct regions of response to tensile loading

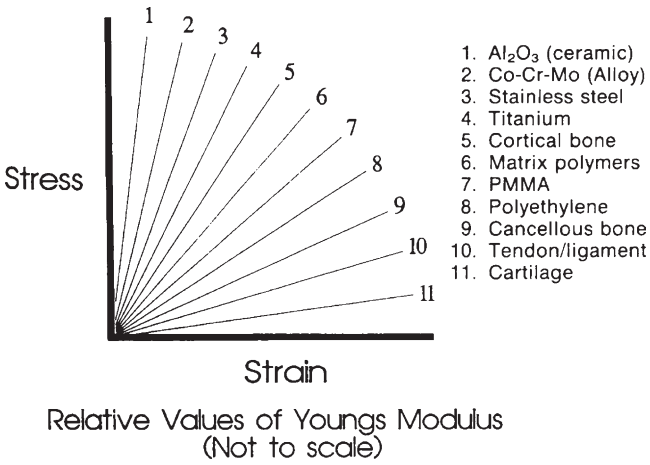

Fig. 9 Comparison of Young's modulus (relative values, not to scale) for various orthopedic materials

annulus is ideally suited for minimizing disk bulging. As tensile properties depend on the pathologic state of tissue, however, annulus degeneration can lead to disk herniation. The nucleus pulposus acts predominantly as fluid under static load, generating large hydrostatic pressures that help to maintain disk height, and support and transfer load.

Mechanical Properties of Cartilage

Similar to the other orthopedic soft tissues described above, cartilage is anisotropic and viscoelastic. It exhibits toe and linear regions in tensile extension (Fig. 8). Its ultimate tensile strength is only 5% that of bone, but it is well suited for compressive loading due to its highly viscoelastic properties.

Tissue Replacement

A comparison of Young's modulus for common artificial materials encountered in orthopedics can be seen in Fig. 9, along with the values of this property associated with biologic tissues. Below is a description of the basic categories into which these replacement materials may fall and a description of their related uses and concerns:

Metals: Metals are used as structural elements in joint prostheses. They demonstrate relatively good corrosion resistance and reasonable fatigue life, and their moduli exceed that of bone. Orthopedic implants are typically made of stainless steel (e.g., 316L), cobalt–chromium (Co–Cr), or titanium alloys. The properties of each, such as modulus (see Fig. 9), are varied and are important when choosing the optimal material for each application. Titanium, for instance, is extremely biocompatible with a high yield strength and a modulus closer to that of bone than stainless steel or Co–Cr. Titanium, however, has poor resistance to wear, raising some concerns regarding its use in implants as the release of corrosion products may incite a macrophage response. Co–Cr alloy generates less metal debris than titanium. Its increased modulus along with that of stainless steel, however, make these metals more likely to induce a condition known as stress shielding, in which normal stress is transferred from the bone to the implant, often with detrimental effects.

Polymers: There are two specific applications in orthopedics in which polymers have proved useful and in both cases, the appropriate mechanical properties of the polymer are of major importance. First, polymers are used as articulating surface components in joint prostheses. Thus, they must have a low coefficient of friction and low wear rate when they are in contact with the opposing surface, which is usually made of metal or ceramic. Second, polymers are used for fixation as a structural interface between the implant component and bone tissue. This usually requires that the polymers be able to minimize plastic deformation and resist creep under the stresses found in clinical situations.

Examples of polymers with orthopedic applications include polyethylene, PMMA, and silicone. Ultra-high molecular weight polyethylene (UHMWPE) is often used to fabricate weight-bearing implant components, such as acetabular cups and tibial trays, owing to its tough, ductile nature as well as its low friction properties and resistance to wear. Wear damage to a UHMWPE articulating surface is most often caused by foreign body inclusions and the associated wear debris is the main factor affecting the longevity of these joint replacements. PMMA is frequently used as a grouting material for fixation of implants and distribution of load at the bone–implant interface. It functions by mechanically interlocking with bone and while

it is strongest in compression, it has poor tensile and shear strength and a low modulus. PMMA wear particles can incite a macrophage response that leads to loosening of the implant. Unlike polyethylene and PMMA, silicones are polymers that are most often found in nonweight-bearing joints. Their poor strength and inability to resist wear can lead to frequent synovitis with prolonged use.

Ceramics and glasses: Ceramics contain metallic and nonmetallic elements and include inert materials, such as alumina (Al_2O_3), as well as bioactive (degradable) substances such as bioglass. These are brittle (no elastic deformation), have a high modulus, high compressive strength, low tensile strength, low yield strain, and exhibit favorable wear characteristics but poor crack resistance. Ceramics and glass ceramics have played an increasingly important role in implants and have been used primarily in two different applications. The first of these is their use as articulating surfaces, for which ceramic properties such as resistance to oxidation (i.e., inertness in the body), high modulus, and low friction and wear rate are highly desirable. Al_2O_3, for instance, has proven quite successful for use in paired femoral head and acetabular components in total hip arthroplasty. The second application takes advantage of the osteophilic surface of certain ceramics and glass ceramics. These materials, termed bioglasses, provide an interface of such biological compatibility with osteoblasts that these cells lay down bone directly next to the material. Several of these compositions have seen wide use as implant materials. The use of bioglass on the metallic stems of hip prostheses provides an alternate approach to fixation instead of using PMMA.

Composites: From the previous description of bone properties and a comparison with the corresponding properties of the various metals, polymers, and ceramics, it is clear that there is considerable disparity among these materials. This mismatch fueled the idea that it might be possible to optimize implant properties by combining materials and thus sparked an interest in composite materials.

An area where composites may provide an interesting and important application is in bone plates. The rigidity and stiffness of the metallic plates generally used are much greater than that of the adjacent bone. Even after healing is well underway, the plate continues to carry a major portion of the load, thereby stress shielding the underlying bone and delaying, if not preventing, full healing. Eventually a second operation is required to remove the plate. This situation is one in which composites may offer a superior solution. For instance, totally bio-resorbable composite plates have been made from polyglycolic acid (PGA) fibers embedded in a polylactic acid (PLA) matrix. As the degradation rate of such composites can be controlled via the design process, it is conceivable to design a plate that would remain stiff and rigid enough to support the loads of physical activity until the bone has healed sufficiently to do so without assistance. Consequently, instead of continuing to divert part of the load away from the underlying bone, the plate would gradually degrade and increasing amounts of load would be transferred to the bone, thus providing the proper loading conditions for full healing to proceed. Another orthopedic application of composites is in replacement of tendons and ligaments. In this capacity, biodegradable polymers such as PLA have acted as a scaffold, allowing ingrowth of collagenous tissue in an attempt to reform the damaged connective tissue.

Engineered (living) tissue: These constructs typically consist of a cell-seeded scaffold, with or without bioactive elements, and are capable of self-adaptation and repair. Growth factors, introduced during fabrication or delivery of the constructs, hold promise for improving repair quality. In addition, the quality of the engineered tissue might be further enhanced through mechanical stimulation of the constructs during the fabrication process. All of these factors, however, are likely to be tissue and site specific and must be delivered thoughtfully and appropriately if tissue engineers expect to stimulate early cell proliferation and subsequent matrix synthesis. This matrix must also be deposited and rapidly organized if the repair is to be capable of resisting the large in vivo forces of daily activities. Scaffolds must also be identified with enough compliance so the cells can organize the construct but with enough stiffness to resist the expected in vivo loading regimes. These materials should initially attract, anchor, and protect the cells, but then degrade at controlled rates that prevent mechanical disruption of the repair and ensure biocompatibility. Many of these treatments are now being investigated and offer exciting potential for the repair of hard and soft tissue injuries.

Selected Reading

1. Brinker MR, O';Connor DP. Basic Science, Chap. 1. In Miller, M. (ed) Review of Orthopaedics, 4th ed. Saunders Publishing, Philadelphia, 2004: 1–153.
2. Buckwalter JA, Einhorn TA, Simon SR (eds). Orthopaedic Basic Science: Biology and Biomechanics of the Musculoskeletal System, 2nd ed. American Academy of Orthopaedic Surgeons, Rosemont, IL, 2000.
3. Moehring HD, Greenspan A. Fractures: Diagnosis and Treatment. McGraw-Hill, New York, 2000.
4. Ratner BD, Hoffman AS, Schoen FJ, Lemons JE (eds). .Biomaterials Science: An Introduction to Materials in Medicine. Academic Press, San Diego, 1996.
5. Li S, Burstein AH. Ultra-high molecular weight polyethylene. The material and its use in total joint implants. J Bone Joint Surg (Am) 1994; 76: 1080–1089.
6. Li P. Bioactive ceramics: state of the art and future trends. Semin Arthroplasty 1998; 9: 165–175.
7. Butler DL, Goldstein SA, Guilak F. Functional tissue engineering: the role of biomechanics. J Biomech Eng 2000; 122(6): 570–575.
8. Burstein AH, Reilly DT, Martens M. Aging of bone tissue: mechanical properties. J Bone Joint Surg 1976; 58A: 82–86.

Chapter 4
Biomechanics – Part II

Solomon Praveen Samuel, George R. Baran, Yen Wei, and Brian L. Davis

Abstract Bone is a self-repairing structural material, which adapts its material properties and shape in response to a number of factors. Healthy bones do not develop spontaneous fractures during voluntary physical activities of life. However, an imbalance between bone strength and the mechanical loads placed on the bones can lead to bone fractures. Bone health is affected by a number of factors including age, gender, physical activity, systemic diseases, and drug treatment for various diseases. This chapter will discuss bone design as it relates to fracture resistance and locomotion, fracture prediction techniques, and fracture prevention.

Keywords Osteoporosis • Trabeculae • Bone mineral density • Load • Matrix • Microgravity • Resorption • Osteon • Haversian system • Axial compression • Flexion • Deformation • Anisotropy, Torque • Dual-Energy X-ray Absorptiometry • Antiresorptive agents • Wolff's law • Osteonal

Introduction

Bones play a major role in locomotion by providing muscle attachment sites and act as a system of levers that either accentuate movement speed (such as a hip flexor causing the lower limb to move rapidly) or force (such as in the biting action of the mandible). They also provide protection of vital organs (e.g., skull and ribs) and serve as a mineral reservoir (involved in the regulation of calcium ion concentration in extracellular fluid). As with any other load-bearing structure, the most obvious mechanical requirement for bone is to avoid fracture. Healthy bones do not develop spontaneous fractures during voluntary physical activities of life (1). Bone is a dynamic tissue that is constantly remodeling itself to avoid failure during locomotion or during muscle activity.

The consequences of bone failure are tragic in humans and animals. Bones usually fail/fracture in two circumstances. Bones fail when a force exerted against the bone in any direction is stronger than the bone can structurally withstand. This type of failure occurs during falls from height, during accidents, or in cases of osteoporotic hip/wrist fractures. Bones also fail when they are subjected to new, strenuous, and repetitive stresses (e.g., fatigue fractures). Fractures of this type usually happen when an individual's relatively sedentary life style suddenly changes to a more active life style as in the case of new military recruits.

The elderly are more susceptible to bone fractures regardless of gender, mainly due to osteoporotic changes in their bones. Osteoporosis is a systemic disease characterized by reduced bone mass and deteriorated bone microarchitecture. There is usually a "quadruple threat" associated with this problem: (i) fewer trabeculae, (ii) thinner trabeculae, (iii) longer trabeculae that are more prone to buckling, and (iv) cracked trabeculae or missing fragments. People with severe osteoporosis are prone to traumatic (during falls) as well as nontraumatic fractures (fractures due to voluntary muscle forces). Most of the osteoporosis-related fractures occur in the hip, spine, or distal forearm (2). Fractures in healthy individuals frequently occur during trauma. These types of fractures happen during sporting activities, high impact loading such as automobile accidents, and falls in children (in children these may take the form of green stick fractures, torus or buckle fractures due to a less mineralized bone).

There are three major factors that interact in a number of ways to cause a fracture: the bone, the patient, and the magnitude and direction of load. Most of the clinical osteoporosis literature portrays bone mineral density (BMD) as the single most important factor in determining fracture risk (3). However, a growing body of evidence indicates that factors other than BMD, such as bone geometry, microarchitecture, molecular structure of inorganic and organic bone components (4), and bone remodeling (3) equally contribute to bone fragility. There are also many patient-related factors that increase the risk of fractures, such as drug treatments (5, 6), systemic diseases, vision problems, gait instability, or nervous disorders. In addition, the magnitude and direction of load as well as the location of a particular bone play an important role in fracture risk. This chapter will discuss some of these issues and how the risk of bone fractures can be predicted in a particular individual. Currently, bone fractures can be predicted with reasonable accuracy and steps can be taken to prevent some of them.

J.S. Khurana (ed.), *Bone Pathology*, DOI 10.1007/978-1-59745-347-9_4,

Bone Composition

The ability of any bone to resist fracture under normal physiological load depends on bone mass, bone geometry, bone architecture, and bone composition. Bone is a composite made up of 65% mineral (mainly hydroxyapatite) and 35% organic matrix (collagen and other noncollagenous protein, bone cells, and water) (7). The inorganic component contributes to bone strength, while the organic matrix is responsible for toughness (i.e., crack resistance). The mechanical properties of any given bone can be fine-tuned according to the loading requirement by changing the ratio of inorganic, organic, and water content (8). Many examples [mineral content (inorganic)] in tooth enamel – 97%, ossicles of the middle ear – 90%, bone – 65%, antler – 30%) can be found in nature where the proportions of these three components are varied to obtain the desired mechanical property. One such interesting example pertains to a child's skeleton: the bones in children are less mineralized than in adults. A less mineralized bone will be more flexible (less brittle) and thus absorbs more energy. This helps children avoid fractures during their frequent falls (9). It is interesting to note that when the same bone mineral content (BMC) *decreases* in adults, the chance of fracture is very high during the first fall. The reason for this will be discussed in the following sections.

Bone Properties and Fracture Mechanics

The mechanical loads applied to bones vary according to an individual's level of activity during adulthood. This means that bones alone cannot depend on their genetic information to maintain structural strength and need constant remodeling to withstand the loads experienced depending on an individual's activity. Bone is a self-repairing structural material, able to adapt its properties and configuration according to changes in mechanical requirements. The most popular early observation regarding bone adaptation was by Wolff (1869), who concluded that the form of bones followed their function. Increased mechanical loading makes bones stronger (10). For example, in tennis players, the total cross-sectional area and, in turn, bone mineral densities were found to be higher in the playing arm when compared to the nonplaying arm (11). Microgravity represents an extreme form of mechanical unloading. Microgravity causes significant bone loss (particularly in the lower limb bones) within 24 h of unloading. Bones rely on an extremely sensitive feedback control system to maintain strength (i.e., to prevent spontaneous fractures). The control system senses mechanical loads applied to the bone and either builds (formation) or removes (resorption) bone accordingly. In a healthy bone, the amount of bone formation and bone resorption is balanced.

Types of Bones and Their Function

There are two types of bone tissue in the skeletal system: cortical (or compact) and cancellous (or trabecular) bone. Adult human skeletal mass consists of 80% cortical bone (porosity 5–30%) and 20% cancellous bone (porosity 30–90%). The cortical bone forms the outer wall of all bones, and trabecular bone is found in the inner parts of bones. The percentage distribution of cortical and cancellous bone varies greatly between individual bones. In cortical bone, the main structural unit is the osteon or Haversian system. The cancellous bone is made up of trabecular plates and rods. The differences in the basic structure of cortical and cancellous bone are shown in Fig. 1 and discussed in Chap. 1.

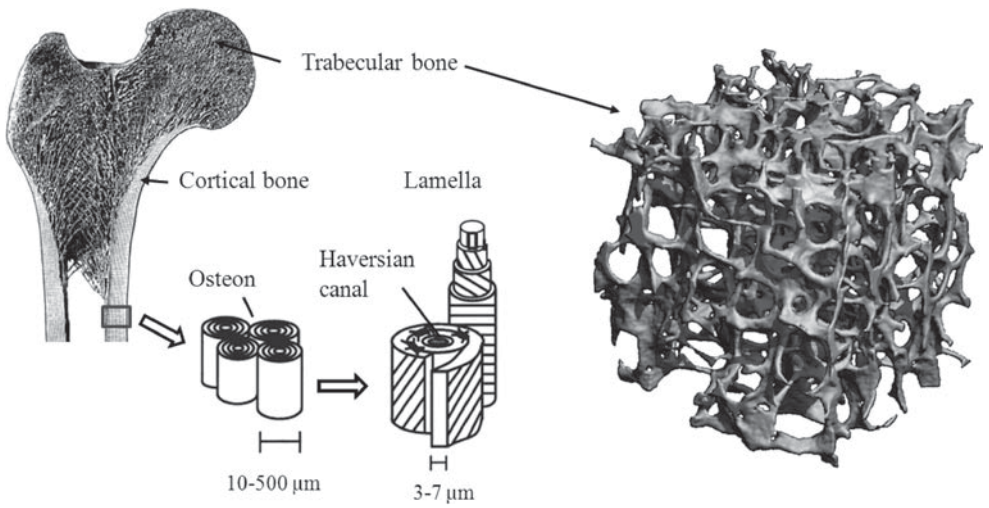

Fig. 1 There are differences in the hierarchical structure between cortical bone (*left*) and trabecular/cancellous bone (*right*, courtesy of SCANCO Medical AG, Switzerland)

Bone Design

Genetic information is responsible for the highly conserved anatomical shape and the type of bones present in each skeletal site. Bone adaptation strengthens or weakens the bone structure according to the loads experienced by the bones in the recent past. Bone as a structure follows sound engineering principles, and therefore engineering analysis can be applied to predict fractures at a particular bone site. For predicting fractures, it is therefore important to understand the function and properties of the two types of bone components and understand how changes in each bone component affects the strength of the whole bone.

An important role of the skeletal system is to enable locomotion. This requires bones to be stiff, crack resistant, and absorb energy during impact loading without fracturing. The other requirement of bone is that it be lightweight (i.e., heavier bone mass could mean higher energy requirement during locomotion). At the macrostructural level, this criterion is met by the proper selection of bone geometry and type of bone (cortical/cancellous bone) in each skeletal site.

An example of how bone geometry and the type of bone are selected to suit the loading condition in a particular skeletal site is discussed below. Long bones (e.g., femur and tibia) of every terrestrial mammal are loaded by a combination of bending and axial compression. The mid shaft of long bones is made up of cortical bone and has a shape in the form of a cylinder. This design serves three purposes: (i) cortical bone is well suited for weight bearing and deformation resistance; (ii) the mineralized tissue mass is placed at a distance from the long axis to resist bending (discussed in detail in the next section – second moment of area); and (iii) a cylindrical structure is much lighter than a solid structure. In terms of resisting bending, however, there are important interactions between bone and muscle. Friedrich Pauwels (1885–1980) examined this issue and concluded that without muscle contractions, a tubular bone subjected to a bending moment will have undesirably high tensile stresses along the convex surface (12). Pauwels showed elegant anatomical principles that resulted in the long bones of the lower extremity having considerably reduced tensile stresses (Fig. 2). These principles included the role of muscles, tendons, and ligaments acting as tension bands along the adjacent bone face, and the fact that the femur and tibia bones are curved so as to bring the body weight vector closer to the long axis of each bone, thereby reducing bending and associated tensile stresses. The use of a tension band is also currently made in fracture fixation in sites such as the olecranon, patella, and malleoli.

Certain weight-bearing skeletal sites benefit from the presence of large amounts of cancellous bones. For example, the vertebral bodies and the calcaneus consist of mostly cancellous bone surrounded by a thin cortical shell (Fig. 3). Cancellous bone offers some advantages in these skeletal sites. First, it tolerates great deformation (peak strains) when compared to cortical bone to accommodate flexion, rotation (in case of spine), and high impact loading (in case of the calcaneus). Second, the porous network makes the material lighter (9).

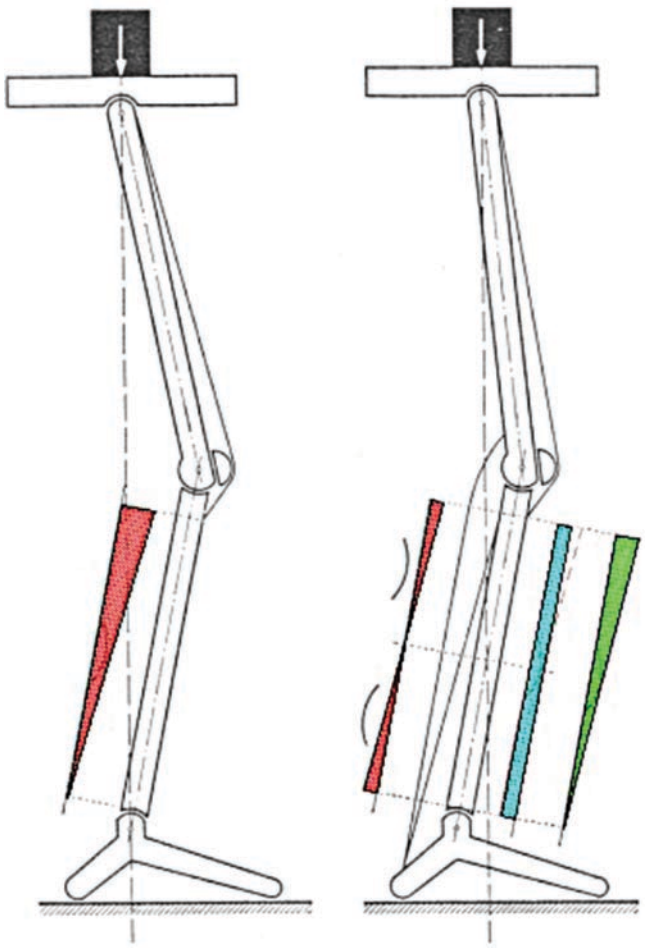

Fig. 2 The work of Pauwels explained how tensile stresses (*shown in red*) are highest where the body weight vector is further away from the long axis of the bone. He also showed how, through muscle contractions in the Triceps Surae (causing stresses *shown in blue*), the resulting tensile stresses (*green*) could be greatly reduced (12). This same principle explains how contractions in the hip abductors can reduce bending stresses in the femoral neck

Apart from having the right type of bone at a particular skeletal site, the bones are also optimally oriented to avoid excessive deformation in the direction of customary loading. Bones exhibit different material properties in different directions and this property is termed *anisotropy*. For example, the trabecular pattern within the calcaneus reflects the stress and strains experienced by the bone (Fig. 3). In the calcaneus, the trabeculae are arranged along the lines of compressive and tensile stresses produced during weight bearing (13).

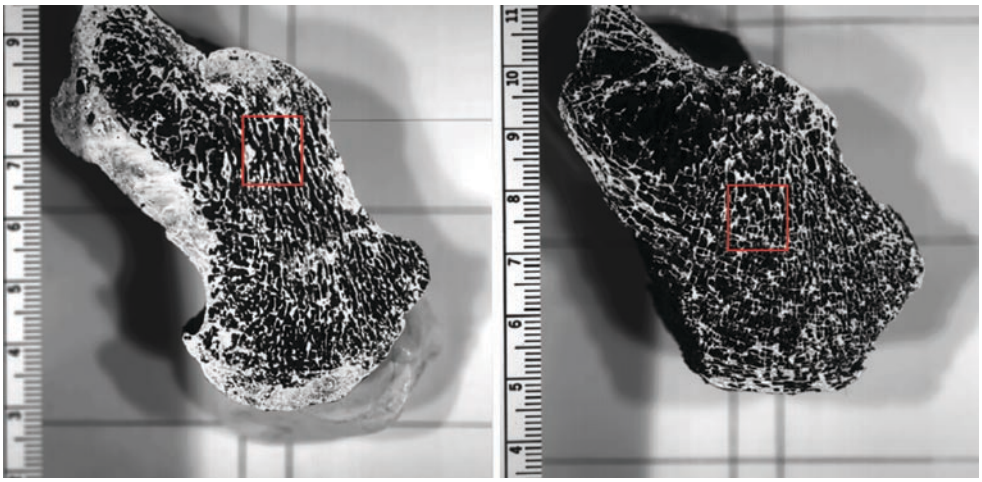

Fig. 3 Healthy calcaneus obtained from 70 kg, 33-year-old male (*left*). Calcaneus obtained from 80 kg, 71-year-old female (*right*)

Role of Age and Gender

All individuals lose bone with advancing age. As described previously, this is mainly due to increased bone mineral loss. Other reasons include deterioration of bone collagen quality (14) and change in bone microarchitecture. There are gender differences in bone size, rate of bone loss, and bone loss pattern. Males have larger skeletons compared to females (15). For example, the vertebral bodies are wider and taller in men than in women. Puberty plays a major role in determining the size of the skeleton. In females, estrogen produced after puberty *limits* the diameter of the bone by inhibiting periosteal bone formation. On the other hand, pubertal androgen in males *increases* periosteal bone formation and bone diameter (9).

The size of the skeleton plays an important role in fracture mechanics. For example, in long bones (cortical), larger cross sections have greater strength in bending and torque than do smaller cross sections with equal amounts of bone. Thus, smaller bone size makes women more vulnerable to fractures than men. Because of the same reason, it is not surprising to observe that long bones usually become wider (periosteal bone formation) and thinner in older adults. This way bones can maintain its strength despite having lesser BMD. This dependence on geometry also explains why tibial fractures tend to occur more distally: not only is the cross-sectional area less, but the resistance to bending (called "second moment of area" in geometric terms) is considerably less at a height corresponding to about a third of the distance between the medial malleolus and the tibial plateau.

The ability of long bones to resist bending is strongly dependent on the distance of the bone mass relative to its central long axis and is explained by the second moment of area. The second moment of area is a geometric property (similar to perimeter or area of a circle) and therefore does not depend on the type of material. This property also explains why a solid plastic rod is easier to bend than a drinking straw, even though both may be made from the same type and amount of material. Let's compare the magnitude of bending deflection of three different cylinders (Fig. 4) made from the same *type* of material and having the same *cross-sectional areas*. The magnitude of bending deflection (D) for a cylinder is given by the equation

$$D = \frac{ML^2}{8EI}$$

where M is the bending moment, L is the length, E is the elastic modulus, and I is the cross-sectional second moment of area.

The second moment of area for a circular cross section is given by the equation

$$I = \frac{\pi}{4}\left[R_o - R_i\right]$$

where R_o is the outer radius and R_i is the inner radius.

One can immediately see from Fig. 4 that the bending resistance increases significantly as the material is placed farther away from the central axis. It should be noted that this trend will be true as long as the buckling ratio $[R_o/(R_o - R_i)]$ is less than 10. If the buckling ratio exceeds 10 (i.e., if the cylindrical wall becomes too thin), then the cylinder will fail due to structural instability.

By age 50, the risk of sustaining fracture is three times greater for women than for men (16). The main reason for this is menopause, that is, bone loss in women increases rapidly once women reach menopause. Postmenopausal bone loss is mainly caused by estrogen deficiency. In addition, the pattern of cancellous bone loss is different in men and women. Cancellous bone loss in men occurs mainly by reduced bone formation and trabecular thinning (17). Cancellous bone loss

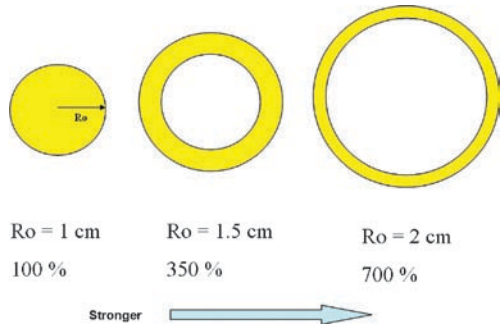

Fig. 4 Bending resistance in cylinders that have identical cross-sectional areas and material properties. For an identical axial force (compression or tension), the ability of the cylinder to resist bending is strongly dependent on the distance of the material relative to the center of the cylinder

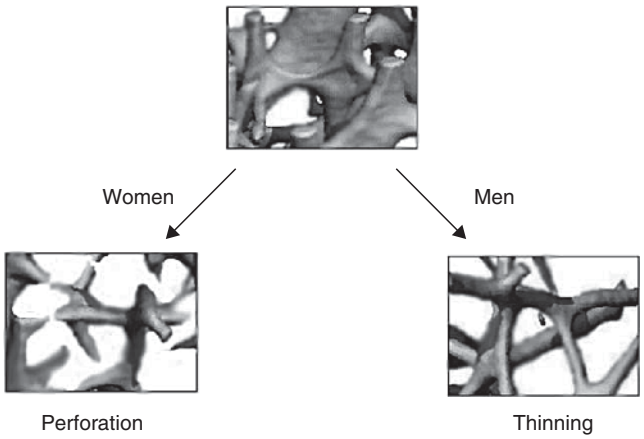

Fig. 5 Mechanisms of loss of trabecular bone in women and trabecular thinning in men

in women is primarily the result of a complete removal of some trabeculae (Fig. 5), leaving those that remain more widely separated and less well connected. Trabecular connectivity is necessary for bone strength. Loss of trabecular connectivity is almost irreversible and leads to permanent alteration in trabecular microarchitecture. Loss of trabecular connectivity makes a larger contribution to the total loss of cancellous bone compared to trabecular thinning (18). Therefore, trabecular bone strength is better preserved in men than in women.

There are also other factors such as race which play a role in fracture risk within same gender. Blacks have greater trabecular and cortical bone thickness when compared to Whites and Asians. It is interesting to note that the higher trabecular bone thickness causes lower bone turnover in blacks. Low bone turnover is due to the lower bone surface-to-volume ratio of the cancellous bone. A reduction in the rate bone turnover could provide a means for preserving bone mass in blacks. In addition, the higher trabecular bone thickness also protects the bone from fatigue damage (19, 20).

Diseases and Bone Fractures

The risk of bone fracture increases with many systemic diseases such as Paget's disease, hypogonadism, rickets, and osteogenesis imperfecta. There are also other disease conditions, such as periodontal disease and diabetes (especially type I) that are detrimental to bone health. Diabetes also causes retinopathy, which increases the risk for fall and diabetic neuropathy is associated with Charcot joints and fractures.

Fracture Prediction

Bone Mineral Density Measurement

Currently, BMD measurement remains the best method for assessing the risk of bone fractures (21). It is well accepted that the amount of mineral is the main determinant of mechanical properties in bone. However, it should be noted that BMD measurements alone can only predict up to ~65–70% of bone strength (22). BMD or bone mass can be measured noninvasively by using X-ray absorptiometry or quantitative ultrasound. X-ray absorptiometry is based on the principle that bone attenuates or absorbs ionizing radiation. Dual-Energy X-ray Absorptiometry (DEXA) is the most commonly used X-ray absorptiometry technique to measure BMD. Even though physical density is defined as mass of the body divided by its volume, bone density in clinical practice is defined differently. BMD measured by using X-ray absorptiometry is defined as the ratio of BMC divided by the two-dimensional projected bone area. The BMD thus measured is areal BMD and is usually expressed in g/cm^2. It should be noted that BMD values are poor indicators of whole bone strength and bone mass (23).

BMD values obtained by DEXA are strongly dependent on bone size and may be obscured by changes in skeletal size. This problem can be avoided by measuring volumetric BMD, as this measurement is independent of skeletal size. Volumetric BMD can be measured by using quantitative computer tomography (QCT) imaging. Computed tomography permits selective measurement of cortical and trabecular density (24).

Quantitative ultrasound (QUS) on the other hand does not measure BMD directly; it is usually described as a measure of bone quality. Quantitative ultrasound measures bone parameters by passing a pulse of ultrasonic waves through the bone. The speed of ultrasonic wave propagation and the extent of attenuation are determined by bone density and bone microarchitecture. The usual site of quantitative ultrasound measurement is the calcaneus. QUS is inexpensive, small, and portable, and does not involve the use of ionizing radiation.

The *T*-score was suggested in order to avoid confusion between different BMD measurement technologies and to simplify the interpretation of BMD measurements. *T*-score compares the measured BMD with the expected young normal value, and one can then immediately determine whether the measured BMD is normal, high, or low. *T*-score is calculated using the following equation and is dimensionless:

$$T \text{ - score} = \frac{\text{BMD} - \text{YN}}{\text{SD}}$$

where BMD is the measured bone density and YN is the expected young normal value. SD is the young normal population's standard deviation. The values of young normal population are usually collected from healthy women aged 20–40 years old, women who have no history of bone fractures or other conditions that affect bone metabolism. A *T*-score of below –2.5 is an indication of severe osteoporosis. The risk of fracture is unacceptably high for these patients (25). It should also be noted that most fractures in absolute numbers happen in individuals with *T*-scores between –1 and –2.5 (26).

Nonskeletal Factors and Fracture Prediction

The risk of future fractures of any type increases twofold in peri-/postmenopausal women with a history of one fracture (27). However, the presence of a vertebral fracture increases the risk of subsequent vertebral fractures by fivefold within the initial year (28). Fractures in the elderly are usually caused by falls (low energy trauma). The best predictor of falling is a previous fall. Some of the other common risk factors for fall include lower limb dysfunction, neurologic conditions, barbiturate use, and impairments in muscle strength, vision, balance, and gait.

Fracture Prevention

There are a number of approaches used to prevent bone fractures. These approaches are aimed at strengthening bones, preventing falls, and protecting bones from trauma. In children, optimal mineralization of the skeleton can be achieved by calcium uptake and physical activity (29). In adults, the goal of osteoporosis treatment is fracture reduction. Osteoporosis can be treated with antiresorptive agents (e.g., alendronate sodium, estrogen) or anabolic agents (e.g., parathyroid hormone, fluoride, prostaglandin E). The majority of the pharmacological treatments now available for osteoporosis work by inhibiting bone resorption. It should be noted that the drug treatments have side effects and hence, it is important to prevent bone loss before the first fracture, particularly in women. In addition, the way to prevent fractures is to maintain bone strength before the first fracture. The reason for this is bone loss is almost largely irreversible (e.g., loss of trabecular connectivity) by the time the first fracture occurs. The best way to prevent bone loss during old age is physical activity and proper diet (30).

Energy absorption is the most important factor that influences the risk of hip fracture. It has been found that the soft tissue thickness in women with hip fractures is reduced. This prompted the use of external hip protectors. Modification of hazards at home including the removal of rugs, safer foot wear, use of nonslip flooring, lighting at night, and addition of stair rails are other methods (31). Advancements in motor vehicle design proved to be more protective of the human chest and head, but less so of the lower extremities (32).

Role of Exercise in Strengthening Bones

As mentioned previously, bones respond to the demands placed upon them in accordance with the well-known "Wolff's law" (33). This principle explains far more than the reorganization of trabecular patterns: it relates to (i) disuse osteoporosis, (ii) the merits of one form of exercise over another in terms of osteogenic potential, and (iii) optimal design of joint replacements and fracture fixation devices.

Disuse osteoporosis: It is well documented that a physiologic effect of musculoskeletal unloading, such as occurs when astronauts spend time in microgravity conditions, or during bedrest, is the loss of calcium from bone [e.g., Whedon et al. (34)]. It is likely that other factors related to bone strength are also affected. For example, Schneider (1989) pointed out that a deterioration of the collagenous matrix of weight-bearing bones would in turn cause an elevated urinary output of hydroxyproline (35). According to Leach and Rambaut (1977) and Rambaut and Goode (1985), this is precisely what occurred during NASA's Skylab missions (36, 37). The latter group reported a 25% increase in hydroxyproline level during the first 30–40 days of spaceflight. Thus, while calcium loss may be a way to track bone loss during periods of disuse, preventing calcium loss alone, if that was possible, is not likely to adequately prevent the deterioration of skeletal integrity.

Both calcium and hydroxyproline excretion have been found to stabilize at elevated levels after 4 weeks of space flight (37, 38). Whedon (1984) has suggested that the process of mineral loss may continue for many months in space, based on the similarity between losses in total body calcium during the Skylab missions and bed-rest studies. Tilton, Degioanni, and Schneider (1980) reported that spaceflight led to a statistically significant loss of bone mineral for as long as 5 years postflight (39). Even if bone reaches a new

homeostatic equilibrium in space, there is the possibility of irreversible osteoporotic changes which could preclude the restoration of normal bone structure in 1G. For example, new trabecular bone can only be deposited on existing scaffolding. Severe osteoporosis can destroy even the basic framework of bone through resorption of trabeculae to the point where they become perforated and then separated (40).

The bones of the lower extremity are particularly at risk during spaceflight (37, 41). Whedon (1984) suggested that a 5% loss in total body calcium over a period of 1 year in space could reflect a 25% loss of calcium in the lower extremities (38). This preferential loss of bone in the lower extremities during weightlessness is in contrast to the conditions of senile osteopenia or osteoporosis that affect patients on Earth. In these cases, the radius is an equally sensitive predictor of mineral loss.

The load-bearing capabilities of bone are directly related to its structural and material properties. Strength is typically proportional to the square of its density (42). Any reduction in density is therefore likely to have a profound effect on bone strength. In a 12-week study involving a sheep model, Thomas et al. (1996) unloaded the calcaneus using an external fixator that still allowed the animals to ambulate (43). They found a 29% decrease of trabecular bone volume in immobilized calcanei compared with nonimmobilized calcanei. This reduction was due to thinning of trabeculae (98.9 vs. 72.4 mm) without any change in trabecular number. This large bone loss was similar to that observed in a previous study (44) that showed a 22% loss in BMC in the calcaneus following 12 weeks of disuse. A study involving humans (45) showed an average loss of bone of 10.4% in six males after 17 weeks of bed rest.

The significance of bone loss following disuse becomes apparent when considering the literature pertaining to osteoporosis of the femoral head. Greenspan et al. (1994) reported that a one-standard deviation reduction in BMD increased the chances of hip fracture 2.4 times (46). In a study of older (59–83 years) and younger (17–51 years) subjects, Courtney et al. (1995) showed that a one standard deviation in the younger group corresponded to 8.5% of the BMD (47). It is also noteworthy that BMD for the older group was 30% lower than for the younger group and that the mean age difference was 41 years. This highlights the fact that losing 22–29% of bone following 12 weeks of disuse may be likened to three decades of aging.

The merits of one form of exercise over another in terms of osteogenic potential: For instance, one study (30) compared cyclists, runners, and control subjects who participated in an exercise experiment over an 18-month period. The results showed that cycling and running had comparable benefits in preserving hip BMD in middle-aged master female athletes (compared with non-exercisers), but at the level of the spine, only running had beneficial effects (i.e., there was no difference between cycling and a sedentary lifestyle as far as BMD of the spine was concerned). This "bone preserving" benefit of relatively high loading on the lower extremity has also been demonstrated in a variety of studies by Snow and her colleagues: (i) 89 prepubescent children participated in a 7-month exercise regimen during the school day, three times per week. The group that performed jumping exercises had significantly higher BMC values at the femoral neck (+4.5%) and lumbar spine (+3.1%) than children who did stretching exercises (48). These gains in BMC were retained even after an equivalent period of detraining (49). (ii) Witzke and Snow (2000) showed that jump training increased BMC of the greater trochanter in adolescent girls (+3.1%) compared with subjects who simply maintained their usual daily activities (+1.9% gain) (50). (iii) A group of 18 postmenopausal women participated in a 32-week/year exercise intervention protocol over a period of 5 years (51). This study showed the bone-protective nature of jumping exercises, since these individuals either maintained their BMD or had slight improvements (e.g., +1.5% at the femoral neck), whereas the control group lost bone at all sites (e.g., –4.4% at the femoral neck level).

From a mechanics point of view, exercises such as walking, running, and jumping are associated with high forces under the feet that range from one to two or three times bodyweight. These forces are largely due to the deceleration of the body as a whole as the lower extremity makes contact with the ground. It is therefore not unreasonable to expect skeletal benefits across the entire axial skeleton during dynamic activities. This is precisely what was shown by a study that involved applying 1.5× bodyweight forces to the right hindlimb of rabbits (52). They found increased osteonal bone formation in the vertebral column extending at least to the cervical spine. Activities such as walking and running, therefore, have benefits that extend beyond the body segment sustaining the initial force that is applied to the human body.

Optimal design of joint replacements and fracture fixation devices: While Wolff's law explains how disuse negatively affects bone density, and how exercise can promote bone health, one might ask how this law relates to the interactions between orthopedic implants and underlying bone. The answer is that bone health can be affected in either a positive or negative manner, depending on the magnitudes of the stresses induced by the implant. If the stresses are too low (similar to the disuse situation but, in the orthopedic implant field, referred to as stress shielding), or too high, then bone can be lost. In the case of the latter, damage accumulation in living tissues occurs when the rate of damage formation exceeds the rate of repair. For high loading rates, bones can develop "stress fractures" due to the growth and coalescence of fatigue-related microdamage (53). Quantitatively, microdamage in lamellar bone can occur when the mechanical

strain exceeds 3,000–4,000 microstrain, corresponding to stresses of 45–60 MPa (54). This explains why, for instance, implants inserted into the tibia of a rabbit model caused bone loss around the implant neck (55). Finite element analyses showed high strains in this region, corresponding with bone modeling and remodeling secondary to microdamage. Similar findings describing crater-like bone defects due to high stresses were reported by Duyck et al. (56).

Summary

As an individual subjects his/her skeletal structures to mechanical loads, microcracks develop over time. While still young, an individual is able to deal with these "wear and tear" problems by activating osteoclasts to remove old bone and by relying on osteoblasts to lay down new bone. The problem can also be dealt with by performing dynamic exercises, since these seem to have beneficial effects across the age spectrum and across multiple skeletal sites. As a person ages, however, there is (i) a tendency to exercise less and (ii) hormonal and physiological process combines to create a negative bone balance. Over time, especially in females, this results in a significantly increased likelihood of developing fractures. This is especially problematic in cancellous bone regions and leads to the well-known problems of hip fractures, spinal collapse, and wrist fractures following a fall. Remedies to the hip fracture epidemic are likely to involve multiple approaches, including but not limited to osteoclast inhibitors, osteoblast activators, and appropriate exercise regimens. Altered life styles (e.g., by wearing padded undergarments) and perhaps modified living arrangements (such as stiff but collapsible bathroom flooring) may be further approaches that benefit particularly high risk individuals.

References

1. Frost HM. From Wolff's law to the Utah paradigm: Insights about bone physiology and its clinical applications. Anatomical Record 2001;262(4):398–419.
2. Melton 3rd LJ. Who has osteoporosis? A conflict between clinical and public health perspectives. 2000:2309–14.
3. Heaney RP. 2003;Is the paradigm shifting? Bone 33(4):457–65.
4. Oxlund H, Mosekilde L, Ortoft G. Reduced concentration of collagen reducible cross links in human trabecular bone with respect to age and osteoporosis. Bone 1996;19(5):479–84.
5. Gage BF, Birman-Deych E, Radford MJ, Nilasena DS, Binder EF. Risk of osteoporotic fracture in elderly patients taking warfarin: Results from the National Registry of Atrial Fibrillation 2. Archives of Internal Medicine 2006;166(2):241–6.
6. Hubbard RB, Smith CJP, Smeeth L, Harrison TW, Tattersfield AE. 2002;Inhaled corticosteroids and hip fracture: A population-based case-control study. American Journal of Respiratory and Critical Care Medicine 166(12):1563–6.
7. Jee WSS. Integrated bone tissue physiology: Anatomy and physiology. In: Cowin SC, Ed. Bone Mechanics Handbook. Second ed. Florida: CRC Press; 2001:1–68.
8. Currey JD. The design of mineralised hard tissues for their mechanical functions. Journal of Experimental Biology 1999;202(23):3285–94.
9. Seeman E. Periosteal bone formation – A neglected determinant of bone strength. New England Journal of Medicine 2003;349(4):320–3.
10. Wolff J. Über die Bedeutung der Architektur der spongiösen Substanz, Zentralblatt für die medizinische Wissenschaft, VI. Jahrgang. 1869:223–34.
11. Haapasalo H, Kontulainen S, Sievanen H, Kannus P, Jarvinen M, Vuori I. Exercise-induced bone gain is due to enlargement in bone size without a change in volumetric bone density: A peripheral quantitative computed tomography study of the upper arms of male tennis players. Bone 2000;27(3):351–7.
12. Pauwels F. Biomechanics of the Locomotor Apparatus. (Translated from German by P. Maquet and R. Furlong). Berlin: Springer-Verlag; 1980.
13. Jhamaria NL, Lal KB, Udawat M, Banerji P, Kabra SG. The trabecular pattern of the calcaneum as an index of osteoporosis. Journal of Bone and Joint Surgery-British Volume 1983;65(2):195–8.
14. Zioupos P, Currey JD, Hamer AJ. The role of collagen in the declining mechanical properties of aging human cortical bone. Journal of Biomedical Materials Research 1999;45(2):108–16.
15. Seeman E. The structural and biomechanical basis of the gain and loss of bone strength in women and men. Endocrinology and Metabolism Clinics of North America 2003;32(1):25–38 (Review).
16. Chevalley T, Hoffmeyer P, Bonjour JP, Rizzoli R. An osteoporosis clinical pathway for the medical management of patients with low-trauma fracture. Osteoporosis International 2002;13(6):450–5.
17. Seeman E. The structural basis of bone fragility in men. Bone 1999;25(1):143–7.
18. Parfitt AM. Implications of architecture for the pathogenesis and prevention of vertebral fracture. Bone 1992;13:S41–S47.
19. Seeman E. From density to structure: Growing up and growing old on the surfaces of bone. 1997:509–21.
20. Han ZH, Palnitkar S, Sudhaker DR, Nelson D, Parfitt AM. Effects of ethnicity and age or menopause on the remodeling and turnover of iliac bone: Implications for mechanisms of bone loss. 1997:498–508.
21. Faulkner KG. Bone matters: Are density increases necessary to reduce fracture risk? 2000:183–7.
22. Aerssens J, Boonen S, Joly J, Dequeker J. Variations in trabecular bone composition with anatomical site and age: Potential implications for bone quality assessment. Journal of Endocrinology 1997;155(3):411–21.
23. Frost HM. Coming changes in accepted wisdom about "osteoporosis". Journal of Musculoskeletal and Neuronal Interactions 2004;4(1):78–85.
24. Augat P, Gordon CL, Lang TF, Iida H, Genant HK. Accuracy of cortical and trabecular bone measurements with peripheral quantitative computed tomography (pQCT). Physics in Medicine and Biology 1998;43(10):2873–83.
25. Watts NB. Fundamentals and pitfalls of bone densitometry using dual-energy X-ray absorptiometry (DXA). Osteoporosis International 2004;15(11):847–54.
26. Karlsson M. Physical activity, skeletal health and fractures in a long term perspective. Journal of Musculoskeletal and Neuronal Interactions 2004;4(1):12–21.
27. Klotzbuecher CM, Ross PD, Landsman PB, Abbott TA, Berger M. Patients with prior fractures have an increased risk of future fractures: A summary of the literature and statistical synthesis. Journal of Bone and Mineral Research 2000;15(4):721–39.
28. Lindsay R, Silverman SL, Cooper C, et-al.. Risk of new vertebral fracture in the year following a fracture. Jama – Journal of the American Medical Association 2001;285(3):320–3.

29. Boot AM, deRidder MAJ, Pols HAP, Krenning EP, KeizerSchrama S. Bone mineral density in children and adolescents: Relation to puberty, calcium intake, and physical activity. Journal of Clinical Endocrinology and Metabolism 1997;82(1):57–62.
30. Beshgetoor D, Nichols J, Rego I. Effect of training mode and calcium intake on bone mineral density in female master cyclist, runners, and non-athletes. International Journal of Sport Nutrition and Exercise Metabolism 2000;10(3):290–301.
31. Tinetti ME. Clinical practice: Preventing falls in elderly persons. 2003;348(1):1–2.
32. Yoganandan N, Pintar FA, Kumaresan S, Boynton M. Axial impact biomechanics of the human foot-ankle complex. Journal of Biomechanical Engineering-Transactions of the Asme 1997;119(4):433–7.
33. Turner CH. On Wolff's law of trabecular architecture. Journal of Biomechanics 1992;25(1):1–9.
34. Whedon GD, L L, Rambaut PC, et-al. Mineral and nitrogen metabolic studies, experiment M071. In: Johnston RS, Dietlein LF, Eds. Biomedical Results from Skylab. Washington: NASA SP-377. NASA; 1977:164–74.
35. Schneider VB. Space medicine considerations: Skeletal and calcium homeostasis. In: Workshop on Exercise Prescription for Long-Duration Space Flight. 1989:47–52.
36. Leach CS, Rambaut PC. Biochemical responses of the Skylab crewmen: An overview. In: Johnston RS, Dietlein LF, Eds. Biomedical Results from Skylab. Washington: NASA SP-377. NASA; 1977:204–20.
37. Rambaut PC, Goode AW. Skeletal changes during space-flight. Lancet 1985;2(8463):1050–2.
38. Whedon GD. Disuse osteoporosis – Physiological aspects. Calcified Tissue International 1984;36:S146–S150.
39. Tilton FE, Degioanni JJC, Schneider VS. Long-term follow-up of Skylab bone demineralization. Aviation, Space, and Environmental Medicine 1980;51(11):1209–13.
40. Parfitt AM. The coupling of bone formation to bone resorption – A critical analysis of the concept and of its relevance to the pathogenesis of osteoporosis. Metabolic Bone Disease and Related Research 1982;4(1):1–6.
41. Zernicke RF, Vailas AC, Salem GJ. Biomechanical response of bone to weightlessness. Exercise and Sport Sciences Reviews 1990;18:167–92.
42. Carter DR, Hayes WC. The compressive behavior of bone as a two-phase porous structure. The Journal of Bone and Joint Surgery 1977;59(7):954–62.
43. Thomas T, Vico L, Skerry TM, et-al.. Architectural modifications and cellular response during disuse-related bone loss in calcaneus of the sheep. Journal of Applied Physiology 1996;80(1):198–202.
44. Skerry TM, Lanyon LE. Interruption of disuse by short duration walking exercise does not prevent bone loss in the sheep calcaneus. Bone 1995;16(2):269–74.
45. Leblanc AD, Schneider VS, Evans HJ, Engelbretson DA, Krebs JM. Bone-mineral loss and recovery after 17 weeks of bed rest. Journal of Bone and Mineral Research 1990;5(8):843–50.
46. Greenspan SL, Myers ER, Maitland LA, Resnick NM, Hayes WC. Fall severity and bone-mineral density as risk-factors for hip fracture in ambulatory elderly. Jama – Journal of the American Medical Association 1994;271(2):128–33.
47. Courtney AC, Wachtel EF, Myers ER, Hayes WC. Age-related reductions in the strength of the femur tested in a fall-loading configuration. The Journal of Bone and Joint Surgery 1995;77(3):387–95.
48. Fuchs RK, Bauer JJ, Snow CM. Jumping improves hip and lumbar spine bone mass in prepubescent children: A randomized controlled trial. Journal of Bone and Mineral Research 2001;16(1):148–56.
49. Fuchs RK, Snow CM. Gains in hip bone mass from high-impact training are maintained: A randomized controlled trial in children. Journal of Pediatrics 2002;141(3):357–62.
50. Witzke KA, Snow CM. Effects of plyometric jump training on bone mass in adolescent girls. Medicine and Science in Sports and Exercise 2000;32(6):1051–7.
51. Snow CM, Shaw JM, Winters KM, Witzke KA. Long-term exercise using weighted vests prevents hip bone loss in postmenopausal women. Journals of Gerontology Series a – Biological Sciences and Medical Sciences 2000;55(9):M489–M491.
52. Burr DB, Martin RB, Martin PA. Lower-extremity loads stimulate bone-formation in the vertebral column – Implications for osteoporosis. Spine 1983;8(7):681–6.
53. Prendergast PJ, Huiskes R. Microdamage and osteocyte-lacuna strain in bone: A microstructural finite element analysis. Journal of Biomechanical Engineering-Transactions of the Asme 1996;118(2):240–6.
54. Frost HM. Mechanical usage, bone mass, bone fragility: A brief overview. In: Kleerekoper M, Krane SM, Eds. Clinical disorders of bone and mineral metabolism. New York: Mary Ann Liebert, Inc.; 1989:15–40.
55. Hoshaw SJ, Brunski JB, Cochran GVB. Mechanical loading of Brånemark implants affects interfacial bone modeling and remodeling. International Journal of Oral & Maxillofacial Implants 1994;9:345–60.
56. Duyck J, Ronold HJ, Van Oosterwyck H, Naert I, Sloten JV, Ellingsen JE. The influence of static and dynamic loading on marginal bone reactions around osseointegrated implants: An animal experimental study. Clinical Oral Implants Research 2001;12(3):207–18.

Chapter 5
The Laboratory in Orthopedic Practice

Vivian Arguello-Guerra and Jasvir S. Khurana

Abstract The laboratory in orthopedic practice is involved in a variety of ways. These include the tissue bank that helps with the storage and retrieval of nucleic acids. The molecular and cytogenetic laboratory is also involved in their analysis and molecular genetic studies for tumors and skeletal diseases and dysplasias. The anatomic pathology laboratory is of course involved in the analysis of biopsy and resection specimens. The clinical chemistry and microbiological laboratory is involved with a variety of tests and assays for metabolic bone disease, infections, and other conditions affecting the skeleton.

Keywords Tissue banking • Calcitonin • Vitamin D • Serum acid phosphatase • Hydroxyproline • Pyridinium cross-links • Parathyroid hormone • Deoxypyridinoline • Osteocalcin • Acid phosphatase • Cytogenetics • Fluorescent in situ hybridization • Immunohistochemistry • Antibody • Electron microscopy

Tissue Banking

This refers to the system of *storage and retrieval of genomic nucleic acids* for study by molecular methods. The setting up of a tissue bank is advantageous for the study of musculoskeletal neoplasms, bone infections, and inherited and genetic diseases of the skeleton.

Although an increasing number of techniques can be applied to formalin fixed, paraffin embedded tissues, these methods suffer from several problems. Fixed tissues suffer from contamination of the processing, and this may be problematic in certain cases. For example, mycobacterial resident in the wax may contaminate the sample in PCR reactions. Additionally, although DNA studies can be attempted on fixed material, frozen tissue is optimal for RNA extraction. Thus, setting up a tissue bank is advised for investigators wishing to carry out such studies. Moreover, material frozen and stored in a tissue bank can be archived and saved for long periods of time for future research or diagnostic use. Frozen tissue can also be shipped, generally in dry ice, which may be needed for collaborative studies.

Tissue banking involves methods for rapid freezing of freshly excised tissues, their storage and archival, as well as a system for cataloguing and rapid retrieval of these.

Tissue freezing is generally accomplished by snap-freezing in dry ice or preferably in liquid nitrogen. Aluminum foil is generally used around the tissue for the process. Tissue thickness should be no more than 0.3 cm. Storage is in plastic cassettes or cryogenic vials. The storage conditions should be below −70°C. Temperatures of −140°C are optimal. Inventory data can be managed on computer programs developed on relational databases.

Extraction of DNA or RNA from *musculoskeletal tissues* is done in a fashion similar to other soft tissues. The modifications needed are only in the initial stage. Since bone cannot be minced, it is important to crush bone for extraction. This can be done when frozen using a hammer, and subsequently using a polytron type instrument. For RNA work (such as RT-PCR reactions), an RNAase free environment is required.

Bone Metabolism Assays

Bone remodeling is essential for stable skeletal architecture and metabolic homeostasis. This process is controlled by hormones like parathyroid hormone, calcitonin, and vitamin D, affecting the concentrations of minerals like calcium, phosphate, and magnesium. However, there are specific markers that indicate bone resorption and formation that may be assessed separately.

Clinical Chemistry

- Markers for bone turnover: serum acid phosphatase, hydroxyproline, pyridinium cross-links
- Markers for bone formation: serum alkaline phosphatase, osteocalcin
- Parathyroid hormone assay
- Vitamin D
- Calcitonin

J.S. Khurana (ed.), *Bone Pathology*, DOI 10.1007/978-1-59745-347-9_5,

Markers for Bone Turnover

A useful serum marker to measure *bone loss* is helpful in monitoring conditions such as osteoporosis. Traditional markers such as serum phosphatases or urinary hydroxyproline are elevated in conditions of very high turnover, such as Paget's disease, but lack the sensitivity for the lower rates of bone loss found in osteoporosis.

Some recent markers available commercially have rectified the situation somewhat. Pyrlinks-D (from Metra Biosystems) measures the urinary excretion of deoxypyridinoline cross-links as a measure of collagen breakdown.

Osteomark (from Ostex International) measures urinary excretion (via immunoassays) of cross-linked N-telopeptides (amino- and carboxyl-terminal collagen fragments) of type I bone collagen, again as a measure of bone turnover. Another pyridinoline assay CrossLapps measures the C-telopeptides with similar results.

A galacto-lysyl hydroxylysine assay is being developed in kit form, but is not yet available at the time of writing.

Measures of bone *formation* include *bone-specific* alkaline phosphatase and osteocalcin.

The major problem with urinary assays, at the moment, is the diurnal variation that occurs in the levels of these substances. This precludes "spot" urine testing, and makes it necessary for 24-h urine collection. This reduces the practicality and ease of the test. Serum assays in general suffer less from this problem. One such test is osteocalcin. This, however, is not generally available commercially.

Since bone resorption and formation are coupled (see section *Remodeling*), it is possible to use a test for bone formation as a surrogate marker for resorption. However, this concept is counterintuitive and has difficulty in acceptance by practicing physicians and laboratorians.

Parathyroid Hormone Assay

Radioimmunoassay

Although described in the early 1960s, the technique of radioimmunoassay (RIA) has become applicable in the automated clinical laboratory only recently. The main problem complicating the introduction has been the heterogeneous nature of the circulating hormone. The biologically active N-terminal part of the hormone is only a small fraction of the circulating hormone. The inactive portions (mid region and C-terminal) are cleared less rapidly and persist longer. The inactive fragments are especially prone to prolonged circulation in renal failure leading to greater concentrations in these patients, since their excretion is by glomerular filtration.

Since the 1970s, attempts have been made to develop antisera with the required regional specificity to allow a meaningful assay. These assays measure the N-terminal fragment or the intact hormone. They are less dependent on renal excretion and can be better applied even in renal failure. Discriminate analysis with simultaneous calcium measurement is required for optimal interpretation.

RIA is not sufficiently sensitive to distinguish subnormal from normal levels. They cannot distinguish hypercalcemia of malignancies (PTH-like species) from true primary hyperparathyroidism.

Noncompetitive Immunometric Assays

Intact PTH can now be measured as immunoradiometric (IRMA), when radiolabeled; or immunochemiluminometric, labeled by a chemiluminescent compound (1). The latter is also known as a two-site antibody assay. The technique utilizes two separate antibodies to the N and the C-terminals; the antibody to the C-terminal is absorbed onto a solid support. This method has an increased sensitivity and specificity over RIA. It is better able to distinguish subnormal levels, and can distinguish PTH-like species from primary hyperparathyroidism.

Vitamin D Assay

Vitamin D measurements are done on its metabolites. Usually the 25-hydroxy (25(OH)D) (most abundant metabolite) or the 1,25-dihydroxy ($1,25(OH)_2D$) (most bioactive form) is chosen. The assays should measure vitamin D2 and D3 because of their similar biological activity. These generally use a three-step process based on deproteinization, chromatographic separation, and quantitation by radioimmunoassay or HPLC (high pressure liquid chromatography) with UV absorption. This is followed by competitive protein binding assays. The cytosolic receptor for the assay is often obtained from animal models. For example, the receptor for 1,25-dihydroxyvitamin D is obtained from the intestinal mucosa of a rachitic chick.

Calcitonin

Calcitonin monomer is the biologically active entity of this hormone that is measurable. Radioimmunoassays have been done in the past, revealing low sensitivity and specificity. Other methods with greater sensitivity, like two-site immunometric assays (EIAs and IRMAs) are being practiced.

Serum Alkaline Phosphatase

Alkaline phosphatase is synthesized in a variety of organs. The measured form of serum alkaline phosphatase in the laboratory is the "*tissue non-specific*" form. This is a product of a gene on chromosome 1. The isoenzymes from bone and liver (all products of the same gene) can be differentiated by electrophoresis.

It is also important to distinguish the tissue non-specific form, from the alkaline phosphatase isoenzymes originating *from other genes*. These kinds of alkaline phosphatases are seen in organs such as the *placenta and the intestine*. Electrophoresis, chemical or immunochemical methods, and thermostability are used for this distinction. For example, the *placental* alkaline phosphatase enzyme is *thermostable* at 65°C for 30 min. *Osseous (bone*) alkaline phosphatase is *thermolabile*, whereas the forms from liver and intestine are of intermediate susceptibility.

Serum alkaline phosphatase is usually estimated by utilizing a substrate *p*-nitrophenyl phosphate. This is cleaved by alkaline phosphatase to chromogenic *p*-nitrophenoxide anion. This is estimated at 405 nm spectrophotometrically. This method generally replaces methods described by Bodansky or King-Armstrong. Bone alkaline phosphatase can be measured by immunoassay after its separation from other isoenzymes through "heat inactivation, wheat-germ agglutinin precipitation, electrophoresis, isoelectric focusing, and two-site immunoradiometric assays."

Serum alkaline phosphatase activity is increased in growing children, pregnancy, healing fractures, Paget's disease, rickets, osteomalacia, hyperparathyroidism, bone-forming tumors, and certain skeletal metastases. It is reduced in hypophosphatasia. It tends to be higher in individuals with blood groups B and O, who are secretors.

Placental	Thermostable
Intestinal	Intermediate
Tissue non-specific	
Osseous	Thermolabile
Liver	Intermediate
Kidney	Intermediate

Osteocalcin

There is no standardized assay for osteocalcin, because different fragments of the protein recognize different antibodies. However, immunoassays may be performed in serum or plasma, on the intact or midmolecule fragment.

Acid Phosphatase

There are two forms of acid phosphatase. One isoenzyme is of prostatic origin, the other is from a variety of tissues including erythrocytes, platelets, and bone. The prostatic acid phosphatase can be differentiated from the latter by its sensitivity to tartaric acid. The action of bone acid phosphatase is not inhibited by tartrate and is referred to as tartrate-resistant acid phosphatase (TRAP).

Measurement of acid phosphatase is generally made by estimating the hydrolysis of thymolphthalein monophosphate into thymol by the enzyme. Thymol is quantitated spectrophotometrically at 595 nm. Immunochemical methods are also available, and may be preferred by laboratories because of ease in automation.

Serum TRAP is increased in Paget's disease, Gaucher's disease, metastatic bone disease, and other conditions of high bone turnover.

Hydroxyproline

Metabolism of this collagen breakdown component happens mainly in the liver. Only 10% is excreted in the urine. Urinary hydroxyproline is measured by HPLC or colorimetry.

Pyridinoline and Deoxypyridinoline

Pyridinium cross-links stabilize collagen chains within the extracellular matrix. Modification of these chains and their proteins results in pyridinoline (Pyd) and deoxypyridinoline (Dpd) as products. Dpd is specific for bone and helps assess (when elevated) individuals with increased risk for bone loss, whereas Pyd is also present in articular cartilage and soft tissue. Both are measured in urine by immunoassays or HPLC.

Cytogenetics, FISH, and Interphase Cytogenetics

Cytogenetics is being applied to musculoskeletal tumors for both diagnostic and prognostic reasons.

Traditional solid tumor cytogenetics relies on the use of in vitro tissue culture, followed by metaphase block and metaphase spreads. These are then stained by Giemsa, Quinacrine, or other stains (G-banding, Q-banding, etc.).

Use of interphase cytogenetics and fluorescent in situ hybridization (FISH) can, in time, eliminate the need for cell

culture. These methods can also be applied to archival (formalin fixed, paraffin embedded material). It is possible to use mapping probes, detect microdeletions, confirm translocations, identify certain marker chromosomes, and detect aneuploidy.

FISH involves three main steps:

- Denaturation of probe and target to single-stranded DNA
- Hybridization of probe and target
- Post-hybridization washes to remove nonspecifically bound probe.

FISH probes are of three types:

- *Painting probes* (covering the whole or part of a chromosome, coatasome). These identify a marker chromosome known to occur in certain neoplasms. The signal is diffuse and difficult to identify in interphase; they are thus used mainly in metaphase spreads.
- *Alpha satellite probes* (identify the centromeric region). They identify marker chromosomes and document loss or gain of chromosomes. These can be used in both interphase and metaphase.
- *Specific probes* (hybridize to a specific region on a chromosome). These identify the presence or absence of these regions. Probes can be combined to form cocktails, which then provide internal controls. This is especially important when deletion of a chromosome region is suspected.

Advantages and disadvantages of FISH:

Advantages	Disadvantages
Rapid (4 h), can be automated	Only get answers to specific questions
Does not require dividing cells	Will not pick up small deletions
Identifies marker chromosomes or small parts of chromosomes	Identifying chromosome where probe goes may be problematic
Examines large populations	Probe sensitivity can be variable
Contamination not a problem	Size limitations

Cytogenetics in Musculoskeletal Tumors

Tabulated below are some examples of characteristic cytogenetic abnormalities consistently associated with musculoskeletal tumors.

Tumor	Abnormality	Molecular defect	Utility
Ewing's sarcoma	T(11;22)(q24;q12)	EWS-FL1 fusion	Diagnostic
	t(21;22)(q22;q12)	EWS-ERG fusion	Diagnostic
Desmoplastic round cell tumor	t(11;22)(p13;q12)	EWS-WT1 fusion	Diagnostic
Alveolar rhabdomyosarcoma	t(2;13)(q35;q14)	PAX3-FKHR fusion	Prognostic
	t(113)(p36;q14)	PAX7-FKHR fusion	Prognostic
Myxoid liposarcoma	t(12;16)(q13;p11)	CHOP-TLS fusion	Diagnostic
Synovial sarcoma	t(X;18)(p11;q11)	SYT-SSX	Diagnostic
Clear cell sarcoma	t(12;22)(q13;q12.2-12.3)	Not known	Diagnostic
Myxoid chondrosarcoma	t(9;22)(q22;q12)	Not known	Diagnostic
Lipoma	Ring chromosome	Not known	Prognostic
Myxoid MFH	Ring chromosome	Not known	Prognostic
MFH	Chromosome 19 abnormalities	Not known	Prognostic

Explanations for Some Selected Tumors of Orthopedic Interest

Ewing's Sarcoma t(11;22) Chromosomal Translocation

This abnormality has been seen in peripheral neuro-ectodermal tumors, thus strengthening the belief that all these tumors are either identical or at the very least related. This test is now used clinically to support the diagnosis of Ewing's sarcoma and to differentiate this entity from tumors that may mimic it on histological grounds alone, such as poorly differentiated carcinomas, lymphomas, and small-round desmoplastic tumors. Whether this translocation also occurs in entities such as small-cell osteosarcomas and mesenchymal chondrosarcomas is not yet known.

By molecular methods, this chromosomal abnormality corresponds to the EWS/FL1 gene fusion. In actual fact, the EWS gene (located on chromosome 22 at q12) is translocated to the FL1 (a gene of the ETS family). This results in the formation of a chimeric protein product, and is seen in ~85% of patients. A second translocation, which has been identified in ~15% of patients is t(21;22) translocation, which fuses the EWS gene with a different member of the ETS family, the ERG gene located on chromosome 21 at q22 (2). This gives a hybrid EWS/ERG product. Whether these two kinds of Ewing's sarcoma (at the molecular level) behave differently clinically is unknown. These two kinds cannot be distinguished at the light microscopic level. Diagnostically, this is a convenient method of confirming or establishing the diagnosis of Ewing's tumor in selected cases.

Synovial Sarcomas

These have been shown to have a t(X;18) translocation. This finding is helpful in the diagnosis of monophasic synovial sarcomas and in the separation of other spindle cell tumors, which might be confused with it on light microscopy alone. Histogenetically, this has been useful in demonstrating that

synovial sarcomas do not "arise" from synovial tissue. This is supported by the finding of similar tumors with similar chromosomal defects in tissues such as the tongue, which do not contain synovium (3).

Cytogenetically, both lipomas and myxoid liposarcomas show alterations at chromosome 12. Some lipomas in particular may show the presence of ring chromosomes which may be associated with a subtype which have an increased tendency to recur. At the molecular level, lipomas differ from the myxoid liposarcomas, in that the methylation patterns are different. Also, a transcription factor called C/EBP homologous protein (CHOP) is rearranged in the myxoid liposarcomas but not lipomas (4–6).

Skeletal Muscle Tumors

The molecular basis of skeletal muscle differentiation is emerging. The attention is focused on the Myo D family of myogenic transcription factors. This family includes Myo D, myf-5, myogenin, and MRF4 (also called herculin and myf-6).

Clonal chromosomal abnormalities have been found in entities such as proliferative fasciitis, desmoid tumors, Peyronie's disease, Dupuytren's contractures, and osteochondroma. Parosteal osteosarcomas have been found to have ring chromosomes; alveolar rhabdomyosarcomas may show a t(2;13) chromosomal translocation. Skeletal muscle tumors with this translocation fall into a prognostically poor group. Clear cell sarcoma shows a distinctive chromosome 22 abnormality. Most often this is a reciprocal 12;22 translocation. This and several such other findings are increasingly being translated into diagnostically useful tests.

At the cytogenetic level, a malignant fibrous histiocytoma appears to be heterogeneous. Those associated with abnormalities of chromosome 19 appear to be prone to frequent recurrences. On the other hand, those associated with ring chromosome are associated with a myxoid histology and a less aggressive clinical behavior.

Similarly, complex chromosomal abnormalities have correlated with a more aggressive behavior in giant cell tumors (GCT) of bone. The histologic grading of such tumors is notoriously unreliable.

Other Applications of Cytogenetics in Orthopedic Pathology

An interesting application of cytogenetics has been the attempt at predicting methotrexate resistance by assessing the numbers of homogeneously staining regions and double minutes. These correspond to repeated copies of dihydrofolate reductase (7). X-chromosome inactivation studies have proven to be a powerful way of assessing clonality. In this technique, lesional tissue is taken from women. X chromosomal genes which show polymorphisms (such as the human androgen receptor gene or HUMARA) are then assessed. The basis of the technique lies in the Lyon hypothesis, that half the X-chromosomes are randomly inactivated in females, and that this is done by methylation. Therefore, most tissues can be expected to have half the inactive X-chromosomes from paternal and half from maternal origin (a problem sometimes encountered is skewed Lyonization). If the inactive chromosomes contain only paternal or only maternal genes, then they are consistent with a clonal origin. Inactive chromosomes can be easily looked for because methylation protects the DNA from the action of certain restriction endonucleases. Primer design and PCR reactions can be designed to amplify the required segments after such endonuclease digestion and the amplicons be assessed for size. Since genes such as HUMARA have sites of variable numbers of tandem repeats (VNTRs) at the polymorphic site, therefore the size difference shows paternal or maternal origin. A technique similar to this has been used by groups to demonstrate that pigmented villo-nodular synovitis and eosinophillic granuloma are both clonal proliferative processes, and thus would better fit "neoplasms" rather than "reactive" processes. This has gone some way toward settling a long standing controversy (8).

VNTRs have also been useful in the technique of molecular "fingerprinting." Such methods may become useful in situations of determining origin. For example, in a multifocal osteosarcoma, the eternal question is whether the lesions represent "metastases" from an initial lesion, or in fact if they are separate tumors. This question can now be addressed. Similarly, a radiation "induced" sarcoma can be probed to see if it is identical to the initial lesion for which the radiation was given. The utility of such techniques expands with the experience gained in using them.

The retinoblastoma gene (Rb) has served as a paradigm of a tumor-suppresser gene. Inactivation or loss of Rb appears to be a key step in the development of retinoblastoma and osteosarcoma. Constitutional deletion of chromosome 13 (bearing the Rb gene) occurs in a subset of patients. In sporadic tumors, a "two-hit" hypothesis is postulated. Additional alterations in p53 gene (another tumor suppressor gene) may be required in most osteosarcomas. A detailed discussion of molecular tests are given in Chapter 5.

Immunohistochemistry

Immunohistochemical analysis in bone tumors is similar in practice to the soft-tissue analogue. It can be applied to determine lineage, differentiation, proliferation, hormone

receptors, oncogenes, tumor suppresser genes, microbiologic agents, and so on.

As a diagnostic tool, immunohistochemistry has had tremendous impact. Between its initial routine of clinical usage in the early 1970s and its widespread, almost routine application in the laboratory today, there has been an explosive increase in availability of antibodies. This has been contributed by the ease in hybridoma technology, allowing the generation of monoclonal antibodies.

Mic 2 (CD 99) has become available for use in formalin fixed, paraffin embedded tissue. This stains the protein expression of a pseudoautosomal gene located on the X and the Y chromosomes.

Markers with osteoblastic differentiation have been developed for reliable identification of bone presence. Some of these are osteocalcin, osteonectin, type I collagen, osteopontin, and proteoglycans I and II. However, only osteocalcin and osteonectin are available for use in paraffin sections. Osteocalcin is available as a monoclonal antibody to aid the diagnosis of osteosarcoma as a marker for osteoid. Osteonectin has lower specificity because it highlights endothelia, fibrocytes, chondrocytes, among other structures. Similarly, histiocytic markers like KP1 (CD 68), lysozyme, a-1-trypsin, a-1-antichymotrypsin, and markers for dendritic and Langerhan's cells such as CD 1A and S100 protein are available for use on routinely processed tissue. These could help in the diagnosis of malignant fibrous histiocytoma, other histiocytic malignancies, infections, and Langerhan's cell histiocytosis. S100 protein is a marker for Langerhan's cells, melanoma, fat, cartilage, and certain neural tissues such as Schwann cells. This staining pattern can be utilized in specific instances.

Markers for muscle differentiation include Myo D, desmin, muscle-specific actin, myoglobin, and so on. These and several other antibodies are routinely applied nowadays to help in the characterization of tumor differentiation. These have reduced the need to employ electron microscopy, which was the only alternative until the 1970s and early 1980s.

Importantly, proliferative markers (such as Mib 1 and PCNA) can give a better idea about the tumor. This is a more reliable measure than the earlier method of counting mitotic figures. These had the disadvantage of being prone to influence of times and kinds of fixatives and processing as well as inter- and intra-observer variability. Immunohistochemical markers for oncogene, apoptosis proteins, and tumor suppresser genes like P53 and Rb are now available. These are expected to be routinely used and give information about the biology of the tumors as well as possible prognostic information.

Some of the more common antibodies of use in musculoskeletal pathology are tabulated below:

Antibody	Utility
Actins	α-Actin (smooth muscle), sarcomeric actin (striated muscle), myofibroblasts
Caldesmon	Smooth muscle and myofibroblasts and myoepithelium
Cytokeratins	Epithelial cells, some mesenchymal tumors, synovial cell sarcoma, chordoma, rhabdoid tumor, epithelioid mesenchymal tumors such as epithelioid sarcoma and epithelioid angiosarcoma
CD 31	Endothelial cells, well-differentiated vascular tumors, Kaposi's sarcoma
CD 34	Endothelial cells, some fibroblasts, well-differentiated vascular tumors, epitheloid sarcoma, Kaposi's sarcoma, dermatofibrosarcoma protruberans, solitary fibrous tumor, leiomyosarcomas
CD 57	(Leu 7; HNK-1) Natural killer cells, T lymphocytes, nerve sheath, and neuroendocrine cells; leiomyosarcoma and synovial sarcoma differentiate between fibrosarcoma and malignant peripheral nerve sheath tumor (MPNST), MFH versus MPNST, and myxoid nerve sheath tumor and non-neural myxoid neoplasms
CD 68	Histiocytes, myeloid cells, MFH, some melanomas, granular cell tumor
CD 99	Cortical thymocytes, Langerhans islet cells, Ewing's sarcoma, lymphoblastic lymphoma
Collagen type IV and laminin	MPNST
Desmin	Smooth and skeletal muscle, desmoplastic round cell tumor
EMA	Epithelia, perineural cells, meningioma
GFAP	Glial fibrillary acid protein seen in some schwannomas
Mib 1	Proliferation marker
Myo D1	Skeletal muscle tumors
NSE	Neural cells, neuroblastic and paraganglionic cells, some smooth muscle tumors, clear cell sarcoma, malignant melanoma
Osteocalcin	Bone, osteoid, osteosarcoma
P 53	Protein product of the P53 gene
Rb	Protein product of the Rb gene
S-100 protein	Schwann cells, melanocytes, Langerhan's cells, Schwannoma, neurofibroma, granular cell tumor, malignant nerve sheath tumor, clear cell sarcoma, malignant melanoma, liposarcoma, cartilage tumors, chordoma
Vimentin	Mesenchymal cells, evaluation of preservation of immunoreactivity
von Willebrand	Endothelial cells, well-differentiated vascular tumors (also called Factor VIII-related antigen)

Electron Microscopy

Valuable diagnostic information can be provided by ultrastructural analysis. Despite the availability of a wide panel of immunohistochemical antibodies, transmission electron microscopy is still of value for diagnosis in selected cases.

Other techniques of ultrastructural analysis such as scanning or immunoelectron microscopy are generally used as research rather than diagnostic tools.

Tumor Feature

Fibrohistiocytic	Histiocytes, fibroblasts, and myofibroblasts, cells with multiple lysosomes
Liposarcoma	Lipid droplets, basement membrane
Vascular neoplasms	Weibel-Palade bodies, pinocytic vesicles, intermediate filaments, vasoformation
Leiomyosarcoma	Actin filaments, dense bodies, basement membrane, pinocytic vesicles, glycogen, intermediate filaments
Rhabdomyosarcoma	Thin and thick filaments, sarcomeres, glycogen, basement membrane
Schwannoma	Cell processes with prominent reduplicated basement membrane, fibroblast-like features
Clear cell sarcoma	Melanosomes, basement membrane
Chondrosarcoma	Scalloped cellular margins, prominent rough endoplasmic reticulum, glycogen
Synovial sarcoma	Biphasic tumors: glands surrounded by basement membrane, lumens lined by microvilli
Monophasic tumors	Frequent cell junctions, primitive gland formation
Epithelioid sarcoma	Intermediate filaments, keratin bundles, complex cell outlines
Ewing sarcoma	Glycogen, desmosomes in some cases

Synovial Fluid Analysis

Synovial fluid (SF) analysis often helps to differentiate between inflammatory, noninflammatory, and traumatic conditions, narrowing the differential diagnosis and permitting early institution of treatment.

Like other body fluids, the essential examination is macroscopic and microscopic, and analysis of biochemical characteristics can be done quickly even in a physician's office laboratory.

Synovial Fluid Work-Up

- *Physical characteristics*: fluid volume, color, clarity, viscosity.
- *Microscopic examination*: Total white blood cells, total red blood cells, differential white blood cell count, evaluation of a wet specimen for crystals.
- *Microbiological studies:* Cultures and Gram's and AFB stains.
- *Additional studies*: Glucose, proteins, lactate dehydrogenase, serology.

Specimen Collection

Arthrocentesis is done avoiding regions of skin infection. The sample is collected in a sterile, clean container. The syringe used may be rinsed with sodium heparin (25 U/ml). Anticoagulants (EDTA, oxalate) that are crystalline in the dry state must be avoided so as to avoid any artifacts while interpreting wet specimens for crystals. Romanowsky stains, wet preparation for analysis for crystals, and culture for pyogenic bacteria and mycobacteria are considered priority tests.

Gross Examination

Volume: Difficulty in obtaining fluid may also be due to insufficient fluid or high viscosity due to high fibrin content, rice bodies, and loculation.
Viscosity: Normal SF is highly viscous because of hyaluronate. When a drop of fluid is suspended from a needle tip or between two glass slides, a "string" is formed about 3–5 cm long. Shorter string formation is due to watery fluid. This is usually associated with inflammation but can also be seen in sudden edema.
Clot formation: Mucin clot formation is assessed with glacial acetic acid. Spontaneous clot formation is abnormal, and implies the presence of high molecular weight coagulation proteins. This is seen in hemarthrosis or in the event of a traumatic tap.
Clarity: Normal fluid is transparent. Cloudy fluid is due to increased proteins and/or cells. Flecks in the SF can be rice bodies, ochronosis where the flecks resemble ground pepper or there may be prosthesis material.
Color: Normal is colorless to a light yellow. It is cloudy or opaque white in inflammations and chylous in chronic arthritis or lymphatic obstruction.

Cell Counts

Normal SF is paucicellular with a WBC count of less than 100 mm^{-3}. Red cell counts help to distinguish frank blood from hemorrhagic effusion.

Normal joint fluid values for cell counts are as under:

Item	Mean	Range
WBC	6 mm^{-3}	1–18 mm^{-3}
Differential counts	(%)	(%)
Neutrophils	7	0–25
Lymphocytes	24	0–78
Monocytes	48	0–71
Histiocytes	10	0–26
Synovial lining cells	4	0–12

A hemocytometer chamber is used for cell counts. SF is diluted with physiological saline and not acetic acid which will polymerize hyaluronic acid. In situations where excessive blood is admixed and erythrocytes are interfering with the counts, RBCs maybe lysed using 0.3% saline instead of acetic acid.

A differential count is done as for peripheral blood. The total white blood cells can be estimated on a smear by averaging the number of WBCs per ten 400× fields and multiplying by 500. Before actually charging the hemocytometer chamber, the SF should be well mixed.

Microscopic Examination

Light Microscopy

Air dried smears on a glass slide stained by any of the Romanowsky stains is adequate for cellular differential counts.

Synovial cells resemble mesothelial cells. Normal cellular elements found in SF include monocytes, lymphocytes, histiocytes, neutrophils, and synoviocytes. The predominant cell type is the monocyte.

- *Abnormal cellular elements suggest a specific diagnosis in some cases:*
- *Erythrophagocytosis, hemosiderin pigment, and hematoidin crystal* suggests hemorrhage. Hematoidin crystals are golden yellow, refractile, and rhomboidal crystals that may be seen intracellularly or extracellularly.
- *Cartilage cells* or their fragments are not normally present in SF and are recognized as individual cells with deep purple cytoplasm and small nucleus surrounded by a halo. Cartilage may be seen following trauma or in osteoarthritis. Iron-laden chondrocytes suggest hemochromatosis. Yellow chondrocytes are described in ochronosis.
- *Ragocytes or RA cells* are neutrophils containing refractile round cytoplasmic inclusions and are best seen in wet preparations using phase contrast microscopy. These cells are seen in inflammatory disorders and are not specific for rheumatoid arthritis. The inclusions represent phagocytosed immunoglobulins, immune complexes, DNA particles, rheumatoid factors, fibrins, and antinuclear factors.
- *Lupus erythromatosus cells* (LE) are neutrophils that contain a phagocytized homogenized nucleus. LE cells have been described in systemic lupus erythromatosus (SLE) and also rheumatoid arthritis (RA). Their absence does not exclude SLE.
- *Reiter's cells* are macrophages containing one or more phagocytized neutrophils. They are not diagnostic of Reiter's syndrome and may be seen in a variety of inflammatory conditions.
- *Lipid-laden macrophages* may be seen in traumatic arthritis as a late finding, in chylous arthritis, and in pancreatitis. Lipid may appear as extracellular or intracellular isotropic fat globules or as anisotropic lipid droplets that show "Maltese cross" birefringence under polarized light. Oil red O or Sudan black B fat stain may be used to identify lipid.
- *Eosinophils* are not found in normal SF. If more than 2% are seen, a variety of disorders can be the cause. These include rheumatic diseases, hypereosinophilic syndromes, bacterial infections, allergic disease, parasitic arthritides, metastatic adenocarcinoma, air and dye arthrography, and acute and chronic urticaria.
- *Marrow fragments* in SF are a clue to fractures with involvement of joint. *Platelets* may be found in rheumatoid arthritis. *Sickled erythrocytes* may provide a clue to underlying sickle cell disease, trait, or a combination of SC and S thalassemia although the presence of sickle erythrocytes does not mean that the hemoglobin is responsible for the joint pathology.
- *Amyloid* appears as amorphous deposits that are green and weakly birefringent when stained with Congo red. Identification of amyloid in SF correlates well with synovial biopsy. Fragments of collagen, and metal or polymer prostheses can be seen in SF.
- *Metastatic and primary malignancies* can involve the joint space. Cells of Hodgkin's or non-Hodgkin's lymphoma, and leukemic blasts can be identified. Metastatic squamous cell carcinoma and adenocarcinoma may be identified (9).

Some medications and radiographic contrast media can affect the leukocyte differential count. Lower number of lymphocytes in patients with rheumatoid arthritis was treated with nonsteroidal anti-inflammatory drugs (NSAIDs); injection of contrast media with epinephrine was associated with a leukocytosis, whereas no inflammatory changes were noted after injection of nonionic contrast media.

Examination of Crystals

Ideally, examination for crystals is attempted in a wet coverslipped preparation under compensated polarized light (10). Crystals should be examined under high power (400 or 1,000×). Weakly birefringent crystals may be difficult to see if the light is not properly adjusted; too bright a background can overexpose the crystals; too little light makes the weak birefringence invisible. Estimation is made by the number of crystals as few, moderate, or many. Their location is noted as intracellular, extracellular, or both. Then the color and shape of the crystal is noted using a red compensator. More than one type of crystal can be present.

- *Monosodium urate (MSU)* crystals are *needle shaped*, 5–25 mm long, strongly negatively birefringent, and may be located intracellularly or extracellularly. When the long axis of the crystal is oriented parallel to the slow axis of the red compensator, the crystal is bright yellow. Rotating the axis of the compensator by 90° causes the crystal to change to blue (Fig. 1). These crystals are usually easy to see under low power with polarized light. Occasionally microcrystals 1–2 mm in length may be found. In the absence of polarized light, MSU crystals are recognized by their size and color in Romanovsky stain.
- *Calcium pyrophosphate dihydrate (CPPD):* These are *rod to rhomboidal shaped*, 1–20 mm in length and up to 4 mm in width, weakly positive birefringent. These are more difficult to see than MSU crystals. These may be either intracellular or extracellular. When the long axis of the crystals is oriented parallel to the slow axis of the compensator, the crystal appears blue. Rotating the axis of the compensator by 90° changes the color to yellow (Fig. 2).

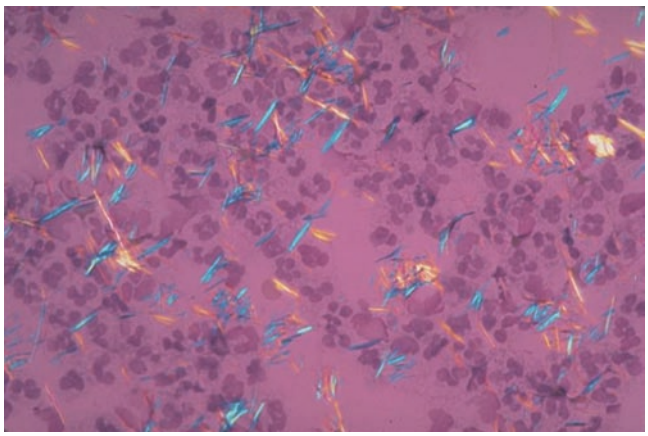

Fig. 1 Crystals of monosodium urate under polarized light (original magnification 400×).

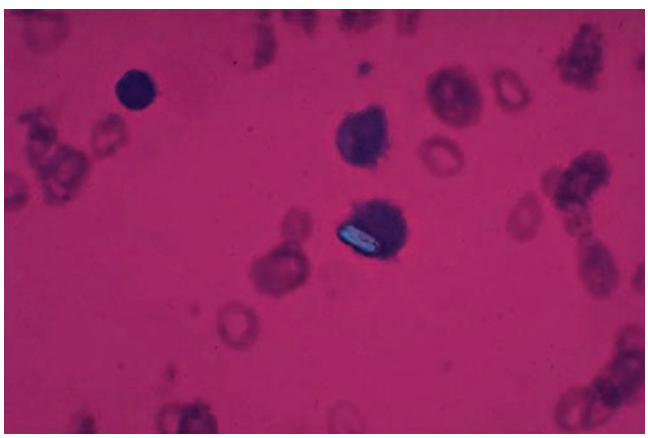

Fig. 2 Calcium pyrophosphate crystals using polarized light with a red compensator at 0° (original magnification 1,000×).

- *Cholesterol crystals* usually appear as large flat rhomboidal plates and have notched corners. These are strongly positively birefringent and are associated with chylous effusion in inflammatory and degenerative arthritis. Negatively birefringent, needle-shaped forms have been described that can resemble MSU. Cholesterol crystals are never phagocytosed and have no known etiologic role in the pathogenesis of arthritis. Both shapes can be seen in the same specimen.
- *Basic calcium phosphate (BCP)* crystals including hydroxyapatite and calcium phosphates are ultramicroscopic in size and can be diagnosed only by scanning electron microscopy.
- *Calcium oxalate (CO)* crystals are pyramidal, 1–2 mm in size, and positively birefringent. These are associated with primary oxalosis as a manifestation of extensive tissue oxalate deposition and chronic renal failure treated with hemodialysis or peritoneal dialysis. Identification of CO crystals is an indication to stop oxalate anticoagulation, if being administered.
- *Corticosteroid*: These crystals mimic the morphology of MSU. Triamcinolone hexacortonide may be seen following intraarticular steroid injection therapy and can persist in SF for months. These crystals are 10–20 mm in length, rectangular to needle shaped, negatively birefringent, and can be phagocytized by neutrophils. In contrast to MSU, these have ragged edges. Steroid crystals may dissolve in alcohol fixatives and examination of a wet preparation is mandatory.
- *Other crystalline objects* have been described such as immunoglobulin, metal fragments, dust, and talc. Some of the artefacts may not be in the same plane as the cellular material when the artefact is picked up during processing.

Chemical Examination

Most chemical tests contribute little to the diagnosis of a joint disorder. Commonly SF protein, glucose, and uric acid may be requested. Other tests are lipids, enzymes, lactate, hyaluronidase, and ferritin (11).

- *Glucose*: Low SF glucose has been used to differentiate infection from inflammatory effusion. SF and plasma specimens should be collected at the same time. Joint fluid glucose equilibrates with serum levels after 6–8 h; fasting levels are most reliable. In noninflammatory diffusion, there is a glucose difference of less than 10 mg/dl between serum and joint fluid. With increasing inflammation, glucose levels in joint fluids fall. Infections should be considered when SF glucose is less than 20 mg/dl. However, the large variations in glucose concentration in

inflammations and infections has minimized the usefulness of this investigation. Glucose levels are low in CPPD in the absence of infection.

- *Protein*: This estimation unlike in serous effusions does not differentiate between transudate and exudate. An increase in protein concentration above 2.5 g/dl is not normal and if more than 4.5 g/dl is suggestive of inflammation. However no specific diagnosis is provided and has no clinical usefulness.
- *Urate*: Urate is not concentrated in joints and SF levels mirror serum levels. Therefore, there is little need to measure joint urate levels.

Microbiological Examination

Gram's stain affords a rapid indication of the pathogen in septic arthritis and gives an immediate indication of the antimicrobial treatment to be offered. In cases where antimicrobial therapy has been instituted prior to the arthrocentesis smear and culture, assessment may be negative or noncontributory. The possibility of fungal, anaerobic infections, and tuberculous arthritis must always be remembered and appropriate specimens collected. For this, appropriate transport media and prior cooperation of the laboratory must be sought. Rapid stains along with fluorescent detection methods have proved useful in selected cases.

Rapid analysis of fungal and bacterial antigens by latex agglutination, analysis of metabolites by gas chromatography, and Limulus lysate assay for bacterial endotoxin are all applicable to SF samples.

Immunological Examinations

There are few immunological tests that are performed on the SF. Of these tests, most pertain to rheumatoid arthritis (RA). Estimations such as IgG, IgM, IgA, rheumatoid factor (RF), and complements have been assessed in relation to clinical usefulness of sensitivity and specificity. Although the finding of RF in SF is specific to RA, the rest do not afford significant advantage. A negative RF in serum may be positive in SF. The other estimations may give similar results in septic arthritis too. Analysis of B- and T-cell subsets in inflammatory disorders is largely a research tool.

Interpretation of Synovial Fluid

Gross examination, WBC, and differential counts can classify the results into one of several broad categories helping to narrow the diagnosis.

Gross	Normal	Noninflammatory	Inflammatory	Septic	Crystal	Hemorrhagic
Volume (ml) (knee)	<3.5	Often >3.5	Often >3.5	Variable	Variable	Variable
Viscosity	High	High	Low	Variable	Variable	Variable
Color	Colorless to straw	Straw to yellow	Yellow cloudy	Yellow to white cloudy	Yellow cloudy	Red xanthochromic
WBC (mm^3)	<200	200–2,000	2,000—75,000	>50,000	2,000–75,000	50–10,000
Neutrophil (%)	<25	<25	Often >50	>75	Often >50	<50
Crystals	No	No	No	No	Yes	No
Culture	Negative	Negative	Negative	Often negative	Negative	Negative
Mucin clot	Firm	Firm	Friable	Friable	Friable	
Glucose (AM fasting)	Nearly equal to blood	Nearly equal to blood	<50 mg% lower than blood	>50 mg% lower than blood	>50 mg% lower than blood	Nearly equal to blood

Synovial fluid findings are often nonspecific, and clinical information and results of other laboratory tests are necessary to establish a specific diagnosis. Essentially a few questions should always be kept in mind that need to be answered at the time a SF analysis is requested:

- *Is this septic or inflammatory arthritis?*
- *Is this crystal-related or septic arthritis?*
- *If crystals are present, is this gout or pseudogout?*
- *Is this a bloody effusion or a traumatic tap?*

The answers are not mutually exclusive as two processes may occur simultaneously.

The highest WBC and neutrophil counts are encountered in septic arthritis. The findings will resemble that of pus and neutrophils will account for 90% of the cells. These findings are modified by previous treatment and this must always be kept in mind when results do not match clinical details. A high neutrophil percentage must always prompt a smear search for bacteria and culture studies advised/performed if the specimen is available, to establish a definite diagnosis. WBC counts in crystal arthritis range from 100 mm^{-3} to greater than 100,000 mm^{-3} with as much as 80% neutrophils and thus resemble septic arthritis. Thus, it is imperative to demonstrate characteristic crystals. Both CPPD and MSU can occur simultaneously.

Inflammatory noncrystal, nonseptic arthritis is characterized by more than 50% neutrophils and WBCs ranging from 2,000 to greater than 100,000 mm^{-3}. Therefore, the diagnosis depends upon the exclusion of organisms and crystals.

Low cell counts only indicate noninflammatory conditions and fluid analysis alone will not usually provide a diagnosis. Macroscopic examination may help in distinguishing between traumatic aspiration and hemarthrosis, xanthochromasia, indicating a long standing hemorrhage.

Interpretation of SF findings must always be done in the appropriate clinical context. Complete information of the clinical situation and previous treatment along with careful and complete evaluation is required for meaningful results.

References

1. McPherson R., Pincus M. Henry's Clinical Diagnosis and Management by Laboratory Methods. 21st ed. China: Elsevier, 2007: 180–182.
2. Sorensen P.H.B., Lessnick S.L., Lopez-Terrada D. et al. A second Ewing's sarcoma translocation, t(21;22) fuses the EWS gene to another ETS-family transcription factor ERG. Nat Genet 1994; 6:146.
3. Bridge J.A., Bridge R.S., Borek D.A. et al. Translocation t(X;18) in orofacial synovial sarcoma. Cancer 1988;62:935.
4. Aman P., Ron D., Mandahl N. et al. Rearrangement of the transcription factor gene CHOP in myxoid liposarcoma with the t(12;16)(q13:p11). Genes Chrom Cancer 1992;5:278.
5. Heim S., Mandahl N., Kristoffersson U., et al. Marker ring chromosome – a new cytogenetic abnormality characterizing lipogenic tumors? Cancer Genet Cytogenet 1987;24:319.
6. Paulien S., Turc-Carel C., Dal C. et al. Myxoid liposarcoma with t(12;16)(q13:p11) contains site-specific differences in methylation patterns surrounding a zinc-finger gene mapped to the breakpoint region on chromosome 12. Cancer Res 1990;50:7902.
7. Scimke R.T. Gene amplification in cultured animal cells. Cell 1984;37:705.
8. Willman C.L., Busque L., Griffith B.B. et al. Langerhans' cell histiocytosis (Histiocytosis X) – a clonal proliferative disease. N Engl J Med 1994;331:154.
9. Fam A.N., Kolin A., Lewis A.J. Metastatic carcinomatous arthritis and carcinoma of the lung. J Rheumatol 1980;7:98–104.
10. Gatter R.A. Use of the compensated polarizing microscope. Clin Rheum Dis 1977;3:9–103.
11. Gatter R.A., Schumacher H.R. A Practical Handbook of Joint Fluid Analysis. 2nd ed. Philadelphia: Lea & Febiger, 1991: 1–122.
12. Carta M., Szakacs J.E., Szakacs M.R. Ewing's sarcoma, extra skeletal and of bone. Case report with ultrastructural analysis. Ann Clin Lab Sci 1974;4(4):306–322.
13. Gao Z., Kahn L. The application of immunohistochemistry in the diagnosis of bone tumors and tumor-like lesions. Skel Radiol 2005;34:755–770.
14. Dabbs D.Diagnostic Immunohistochemistry. Livingstone: Phila delphia, 2002: 60–63, 69–73.

Chapter 6
Genetics and Molecular Biology of Bone and Soft Tissue Tumors

Dolores López-Terrada and John M. Hicks

Abstract Tumors of bone and soft tissue represent a heterogeneous group of biologically and clinically diverse neoplasms. Cytogenetic analysis has identified two broad groups of sarcomas, those with complex unbalanced karyotypes and a second group with characteristic genetic abnormalities, including chromosomal translocations. Common molecular mechanisms of sarcomagenesis include activation of signal transduction pathways, mutations in genes that control the cell cycle, and genes that maintain DNA integrity. Some of the genetic and/or molecular markers identified for these tumors are clinically relevant and used routinely for diagnosis and classification. Integration of cytogenetic analysis, molecular cytogenetics and other molecular assays, as part of diagnostic algorithms, is becoming increasingly common for these tumors, representing an example of how tumor biology is being incorporated and re-defining pathology and clinical practice.

Key words tumor genetics, sarcoma, cytogenetics, signaling pathways, molecular diagnosis, chromosomal translocations

Introduction

During the last decades significant advances have been made in understanding the biology of bone and soft tissue tumors, a heterogeneous group of neoplasms that includes biologically and clinically very diverse types. The great majority of bone and soft tissue tumors are sporadic; however, some have been associated with genetic syndromes. Investigation of somatic genetic changes by cytogenetic analysis of these tumors demonstrated two broad groups of sarcomas: those with complex unbalanced karyotypes and nonspecific genetic alterations, and a second group with simpler karyotypes and characteristic genetic abnormalities, including tumor-specific translocations (Tables 1 and 2).

Among an extensive list of genetic and molecular abnormalities documented in sarcomas, a number of common molecular mechanisms of sarcomagenesis have been recently described, including constitutive activation of signal transduction pathways, and mutations in genes that control cell cycle progression and maintain DNA integrity (1) (Table 3). In this chapter, we will discuss those tumors for which characteristic genetic aberrations and molecular mechanisms of transformation have been identified and genetic and/or molecular markers are clinically relevant.

It is of great importance to remember that, although many tumors require only light microscopy and immunohistochemical testing for a definitive diagnosis, in a proportion of them a multimodal approach is necessary to yield a precise and definitive diagnosis (2). Chromosomal analyses, molecular cytogenetics, and other molecular assays are and will be increasingly available as a diagnostic aid, representing an example of how basic research is being incorporated and redefining pathology and clinical practice. Appropriate triaging of tumor tissue to obtain adequate samples for each diagnostic study and integrated interpretation of all test results, in concert with histologic interpretation and clinical information, should always be part of the diagnosis (Table 4).

Primary Bone Tumors

Osteosarcoma

Cytogenetic analysis of osteosarcomas, in contrast to other sarcomas characterized by nonrandom chromosomal translocations, demonstrated markedly abnormal karyotypes in more than 70% (3–8) and single chromosomal changes present in less than 5% of osteosarcomas (6). Multiple clones with variable ploidy, numerical and complex structural chromosomal abnormalities are often present. These complex

J.S. Khurana (ed.), *Bone Pathology*, DOI 10.1007/978-1-59745-347-9_6,

Table 1 Most common chromosomal rearrangements and resulting fusion genes in sarcomas

Tumor	Translocation	Gene(s)	Frequency (%)	Family
Ewing's family of tumors	t (11;22) (q24;q12)	*EWS-Fli1*	85	Ets domain
	t (21;22) (q22;q12)	*EWS-ERG*	5–10	
	t (7;22) (p22;q12)	*EWS-ETV1*	Rare	
	t (17;22) (q12;q12)	*EWS-E1AF*	Rare	
	t (2;22) (q33;q12)	*EWS-FEV*	Rare	
	t (1;22) (p36;q12)	*EWS-ZFG*	Rare	
	inv (22) (q12;q12)	*EWS-ZFG*	Rare	
	t (2;22)	*EWS-SPE3*	Rare	
	t (16;21) (p11;q22)	*FUS-EFG*	~50	
	Trisomy 8, 12	N/A	~30	
Desmoplastic small round cell tumor	t (11;22) (p13;q12)	EWS-WT1	>90	Zinc-finger
Clear cell sarcoma of soft tissue	t (12;22) (q13;q12)	EWS-ATF1	>75	bZIP protein
Alveolar rhabdomyosarcoma	t (2;13) (q35;q14)	*Pax3-FKHR (FOXO1A)*	~70	Paired box homeodomain
	t (1;13) (p36;q14)	*Pax7-FKHR*	~15	
	t (X;2) (q13;q35)	*Pax3-AFX*	Rare	
	t (2;2) (q35;q23)	*Pax3-NCOA1*	Rare	
Synovial sarcoma	t (X;18) (p11.23;q11)	*SYT-SSX1, 4*	>90 Unknown	Zinc-finger
	t (X;18) (p11.21;q11)	*SYT-SSX2*		
	t (X;20) (p11.2;q13.3)	*SS18L1/SSX1*		
Dermatofibrosarcoma protuberans and giant cell fibroblastoma	t (17;22 (q22;q13), ring chromosomes	PDGFB-COL1A1	>50, ring chromosomes >75	Platelet-derived growth factor B and collagen 1
Congenital fibrosarcoma	t (12;15) (p13;q25)	*ETV6 (TEL)-NTRK3 (TRKC)*	Unknown	
Malignant rhabdoid tumor	del 22 (q11.2)	*hSNF5-INI1*	~50	
Liposarcoma (myxoid and round cell)	t (12;16) (q13;p11)	*TLS (FUS)-CHOP*	>75	bZIP protein
	t (12;22) (q13;q12)	*EWS-CHOP*	Rare	
	t (12;22;20) (q13;q12;q11)	*EWS-CHOP*	Rare	
Atypical lipomatous tumor well-differentiated liposarcoma	12q rings and giant markers	*HMGIC, CDK4,* and *MDM2* amplification	60	N/A
Extraskeletal myxoid chondrosarcoma	t (9;22) (q22;q12)	*EWS-CHN (TEC)*	>75	

Table 2 Sarcomas with complex karyotypes

Fibrosarcoma
Leiomyosarcoma
High-grade undifferentiated pleomorphic sarcoma (malignant fibrous histiocytoma)
Osteosarcoma
Chondrosarcoma
Liposarcoma
– Well differentiated/dedifferentiated (ring, giant, and marker chromosomes)
– Pleomorphic liposarcoma
Rhabdomyosarcoma
– Embryonal
– Pleomorphic
Malignant peripheral nerve sheath tumor (MPNST, malignant schwannoma, neurofibrosarcoma)
Angiosarcoma

karyotypes with multiple marker chromosomes often limit the ability to identify consistent aberrations making conventional karyotyping clinical usefulness very limited for these tumors (8).

The application of FISH and other molecular cytogenetic techniques such as CGH (Comparative Genomic Hybridization), spectral karyotyping (SKY), or multicolor FISH (M-FISH) (Fig. 1) has confirmed the complexity of chromosomal changes present in most osteosarcomas. Chromosomal loci most commonly involved in structural changes seen in these tumors include 1p11-13, 1q11-12, 1q21-22, 6p12-21, 11p14-15, 14p11-13, 15p11-13, 17p, and 19q13. The most common

Table 3 Pathways and gene abnormalities in sarcomas

Tumor suppressor genes
Retinoblastoma gene (RB1, 13q14)
Tumor protein p53 gene (TP53, 17p13.1)
Checkpoint kinase 2 gene (CHEK2, 22q12)
Cyclin-dependent kinase inhibitor – 2A gene (CDKN2A, 9p21)
Wilms tumor gene (WT1, 11p13)
SMARCB1 (hSNF5/INI1, 22q11.2)
Neurofibromatosis type 1 gene (NF1, 17q11.2)
Neurofibromatosis type 2 gene (NF2, 22q12.2)
Adenomatous polyposis coli gene (APC, 5q21)
Beta-catenin gene (CTNNB1, 5q21)
P16 (9p21)
P18 (1q32)
P21 (6p21.1)
Growth factor and signaling pathways
Insulin-like growth factor 1-receptor pathway (IGF1)
Platelet-derived growth factor pathway (PDGF)
Fibroblastic growth factor family (FGF)
C-KIT receptor pathway
C-MET receptor pathway
Wnt pathway
HDM2 (12q13-14)
SAS (12q13-14)
CDK4
P16
Epidermal growth factor, TGF-beta, VEGF, HGF/SF
Stem cell factor (SCF)
V-Sis, C-Sis
Insulin
Nuclear transcription regulators: *c-Myc, c-Myb, Gli, Ras family*
Membrane-bound tyrosine kinases: *c-Erb-b2 (her2), Met, Fms, c-Kit*
Non-receptor tyrosine kinases: *Src, Fes, Abl, Fak*
Congenital syndromes
Beckwith-Wiedemann syndrome (11p15, CDKN1C, IGF2)
Carney complex (17q23-4, PRKAR1AK)
Diaphyseal medullary stenosis (9q21-2)
Familial adenomatous polyposis and (5q21, APC, desmoids)
Myofibromatosis (autosomal recessive, myofibromas)
Neurofibromatosis type 1 (17q11, NF1)
Neurofibromatosis type 2 (22q12, NF2, Schwannoma)
Retinoblastoma (13q14, RB1, osteosarcoma, soft tissue sarcomas)
Rhabdoid predilection syndrome (22q11, SMARCB1, rhabdoid tumor)
Rubinstein-Taybi syndrome (myogenic sarcomas)
Werner syndrome (8p11-12, WRN, bone and soft tissue sarcomas)
Viral Infection
Epstein-Barr virus
Human herpes virus type 8
SV40

Table 4 Triaging of tumor tissue

Frozen tissue with cryopreservative for intraoperative diagnosis
Cytologic, scrape and squash imprints for intraoperative diagnosis
Formalin-fixed tissue for routine histopathology, immunocytochemistry, in situ hybridization and polymerase chain reaction (RT-PCR)
Glutaraldehyde-fixed tissue for electron microscopy
Fresh tissue in tissue culture media for cytogenetics
Frozen tissue without cryopreservative for molecular studies
Fresh tissue for biochemical analyses of tumor-specific products
Cytologic imprints for
Cytogenetic interphase studies: Fluorescent in situ hybridization for cytogenetics (FISH)
Special stains and immunocytochemical phenotyping
Alcohol-fixed tissue for improved cytoplasmic glycogen preservation, immunocytochemistry (requiring such fixation), and microarray gene analysis

numerical abnormalities include gains involving 3q26, 4q12-13, 5p13-14, 7q31-32, 8q21-23, 12q12-13, 12q14-15, and 17p11-12. Losses are most common on 2q, 6q, 8p, 9,10p, 13, and 17 (8–13). Tumor-specific loss of heterozygosity has been reported most frequently for 3q, 13q, 17p, and 18q. An excellent detailed review of reported chromosomal abnormalities in osteosarcomas was recently published by Sandberg and Bridge (8).

Amplified chromosomal areas of particular interest in osteosarcomas include 12q13-q15 and 8q. *MDM2* and *CDK4* are the most generally accepted amplified genes located at the 12q13-q15 region; however, several other targets have been proposed including *GLI*, *CHOP* (or *DDIT3*) *SAS, HMGIC, OS-4, OS-9*, and *PRIM1* (14–17). Tarkkanen and colleagues reported a copy number increase at chromosome 8q that could represent a potential prognostic marker in high-grade osteosarcoma (18). A recent genome-wide array comparative genomic hybridization study defined high-resolution DNA copy number changes and refined amplification (13).

Tumor Suppressor Genes

Molecular genetic analysis of osteosarcomas revealed a variety of recurrent alterations, some involving inactivation of tumor suppressor genes as well as amplification of several oncogenes. The association between *RB1* (retinoblastoma) tumor suppressor gene inactivation and osteosarcoma was first recognized in patients with hereditary retinoblastoma carrying a heterozygous germ line inactivation of this tumor suppressor gene, and up to 1,000 times the incidence of osteosarcoma when compared with the general population (19–21). This tumor suppressor gene located on chromosome13q14, encodes a protein that acts as a major regulator of the G1 to S cell cycle progression. Seventy percent of sporadic osteosarcomas carry alterations of the *RB1* gene, either loss of heterozygosity, structural rearrangements, or point mutations (22). Amplification or overexpression of cyclin-dependent–kinase 4 (CDK4) or cyclin D1 (*CCND1*), also result in functional inactivation of the *RB* signaling pathway, as they form a complex responsible for Rb protein phosphorylation (23, 24).

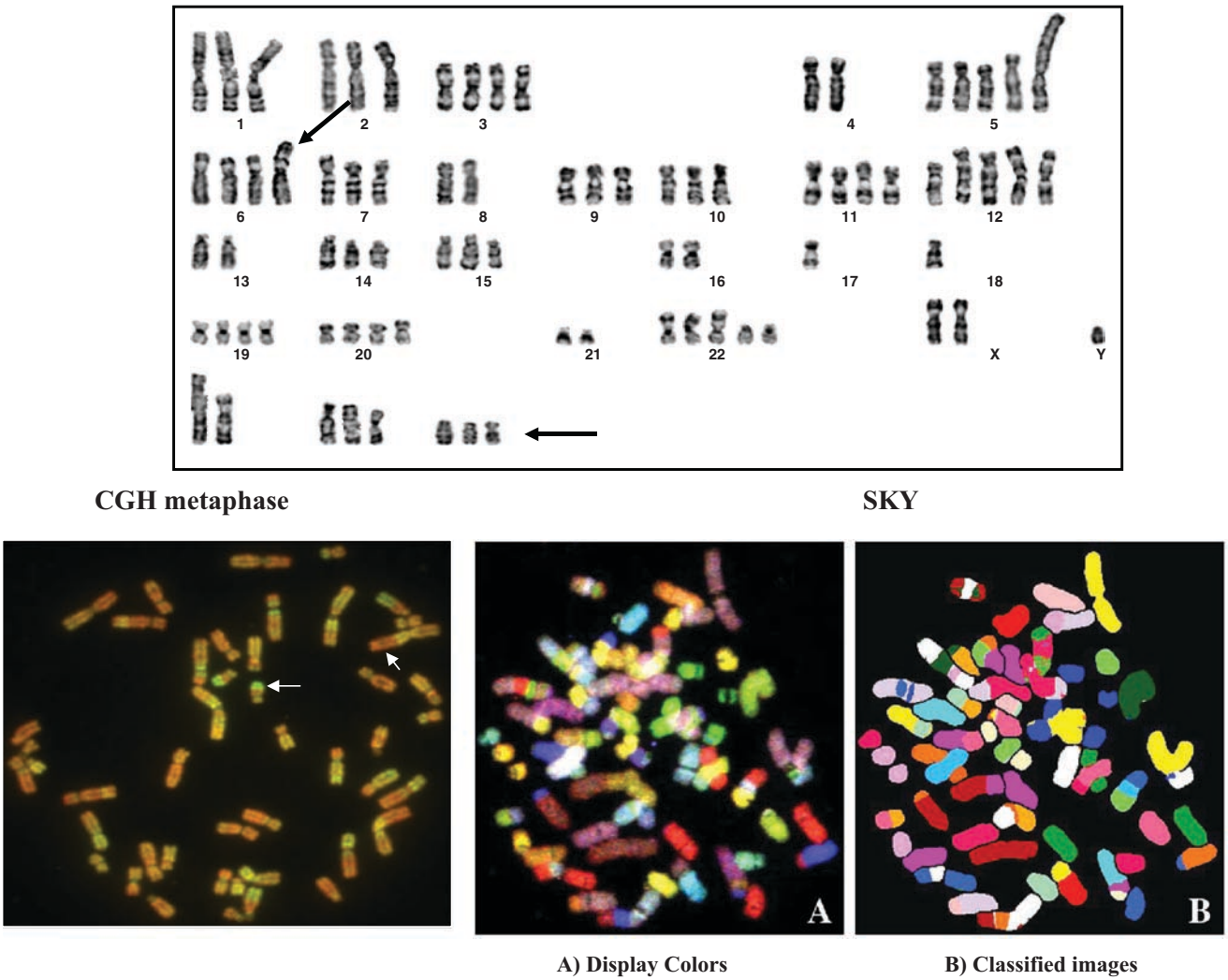

Fig. 1 Osteosarcoma, genetics: Complex Karyotype (G-banding) showing numerous numerical and structural abnormalities, with several marker chromosomes, Comparative Genomic Hybridization (CGH) and Spectral Karyotyping (SKY) of an osteosarcoma case (Images courtesy of Rao Pulivarti, PhD, Texas Children's Hospital Cytogenetics Laboratory)

Another tumor suppressor gene important in the development of osteosarcomas is the *T53* gene located at 17p13 (25). This is the most commonly mutated gene in human cancer which encodes a protein involved in cell cycle control, DNA damage control, and apoptosis (26). P53 protein functions as a nuclear transcription factor that inhibits cell proliferation by activating p21, arresting cells at G1 stage of the cell cycle. P53 protein also binds proteins involved in transcription and DNA repair, and is involved in recognition of DNA damage and induction of apoptosis (27). Patients with Li-Fraumeni Syndrome, characterized by the presence of a germ line mutation of the *P53* gene (28) carry a high risk of bone sarcomas and other tumors. Alterations of TP53 observed in sporadic osteosarcomas include allelic losses, point mutations, and other rearrangements (29–33), with most tumors carrying some combined inactivation of the retinoblastoma and p53 tumor suppressor pathways. Although the presence of p53 mutations in osteosarcomas appears to correlate with high levels of genomic instability in these tumors (34), they appear to have low prognostic significance in sporadic cases (35, 36).

Amplification of the p53 protein binding *MDM2* (Murine Double Minute 2) and the flanking *SAS* (Sarcoma Amplified Sequence) gene, both located on chromosome 12q13–14, also appear to play a role in the biology of osteosarcomas (37, 38). *MDM2* gene encodes a zinc-finger protein that binds p53. Amplification leading to overexpression of MDM2 protein results in suppression of wild-type p53 function, by physically blocking the region responsible for transcriptional activation of important p53 target genes (39).

SV40 (Simian virus 40) is a DNA polyomavirus that inhibits p53 function, promoting cell proliferation. SV40 sequences have been detected in approximately one-third of osteosarcomas tested (40, 41). It is postulated that SV40 large T antigen may inactivate the wild-type *P53* allele in the osteoblasts of susceptible individuals, resulting in tumor development;

however, the precise biologic significance of this finding and its role in the pathogenesis of osteosarcomas, like in other human malignancies, is not completely clear.

Activation of cyclin-dependent kinases (CDKs) by interaction with cyclins regulates progression through the cell cycle and is controlled by CDK inhibitors. Alteration of these tumor suppressor genes that function as cell cycle regulators have been documented to play a role in the development of osteosarcomas. The *CDKN2A* gene (also known as *INK4A*) located in chromosome 9p21 encodes $p16^{INK4a}$ that inhibits *CDK4*. The same gene (*INK4*) also encodes $p14^{ARF}$. Both proteins play an important role in deregulating both p53 and Rb pathways. Genetic and epigenetic abnormalities (deletions and promoter methylation) of the *INK4A/ARF* locus have been documented in osteosarcomas (42), and absence of expression of p16 correlated with decreased survival in pediatric patients (43). Although other genes encoding cell cycle regulating proteins have been involved in the biology of osteosarcomas, their role and clinical significance is still under investigation (44–46).

Oncogenes

A number of oncogene abnormalities have been reported in osteosarcomas. Amplification of *C-MYC*, involved in growth control, DNA replication, and transcriptional regulation, has been reported in a small proportion of osteosarcomas, more commonly in those associated with Paget's disease and cases of patients that relapsed after therapy (47, 48). Overexpression of *FOS* and *JUN* oncogenes has also been reported in osteosarcomas, more frequently in those tumors from patients who developed metastases (48).

Overexpression of *ERBB2* gene (*HER2/neu*, or *c-erbB2*) has also been documented in osteosarcomas, and its significance debated, as it has been associated both with increased probability of survival and with increased risk of pulmonary metastases, in different studies(49, 50).

High levels of aberrant *MET* proto-oncogene expression, encoding the hepatocyte growth factor receptor, have been documented in up to 60% osteosarcomas tested (51) and associated with aggressive behavior in osteosarcomas.

Other Possible Pathogenic Mechanisms in Osteosarcomas: Telomerase and ALT

A potential explanation for the karyotypic complexity and chromosomal instability seen in osteosarcomas is telomere dysfunction. Telomere maintenance to preserve the ability to divide indefinitely is a characteristic feature of neoplastic cells. Two main mechanisms to maintain telomeres have been described: telomerase activity, an enzyme that synthesizes new telomeric DNA, and alternative lengthening of telomeres (ALT). Both mechanisms have been described in osteosarcomas, and telomerase activity has been correlated with the development of metastases (52) a comprehensive study by Ulaner and colleagues demonstrated the correlation between absence of telomere maintenance mechanisms and favorable prognosis in osteosarcoma patients (53).

One of the most significant clinical problems in osteosarcoma is tumor recurrence, likely to be associated with drug resistance. Possible mechanisms of drug resistance include alterations in p-glycoprotein expression, multidrug resistance protein expression, topoisomerase II, glutathione S-transferases, DNA repair, drug metabolism or inactivation, and reduced intracellular influx (54). The Fas cell death pathway has also been implicated in determining chemosensitivity and metastatic behavior in a variety of tumors including osteosarcomas (55). Comprehensive reviews regarding drug resistance mechanisms in these tumors have been published by Ladanyi and Gorlick (54).

During the last few years gene expression profiling of osteosarcomas has been performed by several groups, occasionally in combination with molecular cytogenetic techniques in an attempt to correlate genomic aberrations and gene expression abnormalities (13, 56–58). The main aim of these studies was to identify subgroups of osteosarcomas by expression profiling associated with clinical behavior, mainly response to therapy and metastatic potential. Although some expression patterns and changes on individual gene expression appear to be associated with clinical behavior, the interpretation of these data is still in the beginning. Continuing biological studies of osteosarcoma will be increasingly important in the coming years to identify prognostic factors for treatment stratification and therapeutic targets. If those are successfully identified, selective therapy for specific tumor targets may soon complement systemic chemotherapy and surgery, still the foundation of osteosarcoma treatment (54).

The Ewing Family of Tumors

The peripheral primitive neuroectodermal tumors of childhood (pPNETs) are a group of poorly differentiated malignancies that include Ewing sarcoma of bone and soft tissue, Peripheral Neuroepithelioma, and Askin's tumor (59). These tumors, of debated histogenesis, belong to the so-called group of "Small Round Cell Tumors" of childhood and adolescence.

Ewing sarcoma is the second most common primary bone tumor in children after osteosarcoma, and was the first solid tumor to be defined by a specific chromosomal change, the t (11;22) (q24;q12) translocation (60). Conventional cytogenetic analysis of these tumors preceded and served as the basis

for their molecular characterization (61–65). In addition to the pathognomonic t (11;22) translocation and its variants (Table 1) including those involving a third chromosome, a number of secondary chromosomal abnormalities have been described in these tumors. The most common secondary abnormality are a number of unbalanced translocations involving chromosome 16 usually associated with the t (11;22) translocation (66, 67) most commonly a t (1;16) translocation, leading to a partial trisomy or tetrasomy of chromosome1q. Gain of 1q material appears to be the only recurrent secondary change associated with survival (67–69). The presence of other trisomies, in particular 8 and 12, is also common, probably representing tumor progression (70–72).

Genomic imbalances of the Ewing family of tumors have also been studied by Comparative Genomic Hybridization (CGH). Gains of DNA copies for chromosomes 8, 1q, and 12 have been confirmed by this methodology, and some correlated with clinical parameters. Chromosome region 1q21-22, 8, and 12 copy number increase has been associated with worse outcome in one of these studies (71, 73).

Molecular Genetics of Ewing Family of Tumors

The recurrent t (11;22) (q24;q12) translocation has been described in all members of this group of tumors (60, 61, 74), now designated as the Ewing's Family of Tumors (EFTs). Cloning of this translocation revealed a novel gene *EWS* (*EWSR1)*on 22q12, fused to a member of the ETS family of transcription factors *Fli1*, located on chromosome 11q24 (75, 76). The fusion gene encodes a highly expressed chimeric protein that combines the ETS-binding domain encoded by *Fli1* and the *EWSR1* transactivational properties. The breakpoints associated with this translocation appear to be restricted to exon 7 through 10 for *EWSR1*, but varies widely for the ETS-related genes on the other side of the translocation (Fig. 2a, b). Among the most common rearrangements are those that result in exon 7 of the *EWSR1* gene fused to exons 5 or 6 of the *Fli1* gene, that correspond to the type 1 and type 2 initially described (65, 76).

Numerous biological studies have addressed the tumorigenicity and mechanisms of transformation of the *EWSR1/Fli1* fusion gene as well as its potential target genes (77–80) with a number of pathways being implicated (81–85). Two recent studies have addressed the histogenesis of EFTs using microarray technology and demonstrated that *EWSR1/Fli1* fusion targets genes critical for neural-crest development, responsible for their phenotype (86, 87).

EWSR1/FLI1 fusion gene or chimeric transcripts are present in approximately 85% of Ewing and pPNETs. Another 10% of these tumors carry a second translocation, t (21;22) (q22;q12), which fuses *EWSR1* to a different ETS family member, *ERG*, located on chromosome 21q22. Sequences identical to those found in *EWSR1/Fli-1* fusion transcripts are fused to portions of *ERG* encoding an ETS-binding domain, resulting in the expression of an EWSR1/ERG chimeric protein (88, 89). *ERG* gene had been previously described in the t (16;21) (p11;q22) translocation seen in myelogenous leukemia, fused to *TLS/FUS* gene that, similarly to *EWSR1*, encodes a RNA-binding domain (90). Other much less frequent translocation variants have been described, always involving *EWSR1* gene and a fused ETS family member, all encoding a conserved helix-loop-helix DNA-binding domain, referred as the ETS domain. These translocations include t (7;22) (p22;q12), fusing *EWSR1* to *ETV1*, t (17;22) (q12;q12) encoding *EWSR1/E1AF* fusion gene, t (2;22) (q33;q12), encoding *EWSR1/FEV*, and t (2;22), encoding *EWSR1/SPE3* (91, 92). Four EFTs cases showing t (16;21) (p11;q22) translocations involving *FUS* fused to *ERG* have been reported recently.

ETS family members, known to play an important role in mammalian development and hematopoiesis, have also been cloned in other translocations identified in lymphoblastic and myeloid leukemias (93). *EWSR1* gene is also fused to other genes involved in translocations associated with a number of different neoplasms (Table 1) including *WT1* in Desmoplastic Small Round Cell tumor, *ATF1* in Clear Cell Sarcoma and Angiomatoid Fibrous Histiocytoma, *ERG* in myeloid leukemia, *CHOP* in Myxoid Liposarcoma, and *CHN (TEC,NR4A3)* in Extraskeletal Myxoid Chondrosarcoma (65).

Other oncogenes and tumor suppressor genes have been implicated in the pathogenesis of EFTs. Some of the most relevant include *P53* mutations, which have been described in a subset of cases (94–97) with no apparent association with the presence of *EWSR1* chimeric type. A recent report has also linked p53-dependent growth arrest with EWS-Fli1 expression (81). Deletions of *P16INK4* and *TP15* genes have also been reported, probably representing secondary genetic events. *P16INK4* mutations and deletions and the resulting loss of expression, may represent an adverse prognostic marker in these patients (43, 98). Huang and colleagues reported *P53* mutations or *P16/p14ARF* deletions with a highly lethal subset of these tumors (85). *P27* expression has also been reported as prognostically relevant in these tumors (99). Nogueira and colleagues (100) reported activation of *TRK* gene family members in EFTs, and suggested that Trk A receptor activation as a potential marker of neural differentiation. Expression of VEGF (vascular endothelial growth factor) has also been studied in these tumors as a potential therapeutic target (129).

Other pathways contributing to the malignant and metastatic behavior of EFTs include MEK/MAPk, PI3-K, and WNT/Frizzled (101, 102). cDNA microarray analyses of these tumor family have been recently reported (86, 103, 104) and identified gene expression signatures associated with high risk Ewing's.

From the strictly clinical point of view, the improved understanding of the biology and pathogenic mechanisms involved in EFTs, and in particular, the identification and

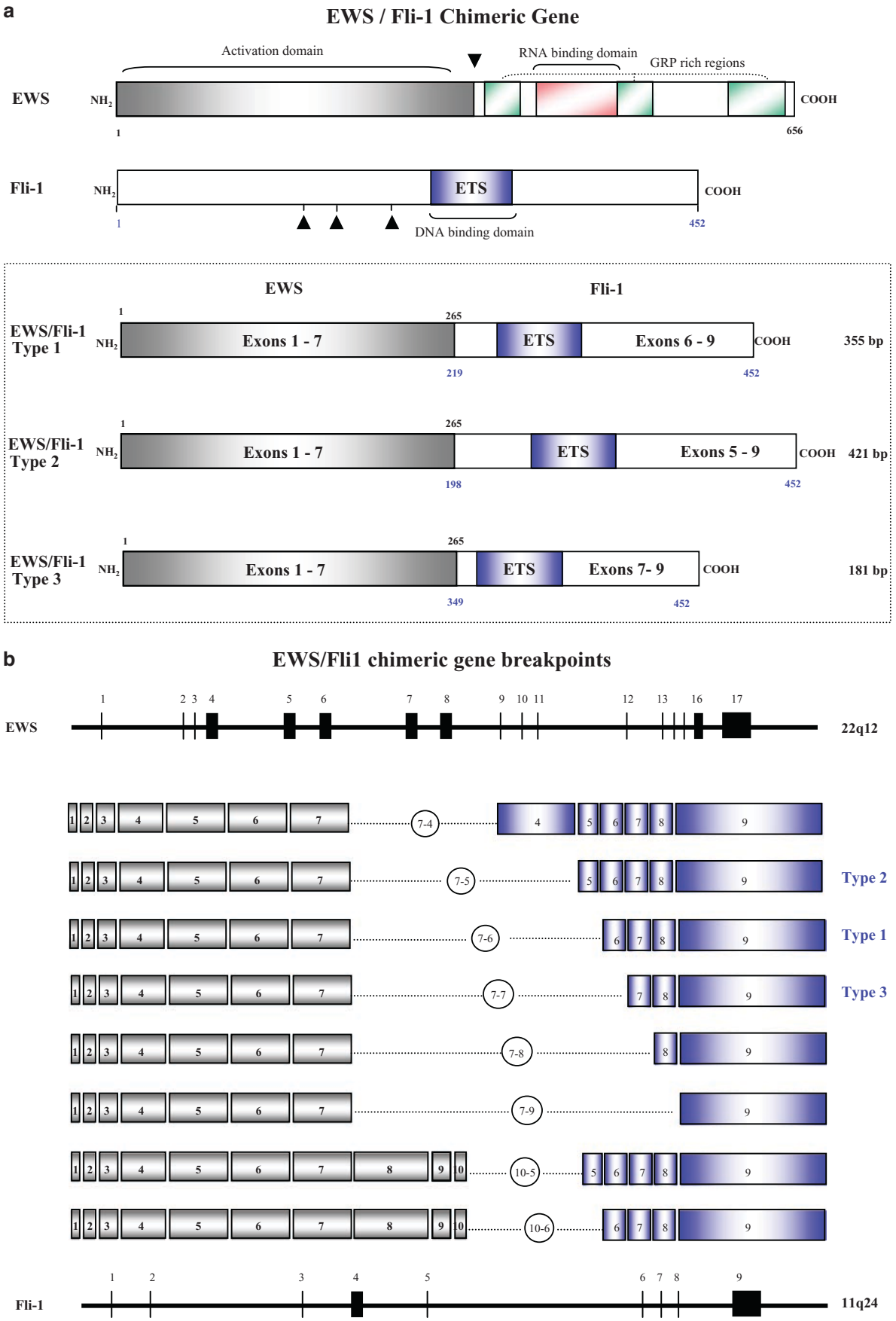

Fig. 2 **a** EWS/Fli-1 Chimeric Genes. **b** EWS/Fli1 chimeric gene breakpoints

cloning of the associated fusion genes, has had a tremendous impact both in the diagnostic algorithms and in the potential therapeutic strategies available for these patients. Cytogenetic and molecular identification of translocations and/or associated fusion genes/transcripts has become part of the routine diagnostic work-up of these tumors. Application of Reverse Transcription, Polymerase Chain Reaction (RT-PCR) (105–109) Fluorescence In Situ Hybridization, and more recently Chromogenic In Situ Hybridization (FISH, CISH) (110–112) assays has allowed the molecular detection of these markers in a variety of specimens, including minute biopsies and formalin-fixed paraffin-embedded samples (FFPE). A number of studies have also addressed the relevance of identifying these fusion transcripts in bone marrow and/or peripheral blood specimens for staging (113) or as a prognostication tool (91, 114–118).

The different *EWSR1* and *Fli1* fusion genes due to the variable breakpoints generate different fusion transcripts. A number of publications have addressed the clinical and biological importance of the molecular transcript variants in these tumors (119–121). An adverse prognosis has been reported in those carrying fusion transcripts other than type I, the most common one. However, it is still uncertain that this phenomenon is not related to other biological factors such as gene interactions, resistance to therapy, or capability of these tumors to metastasize. May and colleagues (122) found no difference in fusion-type tumorigenicity. The true biological meaning of this observation, like in other sarcomas discussed later in this chapter, is still unclear, and its clinical meaning needs to be further explored (65, 123).

Novel and exciting therapeutic strategies are under investigation in EFTs (124, 125) including the use of antisense oligonucleotides against the *EWSR1/Fli1* junction (126) targeting *EWSR1/Fli1* by RNA interference (127, 128), or other potential important genes in these tumors such as vascular endothelial growth factor (129).

Other Bone Tumors

Benign Bone Tumors

Adamantinoma represents 0.5% of all bone tumors, with the anterior diaphysis of the tibia (85%) being the most common site involved (130–132). This tumor is composed of both epithelial and osteofibrous dysplasia components. The epithelial component resembles a conventional ameloblastoma. Cytogenetics with adamantinoma shows recurrent gain in chromosomes 7, 8, 12, 19, and 21 (Table 5). Loss of heterozygosity of TP53 occurs and is restricted to the epithelial component of the tumor.

Table 5 Benign tumors of bone

Adamantinoma	Extra copies 7, 8, 12, 19, 21
Aneurysmal bone cyst	t (16;17) CDH11-USP6 (Tre2, Tre17) t (1;17) AP150-USP6 t (3;17) ZNF9-USP6 t (9;17) Osteomodulin (OMD)/USP6 t (17;17) Collagen1A1 (COL1A1)/USP6 7q, 16p
Clear cell sugar tumor of bone	t (X;2) (q13;q35)
Fibrous dysplasia	GNAS1 Mutations Trisomy 2 12p13
Ossifying fibroma (craniofacial)	t (X;2) (q26;q33) PTHR2-TNFSF5/ZDHHC10 Trisomy 8, 20
Osteofibrous dysplasia	Gains 7, 8,12, 21
Giant cell tumors of bone	Gains 3, 7 Loss 11, 13, 22 Telomeric Fusion at 11p, 13p, 14p, 15p, 19q, 20q, 21q (75%) Rearrangements 16q22, 17p13, ring 11pter
Primary, recurrent, metastatic	LOH 9q, LOH 17p (p53)
Metastatic	LOH 3p26
Recurrent	LOH 3p25
Primary, recurrent	LOH 10q23
Non-ossifying fibroma	t (1;4) (p31;q34)
Osteoid osteoma	22q13.1 Abnormality (deletion, addition) Trisomy 22, 22q monosomy Deletion 17q Monosomy 3, 6, 9, 17, 19, 21
Osteoblastoma	Translocations 15, 17, 20 1q, 1p, 17p deletion 5p, 17q, 22q gain

Aneurysmal bone cyst (ABC) is a cystic lesion that is characterized by fibroconnective tissue septa with intervening blood-filled spaces (130, 131, 133). The fibrous septa contain fibroblasts, giant cells, and reactive bone. Some ABCs have giant cell features as well. The tumor is most often seen in the first two decades of life, but may occur at any age. The most common sites of involvement are the femur, tibia, humerus, and posterior vertebral bodies. Cytogenetic and molecular studies have been extremely helpful in determining that this cyst represents a neoplastic process (130–137). Clonality was initially shown by rearrangement of chromosome 17. Over the past several years, there have been several translocations which involve 17p13 with several other partners. This locus houses the *USP5 (TRE2, TRE17)* gene, which is an ubiquitin-specific protease that represents a potential oncogene and participates in Cdc42/Rac1 Rho GTPase signaling. This signaling pathway affects cell adhesion and actin remodeling. The t (16;17) results in fusion of the *CDH11* (cadherin 11/osteoblast cadherin) gene with *UPS6*. *CDH11* provides a highly active

promoter that upregulates *USP6* transcription. The t (1;17) leads to the *TRAP150* gene promoter being fused to *USP6*. *TRAP150* is located on 1p34.3 and is a thyroid receptor-associated protein. This fusion of an active promoter adjacent to *USP6* allows for unrestricted transcription of USP6. The t (3;17) fuses the ZNF9 promoter to the entire USP6 coding sequence. ZNF9 is a zinc finger transcription factor that is located at 3q21. This gene is also known as *CNBP1* (cellular retroviral nucleic acid-binding protein 1). The t (9;17) positions the OMD promoter adjacent to the entire coding sequence of USP6. OMS (osteomodulin) is located at 9q22 and is a member of the leucine-rich repeat proteoglycan family. This fusion allows for transcription of USP6. The t (17;17) places the entire coding sequence of *USP6* adjacent to the *COL1A1* promoter. The collagen 1A1 (*COL1A1*) gene is located at 17q21.These translocations are found in primary aneurysmal bone cysts and not in "so-called" secondary aneurysmal bone cysts.

Clear cell sugar tumor of bone is a rare mesenchymal tumor of uncertain origin, but evidence points to this tumor being derived from perivascular epithelioid cells (PECs) (130–132, 138). It is likely that this tumor should be reclassified as a PEComa of bone. This is because these tumors express HMB-45, melanA, and smooth muscle markers. Recently, it has been reported that a clear cell sugar tumor of bone displayed a t (X;2) (q13;q35). This was the sole cytogenetic aberration with this particular tumor. Very few PEComas have been evaluated by cytogenetic and molecular means; however, the discovery of this translocation may prove to be important in diagnosis and provide information on pathogenesis.

Fibro-osseous lesions (benign fibro-osseous lesions) comprise a group of clinically distinct entities that have histopathologic overlap (131, 137, 139–142). This group is composed of fibrous dysplasia, ossifying fibroma, and osteofibrous dysplasia. Fibrous dysplasia (fibrocartilaginous dysplasia) affects children and adults with monostotic (85%) and polyostotic (15%) forms. The jaws are the most common sites affected. Other involved sites include long bones, ribs, and skull. This lesion is characterized by a fibrous and osseous component with bland spindle cells and irregular curvilinear trabeculae of woven bone. Occasional psammomatoid bodies may be seen. Cytogenetic studies have demonstrated an activating mutation in *GNAS1* that encodes the alpha subunit of a stimulatory G protein. Clonality has been demonstrated in several lesions, which implies that this disease is neoplastic in origin. Trisomy 2 and structural rearrangement at 12p13 have been demonstrated (Table 5). Ossifying fibroma is confined to the head and neck region and in particular the nasal cavity, paranasal sinuses, craniofacial bones, and jaws (cemento-ossifying fibroma). Cytogenetics has identified translocation between the X chromosome and chromosome 2. This results in fusion of the *PTHR2* gene with the *TNFSF5/ZDHHC10* genes. *PTHR2* encodes for parathyroid hormone receptor 2. *TNFSF5* is a member of the tumor necrosis family, while *ZDHHC10* is a zinc finger transcription factor. All of three of these genes are known to affect tooth development in an adverse manner when mutated or knocked out in animal models. Osteofibrous dysplasia occurs most commonly in the first two decades of life in males and involves the middle third of the tibia (fibrous cortical defect). This entity tends to be self-limiting fibro-osseous lesion, with irregular fragments of woven bone with occasional osteoclasts and bland spindle cells embedded in a myxoid to collagenous background. Cytogenetics demonstrates gains in chromosomes 7, 8, 12, and 21.

Giant cell tumor of bone accounts for about 5% of primary bone tumors and has peak incidence between 20 to 45 years of age (131, 137, 141–146). The most common site involved is the distal femur, proximal tibia, distal radius, and proximal humerus. The tumor is composed of polygonal and elongated mononuclear cells intermixed with osteoclast-like giant cells. The giant cells and stromal mononuclear cells have similar nuclear features. Cytogenetic studies have shown gains in chromosomes 3 and 7, losses in chromosomes 11, 13, and 22, and telomeric fusion in about 75% of cases. Ring chromosome 11pter is a common finding. Rearrangements 16q22 and 17p13 in some tumors have suggested a relationship with aneurysmal bone cysts or a component of aneurysmal bone cysts within some giant cell tumors of bone. More recent loss of heterozygosity studies has characterized giant cell tumors of bone that have certain clinical features, such as non-recurrent, recurrent, and metastatic. These cytogenetic findings may help to predict the behavior of giant cell tumors at initial biopsy, at resection, or at recurrence.

Non-ossifying fibroma (fibrous cortical defect) is a well-demarcated spindle cell lesion with osteoclast-like giant cells and foamy histiocytes, arranged in a storiform pattern (137, 139–142, 147). Typically, this lesion occurs in adolescents in the metaphyseal region of long bones in the lower extremities. A reciprocal translocation involving 1p31 and 4q34 has recently been reported. The 1p31 locus has a common aphidicolin-type fragile site, as well as a zinc finger gene (*ZIS*) and a ras homolog family member (*ARH1*). *ZIS* is a transcription and splicing regulatory gene. *ARH1* is a putative imprinted tumor suppressor gene that is inactivated in ovarian and breast cancer. The 4q34 locus is the site of an apoptotic-related cysteine protease gene, caspase 3 (*CASP3*).

Osteoid osteoma is a small bone-forming tumor that has very limited growth potential and occurs primarily in children and adolescents (131, 137, 141, 142, 148–150). It accounts for 10% of primary bone tumors. These lesions may be found in any bone in the body, but most commonly in long bones, especially the proximal femur. Affected individuals present with pain that increases over time and becomes relentless, often time interfering with sleep. The characteristic

histopathologic appearance is a central nidus of osteoblastic activity. This nidus is surrounded by a zone of sclerotic bone. Cytogenetic studies have shown recurrence chromosome 22 abnormalities (Table 5). These include deletions and additions at 22q13.1, 22q monosomy, and trisomy 22. Certain genes located at 22q13 may play a role in osteoid osteoma development. The *YWAH* gene encodes for a dimeric phosphoserine-binding protein that participates in signal transduction and checkpoint control pathways. PDGF-beta gene produces platelet-derived growth factor that is a potent mitogen for mesenchymal cells and is involved in the transformation process. Additional findings are deletion 17q and monosomy of chromosomes 3, 6, 9, 17, 19, and 21.

Osteoblastoma represents about 1% of primary bone tumors and has a peak incidence between 10 to 30 years of age (80%). It is more commonly seen in males and involves the vertebrae and sacrum most often, although it may be found any bone. The tumor is composed of haphazardly arranged spicules of woven bone lined by a single layer of osteoblasts. The tumors tend to be well demarcated and have a rich vascular bed. Cytogenetic studies have shown translocations with chromosomes 1, 5, 15, 17, 20, and 22. Loss of 17p (site of p53) has also been reported. Several chromosomes have deletions (1q, 1p), while others show gains (5p, 17q, 22q). There are also aberrations at 22q11-13. As noted previously, this is the locus for several genes (*YWAH, PDGF-beta*) associated with cell signaling and transformation. A unique translocation involving chromosomes 1, 5, 17, and 22 has been reported in a large cell telangiectatic osteoblastoma of the mandible with an aggressive behavior.

Table 6 Benign tumors of cartilage

Chondromyxoid fibroma	6q and 6p rearrangements
	Inversion (6) (p25q13)
	Translocation (3;6) and (6;9)
Chondroma	Trisomy 5
	6 Structural abnormalities
	12q13-15 Rearrangement
	4q, 14q, 16q, and 20
Chordoma	Monosomy 3, 4, 10, 13
	1p, 17p, 19, 3p, loss
	5q, 7q, 5q, 12q and 20 gain
	der (6)t (6;13)
	der (9)t (9;11)
	t (19;20) (q13;q11.2)
Parachordoma	Breakpoint on X
	9 loss
Osteochondroma	8q22.1-24 loss (EXT1)
	11p11-12 loss (EXT2)
	19p (EXT3)
	1p36.1 (EXTL1)
	1p21 (EXTL2)
	8p21 (EXTL3)
	1p13-22 breakpoint (inversion, insertion, translocation)
	t (X;13) (q21;q12)
	t (1;8) (q23;q21)
	t (8;8) (p23.1;q24.1)
	t (11;17) (p11.2;p13)
	t (11;22) (p11.2;p11)
Chondroblastoma	Ring Chromosome 4
	Chromosome 5 and 8 abnormalities
Chondromatosis, synovial	Chromosome 6p, 6q Abnormalities
	1p12-21 rearrangement
	Loss of X and Y
	Gain of Chromosome 5

Cartilaginous Tumors

Although not encountered frequently by most surgical pathologist, there are numerous tumors that are derived from cartilage. Most are readily identifiable, while others are quite rare. During the past decade, cytogenetic and genetic alterations in benign cartilaginous tumors have been identified and provide information regarding specific diagnostic categories (Tables 6 and 7).

Benign Tumors of Cartilage

Chondromyxoid fibroma is a benign tumor occurring in children and adults that accounts for 2% of cartilaginous tumors (8, 131, 137, 151–154). It involves primarily metaphyseal regions of long bones, in particular the proximal tibia and distal femur. The tumor is composed of lobules of spindled to stellate cells embedded in an abundant myxoid to chondroid stroma. The periphery of the lobules has dense cellularity with both spindled cells and osteoclast-like giant cells. Hyaline cartilage undergoing ossification with coarse calcification may also be present. The central portion of the lobules is typically hypocellular. This tumor may be mistaken for chondroblastic osteosarcoma or chondrosarcoma. Cytogenetic analyses of this tumor (Table 6) have shown recurring abnormalities with chromosome 6 involving both the long and the short arms. Rearrangements at 6q12-27 have been repeatedly demonstrated, as well as at 6p23-25. Two distinct translocations have been reported, t (3;6) (p12-14;q21-24) and t (6;9) (q25;q22). Interestingly, the type X collagen gene (*COL1OA*) is located at 6q21-22, and the parathyroid hormone/parathyroid hormone-related peptide receptor gene (*PTH/PTHrP*) locus is on 3p. Type X collagen is necessary for normal growth plate formation and function. This gene is also implicated in Schmid-type metaphyseal chondrodysplasia. The *PTH/PTHrP* gene is a member of the G protein-coupled receptor family. Osteoblasts and growth plate chondrocytes possess PTH/PTHrP receptors and secrete PTHrP, implying an autocrine-paracrine regulatory loop. Mutations in this gene are

Table 7 Malignant tumors of cartilage

Chondrosarcoma, conventional	Complex karyotypes
	Abnormalities: 1, 5, 6q, 7, 8q, 9, 11, 12q13-15, 15, 18, 20
	Chromosomal loss: 1p36; 1p13-22, 4, 5q13-31, 6p22-pter, 9q22-pter, 10p, 10q24-pter, 11p13-pter, 11q25, 13q21-pter, 14q24-pter, 18p, 18q22-pter, 221q
	Chromosomal gain: 7p13-pter, 9p, 12q15-pter, 19, 20pter-q11, 21q
	LOH 13q14 RB1
	LOH 17p13 TP53
	LOH 9p21 CDKN2A, CDKN2B
	CGH gains: 20q12pqter (37%), 20q (32%), 8q24-pter (27%), 20p (24%), 14q24-qter (24%), 7, 5q1432, 6p, 12q
	CGH losses: Xcen-q21 (11%), 6cen-q22 (11%), 18cen-q11.2 (11%)
Extraskeletal myxoid chondrosarcoma	t (9;22) (q22;q12) EWS-NOR1 (NR4A3)
	t (9;15) (q22;q21) TCF12- NOR1 (NR4A3)
	t (3;9) (q11-12;q22) TFG/NOR1 (NR4A3)
	der (16)t (1;16) (q21;q13)
	Trisomy 1q, 7, 8, 12, 19
Chondrosarcoma mesenchymal	der (13;21) (q10;q10)
	17p13 TP53
	9p21 CDKN2A
Dedifferentiated chondrosarcoma	t (10;22) (p11.2;q11.2)
	1p36
	5q11.2
	Chromosome 17
	Gains 5, 7, 12, 20
Skeletal myxoid chondrosarcoma	Clonality 1q, 6q, 9p, 12p, 12q
	Loss 4, 6, 9
	Gains 8, 20
	22q11-12
	10q21-23
	Monosomy 10

responsible for Jansen-type metaphyseal chondrodysplasia (short-limb dwarfism). Tumor suppressor genes area also located at 6q25 (LOT-1, lost on transformation-1) and 6q21 (*AIM-1*, absent in melanoma-1).

Chondroma is generally considered to be a group of benign cartilaginous tumors including enchondroma, periosteal chondroma, and enchondromatosis (Ollier disease and Maffucci syndrome) (131, 137, 154–156). These tumors differ in their location and clinical presentation. The tumors appear similar with multiple nodules of cartilage with abundant hyaline cartilage, typical chondrocytes with low cellularity, and lack of vascularity. Enchondroma involves medullary bone and tends to be solitary, accounts for up to 25% of bone tumors, and most commonly involves the tubular bones of the hand. Periosteal chondroma involves the bone surface and is uncommon, accounting for only 2% of all chondromas. It involves primarily the long bones and most frequently the proximal humerus. Enchondromatosis (Ollier disease) is rare and occurs in a young age group. Multiple intraosseous and subperiosteal tumors are present and involve multiple sites, most commonly the hand, as well as foot, femur, humerus, and forearm. Enchondromatosis is a developmental disorder that lacks normal enchondral ossification. When combined with angiomas of soft tissue and rarely viscera, the term Maffucci syndrome is used. Malignant transformation may occur (20–50%) with enchondromatosis. Cytogenetic analyses have revealed certain recurring abnormalities (Table 6). Common findings are trisomy 5, extra copies of chromosome15, rearrangement of 12q13-15, and rearrangement of 6q. It is well known that 6q has certain genes that play a role in chondrocyte differentiation (PTHrP, bcl-2). Detectable levels of PTHrP and bcl-2 have been demonstrated in chondromas. The chromosome 12q13-15 locus is where *MDM2, CDK4, SAS, HMGI-C*, and *CHOP* genes are found. These genes are known to participate in neoplastic and proliferative processes.

Chordoma accounts for 1–4% of bone tumors and occurs along the axial spine, with most being located in the sacrum (131, 137, 154–156). This tumor recapitulates the notochord structure, is lobulated with abundant myxoid stroma, and possesses tumor cells with abundant vacuolated pale cytoplasm (physaliphorous cells). Chordomas may have loss of chromosomes 3, 4, 10, and 13. In addition, there are deletions in segments of certain chromosomes in over 50% of cases (1p11-21, 1p36, 1p31-pter, 3p21-pter, 3q21-qter, 9p23-pter, 17q11-qter). Chromosome 1p36 is the location for several tumor suppressor genes and regulators of the cell cycle. In addition, losses with 3p and 1p, as well as gains in 5q, 7q, 12q, and 20 have also been noted. Translocations have been discovered in isolated cases. In contrast, parachordoma has relatively few chromosomal abnormalities reported (breakpoint on X, 3 and loss of 9, Table 6).

Osteochondroma is characterized as a cartilage capped bony projection that contains a bone marrow cavity that is contiguous with the underlying bone (8, 131, 137, 151, 154, 157–161). It represents about 35% of benign bone tumors. This neoplasm may occur as a solitary lesion (85%) or as multiple lesions (15%). Multiple osteochondromas (osteochondromatosis) has an autosomal inheritance pattern, and may lead to skeletal deformities and disproportionate short stature. The common sites of involvement are the metaphyseal regions of the distal femur, proximal humerus, proximal tibia, and fibula. The tumor is composed of a perichondrium, a cartilaginous cap, and bone. Cytogenetic investigation of these lesions has proven that these tumors are neoplasms and not developmental disorders. Hereditary multiple exostoses (osteochondromatosis) has a prevalence of 1 in 50,000. Two genes have been identified *EXT1* (8q24) and *EXT2* (11p11-12). Linkage to 19p has resulted in the discovery of the EXT3 gene. There are also several EXT-like genes as well (*EXTL1*

1p36.1, *EXTL2* 1p21, *EXTL3* 8p21). *EXT1* and *EXT2* genes encode for a type II transmembrane glycoprotein localized to the endoplasmic reticulum. This glycoprotein is required for heparin sulfate polymerization. Heparin sulfate proteoglycan when linked to a protein core participates in cell signaling pathways (fibroblastic growth factor pathway). This proteoglycan is important for activation of the ttv gene responsible for diffusion of Indian hedgehog. Indian hedgehog and PTHrP are important factors in normal chondrocyte proliferation and differentiation at the growth plate, and both are dependent upon heparin sulfate glycoprotein cell signaling. *EXT1* deletions or rearrangements are often seen in Langer-Giedion syndrome. This syndrome is composed of multiple exostoses, facial dysmorphism, mental retardation, and loss of function of *TRPS1* and *EXT1* genes. DEFECT-11 syndrome has deletions of *EXT2* and *ALX4* genes. This syndrome is characterized by enlarged parietal foramina, multiple exostoses, craniofacial dysostosis, and mental retardation.

Chondroblastoma represents <1% of bone tumors and primarily involves long bones with the most common sites being the epiphyseal and epimetaphyseal regions of the femur, proximal tibia, and proximal humerus (131, 137, 145, 154, 155). The tumor is composed of uniform round to polygonal cells with amphophilic to eosinophilic well-defined cytoplasm. The nuclei often have clefts (reniform) or longitudinal grooves. Osteoclast giant cells may be randomly distributed in the tumor. Hyaline cartilage is seen rarely. Chicken-wire calcifications are usually present. Aneurysmal bone cyst changes may also be noted. These tumors may have a ring chromosome 4, and abnormalities with chromosomes 5 and 8 (Table 6).

Chondroid tumor of undetermined malignant potential (CHUMP) is a recently described category that includes well-differentiated chondroid borderline tumors, lacking definitive features to allow for diagnosis as either a low-grade chondrosarcoma or a benign cartilaginous tumor (154, 160). There are a limited number of these tumors that have had cytogenetic studies performed. So far, the karyotypes in these cases have been normal; however, more extensive studies for cryptic molecular abnormalities have not been initiated.

Synovial chondromatosis arises within the synovium as a benign nodular cartilaginous proliferation involving joints, bursae, and tendon sheaths (8, 151, 154). The knee joint is most commonly involved. These painless nodules adjacent to joints are composed of variably cellular hyaline cartilage with a fine fibrous capsule. Recurrent chromosome 6 abnormalities have been described. Loss of Rab23, an essential negative regulator of the sonic hedgehog signaling pathway, has been demonstrated in synovial chondromatosis. In addition, loss of collagen X and collagen IX genes have been implicated in the pathogenesis. Additionally, loss of chromosomes X and Y and gains in chromosome 5 have been reported. Rearrangement in 1p13-22 has been found in several cases.

Malignant Cartilaginous Tumors

Conventional chondrosarcoma is a malignant bone tumor with hyaline cartilage differentiation that accounts for 20% to 33% of all malignant bone tumors (131, 132, 153, 154, 158, 160, 162). The most common sites are the pelvic bones followed by the proximal femur, proximal humerus, distal femur, and ribs. Typically, the tumors are composed of irregular nodules of cartilage of variable size and shape. The tumors tend to be hypercellular and have a range of differentiation from more typical chondrocytes to chondroblasts with marked pleomorphism. Cytogenetics with conventional chondrosarcomas demonstrate highly complex karyotypes (Table 7). There are many different chromosomes that have abnormalities, losses, and gains, both with conventional cytogenetics and by comparative genomic hybridization. There are also several tumor suppressor (*Rb, TP53*) and cell cycle (*p16 – CDKN2A, p15 – CDKN2B)* genes that undergo loss of heterozygosity. No specific cytogenetic marker has been discovered for conventional chondrosarcoma.

Extraskeletal myxoid chondrosarcoma is a malignant tumor that has a multinodular pattern with prominent myxoid stroma and malignant chondroblast-like cells (132, 147, 154, 162–165). The malignant cells tend to be arranged into cords and nests and embedded in a myxoid matrix. This tumor represents <3% of all soft tissue tumors. Typically, it arises in deep soft tissues of the proximal extremities and the supporting limb girdles. In contrast to conventional chondrosarcoma, tumor-defining translocations have been identified by cytogenetic and molecular means. The most common translocation involves the *EWSR1* gene at 22q12 and the *NOR-1* gene at 9q22. NOR-1 is a member of the steroid and thyroid receptor family and encodes a novel orphan nuclear receptor with a zinc finger DNA-binding domain. The t (9;17) is a cryptic rearrangement of the *RBP56* gene at 17q11, which is closely related to the *EWSR1* gene. This is paired with *NOR1*. It is thought that *RBP56* is a potent transcriptional activator. The t (9;15) results in fusion of the *NOR1* gene with *TCF12* (15q21). *TCF12* has a leucine zipper domain and encodes a bHLH protein that is a ubiquitously expressed transcription factor. This transcription factor plays an important regulatory role in cell growth and differentiation. In general, this protein is a negative regulator of cell proliferation via enhancement of cyclin-dependent kinase inhibitor genes and promotion of cell death (apoptosis). Translocation of the *TCF12* gene interrupts its negative regulatory functions.

Other nontumor-defining cytogenetic findings include trisomy of several chromosomes.

vDedifferentiated chondrosarcoma accounts for 10% of chondrosarcomas and typically involves the pelvis, femur, and humerus (132, 147, 154, 160, 162, 163). The tumor has two components, a well-differentiated cartilaginous tumor (enchondroma, low-grade chondrosarcoma) and a high-grade non-cartilaginous sarcoma (pleomorphic undifferentiated sarcoma, osteosarcoma, rhabdomyosarcoma). Although no tumor defining cytogenetic characteristics have been confirmed, recently a t (10;22) has been reported (Table 8). Karyotypes have been characterized as having structural and numerical aberrations, with chromosomes 1 and 9 being affected most commonly. The gene *STK15 (BTAK)* that encodes a centromere-associated kinase affecting chromosome segregation and aneuploid development may play a role in the pathogenesis of dedifferentiated chondrosarcoma. There is overexpression and amplification of this gene in this tumor and it may be related to tumor progression.

Skeletal myxoid chondrosarcoma is a rare tumor and involved the skull base (8, 132, 147, 154, 162, 163). Clonal chromosomal abnormalities have been reported with several tumors, as well as loss of chromosomes 4, 6, and 9. Additional findings include allelic loss of 22q11-12 and 10q21-23, as well as monosomy 10.

Soft Tissue Sarcomas with Specific Genetic Abnormalities

Rhabdomyosarcoma

Rhabdomyosarcoma (RMS), the most common soft tissue sarcoma in children, is a small round cell tumor of skeletal muscle histogenesis, thought to arise as a consequence of loss of growth control and differentiation of myogenic cells (166). Its differential diagnosis often depends on the identification of rhabdomyoblasts or the detection of muscle-specific proteins in the tumor cells (167, 168). Histologically, three main types of RMS can be identified: Botryoid, Embryonal, and Alveolar, associated with poorer prognosis. Separate categories have been established for undifferentiated sarcoma, anaplastic, and sarcoma NOS (not otherwise specified) subtypes (168–170). Cytogenetic analysis revealed chromosomal abnormalities, primary aneuplodies, in all subtypes of RMS. In the alveolar subtype two specific chromosomal translocations have been identified. The t (2;13) (q35;q14) translocation can be cytogenetically detected in approximately 60% of alveolar RMS (171–173). This translocation juxtaposes the *Pax3* gene on 2q35, a transcription factor functional during early neuromuscular development, to *FKHR* gene (*FoxO1A*)

Table 8 Benign tumors of adipose tissues

Hibernoma	11q13	MEN1
	11q13-21	PPP1A (PPP1CA)
Lipoblastoma	8q11-13	PLAG1
	t (8;8) (q24.1;q11-13)	HAS2-PLAG1
	t (7;8) (q11-13;q22.1)	COL1A2-PLAG1
	der (8)	HAS2/PLAG1
	Ring Chromosome 8	HAS2/PLAG1
	t (7;8)	COL1A2/PLAG1
	t (7;8), t (3;8), t (7;8), other	PLAG1/?
Lipoma (ordinary)	t (12q13-15) (3q28)	HMGIC/LPP
	t (12q13-15) (6p21-22)	HMGIC/HMGI (Y)
	13q deletion	HMG1L
	t (3;12)	HMGIC/LIM
	t (12;13) (q14-22;q21-32)	HMGIC/LHFP
	t (3;6) (q28;-21)	HMAG1
	Other chromosomes 1, 3, 6p, 21	
Intramuscular lipomas	8q11-13, 12q14-15, 13q	
Parosteal lipoma	t (3;12)	HMGA2/LPP
Spindle cell and pleomorphic lipoma	13q deletion	HMG1L
	16q deletion	
Chondroid lipoma	t (11;16)	CD5-PLCB3
Fibrolipoma	t (12;16), t (1;12)	
Angiolipoma	t (X;12)	
Angiomyolipoma	9q34	TSC1
	16p13	TSC2
	Extra Copies 7 and 8	
Angiomyxolipoma	t (7;13), t (8;12)	
Adenolipoma	t (12;16), del (1) (p22)	

on 13q14, a member of the forkhead family of transcription factors (174–176). As a result of this translocation the 5' portion of the *Pax3* gene, including an intact DNA-binding domain, is fused to *FKHR*, resulting in a chimeric transcript and protein containing the *Pax3* DNA-binding domain and the distal half of the forkhead and C-terminal region of *FKHR* (176). A less common variant of the translocation, fusing *Pax7* gene, located on 1p36, to *FKHR*, and resulting in a t (1;13) (p36;q14) translocation, has also been associated with alveolar RMS (177, 178). A third t (2;2) (q35;p23) translocation fusing *Pax3* to *NCOA1* (nuclear receptor coactivator) gene (179) has been recently identified.

Gene expression profiling has demonstrated the activation of a myogenic transcription program by the *Pax3/FKHR* fusion oncogene (180) and it is assumed that these unique fusion genes activate the transcription of downstream genes, ultimately responsible for the transformed phenotype seen in these tumors; however, the exact mechanism is still under investigation (181–183).

Molecular identification of these fusion transcripts, mostly using RT-PCR and FISH assays (Fig. 3), are helpful in diagnosing these tumors, particularly when limited diagnostic material available or when microscopic and immunohistochemical findings are equivocal (107, 113, 184–187). In a recent Children's Oncology Group (COG) study, Pax3-FKHR and PAX7-FKHR fusion transcripts were identified in a majority of alveolar RMSs analyzed (77%), with the first being almost twice as common as the Pax7 fusion in these tumors (188). Pax7 fusion genes are more often associated with lesions in the extremities occurring in younger patients and have a better outcome than those carrying a Pax3 fusion, representing another example of sarcomas with fusion gene variants of apparent clinical relevance (188–190). Barr and colleagues have documented a true "fusion-negative" subset of alveolar RMS represented by a genetically diverse subset of tumors, including low-expressors of the common fusion genes, fusion variants with other genes, and true negative cases (191).

No specific chromosomal abnormality has been associated with Embryonal RMS. Instead, complex numerical and structural abnormalities on chromosomes 2 and 11, and trisomies of chromosome 8 have been reported (192). Loss of heterozygosity of 11p15 locus, the site for *IGF-II* and *MyoD1* genes and genomic imprinting, a mechanism associated with Beckwith-Wiedeman syndrome and Wilms tumors, has also been implicated in Embryonal RMS tumorigenesis (193). Bridge and colleagues documented a number of novel genomic imbalances in embryonal RMS by CGH (Comparative Genomic Hybridization) analysis of 12 tumor specimens (147). Kurmasheva and colleagues recently documented the presence of *Pax3* CpG island methylation in 13 of 15 embryonal RMSs tested, an epigenetic mechanism that appears to be characteristic of this RMS subtype (194).

Abnormalities in a variety of signaling pathways have been reported in RMS.

Isolation of gene members of the *MyoD* family of myogenic transcription factors provided us better understanding of the mechanisms regulating skeletal-muscle differentiation. They all share sequence homology for the basic-helix-loop-helix (bHLH) regulatory motif and a basic domain required for DNA binding. The bHLH motif confers both properties of transcriptional activation of muscle specific genes and inhibition of cell growth. Their function can be suppressed through inhibition of their expression or activity by various growth factor gene products and oncogenes (*FOS, JUN, MYC, RAS, SRC*) (195, 196). Expression of myogenin in rhabdomyosarcoma has been associated with the alveolar subtype and worse prognosis (167, 197).

The investigation of tumor suppressor genes demonstrated the involvement of *RB* and *P53* genes (both in Li-Fraumeni patients and somatic tumor mutations) in RMS (30, 198–200). Mutation of *PTCH, MDM2, CDK4* genes and *MYCN* amplification (201–203) have also been documented, and a correlation between *MYCN* copy number and prognosis in alveolar RMS reported (204). A number of novel genes of potential prognostic and diagnostic relevance for alveolar rhabdomyosarcoma have been recently identified by expression profiling (205).

Desmoplastic Small Round Cell Tumor

Desmoplastic small round cell tumors (DSRCT) are a group of uncommon, poorly differentiated neoplasms of children and young adults, often showing miltilineage differentiation and characteristic desmoplastic stroma. First described by Gerald (206, 207) these tumors are aggressive neoplasms, probably arising from the serosal lining and associated mesenchyme (208, 209). More common in boys, DSRCTs typically present as disseminated lesions in the abdomen or pelvic region, and less frequently in other sites (210, 211).

DSRCT are characteristically associated with the recurrent translocation t (11;22) (p13;q12), first described by Sawyer and colleagues (212) and also recognized by other authors (213), including variants that involve additional chromosomes (214). Gerald and colleagues (215, 216) described the fusion gene that results from the t (11;22) (p13;q12) translocation, and fuses the *EWSR1* gene on 22q12 to WT1 (Wilms) tumor suppressor gene on 11p13. Similarly to other translocations involving the *EWSR1* gene (encoding a protein with a c-terminal region homologous to RNA-binding domains), the fusion product contains the amino terminal domain of *EWSR1* fused to the DNA-binding domain of *WT1*. The chimeric *EWSR1-WT1* product includes

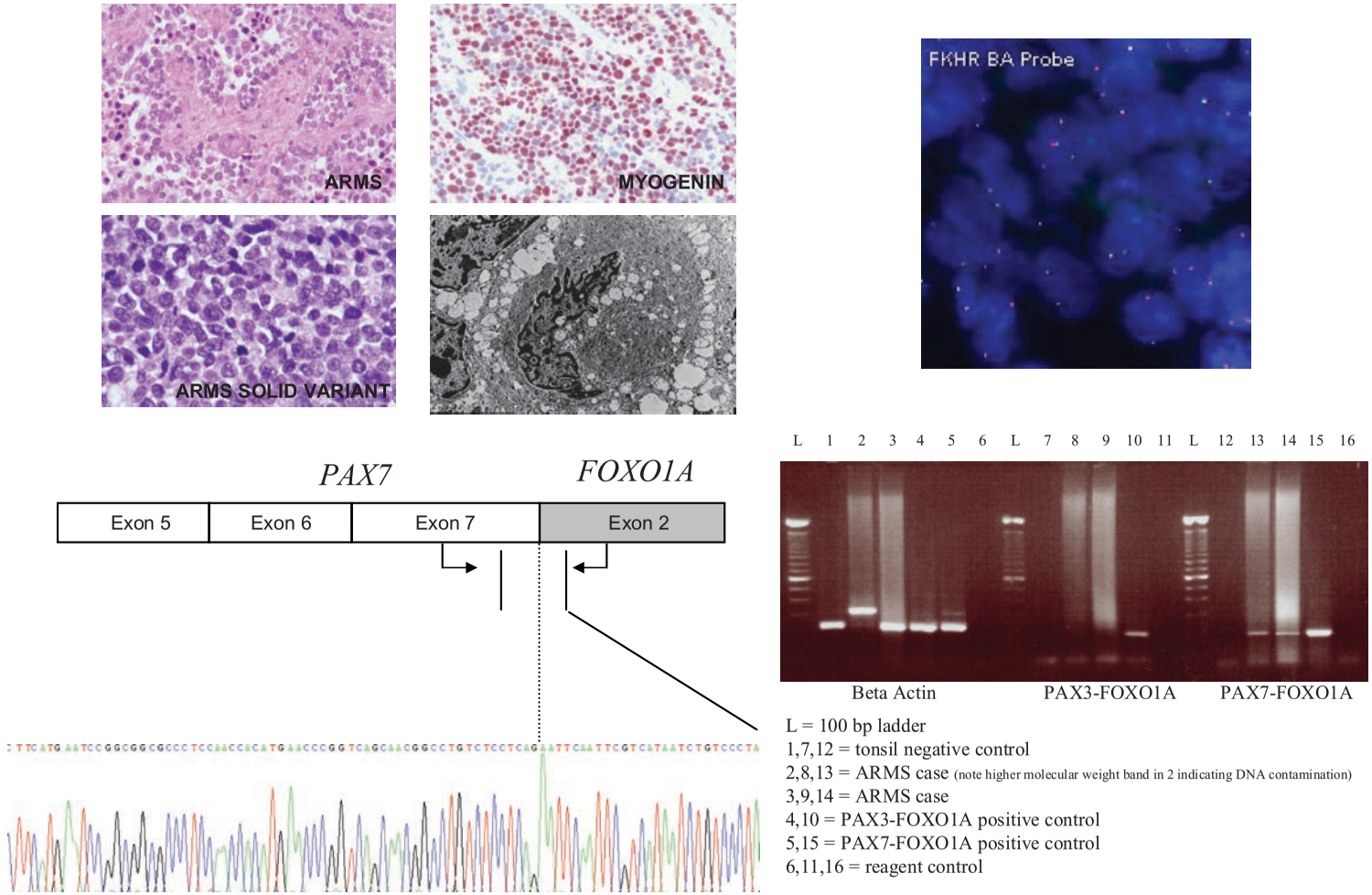

Fig. 3 Alveolar Rhabdomyosarcoma diagnosis: H&E of an alveolar rhabdomyosarcoma (ARMS) and a solid variant ARMS, IHC stain for myogenin, and electron microscopy of the same case (*upper left*), Fluorescence in situ hybridization (FISH) using a breakapart FKHR (FOXO1A) probe (*upper right*), RT-PCR analysis of the case, showing Pax7/FOXO1A chimeric transcript sequence (*bottom, left*), and PCR agarose gel (*bottom, right*)

2 alternatively spliced forms of the zinc-finger domain of WT1, which probably modifies its binding affinities (217).

The t (11;22) (p13;q12) of DSRCTs most commonly results in the fusion of the first seven exons of *EWSR1* to the last three of the *WT1* gene; however, a number of variants have been reported (215, 218–220) demonstrating the molecular heterogeneity of the resulting fusion genes, that encode functionally different transcripts. The clinical significance of the different *EWSR1-WT1* fusion products is still under investigation.

A variety of publications have documented the use of molecular RT-PCR-based diagnostic applications for the identification of the chimeric EWSR1-WT1 transcripts (113, 221, 222), which has become part of the standard diagnostic workup in these tumors. Reports of the translocation by FISH analysis are limited and usually combined with conventional cytogenetics (214, 217, 223).

Synovial Sarcoma

Synovial sarcoma is an aggressive, relatively common sarcoma (approximately 10% of all soft tissue sarcomas) of unknown histogenesis that affects children and young adults, with a slight male predominance (224–226). The most common sites involved are the limbs and particularly areas adjacent to joints, although they can arise in almost any area of the body including the trunk, mediastinum, abdominal wall, head and neck, lung, and pleura (227–231). Histologically, there are two subtypes of synovial sarcoma: the monophasic type composed of spindle cells and the biphasic synovial sarcoma type that also contains areas with variable degrees of epithelial differentiation, form carcinoma-like to "occult" subtle cases. Cytogenetically both monophasic and biphasic synovial sarcomas share a recurrent reciprocal t (X;18) (p11.2;q11.2) translocation. This translocation fuses the *SYT* gene on chromosome 18q11 to either of three homologous genes on Xp11, *SSX1, SSX2*, and rarely *SSX4* (232, 233). The *SSX1* and *SSX2* genes encode closely related proteins with 81% identity. The N-terminal portion of each SSX protein exhibits homology to the Kruppel-associated box (KRAB), a transcriptional repressor. Both the SYT-SSX1 and the SYT-SSX2 hybrid transcripts encode fusion proteins in which the C-terminal 8 amino acids of the normal SYT protein have been replaced by 78 amino acids encoded by an *SSX* gene (234). SYT and SSX proteins appear to be transcriptional regulators primarily through protein–protein interactions, (235) SYT acting as an activator of transcription and SSX as a repressor (236).

Cytogenetic studies on series of synovial sarcomas demonstrated a near-diploid karyotype in a majority of the cases and the t (X;18) (p11.2;q11.2) translocation as the sole cytogenetic abnormality present in approximately a third of synovial sarcomas (213, 237–239). Other chromosomal changes include numerical changes (240, 241) and no other recurrent structural abnormalities.

Molecular detection of SYT-SSX1 and 2 fusions has been demonstrated to be of tremendous clinical value. PCR analysis (Fig. 4) demonstrated the presence of SYT-SSX1 or SYT-SSX2 fusion transcripts in approximately 95% synovial sarcomas examined, indicating that the detection of these hybrid transcripts by PCR may represent a useful diagnostic method. Sequence analysis demonstrated further heterogeneity in the fusion transcripts with the formation of two distinct SYT-SSX1 fusion junctions and two distinct SYT-SSX2 fusion junctions. Coexisting SYT-SSX1 and SYT-SSX2 has been reported in 10% SYT-SSX positive primary tumors (242). Kawai (243) found a relationship between the type of fusion transcript and the histologic subtype (with SYT-SSX1 associated mostly with biphasic and SYT-SSX2 with monophasic types) as well as with prognosis, with a significantly better metastasis-free survival associated with the *SYT-SSX2* subtype. Skytting and colleagues (244, 245) suggested that the base pair differences between the SSX transcripts may have biological significance. The impact of the *SYT-SSX* fusion type on the clinical behavior of synovial sarcoma has since become a subject of scientific debate. Ladanyi and colleagues (246) found fusion type "the single most significant prognostic factor by multivariate analysis in patients with localized disease at diagnosis" for synovial sarcoma. However, a recently published european retrospective analysis found that the most important factor determining the prognosis of these patients is histologic grade, and not SYT-SSX fusion type (247). Further studies, with careful clinical, morphologic, and molecular correlation will be necessary to determine the significance of the molecular fusion type in synovial sarcoma.

Adipocytic Tumors

Benign Adipose Tissue Tumors

Hibernoma is a rare benign adipose tumor representing about 1% of adipocytic tumors. It most commonly occurs in the third and fourth decades of life (132, 156, 163, 248). The common tumor sites are the thigh, trunk, upper extremity, and head and neck. This well-demarcated tumor is composed of brown fat. The adipocytes possess granular and multivacuolated cytoplasm. Cytogenetic analyses have shown recurrent 11p13 and11p13-21 structural rearrangements (Table 9). These sites house the *MEN1* gene and the *PPP1 (PPP1CA)* gene.

Lipoblastoma is a benign adipocytic tumor that typically is discovered during the first 3 years of life and may be

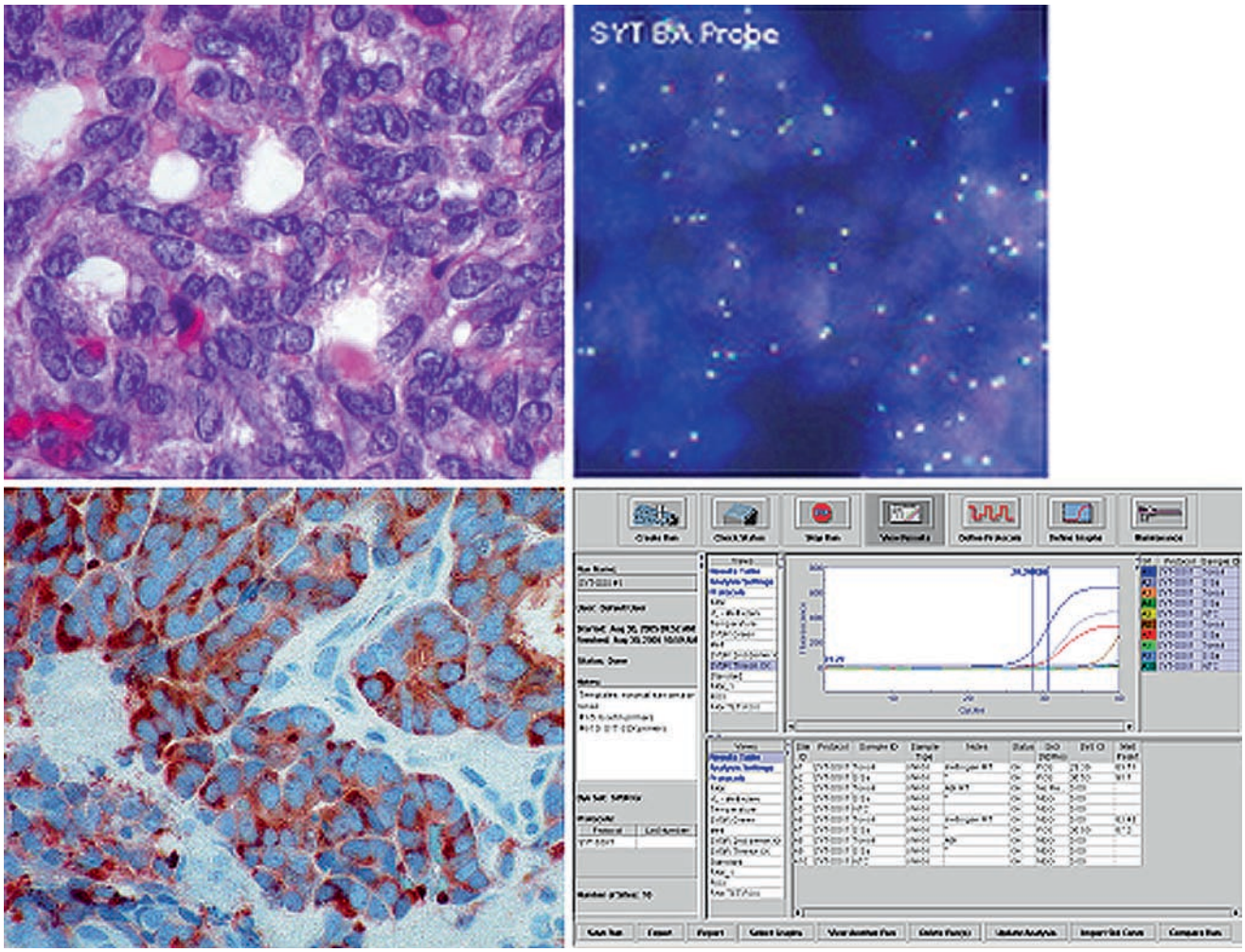

Fig. 4 Synovial sarcoma diagnosis: H&E and EMA immunohistochemistry of a biphasic synovial sarcoma (*left*), Fluorescence in situ hybridization (FISH) using a breakapart SYT probe (*upper right*), and RT-PCR analysis of the case, showing real-time PCR detection of a SYT/SSX1 chimeric transcript (*bottom, right*)

Table 9 Malignant tumors of adipose tissue

Well-differentiated liposarcoma (atypical lipoma or lipomatous tumor)	12q13-15 amplified or rearranged	GLI, CHOP, DDIT3, ATF1 SAS, CDK4, MDM2 HMGA2, HMGC1
	Ring, giant marker chromosomes	
	1q21-23 Amplified	
	3q13.2-225 Amplified	
Dedifferentiated liposarcoma	12q13-15 Amplified	MDM2
	17p	TP53 Mutations
	Ring, giant marker chromosomes	
Myxoid and round cell liposarcoma	T (12;16) (q13;p11)	FUS (TLS)-DDIT3 (CHOP) (95%)
	t (12;22) (q13;q12)	EWS-DDIT3 (5%)
	t (12;22;20) (q13;q12;q11)	EWS-DDIT3
	Trisomy 8	
Pleomorphic liposarcoma	Ring chromosome 12	MDM2
	17p	TP53
	Nonspecific chromosomal gains and losses	
	Amplification of CCND1, GLI, CDK4, MYB, ESR1, A1B1	

lobulated, localized tumors (lipoblastoma), or diffuse (lipoblastomatosis) (132, 156, 163, 248, 249). The trunk and extremities are most commonly involved. These tumors are composed of a mixture of mature and immature adipocytes and may have a myxoid matrix with a plexiform capillary network. This myxoid matrix and capillary network, along with lipoblasts, may cause confusion with myxoid liposarcoma. Cytogenetics is quite helpful in distinguishing lipoblastomas from other adipocytic tumors (Table 9). Translocations involving *HAS2/PLAG1* and *COL1A2/PLAG1* are characteristic found with lipoblastomas. *HAS2* is located at 8q24, *PLAG1* at 8q12, and *COL1A2* at 7q22. Additional copies of chromosome 8 are often times seen with lipoblastomas, as well.

Lipoma (ordinary) is composed of mature adipose tissue and is surrounded by a capsule (132, 156, 163, 248). This is the most common soft tissue tumor in adults. Lipomas may occur in the subcutis (superficial lipoma), within deep soft tissues (deep lipoma), within or between muscle (intramuscular or intermuscular lipoma), or within the periosteum (parosteal lipoma). Cytogenetics with lipomas demonstrates certain recurring abnormalities. There are frequent translocations involving the 12q13-15 region which houses the *HMGIC (HMGA2)* gene. This gene encodes for proteins that form higher order nucleoprotein transcriptional complexes through their ability to modify DNA structure. These genes play critical roles in growth and development. The resulting proteins are associated with transformation and neoplastic proliferations. The *HMGIC* gene fuses with the *LPP, LIM*, and *LHFP* genes in lipomatous tumors. *LPP* (3q28, lipoma preferred partner) allows regulatory flexibility due to the presence of alternative promoters and transcription start sites. *LIM* (3q29, lin-11 isl-1 mec-3) functions in cell signaling and developmental regulation. The *LIM* domain acts as modular protein binding interfaces and acts through protein–protein inactions rather than DNA binding. *LHFP* (13q21-32) is found in about 7–8% of cytogenetically abnormal lipomas. The function of this gene is still being elucidated.

Spindle cell and pleomorphic lipoma most often occurs on the neck or back as a well-circumscribed lesion (132, 156, 163, 248, 249). The spindle cell lipoma is formed by bland spindle cells, hyperchromatic cells, and multinucleated giant cells with thick wavy collagen. The pleomorphic lipoma has similar features, but has floret-like giant cells with occasional myxoid stroma. Cytogenetic studies have shown that over 50% have chromosome 16 aberrations (Table 9). Monosomy or partial loss of 13q is also common.

Chondroid lipoma is a benign tumor containing lipoblasts, mature adipose tissue, and chondroid matrix (132, 156, 163, 248, 249). It most commonly occurs in the proximal extremities and limb girdles, and is deep seated. Two unique translocations have been reported. One translocation is associated with chromosomes 1, 2, and 5. The other translocation results in fusion of *CD5* (11q13) and *PLCB3* (16p12-13). 11a13 abnormalities have also been identified in hibernomas and typical lipomas.

Fibrolipoma are relatively rare tumors that have certain cytogenetic abnormalities that are seen in typical lipomas (Table 5) (156, 249). Several translocations have been reported and these involve the 12q13-14 region (*HMGIC* gene locus), usually seen in typical lipomas.

Angiolipoma are relatively common and occur in the second and third decades of life as subcutaneous nodules composed of mature adipose tissue intermixed with small thin-walled vessels (156, 249). The forearm is the most common site. Recently, a translocation has been identified in this entity involving Xp22 and 12p12. Angiomyolipoma is composed of mature adipose tissue, vascular structures, and smooth muscle cells (156, 249). The common sites of involvement include the kidney, retroperitoneum, liver, and abdomen. These tumors arise sporadically as isolated masses or as part of the tuberous sclerosis complex. Various tumor suppressor genes may be involved in the neoplastic process. *TSC1* (9q34, hamartin), *TSC2* (16p13, tuberin), and 5q33-34 (tumor suppressor locus) are altered in angiomyolipomas. Extra copies of chromosome 7 and 8 and rearrangement of 12 have also been reported.

Angiomyxolipoma is an extremely rare neoplasm that has two translocations that have been discovered (Table 5) (156, 249). One translocation leads to fusion of the 7p12 locus with the 13q21 locus. The second translocation involves an 8q13 and 12p13 loci. The 8q13 (lipoblastoma) is known to be altered in other benign adipocytic tumors.

Malignant Adipose Tissue Tumors

Well-differentiated liposarcoma (atypical lipoma/atypical lipomatous tumor) accounts for 40% to 45% of liposarcomas and is locally aggressive mesenchymal tumor composed of relatively mature adipocytes with variation in size and nuclear atypia with the adipocytes and stromal cells (132, 156, 249). There are scattered lipoblasts. This tumor has no metastatic potential and is locally aggressive. The most common sites for this tumor are deep soft tissues of the extremities, retroperitoneum, paratesticular regions, and mediastinum. Dedifferentiation does occur, most commonly with the retroperitoneum (20%), but is dependent upon site (retroperitoneum) and tumor duration. Cytogenetics (Table 8) have consistently demonstrated certain findings in well-differentiated liposarcoma, including supernumerary ring (circular) chromosomes, giant rod marker chromosomes, and dmin (double minutes) in 80% of tumors. The 12q13-15 region is amplified or rearranged in many of these tumors. This locus is associated with several oncogenes and proliferation factors, *MDM2, GLI1, CHOP (DDIT3), ATF1, SAS, HMGA2 (HMGIC)*, and *CDK4*.

Dedifferentiated liposarcoma are primary tumors in about 90% of cases and arise from a pre-existing liposarcoma or as a recurrence in about 10% (132, 156, 249). The majority involve

the retroperitoneum (75%), while fewer cases involve the extremities (25%). The tumors show transition from well-differentiated liposarcoma to non-lipogenic high-grade sarcoma. These tumors have a metastatic incidence of 15–20% and 5-year survival is about 70%. Other sarcomatous elements may occur with dedifferentiated liposarcoma in 5–10% of cases, such as rhabdomyosarcoma, osteosarcoma, chondrosarcoma, neural and meningothelial components, fibrosarcoma, myxofibrosarcoma, undifferentiated pleomorphic sarcoma, and angiosarcoma. Cytogenetics with dedifferentiated liposarcoma is similar to that for well-differentiated liposarcoma, indicative of the source of origin for dedifferentiated liposarcoma. Ring and giant marker chromosomes and dmin are common findings. In addition, amplification and rearrangement of 12q13-15 and 12q13-21 are frequently reported. *MDM2* is amplified in many of these tumors. TP53 mutation is identified within the dedifferentiated component, as well.

Myxoid liposarcoma (round cell liposarcoma) accounts for one-third of liposarcomas and 10% of soft tissue sarcomas (132, 156, 249). The most common sites for these tumors are the extremities, with two-thirds arising in the deep soft tissues of the thigh. These tumors rarely occur in the retroperitoneum and subcutaneous tissues. Metastases occur in one-third of those affected. The tumor is composed of round to oval primitive cells with variable numbers of lipoblasts in a myxoid stroma with a prominent fine vasculature ("chicken-wire" capillaries). This type of liposarcoma may be predominantly a myxoid pattern, a mixture of myxoid and round cell pattern, or an entirely round cell pattern. The round cell pattern has worse prognosis. Myxoid liposarcoma has a 70% 5 year survival, while round cell liposarcoma has only a 20% 5 year survival. Both myxoid and round cell liposarcoma share identical cytogenetics findings and this indicates that these represent two variants of the same entity (Table 8). The *FUS (TLS)/DDIT3 (CHOP)* translocation is detected in about 95% of myxoid/round cell liposarcoma. This translocation leads to fusion between these two genes. Another tumor defining translocation occurs when *DDIT3* fuses with EWSR1. In contrast to well-differentiated and dedifferentiated liposarcomas, ring and giant marker chromosomes and dmin are lacking in myxoid/round cell liposarcomas. In addition, most myxoid/round cell liposarcomas are diploid.

Pleomorphic liposarcoma is not derived from well-differentiated Liposarcoma and is a high-grade sarcoma with pleomorphic lipoblasts (132, 156, 162, 249). It represents only 5% of liposarcomas. Most occur in patients over 50 years of age and affect the extremities. A metastatic rate of up to 50% is reported and the mortality rate is 40–50%. Cytogenetics lacks specific findings (Table 8). There have been reported cases of *MDM2* amplification, attributed to the presence of ring chromosomes. Mutations in *p53* have also been detected. There are nonspecific chromosomal gains and losses (1p21, 1q21-22, 5p13-15, 7q22, 14q23-24). Additional cases of this rare tumor need to be evaluated before definitive conclusions regarding cytogenetic findings can be made. Comparative genomic hybridization (CGH) evaluation of several dedifferentiated and pleomorphic liposarcomas has shown amplification of certain genes (*CCND1, GLI, CDK4, MYB, ESR1, A1B1*) (Table 8).

Clear Cell Sarcoma (Malignant Melanoma of Soft Parts)

Clear cell sarcoma of the tendons and aponeuroses, also known as Malignant Melanoma of soft parts (CCS/MSP), is a rare sarcoma affecting primarily adolescents and young adults, with slight female predominance. Almost 95% of the times, this tumor arises in the extremities, with a particular predilection for the foot and the ankle, and is often bound to tendons and aponeuroses. Head and neck involvement is more common in children (163, 224, 250, 251). First described by Enzinger (252), this tumor is usually composed of polygonal or spindle shaped cells with abundant eosinophilic or clear cytoplasm, forming nests delineated by fibrous septa. Melanocytic differentiation can be demonstrated by immunohistochemistry or ultrastructural analysis in the vast majority of the cases. Although no genetic relationship with cutaneous malignant melanoma was reported initially (253, 254), recent gene expression profiling studies support the classification of CCS/MSP as a distinct genomic subtype of melanoma (255).

A number of cytogenetic anomalies, including +7, +8, and structural and numerical aberrations of chromosome 22 have been reported in CCS/MSP (256); however, the cytogenetic hallmark of CCS/MSP is the presence of the recurrent t (12;22) (q13;q12) translocation in the majority of cases reported (257–259). This translocation involves *ATF-1* gene on chromosome 12q13, and *EWSR1* on chromosome 22q12 (260). *ATF1* encodes a member of the CREB/ATF basic leucine-zipper type transcription factor family and binds to cAMP inducible promotors. The resulting chimeric protein is composed of the N-terminal domain of *EWSR1* linked to the bZIP domain of *ATF-1* (261) and binds to ATF sites present in cAMP-responsive promoters via the ATF1 bZIP domain. The EWSR1/ATF1 oncoprotein converts ATF1 to a constitutive transcriptional activator that represses p53/CBP-mediated transactivation (262).

Rare cases of CCS/MSP carrying a *FUS-ATF1* and *EWSR1-CREB1* (the predominant gene fusion in angiomatoid fibrous histiocytoma) fusion variants have been also described in, the latest most commonly associated with gastrointestinal location and absence of melanocytic differentiation (263–265).

Fluorescence in situ hybridization-based approaches can be used to demonstrate the t (12;22), using chromosome or gene-specific probes (260). The EWSR1/ATF1 fusion transcript is detectable by RT-PCR in up to 90% of the Clear Cell

Sarcoma cases analyzed (266). Paganopoulus and colleagues (267) identified four types of EWSR1/ATF1 chimeric transcripts, the most frequent one (type 1) resulting in an in-frame fusion of exon 8 of *EWSR1* with exon 4 of *ATF1*. Several cases were found to carry combinations of different fusion transcripts. The reciprocal *ATF1/EWSR1* fusion probably does not contribute to transformation in these tumors, as this type of fusion usually results in an out-of-frame chimeric transcript.

A number of cases of CCS/MSP involving the gastrointestinal tract have been reported (268, 269). Of particular interest for the surgical pathologist is a special subset of gastrointestinal tumors carrying EWSR1/ATF1fusion transcripts, initially diagnosed as metastatic malignant melanoma (270).

Gene expression profiling of CCS/MSP demonstrated that CCS/MSP cluster with melanomas as a distinct group, suggesting the classification of CCS/MSP as a distinct genomic subtype of melanoma (271). Shaefer and colleagues identified critical differentially expressed genes in CCS/MST tumor cells in comparison with other solid tumors affecting children and young. Expression profiling confirmed the neuroectodermal origin of CCS/MST based on their gene expression. *ERBB3* gene (avian erythroblastic leukemia viral oncogene homologue 3) was found to be dramatically upregulated, in addition to genes already known to be highly expressed in CCSST (272).

Regarding other pathways investigated in these tumors, Takahira and colleagues documented overexpression of cyclin D1 and identified rare point mutations/deletions of p16INK4a, p14ARF, and p53 genes associated with high mitotic rate or tumor necrosis, suggesting their potential association with poor prognosis in CCS/MST patients (273).

Angiomatoid Fibrous Histiocytoma

Waters and colleagues (274) identified the fusion of the *FUS* and *ATF-1* genes induced by a chromosomal translocation involving bands 12q13 and 16p11 in angiomatoid fibrous histiocytoma. A second case with a similar rearrangement was documented by Hallor and colleagues (275). Hallor (276) reported a *EWSR1/ATF1* fusion, in one of these tumors. Recent studies have demonstrated the presence of *EWSR1-CREB1* as the predominant fusion gene in this tumor type (264).

Alveolar Soft Part Sarcoma

Alveolar soft part sarcoma (ASPS) is a rare tumor of adolescents and young adults usually presenting as an indolent mass with predilection for the deep tissues of the extremities, and associated with an almost invariable poor prognosis, as it tends to metastasize early (224, 252, 277). First described by Christopherson and colleagues (250), this tumor is characterized by a distinctive histological pattern composed of organoid nests of eosinophilic cells loosely arranged in an alveolar pattern and pathonogmonic PAS positive-diastase resistant rhomboid crystals, recently shown to consist of moocarboxylate transporter 1 (MCT-1)-CD 147 complexes (246). Potential myogenic, neurogenic, neuroectodermal, and melanocytic cell origin have been proposed; however, the histogenesis of ASPS remains uncertain (278–284).

There are only limited numbers of published cytogenetic reports of alveolar soft part sarcomas due to the rarity of these tumors (213). Involvement of chromosome 17 and specifically 17q25 has been documented (284, 285). Comparative genomic hybridization of a few cases of alveolar soft part sarcomas revealed frequent chromosomal gains, most commonly involving chromosomes 1q, 8q, Xp, and 16q (286, 287) Heinman and colleagues described the first case with the recurrent der (17)t (X;17) (p11;q25) unbalanced translocation, characteristic of these tumors, which was validated using FISH (286). A number of reports have corroborated this finding (235, 284, 287, 288). Cloning of the translocation demonstrated the formation of a hybrid gene at the breakpoint involving the *TFE3* gene transcription factor on Xp11 and a novel gene on chromosome 17q25: *ASPL* (289). *TFE3* is a member of the microphtalmia-TFE subfamily of helix-loop-helix leucine zipper transcription factors (290). *ASPL* gene is widely expressed protein of unknown function, likely to be involved in ubiquitylation pathway. *ASPL* is fused in frame to *TFE3* exon 3 or 4, resulting in the translation of a chimeric protein, with the reciprocal most often absent. The formation of this hybrid gene also results in gain of Xp11-pter sequences, loss of heterozygosity in 17q25-qter (213, 235).

Detection of aberrant expression of the *TFE3* gene using immunohistochemistry has been documented by Ladanyi (246) in a series of tumors carrying a *TFE3* fusion genes. Documentation of aberrant TFE3 protein nuclear immunoreactivity in these tumors, using a polyclonal antibody against its C-terminal portion, has been proposed as an alternative and sensitive screening test of potential clinical utility.

A t (X;17) balanced translocation resulting in ASPL-TFE3 fusion transcripts has been described between those involving Xp11.2 in a small group of renal cell carcinomas affecting young children, some of them showing morphological and ultrastructural features resembling those seen in ASPSs, raising the possibility of these two lesions being similar entities in different anatomic sites (291–293).

Dermatofibrosarcoma Protuberans

Dermatofibrosarcoma protuberans (DFSP) is a low-grade malignant neoplasm of the deep dermis with extension to the subcutis, locally aggressive growth, and frequent local recurrence, but rare distant metastases (294–296). It is diagnosed most often on the trunk, in young to middle-aged adults, and

increasingly in children (160, 297, 298). Preprotuberant manifestations, with morphea-like, atrophoderma-like, angioma-like, or other flat or depressed lesions, probably represent early forms and are more frequently recognized in young patients (299).

Classic histologic features of DFSP include a monotonous storiform pattern of spindled cells, with a honeycomb pattern of infiltration into the subcutaneous fat (224, 300). The lesional cells are typically diffusely and strongly positive for CD34 and ApoD and negative for factor XIIIa (301). Of many histological variants described, including its pigmented variant (Bednar tumor), it is worth mentioning those with fibrosarcomatous changes (DFSP-FS) which usually show higher mitotic activity and reduced CD34 staining or lack of it, and have been associated with a significantly more aggressive clinical course than ordinary DFSP (302, 303).

Giant cell fibroblastoma (GCF) (304) occurs predominantly in male infants and children, with a distinct histomorphology, but similar deep dermal location, anatomic distribution, locally aggressive course, and immunohistochemical profile. Other differential diagnostic entities include "indeterminate fibrohistiocytic lesions" (305), "deep penetrating dermatofibroma" (306) cellular dermatofibromas, $CD34^+$ cellular digital fibromas (307), and superficial acral fibromyxomas (308) and related lesions.

The characteristic cytogenetic findings of DFSP are either supernumerary ring chromosomes containing low-level amplified sequences from 17q22-qter and 22q10-q13.1, typically seen in adults, or often unbalanced derivatives of t (17;22) (q22;q13), mostly seen in pediatric cases. Both contain sequences encoding a *COL1A1-PDGFB* fusion gene, which may be cryptic, sometimes within highly complex rearrangements. Few variant translocations involving regions other than 17q22 and 22q13.1 have been published. A variety of additional numerical and structural chromosomal alterations, gains more often than losses, may accompany (309, 310).

Characteristic fusion transcripts that result of these rearrangements in DFSP and GCF involve the *COL1A1* gene on chromosome 17, encoding the a1 chain of type 1 collagen, and the *PDGFB* gene on chromosome 22, encoding platelet-derived growth factor B gene (311). The remarkably constant breakpoint in the *PDGFB* gene is between exon 1 and 2. All identified breakpoints in the *COL1A1* gene are within regions coding for the a helical sequences between exon 7 and 47, and without significant clustering (Fig. 5a) (298, 312). Based on studies with cloned fusion genes (8, 313–317), it is thought that under the regulation of the highly active *COL1A1* promoter, excessive production of mature PDGF-BB drives tumor growth in an autocrine and/or paracrine fashion. Inhibition of the latter has been achieved in cultured cells both by anti-PDGFB (316) and STI571/Glivec (318, 319).

Identification of COL1A1-PDGFB fusion transcripts by RT-PCR, mostly on formalin fixed paraffin embedded (FFPE) tissue, has been reported using a multiplexed set of primers originally reported by Wang and colleagues (320, 321) and modified by other groups (297, 303). A recent publication using a newly designed RT-PCR assay in combination with a FISH assay, identified the fusion in a majority of DFSP cases (Fig. 5b) (322). The presence of COL1A1-PDGFB fusion transcripts has been reported in DFSPs with fibrosarcomatous changes and in Giant Cell Fobroblastomas (165, 297, 321, 322).

FISH has been used to confirm the involvement of chromosome 17 and/or 22 in ring chromosomes (323–325) and in rare variant rearrangements with an alternate partner chromosome (326). *PDGFB* split-apart probes on interphase cells can aid assessment of potential tandem gene amplifications (325). Amplification levels (327), and a variant rearrangement have also been evaluated by comparative genomic hybridization (CGH) (327).

cDNA microarray analysis (328) showed high levels of expression of *PDGFB*, its receptor, *PDGFRB*, CD34, apolipoprotein D (*APOD*), and genes normally expressed during early embryogenesis. With array CHG (aCGH) (329), the 31 genes that were consistently more highly expressed in DFSP than in other soft tissue tumors, were located in the amplified regions of chromosomes 17 and 22 (328). Regarding factors contributing to tumor progression (302) ordinary DFSP compared to fibrosarcomatous areas of DFSP-FS, microsatellite instability (MSI) was consistent with an early event, and p53 mutations with a late secondary event (273).

Wide local surgical excision, preferentially with Mohs surgery (330), remains the mainstay of therapy. Targeted drug therapy with imatinib mesylate (STI571/Glivec, Gleevec), has shown significant clinical activity in several patients with locally aggressive or metastatic disease (324, 325, 331–334). Imatinib has reported clinical activity against DFSP with demonstrable t (17;22); however, fibrosarcomatous variants of DFSP lacking t (17;22) may not respond to this treatment (325).

Congenital Fibrosarcoma

Congenital (infantile) fibrosarcoma is a rare spindle cell sarcoma that most commonly develops in the extremities of children during the first year of life (335). Histologically, these tumors can show some degree of variability and high-grade features (mitoses, hypercellularity); however, its clinical course is usually benign and only rarely metastasizes, raising the importance of differentiating it from other aggressive sarcomas (336).

The main cytogenetic change associated with congenital fibrosarcoma is the t (12;15) (p13;q26) translocation (337) which has not been found in adult fibrosarcomas or other sarcomas (338, 339) and is identical to that described for congenital mesoblastic nephroma (340), a primary tumor of the kidney of newborns and young infants, which most likely represents the same lesion in a different anatomic site. Other cytogenetic abnormalities described in congenital fibrosar-

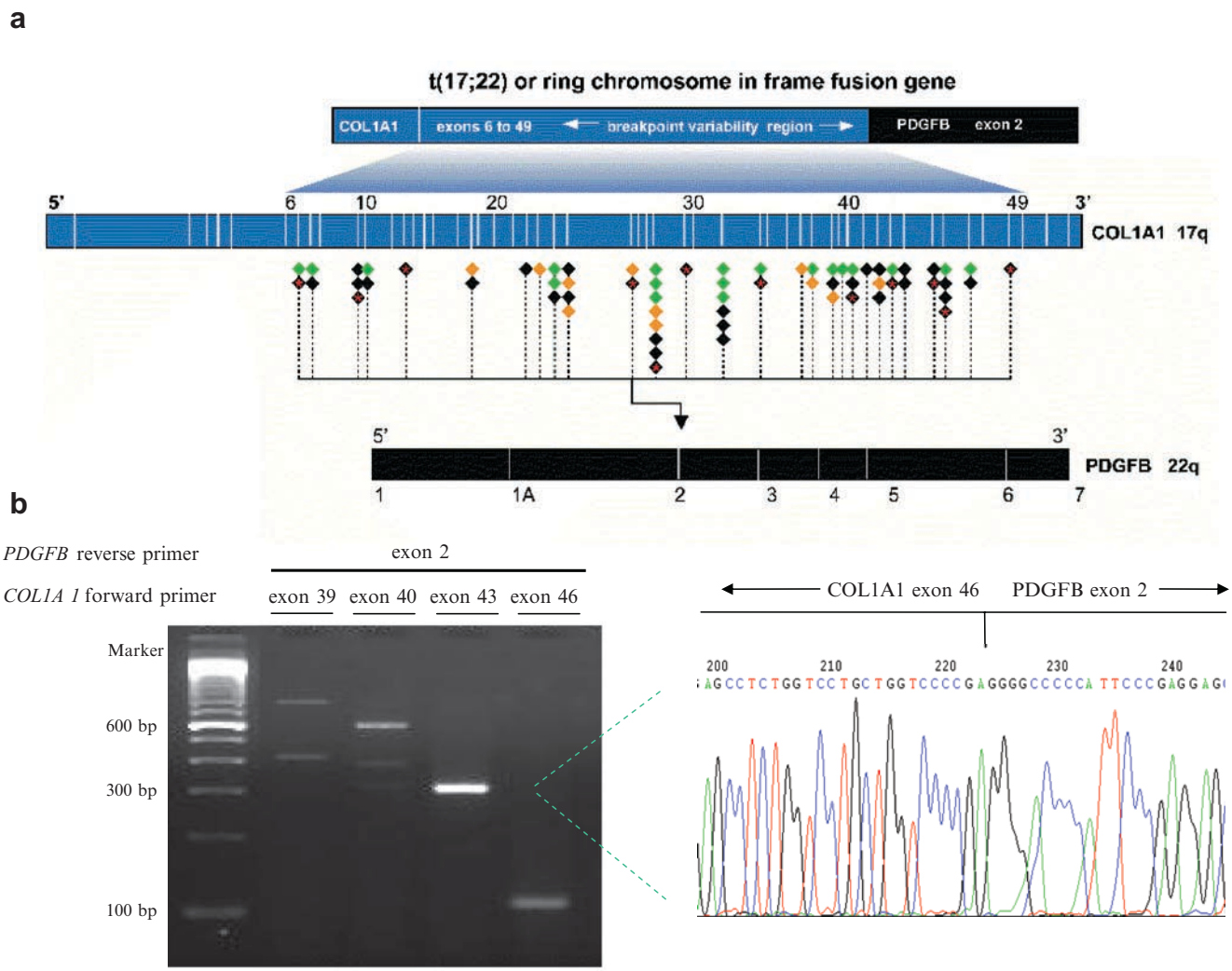

Fig. 5 **a** summary of COL1A1 breakpoints in Dermatofibrosarcoma Protruberans (322). **b** RT-PCR and direct sequencing of a DFSP with a COL1A1/PDGFB rearrangement

coma and mesoblastic nephroma include polysomies of chromosome 11, 8, 10, 17, and 20 (213, 341).

The t(12;15) translocation, present in a majority of congenital fibrosarcoma and cellular mesoblastic nephroma cases, including those with normal karyotypes (342), results in an in-frame fusion of the *ETV6* gene on 12q13 to the neurothrophin 3 receptor gene (*NTRK3 or TRKC*) on chromosome 15q25. *ETV6* gene, also known as *TEL*, is an oncogene containing a helix-loop-helix (HLH) domain, identified initially in translocations associated with hematopoietic malignancies often fused to a partner gene member of the tyrosine kinase family of genes. *NTRK3* is a member of the NTRK family of protein kinase receptors. Fusion transcripts encode ETV6 HLH domain fused to NTRK3 protein kinase domain. The oncogenic mechanism of the chimeric ETV6-NTRK3 protein is believed to involve the HLH domain inducing ligand-independent dimerization and constitutive activation of NTRK3 signaling (338, 339). The t (12;15) translocation is often difficult to identify cytogenetically. Several studies have been published using specific probes for FISH analysis in order to identify this fusion gene, both on metaphase and on interphase cells (338, 339, 342–344). A number of reports have also documented the application of PCR analysis for the detection of this rearrangement. Molecular detection of the fusion transcript by RT-PCR, has been proven superior to cytogenetics as a more sensitive assay, particularly considering the little breakpoint variability (345, 346).

Aggressive Fibromatosis/Desmoid Tumor

Aggressive fibromatosis also known as desmoid tumor is a locally invasive monoclonal proliferation of spindle, fibrocyte-like cells that does not metastasize (347). These tumors can occur as sporadic lesions or about 100 times more frequently, as an extraintestinal manifestation of the familial adenomatous polyposis cancer predisposition syndrome,

caused by germ line mutations of the Adenomatous polyposis Coli (*APC*) gene (348). Approximately 10–25% of FAP patients are thought to develop desmoids, which may represent the leading cause of death among those who have undergone colectomy, usually following one of the two distinct desmoid phenotypes described (349, 350).

APC gene encodes a protein involved in the regulation of beta-catenin, which is a mediator in Wnt signaling, a developmental pathway commonly dysregulated in human malignancies (351). A number of studies have documented that alterations of the APC/beta-catenin pathway with resultant nuclear translocation of beta-catenin, are important in the pathogenesis of both sporadic and FAP-associated fibromatosis (352). Somatic truncating mutations of the APC gene, and elevated beta-catenin protein expression were initially reported in a subset of these lesions (353, 354). Following studies demonstrated that *CTNNB* gene mutations and beta-catenin dysregulation are present in a majority of desmoid tumors, resulting in Cyclin D1 overexpression and APC-beta-catenin-Tcf pathway downstream activation (Fig. 6) (355–358).

The demonstration of nuclear beta-catenin expression appears to be a useful diagnostic tool as it distinguishes desmoids tumors from other benign and malignant fibroblastic and myofibroblastic lesions, (359), as high levels of nuclear beta-catenin staining is present in a very limited subset of mesenchymal tumors, including desmoids (71% of cases), solitary fibrous tumor (40%), endometrial stromal sarcoma (40%), and synovial sarcoma (28%) (360). New therapies for aggressive fibromatosis/desmoid tumors are under investigation, including Imatinib that appears to be an active agent in the treatment of some advanced cases of aggressive fibromatosis, with no apparent correlation between WNT pathway activation status and clinical response (361).

Summary

Tumors of the bone and soft tissue are a heterogeneous group of neoplasms that include very diverse types and are sometimes difficult to definitively classify. Genetic and molecular analyses of these neoplasms have considerably enhanced our understanding of their biology, mechanisms of malignant transformation and response to therapy. Specific genetic abnormalities have been identified for a subset of benign and malignant tumors, including chromosomal abnormalities (translocations), gene mutations, and aberrant activation of signaling pathways, that can be used for diagnosis, and considered as potential targets for therapy.

Traditional methods such as hematoxylin-eosin slide microscopic interpretation, immunohistochemistry, and clinico-pathologic correlation, can often be enhanced by genetic and molecular methods, some of which are increasingly utilized in bone and soft tissue pathology (362, 363). These methods include chromosomal karyotyping, fluorescence-in-situ-hybridization, polymerase chain reaction, and direct DNA sequencing, among others (Figs. 7 and 8).

The pathologist should play an essential role, not only in the diagnosis, but also in assessing the prognosis and understanding of the pathogenesis of benign and malignant neoplasms. Upon receipt of tumorous tissue, it is imperative, particularly in the diagnosis of sarcomas, that appropriate triaging be performed in order to allow for many different diagnostic methods to be employed.

Current DNA/molecular Diagnostics

- Cytogenetics
- Molecular Cytogenetics
  - FISH: Fluorescence in situ Hybridization
  - CGH: Comparative Genomic Hybridization
  - SKY: Spectral Karyotyping
- Immobilized DNA/RNA detection
- DNA Sequencing
- DNA Amplification (PCR, TaqMan)
- *DNA Microarrays: tumor specific genetic profiles*
- *Gene expression profiles*

Fig. 6 Current DNA/Molecular Diagnostics

Detection of tumor specific translocations fusion genes/transcripts

CYTOGENETICS	RT-PCR	FISH/CISH
complete karyotype	frozen, imprints, paraffin	frozen, imprints, paraffin
low resolution	affordable	affordable
need for alive, dividing cells	**fast turn around time**	**fast turn around time**
expensive	**unlimited primer design**	**histological correlation**
slow turn-around time	need for RNA	limited number of probes
may fail to grow	risk of false positives	difficult interpretation
lack of histological context	negatives: non informative	

Fig. 7 Detection of tumor specific translocations fusion gene/transcripts

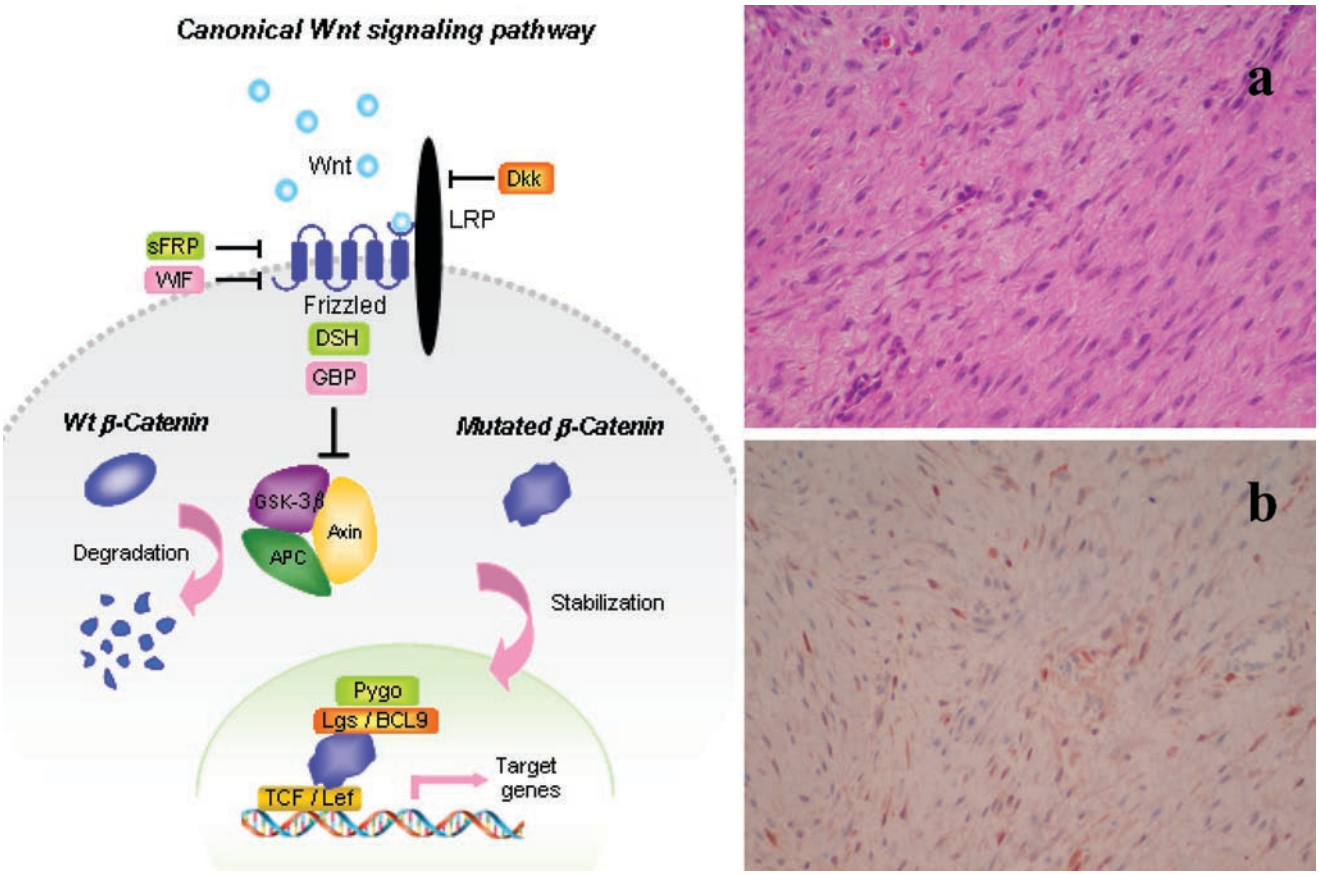

Fig. 8 Canonical Wnt pathway and b-catenin immunohistochemistry: Desmoid tumor **(a)** with a codon, 141 mutation of the CTNNB gene, **(b)** showing nuclear and cytoplasmic staining

Frozen tissue from the tumor may be utilized for immediate intra-operative diagnosis and may guide the surgeon as to the appropriate operative therapy. The residual tissue following frozen section diagnosis and imprint preparations should be retained cryopreserved to allow for diagnosis and future studies that may direct treatment, predict outcome, metastatic potential and recurrence, as well as research studies. Cytologic imprints may be of considerable use with tumors that are difficult to diagnosis on frozen section due to the presence of calcified and/or chondroid components. Cytologic imprints (touch preparations), squash and scrape preparations may allow for immediate evaluation and provide a preliminary diagnosis. Retention of unstained imprints may also be useful for FISH analysis of mutated genes, gene amplification, translocations, and other genetic abnormalities associated with specific tumor types.

Formalin-fixed tissue is essential for routine histopathology, immunocytochemistry, in situ hybridization, RT-PCR evaluation and tissue microarray construction. This type of tissue fixation is the backbone upon which diagnostic surgical pathology is built and has been adapted for many different diagnostic and research tools in pathology.

Cytogenetic analysis may provide valuable information in the diagnosis of tumors. This requires that tumor tissue be submitted in sterile tissue culture media to maintain viable cells that are capable of cell growth and mitotic activity. Ultrastructural evaluation still plays a major role in diagnosis of soft tissue and bone tumors. Finally, the pathologist should also be aware that some tumor tissue may have inflammatory or infectious components. If this is suspected based upon gross examination of the specimen or upon frozen section evaluation, procurement of tissue for microbiologic studies should be performed.

References

1. Matushansky I MR. Mechanisms of Sarcomagenesis Hematology/Oncology Clinics of North America 2005;19:427–49.
2. Triche TJH, Hicks JM, Sorensen PHB. Diagnostic Pathology of Pediatric Malignancies. In: Pizzo PaP, D G, ed. Principles and Practice of Pediatric Oncology. Philadelphia: Lippincott Williams and Wilkins, 2006:185–235.

3. Biegel JA, Womer RB, Emanuel BS. Complex karyotypes in a series of pediatric osteosarcomas. Cancer Genet Cytogenet 1989;38: 89–100.
4. Mertens F, Mandahl N, Orndal C, et al. Cytogenetic findings in 33 osteosarcomas. Int J Cancer 1993;55:44–50.
5. Fletcher JA, Gebhardt MC, Kozakewich HP. Cytogenetic aberrations in osteosarcomas. Nonrandom deletions, rings, and double-minute chromosomes. Cancer Genet Cytogenet 1994;77:81–8.
6. Bridge JA, Nelson M, McComb E, et al. Cytogenetic findings in 73 osteosarcoma specimens and a review of the literature. Cancer Genet Cytogenet 1997;95:74–87.
7. Boehm A, Neff J, Squire J, Bayani j, Nelson M, Bridge JA. Cytogenetic findings in 36 osteosarcoma specimens and a review of the literature. Pediatr Pathol Mol Med 2000;19:359–76.
8. Sandberg AA, Bridge JA. Updates on the cytogenetics and molecular genetics of bone and soft tissue tumors: osteosarcoma and related tumors. Cancer Genet Cytogenet 2003;145:1–30.
9. Tarkkanen M, Karhu R, Kallioniemi A, et al. Gains and losses of DNA sequences in osteosarcomas by comparative genomic hybridization. Cancer Res 1995;55:1334–8.
10. Brinkschmidt C, Blasius S, Burger H, et al. [Comparative genomic hybridization (CGH) for detecting a heretofore undescribed amplified chromosomal segment in high-grade medullary osteosarcoma]. Verh Dtsch Ges Pathol 1998;82:184–8.
11. Tarkkanen M, Bohling T, Gamberi G, et al. Comparative genomic hybridization of low-grade central osteosarcoma. Mod Pathol 1998;11:421–6.
12. Zielenska M, Marrano P, Thorner P, et al. High-resolution cDNA microarray CGH mapping of genomic imbalances in osteosarcoma using formalin-fixed paraffin-embedded tissue. Cytogenet Genome Res 2004;107:77–82.
13. Man TK, Lu XY, Jaeweon K, et al. Genome-wide array comparative genomic hybridization analysis reveals distinct amplifications in osteosarcoma. BMC Cancer 2004;4:45.
14. Roberts WM, Douglass EC, Peiper SC, Houghton PJ, Look AT. Amplification of the gli gene in childhood sarcomas. Cancer Res 1989;49:5407–13.
15. Meltzer PS, Jankowski SA, Dal Cin P, Sandberg AA, Paz IB, Coccia MA. Identification and cloning of a novel amplified DNA sequence in human malignant fibrous histiocytoma derived from a region of chromosome 12 frequently rearranged in soft tissue tumors. Cell Growth Differ 1991;2:495–501.
16. Reifenberger G RJ, Ichimura K, Meltzer PS, Collins VP. Amplification of multiple genes from chromosomal region 12q13-14 in human malignant gliomas: preliminary mapping of the amplicons shows preferential involvement of CDK4, SAS, and MDM2. Cancer Res 1994;54:4299–303.
17. Su YA, Hutter CM, Trent JM, Meltzer PS. Complete sequence analysis of a gene (OS-9) ubiquitously expressed in human tissues and amplified in sarcomas. Mol Carcinog 1996;15:270–5.
18. Tarkkanen M, Elomaa I, Blomqvist C, et al. DNA sequence copy number increase at 8q: a potential new prognostic marker in high-grade osteosarcoma. Int J Cancer 1999;84:114–21.
19. Friend SH, Bernards R, Rogelj S, et al. A human DNA segment with properties of the gene that predisposes to retinoblastoma and osteosarcoma. Nature 1986;323:643–6.
20. Hansen MF, Koufos A, Gallie BL, et al. Osteosarcoma and retinoblastoma: a shared chromosomal mechanism revealing recessive predisposition. Proc Natl Acad Sci U S A 1985;82:6216–20.
21. Dryja TP, Friend S, Weinberg RA. Genetic sequences that predispose to retinoblastoma and osteosarcoma. Symp Fundam Cancer Res 1986;39:115–9.
22. Toguchida J, Ishizaki K, Sasaki MS, et al. Chromosomal reorganization for the expression of recessive mutation of retinoblastoma susceptibility gene in the development of osteosarcoma. Cancer Res 1988;48:3939–43.
23. Ladanyi M, Lewis R, Jhanwar SC, Gerald W, Huvos AG, Healey JH. MDM2 and CDK4 gene amplification in Ewing's sarcoma. J Pathol 1995;175:211–7.
24. Ragazzini P, Gamberi G, Benassi MS, et al. Analysis of SAS gene and CDK4 and MDM2 proteins in low-grade osteosarcoma. Cancer Detect Prev 1999;23:129–36.
25. Hollstein M, Shomer B, Greenblatt M, et al. Somatic point mutations in the p53 gene of human tumors and cell lines: updated compilation. Nucleic Acids Res 1996;24:141–6.
26. Chen PL, Chen YM, Bookstein R, Lee WH. Genetic mechanisms of tumor suppression by the human p53 gene. Science 1990;250:1576–80.
27. Levine RA, Fleischli MA. Inactivation of p53 and retinoblastoma family pathways in canine osteosarcoma cell lines. Vet Pathol 2000;37:54–61.
28. Toguchida J, Yamaguchi T, Ritchie B, et al. Mutation spectrum of the p53 gene in bone and soft tissue sarcomas. Cancer Res 1992; 52:6194–9.
29. Masuda H, Miller C, Koeffler HP, Battifora H, Cline MJ. Rearrangement of the p53 gene in human osteogenic sarcomas. Proc Natl Acad Sci U S A 1987;84:7716–9.
30. Mulligan LM, Matlashewski GJ, Scrable HJ, Cavenee WK. Mechanisms of p53 loss in human sarcomas. Proc Natl Acad Sci U S A 1990;87:5863–7.
31. Diller L, Kassel J, Nelson CE, et al. p53 functions as a cell cycle control protein in osteosarcomas. Mol Cell Biol 1990;10:5772–81.
32. Schreck RR. Tumor suppressor gene (Rb and p53) mutations in osteosarcoma. Pediatr Hematol Oncol 1992;9:ix-x.
33. Scholz RB, Kabisch H, Weber B, Roser K, Delling G, Winkler K. Studies of the RB1 gene and the p53 gene in human osteosarcomas. Pediatr Hematol Oncol 1992;9:125–37.
34. Overholtzer M, Rao PH, Favis R, et al. The presence of p53 mutations in human osteosarcomas correlates with high levels of genomic instability. Proc Natl Acad Sci U S A 2003;100: 11547–52.
35. Gokgoz N, Wunder JS, Mousses S, Eskandarian S, Bell RS, Andrulis IL. Comparison of p53 mutations in patients with localized osteosarcoma and metastatic osteosarcoma. Cancer 2001;92:2181–9.
36. Wunder JS, Gokgoz N, Parkes R, et al. TP53 mutations and outcome in osteosarcoma: a prospective, multicenter study. J Clin Oncol 2005;23:1483–90.
37. Miller CW, Aslo A, Campbell MJ, Kawamata N, Lampkin BC, Koeffler HP. Alterations of the p15, p16,and p18 genes in osteosarcoma. Cancer Genet Cytogenet 1996;86:136–42.
38. Lonardo F, Ueda T, Huvos AG, Healey J, Ladanyi M. p53 and MDM2 alterations in osteosarcomas: correlation with clinicopathologic features and proliferative rate. Cancer 1997;79:1541–7.
39. Ladanyi M, Cha C, Lewis R, Jhanwar SC, Huvos AG, Healey JH. MDM2 gene amplification in metastatic osteosarcoma. Cancer Res 1993;53:16–8.
40. Lednicky JA, Stewart AR, Jenkins JJ, 3rd, Finegold MJ, Butel JS. SV40 DNA in human osteosarcomas shows sequence variation among T-antigen genes. Int J Cancer 1997;72:791–800.
41. Mendoza SM, Konishi T, Miller CW. Integration of SV40 in human osteosarcoma DNA. Oncogene 1998;17:2457–62.
42. Park YB, Park MJ, Kimura K, Shimizu K, Lee SH, Yokota J. Alterations in the INK4a/ARF locus and their effects on the growth of human osteosarcoma cell lines. Cancer Genet Cytogenet 2002;133:105–11.
43. Maitra A, Roberts H, Weinberg AG, Geradts J. Aberrant expression of tumor suppressor proteins in the Ewing family of tumors. Arch Pathol Lab Med 2001;125:1207–12.
44. Obana K, Yang HW, Piao HY, et al. Aberrations of p16INK4A, p14ARF and p15INK4B genes in pediatric solid tumors. Int J Oncol 2003;23:1151–7.

45. Patino-Garcia A, Pineiro ES, Diez MZ, Iturriagagoitia LG, Klussmann FA, Ariznabarreta LS. Genetic and epigenetic alterations of the cell cycle regulators and tumor suppressor genes in pediatric osteosarcomas. J Pediatr Hematol Oncol 2003;25:362–7.
46. Tsuchiya T, Sekine K, Hinohara S, Namiki T, Nobori T, Kaneko Y. Analysis of the p16INK4, p14ARF, p15, TP53, and MDM2 genes and their prognostic implications in osteosarcoma and Ewing sarcoma. Cancer Genet Cytogenet 2000;120:91–8.
47. Ladanyi M, Park CK, Lewis R, Jhanwar SC, Healey JH, Huvos AG. Sporadic amplification of the MYC gene in human osteosarcomas. Diagn Mol Pathol 1993;2:163–7.
48. Gamberi G, Benassi MS, Bohling T, et al. C-myc and c-fos in human osteosarcoma: prognostic value of mRNA and protein expression. Oncology 1998;55:556–63.
49. Onda M, Matsuda S, Higaki S, et al. ErbB-2 expression is correlated with poor prognosis for patients with osteosarcoma. Cancer 1996;77:71–8.
50. Akatsuka T, Wada T, Kokai Y, et al. ErbB2 expression is correlated with increased survival of patients with osteosarcoma. Cancer 2002;94:1397–404.
51. Scotlandi K, Serra M, Nicoletti G, et al. Multidrug resistance and malignancy in human osteosarcoma. Cancer Res 1996;56: 2434–9.
52. Sangiorgi L, Gobbi GA, Lucarelli E, et al. Presence of telomerase activity in different musculoskeletal tumor histotypes and correlation with aggressiveness. Int J Cancer 2001;95:156–61.
53. Ulaner GA, Huang HY, Otero J, et al. Absence of a telomere maintenance mechanism as a favorable prognostic factor in patients with osteosarcoma. Cancer Res 2003;63:1759–63.
54. Gorlick R, Anderson P, Andrulis I, et al. Biology of childhood osteogenic sarcoma and potential targets for therapeutic development: meeting summary. Clin Cancer Res 2003;9:5442–53.
55. Mitsiades N, Yu WH, Poulaki V, Tsokos M, Stamenkovic I. Matrix metalloproteinase-7-mediated cleavage of Fas ligand protects tumor cells from chemotherapeutic drug cytotoxicity. Cancer Res 2001;61:577–81.
56. Wolf M, El-Rifai W, Tarkkanen M, et al. Novel findings in gene expression detected in human osteosarcoma by cDNA microarray. Cancer Genet Cytogenet 2000;123:128–32.
57. Squire JA, Pei J, Marrano P, et al. High-resolution mapping of amplifications and deletions in pediatric osteosarcoma by use of CGH analysis of cDNA microarrays. Genes Chromosomes Cancer 2003;38:215–25.
58. Nakano T, Tani M, Ishibashi Y, et al. Biological properties and gene expression associated with metastatic potential of human osteosarcoma. Clin Exp Metastasis 2003;20:665–74.
59. Unni K, Inwards C, Bridge J, Kindblom L, Wild L. Tumors of the bones and joints. Washington: ARP Press, 2005.
60. Turc-Carel C, Philip I, Berger MP, Philip T, Lenoir G. [Chromosomal translocation (11; 22) in cell lines of Ewing's sarcoma]. C R Seances Acad Sci III 1983;296:1101–3.
61. Aurias A, Rimbaut C, Buffe D, Zucker JM, Mazabraud A. Translocation involving chromosome 22 in Ewing's sarcoma. A cytogenetic study of four fresh tumors. Cancer Genet Cytogenet 1984;12:21–5.
62. Turc-Carel C, Philip I, Berger MP, Philip T, Lenoir GM. Chromosome study of Ewing's sarcoma (ES) cell lines. Consistency of a reciprocal translocation t (11;22) (q24;q12). Cancer Genet Cytogenet 1984;12:1–19.
63. Whang-Peng J, Triche TJ, Knutsen T, Miser J, Douglass EC, Israel MA. Chromosome translocation in peripheral neuroepithelioma. N Engl J Med 1984;311:584–5.
64. Fletcher JA. Cytogenetics and experimental models of sarcomas. Curr Opin Oncol 1993;5:663–6.
65. Sandberg AA, Bridge JA. Updates on cytogenetics and molecular genetics of bone and soft tissue tumors: Ewing sarcoma and peripheral primitive neuroectodermal tumors. Cancer Genet Cytogenet 2000;123:1–26.
66. Hattinger CM, Rumpler S, Ambros IM, et al. Demonstration of the translocation der (16)t (1;16) (q12;q11.2) in interphase nuclei of Ewing tumors. Genes Chromosomes Cancer 1996; 17:141–50.
67. Stark B, Mor C, Jeison M, et al. Additional chromosome 1q aberrations and der (16)t (1;16), correlation to the phenotypic expression and clinical behavior of the Ewing family of tumors. J Neurooncol 1997;31:3–8.
68. Sainati L, Leszl A, Montaldi A, Ninfo V, Basso G. Is the deletion of the short arm of chromosome 1 a prognostic factor in pediatric peripheral primitive neuroepithelioma (PNET)? Med Pediatr Oncol 1996;26:143–4.
69. Hattinger CM, Rumpler S, Strehl S, et al. Prognostic impact of deletions at 1p36 and numerical aberrations in Ewing tumors. Genes Chromosomes Cancer 1999;24:243–54.
70. Trakhtenbrot L, Neumann Y, Mandel M, et al. In vitro proliferative advantage of bone marrow cells with tetrasomy 8 in Ewing sarcoma. Cancer Genet Cytogenet 1996;90:176–8.
71. Armengol G, Tarkkanen M, Virolainen M, et al. Recurrent gains of 1q, 8 and 12 in the Ewing family of tumours by comparative genomic hybridization. Br J Cancer 1997;75:1403–9.
72. Maurici D, Perez-Atayde A, Grier HE, Baldini N, Serra M, Fletcher JA. Frequency and implications of chromosome 8 and 12 gains in Ewing sarcoma. Cancer Genet Cytogenet 1998;100:106–10.
73. Parente F, Grosgeorge J, Coindre JM, Terrier P, Vilain O, Turc-Carel C. Comparative genomic hybridization reveals novel chromosome deletions in 90 primary soft tissue tumors. Cancer Genet Cytogenet 1999;115:89–95.
74. Whang-Peng J, Triche TJ, Knutsen T, et al. Cytogenetic characterization of selected small round cell tumors of childhood. Cancer Genet Cytogenet 1986;21:185–208.
75. Delattre O, Zucman J, Plougastel B, et al. Gene fusion with an ETS DNA-binding domain caused by chromosome translocation in human tumours. Nature 1992;359:162–5.
76. Zucman J, Delattre O, Desmaze C, et al. Cloning and characterization of the Ewing's sarcoma and peripheral neuroepithelioma t (11;22) translocation breakpoints. Genes Chromosomes Cancer 1992;5:271–7.
77. May WA, Arvand A, Thompson AD, Braun BS, Wright M, Denny CT. EWS/FLI1-induced manic fringe renders NIH 3T3 cells tumorigenic. Nat Genet 1997;17:495–7.
78. Rossow KL, Janknecht R. The Ewing's sarcoma gene product functions as a transcriptional activator. Cancer Res 2001;61: 2690–5.
79. Arvand A, Denny CT. Biology of EWS/ETS fusions in Ewing's family tumors. Oncogene 2001;20:5747–54.
80. Ladanyi M. EWS-FLI1 and Ewing's sarcoma: recent molecular data and new insights. Cancer Biol Ther 2002;1:330–6.
81. Lessnick SL, Dacwag CS, Golub TR. The Ewing's sarcoma oncoprotein EWS/FLI induces a p53-dependent growth arrest in primary human fibroblasts. Cancer Cell 2002;1:393–401.
82. Deneen B, Welford SM, Ho T, Hernandez F, Kurland I, Denny CT. PIM3 proto-oncogene kinase is a common transcriptional target of divergent EWS/ETS oncoproteins. Mol Cell Biol 2003;23:3897–908.
83. Takahashi A, Higashino F, Aoyagi M, et al. EWS/ETS fusions activate telomerase in Ewing's tumors. Cancer Res 2003;63:8338–44.
84. Uren A, Tcherkasskaya O, Toretsky JA. Recombinant EWS-FLI1 oncoprotein activates transcription. Biochemistry 2004;43: 13579–89.
85. Huang HY, Illei PB, Zhao Z, et al. Ewing sarcomas with p53 mutation or p16/p14ARF homozygous deletion: a highly lethal subset associated with poor chemoresponse. J Clin Oncol 2005;23: 548–58.

86. Staege MS, Hutter C, Neumann I, et al. DNA microarrays reveal relationship of Ewing family tumors to both endothelial and fetal neural crest-derived cells and define novel targets. Cancer Res 2004;64:8213–21.
87. Hu-Lieskovan S, Zhang J, Wu L, Shimada H, Schofield DE, Triche TJ. EWS-FLI1 fusion protein up-regulates critical genes in neural crest development and is responsible for the observed phenotype of Ewing's family of tumors. Cancer Res 2005;65: 4633–44.
88. Zucman J, Melot T, Desmaze C, et al. Combinatorial generation of variable fusion proteins in the Ewing family of tumours. Embo J 1993;12:4481–7.
89. Sorensen PH, Lessnick SL, Lopez-Terrada D, Liu XF, Triche TJ, Denny CT. A second Ewing's sarcoma translocation, t (21;22), fuses the EWS gene to another ETS-family transcription factor, ERG. Nat Genet 1994;6:146–51.
90. Prasad DD, Ouchida M, Lee L, Rao VN, Reddy ES. TLS/FUS fusion domain of TLS/FUS-erg chimeric protein resulting from the t (16;21) chromosomal translocation in human myeloid leukemia functions as a transcriptional activation domain. Oncogene 1994;9:3717–29.
91. Peter M, Magdelenat H, Michon J, et al. Sensitive detection of occult Ewing's cells by the reverse transcriptase-polymerase chain reaction. Br J Cancer 1995;72:96–100.
92. Wang L, Bhargava R, Zheng T, et al. Undifferentiated small round cell sarcomas with rare EWS gene fusions: identification of a novel EWS-SP3 fusion and of additional cases with the EWS-ETV1 and EWS-FEV fusions. J Mol Diagn 2007;9:498–509.
93. Gilliland DG. Hematologic malignancies. Curr Opin Hematol 2001;8:189–91.
94. Komuro H, Hayashi Y, Kawamura M, et al. Mutations of the p53 gene are involved in Ewing's sarcomas but not in neuroblastomas. Cancer Res 1993;53:5284–8.
95. Hamelin R, Zucman J, Melot T, Delattre O, Thomas G. p53 mutations in human tumors with chimeric EWS/FLI-1 genes. Int J Cancer 1994;57:336–40.
96. Mousses S, McAuley L, Bell RS, Kandel R, Andrulis IL. Molecular and immunohistochemical identification of p53 alterations in bone and soft tissue sarcomas. Mod Pathol 1996;9:1–6.
97. Pellin A, Boix-Ferrero J, Carpio D, et al. Molecular alterations of the RB1, TP53, and MDM2 genes in primary and xenografted human osteosarcomas. Diagn Mol Pathol 1997;6:333–41.
98. Kovar H, Jug G, Aryee DN, et al. Among genes involved in the RB dependent cell cycle regulatory cascade, the p16 tumor suppressor gene is frequently lost in the Ewing family of tumors. Oncogene 1997;15:2225–32.
99. Matsunobu T, Tanaka K, Matsumoto Y, et al. The prognostic and therapeutic relevance of p27kip1 in Ewing's family tumors. Clin Cancer Res 2004;10:1003–12.
100. Nogueira E, Navarro S, Pellin A, Llombart-Bosch A. Activation of TRK genes in Ewing's sarcoma. Trk A receptor expression linked to neural differentiation. Diagn Mol Pathol 1997;6:10–6.
101. Zhang J, Hu S, Schofield DE, Sorensen PH, Triche TJ. Selective usage of D-Type cyclins by Ewing's tumors and rhabdomyosarcomas. Cancer Res 2004;64:6026–34.
102. Uren A, Wolf V, Sun YF, Azari A, Rubin JS, Toretsky JA. Wnt/Frizzled signaling in Ewing sarcoma. Pediatr Blood Cancer 2004;43:243–9.
103. Wai DH, Schaefer KL, Schramm A, et al. Expression analysis of pediatric solid tumor cell lines using oligonucleotide microarrays. Int J Oncol 2002;20:441–51.
104. Ohali A, Avigad S, Zaizov R, et al. Prediction of high risk Ewing's sarcoma by gene expression profiling. Oncogene 2004; 23:8997–9006.
105. Sorensen PH, Liu XF, Delattre O, et al. Reverse transcriptase PCR amplification of EWS/FLI-1 fusion transcripts as a diagnostic test for peripheral primitive neuroectodermal tumors of childhood. Diagn Mol Pathol 1993;2:147–57.
106. Dockhorn-Dworniczak B, Schafer KL, Dantcheva R, et al. [Detection of EWS-/FLI-1 gene fusion transcripts by RT-PCR as a tool in the diagnosis of tumors of the Ewing sarcoma group]. Verh Dtsch Ges Pathol 1994;78:214–9.
107. Barr FG, Xiong QB, Kelly K. A consensus polymerase chain reaction-oligonucleotide hybridization approach for the detection of chromosomal translocations in pediatric bone and soft tissue sarcomas. Am J Clin Pathol 1995;104:627–33.
108. Hill DA, O'Sullivan MJ, Zhu X, et al. Practical application of molecular genetic testing as an aid to the surgical pathologic diagnosis of sarcomas: a prospective study. Am J Surg Pathol 2002; 26:965–77.
109. Bridge RS, Rajaram V, Dehner LP, Pfeifer JD, Perry A. Molecular diagnosis of Ewing sarcoma/primitive neuroectodermal tumor in routinely processed tissue: a comparison of two FISH strategies and RT-PCR in malignant round cell tumors. Mod Pathol 2006;19:1–8.
110. Desmaze C, Zucman J, Delattre O, Melot T, Thomas G, Aurias A. Interphase molecular cytogenetics of Ewing's sarcoma and peripheral neuroepithelioma t (11;22) with flanking and overlapping cosmid probes. Cancer Genet Cytogenet 1994;74:13–8.
111. Kumar S, Pack S, Kumar D, et al. Detection of EWS-FLI-1 fusion in Ewing's sarcoma/peripheral primitive neuroectodermal tumor by fluorescence in situ hybridization using formalin-fixed paraffin-embedded tissue. Hum Pathol 1999;30:324–30.
112. Monforte-Munoz H, Lopez-Terrada D, Affendie H, Rowland JM, Triche TJ. Documentation of EWS gene rearrangements by fluorescence in-situ hybridization (FISH) in frozen sections of Ewing's sarcoma-peripheral primitive neuroectodermal tumor. Am J Surg Pathol 1999;23:309–15.
113. Athale UH, Shurtleff SA, Jenkins JJ, et al. Use of reverse transcriptase polymerase chain reaction for diagnosis and staging of alveolar rhabdomyosarcoma, Ewing sarcoma family of tumors, and desmoplastic small round cell tumor. J Pediatr Hematol Oncol 2001;23:99–104.
114. Toretsky JA, Neckers L, Wexler LH. Detection of (11;22) (q24;q12) translocation-bearing cells in peripheral blood progenitor cells of patients with Ewing's sarcoma family of tumors. J Natl Cancer Inst 1995;87:385–6.
115. West DC, Grier HE, Swallow MM, Demetri GD, Granowetter L, Sklar J. Detection of circulating tumor cells in patients with Ewing's sarcoma and peripheral primitive neuroectodermal tumor. J Clin Oncol 1997;15:583–8.
116. de Alava E, Kawai A, Healey JH, et al. EWS-FLI1 fusion transcript structure is an independent determinant of prognosis in Ewing's sarcoma. J Clin Oncol 1998;16:1248–55.
117. Zoubek A, Kovar H, Gadner H. [Cytogenetic and molecular genetic changes in malignant primary bone tumors]. Radiologe 1998;38:467–71.
118. Avigad S, Cohen IJ, Zilberstein J, et al. The predictive potential of molecular detection in the nonmetastatic Ewing family of tumors. Cancer 2004;100:1053–8.
119. Zoubek A, Kovar H, Kronberger M, et al. Mobilization of tumour cells during biopsy in an infant with Ewing sarcoma. Eur J Pediatr 1996;155:373–6.
120. de Alava E, Lozano MD, Patino A, Sierrasesumaga L, Pardo-Mindan FJ. Ewing family tumors: potential prognostic value of reverse-transcriptase polymerase chain reaction detection of minimal residual disease in peripheral blood samples. Diagn Mol Pathol 1998;7:152–7.
121. Lin PP, Brody RI, Hamelin AC, Bradner JE, Healey JH, Ladanyi M. Differential transactivation by alternative EWS-FLI1 fusion proteins correlates with clinical heterogeneity in Ewing's sarcoma. Cancer Res 1999;59:1428–32.

122. May WA, Lessnick SL, Braun BS, et al. The Ewing's sarcoma EWS/FLI-1 fusion gene encodes a more potent transcriptional activator and is a more powerful transforming gene than FLI-1. Mol Cell Biol 1993;13:7393–8.
123. Fletcher JA. Ewing's sarcoma oncogene structure: a novel prognostic marker? J Clin Oncol 1998;16:1241–3.
124. Longtin R. Ewing's sarcoma: a miracle drug waiting to happen? J Natl Cancer Inst 2003;95:1574–6.
125. Mateo-Lozano S, Tirado OM, Notario V. Rapamycin induces the fusion-type independent downregulation of the EWS/FLI-1 proteins and inhibits Ewing's sarcoma cell proliferation. Oncogene 2003;22:9282–7.
126. Maksimenko A, Malvy C, Lambert G, et al. Oligonucleotides targeted against a junction oncogene are made efficient by nanotechnologies. Pharm Res 2003;20:1565–7.
127. Chansky HA, Barahmand-Pour F, Mei Q, et al. Targeting of EWS/FLI-1 by RNA interference attenuates the tumor phenotype of Ewing's sarcoma cells in vitro. J Orthop Res 2004;22:910–7.
128. Hede K. RNA-based nanoparticle treatment shows promise in Ewing's sarcoma model. J Natl Cancer Inst 2005;97:627.
129. Guan H, Zhou Z, Wang H, Jia SF, Liu W, Kleinerman ES. A small interfering RNA targeting vascular endothelial growth factor inhibits Ewing's sarcoma growth in a xenograft mouse model. Clin Cancer Res 2005;11:2662–9.
130. Borden EC, Baker LH, Bell RS, et al. Soft tissue sarcomas of adults: state of the translational science. Clin Cancer Res 2003;9:1941–56.
131. Bridge JA, Liu J, Weibolt V, et al. Novel genomic imbalances in embryonal rhabdomyosarcoma revealed by comparative genomic hybridization and fluorescence in situ hybridization: an intergroup rhabdomyosarcoma study. Genes Chromosomes Cancer 2000;27:337–44.
132. Slominski A, Wortsman J, Carlson A, Mihm M, Nickoloff B, McClatchey K. Molecular pathology of soft tissue and bone tumors. A review. Arch Pathol Lab Med 1999;123:1246–59.
133. Althof PA, Ohmori K, Zhou M, et al. Cytogenetic and molecular cytogenetic findings in 43 aneurysmal bone cysts: aberrations of 17p mapped to 17p13.2 by fluorescence in situ hybridization. Mod Pathol 2004;17:518–25.
134. Oliveira AM, Hsi BL, Weremowicz S, et al. USP6 (Tre2) fusion oncogenes in aneurysmal bone cyst. Cancer Res 2004;64:1920–3.
135. Oliveira AM, Perez-Atayde AR, Dal Cin P, et al. Aneurysmal bone cyst variant translocations upregulate USP6 transcription by promoter swapping with the ZNF9, COL1A1, TRAP150, and OMD genes. Oncogene 2005;24:3419–26.
136. Oliveira AM, Perez-Atayde AR, Inwards CY, et al. USP6 and CDH11 oncogenes identify the neoplastic cell in primary aneurysmal bone cysts and are absent in so-called secondary aneurysmal bone cysts. Am J Pathol 2004;165:1773–80.
137. Ozaki T, Wai D, Schaefer KL, et al. Genetic imbalances in benign bone tumors revealed by comparative genomic hybridization. Neoplasma 2004;51:456–9.
138. Sawyer JR, Nicholas RW, Parham DM. A novel t (X;2) (q13;q35) in clear cell sugar tumor of bone. Cancer Genet Cytogenet 2004;154:77–80.
139. Bridge JA, Swarts SJ, Buresh C, et al. Trisomies 8 and 20 characterize a subgroup of benign fibrous lesions arising in both soft tissue and bone. Am J Pathol 1999;154:729–33.
140. Nelson M, Perry D, Ginsburg G, Sanger WG, Neff JR, Bridge JA. Translocation (1;4) (p31;q34) in nonossifying fibroma. Cancer Genet Cytogenet 2003;142:142–4.
141. Parham D. USCAP Specialty Conference: case 4. Pediatr Dev Pathol 2005;8:85–7.
142. Parham DM, Bridge JA, Lukacs JL, Ding Y, Tryka AF, Sawyer JR. Cytogenetic distinction among benign fibro-osseous lesions of bone in children and adolescents: value of karyotypic findings in differential diagnosis. Pediatr Dev Pathol 2004;7:148–58.
143. Morgan T, Atkins GJ, Trivett MK, et al. Molecular profiling of giant cell tumor of bone and the osteoclastic localization of ligand for receptor activator of nuclear factor kappaB. Am J Pathol 2005;167:117–28.
144. Oda Y, Sakamoto A, Saito T, et al. Secondary malignant giant-cell tumour of bone: molecular abnormalities of p53 and H-ras gene correlated with malignant transformation. Histopathology 2001;39:629–37.
145. Rao UN, Goodman M, Chung WW, Swalski P, Pal R, Finkelstein S. Molecular analysis of primary and recurrent giant cell tumors of bone. Cancer Genet Cytogenet 2005;158:126–36.
146. Sawyer JR, Goosen LS, Binz RL, Swanson CM, Nicholas RW. Evidence for telomeric fusions as a mechanism for recurring structural aberrations of chromosome 11 in giant cell tumor of bone. Cancer Genet Cytogenet 2005;159:32–6.
147. Bridge JA, Sandberg AA. Cytogenetic and molecular genetic techniques as adjunctive approaches in the diagnosis of bone and soft tissue tumors. Skeletal Radiol 2000;29:249–58.
148. Baruffi MR, Volpon JB, Neto JB, Casartelli C. Osteoid osteomas with chromosome alterations involving 22q. Cancer Genet Cytogenet 2001;124:127–31.
149. Dal Cin P, Sciot R, Samson I, De Wever I, Van den Berghe H. Osteoid osteoma and osteoblastoma with clonal chromosome changes. Br J Cancer 1998;78:344–8.
150. Mascarello JT, Krous HF, Carpenter PM. Unbalanced translocation resulting in the loss of the chromosome 17 short arm in an osteoblastoma. Cancer Genet Cytogenet 1993;69:65–7.
151. Buddingh EP, Krallman P, Neff JR, Nelson M, Liu J, Bridge JA. Chromosome 6 abnormalities are recurrent in synovial chondromatosis. Cancer Genet Cytogenet 2003;140:18–22.
152. Halbert AR, Harrison WR, Hicks MJ, Davino N, Cooley LD. Cytogenetic analysis of a scapular chondromyxoid fibroma. Cancer Genet Cytogenet 1998;104:52–6.
153. Hicks J. USCAP Specialty Conference, case 2: chondroblastic osteosarcoma with features resembling chondromyxoid fibroma. Pediatr Dev Pathol 2005;8:67–73.
154. Tallini G, Dorfman H, Brys P, et al. Correlation between clinicopathological features and karyotype in 100 cartilaginous and chordoid tumours. A report from the Chromosomes and Morphology (CHAMP) Collaborative Study Group. J Pathol 2002;196: 194–203.
155. Buddingh EP, Naumann S, Nelson M, Neffa JR, Birch N, Bridge JA. Cytogenetic findings in benign cartilaginous neoplasms. Cancer Genet Cytogenet 2003;141:164–8.
156. Sandberg AA. Updates on the cytogenetics and molecular genetics of bone and soft tissue tumors: liposarcoma. Cancer Genet Cytogenet 2004;155:1–24.
157. Feely MG, Boehm AK, Bridge RS, et al. Cytogenetic and molecular cytogenetic evidence of recurrent 8q24.1 loss in osteochondroma. Cancer Genet Cytogenet 2002;137:102–7.
158. Pierz KA, Womer RB, Dormans JP. Pediatric bone tumors: osteosarcoma ewing's sarcoma, and chondrosarcoma associated with multiple hereditary osteochondromatosis. J Pediatr Orthop 2001;21:412–8.
159. Porter DE, Simpson AH. The neoplastic pathogenesis of solitary and multiple osteochondromas. J Pathol 1999;188:119–25.
160. Sandberg AA, Anderson WD, Fredenberg C, Hashimoto H. Dermatofibrosarcoma protuberans of breast. Cancer Genet Cytogenet 2003;142:56–9.
161. Sawyer JR, Thomas EL, Lukacs JL, et al. Recurring breakpoints of 1p13 approximately p22 in osteochondroma. Cancer Genet Cytogenet 2002;138:102–6.
162. Swarts SJ, Neff JR, Johansson SL, Bridge JA. Cytogenetic analysis of dedifferentiated chondrosarcoma. Cancer Genet Cytogenet 1996;89:49–51.
163. Hicks J, Mierau GW. The spectrum of pediatric tumors in infancy, childhood, and adolescence: a comprehensive review with empha-

sis on special techniques in diagnosis. Ultrastruct Pathol 2005;29:175–202.
164. Laflamme C, Filion C, Bridge JA, Ladanyi M, Goldring MB, Labelle Y. The homeotic protein Six3 is a coactivator of the nuclear receptor NOR-1 and a corepressor of the fusion protein EWS/NOR-1 in human extraskeletal myxoid chondrosarcomas. Cancer Res 2003;63:449–54.
165. Sandberg AA, Bridge JA. Updates on the cytogenetics and molecular genetics of bone and soft tissue tumors. Dermatofibrosarcoma protuberans and giant cell fibroblastoma. Cancer Genet Cytogenet 2003;140:1–12.
166. Wexler LHJM, W. H.; Helman, L. J. Rhabdomyosarcomas and Undifferentiated Sarcomas. In: Pizzo PaP, D G, ed. Principles and Practice of Pediatric Oncology. Philadelphia: Lippincott Williams and Wilkins, 2006:185–235.
167. Dias P, Chen B, Dilday B, et al. Strong immunostaining for myogenin in rhabdomyosarcoma is significantly associated with tumors of the alveolar subclass. Am J Pathol 2000;156:399–408.
168. Parham DM. Pathologic classification of rhabdomyosarcomas and correlations with molecular studies. Mod Pathol 2001;14:506–14.
169. Qualman SJ, Coffin CM, Newton WA, et al. Intergroup Rhabdomyosarcoma Study: update for pathologists. Pediatr Dev Pathol 1998;1:550–61.
170. Qualman SJ, Morotti RA. Risk assignment in pediatric soft-tissue sarcomas: an evolving molecular classification. Curr Oncol Rep 2002;4:123–30.
171. Turc-Carel C, Limon J, Dal Cin P, Rao U, Karakousis C, Sandberg AA. Cytogenetic studies of adipose tissue tumors. II. Recurrent reciprocal translocation t (12;16) (q13;p11) in myxoid liposarcomas. Cancer Genet Cytogenet 1986;23:291–9.
172. Valentine M, Douglass EC, Look AT. Closely linked loci on the long arm of chromosome 13 flank a specific 2;13 translocation breakpoint in childhood rhabdomyosarcoma. Cytogenet Cell Genet 1989;52:128–32.
173. Douglass EC, Shapiro DN, Valentine M, et al. Alveolar rhabdomyosarcoma with the t (2;13): cytogenetic findings and clinicopathologic correlations. Med Pediatr Oncol 1993;21:83–7.
174. Barr FG, Galili N, Holick J, Biegel JA, Rovera G, Emanuel BS. Rearrangement of the PAX3 paired box gene in the paediatric solid tumour alveolar rhabdomyosarcoma. Nat Genet 1993;3:113–7.
175. Shapiro DN, Sublett JE, Li B, Downing JR, Naeve CW. Fusion of PAX3 to a member of the forkhead family of transcription factors in human alveolar rhabdomyosarcoma. Cancer Res 1993;53:5108–12.
176. Galili N, Davis RJ, Fredericks WJ, et al. Fusion of a fork head domain gene to PAX3 in the solid tumour alveolar rhabdomyosarcoma. Nat Genet 1993;5:230–5.
177. Biegel JA, Meek RS, Parmiter AH, Conard K, Emanuel BS. Chromosomal translocation t (1;13) (p36;q14) in a case of rhabdomyosarcoma. Genes Chromosomes Cancer 1991;3:483–4.
178. Davis RJ, D'Cruz CM, Lovell MA, Biegel JA, Barr FG. Fusion of PAX7 to FKHR by the variant t (1;13) (p36;q14) translocation in alveolar rhabdomyosarcoma. Cancer Res 1994;54:2869–72.
179. Wachtel M, Dettling M, Koscielniak E, et al. Gene expression signatures identify rhabdomyosarcoma subtypes and detect a novel t (2;2) (q35;p23) translocation fusing PAX3 to NCOA1. Cancer Res 2004;64:5539–45.
180. Khan J, Bittner ML, Saal LH, et al. cDNA microarrays detect activation of a myogenic transcription program by the PAX3-FKHR fusion oncogene. Proc Natl Acad Sci U S A 1999;96:13264–9.
181. Sublett JE, Jeon IS, Shapiro DN. The alveolar rhabdomyosarcoma PAX3/FKHR fusion protein is a transcriptional activator. Oncogene 1995;11:545–52.
182. Bennicelli JL, Fredericks WJ, Wilson RB, Rauscher FJ, 3rd, Barr FG. Wild type PAX3 protein and the PAX3-FKHR fusion protein of alveolar rhabdomyosarcoma contain potent, structurally distinct transcriptional activation domains. Oncogene 1995;11:119–30.
183. Bennicelli JL, Edwards RH, Barr FG. Mechanism for transcriptional gain of function resulting from chromosomal translocation in alveolar rhabdomyosarcoma. Proc Natl Acad Sci U S A 1996;93:5455–9.
184. Biegel JA, Nycum LM, Valentine V, Barr FG, Shapiro DN. Detection of the t (2;13) (q35;q14) and PAX3-FKHR fusion in alveolar rhabdomyosarcoma by fluorescence in situ hybridization. Genes Chromosomes Cancer 1995;12:186–92.
185. McManus AP, O'Reilly MA, Jones KP, et al. Interphase fluorescence in situ hybridization detection of t (2;13) (q35;q14) in alveolar rhabdomyosarcoma--a diagnostic tool in minimally invasive biopsies. J Pathol 1996;178:410–4.
186. Anderson J, Renshaw J, McManus A, et al. Amplification of the t (2; 13) and t (1; 13) translocations of alveolar rhabdomyosarcoma in small formalin-fixed biopsies using a modified reverse transcriptase polymerase chain reaction. Am J Pathol 1997;150:477–82.
187. Edwards RH, Chatten J, Xiong QB, Barr FG. Detection of gene fusions in rhabdomyosarcoma by reverse transcriptase-polymerase chain reaction assay of archival samples. Diagn Mol Pathol 1997;6:91–7.
188. Sorensen PH, Lynch JC, Qualman SJ, et al. PAX3-FKHR and PAX7-FKHR gene fusions are prognostic indicators in alveolar rhabdomyosarcoma: a report from the children's oncology group. J Clin Oncol 2002;20:2672–9.
189. Kelly KM, Womer RB, Sorensen PH, Xiong QB, Barr FG. Common and variant gene fusions predict distinct clinical phenotypes in rhabdomyosarcoma. J Clin Oncol 1997;15:1831–6.
190. Anderson MJ, Shelton GD, Cavenee WK, Arden KC. Embryonic expression of the tumor-associated PAX3-FKHR fusion protein interferes with the developmental functions of Pax3. Proc Natl Acad Sci U S A 2001;98:1589–94.
191. Barr FG, Qualman SJ, Macris MH, et al. Genetic heterogeneity in the alveolar rhabdomyosarcoma subset without typical gene fusions. Cancer Res 2002;62:4704–10.
192. Bridge JA, Liu J, Qualman SJ, et al. Genomic gains and losses are similar in genetic and histologic subsets of rhabdomyosarcoma, whereas amplification predominates in embryonal with anaplasia and alveolar subtypes. Genes Chromosomes Cancer 2002;33:310–21.
193. Scrable H, Witte D, Shimada H, et al. Molecular differential pathology of rhabdomyosarcoma. Genes Chromosomes Cancer 1989;1:23–35.
194. Kurmasheva RT, Peterson CA, Parham DM, Chen B, McDonald RE, Cooney CA. Upstream CpG island methylation of the PAX3 gene in human rhabdomyosarcomas. Pediatr Blood Cancer 2005;44:328–37.
195. Crescenzi M, Fleming TP, Lassar AB, Weintraub H, Aaronson SA. MyoD induces growth arrest independent of differentiation in normal and transformed cells. Proc Natl Acad Sci U S A 1990;87:8442–6.
196. Sorrentino V, Pepperkok R, Davis RL, Ansorge W, Philipson L. Cell proliferation inhibited by MyoD1 independently of myogenic differentiation. Nature 1990;345:813–5.
197. Hostein I, Andraud-Fregeville M, Guillou L, et al. Rhabdomyosarcoma: value of myogenin expression analysis and molecular testing in diagnosing the alveolar subtype: an analysis of 109 paraffin-embedded specimens. Cancer 2004;101:2817–24.
198. Felix CA, Kappel CC, Mitsudomi T, et al. Frequency and diversity of p53 mutations in childhood rhabdomyosarcoma. Cancer Res 1992;52:2243–7.
199. Hachitanda Y, Toyoshima S, Akazawa K, Tsuneyoshi M. N-myc gene amplification in rhabdomyosarcoma detected by fluorescence in situ hybridization: its correlation with histologic features. Mod Pathol 1998;11:1222–7.
200. Kouraklis G, Triche TJ, Wesley R, Tsokos M. Myc oncogene expression and nude mouse tumorigenicity and metastasis formation are higher in alveolar than embryonal rhabdomyosarcoma cell lines. Pediatr Res 1999;45:552–8.

201. Driman D, Thorner PS, Greenberg ML, Chilton-MacNeill S, Squire J. MYCN gene amplification in rhabdomyosarcoma. Cancer 1994;73:2231–7.
202. Iolascon A, Faienza MF, Coppola B, et al. Analysis of cyclin-dependent kinase inhibitor genes (CDKN2A, CDKN2B, and CDKN2C) in childhood rhabdomyosarcoma. Genes Chromosomes Cancer 1996;15:217–22.
203. Meddeb M, Valent A, Danglot G, et al. MDM2 amplification in a primary alveolar rhabdomyosarcoma displaying a t (2;13) (q35;q14). Cytogenet Cell Genet 1996;73:325–30.
204. Williamson D, Lu YJ, Gordon T, et al. Relationship between MYCN copy number and expression in rhabdomyosarcomas and correlation with adverse prognosis in the alveolar subtype. J Clin Oncol 2005;23:880–8.
205. Bortoluzzi S, Bisognin A, Romualdi C, Danieli GA. Novel genes, possibly relevant for molecular diagnosis or therapy of human rhabdomyosarcoma, detected by genomic expression profiling. Gene 2005;348:65–71.
206. Gerald WL, Ladanyi M, de Alava E, et al. Clinical, pathologic, and molecular spectrum of tumors associated with t (11;22) (p13;q12): desmoplastic small round-cell tumor and its variants. J Clin Oncol 1998;16:3028–36.
207. Gerald WL, Miller HK, Battifora H, Miettinen M, Silva EG, Rosai J. Intra-abdominal desmoplastic small round-cell tumor. Report of 19 cases of a distinctive type of high-grade polyphenotypic malignancy affecting young individuals. Am J Surg Pathol 1991;15:499–513.
208. Gonzalez-Crussi F, Crawford SE, Sun CC. Intraabdominal desmoplastic small-cell tumors with divergent differentiation. Observations on three cases of childhood. Am J Surg Pathol 1990;14:633–42.
209. Ordonez NG. Desmoplastic small round cell tumor: II: an ultrastructural and immunohistochemical study with emphasis on new immunohistochemical markers. Am J Surg Pathol 1998; 22:1314–27.
210. Young RH, Eichhorn JH, Dickersin GR, Scully RE. Ovarian involvement by the intra-abdominal desmoplastic small round cell tumor with divergent differentiation: a report of three cases. Hum Pathol 1992;23:454–64.
211. Venkateswaran L, Jenkins JJ, Kaste SC, Shurtleff SA, Downing JR, Pappo AS. Disseminated intrathoracic desmoplastic small round-cell tumor: a case report. J Pediatr Hematol Oncol 1997;19:172–5.
212. Sawyer JR, Tryka AF, Lewis JM. A novel reciprocal chromosome translocation t (11;22) (p13;q12) in an intraabdominal desmoplastic small round-cell tumor. Am J Surg Pathol 1992;16:411–6.
213. Sandberg A, Bridge J. Updates on the cytogenetics and molecular genetics of bone and soft tissue tumors: alveolar soft part sarcoma. Cancer Genet Cytogenet 2002;136:1–9.
214. Roberts P, Burchill SA, Beddow RA, Wheeldon J, Cullinane C, Lewis IJ. A combined cytogenetic and molecular approach to diagnosis in a case of desmoplastic small round cell tumor with a complex translocation (11;22;21). Cancer Genet Cytogenet 1999;108:19–25.
215. Gerald WL, Rosai J, Ladanyi M. Characterization of the genomic breakpoint and chimeric transcripts in the EWS-WT1 gene fusion of desmoplastic small round cell tumor. Proc Natl Acad Sci U S A 1995;92:1028–32.
216. Ladanyi M, Gerald WL. Specificity of the EWS/WT1 gene fusion for desmoplastic small round cell tumour. J Pathol 1996;180:462.
217. Kim J, Lee K, Pelletier J. The desmoplastic small round cell tumor t (11;22) translocation produces EWS/WT1 isoforms with differing oncogenic properties. Oncogene 1998;16:1973–9.
218. Liu J, Nau MM, Yeh JC, Allegra CJ, Chu E, Wright JJ. Molecular heterogeneity and function of EWS-WT1 fusion transcripts in desmoplastic small round cell tumors. Clin Cancer Res 2000;6:3522–9.
219. Antonescu CR, Gerald WL, Magid MS, Ladanyi M. Molecular variants of the EWS-WT1 gene fusion in desmoplastic small round cell tumor. Diagn Mol Pathol 1998;7:24–8.
220. de Alava E, Ladanyi M, Rosai J, Gerald WL. Detection of chimeric transcripts in desmoplastic small round cell tumor and related developmental tumors by reverse transcriptase polymerase chain reaction. A specific diagnostic assay. Am J Pathol 1995;147: 1584–91.
221. Argatoff LH, O'Connell JX, Mathers JA, Gilks CB, Sorensen PH. Detection of the EWS/WT1 gene fusion by reverse transcriptase-polymerase chain reaction in the diagnosis of intra-abdominal desmoplastic small round cell tumor. Am J Surg Pathol 1996;20:406–12.
222. Dockhorn-Dworniczak B, Schafer KL, Blasius S, et al. Assessment of molecular genetic detection of chromosome translocations in the differential diagnosis of pediatric sarcomas. Klin Padiatr 1997;209:156–64.
223. Lee SB, Kolquist KA, Nichols K, et al. The EWS-WT1 translocation product induces PDGFA in desmoplastic small round-cell tumour. Nat Genet 1997;17:309–13.
224. Fletcher CDM. Diagnostic Histopathology of Tumors. 2nd ed. London: Churchill-Livingstone, 2000.
225. Weiss S, Goldblum, JR. Enzinger and Weiss's Soft Tissue Tumors. 4th ed. St. Louis, Missouri, 2001.: Mosby-Harcourt Brace Company, 2001.
226. Fletcher CDM, Unni K, Mertens F. Pathology and Genetics Tumours of Soft Tissue and Bone. Lyon, France: IARC Press, 2002.
227. Shmookler BM. Retroperitoneal synovial sarcoma. A report of four cases. Am J Clin Pathol 1982;77:686–91.
228. Shmookler BM, Enzinger FM, Brannon RB. Orofacial synovial sarcoma: a clinicopathologic study of 11 new cases and review of the literature. Cancer 1982;50:269–76.
229. Fetsch JF, Meis JM. Synovial sarcoma of the abdominal wall. Cancer 1993;72:469–77.
230. Roth JA, Enzinger FM, Tannenbaum M. Synovial sarcoma of the neck: a followup study of 24 cases. Cancer 1975;35:1243–53.
231. Zeren H, Moran CA, Suster S, Fishback NF, Koss MN. Primary pulmonary sarcomas with features of monophasic synovial sarcoma: a clinicopathological, immunohistochemical, and ultrastructural study of 25 cases. Hum Pathol 1995;26:474–80.
232. Crew AJ, Clark J, Fisher C, et al. Fusion of SYT to two genes, SSX1 and SSX2, encoding proteins with homology to the Kruppel-associated box in human synovial sarcoma. Embo J 1995;14:2333–40.
233. de Leeuw B, Balemans M, Olde Weghuis D, Geurts van Kessel A. Identification of two alternative fusion genes, SYT-SSX1 and SYT-SSX2, in t (X;18) (p11.2;q11.2)-positive synovial sarcomas. Hum Mol Genet 1995;4:1097–9.
234. Thaete C, Brett D, Monaghan P, et al. Functional domains of the SYT and SYT-SSX synovial sarcoma translocation proteins and co-localization with the SNF protein BRM in the nucleus. Hum Mol Genet 1999;8:585–91.
235. Ladanyi M. Fusions of the SYT and SSX genes in synovial sarcoma. Oncogene 2001;20:5755–62.
236. dos Santos NR, de Bruijn DR, van Kessel AG. Molecular mechanisms underlying human synovial sarcoma development. Genes Chromosomes Cancer 2001;30:1–14.
237. Turc-Carel C, Dal Cin P, Limon J, et al. Involvement of chromosome X in primary cytogenetic change in human neoplasia: nonrandom translocation in synovial sarcoma. Proc Natl Acad Sci U S A 1987;84:1981–5.
238. Orndal C, Mandahl N, Willen H, Rydholm A, Mitelman F. Cytogenetic evolution in primary tumors, local recurrences, and pulmonary metastases of two soft tissue sarcomas. Clin Exp Metastasis 1993;11:401–8.
239. Orndal C, Rydholm A, Willen H, Mitelman F, Mandahl N. Cytogenetic intratumor heterogeneity in soft tissue tumors. Cancer Genet Cytogenet 1994;78:127–37.

240. Sandberg AA, Bridge JA. Updates on the cytogenetics and molecular genetics of bone and soft tissue tumors. Synovial sarcoma. Cancer Genet Cytogenet 2002;133:1–23.
241. Mandahl N, J L, F Met al, . Nonrandom secondary chromosome aberrations in synovial sarcomas with t (X;18). Intl J Oncol 1995;7:495–9.
242. Yang K, Lui WO, Xie Y, et al. Co-existence of SYT-SSX1 and SYT-SSX2 fusions in synovial sarcomas. Oncogene 2002;21:4181–90.
243. Kawai A, Woodruff J, Healey JH, Brennan MF, Antonescu CR, Ladanyi M. SYT-SSX gene fusion as a determinant of morphology and prognosis in synovial sarcoma. N Engl J Med 1998; 338:153–60.
244. Skytting B, Nilsson G, Brodin B, et al. A novel fusion gene, SYT-SSX4, in synovial sarcoma. J Natl Cancer Inst 1999;91:974–5.
245. Skytting BT, Szymanska J, Aalto Y, et al. Clinical importance of genomic imbalances in synovial sarcoma evaluated by comparative genomic hybridization. Cancer Genet Cytogenet 1999;115:39–46.
246. Ladanyi M, Antonescu CR, Drobnjak M, et al. The precrystalline cytoplasmic granules of alveolar soft part sarcoma contain monocarboxylate transporter 1 and CD147. Am J Pathol 2002; 160:1215–21.
247. Guillou L, Benhattar J, Bonichon F, et al. Histologic grade, but not SYT-SSX fusion type, is an important prognostic factor in patients with synovial sarcoma: a multicenter, retrospective analysis. J Clin Oncol 2004;22:4040–50.
248. Hicks J, Dilley A, Patel D, Barrish J, Zhu SH, Brandt M. Lipoblastoma and lipoblastomatosis in infancy and childhood: histopathologic, ultrastructural, and cytogenetic features. Ultrastruct Pathol 2001;25:321–33.
249. Sandberg AA. Updates on the cytogenetics and molecular genetics of bone and soft tissue tumors: lipoma. Cancer Genet Cytogenet 2004;150:93–115.
250. Christopherson WM, Foote FW, Jr., Stewart FW. Alveolar soft-part sarcomas; structurally characteristic tumors of uncertain histogenesis. Cancer 1952;5:100–11.
251. Ordonez NG. Alveolar soft part sarcoma: a review and update. Adv Anat Pathol 1999;6:125–39.
252. Enzinger FM. Clear-cell sarcoma of tendons and aponeuroses. an analysis of 21 cases. Cancer 1965;18:1163–74.
253. Chung EB, Enzinger FM. Malignant melanoma of soft parts. A reassessment of clear cell sarcoma. Am J Surg Pathol 1983;7: 405–13.
254. Langezaal SM, Graadt van Roggen JF, Cleton-Jansen AM, Baelde JJ, Hogendoorn PC. Malignant melanoma is genetically distinct from clear cell sarcoma of tendons and aponeurosis (malignant melanoma of soft parts). Br J Cancer 2001;84:535–8.
255. Segal NH, Pavlidis P, Antonescu CR, et al. Classification and subtype prediction of adult soft tissue sarcoma by functional genomics. Am J Pathol 2003;163:691–700.
256. Limon J, Debiec-Rychter M, Nedoszytko B, Liberski PP, Babinska M, Szadowska A. Aberrations of chromosome 22 and polysomy of chromosome 8 as non-random changes in clear cell sarcoma. Cancer Genet Cytogenet 1994;72:141–5.
257. Bridge JA, Sreekantaiah C, Neff JR, Sandberg AA. Cytogenetic findings in clear cell sarcoma of tendons and aponeuroses. Malignant melanoma of soft parts. Cancer Genet Cytogenet 1991;52:101–6.
258. Lucas DR, Nascimento AG, Sim FH. Clear cell sarcoma of soft tissues. Mayo Clinic experience with 35 cases. Am J Surg Pathol 1992;16:1197–204.
259. Speleman F, Colpaert C, Goovaerts G, Leroy JG, Van Marck E. Malignant melanoma of soft parts. Further cytogenetic characterization. Cancer Genet Cytogenet 1992;60:176–9.
260. Zucman J, Delattre O, Desmaze C, et al. EWS and ATF-1 gene fusion induced by t (12;22) translocation in malignant melanoma of soft parts. Nat Genet 1993;4:341–5.
261. Fujimura Y, Ohno T, Siddique H, Lee L, Rao VN, Reddy ES. The EWS-ATF-1 gene involved in malignant melanoma of soft parts with t (12;22) chromosome translocation, encodes a constitutive transcriptional activator. Oncogene 1996;12:159–67.
262. Fujimura Y, Siddique H, Lee L, Rao VN, Reddy ES. EWS-ATF-1 chimeric protein in soft tissue clear cell sarcoma associates with CREB-binding protein and interferes with p53-mediated transactivation function. Oncogene 2001;20:6653–9.
263. Antonescu CR, Nafa K, Segal NH, Dal Cin P, Ladanyi M. EWS-CREB1: a recurrent variant fusion in clear cell sarcoma--association with gastrointestinal location and absence of melanocytic differentiation. Clin Cancer Res 2006;12:5356–62.
264. Antonescu CR, Dal Cin P, Nafa K, et al. EWSR1-CREB1 is the predominant gene fusion in angiomatoid fibrous histiocytoma. Genes Chromosomes Cancer 2007;46:1051–60.
265. Granville L, Hicks J, Popek E, Dishop M, Tatevian N, Lopez-Terrada D. Visceral clear cell sarcoma of soft tissue with confirmation by EWS-ATF1 fusion detection. Ultrastruct Pathol 2006;30:111–8.
266. Antonescu CR, Tschernyavsky SJ, Woodruff JM, Jungbluth AA, Brennan MF, Ladanyi M. Molecular diagnosis of clear cell sarcoma: detection of EWS-ATF1 and MITF-M transcripts and histopathological and ultrastructural analysis of 12 cases. J Mol Diagn 2002;4:44–52.
267. Panagopoulos I, Mertens F, Domanski HA, et al. No EWS/FLI1 fusion transcripts in giant-cell tumors of bone. Int J Cancer 2001;93:769–72.
268. Taminelli L, Zaman K, Gengler C, et al. Primary clear cell sarcoma of the ileum: an uncommon and misleading site. Virchows Arch 2005;447:772–7.
269. Achten R, Debiec-Rychter M, De Wever I, Sciot R. An unusual case of clear cell sarcoma arising in the jejunum highlights the diagnostic value of molecular genetic techniques in establishing a correct diagnosis. Histopathology 2005;46:472–4.
270. Covinsky M, Gong S, Rajaram V, Perry A, Pfeifer J. EWS-ATF1 fusion transcripts in gastrointestinal tumors previously diagnosed as malignant melanoma. Hum Pathol 2005;36:74–81.
271. Segal NH, Pavlidis P, Noble WS, et al. Classification of clear-cell sarcoma as a subtype of melanoma by genomic profiling. J Clin Oncol 2003;21:1775–81.
272. Schaefer KL, Brachwitz K, Wai DH, et al. Expression profiling of t (12;22) positive clear cell sarcoma of soft tissue cell lines reveals characteristic up-regulation of potential new marker genes including ERBB3. Cancer Res 2004;64:3395–405.
273. Takahira T, Oda Y, Tamiya S, et al. Microsatellite instability and p53 mutation associated with tumor progression in dermatofibrosarcoma protuberans. Hum Pathol 2004;35:240–5.
274. Waters BL, Panagopoulos I, Allen EF. Genetic characterization of angiomatoid fibrous histiocytoma identifies fusion of the FUS and ATF-1 genes induced by a chromosomal translocation involving bands 12q13 and 16p11. Cancer Genet Cytogenet 2000;121:109–16.
275. Raddaoui E, Donner LR, Panagopoulos I. Fusion of the FUS and ATF1 genes in a large, deep-seated angiomatoid fibrous histiocytoma. Diagn Mol Pathol 2002;11:157–62.
276. Hallor KH, Mertens F, Jin Y, et al. Fusion of the EWSR1 and ATF1 genes without expression of the MITF-M transcript in angiomatoid fibrous histiocytoma. Genes Chromosomes Cancer 2005;44:97–102.
277. Lieberman PH, Brennan MF, Kimmel M, Erlandson RA, Garin-Chesa P, Flehinger BY. Alveolar soft-part sarcoma. A clinicopathologic study of half a century. Cancer 1989;63:1–13.
278. Mathew T. Evidence supporting neural crest origin of an alveolar soft part sarcoma: an ultrastructural study. Cancer 1982;50:507–14.
279. Ordonez NG, Ro JY, Mackay B. Alveolar soft part sarcoma. An ultrastructural and immunocytochemical investigation of its histogenesis. Cancer 1989;63:1721–36.

280. Coira BM, Sachdev R, Moscovic E. Skeletal muscle markers in alveolar soft part sarcoma. Am J Clin Pathol 1990;94:799–800.
281. Hirose T, Kudo E, Hasegawa T, Abe J, Hizawa K. Cytoskeletal properties of alveolar soft part sarcoma. Hum Pathol 1990; 21:204–11.
282. Yamaguchi K, Soejima J, Maeda S, Kitamura K. Alveolar soft part sarcoma: a case report with immunohistochemical study. Jpn J Surg 1990;20:476–80.
283. Rosai J, Dias P, Parham DM, Shapiro DN, Houghton P. MyoD1 protein expression in alveolar soft part sarcoma as confirmatory evidence of its skeletal muscle nature. Am J Surg Pathol 1991; 15:974–81.
284. Sciot R, Dal Cin P, De Vos R, et al. Alveolar soft-part sarcoma: evidence for its myogenic origin and for the involvement of 17q25. Histopathology 1993;23:439–44.
285. van Echten J, van den Berg E, van Baarlen J, et al. An important role for chromosome 17, band q25, in the histogenesis of alveolar soft part sarcoma. Cancer Genet Cytogenet 1995;82:57–61.
286. Heimann P, Devalck C, Debusscher C, Sariban E, Vamos E. Alveolar soft-part sarcoma: further evidence by FISH for the involvement of chromosome band 17q25. Genes Chromosomes Cancer 1998;23:194–7.
287. Joyama S, Ueda T, Shimizu K, et al. Chromosome rearrangement at 17q25 and xp11.2 in alveolar soft-part sarcoma: A case report and review of the literature. Cancer 1999;86:1246–50.
288. Craver RD, Heinrich SD, Correa H, Kao YS. Trisomy 8 in alveolar soft part sarcoma. Cancer Genet Cytogenet 1995;81:94–6.
289. Ladanyi M, Lui MY, Antonescu CR, et al. The der (17)t (X;17) (p11;q25) of human alveolar soft part sarcoma fuses the TFE3 transcription factor gene to ASPL, a novel gene at 17q25. Oncogene 2001;20:48–57.
290. Hemesath TJ, Steingrimsson E, McGill G, et al. microphthalmia, a critical factor in melanocyte development, defines a discrete transcription factor family. Genes Dev 1994;8:2770–80.
291. Argani P, Antonescu CR, Illei PB, et al. Primary renal neoplasms with the ASPL-TFE3 gene fusion of alveolar soft part sarcoma: a distinctive tumor entity previously included among renal cell carcinomas of children and adolescents. Am J Pathol 2001;159: 179–92.
292. Heimann P, El Housni H, Ogur G, Weterman MA, Petty EM, Vassart G. Fusion of a novel gene, RCC17, to the TFE3 gene in t (X;17) (p11.2;q25.3)-bearing papillary renal cell carcinomas. Cancer Res 2001;61:4130–5.
293. Ladanyi M, Antonescu CR, Leung DH, et al. Impact of SYT-SSX fusion type on the clinical behavior of synovial sarcoma: a multi-institutional retrospective study of 243 patients. Cancer Res 2002;62:135–40.
294. Bentz BG, Singh B, Woodruff J, Brennan M, Shah JP, Kraus D. Head and neck soft tissue sarcomas: a multivariate analysis of outcomes. Ann Surg Oncol 2004;11:619–28.
295. Chang CK, Jacobs IA, Salti GI. Outcomes of surgery for dermatofibrosarcoma protuberans. Eur J Surg Oncol 2004;30:341–5.
296. Fiore M, Miceli R, Mussi C, et al. Dermatofibrosarcoma protuberans treated at a single institution: a surgical disease with a high cure rate. J Clin Oncol 2005;23:7669–75.
297. Terrier-Lacombe MJ, Guillou L, Maire G, et al. Dermatofibrosarcoma protuberans, giant cell fibroblastoma, and hybrid lesions in children: clinicopathologic comparative analysis of 28 cases with molecular data--a study from the French Federation of Cancer Centers Sarcoma Group. Am J Surg Pathol 2003;27:27–39.
298. Sirvent N, Maire G, Pedeutour F. Genetics of dermatofibrosarcoma protuberans family of tumors: from ring chromosomes to tyrosine kinase inhibitor treatment. Genes Chromosomes Cancer 2003;37:1–19.
299. Martin L, Piette F, Blanc P, et al. Clinical variants of the preprotuberant stage of dermatofibrosarcoma protuberans. Br J Dermatol 2005;153:932–6.
300. Enzinger FM, Weiss SW eds. Soft Tissue Tumors. Fourth Edition. St. Louis: Mosby, 2001.
301. West RB, Harvell J, Linn SC, et al. Apo D in soft tissue tumors: a novel marker for dermatofibrosarcoma protuberans. Am J Surg Pathol 2004;28:1063–9.
302. Sasaki M, Ishida T, Horiuchi H, MacHinami R. Dermatofibrosarcoma protuberans: an analysis of proliferative activity, DNA flow cytometry and p53 overexpression with emphasis on its progression. Pathol Int 1999;49:799–806.
303. Szollosi Z, Nemes Z. Transformed dermatofibrosarcoma protuberans: a clinicopathological study of eight cases. J Clin Pathol 2005;58:751–6.
304. Shmookler BM, Enzinger FM, Weiss SW. Giant cell fibroblastoma. A juvenile form of dermatofibrosarcoma protuberans. Cancer 1989;64:2154–61.
305. Horenstein MG, Prieto VG, Nuckols JD, Burchette JL, Shea CR. Indeterminate fibrohistiocytic lesions of the skin: is there a spectrum between dermatofibroma and dermatofibrosarcoma protuberans? Am J Surg Pathol 2000;24:996–1003.
306. Wick MR, Ritter JH, Lind AC, Swanson PE. The pathological distinction between "deep penetrating" dermatofibroma and dermatofibrosarcoma protuberans. Semin Cutan Med Surg 1999;18:91–8.
307. McNiff JM, Subtil A, Cowper SE, Lazova R, Glusac EJ. Cellular digital fibromas: distinctive CD34-positive lesions that may mimic dermatofibrosarcoma protuberans. J Cutan Pathol 2005;32:413–8.
308. Fetsch JF, Laskin WB, Miettinen M. Superficial acral fibromyxoma: a clinicopathologic and immunohistochemical analysis of 37 cases of a distinctive soft tissue tumor with a predilection for the fingers and toes. Hum Pathol 2001;32:704–14.
309. Minoletti F, Miozzo M, Pedeutour F, et al. Involvement of chromosomes 17 and 22 in dermatofibrosarcoma protuberans. Genes Chromosomes Cancer 1995;13:62–5.
310. Naeem R, Lux ML, Huang SF, Naber SP, Corson JM, Fletcher JA. Ring chromosomes in dermatofibrosarcoma protuberans are composed of interspersed sequences from chromosomes 17 and 22. Am J Pathol 1995;147:1553–8.
311. Fredriksson L, Li H, Eriksson U, Fredriksson L, Eriksson K, Fredriksson L. The PDGF family: four gene products form five dimeric isoforms. Cytokine Growth Factor Rev 2004;15:197–204.
312. O'Brien KP, Seroussi E, Dal Cin P, et al. Various regions within the alpha-helical domain of the COL1A1 gene are fused to the second exon of the PDGFB gene in dermatofibrosarcomas and giant-cell fibroblastomas. Genes Chromosomes Cancer 1998;23:187–93.
313. Simon MP, Pedeutour F, Sirvent N, et al. Deregulation of the platelet-derived growth factor B-chain gene via fusion with collagen gene COL1A1 in dermatofibrosarcoma protuberans and giant-cell fibroblastoma. Nat Genet 1997;15:95–8.
314. Greco A, Fusetti L, Villa R, et al. Transforming activity of the chimeric sequence formed by the fusion of collagen gene COL1A1 and the platelet derived growth factor b-chain gene in dermatofibrosarcoma protuberans. Oncogene 1998;17:1313–9.
315. Shimizu A, O'Brien KP, Sjoblom T, et al. The dermatofibrosarcoma protuberans-associated collagen type Ialpha1/platelet-derived growth factor (PDGF) B-chain fusion gene generates a transforming protein that is processed to functional PDGF-BB. Cancer Res 1999;59:3719–23.
316. Simon MP, Navarro M, Roux D, Pouyssegur J. Structural and functional analysis of a chimeric protein COL1A1-PDGFB generated by the translocation t (17;22) (q22;q13.1) in Dermatofibrosarcoma protuberans (DP). Oncogene 2001;20:2965–75.
317. Ostman A. PDGF receptors-mediators of autocrine tumor growth and regulators of tumor vasculature and stroma. Cytokine Growth Factor Rev 2004;15:275–86.
318. Greco A, Roccato E, Miranda C, Cleris L, Formelli F, Pierotti MA. Growth-inhibitory effect of STI571 on cells transformed by

the COL1A1/PDGFB rearrangement. Int J Cancer 2001;92: 354–60.
319. Sjoblom T, Shimizu A, O'Brien KP, et al. Growth inhibition of dermatofibrosarcoma protuberans tumors by the platelet-derived growth factor receptor antagonist STI571 through induction of apoptosis. Cancer Res 2001;61:5778–83.
320. Wang J, Hisaoka M, Shimajiri S, Morimitsu Y, Hashimoto H. Detection of COL1A1-PDGFB fusion transcripts in dermatofibrosarcoma protuberans by reverse transcription-polymerase chain reaction using archival formalin-fixed, paraffin-embedded tissues. Diagn Mol Pathol 1999;8:113–9.
321. Wang J, Morimitsu Y, Okamoto S, et al. COL1A1-PDGFB fusion transcripts in fibrosarcomatous areas of six dermatofibrosarcomas protuberans. J Mol Diagn 2000;2:47–52.
322. Patel KU, Szabo SS, Hernandez VS, et al. Dermatofibrosarcoma protuberans COL1A1-PDGFB fusion is identified in virtually all dermatofibrosarcoma protuberans cases when investigated by newly developed multiplex reverse transcription polymerase chain reaction and fluorescence in situ hybridization assays. Hum Pathol 2008;39:184–93.
323. Navarro M, Simon MP, Migeon C, Turc-Carel C, Pedeutour F. COL1A1-PDGFB fusion in a ring chromosome 4 found in a dermatofibrosarcoma protuberans. Genes Chromosomes Cancer 1998;23:263–6.
324. Rubin BP, Schuetze SM, Eary JF, et al. Molecular targeting of platelet-derived growth factor B by imatinib mesylate in a patient with metastatic dermatofibrosarcoma protuberans. J Clin Oncol 2002;20:3586–91.
325. McArthur GA, Demetri GD, van Oosterom A, et al. Molecular and clinical analysis of locally advanced dermatofibrosarcoma protuberans treated with imatinib: Imatinib Target Exploration Consortium Study B2225. J Clin Oncol 2005;23:866–73.
326. Sonobe H, Furihata M, Iwata J, et al. Dermatofibrosarcoma protuberans harboring t (9;22) (q32;q12.2). Cancer Genet Cytogenet 1999;110:14–8.
327. Nishio J, Iwasaki H, Ohjimi Y, et al. Overrepresentation of 17q22-qter and 22q13 in dermatofibrosarcoma protuberans but not in dermatofibroma: a comparative genomic hybridization study. Cancer Genet Cytogenet 2002;132:102–8.
328. Linn SC, West RB, Pollack JR, et al. Gene expression patterns and gene copy number changes in dermatofibrosarcoma protuberans. Am J Pathol 2003;163:2383–95.
329. Pinkel D, Albertson DG. Array comparative genomic hybridization and its applications in cancer. Nat Genet 2005;37 Suppl:S11–7.
330. Snow SN, Gordon EM, Larson PO, Bagheri MM, Bentz ML, Sable DB. Dermatofibrosarcoma protuberans: a report on 29 patients treated by Mohs micrographic surgery with long-term follow-up and review of the literature. Cancer 2004;101:28–38.
331. Maki RG, Awan RA, Dixon RH, Jhanwar S, Antonescu CR. Differential sensitivity to imatinib of 2 patients with metastatic sarcoma arising from dermatofibrosarcoma protuberans. Int J Cancer 2002;100:623–6.
332. Labropoulos SV, Fletcher JA, Oliveira AM, Papadopoulos S, Razis ED. Sustained complete remission of metastatic dermatofibrosarcoma protuberans with imatinib mesylate. Anticancer Drugs 2005;16:461–6.
333. Kondapalli L, Soltani K, Lacouture ME. The promise of molecular targeted therapies: protein kinase inhibitors in the treatment of cutaneous malignancies. J Am Acad Dermatol 2005;53:291–302.
334. Jones RL, Judson IR. The development and application of imatinib. Expert Opin Drug Saf 2005;4:183–91.
335. Coffin CM, Jaszcz W, O'Shea PA, Dehner LP. So-called congenital-infantile fibrosarcoma: does it exist and what is it? Pediatr Pathol 1994;14:133–50.
336. Wilson MB, Stanley W, Sens D, Garvin AJ. Infantile fibrosarcoma--a misnomer? Pediatr Pathol 1990;10:901–7.
337. Lowery M, Issa B, Pysher T, Brothman A. Cytogenetic findings in a case of congenital mesoblastic nephroma. Cancer Genet Cytogenet 1995;84:113–5.
338. Knezevich SR, Garnett MJ, Pysher TJ, Beckwith JB, Grundy PE, Sorensen PH. ETV6-NTRK3 gene fusions and trisomy 11 establish a histogenetic link between mesoblastic nephroma and congenital fibrosarcoma. Cancer Res 1998;58:5046–8.
339. Knezevich SR, McFadden DE, Tao W, Lim JF, Sorensen PH. A novel ETV6-NTRK3 gene fusion in congenital fibrosarcoma. Nat Genet 1998;18:184–7.
340. Bolande RP, Brough AJ, Izant RJ, Jr. Congenital mesoblastic nephroma of infancy. A report of eight cases and the relationship to Wilms' tumor. Pediatrics 1967;40:272–8.
341. Speleman F, van den Berg E, Dhooge C, et al. Cytogenetic and molecular analysis of cellular atypical mesoblastic nephroma. Genes Chromosomes Cancer 1998;21:265–9.
342. Rubin BP, Chen CJ, Morgan TW, et al. Congenital mesoblastic nephroma t (12;15) is associated with ETV6-NTRK3 gene fusion: cytogenetic and molecular relationship to congenital (infantile) fibrosarcoma. Am J Pathol 1998;153:1451–8.
343. Schofield DE, Yunis EJ, Fletcher JA. Chromosome aberrations in mesoblastic nephroma. Am J Pathol 1993;143:714–24.
344. Schofield DE, Fletcher JA, Grier HE, Yunis EJ. Fibrosarcoma in infants and children. Application of new techniques. Am J Surg Pathol 1994;18:14–24.
345. Argani P, Fritsch M, Kadkol SS, Schuster A, Beckwith JB, Perlman EJ. Detection of the ETV6-NTRK3 chimeric RNA of infantile fibrosarcoma/cellular congenital mesoblastic nephroma in paraffin-embedded tissue: application to challenging pediatric renal stromal tumors. Mod Pathol 2000;13:29–36.
346. Bourgeois JM, Knezevich SR, Mathers JA, Sorensen PH. Molecular detection of the ETV6-NTRK3 gene fusion differentiates congenital fibrosarcoma from other childhood spindle cell tumors. Am J Surg Pathol 2000;24:937–46.
347. Alman BA, Li C, Pajerski ME, Diaz-Cano S, Wolfe HJ. Increased beta-catenin protein and somatic APC mutations in sporadic aggressive fibromatoses (desmoid tumors). Am J Pathol 1997; 151:329–34.
348. Scott RJ, Froggatt NJ, Trembath RC, Evans DG, Hodgson SV, Maher ER. Familial infiltrative fibromatosis (desmoid tumours) (MIM135290) caused by a recurrent 3' APC gene mutation. Hum Mol Genet 1996;5:1921–4.
349. Couture J, Mitri A, Lagace R, et al. A germline mutation at the extreme 3' end of the APC gene results in a severe desmoid phenotype and is associated with overexpression of beta-catenin in the desmoid tumor. Clin Genet 2000;57:205–12.
350. Sturt NJ, Clark SK. Current ideas in desmoid tumours. Fam Cancer 2006;5:275–85; discussion 87–8.
351. Reya T, Clevers H. Wnt signalling in stem cells and cancer. Nature 2005;434:843–50.
352. Cheon SS, Cheah AY, Turley S, et al. beta-Catenin stabilization dysregulates mesenchymal cell proliferation, motility, and invasiveness and causes aggressive fibromatosis and hyperplastic cutaneous wounds. Proc Natl Acad Sci U S A 2002; 99:6973–8.
353. Li C, Bapat B, Alman BA. Adenomatous polyposis coli gene mutation alters proliferation through its beta-catenin-regulatory function in aggressive fibromatosis (desmoid tumor). Am J Pathol 1998;153:709–14.
354. Alman BA, Pajerski ME, Diaz-Cano S, Corboy K, Wolfe HJ. Aggressive fibromatosis (desmoid tumor) is a monoclonal disorder. Diagn Mol Pathol 1997;6:98–101.
355. Miyoshi Y, Iwao K, Nawa G, Yoshikawa H, Ochi T, Nakamura Y. Frequent mutations in the beta-catenin gene in desmoid tumors from patients without familial adenomatous polyposis. Oncol Res 1998;10:591–4.

356. Tejpar S, Nollet F, Li C, et al. Predominance of beta-catenin mutations and beta-catenin dysregulation in sporadic aggressive fibromatosis (desmoid tumor). Oncogene 1999;18:6615–20.
357. Saito T, Oda Y, Tanaka K, et al. beta-catenin nuclear expression correlates with cyclin D1 overexpression in sporadic desmoid tumours. J Pathol 2001;195:222–8.
358. Saito T, Oda Y, Kawaguchi K, et al. Possible association between higher beta-catenin mRNA expression and mutated beta-catenin in sporadic desmoid tumors: real-time semiquantitative assay by TaqMan polymerase chain reaction. Lab Invest 2002;82:97–103.
359. Lev D, Kotilingam D, Wei C, et al. Optimizing treatment of desmoid tumors. J Clin Oncol 2007;25:1785–91.
360. Ng TL, Gown AM, Barry TS, et al. Nuclear beta-catenin in mesenchymal tumors. Mod Pathol 2005;18:68–74.
361. Heinrich MC, McArthur GA, Demetri GD, et al. Clinical and molecular studies of the effect of imatinib on advanced aggressive fibromatosis (desmoid tumor). J Clin Oncol 2006;24: 1195–203.
362. Lopez-Terrada D. Integrating the diagnosis of childhood malignancies. Adv Exp Med Biol 2006;587:121–37.
363. Lazar A, Abruzzo LV, Pollock RE, Lee S, Czerniak B. Molecular diagnosis of sarcomas: chromosomal translocations in sarcomas. Arch Pathol Lab Med 2006;130:1199–207.

Chapter 7
Grossing of Bone and Soft Tissue (Common Specimens and Procedures)

Jasvir S. Khurana and Vivian Arguello-Guerra

Abstract The chapter addresses the processing of bone and soft-tissue specimens in the surgical pathology laboratory.

Keywords Specimen photography • Specimen radiography • Decalcification • Amputation • Implants • Osteochondroma • Femoral head • Bone and soft-tissue tumors • MSTS (Enneking) system

Introduction

Specimens containing bone are sent to the pathology laboratory for a variety of different reasons. Therefore, a variable amount of information is required from the pathologist.

Specimens such as bunions, menisci, intervertebral disks, and femoral head with degenerative disease are often sent only for documentation. There may, however, be incidental findings. In some cases such as osteonecrosis of the femoral head, there may be a need to confirm a clinical impression because of the implication on the contralateral hip.

On the other hand, the laboratory also receives amputations and resections (limb-salvage procedures) performed for musculoskeletal neoplasms. There may be a need for diagnosis and triaging tissue for appropriate additional studies (such as genetic information or lymphoma work-up). Therapy is frequently based on the pathologist's report, and several important observations (staging information, effects of neoadjuvant therapy) need to be made at the time of pathologic examination.

General Guidelines

Bone specimens are often sharp, and can penetrate gloves. Proper personal protection and frequent handwashing can reduce the risk of transmissible agents. Eye and mucosal protection is often required due to bone dust from the band-saw. Dilute bleach solution should be available on hand, to help clean up after the sectioning of bone on the band-saw.

Specimen Photography

Color pictures are best taken either fresh, or, after brief (few to ten minutes) fixation. The brief immersion reduces distracting glare from reflected light. The color though may be altered if the immersion into formalin is prolonged (hours or days). If immersion is prolonged, return of some color can be achieved by placement in 70% ethanol (alcohol) for 10–15 min.

Specimen Radiography

Specimen X-rays can help in the grossing of tumor resections, indicate the optimal sites for sampling, and serve as teaching material. Bone tumors are often heterogeneous, and X-rays help in locating the optimal areas to sample.

Macerated Specimens

These are used mainly for teaching and can be prepared by immersing a slice of the specimen into a bleach solution after formalin fixation. One to two days may be required. The specimen is then defatted with 70% ethanol.

Rapid (Freeze) Sectioning of Bone Samples

This method is rarely used (except to help with teaching). *The entire specimen* (soft tissues and all) is immersed into a mixture of dry ice and 90% ethanol. After about 10–15 min, the entire amputation or resection specimen can be cut on the band-saw.

Decalcification

1. Bone should ideally be sectioned using a hand or band-saw into slabs of ~3–5 mm thickness. Sections that are thicker than 5 mm take a long time to decalcify and sections that are thinner than 3 mm are at risk of breaking up.

J.S. Khurana (ed.), *Bone Pathology*, DOI 10.1007/978-1-59745-347-9_7,

When slicing through bone it is better to let the saw do the cutting (rather than try and push the bone through). Going slow avoids thermal damage to the bone. Some desktop models often have water to reduce bone dust and thermal damage.

2. It is best at this stage to wash and brush the bone dust off from the cut edges. These are then fixed in formalin and subsequently washed in water before decalcification.
3. The sections should be placed in *fresh* dilute acid (hydrochloric or nitric acid is commonly used) for decalcification. Mixtures of hydrochloric acid, formic acid, and EDTA are alternatives.
4. Commercial decalcifiers (mix well before use): A rapid decalcification solution (RDO) uses hydrochloric acid. Simultaneous fixation and decalcification solutions are available and generally acceptable (Cal-Rite uses formaldehyde and formic acid). Simultaneous formalin fixation and decalcification with RDO should never be attempted (since the mixture is carcinogenic). The decalcification solution to specimen ratio is best kept at 20:1 by volume. It is helpful if the specimen is suspended in the decal solution, so that all sides of it are bathed equally in the solution. It is also preferred that the solution is constantly stirred. This can be best achieved by using a magnetic stirrer and motorized magnetic rotor.
5. Monitoring decalcification is extremely important. Overdecalcification can ruin a specimen, destroy histologic detail, and make the tissue eosinophilic. Monitoring can be done easily by testing for softness using a sharp pin. Decalcification of a 5-mm slice of about 1 × 1 cm should take about a day.
6. After completion of decalcification, it is *critical to trim the specimen to about 3 mm* before cassetting it. This gives a reasonable thickness for processing, and also gets rid of the embedded bone dust. It is also important to *wash the specimen* at the end of decalcifying. This avoids the continuation of decalcification even after embedding, a problem common to several acid decalcifying agents.

Restoration of basophilia to overdecalcified sections is possible, but it is not ideal (it is better to avoid overdecalcification). If needed, it can be attempted by immersion of rehydrated paraffin sections in 5% aqueous sodium bicarbonate. (Alternative solutions are 5% aqueous ammonium sulfide or 5% aqueous periodic acid.)

Some *common problems and artifacts* are tabulated below:

Process	Artifact
Insufficient fixation, under- or overdecalcification	Poor histologic detail, stretching of cells
Incomplete fixation before decalcification	Bubbles of carbon dioxide get entrapped within tissues simulating adipocytes or signet ring cells.
Insufficient decalcification	Hydroxyapatite remains in tissue, unable to assess architecture of collagen, differentiate between woven and lamellar bone or identify cement lines. May miss diseases such as Paget's disease. Microtome may get damaged; tissue may pop off from the block.
Overdecalcification	Bone becomes brittle; cells get digested and may mimic osteonecrosis.
Bone dust	May simulate osteonecrosis, fat necrosis, or degenerative diseases.

Handling of Common Specimens

Nontumor Amputations and Excisions

Limbs amputated for nontumor conditions such as clostridial myonecrosis, nerve deficits, trauma, or ischemic gangrene may occasionally require photographs to document their removal or for medico-legal reasons. Further handling requires knowledge of the information likely to be needed by the managing clinical team. For example, in ischemic gangrene, it may be helpful to document the gangrene, section the supplying vessels to document the underlying disease (atherosclerosis, thromboangiitis obliterans, etc.) and document the soft-tissue margin viability. The latter is perhaps the least valuable, since the correlation between the histologic appearance and the physiologic function is at best imperfect. Benign tumor and tumor-like conditions may have specific considerations; for example, the vascular nidus should be sought (if necessary by specimen X-rays) in a suspected osteoid osteoma. Again, in a case sent as an aneurysmal bone cyst, it is critical to look for solid areas that may represent the precursor lesion.

Amputations for Gangrene, Ulcer, and Trauma

1. Describe the *type of amputation* (toe, ray, fore-foot, mid-foot, hind-foot, below-knee, above-knee) and *state the laterality (right or left)* and give measurements. Indicate whether there have been *prior procedures* (earlier toe amputations, etc.).
2. Describe extent of gangrene, ulcer(s), or trauma.
3. Dissect out vessels (and prior vascular grafts if any) and comment on patency.
4. *Sections*: Vessels (may need decalcification), skin/soft tissue with ulcer or gangrene, and bone under ulcer/gangrene (to look for osteomyelitis).

Exostosis/Osteochondroma

1. Describe and measure the size of the bony fragment(s) and state if they are in continuity with the underlying cortical bone. Indicate if there is a fracture of the stalk.
2. Slice through the osteochondroma on the band-saw and *measure the thickness of the cartilage cap. Ensure that the section is perpendicular to the surface (not tangential, since that would give an incorrect measurement).*
3. Sample the cap, stalk, and base of the osteochondroma.

Femoral Head for DJD and Osteonecrosis

1. Describe size of femoral head and size of neck (and other fragments). Indicate whether prior there are signs of prior procedure (such as a pin tract through the head).
2. Document signs of DJD grossly (erosions, eburnation, osteophytes).
3. Take multiple parallel slices through the femoral head using the band-saw. Evaluate them grossly and (if no focal lesions are seen) select one (that demonstrates the joint changes) to decalcify and process in one or two cassettes.
4. If osteonecrosis (avascular necrosis) is suspected then it may be visible grossly or may need radiographic help. In the latter case, the parallel slices can be X-rayed and one or two slices selected for histological exam after decalcification.

Femoral Head for Fracture/Pathological Fracture

1. Describe size of femoral head and size of neck (and other fragments).
2. The fracture line is usually at the neck (femoral neck fractures can be intra- or extracapsular and may be comminuted). Describe the fracture line (hemorrhage, fragmentation) as well as the articular pathology if any.
3. Sample the base of the neck (two or three cassettes) as well as the additional fragments of bone. Additionally, a section of the articular surface of the femoral head should be included.

If a *pathological fracture* is suspected then the X-rays should be obtained (from the clinician or the radiology department) and the sampling should be more liberal (several cassettes) with emphasis on the fracture line and separate fragments.

Frozen Sections

Frozen sections may be required to diagnose and type bone and soft-tissue tumors and assess margins (or to ensure that lesional tissue is present and obtain tissue for special studies). In surgery for osteoid osteoma, frozen sections can be helpful to identify the nidus. In revision, arthroplasties frozen sections are used to distinguish between infections and aseptic loosening. Generally five polymorphs per high-power field (400×) is considered to be significant and is suggestive of infection, but care must be taken to count in tissues away from vessels or fibrin.

Orthopedic Hardware

Identify if possible the hardware (hip or knee components, plates, screws, intramedullary nail, dynamic hip screw, external fixator, Ilazarov distractor, etc.); if not easily identifiable, describe it in general terms and measure. *Note any failures* of the device (bent hardware, broken or nicked components, cracked plastic).

Resections (and Amputations) for Soft-tissue Tumors

Soft-tissue tumors can be very heterogeneous. Extensive sampling may be required.

1. Resections should be inked and sampled for margins.
2. The sample is then sliced. Describe and measure the tumor. Tissue should be reserved for special studies (electron microscopy and molecular studies).
3. Staging for soft-tissue sarcomas is similar to bone (MSTS/Enneking staging system).

Resection (and Amputations) for Bone Tumors

1. The imaging studies should be reviewed. MRI and bone scan studies are helpful in delineating the extent and identifying skip metastases.
2. Describe the resection sample (measure the overall specimen); ink and sample the margins or use shave margins.
3. Sharply dissect and remove the soft tissues from the bone.
4. Section the specimen using a band-saw. Photograph as needed.
5. Describe the various extensions of the tumor (e.g., cortical breakthrough).
6. If it is a primary excision, the tumor can be sampled at this stage for special studies (molecular studies and electron microscopy).

7. Identify and sample lymph nodes and neurovascular bundles.
8. Sample the tissue – include marrow space proximal to the tumor to look for skip metastases; sample the ligaments around and within the joints, sample the subperiosteal regions, the biopsy tract, and the soft-tissue extension (extracompartmental or T_2 spread). Mesenchymal tumors can be heterogenous – extensive sampling may be needed.
9. Postchemotherapy tumors need to be mapped in order to estimate the percentage of necrosis. In order to do this, the sample is photocopied (after wrapping in see-through plastic) and a central slice is entirely blocked. The blocks are marked on the photocopy to allow reconstruction of the tumor.

The MSTS (Enneking) Staging System

Briefly, the system utilizes the GTM approach (*G*rade, Si*T*e, and *M*etastasis). G refers to grade, and may be G_0, G_1, or G_2 (benign, low, or high grade). T refers to tumor site. The site is particularly important. It is divided into the intracompartmental (T_1) and extracompartmental (T_2) locations. Although nodes are not a feature of the Enneking system, it is known that several sarcomas do in fact go to nodes (albeit infrequently) and these should be assiduously searched for and reported.

T_1 sites include intraosseous, intraarticular, parosseous, and intrafascial locations (such as ray of hand, volar forearm, etc.). T_2 sites are present when there is evidence of soft-tissue or fascial extensions. Certain anatomical locations are always T_2 – such as the popliteal and antecubital fossae, the femoral triangle, mid and hind foot, mid hand, intrapelvic location, and the axilla.

Stage	Grade	Site	Metastasis
IA	Low (G_1)	Intracompartmental (T_1)	None (M_0)
IB	Low (G_1)	Extracompartmental (T_2)	None (M_0)
IIA	High (G_2)	Intracompartmental (T_1)	None (M_0)
IIB	High (G_2)	Extracompartmental (T_2)	None (M_0)
IIIA	G_1 or G_2	Intracompartmental (T_1)	Yes (M_1)
IIIB	G_1 or G_2	Extracompartmental (T_2)	Yes (M_1)

Chapter 8
Bone Histomorphometry and Undecalcified Sections

Mei-Shu Shih

Abstract Bone histomorphometry is a useful tool to understand the cellular and tissue levels of bone activities and to correlate the clinical symptoms for diagnostic and choice of remedy. Experience and training of a histomorphometrist, that usually take months to fully develop and to narrow the coefficient of variation, decide the reliability of the data. Expansion of collective histomorphometric data from cohorts of demographically matched subjects assists the revelation of the disease mechanisms. Although histomorphometric data are limited to represent a short period of bone surfaces cell activities from a focal defined sized biopsy, the reviewer's knowledge and understanding on bone physiology is crucial to decipher them for accurate interpretations. Carefully chosen fluorochrome agents and properly administering them with a known interval aid the demonstration of temporal and spatial relationships of bone surface movement. Estimation on erosion depth in conjunction with the measurement on BMU wall thickness demonstrates the unit bone balance. Derivative estimation on BMU's activation frequency from the bone formation activity parameters enlarges the scope of unit bone balance to examine the alterations in total bone mass. Inclusion of histomorphometric data to subject's medical history and clinical observations on blood chemistry and radiodensitometry completes the evaluation for exploring and explaining subject's clinical symptoms. Histomorphometric data from before and after the treatment regimens can facilitate development of new drugs for a specific disease.

Keywords Histomorphometry • Biopsy • Fluorochrome • Labeling • Formation • Resorption • Balance • Remodeling

Introduction

Bone histomorphometry is the quantitative study of bone. It is most often performed on undecalcified histological sections of bone in order to study generalized skeletal conditions – most often these are metabolic bone diseases. It is a specialized field and several texts are devoted to the subject (1–4). Measurements are taken from bone sections and extrapolated to three dimensions using stereological equations (generally using computer programs). Fluorochrome is made of substances (labels) that are deposited in bone to mark certain features in the biopsy in order to make calculations and correctly classify the condition.

Theoretical Basis of Histomorphometry

To fulfill the biological requirements, bone needs to continuously renew itself. It does so at millions of small regions in the skeleton – these regions are called basic multicellular units (BMUs) (sometimes referred to as bone remodeling units). Cyclic events occur here – involving matrix resorption and formation. Specifically, there is activation of osteoprogenitor cells to proliferate and differentiate (A), resorption of bone matrix by osteoclasts (R), quiescent phase for reversing resorption to formation (F), and formation of bone matrix by osteoblasts (F). The cellular activities are coupled within each BMU's remodeling cycle, that is, A–R–F but appear in different (incoherent) remodeling phases among the BMUs (5–8). Under microscopy, the ideal BMU will have a team of osteoclasts excavating bone matrix that is followed by a team of osteoblasts laying down bone matrix, coupled remodeling. However, on different location of the bone surfaces within a randomly chosen microscopic field of a human iliac crest biopsy, portion of the surfaces may show erosion by osteoclasts, other surfaces may show formation by osteoblast, and the rest of the surfaces may show quiescence of remodeling activity with inactive flat osteoblast coverage. These features suggest that global bone remodeling is incoherent and necessary to maintain the balance of bone mass in whole.

Bone remodeling is controlled in part by the strain induced when bone is loaded and also by nutrition, aging, hormones, drugs, toxic agents, disease, and the genetic make up of the individual (6). It is believed that during remodeling, there is a slight negative balance in the amount of bone matrix being resorbed and formed in each BMU, particularly on the surfaces of corticoendosteum and trabeculae that adjoin the marrow (9). Therefore, bone loss is a natural process as a person ages.

J.S. Khurana (ed.), *Bone Pathology*, DOI 10.1007/978-1-59745-347-9_8

Skeletal activities, such as growth, modeling, and remodeling are key factors in the control of bone anatomy and adaptation. The BMUs operate in periosteum, intracortical Haversian canals, cortico-endosteum, endosteum, and trabeculae at different rates and frequencies (10). The *life span* of a single BMU is sigma (σ) and the *frequency* (*rate) of activation* of a new BMU is mu (μ). Sigma is the summation of phases of resorption (σ_r) and formation (σ_f) during a remodeling cycle, A–R–F.

Introduction to Measurements and Indices

Various anatomical or chemical components of bone are measured in order to provide certain static and dynamic indices. Static indices give information about bone cells and tissue activities captured at the time of biopsy. Dynamic indices are projected information of bone adaptation in response to stimulation exerted from biological factors and biomechanics. Utilization of the scheduled bone labeling schemes can reveal bone mineralization status; and when incorporated with the static data, it can produce an estimation of the rate and the frequency of bone remodeling. In most cases, a single kind of measurement may be misleading and static and dynamic measurements must be combined. For example, the presence of higher than normal amount of osteoid in hyperparathyroidism may be diagnosed as osteomalacia without the identification of a parallel increase in fluorochrome-labeled mineralization of newly formed bone matrix.

Indications for Bone Biopsy

The indications for bone biopsies have been expanded in the past years due to improved instrumentation and now include most metabolic diseases, at a stage where intervention can benefit the patient. These include osteoflurosis, osteoporosis (Fig. 1b), osteomalacia (Fig. 2), and rickets; primary and secondary hyperparathyroidism (Fig. 3); renal osteodystrophies; inherited bone diseases; Paget's disease of bone; and unclassified metabolic bone disease (11). The information obtained from bone biopsies contributes to not only the understanding of pathogenesis of metabolic bone diseases but also the safety and the therapeutic effects of treatment regimens.

Bone Biopsy

Bone biopsies can be performed using manual or powered trephines. The latter is less prone to artifacts of crushing and fragmentation, but more prone to the generation of bone

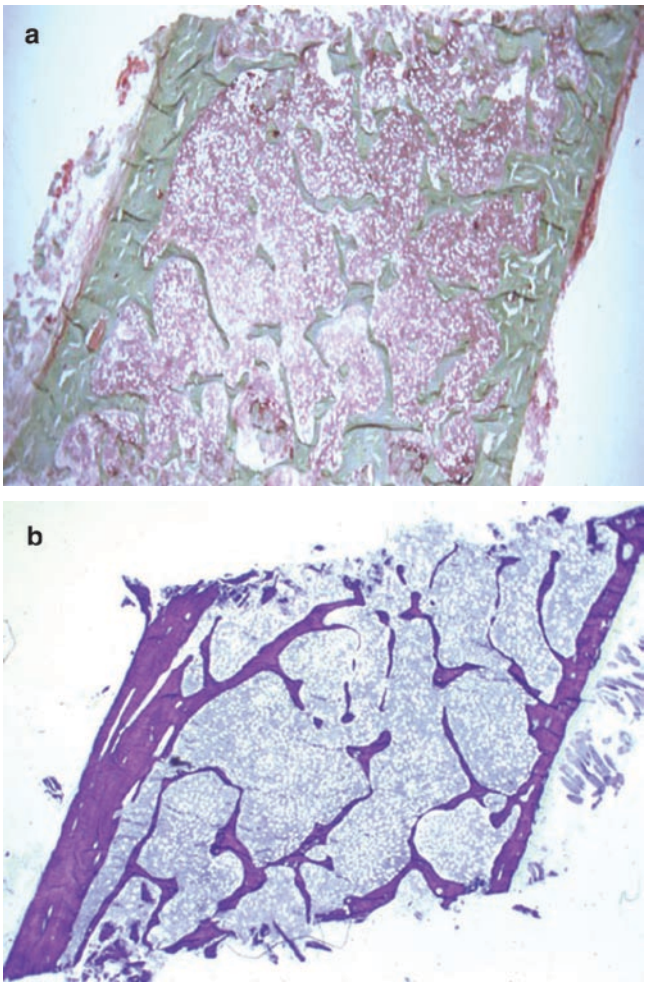

Fig. 1 **a** and **b** Photomicrographs of human iliac crest biopsies are shown with Goldner's trichrome stain on the *top* (**a**) and toluidine blue stain on the *bottom* (**b**). The biopsy from a normal subject (**a**) shows thicker cancellous bone and better network connection than the one from an osteoporotic subject (**b**). 10× magnification enhanced

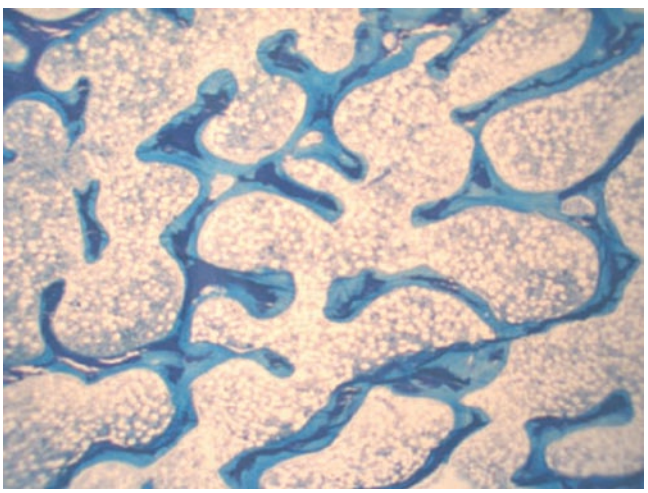

Fig. 2 Photomicrograph shows features with toluidine blue stain in osteomalacia. The mineralized bone stains dark blue, and the thickened osteoid is in light blue. 40× magnification enhanced

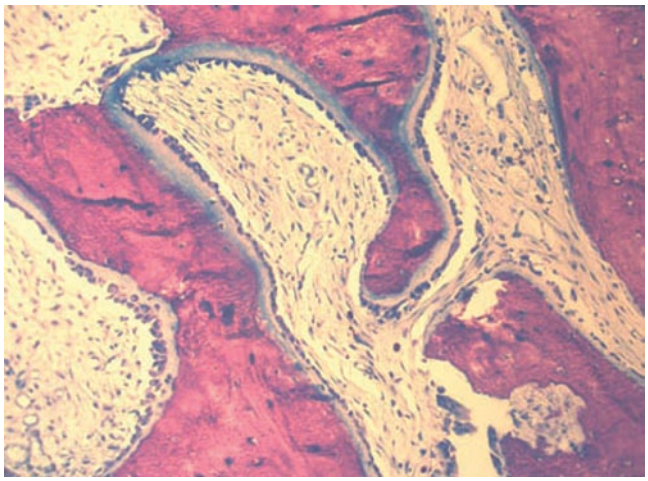

Fig. 3 Photomicrograph shows features commonly observed in bone disease from hyperparathyroidism. Mineralized bone matrix is in magenta and osteoid is in blue. Both bone resorption by osteoclasts (*top left* corner and *bottom right* corner) and bone formation by osteoblast covering osteoid are active. Marrow fibrosis is evident and replaces the normal adipose tissue and hematopoietic cells. 100× magnification enhanced

powder and thermal injury. The most favored site is the anterior iliac crest, for which the most histomorphometric data is available. This site has the advantage of easy accessibility; large histomorphometric database contains both cortical and cancellous bone. The trans-iliac biopsy (as opposed to the vertical iliac crest) produces two cortices besides cancellous bone and is better.

Iliac bone biopsy can be performed in an out-patient setting. Confirming a normal coagulation profile is imperative before the procedure. The usual biopsy site is 2 cm posterior to the anterior superior iliac spine, immediately inferior to the iliac crest. The standard trephine has an internal diameter of at least 7.5 mm in order to obtain an adequate amount of tissue sample. With careful anesthesia, patient tolerance is excellent and many patients are willing to have sequential biopsies. A second biopsy site for a follow-up is preferred to be one of the opposite of the pelvis or at least 2 cm from the first biopsy on the same side if a third biopsy is elected. Complications are rare, and include pain at the biopsy site (non-narcotic analgesia is recommended), hematoma, wound infections, osteomyelitis, and fracture through the iliac crest. Historical data showed that few patients (~0.7%) experienced serious complications (11).

Bone Labels

Bone labels are substances that localize in certain anatomic sites within bone and serve to mark them. The commonest label used currently is tetracycline, which localizes in, and is a marker for, new bone.

Bone has the ability to incorporate phosphate binding elements and heavy metals such as aluminum. The largest naturally occurring form is calcium phosphate. Other known substances that are deposited in bone and can become detectable by radiological image analysis and/or autoradiography are technetium isotopes and plutonium (12). Frost pioneered the use of tetracycline in bone biopsy. The uniqueness of the tetracycline labeling is that it occurs only when the newly formed bone matrices are actively mineralized, and it stays in bone as long as that portion of the bone matrix has not subjected to remodeling activities. It is detectable by fluorescent microscopy under excitation by blue light at a wavelength of 360–490 nm. Therefore, it becomes a landmark for bone microstructural adaptation. Carefully mapping multiple labels in temporal and spatial arrangements can reveal the alterations in physiological and pathological conditions of bone (5).

Different tetracyclines fluoresce in different colors, so it is useful, although not necessary, to use two different tetracyclines (such as oxytetracycline showing gold-yellow fluorescence and declomycin showing green fluorescence) in order to distinguish the first label from the second. If repeat biopsy is warranted in a patient at a short interval after the first biopsy, the use of a different color becomes extraordinarily useful to the histomorphometrist in distinguishing labels of the first biopsy from the second.

There have been many attempts to use bone labeling markers other than tetracycline (Table 1). The general rules are that to be useful a bone label should be nontoxic to the patient, inexpensive, and simple to use that remain stable in situ both within the patient and also throughout the histological preparation of the sample. It must be detectable and the detection process should not alter the marker characteristics of the label. It must localize in new bone (preferably exclusively so) and it must not interfere with osteoblastic function or produce general nonspecific autofluorescence of bone matrices.

Table 1 Other labels used experimentally in comparison to tetracycline

Labeling agent	Labels osteoid	Labels the calcification front	Stable in sections	Good label	Stable in vivo	Stable ex vivo	Toxic to patient	Toxic to osteoblasts	Inexpensive	Reliable
Tetracycline	0	+	+	+	+	+	0	0	+	+
Xylenol Orange	0	+	+	+	+	+	?	+	+	+
Alizarin	0	+	+	+	+	+	+	+	+	0
Calcein	0	+	+	+	+	+	0	0	+	+
Fluorescein	0	+	+	0	0	0	0	?	+	+

Tetracycline Labeling

Tetracycline should be given on an empty stomach. Concomitant antacid preparations (especially those containing aluminum) should be avoided. The dose is usually 250 mg, four times daily, orally in adults. If given parentally, the usual dosage employed is 15 mg/kg/day. It is usual to give this by a slow (5 min) i.v. infusion in a volume of at least 100 ml. Rapid infusions may cause transient (but sometimes fatal) lowering of ionized calcium. Outdated tetracycline is toxic, and does not fluoresce normally. Tetracycline should not be administered to pregnant women or children, because it is incorporated into growing teeth and can cause permanent discoloration. Dairy products and foods, or medications that bind aluminum, iron, magnesium, or calcium can also bind tetracycline and thus be avoided. Patients should be advised to avoid exposure to sunlight or ultraviolet light since some individuals become photosensitive.

Labeling Schedules

The unit of time used is the day. Usually, label is administered for 3 days, followed by a 11- to 14-day drug-free period, after which drug is administered for an additional 3 days. The biopsy is performed, at least, 4 days after the last dose (3-11-3:4 sequence). The order of events is called "staging" and the permissible durations are called "staging limits." The duration of label administration is referred to as the "labeling period" and the time interval between markers is the "label interval."

Optimal staging limits depend on certain characteristics of bone formation at remodeling sites (BMU, also called BRU or basic remodeling units by other authors).

Optimal schedules for the *human Iliac bone–tetracycline system* range between 1-5-1:5 and 3-14-6:14 (although the authors recommend 3 days of label administration). These schedules take into account two main characteristics of this region – namely rate of apposition and length of time taken to complete the formation of a new BMU.

Undecalcified Section Preparation

The biopsy should be fixed in ethanol (70%). Conventional fixatives (formalin, Bouins, Zenker's, glutaraldehyde, etc.) cause tetracycline labels to leach out. The total volume should be at least ten times the volume of the biopsy. A period of 24–48 h fixation is recommended for a full size biopsy. If the subsequent dehydration is done manually, place the biopsy into fresh 70% ethanol for 24 h. This is accompanied by putting the specimen through two changes of 95% ethanol each for 24 h, and then at least three separate passages in pure (100%) ethanol, each lasting 24 h with a magnetic stirrer. There are many brands of tissue processors that can be programmed to shorten the time for these steps by enhancing the fluid exchanges under vacuum.

Embedding (Fig. 4) is usually done in methyl methacrylate (MMA). Other plastics such as bioplastic and glycolmethacrylate are less frequently used. Many methodologies for polymerization exist. It is important to allow thorough infiltration of MMA before polymerization induced by heat or benzoyl peroxide. Use of slow speed rotator or shaker is recommended to facilitate the infiltration of increasing viscosity of the MMA solutions. Slow polymerization at or below 37°C is recommended. The specimens in vials or molds of MMA if placed in oven or water bath should be spaced far enough, at least 3–4 cm apart, to avoid additive heat being released from the polymerization that causes bubbling effect in the tissue block.

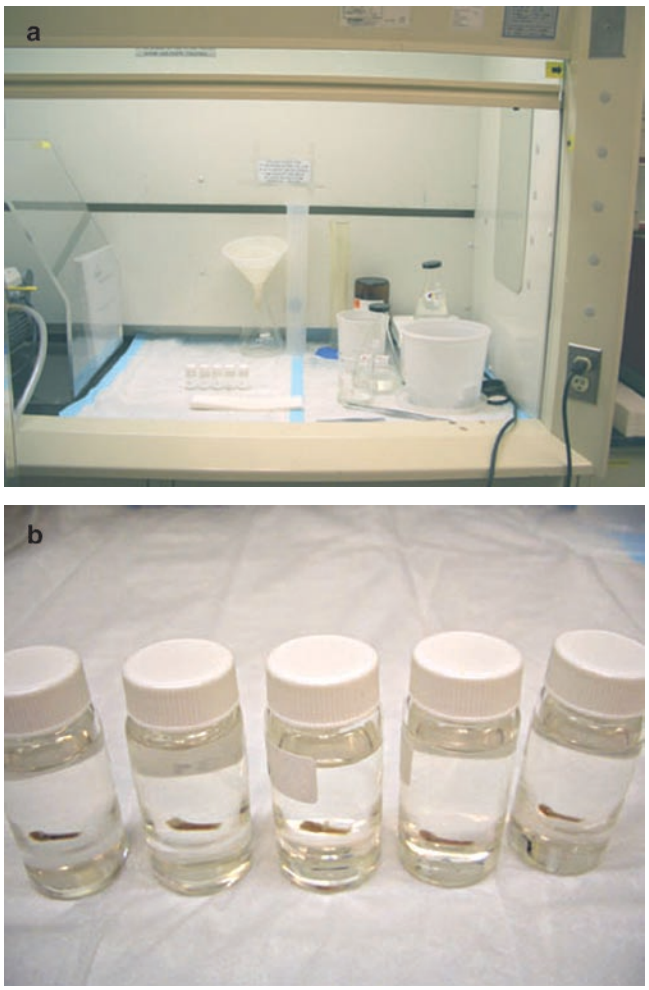

Fig. 4 **a** and **b** Photographs show the embedding of bone specimens in polymethyl methacrylate under a hood. Glassware and measuring cylinder are shown in the background of **a**. In addition, part of a vacuum pump is located on the *left* side of **a**

Special heavy-duty microtomes use diamond coating or tungsten carbide knives, such as the Jung sliding microtome (model K or the Reichert-Jung polycut), are required to cut the specimen. The section thickness of 4–6 μm is readily achievable for the stained section, while 10 μm thick unstained section is recommended for examining fluorochrome labels. Some laboratories stain the entire tissue en bloc, for example, osteochrome, prior to embedding. The common stains utilized include toluidine blue (pH 6.5), Goldner's trichrome, Masson's trichrome, von Kossa, histochemical stains for acid and alkaline phosphatase, and special stains for materials such as aluminum by aurine-tricarboxylic acid and iron by Perl's stain.

Bone Histomorphometry

Bone histomorphometry is a specialized subject. It often entails a steep learning curve to perform consistently and precisely. The operator needs to establish data showing steady intraobserver variation to minimize deviations in repeated histomorphometry on a specimen. The laboratory should document and reduce interobserver variations.

Histomorphometry is often carried out by using computer software, for example, OsteoMeasure™ (OsteoMetrics, Decatur, GA[1]) or BioQuant (R & M Biometrics, Nashville, TN[2]). The video card of the computer converts images projected from a light microscope through lenses of a camera to cause a virtual image to appear on the monitor screen (Fig. 5). The mode of digitizing the images can be through manual tracing of the microscopic objects with a stylus or a mouse or a cursor. The newer version of the software can digitize the images automatically and move the slide-platform by motorized control panel. Nevertheless, classic point-counting method by using ocular grids placed in a microscope is still a viable alternative to the costs of purchasing an image analysis system. The results from both methods are comparable (13). This section will not attempt to deal with the specific techniques of performing the histomorphometry. The intention here will be to introduce some of the parameters that are useful to provide qualitative and quantitative values of bone activities and the interpretations of the results in histomorphometry.

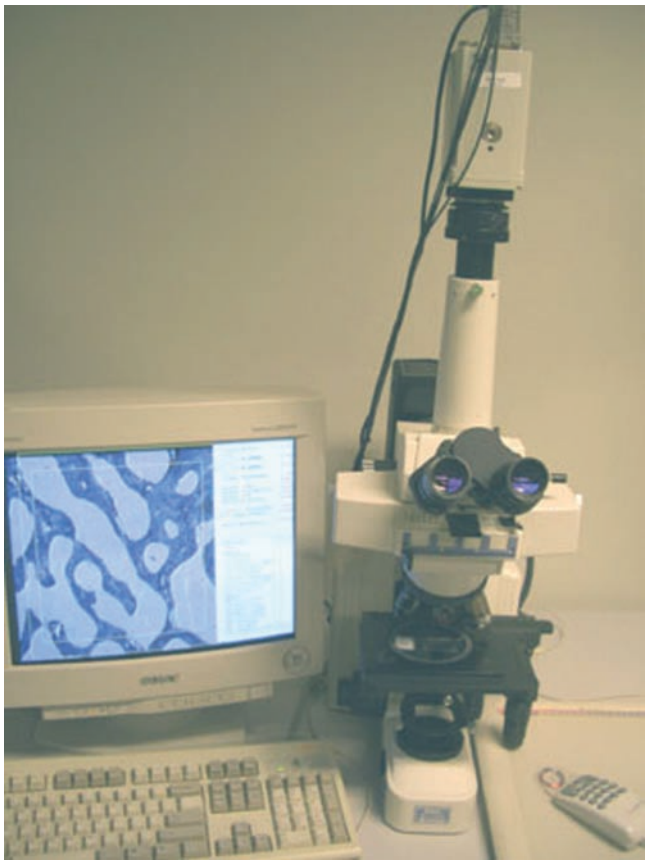

Fig. 5 Photograph shows a system for histomorphometry. The microscope is equipped with a CCD digital camera that can project image of bone from the slide through the video card of a PC. Digitizing board and cursor located on the lower right corner can be used to trace and measure bone structural and cellular indices for static and dynamic parameters. The software program will translate the digitized information to physical values after it is calibrated for unit measurement by using a stage micrometer for the chosen magnification of the objective lens

Evaluation of Undecalcified Bone Histology

Several generalized references are available (14–16). The aim of assessment of biopsies in cases of metabolic bone diseases is to evaluate whether there is disturbed *matrix formation and organization*, disturbed *mineralization*, or disturbed *resorption*. The former is most evident in conditions such as osteopetrosis, osteogenesis imperfecta, and low turnover osteoporosis. Disturbed mineralization or hyper*osteoid*osis may arise in conditions such as rachitic syndromes, osteomalacia, and aluminum and fluoride toxicity. Disturbed resorption is seen in Paget's disease, high turnover osteoporosis, and primary and secondary hyperparathyroidism.

Many laboratories have formed a screening step before commencing a full-scale histomorphometric evaluation. The sections of a biopsy are viewed under microscopy for general alterations in structural, tissue level, and cellular components, as compared to normal values. The parameters focus on trabecular bone volume, cortical width, extent and width of osteoid, extent of fluorochrome label uptakes, separation of labels, extent of resorption, and number of osteoclast and

[1]OsteoMetrics, Inc. 2103 North Decatur Road, Suite 104, Decatur, GA 30033–5305. Tel. 404/876–1004
[2]BIOQUANT Image Analysis Corporation 5611 Ohio Avenue, Nashville, TN 37209. Tel. 800/221–0549

osteoblast. Diagnostic impression is consequently summed to indicate the state of metabolic bone disease of osteoporosis or osteomalacia or hyperparathyroidism, or renal osteodystrophy, or normal or others. In addition, the extent of labeling surfaces assists the estimate of a high or low or normal bone turnover rate.

The clinical laboratory data (blood chemistry, parathyroid hormone, and vitamin D profiles) and bone densitometry together provide more fully the picture of the metabolic stage the patient is in.

The definitions and descriptions of bone biopsy measurements are listed below. In essence, quantification is done for both cortical and cancellous bone including:

Amount of Bone

1. Parameters of bone volume
   a. Cortical bone area – this is the total area of cortical bone in a longitudinal section through the biopsy cylinder, expressed in mm^2.
   b. Porosity of cortical bone – this is the total cross-sectional area of void in the bone, including Haversian canals in osteons at various stages of remodeling and Volkman canals but excluding osteocytes lacunae, expressed as a percentage of the total area of cortical bone.
   c. Relative trabecular bone volume – this is the total area of bone (mineralized + osteoid) in the section, expressed as a percentage of the total bone tissue (including mineralized bone, osteoid, and marrow/porosity).
   d. Relative osteoid volume – this is the total area of osteoid in the section, expressed as a percentage of the total area of bone (mineralized + osteoid).

2. Parameters of thickness
   i. Static
      a. Mean osteoid thickness – this is the width of osteoid, expressed in micrometers.
      b. Mean trabecular thickness – this is estimated indirectly as twice the area to perimeter ratio, expressed in micrometers.

   ii. Dynamic
      a. Distance between labels – this the mean distance between the middle of two fluorescent bands, expressed in micrometers.
      b. Wall thickness – this is the mean thickness of a BMU measuring from the cement line to the quiescent bone surface, expressed in micrometers.
      c. Erosion depth – this is the mean distance from the completed erosion pit to the drawn line joining the adjacent quiescent surface and following the contours of the intact bone surface on either side of the pit (17).

Surface Measurements

1. Static
   i. Osteoid surface – this is the total perimeter length of osteoid, expressed as a percentage of the total + trabecular perimeter.
   ii. Erosion surface – this is the total eroded perimeter on bone, expressed as a percentage of the total bone perimeter.
   iii. Osteoblast surface – this is the length of perimeter adjacent to columnar- and cuboidal-shaped osteoblasts, expressed as a percentage of the total osteoid perimeter.
   iv. Osteoclast surface – this is the total perimeter adjacent to osteoclasts, expressed as a percentage of the total bone perimeter.

2. Dynamic
   i. Mineralizing surface – this is the summation of one half the length of perimeter showing single + the total length of perimeter showing double labels, expressed as a percentage of the total bone perimeter.
   ii. Mineralizing osteoid surface – this is the summation of one half the length of perimeter showing single + the total length of perimeter showing double labels, expressed as a percentage of the total osteoid perimeter.

Bone Formation

1. Mineral appositional rate – this is the mean distance between the labels divided by the number of days between the labels, expressed as μm/day.
2. Adjusted mineral appositional rate – this is the mineral appositional rate being adjusted by multiplying it with the ratio of labeling surface, expressed as μm/day.
3. Mineralization lag time – this is the mean osteoid thickness divided by the mean mineral appositional rate, expressed in days.
4. Bone formation rate – this is the volume of new bone made per mm^3 of an existing bone, expressed as a percentage per year.
5. Formation period – this is the mean wall thickness divided by the adjusted mineral appositional rate, expressed in days.

Bone Resorption

1. Erosion period – this is derived from the formation period by multiplying it with the ratio of erosion perimeter to osteoid perimeter, expressed in days.
2. Erosion rate – this is product of mean erosion depth and the probability that erosion will begin at any point on the surface in a defined time period, that is, activation frequency, expressed as μm/day.

Bone Balance

1. Bone balance at the BMU level – this is the outcome of each remodeling transaction, expressed as the differences between wall thickness and erosion depth in micrometers.
2. Bone balance at the bone volume level – this is derived from the differences between bone formation rate and erosion rate, expressed as percentage of bone volume per year.
3. Activation frequency – this is derived from bone formation rate in reference of total bone perimeter divided by mean wall thickness.

The publication of a set of nomenclature by the American Society for Bone and Mineral Research (ASBMR) has improved communication of histomorphometric data (18). Using the principles of stereoscopy, volumes are reported from area measurements, since they are mathematically equivalent. The histomorphometric parameters listed in Table 2 are most commonly reported in the literatures.

The ranges of normal values of cancellous bone listed in Table 2 for premenopausal and postmenopausal women were a set of reference data obtained and compiled by the author at Henry Ford Hospital from normal volunteers, mostly Caucasian, in and around Detroit, MI, in early 1990s. Other reported normal values of bone remodeling can be found in the literature readily (14, 19–22).

Implications for the Interpretation of Bone formation Indices

The main entities obtained from fluorochrome labeling are the mineral apposition rate (MAR) and the extent of mineralizing surface (MS). The frequency distributions of measurements of these parameters in normal subjects and in patients with osteomalacia indicate that MAR has a measurable lower limit, that is, 0.3 μm/day, but that MS has a true lower limit of zero (23). This is particularly useful when there is complete absence of detectable fluorescent labels in severe case of osteomalacia, MS value is zero, and MAR and its derived indices must be considered as missing data so that it truly reflects the period for bone matrix to be mineralized becomes infinite. Identification of the mineralization front (Fig. 6) can also be accomplished by toluidine blue stainable fine granules that appear at the osteoid/bone interface (24).

Bone formation may temporarily halt (or cease altogether) prior to completing a BMU. The microscopic evidences of this phenomenon are the smooth "resting cement lines" that appear to have similar dark blue stain as reversal cement lines (Fig. 7). The difference between the two lines is that the resting lines are from cessation of osteoblastic activities and the reversal lines are from transition of osteoclastic to osteoblastic activities. Although double labeling with a known interval is now the standard method of gathering bone-forming

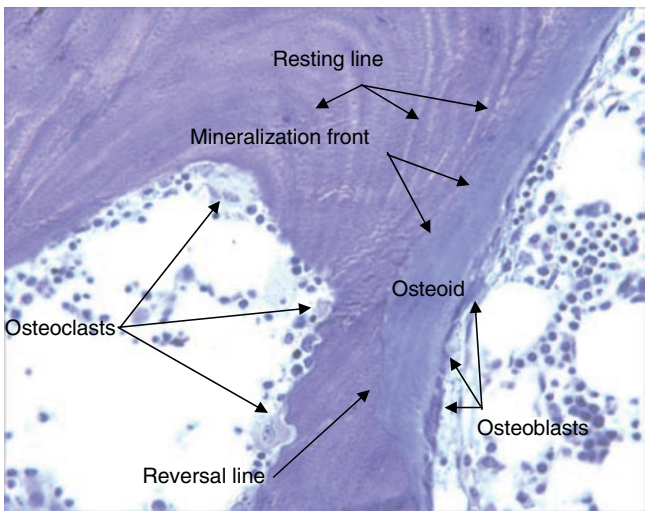

Fig. 6 Photomicrograph shows mineralization front, cement line, and bone surface cell activity with toluidine blue stain. 100× magnification enhanced

Table 2 Common histomorphometric parameters

Term	Abbreviation	Units	Normal premenopausal	Normal postmenopausal
Bone volume	BV/TV	%	12.6–41.2	10.0–31.3
Osteoid volume	OV/TV	%	0.1–0.8	0.1–1.0
Osteoid surface	OS/BS	%	3–21	4–34
Osteoblast surface	Ob.S/BS	%	1–7	0–8
Osteoid thickness	O.Th	mm	7–15	6–16
Eroded surface	ES.BS	%	1–8	2–12
Osteoclast surface	Oc.S/BS	%	0.1–0.9	0.1–1.8
Trabecular thickness	Tb.Th	mm	86–192	83–276
Wall thickness	W.Th	mm	42–56	30–56
Mineralizing surface	MS/BS	%	2–14	3–18
Mineral apposition rate	MAR	mm/day	0.5–1.1	0.4–1.0
Adjusted apposition rate	Aj.AR	mm/day	0.25–0.75	0.15–0.57
Bone formation rate	BFR/BS	mm^3/mm^2/year	5–35	5–40

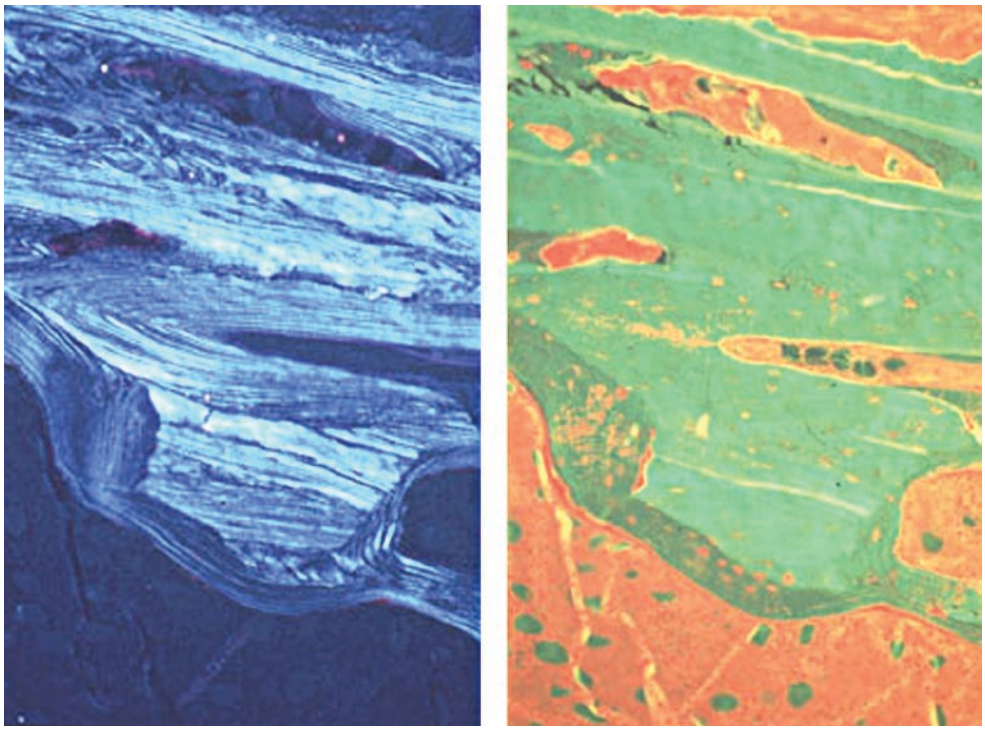

Fig.7 Photomicrographs show the bone lamination under polarization (*left* panel) and under fluorescent (*right* panel) microscopy. The inner margin of the recently formed bone in dark green (*right*) coincides with the reversal line seen under polarization (*left*). Several lines of yellow fluorescent labels indicate the bone formation between them has been continuous with smooth resting lines (*right*) separating several bone formation episodes

activities at tissue level, not all BMUs will take up both labels giving distinct colors from two types of fluorescent agents. In addition, different tetracycline fluorochrome agents give different total length of labeling surfaces (25), where the measured total length of demethylchlortetracycline label is longer than the oxytetracycline label on all bone surfaces of a specimen regardless the order these are administered. Bone formation period in human cancellous bone is calculated to be ~148–228 days (26). The following are plausible explanations to reflect the fluorochrome indices of bone-forming activities during the period.

Labeling Escape Error

Since BMUs are in different stages, it is logical to expect that a certain proportion will not take the first label (because they began to mineralize after it was given). It follows also that a certain proportion will not take the second label (because they have ceased forming prior to its administration). The longer the label interval, the greater the numbers of BMUs which will be single labeled. If the label interval is 40 days, for example, then over 90% of BMUs will show this label escape phenomenon. Lower appositional rates will also increase the occurrence.

Skewed Sampling Error

Individual BMU has individual appositional rate that reflects its stage of forming activities, faster at earlier phase, and gradually declining to barely measurable at final phase. When a label is given at a long label interval, the units in the end of forming period are more likely to take both labels. The units at beginning or middle of forming period tend to miss one of the labels and cause a sampling deviation from the normal frequency distribution. Therefore, the resultant mineralizing surface (MS) is likely to be weighted in favor of slower forming units and be falsely low in this situation. Shorter label intervals help *overcome* this error.

Label Recognition Error

This refers to the error arising from previously administered tetracycline being confused with a current label. The administration could have been due to therapeutic administration (for infections etc.) or for a previous study. The latter case can be a real problem since a previous study would have been administered a double label within a 20- to 60-day period. The presence of overlying osteoid may help establish the recent nature of a label. Also old labels tend to end

abruptly rather than blending together at the edges – but this can still be a major problem in interpretation. Different tetracyclines can be used which fluoresce with a slightly different color as noted above.

Choice of Labeling Agent

This refers to the differences between the fluorochrome compounds in their affinity to bone matrix at the time of mineralization due to physical, chemical, or pharmacokinetic characteristics. For example, label length of oxytetracycline is consistently shorter than that of demethylchlortetracycline regardless the order of administration sequences (25). If the extent of MS is calculated from the mean length of the two labels, either the length of oxytetracycline label should be adjusted by multiplying a factor of 1.18 or the length of the demethylchlortetracycline should be used.

Intermittent Apposition

The vigor of osteoblasts declines during the formation period, and fluorochrome label fixation to the bone matrix at terminal mineralization may be impaired. When osteoid thickness falls below 5 µm, it is possible that there are too few fluorochrome molecules affixed to be visible under fluorescent microscopy (26–28).

Implications for the Interpretation of Bone Resorption Indices

Measurement of erosion depth (Fig. 8) is the counterpart of assessments of wall thickness, the summation output of the osteoblast teams, in the quantum concept of bone remodeling that depicts the resultant focal bone balance. The summation of all such transactions by teams of osteoclasts and osteoblasts determine the spatial and temporal changes in bone surface location (17). To infer erosion depth, it is essential to calculate activation frequency before deriving erosion period in days, erosion rate (µm/day), and surface-based bone resorption rate ($\mu m^3/\mu m^2$/year). Methodologies used in measuring erosion depth vary from counting the number of lamellar that have been eroded adjacent to each cavity with or without cell characterization, to using automatic fitting a smooth line connecting the bone surface on each side of a resorption cavity, and to drawing manually a line joining the adjacent quiescent bone surface of a completed resorption cavity (29).

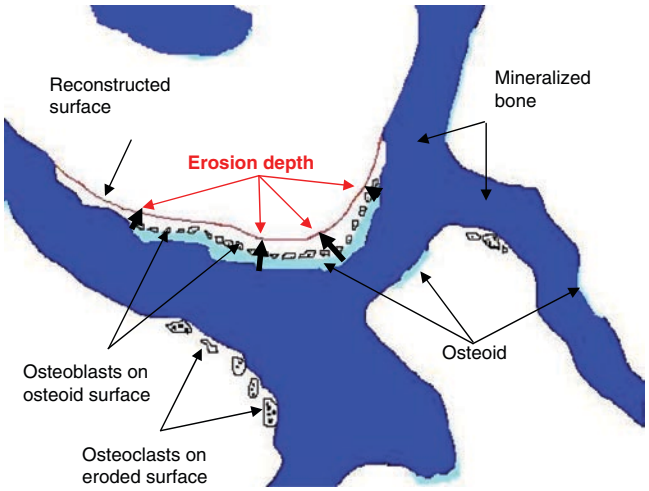

Fig. 8 Drawing depicts the reconstruction of bone surface for erosion depth measurement on toluidine blue stained section. Mineralized bone is in dark blue and osteoid is in light blue. The measurements should be done on remodeling sites that have identifiable reversal line that is covered by osteoid, and eroded lamellar that are still visible at each extremity. For all such sites, a line joining the adjacent quiescent surfaces is drawn on the display screen by following the contours of the intact trabecular surface on either side. Measurements are made at 100× original magnification of orthogonal intercept length between this line and the closest reversal line at intersections

Implications for the Separation of Trabecular Bone from Cortical Bone

It is a well-known fact that cortical bone and trabecular bone behave differently in both normal and disease states. And yet, these are intimately connected to each other in the endocortical zone. Spatial arrangement and alignment of corticoendosteal surfaces adjust constantly, however minute in adult bone, against the biomechanical loads that exceed minimum effective strain. The adjustment function is to maintain a constant and physiological load on entire bone and the end result is to return the load to within the minimum effective strain (8). Coalescing Haversian canals and bone marrow during the adjustments blurs the lines defining cortical versus trabecular bone, which is amplified in osteoporotic bone induced by disuse or by hormonal effects (menopause or hyperparathyroidism) or by senescence. The resultant trabeculation of cortical bone creates conical and cylindrical struts that may or may not be contiguous parts of the cancellous bone network in the bone marrow. A set of criteria has been proposed by Villanueva (personal communication) and used in Bone and Mineral Research Laboratory at Henry Ford Hospital (Detroit, MI). The criteria define that when the height of the strut is less than 170 µm, include it to be part of the cortical bone. When the height of the strut is greater than 170 µm and the base of the strut is less than 340 µm, include it to be part of the cancellous bone. When the height of the

strut is greater than 170 μm and the base of the strut is greater than 340 μm, draw an imaginary line following the contour of the endosteal surface and crossing the strut parallel to the baseline at 170 μm heights.

References

1. Frost HM. Bone Remodeling and Its Relationship to Metabolic Bone Diseases. Charles C. Thomas, Springfield, IL, 1973.
2. Jaworski ZFG. Bone Morphometry. University of Ottawa Press, Ottawa, Canada, 1976.
3. Meunier PJ. Bone Histomorphometry. Armour Montagu, Paris, 1977.
4. Recker RR. Bone Histomorphometry: Techniques and Interpretation. CRC Press, Boca Raton, FL, 1983.
5. Frost HM. Tetracycline-based histological analysis of bone remodeling. Calcif Tiss Res 1969;3:211–37.
6. Parfitt AM. The coupling of bone formation to resorption: A critical analysis of the concept and its relevance to the pathogenesis of osteoporosis. J Metab Bone Dis Relat Res 1982;4:1–6.
7. Frost HM. The skeletal intermediary organization. A review. J Metab Bone Dis Relat Res 1983;4:281–90.
8. Frost HM. The mechanostat: A proposed pathogenic mechanism of osteoporoses and the bone mass effects of mechanical and nonmechanical agents. Bone Miner 1987;2:73–85.
9. Parfitt AM. The cellular basis of bone remodeling: The quantum concept re-examined in light of recent advances in the cell biology of bone. Calcif Tiss Int 1984;36:S37–S45.
10. Balena R, Shih M-S, Parfitt AM. Bone resorption and formation on the periosteal envelope of the ilium: A histomorphometric study in healthy women. J Bone Miner Res 1992;7:1475–82.
11. Rao DS. Practical approach to bone biopsy. In: Recker RR, Ed. Bone Histomorphometry: Techniques and Interpretation. CRC Press, Boca Raton, 1983:3–11.
12. Jee WS, Dell RB, Miller LG. High resolution neutron-induced autoradiography of bone containing 239Pu. Health Phys 1972;226:761–3.
13. Smith JM, Jee WSS. Automated skeletal histomorphometry. In: Receker RR, Ed. Bone Histomorphometry: Techniques and Interpretation. CRC Press, Boca Raton, 1983:285–95.
14. Recker RR, Kimmel DB, Parfitt AM, et al. Static and tetracycline-based bone histomorphometric data from 34 normal postmenopausal females. J Bone Miner Res 1988;3:133–44.
15. Malluche HH, Faugere MC. Atlas of Mineralized Bone Histology. Karger, Basel, 1986.
16. Bullough PG, Bansal M, Di Carlo EF. Morphology of the metabolic diseases of bone, Part I. In: A CPC Series: Cases in Metabolic Bone Disease, vol. 2, number 4. Triclinica Communication, New York, 1987.
17. Cohen-Solal ME, Shih M-S, Lundy MW, et al. A new method for measuring cancellous bone erosion depth: Application to the cellular mechanisms of bone loss in postmenopausal osteoporosis. J Bone Miner Res 1991;6:1331–8.
18. Parfitt AM, Drezner MK, Glorieux FH, et al. Bone histomorphometry: Standardization of nomenclature, symbols and units. J. Bone Miner Res 1987;2:595–610.
19. Courpron P, Meunier P, Bressot C, et al. Amount of bone in iliac crest biopsy. Significance of trabecular bone volume. Its values in normal and pathological conditions. In: Meunier P, Ed. Bone Histomorphometry: Second International Workshop. Armour-Montagu Publishers, Lyon, 1976:39–53.
20. Dahl E, Nordal KP, Halse J, et al. A histomorphometric analysis of normal bone from the iliac crest of Norwegian subjects. Bone Miner 1988;3:367–77.
21. Melsen F, Melsen B, Mosekilde L, et al. Histomorphometric analysis of normal bone from the iliac crest. Acta Pathol Microbiol Scand 1978;86:70–81.
22. Vedi S, Compston JE, Webb A, et al. Histomorphometric analysis of iliac bone biopsies from the iliac crest of normal British subjects. Metab Bone Dis Relat Res 1982;4:231–6.
23. Foldes J, Shih M-S, Parfitt AM. Frequency distribution of tetracycline-based measurements: Implication for the interpretation of bone formation indices in the absence of double-labeled surfaces. J Bone Miner Res 1990;510:1063–7.
24. Villanueva AR, Kujawa M, Mathews CHE, et al. Identification of the mineralization front: Comparison of a modified toluidine blue stain with tetracycline fluorescence. Metab Bone Dis Relat Res 1983;5:41–5.
25. Parfitt AM, Foldes J, Villanueva AR, et al. Different in label length between demethylchlortetracycline and oxytetracycline: Implications for the interpretation of bone histomorphometric data. Calcif Tiss Int 1991;48:74–7.
26. Parfitt AM, Han Z-H, Palnitkar S, et al. Effects of ethnicity and age or menopause on osteoblast function, bone mineralization, and osteoid accumulation in iliac bone. J Bone Miner Res 1997;12:1864–73.
27. Frost HM Bone histomorphometry: Choice of marking agent and labeling schedule. In: Recker RR, Ed. Bone Histomorphometry: Techniques and Interpretation. CRC Press, Boca Raton, 1983:37–52.
28. Frost HM. A method of analysis of trabecular bone dynamics. In: Meunier PJ, Ed. Bone Histomorphometry. Société de la Nouvelle Imprimerie Fournier, Toulouse, 1977:445–76.
29. Bain S, Gross T. Structural aspects of bone resorption. In: Bronner F, Farach-Carson MC, Rubin J. Eds. Bone Resorption. Springer-Verlag, London, 2005:58–66.

Chapter 9
Radiology of the Musculoskeletal System

William R. Reinus, Susan V. Kattapuram, and Jasvir S. Khurana

Abstract Modern orthopedic practice relies heavily on various imaging modalities including plain radiographs, computer-assisted tomography, magnetic resonance imaging and bone scintigrams. These techniques help in diagnosis and management of various orthopedic problems such as trauma, tumor, infections and metabolic skeletal diseases.

Keywords X-rays • Radiogram • CT scan • MRI • CT-guided needle biopsy • Fluoroscopy • Radionuclide imaging • Gallium • Indium • Bone infections • Trauma • Bone tumors • Soft-tissue tumors • Osteoporosis • Fracture • Gadolinium-enhanced MRI • Angiography • Superscans • PET scan • Bone densitometry • Dual energy X-ray absorptiometry (DEXA) • QCT • Ultrasound

Radiology of the Musculoskeletal System

Modern orthopedic practice relies heavily on imaging. Ever since the discovery of the X-ray, plain radiographs have played a major role in diagnosing skeletal trauma. Today radiographs, along with other newer imaging modalities, contribute to the diagnosis, staging, treatment planning, and follow-up of diverse musculoskeletal lesions. The introduction of CT and MR imaging (MRI) permit more accurate preoperative staging of the extent of both bone and soft-tissue involvement by neoplasm. As recent technological advances in CT and MRI have improved the ability to noninvasively stage tumors, limb salvage surgery has become a real possibility without jeopardizing chances of cure. The use of C-arm and bi-plane image intensifiers in operating rooms has allowed accurate positioning of fractured bone fragments and orthopedic implants. The popularity of fluoroscopically and CT-guided needle biopsies has made interventional radiologists a partner in the diagnosis and treatment of musculoskeletal neoplasms. Radionuclide imaging also plays an important role in the work-up of metastatic and multifocal bone disease. In addition, technitium, gallium and indium scanning have found a place in the diagnosis of bone infections. Finally, multiple radiological techniques have been invented to evaluate in vivo bone mass as a means of diagnosing osteoporosis and predicting patients' fracture risk.

Imaging Modalities

Radiography

Radiographs are the primary technology used to detect and characterize most bone pathology. The four major objectives of radiographic imaging are as follows:

- *Detection of pathology*
- *Diagnosis*
- *Staging (including identifying metastatic disease)*
- *Evaluation of treatment*

The choice and sequence of imaging depends upon the type of lesion and clinical objectives. Plain radiographs often suffice to detect, diagnose, and follow bone pathology. For some lesions, more sophisticated modalities are required for diagnosis. For example, MRI is essential to detect internal joint derangements and soft-tissue neoplasms. In other diseases, a combination of imaging may be necessary, for example, plain radiographs, nuclear medicine, and MRI may be necessary to diagnose osteomyelitis. In still other cases, diagnosis relies on clinical laboratory testing but imaging contributes in the evaluation of disease progression and status. These include rheumatological diseases, metabolic diseases, and some anemias. In still other situations, imaging may have characteristic findings but is being supplanted by genomic testing and identification of cellular abnormalities, for example, osteopetrosis. In the following pages, we will provide a description of currently used medical imaging techniques and their applications in diagnosis. This will be followed by a description of the imaging characteristics of various types of pathology where radiological imaging plays an important role in helping the pathologist reach their own diagnoses.

J.S. Khurana (ed.), *Bone Pathology*, DOI 10.1007/978-1-59745-347-9_9,

CT Scan

Modern CT scanners use a rotating gantry containing an X-ray tube and an array of detectors to gather image data (1, 2). The scanner's couch, oriented orthogonally to the gantry, contains a precise positioning system to allow positioning of the patient within the gantry. In modern scanners, the X-ray tube moves continuously in full circles around the gantry and the detectors capture the attenuated beam as the patient on the scaner's couch moves in a controlled fashion continuously through the gantry on the scanner's couch. This technique, known as helical scanning, has replaced the older form of scanning where slices are acquired one at a time in the majority of applications. The data from the helical acquisition is analyzed using fast Fourier transforms and creates a volume of raw data corresponding to the X-ray attenuation of the tissues at each point in the volume that has been scanned. This volume of attenuation data can then be formatted into images in any desired plane. Each image consists of matrices of picture elements, pixels. Each pixel is given a CT number corresponding to the attenuation of the tissue at the location in the volume and displayed on the image as a shade of "gray." The grayscale is designed so that the center of the scale corresponds to water, lower numbers (darker shades of gray) correspond to less dense substances such as fat and air, and higher numbers (lighter shades of gray) correspond to denser tissues including solid organs, bone, and ultimately metals. The operator can manipulate the range of the CT numbers (window width) and the center of the CT numbers (window level) to study specific types of tissue in detail.

The great advantage of helical CT scanners is their ability to acquire and manipulate large volumes of data in seconds. This ability permits these scanners to image volumes of interest multiple times with a single injection of intravenous contrast. As a result, CT scanners can image organs through several phases of enhancement (arterial, capillary, and venous) and create high-resolution angiograms, venograms, and urograms. In addition, the improved resolution of newer helical scanners permits submillimeter imaging. These two capabilities have increased the usefulness of CT to include multiple new tests, including noninvasive evaluation of the pulmonary, cardiac, cerebral, carotid, and visceral arterial trees.

CT is superior to MRI in evaluating the structural integrity of cortical bone. This property makes it useful for the preoperative planning of reduction of complicated fractures and in the evaluation of metastatic disease to bone. CT gives a more accurate portrayal of the amount of cortical bone destroyed by a lesion than MRI and hence the likelihood of a pathologic fracture. Furthermore, the advent of helical CT scanning has enabled scanners to handle high density/low density interfaces with substantially reduced beam hardening artifact. Thus, CT scanners can image fractures in multiple planes and can evaluate healing even in the presence of metal fixation devices. In some situations, CT is preferable to fluoroscopy to guide biopsy of bone lesions. For example, CT is the method of choice to localize biopsy, and treat the nidus of an osteoid osteoma using radiofrequency heat waves (Fig. 1a–d).

Magnetic Resonance Imaging

MRI has gained popularity by its ability to produce images with excellent contrast resolution in any imaging plane. It has become the primary imaging technique for disc disease, internal derangements of the joints, muscle, and tendon injuries as well as staging of bone and soft-tissue tumors (3–6).

The principles and physics behind MRI are complicated, but some familiarity with these is essential to use this modality optimally. Hydrogen atoms (like other atoms with an odd number of protons or neutrons) are dipoles and so exhibit a magnetic moment as they gyrate or spin in space. Normally, these small magnets are randomly oriented, but in the presence of a strong magnetic field they orient themselves parallel or antiparallel to the field – the lowest two possible energy states. Since the parallel orientation has a slightly lower energy state than the antiparallel orientation, slightly more of the hydrogen atoms align with the field. This creates a net magnetic moment along the axis of the magnetic field and hence along the bore of the magnet. Not only do the hydrogen atoms spin on their axes, but also like a slowing spinning top or the earth they gyrate around their axes, a phenomenon known as precession. (The frequency of precession is proportional to the strength of the external field.) Apart from any outside forces, the precession of the hydrogen atoms is randomly phased relative to one another and so the relative wobble summed over the large numbers of atoms present in tissues cancels itself out directionally. This means that the net magnetic moment measured in the scanner will be perfectly aligned with the magnetic field.

In general, the strength of the field is modified by a continuous gradient across a part of the body being imaged. Thus, the position of the signal emanating from the portion of the body being scanned is encoded by a slightly different and known frequency of precession. If a radiofrequency pulse or RF pulse (of frequency equal to the precession frequency) is applied to these nuclei, they deflect from their alignment with the external magnet. The strength of the pulse can be adjusted, to obtain any desired angle of deflection, but the basic MR spin-echo sequence uses 90° and 180° deflections. When the RF pulse is turned off, the nuclei return to equilibrium and as they do so emit signals in accordance with their chemical environments. Receiving coils capture the signals and, as with CT, convert the signal into clinically useful images using fast Fourier transforms. The term *resonance* refers to the synchronization of the radiofrequency pulse with the precession frequency in order to achieve the deflection.

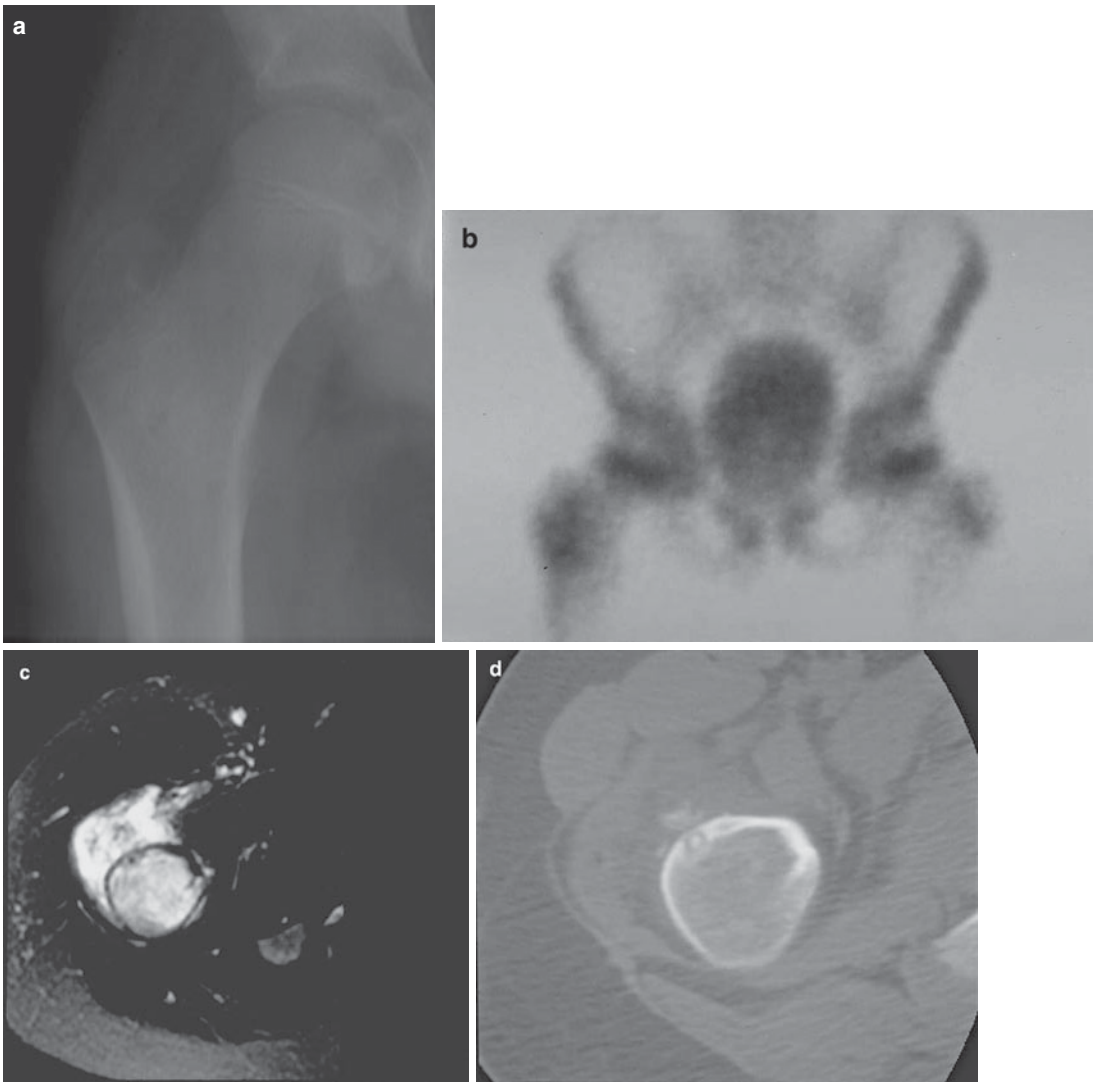

Fig. 1 a-Plain film, b-bone scan, c-T2 weighted MR image and d-CT scan of an osteoid osteoma. The lesion is poorly visualized on plain films. It can be better seen on the bone scan, MR picture and CT scan. The nidus is best seen on the CT scan.

In a standard spin-echo MR imaging sequence, two types of signals can be measured, known as T1 and T2 relaxation. The longitudinal (T1 or spin–lattice) relaxation time is a term given to the time taken for 63% of the deflected nuclei to return to equilibrium after being deflected. The transverse (T2 or spin–spin) relaxation time refers to the time that it takes for randomization of 63% of the ordered precession induced by the deflecting pulse. Once the RF pulse is turned off, the precession of the hydrogen nuclei immediately begins to return to random orientation. The randomizing precession of all the hydrogen atoms within the excited volume are "refocused" back into phase with one another using a 180° RF refocusing pulse so that at a specified time they will come back into coherence and their T2 signals will be maximized.

Both T1 and T2 are "tissue constant" and along with the numbers of free hydrogen nuclei and flow (or movement) of the tissue under study contribute to the amount of brightness the tissue exhibits on the images. Tissues with high water content have *long* T1 times and so appear dark on the T1-weighted sequences, and *long* T2 times and so appear bright on the T2-weighted sequences. Those tissues with *long* T1 and *short* T2 will be dark on T1- and dark on T2-weighted sequences. Examples of this type of tissue include tendons, bone, fibro-connective tissue, and fibrocartilage. Tissues with intermediate T1 and T2 relaxation times include hyaline cartilage and muscle. Fat is bright on T1 and medium signal intensity on T2-weighted sequences. By exploiting these properties, MRI provides high image contrast resolution and some idea of the composition of the tissues or lesions being studied.

The application of sophisticated surface coils has further enhanced MRI quality. Paramagnetic contrast agents that shorten T1 and T2 times (such as gadolinium or Gd-DTPA) are used to examine the vascularity of various tissues. These gener-

ally enhance contrast on T1-weighted sequences. The agents are customized pharmaceutical chelates of a relaxation shortening heavy metal to a carrier molecule. They have been designed to imitate biologically the iodine contrast agents used in CT and so they preferentially localize in vascular areas. Gadolinium contrast agents can help to differentiate necrosis from viable tumor and epidural scarring from recurrent disc herniation.

Contraindications and cautions for MR examination include embedded ferromagnetic substances such as shrapnel in the eye, certain aneurysm clips in the brain, cardiac pacemakers, cochlear implants, and other biomedical devices. Recently, nephrogenic systemic sclerosis had been reported in patients with renal failure who have received gadolinium, particularly if administered in high doses. Because of this, all patients with renal disease receiving gadolinium must have their glomerular filtration rates calculated to determine if it is safe to administer contrast. MR should also be avoided in the first trimester of pregnancy, but it has not been shown to have any teratogenic effects, even then.

MRI has become essential to the practice of musculoskeletal radiology. Its contrast resolution has made it the test of choice for evaluation of the vast majority of joint derangements (Fig. 2a, b). As scanners have improved, so too has the detail with which internal joint abnormalities can be visualized and diagnosed. The addition of MR arthrography with a gadolinium contrast agent instilled into the joint space has further enhanced the detection of small soft-tissue abnormalities within joints.

Today MR plays an increasing role in the evaluation and monitoring of inflammatory arthridities (Fig. 3a–d). The advent of TNF-a antagonists as a therapy for inflammatory autoimmune disease has given rheumatologists an opportunity to prevent joint damage in these diseases. This ability has brought MRI into focus as a sensitive means of evaluating the structure of these patients' joints and assessing the progression of disease.

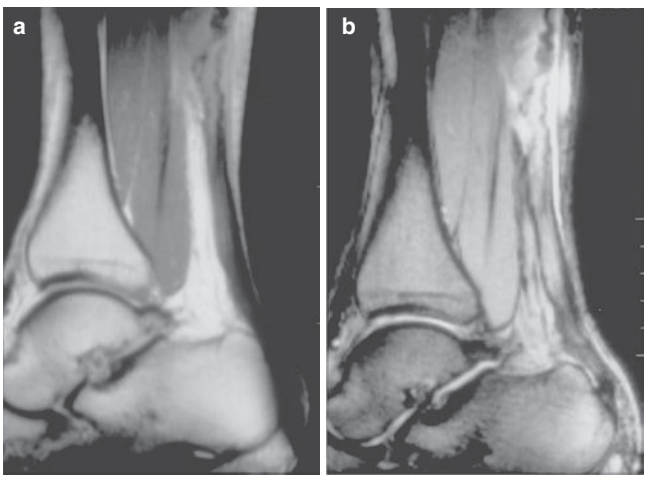

Fig. 2 T1 (**a**) and T2 (**b**)-weighted images demonstrate a tear of the tendo-Achilles. Edema around the zone of injury is particularly well seen on the T2-weighted image

MRI has been shown to be more sensitive and to become positive earlier than nuclear medicine bone scans in the evaluation of occult fractures, particularly in the elderly (7). Similarly, MR is superior to plain radiographs, CT and bone scans in the early detection of AVN (Fig. 4). Differentiation of AVN from infection (in situations predisposing to both, such as in sickle cell disease) can sometimes still be difficult.

MRI also has become a mainstay in evaluating spine pathology. Its ability to image the disks, marrow, spinal ligaments, and the contents of the spinal canal simultaneously have made it the test of choice for evaluation of disk disease, diskitis, and neural canal encroachment from other processes including tumor, hematoma, and abscess. Congenital cord abnormalities can be detected, and this combined with the ease of imaging the entire spine allows the MR to be used as a preoperative screen prior to scoliosis surgery.

MRI has proven to be slightly more sensitive than nuclear medicine bone scans for the diagnosis of osteomyelitis and far more sensitive and specific in the identification of soft-tissue infections and abscesses (8, 9). In the appropriate clinical setting, the essential feature used to diagnose osteomyelitis on any imaging study is evidence of cortical destruction. Since normal bone cortex has no free protons, it normally has no signal on MR imaging. Only a relatively small number of free protons need to invade cortical bone before MRI will not only show some signal but the bone will appear to be completely absent (Fig. 5a–c). Thus, MRI is very sensitive for the detection of early acute osteomyelitis and distinguishing it from soft-tissue infection. On the other hand, this very sensitivity to cortical invasion makes MRI a poor examination to evaluate a tumor-involved bone for impending pathologic fracture. Here CT remains the better test.

MRI has taken a preeminent role in the diagnosis and staging of soft-tissue tumors and in the staging of primary bone tumors. Compared with CT, it has superior ability to define the extent of tumor progression through normal tissues as well as involvement of adjacent vital structures, for example, joint spaces, blood vessels, and musculature that may be required to be saved in order to perform limb salvage surgery (10).

Magnetic resonance signal intensity has been extensively evaluated as a predictor of tumor response. Viable tumor is generally bright on T2-weighted images, but treated tissue may also be bright. In general, MRI signal properties alone, do not allow distinction between viable tumor, tumor necrosis, and edema (11). Decreases in signal on T2 may be seen after effective treatment. Uniform dark signal on T2-weighted images appears to accurately predict complete response, but is uncommonly encountered. Even after administration of intravenous gadolinium, MRI may not distinguish tumor from adjacent reactive tissues (12). Evaluation of static images on gadolinium-enhanced MRI consistently underestimates necrosis.

Because of the nonspecificity of signal intensity changes, the rate of contrast uptake by different tissues also has been

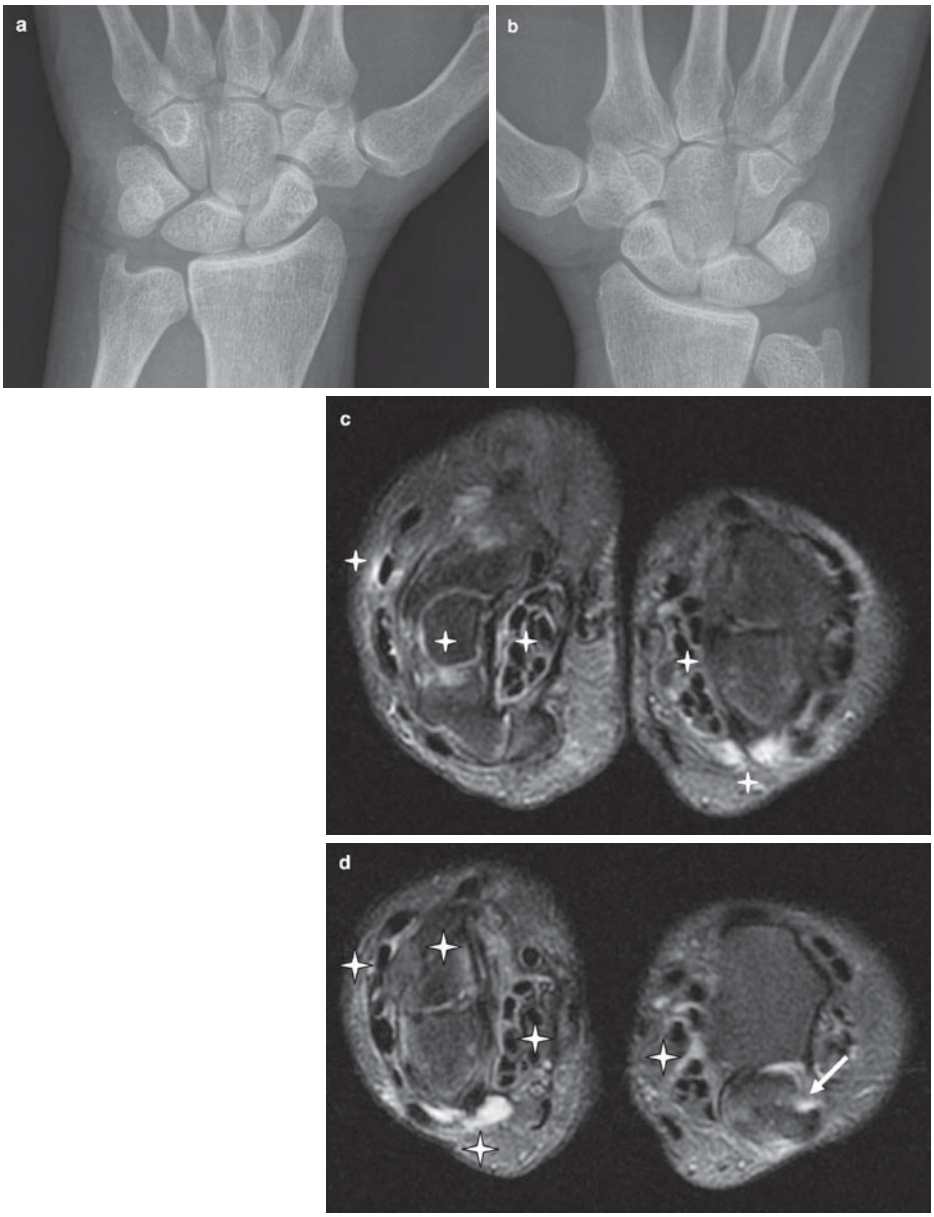

Fig. 3 Plain anteroposterior (AP) radiographs of the left (**a**) and right wrists (**b**) show no visible evidence of abnormality. Axial T2-weighted images through the carpi (**c**) and (**d**) shows evidence of tenosynovitis in multiple compartments and tendon sheaths (*) as well as an early erosion of the left ulnar styloid (*arrow*)

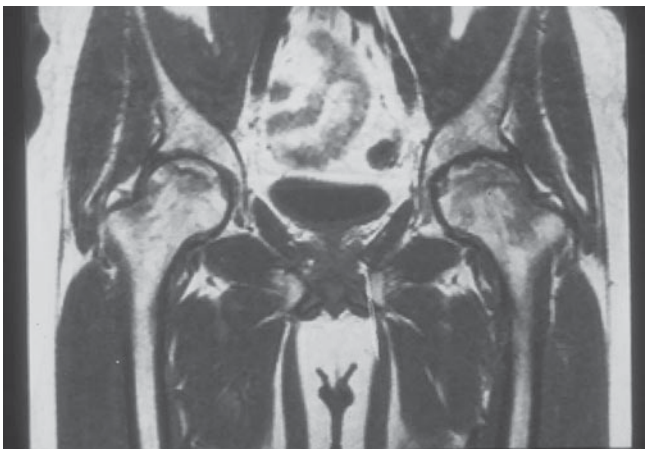

Fig. 4 An MR picture shows avascular necrosis of the hip

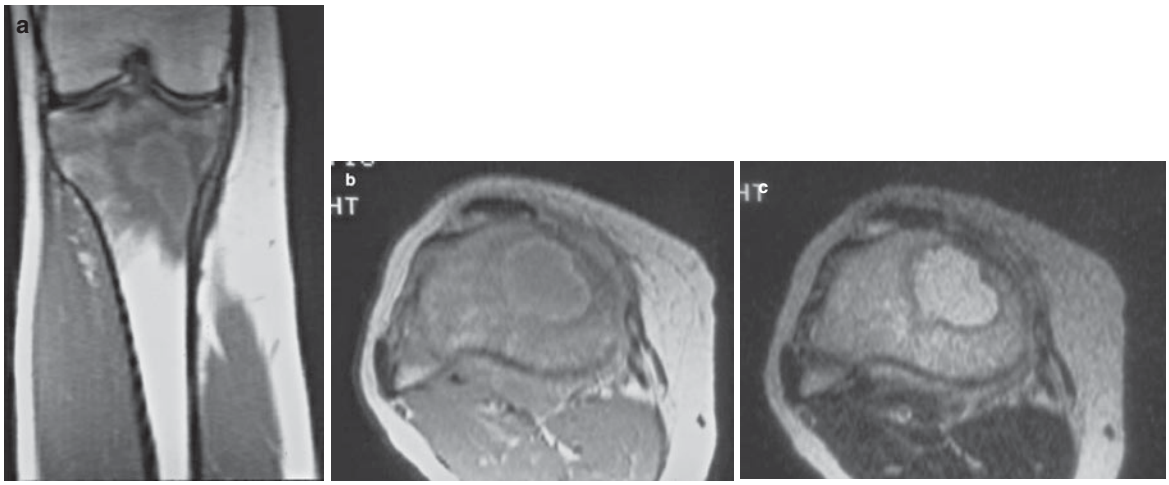

Fig. 5 T1 (**a**) and T2 (**b** and **c**) are utilized to demonstrate a Brodie's abscess in the upper tibia. Although the scanning characteristics are nonspecific, the delineation of the extent of the lesion helps in preoperative planning

investigated. The rationale for this is supported by earlier work that demonstrated that effective chemotherapy of osteosarcoma was accompanied by decreasing vascularity as seen on angiograms (13). Rapid uptake, presumably indicating large vessel blood flow, appears to be primarily a feature of malignant tumors, although some aggressive benign lesions may be similar. Edema can be distinguished from tumor because it takes up gadolinium at a slower rate (14). Preliminary investigations suggest that this methodology holds promise for detection of therapeutic effect, but has not proven reliable enough to be used clinically.

Angiography

A lesion's vascularity may provide important clues to diagnosis and give landmarks for surgical planning (15). Arteriography is, however, no longer the most convenient method to perform this assessment. Instead, CT and MR angiograms have supplanted angiography in this role. Angiography may still be used, however, to identify feeder vessels for surgical planning of resectable bone and soft-tissue lesions or for presurgical tumor embolization (16).

Conventional Tomograms

Conventional tomography has all but disappeared from the practice of modern medicine since the introduction of CT scanning. In particular, the ability of helical scanners to significantly reduce or eliminate beam-hardening artifacts in and around metal fixation devices has put the final nail in the conventional tomography's coffin.

Radionuclide Imaging

The value of radioisotope imaging lies in its ability to scan the entire skeleton and its extreme sensitivity for detection of neoplastic, traumatic, or inflammatory lesions of the bone. The tests most commonly employed in the evaluation of bone today include technetium methylene diphosphonate (MDP) bone scans and indium leukocyte-labeled scans.

To accomplish these scans, a bone-avid radiopharmaceutical, either ^{99m}Tc-MDP or ^{111}In-labeled white cells, is given to the patient intravenously. The patient then lies beneath a γ-camera that captures the photon emissions of the radioactive tracer and forms an image of the activity in the region of the image. The images reflect a function rather than a morphologic entity.

γ-Cameras may take multiple images (of ~40 cm) or be used in conjunction with a moving table to image the entire skeleton. The aperture of the camera's calumniator holes governs the image resolution. The standard cameras can resolve about 2-cm lesions (but high-resolution cameras can resolve down to 1 cm). Tomogram techniques have been applied to radionuclide imaging in the form of SPECT (single energy photon emission computed tomography) that allows the elimination of superimposed images from overlying structures and improves localization of pathology.

Other methods of enhancing the diagnostic yield of bone scans include "three-phase" studies. This gives a "radionuclide angiogram" and blood pool images in addition to the delayed static images obtained with a single-phase scan. The use of gallium scans (^{67}Ga) and indium-labeled white cells (^{111}In), employed in conjunction with standard scans, can detect bone and soft-tissue infections. Leukocytes can be directly labeled by ^{111}In by liphophilic chelating agents and are used in a similar fashion.

The technetium bone scan is the standard of practice for detection of skeletal metastatic disease, and is generally described as sensitive, but not specific for this purpose. Diseases that cause increased bone turnover or increased blood flow (such as osteoarthritis, inflammatory arthritis, Paget's disease, fibrous dysplasia, Ollier's disease) are potential pitfalls in the search for metastatic disease with bone scans. As a result, correlative radiographs are obtained when a new focus of abnormality is identified on a bone scan. Because of the sensitivity of the isotope scan, when radiographs fail to provide an explanation for increased uptake (tumor, osteoarthritis, old fracture, etc.), it is assumed that the isotope scan has detected a metastasis in the preradiographic stage. Some reports have suggested that the MRI scans may have equal or even greater sensitivity.

Bone metastases are occasionally detected on MRI before they are visible on bone scan, CT, or plain films (17, 18). For practical reasons of time and cost, with one exception, MRI is not generally used to screen the entire body for metastatic disease. Radionuclide scans are relatively poor at detecting osseous involvement with multiple myeloma. As a result, MRI is assuming a larger role in the screening of this disease, particularly the axial skeleton (19).

"Superscans" represent another potential pitfall in interpreting bone scans. Here, widespread metastases take up so much radiotracer that individual lesions coalesce and the skeleton appears uniformly abnormal. Superscans caused by severe osseous metastases must be differentiated from other underlying diseases, especially metabolic bone disease such as hyperparathyroidism, renal osteodystrophy, and hypervitaminosis D.

A recent addition to the nuclear medicine armamentarium, positron emission tomography (PET) using flourodeoxyglucose (FDG) has also shown early promise. FDG is a glucose analog that is transported into cells, enters the metabolic cycle-like glucose, and is phosphorylated by hexokinase. FDG-6-phosphate cannot be stored as glycogen and cannot undergo glycolysis. If under aerobic conditions, the FDG is dephosphorylated by glucose-6-phosphatase, it then can be transported out of the cell. Thus, FDG accumulation in cells is related to uptake, rate of glycolysis, and the relative proportions of the enzymes hexokinase and glucose-6-phosphatase. Anaerobic glycolysis predominates in tumor tissues. Therefore, many types of malignant tumors, including mesenchymal soft-tissue sarcomas, show abnormal uptake of FDG. There is a high correlation between the amount of uptake and tumor grade. Demonstration of response to chemotherapy and radiotherapy by PET imaging with FDG has been demonstrated for both primary and metastatic tumors.

Bone Densitometry

Senile osteoporosis is a significant cause of morbidity in the older population, particularly in postmenopausal Caucasian women. As a result, there has been extensive interest over the years in diagnosing this disease and even more importantly in identifying those patients at risk for fracture. To this end, a number of different radiological tests have been developed to evaluate bone mass in living patients. The majority of these tests have the drawback that they measure only bone per unit volume or per unit area and do not account for the microarchitecture of the trabeculae. As a result, the correlation between their actual measurements and the fracture prediction is somewhat imprecise.

Regardless, there are a number of other features that have led clinicians to choose one test over another. These include the accuracy and precision of the test, the radiation dose, and the cost. Accuracy reflects the veracity of the measurement in terms of identifying the actual amount of bone present. Precision reflects the repeatability of the test. These concepts are akin to repeatedly shooting an arrow at a target. The archer can be accurate in that he hits very close to the bull's eye with his arrow but imprecise in that his arrow does not always hit exactly the same location as the one before. On the other hand, the archer may be precise in that his arrow always strikes in the same place but inaccurate in that the arrows are always far from the bull's eye.

Today, based on the criteria of high repeatability (precision), low cost, and low radiation, dual energy X-ray absorptiometry (DEXA) has gained hegemony over other clinical examinations. This test is fast, gives the patient less radiation than a chest radiograph, and costs relatively little. The concept behind this technique is that bone and soft tissue attenuate an X-ray beam differently at different energies. If highly hardened X-ray beams that have narrow energy spectra are shot through a patient, the amount of energy transmitted will depend on the energy of the source beam and the relative amount of bone and soft tissue through which the bone has passed. By using two different energy X-ray beams, one creates two simultaneous equations in two variables – the amount of bone and of soft tissue. These can then be solved deterministically and the amount of bone mineral calculated. Since this technique uses transmission of a beam, it gives results in terms of bone per unit area.

DEXA results are usually given as one of two scores based on normal control data. The first score is the *Z*-score. This gives the results of the test in terms of standard deviations (SD) above or below age- and gender-matched normal controls. The second is the *T*-score which gives results in terms of SD above or below gender-matched controls at peak bone mass (25 years of age). The World Health Organization has adopted standards for reporting the results of this test for women. According to their criteria, patients are normal if their bone mass *T*-score is less than 1 SD below peak bone mass for gender-matched controls. They are osteopenic if their bone mass is between 1 and 2.5 SD below and osteoporotic if their bone mass is more than 2.5 SD below peak

Table 1 Percentage of US Caucasian women in WHO categories

	Age 25 (%)	Age 50 (%)	Age 65 (%)	Age 80 (%)
Normal	84	66	40	10
Osteopenia	15	33	40	35
Osteoporosis	1	1	13	27
Established osteoporosis	1	1	7	27

bone mass for gender-matched controls. If the patient has had a fracture related to decreased bone mass, they are diagnosed with established osteoporosis. The relative percentage of Caucasian women at different age groups that fall into each diagnostic category is given in Table 1.

CT also has been used to measure bone mineral density. Two different methods have been devised: single energy and dual energy quantitative CT (QCT). The former uses software to mark regions of interest within the vertebral marrow, and then compares the density of these regions with the density of several regions of *known* calcium content within a phantom placed below the patient. This method allows quantization of the amount of bone in the vertebral trabecular space. QCT is highly accurate and offers the advantage of incorporating only trabecular bone, metabolically more active than cortical bone, and also not including osteophytes or calcification in vessels in the measurement. DEXA includes all calcium in the path of its beam. On the other hand, QCT is expensive and comparatively high in radiation dose.

Dual energy QCT is identical to single energy technique except that it uses two different hardened energy level X-ray beams, similar to DEXA. As with DEXA, dual energy QCT allows the generation of different curves of attenuation for the various tissues within the marrow (bone and soft tissue). These curves can be analyzed to separate out the soft tissue's effect on the measurement and so provide greater accuracy in quantitating bone. The gain in accuracy is, however, offset to some extent by a loss in reproducibility (precision), making it a better technique for diagnosis, but less useful for follow-up studies.

Ultrasound has also been used to measure bone mineral density by calculating the relative fraction of reflected sound wave from the bone. Generally, this technique is applied to bone in accessible regions such as the patella or the calcaneus. Since bone loss varies according to body site, measurement in these locations may not have the needed clinical relevance that measurement of the spine or hip has. This technique has had limited clinical application and is primarily a research tool.

Finally, some interest has arisen in using MRI as a tool to measure bone mass. Two methods have been developed: one using high-field MRI to measure trabecular bone in a very small three-dimensional sample of bone, and the other method uses the fact that closely placed structures of different magnetic susceptibility alter the magnetic field in the local environment. This susceptibility effect is greater with greater amounts of trabeculae within the marrow space and less with fewer trabeculae. The interest in this technique arises from the fact that the measurement is anisotropic and correlates with the orientation of the trabeculae (20). This means that measurements from this method may provide information relating not only to the amount of bone but also to the underlying architecture of the trabecular bone. Currently, MRI remains an investigational technique, however.

Bone Pathology

Focal Osseous Lesions

Detection of focal osseous lesions is usually not a challenge, as most are readily apparent on routine radiographs. In addition most display features that, when properly analyzed, allow classification of the lesions and at times specific pathologic diagnosis (Table 2).

Features that may be helpful in diagnosis include the bone involved, the portion of the bone involved, the lesion's appearance within the bone (lytic vs. sclerotic; geographic, moth-eaten, or permeative; type of matrix), the lesion's margin with surrounding healthy bone, and its effects on the adjacent soft tissues (including periosteal reaction). These parameters, along with the clinical context (age, sex, symptoms, and preexisting conditions) in which the patient presents can provide specific diagnostic information.

The importance of using bone radiographs in conjunction with biopsy material cannot be overemphasized in forming a pathologic diagnosis of a focal osseous lesion. Biopsy material is often small, and reflects only a sample of the lesion. Radiographs give the gross anatomy of the entire lesion. This is often a safer guide to the growth rate of the lesion even if not completely diagnostic. Several authors consider it malpractice to give a histological opinion on tissue samples in the absence of radiographs. While this may be an extreme view, and not applicable in all cases, there is a certain truth in this hyperbolic belief.

Table 2 Diagnostic approach to radiographs of focal osseous lesions

For the musculoskeletal pathologist, the diagnostic approach to a bone lesion usually follows four steps:

1. Identify the segment of bone involved (epiphysis, metaphysic, or diaphysis).
2. Locate the area of primary involvement: medulla, cortex, periosteum, or soft tissue.
3. Identify whether one or several bones, and whether appendicular or axial skeleton.
4. Characterize the type and margin of each individual lesion. Note any matrix within the lesion. Identify the reaction of the native bone to the lesion.

Lesion Location

The location of the lesion within the skeleton and within the bone (epiphysis, metaphysis, or diaphysis) and part of the bone (medullary cavity, cortex, juxtacortical bone, or periosteum) has a major impact on differential diagnosis. Most primary neoplasms are found in the metaphysis. A few are predisposed to the diaphysis (Ewing's tumor and other small round cell lesions) or the metadiaphysis (nonossifying fibroma). Others are characteristically epiphyseal (chondroblastoma, clear cell chondrosarcoma, giant cell tumors). Some lesions have no anatomical predilection (osteoid osteoma and Langerhan's cell histiocytosis). Some typical locations are given in Table 3.

Basic Radiographic Osseous Anatomy

Bone is composed of cortical and cancellous components. Cancellous bone is found within the medullary cavity of the bone or between the tables of the skull. It is metabolically more active than cortical bone, and considerable remodeling occurs in response to changes in patients' metabolic and structural needs. The trabecular pattern seen on radiographs reflects this remodeling and therefore can be used to assess the underlying stimulus. For example, the trabecular pattern in the femoral neck can be used to follow osteoporotic individuals (Singh's index). Sclerotic margins develop around bone lesions as a result of the Wolff's law. Similarly, subchondral plates thicken in osteoarthritis, reflecting the altered biomechanics of the joint.

Cortical bone is maximal in the diaphysis and is responsible for the majority of the weight bearing. The units of cortical bone are vascular-lined bone segments or "osteons." Remodeling of cortical bone involves osteoclastic resorbtion in the form of "cutting cones" which is then followed by osteon formation. Imbalance in this coupled process, if in favor of resorbtion, gives rise to a tunneled cortex. This is seen radiographically as a "permeated osteolytic" pattern within the cortex itself.

Table 3 Common anatomic locations of focal bone lesions

Epiphyseal lesions	Metaphyseal lesions	Diaphyseal lesions
Chondroblastoma	Chondromyxoid fibroma	Adamantinoma
Giant cell tumor	Chondrosarcoma	Campanacci's disease or osteofibrous dysplasia
Clear cell chondrosarcoma	Fibrosarcoma	
(Langerhan's cell histiocytosis)	osteomielitis	Ewing's tumor
	Osteochondroma	Osteoid osteoma
	Osteosarcoma	Osteoblastoma
	Malignant fibrous histiocytoma	(Metastatic disease)
	Nonossifying fibroma or metaphyseal cortical defect	(Lymphoma/myeloma)
	(Metastatic disease)	(Langerhan's cell histiocytosis)
	(Lymphoma/myeloma)	(Paget's disease)
	(Langerhan's cell histiocytosis)	(Unicameral bone cyst)
	(Paget's disease)	(Hemangioma)
	(Unicameral bone cyst)	(Fibrous dysplasia)
	(Hemangioma)	(Enchondroma)
	(Enchondroma)	
	(Fibrous dysplasia)	

Note: Although no entity is entirely specific to a particular location, those in parenthesis have a greater tendency to be varied in their location.

Lesion Margin

Of the radiographic features that characterize a lesion, its margin provides perhaps the most information. The response of normal bone to any pathologic process is to attempt a return to homeostasis. This means that a bone will attempt to repair itself or at least limit the underlying process. Blastic or lytic processes (such as tumors) *do not affect the bone directly*, but act via the native osteoblasts and osteoclasts within the bone. The signaling mechanisms and the cytokines involved in this process are now beginning to be understood (see Section *Bone Biology*). The balance between the activation of osteoblasts and osteoclasts at the edge of the lesion determine the appearance of the "margin" of the lesion. In essence, the radiographic appearance of a lesion will be the result of competition between the activity of the underlying pathologic process and the bone's attempt to contain that process. Thus, a slow growing lesion will show relatively sharp and well-defined edges while an aggressive lesion will show ill-defined margins. By implication, the "pathologic" margin (or true tumor extent) may extend well beyond the "radiologic margin," especially in certain aggressive neoplasms that cause a permeated or moth-eaten radiographic pattern. In these cases, the actual tumor may extend well beyond the radiographically visible tumor (21).

It is this concept that led Lodwick to suggest that a lesion's rate of growth may be predicted by the pattern of bone destruction at the margin between the lesion and its containing bone (22, 23). Slowly enlarging lesions destroy all the bone in the space that they occupy, producing a "geographic" pattern of bone destruction. Such margins have been termed Type I by Lodwick. Static lesions may become encased by a solid sclerotic boundary as the normal bone responds to the lesion. Lodwick denoted this type of margin as IA (Fig. 6) while those with sharp margins but no surrounding sclerosis

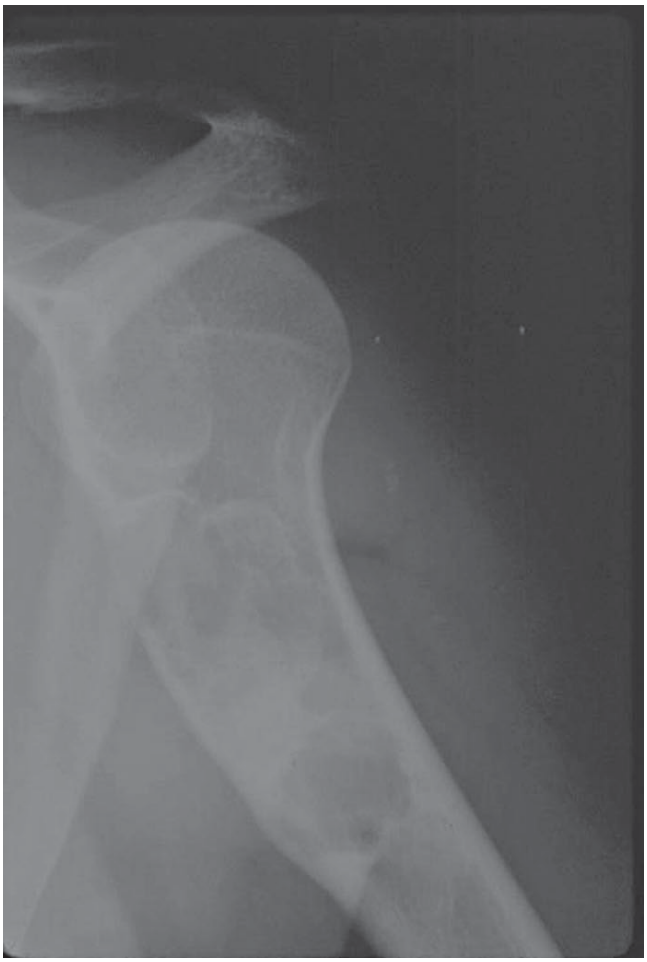

Fig. 6 Nonossifying fibroma. Mixed lytic and sclerotic lesion in the proximal humerus showing a sclerotic margin

are designated as IB. Faster rates of growth result in a "moth-eaten" radiographic pattern, which results from moderately rapid lesion expansion through normal bone giving rise to multiple lucent areas of bone destruction with intervening residual bone (Fig. 7a, b). Margins of this type are termed Lodwick II. The fastest growing lesions "permeate" through existing Haversian systems, resulting in a vague boundary between the normal and abnormal bone (Fig. 8). These are called Lodwick III type margins.

Lesions that typically exhibit IA margins (geographic with sclerotic rim) include simple bone cyst, nonossifying fibroma, chondroblastoma, chondromyxoid fibroma, Brodie's abscess, and fibrous dysplasia. Faster growing lesions such as giant cell tumors are often seen with Type IB margins (geographic with a bare margin). With focal infiltration of the cortical bone, the margins change to IC, such as is seen with some giant cell tumors or some of the relatively slower growing malignant bone tumors. Malignant tumors and rapidly destructive infective lesions, in general tend to have more aggressive margins – Type II or III. A special caveat is that extremely rapid growth may be represented by an "invisible margin." Combinations of patterns around a single lesion are frequent, in which case the clinical implications of the lesion must be taken from its most aggressive appearing margins. Attention to the kinds of margins is extremely useful in assessing bone lesions.

When the underlying bone is osteoporotic, lesion margins may be difficult to appreciate. Furthermore, metabolic bone diseases and posttraumatic osteoporosis may cause aggressive margins and so mimic rapidly growing tumors (24).

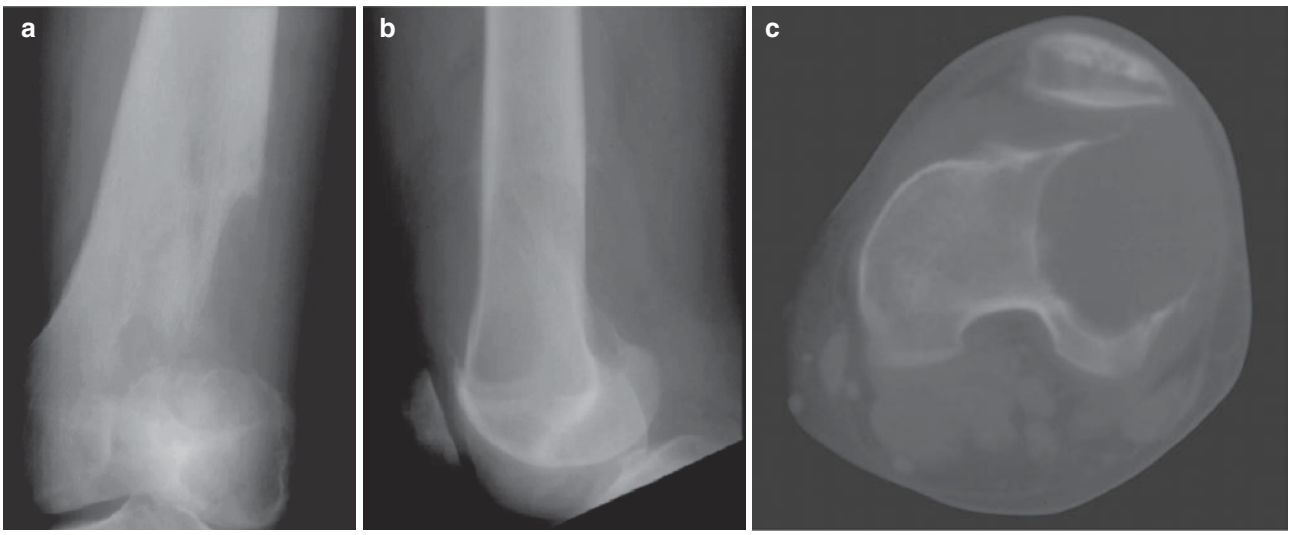

Fig. 7 Geographic pattern of bone destruction. Giant cell tumor, distal femur. **a** Anteroposterior and **b** lateral views of the distal femur show a lytic lesion in the distal femoral metaphysis, which extends to the subarticular bone. **c** Axial CT scan through the distal femoral metaphysis shows an expanded lesion with a thin rim of periosteal shell around the lesion

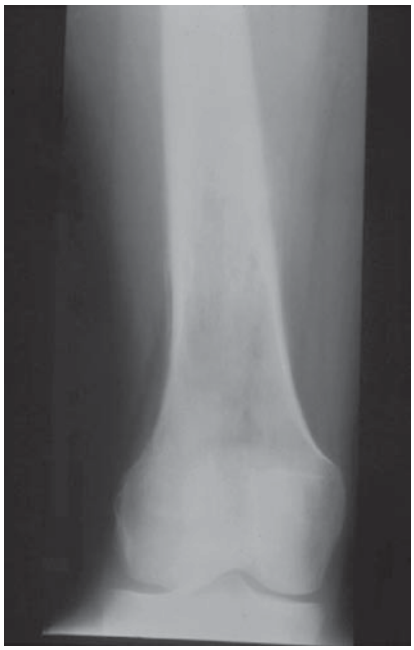

Fig. 8 Aggressive, permeating lesion distal femoral diaphysis. Ewing's sarcoma. A vague area of lysis with linear, aggressive periosteal reaction both medially and laterally is noted

Cortical Destruction

Just as a lesion's margins provide information about the underlying pathological process, so too its pattern of extension through the bone's cortex may provide useful information about the lesion. The highest grade lesions penetrate through the cortical and periosteal bone, leaving an intact or relatively intact-appearing cortex behind. Intermediate grade lesions produce focal cortical defects with an eccentrically located soft-tissue mass (21). Lower grade lesions appear to "expand" the cortex from within as the bone remodels around them. The lowest grade lesions leave the cortex unchanged. Here too, mixtures of patterns are extremely common (Fig. 9a–c) and a lesion's true nature should be estimated from its highest grade of cortical destruction.

In addition, certain lesions cause specific types of cortical destruction that mirrors the pattern of growth of their particular cell type. For example, well and moderately differentiated chondrous lesions tend to grow with a characteristic gross, lobulated mulberry-like pattern. As a result, the endosteal surface of the cortex adjacent to the lesion often displays a scalloped appearance.

Bone Reaction

Bone reaction or proliferation may be medullary or periosteal. Medullary reaction may be in the form of a thin or thick reactive shell around the lesion, indicating slow growth. More aggressive processes may show areas of mottled sclerosis scattered in the adjacent cancellous bone. The most aggressive processes show no medullary reaction as the tumor's growth out-competes any attempt of the native bone to repair itself.

Similarly, as a lesion broaches a bone's cortex, the bone will attempt repair. The appearance of the periosteal new bone formed in response to the lesion will again be the result of the antagonism between the rapidity and type of the lesion's growth and the bone formed in response. Slow growing lesions result in an amorphous (thick) or closely lami-

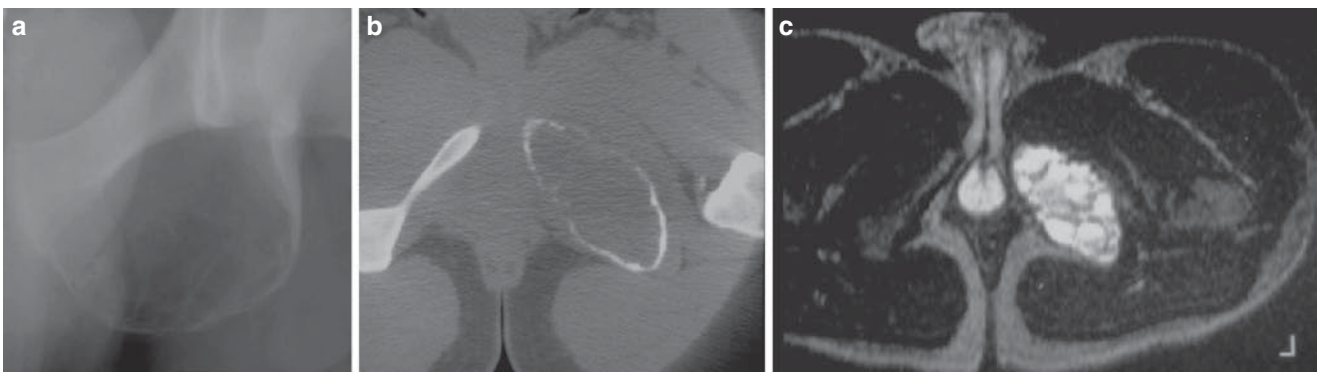

Fig. 9 Aneurysmal bone cyst of the left inferior pubic ramus. **a** Plain film shows an expanded, destructive lesion. **b** Axial CT image through the lesion demonstrates the expansion of the bony margins with a thin rim of bone around the lesion. **c** Axial T2-weighted image shows multiple fluid-fluid levels

nated (layered) periosteal response. Aggressive processes will produce a widely laminated (onion skinned) or spiculated (sunburst) response (Fig. 10a, b). A focal process that alters its growth pattern and breaks through the containing periosteal reaction will leave a characteristic residual of periosteal new bone at its margins known as a Codman's triangle (Fig. 10c). On the other hand, a lesion that has expanded beyond the normal cortex may have a thin layer of periosteal bone replacing the destroyed, old cortex. This is indicative of a relatively slow or well-contained process.

Matrix

Most bone lesions produce no matrix. When lesions do show internal matrix formation, it may arise through several pathophysiological mechanisms. Mineralization may be physiologic (upon cartilage or osseous backgrounds), dystrophic (degenerating fibrous, myxoid tissue, or fat), or metastatic (upon connective tissues altered by a metabolic disease). Osseous matrix may also be formed as a metaplastic process as in fibrous dysplasia (Fig. 11). Another form of osseous matrix formation is the ischemic bone formation of the bone infarcts or ossifying lipoma.

Analysis of internal mineralization or matrix may help to characterize the composition of the lesion. Calcifications may take the form of a diffuse, hazy, "ground-glass" appearance reflecting uniform microscopic deposits of calcium or bone in the lesion. Ossified matrix may be seen as lumps or clouds of densities with fuzzy or sharp margins (Fig. 12a, b). Cartilaginous matrix may show amorphous or the so-called dot- and ring-like calcification. The rings, broken rings, or arcs represent mineralization along the mulberry lobules of cartilage (Fig. 13). Cartilage matrix does not always mineralize; in general however, the more mineral is present, the more mature and well differentiated is the lesion. This rule applies to osteoid-forming lesions as well.

Lesion Size and Shape

The size of a lesion is both a diagnostic and prognostic feature. It has been shown that disease-free survival is much better for lesions less than 100 cm^3 in volume (25). Shape is a subtle clue to interpret. Some lesions tend to be spherical (giant cell tumor, osteosarcoma), whereas others tend to conform in shape to the bone in which they arise (chondrosarcoma), or be shaped by a periosteal envelope (Ewing's sarcoma).

Although many lesions affect a broad age range, knowledge of the age and sex of the patient is helpful in narrowing down the differential (Table 4).

Soft-Tissue Lesions

Unlike the case with focal bone lesions, the anatomy and biologic behavior of soft-tissue lesions generally cannot be assessed from radiographs (16). Indeed, specific diagnosis remains impossible for many soft-tissue lesions regardless of the choice of imaging. MRI, however, is playing an ever-

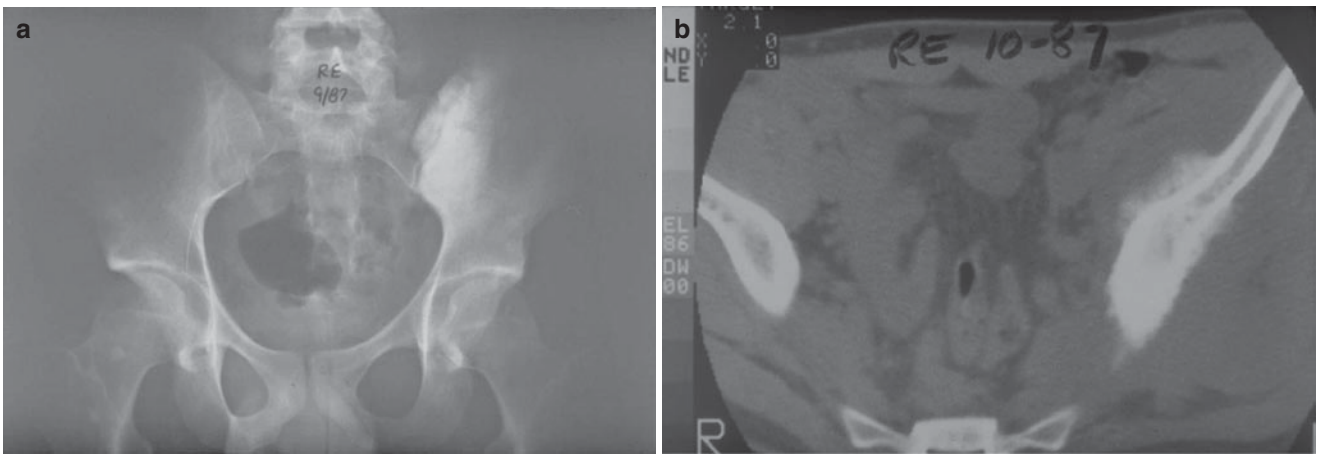

Fig 10 Ewing's sarcoma left ilium. **a** Plain radiograph shows a sclerotic lesion in the left ilium. **b** Axial CT image through the ilium shows a dense, sclerotic lesion with speculated and sunburst periosteal reaction anteriorly and posteriorly suggesting an aggressive growth pattern

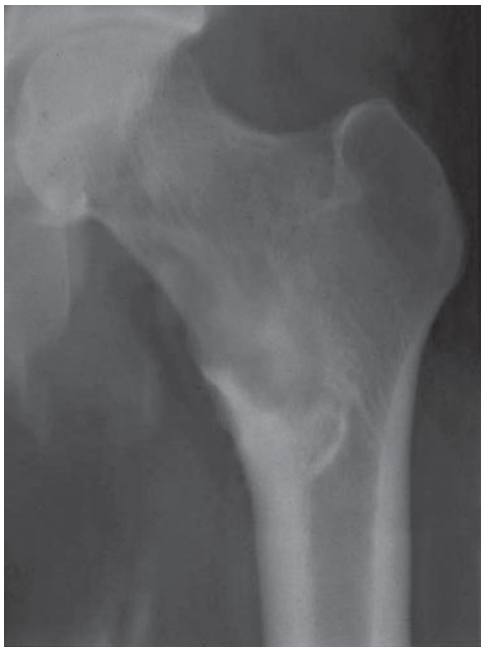

Fig. 11 Osteoid matrix in fibrous dysplasia

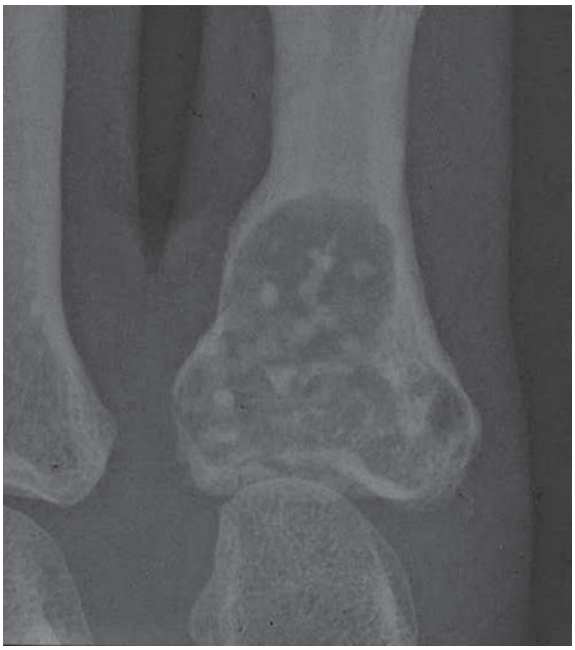

Fig. 13 Rings and arcs of cartilaginous mineralization

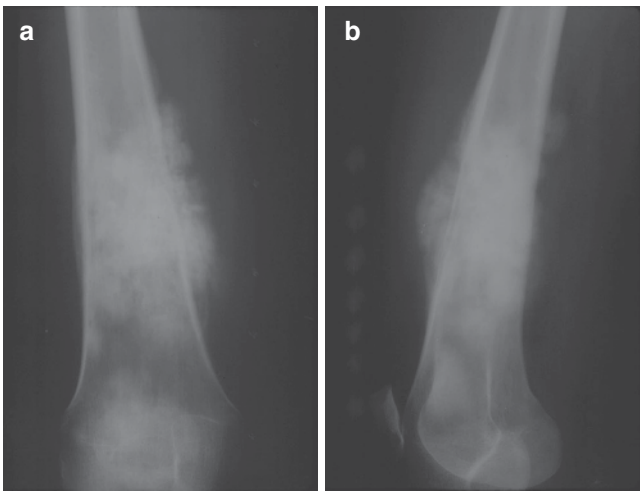

Fig. 12 **a** and **b** Osteoid matrix in osteosarcoma of the distal femur. Anteroposterior and lateral views of the distal femur shows an amorphous, cloud-like matrix in this bone-forming tumor. Also note the periosteal reaction and extension of the tumor into the adjacent soft tissues

Table 4 Imaging and needle biopsies

Image-guided percutaneous needle biopsy plays an increasingly important role in focal lesion diagnosis. Progress in imaging, particularly CT scanning, has made almost any part of the body accessible for needle biopsies. A number of recent review articles have addressed the issue of needle biopsy. In general, biopsy of metastatic disease is highly accurate, yielding an accuracy of 80–95%. Biopsy of primary sarcoma is somewhat less successful, although still frequently useful. It should be undertaken only with consultation among the radiologist, surgeon, and pathologist. Although recent progress in MRI technology has allowed the creation of magnets with more open architecture, MRI is not commonly used to guide needle biopsy because of imaging time and the influence of the magnetic field on the metallic needle. Interpreting needles biopsy material requires experience and expertise (see Section *Bone Tumors*).

increasing role in the assessment of soft-tissue masses. Specific diagnosis is possible for a number of soft-tissue lesions based upon their composition. Such lesions include fatty tumors (Fig. 14a, b), benign vascular tumors (Figs. 15 and 16a, b), pigmented villonodular synovitis (PVNS) (Fig. 17a, b), fibromatosis, hematomas (Fig. 18a, b), and ganglion (Fig. 19a–c).

In some cases, MRI permits an exact diagnosis, for example, lipoma. In others, it can suggest the diagnosis or narrow it down to a small differential. In general, benign lesions are small, have well-defined margins, and a homogenous internal composition (16). Regardless, biopsy remains the mainstay of diagnosis for soft-tissue mass lesions.

Cysts and Fluid

Soft-tissue cysts can be recognized on ultrasound by their characteristic anechoic center and through transmission of the ultrasound beam. On MRI, cysts, regardless of their location, have characteristic features of low signal intensity on T1-weighted images and uniformly bright signal on T2-weighted images. Even so, many solid neoplasms, both benign and malignant, may have cystic components, while many cysts, including aneurysmal bone cysts and Baker's cysts, have internal noncystic components. The relative amount of fluid and soft tissue must be considered

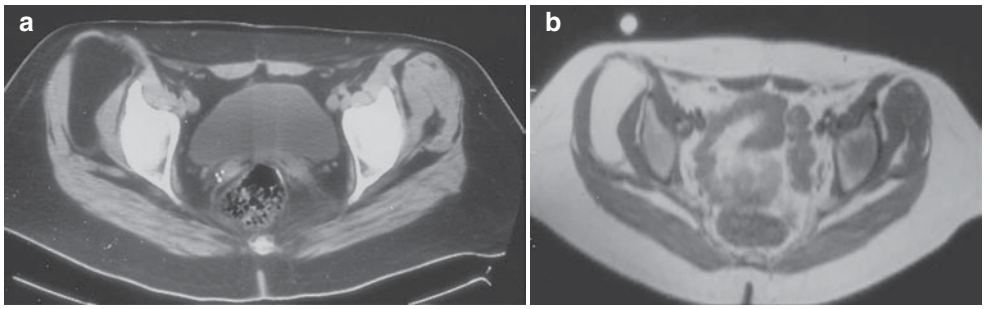

Fig. 14 Lipoma in the anterolateral pelvis. **a** An axial CT image of a lipoma showing a low density mass (black on CT). **b** T1-weighted image showing the lesion with characteristic fat signal within the entire mass, diagnostic of a benign lipoma

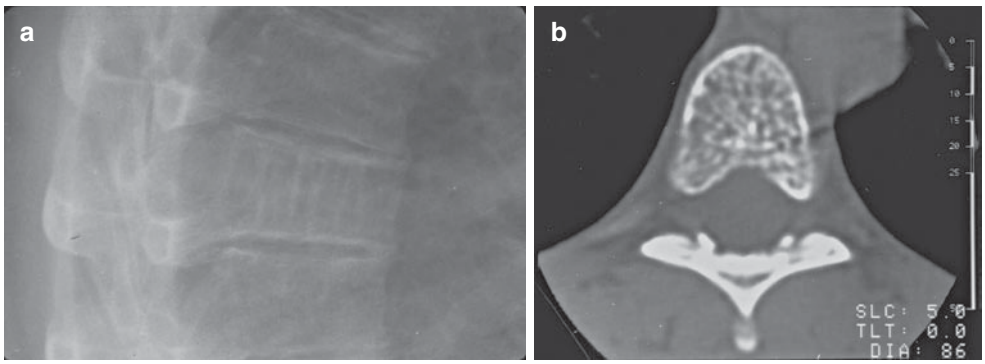

Fig. 15 Hemangioma. **a** Lateral view of the lower thoracic spine shows the typical radiographic pattern of a vertebral body hemangioma. **b** Axial CT scan shows the prominent trabeculations separated by venous pools, a typical CT appearance of a bony hemangioma

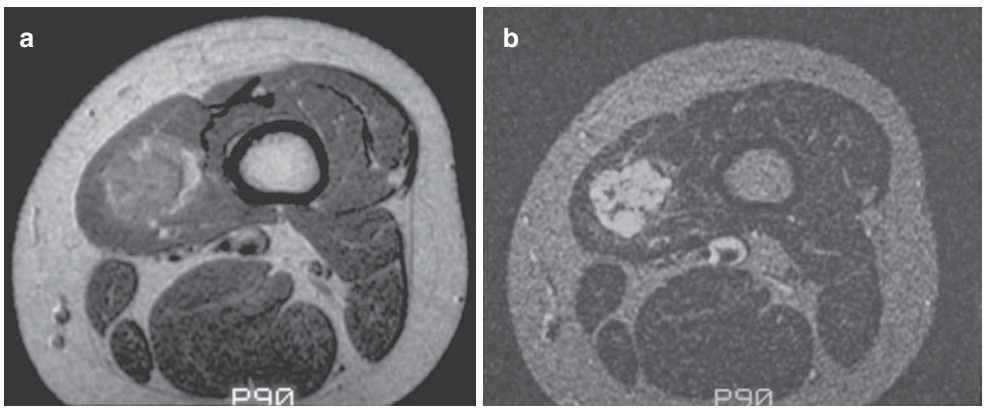

Fig. 16 Soft-tissue hemangioma. Proton density (**a**) and T2-weighted (**b**) axial images through the distal thigh. A soft-tissue mass in the vastus medialis shows heterogeneous signal intensity with signal characteristics of fat blood pooling. On T2-weighted sequences, bright signal with signal void from vessels is noted

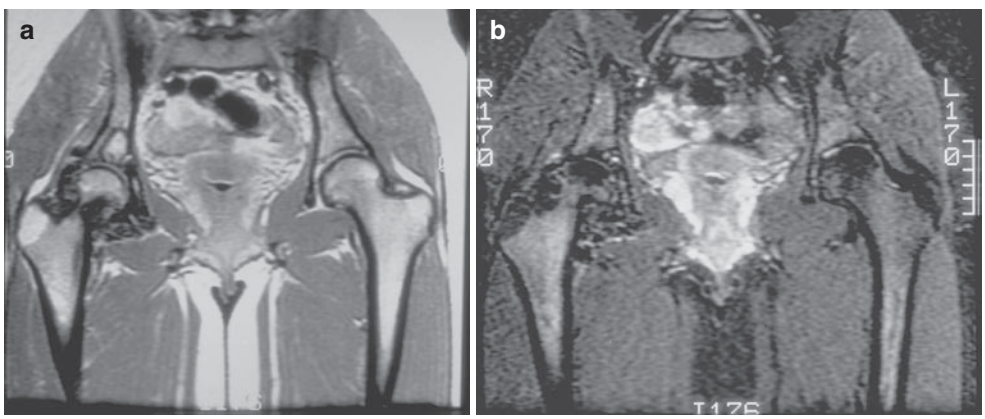

Fig 17 PVNS right hip. Coronal T1 (**a**) and T2 (**b**)-weighted image with fat suppression shows tabulated, dark signal mass within the right hip joint with erosions of the femoral neck causing an apple core deformity of the femoral neck. Dark signal foci on both T1- and T2-weighted images is from hemosiderin deposition and is characteristic of PVNS

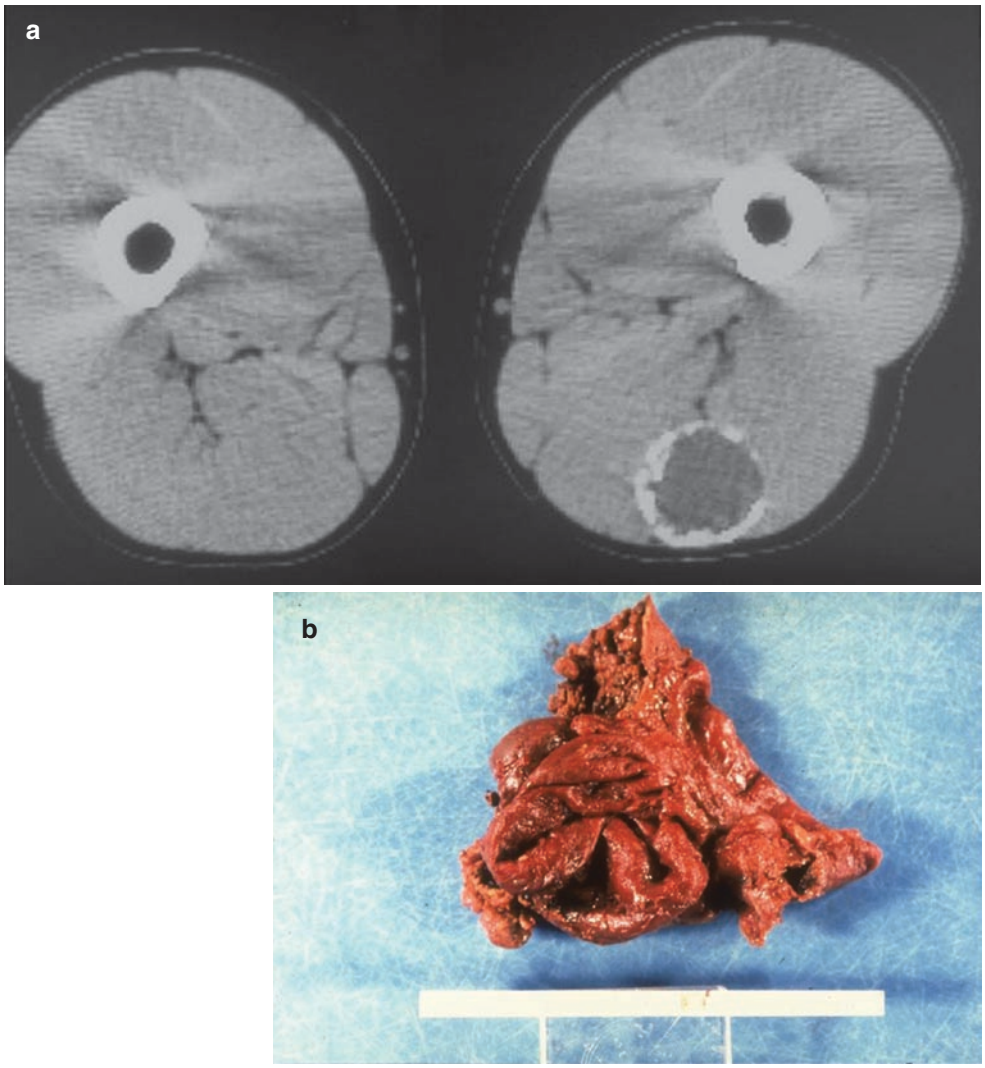

Fig. 18 Hematoma in the posterior thigh. **a** Axial CT scan shows a fairly well-defined low density mass in the posterior compartment with surrounding margin of ossification. **b** Specimen photograph from the same case, showing the hematoma cavity

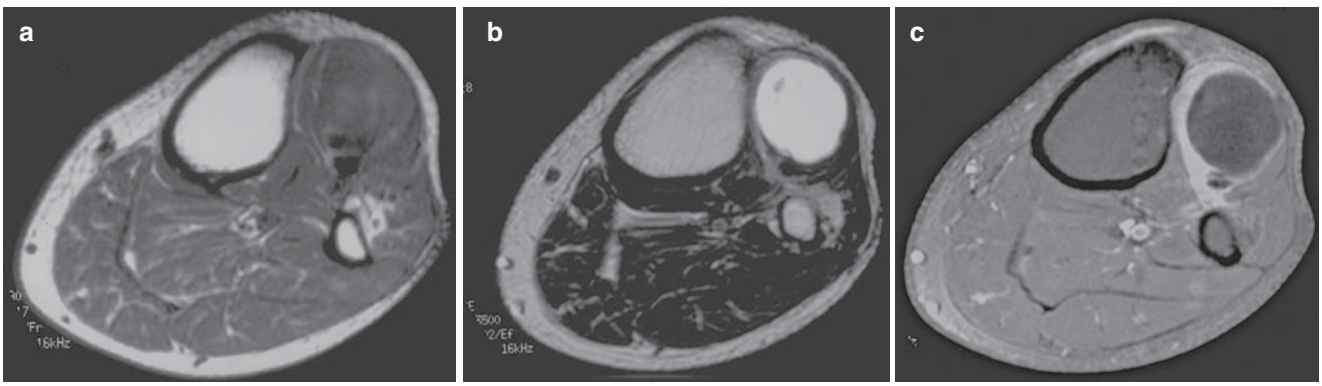

Fig. 19 Ganglion cyst. Axial T1 (**a**), T2 (**b**), and T1 following gadolinium injection (**c**) shows a well-circumscribed mass in the anterior compartment of the lower leg with signal characteristics of fluid. Heterogeneity in the signal intensity was from bleeding into the cyst. Surrounding enhancement is seen

along with other data before the final diagnosis of "cyst" can be attached to a lesion in which noncystic elements are also present.

Fluid-fluid levels are an interesting but nonspecific finding that have been described on MRI in a number of different cystic lesions including aneurysmal bone cyst (Figs. 9c and 20a–d), fibrous dysplasia, simple bone cyst (Fig. 21a–c), MFH, osteosarcoma (Fig. 22), synovial sarcoma, hemangioma, and myositis ossificans (16). Fluid-fluid levels are not diagnostic of any particular tumor.

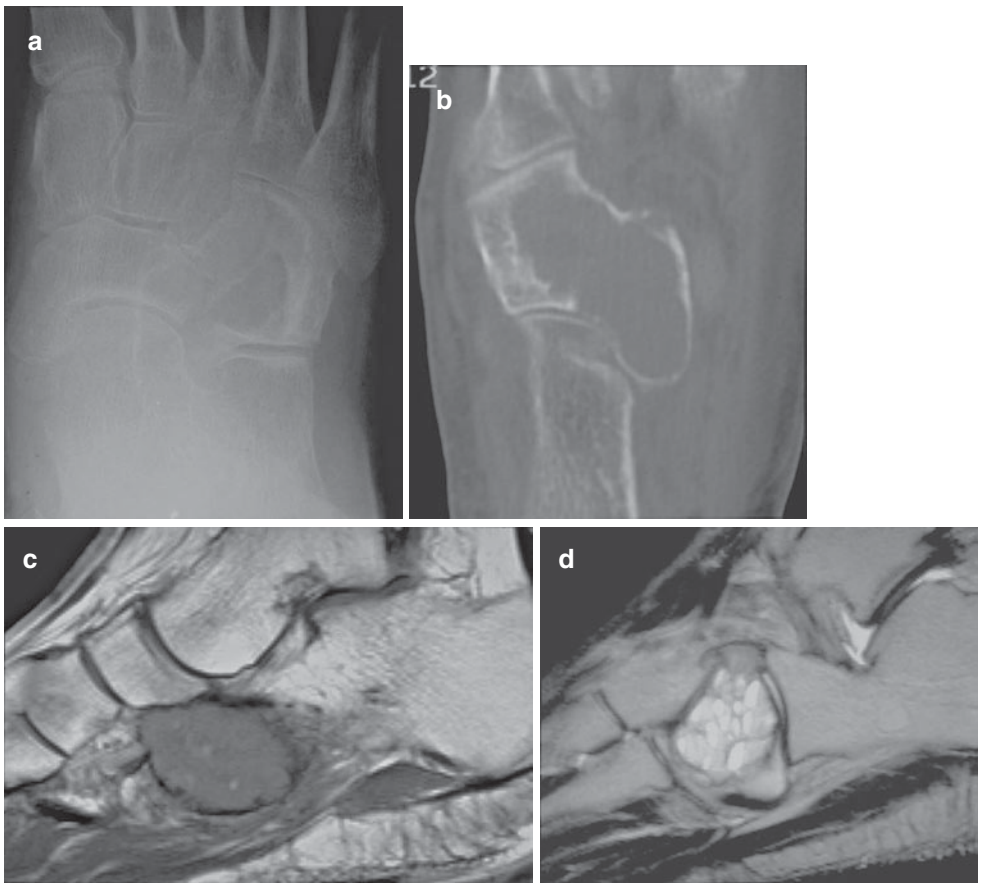

Fig. 20 ABC of the cuboid. **a** Anteroposterior view of the foot shows a lucent area within the cuboid with a sclerotic proximal margin. **b** CT scan shows the significant expansion of the lesion. Fluid-fluid levels can be appreciated. **c** and **d** Sagittal T1- and T2-weighted images show the typical fluid-fluid levels confirming the diagnosis. Bright signal intensity on T1-weighted sequence (10-C) suggests the presence of blood

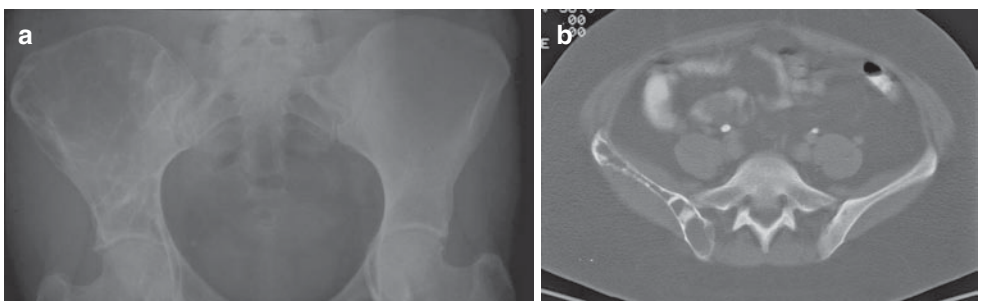

Fig. 21 Bone cyst right ilium. **a** Plain radiograph shows a lucent lesion in the right ilium with sclerotic boundary. **b** Axial CT scan shows a multiloculated, lesion with fluid density. **c** Axial T2-weighted image through the ilium shows bright signal intensity replacing the marrow of the right ilium suggestive of a fluid filled lesion

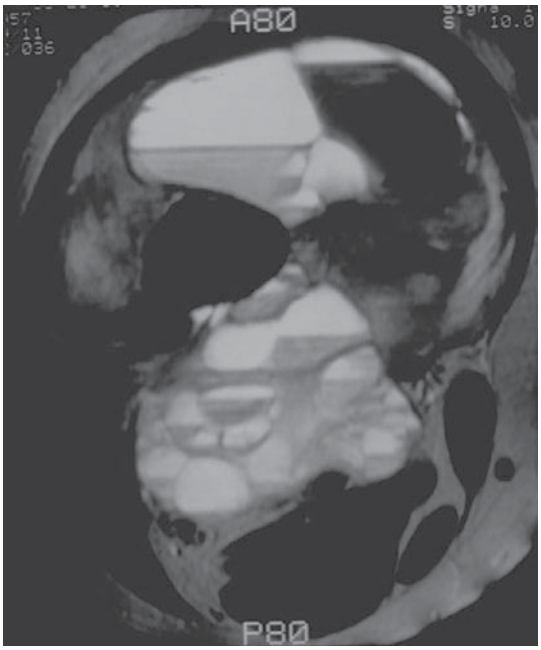

Fig. 22 Fluid-fluid levels from bleeding into a large mass associated with a metastatic osteosarcoma of the femur is seen on this T2-weighted axial image

Fatty Tumors

Benign lipoma is probably the single most common fatty tumor. Liposarcoma is also common, accounting for ~10% of soft-tissue sarcomas. Lipoma is generally easy to identify on imaging studies of all types, being comprised of uniform low attenuation tissue on conventional X-ray studies and CT and showing typical T1 and T2 signal on MR (Fig. 14). Lipomas originating in subcutaneous tissues may be hard to differentiate from adjacent normal fat. A useful technique is to have the patient lie on the affected part during imaging, so that the mass effect of the lesion on the deeper structures may help to identify it. A small amount of internal fibrous tissue is normal in large lipomas; however, larger amounts of nonfatty elements within the lesion raise the possibility of sarcoma (Fig. 23a–c). Indeed, a mixture of fat and soft tissue suggests an atypical lipoma or well-differentiated liposarcoma. Uniform density in the water range (–40 to +30 HU) on CT or water signal on MR may suggest a myxoid liposarcoma. Large areas of necrosis and/or inhomogeneous tumor suggest another diagnosis (being uncommon in liposarcoma). MRI can definitively diagnose lipomas noninvasively using either short tau inversion recovery (STIR) imaging or fat suppression to remove signal from fatty tissue.

Hemangioma

Large venous lakes with slow blood flow result in clusters of high signal areas in hemangiomas on T2-weighted MR images. Hemangiomas often have interposed fatty tissue that shows high signal on T1-weighted images. These features when combined with the occasional presence of phleboliths on plain films are frequently diagnostic. On CT and MRI, hemangiomas display a characteristic pattern of enhancement related to the slow filling of venous channels with contrast agent. This creates a slow, irregular, centripetal enhancement of the lesion.

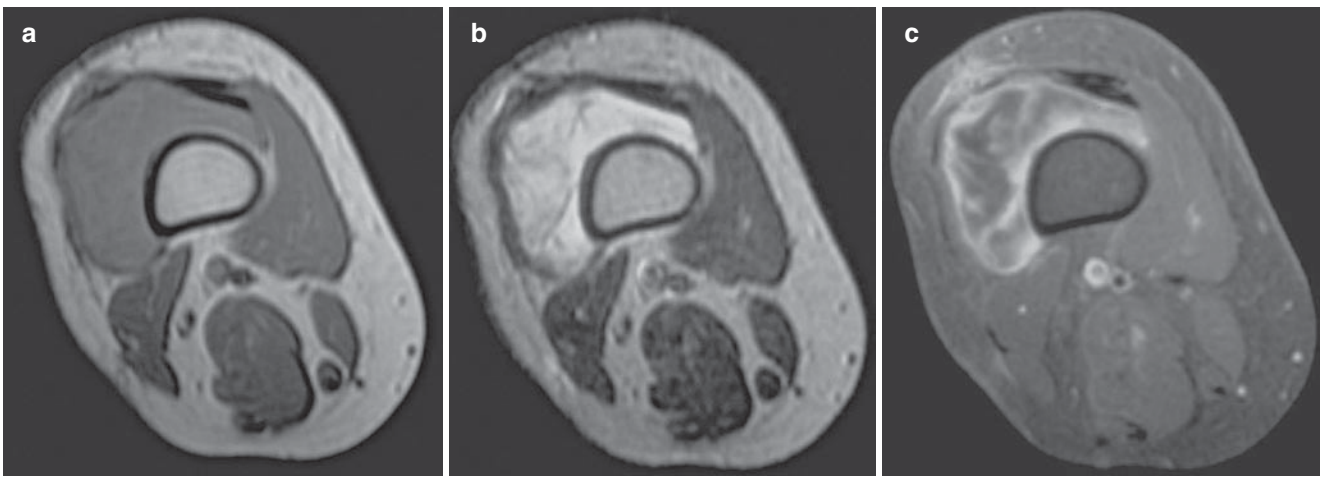

Fig. 23 Liposarcoma anterior distal thigh. Proton density (**a**), T2-weighted (**b**), and post-gadolinium (**c**) images are seen. A large soft-issue mass is noted in the surrounding the anterolateral distal femur. The signal characteristics are not diagnostic of tissue type. The lack of fatty tissue within this liposarcoma probably suggests a higher grade. Gadolinium-enhanced images (**c**) show enhancing tissue within the mass

Pigmented Villonodular Synovitis (PVNS)

Hemosiderin deposition is characterized by low signal intensity on both T1- and T2-weighted images. More important, hemosiderin shows blooming artifact on MRI, particularly gradient echo imaging. In the correct clinical setting, this finding is diagnostic of PVNS (Fig. 24).

Fibromatosis

The MR appearance of fibromatosis is variable. Usually these masses show heterogeneous, rather high signal intensity with low signal areas in between on T2-weighted images. Even so, a spectrum (predominantly high or low signal on T2-weighted sequences) may be encountered. Kransdorf, Sundaram, and various other authors in separate studies have concluded that the relative degree of cellularity of the tumor is of great importance in determining the signal intensity on spin-echo MR images (26, 27).

Hematomas

The signal intensity of hematoma depends on the sequential degradation of hemoglobin, cell lysis, and on the field strength of the magnet (Table 5). In the hyperacute phase of hematoma, oxygenated hemoglobin determines the signal intensities. Oxygenated hemoglobin is not paramagnetic and signal intensities are not characteristic of blood but instead mimic the signal characteristics of cysts. Thus, hyperacute hemato-

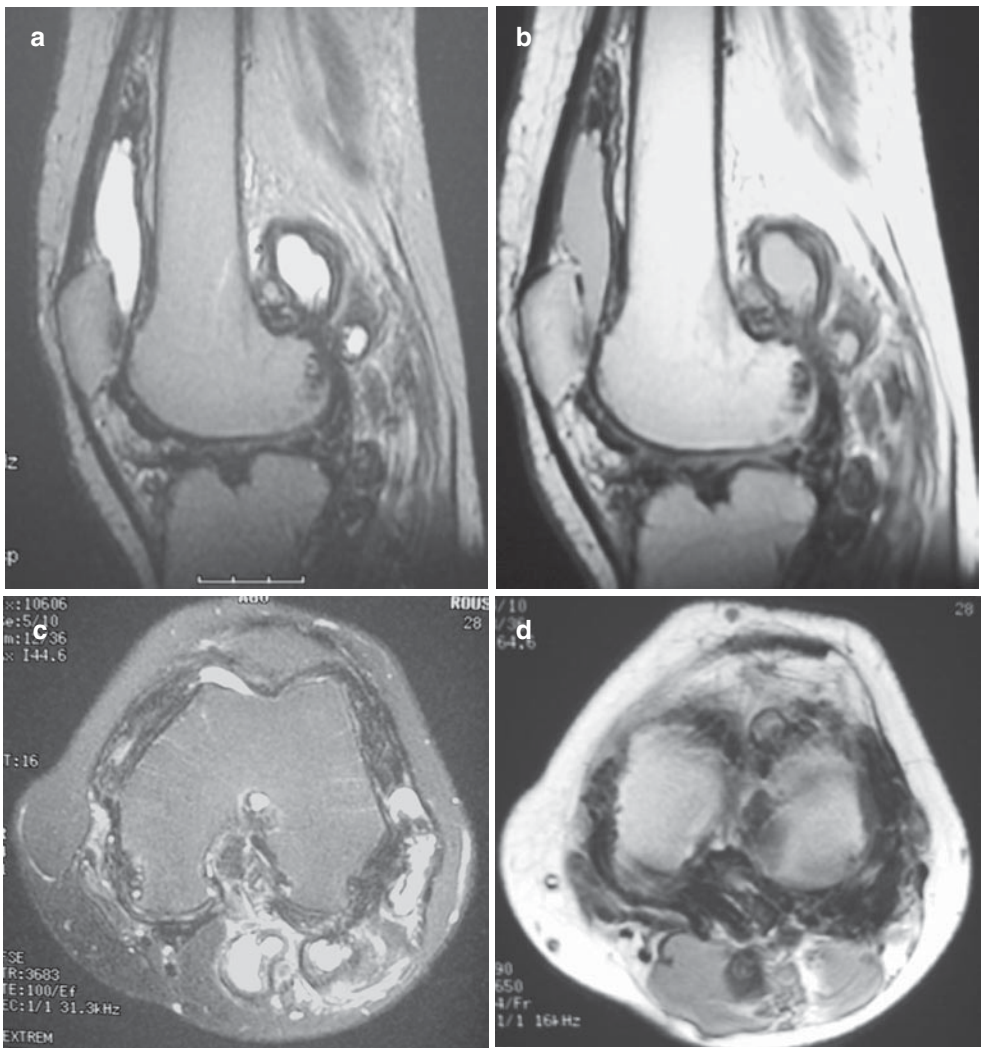

Fig. 24 Pigmented villondular synovitis. Sagittal proton T2-weighted (**a**), proton density (**b**), and axial T2-weighted MR images (**c**) show marked synovial thickening with low signal material on all sequences consistent with hemosiderin deposition along with a joint effusion. An axial gradient echo image (**d**) shows marked "blooming" artifact in and around the synovium confirming the paramagneticity of the low signal material

Table 5 MRI features of hemorrhage

	Signal	
Hemoglobin state	T1-weighted image	T2-weighted image
Intracellular deoxyhemaglobin	Intermediate	Dark
Intracellular methemaglobin	Bright	Dark
Extracellular methemaglobin	Bright	Bright
Ferritin	Dark	Dark

mas show intermediate signal intensity similar to muscle on T1-weighted images and high signal on T2-weighted sequences. In the acute phase, intracellular oxyhemoglobin is converted into intracellular deoxyhemoglobin. This results in low signal intensity on T2-weighted imaging. Subsequently, deoxyhemoglobin is oxidized into intracellular methemoglobin which becomes free with cell lysis. In the subacute phase, this will display a high signal on both T1- and T2-weighted sequences. This high signal intensity is first observed in the periphery of the hematoma and migrates centrally. Over time, hematomas develop a low signal outer rim reflecting the presence of hemosiderin-laden macrophages.

Ganglion

These typically arise adjacent to tendons and joints. They have a characteristic MR appearance. They show a uniform dark signal on T1-weighted images and bright signal on T2-weighted sequences (Fig. 19a–c).

Nerve Sheath Tumors

The neural nature of a tumor can sometimes be recognized, if shown to be closely associated with a nerve (Fig. 25a, b). Classic "dumbbell" neurofibromas may be recognized by their shape, location, and pressure effects on the vertebrae; however, it can be difficult to distinguish benign from malignant peripheral nerve sheath tumors by imaging. Similarly, it may be impossible to tell the difference radiologically between neurofibroma, schwannoma, or ganglioneuroma. On the other hand, Murphy has suggested that neural tumors with centrally located nerves are neurofibromas while lesions that are eccentric to their accompanying nerve are more likely schwannomas (28).

Synovial Sarcoma

Synovial sarcomas show a spectrum of findings on MR scanning. Nevertheless, the possibility of a synovial sarcoma should be high on the list when a relatively well-defined inhomogeneous mass arising near a joint is encountered in a young person. Calcifications can be seen on CT scans or plain radiographs.

Myositis Ossificans

Posttraumatic myositis ossificans (MO) typically presents as a soft-tissue mass with peripheral ossification on radiographs and CT. Over time, the ossification matures from the periphery of the lesion centrally. The lesion may contract over time and in some cases may resolve entirely. Depending upon the age of MO, the MR appearance may vary (29). In the early phase before visible ossification, the lesions are isointense to muscle on T1-weighted sequences. On T2-weighted images, the mass shows a central high intensity with diffuse peripheral edema. In the subacute stage, a low-density rim representing peripheral ossification is visible around all or part of the lesion. In chronic stages, the ossification may show features of more mature bone.

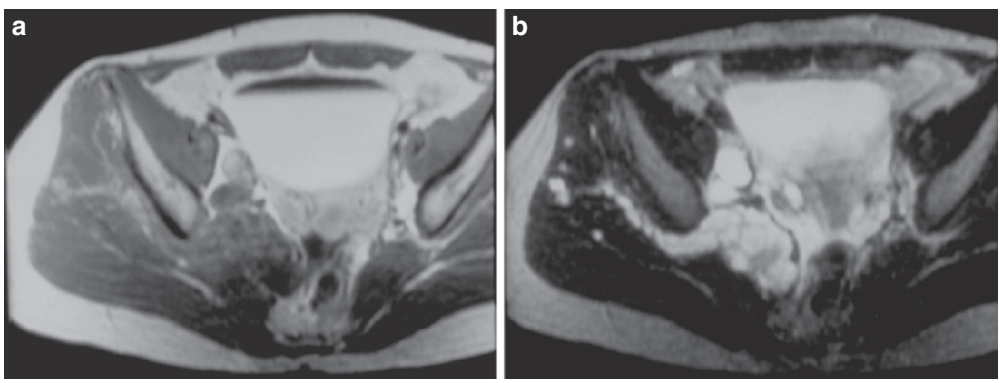

Fig. 25 T1 (**a**) and T2 (**b**)-weighted images showing a peripheral nerve sheath tumor exiting along a nerve root. Histologically, this neoplasm was confirmed to be a neurofibroma

References

1. Cody DD. AAPM/RSNA physics tutorial for residents: topics in CT: image processing in CT. RadioGraphics 2002; 22: 1255.
2. Flohr TG, Schaller S, Stierstorfer K, Bruder H, Ohnesorge BM, Schoepf UJ. Multi-detector row CT systems and image-reconstruction techniques. Radiology 2005; 235: 756–773.
3. Kattapuram SV, Khurana JS, Rosenthal DI, Ehara S. Musculoskeletal applications of MRI. Rad Med 1989; 7: 47–54.
4. Kattapuram SV. Imaging of musculoskeletal tumors. Curr Opin Orthop 1991; 2: 781–787.
5. Kattapuram SV, Rosenthal DI. Diagnostic imaging of musculoskeletal tumors. In Simon M, Springfield D (Eds). Surgery for the Musculoskeletal Tumors. Philadelphia: JB Lippincott Company, 1995, Chap. 13.
6. Herman G, Rose JS, Strauss L. Tumor infiltration of the bone marrow: comparative study using computed tomography. Skel Radiol 1984; 11: 17.
7. Imhof H, Breitenseher M, Trattnig S. Imaging of avascular necrosis of bone. Eur Radiol 1997; 7(2): 180–6.
8. Love C, Patel M, Lonner BS, Tomas MB, Palestro CJ. Diagnosing spinal osteomyelitis: a comparison of bone and Ga-67 scintigraphy and magnetic resonance imaging. Clin Nucl Med 2000; 25(12): 963–77.
9. Nigro ND, Bartynski WS, Grossman SJ, Kruljac S. Clinical impact of magnetic resonance imaging in foot osteomyelitis. J Am Podiatr Med Assoc 1992; 82(12): 603–15.
10. Vanel D, Verstraete KL, Shapeero LG. Primary tumors of the musculoskeletal system. Radiol Clin North Am 1997; 35(1): 213–37.
11. Sanchez RB, Quinn SF, Walling A, Estrada J, Greeberg H. Musculoskeletal neoplasms after intra-arterial chemotherapy: correlation of MR images with pathologic specimens. Radiology 1990; 174: 237.
12. Lemmi MA, Fletcher BD, Marina NM, et al. Use of MR imaging to assess results of chemotherapy in Ewing's sarcoma. AJR 1990; 155: 343.
13. Carrasco CH, Charnsangvej C, Raymond AK, Richli, WR, Walllace S, Chawla SP, Ayala AG, Murray JA, Benjamin RS. Osteosarcoma: angiographic assessment of response to preoperative chemotherapy. Radiology 1989; 170(3 Part 1): 839–42.
14. Erlemann R, Reiser MF, Peters PE, et al. Musculoskeletal neoplasms: static and dynamic Gd-DTPA enhanced MR imaging. Radiology 1989; 171: 767.
15. Bloem JL, Taminiau AHM, Eulderink F, Hermans J, Puwels EK. Radiologic staging of primary bone sarcoma: MRI, scintigraphy, angiography and CT correlated with pathologic examination. Radiology 1988; 169: 805.
16. Kransdorf MJ, Jelinek JS, Moser RP. Imaging of soft-tissue tumors. Radiol Clin North Am 1993; 31: 359.
17. Kattapuram SV, Khurana JS, Scott JA, el Khoury GY. Negative scintigraphy with positive magnetic resonance imaging in bone metastasis. Skel Radiol 1990; 19(2): 113–6.
18. Vanel D, Couanet D, Leclere J, Patte C. Early detection of bone metastases of Ewing's sarcoma by magnetic resonance imaging. Diag Imag Clin Med 1986; 55: 381.
19. Angtuaco EJC, Fassas ABT, WalkerR, Sethi R, Barlogie B. Multiple myeloma: clinical review and diagnostic imaging. Radiology 2004; 231: 11–23.
20. Yablonskiy DA, Reinus WR, Stark H, Haacke EM. Quantitation of T2' anisotropic effects on magnetic resonance bone mineral density measurement. Magn Reson Med 1997; 37(2): 214–21.
21. Brown KT, Kattapuram SV, Rosenthal DI. Computed tomography analysis of bone tumors: patterns of cortical destruction and soft-tissue extension. Skel Radiol 1986; 15: 448.
22. Lodwick GS. Atlas of Tumor Radiology: The Bones and Joints. Chicago: Yearbook Medical Publishers, 1971.
23. Lodwick GS, Wilson AJ, Farrell C, et al. Determining growth rates of focal lesions of bone from radiographs. Radiology 1980; 134: 577.
24. Kattapuram SV, Khurana JS, Ehara S, Ragozzino M. Aggressive post-traumatic osteoporosis of the humerus simulating malignant neoplasms. Cancer 1988; 62: 2525–7.
25. Jurgens H, Exner U, Gardner H, et al Multidisciplinary treatment of primary Ewing's sarcoma of bone. Cancer 1988; 61(1): 23–32.
26. Kransdorf MJ, Jelinek JS, Moser RP, et al Magnetic resonance appearance of fibromatosis. A report of 14 cases and review of literature. Skel Radiol 1990; 19: 495.
27. Sundaram M, McLeod RA. MR imaging of tumor and tumor like lesions of bone and soft tissue. AJR 1990; 155: 817.
28. Robbins MR, Murphy MD, Temple HT, et al. Imaging of musculoskeletal fibromatosis. Radiographics 2001; 21: 585–600.
29. De Smet AA, Norris MA, Fisher DR. Magnetic resonance imaging of myositis ossificans: analysis of seven cases. Skel Radiol 1992; 21: 503–7.

Chapter 10
Skeletal Trauma and Common Orthopedic Problems

Harish S. Hosalkar, Jesse T. Torbert, Jennifer Goebel, and Jasvir S. Khurana

Abstract Our understanding of the biology of fracture healing has evolved over the decades and basic science research as well as clinical outcomes studies continue to add to the existing knowledge. This review outlines the physiology and pathology of healing of fractures including those in children as well as fracture configurations with basic modalities of fixation and treatment.

Keywords Pathology • Bone • Fracture • Healing • Fixation

Healing of Musculoskeletal Tissues

The pathology and pathophysiology of bone healing is important from several aspects. For the surgical pathologist, it is critical to be able to distinguish normal fracture healing in bone from disordered healing and from bone neoplasms. For the orthopedic surgeon and the scientific investigator, the histologic appearances of healing allow a qualitative and quantitative assessment of the process. This permits, for example, the comparison of different methods of treatment. Additionally, an understanding of the cellular signals operating in bone healing, allows the clinician to manipulate and promote or modify osseous union.

Healing of Bone: Fractures

Traumatic disruption of bone, such as in fractures or surgical osteotomies, can have several different end points. The result is dependent on the mechanism of disruption, the pattern of fracture/osteotomy, the type of fixation utilized, and the mechanical and biologic environment to which the bone is subject. For instance, fractures under semi-rigid conditions go on to form an external and internal callus and reunite via a cartilage model. Under several unfavorable conditions, this process may get disrupted and go on to "nonunion." Under rigidly fixed conditions, there may be no visible external callus and no transitional cartilage formation. If there are tensile forces acting such as in callotasis or distraction osteogenesis, then a different sequence of events follows. The cellular mechanisms that operate in these different situations have only recently begun to be elucidated.

Types of Fractures

Full understanding of bone healing first requires an understanding of the process of disruption. The type of fracture often provides insight into the mechanism and characteristics of the fracture. In describing the type of fracture, the particular bone and location are named first (Table 1). The location is described by proximal, mid-, or distal and the portion of bone (epiphysis, growth plate [in the skeletally immature], metaphysis, or diaphysis). Skin integrity overlying the fracture is extremely important. Open fractures are those that expose the fracture through defects in the soft tissue and skin. Closed fractures do not penetrate the skin. Open fractures can range from a small puncture wound caused by a bony spicule to large fragments of bone exposed without any soft-tissue coverage. All open fractures carry the risk of contamination with bacteria and subsequent infection. Therefore, open fractures are orthopedic emergencies and should undergo irrigation and debridement.

The extent of the fracture is complete when the fracture extends completely across the bone and incomplete when the fracture crosses only portion of a cortex. Incomplete fractures are more often seen in the pediatric population as greenstick fractures or as stress fractures in adults. Displacement refers to the degree of translation that between major fragments, and by convention, the distal portion is described in relation to the proximal portion. Displacement can consist of anterior, posterior, medial, and lateral directions as well as proximal (shortening/overlap) or distal (lengthening/gapping) components. Angulation, by convention, is described based on the apex of the

J.S. Khurana (ed.), *Bone Pathology*, DOI 10.1007/978-1-59745-347-9_10,

Table 1 Common terms used to describe fractures

Fracture descriptor	Examples
Bone	Femur, radius
Location	Proximal, mid-, distal Epiphyseal, physeal, metaphyseal, diaphyseal
Skin integrity	Open, closed
Extent	Complete, incomplete
Displacement	Anterior, posterior, medial, lateral 1 cm proximal (overlap)
Angulation	Apex anterior, apex posterior, apex medial, apex lateral
Rotation	Internally rotated, externally rotated
Morphology	Transverse, oblique, spiral, butterfly, buckle, corner, greenstick
Energy	Low energy/simple fracture, high energy/comminuted
Joint involvement	Extraarticular, intraarticular

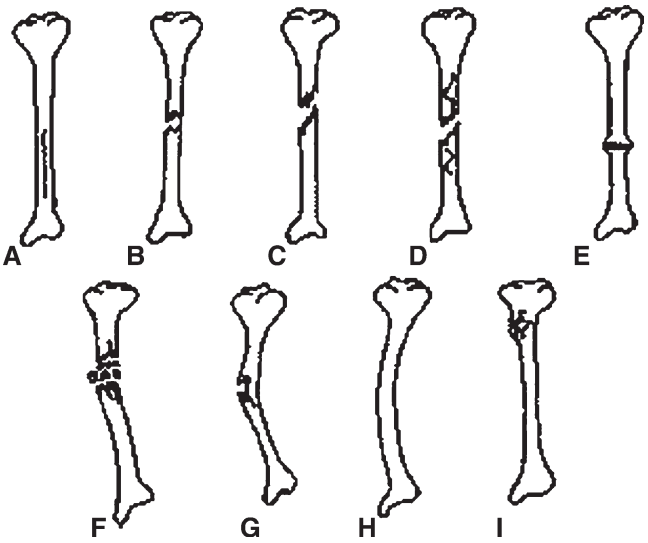

Fig. 1 Illustration of fracture patterns. **a** Longitudinal fracture line parallel to bony axis. **b** Transverse fracture line perpendicular to bony axis. **c** Oblique fracture line at angle to bony axis. **d** Spiral fracture runs a curvilinear course to the bony axis. **e** Impacted fractured bone ends compressed together. **f** Comminuted fragmentation of bone into three or more parts. **g** Greenstick bending of bone with incomplete fracture of convex side. **h** Bowing bone plastic deformation. **i** Torus buckling fracture

angulation and can be present in two planes. Rotational deformity is important, and again the distal fragment is described in relation to the proximal fragment as internally rotated or externally rotated.

The morphology of the fracture is often a clue to the mechanism of injury (Fig. 1). Transverse fractures (b) are a result of bending and are typically low in energy. Butterfly fractures are caused by a combination of bending and compression, and the butterfly or triangular fragment occurs on the convex side of the fracture. Oblique fractures (c) are often a result of a combination of compression, bending, and torsion. Spiral fractures (d) are caused by a torsional load. The bone of a child is to some degree able to deform plastically, or bend without breaking. Thus, children have a higher probability of sustaining incomplete fractures. The greenstick fracture (g) occurs in cortical bone and is typically the result of bending load which causes a crack on the convex, or tension side, of the diaphysis with intact, but bent cortex on the concave side. The buckle, or torus fracture, occurs in pediatric cancellous bone and failure is seen on the concave or compression side of the bone. Corner fractures, also known as bucket-handle fractures, often occur secondary to violent shaking or traction injuries to the extremity and are suggestive of child abuse, with their incidence in large series of abused children ranging from 15 to 32%. Kleinman et al. found that these fractures were complete metaphyseal fractures extending through the primary spongiosa of bone just above the zone of provisional calcification (1).

Often times the amount of energy required to create fractures can be determined by the fracture pattern. For instance, highly comminuted fractures are likely due to high energy mechanisms such as motor vehicle accidents or a fall from significant height. Simple fractures are more likely to be a result of lower energy trauma; however, osteoporotic bone and pathologic bone are weaker and more susceptible to comminution in low energy settings. The extension of fractures into joints often makes the treatment more difficult as anatomic reduction is ideal to eliminate step-offs in the articular surface.

Unique Characteristics of Pediatric Fractures

Fracture Remodeling

Remodeling is the third and final phase in biology of fracture healing preceded by inflammatory and reparative phase. This occurs from a combination of appositional bone deposition on the concavity of deformity, resorption on the convexity, and asymmetrical physeal growth. Considering this unique feature of biology reduction is somewhat less important than in adults (Fig. 2).

The major factors that have bearing on the potential for angular correction are skeletal age, distance to the joint,

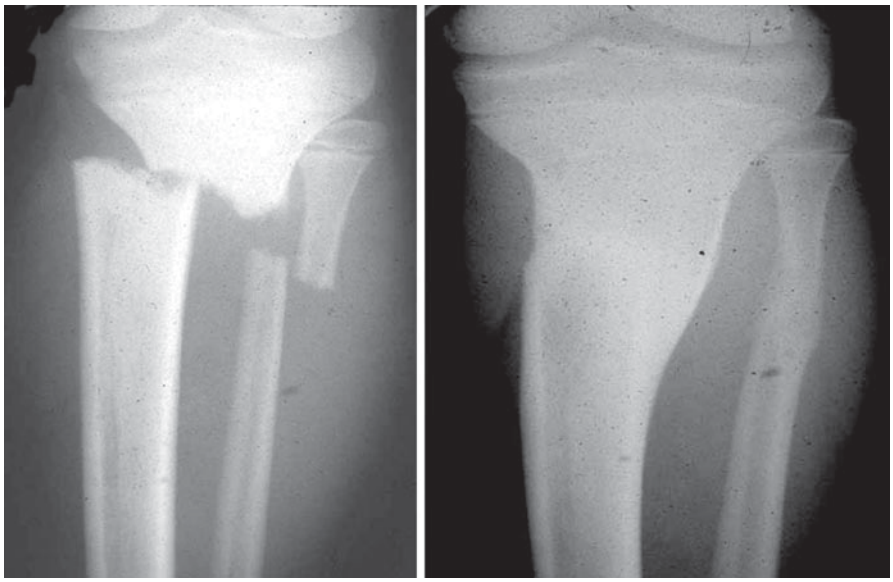

Fig. 2 Radiographs of a healing fracture of proximal tibia–fibula demonstrating remodeling from a combination of appositional bone deposition on the concavity of deformity and resorption on the convexity

and orientation to the joint axis. The rotational deformity and angular deformity not in the axis of the joint motion is less likely to remodel. The amount of remaining growth provides the basis for remodeling and therefore younger children have greater remodeling potential. Fractures adjacent to a physis undergo the greatest amount of remodeling, provided that the deformity is in the plane of axis of motion for that joint. The fractures away from elbow and closer to knee joint have greater potential to remodel as this physes provide maximum growth to the bone. In general, one can expect remodeling to occur over the next several months following injury throughout skeletal maturity.

Overgrowth

Physeal stimulation from the hyperemia associated with fracture healing causes overgrowth. It is usually prominent in long bones such as femur. Femoral fractures in children younger than 10 years of age frequently overgrow by 1–3 cm. Bayonet apposition of bone (Fig. 3) is preferred to compensate for the expected overgrowth.

This overgrowth phenomenon will result in equal or near equal limb lengths at the conclusion of fracture remodeling. After 10 years of age, overgrowth is less of a problem and anatomic alignment is recommended. In physeal injuries, growth stimulation is associated with use of implants or fixation hardware that may cause chronic stimulus for longitudinal growth.

Progressive Deformity

Injuries to the physes can be complicated by progressive deformities with growth (Fig. 4). The most common cause is complete or partial closure of the growth plate. As a consequence, angular deformity, shortening, or both, can occur. The partial arrest may be peripheral, central, or combined. The magnitude of deformity depends on the physis involved and the amount of growth remaining.

Rapid Healing

Children's fracture heals quickly as in comparison with adult fracture healing. This is due to children's growth potential and thicker, more active periosteum. As children approach adolescence and maturity, the rate of healing slows and becomes similar to that of an adult (Fig. 5).

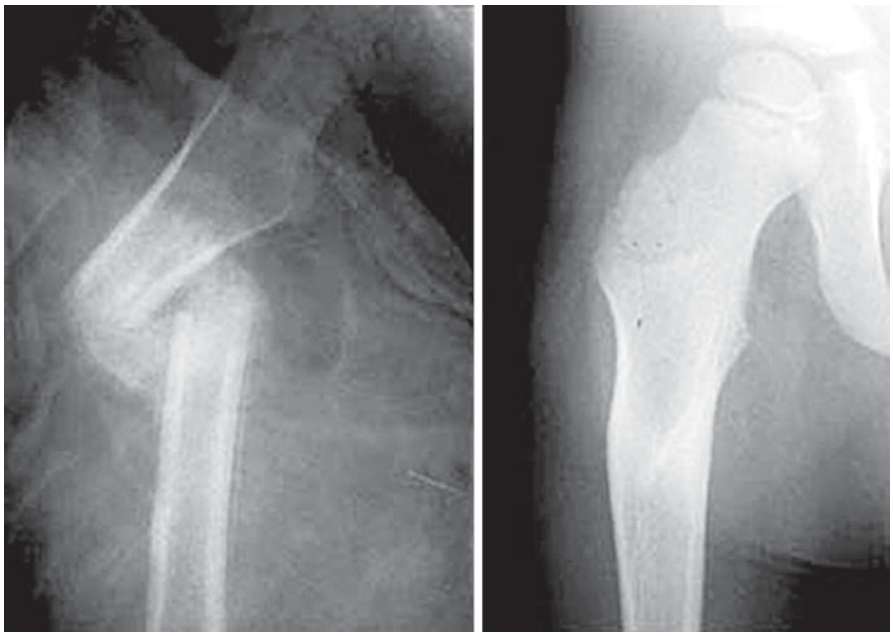

Fig. 3 Femur fracture in a child where bayonet opposition is accepted for reduction in anticipation of expected overgrowth and remodeling

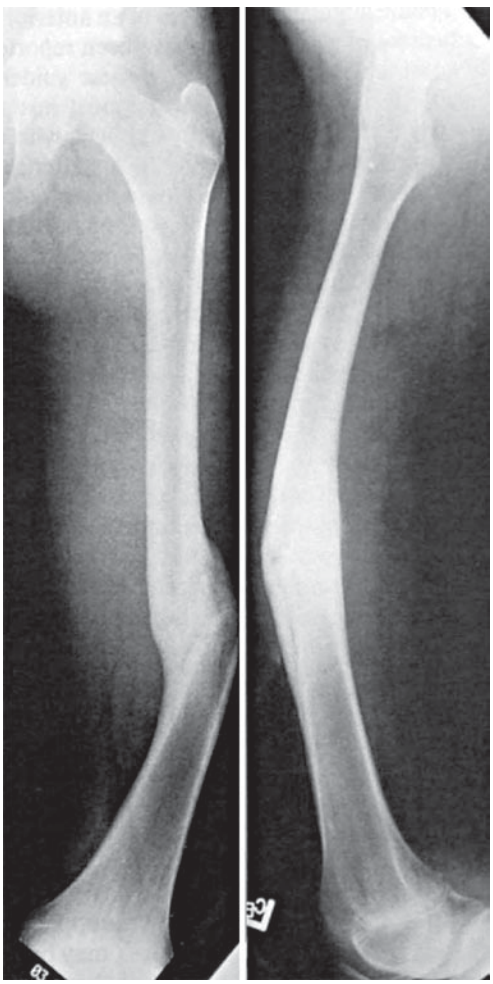

Fig. 4 Radiographs of femur fracture with associated distal physeal injury demonstrating progressive angular deformity at the malunion site with growth

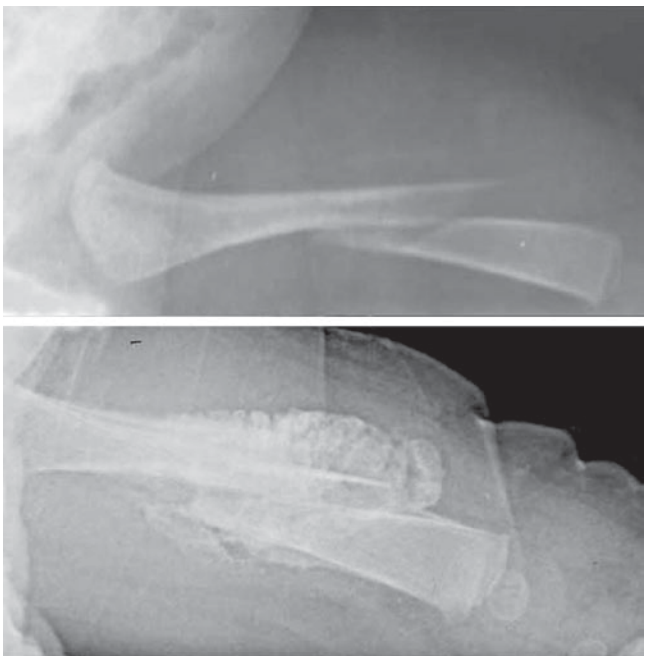

Fig. 5 Rapid healing of neonatal femur fracture due to excellent and rapid bridging callus formation

Pediatric Fracture Patterns

The different pediatric fracture patterns are the reflection of child's characteristics skeletal system. The majority of pediatric fractures can be managed by closed methods and heal well.

Plastic Deformation

Plastic deformation is unique to children. It is most commonly seen in ulna and occasionally, the fibula. The fracture occurs due to a force, which produces microscopic failure on the tensile side of bone and does not propagate to the concave side. The concave side of bone also shows evidence of microscopic failure in compression. The bone is angulated beyond its elastic limit, but the energy is insufficient to produce a fracture. Thus, no fracture line is visible radiographically (figure 6). The plastic deformation is usually permanent and a bend in ulna of less than 20° in a 4-year-child is expected to correct with growth.

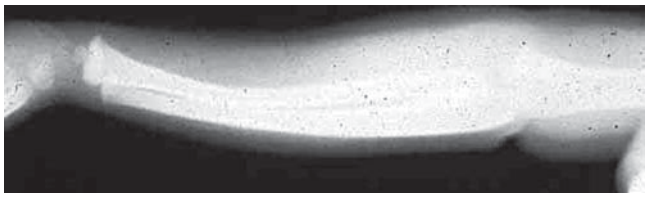

Fig. 6 Radiograph of forearm fracture in a child with plastic deformation of the radius and ulna

Buckle or Torus Fracture

It is a compression failure of bone that usually occurs at junction of metaphysis and diaphysis, especially in the distal radius. This injury is referred to as torus fracture (figure 7) because of its similarity to the raised band around the base of a classical Greek column. These are inherently stable and heal in 3–4 weeks with simple immobilization.

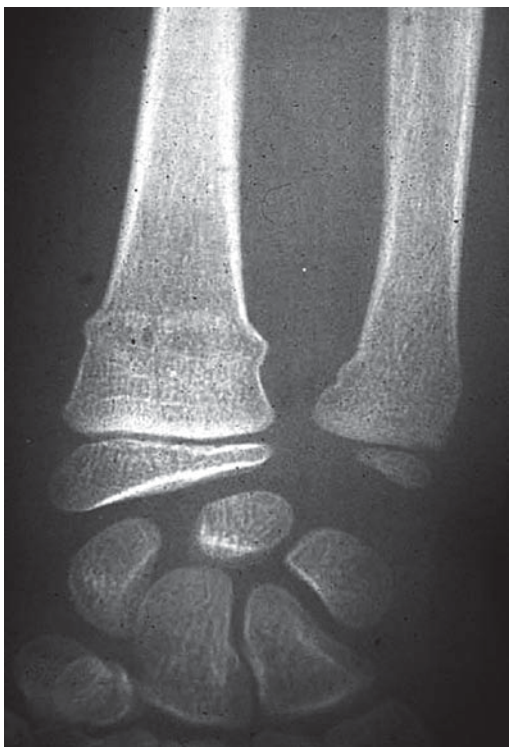

Fig. 7 Radiograph demonstrating torus fracture of distal end of radius in a child

Greenstick Fracture

These fractures occur when bone is bent and there is failure on the tensile (convex) side of the bone. The fracture line does not propagate to the concave side of the bone. The concave side shows evidence of microscopic failure with plastic deformation. It is necessary to break the bone on the concave side as the plastic deformation recoils it back, to the deformed position.

Complete Fractures

Fractures that propagate completely through bone are called complete fractures. These fractures may be classified as spiral, transverse, or oblique, depending on the direction of the fracture lines. A rotational force usually creates the spiral fractures and reduction is easy due to presence of intact periosteal hinge. Oblique fractures are in diaphysis at 30° to the axis of bone, and are inherently unstable. The transverse fractures occur following a three-point bending force and are easily reduced by using the intact periosteum from the concave side.

Epiphyseal Fractures

The injuries to epiphysis involve the growth plate. There is always a potential for deformity to occur and hence long-term observation is necessary. The distal radial physis is the most frequently injured physis. Salter and Harris (SH) classified epiphyseal injuries into five groups (Fig. 8). This classification helps to prognosticate on the outcome of the injury and offers guidelines in formulation of the treatment. The SH Type I and II fractures usually can be managed by

Fig. 8 Diagrammatic illustration of the Salter–Harris classification of physeal fractures in children

closed reduction techniques and do not require perfect alignment, as they tend to remodel with growth. The SH Type II fractures of distal femoral epiphysis need anatomic reduction. The SH Type III and IV epiphyseal fractures involve the articular surface and require anatomic alignment to prevent any step-off and realign the growth cells of the physis. SH Type V fractures are usually not diagnosed initially. These fractures present in future with growth disturbance. Other injuries to the epiphysis are avulsion injuries of tibial spine and muscle attachments to the pelvis. Osteochondral fractures are also defined as physeal injuries that do not involve growth plate.

Types of Fixation

Sticks, mud, and cloth have been used to immobilize fractures for millennia. Hippocrates described the splint in 400 B.C. Plaster of Paris impregnated linen cloth was first described in 1852 by a Flemish army surgeon (3). Regardless of the materials used, splints, traction, and casts offer relative stability. They provide a noninvasive, nonrigid stabilization that can be temporizing until surgical fixation is obtained or, as in many pediatric fractures, the definitive form of immobilization (Fig. 9).

Screws are the most commonly used implant in the treatment of fractures (Fig. 10). In the simplest form, screws can alone be used to achieve interfragmentary compression, or compression between two fragments. Although implants reduce mobility and displacement under functional load, the only technique which will effectively abolish motion at the fracture site is interfragmentary compression. This is referred to as absolute stability and diminishes the strain at the fracture site enough to allow for direct healing without visible callous. Examples of interfragmentary compression include the use of screws to fix a proximal femur transcervical femoral neck fracture and the use of a single screw to compress a transverse fracture of the scaphoid. Screws are also commonly used to fix a plate to bone.

Orthopedic plates vary tremendously in regard to their design and use (Fig. 11). The role of the orthopedic bridging plate is to stabilize the fracture site and transmit the force from one end of the bone to the other, thereby bypassing the fracture site. Buttress plates are placed on the surface of the bone to act as a buttress and prevent fragments of bone from being displaced. An example of this is a medial tibial plateau fracture that is prevented from sliding off medially by medial tibial plate. The bridging and buttress plates allow some degree of motion under weight bearing conditions, and are therefore classified as semi-rigid constructs.

Plates can also act as additional support (neutralization plate) to the interfragmentary screw by neutralizing the forces that would cause rotation about the long axis of the interfragmentary screw, further enhancing a rigid construct. Dynamic compression plates (DCPs) are shaped in a way that when the screws are inserted, interfragmentary compression is achieved and can thus be used to build a rigid construct.

Traditional plates relied on the friction of the bone/plate interface to minimize motion. The pressure caused by the plate contact on the periosteal surface of the bone causes damage to the periosteal blood supply to the bone. Unlike traditional plates, the newer locking plates have threaded holes in the plate, which accommodate screws with threaded heads. By locking the head of the screw into the plate, the locking plate construct acts as a fixed angle device and results in angular stability and increased load-carrying capacity without the requirement of pressure and friction between the plate and bone. Locking plate designs are now incorporating minimal contact designs to reduce the area of bone/plate contact to preserve periosteal blood supply.

Intramedullary rods are placed in the intramedullary canal of long bones at a site distant to the fracture site and are generally considered the standard treatment for long bone diaphyseal fractures (Fig. 12). Depending on the bone anatomy, the insertion can be anterograde or retrograde. Rods can be

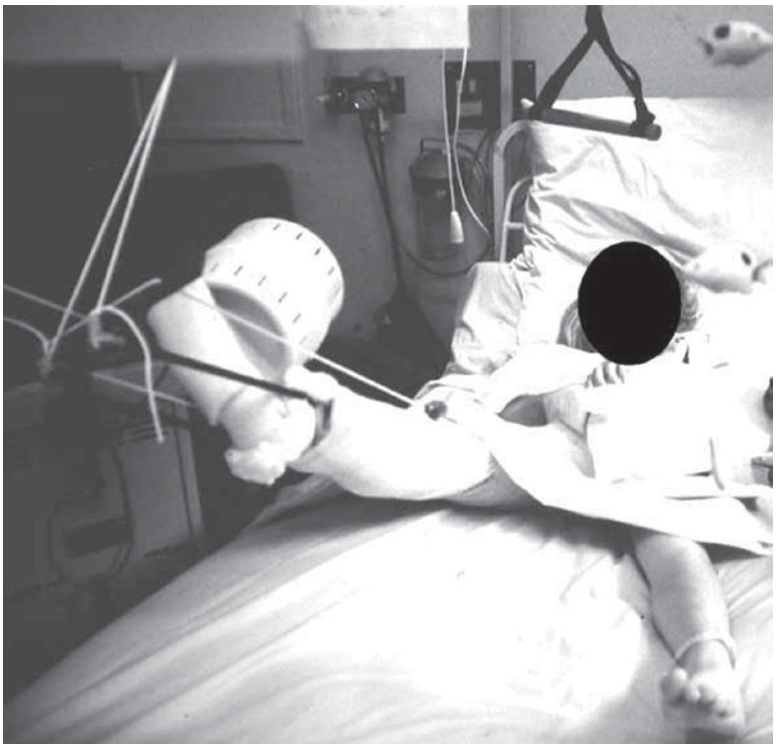

Fig. 9 Use of a traction assembly for treatment of femur fracture in a 9-year-old girl

placed with or without intramedullary reaming. Reaming the medullary canal increases the diameter of the nail that can be used, and thus, the strength of the rod and the area of contact between the rod and bone. The process of reaming has some deleterious effects: rise in the intramedullary pressure leading to fat emboli and temperature increase leading to bone necrosis. Intramedullary rods are considered load-sharing devices and result in semi-rigid conditions.

External fixation provides stabilization to bones based on the principle of splinting. This is done using either threaded large-diameter pins or tensioned small-diameter wires or the combination of both. The pins/wires secure both proximal and distal fragments which are then connected by external rods. External fixators result in semi-rigid constructs (Fig. 13a, b).

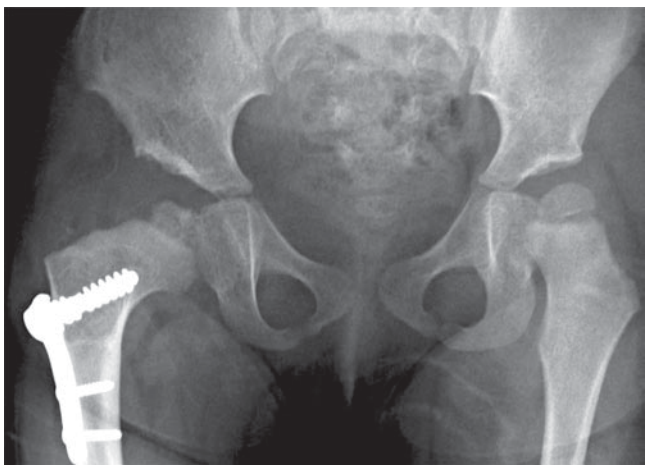

Fig. 10 Hip screw and side-plate being used for fixing a proximal femoral derotation osteotomy/fracture

Biology of Semi-Rigid Conditions

Under semi-rigid conditions, there are three recognizable stages of healing. These are termed the inflammatory, reparative, and remodeling stages. With disruption of the blood supply and the formation of a hematoma at the fracture site, there is a variable amount of necrosis of tissues in the immediate vicinity of the traumatic disruption. Blood and plasma infiltrate the surrounding tissues which become swollen and friable (thus delaying surgery beyond a few hours leaves the surgeon dealing with

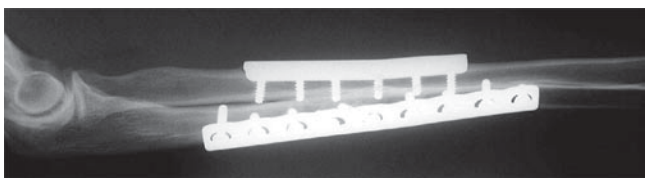

Fig. 11 Use of dynamic compression plates (DCPs) for fixation of diaphyseal forearm fractures

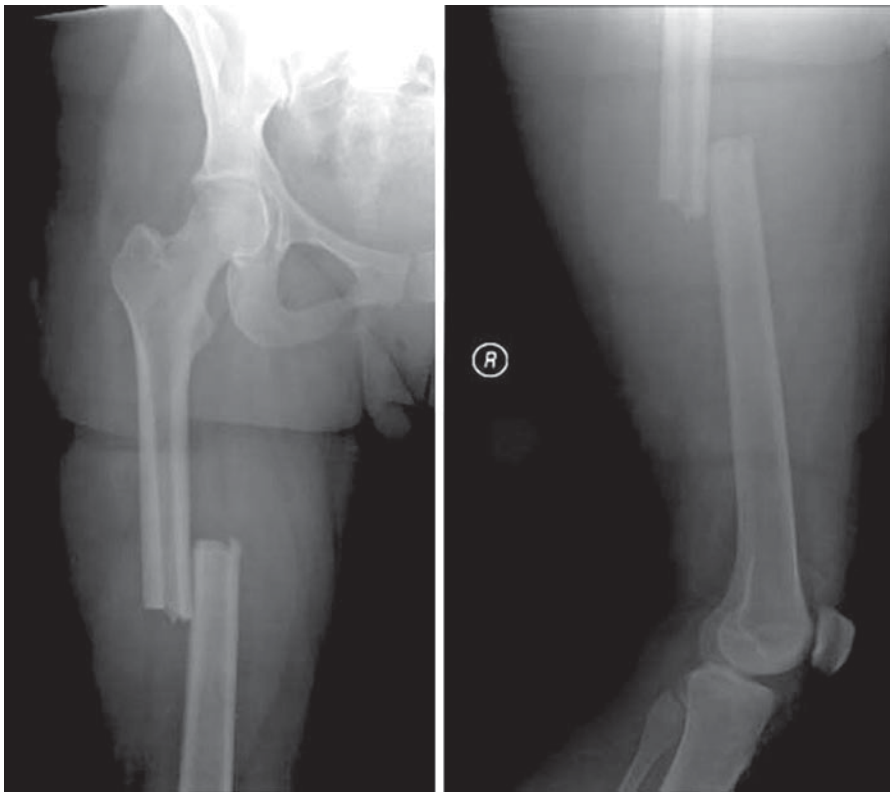

Fig. 12 Plain radiographs of mid-shaft femur fracture

swollen tissues which often "cut through" when sutured). The necrotic tissue chemotactically attracts primitive mesenchymal elements, which differentiate into osteoblasts and chondrocytes. These produce collagen II and considerable amounts of collagen III, contributing to the external callus. This is the start of the reparative stage. The majority of the proliferating osteoblasts appear to be localized under the periosteum which gets "lifted." Some, however, almost certainly appear to be arising from the endosteum or the marrow cavity.

The Type III collagen has a loose network of argyrophilic fibrils and is weakly birefringent. It serves as a loose network for fibroblast in-growth and supports capillary proliferation which ensues. Osteoblasts (especially close to the original bone and within the well-vascularized tissue) start to produce trabecular bone (and collagen I). A variable amount of cartilage is formed between this well-vascularized tissue and the covering periosteum. In this region, collagen II can be localized. Thus, a variable amount of enchondral ossification occurs. Soon thereafter, collagen I starts to predominate. At this point, the two collars of bone from each end have advanced toward each other and a "bridge" of initial union is complete. The cartilage of the initial callus is completely replaced by a process of enchondral ossification. This is referred to as the remodeling stage. The internal callus (endosteal callus) is the chief source of union between the fragments as the callus disappears. This callus is predominantly made up of woven bone and the collagen species localizable is collagen I in this callus. With the passage of time, the entire callus gets remodeled, and woven cancellous bone gives way to mature (lamellar) compact bone.

A number of growth factors and other bone cytokines play a role in this process. The exact mechanisms and their individual contribution are being studied and are not fully understood at present. A number of studies have shown conflicting results. This is possibly due to species variation in the experimental model used. Another potential reason for conflict could be that combining various growth factors may result in additive, potentiative, or subtractive effects. Also, in vitro and in vivo results have been at variance. Additionally, doses, purity of extraction, and other variables have added to the questions pertaining to the effects of these factors.

From the available data, it seems that TGF-β may have a prominent role in fracture healing. It may cause an increase in the synthesis of collagen Type I (4). Platelet-derived growth factors (PDGFs) have also been studied and may have a role in the healing process. Insulin-like growth factors (IGF-I and -II) have been demonstrated to be involved in fracture healing and in distraction osteogenesis (4–7).

Biology of Rigid Conditions

Under conditions of rigid internal fixation, repair occurs by the internal (endosteal) callus alone. Metal fixation of

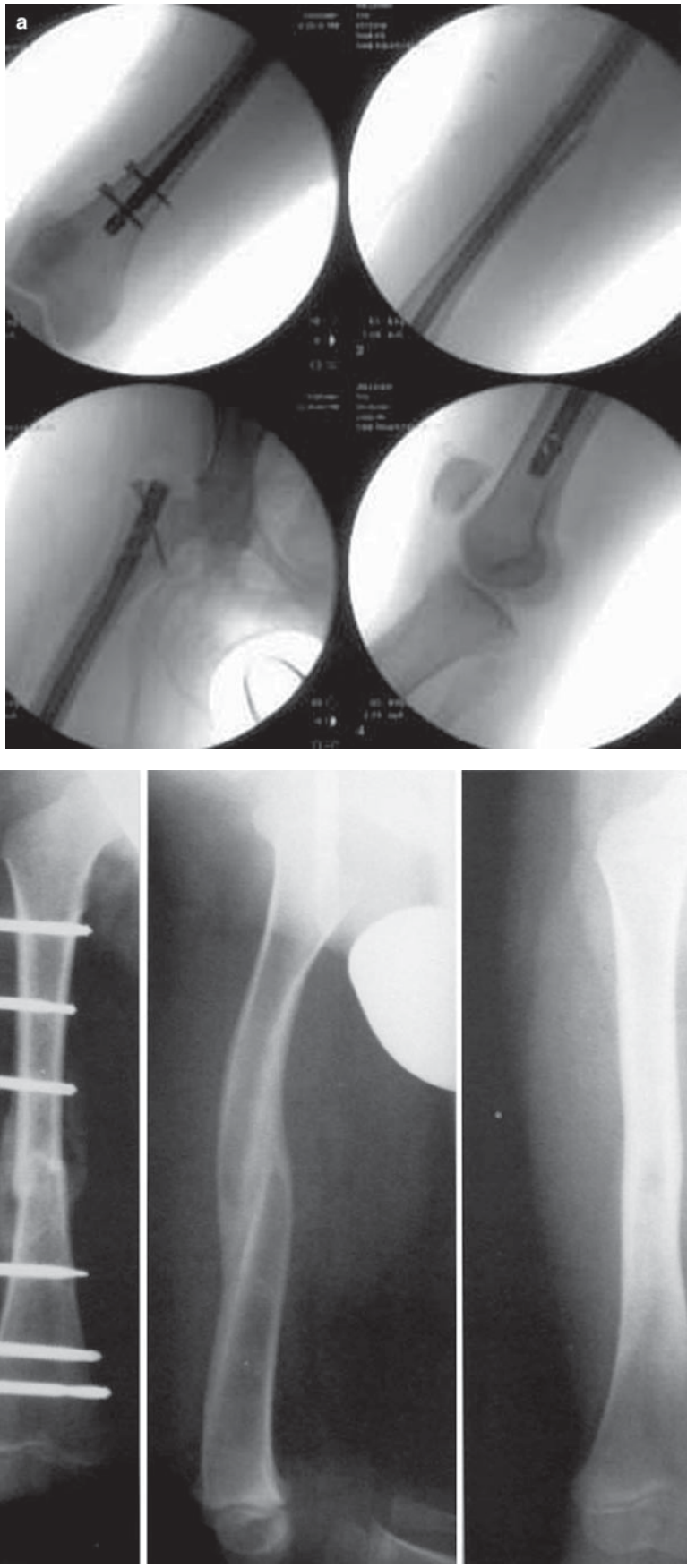

Fig. 13 **a** Fluoroscopic views of locked intramedullary nailing and fixation. **b** Mid-shaft femoral fracture treated with external fixator. Sequential films demonstrating healing of fracture and remodeling

fractures was used as early as the late nineteenth century. But the recent enthusiasm for internal fixation was in part the result of pioneering studies on the biology of rigidly fixed bone fragments, carried out by the AO-ASIF group (Arbeitgeminschaft fur osteosynthesisfragen) in Germany and in Switzerland. These studies showed that union of rigid fixation resembled native bone histologically.

The AO studies also highlighted the importance of the periosteum and the vascular supply in fracture union. The notion that the outer half of the diaphysis is dependent on the periosteal supply, is the basis for the tendency of some surgeons to apply orthopedic hardware extraperiosteally rather than subperiosteally.

The kind of union seen in rigidly fixed fractures resembles the physiologic process of remodeling. It is important to note that bone resembling native bone histologically does not automatically translate into strong union biomechanically. There may be a certain time lag when this callus consolidates and achieves the strength of original bone.

Complications

Nerve and vascular injuries can occur at the time of initial injury, during closed reduction maneuvers, and during operative fixation. For instance, the most common nerve complication of humeral shaft fractures is radial nerve palsy. This is typically due to contusion or stretching of the nerve at the time of injury as the nerve lies on the humerus in the spiral groove. The nerve can also be lacerated or impinged upon during reduction if it is displaced between two fracture fragments. Open reduction and internal fixation with a plate can also result in nerve injury secondary to traction during the time of surgery or compression by the plate.

Blood loss is common in the orthopedic trauma patient. This can range from a small hematoma at the fracture sight to loss of the entire blood volume in a pelvic fracture, which results in the demise of the patient. Blood loss can be external blood loss at the scene of injury, continuous external loss, operative blood loss, and internal blood loss. Resuscitation is vitally important in the trauma patient and is often the difference between life and death.

Compartment syndrome is a condition in which the pressure within a compartment rises to a level that decreases the perfusion gradient across tissue capillary beds, leading to cellular anoxia, muscle ischemia, and irreversible muscle damage. A variety of conditions may initiate compartment syndrome (contusions, bleeding disorders, burns, postischemic swelling, trauma, fracture fixation, constriction caused by a tight cast), although the most common cause of compartment syndrome is fracture. One large series showed that 70% of compartment syndromes were caused by fracture (8). Compartment syndrome is not uncommon after intramedullary nailing of tibial fractures. This is multifactorial with swelling due to the initial injury and surgical manipulation, traction which decreases the compartment volumes, reaming which forces blood and marrow into the compartments, and outflow restriction caused by limb supports contributing to the development of increased compartment pressures. The treatment is surgical release of the fascial compartments and skin. The skin is closed when the swelling diminishes.

Fat embolism is the extravasation of fatty marrow into the venous system upon fracture and can be worsened during introduction surgical instruments and implants into the intramedullary canal. Fat emboli syndrome can result from this introduction of fat into the blood stream. Fat emboli syndrome consists of respiratory symptoms or signs (shortness of breath, tachypnea, and hypoxia), neurologic signs (agitation, delirium, stupor, and coma), and a nonpalpable petechiae developing over the upper body, particularly in the axillae. The predominant theory regarding fat emboli syndrome is that fat droplets produce ischemia and inflammation, with concomitant release of inflammatory mediators. Symptoms typically appear 48 or more hours after the insult. Fat emboli syndrome can resolve without any permanent sequeli or can lead to death.

Deep venous thrombosis (DVT) is quite prevalent (60%) in patients admitted for orthopedic fractures (9). DVT exists in a spectrum of disease that includes asymptomatic DVT, symptomatic DVT, asymptomatic pulmonary embolism (PE), symptomatic PE, and death due to PE. The incidence of death from PE is rare, approximately 1–2%. The cause of DVT is multifactorial. As described by Virchow, damage to vessel walls, stasis, and hypercoagulability are factors that lead to thrombosis, and all are likely found in patients with fractures. Doppler ultrasonography of the deep veins of the lower extremities is commonly performed for fracture patients with symptoms, and in some centers, as a screening tool in multiply injured patients. Patients with lower extremity fractures or multiply injured patients who are nonambulatory are usually given prophylactic pharmacologic (heparin, low molecular weight heparin, or warfarin) and mechanical (pneumatic compression devices or stockings) anticoagulation.

Nonunion is the absence of bony union within a defined amount of time. Typically this is 6 months, but can be up to a year for certain fractures such as the femoral neck fracture. Two types of nonunion exist. Atrophic nonunions occur when little or no callus is formed and are often attributed to a lack of blood supply. Hypertrophic nonunions are characterized by a large volume of callus without union. These often develop due to inadequate fixation and motion that exceeds the limit required for bony union. Several adverse conditions can occur that delay or prevent union. These conditions include the presence of an extensive gap between the fragments (or interposition of soft tissues), loss of blood supply, or abnormal

biomechanics such as increased mobility or the presence of shearing forces. Additional problems may be contributory to these such as infection or a pathologic fracture, extensive comminution, or the presence of a systemic metabolic disturbance. Loosening or mechanical failure of internal fixation may be a late complication in the nonunited fracture. However, loosening is often an issue in the treatment of severely osteoporotic fractures.

Malunion is bony union with a deviation from the anatomic length, alignment, and rotation. This can occur with both nonsurgical and surgical treatment. Deviations are better tolerated in the child due to remodeling potential. Guidelines are present for acceptable deformities in children and adults and depend on the bone, location within the bone, plane of deformity, and amount of time left before skeletal maturity. Pediatric fractures that involve the growth plate can develop deformities. Decrease in growth can result from injury to the physis. This can result in a limb length inequality or angular deformity if the damage is asymmetric.

Infection is a risk in open fractures and in operative fixation of fractures. The presence of infection does not allow fracture healing at the maximal rate due to an attempt of the body to wall off and eliminate the infection. Infection causes necrosis, edema, and thrombosis of blood vessels which slow or prevent healing. However, infected fractures can heal if these are stabilized and the infection is suppressed. If possible, hardware is left in place and antibiotics are used to promote fracture healing. Because an infected union is better than an infected nonunion, the hardware and any areas of necrotic, infected bone are removed after bony union.

Distraction Osteogenesis (Callotasis or Ilizarov Lengthening)

This is a technique of achieving bone lengthening. The technique involves, creating a cortical disruption (often with preservation of the endosteum), waiting for a primary callus to form, and then gradually moving the two ends of the bone away. This results in an increase in length of the bone and its' surrounding soft tissues (Fig. 14).

Gavaril Ilizarov, a Russian orthopedist, has popularized distraction osteogenesis (in its modern sense). His technique consists of using a corticotomy, a very rigid construct providing stability to the distracted fragments, a short delay before starting, slow but high frequency movement and functional use of the limb during the lengthening.

With continuous tensile forces, there is early linear organization of collagen bundles. Type I collagen is the only collagen formed, with undetectable amounts of Type II or III. There is direct synthesis of mature fibrous organic matrix of bone without an intervening cartilage model. If the fragments take a curved path, there is more bone formation on the internal side of the arc. This tissue has been found to be rich in PDGFs A and B, as well as IGF-I and possibly -II. Additionally, patients undergoing distraction seem to produce mitogenic cytokines which are different to patients with skeletal fractures alone (10).

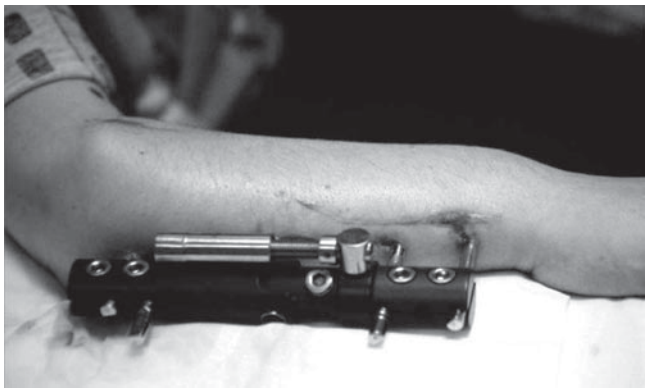

Fig. 14 Demonstration of ulnar distraction osteogenesis using monolateral external fixator assembly

An important histologic difference from fracture healing is the absence of cartilage formation in distraction osteogenesis. In fact, if the pathologist visualizes cartilage, it can be inferred that instability of the construct or fracture of the regenerate bone may have occurred. Experiments conducted by Dr. Ilizarov have suggested that the process of distraction results not only in bony lengthening but also true hyperplasia (rather than mere stretch) of soft tissues, blood vessels, and nerves – provided the technique is carried out meticulously and at an optimal rate of distraction. Failure to pay attention to detail can result in disaster for the patient, with complications such as infection, non- or malunion, nerve palsies, or blood vessel spasm, and may lead to salvage by amputation of a useless limb.

Healing of Tendons and Ligaments

Ligament repair is similar in many respects to bone. Collagen fibrils are formed early in repair; there is considerable formation of Type III collagen in scar tissue, and finally a stage of remodeling. Studies done on the healing of tendon have sup-

> Gavril Abramovitch Ilizarov (1921) – Gavril Ilizarov was born in June 1921 to a poor family in a village near Vitebsk, Russia. He was the oldest of eight children. As a boy, his family moved to the Caucasus mountain region, but poverty precluded schooling till the age of

11. He caught up quickly however, and was accepted to the Simpherol medical school in Crimea, in 1939. While studying basic sciences, the war between Germany and Russia broke out. This caused relocation of the medical school, and he graduated in 1944 from Kzyl-Orda. He was sent to work in the Kurgan district of Western Siberia. He became self-trained obstetrician, surgeon, internist, and orthopedician to the district, with primitive working conditions. He tended thousands of war invalids with war wounds, and without the help of antibiotics and only minimal surgical equipment. With trial and error, he developed from piano wires (Kirschner wires) and metal struts, an apparatus which provided rigid fixation, thus reducing the number of complications of these injuries. He received the Soviet patent for this device, one of the world's first tension wire skeletal fixators. He also discovered that a corticotomy allowed distraction and limb lengthening. Despite achieving considerable success with this device, he was not recognized by the Ministry of Health at the time. In 1967 however, he treated Valery Brumel (a Soviet high jumper) who had sustained a fracture in a motorcycle accident, and had been deemed untreatable by Moscow physicians. Following Brumel's treatment, he was granted an orthopedic hospital in Kurgan staffed by 350 surgeons. In the 1980s, his work became known to the Western world following visits by Italian and American surgeons to this hospital. In 1987, Ilizarov was awarded the Lenin Prize and made a member to the National Academy of Sciences of the USSR and shortly thereafter a People's Deputy, that is, a member of the Soviet parliament.

ported the similarity of stages of inflammation, proliferation, and remodeling. There is evidence that tendon never regains its original strength or chemical composition (4). In intrasynovial tendons, epitenon cells migrate to the site of rupture and may be responsible for the synthesis of Type I collagen (11). In intraarticular tendon graft repair (patellar tendon model), there is a stage of necrosis (where the graft depends on the integrity of surgical repair), followed by synthetic migratory cells of likely synovial origin. This is accompanied by revascularization which normally decreases with time. Persistent neovascularity may portend graft ill health. This is followed by "ligamentization" of the tendon, with poorly oriented fibers (12). The application of tension to healing tendons may enhance the process of healing. Such tissues have been shown to be more organized, and have numerous interfibrillar cross-links. The cytokines involved with the healing of tendons and ligaments appear to include PDGFs, IGF, and TGF-β.

There is less known about the healing of soft tissues to bone or of the so-called "extra-cortical fixation" in which metal is joined to bone.

Strategies to Enhance Fracture Healing

Several biologic and physical/mechanical techniques have been applied to the instances where the normal process of healing has been delayed or has undergone a complete cessation. The focus until recently has been on the physical and mechanical means of enhancing union in situations of delayed union, nonunion, or bone gap. Currently, there has been a search for specific molecules that can enhance the process selectively at various stages. Additionally, there is an understanding on the need to develop delivery systems for these molecules.

The delivery may be systemic or local. Safe systemic biologic methods of treatment have the advantage of eliminating surgery and the risks associated with surgical implants and bone grafts. Additionally, if successful, such strategies may be applied to nontraumatic conditions such as osteoporosis. Again, the understanding of the cellular mechanisms involved in bone formation and healing may allow rational treatment of conditions such as myositis ossificans progressiva. Unfortunately, these systemic methods are not as yet generally available. Local methods both biologic and physical/mechanical on the other hand have proved to be effective. Local biologic methods have recently been applied to clinical situations with encouraging results.

Biologic Enhancement

Systemic Strategies

Interest in these developed with the observation that patients with fractures and simultaneous head injuries develop exuberant callus in the fractured bones. They are also prone to develop heterotopic ossification, presumably at the site of additional soft-tissue injuries. This led to the search of systemic factors involved in the increased osteogenic response. The search has included the testing of peptide signaling molecules (such as TGF-β and fibroblast growth factors). There has been no conclusive result on the role of any factor as yet.

Interest has also developed in the systemic use of prostaglandins (several compounds are being tested with the best known being E_1 and E_2). Some preliminary encouraging results have appeared in literature. Additionally, there is the observation that prostaglandin inhibitors may reduce the osteogenic response (13).

Local strategies to improve fracture healing can be divided into osteogenic, osteoconductive, and osteoinductive. Osteogenic methods utilize naturally occurring materials (autogenous, allogenic, or demineralized allogenic bone grafts). Bone grafting has been in practice since the late nineteenth century. The idea that bone grafts may contain an osteogenic factor has been around for over a hundred years. Autogenous bone grafts heal by the stages similar to fractured bones, that is, by hematoma formation, release of bioactive molecules and cytokines, necrosis, inflammation, and fibrovascular proliferation followed by resorption of the graft by osteoclasts and replacement by host cells. The graft then behaves in an "osteoconductive" manner. Since the bone contains osteoprogenitor cells, a small "osteogenic" effect is also possible. Noted differences in the kinds of healing between cortical and cancellous grafts may be more a result of the physical properties (faster revascularization in cancellous grafts) rather than an innate biologic difference. There are, however, some differences in the rates of incorporation based upon the origin of the graft (cortical vs. cancellous as well as enchondral vs. membranous) and the methods used to fix the graft to the site of fracture. Less is known about allogenic grafts. Lyophilization (freeze-drying) has been used to reduce the immunogenicity of these grafts, and thus negate the effect of their histocompatibility antigens. There is, however, a risk of transmission of disease through such grafts. Processing of these grafts to overcome these problems may have effects on the mechanical integrity (and load-bearing capacity) of these grafts. Such processing also eliminates their osteogenic properties and so these grafts act in a osteoconductive manner. Autogenous marrow grafts have also been successful in treating delayed union in fractures. This kind of graft relies upon the osteogenic rather than the osteoconductive properties. Technical refinements of these kinds of grafts are being attempted to enhance their osteogenicity. These include improvements in isolation, purification, and cultural expansion of the osteoprogenitor pool. Selective adhesion techniques hold promise in this attempt. In animal models, this has been combined with calcium–phosphate–ceramic delivery system with good results (13).

Osteoconductive methods are those that support the growth of capillaries, perivascular tissues, and osteoprogenitor cells from the host into the implant or graft. They do not induce bone formation per se. Materials like ceramics including hydroxyapatite (Interpore), tricalcium phosphates, and bioactive glasses as well as certain synthetic polymers are some such examples. Some are combinations such as Collagraft (hydroxyapatite, tricalcium phosphate, fibrillar collagen). Questions are asked from time to time regarding their safety in the body and effect on the strength and remodeling of native bone if not completely resorbed.

A new strategy based upon this group of materials is dahlite – a material formed from a combination of inorganic calcium and phosphate to form a paste which can be injected into the fracture site. Animal experiments have suggested that the material can undergo remodeling and is completely resorbed and replaced by host bone.

Osteoinductive methods involve processes that support the mitogenesis of undifferentiated perivascular mesenchymal cells, leading to the formation of osteoprogenitor cells. Osteoinductive substances can lead to bone formation in extraskeletal sites in contradistinction to osteoconductive substances. Several factors may act together to potentiate the total effect. Some such substances thought to have an osteoinductive effect include TGF-β superfamily (including bone morphogenetic proteins (BMPs) 2–10 and related molecules), fibroblast growth factors, PDGFs, and certain immunoregulatory cytokines (IL1, IL6). (Please see Section *Bone Biology*.)

TGF-β, demineralized bone (a source of BMPs), and several such substances have been used to treat fractures, phalangeal and maxillofacial cysts, bone defects, and so on. The major problem with the use of demineralized bone has been the enormous quantities required for osteoinduction. About 1 μg of pure BMP is extracted from 1 kg of bovine bone.

Another approach has been to extract the bone-inducing factors from certain neoplastic cell lines such as the Saos-2 human osteosarcoma line. Although such lines produce considerable quantities of BMPs and although living Saos-2 cells are nonaggressive and do not survive implantation, there is still fear of using tumor produced products in the minds of the patients and public. The ability to extract this product in a "cell free" manner has not been effective in reducing this apprehension.

Recently, BMPs prepared by recombinant DNA techniques delivered in collagen carriers have been tested (13, 14). Results of radiologic and histologic union as well as mechanical strength studies in some of these studies have been positive. Locally delivered acid and basic fibroblast growth factors have also been tried in experimental situations. Results in these studies have suggested that positive or negative effects on healing may occur depending on the timing, delivery schedule, or ionic environment of the local site. Similarly, the application of PDGF has shown contradictory results (13). Some of these factors (such as TGF-β) may be osteoinductive only in combination with other proteins such as BMP or work to enhance and potentiate their effects. Collagen Corp. has used three substances: BMP 2 and 3 along with TGF-β2 to induce bone formation (15).

A problem in the use of such osteoinductive agents is the availability of suitable delivery systems. Carriers for the osteoinductive agents must be biocompatible. That means that the carrier (and its degradative product) must be nontoxic, nonimmunogenic, and nonreactive. Additionally, the carrier should withstand sterilization, have dose flexibility (for titrating doses), and be capable of allowing timed release

of the active agent. In its use in bridging bone gaps, the carrier should have rigidity (ideally similar to bone) and have no risk of transmitting infectious agents. Demineralized bone and synthetic biodegradable polymers are currently the options available. Of the latter, the ones frequently used include collagen, fibrin, poly-lactic acid, poly-glycolic acid, and poly-ortho ester. Hydroxyapatite and other osteoconductive materials could also potentially be used.

Mechanical and Biophysical Enhancement

Instability, excessive distraction, and other mechanical factors are some of the commonest reasons for the delay or cessation of fracture union. It was not unreasonable then, for interest to have developed in the treatment of fractures to focus on correcting and controlling these variables.

There are several observations. Electrical and electromagnetic stimulation may under certain conditions positively affect bone healing. It has also been seen that weight bearing or controlled rhythmic distraction has a beneficial effect on fracture healing. The healing response in rigidly internally fixed fractures is different from those which are casted or those treated by intramedullary nailing. Again, bone subjected to Ilizarov distraction heals under certain special conditions of optimal rates and forces.

These observations then point to the enormous role of the physical environment. However, advancement and scientific investigation into the role of the mechanical environment has been hampered by a lack of understanding on the translation of forces into cellular and molecular events. There are also differences (recognized at the clinical, but unexplained at the cellular levels) between the responses of fresh fractures to those that have gone on to nonunion.

Mechanical Stimulation

Studies by Page (16, 17) have suggested that in mechanically stable fractures, the initially produced Type III and V collagens are replaced at about 5–7 days by gradually increasing amounts of Type I collagen. There is a presence of chondroitin-4 sulfate, chondroitin-6 sulfate, and keratan sulfate. In mechanically unstable conditions however, there are smaller quantities of Type I collagen, larger quantities of Types II and IX collagen, and the glycosaminoglycans are of similar types but are very highly sulfated. These observations would fit in with the histologic observations of the increased amounts of cartilage seen in the latter situations.

Despite Wolff's observation that the structure of bone adapts to changes in its stress environment over a hundred years ago, there has been very little understanding of this relationship at the cellular level (18).

Sarmiento et al. have observed a beneficial effect of weight bearing on healing; however, this has been disputed by other workers (19, 20). The idea that disuse may be partly responsible for the discrepant results in some of these situations has been proposed. Bone healing in microgravity situations such as on a space shuttle flight has also been studied (21). Although differences have been found in the healing under conditions of reduced gravity, it has been exceedingly difficult to separate the effects of the gravity from the metabolic effects of the space environment. Additional experiments with appropriate controls to address this problem may be needed.

The notion that interfragmentary strain is of extreme importance in the healing of tissues has had circumstantial and experimental support. The former has come by the way of the sequence of healing and the idea that tissues such as cartilage and fibrous tissue allow less strain (essential later in healing) than granulation tissue (earlier in healing) which has a greater tolerance. Biomechanical studies by Blenman et al. and Carter et al. have resulted in a unified theory. This relates mechanical loading to tissue differentiation. Using two-dimensional finite analysis in an osteotomy model, these authors identified two mechanical parameters as key. These are the "cyclical hydrostatic stress" or pressure and cyclical tensile strain. According to these studies, there are associations between intermittent compressive hydrostatic stress and chondrogenesis, between intermittent strain and fibrogenesis, and between low levels of mechanical stimulation and either osteogenesis (good vascularity) or chondrogenesis (poor vascularity). Additionally, once cartilage has formed, cyclical tensile strain (distortional strain) accelerates enchondral ossification. Local cyclical hydrostatic stress, however, delays enchondral ossification, possibly by inhibition of revascularization (22, 23).

On the basis of investigations into the role of mechanical environment, several workers have attempted to design systems in which mechanical input stimulates fracture healing. Controlled micromotion has been successful in experimental models and has been applied to clinical situations (13, 24). Some devices have been fabricated which allow micromotion controllable in the numbers of cycles and frequency using transfixon pins, sliding clamps, and pneumatic pumps.

Electrical Stimulation

Although interest in electrically stimulating the healing of bony union has been around since the middle of the nineteenth century, it is only in the past 30 years or so that objective

evidence has been gathered about its application. Devices began being used in the 1970s in clinical situations in the mainstream physician practices. In general, three kinds of devices are used: constant direct current (using percutaneous or implanted electrodes); time-varying inductive coupling produced by a magnetic field (noninvasive); and capacitative coupling (noninvasive).

Constant direct current produces osteogenesis in a dose–response manner above a minimal threshold and may cause tissue necrosis in excess. In electromagnetic stimulation, a time varying magnetic field is generated, which in turn generates a (time varying) electric field in the tissues. In capacitative coupling, an electric field is induced by an external capacitator.

Most instances of electric stimulation in clinical practice have been on patients with nonunions. The data from several such trials (including double-blind trials) has been excellent and the procedure is now firmly established as a valid clinical modality (Fig. 15). There, however, is less information available with regard to fresh fractures. Additionally, an understanding of the processes involved at the cellular level is still in its infancy.

Ultrasound Stimulation

While the diagnostic applications of ultrasound require very low intensities (milliwatts per square centimeter), the physical therapists have used higher intensities (1–3 W/cm^2) to heat tissues. This has been shown to have beneficial effects on joint stiffness, muscle spasm and muscular mobility. Early studies showing its efficacy in bone union were done in the 1980s (25).

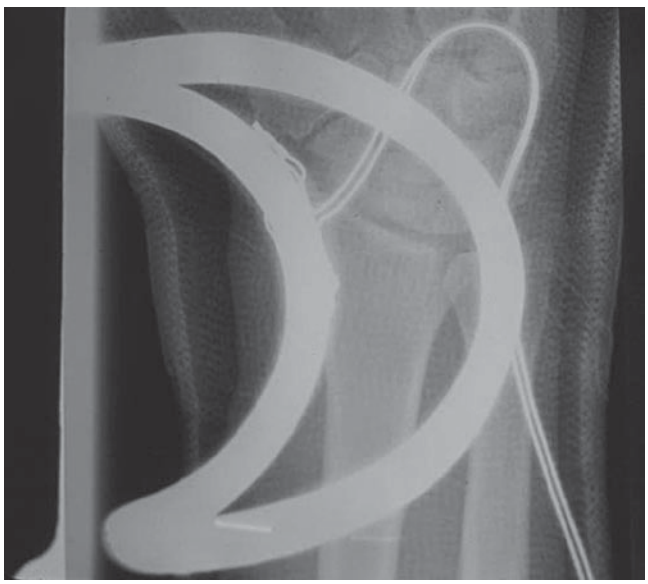

Fig. 15 Electrical stimulation using a standard electromagnetic coil for a nonunion of a scaphoid fracture

Subsequently, several studies and clinical trials have confirmed the earlier reports leading to approval by the US Food and Drug Administration for its use in certain situations (13).

In summary, although several advances have been made in fracture union in the mechanical and biophysical methods, there is only a recent interest in the biologic methods of therapy. Future directions will probably continue to focus on the cellular understanding of these processes. The day, however, that gene therapy will allow the insertion of "helpful" promoter sequences or receptor agonists to aid healing is still some distance away. A problem in the understanding of the efficacy of therapies has been the difficulty in quantifying fracture healing. Another is identifying fractures which are at risk for problems in union.

Common Problems in Orthopedic Surgery

Discussed are common conditions in orthopedic surgery. These two problems are indirectly related to bone trauma. The help of the musculoskeletal pathologist is frequently requested in the management of these conditions. It is therefore advantageous to be familiar with these entities and with the concerns of the surgeon.

- Heterotopic ossification
- Myositis ossificans
- Reflex sympathetic dystrophy (algodystrophy)
- Avascular necrosis
- Other osteochondritides
- Legg-Calve-Perthes Disease

Heterotopic Ossification (HO)

This refers to the presence of bone formation within the soft tissues. It is to be distinguished from the metastatic calcification that occurs in conditions such as hyperparathyroidism. It must also be distinguished from traumatic ossification (myositis ossificans). The site of most concern to the orthopedic surgeon is the hip, in the context of postoperative ossification following total hip arthroplasties. The prevalence of HO varies from 2 to 90% depending upon the population operated and the diagnostic criteria used. Severe HO results in restriction of movement and an unsatisfactory result.

In the most common region, the hip, there are two basic forms of HO: the central type (that develops around the neck of the femoral component) and the lateral type (that develops around the greater trochanter). The lateral type is associated with the lateral surgical approach (McFarland approach), and therefore would represent a form of traumatic (myositis-type) ossification.

The central ossification appears to be individual specific and is unrelated to surgery. It is unrelated to the kind of local procedure, prior operations, preoperative hip motion, prosthesis cement, or operative approach. This suggests that systemic and genetic rather than local factors may be more important in the causation of HO.

The amount of HO can be quantitated on X-rays by several schemes (26). Methods to prevent or reduce the amount of HO include anti-inflammatory drugs and irradiation.

The role of the pathologist is in confirming the diagnosis and distinguishing it from other possible causes of soft-tissue ossification, including neoplasms. The pathologist is also important in the teams investigating the nature and pathogenesis of this condition.

Myositis Ossificans

This is a time honored term and continues to be used despite being neither a muscle nor an inflammatory disorder. It refers to the reaction to trauma, seen most often in soft tissues, but also in a subperiosteal location (subperiosteal hematoma). The entity most often represents a localized tissue disruption, followed by a hematoma. This hematoma gets organized in a fashion similar to a healing fracture. Ossification commences from the outside to within. Eventually, the entire mass may get ossified. From the point of the surgical pathologist, this can present a problem, since it may clinically present as a painful mass and be biopsied under the clinical impression of it being a soft-tissue tumor. In these situations, the central fibroblastic repair reaction can be alarming (Figs. 16a–d and 17).

Mistakes can be avoided by paying attention to the characteristic radiologic and histologic clues. By CT scan, it is often possible to see a peripheral rim of bone formation. This sign may be absent very early or very late in the evolution of the lesion. When present, however, it is a valuable sign and serves to differentiate it from bone-forming tumors such as extraskeletal osteosarcomas. Tumors in general tend to have bone formation centrally or more haphazardly placed.

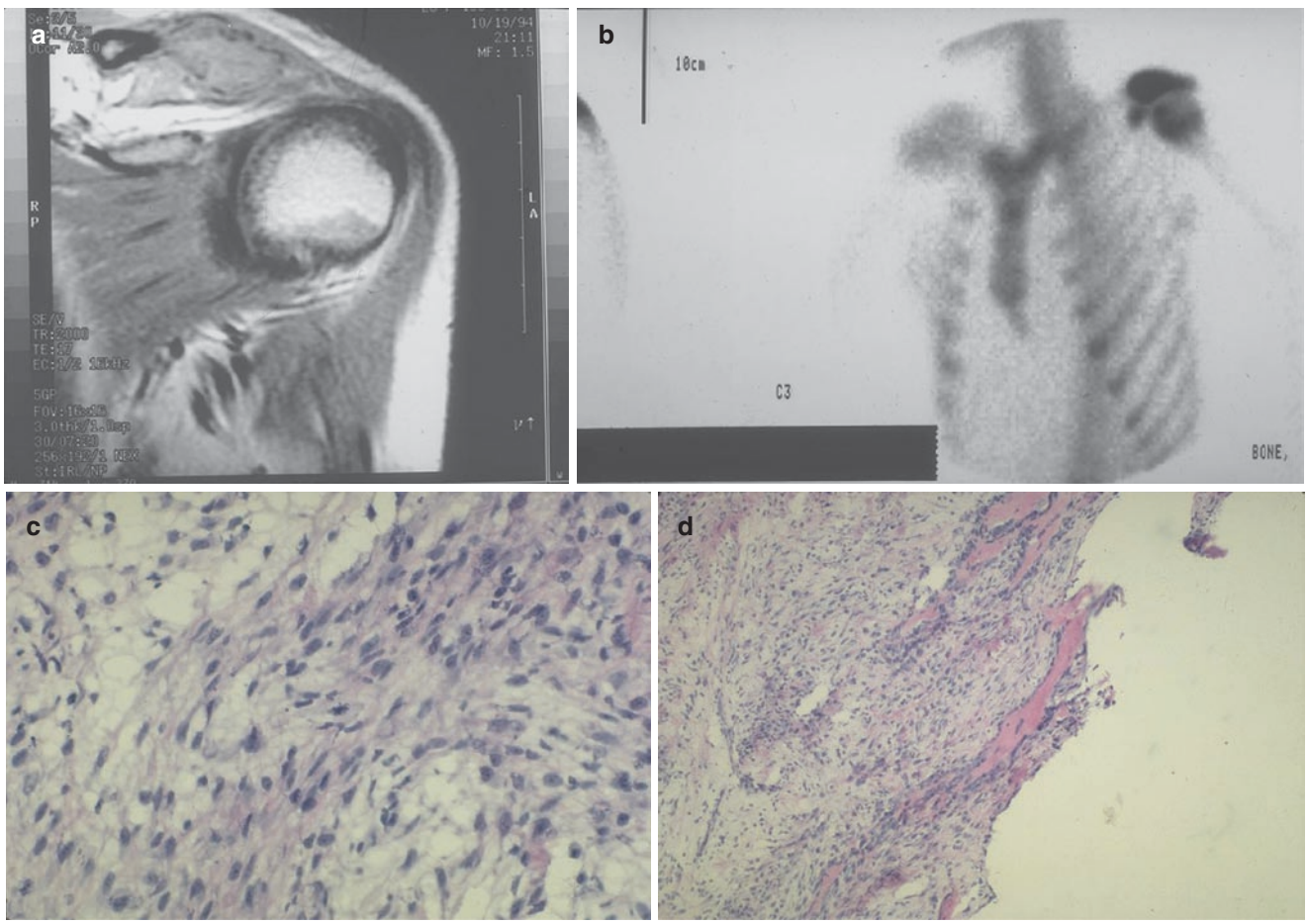

Fig. 16 **a** An MRI from a 13-year-old girl who presented with a mass in the clavicle which clinically mimicked a malignant bone tumor. **b** The mass was hot on bone scan. A tentative diagnosis of osteosarcoma was made and the patient was biopsied. **c** A frozen section revealed a hypercellular central portion with numerous mitotic figures. **d** Peripherally, there was woven bone and a low-power architecture suggesting an encasing rim (zonation phenomenon). A tentative diagnosis of myositis was rendered and subsequently confirmed on permanent sections

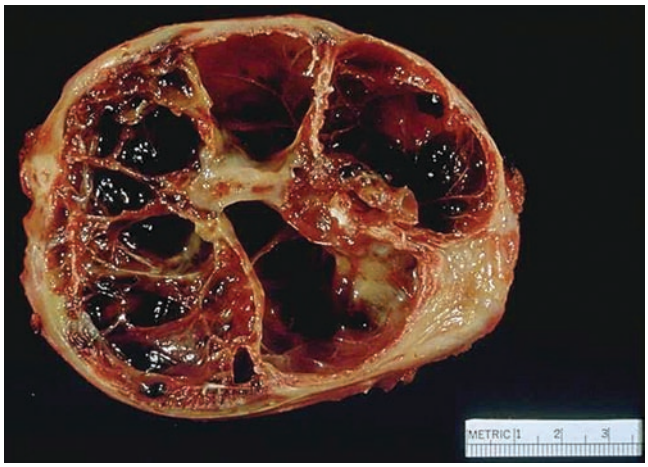

Fig, 17 Myositis ossificans forming a peripheral shell of bone around a central area of hemorrhage and repair

Histologically, myositis shows a zonation phenomenon. This corresponds to the peripheral rim of ossification seen radiologically and is its microscopic equivalent. The finding of mature tissues situated in an organized fashion on the outer side of the lesion, with a fibroblastic or immature, reactive, spindle-cell center is extremely suggestive of myositis ossificans.

Myositis ossificans of this type described above is often referred to as "traumatic myositis ossificans" to differentiate it from the congenital type of myositis ossificans or myositis ossificans progressiva. The latter term is also a misnomer and would best be abandoned altogether in favor of fibrodysplasia progressiva (see Section *Inherited Diseases of the Skeleton*).

Reflex Sympathetic Dystrophy (Algodystrophy), Now Known as Complex Regional Pain Syndrome (CRPS)

This term refers to a condition of severe regional, patchy, osteopenia and often pain, following trauma. The condition is associated with trophic skin changes, edema of the extremity, and psychological disturbances in the afflicted patients. Most often, a peripheral portion of an extremity is involved (hand or foot), but proximal parts of the appendicular skeleton and the axial skeleton are not immune. Occasionally, the condition can arise in the absence of trauma, and even less often, in association with pregnancy. The condition is infrequent, and afflicts a minority of posttrauma patients, but can prove severely disabling.

Reflex sympathetic dystrophy must be differentiated from other forms of osteopenia such as bone marrow edema, transient osteoporosis, migratory osteolysis, and idiopathic regional osteoporosis. These latter entities are benign, self-limited forms of osteopenia that are not accompanied by loss of function of the limb, or by pain. The underlying path physiology, however, may perhaps be related (27). In cases where this condition is suspected, MR imaging can prove a sensitive tool for early detection (loss of signal on T1-weighted images, along with an increased signal on T2-weighted images). Rest, analgesics, sympathetic blockade, and core decompression have been used to treat the condition. Histologically, there is a proliferation of fibroblasts within the marrow space, but there is little that is characteristic or diagnostic of the condition. Some authors have noted bone necrosis and new bone formation as well.

Osteonecrosis (Avascular, Aseptic, Ischemic Necrosis)

Osteonecrosis refers to the in situ death of bone, presumably from one or more vascular insults. Although the pathology of osteonecrosis is well worked out, the pathogenesis remains an enigma. It may be related to disruption of the blood supply to bone, either by blockage, trauma, or increased intraosseous pressure.

Osteonecrotic bone may either repair (favorable outcome) or undergo failure and collapse (unfavorable outcome). The latter event occurs when remodeling and renewal are absent or insufficient. The combination of constant mechanical insult then causes the bone to eventually fail.

Two Main Forms of Osteonecrosis

- Medullary infarction (marow cavity and trabecular bone). This is usually silent.
- Cortico-medullary infarction (cortex also involved). This may be painful and progressive.

Conditions predisposing to osteonecrosis include trauma, infection, fatigue fractures, alcohol abuse, dysbarism, Gaucher's disease, connective tissue disorders, vasculitides, hemoglobinopathies, coagulopathies, radiation injury, corticosteroid therapy, pregnancy, aging, gout, fat embolism, hypersensitivity reactions, infections, thromboplastin release in malignancies and inflammatory bowel disease, pancreatitis, and childhood "osteochondritides" such as Perthe's, Keinbock's, Sever's, Kohler's, Larsen's, Blount's, or Panner's diseases. The mechanisms of blood supply interruption are included in Table 2.

Six arterial groups supply the long bone. Epiphyseal, metaphyseal, and diaphyseal (one set from each end of bone). These systems anastomose. In addition, there is anastamosis between the medullary, periosteal, and soft-tissue vasculature. The medullary supply originates in the diaphyseal nutrient

Table 2 The four main mechanisms of damage to the vascular supply of bone and some examples

Mechanism	Example
Mechanical interruption	Fractures and dislocations
Thromboembolism	Nitrogen gas bubbles, fat, abnormal (sickle) red cells
Vessel injury or pressure	Vasculitis, radiation, angiospasm producing substances (Gaucher's disease), extravasated blood, marrow-packing disorders
Venous occlusion	Chandler's disease, when the joint is distended with fluid

vessels and provides supply to the bone marrow, trabecular bone, and the inner half of the endosteum. The periosteal, muscular, metaphyseal, and epiphyseal vessels supply the outer one third to half of the cortex.

The condition is suspected on the basis of history, physical findings, X-rays, and scanning techniques. MRI is an especially sensitive method. Early scans show a photon deficiency (doughnut sign) at the site of the necrosis with surrounding hyperemia. Within a matter of weeks, this becomes a uniform signal. This is reduced on both T1- and T2-weighted images. With time, this signal may vary to reflect that revascularization is occurring.

The diagnosis of osteonecrosis is confirmed by biopsy. Necrotic bone is identified by anucleate bony trabeculae often in the context of marrow infarction. Early in the course of healing of osteonecrosis, there is reactive hyperemia. Vascular fibrous repair tissue proliferates adjacent to bone. The dead bone gets walled off by this tissue, in a fashion similar to sequestrum formation in osteomyelitis. Revascularization of dead bone occurs in a few weeks. Cutting cones carrying blood vessels enter the dead bone. These vessels remove dead bone by osteoclastic resorption. At the same time, osteoblasts lay down bone on the top of this necrotic fragment (creeping substitution). The next stage is unpredictable, and probably depends upon the site and extent of damage. It may culminate in restitution (complete healing). Or, it may lead to the relentless continuation of the repair process that damages the integrity of bone. This second course, leads to fatigue fractures, collapse of the subchondral bone, cartilage disintegration, and joint deformity (Fig. 18a, b).

Depending upon the cause of osteonecrosis, supportive management of the primary problem may be required. This is especially true in conditions such as Gaucher's disease, dysbarism, and sickle cell anemia. Short-term immobilization, anti-inflammatory drugs, exercises, and limiting weight bearing are additional supportive measures.

Drilling of the segment has been attempted in an effort to "decompress" the area, and to bring vascular supply to it. This can be combined with a core biopsy, which would then serve both diagnostic and therapeutic measures. Despite the popularity of this procedure however, there is very little proven benefit of drilling.

Electrical stimulation and vascularized fibular grafts have also been attempted. The results of such procedures suffer from insufficient numbers for analysis. Osteotomies to alter "coverage" in the hip have had waves of popularity from time to time. The end result of osteonecrosis, a deformed joint, may ultimately require prosthetic replacement.

Perthes Disease (Legg-Calve-Perthes Disease)

This condition refers to the osteonecrosis of the femoral head occurring in children. Most often this occurs in the ages between 3 and 12 years. This osteonecrosis is associated with a constitutional delay in growth, and perhaps altered skeletal proportions. The presentation is with pain, shortening, Trendlenburg gait, and limitation of abduction and internal rotation. The eti-

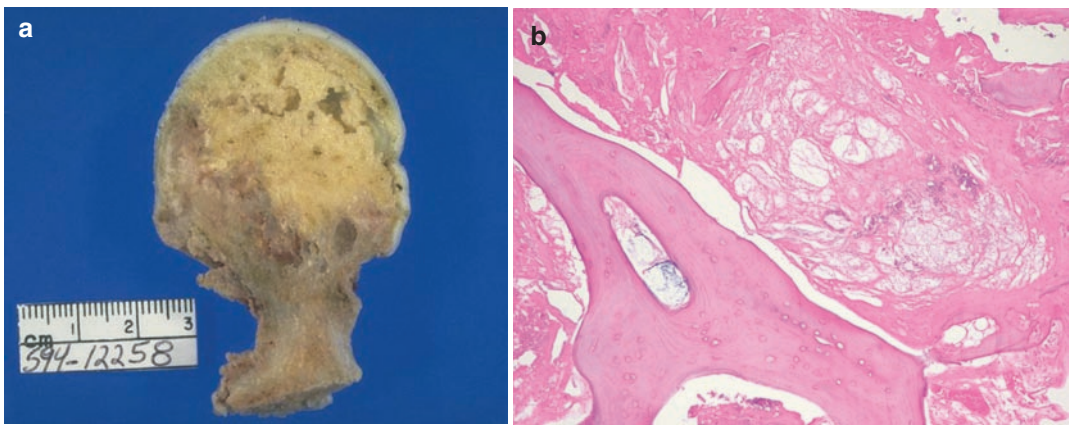

Fig. 18 **a** Femoral head with avascular necrosis and collapse. **b** Avascular necrosis showing anucleate bony trabeculae. The surrounding marrow is necrotic

ology is not understood, but may be related to an acute transient synovitis with secondary compression of the retinacular blood vessels supplying the femoral head. The disease may be a local manifestation of a systemic disorder, in that there is primary thickening and disorganization of the growth plate in these patients. This could render the femoral head more likely to suffer an avascular insult. Cartilaginous dysplasia has been found by epidemiological studies in these children. These children are shorter and tend to have small feet (28).

Technetium bone scans and MR scans are utilized in the early diagnosis of this condition. The classification of the extent of the disease has been based upon the plain X-ray features. The commonly used schemes are those of Catterall and Salter–Thompson (28) or the lateral pillar classification scheme. Quantitative methods such as Mose's rings may be more accurate than these traditional schemes, but are applicable to the late stage. The management is directed toward improvement in motion in the synovitis stage, along with symptomatic treatment.

Methods to achieve coverage of the femoral head, as well as the benefit of containment are controversial. Containment refers to the attempt at improving coverage of the femoral head in the acetabulum. This attempt is said to improve the outcome, but are utilized only in the more severely affected cases, or those at risk for complications. Numerous nonoperative and operative methods are utilized in order to achieve this result. Long-term complications are managed by osteotomies or arthroplasties.

Other Osteochondritides

Osteochondritis "juvenalis" refers to the earlier set of eponymic names for avascular necrosis occurring in certain bones. This includes conditions such as Perthe's, Sever's, Kohler's, Keinbock's, Larsen's, Blount's, or Panner's diseases. With the exception of Perthes disease (which may be associated with constitutional skeletal abnormalities), these conditions are no different to the musculoskeletal pathologist than the osteonecrosis occurring in the noneponymic locations.

References

1. Kleinman PK, Marks SC. The metaphyseal lesion in abused infants: a radiologic-histopathologic study. Am J Roentgenol 1986; 146: 895–905.
2. Nelson Textbook of Pediatrics. Part XXXI – Bone and Joint Disorders, Section 1: Orthopaedic Problems 2008; 18: 2771–811.
3. Rang M. Rang's Children's Fractures. 3rd ed. Lippincott, Philadelphia, 2005.
4. Liu SH, Yang R, Al-Shaik R, et-al.. Collagen in tendon, ligament and bone healing. Clin Orthop Rel Res 1995; 318: 265–78.
5. Lynch SE, Buser D, Hernandez RA, et-al.. Effects of platelet derived growth factor/insulin like growth factor 1 combination on bone regeneration around titanium dental implants. J Periodontol 1991; 62: 710–6.
6. Lynch SE, DeCastill GR, Williams RC, et-al.. The effect of short term application of platelet derived and insulin like growth factors on peridontal wound healing. J Periodontol 1991; 62: 458–67.
7. Andrew JG, Hoyland J, Andrew SM, et-al.. Demonstration of TGF-beta1 mRNA by in situ hybridization in normal human fracture healing. Calcif Tissue Int 1993; 52: 74–8.
8. McQueen MM, Gaston P, Court-Brown CM. 2000; Acute compartment syndrome: who is at risk? JBJS(B) 82: 200–3.
9. Geerts WH, Code KI, Jay RM, et-al.. A prospective study of venous thromboembolism after major trauma. N Engl J Med 1994; 331: 1601–6.
10. Holbein O, Neidlinger-Wilke C, Suger G, et-al.. Ilizarov callus distraction produces systemic bone cell mitogens. J Orthop Res 1995; 13: 629–38.
11. Gelberman RH, Amiel D, Harwood F. Genetic expression for type I procollagen in the early stages of flexor tendon healing. J Hand Surg 1992; 17A: 551–8.
12. Amiel D, Kleiner JB, Doux RD, et-al.. The phenomenon of ligamentization: anterior cruciate ligament reconstruction with autogenous patellar tendon. J Orthop Res 1986; 4: 162–72.
13. Einhorn TA. Enhancement of fracture healing. JBJS(A) 1995; 77: 940–56.
14. Cook SD, Wolfe MW, Salkeld SL, et al. Effect of recombinant human osteogenic protein-1 on healing of segmental defects in non-human primates. JBJS(A) 1995; 77(5): 734–50.
15. Bentz H, Thompson AY, Armstrong R, et-al.. Transforming growth factor-beta 2 enhances the osteoinductive activity of a bovine bone derived fraction containing bone morphogenetic protein-2 and protein-3. Matrix 1991; 11: 269–75.
16. Page M, Hogg J, Ashhurst DE. The effects of mechanical stability on the macromolecules of the connective tissue matrices produced during fracture healing. I: The collagens. Histochem J 1986; 18: 251–65.
17. Page M, Ashhurst DE. The effects of mechanical stability on the macromolecules of the connective tissue matrices produced during fracture healing. II: The glycosaminoglycans. Histochem J. 1987; 19: 39–61.
18. Wolff J. Das Gaesetz der Transformation der Knochen. Hirchwald, Berlin, 1892.
19. Sarmiento A, Schaeffer JF, Beckerman L, et-al.. Fracture healing in rat femora as affected by functional weight-bearing. JBJS(A) 1994; 76: 820–6.
20. Riggins RS, Simanonok C, Lewis DW, et-al.. Weight bearing: its lack of effect on fracture healing. Int Orthop 1985; 9: 199–203.
21. Kirchen ME, O'Conner KM, Gruber HE, et-al.. Effects of microgravity on bone healing in a rat fibular osteotomy model. Clin Orthop Relat Res 1995; 318: 231–42.
22. Blenman PR, Carter DR, Beupre GS. Role of mechanical loading in the progressive ossification of a fracture callus. J Orthop Res 1989; 7: 398–407.
23. Carter DR, Blenman PR, Beupre GS. Correlation between mechanical stress history and tissue differentiation in initial fracture healing. J Orthop Res 1988; 6: 736–48.
24. Goodship AE, Kenwright J. The influence of induced micromovement upon the healing of experimental tibial fractures. JBJS(B) 1985; 67: 650–5.
25. Duarte LR. The stimulation of bone growth by ultrasound. Arch Orthop Trauma Surg 1983; 101: 153–9.
26. Kjaerssgaard-Anderson P, Ritter MA. Prevention of formation of heterotopic bone after total hip arthroplasty: current concepts review. JBJS(A) 1991; 73: 942–7.
27. Doury P. Bone marrow oedema, transient osteoporosis and algodystrohy. JBJS(B) 1994; 76: 993–4.
28. Wenger DR, Ward WT, Herring JA. Legg-Calve-Perthes disease – current concepts review. JBJS(A) 1991; 73: 778–88.

Chapter 11
The Surgical Pathology of Bone Infections

Jasvir S. Khurana

Abstract Infections and inflammations of bone (osteitis) and the bone marrow space (myelitis) are among the most commonly encountered problems in orthopedic surgical pathology. The majority of infections are limited to pyogenic, tubercular, and fungal organisms. Viral, rickettsial parasitic, and other infections are much less commonly seen. With the AIDS epidemic, however, several organisms that were previously considered rare are being increasingly seen. Viral, rickettsial, and other organisms have been reported.

Keywords Infection • Pyogenic • Osteomyelitis • Osteitis • Myelitis • AIDS • Tuberculosis • Fungi • Viruses • Parasites • Hematogenous • Aerobic • Anaerobic • In volucrum • Sequestrum • Cloacae • Brodie's abscess • Sinus tract • Sclerosing osteomyelitis • Garre's osteomyelitis • Chronic multifocal Osteomyelitis • Syphilis

Pyogenic Osteomyelitis

Infections can reach the bone either by the *hematogenous route* or by *direct extension* of a focus of infection. The former is by far the most common. In this situation, an antecedent focus of infection may be present elsewhere. The latter is seen in situations of trauma, following manipulations, or compound fractures and occasionally in iatrogenic implantation of infective material.

Most cases of hematogenous osteomyelitis are seen in the long tubular bones in children. In this situation, the infection is most frequently seen predominantly in a metaphyseal location. In adults, hematogenous osteomyelitis is less frequent, and flat bones contribute a considerable number. Even in adults, metaphyseal long bone involvement is the more common form of involvement. The metaphyseal location is often explained by Trueta's hypothesis, which suggests that the blood flow is sluggish in the metaphysis as the supplying vessels take a bend in that region. The region is of course richly supplied by blood and is the site of the majority of the cancellous bone and bone marrow. Phemister showed that the rates of infection correlate with periods of maximal growth.

Osteomyelitis by direct extension by contrast has no such predisposition whether in children or in adults. In children, the physeal plate and the articular cartilage form relatively efficient barriers to the infection and tend to limit the infection to the bone, thereby preventing extension into the joint. Secondary joint infection although infrequent may occasionally be seen, especially in situations where the metaphysis is intra-articular (such as in the hip).

Commonly encountered organisms include *Staphylococcus aureus* followed by *Escherichia coli*, *Klebsiella* species and Pseudomonas species. Patients with sickle cell may get a cortically based osteomyelitis caused by *Salmonella* (choleraesuis, paratyphi B, and typhimurium). Neonates are prone to *Treponema* (periostitis), Gram-negative rods, *Streptococci*, *Hemophylis influenzae*, and *Listeria* species. Pseudomonas infections are not infrequent in addicts abusing intravenous street drugs. This kind of infection may occur in locations such as the clavicle and the sternoclavicular joint. Pseudomonas is also a frequent organism found subsequent to puncture wounds from sharp objects, such as a nail wound through a sneaker.

Acute Infections

Osteomyelitis usually starts in an "acute" fashion. The infection may resolve spontaneously, but much more frequently requires aggressive (and often long-term) antibiotic therapy. The patient is usually very sick, often blood cultures are positive. In the treatment, antibiotics should be chosen with care, since the bone levels of many drugs are less than the serum levels. Cloxacillin, nafcillin, third-generation cephalosporins (ceftriaxasone, etc.), ciprofloxacillin, and so on. are frequently employed. The clinician is usually guided by the culture and sensitivity reports and the minimum inhibitory concentration demonstrated by the drug in the specific infection.

Plain X-rays in early stages may be negative, three-phase bone scans (sometimes with concomitant Gallium or Indium scanning, MRI or other studies may be needed to help make the diagnosis). Later, the X-rays can show prominent periosteal reaction, mimicking bone neoplasms such as Ewing's sarcoma.

J.S. Khurana (ed.), *Bone Pathology*, DOI 10.1007/978-1-59745-347-9_11,

The role of surgery in very early infections is possibly limited. However, in the event of even minimal bone destruction, abscess formation, localization of infection, and so on surgical debridement and drainage may serve to limit the further extension of established infection.

Surgical Pathology

Grossly, the changes may be minimal or marked. In the obvious cases, there is pus within the bone. The bone may be lifted off, or clearly necrotic.

Microscopically, bone destruction, polymorphonuclear leukocytes, and cell debris are seen. The region is often intensely hyperemic. The pressure exerted by the pus may compress smaller vessels. This possibly results in additional ischemic damage to bone. The exudate follows the path of least resistance and exits through the Volkmann canals into a subperiosteal location. In the neonatal age group, the Sharpey's fibers are less developed and considerable subperiosteal spread may occur. Medullary spread causes additional damage. In severe cases, the combination of subperiosteal and intramedullary spread can cause the entire diaphysis to become necrotic, forming a "ring sequestrum." The role of decompressive surgery in such situations is obvious. Fortunately, these situations are infrequent.

Dead bone is absorbed by granulation tissue and osteoclastic activity on its surface. When the dead bone is large, it is gradually separated from the living bone by the granulation tissue. In this situation, it is called a *sequestrum*. This bone is avascular and usually stands out on X-ray examination as being *dense* in comparison to the surrounding hyperemic and decalcified bone. By this time, the disease has passed into chronicity. (The distinction between acute and chronic osteomyelitis is somewhat arbitrary and is often based on clinical grounds). It should be remembered in this context, that polymorphonuclear leukocytes can remain in bone for long periods of time (several weeks), and may not be a good guide to the acuteness of the process. Some pathologists use these to define acute osteomyelitis, and if this is the practice, then good communication is essential between the treating team and the pathologist to prevent misunder-standing.

Course: The infection may heal (either spontaneously or more often as a result of treatment). Untreated cases, or suboptimally treated cases usually progress into chronicity. Organisms of lesser virulence often get walled off by a ring of dense bone (Brodie's abscess). The infection in this situation can reactivate at any time, or the organisms may die, leaving behind a sterile cavity filled with fluid or fibrous tissue. Late recrudescence is not infrequent.

Chronic Infections

Although chronic bone infections can start de novo, the majority, are a result of unresolved acute osteomyelitis. Chronic osteomyelitis is a frequent problem in developing countries.

Patients with chronic bone infections have a protracted course, interspersed with acute exacerbations. The organisms may be present in very low levels and the cultures are often returned as "sterile." Common organisms include *S. aureus*, *Streptococci* (group A is more frequent), *Klebsiella* (which causes extensive bone damage), *Aerobacter*, *Proteus*, *Brucella*, *Staphylococcus epidermidis*, and *Bacteroides*. These infections are notoriously resistant to antibiotic therapy except in the exacerbation (Fig. 1).

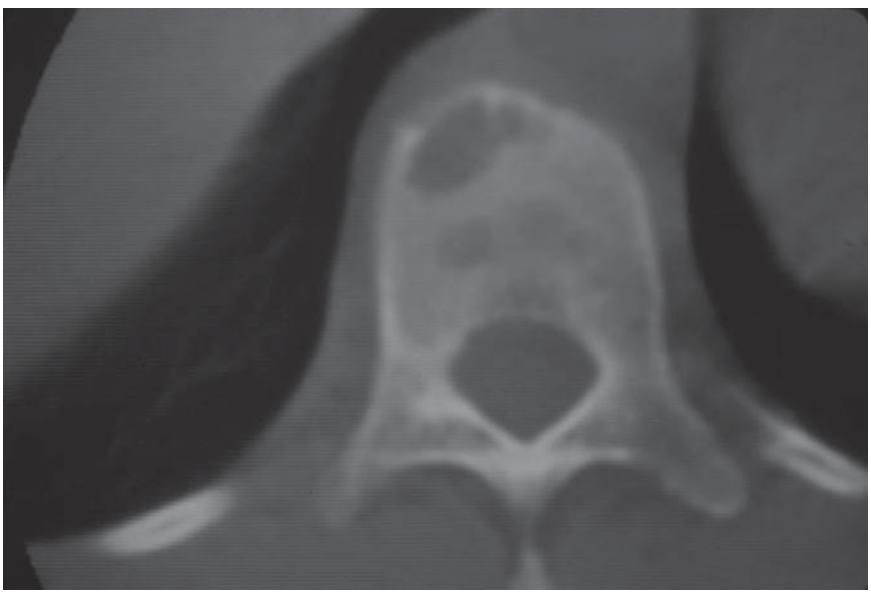

Fig. 1 Brucella involving the vertebra and the adjacent disk space

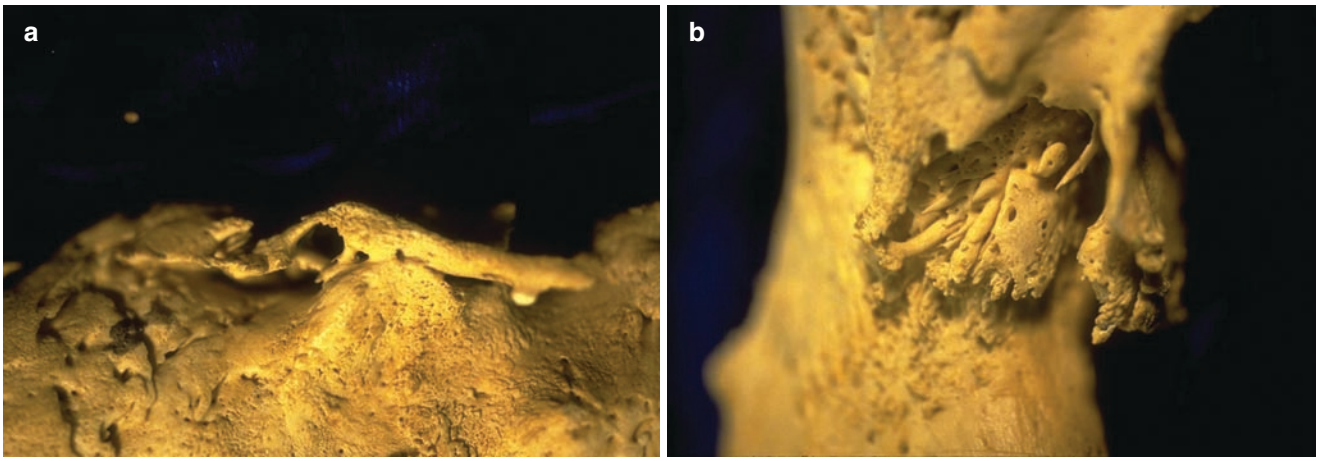

Fig. 2 Chronic osteomyelitis showing markedly (**a**) irregular bone thickening and (**b**) residual sinuses

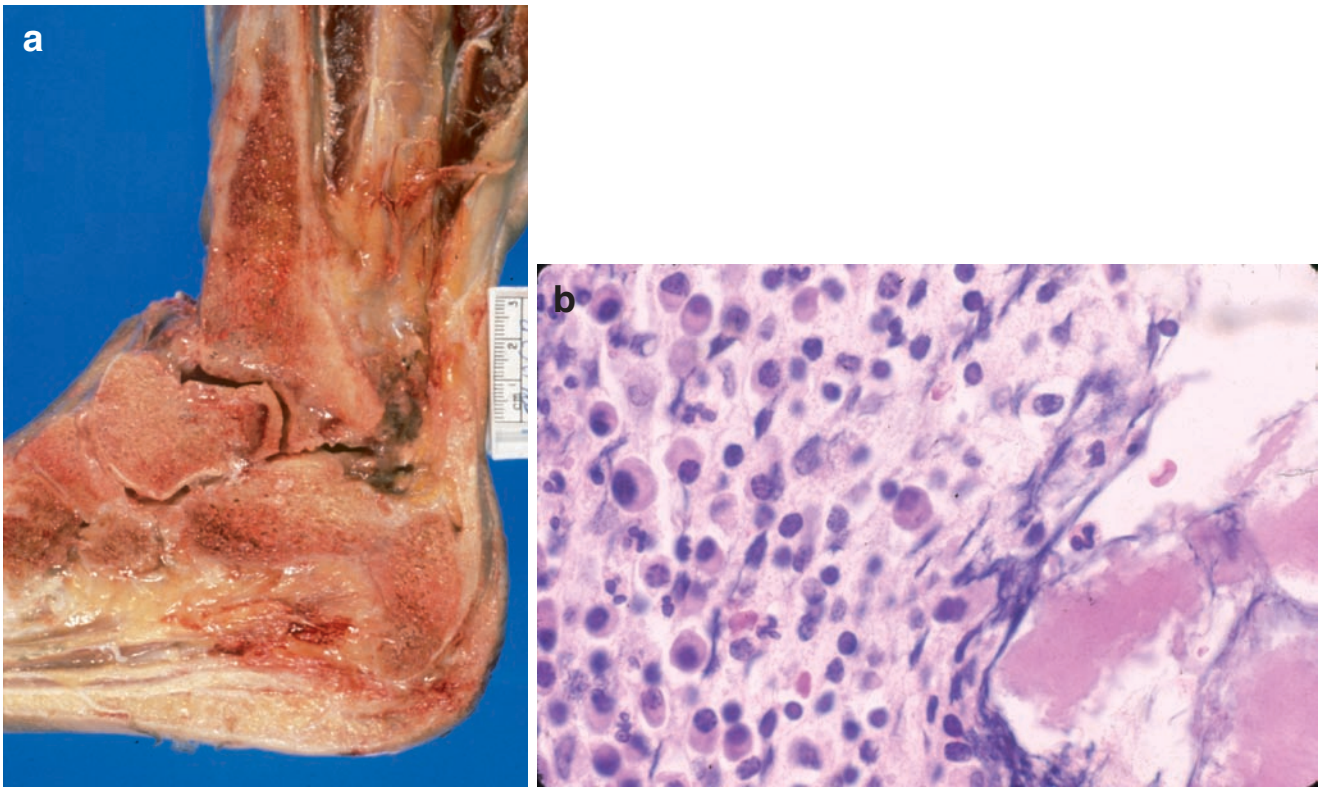

Fig. 3 **a** Chronic osteomyletis involving multiple bones of the foot and the ankle space. The pus has lifted the periosteum and has penetrated it, to lie free in the ankle joint and the surrounding soft tissues. **b** Chronic osteomyelitis characterized by ragged, anucleate, necrotic bone and a lympho-plasmacytic inflammatory infiltrate

Surgical Pathology

Grossly, there may be sequestrated necrotic bone, new bone (involucrum), and draining sinuses (Fig. 2a, b and 3a). Not infrequently, the chronic infections show the presence of necrotic bone, which persists and is surrounded by granulation tissue (the sequestrum). Separation of the sequestrum generally takes months to complete. This bone is usually of cortical origin, since the cancellous bone is much more easily absorbed and replaced by viable bone. The sequestrum can be recognized on plain X-rays as being radiodense, and more accurately by CT scanning as being a fragment of bone lying in a cavity separate from the main cortex. The bone surrounding a focus of chronic osteomyelitis is often dense, and is referred to as the "involucrum." The involucrum is often of periosteal origin. The involucrum frequently has several openings or "cloacae" through which exudate, bone debris, and sequestra exit and pass through sinus tracts to the surface. Constant destruction of the neighboring soft tissues leads to scarring, and squamous metaplasia of the sinus tract.

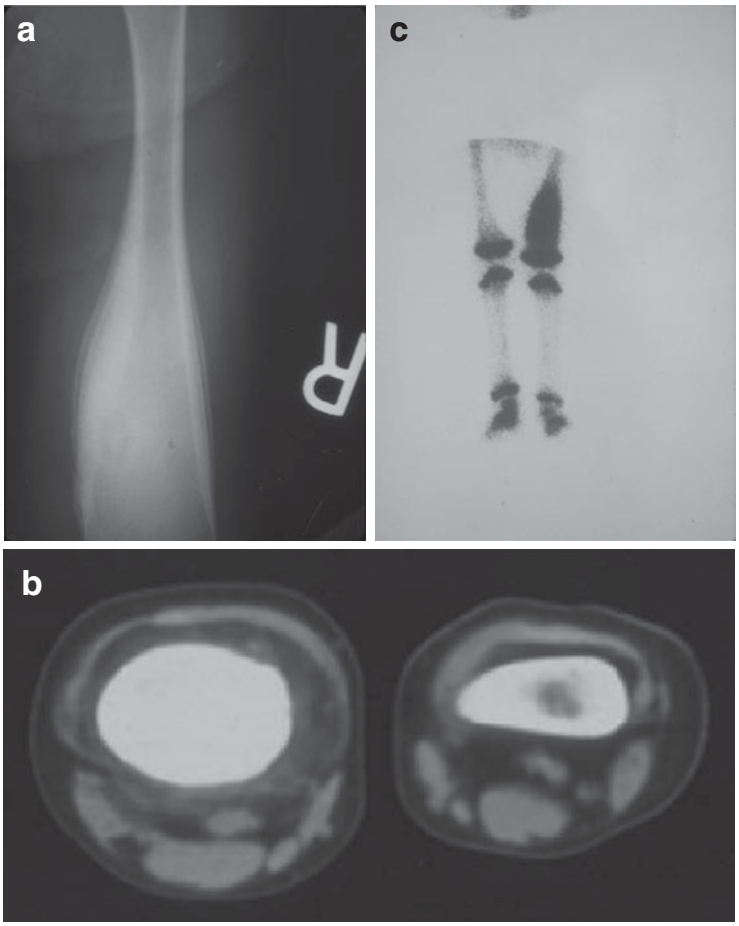

Fig. 4 **a** Low-grade chronic osteomyelitis characterized by cortical bone thickening due to periosteal new bone. **b** There was a homogenous marrow and cortical signal on MR images, suggesting that there were no abscesses. **c** The signal on the radionuclide bone scan went superior to the changes seen on the X-rays. This is a frequent finding in bone infections as well as neoplasms

This is a further impediment to resolution. Persistent infection in a localized area is a rare cause of secondary squamous cell carcinoma, which may develop in a long-standing sinus. Equally, infrequent is the systemic secondary amyloidosis, which may develop in long-standing chronic osteomyelitis.

The microscopic diagnosis of chronic osteomyelitis is usually straightforward. Sometimes, however, the inflammatory infiltrate is often sparse and may mimic the normally found elements of the marrow space. A clue often found useful in making this distinction is the normal fat pattern of marrow is lost in osteomyelitis and instead there is a fibrous background. Microscopic recognition of the sequestrum can be very helpful if the diagnosis of infection is in doubt (Fig. 3b). The sequestrum is recognized by virtue of its anucleate nature, often the edges are jagged owing to the action of proteolytic enzymes and osteoclastic action.

Course: The course is usually chronic, interspersed with acute exacerbations. The bone becomes thickened irregular and deformed. Sinuses may drain for extended periods of time. Low-grade infections can smolder on, in a chronic fashion (Fig. 4a–c), resolve and heal or undergo acute relapses. Relapses are caused by and in turn contribute to debilitation, malnutrition, and reduced immunity. Joint contractures and scarring may occur. Epiphyseal destruction may cause malaligned limbs if asymmetric or shortening if complete. Epiphyseal hyperemia is an infrequent but dramatic cause of limb lengthening. Special problems in orthopedic practice involve treating osteomyelitis in the presence of foreign material (either orthopedic hardware or a fragment of sequestrum).

Management: Surgical management under antibiotic cover forms the main therapeutic strategy. The planning and timing of surgery depend on the prevailing situation at that time. Surgical debridement and drainage are the usual procedures. This may take the form of saucerization, excision, or other resections followed by drainage, closed suction-drainage, muscle pedicle cover, or packing. Antibiotic beads, or bone graft packing, are occasionally needed.

Sclerosing Osteomyelitis, Sclerosing Osteitis

This refers to the condition of bony sclerosis, which is gradual, usually unilateral and often associated with pain. Constitutional symptoms are infrequent. The condition usually affects children. The tibia, jaws, and clavicle are frequent

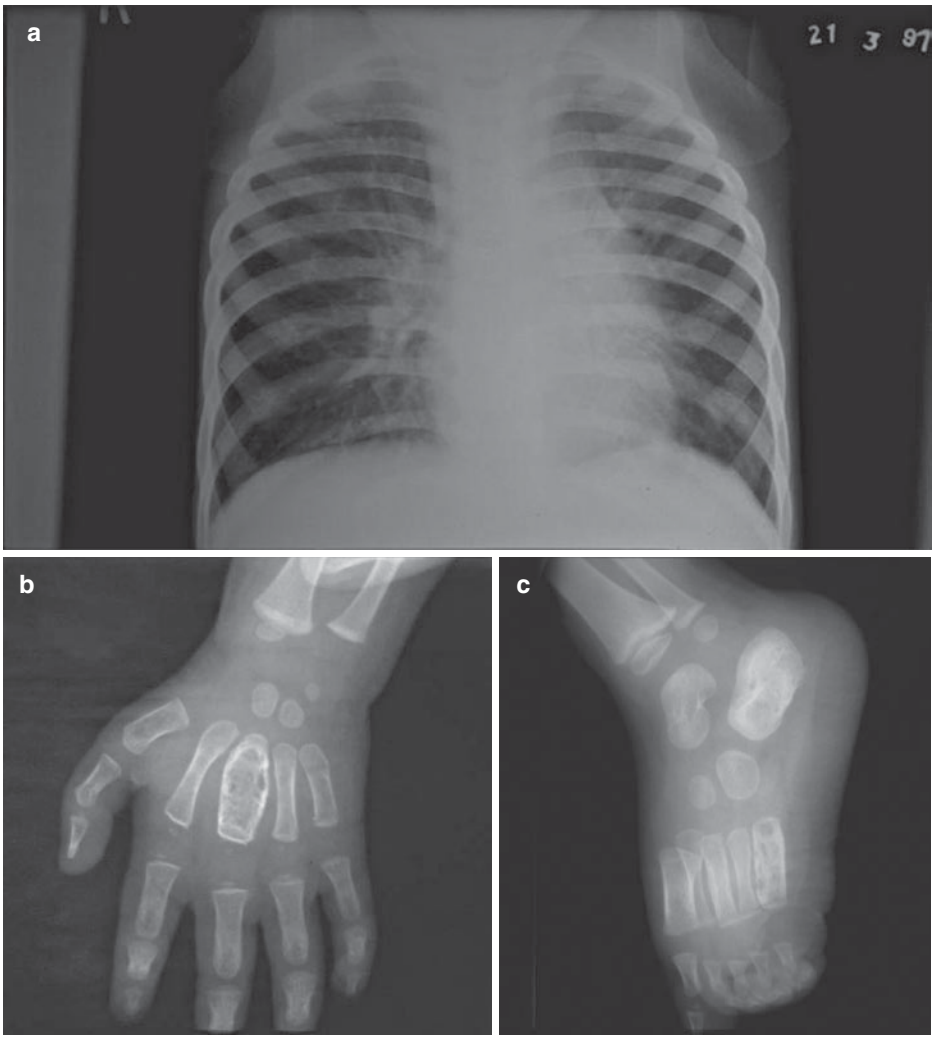

Fig. 5 **a** Rib involvement in a child with multifocal tuberculosis affecting joints and bones. **b** Hand involvement in the same child. The thickening and expansion of the short tubular bones of the hands is characteristic of tubercular dactylitis, but is infrequent in the long tubular bones, where the infection tends to be lytic without bony expansion. The expanded type of involvement in the hands is sometimes referred to as spina ventosa. **c** Ankle and foot involvement in the same child. Involvement of the calcaneus and metatarsals was particularly severe

sites in children. The biopsy fails to show inflammation and bacteriologic work-up is often negative. Some of these cases respond to empirical antibiotic therapy. Hence, although unsatisfactory from a theoretical basis, the lesions are often ascribed to infections.

Chronic Multifocal Recurrent Osteomyelitis

This is a condition where patients present with recurrent episodes of bone pain, erythema, and swelling. X-rays and bone scans are consistent with osteomyelitis. Bone biopsies confirm the suspicion, but organisms are usually not isolated. Antimicrobial therapy is not helpful. There may be a poorly related association with the sero-negative spondyloarthropathies. The condition usually resolves with time.

Tubercular Osteomyelitis

The disease may affect the bone, the joints, or not infrequently, both (Fig. 5a–c). Often it occurs in the form of a hematogenous spread. This is usually a reactivation in a patient with a preexisting primary focus in the lung. The emergence of multidrug resistant tuberculosis and the AIDS epidemic have reemphasized the infections with the mycobacteria. Especially in the latter situation, atypical mycobacteria may be seen. These organisms may require different treatment protocols, making it important to get culture reports on all cases of tuberculosis.

Like the pyogenic osteomyelitis, tubercular osteomyelitis is frequent in children, in whom it occurs in bones such as vertebrae, or in long tubular bones in a metaphyseal location. In adults, vertebrae or epiphyses of the long bones

may be involved. Secondary joint involvement from an osteomyelitis is uncommon except in situations such as the hip where the metaphysis is intra-articular. The course is frequently chronic, although a rapid acute infection with widespread (miliary) form is described.

Surgical Pathology

For purposes of description, the disease has traditionally been divided into the "granular" and the "exudative" types. In reality, both forms overlap.

Grossly, the disease is characterized by reactive tissue, which can be extensive in the exudative forms, or sparse in the granular (dry) forms.

The characteristic histological findings are those of a granulomatous inflammation, often with Langhan-type giant cells (Fig. 6). Special stains reveal organisms, which fluoresce with auramine–rhodamine, and are acid-fast. It must be remembered that giant cells are common in the marrow space. Foreign body giant cells, osteoclasts and megakaryocytes should not be confused with a tubercular reaction. Looking for epitheloid histiocytes and granuloma formation should help in establishing the correct diagnosis. Organisms should be sought, since fungi can have a granulomatous reaction similar to tuberculosis.

Acid-fast organisms may be sparse, and special methods to confirm the diagnosis include tests based on the polymerase chain reaction technology as well as culture methods. The emergence of BACTEC instruments has improved the yield and turn-around time of the latter method.

Management is based on multidrug chemotherapy along with the appropriate surgical approach. The latter is dependent on the site and clinical situation. For example, vertebral tuberculosis may be treated with drugs alone, but if associated with a progressive neurologic deficit or a rapidly developing cauda equina syndrome, then surgical intervention must be considered. Several different types of operations are described depending on the location and type of the infection.

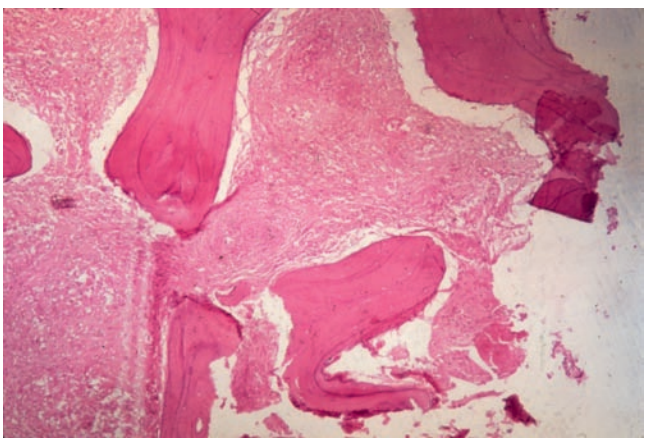

Fig. 6 The classic histological features of tuberculosis are seen, with granulomatous inflammation and a Langhan's-type giant cell reaction

Syphilitic Osteomyelitis

Osseous syphilis is no longer a common infection in most parts of the world. There are pockets, however, where significant syphilis persists. The causative spirochete, Treponema pallidum is highly susceptible to penicillin.

Surgical Pathology

The infection is usually spread by the hematogenous route. The spirochete lodges within the medulla in the metaphysis. They incite a low-grade inflammatory response, most prominent about blood vessels. In *favorable conditions*, healing by fibrosis occurs, imparting a characteristic yellow color to the medulla. In *unfavorable conditions*, tissue necrosis occurs. Characteristically, foci of yellow-gray necrosis are surrounded by mononuclear cells. These in turn are surrounded by fibrovascular granulation tissue and reactive woven bone. This pattern of necrosis is referred to as a gumma. Spread through the Haversian and Volkmann systems results in considerable subperiostal spread, and sometimes periosteal lifting. There is therefore a characteristic periosteal thickening. Extension into underlying organs or overlying soft tissues may occur. Joint involvement is infrequent. When present, there is often extensive gummatous destruction of the bone, which is centered about the epiphysis.

Early Congenital Syphilis (Parrot's Pseudoparalysis)

Skull, nasal bones, and long bones are the favored sites. The neonate is irritable, with a tender limb. Other stigmata of syphilis may be present such as snuffles, keratitis, skin or mucous lesions, or a positive serology.

Histologically, the metaphyseal medulla is invariably involved. This causes disordered enchondral ossification, wide epiphyseal plates, increased accumulation of calcified cartilage, and a propensity to fracture at this site. Healing frequently occurs by a few months of age, along with reactive periosteal new bone. The changes have to be differentiated from rickets or scurvy.

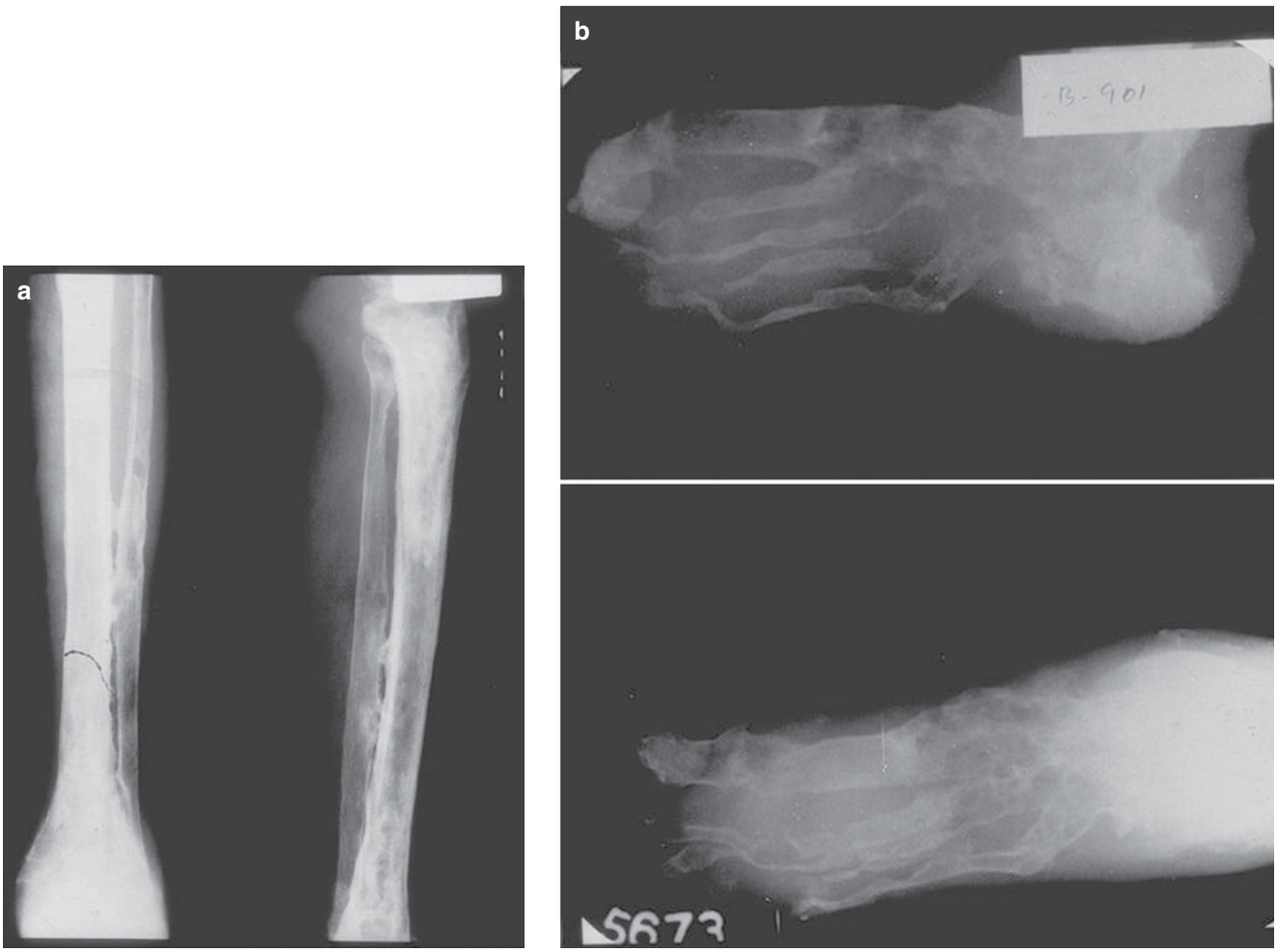

Fig. 7 Maduramycosis mycetoma involving the (**a**) leg and (**b**) foot of a young man

Late Congenital Syphilis

This is the tertiary form of congenital syphilis. It occurs around the second or third year. Periosteal new bone is the hallmark of this stage; however, occasionally destructive gummatous lesions may be seen. Syphilitic dactylitis refers to the periosteal new bone causing enlargement of the tubular bones of the hands. Additional stigmata such as Hutchinson's triad or central nervous system involvement may be present. Clutton's joints (symmetrical synovitis) may be seen between 8 and 18 years of age.

Fungal Osteomyelitis

Fungal infection of bone is very uncommon. Blastomycosis, Coccidioidomycosis, Actinomycosis, Maduramycosis and Sporotrichosis are the more common infections seen. Blastomycosis may be relatively more frequently seen in the midwestern parts of the United States but is still very rate. Often these infections involve the hands, feet, or the craniofacial skeleton (Fig. 7a, b).

The AIDS epidemic has changed the face of such infections considerably, and increased their incidence. Identification of the organisms using standard pathologic techniques (such as silver or periodic acid Schiff stains) and standard culture techniques in the laboratory form the basis of diagnosis. Therapy is directed toward the clinical problem often under appropriate drug cover. Wide surgical excision may sometimes be required.

Parasitic Osteomyelitis

Although rare in the west, parasitic osteomyelitis is not infrequently encountered in certain pockets of the world. In parts of the Middle East, South Asia, and certain African countries, there is a high incidence of hydatid disease of bone (Fig. 8).

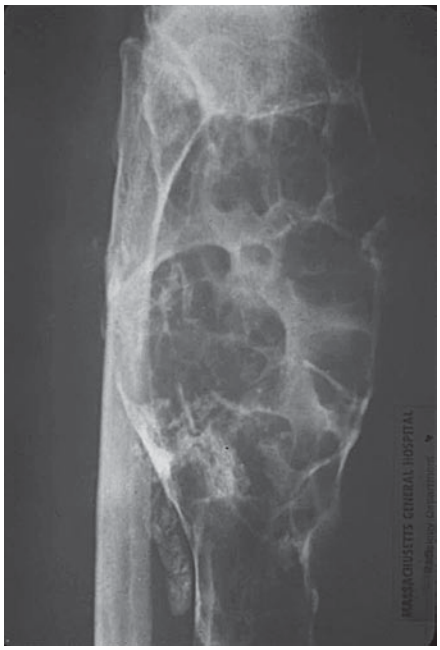

Fig. 8 Hydatid disease of bone

Bone Infections in AIDS

It is likely that *rare organisms* will be seen in patients with HIV infection or with AIDS, in addition to the more common organisms. A pseudoneoplastic condition of the bone has been described occurring in the bone, due to the cat scratch bacillus. The histology of this case resembled the bacillary angiomatosis described with Bartonella henselae infections. There is, however, no morphologically diagnostic picture for a specific organism and microbiological correlation is needed in almost all cases. Most reports dealing with exotic or opportunistic organisms causing bone infections in HIV have been those involving the bone marrow rather than bone.

Chapter 12
Arthropathies

William R. Reinus, Mary F. Barbe, Steven Berney, and Jasvir S. Khurana

Abstract Arthropathies are joint-centered diseases that arise from a variety of causes but show certain clinical and radiological similarities with one another. This chapter is concerned with a systematic approach to the understanding of these conditions so that an accurate diagnosis can be made with obvious implication on the management

Keywords Arthritis • Loose bodies • Neuropathic arthropathy • Gout • Hemophilia • Hemochromatosis • Ochronosis • Synovial arthropathy • Bacterial arthropathy • Pigmented villonodular synovitis (PVNS)

Common Features of Arthropathies

Arthropathies, by definition, are primarily joint-centered in that they cause changes within the joint and bones around the joint in more or less equal proportion. If only one side of the joint is affected, the disease process is unlikely to be a primary arthropathy – for example, in osteonecrosis of the femoral head, only one side (femoral side) of the joint is affected. Thus, it is not considered an arthropathy although it may lead to secondary osteoarthritis.

Hyaline cartilage that lines the synovial joint surfaces is critical for proper function of the joint. Its loss is a common finding in most arthropathies. Radiographically, this loss is seen as reduction in joint space. On magnetic resonance imaging (MRI), the cartilage may be imaged and evaluated directly. In most arthropathies, there is also a variable amount of inflammatory destruction of the cartilage and synovial lined joint capsule (inflammatory pannus). This may be marked (rheumatoid arthritis, RA) or minimal (primary osteoarthritis). Depending on the severity and duration of the inflammation, the joint may be destroyed, ankylose, or ultimately go on to develop osteoarthritis.

With loss of cartilage comes the rubbing of bare bones against each other, leading to new bone formation (termed eburnation when described grossly and seen as subchondral new bone formation on radiographs). In addition, as a response to abnormal stresses across the joint as a result of cartilage loss the joint attempts to maintain pressure homeostasis and so increases its surface area through osteophyte formation. This end stage is called osteoarthritis. The radiographic sine qua non for osteoarthritis (whether primary or secondary to other arthritidies or disease processes) is the trio of joint space narrowing, subchondral sclerosis, and osteophyte formation.

Animal Models of Arthritis

Several animal models have been developed for the study of rheumatoid and osteoarthritic conditions on joint tissues. These models use injections of monoiodoacetate (MIA), collagen (bovine type II collagen in the presence of incomplete Fruend's adjuvant), bacteria (*Lactobacillus*), and a variety of growth factors into joints, intraperitoneally or intracutaneously to create inflammation-induced arthritis (Table 1)(1–4). The collagen-induced arthritis (CIA) is used as a human RA model (3). Inflammatory arthritis can also be induced via autoreactive immunoglobulin (Ig) transfer in which arthritogenic serum from KRN-TCR (K/B) transgenic mice is injected intraperitoneally into normal mice to induce knee and ankle joint arthritis (5). In each of these types of inflammatory arthritis, cartilage thinning and joint erosion occurs due to the induction of various inflammatory responses such as macrophage infiltration and proinflammatory cytokine upregulation. Cyclical loading has also been used to create cartilage thinning in animal knee joints to simulate overuse-induced osteoarthritis seen in humans (6). Various examples of these models are described further in Table 1 These models can be used to examine the effectiveness of pharmaceutical interventions or the role of various molecules in inducing or protecting against joint damage. In the latter case, transgenic mice lacking one or more known proteins can be examined after the induction of arthritis to understand the underlying mechanisms by which the protein(s) modulate the pathophysiology of the arthritic condition. For example, transgenic mice lacking each of the four known prostaglandin E2 (PGE2) receptors (PGE2 is an inflammatory molecule associated with edema and cartilage erosion) were examined for arthritic joint changes after generation of CIA (7). Deletion of three of the PGE2 receptors (EP1, EP2, or EP3 receptors) did not affect

J.S. Khurana (ed.), *Bone Pathology*, DOI 10.1007/978-1-59745-347-9_12,

Table 1 Examples of animal models of experimental arthritis

Type of arthritis	Induction/generation mode	Pathological presentation
Inflammatory: collagen-induced arthritis, used as a RA model (1,3)	Two intraperitoneal injections of bovine type II collagen and incomplete Freund's adjuvant into Wistar rats, or into Dark Agouti rats	Synovial inflammatory cytokine expression (TNF and IL-1b), then inflammatory cell infiltration into joints by >1 week. Macrophage-pacifying agent CNI-1493 reduced TNF and IL-1b expression and increased anti-inflammatory cytokine TGF-b
Inflammatory: bacterial induction, used as a RA model (2)	Intraperitoneal injections of arthritogenic species of Gram-positive bacteria (*Lactobacillus*)	Erythema, edema, pain, functional disorders of ankle, write and metatarsal joints; Production of IL-10, TNF-a, IL-1b, IL-4 in serum
Inflammatory: transgenic mice with human TNF; similarities to RA (7)	Generation of transgenic mice expressing human TNF (hTNFtg, i.e., overexpression of TNF) crossed with osteopetrotic *c-fos*-deficient mice lacking osteoclasts: *c-fos-/hTNFtg* mice	Paw swelling, reduction in grip strength; no osteoclasts, knee cartilage damage, expression of MMP-3 and MMP-13, but no bone erosion indicating that osteoclasts mediate joint destruction
Inflammatory: collagen antibody-induced arthritis in transgenic mice lacking PEG2 receptors (6)	Generation of transgenic mice lacking each of the four known PEG2 (EP) receptors, then intraperitoneal collagen monoclonal antibody cocktail injection to induce arthritis	Collagen antibody injection induced multiple joint bone erosion, proteoglycan loss, and type II collagen breakdown; EP4 receptor-deficient mice had decreased incidence of joint disease indicating PGE2 contributes to disease progression through EP4 receptor
Inflammatory: transgenic mice with human IL-1a (8)	Generation of transgenic mice overexpressing human IL-1a (hIL-1a), the membrane associated form of IL-1 (MA-IL-1)	Chronic synovitis with macrophage-like and fibroblast-like synoviocytes constitutively producing MA-IL-1; synoviocyte proliferation; cartilage destruction
Inflammatory: mouse model of autoreactive Ig transfer (5)	Mouse model; autoreactive Ig transfer that engenders arthritis. KRN-TCR transgenic mice bred on a B6 background. Serum obtained from K/BxN mice	Numerous osteoclasts in articular joint tissue associated with progressive periarticular osteolytic lesions; cells from joints exhibit heightened NF-kB activity, which when replaced with a mutant form reduces arthritis. This indicates that NF-kB has a role in inflammatory-osteolytic arthritis
Spontaneous arthritis type of RA (10,11)	KRN mouse model using transgenic mice for a TCR recognizing an epitope of bovine RNase	Severe destructive arthritis and joint inflammation initiated by T cell and pathogenic Ig recognition of a ubiquitously expressed self-antigen (glucose-6-phosphate isomerase, a glycolytic enzyme); once initiated, pathology is driven almost entirely by Igs
Experimental osteoarthritis (OA) – relevant to metabolic as well as biomechanical aspects of OA (4)	Intra-articular (knee) injection of monoiodoacetate (MIA) in Wistar rats	Knee proteoglycan synthesis inhibition and increased gelatinize activities in weight-bearing areas of cartilage; increased IL-1-b and iNOS in cartilage at time of maximal proteoglycan synthesis inhibition
Experimental OA	TGF-b injections into normal murine knees with or without a 7 days prior injection of clodronate-laden liposomes (the latter selectively removes macrophage-like synoviocytes)	TGF-b induces knee osteophyte formation; prior clodronate removal of macrophages dramatically reduced osteophyte formation, indicating macrophages produce TGF-b and other chondrogenic factors
Ectopic crystal deposition in joints due to lack of *Ank* gene (12)	Anknull/Anknull transgenic mice (null mice for joint only)	Severe ectopic postnatal crystal deposition in almost every joint in body, leading to eventual joint fusion and loss of mobility
Cyclical joint mechanical overloading, similar to osteoarthritis (6)	Repetitive forepaw joint flexion and loading (metacarpophalangeal joints)	A decrease in uncalcified cartilage, increased cells expressing osteopontin in the uncalcified cartilage

EP PGE2 receptor, *Ig* immunoglobulin, *IL-1* interleukin 1, *MMP* matrix metalloproteinase, *iNOS* inducible nitric oxide synthase, *NF-kB* nuclear factor-kappa B, *PGE2* prostaglandin E2, *RA* rheumatoid arthritis, *tg* transgenic mice, *TGF-b* transforming growth factor beta, *TNF* tumor necrosis factor, *TCR* T cell receptor.

the development of arthritis. However, deletion of the EP4 receptor reduced bone destruction, proteoglycan loss, and type II collagen breakdown in cartilage following CIA, compared to EP4 wild-type mice. The findings of this last study showed that PGE2 contributes to the progression of RA in part by binding to the EP4 receptor. Development of an EP4 antagonist might provide an effective pharmacological intervention against joint disease in patients with RA.

Radiological Aspects of Arthropathies

From a radiological point of view, then, there are four possible appearances of arthritis: destructive, productive, both destructive and productive, and those that are neither. Two of these appearances – those that are productive, the osteoarthroses, and those that are destructive, the inflammatory arthropathies – account for the majority of arthritidies.

Radiologically, it is important to evaluate *A*lignment, *B*ones, *C*artilage spaces, *D*istribution of disease, other *E*xtraordinary findings and the *S*oft tissues: the so-called ABCDES of arthritis.

Alignment

Misalignment of bones may occur in a consistent and predictable fashion in some arthritidies as a result of inflammation-induced destruction or dysfunction of tendons and muscles. For example in RA, ulnar deviation of hand and bones of the hands is common. Swan neck and boutonnière deformities are other examples of malalignments and are often seen in inflammatory arthritidies, especially RA. In the case of a swan neck deformity, there is a lateral subluxation of the lateral bands of extensor mechanism, from inflammatory shortening of these bands and/or rupture of the superficial flexor digitorum tendon, this leads to hyperextension at the proximal interphalangeal (PIP) joint and hyperflexion at the distal interphalangeal (DIP) joint. The opposite deformities occur in a boutonniere deformity – hyperflexion at the PIP joint and hyperextension at the DIP joint (Fig. 1a, b).

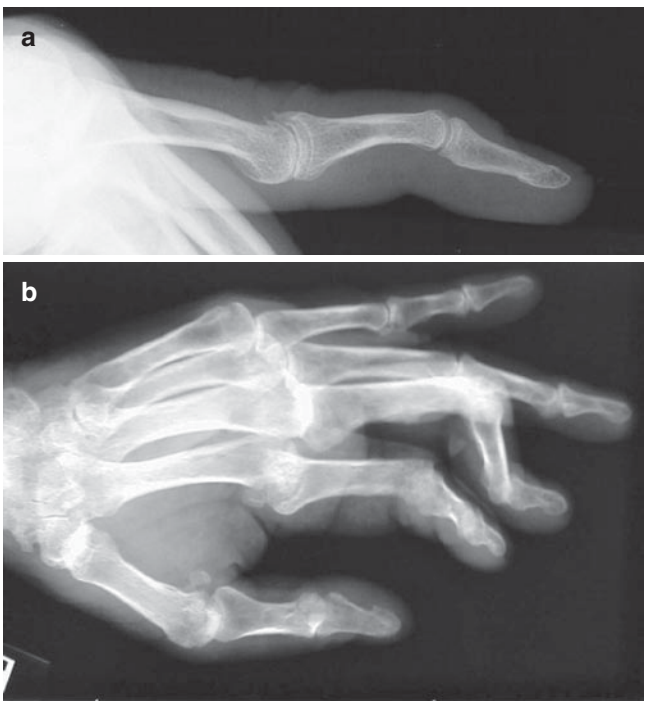

Fig. 1 Lateral radiographs showing (**a**) a swan neck deformity with hyperextension at the proximal interphalangeal (*PIP*) joint and flexion at the distal interphalangeal (*DIP*) joint of a patient's second digit and (**b**) showing a boutonniere deformity of another patient's third digit – flexion at the PIP joint and hyperextension at the DIP joint

Bones

Bones may develop either osteopenia from disuse or inflammation-induced hypervascularity (e.g., RA) or sclerosis (as seen in the phalanges in psoriasis). Periosteal reaction may also occur along the diaphysis of bones affected by inflammatory arthropathies, particularly psoriatic arthritis and Reiter's disease (also now called reactive arthritis).

Cartilage

Cartilage space narrowing is seen as an end result of most arthropathies. Erosions are often seen in the cartilage space as the result of inflammatory destruction of the underlying bone. Some diseases, for example, RA, cause marginal erosions (at least initially) while others show uniform erosive changes (such as erosive osteoarthritis). In general, inflammatory arthropathies tend to be destructive and as such show erosions along the joint margins within the cartilage space. For example, RA, because of its changes in the degree of inflammation (the so-called "relapses and remissions") typically will cause marginal erosions of different ages that also vary in their progression toward the center of the joint (Fig. 2) Psoriatic arthritis, in its more aggressive forms, is more likely to result in pencil-in-cup deformity of the joint than RA (Fig. 3). Erosive osteoarthritis tends to show gull-wing-shaped erosions all the way across the joint at once since the hyaline cartilage is generally completely lost early in the disease (Fig. 4). In gout, the erosions start juxtarticularly in the metaphysis and give rise to a peculiar clasp-like erosion with overhanging edges (Fig. 5), so-called Granger's overhanging edges. In psoriatic arthritis, there is often total obliteration of the cartilage space and ankylosis. In other conditions (collectively referred to as the chondrocalcinoses), there is calcification of joint cartilage. Such conditions include calcium pyrophosphate dihadrate deposition, hyperparathyroidism, hemochromatosis, and alkaptonuria (Ochronosis).

Distribution

Knowing the distribution of disease is critical in diagnosis. The spondyloarthropathies and alkaptonuria both primarily involve the spine; the spondyloarthropathies also involve the sacroiliac joints. Gout predominates in the distal parts of the appendicular skeleton (the acral skeleton, and frequently involves the feet and knees). RA tends to be symmetric whereas psoriatic arthritis and Reiter's disease tend to be asymmetric. Infections and gout may affect a single joint while the other inflammatory arthritidies tend to involve more

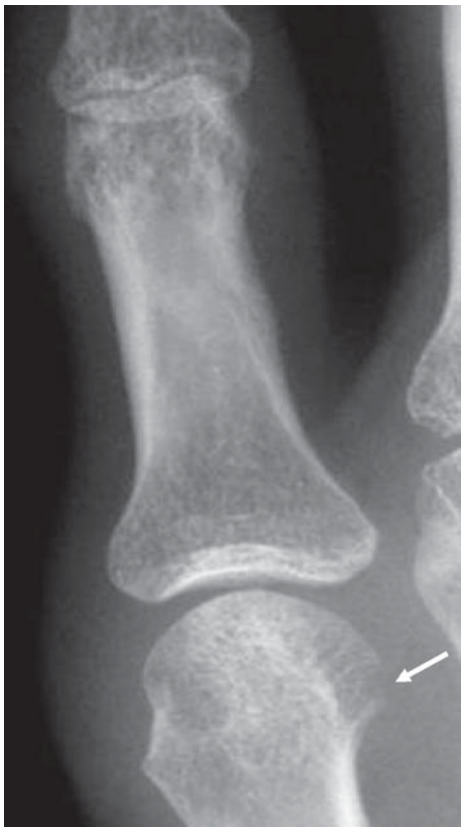

Fig. 2 Anteroposterior (AP) coned-down radiograph showing a periarticular erosion of the radial aspect of the fifth metacarpal head (*arrow*)

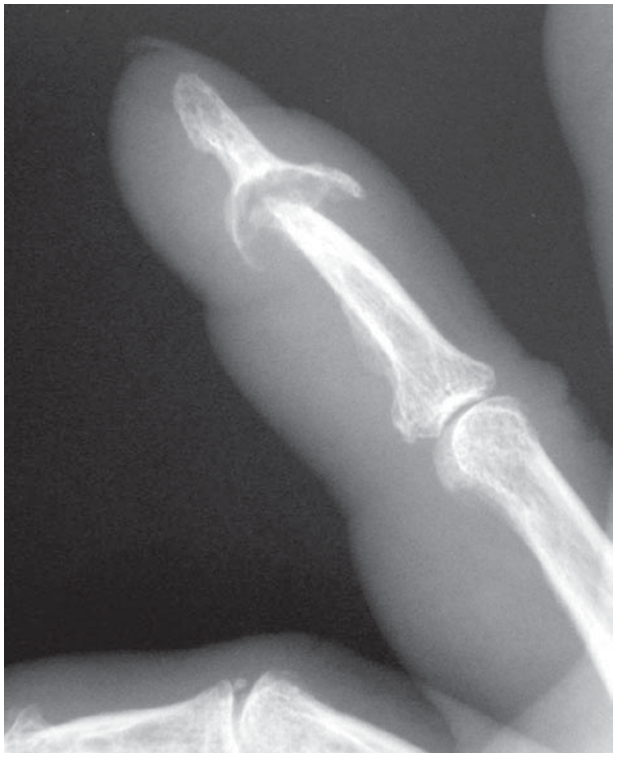

Fig. 3 Lateral radiograph of the second digit showing pencil in cup deformity of the proximal interphalangeal (*PIP*) joint caused by psoriatic arthritis

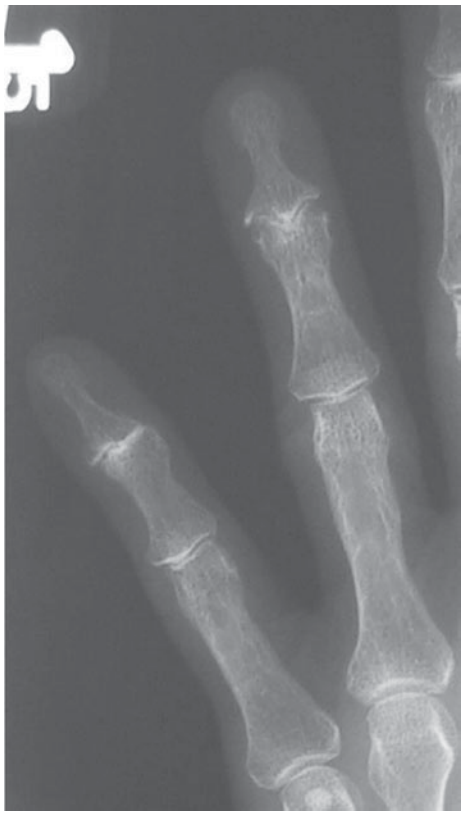

Fig. 4 AP radiograph of the second and third digits of the hand in a patient with erosive osteoarthritis. The distal interphalangeal (*DIP*) of the third digit shows characteristic gull-wing shaped erosions seen in this disease

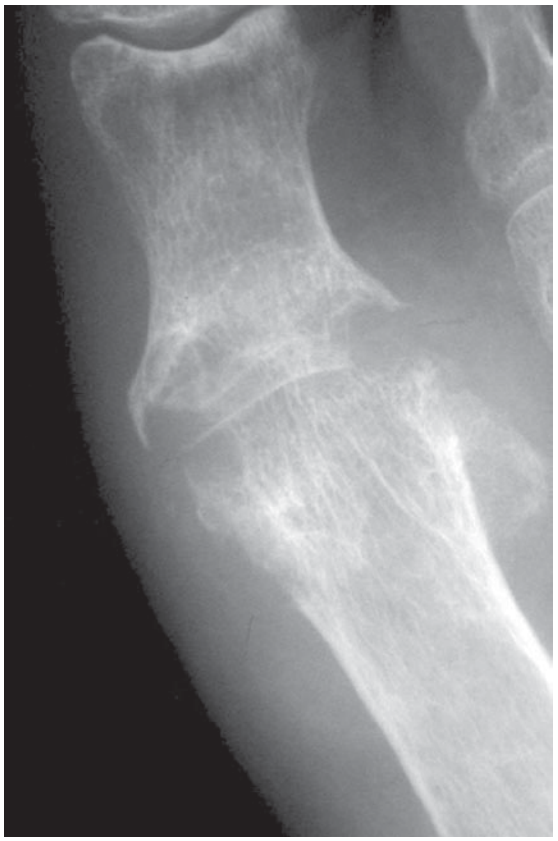

Fig. 5 AP coned-down radiograph of the first metatarsophalangeal joint in a patient with gout. Note the deep erosions with clasp-like overhanging edges, Granger's overhanging edge

than one joint. Thus, a bilaterally symmetric destructive arthropathy involving the carpi and the metacarpophalangeal joints strongly suggests RA. Productive arthritis involving the patellofemoral joint out of proportion to other compartments of the knee joint may indicate calcium pyrophosphate dihydrate (CPPD) deposition arthropathy. Similarly, a productive arthritis that involves primarily the second and third metacarpophalangeal joints and shows large radial hook-like osteophytes suggests the possibility of hemochromatosis.

Extraordinary Findings

In addition, peculiarities of the radiographic appearance and distribution of some arthropathies help to narrow the differential and lead to definitive diagnosis. For example, the presence of spontaneous joint ankylosis or an ivory phalanx is strongly suggestive of psoriatic arthritis. Chondrocalcinosis, though caused by many conditions, is frequently although not always present in CPPD deposition disease. Atlantoaxial subluxation is common in RA but unusual in psoriatic arthritis and Reiter's disease. Soft tissue nodules occur primarily in three arthropathies: RA with rheumatoid nodules, gout with tophi and multicentric reticulohistiocytosis with xanthomas. Finally, interstitial lung disease is common in some of the conditions associated with arthritis, for example, RA and ankylosing spondylitis.

Soft Tissues

Soft tissues may be involved in the form of capsular or joint swelling or masses as seen in gout, RA or multicentric reticulohistiocytosis (a form of histiocytic proliferation). There may also be considerable soft tissue atrophy in such diseases as RA or lupus.

Specific Arthritidies

Part I The Productive Arthritidies

Osteoarthritis

Osteoarthritis (degenerative joint disease) is the prototypical productive arthropathy. It may be the end result of one of several arthritidies (secondary osteoarthritis) or occur in the absence of other known arthritis (idiopathic or primary osteoarthritis).

Osteoarthritis is considered to be one of the most important contributors to old age morbidity and medical expense. Over 80% of patients over the age of 75 years have clinically symptomatic osteoarthritis. It affects women about twice as often as men, but this ratio depends on the joint in question. For example, women have involvement of the small joints of the hand much more frequently than men, but hip involvement is equally common between the genders. Racial differences also exist, for example, osteoarthritis of the hip is more common in Caucasians than it is in Blacks and Asians.

Pattern of involvement: Overall, primary osteoarthritis is most common in the major weight-bearing joints, the hip, knee, and to a lesser degree the ankle. It is also common in the frequently used small joints of the hands and wrists, particularly the first carpometacarpal joints at the base of the thumbs. Often the dominant hand is more severely affected than the nondominant hand. The facet joints of the cervical and lumbar spine are also commonly affected. Typically, the shoulder and elbow are relatively spared.

Clinical presentation: Clinically, patients with osteoarthritis complain of joint pain, crepitus, and stiffness after periods of inactivity that eases with use. Normally, the pain is relieved by rest but may become continuous late in the disease.

Osteoarthritis is not relentless in its symptoms. It undergoes relative periods of symptomatic improvement and worsening, the latter related to periods of reactive synovitis and joint effusion. Advanced disease is often accompanied by disuse atrophy of muscles. As the disease progresses, the joints begin to show clinical enlargement. In the fingers, these enlarged areas are known as Heberden's and Bouchard's nodes in the DIP and PIP joints, respectively. With enlargement of the facet joints in the spine, the neuroforamina may become encroached, resulting in radiculopathy or development of spinal stenosis.

Etiology: Various causes of osteoarthritis have been investigated. Aging, trauma, and repetitive joint use are all risk factors for (secondary) osteoarthritis, which can also result as an end result from other arthritidies as well as many deposition and endocrine diseases. Thus, the shoulder and elbows of baseball pitchers, knees of basketball players, metacarpophalangeal joints of boxers and ankles of ballet dancers are all at increased risk of osteoarthritis. Obesity plays a role, whether from the effects of increased trauma/overuse of weight bearing, or from a metabolic imbalance is not settled. Many cases of idiopathic osteoarthritis of the hip may be due to congenital or developmental defects, such as congenital subluxation/dislocation, acetabular dysplasia, Legg-Calve-Perthes disease, slipped capital femoral epiphysis, or other conditions that decrease joint congruity and concentrate loads. Screening and treatment of newborns and infants for congenital hip disease has led to marked decrease in the prevalence of hip osteoarthritis. Diseases that reduce the ability of the cartilage or subchondral bone to deform are also associated with development of osteoarthritis. Patients with ochronosis accumulate homogentisic acid polymers, which leads to stiffening of the cartilage. In osteopetrosis,

stiffness of the subchondral trabeculae occurs. In both, severe degeneration of cartilage is present by 40 years of age.

The etiology of primary osteoarthritis is less well characterized. A genetic basis appears possible. The mother of a woman with DIP joint involvement (Heberden's nodes) is twice as likely to exhibit osteoarthritis in these joints, and the proband's sister three times as likely as the mother and sister of an unaffected woman. Investigations have implicated mutations in the gene for collagen II.

Pathogenesis: Osteoarthritis is thought to occur when there is an imbalance between the catabolic and anabolic pathways in cartilage metabolism. The catabolic pathways are commonly associated with proinflammatory proteins, including interleukin 1 alpha (IL-1α), tumor necrosis factor alpha (TNF-α), IL-17, macrophage inflammatory protein-1a (MIP), and monocyte chemoattractant protein-1 (MCP-1). Proteinases (such as cysteine proteinases, metalloproteinases, and serine proteinases) also become upregulated. Proinflammatory cytokines, chemokines, and extracellular matrix fragments propagate the elevated synthesis of metalloproteinases and additional inflammatory cytokines/chemokines. The catabolic pathways also alter the chondrocyte phenotype and impair the production of new extracellular matrix proteins. In contrast, anabolic pathways related to anti-inflammatory proteins, such as IL-4, IL10, IL-13, and IL-1ra, are suppressed.

In response to trauma or insult and inflammatory mediators (especially IL-1), chondrocytes are thought to undergo cell division ("cloning") and become metabolically active, producing increased quantities of collagen, metalloproteinases, and proteoglycans. Ultrastructurally, the osteoarthritic chondrocytes are characterized by hypertrophy, impaired mitochondrial function, dysfunctional Golgi apparatus, decreased free ribosomes, and increased intracellular filaments. This leads to thickening of cartilage in the very early stages of osteoarthritis (because of increased proteoglycan accumulation). Eventually, however, because of continuing cell damage and the release of cathepsins and metalloproteinases there is a loss of cartilage. There is also a change in the arrangement and size of the collagen fibers. Synovitis may occur, due to phagocytosis of shards of cartilage and bone from the abraded joint surface, the release from the cartilage of soluble matrix macromolecules (glycosaminoglycans, proteoglycans), or the presence of crystals of calcium pyrophosphate or calcium hydroxyapatite. Immune complexes containing antigens derived from cartilage matrix may be sequestered in collagenous tissue of the joint and their release may contribute to a low-grade chronic synovitis. It should be remembered, however, that the inflammatory component is minimal or mild in comparison to other inflammatory arthritidies. Along with the changes in cartilage, metabolic changes in the synovial membrane lead to decreased concentration and viscosity of the synovial fluid, aggravating cartilage degradation due to a loss of appropriate lubrication and cushioning.

In addition, the body attempts to reduce the pressure across the joint back to its homeostatic set point through development of peripheral osteophytes. Excessive endogenous production of growth factors such as transforming growth factor β (TGF-β) and bone morphogenetic proteins (BMPs) have been implicated in driving osteophyte formation and synovial thickening associated with osteoarthritis. As a result, joints affected will have large osteophytes in due course, giving the characteristic appearance of a productive arthritis.

Surgical pathology: The most striking changes are usually seen in load-bearing areas of the articular cartilage. In the early stages, the cartilage is thicker than normal but with progression of the disease, the joint surface thins, the cartilage softens, the integrity of the surface is breached, and vertical clefts develop. This gives the cartilage a resemblance to velvet and is termed fibrillation (Fig. 6). Deep cartilage ulcers, extending to bone, may appear. Areas of fibrocartilaginous repair may develop. Fibrocartilage, however, is inferior to the original hyaline articular cartilage in its ability to withstand mechanical stress. The articular cartilage is metabolically very active and the chondrocytes replicate forming clusters – a finding called "cloning." Later, the cartilage becomes hypocellular. Remodeling and hypertrophy of bone are also major features. Appositional bone growth occurs in the subchondral region leading to an opaque rim seen radiologically. The abraded bone under a cartilage ulcer may take on the appearance of ivory or of shiny wood and is termed "eburnation." Growth of cartilage and bone at the joint margin leads to osteophytes (spurs), which alter the contour of the joint restricting movement. Thickening of the joint capsule along with chronic synovitis also occurs in some cases, but the inflammation is not usually very prominent.

Osteochondral Loose Bodies

Separated fragments of bone and cartilage from a damaged joint surface (osteoarthritis trauma, osteoarthritis dissicans, etc.) can incorporate within the synovial membrane, resorb, or remain in the joint as free "loose bodies." Under certain conditions, proliferation of cells may occur on the surface of these loose bodies and consequently they may grow larger. The centers of such fragments, sometimes, become calcified or necrotic. The growth can be identified by the presence of telltale concentric rings, which appear as the loose body grows. Sometimes, the body reattaches to the synovium and develops its own vascular supply. In this situation, enchondral bone formation can follow and lead to complete ossification.

Numerous loose bodies are a feature of synovial chondromatosis, a condition in which literally hundreds of loose bodies can be present. It should be remembered, however, that conditions such as osteoarthritis can also have multiple

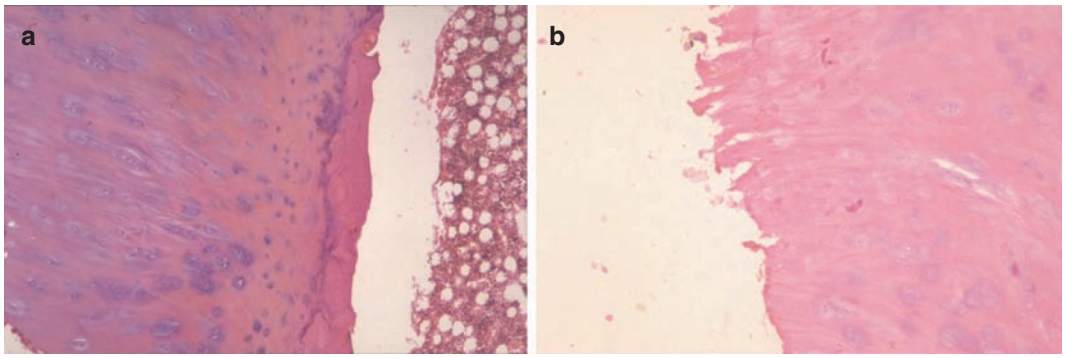

Fig. 6 Early osteoarthritis. **a** There is cloning of the chondrocytes along with vertical prominences of cartilage (fibrillation). **b** Shortly thereafter, small tears begin on the surface of the cartilage (clefting). These can eventually develop into ulcers going the entire length of the cartilage. Still later, the cartilage will wear away

loose bodies. Numerous "rice bodies" made up of fibrin can be seen in chronic synovitis such as tuberculosis and RA, but these should be distinguished from true osteochondral bodies.

Surgical pathology: Pathological findings neuropathic arthropathy include severe degeneration and fragmentation of the joint surfaces with extensive detiritic synovitis, resulting from particles of bone and cartilage embedded in the synovium.

Neuropathic Arthropathy (Charcot's joints)

Neuropathic arthritis is an extreme form of posttraumatic osteoarthritis. In neuropathic arthropathy, the involved joints lack proprioception and deep sensation. As a result, joint movement is not inhibited and tends to cause unintentional repetitive minor trauma. Ultimately, this constant trauma causes repetitive fracture and fragmentation of the joint and eventually biomechanical instability and severe osteoarthritis.

Neuropathic joint disease was first described by Jean-Martin Charcot in 1868 as an extremely destructive joint disorder in patients of neurosyphilis as a consequence of damage to sensory innervation to the joint. With decline in tertiary syphilis, other causes of neuropathic joints have now become more important. These include diabetes (especially the foot and ankle), syringomyelia (in the shoulder), amyloid, alcoholic neuropathies, and leprosy. The commonest cause in the United States is diabetes.

Radiology: The radiographic hallmark of neuropathic arthritis is one of "osteoarthritis with a vengeance." Not only will affected joints show narrowing, sclerosis, and osteophytes but they will show these with such exuberance that the appearance is one of marked increased Density about the joint, Disorganization of the joint structures, Debris surrounding and within the joint, Destruction of the joint surfaces, and Dislocation of the joint. This collection of "D" word descriptors should bring the diagnosis to mind. Thus, the viewer must be vigilant to make the diagnosis, especially since neuropathic arthritis may have a wide range from the purely productive arthropathy to one that resembles an aggressively destructive process. Because of this, septic arthritis with or without osteomyelitis is often in the differential diagnosis of neuropathic arthritis, particularly in the diabetic foot, where the two may coexist.

Charcot, Jean Martin (1825–1893) – Charcot was born in Paris in 1825. His father was a coach builder. He qualified in medicine at the age of 23 and joined Saltpetriere, on the left bank of the Seine. He became chief after his doctoral thesis differentiating gout from other forms of rheumatism. Saltpetriere (once the arsenal and gunpowder store of Louis XIII), was a hospice to over 5,000 indigent patients. Charcot gave descriptive diagnoses to several entities here, and founded the *Archives of Neurology Journal*. He became professor of pathological anatomy at the university of Paris, and the first chair of Neurology. Charcot employed a housemaid with disseminated sclerosis with a view to later obtaining her autopsy! He employed theatrical techniques for teaching – including floodlights and demonstrations. His interests included hypnosis, and admirers included Sigmund Freud, Jules Dejerne, Pierre Marie, and Joseph Babinski. Following the Franco-Prussian war of 1871, he became occupied with epidemics of typhoid and small pox, but retained an interest in mental diseases such as hysteria. He developed angina and died of pulmonary edema in 1893. He is known for descriptions of peroneal muscular dystrophy (Charcot-Marie-Tooth disease), Charcot joints and Charcot disease (disseminated sclerosis).

Calcium Pyrophosphate Dihydrate Crystal Deposition Disease

Synonyms: pseudogout, chondrocalcinosis.

In CPPD deposition arthropathy, there is excess calcium and pyrophosphate solute with the joint such that crystal precipitates out into the joint spaces and is deposited within the

synovium and articular cartilage. This material causes an inflammatory reaction within the joint that leads to destruction of the articular cartilage and symptomatic joint effusion.

Clinically, CPPD affects a similar population to that of osteoarthritis. It becomes more prevalent with age and affects about 5% of the population. The clinical features in many cases are very similarly to osteoarthritis: joint pain, crepitus, and stiffness after prolonged rest. CPPD also has a tendency to present with occasional flares where patients develop acute inflammation in the joint, swelling from a joint effusion and erythema. This presentation may be very similar to gout and has been referred to clinically as pseudogout.

There are three types – sporadic, hereditary, and secondary. The secondary form occurs in conditions such as hyperparathyroidism, hemochromatosis, hypomagnesemia, hypophosphatasia, gout, X-linked hypophosphatasia rickets, hypothyroidism, Ochronosis, and diabetes.

Radiology: The deposition of calcium pyrophosphate within the articular structures, primarily the hyaline cartilage and the meniscal fibrocartilage, can become radiographically visible (Fig. 7).

CPPD has a predilection for different joints from typical osteoarthritis. These include the radioscaphoid joint, the scaphotrapeziotrapezoidal (STT) joint, the metacarpophalangeal joints (particularly the second and third) (Fig. 8), the patellofemoral joint (Fig. 9), and the talonavicular joint. The inflammatory component may contribute to some radiographically

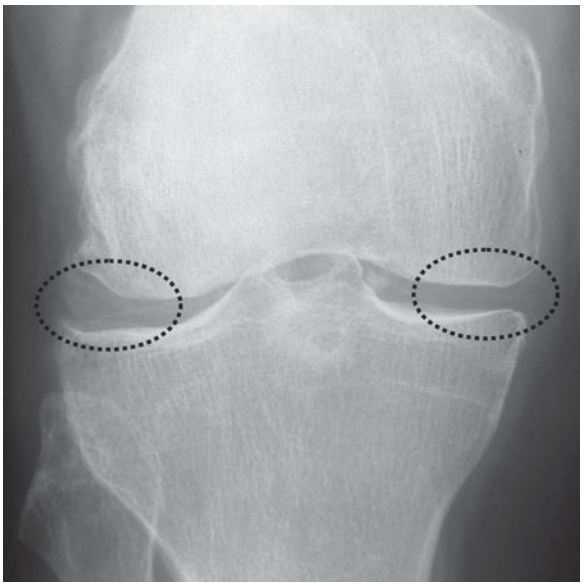

Fig. 7 AP radiograph of the knee showing calcification in the articular cartilage and the fibrocartilage of the menisci (*dotted ovals*). This is known as chondrocalcinosis

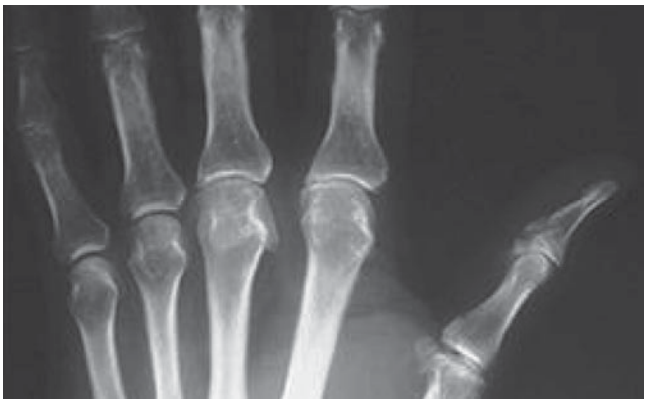

Fig. 8 AP radiograph of the metacarpophalangeal joints of the left hand showing joint space narrowing and osteophytes involving the second and third metacarpophalangeal joints in a patient with calcium pyrophosphate dihydrate (*CPPD*) arthritis

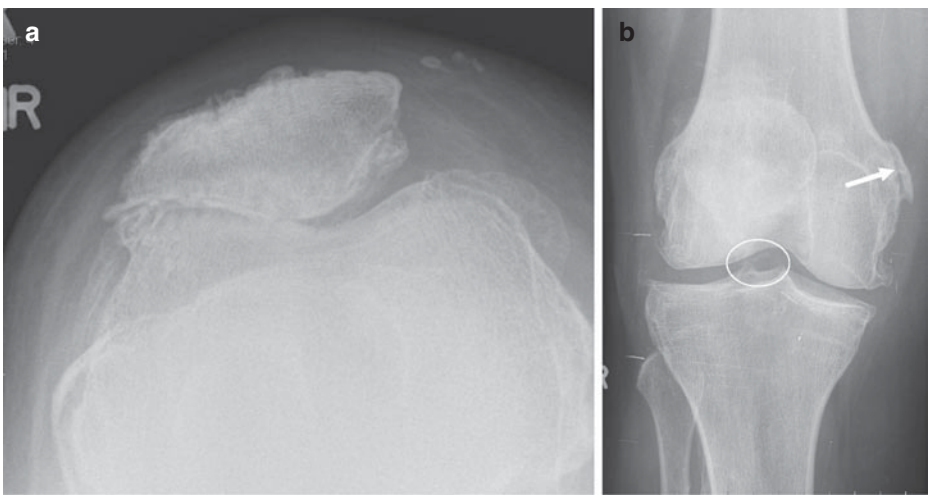

Fig. 9 Calcium pyrophosphate dihydrate (*CPPD*) showing disproportionate narrowing of the patellofemoral joint (**a**) compared with the medial and lateral compartments of the knee (**b**). Note the chondrocalcinosis in the femoral notch (*oval*) consistent with a diagnosis of CPPD and the Pellegrini Stieda, suggesting prior medial collateral ligament injury (*arrow*)

identifiable erosion at the joint surfaces, particularly in the radioscaphoid joint.

The pathogenesis of CPPD is not quite understood. Possibly, there is altered activity of the cartilage matrix enzyme that produces and degrades pyrophosphate resulting in its accumulation and eventual, crystallization. The crystals are 0.5–5 mm in the greatest diameter. They first develop in the articular matrix, menisci, and intervertebral discs. The deposits later enlarge into large chalky white friable masses. They are distinguishable from gout by their positive birefringence under polarized light (gout contains uric acid crystals that are negatively birefringent).

Hemophilia

Hemophilia is one of the oldest recorded diseases. It affects about 400,000 people worldwide and 20,000 in the United Sates. Common usage in orthopedic and radiology literature of this bleeding diathesis often includes hemophilia A (a lack of clotting factor VIII), and hemophilia B or Christmas disease (resulting from a lack of clotting factor IX). Both are sex-linked diseases, making women asymptomatic carriers of the gene (if heterozygous). Until the development of clotting factor replacement therapy, life expectancy for patients with hemophilia was around 11 years. Since the 1980s, replacement therapy has lengthened patients' lives to 50 or even 60 years.

Regardless, hemophilia is a serious disease where minor trauma permits not only life-threatening external bleeding but also bleeding into the body's potential spaces. Joints undergo continual minor daily trauma and so are prone to bleeding. In fact, hemarthroses occur in 75–90% of patients with hemophilia. The knee, ankles, and elbows are the joints most commonly affected. For obscure reasons, joints distal to the elbow and ankle are rarely affected. Patients may also develop hemorrhage into their marrow space, resulting in pseudotumors of bone (Fig. 10). These are generally isolated lytic lesions with well-defined margins that may be confused radiographically with other true neoplastic lesions of bone. There have been disastrous instances where these pseudotumors were amputated in the belief that the patient had an osteosarcoma.

Radiology: Recurrent hemorrhage into a target joint leads to immediate inflammation and eventual deposition of ferritin within the joint. MRI is extremely sensitive to this intra-articular hemosiderin deposition since the iron alters the local magnetic field and causes signal loss (Fig. 11). Episodes of hemorrhage cause (generally beginning around the age of 2 years) increased blood flow to the bone around the joint. This increased flow in turn causes overgrowth of the adjacent epiphyses (Fig. 12) and early leg length discrepancies with the involved leg becoming longer than the uninvolved leg. Overgrowth of the femoral condyles leads to widening of the intercondylar notch and overgrowth of the patella causes the appearance of squaring of its inferior pole. This finding is evident in about 20–30% of juvenile patients with hemophilia (similar hyperemic changes from inflammation may lead to epiphyseal overgrowth in children with juvenile

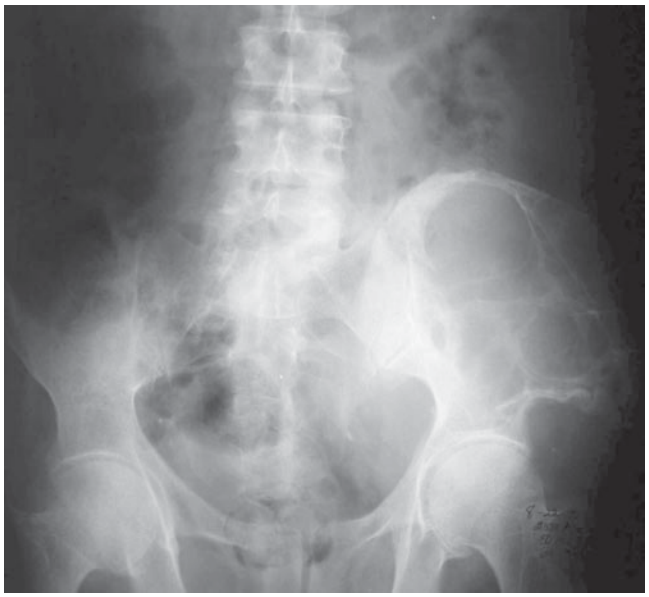

Fig.10 AP pelvic radiographs showing a large lytic lesion in the left iliac wing secondary to a hemophilic pseudotumor

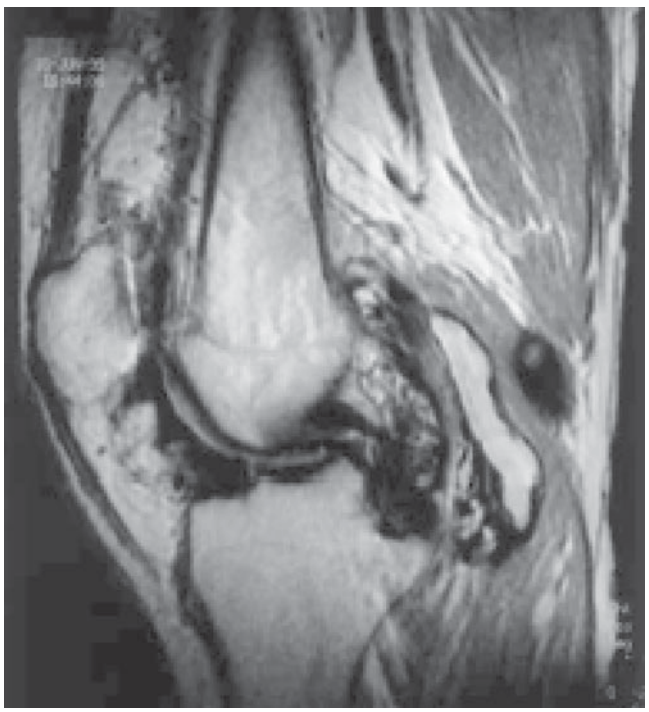

Fig. 11 Sagittal T2-weighted MR image of the knee showing marked hemosiderin deposition about the joint in a patient with hemophilia and recurrent hemorrhages

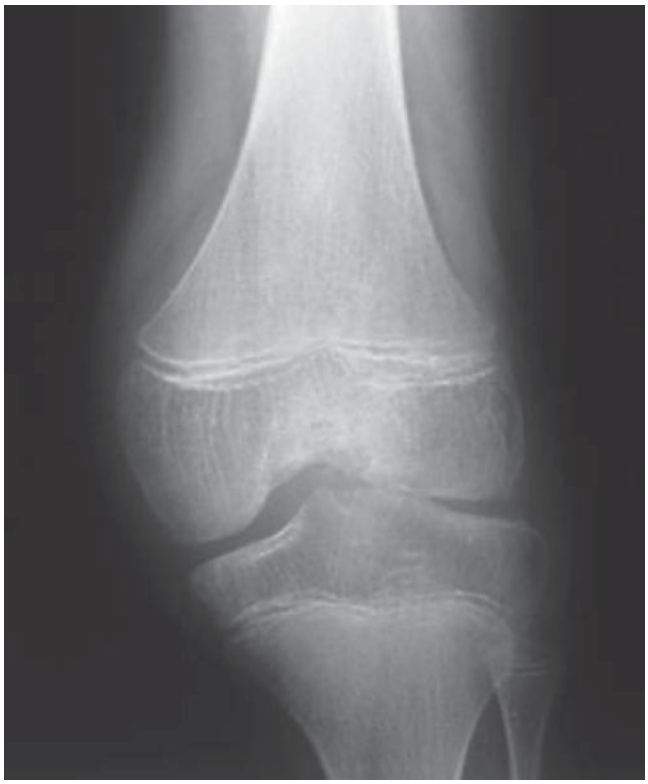

Fig. 12 AP radiograph of the knee in a young patient with hemophilia showing overgrowth of the distal femoral epiphysis related to increased blood flow and inflammation from recurrent hemorrhage into the joint

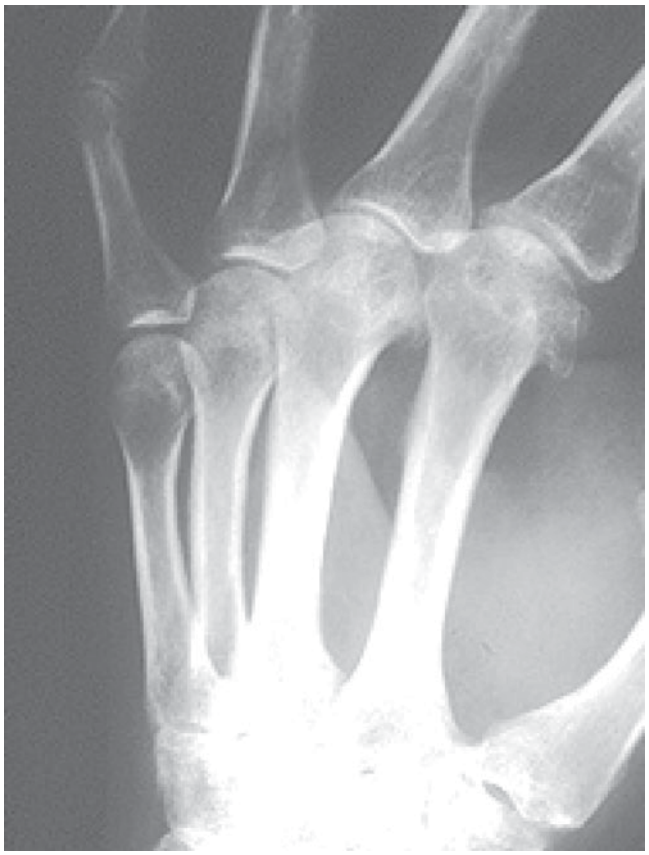

Fig. 13 Oblique radiograph of the left hand in a patient with hemochromatosis showing large osteophytes arising from the radial aspect of the second and third metacarpal heads

chronic arthritis). Ultimately, bones around involved joints undergo premature epiphyseal fusion and as a result the mature limb length is shorter than the normal. Eventually, these patients develop secondary osteoarthritis secondary to loss of their articular cartilage and abnormal biomechanics.

Hemochromatosis

Hemochromatosis has two major forms, one an autosomal recessive type (associated with low transferrin), and the other an acquired form from exogenous iron overload as might result from transfusions for hemolytic anemias or among the Bantu who use iron cookware exclusively. Iron is deposited in many organs, most prominently the liver, spleen, pancreas, brain, joints, and the skin (hyperpigmentation).

The genetic form of the disease is most common among northern Europeans and is more common in men than women. Symptoms may not appear for 30–50 years. Complications include iron-induced cirrhosis, hepatocellular carcinoma, type I diabetes, cardiomyopathy, and pituitary apoplexy. Joint involvement may manifest itself as chondrocalcinosis or osteoarthritis. Similar to CPPD, hemochromatosis has a predilection for the second and third metacarpophalangeal joints. Unlike CPPD, hemochromatosis arthropathy has a tendency to cause large "hook-like" osteophytes from the radial aspect of the metacarpal heads (Fig. 13).

Ochronosis (Alkaptonuria)

Ochronosis is a rare autosomal recessive genetic disease with ineffective homogentisic acid oxidase in the pathway of tyrosine catabolism. Lack of this enzyme leads to excessive production of homogentisic acid (*ortho-meta-* dihydroxyphenylacetic acid). The kidneys rapidly clear this material and only a small amount remains in the tissues, but eventually it begins to accumulate, particularly in tissues with high cartilage content, that is, synovial joints, intervertebral disk spaces, the sclera of the eye, and the pinna of the ear. Homogentisic acid is reactive on exposure to air and will oxidize into a black polymer. By the fourth decade, these deposits begin to calcify causing the synovial joints to show chondrocalcinosis. The intervertebral disks also calcify as do other cartilage structures, including the pinna of the ear. Eventually, the patients develop secondary osteoarthritis and spondylosis related to disk

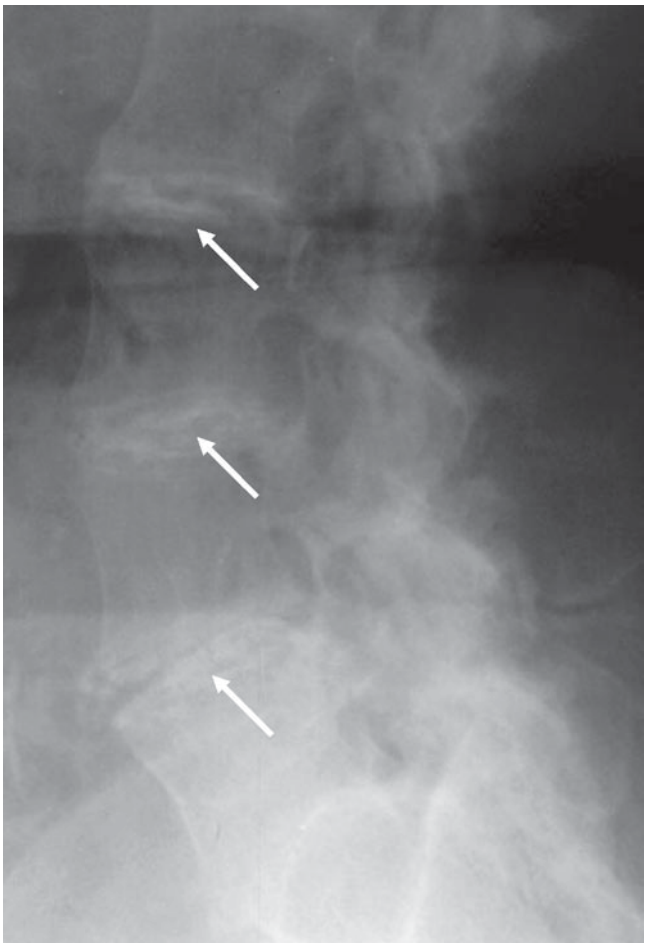

Fig. 14 Lateral coned-down lumbar spine in a patient with ochronosis showing severe disk space narrowing with calcification within the disk spaces (*arrows*). This is a late finding in the disease

degeneration caused by the deposition of homogentisic acid in cartilage (Fig. 14). There is no involvement of the sacroiliac or apophyseal joints, distinguishing it from ankylosing spondylitis.

Part II. The Destructive (Inflammatory) Arthritidies

Rheumatoid Arthritis

RA is considered to be an autoimmune disease that may involve multiple organ systems. Joint involvement predominates in most patients. The disease occurs more often in women than men in a ratio of about 2–3:1. It may appear at any time during life but has its peak incidence between 35 and 50 years of age.

The majority of patients afflicted with RA have ongoing, progressive disease with periods of reduced activity. Only about 5–10% have spontaneous remissions. Since the severity and behavior of RA varies from patient to patient, diagnosis can be difficult. The American College of Rheumatology has established a set of clinical criteria to establish the diagnosis.

Etiology: RA is a systemic disease that manifests as a synovial arthropathy. An antigen-antibody reaction, or a state of hypersensitivity, initiates the inflammatory process. The antibody, a gamma globulin (rheumatoid factor), is produced in lymph nodes and coats the cell membranes of lymphocytes and plasma cells, which travel to the synovium where they react with the antigen causing acute inflammatory reaction. Several factors including genetics (human leukocyte antigen, HLA DR4 and DR1) and infections have been studied, and may contribute in a multifactorial fashion. Key pathogenic factors include increased production of cytokines, such as TNF-α and IL-1. The infiltrating T cells and macrophages release another inflammatory cytokine into the synovial fluid, oncostatin M (related to the IL-6 family) (9) as well as additional IL-1. TNF-α and oncostatin M work together to induce production of collagenases called matrix metalloproteinases (MMPs) by the diseased synoviocytes and chondrocytes. If produced in excess, the MMPs result in excessive collagen degradation and can lead to cartilage matrix collapse. Furthermore, the infiltrating macrophages have the ability to differentiate into osteoclasts, which play a role in the bone erosion associated with RA

Clinical features: RA is a symmetrical multijoint inflammatory arthropathy, potentially involving every joint in the body with the exception of the DIP joints. There are usually accompanying constitutional symptoms such as stiffness, fatigue, malaise, anorexia, and weight loss. Other organs and systems can be involved in the inflammatory process, including the formation of rheumatoid nodules, which are pathognomonic of the condition. The diagnosis is usually one of exclusion, since other causes for the clinical appearance must be ruled out. Increased rheumatoid factor and anticyclic citrullinated antibody titers are helpful in confirming the diagnosis.

Radiological features: RA is a destructive arthritis, with the most severe initial changes being erosions in the bone at the periphery of the involved joint. With progression of disease, the central articular cartilage of the joints erodes and the subchondral bone shows erosions and subchondral cysts. The distribution of RA is generally symmetrical. The one exception to this rule is in patients with paralysis where, for unknown reasons, the disease tends not to involve the paralyzed limb. Despite long-standing disease, ankylosis of joints usually does not occur – the major exception being the wrist.

Tendons are often involved by inflammatory pannus in RA. MRI is very sensitive for detecting early involvement of

tendon sheaths and other synovial-lined spaces. Subcutaneous nodules can also be seen clinically and by radiological imaging, and are a pathognomic feature if seen.

Tendon and ligament inflammation often lead to joint misalignment including prominent ulnar drift at the metacarpophalangeal joints of the hands (the feet may also show similar deformities). Boutonniere deformities (flexion deformity at the PIP and hyperextension at the DIP) and swan neck deformities (hyperextension at the PIP and flexion at the DIP) also occur frequently.

The bone adjacent to involved joints shows marked osteopenia caused by increased local blood flow, so called periarticular osteopenia. Periosteal reaction, while common in psoriatic arthritis, is rare in RA.

RA affects the metacarpophalangeal joints, the wrists, the knees, the subtarsal joints, and the metatarsophalangeal joints in more than 80% of patients. It affects the hips, shoulders and acromioclavicular joints, elbows, the ankle and subtalar joints, and the cervical spine, particularly the atlantoaxial joint (Fig. 15–18) in about 50% of patients. The temporomandibular joints and the sternoclavicular joints are affected in about a third of patients. The sacroiliac joints, on the contrary, are involved in less than 5% of patients, a distinguishing feature from the spondyloarthropathies.

Surgical pathology: In the early stages of RA, the capsule of the joint especially the juxta-synovial layer shows non-suppurative chronic inflammation. This is characterized by hypertrophy and hyperplasia of the synovial cells resulting grossly in a papillary pattern on the surface of the synovium.

Marked increase in vascularity occurs and the tissue is edematous and infiltrated with large numbers of cells, especially plasma cells and lymphocytes, the former frequently containing eosinophilic inclusions of gamma globulin. These cells form "rosettes" or cuffs around blood vessels and may form lymphoid follicles (Allison-Ghormeley bodies). In time, the collections of lymphocytes often develop germinal centers (Fig. 19). Synovial villi can get engulfed in the lymphocytes; also, the hypertrophic synoviocytes can develop into giant cells.

Immature mesenchymal cells proliferate. There is fibrinous exudation at the surface and within the synovium (rice bodies). Disruption of the synovial border of the inner aspect of the capsule occurs and there is extravasation of inflammatory cells into the joint. The amount of joint fluid is markedly increased.

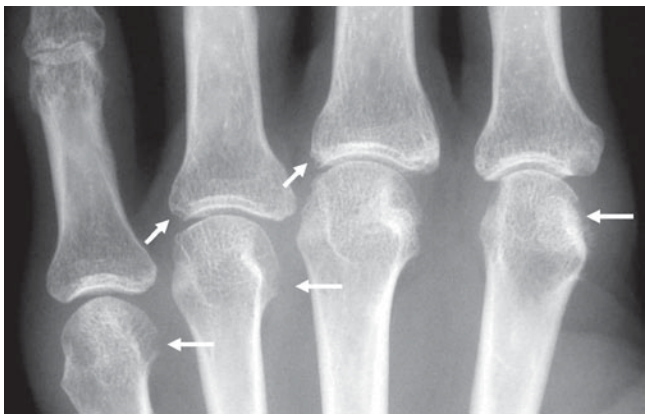

Fig. 15 Posteroanterior (*PA*) radiograph of the metacarpophalangeal joints showing early marginal erosions (arrows) in a patient with rheumatoid arthritis (*RA*)

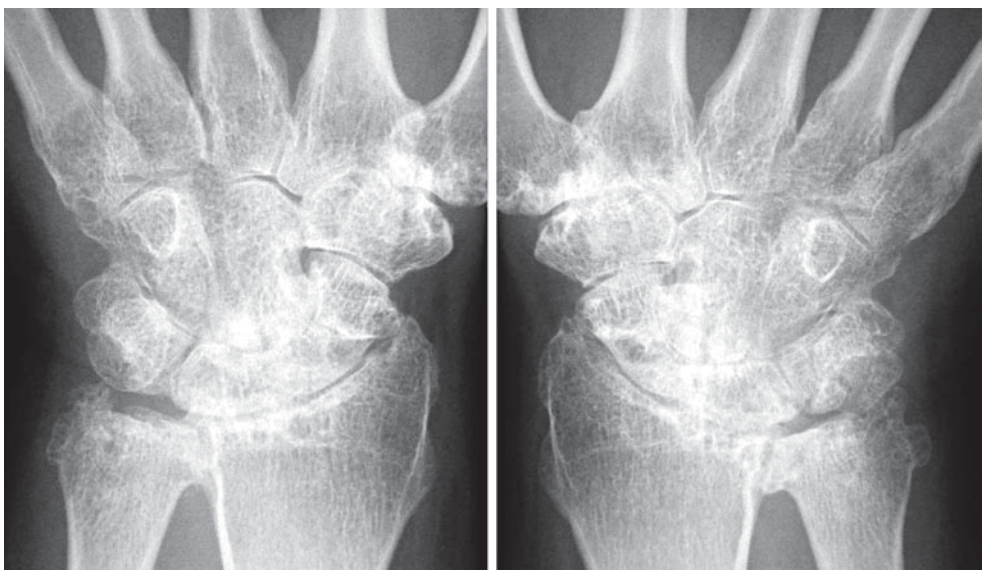

Fig. 16 Bilateral posteroanterior (*PA*) views of the wrist in a patient with moderately advanced rheumatoid arthritis (*RA*) showing diffuse intracarpal joint space narrowing, subchondral lucencies, and evidence of erosion

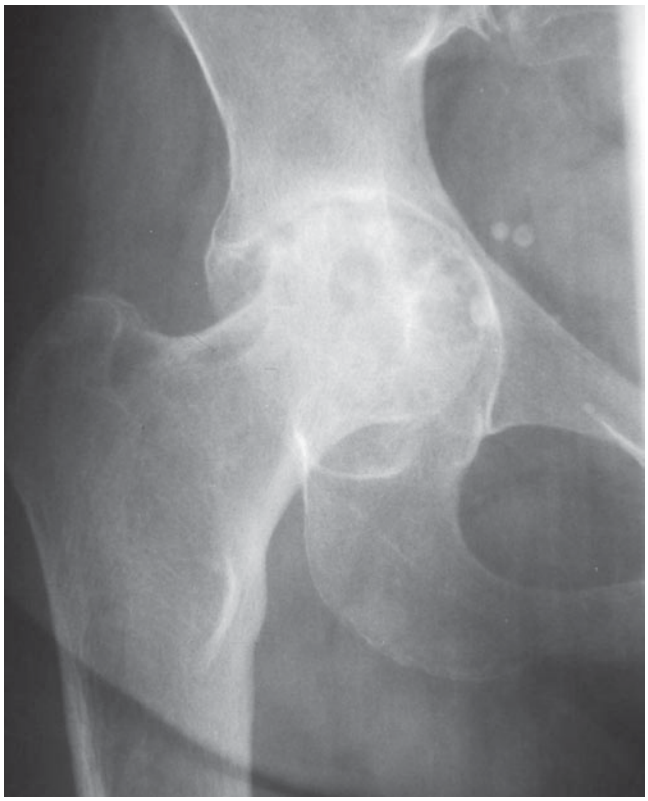

Fig. 17 AP radiograph of the right hip showing axial joint space narrowing with irregular erosions along the femoral head and large lucencies consistent with geodes in a patient with rheumatoid arthritis (*RA*)

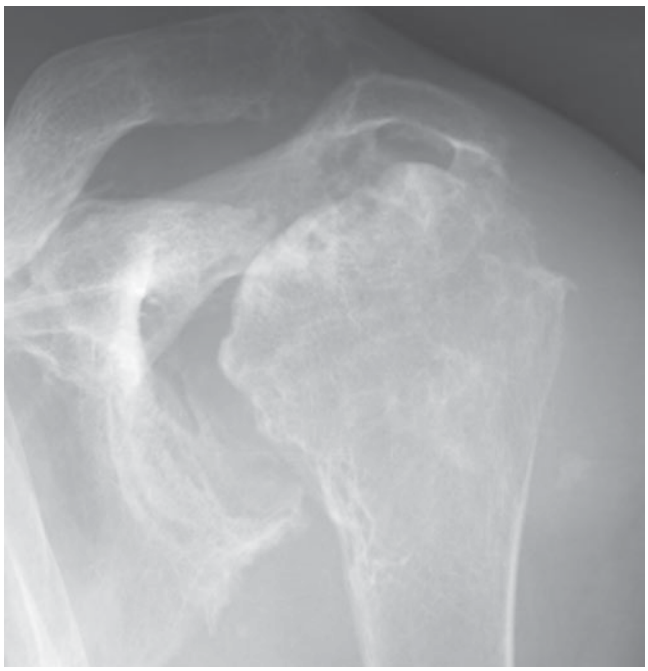

Fig. 18 AP radiograph of the left shoulder in a patient with rheumatoid arthritis (*RA*) showing marked destruction of the glenohumeral joint and resorption of the distal end of the clavicle

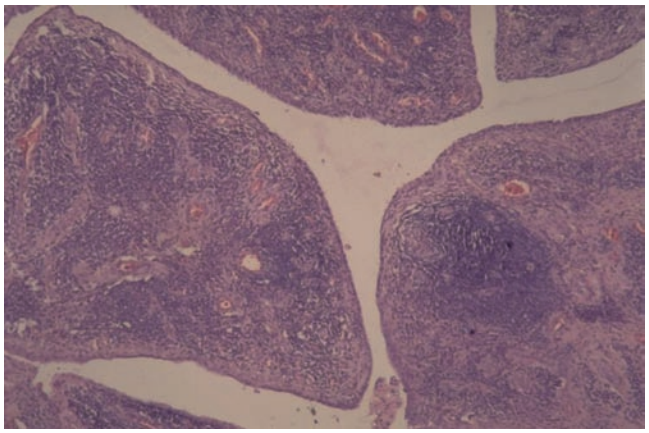

Fig. 19 Rheumatoid arthritis (*RA*). The microphotograph shows synovium with papillary architecture, and a prominent lymphoplasmacytic infiltrate. The lymphocytes are aggregated into nodules and the beginning of germinal center formation can be appreciated

Later, pannus forms. This is a combination of proliferating mesenchymal cells and granulation tissue starting at the periphery of a joint and invading it covering and destroying the articular cartilage and the subchondral marrow spaces beneath the articular cartilage. Pannus destroys the internal structures of the affected joint. Pannus grows into the articular surface, which is why it is difficult to eradicate it completely using mechanical means. Pannus activates various enzymes in the inflammatory cascade and destroys the joint enzymatically. The enzymes come from the lysosomal sacs of neutrophils and the chondrocytes and result in chondrolysis.

Chronic Synovitis

The surgical pathologist is often confronted with samples that show proliferative changes, mild -to -moderate chronic inflammation and non-specific reactive changes. A host of conditions may cause these changes. Attention paid to some of the common entities listed can help the work-up of such patients. Certainly, infections, crystal arthropathies, and so on, etc. are in the differential. Sometimes, however, despite the best efforts, a specific diagnosis cannot be reached. Under such circumstances, the clinical work-up using laboratory methods can be more helpful than the histopathologic clues (which are common to a variety of etiologies). This must be recognized, and it must not be considered wrong to diagnose a sample as chronic or proliferative synovitis. For example, hemosiderin deposition in the joints, can be due to trauma, bleeding diathesis, tumors such as pigmented villonodular synovitis (PVNS), and hemangiomas. etc. All these can result in chronic hemosiderotic synovitis (Fig. 20).

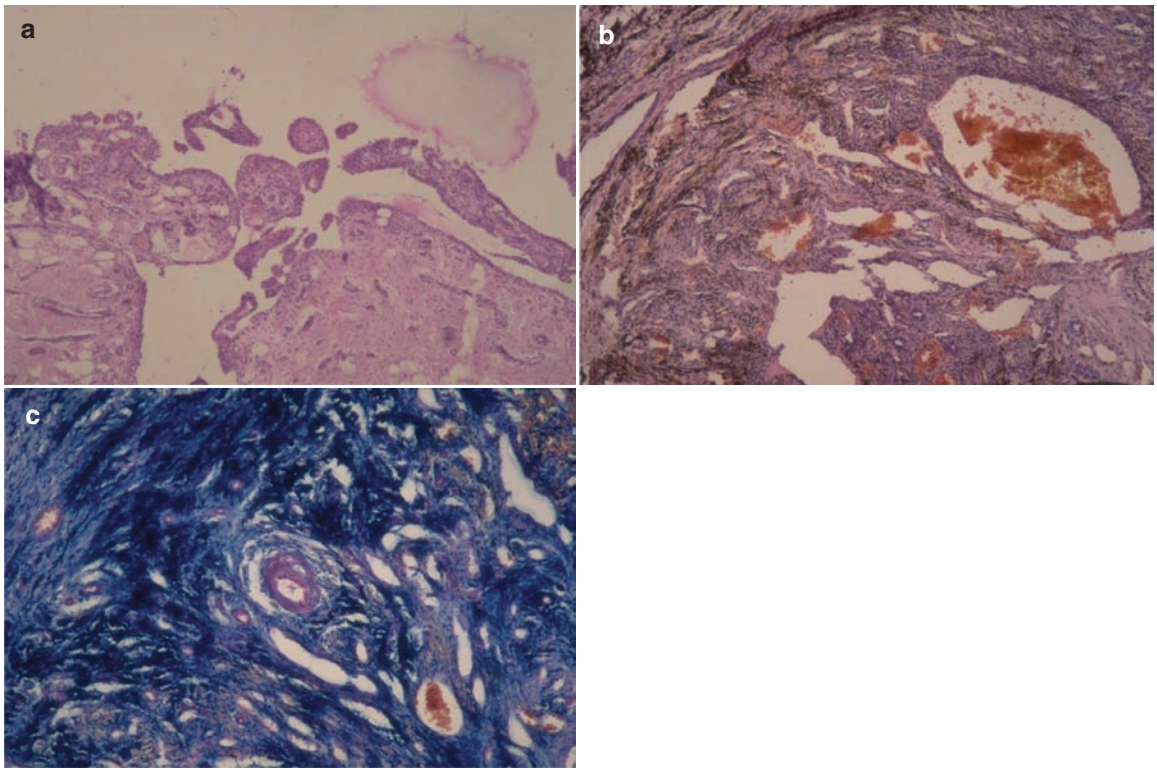

Fig. 20 **a** Chronic nonspecific synovitis. There are some proliferative changes and minimal nonspecific lymphocytic infiltration. **b** Chronic hemosiderotic synovitis due to an arteriovenous malformation (hematoxylin and eosin). **c** Chronic hemosiderotic synovitis (Prussian blue stain)

Juvenile Rheumatoid Arthritis (Juvenile Chronic Arthritis)

Juvenile rheumatoid arthritis (JRA) is usually seen in individuals before the age of 16. As with adult RA, it affects girls more often than boys in a 2:1 ratio. It often resolves with age but may leave significant residual joint damage. JRA has three main forms: pauciarticular (less than 5 joints involved), polyarticular, and Still's disease.

Clinical features: Patients with JRA complain of swollen, stiff, and painful joints, especially in the morning or after a nap. The affected joints show warmth and redness. Patients often complain of fatigue, decreased appetite, poor weight gain, and show slow growth. They may have ocular inflammation.

Radiographic features: Radiographs in pauciarticular JRA may show periarticular soft tissue swelling, osteopenia, periosteal new bone formation, and overgrown epiphyses. As with hemophilia, the knee may show widening of intercondylar notch, but squaring of the inferior pole of the patella is less common than in hemophilia. The inflammation may eventually lead to premature skeletal maturation. This in turn causes leg length discrepancies, small vertebral bodies, tibiotalar slant in the ankle, or Madelung's deformity in the wrist (Figs. 21 and 22) from premature closure of part of the physis.

Erosions are often a late finding in JRA, and unlike adult RA, joint fusion may be a prominent complication in severe cases. As with adult RA, atlantoaxial subluxation may be a problem. Polyarticular JRA is essentially the adult type of RA occurring in younger patients. As with adult RA, its distribution is generally symmetric. It is also more likely to persist into adulthood than pauciarticular JRA. Still's disease is the most serious form of JRA. It affects not only the joints but has systemic manifestations including fever and diffuse lymphadenopathy. It affects multiple organ systems including the heart and pericardium, the pleura, and the spleen.

Septic Arthritis

Infectious arthritis is a serious problem in spite of the wide range of potent antibiotics that are available. Sometimes these infections arise in individuals who are immune compromised. In some cases, the joint infection is secondary to overwhelming infection primary to some other system of the body. In other cases, there may be contiguous infection or a penetrating injury into the joint. The problem of infectious arthritis is further aggravated by poor diffusion of antibiotics into the joint space. Septic arthritis may cause considerable morbidity if treatment is delayed. Early intervention in the

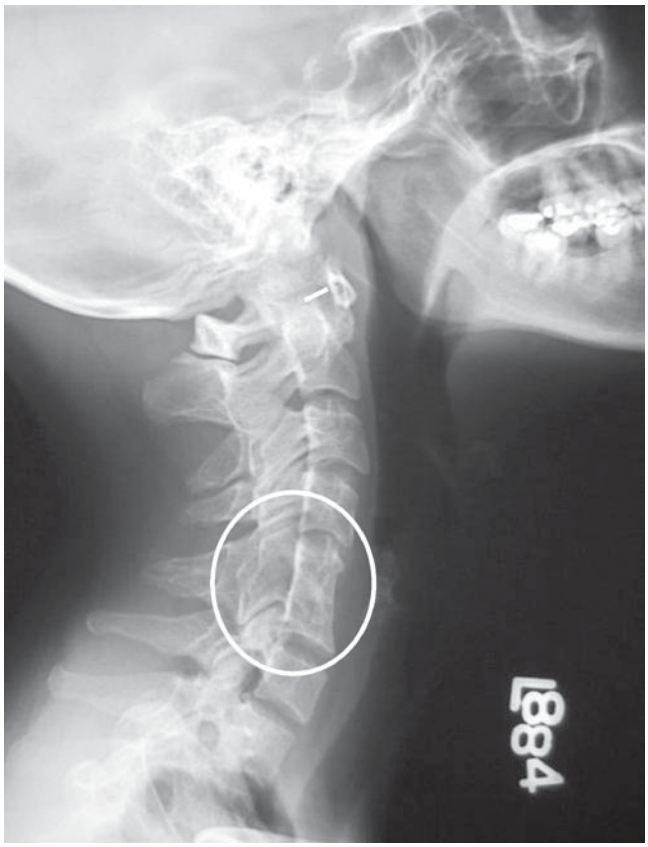

Fig. 21 Lateral radiograph of the cervical spine showing widening of the atlantoaxial joint (*line*) and fused anterior and posterior elements of C5 and C6 related to underlying juvenile rheumatoid arthritis (*JRA*).

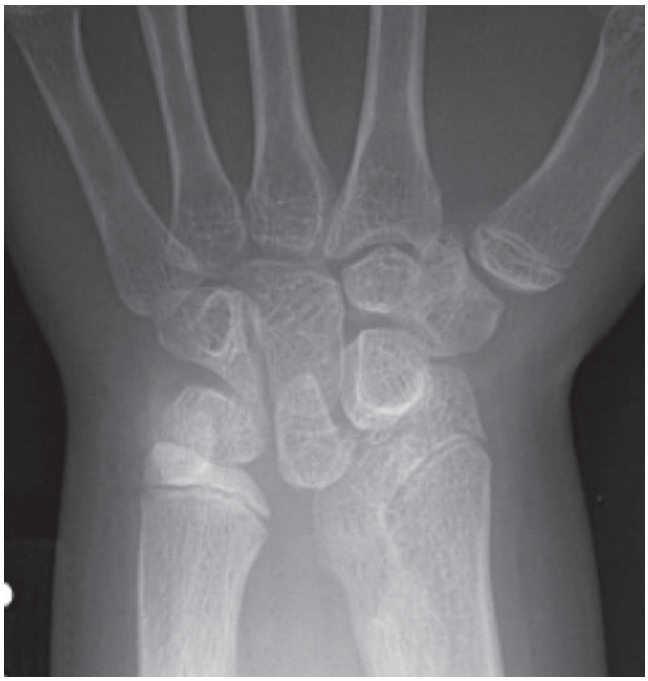

Fig. 22 Posteroanterior (*PA*) radiograph of the wrist showing a Madelung's deformity in a patient with juvenile rheumatoid arthritis (*JRA*) and premature closure of the ulnar aspect of the distal radial physeal plate

form of arthrotomy or arthrocentesis for diagnosis and therapeutic washout is important.

Besides direct involvement of the joint by a pathogen, arthritis may occur by an immune response to a pathogen causing a reactive arthritis as is seen in Chlamydial (Reiters syndrome), some enteric, and sometimes with treponemal and fungal systemic infections. These immune forms of arthritis, however, are generally discussed separately and excluded from discussion of infectious arthritis and discussed.

*Pathogenesis***:** Infection reaches the joint by hematogenous or lymphatic routes. The hematogenous route is common in most forms of arthritis including viral. Infection to the joint may also be by direct spread from neighboring soft tissue or bone. Penetrating injuries are especially important as a cause of fungal septic arthritis.

Pathology: The basic inflammatory process in infection of the joint is marked by hyperemia of the synovium, infiltration by leukocytes, lymphocytes and macrophages and plasma cells. An associated exudate develops which may be purulent, serous, or fibrinous. With persisting infection and inflammation, granulation tissue (pannus) results and subsequently adhesions occur. Pyogenic infections may result in pyoarthrosis which is extremely resistant to antibiotic therapy and requires surgical drainage or repeat arthrocentesis – often emergently.

The sequelae of septic arthritis can be severe and leave lasting scars. These are fibrinous adhesions and fibrous ankylosis, articular erosion by pannus (chondrolysis), destruction of the stabilizing ligaments, and intra-articular disks. Erosion of the articular cartilage by pannus may extend to the subchondral bone and lead to secondary osteoarthritis. Lasting damage is frequent in bacterial and fungal arthritis.

Chondrolysis is a significant feature of bacterial, mycobacterial, and fungal arthritis. In all probability, cytokines and the release of lytic enzymes and less likely the physical effect of the pannus mediate the chondrolysis. In effect, inflammation upsets the balance of regeneration and erosion that occurs in normally functioning cartilage. The inflammatory reaction produces IL-1 and TNF-α. These act in concert, inducing the chondrocytes into the release of degrative enzyme, metalloproteinases. These, in concert with granulocytic hydrolytic enzymes, cause rapid destruction of the articular surface. The late sequela of septic arthritis is secondary osteoarthritis.

Bacterial arthritis: The type of organism and pattern of joint involvement often depend on the age (the elderly are at greater risk) of the patient, preexisting arthropathy, immune status, and habits, particularly intravenous drug abuse. Dermal nosocomial bacteria are the most frequent pathogens (*Staphylococci*, *Streptococci*, Pseudomonas) and Enterobacteriaceae less so. *Neisseria gonorrhea* is suspected most often in septic arthritis in young sexually active individuals, particularly females.

The clinical course can be prolonged with staphylococcal arthritis being the most destructive. Diagnosis is by way of clinical presentation and smear and culture evaluation of synovial fluid. However, synovial fluid may not always offer a diagnosis especially in partially treated patients.

Infection can also complicate prosthetic joints. In this case, it may be acute (pyogenic and enteric bacteria) or chronic (coagulase negative staphylococci or diphtheroids, etc.). The diagnosis in such cases can be difficult, and requires clinical, laboratory, and radiological input.

Loosening of endoprosthetic components can occur from a variety of causes (infection, metal reaction, rejection, wear reaction, etc.). Separating infection from all the other non-infectious causes is important, since the foreign material acts as a nidus for infection and perpetuates it in a vicious cycle. Removing the endoprosthesis is often considered an important part of the management. It may subsequently be replaced later or a procedure such as an excision or interposition arthroplasty be used instead (such as a Girdlestone arthroplasty of the hip).

Estimation and quantization of the acute inflammatory response is the usual way of suspecting infection. Tissue from around the prosthesis is taken. The number of polymorphs per 40X× field (400X magnification) are counted and averaged over at least 5 fields (taking care to avoid counting cells within vessels, fibrin, and inflammatory exudate). Counts of 5 polys/high-power fields are suspicious ("Mirra's criteria") and correlate with the presence of infection (sensitivity 0.4–0.9 and specificity 0.7). Counts of 10 polys/high-power field are, however, much more likely to be infection (sensitivity 0.86 and specificity 0.85) (13). Whether or not this method still applies in specialized situations such as patients with rheumatoid arthritis (RA) is uncertain (14).

Mycobacterial arthritis: Mycobacterial arthritis and spondylitis deserve separate mention because they usually are diagnosed late and can be extremely destructive. Mycobacterial infections to the synovium are mostly hematogenous. At times, they may be spread contiguously from the bone marrow. Joint infection can be either exudative or dry (caries sicca). The latter is frequent in the shoulder (Fig. 23). Spinal involvement is frequent. Next in frequency is the knee and hip.

Spinal tuberculosis (Pott's disease) generally presents as persistent backache followed by a gibbus deformity of the spine. Tuberculosis of the spine causes vertebral destruction but usually the intervertebral disk is spared. If treatment is delayed, vertebrae may collapse, and cause spinal cord compression. Alternatively, patients may develop intraspinal, epidural abscesses. Pott's paraplegia, may result from, osseous compression, kinking of the cord, or mass effect from a paraspinal abscess. Radiologically, in spinal disease, there is usually a paraspinal abscess, and often evidence of vertebral destruction. In other joints, there is often a narrowing and periarticular osteopenia.

Early diagnosis and treatment is important, since the disease can be extremely destructive. A combination of clinical evidence, radiological findings, smears, and culture of synovial fluid and an aspirate from a paraspinal abscess, help in arriving at the diagnosis. In cases where tissue is available (synovial biopsy or abscess wall), the classical features of caseating and noncaseating epithelioid cell granulomas with mononuclear cell infiltrate are seen.

In human immunodeficiency virus (HIV)-associated mycobacterial infections, the causative organism is most commonly *Mycobacterium tuberculosis*. Atypical mycobacterial species involve the bone marrow and tendon sheaths (tenosynovitis).

Spirochetal arthritis: Syphilitic involvement of the joint is important both in congenital syphilis and in adults as also in patients with HIV. Organisms are detected in the early lesions and in paresis, but only rarely in other late lesions.

Congenital syphilis may result in stillbirth or neonatal death. The basis of the lesions is an ischemia resulting from an endarteritis, along with a granulomatous reaction often rich in plasma cells (gumma). Characteristically, there is cortical destruction indicating osteomyelitis and nonspecific periostitis as well. Likewise, there may be inflammation of the epiphyseal and articular cartilage of the humerus and tibia. A Clutton's joint is a chronic hydrarthrosis of the knee joints and is a late manifestation of congenital syphilis.

In acquired syphilis, bone infection overshadows the joint involvement. In tertiary syphilis, gummatous lesions of paraarticular connective tissues may rupture into the joint space, resulting in large painless effusion mimicking neuropathic arthropathy. The synovium will show villous hypertrophy, perivascular lymphoid and plasma cell infiltrate, and endothelial proliferation. Syphilitic polyarthritis is described in patients with AIDS.

Borrelia burgdorferi causes a nontreponemal arthritis typified by Lyme's disease. The disease is inoculated by the tick, Ixodes. There may be large joint involvement (either

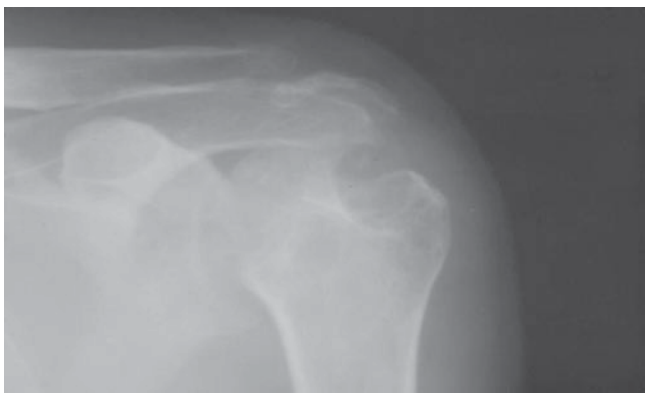

Fig. 23 Caries sicca involving the shoulder. The X-ray demonstrates reduction in the joint space and bony destruction

mono- or polyarticular) or arthralgias for varying periods of time. HLA-DR4 is particularly associated with a prolonged course and refractoriness to therapy. Polymerase chain reaction methods allow the detection of microbial DNA. This is useful in diagnosis as well as therapy. Arthritis occurs in the tertiary stage.

Viral arthritis: Systemic viral diseases can cause transient arthritis as a part of the clinical complex. These viruses include infectious mononucleosis, influenza, mumps, parainfluenza, and respiratory syncytial virus. Prolonged involvement may be noticed in rubella where arthritis may last persist up to 4 weeks. Arthritis occurs frequently in hepatitis B and hepatitis C virus infection, where it is polyarticular with a nonspecific synovitis. Joint involvement also occurs in infections with HIV and parvovirus.

Fungal arthritis: Fungal arthritis is uncommon. Involvement of the joint is by hematogenous or direct spread from soft tissue lesions or from osteomyelitis. AIDS predisposes to fungal arthritis but even then it is rare.

Parasitic arthritis: Several organisms, such as the guinea worm (Dracunculus), hydatid cyst (Echinococcus), schistosoma, strongyloides, and hookworm have been associated with arthritis.

Gout

Gout is one of the oldest recognized arthropathies (described by Thomas Sydenham in 1683). It affects about 2 million individuals in the United States, roughly the same number as are afflicted by RA. Primary gout is predominantly a disease of adult men with a 4:1 male to female ratio. In fact, gout is the major cause of inflammatory arthritis in men over the age of 30. When it does occur in women, they are usually postmenopausal or secondary to other hyperuricemia-producing conditions.

Gout arises from precipitation of urate crystals into joint spaces, the marrow and the soft tissues. The first causes an inflammatory arthropathy within the joint, the second causes intraosseous tophi that may lead to para-articular erosive changes, and the last causes soft tissue tophi and inflammatory masses in the soft tissues. Some patients with chronic gout also develop urate nephropathy.

Uric acid (urate) crystallizes at a level that exceeds 6.8 mg/dL (with slight variation in temperature and pH). High concentrations of uric acid may result from underexcretion or from overproduction of uric acid. The former, known as primary gout, accounts for 90% of cases. Overproduction most commonly results from high rates of tissue degradation as one may see in patients on chemotherapy for neoplasms or myeloproliferative diseases or ethanol abuse. This form of gout is secondary and accounts for only 10% of patients. Some rare enzymatic deficiencies result in overproduction of uric acid. These include patients with Lesch-Nyhan syndrome (hypoxanthine-guanine phosphoribosyl transferase deficiency), Von Gierke's disease (glucose-6-phosphatase deficiency), and patients with PP-ribose-P synthetase variants. Synovial fluid is a poor solvent of monosodium urate crystals because of a low pH. Thus, urate in joint fluids become supersaturated much before plasma does especially in peripheral joints where the temperature is lower (such as the foot, where gout is prone to manifest).

Uric acid is the end point of purine metabolism. The synthesis of purine is by two pathways: One is synthesis from non-purine precursors. The other is the salvage of free purine bases derived from the breakdown of nucleic acids of endogenous and exogenous origin. Little uric acid is produced by the operation of the salvage pathway, with the synthesis of purine from non-purine precursors contributing the bulk. In any situation where the salvage mechanism is less efficient and greater synthesis is from non-purine precursors, uric acid production is increased and gout may result.

Factors that may result in the conversion of hyperuricemia into primary gout are as follows:

- Gender
- Duration of the hyperuricemia – gout rarely appears before 20 to –30 years.
- Genetic predisposition: the X-linked abnormalities of hypoxanthine guanine phosphoribosyl transferase (HGPRT) and gout following multifactorial inheritance running in families.
- Heavy alcohol consumption
- Obesity
- Thiazide diuretics, low-dose aspirin or chronic renal failure

Surgical pathology: The progress of gout can be divided into (1) asymptomatic hyperuricemia, (2) acute arthritis, (3) intercritical periods, (4) chronic tophaceous arthritis, and (5) gouty nephropathy.

Acute arthritis: The synovium and the synovial fluid show a dense infiltrate of polymorphonuclear leukocytes. The synovium and neutrophils may show small clusters of monosodium urate crystals. These are slender, long, needle like, and negatively birefringent. In response to the inflammation, there is edema and congestion of the synovium. Besides the dense neutrophil aggregates, some lymphocytes, plasma cells and macrophages are also seen. The acute attack abates when the crystals go into solution and as a result the inflammatory response ceases.

Chronic tophaceous arthritis: Repeated acute attacks lead to precipitation of monosodium urate crystals until visible deposits form. The synovium in response becomes progressively more fibrotic and thickened, with pannus formation. This pannus destroys the underlying bone. The fibrosis and articular destruction progress to progressive articular functional impairment. Since uric acid crystals are water soluble, when tissue is placed in 10% formalin they will dissolve out

(and so polarization microscopy will not reveal the crystals). Diagnosis can still often be made by identifying the needle-shaped empty spaces where the crystals once resided. If visualizing the crystals is needed, the tissue should be fixed in ethanol.

Gouty nephropathy: The deposition of monosodium urate crystals in the interstitium of the kidney ultimately results in the formation of tophi and attendant inflammation ensues. The crystalline material is also deposited in the tubular epithelium. The third feature is the formation of uric acid calculi (not radio-opaque) and resultant obstructive nephropathy which may include chronic pyelonephritis.

Tophi: A tophus is an aggregate of monosodium urate crystalline material with its accompanying inflammation including foreign body type of giant cells. This is the pathognomonic hallmark of this disorder *Caries sicca involving the shoulder***.** The X-ray demonstrates reduction in the joint space and bony destruction. Tophi can be seen in the articular cartilage, periarticular ligaments, bone, tendons, and soft tissue such as olecrenon and patellar bursae, kidneys, nasal cartilage, skin of the finger tips, palms, and soles. They may cause superficial swelling if large enough, overlying ulceration (Fig. 24).

Radiology: Gout classically affects the first metatarsophal phalangeal joint of the feet, a condition known as podagra. It also often affects other joints in the feet as well as the wrist and small joints of the hand. The knee and elbow are less commonly affected. Typical early gout shows deposition of mildly hyperdense material in the soft tissues adjacent to joints. These represent soft tissue tophi. Over time and with repeated attacks, the bones may develop para-articular erosions related to osseous tophi that punch out into the surrounding tissues. At the same time, intracapsular urate deposition leads to an inflammatory synovitis and destructive changes within the joint. The appearance of clasp-like erosions in a distribution that is typical for gout is nearly pathognomonic. The disease does not always follow a classic course, however, and may give myriad less typical appearances.

Clinical course: The initial symptoms are most often at the first metatarsophalangeal joint. Besides this, the other common sites of gouty attacks include instep of the feet, ankle, heel, knee wrist, finger, and elbows. Early attacks last from that of a few hours to a few weeks. Subsequent attacks may occur in months or years later. Progressively, the symptoms fail to resolve, and a chronic phase sets in.

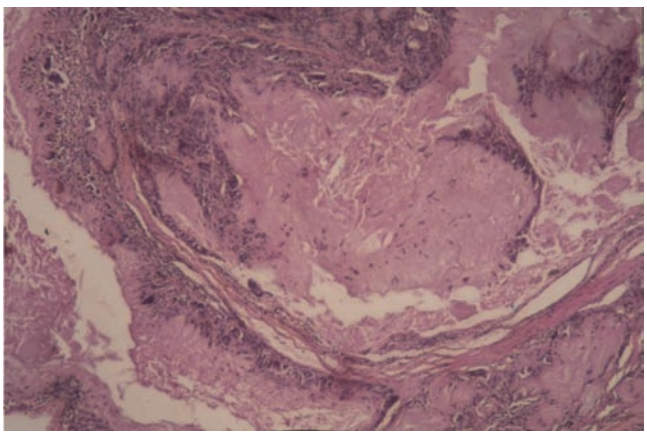

Fig. 24 Gout. Uric acid tophus in the soft tissues with a giant cell reaction. This material can often dissolve during processing

Psoriatic Arthritis

About 5–10% of patients with cutaneous psoriasis develop arthropathy, a subset of which may be severe, deforming, and progressive. In some cases, the arthropathy precedes the skin disease, and in some cases of familial psoriasis, the skin manifestations may be entirely absent for a generation. Five basic patterns of psoriatic arthritis have been described:

1. Asymmetric distal oligoarthritis involving the small joints of the digits (55–70%).
2. Asymmetric DIP arthritis, often with paronychial swelling and nail changes (5–10%).
3. Sacroiliitis and spondylitis (5%).
4. Symmetric polyarthritis that resembles RA (10–30%).
5. Arthritis mutilans with severe opera glass hand deformity (“main en lorgnette”) (3–5%).

Of these five types of psoriatic arthritis, the asymmetric oligoarthritis is most common; the mutilans form of the disease is the least common. Psoriatic arthritis is among a group of diseases associated with a spondyloarthritis. Four diseases, ankylosing spondylitis, spondyloarthropathy of inflammatory bowel disease, psoriasis, and reactive arthritis may all cause an arthritis that primarily affects the sacroiliac joints and the spinal column (especially in patients who are HLA B-27 positive).

Reactive Arthritis

Reactive arthritis occurs more commonly in young adults (20–40 years) with a male predominance and is strongly associated with HLA B-27. The syndrome consists of inflammatory arthritis, mucosal lesions, conjunctivitis, urethritis or cervicitis, skin rash, and keratodermia blenorrhagicum (a rash that occurs on the soles of the feet and the palms of the hands that resembles pustular psoriasis). The condition is called reactive arthritis because it frequently follows dysentery or a sexually transmitted disease. Several bacterial triggers have been identified that may initiate the onset of disease. These include *Shigella*, *Salmonella*, *Yersinia enterocolitica*, *Chlamydia trachomitis*, *Campylobacter jejuni*, and *Lymphogranuloma venereum*.

Radiographically, reactive arthritis is virtually indistinguishable from psoriatic arthritis. There is a bilateral asymmetric and distal arthritis with fusiform digital swelling, peripheral erosions, bone proliferation, and enthesopathy. It even causes an asymmetric spondyloarthropathy that is virtually identical to psoriatic spondyloarthropathy. It differs from psoriasis in the frequency with which joints are involved. Reactive arthritis involves the feet, ankles, and knees most frequently. The hands, hips, and sacroiliac joints are much less frequently involved.

Ankylosing Spondylitis

Ankylosing spondylitis (Marie-Strumpell disease or Morbus Bechterew) most common of the spondyloarthropathies and has the highest association with the HLA-B27 antigens (over 95% of patients are HLA B27 positive). As with many arthropathies, it is a systemic disease so it not only affects the spine and sacroiliac joints but also causes aortitis and aortic insufficiency late in the disease in about 5–10% of patients, rare upper lobe predominant interstitial restrictive pulmonary disease (1%) and iridocyclitis (25%) or uveitis (20%). About 10% of patients with ankylosing spondylitis will develop secondary amyloidosis.

Ankylosing spondylitis is insidious in onset and usually begins between ages 16 and 45 years, although 10% of patients may have had an earlier onset in a juvenile form of the disease. It progresses to significant disability in about 20% of those affected. Clinically, it affects men nine times more often than women, but radiographic survey studies have shown an equal prevalence, suggesting that women are less symptomatic. Patients complain of low back pain, morning stiffness, and fatigue. They may have intermittent fever. Many patients have enthesopathy/tendonitis. Typically, ankylosing spondylitis starts in the sacroiliac joints (from inferior to superior with later fusion of the joint) and slowly ascends the spine. There may be reactive bone formation in the ring apophyses with erosions of the margins and later, squaring of the bodies of the vertebrae. There is a prominent calcification of the posterior longitudinal ligament of the spine. There is prominent vertebral syndesmophyte formation. In late stages, the spine may appear fused, with a fixed kyphosis (the so-called bamboo spine).

Pigmented Villonodular Synovitis

PVNS is considered to be the diffuse counterpart of giant cell tumor of tendon sheath, with which it shares morphological and genetic features. It is an uncommon proliferative disease of the synovium that arises most frequently in patients aged 20–50 years. This disease may affect the synovium of the joints, bursae, and tendon sheaths and is most common in the hips, knees, and ankles. Rare cases have occurred in the temporomandibular joint and the facet joints of the spine. Extraarticular tumors of the soft tissue and muscle have also been described. Typically, it causes nodular synovitis throughout the joint but rarely may give rise to a focal nodular form. The proliferative nodules have a tendency to bleed, and over time hemosiderin is deposited in the joint giving rise to the characteristic pigmentation of the nodules and the "crank case oil" appearance of the affected joint fluid. Clonal abnormalities and the capacity for autonomous growth have supported PVNS as being a true neoplasm.

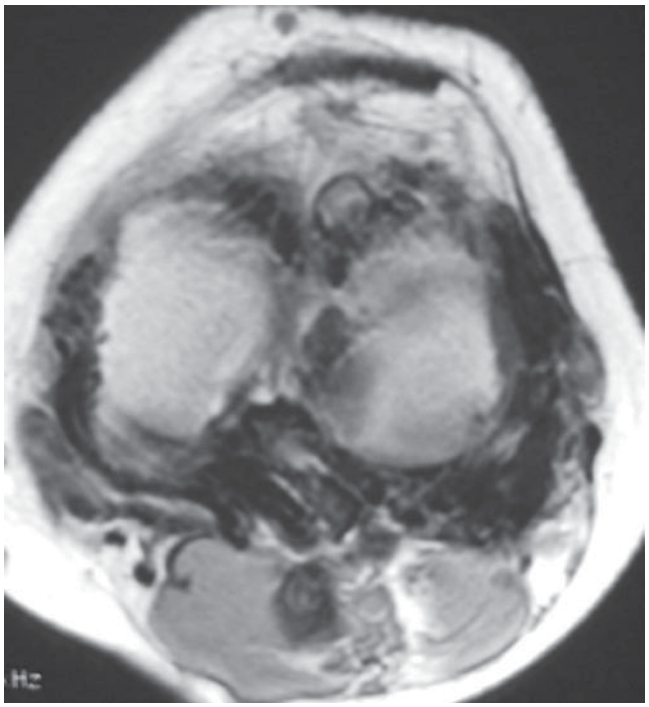

Fig. 25 Axial T1-weighted image from a knee MR of a patient with pigmented villonodular synovitis (*PVNS*). As with hemophilia, the large amount of hemosiderin deposition causes signal dropout and dark areas on the image in the region of the synovium

Early in the disease, the nodules may cause recurrent hemarthroses, saucerized erosions, and subchondral cysts on either side of the joint. Radiographically, these phenomena are seen as hyperdense effusions and smooth corticated saucerizations with relative preservation of the joint space. MRI has proven very useful to make the diagnosis because of the paramagnetic effects of hemosiderin (dark on T1 and T2). MRI shows joint effusion with dark signal lining the synovium and internal structures of the joint (Fig. 25). This material shows susceptibility effects on gradient echo imaging resulting in "blooming" of the low signal. Calcification is rare in cases of PVNS and if present, alternative diagnoses should be considered, particularly synovial sarcoma.

Surgical pathology: The tumors are large (often more than 5 cm), red or brown, and a villous pattern can often be seen grossly. Microscopically, one can see variably cellular, diffuse, expansile, and somewhat infiltrative sheets small ovoid or spindle cells admixed with larger and a few multinucleated cells. Cleft-like spaces and blood-filled spaces are generally prominent. The smaller cells are histiocyte like and often display grooved nuclei. The larger mononuclear cells frequently have a densely eosinophilic cytoplasm and sometimes have a peripheral rim of hemosiderin granules. Sheets of foam cells can also be observed. There is variable amount of fibrosis and lymphocytic infiltrate. Mitoses can be quite frequent. Rare malignant cases have shown very frequent mitotic activity (more that 20 per 10 HPF) and necrosis; although there are no definite histological criteria for malignancy, since some histologically banal cases have metastasized. Both the mononuclear and multinucleate cells can be positive for CD 68. There may be focal desmin positivity.

Chromosomal studies show that translocations involving chromosome 1p11-13 are common in PVNS and giant cell tumor of tendon sheath. More recent studies have found the overexpression of colony stimulating factor 1 receptor (CSF1R) in both these lesions (the location for CSF1 is chromosome 1). It is currently thought that many cases have translocations involving CSF1 and the collagen gene COL6A3 (which resides on chromosome 2q35).

PVNS is considered a benign disease; the treatment usually consists of synovectomy. The disease has a tendency to recur (around 20–30%), sometimes requiring extensive synovectomy and total arthroplasty. Malignant (metastasizing) PVNS is extremely rare (a few case reports). If left untreated, PVNS eventually causes joint destruction and secondary osteoarthritis.

Productive and Destructive Arthropathies

This class of arthropathies shows both erosive and productive changes together in the same joint. Erosive osteoarthritis is the prototype of this type of arthritis. A similar imaging pattern becomes apparent is in cases of old burned out destructive arthropathies where, for reasons of altered biomechanics, the joints develop secondary osteoarthritis. Gout, too, though typically destructive, may give an appearance of a combination of destruction and production. This may, in part, be the result of bone production in the healing phase between acute attacks, the loss of hyaline cartilage to synovitis and bone production induced by urate. On the other side of the coin, neuropathic arthritis may cause so much joint disintegration that it may appear destructive as well as productive.

Nondestructive and Nonproductive Arthropathies

Although these diseases do not actually cause morphological alterations in joint architecture and hence technically are not arthropathies, a few conditions are traditionally placed in this category. These include the joint-related abnormalities of systemic lupus erythematosis (SLE), scleroderma, Ehlers Danlos syndrome, agammaglobulinemia, and those associated with rheumatic fever, Jaccoud's arthropathy.

Miscellaneous Joint-Related Conditions

Although not actually arthropathies, a few conditions occur around joints or bursae, that is, diffuse idiopathic skeletal hyperostosis (Forestier's disease), Haglund's disease (retrocalcaneal bursitis) or within the joint space with the potential to lead to arthritis, that is, synovial chondromatosis, osteochondritis dissicans, and chondromalacia patella.

Osteochondritis Dissicans

More frequently seen in males, this lesion is characterized by variable number of (but fewer compared to synovial chondromatosis) loose bodies composed of bone and cartilage within the joint cavity often referred to as joint mice. They can measure up to 2 cm. The articular surface shows grooves and discontinuities in the articular margins probably from where the bodies were detached. The underlying bone is sclerotic. The knee is most frequently involved followed by hip, elbow, and shoulder joints. Although a trauma history is frequently elicited, the role of developmental and circulatory factors cannot be ignored. It is believed, that the lesions can heal in skeletally immature individuals, but not in adults.

Synovial Chondromatosis (Synovial Chondrometaplasia)

Synovial chondromatosis is a benign nodular cartilaginous proliferation arising in the synovium of joints, bursae, or tendon sheaths. It occurs often in adults. Joints involved include the knee and less commonly the hip, elbow, wrist, ankle, shoulder, or the temporomandibular joint. Presentation is with pain, mass or both.

Grossly, there are multiple (many) nodules of cartilage either free within the joint or attached to the synovium that vary from a few millimeters to a few centimeters. The nodules

are variably cellular with the chondrocytes present in clusters (a very characteristic finding). Mitoses are uncommon. There may be ossification.

Chondromalacia Patella

Chondromalacia patella occurs in younger often female patients and is a form of chondrolysis. The patellar cartilage surface becomes softened and may develop fissures or be lost altogether. MRI has become a useful tool to evaluate the hyaline cartilage in joints and on the posterior aspect of the patella. Most believe that chondromalacia patella is the final common pathway to a number of problems including trauma, patellar tracking abnormalities, chronic muscle imbalance about the knee, and patellar hypermobility.

References

1. Palmblad K, Erlandsson-Harris H, Tracey KJ, Andersson U. Dynamics of early synovial cytokine expression in rodent collagen-induced arthritis: a therapeutic study using a macrophage-deactivating compound. Am J Pathol. 2001;158(2):491–500.
2. Simelyte E, Isomaki P, Rimpilainen M, Zhang X, Toivanen P. Cytokine production in arthritis susceptible and resistant rats: a study with arthritogenic and non-arthritogenic Lactobacillus cell walls. Scand J Immunol. 2001;53(2):132–8.
3. Kameyama Y, Hagino H, Okano T, Enokida M, Fukata S, Teshima R. Bone response to mechanical loading in adult rats with collagen-induced arthritis. Bone. 2004;35(4):948–56.
4. Dumond H, Presle N, Pottie P, Pacquelet S, Terlain B, Netter P, Gepstein A, Livne E, Jouzeau JY. Site specific changes in gene expression and cartilage metabolism during early experimental osteoarthritis. Osteoarthritis Cartilage. 2004;12(4):284–95.
5. Clohisy JC, Roy BC, Biondo C, Frazier E, Willis D, Teitelbaum SL, Abu-Amer Y. Direct inhibition of NF-kappa B blocks bone erosion associated with inflammatory arthritis. J Immunol. 2003;171(10):5547–53.
6. King KB, Opel CF, Rempel D. Cyclical articular joint loading leads to cartilage thinning and osteopontin production in a novel in vivo rabbit model of repetitive finger flexion. Osteoarthritis Cartilage. 2005;13(11):971–8.
7. McCoy JM, Wicks JR, Audoly LP. The role of prostaglandin E2 receptors in the pathogenesis of rheumatoid arthritis. J Clin Invest. 2002;110(5):651–8.
8. Niki Y, Yamada H, Kikuchi T, Toyama Y, Matsumoto H, Fujikawa K, Tada N. Membrane-associated IL-1 contributes to chronic synovitis and cartilage destruction in human IL-1a transgenic mice. J Immunol 2004;172:577–584.
9. Redlich K, Hayer S, Ricci R, David JP, Tohidast-Akrad M, Kollias G, Steiner G, Smolen JS, Wagner EF, Schett G. Osteoclasts are essential for TNF-alpha-mediated joint destruction. J Clin Invest. 2002;110(10):1419–27.
10. Kyburz D, Corr M. The KRN mouse model of inflammatory arthritis. Springer Semin Immunopathol. 2003;25(1):79–90.
11. Matsumoto I, Staub A, Benoist C, Mathis D. Arthritis provoked by linked T and B cell recognition of a glycolytic enzyme. Science. 1999;286(5445):1732–5.
12. Gurley KA, Chen H, Guenther C, Nguyen ET, Rountree RB, Schoor M, Kingsley DM. Mineral formation in joints caused by complete or joint-specific loss of ANK function. J Bone Miner Res. 2006;21(8):1238–47.
13. Wong et al. Journal of Arthroplasty. 20(8):1015–20, 2005 Dec., Abdul-Karim et al. Modern Pathology. 11(5):427–31, 1998 May, Mirra et al. Clinical Orthopaedics & Related Research. (170):175–83, 1982 Oct.
14. Kataoka et-al. Clinical Rheumatology. 21(2):159–63, 2002 May.

Chapter 13
The Surgical Pathology of Prosthetic Materials

Jasvir S. Khurana and Vivian Arguello-Guerra

Abstract Although implants and prosthetic materials are very commonly received in the surgical pathology laboratory, extracting the most information from them remains under the purview of specialized laboratories. Understanding the various issues involved with their failure will assist the proper management of patients. Additionally, the pathologist is frequently asked to identify possible implant-associated infection. Understanding the difficulties and problems of such a diagnosis will be helpful to the clinical team.

Keywords Prosthetic materials • Biomaterials • Implants • Metals • Polymers • Ceramics • Composites • Implant failure • Aseptic loosening • Infection • Carcinogenicity Osteolysis

The surgical pathologist often encounters implants and other surgical specimens containing biomaterials, although, generally, handling these specimens is a specialized field at present. Most often, these implants are removed with certain specific questions and protocols in mind. These questions often involve biomechanics, engineering, or biocompatibility. In the surgical pathology setting, one is often concerned only with the latter or with implant failure resulting from infection.

The aim of examining such materials is to recognize complications, device development, and elucidate mechanisms of interaction of tissue and biomaterials (1). Various techniques are used for the biocompatibility analysis. These include flurochrome labeling, microradiography, transmission and scanning electron microscopy, energy dispersive X-ray analysis for implant interface analysis, cement thickness, and cement penetration studies (2,3).

Biomaterials

These are synthetic or modified biologic materials that are used to augment or replace abnormal body structures. They include polymers, metals, ceramics, carbons, collagen, tendons, and so on. The life and proper function of these materials is dependent usually on their biomechanical and biologic properties.

Biomechanical properties of these materials include optimal strength, modulus (elasticity or stiffness), creep resistance (ability to maintain shape under stress from constant loading), fatigue resistance (ability to undergo cyclic stress without crack propagation), permeation (diffusivity), and water absorption. One of the major problems of implanted prostheses is that of wear debris. This can be voluminous, and may cause osteolysis and loosening. This wear may be due to abrasion, adhesion, or fatigue. It has been thought that wear acts as a stress concentrator and produces secondary three-body wear.

Biologic properties include biostability (maintain properties in situ and resist degradation), bioresorbability (useful in drug delivery), and bioactivity (ability to participate in biologic reactions such as bone induction) (Table 1).

Preimplant Analysis

Implant manufacturers usually carry out such tests. This kind of testing includes *bulk* and *surface* analyses. *Bulk analysis* is used to characterize the substance, identify possible toxic leachables, and classify polymers in accordance with structural properties such as density, porosity, or solvent interaction. *Surface analysis* is used to study the contact surface and the structural or conformational changes occurring here. The attempt is to understand the surface chemistry. Properties studied include surface energy and charge, structure and chemical function, defects in structure and degradation (corrosion) potential. The techniques utilized for surface analysis includes the following:

- Contact angles (liquid wetting studies)
- Electron spectroscopy (via X-rays)
- Auger electron spectroscopy
- Secondary ion mass spectroscopy (using ion bombardment)
- Attenuated total reflection infrared (using infrared light to excite molecular vibrations)
- Scanning tunneling microscopy (measuring tunneling current from a metal tip to surface)
- Scanning electron microscopy

J.S. Khurana (ed.), *Bone Pathology*, DOI 10.1007/978-1-59745-347-9_13,

Table 1 Commonly used biomaterials

General group	Examples
Metals	Stainless steel (F138, F621, F745, F1314), Cobalt-based alloys (F75, F90, F562, F563), Titanium (F67), Titanium-based alloys (F136, F620)
Polymers	Ultrahigh molecular weight polyethylene (F648), polymethylmethacrylate (F451)
Ceramics	Alumina (F603), b-tricalcium phosphate (F1088), Calcium hydroxyapatite (F1185)
Composites	Polysulfone (F702), carbon fiber

Standard designations of the American Society for Testing Materials (ASTM numbers) are given in parentheses. Table modified from Friedman et al. (1).

Implant Examination

A careful gross examination is essential. Attention must be paid to gross alterations of shape and surface. The exam must be supplemented by careful photography.

For joint arthroplasties, an evaluation includes an assessment of the *interface membrane*. This is done by light and polarized light microscopy as well as enzyme histochemistry and molecular studies. The attempt is to evaluate the nature of the infiltrating cells, asses their activation status, characterize the molecular signals, and cytokines involved and characterize the wear debris particles. Additional studies often undertaken include tissue culture and undecalcified sections for viewing the histology of the bone–membrane histology.

Special studies: Studying the implant–bone and implant–membrane histology is more complicated and usually done by the manufacturers or other specialized laboratories. Also, porous ingrowth type of implants (sintered) may be studied by backscatter electron microscopy. Scanning electron microscopy is used to study erosion and wear.

These studies are improving our understanding of implant failures, and have additional medicolegal importance.

Implant Failure

Implants may fail and cause problems in the host. A mandatory requirement of implants in most situations is biocompatibility. Its breakdown is associated with biochemical and metabolic effects. Implant-associated neoplasia may be another possibility. Other deleterious effects of the implant on the host include complications from rupture, cracking or distortional types of mechanical failure. Improper implant usage may lead to several complications. For example, inappropriate sterilization procedures (heat, ethylene oxide, radiation, etc.) may cause implant failure. Bacterial, endotoxin, particulate, and pathogen contamination may have profound effects on the host.

On the contrary, the host may adversely affect the implant. Thus, excessive stress may cause abrasive wear, release of wear debris, and fatigue. Certain body fluids may cause implant corrosion resulting in pitting, crevices, and stress. Certain materials can be biodegradable (cellulosic esters, nylons, etc.) and be susceptible to hydrolytic degradation. Organic polymers may undergo autoxidation in vivo. This may result in pelletization, extrusion, or molding. This reaction is particularly favored in the setting of inflammation and foreign-body-type reactions.

Complications of Prosthetic Devices

- Infection
- Toxicity and tumorigenesis
- Systemic reaction
- Aseptic loosening

Orthopedic devices have been used in extremely large numbers. On the whole, they have been free from major complications, at least in significant numbers. The biomaterials used have proved to be relatively inert. The extremely small numbers of problems (as a percentage of implants inserted) has made the study of complications difficult.

Infection

Implants and biomaterials may aid the development of deep infections. This may especially be true of polymethylmethacrylate cement cured in situ. More importantly, once an infection is established, the presence of the implant acts as a foreign body and contributes to the refractoriness to its treatment.

Improvements in implant design and surgical technique have reduced the incidence of this complication. It, however, remains as one of the most serious problems in orthopedic surgery. Many centers currently report figures in the order of 1% of all total arthroplasties performed. The use of ultraclean operating rooms with laminar flow, prophylactic antibiotics, incorporation of antibiotics into methylmethacrylate cement, and so on are some of the measures used by certain centers to decrease the incidence of this problem.

Increased rates of infections are seen in patients with collagen vascular diseases, diabetes mellitus, obesity, and arthroplasties or revisions in previously infected joints. The most commonly isolated organisms are bacterial, among which *Staphylococcus aureus* and *Staphylococcus epidermidis* predominate.

Deep-seated infections following total hip arthroplasty may be thought of as three clinical stages. Stage I corresponds to

infected hematomas and are amenable to treatment with debridement and antibiotics. Stage II infections are characterized by persistent hip pain 6 months to 2 years after surgery and are difficult to separate from aseptic loosening. Stage III infections occur after 2 years, and are often secondary to other remote infections. Similar principles can be extrapolated to orthopedic implants at other sites.

Investigations: The problem of separating deep-seated implant infections from aseptic loosening can be extremely problematic. Plain X-rays may show similar features, and imaging studies are prone to metal artifact. The major investigative procedures therefore are joint arthrography (which also obtains material for microbiological studies) and Gallium or Indium isotope scans. Laboratory investigations such as culture and special techniques such as polymerase chain reaction (PCR) for organisms may be adjunctive and useful in selected situations.

Biopsy interpretation: This can be equally difficult. Requests for this diagnosis often arise as frozen sections at the time of surgery or revision. Mirra has suggested criteria that utilize the assessment of numbers of polymorphonuclear neutrophils (PMNs) (4). Although it is true that the probability of infection is correlated with five or more PMNs per single high-power microscopic field, rigid criteria may not always be applicable. In low-grade and chronic infections, or in cases where the organisms are of low virulence, relying on these criteria may underdiagnose infection. The same is true in cases, which have received antibiotics. Another caveat is that focal collections of PMNs may occur in patients with rheumatoid arthritis. In this situation, overdiagnosis may result.

Mechanisms and factors in implant infection: An implanted foreign body is conducive to the development of infection by a variety of postulated ways. Tissue damage may occur from liberated enzymes, inflammatory mediators, and oxygen-free radicals. Reactive metals, like cobalt or copper may incite a sterile infection or a sterile abscess. Bioreactivity of otherwise inert materials may be enhanced with wear. Implants may adversely affect the host immune defenses, especially the phagocytic and bactericidal abilities. An important mechanism appears to be the production of bacterial glycocalyx (slime or biofilm) by organisms such as *S. epidermidis*, *Streptococcus viridans, Pseudomonas aeruginosa*, and *S. aureus*. This material may inhibit phagocytosis, neutrophil chemotaxis, mononuclear responses, CD4 T cells, natural killer cells, and immunoglobulin synthesis. Fibronectin and collagen may increase bacterial adherence to implants.

Toxicity and Tumorigenicity

The occurrence of these complications is controversial. Also the establishment of cause–effect relationships in implant toxicity and tumorigenesis is extremely difficult.

Toxicity can be generated from implants by release of biologically active leachables, physical contact with the material, and/or biodegradation with the subsequent production of bioactive molecules. Biologic reactivity depends on the intracellular incorporation of small particles. Low molecular weight substances can readily permeate cell membranes and may be more active. In vitro cell culture methods are used to assess toxicity.

Carcinogenicity is a time-honored term. Since a variety of neoplasms other than carcinomas have been implicated, tumorigenesis may be a better term. The relationship between biomaterials and tumors is complex. Clear-cut cause–effect relationships are difficult to establish. There are, however, some suggestions that the metals, plastics, cement, and so on used in orthopedic surgery may be tumorigenic (5,6). Chemicals that have been linked to neoplasia include cobalt, cadmium, nickel, cobalt-chromium-molybdenum alloys, and chromates. On the contrary, zinc, tungsten, iron, copper, manganese, and molybdenum in their pure forms are thought to be nontumorigenic. Metal wear products may also be tumorigenic (7). It has also been shown that some of the wear products, for example, cobalt–chromium products can be absorbed systemically (8). Studies have looked at the effects of anodic-back electromotive force, particle size, surface finish, solubility, environmental pH, corrosion, and magnetization of metals on tissue. Host factors such as immunity, contact inhibition, metal allergy, and foreign body giant cell reactions have also been investigated. There have, however, been no definite results or conclusions. Inspite of this lack of consensus, the debate continues.

Systemic Reaction

Orthopedic devices may have interactions with the host in sites remote from the point of insertion. Such reactions include absorption of wear particles, and the long-term effects of these. The metabolic effects of such wear particles, including heavy metals, is not fully elucidated at present. Metal allergy and immune responses to biomaterials are other problems. Documented allergy to nickel or chromium may form a contraindication to the use of stainless steel or cobalt-based alloys.

Aseptic Loosening (Osteolysis)

This complication is the most common cause of failure of total hip arthroplasty (Fig. 1). It may occur in up to 10% of cases, in many centers. The exact sequence of events involved in loosening are unknown but is related to the presence of

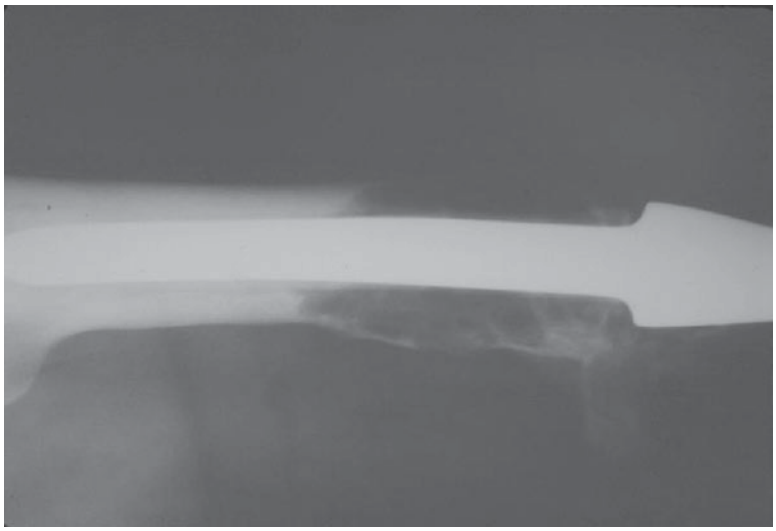

Fig. 1 Osteolysis around the distal femoral portion of a custom made prosthesis in a patient who had undergone limb salvage surgery for a femoral osteosarcoma

wear debris causing a local reaction. Wear debris is a direct result of micromotion between the prosthesis, cement, and bone interfaces.

Presumed factors leading to micromotion at the bone–cement interface have thought to include differences in the elastic modulus of bone and cement, bone necrosis from thermal trauma (during bone preparation or cement insertion), and poor cement fixation. Small particles from various sources, including polyethylene liners, may be responsible (as the problem occurs in noncemented hips also).

Clinical Features

Aseptic loosening manifests itself with bone pain and disability. The time interval between surgery and presentation is usually between 40 and 170 months. Radiographically, it can take the form of either diffuse femoral cortical thinning or a focal cystic lesion. Predisposing or exacerbating factors include obesity, increased physical activity, and improper stem placement. The mechanism of action of these exacerbating factors is probably increased stress at the implant–bone interface.

Basis of Aseptic Loosening

Wear debris (from ultra-high-molecular-weight polyethylene or UHMWPE and from polymethylmethacrylate cement) not only *indicates* micromotion but may *contribute to* further loosening, in a vicious cycle. Thus, *micromotion (directly and through wear) may activate macrophages*. These in turn produce acid phosphatase, collagenase, Tumor necrosis factor, IL-1, and prostaglanding E_2. These substances cause osteoclastic resorption of bone, further loosening, and additional motion. The term "cement disease" was given to this in the belief that polymethylmethacrylate cement was the main cause of this reaction. It is now the feeling that UHMWPE contributes at least equally if not more to aseptic loosening. Thus, aseptic loosening can be seen in uncemented prostheses as well as cemented ones.

Surgical pathology of the interface membrane: A thin membrane forms at the bone–implant interface in failed (loose) arthroplasties. The appearance of this membrane differs slightly in cemented and noncemented implants. Membranes from *cemented* prostheses show the following three zones (starting from the prosthesis interface):

1. Superficial zone (synovial-like cells along with fibrin and necrosis).
2. Midzone [fibrovascular with histiocytes and giant cells) the giant cells and macrophages contain particles of cement and UHMWPE]
3. Deep fibrous zone (bone interface)

Membranes from noncemented, ingrowth type prostheses lack the superficial zone. In these specimens, the interface membranes contain macrophages which are present in a loosely organized fibrous tissue and there may be focal woven bone.

An *aggressive granulomatous reaction* has also been described, which occurs in a few cases. Radiologically, there is a large, tumor-like ovoid lytic area which progresses rapidly. Histologically, these lesions consist of large sheets of histiocytes and giant cells.

Acetabular loosening has received less attention but occurs in a fashion similar to femoral loosening. It too has been associated with cemented and noncemented acetabular components. By X-ray, the lesions can be divided into "periacetabular type" and "retroacetabular type." The periacetabular lesions have been ascribed to the particles originating in the joint cavity. The retroacetabular lesions may be directly related to the acetabular component. The histologic features of these lesions are similar to those of the femoral ones.

Identifying the foreign material responsible for inciting the reaction and its origin if possible can help identify the problem in many cases, and has been helpful to the prosthesis designers. This, however, may require special techniques.

Material	*Surgical pathology*
Methylmethacrylate	Methylmethacrylate is not seen in histologic sections as it is dissolved during processing. It appears as cleared out spaces of varying sizes. Often these are present within multinucleate giant cells. Barium sulfate is often present within cement and may contribute to the granular appearance. In unstained frozen sections, it can be seen as glassy and granular material. It is not birefringent by polarization.
Polyethylene	The debris is generated by abrasion, three-body wear and surface fatigue damage. Microscopy shows a cellular infiltrate of macrophages and giant cells in a granulomatous pattern (Fig. 2). The polyethylene is seen in the form of variably sized shards of glassy refractile material. It can be overlooked in transmitted light, but polarization highlights the particles. Larger pieces may be surrounded by fibrous tissue, smaller ones are surrounded by or engulfed by giant cells. It may be present deep within bone or in bone marrow, at a considerable distance from the implant.
Metal	Chemical corrosion causes coarsely granular brown-black debris (Figure). Much more common are the metallic particles generated by wear. Microscopically, it is usual to identify small irregular black fragments 1–3 mm or so. Although opaque in transmitted light, they are nevertheless highlighted by polarization. Many fragments are located within macrophages. Heavy deposition may be present in sites of metal fracture or areas of articulation of metal. Titanium-aluminum-vanadium alloy is particularly prone to give metal reactions of this type (Fig. 3).
Ceramic	The major feature is a thick membrane with necrosis, fibrosis, and macrophages. Small gray-black debris particles of around 5m are seen, often within macrophages. Aluminum can often be demonstrated by special techniques.

Work-Up of Submitted Material

A *simplified protocol* adaptable to the laboratory has been suggested by Singh et al. (9). This advocates the histologic study of tissues around the implant by routine processing and histochemical staining (Hematoxylin-Eosin, Phosphotungstic acid Hematoxylin, Prussian blue, Periodic acid Schiff, and Alcian blue stains) along with the analysis of implant. The tissue is assessed for

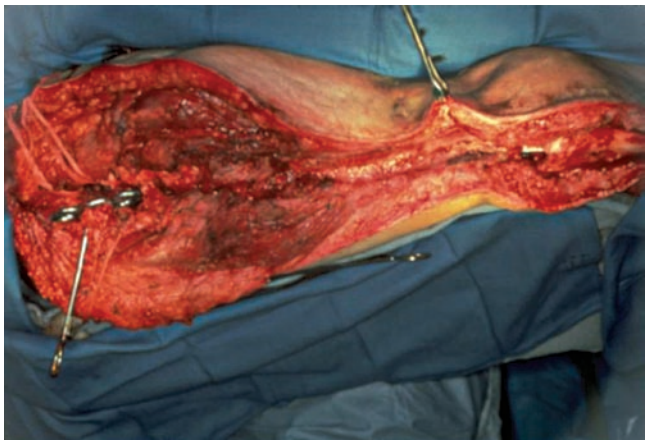

Fig. 2 Implant failure in a patient with sialastic granulomas and sialastic synovitis. The reaction was severe. It required removal of the implant, replacement with an allograft, and fusion of the knee

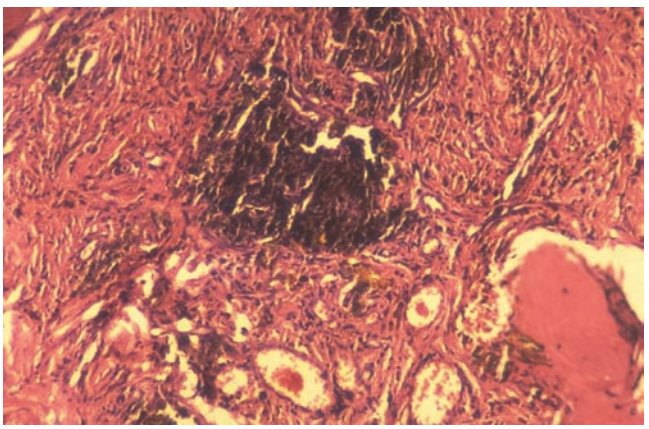

Fig. 3 The section corresponds to a type III (of III) metal deposition, with a grade 2 (of 5) tissue response

- Inflammatory response
- Metal debris
- Fibrosis
- Necrosis

The implant is assessed grossly as follows:

- Corrosion (Graded as 0 if there is no corrosion, 1 if mild corrosion discernable only by microscopy, 2 if moderate, and 3 if severe corrosion showing eaten up areas grossly)
- Loosening (Graded as 0 if there is no loosening, 1 if loosening is detected at surgery, and 2 if detected both at surgery and radiologically)
- Mechanical damage (Graded as 0 if the implant is neither bent nor broken, 1 if a component is bent, 2 if a component is broken, and 3 if a component is both bent and broken)

This is followed by destructive testing utilizing chemical analysis, metallography, scanning electron microscopy, and mechanical testing in specialized laboratories.

Histologic sections estimate:

- The amount and kind of metal deposition (Type I deposit consists of small fragments of stainless steel related to wear but not corrosion, Type II associated with acellular or necrotic collagen tissue response, and Type III associated with varying degrees of tissue response associated with corrosion)
- The tissue reaction is graded for better communication (Fig. 4) (Grades 0 if only a thin fibrous membrane containing lipid cells, 1 if a mildly fibrous membrane, 2 if there is mild chronic inflammation, 3 if moderate chronic inflammation, 4 if there is heavy chronic inflammation with giant cells and/or granulomas, and 5 if severe inflammation is accompanied by giant cells, granulomas and necrosis)

The Surgical Pathology of Allografts

The use of musculoskeletal allografts is increasing. Such allografts include bone, nerves, ligaments, and tendons. The following discussion will pertain to bone, which is the substance most utilized as an allograft.

The advantages of shape, attachment sites for soft tissues, strength, and osteoconductivity have served to popularize bone allografts. The disadvantages include the potential transmission of infective diseases and the newly recognized but poorly understood phenomenon of rejection. Immunogenicity of bone allografts has been decreased by the techniques of preservation, such as lyophilization. It has, however, become clear that allografts do undergo rejection, albeit to a lesser extent than found in parenchymal organs (10).

Complications and Problems with Allografts

There are several clinical complications. From the point of view of the pathologist, however, the major problems include *nonunion, infection, and rejection*.

Infection can be subtle and difficult to assess. It must be differentiated from rejection. This may require additional laboratory input, such as microbiologic cultures.

Studying and quantifying allograft rejection can be equally difficult. Clinically, such grafts undergo resorption, or fail at soft-tissue attachments. Biopsy methods have been limited by the focal nature of the inflammatory infiltrate that occurs in rejecting bone. The gold standard of comparative studies for rejection of allografts has been autogenous bone grafts. The latter would be expected to show the effects of healing, without the effects of rejection. Autogenous and perfectly healed allografts ideally would show incorporation, healing, revascularization, and substitution of bone with host bone, with no loss in function or strength.

Healing and Revascularization Under Ideal Situations

Autogenous cortical grafts as well as allografts start the process of incorporation with the formation of a hematoma. This hematoma is rich in cytokines and growth factors. These substances may be responsible for attracting undifferentiated mesenchymal and osteoprogenitor cells to the allograft. The first 2 to 3 weeks is marked by the intense inflammatory response seen in the allograft. This may abate, or lapse into chronicity. In any event, within days, there is an ingrowth of fibrovascular stroma. This utilizes the preexisting Haversian and Volkmann systems to allow vascular channels and the ingression of osteogenic cells. Osteoclastic resorption of the graft is initiated at the same time, and this is generally coupled with bone formation. This is the start of remodeling and substitution of graft with host bone. Even before the graft is substituted, clinical healing is said to have occurred, provided the graft–host interface is united and the graft is able to painlessly function or bear weight.

Rejection

The first 4 weeks of allografts are critical in incorporation. Signs of impending rejection often manifest during this period. Allograft osteoblasts have been thought to express Class I and II, major histocompatibility complex (MHC) antigens. These are responsible for T cell and monocyte–macrophage responses that characterize rejection. Tissue culture studies have suggested the MHC expression of HLA-DR can be upregulated by interferon or 1,25-dihydroxyvitamin D_3. Under normal circumstances, the processes of freezing and freeze-drying kills the bone cells, thereby reducing their expression. Escape mechanisms that have been postulated in allograft rejection therefore include the following:

- Release of antigens by dead cells that can be directly recognized by T cells
- Release of antigens by dead cells that are taken up by live cells and then presented to T cells
- Survival of some graft cells because of tissue cryoprotectants such as dimethylsufoxide

The histologic findings in rejection are not well worked out. Persistent lymphocytic infiltrate is a worrisome finding.

This, however, can be focal, and is difficult to quantify. Additionally, making a distinction between infection and rejection can be extremely difficult in many cases.

References

1. Friedman RJ, Black CJ, Galante JO, Jacobs J and Skinner HB—Orthopaedic biomaterials and implant fixation. J Bone Joint Surg (1993) 75-A (7):1086–1109.
2. Jansen J—Histological Analysis of Bone-Implant InterfaceIn Handbook of Histology Methods for Bone and Cartilage. EditorsYuehuei An and Kylie Martin. Humana Press, New Jersey 2003. Pages 353–360.
3. Wang J, Gonzalo G, Valdivia MJ, Rorabeck, CH, Bourne RB and Maher, S—Histomorphometric Analysis of Bone-Cement and Cement–Metal Interface InHandbook of Histology Methods for Bone and Cartilage. EditorsYuehuei An and Kylie Martin. Humana Press, New Jersey 2003. Pages 361–375.
4. Mirra JM, Marder RA and Amstutz HC—The pathology of failed total joint arthroplasty. Clin Orthop (1982) 170:175.
5. Khurana JS, Rosenberg AE, Kattapuram SV, Fernandez OS and Ehara S—Malignancy superveinging on an intrameduallary nail. Clin Orthop (1991) 267:251–254.
6. Memoli VA, Urban RM, Alroy J and Galante JO—Malignant neoplasms associated with orthopaedic implant materials in rats. J Orthop Res (1986) 4:346.
7. Heath JC, Freeman MAR and Swanson SAV—Carcinogenic properties of wear particles from prostheses made in cobalt chromium alloy. Lancet (1971) 1:564.
8. Coleman RF, Herrington J and Scales JT—Concentration of wear products in hair, blood and urine after total hip replacement. Br Med J (Clin Res) (1973) 1:527.
9. Singh AP, Saxena RK, Raj GA, Guha SK, Sural A and Vishwakarma GK—Orthopaedic Implants and FailuresIn Biomechanics. EditorsSahay KB and Saxena RK. John Wiley, New York(Chapter 24) 1989.
10. Stevenson S and Horowitz M—The response to bone allografts (Current Concepts Review). J Bone Joint Surg (1992) (74-A): 939–950.

Chapter 14
Osteoporosis and Metabolic Bone Disease

Jasvir S. Khurana and Lorraine A. Fitzpatrick

Abstract The chapter discusses bone metabolism and regulation under normal conditions. It also discusses disease conditions that affect the skeleton as a whole including osteoporosis, rickets, osteomalacia, scurvy, renal osteodystrophy, hyperparthyroidism, storage disorders and amyloidosis. Paget disease is also discussed here because of tradition and its similarity to other generalized skeletal disorders despite some evidence that it might be due to an infective viral agent. Similaryly, largely because of tradition, osteopetrosis, pycnodysostosis and osteogenesis imperfecta are discussed although they could be discussed amongst genetic disorders (inherited and dysplastic conditions) of the skeleton.

Keywords Metabolic bone diseas; • Osteoporosis • Rachitism • Osteomalacia • Scurvy • Hyperparathyroidism • Hypop hosphatemia • Hyperphosphaturia • Hypercalciuria • Paget disease • Amyloidosis • Osteopetrosis • Osteogenesis imperfecta • Mucopolysacharidoses • Gaucher disease • Parathyroid hormone • Vitamin D • Hypocalcemia • Hypercalcemia • Hyperreflexia • Crystallysis • DEXA scan • Calcitonin • Serum alkaline phosphatase • Gastric rickets • Biliary rickets • Enteric rickets • Phosphatonin • Renal osteodystrophy • Albers- Schonberg marble bone disease • Glycosaminoglycanosis • Glucocerebrosidase

Biochemical Basis of Metabolic Bone Disease

The term "metabolic bone disease" is used to encompass a variety of differing conditions that focus on pathology of bone tissue. Conventionally, they include the diseases resulting from disorders of bone formation and/or resorption, resulting in changing rates of bone turnover. Bone is a specialized connective tissue composed of mineral and organic matrix. The inorganic mineral is made up of calcium hydroxyapatite-like crystals and provides stiffness to the organ. The matrix provides elasticity, so that bone can be both tough and yet bend. These two properties are critical, since if bone is too stiff, it cannot bend. Bone can become very dense with an abundance of mineral, but it may become brittle and fragile. At the other end of the spectrum, if bone has not enough mineral and is made up of matrix, it becomes too weak to be structurally intact. Most metabolic bone diseases affect either the mineral or matrix components, resulting in a more fragile bone.

The cellular components of bone, osteoclasts, osteoblasts, and osteocytes, are involved in bone modeling and remodeling and determine the mineral and matrix composition. Abnormalities in the rate or balance of bone remodeling can lead to bone loss and fragility. The cells within bone are under the influence of several hormones and cytokines which are discussed below.

Parathyroid Hormone

Parathyroid hormone (PTH) is an 84 amino acid, single-chain polypeptide (designated PTH 1–84) that is produced by the chief cells of the parathyroid gland. PTH is essential for the maintenance of calcium homeostasis through its indirect actions on the gastrointestinal tract and its direct actions on bone and kidney. The principal form of biologically active PTH is the intact molecule, PTH (1–84), although an independent role for carboxyterminal fragments has been proposed (1). PTH exerts its actions on bone to release calcium into the extracellular fluid during the process of bone remodeling. The three key regulators of PTH secretion and synthesis are extracellular calcium, phosphate, and 1, 25 dihydroxyvitamin D3. In response to falling extracellular calcium levels, increases in extracellular phosphate and/or reductions in 1, 25 dihydroxyvitamin D3 the chief cell synthesizes and secretes PTH. Calcium ions control the release of PTH though a G protein-coupled receptor, called the calcium-sensing receptor.

In bone, PTH stimulates the release of phosphate and calcium, and in the kidney, PTH stimulates tubular reabsorption of calcium and inhibits the reabsorption of phosphate. PTH has another effect on the kidney as it stimulates the production of 1, 25 dihydroxyvitamin D3 through its actions on 1-α hydroxylase.

In bone, PTH mediates release of calcium initially from a pool of calcium near the surface of bone. Chronic administration of PTH results in an increase in osteoclast cell number and activity. Intermittent administration of PTH results in anabolic actions through stimulation of osteoblasts. PTH can

J.S. Khurana (ed.), *Bone Pathology*, DOI 10.1007/978-1-59745-347-9_14,

increase the number of osteoprogenitors cells and reduce apoptosis of preosteoblasts and osteoblasts, and increase osteoblast proliferation. Continuous administration of PTH increases osteoclast-mediated bone resorption. Intermittent administration results in stimulation of bone formation resulting in an overall anabolic effect on bone. Thus, the effect of PTH can be catabolic or anabolic to bone, depending on the timing of the administration of this hormone.

For interpreting the various diagnostic tests, it is important to understand the metabolism of PTH and the generation of its fragments. Clearance of PTH occurs rapidly in the liver (60–70%), kidney (20–30%), and, to a much lesser extent, in other organs (2, 3). Hepatic clearance results in uptake of PTH by Kuppfer cells which cleave the hormone into C-terminal fragments that are recirculated. The C-terminal fragments are longer lived than the intact hormone, and are cleared by the kidney. However, the metabolism is rapid leaving the hormone receptor available to respond to immediate changes in serum calcium levels. PTH is also degraded intracellularly within the parathyroid gland, resulting in release of circulating levels of amino- and carboxyterminal fragments. Biologic activity may be measured directly by bioassays, but these are cumbersome and not generally used currently.

Vitamin D

Vitamin D is a secosteroid that is made in the skin, by the action of sunlight. Vitamin D is inert and undergoes two hydroxylations, one is in the liver (to 25-hydroxyvitamin D) and the second is in the kidney (to 1,25 dihydroxyvitamin D). The latter is the biologically active form. 1, 25 dihydroxyvitamin D3 controls calcium metabolism in the gastrointestinal tract, proximal tubule, and bone. Receptor sites of 1, 25 dihydroxyvitamin D3 have been identified on multiple cell types. Several forms of rickets have been found to occur with errors of these receptors, or receptor signaling.

The major function of vitamin D is to increase the efficiency of the small intestine to absorb dietary calcium. 1, 25 dihydroxyvitamin D3 directly effects the entry of calcium through the plasma membrane into the intestinal absorption cell, enhances the movement of calcium through the cytoplasm, and transfers calcium across the basolateral membrane to the circulation. During times when additional calcium is necessary such as during a growth spurt or pregnancy, circulation concentrations of 1, 25 dihydroxyvitamin D3 increase which, in turn increases the efficiency of the small intestine to absorb calcium as much as 50–80%. In bone, vitamin D enhances the mobilization of calcium stores when dietary calcium is inadequate to maintain serum blood calcium within the normal range. 1, 25 dihydroxyvitamin D3 stimulates the preosteoclast to mature and dissolve bone mineral and matrix, releasing calcium into the extracellular space. 1, 25 dihydroxyvitamin D3 induces stem cells in the bone marrow to differentiate into osteoclasts. Vitamin D has been recognized as important for bone mineralization, but there is little knowledge of the actual role 1, 25 dihydroxyvitamin D3 plays in the process.

When serum calcium levels decrease, PTH is secreted and regulates calcium homeostasis by enhancing the renal conversion of 25 hydroxyvitamin D to 1,25 dihydroxyvitamin D by stimulation of 1-α- hydroxylase in the kidney. This effect is indirect and is the result of the decreased renal reabsorption of phosphorus leading to decreased serum levels of phosphorus. Hypophosphatemia and hyperphosphatemia are associated with increased and decreased circulating levels of 1, 25 dihydroxyvitamin D3, respectively.

Calcium

Calcium absorption occurs mainly in the duodenum and jejunum, and is dependent on the presence of 1, 25 dihydroxyvitamin D3. Decreased absorption occurs in the presence of chelating agents (phytate, oxalate). Similarly, the presence of excessive phosphate as a result of dietary intake of free fatty acids in biliary disease retards absorption.

Calcium ion concentrations are maintained by the combined control of the kidney and bone. In the kidney, there are glomerular filtration and tubular reabsorption (under the control of 1, 25 dihydroxyvitamin D3 and PTH). In the bone, there is formation and resorption – both dependent on PTH and to a lesser extent, on vitamin D_3. If Calcium ion concentrations fall, there is increased release of PTH, which in turn increases production of vitamin D_3. Acting together, these two hormones increase the absorption of calcium from the gastrointestinal tract and the tubular resorption in the kidney.

Phosphorus

The management of phosphorus within the body is relatively simple. Phosphorus absorption occurs mainly in the distal jejunum. The majority of the absorbed phosphorus enters the extracellular space. Excess calcium or aluminum absorption (such as in excessive antacid therapy) may interfere with the absorption of phosphorus. Bone resorption adds to the available phosphorus. Increases or decreases in dietary phosphorus are reflected in the serum levels of phosphorus.

The synthesis of hydroxyapatite, $Ca_{10}(PO_4)_6(OH)_2$ requires six phosphate for ten calcium ions. The principal control on phosphorus is renal. Phosphorus is regulated by tubular maximum, tubular secretion, and tubular resorption in the kidney and is under the influence of parathyroid hormone (PTH). Thus, increased PTH results in a phosphate diuresis. In conditions such as rickets, osteomalacia, and renal osteodystrophy, there is often hypocalcemia and therefore secondary hyperparathyroidism; this results in hyperphosphaturia and hypo-

phosphatemia. This mechanism is clearly protective, or else these patients would have extensive soft tissue calcification

Calcitonin

Calcitonin is a 32 amino acid peptide that is secreted by thyroid C-cells and inhibits osteoclast mediated bone resorption. Onset of action is rapid and calcitonin causes the osteoclast to shrink in size and inhibits bone resorbing activity. In rare cases, if bone turnover is sufficiently high, calcitonin administration can result in hypocalcemia and hypophosphatemia.

Ambient calcium concentration is the most important regulator of native calcitonin secretion. When serum calcium levels increase, there is proportional increase in calcitonin secretion. Musculoskeletal disease has not been conclusively attributed to abnormalities in calcitonin although gender-related differences in calcitonin levels have been described. Several forms of calcitonin are available as agents to inhibit osteoclast activity for the treatment of metabolic bone diseases.

PTH-Related Protein

Parathyroid hormone-related protein (PTHrP) is a complex protein that was purified from the tumors of patients with humoral hypercalcemia of malignancy. The amino acid sequence is homologous to PTH in the amino terminal region. The gene encoding PTHrP, unlike the gene for PTH, is expressed in many different tissues of the body and PTHrP functions in an autocrine or paracrine manner. The role that PTHrP plays is incompletely understood, but its wide expression suggests it may play an important role in normal physiology.

Certain fragments of PTHrP may have significant physiologic relevance. For example, a midregion fragment, PTHrP (amino acid 67–86) stimulates a placental calcium pump. The carboxy-terminal region PTHrP (amino acids 107–111) inhibits osteoclast-mediated bone resorption. Tumorsexpressing PTHrP causes hypercalcemia by secreting large amounts of PTHrP containing the amino terminal region, which binds to and stimulates the PTH/PTHrP receptor in bone and kidney. PTHrP is expressed in cartilage where it functions in growth and development. Other tissues that PTHrP may have a seminal role include bone, mammary epithelium, teeth, and skin.

Fibroblast Growth Factor 23

Fibroblast Growth Factor 23 (FGF23) is the principal phosphaturic hormone and is produced by osteocytes in bone. The principal actions of FGF23 are to inhibit sodium-dependent phosphate reabsorption and 1-α-hydroxylase activity in the proximal tubule of the kidney, with resulting phosphaturia and suppression of 1, 25 dihydroxyvitamin D3 levels (4). Excess FGF23 mediates renal phosphate wasting in three hereditary human hypophosphatemic disorders: X-linked hypophosphatemia, autosomal recessive hypophosphatemic rickets, and autosomal dominant hypophosphatemic rickets. An excess of FGF23 leads to phosphaturia and interferes with normal mineralization of bone resulting in rickets or osteomalacia. Elevated levels of FGF23 have been noted in several acquired disorders as well. Tumor-induced osteomalacia or oncogenic hypophosphatemic osteomalacia is associated with increased production of FGF23 by tumors. A subset of patients with McCune-Albright syndrome and polyostotic fibrous dysplasia have elevated FGF23 levels (5). Mutations leading the loss or decreased concentrations of FGF23 result in tumoral calcinosis.

Osteoporosis

Osteoporosis is the most common metabolic bone disease. Osteoporosis was defined at a Consensus Conference as "a disease characterized by low bone mass and microarchitectural deterioration of bone tissue, leading to enhanced fragility and a consequent increase in fracture incidence" (6). The World Health Organization provided an operational definition based on the T-score, or standard deviation beyond the young adult mean bone mineral density as determined by dual energy x-ray absorptiometry (DXA). Osteoporosis can be primary or secondary and secondary osteoporosis can be seen in a variety of conditions such as osteogenesis imperfecta (OI), Turner syndrome, rheumatoid arthritis, glucocorticosteroid use, systemic mastocytosis, hyperthyroidism, adrenal disease, malignancy, steroid or anticoagulant therapy, chronic alcoholism, multiple myeloma, and immobilization. Secondary osteoporosis accounts for up to 40% of cases in men, and 12–30% of cases in women. In this section, the discussion is limited to primary osteoporosis, which is a diagnosis of exclusion.

Osteoporosis has varying incidences in different populations. The incidence is higher in Caucasian and Asian populations and in women. There is an association with lower body mass index, smoking, sedentary lifestyle, and early menopause. For some reason, osteoporosis is rare in patients with widespread osteoarthrosis. It is an extremely common condition, among the overall US population it is thought that one in three women and one in six men over the age of 80 years will develop a hip fracture. This makes osteoporosis one of the most common conditions of the elderly. In the United States, the cost of treating patients with osteoporosis is estimated to be about $7 billion each year in the mid-1980s and is estimated to rise to $60 billion by 2000 (7, 8).

Patients with the disease are asymptomatic, until they suffer a fracture (Fig. 1a–c). Spinal vertebral crush fractures are associated with a loss in height, but two-thirds of vertebral fractures are without symptoms. Hip fractures can be particularly devastating in an elderly population. Colles' or other fractures of the distal radius may be seen with an increased frequency.

Bone Quality

Bone quality is a term that has been used to encompass bone mineral density and other aspects of bone which make up the risk to fracture. The sum of these characteristics influences the ability of the bone to fracture. The strength of bone is due to its material composition and structure. Although bone mineral density is used clinically for assessment of fracture risk, there are many other parameters that comprise the quality of bone. These include bone geometry, micro- and macroarchitecture, and matrix composition.

Bone Mineral Density (BMD) Measurements and Fracture Risk

Bone mineral density measurements can stratify patients on the basis of fracture risk. Bone density measurements of the spine, radius, os calcis, spine, and femur can all predict the probability of fractures. Dual energy X-ray Absorptiometery (DXA) is a standard method for measurement of bone mineral density at the hip, spine, or forearm. Using this technique, for each one standard deviation decrease in bone mass, age-adjusted relative risks in fracture range from 1.4 to 1.6. Measurement at a particular site may be best for the ascertainment of risk of a specific type of fracture. In contrast, assessment of clinical risk factors only explain about 20–35% of the variance in bone mineral density and have a low predictive power for fracture.

Risk Factors for Osteoporosis

Numerous studies have evaluated risk factors for osteoporosis. Recently, the World Health Organization has selected and validated a group of risk factors to determine the probability of fracture. These risk factors include: current age, gender, personal history of a fracture, femoral neck BMD, low body mass index, use of oral glucocorticoid therapy, secondary osteoporosis (e.g., rheumatoid arthritis), parental history of hip fracture, current smoking, and alcohol intake of three or more drinks per day (9).

There are three diagnostic approaches to quantitating osteoporosis: radiological studies, laboratory studies, and bone biopsy. It is important to utilize one or more of these strategies, not only to accurately diagnose bone loss but also to exclude other secondary causes of osteoporosis and also to monitor therapy. Radiologic approaches include older diagnostic tests such as radiograms to assess the trabecular pattern (Singh's index), radiogrammetry, and single energy photon absorptiometry. New techniques include the gold standard (DXA), but bone density or mass can also be determined by computed tomography or ultrasound measurements. These techniques are discussed in the section on musculoskeletal radiology. Laboratory investigations include the exclusion of other metabolic diseases by assessing serum calcium, phosphate, alkaline phosphatase, PTH, 25 hydroxy- and 1, 25 dihydroxyvitamin D3, thyroid-stimulating hormone, serum protein electrophoresis, and urinary calcium. Other tests may be indicated depending on physical examination or symptoms. There are some biologic markers that have recently been introduced for assessing bone turnover. Bone resorption can be measured by serum or urine assessment of C-terminal of cross-linked telopeptide, a breakdown product of type I collagen. Bone formation can be assessed by serum levels of bone-specific alkaline phosphatase, serum osteocalcin, or amino terminal propeptide of type I collagen. These are discussed in the section on the Laboratory in Orthopedic Practice.

Management of Osteoporosis

It is critical to rule out secondary causes of osteoporosis which may be reversible. Once the diagnosis is established, several different strategies are used. A sensible weight-bearing exercise program suited to the patients' age (and other medical problems) has been shown to be helpful. Although weight-bearing exercise will not build bone, the increased muscle strength can improve balance and prevent falls that lead to fracture. Many patients benefit from calcium and vitamin D supplementation (see Table 1). Antiresorptive agents include estrogens, selective estrogen receptor modulators (SERMs), calcitonin, and bisphosphonates. Strontium ranelate is available in some areas and may have dual actions on the osteoclast and osteoblast. Anabolic agents such as PTH can stimulate osteoblasts and enhance bone formation when given intermittently.

Mechanism and Pathogenesis of Osteoporosis

Bone in the adult is continuously undergoing *cycles of remodeling*. Each cycle takes several months and involves an initial resorption phase that lasts several days. The completion of the cycle allows a renewal of bone. The amount of bone added in each remodeling cycle, however, reduces

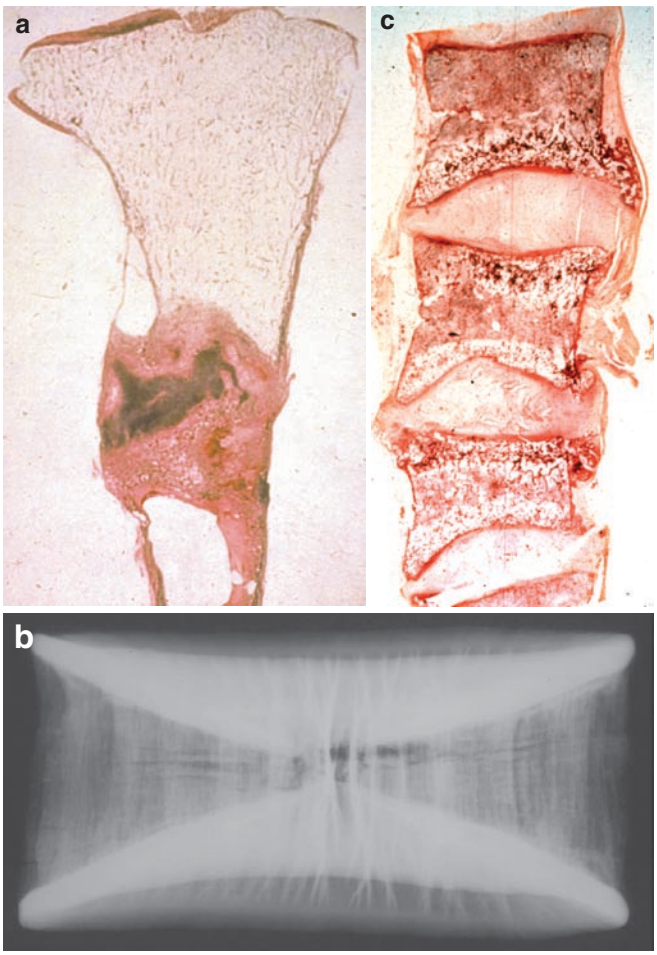

Fig. 1 **a** Osteoporotic bone with fracture. There is a paucity of trabeculae within the marrow space, associated with cortical thinning. **b** Specimen radiograph of a shark vertebra showing a reduced trabecular bone and wide end plates as compared to human vertebrae. The end plates have a biconcave appearance. Osteoporotic vertebrae in humans attain this appearance when the condition is advanced, and are then prone to fracture. **c** Autopsy preparation of the vertebral column from a patient with severe osteoporosis showing several "fish" vertebrae

Table 1 Optimal calcium requirements (6)

Group	Optimal daily intake (in milligram of elemental calcium)
Infants	
Birth–6 months	400
6 months–1 year	600
Children	
1–5 year	800
6–10 years	800–1200
Adolescents/young adults	
11–24 years	1200–1500
Men	
25–65 years	1000
Over 65 years	1500
Women	
25–50 years	1000
Over 50 years (postmenopausal)	
On estrogens	1000
Not on estrogens	1500
Over 65 years	1500
Pregnant and nursing	1200–1500

slightly with age. Through the remodeling process, adults reach their peak bone mass in their early 20s. At the time of the menopause, estrogen deficiency increases bone remodeling so that women can lose up to 10% of their bone in the first few years of menopause. Estrogen deficiency results in an increase in a number of cytokines such as interleukin-6, interleukin-1, and tumor necrosis factor which are implicated in bone loss (7, 8).

Genetics plays an important role in the development of peak bone mass. However, different populations include different factors like ethnicity and environmental factors, which makes osteoporotic genetics more complex to study (10). Several studies have evaluated polymorphisms in various receptors such as vitamin D (11), estrogen, or androgen receptors. A recent study suggests that specific alleles of the type I collagen (COL1A1 gene) may be predictive of bone density. Specific mutations in COL1A1 and COL1A2 genes (chromosomes 17q and 7q, respectively) have been described in cases of idiopathic osteoporosis at an early age. Studies have shown that G-to-T polymorphism have lower bone mineral density than G-to-G polymorphisms. Even though further studies are needed to assess the clinical significance of such findings, this can be helpful as a future marker to determine those patients with decreased bone mass and increased risk for osteoporosis (12). Additional studies in various populations will be important to validate this concept.

Bone densitometry studies have confirmed that bone loss occurs at varying rates in different parts of the body, and differs at different stages in life. In the immediate postmenopausal period, there is a precipitous fall in bone density from several regions, but most seen in the trabecular bone from the vertebra. In this location, the bone loss may reach rates up to 10% per year (compared to cortical bone from the radius where it is 2–3% per year).

It has been estimated that bone mass reaches a peak about 10 years after linear growth stops. Peak mineral density is lower in women, especially Caucasian women as compared to Black women and men. Women can expect to lose 35% of cortical and 50% of trabecular bone with age. Men can expect to lose about two-thirds of these values. In women, about half the loss can be ascribed to menopause. Cancellous bone may constitute up to 66% of the total bone in the lumbar vertebra, 50% in the intertrochanteric and 25% in the intracapsular neck region of the femoral neck. It is as little as 5% in the mid radius. Cortical bone is removed mainly by endosteal tunneling in the Haversian system as opposed to trabecular perforation, fragmentation, and thinning in the cancellous regions.

Bone Biopsy: In osteoporosis, cortical bone is remarkable for enlarged Haversian and Volkmann's canals which larger because of tunneling by osteoclasts. The cortex is thinned (caused by a resorption of the subperiosteal and endosteal surfaces). Endosteal resorption results in a blurring of the cortical–cancellous border, referred to as "trabecularization" of the cortex. Trabecular bone shows thinning and perforation of the trabeculae. Perforation is an irreversible process, which occurs when an osteoclast resorbs all the way through a trabeculum, or when two osteoclasts fortuitously located at opposite ends of the trabeculum meet midway. These thin trabeculae seem to "float" in the marrow space. In "high turn-over" osteoporosis, there is increased osteoclastic activity. Low-turnover osteoporosis is characterized by diminished osteoclastic and osteoblastic activity.

Rickets and Osteomalacia

Rickets and osteomalacia are characterized by a defect of mineralization due to calcium and phosphate deficiencies. This could be due to inadequate absorption by the gastrointestinal tract, lack of sunlight exposure, or disorders of vitamin D metabolism such as hydroxylation defects, increased renal excretion, increased catabolism, or drug induced (e.g., fluoride, etidronate). The lack of vitamin D results in a fall in serum calcium concentration and bone mineralization becomes defective. In contract, in phosphate deficiency, osteomalacia can also occur due to the lack of mineralization. Pathophysiologically, there is a failure of normal mineralization of bone and epiphyseal cartilage resulting in clinical deformities.

The prototype of the disease is vitamin D deficiency (nutritional) rickets. Historically, this was one of the earliest syndromes to be described – a treatise in Latin having been written on it by Daniel Whistler in 1645 (13). The previously less common forms of vitamin D-resistant and vitamin D-dependent rickets, along with renal osteodystrophy, are recognized. The central theme of all these defects is the lack of available calcium and/or phosphorus for mineralization. The discovery of the cause of the various forms of rickets, its association with sunlight and pollution, the recognition of non nutritional forms, the synthesis of vitamin D, and the modern molecular studies form an exciting story. More has been learnt about the disease in the past 20 years than in the preceding 200 years.

In rickets (which occurs in children), both bone and epiphyseal cartilage are involved (Fig. 2a). There is a lack of mineral at the zone of provisional calcification, with a subsequent loss of strength of the bone produced. This results in a deformed epiphyseal plate (metaphyseal flaring).

Osteomalacia, an adult disease, is characterized on undecalcified bone biopsy by osteoid thickness (O.Th) of more than 15 mm and mineralizing lag time (Mlt) of more than 100 days. Osteoid surface and thickness are also increased (Fig. 2b). Bone histology after tetracycline labeling is useful to determine the presence or absence of mineralization. Radiographic features include pseudofractures, biconcave (fish) vertebrae, similar to those seen in osteoporosis (Fig. 1b, c), triradiate pelvis, and protusio acetabuli.

The histological features of all the rachitic and osteomalacic syndromes are similar. The distinction of the various types is not made on histological features – instead, a combination of clinical and laboratory tests are used to distinguish between the types of rickets and determine their etiology.

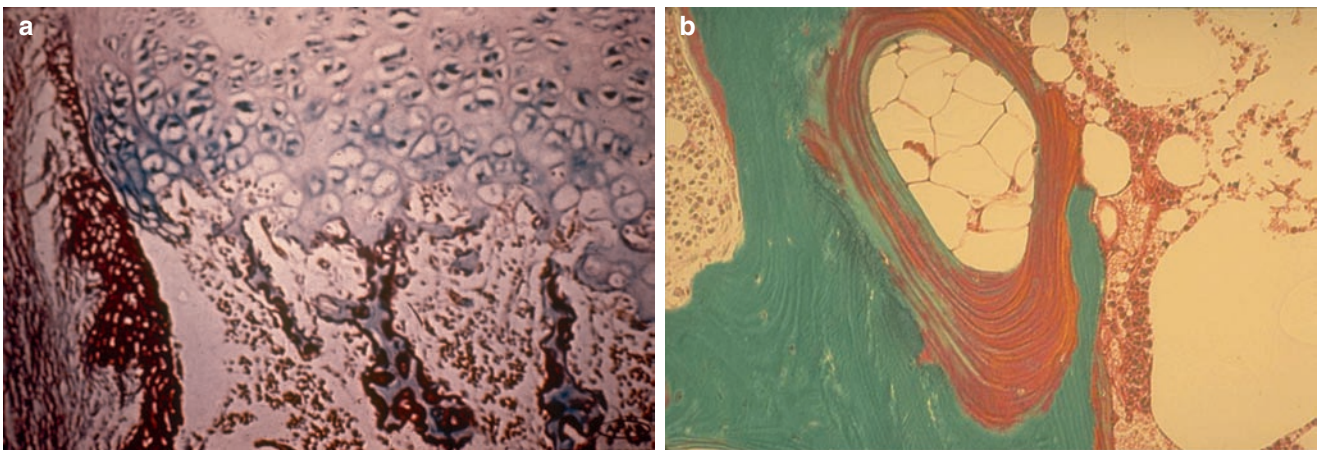

Fig. 2 **a** Growth plate showing orderly maturation. The zones of proliferation and hypertrophy are seen above a zone of provisional calcification where residual enchondral ossification is occuring. In rickets, there is an increase in width of the zone of hypertrophy and a deformation in the shape of the cartilage–bone interface. This results in the metaphyses being "flared". **b** Severe osteomalacia. Wide, unmineralized osteoid seams are represented by red-orange unmimineralized bone in this undecalcified biopsy preparation

Causes of Rickets and Osteomalacia

- Deficiency states (vitamin D, calcium, and phosphorus)
- Gastrointestinal causes
- Genetic disorders
- Renal tubular causes
- Miscellaneous and unusual causes

Deficiency States

These can occur in three situations. The first is dietary deficiency of vitamin D (by far the commonest cause and often coupled with a lack of exposure to sunlight). The second is from bizarre diets which supply a large amount of chelaters in the diet (these include calcium binders such as phytate (coarse cereals), oxalate (from spinach), and phosphates. The third situation is from phosphorus deficiency most often due to binding by aluminum hydroxide (present in antacids) or beryllium (an industrial toxin).

Clinical features: Children with this disorder have deformities (usually by the age of 1 year), including difficulty in walking and weakness. They may have stunted growth, irritability, and apathy. There may be an enlarged abdomen (Buddha belly), softening of the skull (craniotabes), prominence of the skull suture lines (hot cross bun), and frontal bossing. Defects of tooth enamel and dental caries are common. A prominence of the costochondral junctions (rachitic rosary) and a pectus carinatum may also be seen. A thoracic kyphosis (rachitic cat back) and a prominent indentation of the lower rib cage (Harrisons's sulcus) are additional classic signs. Added to these are bowing deformities of the limbs and flaring of epiphyses that result in prominent wrists, ankles, and knees to complete the full-blown picture of traditional rickets. Muscle hypotonia may occur with a delay in developmental milestones.

Adults may have few localizing signs. Diffuse bone and muscle pain is the most common manifestation. Although the reason for the pain is not clear, it has been suggested that it may be due to the swelling of the collagen-rich osteoid that is laid down on the periosteal surface, which puts pressure on the periosteal covering, which is innervated. The vitamin D receptor has been identified in skeletal muscle tissue, and low serum 25 hydroxyvitamin D has been associated with reversible myopathy in patients with osteomalacia. Patients may complain of malaise, or tenderness, sometimes localizing to the hip. The tenderness may be extreme, and may lead the examiner to question a psychological basis for the symptoms. Proximal muscle weakness may lead to an antalgic gait.

The mechanism of disease is as follows. Reduced vitamin D causes a diminution in the absorption of calcium from the gastrointestinal tract. This in turn leads to a lowering of calcium in the blood. This ends up inciting a secondary hyperparathyroidism which brings the calcium to a low-normal level, but at the expense of bone loss and a phosphate diuresis (14).

Table 2 Chemical changes in the blood (deficiency states)

Serum measurement	Serum value (change compared to normal)
Serum calcium	Low to normal
Serum phosphate	Low
Urinary calcium	Low
Percent tubular resorption of phosphate	Low
Serum alkaline phosphatase	High
Parathyroid hormone	High
1,25 Dihydroxyvitamin D	Low

Gastrointestinal Causes

- Gastric rickets (or osteomalacia)
- Biliary rickets (or osteomalacia)
- Enteric rickets (or osteomalacia)

Gastric rickets: This unusual entity has seen a marked decline since the decrease in the frequency of gastric operations for duodenal ulcers. In the years past, this followed (often quite subtly) a Polya or a Bilroth II gastrectomy. The cause is not well known, but is thought to result from a diminished acid content in the stomach (calcium salts are more soluble in acid medium). Additionally, the rapid motility of gastrointestinal contents – the so-called dumping syndrome may have contributed and prevent absorption of calcium and/or vitamin D.

Biliary rickets: The cause is essentially due to an abnormal fat metabolism. It is seen with a failure to emulsify fats by bile salts or the presence of free fat in the intestinal tract. The absorption of vitamin D (a fat-soluble vitamin) is reduced. Ionic calcium may serve as the counterion for fatty acids resulting in an insoluble soap formation. Vitamin D deficiency osteomalacia has also been seen in alcoholics and in patients with biliary cirrhosis. In these situations, altered intrahepatic handling of vitamin D is the suspected cause of the problem.

Enteric rickets: This is associated with a diffuse injury to the small bowel (celiac disease, Crohn's disease, short loop bowel, gluten enteropathy, tropical sprue, etc.). There is also a form associated with total parenteral nutrition.

Table 3 Chemical changes in the blood (gastrointestinal causes)

Serum measurement	Serum value (change compared to normal)
Serum calcium	Low
Serum phosphate	Low
Urinary calcium	Low
Percent tubular resorption of phosphate	Low
Serum alkaline phosphatase	High
Parathyroid hormone	High
1,25 Dihydroxyvitamin D	Low to normal

Classification of Genetic-Based Rickets

- Hypophosphatemic rickets or osteomalacia: X-linked rickets (related to PHEX mutations)
- Type I vitamin D-dependent rickets or osteomalacia (related to 1-alpha hydroxylase deficiency)
- Type II vitamin D-dependent rickets or osteomalacia (related to vitamin D receptor mutations)

X-Linked Hypophasphatemic Rickets

X-linked hypophasphatemic rickets is the pure hypophosphatemic form of rickets (Albright syndrome, phosphate diabetes, classic vitamin D-deficient rickets). The signs of rickets usually manifest only after 3 years of age. A family history is often available and is helpful in the diagnosis. The most prevalent form (described by Albright in 1937) is an X-linked dominant condition and is due to a diminished tubular resorption of phosphate.

The classic triad consists of hypophosphatemia, lower limb deformities, and stunted growth rate. There is no enamel hypoplasia, as is usually seen in hypocalcemia rickets. Dentin defects may be present and manifest as dental decay and dental abscesses in the adult. Bone histology varies, depending on the presence or absence of hyperparathyroidism. There is an accumulation of undermineralized osteoid with no evidence of increased osteoclast activity and excessive bone resorption.

The genetic defect (an inactivating mutation of PHEX-phosphate regulating gene with homologies to endopeptidases on the X chromosome) is localized to the X chromosome, located at Xp22.1-22.2. This gene encodes a membrane-bound endopeptidase primarily expressed in osteoblasts, osteocytes, odontoblasts, muscle, lung, and ovary. More than 180 *PHEX* mutations have been identified.

In other cases (perhaps unrelated to PHEX mutations), the proximal tubular defect may be more extensive and may show (in addition to phosphaturia) the presence of glycosuria and aminoaciduria. The molecular/genetic basis for these defects is under investigation. If the defect is present in all three (glucose, amino acids and phosphate), then the condition is known as the Fanconi's proximal tubular (Fanconi's type I) syndrome. Fanconi's type II or the Debre-de Toni-Fanconi syndrome, a broader defect, extends to the distal tubule and results in a failure to reabsorb water, fixed base, and hydrogen. The latter state may be associated with systemic cystinosis with deposition of cystine crystals in various organs. In this situation, it is known eponymically as the Lignac-Fanconi syndrome. Patients respond to oral phosphorus supplements and 1, 25 dihydroxyvitamin D3.

Hypophosphatemic Rickets (Hyp) due to PHEX mutations

Contemporary molecular genetics have linked the gene thought to be responsible for this condition to the short arm of chromosome X (Xp22.1-Xp22.2), but there is evidence for possible locus heterogeneity. The Hyp mouse is a model to study the disease. The defect is less severe in the female heterozygotes than it is in male hemizygotes and this gene dose effect indicates that the observed defect is close to the abnormal gene product.

Studies in both man and mouse indicate that the defective bone formation in X-linked hypophosphatemia is due to an intrinsic osteoblast defect. Hypomineralization occurs and therapy is based on aggressive phosphorus replacement. A severe secondary hyperparathyroidism occurs and large amounts of vitamin D result in an improvement in growth rates and evidence of healed rickets on radiographs.

Two murine models (the Hyp and the gyro mice) have also been studied. In the murine model, there is evidence of increased catabolism of 1, 25 dihydroxyvitamin D3. In the mouse model (Hyp), phosphorus transport in the proximal convulated tubule is defective. Moreover, parabiotic mouse experiments have raised the possibility of a phosphorus-controlling hormone that might be responsible for some of these abnormalities. Interestingly, in Hyp mice, bone abnormalities are not corrected, by correcting the metabolic defect. This suggests that there may be an additional primary osteoblast defect as well (15). Whether all these factors and mechanisms are operative in human patients afflicted with this disease remains to be seen

The use of 1, 25 dihydroxyvitamin D3 allows for more precise control of the secondary hyperparathyroidism and appears to give better healing on bone biopsy.

Fuller Albright (1900–1969): Albright had a distinguished career at Harvard and contributed to several discoveries in endocrinology and bone diseases. He was born on January 12, 1900, in Brookline, MA. His father was a fancier and philanthropist. He studied at Harvard and did his medical training at Johns Hopkins hospital in Baltimore, and in Vienna. He joined the Massachusetts General Hospital in 1930, where he developed a department of endocrinology. He was stricken by Parkinson's disease at this time but continued to work on many aspects of bone disease, sex hormones, and steroids. Following a stereotactic brain biopsy in 1956, he became an invalid. His name is associated with descriptions of pseudo-hypoparathyroidism, pseudo-pseudo-hypoparathyroidism and the Albright hereditary osteodystrophy. His name is also associated with a kind of polyostotic fibrous dysplasia (McCune-Albright syndrome). Another notable eponym is the Albright-Butler-Bloomberg syndrome (vitamin D-resistant rickets).

Guido Fanconi (1892–1979): Fanconi was a professor of pediatrics at the University of Zurich. He was born on January 1, 1892, in Poschiavo, Grisons, Switzerland. He trained in Zurich, Lusanne, Munich, and Berne. He obtained postgraduate experience at several centers in Europe. He was responsible for applying biochemistry to pediatrics. He spoke several languages and was on a number of committees on pediatrics. He also took a keen interest in the problems of children in the less-developed countries of the world. His name is attached to over 15 genetic syndromes, a cause of considerable confusion. The best known, however, is the syndrome previously described by Guido di Toni, and often referred to as the di Toni-Fanconi syndrome.

Table 4 Chemical changes in the blood (phosphaturic rickets)

Serum measurement	Serum value (change compared to normal)
Serum calcium	Normal
Serum phosphate	Low
Urinary calcium	Normal*
Percent tubular resorption of phosphate	Low
Serum alkaline phosphatase	High
Parathyroid hormone	Normal

**May have glycosuria, aminoaciduria etc. (Fanconi I syndrome)*

Table 5 Chemical changes in the blood (type I vitamin D-dependent rickets)

Serum measurement	Serum value (change compared to normal)
Serum calcium	Low
Serum phosphate	Low
Urinary calcium	Low
Percent tubular resorption of phosphate	Low
Serum alkaline phosphatase	High
Parathyroid hormone	High

Vitamin D-Dependent Rickets Type (1-α-hydroxylase Deficiency) I

The incidence of this autosomal recessive inherited syndrome has been estimated to be in the order of 1:20,000. In this disease, there is a failure to convert 25 hydroxyvitamin D to its 1,25 dihydroxy form in the renal tubule. These individuals have inactivating mutations in the 1-α-hydroxylase gene. This is manifest often during the first 6 months of life and often presents with seizures. Patients develop secondary hyperparathyroidism and hypophosphatemia due to the increased renal phosphate clearance. Amino aciduria may also be observed. Patients have normal-to-elevated levels of 25 hydroxyvitamin D and markedly reduced or undetectable concentrations of 1, 25 dihydroxy vitamin D. Patients do not respond to 25 hydroxyvitamin D therapy but normalize with the 1, 25 dihydroxyvitamin D3. Complete remission can be obtained with high doses of vitamin D but is dependent on continuous therapy. Healing of the rickets has been noted within several months of initiation of therapy.

Type II Vitamin D-Dependent Rickets

These patients present with hypocalcemia, osteomalacia, and elevated levels of 1, 25 dihydroxyvitamin D3. Treatment with vitamin D results in correction of the hypocalcemia and the term "hereditary resistance to 1, 25 dihydroxyvitamin D3" may be more appropriate. These patients have mutations of the vitamin D receptor, making these appear resistant. This is an autosomal recessive disorder, and children may present with tetany or seizures. One distinguishing feature is the development of alopecia in the first year of life, resulting in alopecia totalis. Additional ectodermal abnormalities such as epidermal cysts, multiple milia, and oliogodontia may be present. Parental consanguinity in multiple siblings with the same defects occurs in about half of the reported kindreds with vitamin D-dependent rickets type II (VDDR-II). These children have very high levels of 1, 25 dihydroxyvitamin D3, due to the secondary hyperparathyroidism. The elevated levels of PTH drive 1-α-hydroxylase to produce more 1, 25 dihydroxyvitamin D3.

Several cellular and molecular defects of the vitamin D receptor–effector system have been described in different kindreds with VDDR-II. Three different classes of intracellular defects have been identified and include hormone-binding defects such as decreased capacity or decreased hormone-binding affinity, deficient nuclear localization, and normal or near-normal tritiated 1, 25 dihydroxyvitamin D3 binding to soluble cell extract in nuclei but decreased affinity of the hormone–receptor complex to heterologous DNA. Induction of 25 hydroxy-24-hydroxylase by 1,25 dihydroxyvitamin D in cultured dermal fibroblasts shows a correlation to the therapeutic response in two vitamin D metabolites in vivo in kindreds in which this was tested. Although not all individuals with VDDR-II have been tested, adequate therapeutic trails must include administration of pharmacological doses of vitamin D daily (1,25 dihydroxyvitamin D or 1-α-hydroxy vitamin D) at doses in the range up to 6 mg/kg of body weight, supplemental calcium up to 3 g elemental calcium per day, and a duration of therapy (3–5 months) sufficient to mineralize depleted bones. In rare cases, intravenous calcium infusions have been required to normalize serum calcium. Catch-up growth and histological healing of defective osteoid mineralization has been described in individual patients (16).

Table 6 Chemical changes in the blood (type II vitamin D-dependent rickets)

Serum measurement	Serum value (change compared to normal)
Serum calcium	Low
Serum phosphate	Low
Urinary calcium	Low
Percent tubular resorption of phosphate	Low
Serum alkaline phosphatase	High
Parathyroid hormone	High
1,25 Dihydroxyvitamin D	Normal to high

Renal Tubular Acidosis

Fanconi syndrome is a disorder of renal proximal tubules, with decreased resorption of phosphorus, glucose, and amino acids. The syndrome can be acquired, drug-related, due to heavy metal poisoning, or part of a heritable disorder. Laboratory finding includes hypophosphatemia, phosphaturia, and low tubular maximum of inorganic phosphate, glycosuria with normal plasma glucose, generalized aminoaciduria, hypobicarbonatemia, excessive bicarbonate excretion in the urine, and elevated serum alkaline phosphatase. Children present with growth failure and rickets. In adults, multiple myeloma is the most common cause of Fanconi syndrome.

The syndrome (regardless of etiology) is thought to be a result of a failure to substitute hydrogen ion for a fixed base or "bicarbonate wastage." It results in a hyperchloremic, hyponatremic, hypokalemic acidosis with alkaline urine, and a notable loss of fixed base including calcium ion. This results in rachitic findings and renal calculi. Renal tubular acidosis cannot be effectively treated with vitamin D or phosphorus alone. It requires alkalinization of the extracellular fluid with the use of sodium bicarbonate (or equivalent) solutions.

Table 7 Chemical changes in the blood (renal tubular acidosis)

Serum measurement	Serum value (change compared to normal)
Serum calcium	Low
Serum phosphate	Low
Urinary calcium	High*
Percent tubular resorption of phosphate	Low
Serum Alkaline phosphatase	High
Parathyroid hormone	High
1,25 Dihydroxyvitamin D	Normal to high

**Lowlevels of sodium and potassium, high levels of chloride acidosis and alkaline urine*

Unusual Causes of Rickets

Fibrous Dysplasia

Rickets or osteomalacia may occur (very rarely) as an osteoendocrine manifestation of florid fibrous dysplasia. Fibrous dysplasia is due to increased levels of FGF23, a potent phosphaturic agent. The degree of phosphate wasting correlated with the degree of elevation of FGF23. The elevated levels of FGF23 correlate with the burden of skeletal disease in these patients. In these patients, the fibrous dysplasia in bone is the source of elevated levels of FGF23 which, in turn, acts on the kidney to lower serum phosphorus and 1, 25 dihydroxyvitamin D3 and the low serum phosphorus at least contributes to the worsening of the osteomalacia that is seen in this disorder (17, 18).

Bone and Soft Tissue Tumors (Oncogenic Osteomalacia)

Oncogenic osteomalacia is a relatively rare disorder and is characterized by unexplained osteomalacia in association with a concurrent neoplasm elsewhere. This is a paraneoplastic syndrome of phosphate wasting and resembles the genetic forms of hypophosphatemic rickets. There is remission of the bone disease after resection of coexisting tumor.

Patients present with bone and muscle pain, muscle weakness, and recurrent fractures. Additional symptoms are similar to those found in classic vitamin D deficiency rickets. Age at the time of diagnosis is variable with a wide range (7–74 years), although the majority of patients are in their sixth decade. An average of 5 years elapses from the time of onset of symptoms to the identification of the underlying tumor.

Biochemical findings including hypophosphatemia and abnormally low renal tubular maximum for resorption of phosphorus per liter of glomerular filtrate (TMP/GFR) are indicative of phosphate wasting. Serum phosphate values range from 0.7 to 2.0 mg/dL and after removal of the tumor, biochemical parameters return to normal. Serum 25 hydroxyvitamin D may be normal and serum 1,25 dihydroxyvitamin D overtly lower or inappropriately normal relative to hypophosphatemia. Aminoaciduria is occasionally present. Biochemically, therefore, these patients are similar to patients with vitamin D-dependent rickets.

The osteomalacia-inducing tumors are frequently of mesenchymal origin in the majority of patients. Mostly, these have been soft-tissue tumors with a hemangiopericytomatous pattern. Other tumors that have caused osteomalacia include neurofibromas, fibrous dysplasia, a variety of bone tumors containing giant cells, or having a chondroblastoma-like pattern (Fig. 3a, b). However, tumor-induced osteomalacia may be concurrent with cancers such as breast, prostate, oat cell, small cell carcinomas, and multiple myeloma or chronic lymphocytic leukemia.

Investigators agree that tumor production of a humeral factor, designated FGF23 (phosphatonin), alters the function of the proximal renal tubular phosphate resorption, and downregulates 1-α-hydroxylase. Circulating levels of FGF23 are elevated in these patients.

Diagnosis of oncogenic osteomalacia is dependent on all the classical, biochemical, and radiographic criteria of hypophosphatemic osteomalacia. In this setting, a diligent search for tumors is recommended. In the absence of tumor or family history of disease, exclusion of common causes of osteomalacia must be considered.

Treatment is complete resection of the associated tumors but occasionally this is not possible. Pharmacological doses of vitamin D and oral phosphate supplementation have resulted in symptomatic resolution of the disease although biochemical abnormalities may remain. Large doses of phosphorus may be necessary (2–4 g per day) and calcitriol (1.5–3.0 mg/day) replaces the insufficient renal production and enhances phosphate resorption.

Chronic Anticonvulsant Therapy

Initial reports of bone disease in patients with epilepsy often included institutionalized patients who might be at risk due to reduced sunlight exposure and poor nutrition. However, osteomalacia and bone loss have been reported in ambulatory, well-nourished individuals. The original focus of anticonvulsant therapy bone loss was on agents that induce the hepatic cytochrome P450 enzyme system which increased the metabolism of vitamin D. More recently, the mechanisms of antiepileptic drug-induced bone loss are multiple and all types of these agents have been implicated. Besides the effects on vitamin D, there is evidence that these drugs may have direct effects on bone cells, resistance to PTH, inhibit calcitonin secretion, and impair calcium absorption (19).

Fluorosis

The effect of fluoride is dose dependent, such that low doses prevent dental caries but high doses can interfere with bone mineralization. Skeletal fluorosis can occur with chronic ingestion of fluoride, which is endemic in the water in some parts of the world. Skeletal fluorosis causes bone pain, stiffness, and deformities of the spine and limbs. Bone mass in increased, but due to the brittleness of the bone, bone strength is decreased. Fluoride is incorporated into the crystalline lattice of hydroxyapatite, changing the structure and the interface between the

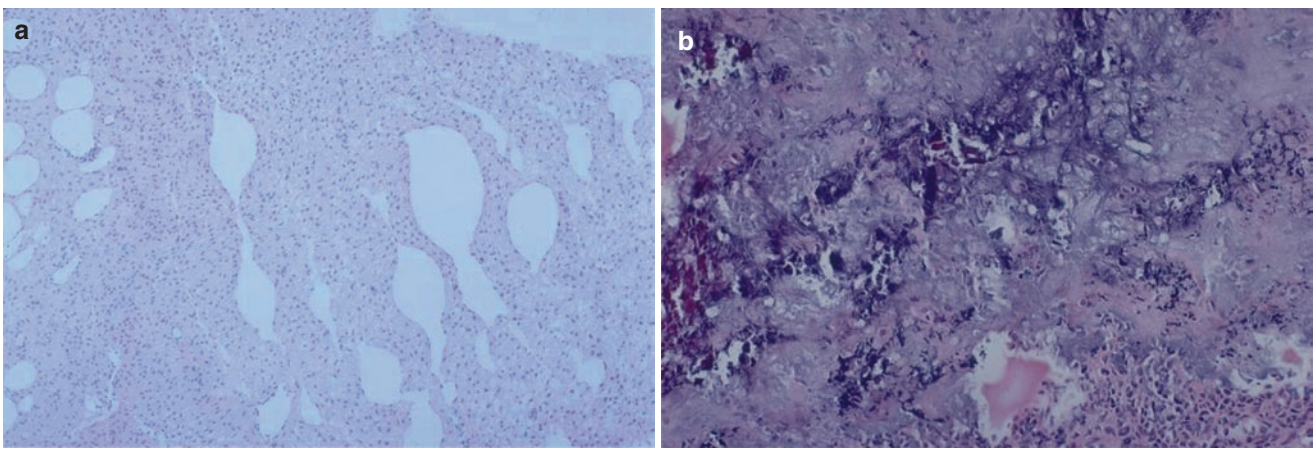

Fig. 3 **a** Oncogenic osteomalacia was caused by this tumor with a hemangiopericytomatous pattern. **b** Oncogenic osteomalacia was caused by this tumor with a chondroblastoma-like pattern with heavy mineralization. The tumor subsequently metastasized to the lung, but the patient lived on with multiple resections for more than 20 years

mineral and the matrix. Histomorphometric analysis of iliac crease bone biopsies is consistent with skeletal osteosclerosis with an increase in bone formation. Mineralization defects are present, and occasionally woven bone is observed (20).

Pathology of Rickets and Osteomalacia

The changes of rickets and osteomalacia vary according to the age of the patient and the severity of the disorder.

Rickets is a disease of the growing skeleton and affects the epiphyseal plate and bones of children. The clinical finding of bones which are defective in strength and deformed is probably not (as was earlier believed) due to "softening." In fact, the poorly mineralized bones are more prone to stress "micro-fractures" and these heal with the resultant deformities. This hypothesis has support histologically.

Osteomalacia is the adult counterpart, after the growth cartilage has fused and the epiphysis is obliterated. In many respects, however, the changes of osteomalacia are similar (but often less prominent since the adult skeleton is metabolically less active).

In both instances, there is insufficient ionized calcium, inorganic phosphorus (or both) to mineralize the skeleton. There is thus less mineralized bone per unit volume of bone. There may in fact be less bone overall, but more strikingly, the bone that there is fails to mineralize properly. Trabeculae are surrounded by unmineralized osteoid in the form called "osteoid seams." Osteoid seams, however, are not pathognomic of osteomalacia/rickets and may be seen in hyperparathyroidism, fibrous dysplasia, and several bone-forming tumors. But, contrary to the other conditions, these are very prominent in rickets and in osteomalacia and are considered an important diagnostic clue. Bone histomorphometry has shown that the mineralization lag time is greater than 100 days in rickets or in osteomalacia (normal 80–90 days). Also, such studies have determined that osteoid seams of greater than 15 mm are virtually diagnostic of this syndrome. It is important to recognize that all rachitic syndromes have similar histology and the individual diagnosis cannot be made on the basis of a bone biopsy. Additional studies, however, may be useful in certain conditions, for example, histological stains for aluminum may be considered in rare cases of renal osteodystrophy due to aluminum toxicity (Fig. 4).

In rickets, pressure effects cause deformity at the epiphysis–metaphysis junction, resulting in metaphyseal flaring and a disordered physis. The radiologic finding of Looser's lines (or Milkman's pseudofractures) is represented histologically by focal collections of osteoid. These produce characteristic ribbon-like radiolucency, and are seen most commonly on the concave side of long bones, or the axillary side of clavicles. On occasion, they may propagate and become true fractures.

Fig. 4 Acid Solochrome Azurine (ASA) stain for aluminium in a patient with aluminium associated renal osteodystrophy.

Management of Patients with Rickets or Osteomalacia

This is a specialized topic and is discussed in the appropriate orthopedic and endocrinology texts. The therapeutic armamentarium includes vitamin D and its synthetic analogues and active metabolites such as 1, 25 dihydroxyvitamin D3, calcium infusions, neutral phosphate. From the orthopedic standpoint, fractures and slipped capital epiphyses must be treated, deformities be corrected by bracing or osteotomy and damaged joints be realigned or replaced. Overtreatment by vitamin D and unnecessary immobilization should be avoided, especially in the refractory syndromes. The therapy should be directed at the underlying cause of the disorder.

Scurvy

Scurvy is a result of decreased vitamin C intake. This is a condition that is largely of historical interest only. The surgical pathology of this condition, however, is instructive. In its usual form, it is seen in infancy, especially in the age group 5–10 months of age. Elderly people or those on unusual diets may also develop subclinical, or rarely, clinical scurvy.

Infants affected are restless, febrile with tender limbs (pseudoparalysis). Petichae, hemorrhages, hematemesis, and hematuria may be prominent. Bleeding gums are usual, pathologic fractures or epiphyseal separation may be seen.

Surgical Pathology

The connective tissue matrix and the endothelium are affected. Capillary hemorrhages particularly beneath mucous membranes, may occur. Common sites are bones, gums, intestine, conjunctivae, skin, bladder, and kidneys.

Subperiosteal hemorrhage is characteristic. This may be large, and cause ballooning of the periosteum in the form of a mass overlying the bone. If vitamin C is supplied, healing occurs by fibrosis and ossification. The healing occurs from the outside to the center, mimicking myositis ossificans. Eventually, the healed bone is resorbed.

Metaphyseal hemorrhage interferes with the ingrowth of osteoblastic tissue. Endochondral ossification proceeds normally only up to the zone of provisional calcification. The calcified cartilage persists and accumulates. There is a paucity of osteoblastic and osteoclastic activity in this region as seen on histological material. The broadened layer of calcified cartilage is referred to as the "white line of Fraenkel" on X-rays. The metaphysis is also extremely hyperemic in response to the hemorrhage. The resultant increased resorption of bone accentuates the white line of Fraenkel. It also leads to deficient bone and epiphyseal separation. The buttressing bony spur protruding from the metaphysis to prevent epiphyseal separation is known radiologically as the Pelkan spur.

Within the epiphysis, a zone of calcified cartilage accumulates about the bony centrum (secondary centers of ossification). This encircling dense ring is known as the Wimberger's line. Within the marrow space, fibrous replacement of the marrow is present. Secondary anemia may therefore ensue. Osteogenesis is interfered with, the cortices become thinner and there is poor trabeculation. Pathologic metaphyseal and diaphyseal fractures may occur.

For the same reason, alveolar resorption may cause loose teeth. Pulp hemorrhage, reduced dentine formation with normal enamel production is characteristic. The gums consequently become hemorrhagic and swollen.

Renal Osteodystrophy

The term renal osteodystrophy has been used to include bone diseases observed with renal failure. Currently, more specific terms are preferred for each component – for example, secondary hyperparathyroidism-associated osteitis fibrosa and aluminum-related bone disease. On the basis of tetracycline double-labeled bone biopsy, the set of diseases (renal osteodystrophies) can be divided into high turnover, low turnover, and mixed types of bone disease. Secondary hyperparathyroidism is an example of high and osteomalacia is an example of low-turnover types (21).

Improved management of renal bone disease has decreased the incidence of renal osteodystrophy. The kidney plays a role in the conversion of 25 hydroxyvitamin D to its potently active 1,25 dihydroxy form. In addition, it is the target organ for the action and degradation of PTH. It is also responsible for elimination of aluminum.

In high-turnover renal osteodystrophy, PTH levels are persistently elevated. In low-turnover renal osteodystrophy, PTH may be low, normal, or slightly elevated. High-turnover osteodystrophy is the most common form. Phosphate retention in renal failure plays an important role in the pathogenesis of secondary hyperparathyroidism.

High-Turnover Osteodystrophy

High-turnover renal osteodystrophy is due to elevated levels of PTH on bone. Hyperplasia of the parathyroid glands can occur. Glomerular disease (decreased filtration) results in phosphorus retention. Hyperphosphatemia resulting from this is key in the development of high-turnover osteodystrophy and metastatic calcification. Hyperphosphatemia (along with a reduction in kidney mass) also results in a reduced synthesis of 1, 25 dihydroxyvitamin D3. This in turn decreases the absorption of calcium through the gut. As can be expected, this leads to a secondary hyperparathyroidism and calcium rises to near normal values at the expense of bone resorption. Other factors contributing to the secondary hyperparathyroidism include a shift of the parathyroid "set point," so that a higher serum calcium level is needed to suppress the PTH secretion in some patients, and reduced degradation of PTH. In addition, phosphate retention may be associated with an increase in FGF23, which is a potent inhibitor of 1-α-hydroxylase.

Osteitis fibrosa cystica is a common manifestation of renal osteodystrohy. There is histological evidence of active bone resorption with an increase in the number and size of osteoclasts and the percentage of surface eroded. Marrow fibrosis is apparent adjacent to the bony trabeculae and accumulates throughout the marrow space. In advanced cases, the bone marrow may be completely replaced by fibrous tissue. Osteoblast activity is increased and the rates of bone formation are often above the upper limits of normal. A greater proportion of cancellous bone is covered with newly formed osteoid and the osteoid appears woven. Subperiosteal erosions are a consistent histological and radiographical finding in patients with secondary hyperparathyroidism. Osteosclerosis may also account for the "rugger jersey" appearance of the spine on lateral views of the thoracic vertebrae and the "salt-and-pepper" appearance of the skull. Slipped epiphyses are a striking clinical and radiographical finding in children. Gross deformities of the

skeletal including ulnar deviation of the hands and gait abnormalities may be found in the growing child.

Weakness of the proximal muscles also occurs and can be debilitating. Spontaneous rupture of tendons has been noted in those with long-standing kidney disease.

Extracellular calcifications include calcification of the vascular system, including the coronary arteries, aorta, femoral, and carotid arteries (22). Dystrophic calcification can occur around joints. In the extreme, small vessel calcification can result in the syndrome of calcific uremic ateriolopathy, or calciphylaxis. This is manifest as painful areas of the lower extremities and trunk that become violaceous, indurated, and mottled. It has been suggested that decreased levels of the calcification inhibitor, fetuin A, may play a role in this syndrome. The deposition of β-2 microglobulin in articular and periarticular tissues may result in disabling arthropathy. Large bone cysts may be seen, particularly in the vertebrae.

Low-Turnover Renal Osteodystrophy

Low bone turnover can be seen in association with kidney disease and is associated with very low rates of bone formation, even to the point of an increased volume of unmineralized bone matrix or osteomalacia. The majority of cases with this picture have been caused by accumulation of aluminum at the mineralization front. But with the discontinuation of the use of aluminum-based phosphate binders, this is becoming a rare entity. There remains a substantial population of renal dialysis patients who have low bone turnover not associated with osteomalacia, or "adynamic bone." This is more prevalent in patients on peritoneal dialysis. Many factors are responsible for the development of low-turnover renal osteodystrophy, and most decrease the ambient levels of PTH.

Low-turnover renal osteodystrophy can be subdivided on the basis of osteoid volume into osteomalacia and aplastic bone disease. Histological features of osteomalacia secondary to renal disease are similar to the characteristics of other types of osteomalacia.

The histological appearance of "adynamic" or "aplastic lesion of renal osteodystrophy" presents as reduced amount of osteoid, the absence of tissue fibrosis, and diminished numbers of osteoblasts and osteoclasts. The number of patients with adynamic bone disease who have no evidence of bone aluminum deposition has increased substantially and attributed to the increased use of vitamin D steroids and calcium in the treatment of patients with renal failure (21).

Currently, renal osteodystrophy is treated by maintenance of normal serum calcium and phosphorus levels to prevent hyperplasia of the parathyroid glands, avoidance of exposure to toxic agents such as aluminum, prevention of extraskeletal calcification, and judicious use of vitamin D steroids. Chelating agents such as furoxamine are administered when appropriate for aluminum intoxication.

Primary Hyperparathyroidism

This is a common disorder due to an adenoma of the parathyroid glands. Less commonly, parathyroid hyperplasia (~15–20% of cases) or rarely, carcinoma (less than 1% of all cases) is present. Excessive amounts of PTH are released from the gland, resulting in hypercalcemia. In the past 30 years, the widespread application of multichannel screening tests has led to the detection of asymptomatic disease, which is the most common presentation. Primary hyperparathyroidism is the most common cause of hypercalcemia and involvement of the skeleton (osteitis fibrosa cystica), kidneys (nephrolithiasis, nephrocalcinosis), and neuromuscular dysfunction (specific muscle weakness) is less common. Serum levels of PTH can help establish the diagnosis.

Hereditary disorders of hyperparathyroidism include multiple endocrine neoplasia types I and II, hyperparathyroidism-jaw tumor syndrome, familial isolated hyperparathyroidism, familial hypocalciuric hypercalcemia, and neonatal severe primary hyperparathyroidism (23).

It has been suggested that primary hyperparathyroidism is a biphasic disease. The first phase is notable for increased levels of PTH, without an increase in serum calcium levels. It is during this phase that cortical bone is affected by the elevated levels of PTH. The second phase consists of the clinically apparent, albeit usually asymptomatic disease with elevated levels of serum calcium. The first phase has been named "normocalcemic primary hyperparathyroidism" and these subjects have more substantial skeletal involvement and more complications over time than is typically noted in primary hyperparathyroidism (24).

Classic radiographic findings are rarely seen today. These include osteopenia, a "salt-and-pepper" skull, loss of lamina dura, erosion of the outer clavicle, osteopenia of the medial aspect of the tibia, and subperiosteal resorption of the radial side of the digital tufts and phalanges. In advanced cases, brown tumors and pathologic fractures elsewhere may occur. Bone mineral density may be decreased, with cortical bone at the distal third of the radius being the most predominant site of bone loss. Lumbar spine bone mineral density, which largely reflects trabecular bone, is minimally reduced (23).

Renal calculi may be present and in recent studies the incidence is 15–20% of all patients. Patients may also have hypercalciuria, which is noted in about 40% of patients or nephrocalcinosis. With high calcium values, ectopic calcification may rarely occur.

There may be calcification of the triangular fibrocartilage of the radioulnar joint, articular cartilage, and the menisci. On radionuclide imaging, there is typically a "patchy" increased uptake. The classic presentation of "bones, stones and groans" is vanishingly rare. The term "bones" used to refer to the bone changes of the disease – especially brown tumors and pathologic fractures. "Stones" were renal calculi and groans referred to the mental aberrations of hypercalcemia,

along with the pain from the accompanying peptic ulcerations and pancreatitis of the full-blown picture. Today, the presentation is usually more subtle, the patient is usually asymptomatic. Nonspecific complaints include weakness and easy fatigability.

von Reclkinghausen, Friedrich Daniel (1833–1910): von Recklinghausen was an eminent German pathologist, who was born in Gutersloh, Westphalia, Germany in 1833. He studied in Bonn, Wurzburg, and Berlin and qualified in 1855 having written a thesis in Latin on pyemia. He was appointed assistant to Professor Rudolf Virchow at the Pathological Institute in Berlin, and later moved to Strasbourg, Alsace where he became Rector of the university. He achieved fame and success but rarely spoke to his students. He died at the age of 77. His name is associated with neurofibromatosis (cafe-au-lait spots, neurofibromas, etc.), and also with the bone changes associated with hyperparathyroidism. He included two cases in this, which are now recognizable as Albright's disease.

Pathology: The major skeletal manifestations are caused by increased bone remodeling rates, with increased bone resorption and augmented bone formation rates. Cancellous bone volume is maintained but cortices are thinner and more porous. The bones are characterized by marrow fibrosis, osteoclastic resorption, active osteoblasts on new and often incompletely mineralized lamellar bone trabeculae and rarely, "brown tumors"(Fig. 5a–c). The latter are areas of granulation tissue, inflammatory cells, and macrophages containing hemosiderin and giant cell formation. There is virtually no bone present in the area. Occasionally, cystic change may supervene. The increased osteoclastic activity is seen in subperiosteal, intracortical, endosteal, subchondral, and trabecular surfaces. Intracortical resorption is characterized by groups of osteoclasts (known as cutting cones) that tunnel through the cortex enlarging the Haversian and Volkmann's canals. These channels are often expanded to 1 mm or more in some cases, and may be seen radiographically as lucent lines within the cortex. Endosteal resorption is also visible radiographically as "scalloping" of the cortex at its marrow interface. Subchondral resorption results in microfractures and joint abnormalities. Atrophy of type II muscle fibers suggests a reason for neuromuscular complaints. Cardiovascular manifestations include hypertension, left ventricular hypertrophy, and arrhythmias (23).

Surgical success rates of extirpation of the single parathyroid adenoma are 95% and is usually curative. Surgery leads to an improvement in bone mineral density of up to 10% at the lumbar spine and femoral neck. Other medical measures include antiresorptive agents and calcimimetics.

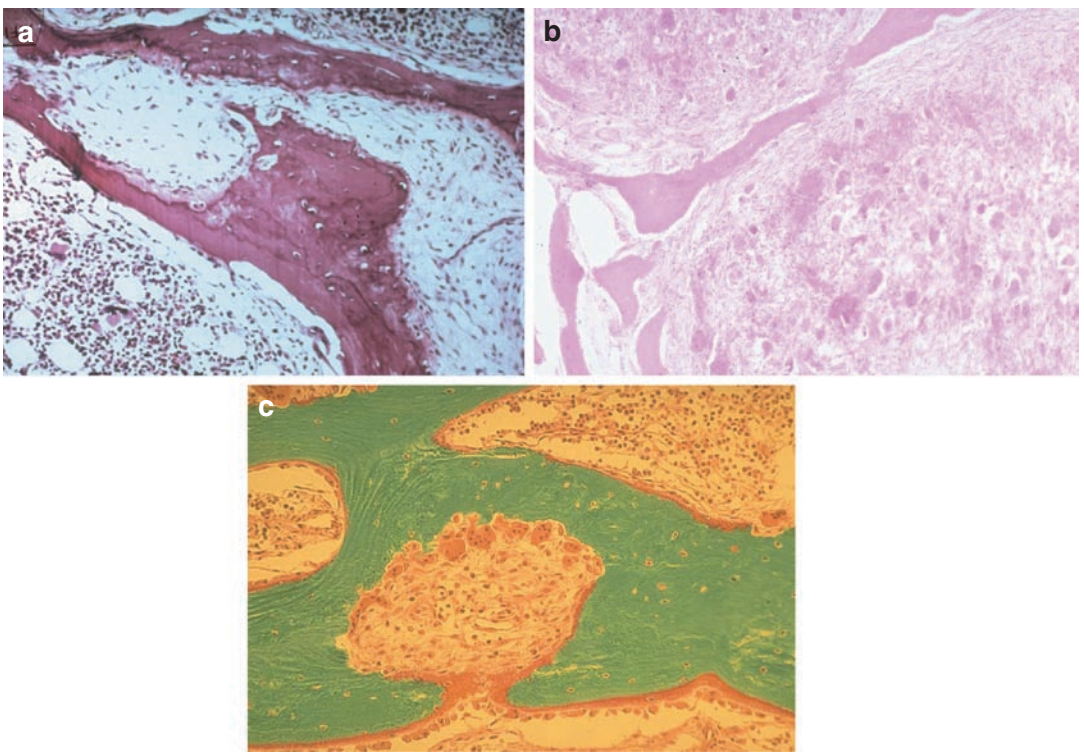

Fig. 5 **a** Osteitis disicans – where fibrous tissue insinuates between the bone trabeculae in hyperparathyroidism. Active osteoclastic activity is seen by the presence of numbers Howship's lacunae on the trabecular surface. **b** Brown tumor containing numerous giant cells and hemorrhage. **c** Undecalcified section of bone from a patient with severe hyperparathyroidism. There is prominent marrow fibrosis along the bone trabeculae, active bone formation is also seen, and there are numerous plump active osteoblasts seen. Activated osteoclasts can be seen in the center, within a Howship's lacuna

Paget Disease (Osteitis Deformans)

Paget disease of bone has been termed a "collage of metabolic madness" in a graphic description of the histological features. This is a localized disorder of bone, with increased bone remodeling, bone hypertrophy, and abnormal structure. Epidemiologically, it is seen in patients above the fourth decade, with a slight male predominance. It is common among the white population of England, France, Austria, Germany, Australia, New Zealand, and the United States (with an estimated incidence of 3%). It is rare in Scandinavia, China, Japan, and Africa.

The basis for the pathophysiology remains unknown. There is a strong genetic predisposition. Paget's disease occurs commonly in families and can be transmitted vertically between generations in an affected family. Several genetic loci have been linked to familial Paget's disease. These genes have included one family with a locus that on chromosome 13 which contains the RANKL gene. Another family has a mutation that was mapped to a gene which encodes an ubiquitin-binding protocol, sequestasome-1, associated with the NFκB signaling pathway (25).

Studies have suggested that Paget's disease may result from a chronic paramyxoviral infection based on ultrastructural studies. Nuclear and cytoplasmic inclusions similar to nucleocapsides from paramyxoviruses were present in osteoclasts from patients with Paget's disease. The role of a chronic paramyxoviral infection in this disorder remains controversial (26).

Clinically, the disease may be uni- (monoostotic) or multi- (polyostotic) focal and is characterized by asymmetry. The disease may be asymptomatic and discovered incidentally in a large proportion of patients but can present with pain. The axial and the proximal appendicular skeleton are frequently involved. Involvement of the ribs, fibulae, and bones of the hands and feet are less often seen. Pain or increased width of bone are the most common presenting complaints. Weight-bearing bones may be bowed or deformed. Hyperdynamic circulation that occurs in these patients may lead to high-output cardiac failure. Secondary malignancies have been described in long-standing Paget disease, the commonest of which is osteosarcoma. Bone fragility results from the accelerated bone turnover and disorganization of the matrix. Bone is fragile in spite of the increase in bone density and size.

Radiographically, three phases of the disease can be discerned. These are the lytic, mixed, and blastic phases. These correspond to the predominant bone activity occurring at the time. Eventually, the disease "burns out" in that particular site.

The laboratory investigations reflect this increased bone turnover, and are characterized by increased levels of bone markers including serum alkaline phosphatase, osteocalcin, and the propeptide of type I collagen.

Histology: Paget disease is a focal process. The initiating lesion is increased bone resorption and Pagetic osteoclasts are more numerous than normal and contain substantially more nuclei than normal osteoclasts. The hallmark of this disease is mosaic lamellar bone (woven bone), but this is not specific for Paget disease (Fig. 6a, b). This jigsaw-like pattern is produced by haphazard cement lines. In the lytic phase of the disease, there are waves of osteoclast activity and numerous resorptive pits. In the mixed phase, the osteoclasts are admixed with osteoblasts, which line the bone surfaces. The marrow adjacent to bone gets replaced by loose vascularized, connective tissue. The newly formed bone is initially woven but soon is remodeled into lamellar bone. As the mosaic pattern becomes prominent, cell activity ceases. The fibrovascular tissue is replaced by normal marrow in the burnt-out phase. Eventually, the bone is larger, with thick irregular trabeculae, porous cortices, and weakness due to the irregular orientation of the bone units.

Neoplastic degeneration of pagetic bone is rare but has a grave prognosis. The most common site of sarcomatous changes is the pelvis, and osteogenic sarcoma, fibrosarcoma, and chondrosarcomas have been described. Benign giant cell tumors may present as localized masses.

Biochemical features include increased markers of bone formation and resorption, and reflect the extent of the severity of the abnormal bone turnover. There is a 15–20% prevalence of secondary hyperparathyroidism in Paget disease. Potent bisphosphonates will normalize (or near normalize) the bone turnover markers and bring relief to those who are symptomatic. Treatment is usually recommended for symptomatic relief or to prevent future complications.

Paget, James (1814–1899) – Paget was born in Yarmouth in 1814. His father was a brewer, shipowner, chandler, and sometime mayor. He was the eighth of 16 siblings. At the age of 16, he was apprenticed to a local surgeon, and 4 years later he entered St. Bartholomew's Hospital, London. Paget obtained his qualification in 1836 and was appointed curator of the anatomy museum. He supplemented his income by translating books and papers. He went on to a surgical career and eventually became president of the Royal College of Surgeons. After narrowly escaping death from an accidental cut during a postmortem, he resigned from St. Bart's hospital and restricted himself to consultation practice. He was tactful and polite, methods guaranteeing a flourishing practice. He became surgeon to Queen Victoria, a baronet and a member of the leading medical societies. He was a gifted orator, his friends included Gladstone, Huxley, Darwin, and Florence Nightingale. He died in London in 1899. His name is linked to osteitis deformans – a condition he described in 1856. His patient's enlargement of the head to a point where it would no longer fit his Yeomanry helmet impressed Paget. This patient developed a simian

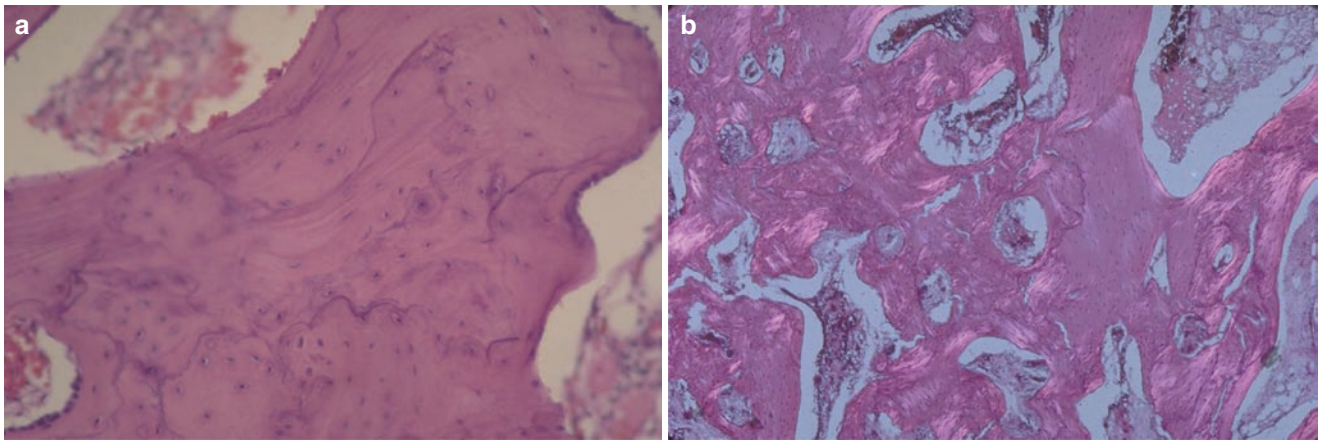

Fig. 6 **a** Mosaic bone seen in Paget's disease. **b** Semipolarized light utilized to highlight the haphazard nature of bone in Paget's disease

stance, bowing of the legs, retinal hemorrhage, and deafness; at autopsy, his bone was soft enough to cut with a razor. He linked these to an infective etiology, a view which is now resurfacing. His name is also linked to familial hyperphosphatasia (Juvenile Paget disease), mammary carcinoma (Paget disease of skin), bone necrosis, and traumatic thrombosis of the axillary vein.

Skeletal Diseases Arising from a Metabolic Defect

Amyloidosis of Bone (Amyloid Tumor)

Amyloidosis is a heterogeneous group of diseases, linked by the deposition of fibrillar, β-pleated proteins. These proteins are chemically different, by site and condition, but share properties based on their β-pleated nature such as congophilia (reaction with the Congo red dye). The diseases associated with amyloid are diverse and can be acquired or hereditary, neoplastic, infectious, degenerative, or associated with ageing. Amyloid deposits can be derived from more than 25 different types of proteins and the current classification of amyloid is based on the amyloid fibril protein type (27).

Deposition in bone is no different from the kind of amyloidosis found in other parts of the body, as far as the surgical pathologist is concerned. Large deposits may present as masses and mimic bone tumors, both radiologically and clinically. A panel of antibodies can aid in amyloid typing, particularly important in distinguishing between hereditary amyloidosis and low-grade monoclonal gammopathy. Biochemical typing can be performed on formalin-fixed, paraffin-embedded specimens.

Therapy is directed toward the systemic condition and radical and aggressive treatments have been used (28). The approach is dependent on the molecular type of amyloid protein and may involve chemotherapy, transplantation, and use of small molecules for specific therapy.

Osteopetrosis (Albers-Schonberg Marble Bone Disease)

This term refers to a group of heterogeneous diseases characterized by diffuse osteosclerosis. The term refers to the diffuse, symmetric, stone-like, skeletal sclerosis. There are several types described that include the traditional types I and II, an intermediate form, a type associated with renal tubular acidosis and cerebral calcification (due to carbonic hydrase II deficiency), osteopetrosis associated with a neuronal storage disease, and a new syndrome of osteopetrosis, lymphedema, anhydrotic ectodermal dysplasia, and immunodeficiency. Drug-induced osteopetrosis has also been described. The histopathological marker in all of these syndromes is the failure of osteoclast-mediated bone resorption, resulting in persistence of the primary spongiosa.

The autosomal recessive infantile (malignant) type I and the autosomal dominant (benign) type II are the classic examples of osteopetrosis. Clinically, the patients with the infantile form have a high postnatal mortality. In this form, malformation of the mastoid and paranasal sinuses is often an early symptom. Cranial foramina do not widen and palsies of the optic, ocular motor, and facial nerves can occur. Dentition is delayed and although bones can appear dense on radiograph, they are actually fragile and prone to fracture. Overall, patients present with short stature, frontal bossing, and adenoid appearance, nystagmus, hepatosplenomegaly (due to extramedullary hematopoesis), and genu valgum. Untreated children usually do not survive

the first decade of life. The skeleton may be uniformly dense, but alternating sclerotic and lucent bands are noted in the iliac wings. There may also be an Erlenmeyer-flask deformity at the junctions of the metaphysis and diaphysis. These children have anemia, frequent infections, and bleeding due to insufficient bone marrow space. Cranial nerve deficits, fractures, and hydrocephalus may also occur (20). Serum acid phosphatase levels may be increased and presence of the brain isoenzyme of creatine kinase in serum is a biochemical marker (29). The infantile form of osteopetrosis is often found to have an inactivating mutation of the a3 subunit of the vacuolar H^+ pump (30).

In adult osteopetrosis, radiographic abnormalities, fractures, or vision or hearing deficits may be presenting symptoms. Facial palsy and osteomyelitis of the mandible are additional clinical problems. This type is due to inactivating mutation of the chloride-7-channel gene necessary for acidification of the resorptive site and dissolution of mineral. Collagen and mineral are normal, but the continued accretion of mineral leads to abnormal crystallization and decreased biomechanical strength.

Histology: There is an increased mass of bone with thick cortices and thick trabeculae. The primary spongiosa (which consists of ossifying cartilage, and should be resorbed under normal circumstances by osteoclasts) persists. This causes the characteristic changes of islands or bars of calcified cartilage within mature bone. The medullary cavity contains little or no hematopoietic elements since there is overgrowth and accumulation of the primary spongiosa. Marrow fibrosis may be prominent. The bone is mainly woven, and lacks remodeling. The numbers of osteoclasts may be normal, increased, or decreased. Microscopically, these osteoclasts are unremarkable, although in the infantile form, electron microscope findings may show an absence of a ruffled border and clear zone. The adult form (type II) may be distinguished from the childhood form of the disease by increased resorptive surface with numerous and multinucleated osteoclasts and decreased resorption at the cell level (31). Both types represent decreased bone turnover due to decreased bone resorption.

Bone marrow transplant has improved patients with the infantile form of the disease, but early intervention is necessary due to the crowding of the bone marrow space by sclerotic bone. Some success has been reported with a calcium-deficient diet. Administration of recombinant human interferon γ-1b has provided clinical, laboratory, and histopathological benefit.

Albers-Schonberg, Heinrich E (1865–1921) – Albers-Schonberg was born in Hamburg in 1865. He attended the University of Tubingen and qualified in medicine from Leipzig. After a few years in several other cities, he settled in Hamburg to practice as a radiologist. He founded a radiology journal and authored an atlas on normal and abnormal radiologic anatomy. The text saw 33 editions. He also authored a text on radiographic techniques, which saw several translations and editions. In 1905, he became head of the department of radiology at the Hamburg hospital. He moved to St. George's hospital in Hamburg as head to start a new department. He received a Red Cross medal for his contributions during the First World War. Later, he unfortunately developed radiation-induced tumors on his hands, thorax, and shoulder. Eventually, he lost use of his arms, and was in severe discomfort. He died at the age of 56, in 1921 leaving his body to autopsy. In 1904, he published radiographs of a rare bone disease in a 26 years old with skeletal sclerosis and multiple fractures. In 1921, Schulze popularized his finding eponymically, and used the name Marmorknochen (marble bone). In 1926, Karshner introduced the term osteopetrosis.

Pycnodysostosis

The rare autosomal recessive bone disorder is due to a deficient activity of cathepsin K, a key enzyme for degradation of bone collagen. Affected individuals are diagnosed during childhood with short stature, dysmorphic features of skull, narrow thorax, short hands and fingers and increased lumbar lordosis. Radiographically, bone is sclerotic, and the anterior fontanel and other cranial sutures are usually open. Recurrent fracture may occur of the lower limbs. Histologically, bone contains thick cortices and trabeculae. Collagen is mildly disorganized with inclusion of mineralized cartilage within calcified bone. There is no sign of active osteoclasts, and bone turnover is low (20).

Osteogenesis Imperfecta or Brittle Bone Disease

Osteogenesis imperfecta (OI) is characterized by increased bone fragility with recurrent fractures. The phenotype of the disease ranges from being fatal in the perinatal period to mild forms diagnosed late in adulthood. Abnormalities in collagen are due to mutations in two of the type AI collagen genes, COLIA1 and COLIA2. Over 200 mutations have been reported, making this a heterogeneous disorder, represented by decreased bone formation. Bone turnover is high in children and low in adults (20).

Two main types of type I collagen mutations have been reported. The first "null allele" mutation affects the pro-α1(I) or pro-α2(I) alleles that impair transcription and mRNA

stability, with the production of low amounts of secreted heterodimer. The second mechanism results in structurally abnormal pro-α1(I) chains. Most mutations occur de novo. Sillence has classified this group into four types (I-IV) based on clinical presentation and outcome. Types I and II are the more commonly encountered.

Type I O I is the mildest form and presents with short stature, thin bone cortices, bowing, biconcave flattening of the vertebrae, small facial bones, hyperextensible joints, susceptibility to infection, abnormal placement and late eruption, thin skin, and sclerae leading to blue sclerae, otosclerosis, and an increased bleeding tendency due to capillary fragility. Early mortality may occur mainly from bronchopneumonia. Beyond infancy the outlook is good. Increased amounts of fractures are seen especially until skeletal maturity. Otosclerosis and subsequent deafness cause problems in older patients. A subset may have dentogenesis imperfecta (hypoplasia of dentin and pulp, translucency of teeth).

Type II OI is the most severe form and is characterized by short limbs, broad long bones, flattened vertebrae, hypotonia, variable hydrocephalus, and hydrops. Scleras are blue-gray. The majority of patients die in the perinatal period.

Type III OI is known as the progressive deforming type and presents with shortness, bowing, and multiple fractures. Normal sclerae and scoliosis occur in those that pass puberty. There may be metaphyseal flaring. These patients are prone to nonunions and have extreme growth deficiency. Dentinogenesis imperfecta and hearing loss are common.

Type IV OI is moderately severe with variable scleral hue. All have short stature and respond to growth hormone.

Types V–VII OI have been proposed and are based on bone histology. Phenotypically, they would be included in the Sillence classification type IV and do not have defects in type I collagen (32).

Surgical pathology: The amount of osseous tissue is decreased. There may be fibromembranous tissue with foci of bone, especially in the severe forms of OI (Fig. 7). This kind of finding is more common in the skull (33). In the long bones, the cortices are thin, except at a fracture site. The medullary cavity is likewise made up of very sparse trabeculae. The periosteum is normally present and the inner (cambium) layer may be more prominent than normal. The osteoblasts lining the bone trabeculae tend to be less plump, and more spindled than normal. Osteoclasts are quite sparse. The growth plates are normal and ossification is not delayed, but the ossification centers may be smaller than normal. The chondrocytes and cartilage matrix are also within normal limits of microscopy (33). The teeth are abnormal; the mesodermal component is more severely affected and may be deficient. The ectodermal component is usually normal.

Diagnosis of the collagen biochemistry can be made from cultured fibroblasts in some but not all of the mutations. Mutation detection by direct sequencing is more sensitive but does not provide functional information.

Early rehabilitation is recommended to maximize physical potential of patients with OI patients. Orthopedic care is important with emphasis on correction of deformity for ambulation. Coordinated care programs are essential for those with hearing loss, visual loss, growth deficiency, and dental issues. Bisphosphonates have been used with both benefits and limitations. The effect on trabecular bone supports improved strength but the effect on cortical bone has been more equivocal due to increased stiffness which can reduce bone quality.

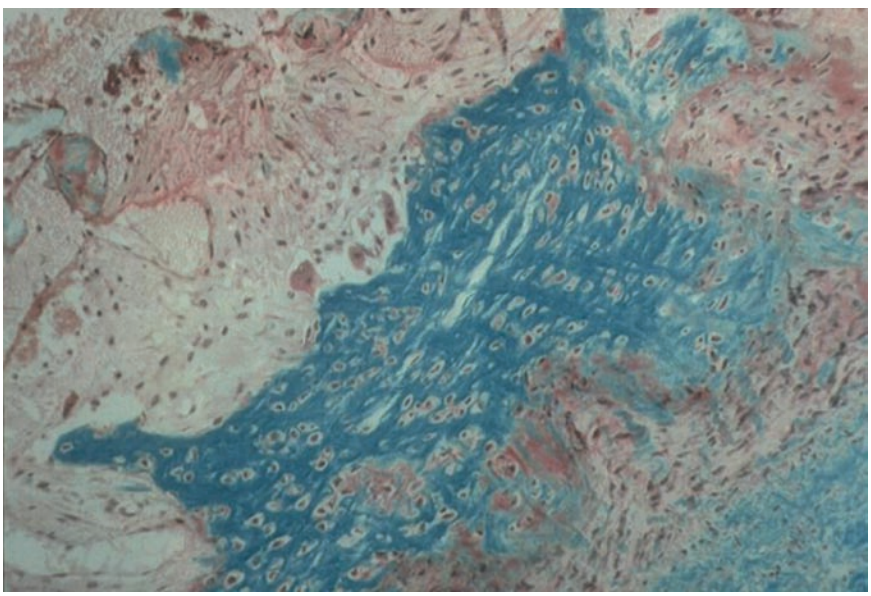

Fig. 7 Bone biopsy from a child with osteogenesis imperfecta, stained with Goldner Masson trichrome stain. The hallmark of the disease is the osteocytes present in enlarged lacunae. The lack of lamellar structure is evident from the disorganization of the osteocyte alignment

Mucopolysaccharidosis or Lysosomal Storage Diseases

Lysosomal storage diseases are a heterogeneous group of inborn errors of metabolism caused by decreased activity, processing, or synthesis of lysosomal enzymes that degrade glycosaminoglycans. Each disorder is represented by a wide variety of manifestations and severity that are the result of accumulation of complex carbohydrates in most cells (34). These disorders are inherited as autosomal recessive diseases except for three disorders which are inherited as X-linked-recessive or X-linked dominant syndromes (35). Classification is confusing as older terminology was based on clinical sign and symptoms and biochemical basis, while newer classification is based on genetic findings. Since cartilage has the largest proportion of glycosaminoglycans, it tends to be severely affected. Multidisciplinary care is required for these patients, and enzyme replacement therapy or stem cell transplant may improve the outcome.

Histology: Most of the disorders show similar changes in the cartilage. Resting cartilage consists of uniformly stained matrix. It contains chondrocytes which are larger than normal. These cells can be stained positively for glycosaminoglycans. Scattered through the resting cartilage, there are large areas of loose, somewhat foamy connective tissues. These can be stained with the Alcian blue stain. In many areas, these show a regular transition into cartilage. In type I and type IV glycosaminoglycanosis (Hurler and Morquio syndromes), these show a focal disruption of the growth plate. In type I (Hurler) disease, the trabeculae are coarse, wide, and fuse horizontally. They contain a loose connective tissue between the calcified connective tissue (36).

Gaucher Disease

This is a group of conditions that result from different allelic mutations in the structural gene for the enzyme β-glucosidase. This gene is located on chromosome 1q21. The enzyme cleaves glucose from ceremide. In Gaucher disease, glycosylceramide accumulates in the phagocytic cells and in some forms in the cells of the central nervous system. There are three clinical types, the commonest is type I, which has the dominant involvement in the skeletal system and the spleen. This type is associated with the mutation at nucleotide 1226 of the cDNA of the gene. Type II (acute neuronopathic) is a form dominated by progressive central nervous system involvement, along with hepatosplenomegaly. Death occurs at an early age. Type III is a hereditary disorder with a pattern in-between these two, but usually involves the central nervous system.

Type I is the form most commonly of concern to the orthopedic surgeon and the musculoskeletal pathologist. In these cases, skeletal disease is a cause of considerable morbidity. Skeletal manifestations include the Erlenmeyer-flask deformity of the femur, osteonecrosis of the femoral head, bone infarcts, and pathologic fractures.

MRI examination is a sensitive method of diagnosing the skeletal involvement by Gaucher's disease. Laboratory diagnosis is usually made with the estimation of b-glucosidase activity of leukocytes. Levels of certain enzymes such as serum acid phosphatase and angiotensin-converting enzyme are ancillary tests. The common mutations at nucleotides 84, 1226, and 1448 can now be detected using the polymerase chain reaction.

Histology: Distended phagocytic cells (Gaucher cells) are seen throughout the body, especially in the spleen, liver, bone marrow, lymph nodes, tonsils, thymus, and mucosa-associated lymphoid tissues. Macrophages may be engorged with lipid giving a classic "crumpled silk" appearance. The PAS stain highlights the cells. Within the bone, the cells are present maximally in the marrow space, and may be present as "deposits." These are important in that they may cause bone erosion or fracture.

Management is symptomatic and includes correction of hematologic disorder (correction of thrombocytopenia and anemia), partial splenectomy, and the orthopedic management of Gaucher's crises as well as infections. Long-term disability from joint damage due to osteonecrosis may require arthroplasties. Systemic treatment includes the administration of enzyme replacement, substrate reduction therapy, and bone marrow or stem cell transplants have been used with some success.

Phillipe Charles Ernest Gaucher (1854–1918): Gaucher was a French dermatologist, born in Nievre, France. His father was an architect. He spent his childhood with an uncle who was a general practitioner. Gaucher underwent military training in army hospitals, and on return to civil life failed his university entrance examinations. He thus entered medical school as a second alternative. He rose to chair the dermatology department at the University of Paris. He developed the fixation that appendicitis, polio, and several congenital deformities were the result of venereal disease. He died from pneumonia at the age of 73. His description of a man with an enlarged spleen filled with abnormal cells became known after his name – but he ascribed the condition to a neoplasm.

References

1. Murray TM, Rao LG, Divieti P, Bringhurst FR. Parathyroid hormone secretion and action: Evidence for discrete receptors for the carboxyl-terminal region and related biological actions of carboxyl-terminal ligands. Endo Rev 26:78–113, 2005.
2. Bringhurst FR, Stern AM, Yotts, M, Mizrahi N, Segre GV, Potts JT, Jr. Peripheral metabolism of PTH: Fate of biologically active amino terminus in vivo. Am J Physiol 255:E886–E893, 1988.
3. Friedman PA, Goodman, WG. PTH(1–84/PTH(7–84): A balance of power. Am J Physiol Renal Physiol 290:F975–F084, 2006.
4. Liu S, Gupta A, Quarles LD. Emerging role of fibroblast growth factor 23 and in a bone-kidney axis regulating phosphate homeostasis and extracellular matrix mineralization. Curr Opin Nephrol Hypertens 16:329–335, 2007.
5. Imel EA, Econs MJ. Fibrous dysplasia, phosphate wasting and fibroblast growth factor 23. Pediatr Endocrinol Rev 4:434–439, 2007.
6. Consensus development conference: diagnosis, prophylaxis, and treatment of osteoporosis. Am J Med 94:646–650, 1993
7. Raisz L. Pathogenesis of osteoporosis: Concepts, conflicts and prospects. J Clin Invest 115:3318–3325, 2005.
8. Rosen CJ. Postmenopausal osteoporosis. N Engl J Med 353:595–603, 2005.
9. WHO Technical Report Series 921 Prevention and management of osteoporosis, 2000.
10. Giguere Y, Rousseau F. The genetics of osteoporosis: Complexities and difficulties. Clin Genet 57:161–169, 2000.
11. Morrison NA, Qi JC, Tokita A, Kelly PJ, Crofts L, Nguyen TV, Sambrook PN, Eisman JA. Prediction of bone density from vitamin D receptor alleles. Nature 367:284–216, 1994.
12. Uitterlinden AG, et-al. Relation of alleles of the collagen type I-alpha-1 gene to bone density and the risk of osteoporotic fractures in postmenopausal women. N Engl J Med 338:1016–1021, 1998.
13. Mankin HJ. Rickets, osteomalacia and renal osteodystrophy Part I. J Bone Joint Surg 56-A (1):101–128, 1974.
14. Holick MF. High prevalence of vitamin D inadequacy and implications for health. Mayo Clin Proc 81:353–373, 2006.
15. Bielesz B. Emerging role of a phosphatonin in mineral homeostasis and its derangements. Eur J Clin Invest 36 (Suppl 2):34–42, 2006.
16. Hochberg Z. Vitamin-D-dependent rickets type 2. Hormone Res 58:297–302, 2002.
17. Collins MT. Spectrum and national history of fibrous dysplasia of bone. J Bone Miner Res 21 (Suppl 2):P99–P104, 2006.
18. Riminucci M, Gehron Robey P, Biano P. The pathology of fibrous dysplasia and the McCune-Albright syndrome. Pediatr Endocrinol Rev 4:401–411, 2007.
19. Fitzpatrick LA. Pathophysiology of bone loss in patients receiving anticonvulsant therapy. Epilepsy Behav 5:S3–S15, 2004.
20. Chavassieux P, Seeman E, Delmas PD. Insights into material and structural basis of bone fragility from diseases associated with fractures: How determinants of the biochemical properties of bone are compromised by disease. Endo Rev 28:151–164, 2007.
21. Gal-Moscovici A, Sprague SM. Bone health in chronic kidney disease-mineral and bone disease. Adv Chronic Kidney Dis 14(1):27–36, 2007.
22. Hruska KA, Saab G, Mathew S, Lund R. Renal osteodystrophy, phosphate homeostasis, and vascular calcification. Semin Dial 20(4):309–15, 2007.
23. Silverberg SJ, Bilezikian JP. The diagnosis and management of asymptomatic primary hyperparathyroidism. Nat Clin Pract Endocrinol Metab 2:494–503, 2005.
24. Lowe H, McMahon DJ, Rubin MR, Bilezikian JP, Silverberg SJ. Normocalcemic primary hyperparathyroidism: Further characterization of a new clinical phenotype. J Clin Endocrinol Metab 92:3001–3005, 2007.
25. Layfield R, Shaw B. Ubiquitin-mediated signaling and Paget's disease of bone. BMC Biochem 8 (Suppl 1):1–7, 2007.
26. Siris ES, Roodman GD. Paget's Disease of Bone. In: Primer on the Metabolic Bone Disease and Disorders of Mineral Metabolism. 6th edition. Edited by M.J. Favus. American Society for Bone and Mineral Research, Washington, D.C. pp. 320–330, 2006.
27. Picken MM. New insights into systemic amyloidosis: The importance of diagnosis of specific type. Curr. Opin. Nephrol. Hypertens. 16:196–203, 2007.
28. Comenzo RL. Current and emerging views and treatment of systemic light-chain (AL) amyloidosis. Contrib Nephrol 153:195–210, 2007.
29. Whyte MP, Chines A, Silva DP, Landt Y, Ladenson JH. Creatine kinase brain isoenzyme (BB-CK) presence in serum distinguishes osteopetrosis among the sclerosing bone disorders. J Bone Miner Res 11:1438–1443, 1996.
30. Tolar J, Teitelbaum SL, Orchard PJ. Osteopetrosis. N Engl J Med 351:2839–2849, 2004.
31. Brockstedt H, Bollerslev J, Melsen F, Mosekilde L. Cortical bone remodeling in autosomal dominant osteopetrosis: A study of two different phenotypes. Bone 18:67–72, 1996.
32. Marini J. Osteoporosis Imperfecta. In: Primer on the Metabolic Bone Disease and Disorders of Mineral Metabolism. 6th edition edited by M.J. Favus. American Society for Bone and Mineral Research, Washington, D.C. pp. 418–421, 2006.
33. Jaffe HL. Osteogenesis Imperfecta. In: Metabolic, Degenerative and Inflammatory Diseases of Bones and Joints. Lea Febige, Philadelphia, 1972.
34. Muenzer J. The mucopolysaccharidoses: A heterogeneous group of disorders with variable pediatric presentations. J Pediatr 144:S27–S34, 2004.
35. Vellodi A. Lysosomal storage disorders. Br J Haematol 128:413–431, 2004.
36. Rimoin DL, Silberberg R, Hollister DW. Chondro-osseous pathology in the chondrodystrophies. Clin Orthop 114:137–152, 1976.

Chapter 15
Inherited and Dysplastic Conditions of the Skeleton

Vivian Arguello-Guerra, Eileen M. Shore, Fredrick S. Kaplan, and Jasvir S. Khurana

Abstract The diagnosis of skeletal dysplasias is changing rapidly as molecular biology contributes to our understanding of their basis. Although the total number of dysplastic and inherited skeletal conditions is enormous, a few important ones with interest to the skeletal pathologist, radiologist, and surgeon are selected here for discussion.

Keywords Spondyloepiphyseal dysplasia • Thanatropic • Metaphyseal chondrodysplasia • Metatropic • Dysostoses • Fibrodysplasia ossificans progressiva • Melorheostosis • Dyschondroplasia • Osteopoikilosis • Engelman's disease • Pycnodysostosis • Heterotopic ossification • Fibro matosis • Bone morphogenetic protein-4 (BMP-4) • Activin receptor IA/activin-like kinase-2 (ACVR1;ALK2) gene • Progressive osseous heteroplasia • Albright hereditary osteodystrophy • Adenylate cyclase • Achondrogenesis • Fibrochondrogenesis • Thanotropic dwarfism • Metatropic dwarfism • Kniest syndrome • Achondroplasia • Hypochon droplasia • Diastrophic dwarfism (dysplasia) • Chondrodysplasia punctata • Metaphyseal chondrodysplasia • Multiple epiphyseal dysplasia • Parenti-Fraccaro • Langer-Saldino • COL2A1 gene • Platyspondyly • Talipes equinovarus • Rhizomelic • Schmid type • McKusick type • Jansen type • Shwachman type • Osteogenesis imperfecta • Osteo petrosis • Campanacci's disease

This is a group of diverse, conditions, which have in common only our limited understanding of their basis. An increasing number of these are syndromic inherited conditions which are becoming amenable to modern genetic investigations. Skeletal dysplasia is a time-honored term, which should not be confused with the preneoplastic connotation given to the word dysplasia in some organ systems. These are not preneoplastic but instead are characterized by a altered or disorganized formation of skeletal components.

Surgical pathologists are not commonly called upon to help in the diagnosis of many of these conditions although some chondrodystrophies have certain characteristic morphology. The diagnosis is currently clinical and radiological although molecular diagnosis has the potential to help demystify many of these problems. A major problem is the changing terminology of the diseases. This has resulted in older literature describing several entities which would be considered differently today. It is thus important to keep this in mind when reviewing older texts for the histological features of some of these conditions.

Terminology: The terminology and the classification are usually based on the clinicoradiological picture. Before the 1960s, most disproportionate dwarfs were termed either achondroplastics (those with short limbs) or having Morquio-Brailford's disease (those with short trunks). In the late-1960s, the radiological classification became popular. The part of the skeleton affected maximally was used to designate the condition. Thus, for example, spondyloepiphyseal dysplasia (SED), metaphyseal chondrodysplasia, diastrophic (twisted) dwarf, thanatropic (death seeking) dwarf, or metatropic (changing) dwarf became common.

In 1970, the Paris conference attempted to classify the inherited conditions into those having abnormalities of cartilage and/or bone development and growth (osteochondrodysplasias); and those having malformations of bone (dysostoses).

Selected Inherited Conditions

- Fibrodysplasia (Myositis) Ossificans Progressiva
- Progressive Osseous Heteroplasia
- Chondrodystrophy and Ostoechondrodysplasia
- Melorheostosis
- Dyschondroplasia
- Osteopoikilosis
- Engelman's disease
- Pycnodysostosis
- Osteogenesis imperfecta
- Osteopetrosis
- Hypophosphatasia
- Congenital deficiencies

Fibrodysplasia Ossificans Progressiva (Myositis Ossificans Progressiva)

Fibrodysplasia ossificans progressiva (FOP) is a rare autosomal dominant disorder of connective tissue characterized by congenital malformations of the great toes, progressive heterotopic endochondral ossification (1, 2), and disease

J.S. Khurana (ed.), *Bone Pathology*, DOI 10.1007/978-1-59745-347-9_15,

progression in well-defined temporal and spatial patterns (3, 4). Impending heterotopic ossification is signaled by the appearance of large painful swellings of highly vascular fibroproliferative tissue (1, 5) involving tendons, ligaments, and skeletal muscle. Soft-tissue lesions appear spontaneously, or may be precipitated by minor trauma including intramuscular childhood immunizations, blunt muscle trauma from falls, or influenza-like illnesses (6–8).

The lesions in FOP mature through an endochondral pathway to form normal lamellar bone. Progressive episodes of heterotopic ossification lead typically to ankylosis of all major joints of the axial and appendicular skeleton (1, 2). Although the rate and the severity of disease progression is variable (9), most patients are confined to a wheelchair by their early twenties and require lifelong assistance in performing activities of daily living. Death often results in adulthood from complications of severe restrictive disease of the chest wall. At present, there is no effective prevention or treatment.

Clinical observations of FOP skeletal malformations and progressive heterotopic ossification suggested that the primary molecular pathology involves the BMP signaling pathway (2). FOP cells exhibit dysregulation of BMP4 expression as well as expression of some BMP antagonists (16). In addition, defects in internalization of at least some BMP receptors, coupled with increased activation of BMP downstream signaling has been observed (17, 18).

Although inheritance of FOP is rare due to low reproductive fitness, when it occurs, genetic transmission is autosomal dominant (19, 45, 46). Recently, genetic linkage analysis using five small families was used to map the mutant FOP gene to chromosome 2. Subsequently, a recurrent heterozygous single nucleotide substitution (c.617G > A) was identified in the activin receptor IA/activin-like kinase-2 (*ACVR1; ALK2*) gene of all sporadic and familial cases of classic FOP (19, 46). This mutation causes an amino acid substitution in codon 206 (R206H) in the glycine-serine (GS) activation domain, a highly conserved and functionally important domain of the receptor.

Both genetic and environmental factors affect the phenotype of FOP. A study of three pairs of monozygotic twins with FOP found that within each pair, congenital toe malformations were identical. However, postnatal heterotopic ossification varied greatly depending on life history and environmental exposure. This study indicated that genetic determinants strongly influence disease phenotype during prenatal development and that environmental factors strongly influence postnatal progression of heterotopic ossification (20).

Surgical Pathology: Biopsy specimens of developing FOP lesions are exceedingly rare, since surgical trauma associated with the resection of heterotopic bone often leads to exacerbation of ossification (1, 2, 10, 11). Histological examination of early FOP lesions reveals an intense perivascular lymphocytic infiltration followed by lymphocytic invasion into muscle and robust development of fibroproliferative tissue with extensive neovascularity (12, 13). A role for hematopoietic cells in heterotopic osteogenesis had been suggested (14).

Immunohistochemical evaluation of lymphocyte markers revealed a predominance of perivascular B-lymphocytes and a mixed population of B-lymphocytes and T-lymphocytes invading the skeletal muscle (10, 12). Whether the early lymphocytic infiltrate is a causative event, a reaction to it, or both, cannot be determined from the observations in a small sample of patients. The intermediate stage lesions are histologically indistinguishable from aggressive juvenile fibromatosis, a condition that does not progress to form bone (5). However, two recent studies document the expression of bone morphogenetic protein-4 (BMP-4) in cultured fibroproliferative cells and in intact tissue specimens from preosseous lesions in patients with FOP (5, 15). Tissue from FOP lesions at a later stage shows characteristic features of endochondral ossification including chondrocyte hypertrophy, calcification of cartilage, and formation of woven bone with marrow elements.

Progressive Osseous Heteroplasia

Progressive osseous heteroplasia (POH) is a developmental disorder of mesenchymal differentiation characterized by dermal ossification during infancy and by progressive heterotopic ossification of cutaneous, subcutaneous, and deep connective tissue during childhood (21). The disorder can be distinguished from FOP by the presence of cutaneous ossification, by the absence of congenital skeletal malformations, by the asymmetric mosaic distribution of lesions, by the absence of predictable regional patterns of heterotopic ossification, and by the predominance of intramembranous rather than endochondral ossification (21, 49).

The cutaneous and subcutaneous ossification in POH is similar to that observed in some cases of Albright hereditary osteodystrophy (AHO) and pseudohypoparathyroidism type IA (22) but is significantly more severe and involves deep skeletal muscles. In addition, patients with POH do not exhibit the hormone resistance that is commonly associated with pseudohypoparathyroidism IA. However, like AHO and PHP1a, heterozygous-inactivating mutations in the *GNAS* gene, which encodes the alpha subunit of the G stimulatory protein of adenylate cyclase, have recently been associated with POH (23). POH can be inherited through an autosomal dominant pattern of inheritance; however, POH pedigrees have uniformly shown inheritance from fathers (23). This observation is consistent with *GNAS* as an imprinted genetic locus.

The results of laboratory analysis in POH are usually normal, although elevated levels of serum alkaline phosphatase have been observed during phases of progressive heterotopic osteogenesis. Typically, serum levels of calcium, inorganic phosphate, parathyroid hormone, and vitamin D metabolites are normal, although transient abnormalities have rarely been noted

(28). Elevated serum levels of lactate dehydrogenase (LDH) and creatine phosphokinase (CPK) have been observed, and may reflect bone deposition in skin and skeletal muscle (26, 28).

*Surgical Pathology:*Heterotopic ossification in POH occurs predominantly through an intramembranous pathway (21, 24–27). Initial bone formation in patients is typically within dermal fat. Progressive bone formation in skeletal muscle is diffuse and web-like. Heterotopic ossification through an endochondral pathway has also been described following unsuccessful attempts at surgical ablation of deep heterotopic ossification (21, 47).

Chondrodystrophy and Osteochondrodysplasias

- Achondrogenesis
- Fibrochondrogenesis
- Thanotropic dwarfism
- Metatropic dwarfism
- Kniest syndrome
- Achondroplasia
- Hypochondroplasia
- Diastrophic dwarfism (dysplasia)
- Chondrodysplasia punctata
- Metaphyseal chondrodysplasia
- Spondyloepiphyseal dysplasia
- Multiple epiphyseal dysplasia (Dysplasia epiphysealis multiplex)

This is a partial list of conditions sometimes included in this large category (29). The surgical pathology of these conditions is unclear, mainly because of the lack of a "gold standard" for the diagnosis. In general, clinical, radiological, and genetic characteristics have been used, leading to considerable heterogeny in the pathologic findings (30). Studies on the pathology and molecular biology of these conditions may help clarify some of the entities.

Achondrogenesis

This group of conditions, initially cataloged as autosomal recessive, was identified to be an autosomal dominant trait caused by a de novo mutation. It is marked by severe cartilage dysplasia and severe defects, having most deaths in utero or early neonatal period. Most manifest with short trunks, prominent abdomens, and micromelia. Bones are poorly ossified, crenated, or stellate.

Two forms of achondrogenesis have been identified and classified as follows:

- Type I-Parenti-Fraccaro type. Characterized by thin ribs with multiple fractures. Gene identification has been linked to the DTDST gene on chromosome 5q32–33, linked to the SLC26A2 sulfate transporter.
- Type II-Langer-Saldino type. Described to have longer gestational period with fewer stillbirths. These babies are characterized by virtual absence of ossification in the vertebral column, sacrum, and pubic bones, with craniofacial features. Genetic linkage analysis mapped the sequence to COL2A1 gene located on chromosome 12q13.1, with a defect in biosynthesis of type II collagen or in chondrocyte differentiation.

Surgical Pathology: The cartilage may be hypervascular and hypercellular. The chondrocytes contain round cytoplasmic inclusions and are present in large lacunae.

Fibrochondrogenesis

This is a rare autosomal recessive disease of severe dysplasia, with rhizomelic shortening, broad irregular metaphyses, and skeletal deformities, resulting in neonatal death.

Surgical Pathology: Changes in the growth plate with fibroblastic dysplasia of chondrocytes and distinctive fibrosis, characterized by an interwoven fibrous septa.

Thanatophoric Dwarfism

Thanatophoric dwarfism or dysplasia (TD) is an entity of autosomal dominant inheritance characterized by skeletal dysplasia and early death. The patient has short extremities narrow short ribs, flattened vertebrae with absence of caudad spinal canal narrowing (H-shaped on X-ray), small square scapulae and pelvis, and associated brain, kidney, and other parenchymal organ abnormalities. The child is usually hypotonic has severe growth retardation, a large cranium (cloverleaf skull), and femurs shaped like telephone receivers.

TD has been subtyped according to the presence or absence of curved femurs:

- Type I: short and curved femurs, with or without cloverleaf skulls
- Type II: straight, long femurs with severe cloverleaf skulls

Because of phenotypic similarities, it is important to rule out other skeletal dysplasias. It is suggested that the gene mutation is located in chromosome 1 or 10 (31). Studies have proved that TD and achondroplasia have the same mutant gene and locus map (4p16.3), affecting fibroblast growth factor receptor-3 (FGFR3) gene; reason for which such phenotypic similarities are shared.

Surgical Pathology: There is a lack of ossification in the secondary centers at the knee as well as disorganized chondrocytes and bony trabeculae in central epiphyseal–metaphyseal regions.

Metatropic Dwarfism

This is a condition, in which newborns exhibit short extremities with relatively long trunks. This disproportion gets corrected in early infancy, but by late infancy a kyphosis develops which renders the trunk short. Infant mortality is high but survival into adulthood is not uncommon. The hands and feet are short and hyperextensible. There is a peculiar tail-like fold over the sacrum. There is marked platyspondyly (flattened vertebrae). The long bones are short with irregular expanded metaphyses. There are three forms of the disease a nonlethal form, autosomal recessive form, a non-lethal dominant, and a lethal autosomal recessive form that results in in utero death or shortly after birth.

Surgical Pathology: The epiphyses are widened and club-shaped. Bronchial and tracheal cartilages are hyperplastic but normal in appearance. The ossified portions of the vertebrae are very narrow (about one-sixth the thickness of the unossified vertebral cartilage). Resting cartilage appears normal. The growth plate is irregular with uneven vascular penetration and foci of unossified cartilage extending into the metaphysis. The bony trabeculae are irregular.

Kniest Syndrome

This is an unusual form of short-trunk dwarfism. The syndrome has also been called metatropic dwarfism type II, owing to certain radiological similarities. There is disproportionate dwarfism, kyphosis, flat facies, cleft palate, hearing loss, myopia, limited joint motion, lumbar lordosis, bowing of long bones, enlargement of joints, and flexion contractures. Radiological findings show vertebral, epiphyseal, and metaphyseal abnormalities. There is dumbbell-shaped femurs with pelvic hypoplasia in the newborn period. The ends of the bones show irregular epiphyses. The spine is platyspondylic with a cloud-like radiodensity. The intervertebral disk spaces are narrow. The odontoid may be enlarged. The hands show a squaring of the metacarpophalangeal joints. Fragmented accessory centers of the proximal phalanges are seen. These patients are characteristically incapable of making a tight fist. Their palms tend to have a bluish coloration.

It is important to clinically distinguish among other chondrodysplasias. Kniest syndrome falls within the type II collagen mutating diseases located in the COL2A1 gene (gene map locus 12q13.11-q13.2) (32, 33). There are approximately ten different collagen mutations, involving a deletion within exons 12–24, resulting in a shorter monomer. The type II procollagen lacks the C-propeptide, a component required for adequate fibril formation.

Surgical Pathology: Biopsied cartilage is soft and has a distinct histological morphology. Resting cartilage contains large chondrocytes, which lie in a very loosely woven myxoid matrix containing numerous empty spaces (Swiss cheese cartilage). With the Alcian blue-Periodic acid-Schiff (PAS) stain, the resting cartilage is seen to be markedly abnormal. There are patchy areas of light and dark staining matrix filled with cells of various sizes. There are also many empty spaces within the matrix. At the growth plate, the abnormality varies with the age of the patient. In the young, the growth plate is extremely hypercellular. Chondrocytes are large, with little intervening matrix. Vascular penetration is patchy. With increasing age, there is an attempt at column formation. There is, however, always some irregularity of the hypertrophic zone. Weis et al. (33) stated that exon 24 mutation showed the following electron microscopy findings. Thin collagen fibrils surrounding chondrocytes with thick fibrils at its periphery. The chondrocytes had inclusion bodies of rough endoplasmic reticulum, which appears swollen with a granular material that appears to be abnormal type II collagen.

Achondroplasia

This is a relatively common form of chondrodysplasia, transmitted as an autosomal dominant trait; however many are de novo mutations. It is characterized by a short stature, megalocephaly, foramen magnum narrowing, low nasal bridge, small cuboidal-shaped vertebral bodies, thoracolumbar kyphosis, small iliac wings, shortening of the tubular bones, and late overgrowth of the fibula. Achondroplasia is a disease that does not hinder the patient to grow and allows life with minor disabilities. At birth, they may manifest mild hypotonia and motor milestones may be delayed; however, their intelligence is generally not affected. In some cases there is increased intracranial venous pressure, leading to hydrocephalus due to sinus stenosis at the foramen. Speech delay has been described when associated with middle ear disease, which may progress to hearing loss. Early deaths are associated with neurologic deficits associated with hydrocephalus and respiratory compromise.

Genetic linkage has been mapped to a mutation in the FGFR3, located at 4p16.3. There is a substitution to a glycine at position 380 of the mature protein (G380R mutation) (34, 35). This results in a gain-of-function of the FGFR3 receptor, leading to chondrocyte proliferation of the growth plate. Transmission is with complete penetrance. Sporadic cases have been associated with increasing paternal age but less severe phenotype.

Surgical Pathology: There is regular arrangement of the rows and columns of cells, including its major constituents, in the growth plate cartilage, but the rate of enchondral ossification may be reduced (30). Horton et al. investigated that these patients showed mutation dosage effects on the to

thickness of the growth plate (shorter than normal); with a shorter growth plate in homozygous versus heterozygous patients. Periosteal bone may extend past the growth plate onto the perichondrium of the resting cartilage. This is the basis for the cupping seen in the growth ends on X-rays. Membranous ossification is also abnormal, resulting in the unusual shapes of bones, especially those of the cranium.

Hypochondroplasia

This is a condition similar to, but milder than achondroplasia with the same transmission and genetic classification. It is differentiated from achondroplasia by the absence of craniofacial abnormalities, tibial bowing, and fibular extension. The mutation is within the FGFR3 gene (36).

Surgical Pathology: There is regular well-organized enchondral ossification, which may, however, be quantitatively reduced. Overgrowth of periosteal bone is not a feature of this condition and differentiates it from achondroplasia.

Diastrophic Dwarfism

This is characterized by scoliosis, short tubular bones (especially the first metacarpal; "hitchhiker thumb," broad metaphyses, hypertrophied articular cartilage with joint limitation, bilateral talipes equinovarus, and accelerated carpal ossification. There is 25% mortality in early infancy, but the survivors have normal intelligence and a reasonable outcome. Gene identification has been linked to the DTDST gene on chromosome 5q32-q33.1, linked to the SLC26A2 sulfate transporter.

Surgical Pathology: The resting cartilage is distinctly abnormal. Moreover, these abnormalities are generalized over the various parts of the body. There is nonuniform staining of the matrix and an irregular distribution of the cells, with focal acellularity. The chondrocytes appear larger than normal. They are surrounded by matrix which stains densely blue with the Alcian blue-PAS stain. These acellular foci are thought to progress with time to be replaced by fibrous tissue. Cystic areas may also occur, which later get replaced by fibro-osseous scar tissue. The growth plates also stain intensely with Alcian blue-PAS. They may be partly disrupted by scar tissue encroaching from resting cartilage.

Chondrodysplasia Punctata

This is a heterogeneous group of conditions, with punctate mineralization of the epiphyses. In the Conradi-Hunermann type, there is asymmetric limb shortness, flat facies, punctate mineralization in the epiphyses, scoliosis, follicular atrophoderma with large skin pores. There is often failure to thrive and frequent infections in infancy. Chances of survival improve remarkably after the first few months. In the rhizomelic type, there is shortening of the humeri and femora, coronal clefting of the vertebra, microcephaly, and icthyosiform skin dysplasia. The patients usually die by the age of 2 years. The rhizomelic form has been associated with a peroxisomal disorder. In these patients, there are three biochemical defects. These are in the plasmalogen biosynthesis, phytanic acid oxidation, and 3-oxoacyl-coenzyme A thiolase pathways. The other forms of chondrodysplasia punctata are far less frequent. There is a X-linked dominant as well as an X-linked recessive form. The latter is associated with a steroid sulfatase activity defect.

Surgical Pathology: In the Conradi-Hunermann variant, there is focal disruption of the growth plate by fibrous tissue. Spicules of bone arise from this and extend into the metaphysis. Enchondral ossification is altered into a semicircular array around this fibrous tissue. This may account for the asymmetric nature of growth retardation (30). Other descriptions of this disorder have mentioned a "disordered" growth plate without commenting on the presence or nature of the fibrous tissue. The resting cartilage in this variant contains areas of mucoid degeneration and cyst formation with calcification and fibrous tissue invasion. The calcification corresponds to the punctate, stippled densities seen on X-ray.

In the rhizomelic variant, the enchondral growth is markedly disordered. There is decreased vascular invasion and diminished mineralization of the matrix. Tongues of cartilage extend into the metaphysis. The metaphysis is also abnormal, in that it contains a diminished number of trabeculae. The resting cartilage has foci of mucoid degeneration, vascularization, and ossification.

Metaphyseal Chondrodysplasias (dysostoses)

This is a heterogeneous group of conditions, associated with short-limbed dwarfism and irregularity of the metaphyses. The epiphyses and the spine are normal. Several eponymic forms are described. In the Schmid type, there is mild shortening, evident in the second year. Improvement occurs with time. In the McKusick type, there is a greater degree of shortening. Additionally, the hair is fine and sparse and there may be loose jointedness. In the Jansen type, there is severe shortening, micrognathia, flexion deformities especially at the hip and knee, a small thorax, and possible hypercalcemia. In the Shwachman type, there is associated pancreatic insufficiency, diarrhea, and periodic neutropenia.

Surgical Pathology: The histology from the several different types of metaphyseal chondrodysplasias seems to be similar. There is a disorganized growth plate, extension of

the cartilage into the metaphysis, and uneven staining of the resting cartilage.

The growth plate shows the proliferating chondrocytes to be arranged in balls of cells, surrounded by densely staining cartilage. In between these, there is a fibrillar cartilage. Vascular invasion of the cell clusters is irregular. This results in wide spicules of calcified cartilage and bone. In nonvascularized areas, tongues of cartilage extend into the metaphysis. These correspond to the radiolucent linear metaphyseal streaks found in these disorders.

Resting cartilage stains unevenly with the Alcian blue-PAS, as well as the trichrome stain and has a fibrillar appearance. The chondrocytes are larger and clustered. There may be bi- or multicelled lacunae.

Spondyloepiphyseal Dysplasias

This is a group of disorders representing several distinct clinical syndromes but having certain radiological features in common. The prototype traditionally considered is the SED-congenita, a type II and XI collagenopathy, with autosomal dominant inheritance; referred to as a milder form of achondrogenesis type 2 and hypochondrogenesis. As the name indicates, it is dysplasia of the spine and epiphysis. This is characterized by a short trunk with progressive lordosis and kyphoscoliosis, malar, and odontoid hypoplasia leading to cleft palate, lag in mineralization of epiphyses, weakness, hearing loss, and myopia. Other skeletal structural signs may include platyspondyly (flattened vertebrae) and coax vara (inward rotation of upper leg bones, resulting in hip joint deformity)

Genetic linkage analysis mapped the sequence to COL2A1 gene located on chromosome 12q13.1, with a defect in biosynthesis of type II collagen.

Surgical Pathology: Sufficient numbers of cases of SED have not been examined. In SED-congenita, there is a regular enchondral ossification at the costochondral junction, with some blunting and irregularity of spicule formation. Abnormal ossification is observed at the iliac crest, with hypocellularity of the matrix, irregular growth plate, and irregular broad short spicules of calcified cartilage and bone. There may be microcystic changes. Chondrocytes of the resting cartilage may be enlarged and vacuolated. PAS stain shows a nonpathognomonic intracytoplasmic inclusion in chondrocytes. It is noted to be a fine granular material located within dilated cisterns of rough endoplasmic reticulum on ultrastructural examination. Differential diagnoses include achondrogenesis, Kniest syndrome, pseudoachondroplastic dysplasia, and a type of short rib-polydactyly syndrome. Other forms of SED examined seem to be very heterogeneous. There may be hypocellularity and lack of spicule formation. The cartilage may, in some cases stain slightly heterogenously.

Multiple Epiphyseal Dysplasia (Dysplasia Epiphysealis Multiplex)

There are ten types or variants of this disease, with a range of mild (Ribbing) to severe (Fairbank) forms. Fairbank type was the first described; later came Ribbing, which was subdivided into pseudoachondroplastic and tarda form. All are autosomal dominant, except for type IV, which is autosomal recessive. The abundant amount of variants makes it hard to classify this entity to a specific genetic mutation and gene locus. Most are due to a gene mutation for cartilage oligometric matrix protein (COMP) (37). However, other genes involved are COL9A1, COL9A2, COL9A3, MATN3, and DTDST. The latter one is correlated to multiple epiphyseal dysplasia (MED) type IV.

The features of this disease are extremity-dependent short stature (resembles achondroplasia, but dwarfism is not present), without vertebral participation and brachydactyly. Clinical detection arises at the age when the child starts to walk. Several epiphyses of the body are affected. The lower limbs and hips have the more pronounced disease, with bowleg deformity (curved tibia with knock-knee). There is delay of ossification (irregular ossification centers on X-ray), and abnormalities of physeal growth. There may be overgrowth of cartilage, causing subluxations of joints. The femoral heads may develop a mushroom shape, coxa vara, and osteoarthrosis.

Histology: The clinical features are reflected in the histology. There are physeal, matrix, and chondrocyte abnormalities to varying degrees. MED type IV shows chondrocytes with inclusions that have granular or filamentous material. These inclusions are thought to be of lysosomal origin.

Involvement of wrists and hands are used to distinguish between some types. Ribbing type often has normal wrists and hands, while Fairbank type shows short and stubby hands (38). On the contrary, MED type IV is characterized by a lack of irregularities in the wrists and hands and a presence of a flat femoral head.

Melorheostosis

This is a condition where dense bone forms, around the diaphyseal cortex of a tubular bone. Forming irregular and asymmetrical linear longitudinal thickenings that protrude intramedullary and externally, below the periosteum. These may extend distally throughout the length of the bone and into joints, as well as, overlying soft tissue. Shortening of extremities with premature closing of epiphysis may be seen when the condition is severe and has an early onset. The bone formed in this situation resembles the dripping of a candle on roentgenograms.

The etiology is unknown. No mendelian basis has been established. The age of onset is usually in childhood. The

patients present with chronic pain, limitation of motion, and sometimes palpable thickening of bone. The skin may be erythematous, shiny with induration of skin (scleroderma), and subcutaneous tissue. Underlying muscle may atrophy. Progression may lead to malformations, decreased motion or ankylosis, sensory disturbance, and edema due to nerve and vascular compression. Changes are no longer seen once the bone reaches its mature state, without regression of lesions.

The condition may be associated with other dysplasias, such as osteopoikilosis, or with soft-tissue contractures or ossification or vascular anomalies. Studies have suggested a somatic mutation in the same locus (LEMD3) that causes osteopoikolisis.

Surgical Pathology: Histologically, there is compact, overcrowded lamellar bone, interlaced with woven bone.

Osteopoikilosis

This is a condition characterized by the development of symmetrical but unequal distribution of multiple dense spots in many bones. The spots are particularly numerous in the epiphyses and metaphyses of the long tubular bones. But most commonly found in bones of the carpus and tarsus. The pelvis may also be involved.

It is an autosomal dominant disease with mutation of LEMD3 gene in chromosome 12q14. Osteopoikilosis may occur as an isolated process or in association with other skin (Buschke-Ollendorff syndrome, BOS) or bone (melorheostosis) abnormalities.

Surgical Pathology: Is identical to multiple enostoses and is essentially that of normal appearing lamellar bone..

Engelman's Disease (Progressive Diaphyseal Hyperostosis)

This is an autosomal dominant disease with increased bone turnover and symmetrical fusiform enlargement with sclerosis of the shafts of major long bones. Flat bones (trunk, skull, and face) have multiple areas of thickening. One or several bones may be involved.

This disease is first noticed in early childhood. The bones that are most commonly affected are usually the femur and tibia, manifesting with waddling or shuffling gait, pain, and muscular weaknesses. Hyperostosis may lead to nerve compression (facial paralysis, hearing abnormalities, and vision loss) and frontal bossing. Gene mapping has linked this disease to mutations in the TGFB1 gene in locus 19q13.1.

Caffey's disease must be differentiated (infantile cortical hyperostosis). This latter condition is an autosomal dominant disease, linked to chromosome 17q21–22, seen within the first year of life, and accompanied by fever. The increase in density is unilateral, and mandibular involvement is common in Caffey's disease.

Histology: The cortices are thickened. The medullary canal is encroached. The bone is of the normal lamellar type.

Pycnodysostosis

Pycnodysostosis is a rare autososmal recessive disorder characterized by inadequate resorption, causing short stature and increased tendency to fractures. The disease was first described by Maroteaux and Lamy in 1962. The word derives from the Greek, meaning, "pyknos = dense," "dysostosis = abnormal bone formation."

The features are prominent skull deformity with open sutures, short fingers due to deterioration of distal phalanges (acroosteolysis), osteosclerosis, and dense and abnormal brittle bones. Other abnormalities involve the head and face, teeth (hypodontia), collar bones (scoliosis), skin, and nails.

Genetic linkage analysis has mapped this disease to chromosome region 1q21. Subsequent studies identified the gene as Cathepsin K gene (CTSK). Cathepsin K is a cysteine protease, responsible for osteoclastic function and bone resorption. Parental consanguinity has been reported in many cases since the 1950s. An association with defective growth hormone secretion and low insulin-like growth factor-1 (IGF1) has been reported (39); without evidence of abnormal hypothalamic-pituitary-gonadal axis. These patients have normal sexual development and thyroid and adrenal function.

There is no cure for this disease. However, measures must be taken (e.g., alternate exercise like swimming) to avoid any activity that may lead to fractures. Physiologic replacement with growth hormone has proven to improve linear growth of children, while increasing IGF1 concentration.

Surgical Pathology: Histological examination shows normal amount and morphology of osteoclasts with increased area of demineralized bone surrounding the osteoclasts. Ultrastructural examination reveals large, abnormal cytoplasmic vacuoles with bone collagen fibrils. This suggests that osteoclasts cannot remodel bone efficiently because of inadequate resorption.

Osteogenesis Imperfecta

This is a disease with a wide spectrum of clinical findings characterized by skeletal fragility and multiple fractures due to a defect in adequate collagen type I production. Hence, any part of the body depending on collagen production will also be affected. The severity of presentation varies from stillborn to neonatal death with survival of up to fifth and sixth decades with minimal affection. All types of fractures

may occur often with minimal or no evidence of trauma. Other signs include variation in coloration of sclerae (most commonly blue) in about two-thirds of patients, fragile, discolored, and translucent teeth (dentinogenesis imperfecta), laxity of ankles and wrists, neurologic problems associated with herniation and compression of brain stem, cardiac valve insufficiency, among others.

Osteogenesis imperfecta has been classically classified into four types: type I (Tarda), type II (Congenita), type III and type IV (Tarda) with predominant autosomal dominant inheritance (except type III). However, variations have been found within type IV, extending the classification to a total of seven types (types V and VI being autosomal dominant) (Table 1) (41–45).

The mutations in the collagen protein may lead to decreased amounts of normal collagen (type I) or production of structurally abnormal collagen (types II, III, and IV). The genetic basis for types V and VI is still to be determined. However, studies involving collagen type I protein have been found to be normal.

Table 1 Clinical and genetic features of osteogenesis imperfecta.

Type	Clinical features	Gene	Locus
I	Mild-to-moderate severity; dentinogenesis imperfecta may be present; blue sclerae	COL1A2[a]	17q21–22
		COL1A2	7q22.1
II	Severe; stillborn or neonatal death	COL1A2	17q21–22
		COL1A2	7q22.1
III	Severe; antenatal fractures, progressive deformity with growth impairment, dentinogenesis imperfecta, and occasional blue sclerae	COL1A2	17q21–22
		COL1A2	7q22.1
IV	Mild-to-moderate severity; growth impairment, blue sclerae in early childhood (white sclerae later)	COL1A2	17q21–22
		COL1A2	7q22.1
V	Moderate-to-severe; long bone and vertebral fragility, hyperplastic callus, limitation in range of pronation/supination of forearms	Not associated with collagen type I	
VI	Moderate-to-severe; white or faint blue sclerae, osteoid accumulation due to mineralization defect in the absence of mineral metabolism	Not associated with collagen type I	
VII	Moderate-to-severe; fractures at birth, blue sclerae, lower extremity deformity, coxa vara, rhizomelia, and osteopenia	(CRTAP2)	3p22–24.1

[a]Collagen 1 alpha-1 chain and Collagen 1, alpha-2 chain.
[b]Cartilage-associated protein.

Osteopetrosis

Increase in bone density results in osteopetrosis, due to inadequate bone resorption. Osseous homeostasis is maintained by osteoblastic (bone formation and osteoclast stimulation) and osteoclastic function. Osteoblasts are responsible for osteoclast differentiation by production of macrophage colony-stimulating factor (M-CSF), granulocyte macrophage colony-stimulating factor (GM-CSF), interleukin-1 (IL-1), interleukin-1 (IL-6) via the RANKL pathway. Any disturbance in this process leads to osteclast dysfunction and to increased bone density. The medullary cavity is filled with endochondral new bone formation, therefore leaving no room for hematopoietic structures, leading to the common serological and clinical presentation of hepatosplenomegaly (extramedullary hematopoiesis) and pancytopenia. Other laboratory findings include increased acid phosphatase, creatine kinase BB (type II), and levels of 1,25-dihydroxyvitamin D.

Radiological findings are described as "bone within a bone" with indistinguishable medullary cavity; instead, there are transverse radiolucent bands.

Bone resorption is a two-way process: acidification of the surface and digestion of bone via enzyme secretion. In the cytoplasm of osteoclasts, carbonic anhydrase II forms carbonic acid (H_2CO_3) from carbon dioxide (CO_2) and water; the H_2CO_3 is dissociated to bicarbonate (HCO_2^-) and a proton (H^+), which are released extracellularly decreasing the pH. Acidification is needed to initialize the degradation of the mineral component of bone, which is composed primarily of hydroxyapatite (40). For acid–base balance, a chloride channel (present in the membrane of the osteoclast) exchanges the excess bicarbonate produced in this process. The digestion of the organic component is done by released vesicles, through exocytosis, containing enzymes like cathepsin K and tartrate-resistant acid phosphatase (TRAP).

Multiple genetic studies in mice have revealed a number of linked genes and proteins. However, only a few have been confirmed in humans, mainly involving the pathways associated with acidification.

This disease is sub-classified as malignant (type I) and intermediate with autosomal recessive inheritance, and benign (type II) with autosomal dominant inheritance. The genes involved are the following (40):

- TCIRG1 – subunit of ATPase proton pump; locus 11q13
- CLCN7 – chloride channel; locus 16p13
- GL (OSTM1) – Grey lethal, osteopetrosis associated transmembrane protein; locus 6q21
- CAII – carbonic anhydrase II; locus 8q22
- LRP5 – low-density lipoprotein receptor-related protein 5; locus 11q13.4

The best treatment involves bone marrow transplantation. There is a 79% survival for 5 years for HLA-identical sibling donor. Better results are seen the earlier the transplant is done.

Surgical Pathology: There is persistence of the primary spongiosa characterized by interweaving bony trabeculae with persisting plates of hyaline cartilage with minimal medullary contents.

Hypophosphatasia

This disease has been described as a rickets-like disease (clinical and radiological similarities), characterized by increased fracture incidence, deformity, poor weight gain, and pain of extremities. There are four types (perinatal, infantile, childhood, and adult) with better life expectancy and decreased severity with age. These patients characteristically have low plasma concentration of alkaline phosphatase. Other common serology findings are hypercalcemia, hypercalciuria, and hyperphosphataemia.

Hypophosphatasia results from a mutation of the ALPL gene on chromosome 1 (locus 1p36.1-p34), which codes for the tissue-nonspecific alkaline phosphatase isoenzyme.

Congenital Deficiencies

There are a variety of focal deficiencies and supernumerary defects in the skeleton. These are of importance to the orthopedic surgeon, but the details of the genetic alteration are not yet available. It is thought that there may be a number of limb patterning genes that are responsible (see Chap. 5, section on developmental molecular biology of limb formation).

There are no characteristic histological features that may be utilized for prediction, diagnosis, or prognostication of these defects. Such defects include the proximal focal femoral deficiency, tibial hemimelia, fibular hemimelia, and so on. Certain conditions, which had been included earlier in this group such as nerve, oriented macrodactyly, or congenital pseudarthrosis of the tibia, have now been excluded on the basis of their known etiologies. For example, neurofibromatosis may be associated with either of these. Tibial pseudarthrosis could also be associated with a desmoid, Campanacci's disease, and so on. These conditions are discussed in the appropriate sections in the compendium.

The molecular defects causing many of these disorders are now known or under intense investigation. Using the on-line "Mendelian Inheritance in Man (OMIM)" through the **W**eb site from the National Center for Biotechnology Information from the NIH is a good source for update on these disorders (www.ncbi.nlm.nih.gov)

References

1. Kaplan FS, Tabas JA, Gannon FH, Finkel G, Hahn GV, Zasloff MA (1993) The histopathology of fibrodysplasia ossificans progressiva. An endochondral process. J Bone Joint Surg (Am) 75:220–230.
2. Kaplan FS, Glaser DL, Shore EM, Deirmengian GK, Gupta R, Delai P, Morhart R, Smith R, LeMerrer M, Rogers JG, Connor JM, Kitterman JA (2005a) The phenotype of fibrodysplasia ossificans progressiva. Clin Rev Bone Min Metab 3:183–188.
3. Cohen RB, Hahn GV, Tabas JA, Peeper J, Levitz CL, Sando A, Sando N, Zasloff M, Kaplan FS (1993) The natural history of heterotopic ossification in patients who have fibrodysplasia ossificans progressiva. A study of forty-four patients. J Bone Joint Surg (Am) 75:215–219.
4. Rocke DM, Zasloff M, Peeper J, Cohen RB, Kaplan FS (1994) Age- and joint-specific risk of initial heterotopic ossification in patients who have fibrodysplasia ossificans progressiva. Clin Orthop 301:243–248.
5. Gannon FH, Kaplan FS, Olmsted E, Finkel GC, Zasloff M, Shore E (1997) Bone morphogenetic protein (BMP) 2/4 in early fibromatous lesions of fibrodysplasia ossificans progressiva. Hum Pathol 28:339–343.
6. Lanchoney TF, Cohen RB, Rocke DM, Zasloff MA, Kaplan FS (1995) Permanent heterotopic ossification at the injection site after diphtheria-tetanus-pertussis immunizations in children who have fibrodysplasia ossificans progressiva. J Pediatr 126:762–764.
7. Glaser DL, Kaplan FS (2005) Treatment considerations for the management of fibrodysplasia ossificans progressiva. Clin Rev Bone Min Metab 3:243–250.
8. Scarlett RF, Rocke DM, Kantanie S, Patel JB, Shore EM, Kaplan FS (2004) Influenza-like viral illnesses and flare-ups of fibrodysplasia ossificans progressiva. Clin Orthop 423:275–279.
9. Janoff HB, Tabas JA, Shore EM, Muenke M, Dalinka MK, Schlesinger S, Zasloff MA, Kaplan FS (1995) Mild expression of fibrodysplasia ossificans progressiva: A report of 3 cases. J Rheumatol 22:976–978.
10. Kaplan FS, Shore EM, Gupta R, Billings PC, Glaser DL, Pignolo RJ, Graf D, Kamoun M (2005b) Immunological features of fibrodysplasia ossificans progressiva and the dysregulated BMP4 pathway. Clin Rev Bone Min Metab 3:189–193.
11. Kaplan FS, Shore EM, Zasloff MA (1996) Fibrodysplasia ossificans progressiva: searching for the skeleton key. Calcif Tissue Int 59:75–78.
12. Gannon FH, Valentine BA, Shore EM, Zasloff MA, Kaplan FS (1998) Acute lymphocytic infiltration in an extremely early lesion of fibrodysplasia ossificans progressiva. Clin Orthop 346:19–25.
13. Pignolo RJ, Suda RK, Kaplan FS (2005) The fibrodysplasia ossificans progressiva lesion. Clin Rev Bone Min Metab 3:195–200.
14. Buring K (1975) On the origin of cells in heterotopic bone formation. Clin Orthop 110:293–302.
15. Shafritz AB, Shore EM, Gannon FH, Zasloff MA, Taub R, Muenke M, Kaplan FS (1996) Overexpression of an osteogenic morphogen in fibrodysplasia ossificans progressiva. N Engl J Med 335:555–561.
16. Kaplan FS, Fiori J, LS DLP, Ahn J, Billings PC, Shore EM (2006) Dysregulation of the BMP-4 signaling pathway in fibrodysplasia ossificans progressiva. Ann NY Acad Sci 1068:54–65.
17. de la Pena LS, Billings PC, Fiori JL, Ahn J, Kaplan FS, Shore EM (2005) Fibrodysplasia ossificans progressiva (FOP), a disorder of ectopic osteogenesis, misregulates cell surface expression and trafficking of BMPRIA. J Bone Miner Res 20:1168–1176.
18. Fiori JL, Billings PC, Serrano de la Peña L, Kaplan FS, Shore EM (2006) Dysregulation of the BMP-p38 MAPK signaling pathway in cells from patients with fibrodysplasia ossificans progressiva (FOP). J Bone Miner Res 21:902–909.
19. Shore EM, Kaplan FS (2005) Fibrodysplasia ossificans progressiva and progressive osseous heteroplasia: two genetic disorders of heterotopic ossification. Clin Rev Bone Min Metab 3:257–260.

20. Hebela N, Shore EM, Kaplan FS (2005) Three pairs of monozygotic twins with fibrodysplasia ossificans progressiva. Clin Rev Bone Min Metab 3:205–208.
21. Kaplan FS, Craver R, MacEwen GD, Gannon FH, Finkel G, Hahn G, Tabas J, Gardner RJ, Zasloff MA (1994) Progressive osseous heteroplasia: a distinct developmental disorder of heterotopic ossification. Two new case reports and follow-up of three previously reported cases. J Bone Joint Surg (Am) 76:425–436.
22. Levine MA (1996) Pseudohypoparathyroidism. In: Bilezikian JP, Raisz LG, Rodan GA (eds) Principles of Bone Biology. Academic Press, New York, pp 853–876.
23. Shore EM, Ahn J, Jan de Beur S, Li M, Xu M, Gardner RJ, Zasloff MA, Whyte MP, Levine MA, Kaplan FS (2002) Paternally inherited inactivating mutations of the GNAS1 gene in progressive osseous heteroplasia. N Engl J Med 346:99–106.
24. Schmidt AH, Vincent KA, Aiona MD (1994) Hemimelic progressive osseous heteroplasia. A case report. J Bone Joint Surg (Am) 76:907–912.
25. Rosenfeld SR, Kaplan FS (1995) Progressive osseous heteroplasia in male patients. Two new case reports. Clin Orthop 317:243–245.
26. Miller ES, Esterly NB, Fairley JA (1996) Progressive osseous heteroplasia. Arch Dermatol 132:787–791.
27. Urtizberea JA, Testart H, Cartault F, Boccon-Gibod L, Le Merrer M, Kaplan FS (1998) Progressive osseous heteroplasia. Report of a family. J Bone Joint Surg (Br) 80:768–771.
28. Rodriguez-Jurado R, Gonzalez-Crussi F, Poznanski AK (1995) Progressive osseous heteroplasia, uncommon cause of soft tissue ossification: a case report and review of the literature. Pediatr Pathol Lab Med 15:813–827.
29. Jones KL– (1988) Osteochondroplasias In Smith's Recognizable Patterns of Human Malformation. W.B Saunders Company, Philadelphia. 4th Edition, pp 278–352.
30. Rimoin DL, Silberberg R, Hollister DW (1976) Chondro-osseous pathology in the chondrodystrophies. Clin Orthop 114:137–152.
31. Hersh, JH, Yen FF, Peiper SC, Barch MJ, Yacoub OA, Voss DH, Roberts JL (1995) De novo 1;10 balanced translocation in an infant with thanatophoric dysplasia: a clue to the locus of the candidate gene. J Med Genet 32:293–295.
32. Mortier GR, Wilkin DJ, Wilcox, et al. (1995) A radiographic, morphologic, biochemical and molecular analysis of a case of achondrogenesis type II resulting from substitution for a glycine residue (Gly691-to-Arg) in the type II collagen trimer. Hum Molec Genet 4:285–288.
33. Weis MA, Wilkin D, Kim Het al., (Feb 20 1998) Structurally abnormal Type II collagen in a severe form of Kniest Dysplasia caused by an exon 24 skipping mutation. J Biol Chem 273(8):4761–8.
34. Rousseau F, Bonaventure J, Legeai-Mallet L, Pelet A, Rozet J-M, Maroteaux P, Le Merrer M, Munnich A (1994) Mutations in the gene encoding fibroblast growth factor receptor-3 in achondroplasia. Nature 371:252–254.
35. Shiang R, Thompson LM, Zhu Y-Z, Church DM, Fielder TJ, Bocian M, Winokur ST, Wasmuth J J (1994) Mutations in the transmembrane domain of FGFR3 cause the most common genetic form of dwarfism, achondroplasia. Cell 78:335–342.
36. Heuertz S, Le Merrer M, Zabel B, et al. (2006) Novel FGFR3 mutations creating cysteine residues in the extracellular domain of the receptor cause achondroplasia or severe forms of hypochondroplasia. Europ J Hum Genet 14 1240–1247. Note: Erratum: Europ. J. Hum. Genet. 14: 1321 only, 2006.
37. Hecht JT, Nelson LD, Crowder E, et al. (1995) Mutations in exon 17B of cartilage oligomeric matrix protein (COMP) cause pseudoachondroplasia. Nature Genet 10:325–329.
38. Stanescu R, Stanescu V, Muriel M-P, Maroteaux P, (1993) Multiple epiphyseal dysplasia, Fairbank type: morphologic and biochemical study of cartilage. Am J Med Genet 45:501–507.
39. Soliman AT, Rajab A, AlSalmi I, Darwish A, Asfour M (1996) Defective growth hormone secretion in children with pycnodysostosis and improved linear growth after growth hormone treatment. Arch Dis Child 75:242–244
40. Tolar J, Teitelbaum S, Orchard P, Osteopetrosis (2004) N Engl J Med 351:2839–49.
41. Glorieux FH, Rauch F, Plotkin H, et al. (Sep 2000) Type V osteogenesis imperfecta: a new form of brittle bone disease. Bone Miner Res 15(9):1650–8.
42. Glorieux FH, Ward LM, Rauch F, et al. (Jan 2002) Osteogenesis imperfecta type VI: a form of brittle bone disease with a mineralization defect. J Bone Miner Res 17(1):3–8.
43. Ward LM, Rauch F, Travers R, et al. (Jul 2002) Osteogenesis imperfecta type VII: an autosomal recessive form of brittle bone disease. Bone 31(1):12–8.
44. Paterson C (1997) Osteogenesis imperfecta and other heritable disorders of bone. Balliere's Clin Endo and Metabolism 11(1):195–209.
45. Shore EM, Feldman GJ, Xu M, Kaplan FS (2005) The genetics of fibrodysplasia ossificans progressiva. Clin Rev Bone Min Metab 3:201–204.
46. Shore EM, Xu M, Feldman GJ, Fenstermacher DA, Consortium FOPIR, Brown MA, Kaplan FS (2006) A recurrent mutation in the BMP type I receptor ACVR1 causes inherited and sporadic fibrodysplasia ossificans progressiva. Nat Genet 38:525–527.
47. Glaser DL, Rocke DM, Kaplan FS (1998) Catastrophic falls in patients who have fibrodysplasia ossificans progressiva. Clin Orthop 346:110–116.
48. Kaplan, F.S. and E.M. Shore (2000). Progressive osseous heteroplasia: a perspective. J. Bone Min. Res. 15, 2084–2094.
49. Horton WA, Rimoin DL - Kniest dysplasia. A histochemical study of the grown plate. Pediatr. Res. 1979 November 13(11):1266–70
50. Weis MA. Wilkin DJ. Kim HJ. Wilcox WR. Lachman RS. Rimoin DL. Cohn DH. Eyre DR. Structurally abnormal type II collagen in a severe form of Kniest dysplasia caused by an exon 24 skipping mutation. [Journal Article. Research Support, U.S. Gov't, P.H.S.] Journal of Biological Chemistry. 273(8):4761-8, 1998 Feb 20. UI: 946

Chapter 16
Musculoskeletal Neoplasms: An Introduction

Harish S. Hosalkar, Jennifer Goebel, Jasvir S. Khurana, and Richard D. Lackman

Abstract Our understanding of the biology of tumors, approach to their diagnosis, and management strategies has dramatically evolved over the decades and basic science research as well as clinical outcomes studies continue to add to the existing knowledge. This chapter outlines the current approach to musculoskeletal tumors including their diagnosis, staging, biopsy, and management strategies as well as zone-specific approach to limb tumors including discussion on pathologic fractures.

Keywords Musculoskeletal tumors • Sarcomas • Staging • Biopsy • Approach • Surgery • Limb salvage • Pathologic fractures

Introduction

Vast improvements in the diagnosis, staging, medical management, and thus outcome of patients with sarcoma have spurred interest in limb salvage procedures. Thus, limb-sparing surgery (LSS) for primary bone and soft tissue malignancies is an acceptable option of surgical treatment in most cases today. However, performing reconstructions that preserve function after musculoskeletal tumor resection can be extremely challenging. Early recognition, appropriate evaluation, and management are essential to optimize survival and function. Diagnostic and treatment strategies for patients with musculoskeletal sarcoma are continually evolving. Thirty years ago, it was estimated that around 70% of patients with bone and soft tissue sarcomas would die whereas now around 70% live. Additionally, 30 years ago most of the patients had amputations, whereas now most have LSS (1).

Staging and Biopsy

It is usual to undertake the staging of the tumor in patients with suspected sarcoma before any biopsy since is important to learn as much about a lesion and its differential diagnosis before the biopsy so as to avoid wrong decisions that may alter the eventual outcome of management. Staging includes a total body scan, a CT scan of the chest, and an magnetic resonance imaging (MRI) of the primary lesion. MRI should include the involved portion of the extremity, including the joint above and below.

Musculoskeletal Tumor Society (MSTS) adopted the Enneking Surgical Staging System for bone sarcomas. The Enneking's staging system is based on the GTM classification: grade (G), tumor site (T), and metastases (M) (Table 1) (2).

Biopsy

Not all lesions may require a biopsy as many benign and inactive lesions may be diagnosed via imaging studies alone. The ideal biopsy is one that provides sufficient tissue needed for a histologic diagnosis without affecting subsequent management (3). It is important that the treating surgeon should be very familiar with the guidelines concerning type of biopsy performed and biopsy techniques.

Current biopsy options include both open and needle techniques (3). The advantage of percutaneous needle biopsies is that they cause little soft tissue contamination and require little or no anesthesia. They are frequently performed under CT scan or ultrasound guidance (Fig. 1). The main disadvantage of this technique is that it provides only a small amount of tissue for the pathologist to review and as such, it can frequently be nondiagnostic. More importantly, it must be remembered that primary bone tumors are notoriously heterogeneous, thereby creating a great potential for sampling error with closed techniques. Needle biopsies are optimal for initial sampling of lesions in anatomically inaccessible areas such as the spine or pelvis. In most locations, however, the carefully performed open biopsy is still the gold standard. The *rules for open biopsy* are as follows (3):

- Use as small an incision as possible placed over the lesion.
- The incision should be longitudinal on the extremities and well planned on the trunk to be part of a resection incision.
- While it is fine to use an extremity tourniquet above an extremity tumor, use of an Esmarch bandage over a tumor may rupture the tumor into the surrounding tissues and should be avoided.

J.S. Khurana (ed.), *Bone Pathology*, DOI 10.1007/978-1-59745-347-9_16,

Table 1 Surgical staging system for bone sarcomas (2).

Stage	Grade	Site
I	Low	A Intracompartmental B Extracompartmental
II	High	A Intracompartmental B Extracompartmental
III	Any grade with regional or distant metastasis	Any

[a] By *compartment* is meant an anatomic structure or space bounded by natural barriers to tumor extension. A whole bone, a joint, and a functional muscle group are each considered compartments in this staging system.

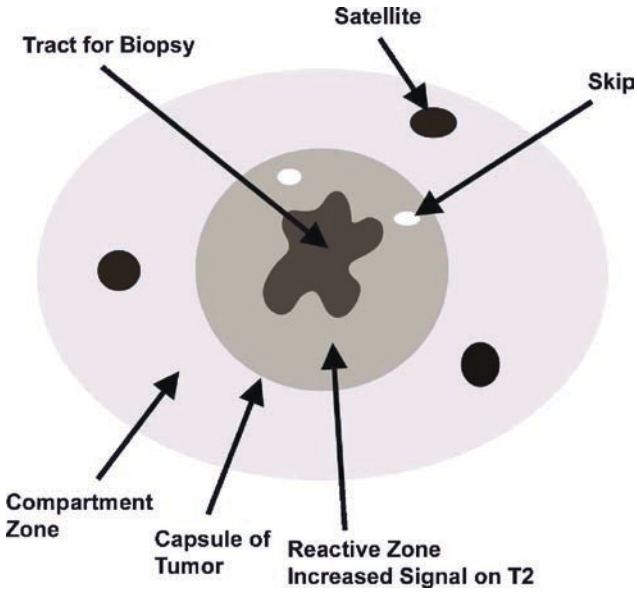

Fig. 1 Diagrammatic illustration of tumor zones and tract for biopsy

- Use a small incision into the capsule of a tumor so that it can be closed easily. This is especially important when there is no tourniquet used as bleeding may be appreciable and difficult to control with a large incision.
- Try not to directly contaminate a neurovascular bundle when possible.
- Try not to violate major flap structures (e.g., Gluteus maximus) or functionally important structures (e.g., Rectus femoris).
- Utilize minimal retraction to limit soft tissue contamination.
- It is better to go through a single muscle belly if it is large enough than to go between two structures that contaminates both.
- Obtain good hemostasis by a meticulous multilayered watertight closure. This is an essential step. Many large tumors put the closure under pressure and the vascularity commonly seen predisposes to subsequent drainage. Any wound complication will increase the risk of secondary infection and may delay subsequent chemotherapy or radiation.
- Drains should not be used routinely. If needed they should be thin and brought out 1–2 cm beyond one end of the incision so that the drain track can be easily resected with the biopsy track.
- Obtain a frozen section when feasible to insure that diagnostic material has been obtained. Tumors can often be very necrotic and it may rake a large volume of tissue before diagnostic material is encountered. It is certainly easier to get more tissue while the patient is still prepped and draped in the operating room than several days later if the biopsy was insufficient.
- Whenever feasible during a diagnostic open biopsy, the operating surgeon should accompany the specimen to the pathology department with imaging studies in hand. In this way, the pathologist can review the specimen and frozen section slides with the surgeon in light of the imaging studies and clinical history.

Surgery for Local Tumor Control: Margins

A precise definition and classification of surgical margins is useful for evaluation, planning, and treatment in the care of musculoskeletal tumors. There are four different kinds of surgical oncologic wound margins: *intralesional, marginal, wide, and radical* (4).

Intralesional margins involve removing a portion of the lesion. With an intralesional margin, portions of the lesion, the reactive zone containing satellites, and skip lesions in the surrounding normal tissues are all left behind. Marginal margins involve removing the lesion en bloc with an extracapsular plane of dissection through the reactive zone of inflammation. Satellite and skip lesions are left behind in the normal surrounding tissue. Wide margins require en bloc excision of the lesion in a plane of dissection that is peripheral to the reactive zone through normal tissue. The distance away from the tumor required to achieve this margin depends on factors including which tissue is involved, what the boundary tissue is (e.g.,cartilage, bone and thick fascia are more resistant to spread as compared to loose areoalar tissue or fat), type of tumor, response to chemotherapy, and so on. With better imaging and the development and progress of limb salvage surgery, decreasing distances from the tumor while still maintaining a cuff of normal tissue around the tumor are being accepted. Finally, radical margins involve removing the entire compartment(s) in which the tumor has extended.

Surgical Procedures

The margin of the wound is the criteria by which the procedures are defined (4). Margin may be obtained by either a local or an ablative procedure. Since there are four possible

Table 2 Surgical margins

Surgical margins	Limb salvage	Amputation	Histology
Intralesional	Curettage, piecemeal resection within lesion	Through tumor	Tumor at margin
Marginal	Marginal excision through reactive tissue	Along reactive tissue	Reactive tissue +/– satellites
Wide	Wide excision through normal surrounding tissue	Through normal tissue in compartment	Normal tissue +/– skip lesions
Radical	Radical resection with entire compartment	Extracompartmental amputation or disarticulation	Normal tissue

margins, there are eight distinct oncologic surgical procedures possible (Table 2) (4).

Surgical Intentions

There are four different reasons for doing oncosurgical procedures: diagnostic, palliative, adjunctive, and definitive (4).

A diagnostic procedure may be performed open or closed by incision or needle. It could also be accomplished by marginal excision. A palliative procedure is undertaken to relieve pain or to improve function temporarily. There is no intent to cure and recurrence is accepted as inevitable. The benefits of palliative procedure are accepted as temporary and are generally performed when no alternate surgical methods are desirable. An adjunctive procedure is done with the intent of local control and is usually followed by a definitive modality of treatment. Finally, a definitive procedure is done with the intent of local control by the procedure itself. Nonsurgical modalities may be used as adjuncts in these cases.

Current Indications for Limb-Sparing Surgery (1)

The two broad criteria that should be satisfied before considering LSS are as follows:

1. Satisfactory surgical margin must be possible so that the risk of local recurrence is low (<10%).
2. Functional outcome should be better than or equal to that achieved by amputation and prosthetic fitting.

Limb-sparing resections are most frequently indicated for sarcomas that do not involve major neurovascular structures.

Table 3 Contraindications to limb salvage procedures.

Contraindications to limb salvage procedures
Inability to achieve wide surgical margins
• Invasion of major neurovascular structures.
• Involvement or contamination of multiple compartments with extensive muscle involvement.
• Patients with extensive skin involvement.
• Pathologic fractures where the risk of recurrence increases several folds.
• Sepsis jeopardizing the effectiveness of adjuvant chemotherapy.
• Inappropriate or improper biopsy contaminating normal tissue planes and compartments.

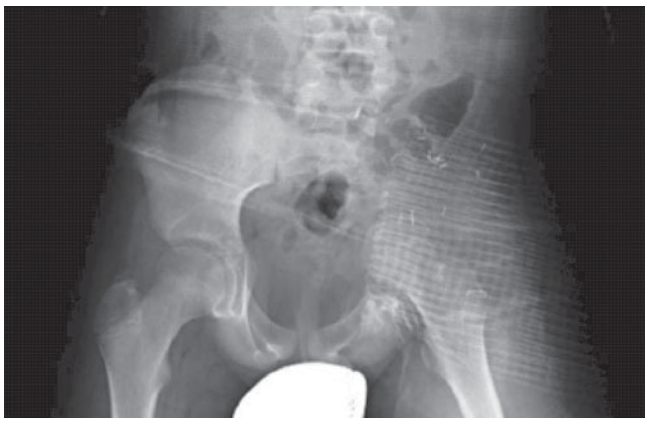

Fig. 2 Postoperative posteroanterior radiograph of a type II resection of the pelvis (internal hemipelvectomy), with cerclage tape stabilizing the proximal end of the femur and attaching it to the pubis

Loss of function can occur based on the extent and location of the muscular resection. Decisions are individualized based on the location, extent of the tumor, and the psychosocial characteristics of the patient. Relative contraindications for limb salvage include those mentioned in Table 3 (1).

Changes in Management Approach

Improvement in mortality was seen in the 1960s and 1970s. This led to interest in improving quality of life, and thus generated interest in limb salvage for primary tumors of the appendicular skeleton. The introduction of plastic surgery techniques and the incorporation of muscle transfers allowed the use of standard orthopedic reconstruction in the relatively large gaps that develop after tumor resection. Surgeons today routinely use muscle pedicle flaps and vascularized bone transfers. Some older methods of resection arthrodeses, turndown and turnup plasties, Tikhoff-Lindberg resections and internal hemipelvectomies may still have a role today (Fig. 2). Allografts, alloprosthetic composites (APCs), and endoprosthesis (both modular and custom-made) are some of the standard options available today.

Reconstruction After Resection of Extremity Sarcoma

During the late 1970s, two primary advances occurred that generated surgeons interest in limb salvage for at least a limited number of patients. First, early chemotherapy results were demonstrating that the drugs of that day could have a positive effect on bone sarcomas and some early limb salvage techniques became available for clinical use. Using osteosarcoma as an example, the 5-year survival rate in the early 1970s was ~20%. With the advent of neoadjuvant chemotherapy and advances in radiation therapy techniques, the 5-year survival rate has improved to ~60–70% (5). These limb salvage techniques included bone turnup or turndown procedures, as were originally described by Enneking (6).

The turndown and turnup procedures were described for tumors about the knee and involved resection of either the distal femur or proximal tibia followed by a sagittal split through either the remaining proximal tibia or distal femur. The split piece would be rotated up or down to span the gap and would then be fixed in place and augmented with an intramedullary rod from the hip to the knee with bone graft inserted at the junctions. Figure 3 demonstrates such a procedure performed for a large giant cell tumor of the proximal tibia. While this procedure was technically considered limb salvage, the limitations of knee fusion prevented this surgical option from being a popular operation with patients.

Another technical advance that occurred during the late 1970s was the availability of primitive segmental replacement prostheses. These included proximal femoral replacing bipolar or total hip prostheses and segmental replacement Guepar-style total knee prostheses. The proximal femoral prostheses were one-piece units with varying body lengths and typically one stem option, which was a fixed diameter and length. The Guepars were fixed hinge (Fig. 4), complete constrained versions of the standard Guepar knee prosthesis, which had been modified for segmental replacement. Because of their fixed "door hinge" design, these prostheses were subject to a high rate of loosening and breakage and did not constitute a viable long-term solution.

Since the early 1980s, segmental replacement prostheses have evolved significantly and have become available for many anatomic locations, including the humerus, femur, and tibia to provide functional shoulder, elbow, hip, and knee prostheses. Total bone replacement has also become a possibility for the femur and humerus, though these are rarely indicated. The other major segmental replacement reconstructive option that arose in the 1980s was the use of osteoarticular allografts (Fig. 5a, b). These grafts were met with initial early enthusiasm as they represented a "biologic" alternative to massive metallic prostheses. The use of these grafts paralleled the evolution of bone banking techniques along with the availability of these grafts from a number of

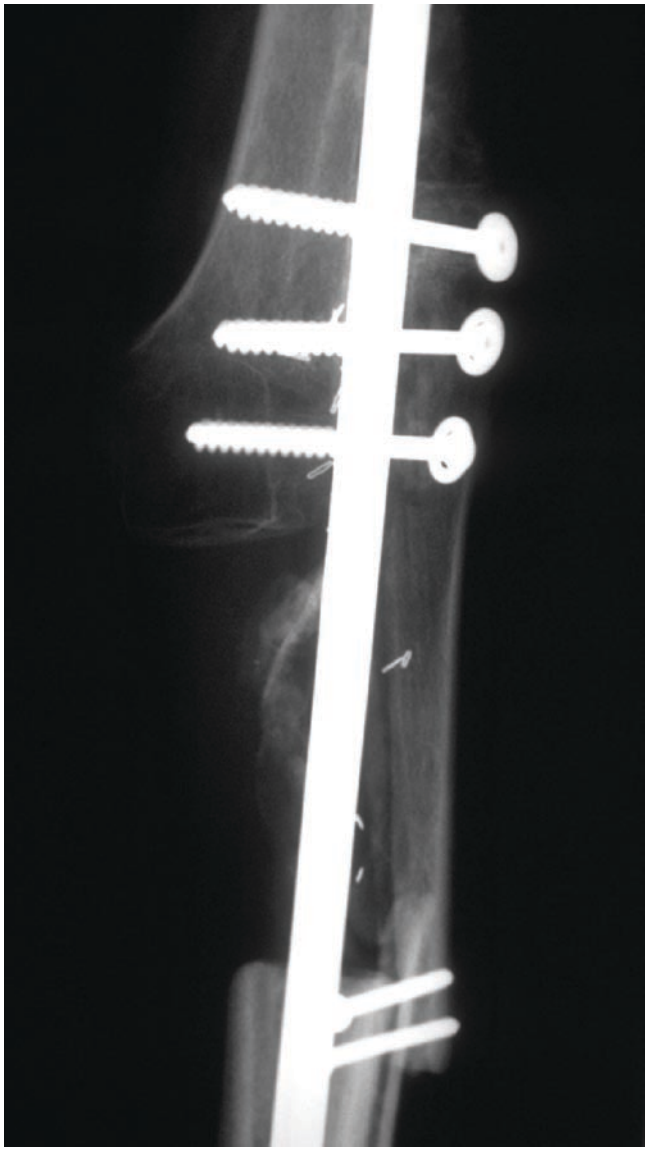

Fig. 3 Postoperative anteroposterior radiograph of turndown procedure performed on a patient with a large giant cell tumor of the proximal tibia

Fig. 4 Complete constrained standard Guepar knee prosthesis

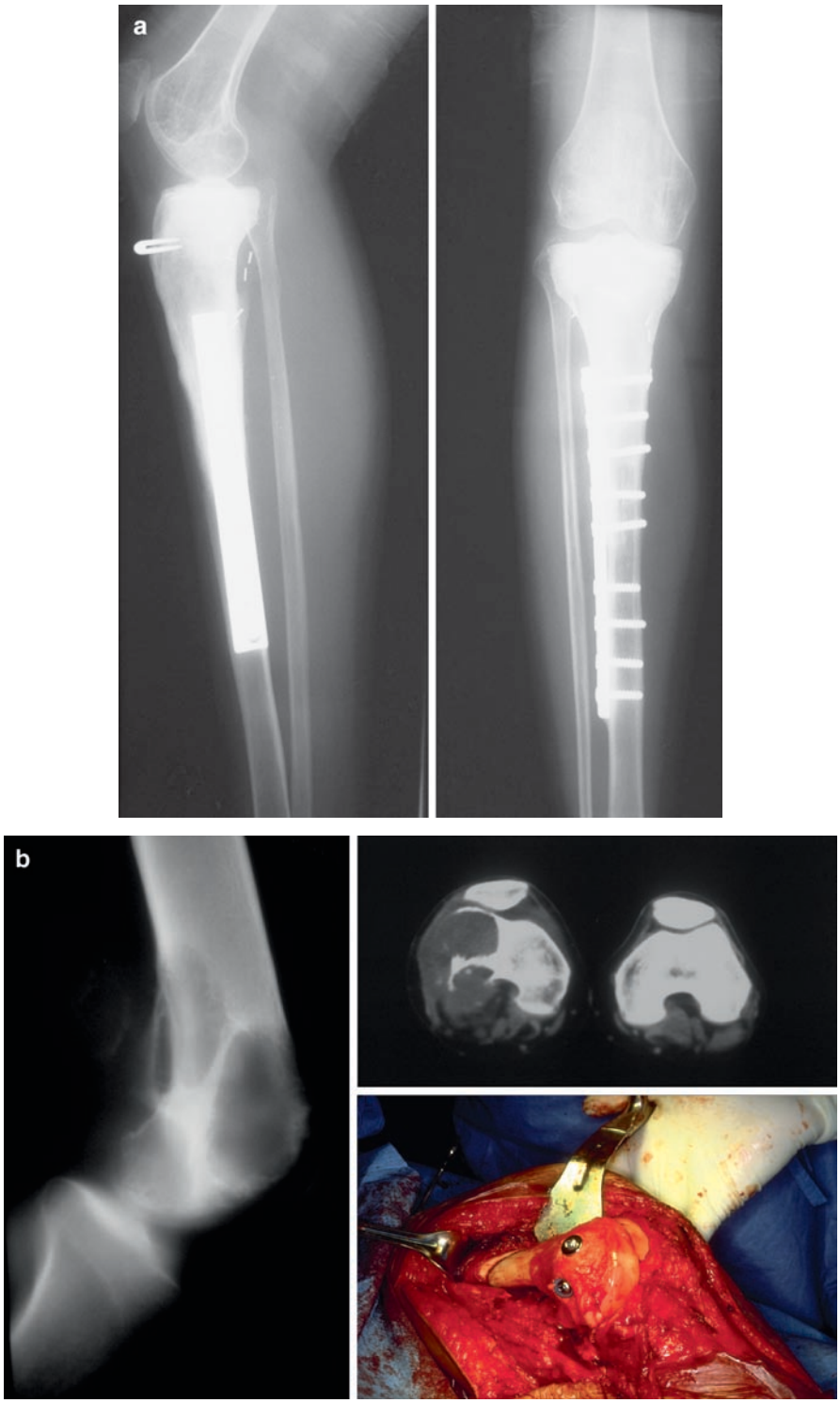

Fig. 5 **a** Postoperative anteroposterior and lateral radiographs demonstrating segmental reconstruction of the proximal tibia utilizing osteoarticular allograft. **b** Distal femoral osteosarcoma treated with wide resection and osteoarticular allograft

bone banks. Their use for tumor reconstruction in the United States was pioneered by a variety of people, but was extensively studied by Henry Mankin and his associates (7). These osteoarticular allografts demonstrated early positive results with good joint function and a reasonable complication rate. Over time, however, the complications of fracture, nonunion, infection, dislocation, and arthritis rose to a level that decreased the overall enthusiasm for this technique in the

lower extremity, where weight-bearing stresses made it difficult for the grafts to heal. However, osteoarticular grafts remain a popular option for nonweight-bearing applications such as the proximal humerus and distal radius, which are sites of frequent tumor involvement. In these locations, the stresses to which the grafts are subjected are much less than those experienced in weight-bearing applications, thereby increasing the longevity of the graft.

Recent research by Mankin et al. demonstrates a fourfold increase in the number of endoprosthetic reconstructions performed at their institution over the last decade compared with a concomitant 50% decrease in the use of allograft reconstructions for limb preservation surgery. In perhaps the largest published series of allografts (718 total, 386 of which were osteoarticular), the authors reported a 19% fracture rate, 17% nonunion rate, 11% infection rate, and a 6% rate of joint instability, with most of these complications occurring within the first 3 years of implantation (7). If the allograft managed to survive the first 3 years, osteoarthritis typically became a problem for the osteoarticular allografts at around 6 years postoperatively. Despite the fact that 16% of the osteoarticular allografts ultimately required conversion to total joint arthroplasty, ~75% of the grafts were retained by the patient and were considered successful for more than 20 years following implantation (7).

In our experience at a tertiary level, orthopedic oncology university referral center, we have found endoprosthetic reconstruction to be a very reliable technique for restoration of segmental defects following wide resection of sarcomas. We recently reviewed the long-term survival of 139 endoprosthetic reconstructions performed over an 8-year period to achieve a better understanding of the factors affecting endoprosthetic survival (8). Kaplan-Meier event free survivorship analysis revealed that endoprosthetic survival was 86%, 80%, and 69% at 3, 5, and 10-year follow-up. The location and periprosthetic infection had a statistically significant effect on survival. Interestingly, the patient age or type of reconstruction (primary vs revision) did not affect the survival outcomes. There was a low early wound complication rate (3 out of 129 patients, that is, 2.3% developed early infections), all of which occurred following proximal tibia replacements (9). These studies help substantiate the evolution of this procedure and demonstrate the reliability of current techniques.

Categorization Based on Anatomical Zones

Proximal Femur

Probably the simplest site for segmental replacement early designs was the proximal femur. In light of the early success of hemiarthroplasty and total hip replacement, the only necessary development was the longer body component and a stem to fit the diaphyseal location, since that is where most of these stems were placed given the common segmental replacement lengths of 60–160 mm.

Initially, early models were one-piece femoral components that could be utilized for treatment with either total hip or hemiarthroplasty (Fig. 6a, b). Cemented stems were used most commonly. The most difficult engineering challenge was the design of the attachment site for the greater trochanter. Early designs used a metal loop for trochanteric attachment, which was not optimal. The most common surgical technique utilized multistrand cables or thick nonmetallic sutures around the trochanter and through the prosthetic loop. The acute turn of the wire or suture around the loop compounded with the stress concentration and wear characteristics of this design caused cable or suture breakage and subsequent proximal migration of the trochanter.

Most modern designs have replaced the prosthetic loop with holes through the prosthesis for use with wire or heavy suture. Further accommodations for trochanteric reattachment vary between manufacturers. All current designs are modular with varying body sizes and stem diameters (Fig. 7). Several studies document the early success and long-term durability of these prostheses. The most common application for tumor replacements has been the use of these prostheses in association with a hemiarthroplasty and a cemented stem. The rationale for the use of a hemiarthroplasty has been the fact that in most of these patients the acetabulum is normal with regard to subchondral bone and articular cartilage. Another advantage of the hemiarthroplasty was the increased inherent stability of a large ball in a deeper socket when compared to a total hip prosthesis.

In Europe, Kotz has reported on the use of a bone ingrowth stem with an associated side plate (Fig. 8) (10). Complications with this system have included stress shielding and bone-collar resorption secondary to particulate debris. A novel spring-loaded, titanium-alloy uncemented implant was recently developed to address the problem of loosening secondary to stress shielding in patients managed with tumor prostheses (11).

More recently, the US market has seen the introduction of other cementless stem designs, although no data on the potential long-term success of these cementless designs is available to date. The question of whether these particular designs will eventually perform better or worse than cemented stems remains to be seen. As always, surgeons should carefully consider integrating any novel technology unsupported by long-term data into their practice.

Distal Femur and Proximal Tibia

Probably the most common use of segmental replacement prostheses has involved the knee, with the distal femur accounting for the largest share of these procedures in light of this area being a common site for primary and metastatic tumors.

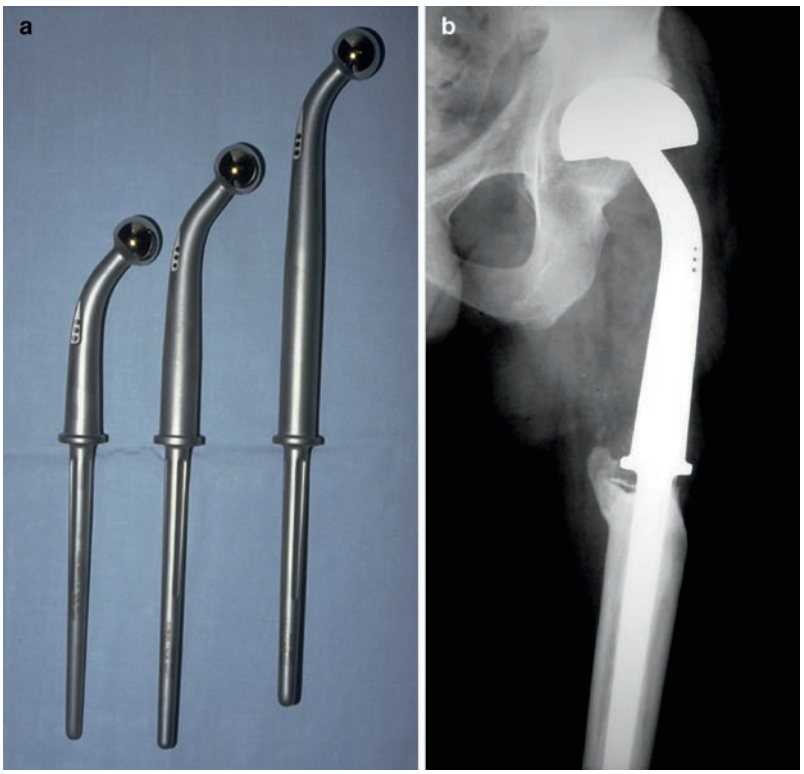

Fig. 6 **a** Early proximal femoral segmental replacement prosthesis. **b** Postoperative radiograph of patient who underwent proximal femoral segmental replacement

Fig. 7 A current modular proximal femoral segmental replacement prosthesis demonstrating variety of body sizes and stem diameters

Fig. 8 Segmental replacement prostheses with associated compression side plates to facilitate prosthetic fixation about the hip and knee

The real success of these designs dates back to the invention of the rotating hinge total knee, which was a fixed hinge knee prosthesis that was introduced by Walldius in 1953 for use in primary total knee arthroplasty (12). As mentioned previously, initial hinged knee designs utilized constrained "door hinge" technology. This design transmitted tremendous stresses to the prostheses and the bone–cement interfaces, which made early failure inevitable. This design utilized a hinge in the femoral component but was connected to the tibia with a rotating bearing component (Fig. 9). As such, the bearing component could toggle up and down within the tibial component and also allowed rotation. Thus, varus and valgus stresses were relieved by flexion-rotation and distraction forces were relieved by slight pistoning of the bearing component. This design allowed far less stress to be delivered to the prosthetic components themselves, as well as the bone–cement interfaces. This design has been altered to some extent by a variety of manufacturers, but all current designs remain true to the basic plan of the original rotating hinge.

Several design evolutions have occurred over the past two decades since segmental replacement designs became available. These changes have involved modularity, stem design, patellofemoral joint mechanics, patellar tendon attachment, prosthetic size, bearing component geometry, and jig improvements.

With regard to modularity, initial designs were one-piece custom-ordered items with primitive stem designs that afforded no intraoperative flexibility (Fig. 10). Current systems are completely modular with varying stem, body, and joint component sizes (Fig. 11). This variety affords the surgeon a myriad of intraoperative choices, which can optimize prosthetic placement, function, and stability. Body sizes that are inserted between the stem and the articular components (Fig. 12) replace lost bone stock and usually vary every 1–2 cm depending on the manufacturer. These are simple shafts with Morse tapers and design differences are typically not an issue.

Fig. 9 Standard nonsegmental rotating hinge knee assembly

Stem design is probably an important consideration, although there are no studies investigating which parameters of individual designs are effective. It is probably reasonable to assume that avoiding stems with very small diameters will decrease stem breakage. As such, stems used for lower extremity reconstructions should probably be at least 13 mm in diameter, although surgical judgment for individual cases is always essential and excessive reaming of normal bone is not desirable.

Similar to proximal femoral segmental replacement prostheses, both cemented and noncemented stem designs exist. Certainly, there is more data regarding the long-term survival of cemented stems than there is for noncemented designs. As such, it is up to each surgeon to review design and outcome parameters before making implant decisions. Beyond that, the stem designs used for the proximal femur are usually the same provided by most manufacturers for the distal femur and proximal tibia as well.

One of the most critical areas of concern with any knee design is patellofemoral articulation. This is an area of extreme stress concentration and a site where misalignment can result in pain and instability. Two important issues here are inherent patellofemoral design stability and proper component insertion. In terms of design, several products on the

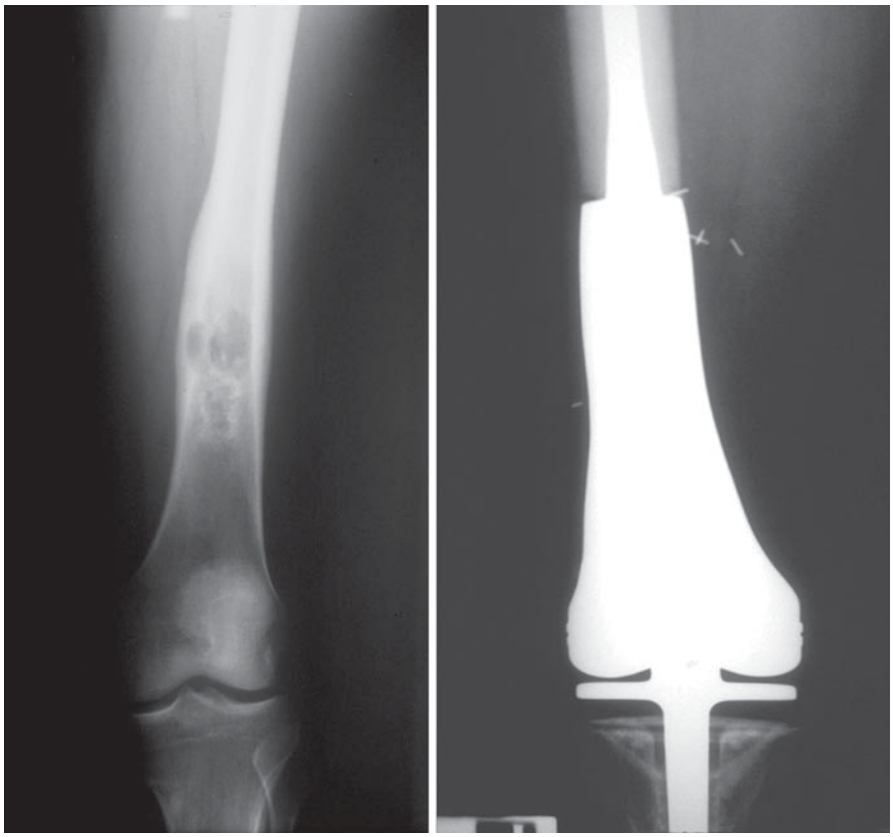

Fig. 10 One-piece distal femoral replacement prosthesis. Pre- and postoperative anteroposterior radiographs demonstrate total knee replacement utilizing a long-stem femoral component

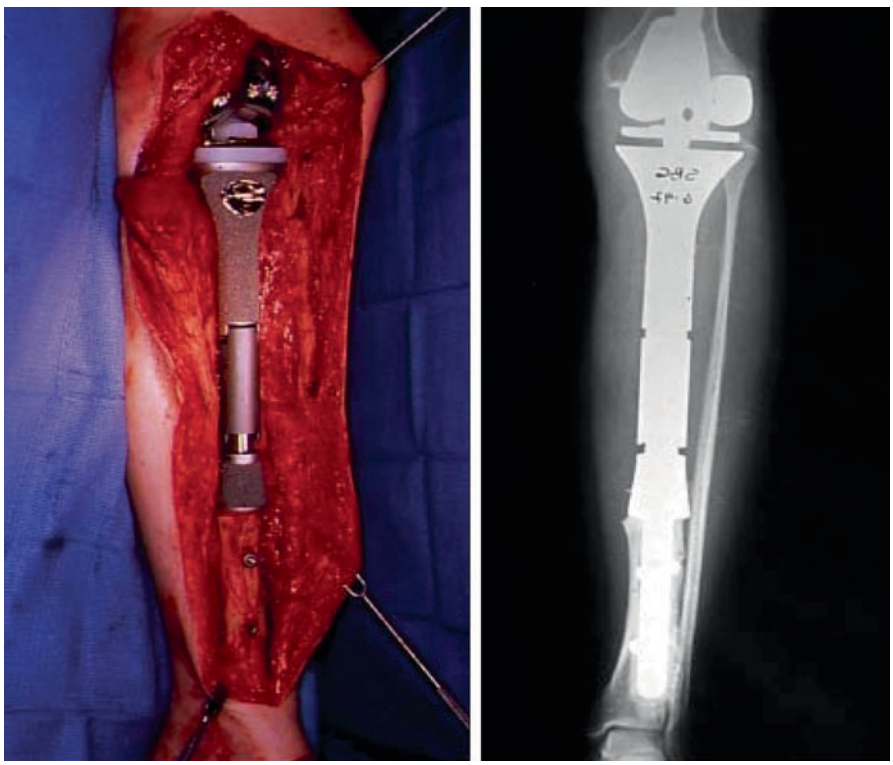

Fig. 11 A tibial segmental replacement prosthesis with a modular hinge prosthesis and a distal femoral component

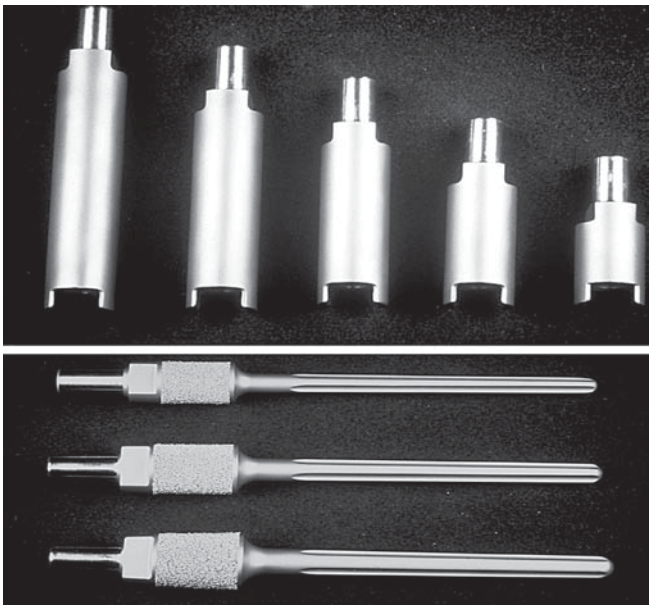

Fig. 12 Varying body segments that allow for varying the length of segmental replacement at 2-cm increments

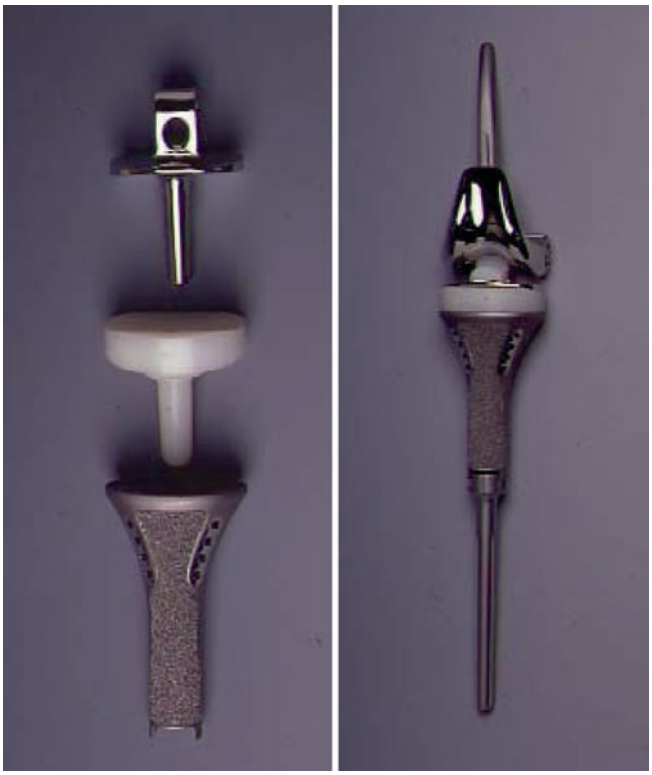

Fig. 13 Proximal tibial segmental prosthesis demonstrating frayed anterior surface to facilitate soft tissue ingrowth

market have developed improved patellofemoral stability by widening and deepening the trochlear notch on the distal femoral component. This has gone a long way toward making the articulation less precarious and also added significant inherent stability to the patellar component as it rides in the trochlear notch.

The other factor that remains important to proper function is proper version on the femoral and tibial components. In terms of the distal femur, the components are usually placed in anatomic position with neutral version, or may have jigs to impart slight external rotation. The more critical prosthetic position involves the tibial component. This is usually placed in "slight" external rotation so that during flexion, the tibia is slightly rotated internally, which brings the patella up on top of the femoral component and prevents lateral patellar dislocation. Typically, about 10–15° of external rotation of the tibial component is adequate, although individual situations may call for more, especially when used in the context of a failed standard total knee replacement.

Patellar tendon reattachment and soft tissue coverage are the major challenges inherent to proximal tibial segmental replacement total knees. In terms of patellar tendon reattachment, no clear solution exists at present. Several designs are available, most of which utilize a sintered surface on the anterior aspect of the tibial component to facilitate soft tissue ingrowth (Fig. 13). This process aids in scar formation and adhesion of the patellar tendon to the surface of the prosthesis. Usually, this is performed in association with drilling holes in the tibial component to allow insertion of large sutures to help stabilize the patellar tendon repair during healing. Protection of this repair is achieved by keeping the knee in extension in a knee immobilizer or cylinder cast for 5–6 weeks following surgery. Most patients treated in this manner regain greater than 90° of flexion with the help of gentle physical therapy. Many patients will eventually develop an extensor lag, though this is usually less than 20° and may be absent altogether. Rarely does this lag cause knee instability, but if it does a drop lock brace can be used to maintain the knee in extension during ambulation.

In terms of soft tissue coverage for the proximal tibia, there are two important rules:

1. Be mindful to handle the soft tissue flaps with care to avoid necrosis.
2. Never close the wound with the tissues in tension.

In many cases, flap coverage is unnecessary as primary closure over the tibial component is possible (13). In cases where the soft tissue is not adequate for primary closure, a medial gastrocnemius flap with or without a split thickness skin graft will provide adequate coverage.

The other factor that facilitates ease of closure is the use of a downsized tibial component. Some manufacturers include regular and small versions of the rotating hinge tibial component in their sets. This may make closure much simpler and help avoid the need for flap coverage. Finally, appropriate jigs

will facilitate proper prosthetic insertion, especially in the hands of the occasional user. As such, it may be helpful for the occasional surgeon to review the techniques involved via a "saw bones" knee and closely review all jigs along with their proper use and placement.

Total Femoral Replacement Prostheses

Occasionally, it becomes necessary to resect and replace the entire femur with a new articulation at the hip and the knee (Fig. 14). This is most commonly indicated in patients with extensive tumor involvement of the femur, but also occasionally in patients with multiple hip and knee prostheses revision on the involved side.

Extendable reconstruction devices (Fig. 15) for replacing the entire femur offer skeletally immature patients with malignant bone tumors the opportunity of a nearly normal development by overcoming an expected leg length discrepancy.

In patients undergoing total femur replacement, the hip and knee considerations are similar to those involved with segmental replacement of either end of the bone. Hip stability can be a major issue and a constrained liner is a worthwhile consideration.

These total femur replacements are less functional than either the proximal or distal femoral replacements individually, but still can be a major improvement over high-level amputations in these patients.

With regard to future trends for these prostheses, several avenues of research are currently in progress. One of the most promising of these studies is metal foam, which will facilitate and enhance soft tissue attachment to metallic components. This will hopefully improve the outcome with regard to abductor attachment to the proximal femur and patellar tendon attachment to the proximal tibia.

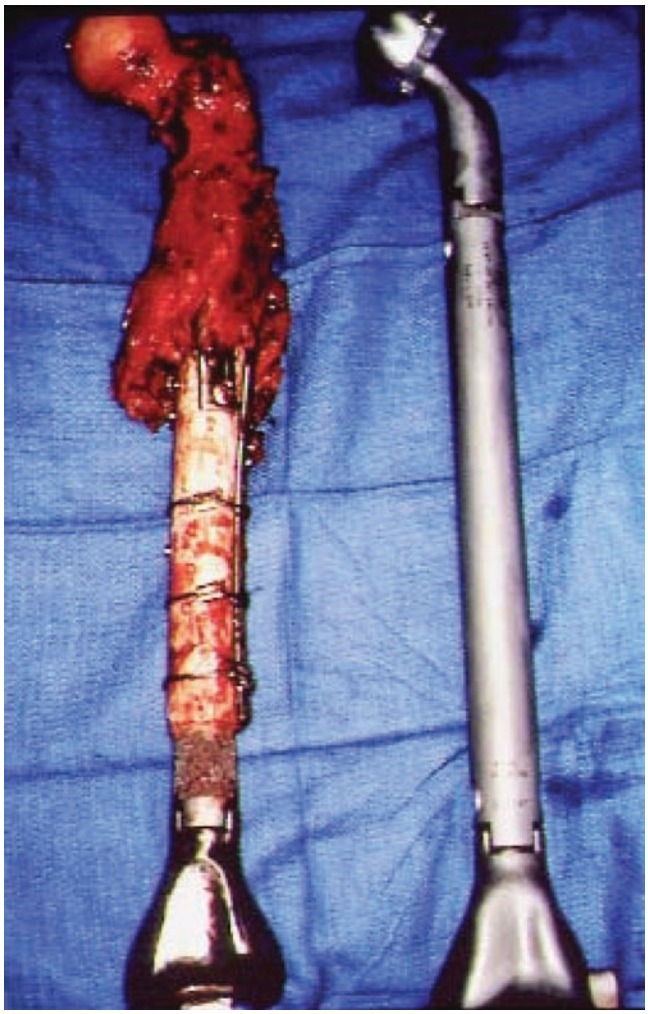

Fig. 14 Resection of prior tumor endoprostheses to be replaced with total femoral replacement prostheses

Fig. 15 Extendable total replacement prostheses facilitate replacement of the entire femur in skeletally immature patients

Classification of Pelvic Resections (14)

Terminology (14)

Classical hemipelvectomy: Also known as hindquarter amputation (v/s forequarter for upper extremity) involves resection of the entire or a portion of the hemipelvis with the lower extremity. This can be performed using either the standard posterior or anterior myocutaneous flaps. Alternative approaches with creative options for soft tissue flap coverage exist, based on individual presentations in given situations and may give satisfactory results.

Internal hemipelvectomy: This procedure involves the resection of the entire or a portion of hemipelvis (innominate bone) with preservation of the ipsilateral extremity.

Extended hemipelvectomy: This procedure includes sacral transection through the neural foramina.

Compound hemipelvectomy: Involves resection of a viscus in addition to the hemipelvis.

Sacrectomy: Involves excision of entire or a portion of (partial sacrectomy) the sacrum and is reserved for primary sacral tumors like chordoma or secondary spread of pelvic tumors to sacrum.

The *classification of internal hemipelvectomies* is based on the resected region of the innominate bone from posterior to anterior (15, 16) (Fig. 16a, b):

Type I: Resection of the ilium
Type II: Resection of the periacetabular region.
Type III: Ischiopubic region resection.
Type IV: En bloc excision of the sacral ala is termed as extended type I or type IV resection.
Note: The capital A indicates a more aggressive resection:
IA: The buttock is resected en bloc with the iliac wing.
IIA: The proximal femur and hip capsule are resected with the periacetabulum.
IIIA: The femoral neurovascular bundle is resected with the pubic rami.

Reconstruction After Resection

Reconstruction (i.e., rebuilding the extremity to accommodate the loss of the structures removed for surgical control of the local tumor) remains an important aspect after resection of pelvic sarcomas with limb-sparing techniques depending on the type of resection. This may be achieved by reconstruction with custom endoprosthetic devices, allograft reconstruction (with or without fusion of joints), autograft reconstruction (either vascularized or nonvascularized) or combinations of endoprostheses and bone grafts. Reconstructive plastic surgical procedures

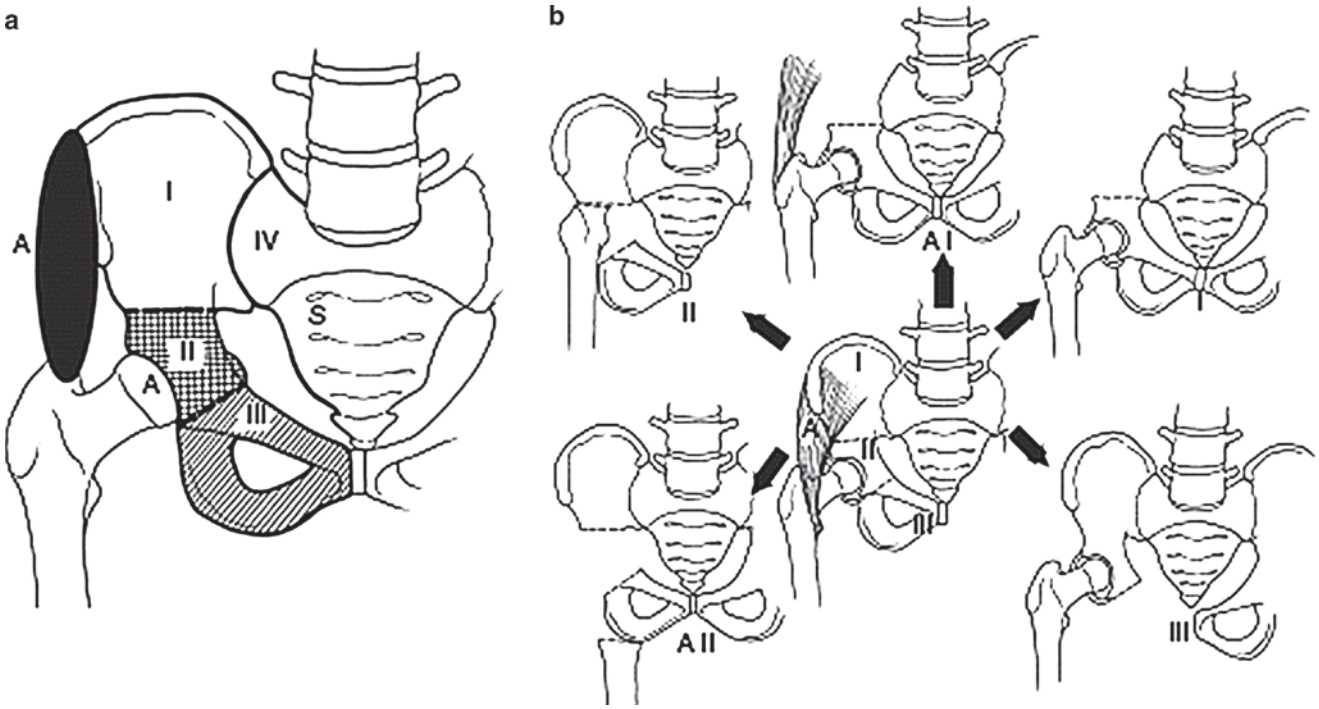

Fig. 16 **a** Types of pelvic resection. The black oval indicates the gluteus medius muscle. **b** Enneking's classification of pelvic resections. *Type I* resection of the ilium. *Type II* resection of the periacetabular region. *Type III* resection of the ischiopubic region. *Type IV* en bloc excision of the sacral ala. *A* aggressive resection, *S* sacrum

such as vascularized free flaps are occasionally required for management of soft tissue defects. Titanium alloy implants may be utilized for reconstruction for ease of monitoring postresection recurrence and MR imaging. Because of ferromagnetic properties of conventional stainless steel implants, MRI performed to determine completeness of the resection and later for recurrence of the tumor becomes difficult.

Iliac Reconstructions

Type I resections of the ilium usually create defects extending from the sacroiliac joint to the supra-acetabular part of the ilium. Reconstruction may be considered *anatomic* when the hip joint is restored to its anatomic level and the pelvic ring is reconstituted, or *nonanatomic* when the iliac stump is approximated to the sacrum. The various options of reconstruction include primary arthrodesis and bone grafting with vascularized or nonvascularized autografts, allografts, or custom implants and endoprosthesis (15). The ends of the resection could be fixed with a cerclage wire or other implantable device as demonstrated (Fig. 17). *Autograft reconstruction* using either vascularized or nonvascularized autografts are reasonable options for reconstruction of pelvic skeletal defects after resection of pelvic sarcoma (16). Vascularized autografts are most commonly harvested from the fibula or the iliac crest (17). Double-barreled vascularized fibulas have been successfully used for reconstruction of pelvic defects after type I resections (Fig. 18) (18). Nonvascularized autogenous bone grafts are commonly obtained from iliac crest, fibula, anterior tibia, and sometimes the patella.

Acetabular Reconstructions

Acetabular resections can be dealt with in different ways.

Left Flail Without Any Formal Reconstruction

In their follow-up of five cases of flail hip joint after resection of primary bone tumors of the pelvis, Takami et al. (19) noted that when a thick portion of the supra-acetabular pelvic neck was left in place, the operated legs functioned well regardless of whether the head of the femur was placed anterior or posterior to the iliac wing. They noted favorable healing of the operative wound in all cases and suggest consideration of this procedure for women or sedentary patients with primary bone tumor of the pelvis involving acetabular region.

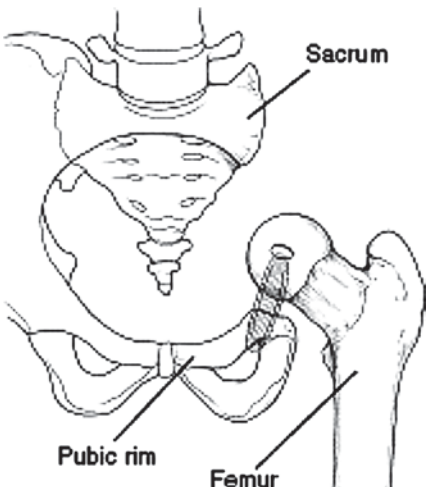

Fig. 17 Type I and II pelvic resection with cerclage reapproximation

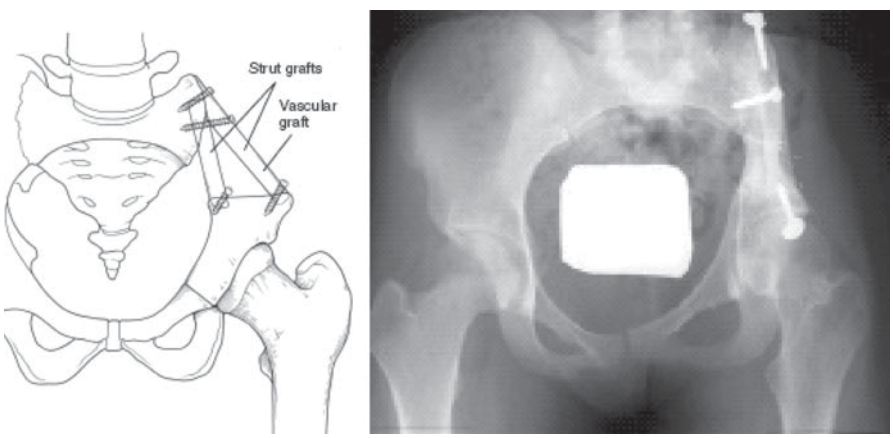

Fig. 18 Type I resection with an A-frame reconstruction. Anteroposterior plain radiograph of the fibular grafts after double-barreled reconstruction demonstrating the grafts 4 years after surgery with good results

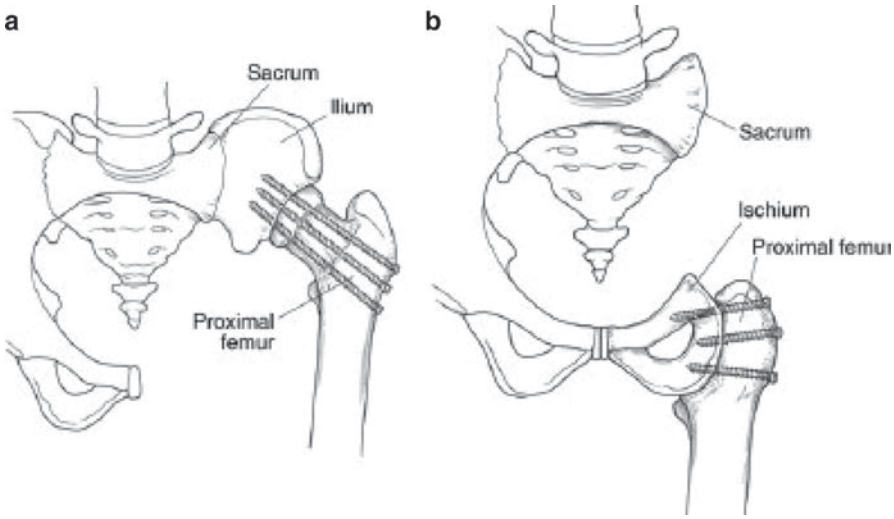

Fig. 19 Iliofemoral (**a**) and ischiofemoral (**b**) arthrodesis

Reconstructed with an Arthrodesis of the Ipsilateral Proximal Femur

Arthrodesis of the proximal femur to the resected pelvis remains an acceptable option for reconstruction if there is sufficient bone stock. Depending on the level of resection the procedure offered could be iliofemoral or ischiofemoral arthrodesis (Fig. 19a, b) (20). Although the fusion rates reported are less than 50%, a stable and painless pseudarthrosis may develop in most patients who fail to achieve a bony arthrodesis. Functional results may be comparable to other procedures including endoprosthetic reconstruction and APCs (20). The advantage of this procedure is that it provides a stable and durable reconstruction. Shortcomings may include leg shortening, prolonged period for consolidation, and permanent lack of hip mobility. The long lever arm of the lower limb acting at the site of arthrodesis and possibly decreased contact area may sometimes compromise the outcome of a successful arthrodesis. Also the local blood supply may be compromised by the surgical resection and possible radiotherapy.

Reconstructed with a Hip Arthroplasty

- Using saddle endoprosthesis.
- Using composite iliac allograft and a total hip arthroplasty.
- Using a customized acetabular construct with cortical fixation to the remaining pelvis.

Reconstruction using *endoprosthetic devices* has provided many surgical alternatives to children and teenage individuals with limb-threatening malignancies. Matching the implant to the recipient may be difficult and most implants are therefore custom-made. Endoprosthetic reconstruction has advantages

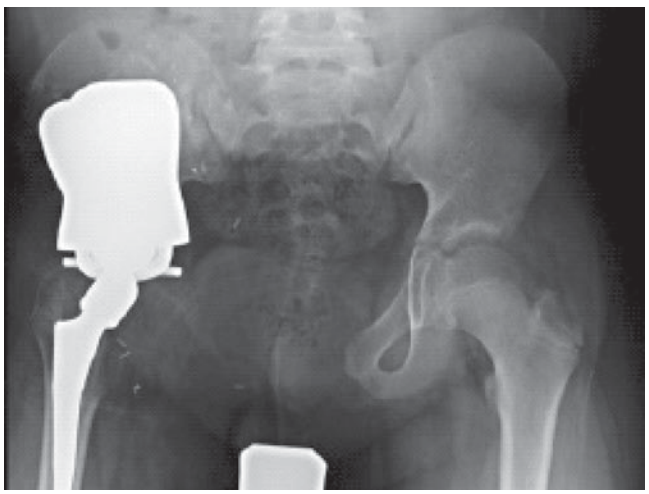

Fig. 20 Radiograph of a pelvic resection followed by placement of saddle endoprosthesis

in that it involves immediate weight bearing with early rehabilitation and return to function and a quick postoperative recovery.

The saddle prosthesis has been widely used for reconstruction following periacetabular resection particularly following type II and II/III resections, despite the potential problems of a large residual dead space and a nonanatomic hip center (21) (Fig. 20). The surgical requirements for implantation of the saddle endoprosthesis could be outlined as follows: retaining of a reasonable segment of ilium subsequent to the tumor resection (at least 2 cm), creating a notch within the remaining ilium located preferably in the thickest part of the bone, retaining the hip abductors and the iliopsoas muscles, and optimizing the pelvic-femoral tension (22). If the ilium has been resected completely, it may be possible to

construct an articulation using allograft or cement fixed to the sacrum (21).

Sometimes in type II resections when reconstruction is difficult one may use a cerclage tape or wire and stabilize the proximal migration of the femoral head by transfixing the cable/wire/tape through the femoral head at one end and the pubic symphysis/ramus/obturator foramen at the other end. This helps in early postoperative mechanical stabilization and the reactive fibrosis and soft tissue thickening at a later stage possibly helps in preventing proximal migration.

Allograft reconstruction (intercalary or osteoarticular: with joint fusion) can also be an option for reconstruction of defects after wide resection following pelvic sarcomas (20). The main advantage is that allograft is readily available. Disadvantages include joint degeneration and instability of joints for osteoarticular allografts, and higher risk of infection and fracture.

APC reconstruction can also be considered after wide resection of pelvic sarcomas. These have better results when there is an adequate remaining ilium and pubis for fixation of the graft or endoprostheses (20). The possible advantages of this technique include healing to and partial replacement by host bone and the ability to shape the allograft to fit the defect during the resection. Main disadvantages are high rate of infection, risk of viral transmission, risk of allograft fracture, and subsequent development of pelvic instability.

Concepts in Surgical Management of Metastatic Lesions

Management of Metastases to the Extremities

Indications for Surgery

Surgical intervention is necessary for pathologic fractures and impending fractures (23). A pathologic fracture can be devastating in a patient with cancer and is a clear indication for surgical intervention. Because pathologic fractures are so devastating and prophylactic s urgical treatment of impending fractures has been shown to improve outcomes (24, 25), a system is needed to determine which extremity metastases are impending fractures and how these lesions should be managed to avoid this complication. Mirels developed a scoring system designed to predict the risk of pathologic fracture in the extremities (26). It is based on the degree of pain, lesional size, lytic versus blastic nature, and anatomic location, as shown in Table 4.

The highest total score is 12 and represents lesions most likely to result in fracture. This is the most helpful scoring system available to date, but it still has practical limitations. Although Mirels' scoring is based on objective criteria, the variability in quality of surrounding bone, behavior of metastases from different primaries, response of these metastases to radiation therapy, patient activity level, and life expectancy create problems in predicting the risk of fracture (27). Although this system is helpful, these authors feel that the most reliable indication of the need for prophylactic fixation is the presence of mechanical pain. Mechanical pain is a physiologic indicator that the involved bone cannot withstand the physical stresses it is subjected to and is therefore at risk of fracture. As a result, all metastatic lesions in the extremities that exhibit mechanical pain should be considered for prophylactic fixation. Patients with lesions producing little or no pain can be evaluated according to Mirels' system, which is a further guide to the potential need for prophylactic surgery in this group. Lesions with a risk of fracture too low to necessitate surgery should be treated initially with radiation, which may negate the need for subsequent surgical intervention.

Table 4 Demonstration of the scoring system proposed by Mirels (26).

Score	1	2	3
Pain	Mild	Moderate	Functional
Lesion size/diameter of bone involved	<1/3	1/3 – 2/3	>2/3
Lesion type (blastic/lytic)	Blastic	Mixed	Lytic
Anatomic site	Upper limb	Lower limb	Peritrochanter

[a]Prophylactic fixation is indicated for a total score of ≥9.

Principles of Surgical Management

The use of the following principles in the surgical management of both extremity and pelvic metastatic lesions helps to increase the efficacy and improve the outcomes of surgical procedures (23).

1. Understand the patient's prognosis.
2. Embolize all suspected vascular lesions preoperatively, when possible.
3. Provide adequate perioperative antibiotic coverage and optimize the patient's medical condition before surgery.
4. In the face of prior radiation fields, ensure adequate soft tissue coverage and carefully avoid unnecessary trauma to soft tissue flaps.
5. Verify histology in lesions that present as the first skeletal metastasis.
6. Remove as much of the lesion as possible without negatively affecting the ability to provide proper fixation.
7. Use internal fixation bone cement or cemented prosthetic placements as indicated to create a stable, durable construct and to fulfill the goal of immediate return to function.

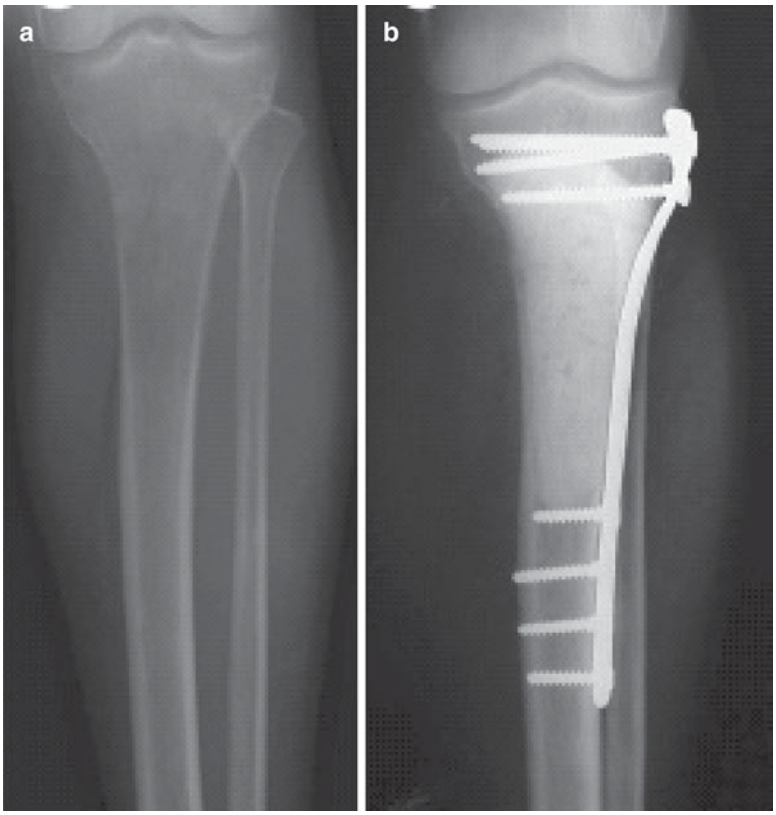

Fig. 21 A plain film of a metadiaphyseal tibia lesion (**a**) that has been appropriately treated with cementation and plate fixation (**b**)

8. Use adjuvant therapy in the form of postoperative radiation therapy and/or chemotherapy when indicated.

Surgical Management

The goal of surgery, whether for an impending or pathologic fracture, is to reinforce or replace the compromised bone with a rigid and durable construct, providing functional stability and pain relief. The concept of a durable construct is important in orthopedic oncology because fixation in this setting must persist for the life of the patient, because the bone involved in metastatic lesions may not heal. With regard to surgical margins, intralesional margins are appropriate in metastatic skeletal lesions requiring fixation, because the intent of such procedures is to mechanically reinforce rather than to surgically cure.

The rational treatment of impending pathologic fractures depends on the appreciation of stress distribution mechanisms in diaphyseal and metaphyseal bone. In metaphyseal bone, it is the prominent cancellous trabeculae that provides most of the mechanical support. Thus, it is this aspect of the bone that must be replaced or reinforced if involved. Most metaphyseal lesions that are candidates for prophylactic internal fixation require the application of bone cement to correct the loss of metaphyseal medullary bone. This cement is usually reinforced either by a plate or by an intramedullary rod (Fig. 21a, b).

In the surgical treatment of metastatic bone lesions, one of the most frequent errors encountered is the treatment of pathologic fractures as if they were ordinary traumatic fractures. To adequately treat pathologic and impending fractures and avoid undertreatment, the surgeon should always ask, "Where can I put the bone cement?" Internal fixation of metaphyseal impending fractures without the adjunctive use of bone cement should be reserved for minimal lesions that are still candidates for fixation according to the classifications discussed. In contrast to metaphyseal bone, diaphyseal bone receives most of its inherent strength from the cortical bone. Therefore, diaphyseal lesions involving the cortex should be reinforced with intramedullary devices, typically a locked intramedullary rod, and defects should be filled with bone cement. Medullary diaphyseal lesions without cortical destruction rarely qualify as impending lesions. However, these lesions should be treated with an intramedullary device if they cause mechanical pain or otherwise fit the Mirels' classification for surgical intervention. In most of these cases, cement augmentation is not needed (Fig. 22).

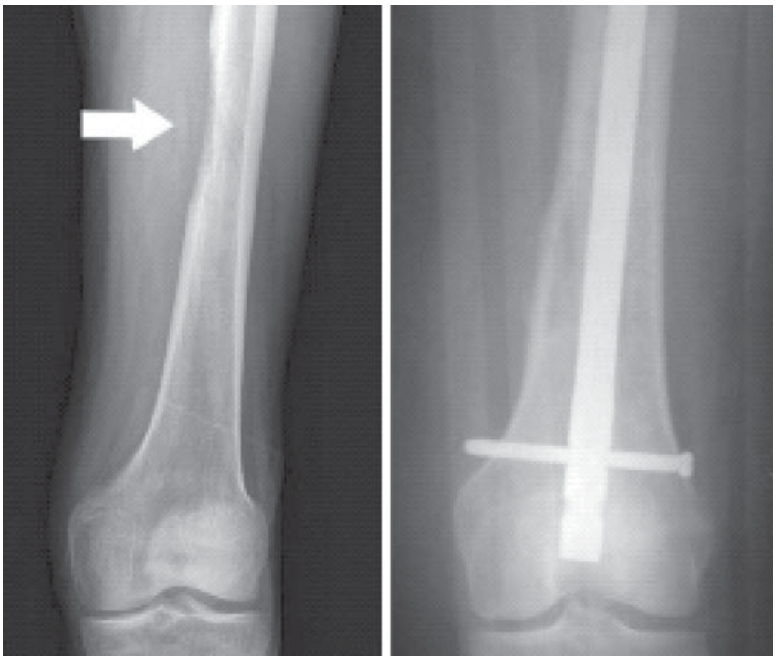

Fig. 22 A diaphyseal lesion with cortical involvement but continued cortical continuity; it was fixed appropriately with the placement of an intramedullary rod without the need for cement augmentation

Pathologic Fractures

Once a pathologic fracture occurs, the decision must be made between internal fixation and resection. An important rule to keep in mind is that one would like to perform a single operation that provides adequate mechanical stability throughout the patient's remaining life. Therefore, a judgment is required regarding the ability to reinforce the area of bone involved versus the need for resection. Although most pathologic fractures can be successfully treated with internal fixation, a significant number will require resection and prosthetic replacement. This is sometimes difficult to predict preoperatively and, as such, it is wise for the treating surgeon to have devices for either eventuality available at the time of surgery. In any case, in the interest of patients with progressive disease, it is desirable for the surgeon to perform the last operation first.

Patients with pathologic fractures require rapid restoration to an acceptable level of function. Thus, internal fixation of pathologic fractures differs from that of normal traumatic fractures, where a significant time period can be devoted to fracture healing in light of the patient's otherwise good health. Therefore, pathologic fractures require an immediately stable and durable mechanical construct. Ideally, these patients should be stable enough to begin activity without restrictions. To achieve this end, the surgeon again must always ask, "Where can I put the bone cement?" In situations where there is no large gap and weight-bearing continuity can be assured with a device alone, then cement augmentation is unnecessary. However, many metaphyseal and diaphyseal pathologic fractures will present with large areas of bone loss. In these cases, cement augmentation of the internal fixation device is critical (Fig. 23).

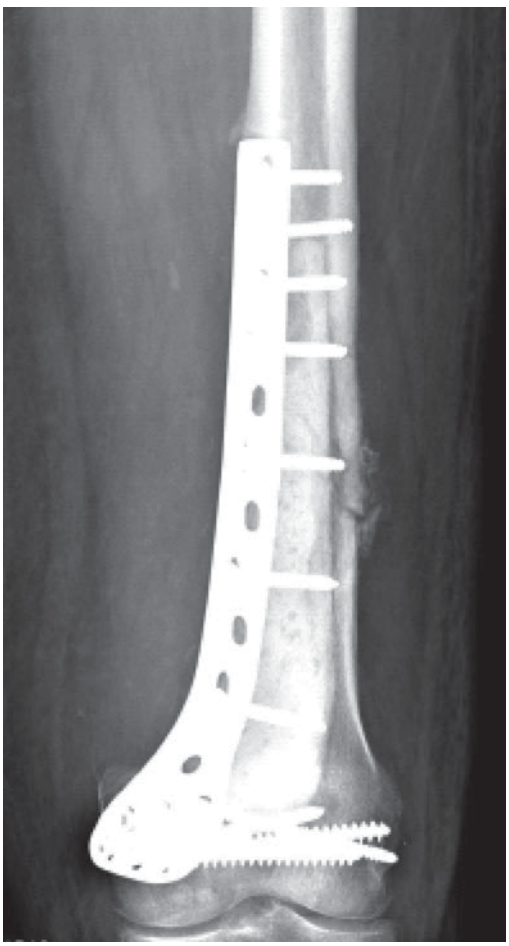

Fig. 23 A pathologic metadiaphyseal femur fracture treated with cementation and a plate. Treatment of this lesion with a plate alone would provide inadequate stabilization and be subject to a high rate of failure

One important caveat to any surgeon considering operative intervention for a suspected metastasis in bone is to recognize the possibility of an unrelated tumor in a patient with a previously diagnosed malignancy. Multiple primary tumors occur frequently in our current cancer population and represent a further challenge to correct diagnosis. A good general rule is that the first time a tumor presents with metastasis to bone, histologic confirmation should precede definitive surgical intervention. This can include a frozen section at the time of surgery. In these cases, if the pathologist can state that the lesion is either a metastatic carcinoma or a round cell tumor such as plasmacytoma, then immediate internal fixation is reasonable. If concern for a potential sarcoma persists despite the frozen section, then definitive surgery should be postponed. Passing an intramedullary nail through a sarcoma involves the entire bone and will frequently necessitate amputation.

References

1. Hosalkar HS, Dormans JP. Limb sparing surgery for pediatric musculoskeletal tumors. *Pediatr Blood Cancer*. 2004 Apr; 42(4):295–310.
2. Enneking WF. Staging musculoskeletal tumors. In: Enneking WF, editor. *Musculoskeletal tumor surgery*. New York: Churchill Livingstone; 1983. pp 68–88.
3. Hosalkar HS, Torbert JT, Carolan G, Lackman RD. Musculoskeletal tumors. In: Chin KR, Mehta SM, editors. *Key Review Concepts*. Philadelphia: Wolters Kluver/ Lippincott Williams and Wilkins; 2007.
4. Enneking W. Surgical prodcedures. In: Enneking WF, editor. *Musculoskeletal tumor surgery*. New York: Churchill Livingstone; 1983. pp 89–122.
5. Zeegen EN, Aponte-Tinao LA, Hornicek FJ, Gebhardt MC, Mankin HJ. Survivorship analysis of 141 modular metallic endoprostheses at early follow-up. *Clin Orthop Relat Res*. 2004 March; 420:239–250.
6. Enneking WF. Modification of the System for Functional Evaluation of Surgical Management of Musculoskeletal Tumors. In: Enneking WF, editor. *Limb Salvage in Musculoskeletal Oncology*. New York: Churchill Livingstone; 1987. pp 626–639.
7. Mankin HJ, Gebhardt MC, Jennings LC, et-al.. Long-term results of allograft replacement in the management of bone tumors. *Clin Orthop Relat Res*. 1996; 324:86–97.
8. Torbert JT, Fox EJ, Hosalkar HS, Ogilvie CM, Lackman RD. Endoprosthetic reconstructions: results of long-term follow-up of 139 patients. *Clin Orthop Relat Res*. 2005 Sep; 438:51–9.
9. Ogilvie CM, Torbert JT, Hosalkar HS, Fox EJ, Lackman RD. Incidence and outcomes of early infection after endoprosthetic reconstruction. *The University of Pennsylvania Orthop J*. 2004; 17:31–33.
10. Kotz R, Pongracz N, Fellinger EJ, Ritschl P. Uncemented hinge prostheses with reinsertion of the ligamentum patellae. In: Yamamuro T, editor. *New developments for limb salvage in musculoskeletal tumours*. New York: Springer Verlag; 1989. pp 605–10.
11. Bini SA, Johnston JO, Martin DL. Compliant prestress fixation in tumor prostheses: interface retrieval data. *Orthopedics*. 2000; 23:707–12.
12. Barrack RL, Lyons TR, Ingraham RQ, Johnson JC. The use of a modular rotating hinge component in salvage revision total knee arthroplasty. *J Arthroplasty*. 2000 Oct; 15(7):858–66.
13. Abboud JA, Patel RV, Donthineni-Rao R, Lackman RD. Proximal tibial segmental prosthetic replacement without the use of muscle flaps. *Clin Orthop Relat Res*. 2003; 414:189–196.
14. Hosalkar HS, Dormans JP. Surgical management of pelvic sarcoma in children. *J Am Acad Orthop Surg*. 2007 Jul; 15(7):408–24. Review.
15. Enneking W. Pelvis. In: Enneking WF, editor. *Musculoskeletal tumor surgery*. New York: Churchill Livingstone; 1983. pp 483–529.
16. Conrad EU, Springfield D, Peabody TD. Pelvis. In: Simon MA, Springfield D, editors. *Surgery for bone and soft-tissue tumors*. Philadelphia: Lippincott-Raven Publishers; 1998. pp 323–341.
17. Springfield D. Autograft reconstructions. *Orthop Clin North Am*. 1996; 27:483–492.
18. Dormans JP. Limb-salvage surgery versus amputation for children with extremity sarcomas. In: Herring JA, Birch JG, editors. *The child with a limb deficiency*. Rosemont, IL: American Academy of Orthopaedic Surgeons; 1998. pp 289–302.
19. Takami M, Ieguchi M, Takamatsu Ket-al., . Functional evaluation of flail hip joint after periacetabular resection of the pelvis. *Osaka City Med J*. 1997; 43:173–183.
20. Conrad EU, Springfield D, Peabody TD. Pelvis. In: Simon MA, Springfield D, editors. *Surgery for bone and soft-tissue tumors*. Philadelphia: Lippincott-Raven Publishers; 1998. pp 323–341.
22. Aboulafia AJ, Buch R, Mathews Jet-al., Reconstruction using the saddle prosthesis following excision of primary and metastatic periacetabular tumors. Clin Orthop. 1995; 314:203213.
22. Malawer M. Periacetabular resections. In: Malawer MM, Sugarbaker PH, editors. *Musculoskeletal cancer surgery*. Norwell, Massachusetts: Kluwer Academic Publishers; 2001. pp 425–438.
23. Lackman RD, Torbert JT, Hosalkar HS, Fox EJ, Ogilvie CM. Treatment of Metastases to the Extremities and Pelvis. In Operative Techniques in Orthopedics, Elsevier Inc, Philadelphia. 2004.
24. Ward WG, Holsenbeck S, Dorey FJ, et-al.. Metastatic disease of the femur: surgical treatment. *Clin Orthop*. 2003; 415 (suppl):S230–S244.
25. Hardman PD, Robb JE, Kerr GR, et-al.. The value of internal fixation and radiotherapy in the management of upper and lower limb bone metastases. *Clin Oncol. (R Coll Radiol)* 1992; 4:244–248.
26. Mirels H: Metastatic disease in long bones. A proposed scoring system for diagnosing impending pathologic fractures. *Clin Orthop*. 1989; 249:256–264.
27. Jacofsky DJ, Papagelopoulos PJ, Sim FH: Advances and challenges in the surgical treatment of metastatic bone disease. *Clin Orthop*. 2003; 415 (suppl):S14–S18.

Chapter 17
The Medical Management of Sarcomas

Richard B. Womer

Abstract Sarcomas can be classified into those usually found in children and adolescents (osteosarcoma, Ewing sarcoma, and rhabdomyosarcoma), and the non-rhabdomyosarcoma soft tissue sarcomas (NRSTS) found primarily in adults. Chemotherapy and multidisciplinary care are essential for cure in the first group, while management of the second group is controversial. Evaluation involves imaging of primary and possible metastatic sites, biopsy and diagnosis (often using molecular tools), and marrow evaluation (in Ewing sarcoma and rhabdomyosarcoma). Most children with sarcomas are entered on clinical trials, with chemotherapy to prevent the emergence of metastases. Neo-adjuvant chemotherapy has become the standard approach to osteosarcoma, Ewing sarcoma, and most rhabdomyosarcomas. Primary tumor treatment is surgical in osteosarcomas, but may include surgery, radiation, or both in rhabdomyosarcoma and Ewing sarcoma. About two-thirds of patients with localized tumors are cured with current approaches, but the outlook for patients with metastases is much poorer. The role of chemotherapy in the treatment of patients with NRSTS is uncertain, and practice varies widely. Treatment of sarcomas has many acute toxic effects, as well as many late effects including second malignant neoplasms, growth disturbances, reduced fertility, and organ dysfunction.

Keywords Osteosarcoma • Ewing's sarcoma • Rhabdomyosarcoma • Chemotherapy

Introduction

For clinical purposes, sarcomas fall into two broad categories. The first category is the three sarcomas usually found in children, adolescents, and young adults: osteosarcoma, Ewing sarcoma, and rhabdomyosarcoma. These three tumors are relatively sensitive to chemotherapy, and multidisciplinary care including chemotherapy is essential for successful treatment. The second category comprises the myriad sarcomas found primarily in adults, but also affecting adolescents and some children, the nonrhabdomyosarcoma soft tissue sarcomas (NRSTS). These tumors include synovial sarcomas, malignant peripheral nerve sheath tumors, fibrosarcomas, and malignant fibrous histiocytomas, among many others. Treatment of these diseases relies primarily on surgery and radiation therapy, and the role of chemotherapy is uncertain.

The prognosis of patients with nonmetastatic osteosarcomas, Ewing sarcomas, and rhabdomyosarcomas has improved dramatically in the last 30 years: Before the beginning of chemotherapy and multidisciplinary care in the 1970s, only about 10–20% of patients with these diagnoses survived. With current treatment, approximately two-thirds of patients with localized tumors are cured. This change reflects the relative sensitivity of these tumors to chemotherapy, and the enrollment of the majority of patients in large multi-institutional randomized controlled trials.

There has not been a similar change in the prognoses of patients with NRSTS, probably because of their limited sensitivity to available chemotherapy, the slow adoption of multidisciplinary care in their treatment, and a paucity of large randomized clinical trials. About two-thirds of patients with localized tumors survived in the 1970s, and the same is true now.

For patients with metastases at diagnosis, the situation was grim 30 years ago and remains so today. Although about one-third of patients with small numbers of pulmonary metastases can be cured, survival with widespread metastases is very rare. Chemotherapy may prolong survival in these patients, but seldom leads to cure.

There is much more knowledge about sarcomas in children and adolescents (mostly osteosarcoma, Ewing sarcoma, and rhabdomyosarcoma) than about sarcomas in adults because of the strong tradition of cooperative group clinical research in pediatrics. The majority of North American and European children with cancer are enrolled in multi-institutional clinical trials. In North America, most of these are sponsored by the Children's Oncology Group (COG), which was formed in 2001 by the merger of the Children's Cancer Group (CCG), the Pediatric Oncology Group (POG), the Intergroup Rhabdomyosarcoma Study

J.S. Khurana (ed.), *Bone Pathology*, DOI 10.1007/978-1-59745-347-9_17,

Group (IRSG), and the National Wilms Tumor Study Group. In Europe, there are now pan-European studies in rhabdomyosarcoma, through the European Pediatric Soft Tissue Sarcoma Study Group (EPSSG) and Ewing sarcoma (Euro-EWING99). Previously, a variety of organizations sponsored studies, particularly the International Society of Pediatric Oncology (SIOP), the German CWS (soft tissue sarcoma), CESS (Ewing sarcoma) and COS (osteosarcoma) consortia, and other groups in Scandanavia, the UK, and Italy.

Clinical Evaluation of Patients with Sarcoma

The clinical evaluation of a patient with a probable sarcoma has three elements: making the diagnosis, determining the extent of spread (staging), and identifying other medical problems. All of this work is best done at a center experienced in the diagnosis and treatment of sarcomas.

Diagnostic Imaging

Although patients with suspected sarcomas often have a plain radiograph as their first diagnostic image, other imaging methods have become indispensable in evaluation. The extent of the primary tumor is best determined with a contrast-enhanced MRI, which displays soft tissues much better than CT. In some anatomic locations, such as the sinuses and skull base, the superior bone imaging of CT can clarify questions of bone involvement raised by an MRI.

Since all sarcomas can metastasize to the lungs, a chest CT scan is a central component of staging. Contrast enhancement is not necessary unless one suspects involvement of hilar nodes or mediastinal structures.

Ewing sarcoma, rhabdomyosarcoma (especially alveolar histology), osteosarcoma, and occasionally NRSTS can metastasize to the skeleton. A radionuclide bone scan is the current method for detecting bony metastases, but since the imaging agent is taken up by reactive or growing bone rather than by tumor cells themselves (except in the case of osteosarcoma), there are occasional false-negative scans. A lytic skeletal metastasis may be invisible on a scan performed at diagnosis, but appear on a scan after initial chemotherapy as the bone heals.

PET (positron emission tomography) and whole-body MRI are new imaging methods whose roles in diagnosis and staging are evolving. PET using 18-fluorodeoxyglucose (FDG) has been reported to be highly sensitive and specific in soft tissue sarcomas, but FDG uptake is variable (1). Early comparisons of FDG-PET with radionuclide bone scanning and computed tomography show that PET may complement the older imaging methods, but is not yet ready to replace them (2, 3). A recent systematic, prospective comparison of FDG-PET with conventional imaging (chest CT, radionuclide bone scan, and MRI of the primary tumor) in 46 pediatric sarcoma patients found that PET was superior in detecting lymph node and skeletal involvement, while chest CT remained superior in detecting pulmonary metastases(4). In combination with CT scanning of primary tumors, FDG-PET may be able to distinguish areas of viable tumor from areas of necrosis, thus improving the yield of biopsies, and serial scans may reflect histologic response of a tumor to therapy.

Whole-body MRI scanning appears to be more sensitive than current methods of detecting skeletal and marrow metastases in patients with osteosarcoma, Ewing sarcoma, and Langerhans cell histiocytosis, though MRI detected fewer than half the lesions found with the two modalities combined (5). A comparison of whole-body MRI, FDG-PET, and bone scintigraphy in 39 children with a variety of tumors found that PET was the most sensitive, but also had the highest false-positive rate (6). Results from a prospective multi-center study by the American College of Radiology Imaging Network are pending.

The open question is whether the information from these techniques will be of practical use in assignment of treatment or prognosis. Answering this will require careful prospective clinical trials.

Biopsy

If possible, the surgeon who will perform the definitive excision of the tumor should perform, or at least supervise, the diagnostic biopsy of a suspected sarcoma. Violation of tissue planes or neurovascular structures with inexpertly placed biopsy tracts, whether closed or open, may limit excision and reconstruction options, prevent limb salvage procedures or increase the chances of local recurrence. Since sarcomas are often highly heterogeneous and contain large areas of necrosis, and since molecular techniques are often helpful in the diagnosis of many sarcomas, generous specimens are important. If closed techniques are used, many passes of the needle may be required, and frozen section confirmation of specimen adequacy is important before the procedure ends.

Bilateral marrow aspirates and biopsies are the traditional method for identifying marrow metastases of Ewing's sarcomas and rhabdomyosarcomas (especially alveolar). It is possible that whole-body MRI or FDG–PET will supplant these histologic methods, but prospective evaluations are necessary.

Osteosarcoma and Ewing Sarcoma

Adjuvant and Neoadjuvant Chemotherapy

Before the 1970s, the treatment of osteosarcoma and Ewing's sarcoma was limited to amputation or (for Ewing's sarcomas) irradiation; between 80% and 90% of patients died of metastases within 2–3 years. In the 1970s, some patients with recurrences were seen to respond to chemotherapy, and the first prospective clinical trials of adjuvant chemotherapy began.

Localized Osteosarcoma

In osteosarcoma, initial studies of adjuvant high-dose methotrexate or doxorubicin soon led to adjuvant multiagent chemotherapy regimens, including as many as seven agents. Unfortunately, none of these trials was large or randomized, and though the prognosis seemed to be improving it was unclear whether the chemotherapy deserved the credit, or whether improved imaging (CT scanning and radionuclide scanning) was identifying a lower-risk patient population (7). The Multi-Institutional Osteosarcoma Study (MIOS, 1982–86) settled the question. Patients with localized osteosarcomas underwent surgery (usually amputation), and were assigned at random to chemotherapy with seven agents, or observation; patients assigned to observation received chemotherapy in the event of a recurrence. Relapse-free survival was 63% in the chemotherapy group, and 17% in the observation group at 5 years (8); with longer follow-up, the overall survival statistics are similar.

While many centers participated in the MIOS, others assumed the effectiveness of chemotherapy and began exploring "neo-adjuvant" treatment, in which surgery followed a period of initial chemotherapy. Initially, this was designed to permit construction of custom endoprostheses for limb-sparing tumor excisions, though oncologists rationalized that it also began treatment of the likely pulmonary micrometastases without the 2- or 3-week delay previously required for surgery. A POG randomized study comparing adjuvant and neoadjuvant chemotherapy detected no difference in outcome, though poor participation limited its statistical power (9). Neoadjuvant chemotherapy gradually became the standard approach, largely because of its advantages in aiding limb-sparing excisions and reconstructions. Various large clinical trials, both in North America and Europe, gradually narrowed the chemotherapy to the current combination of high-dose methotrexate, doxorubicin, and cisplatin.

Recently, a COG randomized controlled trial showed that ifosfamide does not contribute to the efficacy of methotrexate, doxorubicin, and cisplatin (10). A European-American osteosarcoma study (EurAmOS) testing whether high-dose ifosfamide and etoposide can improve the prognosis for patients with a poor histologic response to initial chemotherapy is underway.

A biologic agent thought to stimulate pulmonary macrophages, MTP-PE, was also tested in the COG study, and shown to improve survival (10). The EurAmOS study is evaluating another biologic agent, pegylated interferon alfa-2b, in patients who have a good histologic response to initial therapy.

Localized Ewing Sarcoma

The evolution of chemotherapy in Ewing sarcoma was more systematic. The first Intergroup Ewing's Sarcoma Study (IESS-I, 1973–1978) was a North American collaboration comparing vincristine, dactinomycin, and cyclophosphamide (VAC) with the same three drugs plus whole-lung irradiation, or the same three drugs with added doxorubicin. The doxorubicin-containing arm was clearly superior, the VAC arm clearly inferior, and the VAC + radiation arm in between (11). The second IESS study (1978–1982) compared the winning regimen from IESS-I with a regimen incorporating more doxorubicin earlier in therapy; more and earlier doxorubicin proved superior (12). After a hiatus of several years, a CCG–POG cooperative study demonstrated that the addition of ifosfamide and etoposide to the then-standard combination of vincristine, doxorubicin, dactinomycin, and cyclophosphamide led to a striking improvement in survival (13). The regimen of alternating vincristine–doxorubicin–cyclophosphamide and ifosfamide–etoposide has become the standard therapy for Ewing sarcoma in North America.

Recent clinical trials have focused on improving outcomes by improving the delivery of the regimen in patients without metastases at diagnosis. A second CCG–POG study compared five-agent alternating chemotherapy given at standard doses every 3 weeks for 42 weeks with the same chemotherapy given in higher doses every 3 weeks for 30 weeks, with the same total doses in each arm; there was no difference in outcome, apart from higher toxicity in the high-dose arm (14). The first study under the auspices of the COG (formed by the merger of the pediatric cooperative groups, including CCG and POG) compared every-three-week chemotherapy with every-two-week chemotherapy, again with the same total doses in each arm. The every-two-week arm was more effective than the every-three-week arm (76% v. 65% event-free survival), with no increase in toxicity (15).

In European studies, the standard approach to Ewing's sarcoma incorporates the same drugs, but uses them all at once rather than in an alternating design. The results do not appear markedly different. The ongoing EuroEWING-99 study has a complex design including risk classification

based on the presence or absence of metastases; the location of metastases; the volume of the primary tumor, and the histohgic response of the tumor to initial chemotherapy. The randomized questions are a comparison of cyclophosphamide with ifosfamide in continuing chemotherapy for low-risk patients; and a randomized comparison of chemotherapy with autologous stem cell transplant using busulfan and melphalan chemotherapy for patients with a poor histologic response to initial chemotherapy, or with lung metastases at diagnosis.

Metastatic Bone Tumors

Patients with widespread metastases of osteosarcoma or Ewing sarcoma at diagnosis have a grim prognosis. Approaches that have improved survival for patients with localized tumors (such as the addition of ifosfamide and etoposide to Ewing sarcoma chemotherapy) have had no impact at all on outcome for patients with metastases (16–18). High-dose chemotherapy with stem cell transplant has had no demonstrable effect on outcome in metastatic Ewing sarcomas (15). These patients are usually treated on research protocols; studies now in development incorporate new biologically targeted agents along with chemotherapy.

Primary Tumor Treatment

Chemotherapy alone is insufficient to treat either osteosarcoma or Ewing sarcoma. For osteosarcoma, complete excision of all tumor, with negative margins, is essential for cure. Some patients with unresectable osteosarcomas (such as spine or skull base lesions) have been treated with radiation therapy, but the risk of local failure is high. The large majority of patients with osteosarcoma now undergo limb-sparing excisions rather than amputations, though there are some situations in which amputation is preferable (lesions of the distal tibia or fibula, for example, or in patients who will not tolerate the limitations a fragile reconstruction imposes on their activities) or essential (such as cases of neurovascular entrapment in the tumor).

The primary tumors of patients with Ewing sarcoma may be treated with either surgery or radiation. During the last 15 years, there has been a trend toward surgery, as two drawbacks of radiation therapy have become apparent: a high local failure rate, and an apparently lifelong risk of secondary osteosarcoma in the radiation field (see section on Late Effects below). Many patients are currently treated with gross surgical excision followed by irradiation of microscopic residual disease, an approach that makes possible limb preservation while avoiding irradiation of the tumor-bearing bone. Some centers, especially in Europe, make use of preoperative radiation therapy.

Histologic Assessment of Tumor Response

In osteosarcomas, patients whose tumors are mostly or entirely necrotic upon excision (after neoadjuvant chemotherapy) have a better prognosis than those whose tumors have less necrosis (20–22). There is currently no evidence that modifying the chemotherapy of patients with poor histologic responses has any impact on prognosis, though the first randomized controlled trial testing this approach (the European–American Osteosarcoma Study, or EURAMOS) is now underway. It provides patients without metastases initial treatment with methotrexate–doxorubicin–cisplatin. Patients with a good histologic response at primary tumor excision continue the same chemotherapy. Patients with a poor histologic response are randomly assigned to continue the initial chemotherapy, or to receive a more intense regimen including high-dose ifosfamide and etoposide.

When assessing response to chemotherapy, it is important to remember that osteosarcomas do not usually shrink. Ewing sarcomas often shrink as they respond, making the calculation of tumor response more problematic. Thus, for Ewing sarcoma, the relationship between histologic response and prognosis is not as clear. There is again no evidence that modification of therapy improves the prognosis of poor histologic responders, and no clinical trials of the concept are underway or planned.

Rhabdomyosarcoma

Risk Classification

Rhabdomyosarcomas are a family of tumors which are remarkably complex in diagnosis, classification, and treatment. Within a single pathologic diagnosis, the treatment and prognosis can vary widely depending on several variables with complex interctions. Different clinical trial groups have analyzed and combined criteria differently to develop different classifications, but a few variables consistently emerge.

Histology

For clinical purposes, the important histologic distinction is between embryonal and alveolar tumors, as they have considerably different clinical characteristics (Table 1). Molecular diagnosis has greatly aided the identification of alveolar rhabdomyosarcomas, but has raised the practical problem that about one-quarter of histologically alveolar tumors lack a detectable PAX-FKHR rearrangement (FKHR is also known as FOXO1A). Work to understand the biology and behavior of these “fusion-negative alveolar tumors” using gene expression profiling, proteomic analysis, and clinical data are underway (23).

Table 1 Clinical differences between embryonal and alveolar rhabdomyosarcomas.

	Embryonal	Alveolar
Age	Younger	Older
Location	Central (head, GU)	Peripheral (muscular trunk, limbs)
Invasiveness	Low to moderate	High
Metastases	Lung, regional nodes	Lung, regional nodes, distant nodes, bones, marrow, and other
Prognosis	50–90 + % progression-free survival	0–60% progression-free survival

Table 2 Rhabdomyosarcoma group and stage (IRS and COG)

Group I: Complete excision No gross or microscopic residual disease	Stage 1: Favorable site Orbit, superficial head and neck, bilary tree, paratestis, vagina
Group II: Microscopic residual disease IIa: Microscopically positive excision margins IIb: Excision margins negative; involved nodes but completely excised; most distant node negative IIc: Microscopically positive margins at primary site or grossly excised nodes; or most distant node positive	Stage 2: Unfavorable site *and* diameter ≤ 5 cm, *and* nodes clinically negative or unknown All sites except the favorable ones above are unfavorable.
Group III: Gross residual disease Biopsy only or incomplete excision	Stage 3: Unfavorable site, and: diameter > 5cm *or* clinically involved nodes
Group IV: Distant metastases	Stage 4: Distant metastases

IRS Intergroup Rhabdomyosarcoma Study, *COG* Children's Oncology Group.

The distinction between embryonal and alveolar histology has therapeutic implications for chemotherapy and radiotherapy. A tumor with favorable characteristics, but alveolar histology, is considered "intermediate risk" rather than "low risk," and is treated with more intense chemotherapy. Also, in COG studies, patients with alveolar histology tumors in Clinical Group I (histologically complete excision before beginning chemotherapy) receive local radiation therapy because of a significant risk of local recurrence, unlike their counterparts with embryonal histology tumors.

Site

The clinical behavior and prognosis of rhabdomyosarcomas varies greatly with the site of the primary tumor. For example, an embryonal rhabdomyosarcoma of the orbit is almost always curable, while an embryonal tumor arising in the ethmoid sinus, just a few centimeters away, carries about 25% mortality despite more intense therapy. The favorable sites for rhabdomyosarcoma are the orbit, superficial head and neck, biliary tree, vagina, and paratestis; all other sites are considered unfavorable. Site is the principal determinant of Stage in rhabdomyosarcoma (Table 2).

Age

The prognosis for patients with rhabdomyosarcoma is best in preschool and middle childhood, and worse for infants and adolescents and adults. The changes in prognosis with age vary gradually, however, and the boundaries of the good prognosis group have somewhat arbitrarily been set at 1 and 10 years.

Invasiveness

Invasive tumors, those which cross tissue planes or extend beyond the organ of origin, have a worse prognosis that noninvasive tumors. European studies have used this variable for risk classification, but North American clinical trials have not, largely because of difficulty in arriving at a workable definition of invasiveness that would be usable in a large cooperative group. Size is nearly as potent a variable as invasiveness in multivariate analyses, and is the variable used for classification in the IRSG and COG trials.

Clinical Group

The extent of tumor when chemotherapy begins determines the clinical group (Table 3). The first Intergroup Rhabdomyosarcoma Study (IRS-I) showed clinical group to be a powerful prognostic variable, but it is a complex one: site, invasiveness, the aggressiveness of the surgeon, the attitude of the family toward mutilating surgery, and the confidence of the treating team in chemotherapy and radiation therapy can all influence whether a tumor is excised with negative margins at diagnosis (Group I) or only biopsied (Group III).

Interactions

All of these variables interact, which complicates classification. For example, large extremity primary tumors are often alveolar histology and often occur in teenagers, and alveolar rhabdomyosarcomas are usually invasive. The most extensive multivariate analysis, based on combined European and North American data, identified site and invasiveness as the most important variables for nonmetastatic tumors (24). Since invasiveness is a difficult variable to define or score, size is used in North American staging instead.

Many different risk classification schemes exist for rhabdomyosarcomas, and they change from one clinical trial to another. In the system currently used by the COG, Stage, Clinical Group, histology, and age are combined to produce

Table 3 Risk group in Rhabdomyosarcoma (Children's Oncology Group)

	Low Risk	Intermediate Risk	High Risk
Metastases	No	No	Yes
Histology	Embryonal	Any	Any
Stage	Any if Group I or II ; 1 if Group III	1, 2, or 3 if alveolar histology; 2 or 3 if embryonal histology	4
Group	I, II, or III if Stage 1; I or II if Stage 2 or 3	III is Stage 2 or 3; I, II, or III if alveolar histology	IV

a three-way risk classification (Table 3). The primary site and tumor size determine the stage. Patients with small embryonal tumors in favorable locations are classified as low risk. Patients with metastatic alveolar tumors, or patients over age 10 years with metastatic embryonal tumors, are considered high risk. All other patients are intermediate risk.

Principles of Treatment

Successful treatment of rhabdomyosarcomas depends on integrated systemic chemotherapy and primary tumor treatment. The first randomized controlled trial of chemotherapy in rhabdomyosarcoma randomly assigned patients with completely excised tumors to a chemotherapy arm, treated with vincristine and dactinomycin, or a control arm. Patients with microscopic residual tumor were nonrandomly treated with chemotherapy, as their survival was historically so poor. The chemotherapy-treated patients had much better disease-free survival than the controls (83% vs 47%), and the patients with microscopic residual disease also benefited greatly from chemotherapy (90% vs 8% for historical controls) (25).

There have been three thematically distinct approaches to rhabdomyosarcoma in the past 20 years: the IRS Studies in North America focused on maximizing disease-free survival (the "IRS" structure is now part of the Children's Oncology Group, or COG). In Europe, the SIOP trials have sought to use chemotherapy to minimize primary tumor treatment, particularly radiation, and its attendant late effects. Finally, the German-based CWS series has focused on using the response of the primary tumor to initial chemotherapy to guide the intensity of primary tumor treatment and subsequent chemotherapy.

Chemotherapy

In the IRS–COG studies, the lowest-risk patients receive chemotherapy with vincristine and dactinomycin alone (VA). In intermediate and high-risk studies, no regimen has proven superior to VAC (vincristine–actinomycin–cyclophosphamide). The IRS-IV study (1991–1997) compared VAC to the European standard IVA (ifosfamide–vincristine–dactinomycin) and VIE (vincristine–ifosfamide–etoposide) in a three-way randomization in intermediate risk patients, and the result was a tie. Most recently, a randomized comparison of VAC with an alternating regimen of VAC and vincristine-topotecan-cyclophosphamide yielded another tie, with about 75% failure-free survival in each arm (26).

Comparisons of VAC with a wide variety of alternative regimens in high-risk patients have yielded similar results, though with much worse survival. No regimen, including high-dose therapy with autologous stem cell rescue, has had an appreciable impact on the prognosis of patients with widely disseminated alveolar tumors.

The new generation of COG trials, which opened in 2005–2006, calls for treating all low-risk patients with four cycles of VAC followed by VA for a total of 6 or 12 months, depending on age, stage, and group. For intermediate-risk patients, there is a randomized comparison of VAC with a regimen incorporating VAC and irinotecan. High-risk patients will be treated on a single-arm study using vincristine, irinotecan, and Ewing sarcoma-like chemotherapy given every 2 weeks.

The three European soft tissue sarcoma study groups have merged to form the European Pediatric Soft Tissue Sarcoma Study Group (EPSSG), which is launching a comprehensive study, RMS2005. A complex scheme sorts patients into low, standard, high, and very high-risk groups. The key randomized chemotherapy questions are whether the addition of doxorubicin to IVA early in therapy will improve outcomes, and whether a "maintenance" regimen of vinorelbine and low-dose cyclophosphamide after nine cycles of standard chemotherapy is beneficial.

Analysis of Specimens After Chemotherapy

Rhabdomyosarcomas respond to chemotherapy in a variety of ways: necrosis with shrinkage of the mass; necrosis with replacement of the tumor cells with inflammatory and fibrotic tissue, and little or no shrinkage; or differentiation of malignant cells into nonmitotic rhabdomyoblasts; or any combination of these responses. This wide repertoire makes histologic assessment of response difficult, and it is not incorporated in any planned or current trials. It is now clear that persisting rhabdomyoblasts after chemotherapy and radiation do not portend relapse, however (27).

Nonrhabdo Soft Tissue Sarcomas

The nonrhabdo soft tissue sarcomas have been a frustrating group of tumors to study. There is a wide variety of diagnoses, which may respond differently to therapy. In childhood and adolescence, the overall incidence is roughly equal to that of rhabdomyosarcoma, making any one histologic type very rare. Although these tumors are more common in adults than in children, there have been very few randomized clinical trials.

Spectrum of Disease

The NRSTS include synovial sarcomas, malignant peripheral nerve sheath tumors (also known as neurofibrosarcomas or malignant schwannomas), fibrosarcomas, chondrosarcomas, malignant fibrous histiocytomas, alveolar soft part sarcomas, epithelioid sarcomas, and others. About three-quarters of patients have localized tumors at diagnosis; metastases occur primarily in the lungs, though some (such as clear cell sarcoma and epithelioid sarcoma) also spread to regional nodes. Metastatic recurrences can happen remarkably late, as much as 20 years after treatment for alveolar soft part sarcoma, for example.

Prognostic Variables

Many studies have analyzed prognostic variables in NRSTS. Those that consistently emerge from analyses are histologic grade; tumor size (over 5 cm is the usual criterion for unfavorable prognosis); and IRS clinical group (which encompasses extent of initial excision and presence of metastases). Patients in the best prognostic group, with low-grade, small, completely excised tumors, are almost always cured with surgery alone. Patients with unresectable tumors or metastases at diagnosis rarely survive.

Principles of Treatment

NRSTS remain primarily surgical diseases. Patients whose primary tumors or metastases are unresectable seldom survive, as radiation therapy seldom sufficient for local treatment. Complete excision with clear margins, or excision with microscopically positive margins followed by radiation therapy, are generally necessary for cure.

Role of Chemotherapy

NRSTS treated with adjuvant chemotherapy often shrink. However, there is no good evidence that chemotherapy reduces the risk of recurrence. The generally good prognosis, variety of histologies, and rarity of these tumors have made randomized controlled trials difficult. A POG study found no difference between groups of patients with NRSTS randomly assigned to chemotherapy or observation, but poor accrual severely limited the trial's statistical power (28). A multivariate analysis of 219 children and adolescents with synovial sarcoma from a variety of cooperative groups and institutions showed a weak association between chemotherapy responsiveness and survival, but there were too few patients who received local therapy alone to assess the impact of chemotherapy on survival overall (29). A retrospective analysis of 356 adult patients with NRSTS treated at two institutions over a 25-year period showed a survival advantage for those receiving neoadjuvant chemotherapy (ifosfamide and doxorubicin), though such a study design has many confounding variables (30).

When chemotherapy is used, it is usually a combination of doxorubicin and ifosfamide. Clinical trials are in development for both children and adults that will involve centrally reviewing pathology, applying molecular diagnostic techniques, uniformly assigning risk groups, and treating intermediate and high-risk patients with chemotherapy. While not randomized, these studies should significantly enhance our understanding of these diseases.

Acute and Late Effects of Sarcomas and Their Treatment

Acute Effects of Chemotherapy

The chemotherapy of sarcomas, like other cancer chemotherapy, has a variety of well-known side effects, including nausea and vomiting, hair loss, myelosuppression, and mucositis. Different regimens cause different toxicities in different patients, making any one patient's reactions unpredictable.

Cisplatin, used in osteosarcoma chemotherapy, is particularly potent at causing nausea and vomiting, which may last for several days after treatment. It can also cause acute (and chronic) renal electrolyte wasting. High-dose methotrexate with leucovorin "rescue" can cause acute renal failure if not properly administered, and may do so idiosyncratically as well. Cyclophosphamide and ifosfamide are metabolized to compounds that are toxic to the urinary bladder mucosa, and may produce hemorrhagic cystitis; mesna is often given with cyclophosphamide and

ifosfamide to chemically neutralize these metabolites. Etoposide carries a high risk of acute allergic reactions, including anaphylaxis.

Late Effects of Therapy

The intense chemotherapy, surgery, and radiation therapy used to treat sarcomas have many late effects as well. Although some are attributable to a single treatment modality, there are also interactions. The study of late effects in children has been ongoing for two decades but is just beginning in adults.

Late effects are a problem of considerable magnitude: The Childhood Cancer Survivor Study compared 10,397 childhood cancer survivors an average of 17.6 years from their diagnosis with 3034 siblings, and found that survivors were 3.3 times as likely as their siblings to have a chronic health condition, 4.9 times as likely to have multiple chronic health conditions, and 8.2 times as likely to have severe, disabling, or life-threatening conditons. Bone tumor survivors were at the highest risk (relative risk 38.9). The cumulative incidence of severe, disabling, life-threatening, or fatal conditons was 42.4% at 30 years. The problems included major joint replacement (not part of original therapy), congestive heart failure, second malignancies, cognitive dysfunction, strokes, renal failure, hearing or vision loss, and ovarian failure. Some of the treatments most associated with later problems included chest radiation plus an anthracycline (such as doxorubicin), or an alkylating agent (such as cyclophosphamide or ifosfamide) plus an anthracycline—both common in sarcoma patients (31).

Second Malignancies

Second malignancies are multifactorial in origin, just as primary malignancies are. Thus, hereditary predisposition, environmental factors, chemotherapy, radiation therapy, and influences unknown interact to produce second malignancies.

The most common types of second malignant neoplasms, are secondary acute myeloid leukemia or myelodysplasia (AML/MDS), and secondary sarcomas. AML/MDS can arise from treatment with alkylating agents (such as cyclophosphamide and ifosfamide), etoposide, or doxorubicin, and the risk may be further increased by radiation therapy. It tends to occur in the first 5–7 years after the completion of treatment. Studies of Ewing sarcoma survivors have found the incidence of AML/MDS to be about 2%, though patients treated with high-dose regimens may have a higher risk. Secondary AML/MDS appears to be more resistant to treatment than the sporadic forms, and only about one-third of patients survive.

Secondary sarcomas, especially osteosarcoma, usually occur in radiation fields, and the risk is increased by chemotherapy (32, 33). The interval between the treatment and the emergence of the second tumor is generally at least 5 years. In Ewing sarcoma, there appears to be roughly a 5% risk of secondary sarcoma in the irradiated bone per decade of survival, varying with the radiation dose, and it does not appear to diminish with time (34).

Growth Disturbances

Global decreases in linear growth from childhood cancer therapy appear to be unusual. Many children grow more slowly than previously while receiving treatment, but appear to have a period of catch-up growth when treatment ends. The exceptions are patients who receive radiation therapy to the pituitary, who may have growth hormone deficiency leading to short stature, and these who experience puberty during therapy.

Decreased growth of irradiated body parts is common, however, and may be potentiated by chemotherapy. Childhood tissues irradiated to a dose of 20Gy or more grow very little, if at all, potentially leading to severe deformity and disability. Patients with heritable retinoblastoma have a particularly high risk of secondary sarcomas in radiation fields. Other solid tumors in survivors of childhood sarcomas are associated with both radiation therapy and chemotherapy, and include carcinomas of the breast, thyroid, head and neck, bladder, and colon (35).

Organ-Specific Chemotherapy Late Effects

Doxorubicin can cause a cardiomyopathy leading to arythmias or congestive heart failure, which may occur many years after treatment. The risk seems to vary with the patient's age at the time of treatment and sex but is roughly 2–5% over 20 years. Cisplatin can cause irreversible high-frequency hearing loss; the risk is greatest with high cumulative doses and younger age at treatment (36). Cisplatin and ifosfamide can both cause chronic nephropathies with electrolyte wasting.

The effects of sarcoma chemotherapy on fertility are just emerging, because of the often long interval between treatment and attempted parenthood. The ovaries appear to be highly resistant to chemotherapy, though there may be a tendency toward early menopause. The testes are highly sensitive, with a high risk of permanent azoospermia in most males treated with sarcoma chemotherapy.

Medical Management of Skeletal Metastases

Many malignancies can metastasize to the skeleton; in addition to sarcomas, they include carcinomas, melanoma,

myeloma, and lymphomas. Some brain tumors can metastasize to bone, usually after gaining access to the peritoneum or vasculature through a shunt. In childhood, retinoblastoma bone and soft tissue sarcomas, neuroblastoma, lymphoma and clear cell sarcoma of the kidney can have skeletal metastases. Most patients with bone metastases do not have hypercalcemia, but the lesions can be very painful and lead to pathologic fractures.

Individual bone metastases are often treated with radiation therapy or surgery. Widespread bony metastases generally require systemic treatment. While such treatment usually targets the cancer cells (chemotherapy or hormonal therapy), there is increasing use of agents targeting the bone itself. Metastatic tumor cells generally destroy bone by stimulating osteoclasts. Bisphosphonates are a class of drugs (including pamidronate, etidronate, zolidronate, and several others) which bind to bone matrix and decrease the activity of osteoclasts; they have been shown to increase bone density, slow the growth of established skeletal metastases, and inhibit the development of new skeletal metastases (30). Ideally, patients with bone metastases, or at high risk for them, should receive multidisciplinary care.

References

1 Aoki, J., H. Watanabe, et al. (2001). "FDG PET of primary benign and malignant bone tumors: standardized uptake value in 52 lesions." *Radiology* **219**(3): 774–7.

2. Franzius, C., J. Sciuk, et al. (2000). "FDG-PET for detection of osseous metastases from malignant primary bone tumours: comparison with bone scintigraphy." *European Journal of Nuclear Medicine* **27**(9): 1305–11.

3. Franzius, C., H. E. Daldrup-Link, et al. (2001). "FDG-PET for detection of pulmonary metastases from malignant primary bone tumors: comparison with spiral CT." *Annals of Oncology* **12**(4): 479–86.

4. Volker, T., T. Denecke, et al. (2007) "Positron-Emission Tomography for staging of pediatric sarcoma patients: Results of a prospective multicenter trial." *Journal of Clinical Oncology* **34**(25): 5435-5441.

5. Mentzel H.-J., K. Kentouche, et al. (2004). "Comparison of whole-body STIR-MRI and 99mTc-methylene-diphosphonate scintigraphy in children with suspected multifocal bone lesions." *European Radiology* 14:2297–2302

6. Daldrup-Link, H. E., C. Franzius, et al. (2001). "Whole-body MR imaging for detection of bone metastases in children and young adults: comparison with skeletal scintigraphy and FDG PET." *AJR American Journal of Roentgenology* **177**(1): 229–36.

7. Lange, B. and A. S. Levine (1982). "Is it ethical not to conduct a prospectively controlled trial of adjuvant chemotherapy in osteosarcoma?" *Cancer Treatment Reports* **66**(9): 1699–1703.

8. Link, M. P., A. M. Goorin, et al. (1986). "The Effect of adjuvant chemotherapy on relapse-free survival in patients with osteosarcoma of the extremity." *New England Journal of Medicine* **314**(25): 1600–6.

9. Goorin, A. M., D. J. Schwartzentruber, et al. (2003). "Presurgical chemotherapy compared with immediate surgery and adjuvant chemotherapy for nonmetastatic osteosarcoma: Pediatric Oncology Group Study POG-8651.[see comment]." *Journal of Clinical Oncology* **21**(8): 1574–80.

10. Meyers P.A., C. Schwartz, et al. (2008) "Osteosarcoma: The addition of muramyl tripeptide to chemotherapy improves overall survival—A Children's Oncology Group study. *Journal of Clinical Oncology* **26**:633-638.

11. Nesbit, M. E., E. A. Gehan, et al. (1990). "Multimodal therapy for the management of primary, nonmetastatic Ewing's sarcoma of bone: a long-term follow-up of the first intergroup study." *Journal of Clinical Oncology* **8**(10 October): 1664–1674.

12. Burgert, E. O., M. E. Nesbit, et al. (1990). "Multimodal therapy for the management of nonpelvic localized Ewing's sarcoma of bone: intergroup study IESS-II." *Journal of Clinical Oncology* **8**(9 September): 1514–1524.

13. Grier, H. E., M. Krailo, et al. (2003). "Addition of ifosfamide and etoposide to standard chemotherapy for Ewing's sarcoma and primitive neuroectodermal tumor of bone." *New England Journal of Medicine* **348**(8): 694–701.

14. Granowetter, L., R.B. Womer, et al. (2009). "Dose-intensified compared with standard chemotherapy for nonmetastatic Ewing sarcoma family of tumors: a Children's Oncology Group Study." *Journal of Clinical Oncology* **27**: 2536–2541.

15. Womer R.B., D.C. West, et al. (2008) "Randomized comparison of every-two-week v every-three-week chemotherapy in Ewing sarcoma family tumors (ESFT)" *Journal of Clinical Oncology* 26 (Suppl.), No. 10504.

16. Meyers, P. A., G. Heller, et al. (1993). "Osteogenic sarcoma with clinically detectable metastasis at initial presentation." *Journal of Clinical Oncology* **11**(3): 449–53

17. Kager, L., A. Zoubek, et al. (2003). "Primary metastatic osteosarcoma: presentation and outcome of patients treated on neoadjuvant Cooperative Osteosarcoma Study Group protocols." *Journal of Clinical Oncology* **21**(10): 2011–8.

18. Miser, J., M. Krailo, et al. (2004). "Treatment of metastatic Ewing's sarcoma or primitive neuroectodermal tumor of bone: evaluation of combination ifosfamide and etoposide—a Children's Cancer Group and Pediatric Oncology Group study." *Journal of Clinical Oncology* **22**(14): 2873–2877.

19. Marina, N. and P. Meyers (2005). "High-dose therapy and stem-cell rescue for Ewing's family of tumors in second remission." *Journal of Clinical Oncology* **23**(19): 4262–4264.

20. Meyers, P. A., G. Heller, et al. (1992). "Chemotherapy for nonmetastatic osteogenic sarcoma: the Memorial Sloan-Kettering experience." *Journal of Clinical Oncology* **10**(1): 5–15.

21. Bielack, S. S., B. Kempf-Bielack, et al. (2002). "Prognostic factors in high-grade osteosarcoma of the extremities or trunk: an analysis of 1,702 patients treated on neoadjuvant cooperative osteosarcoma study group protocols.[see comment]." *Journal of Clinical Oncology* **20**(3): 776–90.

22. Meyers, P. A., C. L. Schwartz, et al. (2005). "Osteosarcoma: a randomized, prospective trial of the addition of ifosfamide and/or muramyl tripeptide to cisplatin, doxorubicin, and high-dose methotrexate.[see comment]." *Journal of Clinical Oncology* **23**(9): 2004–11.

23. Barr, F. G., S. J. Qualman, et al. (2002). "Genetic heterogeneity in the alveolar rhabdomyosarcoma subset without typical gene fusions." *Cancer Research* **62**(16): 4704–10.

24. Rodary, C., E. A. Gehan, et al. (1991). "Prognostic factors in 951 nonmetastatic rhabdomyosarcoma in children: a report from the international rhabdomyosarcoma workshop." *Medical and Pediatric Oncology* **19**: 89–95.

25. Heyn, R. M., R. Holland, et al. (1974). "The role of combined chemotherapy in the treatment of rhabdomyosarcoma in children." *Cancer* **34**: 2128–2142.

26. Arndt C.A., D.S. Hawkins, et al. (2007) "Randomized phase III trial comparing vincristine, actinomycin, cyclophosphamide (VAC) with VAC/V topotecan/cyclophosphamide (TC) for intermediate

risk rhabdomyosarcoma (IRRMS). D9803, COG study." *Journal of Clinical Oncology* 25(18 Suppl.), No. 9509.
27. Ortega, J. A. R. J et al., (2000). "Presence of well-differentiated rhabdomyoblasts at the end of therapy for pelvic rhabdomyosarcoma: implications for outcome". *Journal Pediatric Hematology/Oncology* **22**(2): 106–111.
28. Pratt, C., A. Pappo, et al. (1999). "Role of adjuvant chemotherapy in the treatment of surgically resected pediatric nonrhabdomyosarcomatous soft tissue sarcomas: a Pediatric Oncology Group study." *Journal of Clinical Oncology* **7**: 1219–1226.
29. Okcu, M. F., M. Munsell, et al. (2003). "Synovial sarcoma of childhood and adolescence: a multicenter, multivariate analysis of outcome." *Journal of Clinical Oncology* **21**(8): 1602–11.
30. Grobmyer, S. R., R. G. Maki, et al. (2004). "Neo-adjuvant chemotherapy for primary high-grade extremity soft tissue sarcoma." *Annals of Oncology* **15**(11): 1667–72.
31. Oeffinger K.C., A.C. Mertens, et al. (2006) "Chronic health conditions in adult survivors of childhood cancer." *New England Journal of Medicine* **355**(15):1572–1582.
32. Tucker, M. A., G. J. D'Angio, et al. (1987). "Bone sarcomas linked to radiotherapy and chemotherapy in children." *The New England Journal of Medicine* **317**: 588–593.
33. Neglia, J. P., D. L. Friedman, et al. (2001). "Second malignant neoplasms in five-year survivors of childhood cancer: childhood cancer survivor study." *Journal of the National Cancer Institute* **93**(8): 618–29.
34. Kuttesch, J. F. J., L. H. Wexler, et al. (1996). "Second malignancies after Ewing's sarcoma: radiation dose-dependency of secondary sarcomas." *Journal of Clinical Oncology* **14**(10 (October)): 2818–2825.
35. Bassal M., A.C. Mertens, et al. (2006) "Risk of selected subsequent carcinomas in survivors of childhood cancer: A report from the Childhood Cancer Survivor Study." *Journal of Clinical Oncology* **24**:476–483.
36. Li, Y., R. B. Womer, et al. (2004). "Predicting cisplatin ototoxicity in children: the influence of age and the cumulative dose.[see comment]." *European Journal of Cancer* **40**(16): 2445–51.
37. Berenson, J. R. (2005). "Recommendations for zoledronic acid treatment of patients with bone metastases." *Oncologist* **10**(1): 52–62.

Chapter 18
Radiation Therapy for Sarcomas

Amit Maity

Abstract The use of radiation therapy for the management of sarcomas is time honored; however, newer advances in the field and understanding of its limitations and problems have changed the application considerably. This chapter discusses some of these changes and then addresses certain specific bone and soft tissue tumors.

Keywords Radiation therapy; • Oncology • Rad • Gy, cGy: Brachytherapy • Teletherapy • High-energy linear accelerator • Electrons • Proton beam • Survival fraction • Hyperfractionation • Three-dimensional conformal radiation therapy • Multileaf collimator • Intensity-modulated radiation therapy • Ewing's sarcoma • Rhabdomyosarcoma

Introduction

Shortly after their discovery in 1895 by Wilhelm Roentgen, the biologic effects of X-rays were recognized, leading to their rapid adoption in the treatment of cancer. Cures were reported by 1899, and the discipline of radiation oncology developed rapidly thereafter. There have been many changes over the past century, driven by both technological advances in the delivery of radiation and by improved understanding of biology. Radiation therapy is now an integral component of the overall management of many patients with cancers, in particular sarcomas.

Physical Aspects of Radiation Therapy

Historically, the "rad" was the unit for radiation therapy dose but has now been supplanted by the gray (Gy), the International System of Units (SI units) standard unit of measurement. One Gy is equivalent to one joule of absorbed energy per kilogram mass. By definition, 100 rad is equivalent to a Gy and, therefore, one rad equals one centigray (cGy).

Brachytherapy and external beam radiation therapy (teletherapy) are the two primary means of delivering therapeutic irradiation. Brachytherapy involves the implantation of a radioactive source in the region of the tumor. The advantage of brachytherapy over teletherapy is that because of the inverse square law, there is a very rapid falloff of dose from the radioactive source, resulting in less radiation to normal tissues that are several centimeters away from the sources. For brachytherapy in sarcomas, often catheters are laid in the tumor bed at surgery, and then approximately a week later, radioactive sources are threaded into the catheters (afterloaded) to deliver the radiation over several days. A number of different radioactive sources have been used for brachytherapy, with differing half-lives and types of radioactivity emitted. There is substantial literature (on the use of) brachytherapy for sarcomas, especially of the extremities. However, this technique is used less commonly than it might because it requires close cooperation between the surgeon and radiation oncologist, specialized skill on the part of the radiation oncologist, and significant physics support.

The vast majority of patients who undergo radiotherapy receive external beam radiation. High-energy linear accelerators (linacs) are the workhorses of modern day radiation oncology departments. The linear accelerator is typically mounted on a gantry that can rotate 360° around a patient (Fig. 1). The patient lies on a "couch" that has limited rotation capability. Therefore, there are many angles through which the radiation beam can be directed. Linear accelerators generally have the capability of delivering both high-energy X-rays and electrons. The physical properties of X-rays and electrons differ in major ways. High-energy X-rays will penetrate further into tissues and display more skin sparing than electrons. However, in cases in which it is desirable to deposit much of the energy at or near the skin surface, for example, in treating skin cancers or superficial lymph nodes, electrons are preferred.

Although X-ray and electron beams are by far the most common forms of radiation in use today for the treatment of cancer, other types of atomic particles have also been used clinically. Protons and even heavier ions (such as carbon) have also been used in selected centers. These particles have an unusual physical characteristic when compared to X-rays in that their energy deposition peaks many centimeters at depth from the skin and then rapidly falls off distal to this region. Therefore, with proton beam therapy it is possible to

J.S. Khurana (ed.), *Bone Pathology*, DOI 10.1007/978-1-59745-347-9_18,

Fig. 1 Linear accelerator used for clinical radiotherapy. Patient lies on platform around which a gantry can rotate 360° to deliver external beam radiation. The couch can also be moved to increase the variety of angles at which radiation can be delivered

have lower radiation doses to normal tissues than with X-rays. The main drawback of proton beams is their expense; hence, there are only a handful of proton beam centers currently in operation in the United States with several more facilities planned for opening in the next 5 years.

Biologic Principles of Radiation Therapy

Ionizing radiation is thought to kill cells primarily by causing DNA damage (1). Approximately a third of this damage results from direct damage to the DNA; the remainder occurs indirectly by interaction of radiation with water molecules to generate free radicals that react with DNA. Double-strand breaks (DSBs) result when breaks occur close together on both strands of a DNA molecule. DSBs are thought to be the primary lesion that leads to cell death. Some studies have found a correlation between the number of DSBs generated and the level of cell killing. If a cell sustains more DNA damage than it can repair, it may die either while undergoing mitosis (mitotic cell death) or by programmed cell death (apoptosis).

A clonogenic survival assay is typically used to measure the sensitivity of a cell to the effects of ionizing radiation. Known numbers of cells are seeded in different plates, then the plates are irradiated with different doses of radiation. Weeks later, the plates are stained and the number of colonies counted. The survival fraction is the ratio of the number of colonies that grow divided by the number of cells seeded. When the survival fraction is plotted versus the dose, a cell survival curve is generated (Fig. 2). Generally, there is a "shoulder" in the low-dose region due to the ability of cells to repair sublethal DNA damage. Tumor cells often display a reduced "shoulder" width compared to their counterpart normal cells. Fractionated radiotherapy exploits this difference in the "shoulder" region to increase the therapeutic index. By adding low doses together in this manner, therapeutic advantage can be magnified.

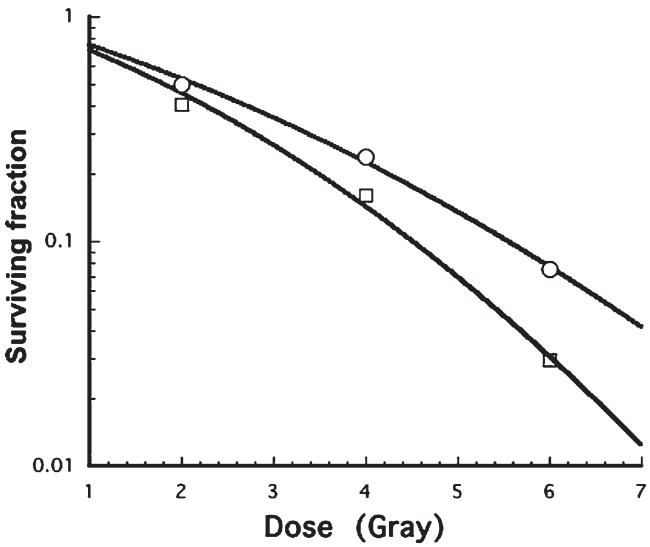

Fig. 2 Cell survival curves for mammalian cells. The fraction of cells surviving is plotted on a logarithmic scale against dose on a linear scale. Typically, cells have a shoulder corresponding to low radiation doses, which is presumed to be due to the ability of most cells to repair sublethal DNA damage

Patients who are treated definitively with the expectation of cure generally receive 1.8–2.0 gray (Gy) per day. Daily (Monday through Friday) radiation treatments are given over the course of many weeks. The total cumulative dose varies for different tumor types, but for common cancers in adults, often 60–70 Gy are given over a 6–8-week course of treatment. Altered fractionation schemes have been used in an attempt to further exploit the differential response of tumor versus normal cells to radiation in the low-dose region. One example is hyperfractionation using 1.0–1.2 Gy twice a day. In theory, hyperfractionation can further increase the therapeutic index compared to standard fractionation, either by permitting the delivery of higher tumor doses with similar late normal tissue toxicity or by comparable tumor doses with a concomitant decrease in late normal tissue toxicity. However, in clinical trials hyperfractionation has not lived up to its theoretical promise; therefore, it is rarely used outside of a study setting.

Tumor oxygenation is another factor that can alter the response of tumors to radiation therapy. Oxygen is required for radiation-induced free radical formation, which accounts for the majority of the damage to DNA. Approximately 2.5–3 times as much radiation dose is necessary to cause the same level of cell killing in cells irradiated in complete anoxia compared to cells irradiated in well-oxygenated conditions. Hypoxia is associated with a poorer outcome in many tumor types, including sarcomas. Part of this may be because hypoxia is associated with increased biologic aggressiveness, but the fact that hypoxic tumors are more resistant to radiation therapy may also play a role.

Radiation Therapy: Clinical Issues

Planning and verification steps need to be undertaken before a patient can undergo radiotherapy. The first step in this process involves "simulation" of the proposed radiation beams, generally using a planning CT scan. At the start of simulation, the patient must be placed in the optimal position so that subsequent treatments can be delivered reproducibly while minimizing dose to normal tissues. The position will vary depending on the site of the tumor. For a patient with a sarcoma of thigh, this may involve placing the leg in a frog-leg position, which separates the anterior thigh from the flexor and adductor compartments. For a patient with a sarcoma of the calf, elevating the affected leg above the other allows easy access to the posterior compartment of the leg with the tumor while sparing the other leg altogether. Custom-made foam cradles or thermoplastic casts are often used to maintain the patient in the proper position.

The patient then undergoes CT scanning in the treatment position. Once the CT scanning is completed, the target volume is outlined on the CT scan slices. In some cases, this can be accomplished by merging the treatment planning CT with a diagnostic MRI scan of the region. In the 1990s, the most complex treatment planning was done using three-dimensional conformal radiation therapy (3D-CRT). Beams are chosen with the aid of commercially available treatment planning software to optimize coverage of the target volume while minimizing dose to normal tissues. The simplest arrangements utilize beams of radiation that originate from simple, easily verifiable directions (e.g., anterior/posterior, laterals); however, more complicated beam arrangements with noncoplanar beams approaching at oblique angles can also be used. Historically, each of the radiation field from each beam was shaped with custom-made blocks that were made from a low-melting weight alloy and were mounted in the head of the machine. A modern alternative is the multileaf collimator, in which movable leaves are controlled by a computer to create different blocking patterns (Fig. 3).

3D-CRT is still used; however, over the past few years, intensity-modulated radiation therapy (IMRT) has been used for the most complicated cases. The planning for IMRT is far more involved than for 3D-CRT. Instead of simply deciding on beam arrangements and calculating doses to normal tissues, with IMRT, the physician must specify dose–volume constraints for various critical structures as well as for the target volume. Sophisticated computer software is then used that goes through thousands of iterations to determine a plan than optimizes coverage of the target while adhering to the constraints selected. IMRT plans generally utilize more beams than 3D-CRT plans. Furthermore, with IMRT, as the

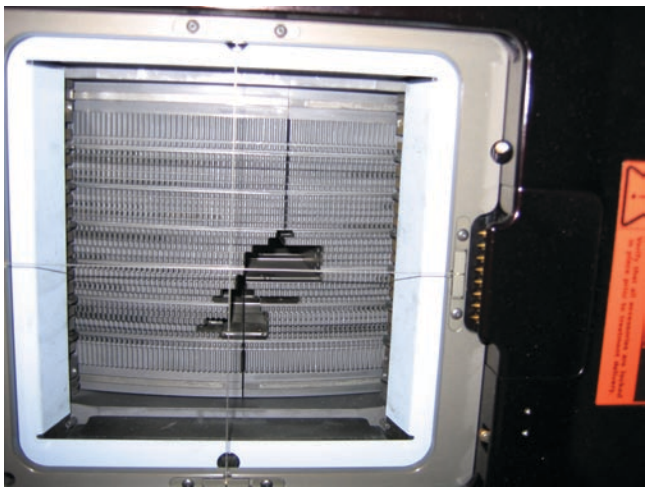

Fig. 3 Multileaf collimator mounted on the head of linear accelerator. As X-rays leave the linear accelerator, they pass through a collimator. Metal "leaves" in the collimator block the transit of X-rays to the patient, allowing for shaping of the beam. Movement of the leaves is computer controlled, so that the pattern of blocking can be changed rapidly, allowing for multiple modulations of the beam. The ability to alter the shape of the radiation beam by computer is essential for intensity-modulated radiotherapy (*IMRT*)

radiation is being delivered via a specific beam orientation, it may be modulated many times by using the multileaf collimators . The result from all this complexity is that for tumors in certain locations that IMRT plans give more conformal dose distributions than 3D-CRT plans, thereby reducing both acute and late toxicity.

After a plan has been devised, the next step involves patient setup during which films are taken on the treatment machine to confirm that the patient is positioned correctly and the beams are set up properly. Once this has been done, the patient is ready to start treatment.

Radiation Therapy for Ewing's Sarcoma

Doses greater than 60 Gy, sometimes as high as 75 Gy were used in the 1960s to achieve local control in Ewing's sarcoma. The severe late effects following such doses, especially in children, led to the lower doses in current use. A German cooperative group study reported that patients who received ~60 Gy of radiation using either standard once daily X-ray therapy (XRT) or a split-course twice-a-day hyperfractionated regimen had equivalent local control rates; 82% and 86%, respectively. Patients in a British trial who received 55 Gy had a similar local control rate (82%). Attempts have been made to further reduce the XRT dose. At St. Jude Children's Research Hospital, 30–36 Gy was used for patients with a good response to induction chemotherapy and 50–60 Gy for those with a poor response with an overall local control rate of only 68% (2)**.** However, for patients treated with the lower doses, local control rate was significantly higher if tumor was less than 8 cm (90% vs 52%; $p = 0.05$). Therefore, selected patients may be treated with lower radiation doses without compromising local control. However, standard therapy remains 55–60 Gy for gross disease. On recent CCG (Children's Cancer Group) and COG (Children's Oncology Group) studies for Ewing's sarcoma, the recommended dose for gross disease was 55.8 Gy in 1.8 Gy fractions for most cases. Exceptions include lesions adjacent to critical structures that could not tolerate this dose; for example, tumors of the vertebral body were treated to 45 Gy to prevent damage to the spinal cord.

Over time, there has also been a reduction in the volume of bone that is irradiated. In the 1960s and early 1970s, it was common to treat the entire bone to 60 Gy. The practice was based partly on the inability of plain films to define accurately the volume of bone affected by tumor. However, with the advent of CT and MRI scans, it is now possible to more accurately define the extent of bone involvement as well as the extraosseous soft tissue extension. In a POG (Pediatric Oncology Group) trial, patients were randomized to receive either 39.6 Gy to the whole bone followed by a 16.2 Gy boost to the involved portion or 55.8 Gy to the involved bone only (3). No difference in local control was found with most failures occurring centrally within the XRT fields.

Recent CCG and COG protocols recommend that XRT start after 12 weeks of chemotherapy. By this time, the soft tissue component has often shrunk significantly. These protocols suggest that the entire prechemotherapy volume (both soft tissue mass and osseous tumor extent) with a 1.5 cm margin be treated to a dose of 45 Gy. After this, most lesions receive an additional 10.8 Gy to a smaller boost volume that includes the entire *pre*chemotherapy osseous tumor volume, but the residual *post*induction chemotherapy soft tissue tumor volume. In general, radiation ports for Ewing's sarcoma should exclude the epiphysis to minimize leg shortening, unless absolutely necessary. They should not extend across the joint space, to prevent joint dysfunction. Furthermore, a strip of subcutaneous tissue should be excluded to avoid circumferential high-dose XRT to help avoid lymphatic obstruction that can occur through post-XRT scarring and a tourniquet effect.

XRT for Ewing's sarcoma can lead to induration, fibrosis, impaired bone growth, and increased risk of fracture; however, the most serious complication is the occurrence of a second malignant neoplasm (SMN). The most common SMN following radiation for Ewing's sarcoma is osteosarcoma, but soft tissue sarcoma and other cancers such as brain tumors, lung cancer, and skin cancer have also been reported. In a study from the Late Effects Study Group, the risk of SMN following treatment of Ewing's sarcoma was 22% at 20 years; however, many of these patients had received doses greater than 60 Gy (4). In one multi-institutional study, the estimated cumulative incidence rates at 20 years for any SMNs and for secondary sarcomas were 9.2% and 6.5%, respectively (5). All secondary sarcomas occurred at or near the primary tumor site and within the primary radiation field. The cumulative incidence rate of secondary sarcoma was radiation dose-dependent with no secondary sarcomas developing in patients receiving less than 48 Gy. In German cooperative group studies, no secondary sarcomas developed in 162 patients who underwent surgery without radiation, but the cumulative incidence of secondary sarcoma was 3–6% at 15 years in 486 patients treated with definitive or postoperative radiation (6).

Radiation therapy was once the standard modality for local control in Ewing's sarcoma. A number of factors since the 1980s including innovations in orthopedic techniques, doubts regarding the efficacy of radiation therapy in controlling larger tumors, and the realization of the high incidence of SMNs following radiation have led to a resurgence of interest in surgery. For certain expendable bones, such as the fibula, clavicle, and rib, surgery is clearly preferred since removal of these bones causes relatively little morbidity. For sites such as the vertebrae or nasopharynx where total

resection is impossible or cosmetically disfiguring, XRT is preferred. In most other cases, the decision between radiation and surgery must be made on an individual basis, weighing their respective risks of complication. These modalities have never been compared in a randomized trial. In a compilation of a number of series, the local control following XRT alone using doses between 45 and 65 Gy ranged from 53% to 88% (7, 8). As mentioned previously, some large cooperative studies have found local control rates in the 80–85% range with radiation. Most series using surgery alone for local control have reported higher local control rates, ranging from 90% to 95%. However, the advantage of surgery may not be as great as the numbers suggest at first glance due to an inherent selection bias in favor of surgery. Smaller, easier to resect tumors are more likely to have undergone surgery whereas larger, harder to resect tumors (i.e., pelvic bones) are more likely to be treated definitively with radiation. Furthermore, the XRT used in some of the series showing particularly low rates of local control may have been suboptimal by today's standards due to poor imaging of the tumor. In a POG study, the quality of XRT, as determined by central review, dramatically influenced local control: 80% for patients with appropriate radiotherapy to 48% and 16% for those with to minor or major protocol violations, respectively.

There are cases in which surgery is performed with the intention of achieving a complete excision, but the pathology shows close or positive margins. In these cases, postoperative radiation therapy is often given, usually within a few weeks of surgery. In recent CCG and COG studies, the recommended dose for microscopic residual disease in the postoperative setting has been 50.4 Gy; however, other groups have used 45 Gy in these cases with excellent local control. Limited data suggest that doses as low as 30 Gy may be effective for local control in patients who have only microscopic positive margins. In addition to its use for close or positive margins, some investigators have advocated postoperative XRT for patients who have undergone resections with wide margins if the pathology shows a poor histologic response to chemotherapy.

Radiation Therapy for Rhabdomyosarcoma

Rhabdomyosarcomas are often treated with radiation therapy for local control. In the 1960s, doses as high as 60–65 Gy were used, but this led to serious late effects. Over the decades, the XRT doses have been lowered. On Intergroup Rhabdomyosarcoma Study (IRS) IV, patients with gross residual disease following initial surgery were randomized to receive either 50.4 Gy in conventional fractionation or 59.4 Gy with hyperfractionation (9). The overall 5 year local relapse rate was 13% and the regional relapse rate was 3%. To date, there has been no difference in local control, freedom from relapse, or overall survival.

Some patients with rhabdomyosarcoma may be able to forego XRT without a compromise in local control. In a retrospective analysis of patients with Group I disease (completely resected with negative margins) treated on several IRS trials, children with alveolar or undifferentiated rhabdomyosarcoma who had been treated with radiation were found to have fared much better than their nonirradiated counterparts (10). However, Group I patients with embryonal histology did not benefit from XRT.

Some have questioned whether radiation can be avoided in patients with Group II disease (microscopic residual). In an analysis of several German cooperative group trials, the local control rate was 83% in children with Group II disease who received XRT (median dose 45 Gy) versus 65% for those who did not ($p < 0.004$) (11). Data from St. Jude and Memorial Sloan-Kettering Cancer Center (MSKCC) suggest that it may be possible to lower the dose to 30–40 Gy in patients with Group II disease and still achieve excellent local control.

There are also European data detailing the outcome of children with Group III (gross residual) disease in whom XRT was omitted, generally because of young age or a complete response to chemotherapy and/or second look surgery. These studies, coming from German cooperative groups and SIOP (International Society of Pediatric Oncology), have found a higher than expected local relapse rate in patients in whom XRT was omitted. Another study analyzed the outcome of 306 children with orbital rhabdomyosarcomas, mostly group III, combining data from trials from four international cooperative groups (12). This report found local relapse rates of 8% and 44%, respectively, in those who did and did not initially receive XRT. However, this did not translate into an overall survival advantage for patients who received upfront XRT because of effective salvage therapy.

In the United States, there has been a reluctance to eliminate XRT in the treatment of rhabdomyosarcoma. Commonly, accepted doses are ~50 Gy for most patients with Group III disease and 41 Gy for those with Group II disease. Group III embryonal orbital rhabdomyosarcomas have been treated to 45 Gy with excellent local control.

Through the decades, the timing of XRT in relation to the start of chemotherapy has changed on IRS studies. In IRS IV, most patients received XRT at week 9 of chemotherapy. In IRS V, radiotherapy was given at week 3 in low-risk patients or at week 12 in intermediate-risk patients. In general, the trend has been to give XRT later to allow for chemotherapy to be delivered to address micrometastatic disease. The only patients who currently receive XRT emergently at the time of diagnosis are those with intracranial extension of their disease.

Numerous late complications attributable to XRT have been described in children treated on IRS studies, most commonly hypoplasia within the irradiated region. The peak incidence for rhabdomyosarcomas is between 2 and 5 years of age when children are particularly susceptible to radiation-induced growth delay. For those irradiated to the head and neck region, short stature (pituitary irradiation), poor dentition, malformed teeth, cataracts, corneal changes, optic atrophy, and decreased hearing acuity can occur. It is interesting to note that SMNs, which occur at such a high frequency after XRT for Ewing's sarcoma, are much less common following therapy for rhabdomyosarcoma. In the latter, the estimated rate is only 1.7% at 10 years, in spite of the fact that similar radiation doses have been used for both types of sarcomas (13).

Radiation Therapy for Nonrhabdomyosarcomatous Soft Tissue Sarcoma

There is a group of soft tissue sarcomas including malignant fibrous histiocytomas, liposarcomas, leiomyosarcomas, synovial sarcomas, fibrosarcomas, and angiosarcomas, which, unlike Ewing's sarcomas and rhabdomyosarcomas, (i) occur mostly in adults and (ii) are not nearly as responsive to chemotherapy and radiotherapy. The majority of these tumors occur within the muscle groups of the extremities, with the thigh a particularly common site of origin. However, soft tissue sarcomas can also occur in the trunk, in the retroperitoneum, and in the head and neck region.

Before the 1980s, amputation of a limb was commonly performed for local control of extremity sarcomas. In the 1970s, the National Cancer Institute (NCI) conducted a randomized trial in which patients with high-grade sarcomas of the extremity underwent either amputation or limb-sparing surgery with adjuvant XRT (14). All patients received postoperative chemotherapy. None of 16 patients undergoing amputation had a local recurrence, and 4 of 26 patients undergoing limb-sparing surgery and radiation had a local recurrence. However, the disease-free survival and overall survival rates between the two groups were the same. In another randomized trial from the NCI, patients with extremity sarcomas who had tumors amenable to limb-sparing surgery underwent surgery and were then randomized to postoperative XRT versus none (15). There was a highly significant reduction in the local failure rate in patients who received postoperative XRT although this did not translate into a difference in overall survival. Based on these trials and single-institutional series, the standard of care has moved to limb-sparing surgery, when possible, along with adjuvant XRT. In contrast to Ewing's sarcomas and rhabdomyosarcomas, these soft tissue sarcomas are infrequently controlled when gross disease remains after surgery; therefore, it is imperative that if limb-sparing surgery is selected that the goal is to perform a gross total resection, preferably with wide margins, to maximize the chance for local control.

The likelihood of local control following surgery is dependent on the grade of the sarcoma and its size as well as the extent of resection. For *low-grade* soft tissue sarcomas that are resected with a wide excision, there is some controversy as to whether postoperative XRT is required. Small low-grade sarcomas seem to do very well following surgery alone. However, certainly for intermediate and high-grade soft tissue sarcomas, the standard is to use adjuvant XRT. A number of different strategies for combining radiation with surgery have been used successfully. At the Massachusetts General Hospital (MGH), there has been extensive experience with preoperative XRT (16). This approach allows for the radiation volume to be smaller than in the postoperative setting; however, one drawback is that radiation can impair wound healing after the subsequent surgery. Typically, the entire preoperative volume is treated to a dose of 45–50 Gy. Generally, patients are given 10–20 days to recover after the completion of XRT before surgery is performed. If the pathology from the surgery shows microscopically positive margins or if there is gross residual disease, a postoperative XRT boost is given ranging from 15 to 25 Gy depending on the extent of residual disease.

MSKCC has a large experience using surgery and brachytherapy (without external beam radiation) for higher-grade soft tissue sarcomas (17). Catheters are placed at surgery and approximately a week later, the catheters are loaded with radioactive sources to deliver 45 Gy over 4–6 days. Other institutions have combined brachytherapy with postoperative external beam radiation. A different approach is to use intraoperative radiotherapy (IORT) to deliver a single dose of radiation to the tumor bed during surgery. Both brachytherapy and IORT have the advantage that there is less radiation dose to surrounding tissues because radiation is applied directly to the tumor bed. However, both techniques require very close cooperation between the surgeon and the radiation oncologist as well as specialized expertise. Furthermore, IORT machines are not available in most medical centers.

Most centers use postoperative XRT for soft tissue sarcomas. This has the advantage over preoperative XRT of pathologic evaluation of the entire specimen and fewer radiation-induced wound healing problems. The disadvantage is that the radiation volume may be increased due to the necessity of treating scars and drainage sites from the surgery. There are some who advocate including the entire muscle group in the radiation field because of the possibility that tumor cells

may have tracked throughout the muscle group during surgery. Others advocate using a 5–15 cm margin on the initial tumor volume and treating this to a lower dose (45–50 Gy), then using a shrinking field technique to treat the tumor bed with a 2–4 cm margin to a higher dose. Some centers vary the extent of the margin based on the grade of the sarcoma and its size. The total tumor bed dose is generally 60–66 Gy depending on whether the margins at surgery were negative or microscopically positive. Radiotherapy should be delayed 10–20 days following surgery to allow for sufficient healing to occur.

The results from a number of large series using conservative surgery and adjuvant XRT (preoperative, brachytherapy, IORT or postoperative) from MGH, MSKCC, and M.D. Anderson have been similar with local control rates in the 80–90% range when retroperitoneal sarcomas have been excluded (16–18). Unfortunately, disease-free survival rates are 20–30% below these local control rates because of the high incidence of distant metastases in intermediate and high-grade sarcomas. The results for patients who receive XRT for gross residual disease are far poorer, even though doses as high as 70–75 Gy are used. Local control rates in series from MGH and M.D. Anderson have been in the 30% range for these patients. Therefore, surgery is essential for obtaining optimal local control in sarcomas, and radiotherapy alone should be reserved for patients with unresectable lesions or who are medically inoperable.

Most soft tissue sarcomas occur in the extremities, and most of the data discussed above come from series that include predominantly or exclusively these lesions. Retroperitoneal soft tissue sarcomas are much rarer and have a poorer outcome. These are generally very large (>10 cm) and highly infiltrative by the time they are diagnosed, therefore difficult to completely resect. Postoperative radiation in these cases is often limited by small intestinal toxicity, the probability of which increases significantly when doses greater than 45–50 Gy are given to a large volume of bowel. In a study from MGH of 37 patients with retroperitoneal sarcomas who received preoperative XRT (45 Gy) followed by surgery and in some cases IORT (10–12 Gy), the overall 5-year overall survival rate was only 50% and the local control rate 59% (19). For 16 patients who were able to undergo a gross total resection and then received IORT, the 5-year overall survival and local control rates were 74% and 83%, respectively, again highlighting the importance of not leaving behind gross disease when performing surgery for these sarcomas.

Needless to say, with the high doses of radiation used for soft tissue sarcomas, there can be many complications. Wound healing problems are more common in patients who receive preoperative radiotherapy or brachytherapy. Late complications include decreased range of motion, decreased muscle strength, contractures, bone fracture, and arthritis. In particular, irradiation through a joint space can cause significant problems; therefore, it is important to adjust the fields to avoid the joint space after 40–45 Gy, if possible. Lymphedema of an extremity and severe fibrosis is also a risk, especially if the entire circumference of an extremity is treated, hence it is customary to keep a strip of skin and subcutaneous tissue out of the radiation field.

References

1. HallE. Radiobiology for the Radiologist. Philadelphia: Lippincott, Williams and Wilkins; 2000.
2. Arai Y, Kun LE, Brooks MT, et al.. Ewing's sarcoma: local tumor control and patterns of failure following limited-volume radiation therapy. Int J Radiat Oncol Biol Phys 1991;21(6):1501–8.
3. Donaldson SS, Torrey M, Link MP, et al. A multidisciplinary study investigating radiotherapy in Ewing's sarcoma: end results of POG #8346. Pediatric Oncology Group. Int J Radiat Oncol Biol Phys 1998;42(1):125–35.
4. Tucker MA, D'Angio GJ, Boice JD, Jr., et al. Bone sarcomas linked to radiotherapy and chemotherapy in children. N Engl J Med 1987;317(10):588–93.
5. Kuttesch JF, Jr., Wexler LH, Marcus RB, et al. Second malignancies after Ewing's sarcoma: radiation dose-dependency of secondary sarcomas. J Clin Oncol 1996;14(10):2818–25.
6. Dunst J, Ahrens S, Paulussen M, et al. Second malignancies after treatment for Ewing's sarcoma: a report of the CESS-studies. Int J Radiat Oncol Biol Phys 1998;42(2):379–84.
7. Donaldson SS. Ewing sarcoma: radiation dose and target volume. Pediatr Blood Cancer 2004;42(5):471–6.
8. Dunst J, Schuck A. Role of radiotherapy in Ewing tumors. Pediatr Blood Cancer 2004;42(5):465–70.
9. Donaldson SS, Meza J, Breneman JC, et al. Results from the IRS-IV randomized trial of hyperfractionated radiotherapy in children with rhabdomyosarcoma—a report from the IRSG. Int J Radiat Oncol Biol Phys 2001;51(3):718–28.
10. Wolden SL, Anderson JR, Crist WM, et al.. Indications for radiotherapy and chemotherapy after complete resection in rhabdomyosarcoma: a report from the Intergroup Rhabdomyosarcoma Studies I to III. J Clin Oncol 1999;17(11):3468–75.
11. Schuck A, Mattke AC, Schmidt B, et al. Group II rhabdomyosarcoma and rhabdomyosarcomalike tumors: is radiotherapy necessary? J Clin Oncol 2004;22(1):143–9.
12. Oberlin O, Rey A, Anderson J, et al. Treatment of orbital rhabdomyosarcoma: survival and late effects of treatment—results of an international workshop. J Clin Oncol 2001;19(1):197–204.
13. Heyn R, Haeberlen V, Newton WA, et al. Second malignant neoplasms in children treated for rhabdomyosarcoma. Intergroup Rhabdomyosarcoma Study Committee. J Clin Oncol 1993;11(2):262–70.
14. Rosenberg SA, Tepper J, Glatstein E, et al. The treatment of soft-tissue sarcomas of the extremities: prospective randomized evaluations of (1) limb-sparing surgery plus radiation therapy compared with amputation and (2) the role of adjuvant chemotherapy. Ann Surg 1982;196(3):305–15.
15. Yang JC, Chang AE, Baker AR, et al. Randomized prospective study of the benefit of adjuvant radiation therapy in the treatment of soft tissue sarcomas of the extremity. J Clin Oncol 1998;16(1):197–203.

16. Spiro IJ, Rosenberg AE, Springfield D, Suit H. Combined surgery and radiation therapy for limb preservation in soft tissue sarcoma of the extremity: the Massachusetts General Hospital experience. Cancer Invest 1995;13(1):86–95.
17. Alektiar KM, Leung D, Zelefsky MJ, Healey JH, Brennan MF. Adjuvant brachytherapy for primary high-grade soft tissue sarcoma of the extremity. Ann Surg Oncol 2002;9(1):48–56.
18. Zagars GK, Ballo MT, Pisters PW, et al. Prognostic factors for patients with localized soft-tissue sarcoma treated with conservation surgery and radiation therapy: an analysis of 225 patients. Cancer 2003;97(10):2530–43.
19. Gieschen HL, Spiro IJ, Suit HD, et al. Long-term results of intraoperative electron beam radiotherapy for primary and recurrent retroperitoneal soft tissue sarcoma. Int J Radiat Oncol Biol Phys 2001;50(1):127–31.

Chapter 19
The Surgical Pathology of Bone Tumors and Tumor-Like Lesions

Jasvir S. Khurana

Abstract Primary bone tumors, especially malignant ones, are rare and so unfamiliarity on a day-to-day basis with the various entities adds to the difficulty with their diagnosis and management within the entire clinical team including the surgeon, radiologist, pathologist, and internist or medical oncologist. This chapter takes an overview of the most important of the benign and malignant primary bone tumors. A section on differential diagnosis is included to help the surgical pathologist in diagnosis. This chapter emphasizes a good coordination with radiologists, clinicians, and pathologists to come to the correct diagnosis.

Keywords Unicameral bone cyst • Aneurysmal bone cyst • Synovial cyst • Intraosseous ganglion • Enostosis • Osteoma • Osteoid osteoma • Osteoblastoma • Osteosarcoma • Periosteal osteosarcoma • Parosteal osteosarcoma • Secondary bone tumors • Telangiectatic osteosarcoma • Chondroblastic • Osteoblastic • Fibroblastic • Giant cell rich • Low-grade intraosseous • High-grade surface • Neoadjuvant chemotherapy • Small cell • Osteochondroma • Nora's lesion • Chondroma • Chondroblastoma • Chondromyxoid fibroma • Chondrosarcoma • Exostosis • Enchondromatosis • Ollier's disease • Clear cell chondrosarcoma • Mesenchymal chondrosarcoma • Dedifferentiated chondrosarcoma • Hemangioma • Angiomatosis • Gorham's disease • Epitheloid hemangioendothelioma • Angiosarcoma • Hemangiopericytoma • Solitary fibrous tumor • Glomus tumor • Giant cell tumor (GCT) • Giant cell reparative granuloma • Desmoplastic fibroma • Fibrosarcoma • Benign fibrous histiocytoma • Nonossifying fibroma (NOF) • Malignant fibrous histiocytoma • Fibrous dysplasia (FD) • Osteofibrous dysplasia • Adamantinoma • Ewing's sarcoma • Intraosseous lipoma • Intraosseous liposarcoma • Leiomyosarcoma • Intraosseous schwannoma • Chordoma • Chondroid chordoma • Plasma cell myeloma • Leukemia • Granulocytic sarcoma • Non-Hodgkin's disease • Hodgkin's disease • Langerhans cell histiocytosis (LCH) • Erdheim-Chester disease

Introduction

The list of entities to be included in this broad category is sometimes controversial. In general, we have used a traditional approach, based on the WHO 2002 classification. The emphasis has been to study lesions based on the clinicoradiological appearance. Only entities of concern to the surgical pathologist, a musculoskeletal tumor surgeon, or oncologist are included.

Bone Tumors and Tumor-Like Lesions

- Cystic lesions
- Bone-forming lesions
- Cartilaginous lesions
- Vascular lesions
- Giant cell lesions
- Fibrous lesions
- Fibrous histiocytic lesions
- Other mesenchymal lesions
- Hematopoietic lesions
- Metastatic bone disease

Cystic Lesions

- Simple bone cyst
- Subchondral bone cyst
- Intraosseous ganglion cyst
- Aneurysmal bone cyst

Simple (Unicameral) Bone Cyst

A simple (unicameral, juvenile, or essential) cyst of bone is an intramedullary lesion, comprising of a generally unilocular cystic cavity, which is generally filled with clear or straw-colored

J.S. Khurana (ed.), *Bone Pathology*, DOI 10.1007/978-1-59745-347-9_19,

fluid. It is lined by a thin fibrovascular tissue membrane. Following trauma, the cavity may contain blood and with healing, it may get some septations.

It has been speculated that simple cysts are either a developmental abnormality or may result from a venous obstruction. Little is known about the genetic alterations in simple cysts, complex clonal structural rearrangement has been found in chromosomes 4, 6, 8, 16, 21, and both chromosomes 12 in one study (1).

Clinical Features: There is a predilection for long bones (proximal humerus, proximal femur, and proximal tibia), but some flat bones (especially the ilium) and short tubular bones (calcaneus) are also frequent. About 80% of cases are seen in either the humerus or femur. The presentation is with pain, stiffness, pathologic fracture, or sometimes as an incidental finding on X-rays. Most patients are within the first two decades of life.

Radiologically, unicameral bone cysts (UBCs) are often metaphyseal and may encroach the epiphysis in skeletally immature individuals. As the bone lengthens at the physeal end, the cyst may appear to "move" into a diaphyseal location. The cysts size varies from a few to several centimeters. Fragments of bone may be present within the cyst and can be visualized as "fallen fragments" by X-ray (2).

It has been reported that hemodynamic data may help in the diagnosis of UBCs, and serve to separate them from other entities which may be confused radiologically such as aneurysmal bone cysts (ABCs), giant cell tumor (GCT), eosinophilic granuloma, fibrous dysplasia (FD), and enchondroma. The typical transduced pressures have ranged from 15 to 40 mm Hg. The curves obtained, show a systolic, diastolic, and dichrotic notches. This compares with a normal intraosseous pressure of 5–15 mm Hg. Curves from normal bone show smooth, unnotched tracings. ABCs, typically have much higher mean pressures and range 80–200 mm Hg (3).

Surgical Pathology: It is most unusual to receive intact gross specimens, since these lesions are rarely resected. Curetted material if received often consists of irregular fragments of membranous fibrovascular tissue, often with reactive bone. Hemosiderin, granulation tissue, a few giant cells or mild focal chronic inflammatory cells may be present. Some cases have pink cementum-like rounded material (Fig. 1a, b). These may be the result of diffusion and precipitation of supersaturated solutions from the cavity, or, perhaps a peculiar reactive osteoid.

Management and Prognosis: Many unicameral cysts go on to heal either spontaneously or following trauma. Some cases may progress to fracture and may be treated when a fracture is impending. Aspiration of the cyst followed by steroid injections is the currently most popular method of treatment. Some cases may require other intralesional procedures (curettage, with our without bone grafting or cement placement), or rarely, excision, especially in cases that have recurred following prior curettage (which may occur in about 10% of cases).

Subchondral (Synovial) Cyst

These are small cysts, usually adjacent to the articular cartilage and associated with degenerative joint disease. These are seen in surgical pathology material only as incidental findings of joints removed for other reasons (such as arthroplasties).

Radiologically, they are sharply defined lesions in a subchondral location within a joint affected by osteoarthritis.

Surgical Pathology: Microscopically, they appear as defects in the bone, often with no discernible lining. The lesion is important, only in that it may be radiologically confused with entities such as chondroblastoma or GCT.

Management: If recognized, these lesions require no specific therapy.

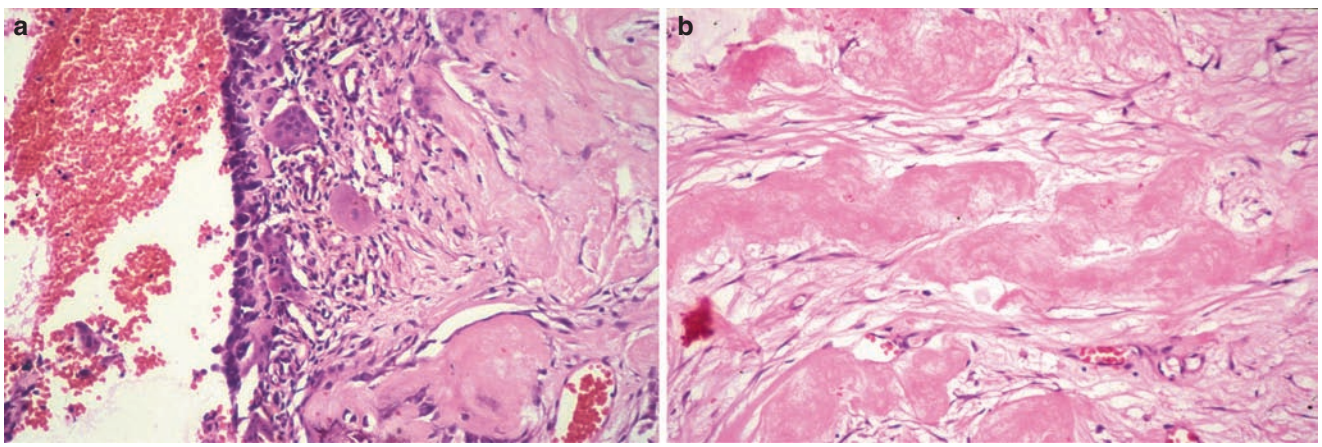

Fig. 1 **a** Unicameral cyst showing a fibrous background and a few scattered osteoclast-type giant cells, hemosiderin and mild chronic inflammation. **b** Unicameral cyst showing the characteristic cementum-like material. The same material may sometimes be seen in aneurysmal bone cysts and while characteristic it is not specific to this entity

Intraosseous Ganglion Cyst

An intramedullary, mucin-filled, fibrous-lined lesion. The relationship to a soft tissue ganglion cyst is unclear. There is a wide age range; the presentation is often with pain or as an incidental finding. The distal and proximal tibia, femur, ulna, and the hands and feet are commonly involved. Some lesions are bilateral.

Radiologically, these are epiphyseally located, and show well-defined sclerotic margins. The joint articular surface is usually normal (as opposed to subchondral cysts where the joint has osteoarthritis).

Surgical Pathology: Microscopically, the tissue is mainly myxoid, mixed with fibroblasts, but the typical stellate cells of true myxomas are not seen. Fibrous tissue may be haphazardly interspersed or be arranged in the form of septa. The outer layer is often heavily collagenized. The differential includes intraosseous fibromyxoma [generally seen in the gnathic (jaw) bones], chondromyxoid fibromas and subchondral cysts.

Management: Intraosseous ganglion may be treated non-operatively if asymptomatic and recognized as such, or may require local intralesional procedures only.

Aneurysmal Bone Cyst (ABC)

An aneurysmal bone cyst (multilocular or hematic cyst) is a benign multicystic lesion of bone, which is composed of blood-filled spaces, separated by connective tissue septae containing giant cells and reactive bone.

The histogenesis of the lesion has been controversial. Some advocate the possibility of this representing a change secondary to an arteriovenous malformation. Others have suggested that the many, if not most of these lesions are secondary to a variety of different bone neoplasms. These lesions include giant cell tumor (GCT), nonossifying fibroma (NOF), giant cell reparative granuloma, fibrous dysplasia (FD), chondromyxoid fibroma, chondroblastoma, osteoblastoma, unicameral bone cyst, hemangioma, and even osteosarcoma. These lesions should always be looked for in every case, the diagnosis of ABC is essentially that of exclusion. Even with the exclusion of secondary neoplasms, however, there remain a number of lesions that correspond to an ABC. Some of these lesions spontaneously regress, suggesting that they may be nonneoplastic.

Recent cytogenetic studies, however, have suggested that ABCs are true neoplasms and have a repeated genetic abnormality, associated with the short arm of chromosome 17 (most likely involving the coding sequence of the ubitquitin protease gene USP 6. The commonest translocation is t(16;17) (q22;p13), but there are several variations. These genetic changes seem to be absent in secondary ABCs further supporting the evidence that this is a definite pathological entity (4, 5).

Clinical Features: The lesion is common in the first two decades (but there is a wide age range). It can affect any bone, it is often metaphyseal in long bones (femur, tibia, and humerus are more common). It may affect the vertebrae, especially the posterior elements. Secondary ABCs follow the sites of predilection of their primary lesions.

Presentation is with pain and swelling, sometimes with a pathological fracture. In the vertebrae, there can be compressive neurological symptoms.

Radiologically, the ABCs of long bones may be eccentric (often seen in long bones), central or parosteal (an uncommon location). In the initial (or incipient phase), there is a small lytic lesion, that does not expand the bone and may have a worrisome permeative margin. In the growth phase, there is rapid growth and lysis of bone. Codman's triangles may be prominent or there may be cortical "blowout." The intramedullary component, however, is usually well circumscribed, and this may help establish the diagnosis. In the stable phase, the X-rays have a characteristic picture with expanded bone and a "shell" around the lesion along with trabeculations coursing within it. Finally, there is a healing phase, in which there is progressive ossification, resulting in a coarsely trabeculated bony mass. In some ABCs, there may be some matrix production – usually this is mineral or bone. Fluid/fluid levels on CT scan or MRI are common, and a characteristic finding (Fig. 2a, b).

Surgical Pathology: Grossly, if intact, the lesions can be seen to have a thin osseous bony shell surrounding a honeycombed mass with cavernous vascular spaces that ooze blood like a sponge. Older cysts may have serosanguinous fluid rather than blood. A careful search should be made for solid areas that may represent the solid portion of an ABC or the precursor lesion in a secondary ABC.

Microscopically, the main feature is the presence of cavernous spaces that are filled with blood but lack the smooth muscle wall and endothelial cells of blood vessels. The fibrous walls contain fibroblasts, osteoid, chondroid, and giant cells in varying proportions. The cysts of an ABC may invaginate into normal bone at the periphery of the lesion or extend into the soft tissue.

The fibroblastic stromal cells lack atypia, atypical mitoses, and anaplasia. These are important features to search for, since if found, the possibility of telangiectatic osteosarcoma must be considered. Sometimes, the mineralizing component has a chondroid aura. Osteoid may arise in a metaplastic fashion, like FD, or may be surrounded by chondroid. The osteoid often follows the contours of the septate. It has been likened to a crinkled paper in appearance and frequently occurs in long, linear depositions. Chondroid within these lesions is said to have a fibrillary or chondromyxoid quality. It may be focally calcified. Mitotic figures may be numerous, particularly in the areas of osteoid formation. Atypical mitoses, however, should

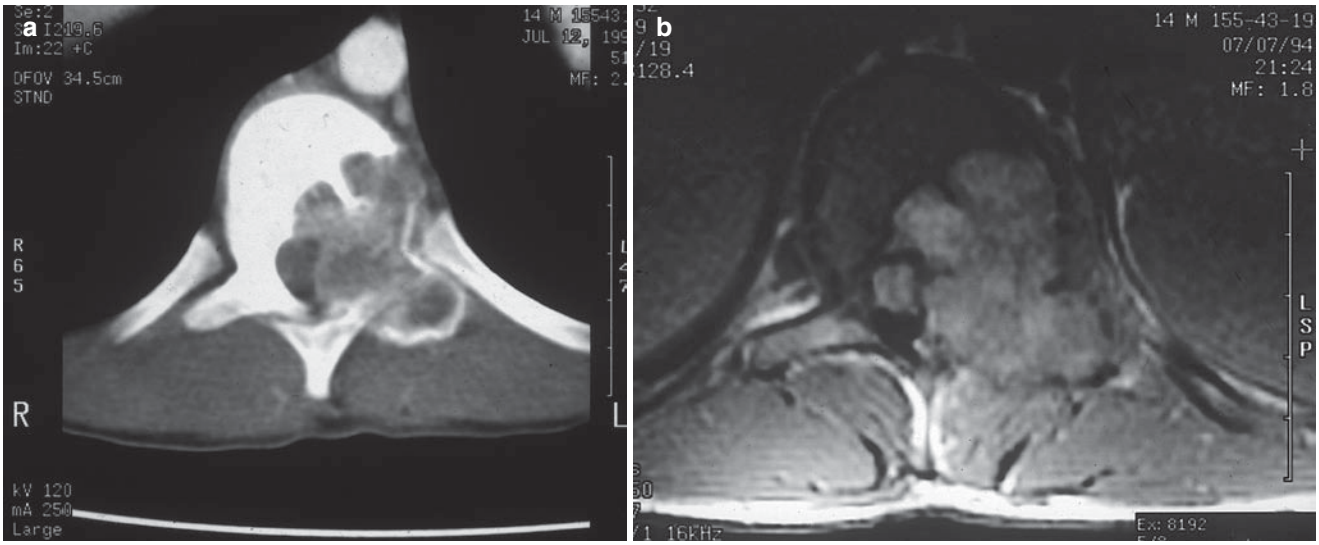

Fig. 2 **a** CT scan showing an aggressive aneurysmal bone cyst of the vertebrae that has caused marked cortical expansion into the adjacent soft tissues. The lesion remains quite well delineated. **b** An MR picture showing fluid–fluid levels

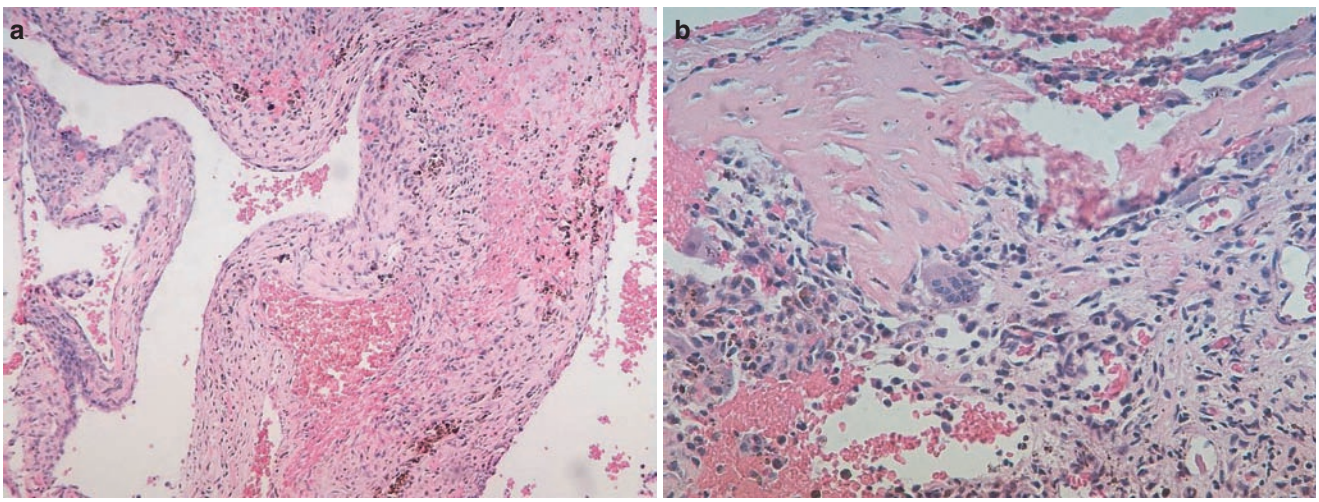

Fig. 3 **a** A low-power photomicrograph showing a hypocellular lesion with septations composed of fibroblasts and fibrocollagenous matrix. **b** A sprinkling of giant cells and osteoid is visible

not be seen. Necrosis too, is generally absent, except in regions around a pathological fracture (Fig. 3a, b).

A solid variant of an ABC has been described which may be related (if not identical) to a reparative giant cell granuloma (6). Grossly, these lesions are completely solid. Microscopically, a spindle cell proliferation with a loose arrangement is seen. Giant cells occur in clusters, and are often arranged around areas of hemorrhage. Characteristically, there is abundant reactive new bone formation with osteoblastic activity similar to that of the heterotopic ossification (Fig. 4a, b). Some authors consider these lesions identical to giant cell reparative granulomas. The finding of translocations involving USP6 gene in both these lesions supports the idea that both the lesions are at least closely related if not identical.

Differential Diagnosis: A telangiectatic osteosarcoma should be excluded. The diagnosis rests on the presence of anaplastic cells in osteosarcoma. A primary tumor with secondary ABCs should always be considered and such areas be sought for. Ossifying hematoma and pseudotumor of hemophilia are other differentials. These entities are examples of subperiosteal hematomas, and may mimic radiographically an ABC. Hemosiderin, zonation, and an organized appearance of bone may help establish the diagnosis of hematoma.

Management: Intralesional procedures such as curettage followed by cement or bone grafting, sclerotherapy via feeding vessels, radiation, cryotherapy, and other forms of therapy have been advocated. In a few cases, spontaneous regression has occurred. Radiation has a risk of postradiation sarcoma transformation. The other forms of treatment

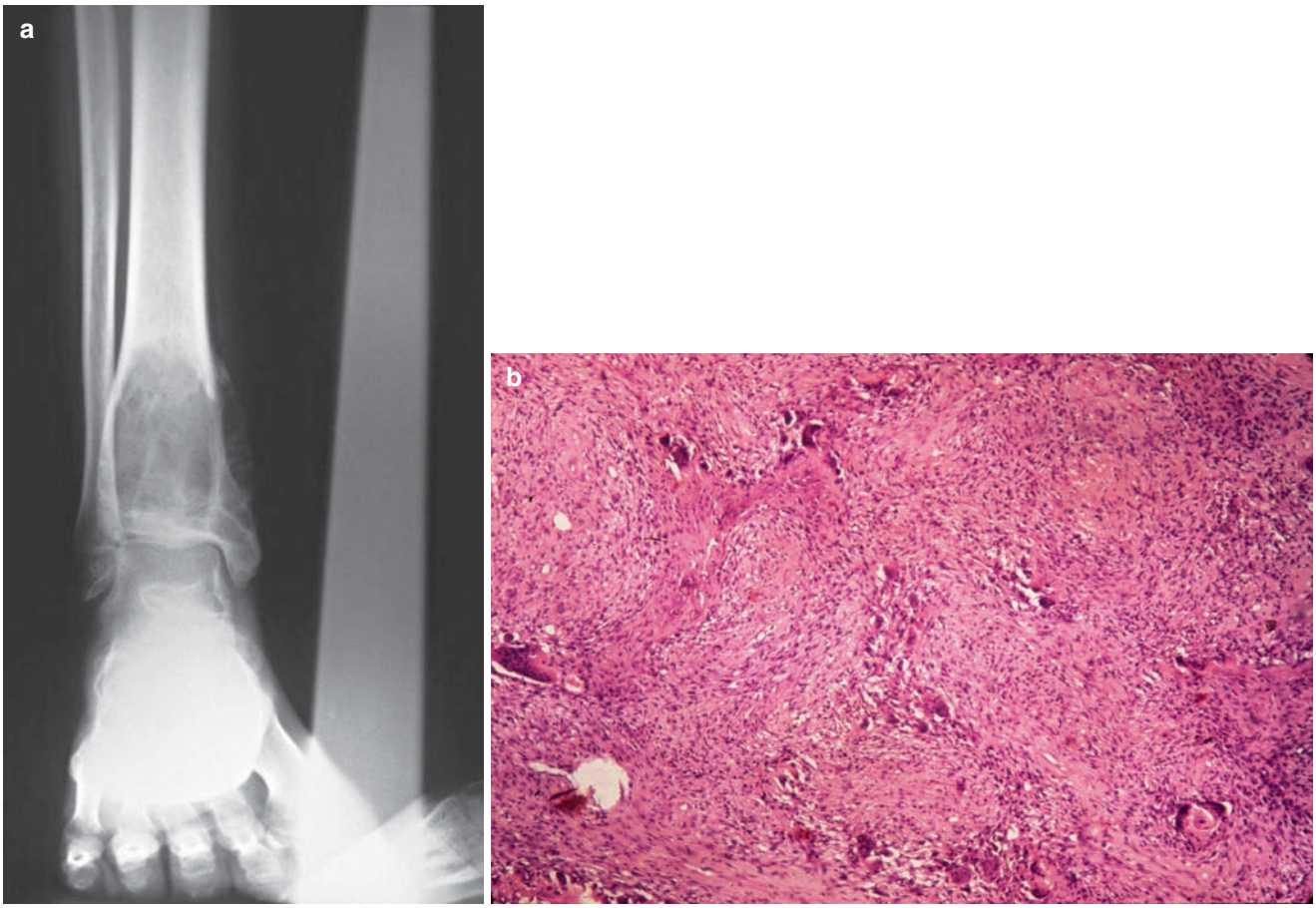

Fig. 4 **a** Solid aneurysmal bone cyst. The X-ray appearance is unable to differentiate between the solid and the usual variant. MRI scans, however, failed to show fluid in the solid variant (*not shown*). **b** Histologically, the lesion showed aggregates of giant cells, cytologically bland stromal cells arranged loosely, reactive woven bone, and focal hemosiderin deposition

(such as wide excision) have to be tailored to the individual situation, location, and operator preference.

Bone-Forming Lesions

- Enostosis
- Osteoma
- Osteoid osteoma
- Osteoblastoma
- Osteosarcoma and related variants

Enostosis (Bone Island)

These are small (0.2–2 cm) sclerotic lesions occurring in the diaphysis of adults. The lesions are usually cold on bone scans, and generally diagnosed on plain radiograms. A round to oval sclerotic lesion with a subtle "brush" border sign is suggestive. The lesions may enlarge or disappear with time. Their importance lies in the distinction from metastatic disease or the well-differentiated intraosseous osteosarcoma.

Surgical Pathology: Grossly, the enostoses are sharply demarcated and hard. Microscopically, they are composed of lamellar bone and have a well-developed Haversian system. The spicules of cortical bone blend into the adjacent spongiosa. Woven bone, if present is a minor component. Osteopoikilosis (spotted bone disease) is an autosomal dominant condition characterized by multiple enostoses.

Osteoma

A tumor-like mass of abnormally dense (cortical) lamellar bone, occurring almost exclusively in the craniofacial bones of adults. Multiple osteomas, especially those of the appendicular skeleton osteomas should raise the possibility of Gardeners syndrome. Sinus osteomas have a male predominance, whereas the reverse is true of the jaw.

Surgical Pathology: Osteomas are composed primarily of lamellar bone. Some amount of woven bone is acceptable (Fig. 5a, b). A spongy variant of the osteoma has been

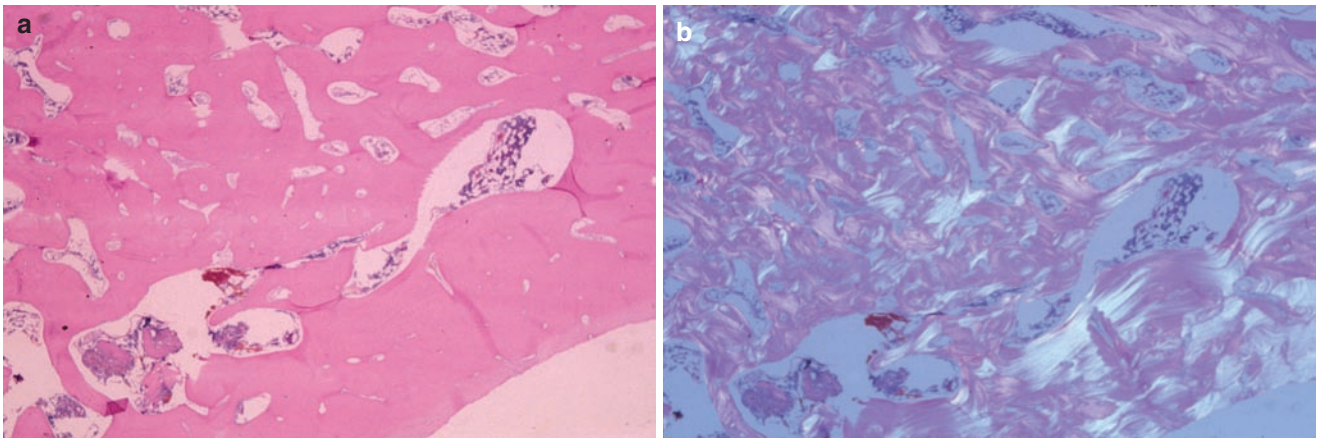

Fig. 5 **a** Osteoma, the lesion is composed of dense cortical-type bone. **b** Under semipolarized light, the bone is seen to be a combination of lamellar and woven bone

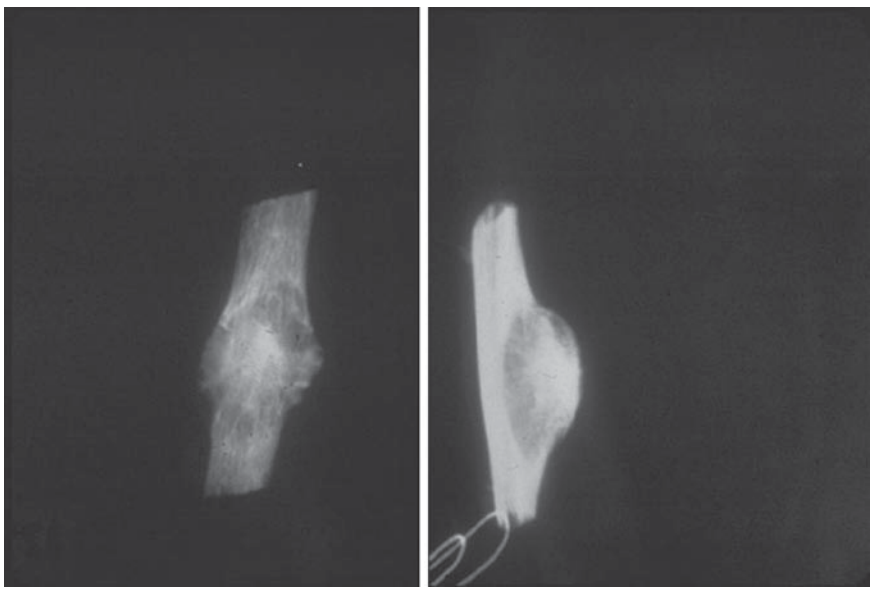

Fig. 6 Osteoid osteoma, specimen X-ray shows a sharply delineated, small, cortical lesion

described which contains a fibrofatty or hematopoietic medullary component.

Differential Diagnosis: Differentiation should be made between osteomas and dense bone lesions such as reactive (post traumatic or post infectious) sclerosis, neoplasm-induced bony overgrowth (such as with meningiomas), eburnated osteochondromas, ossified FD, solid odontomas, and parosteal osteosarcomas.

Osteoid Osteoma

An osteoid osteoma is a benign neoplasm, clinically characterized by small size and disproportionate pain, histologically consisting of a nidus, and surrounding reactive, sclerotic bone. The nidus is a *highly vascular, sharply defined osteoblastic proliferation* that is usually less than 1.5 cm.

Clinical Features: The majority of osteoid osteomas are found within the first three decades of life. The classic presentation of the patient is with severe, unremitting pain (initially mostly nocturnal pain). Relief of pain, by aspirin is seen in the majority of patients. The demonstration of unmyelinated nerve fibers and high levels of prostaglandin E_2 within the lesion may explain this observation. Undiagnosed osteoid osteomas may present with scoliosis or joint flexion contractures. Although almost any bone can be affected (except perhaps the sternum), the most classic location is in the long bones where it often has sclerotic borders on X-rays (Fig. 6). Classically, the nidus is lucent which in turn may have a small central radiodense spot of calcification. The nidus may require

tomograms or CT scans to demonstrate. Osteoid osteomas are characteristically located in the cortex of the diaphysis when they are present in long bones. They have a more variable (periosteal or intramedullary) location in the short tubular bones or when present within joints. Osteoid osteomas of the joints can be difficult to detect by plain films. Since osteoid osteomas are "hot" on Technetium pyrophosphate bone scans, this modality becomes useful in many atypical cases.

The pathologist is most often concerned with locating the nidus. This is diagnostic, and also confirms that the *lesion has been removed*. Recurrence may follow (or the symptoms are unrelieved) if the nidus is not completely excised.

Since the location is difficult to achieve intraoperatively, several different approaches have been tried. The best established is the fine detail (overpenetrated) X-ray. Alternatively, but perhaps with less sensitivity, preoperative tetracycline can be given, and the nidus looked for under ultraviolet light. Another technique has been to utilize a portable gamma camera and use an intraoperative bone scan. CT scan identification and microwave ablation or intrascan marking are other strategies. Once the nidus is located, frozen section diagnosis from the diagnostic area can be used to confirm the impression.

Surgical Pathology: Grossly, the nidus is red, spherical, and gritty. Classically, it can almost always be "shelled" out from the surrounding bone. This forms an important diagnostic clue.

Microscopically, there is a *sharp demarcation* of the nidus from the surrounding sclerotic bone. The nidus may be poorly ossified, with a richly vascularized stroma, or, it may be ossified, with calcific or lacy osteoid composed of osteoid rimmed with osteoblasts. The osteoblasts of osteoid osteomas are usually plump and active. They may have occasional mitoses, but there should be no atypical mitotic figures. The woven bone shows prominent osteoblastic rimming. Cartilage is absent unless there has been a fracture, previous surgery, or if the lesion is intra-articular. Marrow hematopoietic elements and fat are also absent. Scattered lymphocytes and plasma cells are found, but acute inflammation is absent (Fig. 7a, b). Surrounding the nidus is a 0.1–0.2 cm zone of less trabeculated fibrovascular tissue. Outside this, is sclerotic compact or spongy lamellar bone. The previously termed "giant" osteoid osteomas (larger than 2 cm) were probably examples of osteoblastomas.

There have been very few genetic studies. Very limited cases have suggested the involvement of chromosome 22q13 and loss of part of chromosome 17q (7).

Differential Diagnosis: The differential diagnosis on clinical and radiological grounds is with a variety of entities: intracortical abscess (such as salmonella infection), osteosarcoma, sclerosing osteomyelitis (of Garre), enostosis, aseptic necrosis, stress fracture, Langerhans cell histiocytosis (LCH), and metastasis.

To this can be added, on histologic grounds, osteoblastoma. Osteoblastomas may have a lobulated margin, a feature not found in osteoid osteomas. Again, the degree of haphazardness in the trabecular arrangement of osteoblastomas should be contrasted with the orderly zonal pattern of central ossification in the osteoid osteoma. However, it is rare for this exercise in differentiation to be required, since these two entities are easily differentiated on radiological studies. Again, the size criteria should be kept in mind. Lesions below 1 cm are almost always osteoid osteomas, and those above 2 cm, almost always osteoblastomas.

Osteosarcomas are only rarely smaller than 1 cm. Moreover, they are generally medullary and it is very rare for them to be completely intracortical. Microscopically, osteosarcomas are generally obviously malignant.

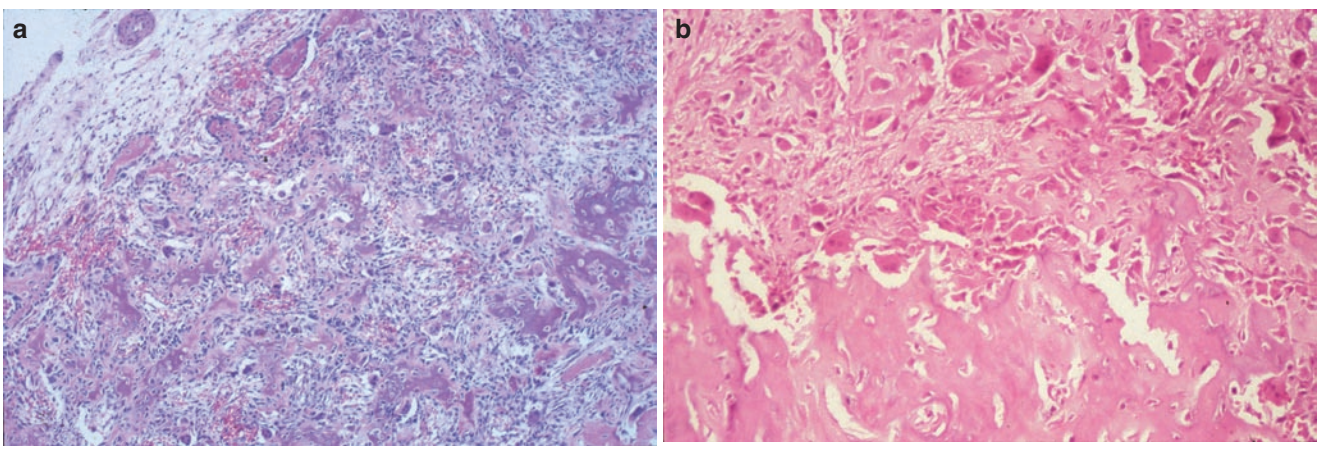

Fig. 7 The center of the lesion shows a fibrovascular tissue (*the nidus*). The periphery shows a sharply delineated bone-forming lesion. The trabeculae are rimmed by benign-appearing osteoblasts

Intracortical abscesses have an irregular contour, lack the prominent vascularity, and may contain a sequestrum. Sclerosing osteomyelitis may produce dense bone but lacks a nidus. Enostoses are asymptomatic, inert on radio isotopic scans, and lack the nidus of osteoid osteomas. Similarly, LCH and metastatic disease can be differentiated on histologic grounds.

Management: Although there is evidence to suggest that osteoid osteomas may regress spontaneously (after many years), the majority of them are exquisitely painful. Therefore, most osteoid osteomas are managed operatively. Marginal excision is adequate in most cases. The entire nidus should be removed. CT-guided drilling or microwave ablation are other additional approaches which may serve to ablate the nidus. Some osteoid osteomas have been treated with long-term salycilates.

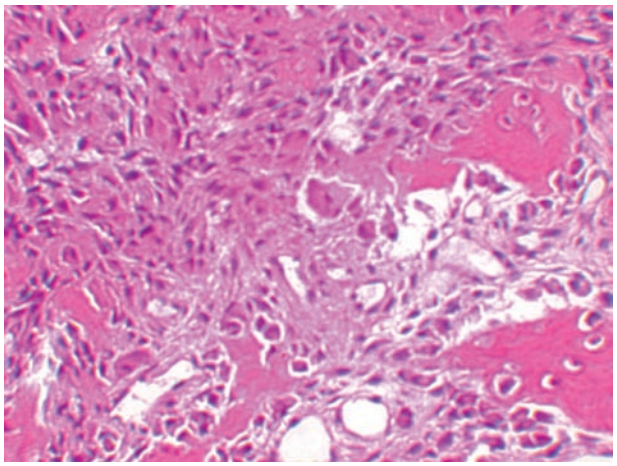

Fig. 8 Osteoblastoma is a well-circusmscribed bone-forming neoplasm with woven bone, osteoblasts and a fibrovascular stroma, similar to osteoid osteoma. They are, however, larger than osteoid osteomas, often more than 2 cm

Osteoblastoma

Osteoblastomas (giant osteoid osteoma, ossifying GCT, cementoblatoma of jaw) are benign or sometimes locally aggressive osseous lesions, with microscopic similarity to osteoid osteomas.

The majority of these tumors are seen in patients below the age of 30 years, with a male predominance. The presentation is with pain but often less intense than that of osteoid osteoma. There is a predilection for the axial skeleton, with a majority of cases affecting the posterior elements of the spine. Osteoblastomas can be metaphyseal or diaphyseal. Epiphyseal osteoblastomas are extremely uncommon, occasional examples have involved the short tubular bones of the hands and feet. The so-called cementoblastoma of jaw is considered to be an osteoblastoma, rather than a separate entity.

Radiologically, most lesions are between 4 and 6 cm, uniform, geographic, expansile lucent lesions. Most lesions are cortical, about a third may be intramedullary. There may be a stippled calcification in the matrix of the lesion.

Surgical Pathology: Grossly, the lesions show circumscription and typically measure 2–10 cm. A secondary cystic change (ABC) may supervene in some of these tumors.

Microscopically, they are identical to osteoid osteomas, being composed of anastomosing bony trabeculae in a fibrovascular stroma (Fig. 8). Osteoblastomas are often well circumscribed, with the edges merging into the adjacent bone. This gives an appearance of maturation.

The bony trabeculae are variably calcified. Some lesions are heavily mineralized, whereas others may be made of just osteoid. There is considerable intralesional variation in trabeculum size. In the majority of cases, the trabeculae are thick. In a small number, thin, lace-like trabeculae are present, raising the differential diagnosis of osteosarcoma. Plump, mitotically active osteoblasts line these trabeculae. This rimming is considered an important feature in favor of benignity. Early lesions may be rich in giant cells. Chondroid differentiation can occur but is unusual in the absence of fracture. Bizarre pleomorphic nuclei may occur in some cases. These are thought to represent a secondary degenerative change, similar to that seen in neurilimommas. In such nuclei, the nuclear features are not crisp. Secondary ABC-like change occurs in about 10% of cases.

A subgroup of "*aggressive*" *osteoblastomas* has also been recognized. These have been termed "malignant" osteoblastomas or "low grade osteosarcomas" by some authors. These variants contain a trabecular pattern of osteoid similar to that of the "conventional" osteoblastoma; however, there is a tendency to wider and more irregular forms. There may be occasional areas of nontrabecular (lace like) osteoid, but this component is minor. The osteoblasts present are large (almost twice the size of normal osteoblasts) and have an *epitheloid* quality. The nuclei may have a vesicular "histiocyte like" appearance. Although many of these aggressive variants develop in patients over the age of 30 years, some have been seen in younger age groups as well. Radiologically, they are larger in size but can occur in a variety of bones. The propensity of these tumors to recur is the reason for separating out this subgroup.

Differential Diagnosis: The differential diagnosis includes osteoid osteomas (differentiated based on the size criteria, see above) and low-grade (osteoblastoma-like) osteosarcoma. The relationship between such osteosarcomas and osteoblastoma is still unclear. In limited material, the distinction between osteoblastoma and osteosarcoma

can be impossible. Features that favor benignity include sharp circumscription, loose arrangement of the tissue with trabeculae that seem embedded in it, and the osteoblastic rimming around the trabeculae. If sheets of osteoblasts are seen, then the diagnosis of osteosarcoma should be considered. The single most important feature, however, is permeation. Permeation, if present, helps make the diagnosis of osteosarcoma over osteoblastoma.

The difficulty in recognizing osteosarcoma has led to descriptions of aggressive or malignant ostoeblastomas; both these entities may actually represent underdiagnosed osteosarcomas.

In some cases, the differential may include a GCT or ABC. Generally, the epiphyseal location of appendicular GCTs and the favored anterior body location of the vertebral GCTs should be kept in mind when faced with this problem. Osteoblastomas do not contain the sheets of large giant cells and stromal cells of the true GCT; however, a few osteoclast-like giant cells can be found. Although the ABC and osteoblastomas share several radiographic features, they can be usually separated microscopically. Several cases occur, however, with secondary ABC-like changes supervening on an osteoblastoma, and these lesions should be interpreted as such.

Management: The mainstay of treatment is operative. Wide local resection is preferred, but thorough curettage is acceptable in many locations. Adjunct treatment modalities such as cryosurgery or methylmethacrylate packing may be considered. Lesions not amenable to surgery have on occasion been irradiated. This method of treatment is, however, controversial and the possibility of postradiation sarcoma induction should be kept in mind.

Osteosarcoma and Its Variants

Osteosarcomas (also known as osteogenic sarcoma) are malignant neoplasms of bone that are composed of proliferating cells that produce osteoid, at least focally. Since the production of osteoid is quite focal, it may not be recognized, in biopsies with limited sampling. It is thus reasonable to make the diagnosis, in cases that are otherwise classic, but show no osteoid on the biopsy sample.

There are several subtypes of osteosarcoma. The common type is the conventional osteosarcoma (high grade, intramedullary) variant. In this variant, there are several histologic patterns: chondroblastic, osteoblastic, fibroblastic, fibrohistiocytic (malignant fibrous histiocytoma like or MFH-like), giant cell rich, and osteoblastoma like. Such descriptors of the predominant patterns most likely have no prognostic significance.

Other variants include small cell osteosarcoma, telangiectatic osteosarcoma, low-grade intramedullary, intracortical, surface (parosteal, periosteal and high-grade surface), and multifocal osteosarcoma.

- Conventional osteosarcoma
- Secondary osteosarcoma
- Multifocal osteosarcoma
- Small cell osteosarcoma
- Telangiectatic osteosarcoma
- Intramedullary low-grade osteosarcoma
- Intracortical osteosarcoma
- Parosteal osteosarcoma
- Periosteal osteosarcoma
- High-grade surface osteosarcoma

Conventional Osteosarcoma

Osteosarcomas may arise de novo or develop *secondarily* on other lesions such as Paget disease, osteogenesis imperfecta, bone infarct, chronic osteomyelitis, fibrous dysplasia, giant cell tumor or osteoblastoma. Traditionally, however, osteosarcomas that have arisen upon an underlying low-grade chondrosarcoma have been termed dedifferentiated chondrosarcoma rather than include them as examples of secondary osteosarcomas. There is also an association with prior radiation therapy and possibly with metallic or other orthopedic implants. There may be a relationship with trauma, but if so it is poorly documented and understood.

Some cases of osteosarcoma may be familial. Children with bilateral retinoblastomas have an incidence several hundred fold that in the normal control population. Such cases show loss of heterozygosity at 13q (corresponding to the Rb gene). There is also a predisposition to osteosarcoma in the Li-Fraumeni syndrome. These cases have a loss of heterozygosity in 17p (TP 53 mutations are seen in about 30% of these patients).

The majority of the patients with conventional de novo osteosarcoma are below the age of 30 years (over 85%). The long tubular bones, in the active growth phase (second decade) appear most at risk (about three quarters of all tumors). The metaphyseal region is the site of over 85% of these tumors, the diaphysis being the primary site in about 10%. Epiphyseal location is rare.

In secondary osteosarcomas, the incidence of flat bone and diaphyseal involvement is much higher. The incidence of osteosarcoma (in fact of all malignant bone tumors) in the distal appendicular skeleton, such as the hands and feet is very low.

Pain is the most frequent presenting symptom, followed by pain and swelling. The duration of the symp-

toms is usually less than 1 year, most often only a few weeks to months. Pathologic fractures may be the presentation in about 5%.

The serum alkaline phosphatase may be raised in the more heavily osteoblastic tumors but is often normal in the lytic examples. A rise in alkaline phosphatase following excision may herald a recurrence. Lactate dehydrogenase has also been found to be useful to monitor recurrence. A case has been reported of an osteosarcoma producing Beta human chorionic gonadotropin (8).

Radiographic appearances are diagnostic in about two-thirds of osteosarcomas (Fig. 9a–c). The classic radiograph is that of an intramedullary, lytic, and sclerotic lesion, which demonstrates cortical breakthrough and is associated with matrix bone formation. Some lesions may be purely lytic or purely sclerotic. The margins are generally those of an aggressive lesion, but rarely are they permeative as seen in the rapidly growing Ewing's tumor. The periosteum is often lifted to form a Codman's angle (often called a Codman's triangle) but may show other patterns associated with rapid growth such as onion skinning (see section on bone radiology).

Most osteosarcomas show foci of cortical breakthrough. These therefore correspond to Enneking Stage IIB. Examples limited to the bone alone (Enneking Stage IIA) are unusual (please see section on grossing of bone specimens for the Enneking-staging system).

Rare cases can be deceptively bland on X-rays. There are examples of telangiectatic osteosarcomas, which have simulated ABCs on radiological studies.

Surgical Pathology: Osteosarcomas are often large lesions, generally over 5 cm. The conventional osteosarcomas are intramedullary and centered in the metaphysic. Grossly, the vast majority of osteosarcomas demonstrate penetration of the cortex, with an extraosseous soft tissue extension (Fig. 9d). The intramedullary extension can be extensive and may be underestimated by conventional X-rays, although MRI studies are better at estimating their true extent. Distant foci, within the marrow cavity of the same bone may be found (at a distance from the main tumor mass) and are termed "skip" lesions or skip metastases. Skip lesions are uncommon findings but are important potential causes of recurrent disease.

The gross appearance of the tumor is variable depending on the predominant differentiation, and is frequently variegated. Thus, areas of lobular cartilaginous growth and gritty bone may be found within the same mass. Foci of hemorrhage and necrosis are common. Large blood-filled areas may represent a telangiectatic component. The periosteal reaction is frequently visible as spicules or lamellae of bone. Epiphyseal penetration is uncommon especially at the gross (macroscopic) level, and should be assessed microscopically. Joint extension may occur; sometimes this is along the intra-articular ligaments (ligamentum teres in the femoral head, or the cruciate ligaments in the knee). Because preoperative chemotherapy is commonly utilized, it is rare to see osteosarcomas nowadays in their native viable form.

Microscopically, osteosarcomas are high-grade, anaplastic tumors and frequently show unequivocal osteoid production. Osteoblastic, chondroblastic, and fibroblastic differentiation is commonly admixed (Fig. 10a–d). Sometimes the amount of osteoid production can be minimal or absent in otherwise typical osteosarcomas. However, such lesions may produce heavily ossified metastases, justifying the use of osteosarcoma, even though the primary tumor has little or no bone production.

Osteosarcomas of the jaw bones (gnathic osteosarcomas) are frequently chondroblastic and are reputed to have a somewhat better outcome. The average age of such patients is usually higher than seen in conventional osteosarcomas. The tumors tend to have less anaplasia, and are often diagnosed as a lower grade. The differentiation from benign lesions may be difficult in many cases. The better outcome of jaw osteosarcomas, however, does not extend to skull osteosarcomas, since the latter are highly malignant tumors.

The neoplastic cells of the osteosarcoma may be plasmacytoid, epitheloid, spindled, or oval. They often have marked nuclear pleomorphism, a high mitotic rate, and atypical mitotic forms. These cells are easier to identify in the areas away from the bone trabeculae or osteoid formation. Occasional osteosarcomas, however, are bland cytologically. This makes small fragmented biopsies treacherous to interpret, and the clinical context must be taken into account. A well-recognized phenomenon known as *normalization* is seen in most osteosarcomas. This refers to the tendency of the osteoblasts to become smaller and less pleomorphic as they get incorporated into the osteoid. An additional feature that may be helpful is the presence of osteoid lacking an osteoblastic rimming. This can be helpful in differentiating neoplastic from reactive osteoid or woven bone.

Osteoid may have variable thickness and degrees of mineralization. A thin, highly mineralized pattern (the filigreed pattern) is quite suggestive of neoplastic osteoid if found. Other tumors can be very heavily ossified. Some osteosarcomas can resemble osteoblastomas (see previous section).

Although the chondroblastic, fibroblastic and MFH-like osteosarcomas are familiar to most pathologists, one histologic subtype is particularly troublesome. This is the giant cell rich type – characterized by a proliferation of bland giant cells amid a sarcomatous stroma. Osteoid pro-

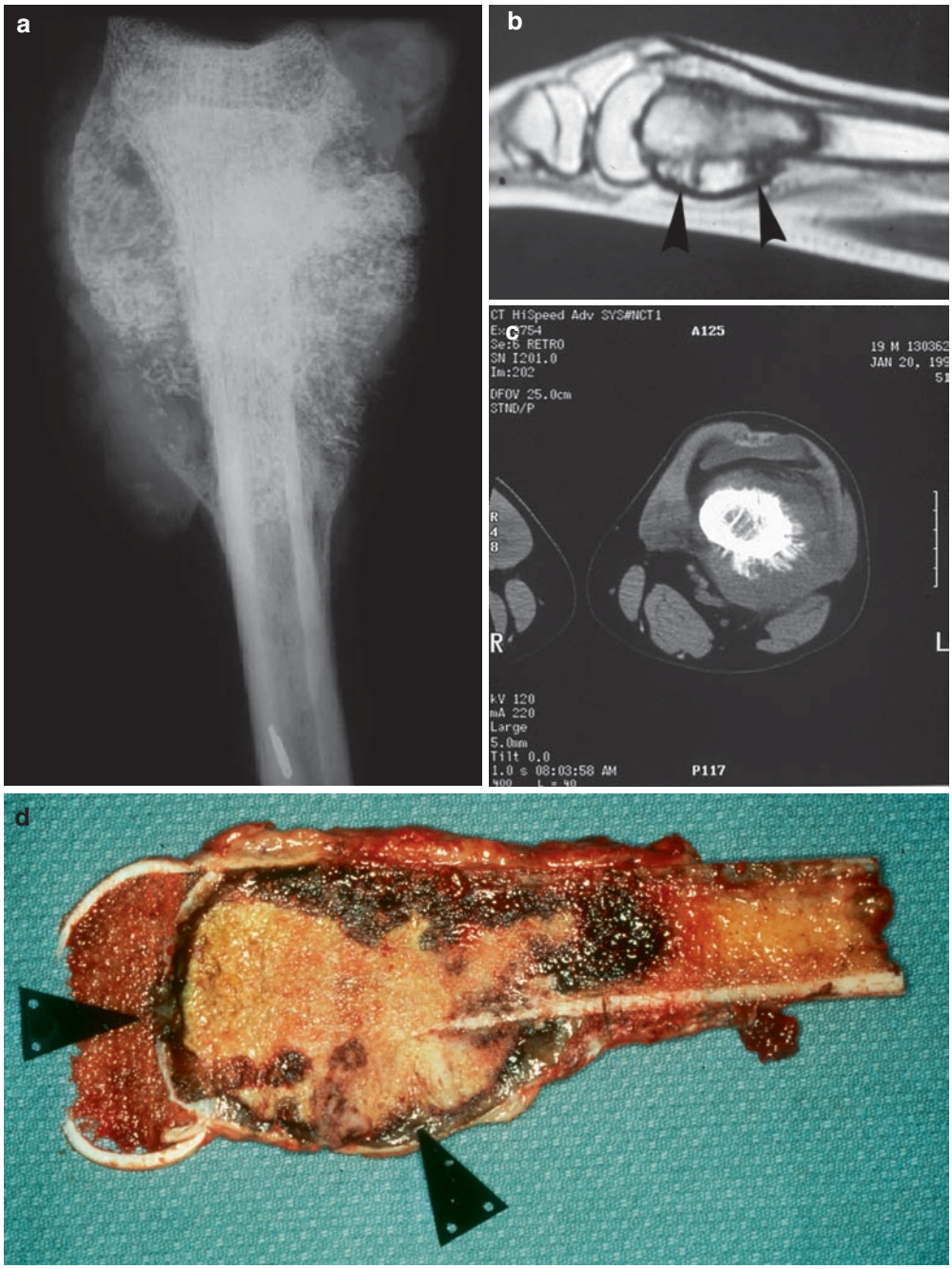

Fig. 9 **a** Specimen X-ray of an osteosarcoma. There is a characteristic lifting of the periosteum by the tumor producing the Codman's angles. The tumor can be seen to be producing osseous matrix. **b** Osteosarcoma, MRI shows the lesion located in the metaphysis. It does not cross into the epiphysis. There is cortical breakthrough and a soft tissue extension (*marked with arrows*). **c** CT scan of the same patient as Fig. 6B, it shows the typical appearance of an osteosarcoma. The bone production is evident and it extends into the soft tissues. **d** Gross specimen from the same patient as Fig. 6b, c. The tumor shows extensive necrosis (the patient had received preoperative chemotherapy)

duction is usually sparse. If attention is not paid to the stromal anaplasia, an incorrect interpretation of this lesion as a GCT will result. Usually, but not always, these tumors are metaphyseal (like conventional osteosarcomas) rather than epiphyseal (like other GCTs). This location gives a clue to its true nature. Unfortunately, there are examples, of some tumors that have had all the X-ray features of GCTs.

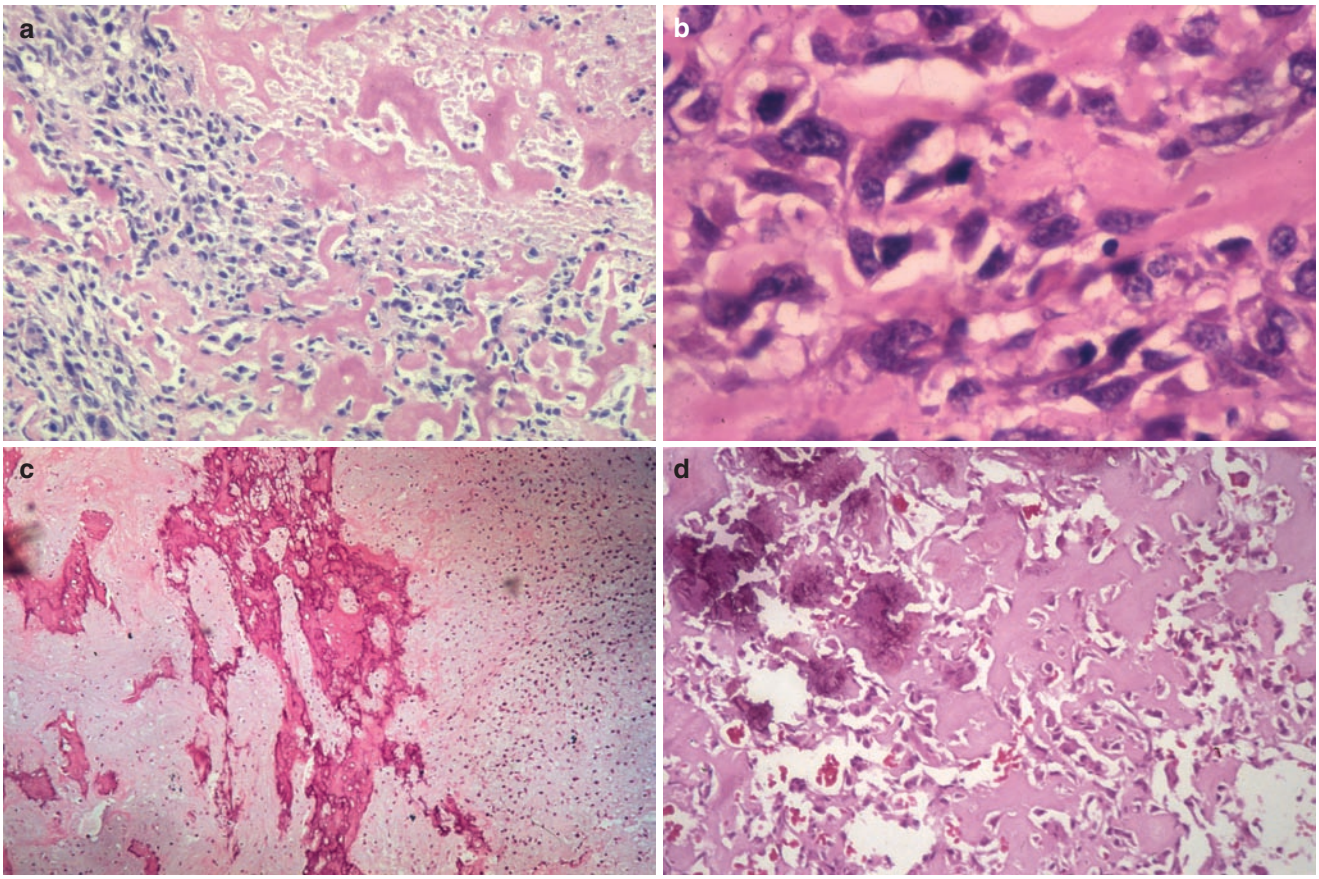

Fig. 10 The figures show various patterns of osteosarcoma. **a** Thin lacy osteoid. **b** Highly anaplastic cells. **c** Chondroblastic and mineralized areas. **d** Thicker trabeculae of well-formed bone

Rarely, an osteosarcoma that resembles a chondroblastoma is seen. Such tumors can be diagnosed if attention is paid to the permeative nature. Seeing sheets of cells should be a clue to its malignant nature, since chondroblastomas have a loose arrangement of cells. Frequently, however, the diagnosis is only made with the benefit of hindsight, when a tumor diagnosed as a chondroblastoma recurrs or metastasizes, and the metastasis has a more typical appearance of an osteosarcoma.

Some osteosarcomas are composed of epitheloid looking cells. A rosette formation may give the appearance of gland formation, and immunohistochemical markers may be positive for epithelial differentiation. Such osteosarcomas can be also seen as part of the sarcomatous component of a dedifferentiated chondrosarcoma.

Chemonecrosis of the tumor (following neoadjuvant therapy) is important to recognize and quantitate. The appearance of the tumor after chemotherapy depends on its original morphology. Chondroblastic foci appear acellular-like chondroid, often with ghost cells in the lacunae. Telangiectatic foci appear as acellular blood-filled cysts (Fig. 11). Osteoblastic foci appear as acellular osteoid matrix. Atypical stromal cells may be scattered in all of these foci, and the biologic significance of these cells is unclear.

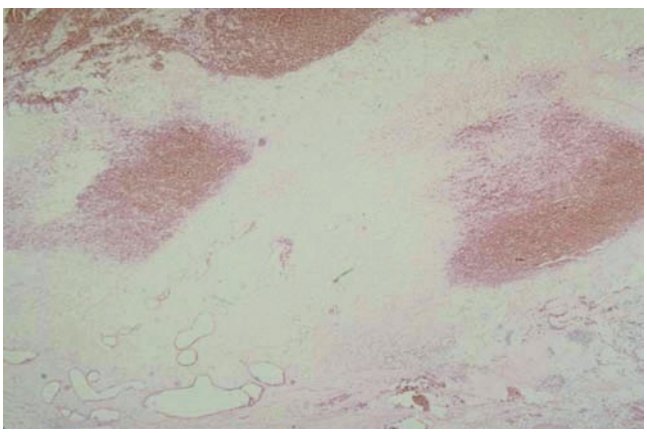

Fig. 11 Osteosarcoma following chemotherapy. The washed out, necrotic appearance is typical. Blood-filled lakes are seen in this telangiectatic osteosarcoma

Differential Diagnosis: Osteoblastomas – About 10% of osteosarcomas may appear radiologically benign, and conversely about a quarter of osteoblastomas may be worrisome on X-rays. Typical osteoblastomas are composed of trabeculae and intervening stroma, the two components being frequently of equal width. Aggressive osteoblasto-

mas lack this feature, but in this instance often have an epitheloid cytomorphology. Osteoblastic rimming goes in favor of osteoblastomas, whereas extensive pleomorphism and atypical mitotic figures would be features warranting the diagnosis of osteosarcoma. While interpreting woven bone with osteoblastic rimming it is important to distinguish diagnostic areas from the surrounding woven reactive bone, which is present in several lesions, whether benign or malignant. An important feature to assess is infiltration. This feature goes strongly in favor of osteosarcomas when demonstrable. Osteoblastomas on the contrary grow in a "pushing" fashion.

Fracture Callus: Callus can be extremely hypercellular, form compact masses of osteoid and contain a mitotically active stroma. The finding of zonation (a pattern of peripheral ossification with a fibrous or less ossified center), or osteoblastic rimming can be helpful in recognizing callus. Cartilage can be present in both entities, but recognizing atypical or frankly malignant cartilage would favor osteosarcoma.

Giant cell tumor (GCT): Clues to the sarcomatous nature of tumors containing osteoclastic giant cells come from the radiograms. Evidence of destruction, infiltration, and the lack of an epicenter in the epiphysis should make the observer reconsider a diagnosis of GCT. Histologically, the presence of a sarcomatous stroma and osteoid is diagnostic, and the reactive osteoclasts should be ignored.

Malignant Fibrous Histiocytoma: The differentiation from this entity may be arbitrary. Several cases occur where the amount of osteoid is small and the MFH pattern is extensive.

Osteogenic Melanoma: A few cases of melanoma are characterized by bone formation. The background is that of spindle melanoma cells. A stain for S-100 is often positive in the melanoma cells (although other markers including HMB 45, melan A, MiTF may or may not be positive). Knowledge of the entity, its atypical radiological location, and a high index of suspicion are helpful in making the diagnosis.

Management: Untreated osteosarcoma is uniformly fatal. Lung and or widespread metastases are the usual cause of death. Animal models and molecular markers are being developed to help understand this problem; however, the data from these are very preliminary (9, 10). Wide resection along with neoadjuvant and adjuvant chemotherapy is currently utilized in treatment. The current survival of conventional, nonmetastatic osteosarcoma is approaching 80% survival at 10 years. Because of late adverse events, long follow-up periods are suggested (11). Necrosis following neoadjuvant chemotherapy is used by many as a prognostic marker and to tailor the postoperative chemotherapy regime. Low-grade and chondroblastic osteosarcomas may not respond well to chemotherapy.

Secondary Osteosarcoma

Secondary osteosarcomas are bone forming sarcomas that arise in bones affected by other abnormalities such as Paget disease. Radiation associated osteosarcoma is also included in this category. It is estimated to occur in about 1% of patients with Paget disease. The incidence of radiation associated osteosarcoma has been difficult to estimate since the latent period can be long (several years). Other rare instances of secondary osteosarcomas have included cases arising on bone infarcts, endoprostheses and fibrous dysplasia. The prognosis of secondary osteosarcomas is in the order of about 70% 5 year survival for extremity lesions and about 30% 5-year survival for axial lesions.

Multifocal Osteosarcoma

This is a small but distinct subgroup of osteosarcomas, which has traditionally been divided into the synchronous and the metachronous types. Synchronous lesions appear to arise (or are discovered), more or less simultaneously (or at least within 6 months of each other). These could represent multifocal primary osteosarcomas, and are subdivided into the "juvenile" and "adult" types. Synchronous osteosarcomas are often bilaterally symmetrical.

The juvenile (or childhood–adolescent) form is typically found in the age group 5–17 years. The lesions are osteoblastic and of high grade. The lesions are often Enneking Stage IIA at presentation but uniformly rapidly fatal with a mean survival of 8 months.

The adult form of synchronous multifocal osteosarcoma occurs at a mean age of 37 years, the tumors are better differentiated (they resemble the low-grade intraosseous osteosarcoma) but are again uniformly fatal. The mean survival is somewhat longer (30 months).

Asynchronous (metachronous) multifocal osteosarcoma is more common than the synchronous variant. Several long-term survivors of this form are known, and the patients should not be assumed to have a fatal disease.

The problem of whether these lesions represent multiple primary sarcomas or whether they are metastatic deposits of a single primary tumor, can now hopefully, be answered with the currently available DNA fingerprinting technology.

Surgical Pathology: The individual lesions of multifocal osteosarcoma resemble the conventional osteosarcoma (see above).

Differential Diagnosis: As is obvious, the presence of multiple radiographically evident bony lesions should be investigated to rule out the more likely possibility of metastatic disease to the skeleton, rather than the rare multifocal osteosarcoma. Sarcomatoid carcinomas, especially sarcomatoid

renal cell carcinoma may mimic osteosarcoma, and may need immunohistochemical staining to diagnose (they are positive for epithelial markers such as cytokeratins and epithelial membrane antigen).

Management: The management of widespread multifocal osteosarcoma relies on chemotherapy and radiation. Surgical treatment is on a case by case basis, mainly depending on the location and the problem caused by the particular deposit of tumor locally.

Small Cell Osteosarcoma

A microscopically distinct variant of a high-grade intramedullary osteosarcoma consisting of small round cells but showing at least focal osteoid production.

Although around 70% of the patients are in the first two decades of life, cases upto the age of 80 have been reported. The presentation and sites of the lesions are similar to those of the conventional osteosarcoma.

Radiologically, the lesions show permeative margins and cortical destruction. Extraosseous extension is common. Although largely lytic, many cases may exhibit focal blastic matrix patterns on X-ray.

Surgical Pathology: Grossly, the lesions cannot be differentiated from the conventional variant. On microscopy, osteoid is found in the context of a small round cell proliferation (Fig. 13a, b). Chondroblastic differentiation occurs in about a third of cases. Sheets of neoplastic cells are often found; focal hemangiopericytoma-like areas may be seen. Necrosis and mitotic figures may be seen, or occasionally be rare. The nuclear characteristics of these cells may vary. The majority of cases have cells with hyperchromatic rounded nuclei. Other examples have closely packed spindle shaped cells with scant amounts of indistinct cytoplasm.

The cells of the small cell osteosarcoma have glycogen. This finding therefore cannot be utilized to make a distinction from Ewing's sarcoma. There is, however, abundant reticulin, which surrounds the neoplastic cells and this feature differs from the sparse reticulin seen in Ewing's tumor. Stains for CD 99 and osteocalcin show variable staining, thus there are currently no immunohistochemical markers available which can be used to confirm the diagnosis.

Ultrastructurally, the features are similar to those of Ewing's tumor and mesenchymal chondrosarcoma, and show small cells with scant cytoplasm and organelles. There are frequent free ribosomes and variable numbers of mitochondria, rough endoplasmic reticulum, Golgi and filaments.

The characteristic 11:22 translocation of Ewing's sarcoma is not seen in small cell osteosarcoma. By molecular methods, the EWS/FLI1 or EWS/ERG fusion product is absent.

Differential Diagnosis: Ewing's tumor is distinguished by the absence of osteoid, as opposed to at least focal osteoid production in the small cell osteosarcoma. Mesenchymal chondrosarcoma favors the axial skeleton and has sharply demarcated *low*-grade cartilage amid a small cell proliferation. Small cell osteosarcoma, if it has cartilage, tends to be in the form of high-grade chondrosarcoma-like areas. Lymphomas can be distinguished by a panel of lymphoid and pan-leukocyte markers such as the leukocyte common antigen (CD 45). Neuroendocrine markers can be utilized to distinguish neuroectodermal tumors of bone. These include neuron-specific enolase, chromogranin, and synoptophysin.

Management: The therapy of these lesions includes surgery in association with chemotherapy. However, while some

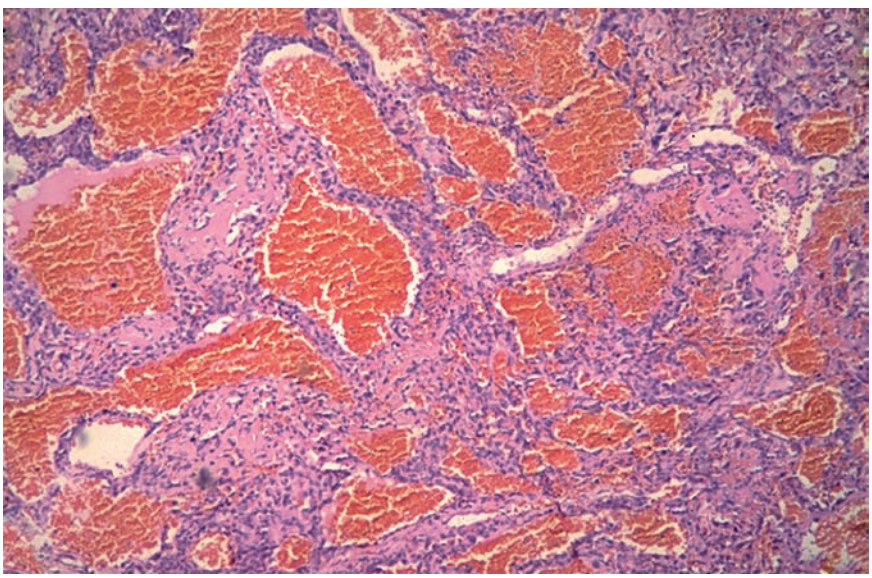

Fig. 12 Telangiectatic osteosarcoma. There are large vascular spaces lined by anaplastic sarcomatous cells

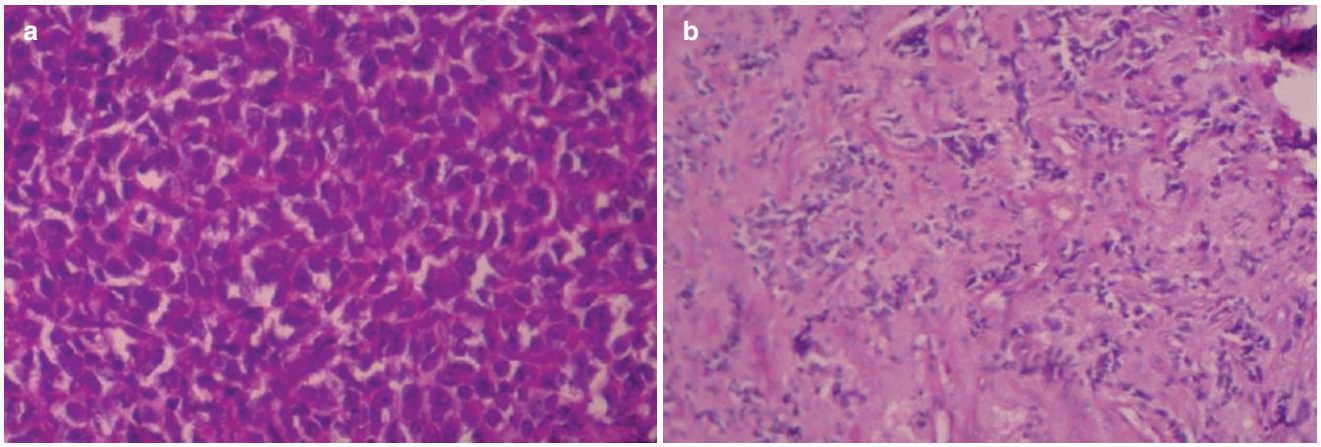

Fig. 13 Small cell osteosarcoma. The majority of the lesion was composed of a small cell population as illustrated **a** in this microphotograph. In some areas **b**, there was osteoid and bone formation by the malignant cells, illustrating the osteosarcomatous nature of the neoplasm

centers manage these cases on protocols designed for osteosarcoma others have opted for treating them on protocols for small cell tumors such as Ewing's. Comparative studies have not been done.

Telangiectatic Osteosarcoma

The diagnostic criteria for this entity have been very varied. Some authors have been extremely liberal with the diagnosis of this variant. The incidence therefore is difficult to estimate but is probably less than 10% of all osteosarcomas. Patients with the telangiectatic variant are more prone to present with a pathologic fracture than those with a conventional osteosarcoma (around 25%). The age and the location of the tumors are, however, similar to those of the conventional variant.

Radiologically, these tumors are purely lytic. They present features of rapid growth, such as permeative margins, cortical destruction, and soft tissue extension. An ABC-like appearance may be seen in some cases. Any sclerosis on the X-ray should preclude the diagnosis of telangiectatic osteosarcoma.

Surgical Pathology: Grossly, the tumor may appear as a blood clot, be a hemorrhagic–necrotic mass or be multicystic with blood-filled spaces or ABC-like.

Microscopically, two variants are described, corresponding to the gross appearances. These are the hemorrhagic-necrotic and the ABC-like variants (Fig. 12). In the hemorrhagic–necrotic variant; malignant cells are present, widely separated in a background of blood and necrotic debris (several levels and slides may have to be viewed to diagnose this variant). Osteoid matrix may be minimal. Frequently, the combination of radiologic–microscopic findings are needed.

In the second (ABC like) variant, the low power view is that of an ABC. Necrosis is sparse or absent. It is only at high power that one begins to appreciate the overtly malignant cells within the cyst wall. Benign giant cells are present and serve to further obscure the malignant nature of this entity. The osteoid is usually delicate, contrast to the coarse osteoid seen in ABC.

Differential Diagnosis: Conventional osteosarcomas with focal telangiectatic change should be separated out from the purely telangiectatic ones. The latter are entirely lytic lesions on X-rays, lack a solid component on gross examination, and fulfill the microscopic criteria discussed above. This will yield a pure entity, which can then be studied for its biologic behavior. The potential misdiagnosis of a telangiectatic osteosarcoma as an ABC has been alluded to earlier.

Management: The treatment is similar to that of the conventional osteosarcoma. The biologic behavior and spread of this variant appear similar, according to presently available data, to a conventional osteosarcoma. The data, however, are clouded with the problem of variability in the application of diagnostic criteria.

Intramedullary Well-Differentiated Osteosarcoma

Intraosseous (or central) well-differentiated osteosarcoma is a term given to an intramedullary variant composed of low-grade, fibrous and osseous tissue with only minimal cytologic atypia. Although the number of cases studied in most series is small, it is important to recognize this subtype, since the patients tend to do much better than those with the conventional osteosarcomas.

There is a tendency to a slightly older age, and slightly longer symptomology, as compared to the conventional oste-

osarcoma. However, the sites of involvement and other clinical features are similar.

Radiographically, the lesions are intramedullary, some may be slightly eccentric. Many cases show at least a focal suggestion of malignancy; however, in many cases the margins are often well defined rather than aggressive, and may occasionally also be sclerotic (12). A mineralized matrix is present in the majority of cases; about a quarter are entirely lucent.

Surgical Pathology: Grossly, the tumors are often well demarcated and gritty or whorled, resembling the gross appearances of a desmoid tumor. Cortical breakthrough and soft tissue extension may be seen.

Microscopically, fibrous tissue and variable amounts of osteoid form the bulk of the tumor. Cartilage differentiation is infrequent. A pattern of infiltration into the preexisting lamellar bone or fatty marrow is diagnostic (Fig. 14). There is only slight atypia and the mitotic rate is low (1–2 per 10 high-power fields). The osteoid component may be mineralized and appear mature (lamellar). About one third have a fibroblastic stroma that resembles a desmoid or desmoplastic fibroma. Uncommonly, a FD-like pattern of "Chinese alphabets"-like bone may be seen embedded in a fibrous stroma. The most important histologic finding is that of a permeative growth pattern.

Differential Diagnosis: Conventional osteosarcomas often have better differentiated, innocuous "normalized" areas. These should not be underdiagnosed as this variant since biologically they behave in accordance with their more aggressive foci. Desmoplastic fibromas may infiltrate the bone and prove diagnostically challenging. Osteoid production should be sought in these cases. Radiographic evidence of matrix production is helpful in establishing the correct diagnosis. FD can be another potential mimicker of the well-differentiated osteosarcoma. Radiographically, however, FD is homogenous (the matrix is referred to as ground glass to emphasize this quality) whereas the well-differentiated osteosarcoma is less so, and may in fact show trabeculations. Microscopically, the trabeculae of FD tend to be rather short and curled, whereas those of the well-differentiated osteosarcoma are longer, and may be arranged in parallel arrays. Again, cytologic atypia in the stroma should be sought and is diagnostic if found.

Management: The surgical management of this entity differs little from the conventional osteosarcoma. Chemotherapy, however, is often withheld, since these tumors are often nonresponsive. The outcome is usually very favorable. Cases that have transformed into high-grade lesions are on record, and in such an instance the treatment regimen should be altered to reflect this.

Intracortical Osteosarcoma

Intracortical osteosarcoma is a rare variant, which arises within and is confined to the cortex of a long bone. The number of cases is too small to draw conclusions, but there is a tendency to involve the diaphysis of a lower extremity. The radiographic appearance is that of a lucency surrounded by a zone of sclerosis. CT scans may demonstrate cortical permeation. However, the radiographic findings have usually suggested a benign lesion – such as FD, adamantinoma, Brodies' abscess, and osteoblastoma.

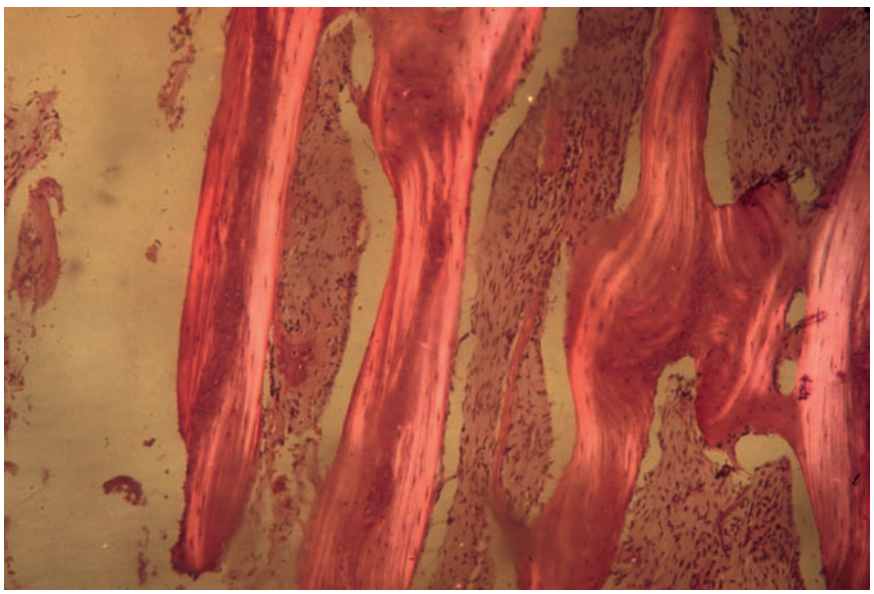

Fig. 14 A low-grade, fibroblastic, intraosseous osteosarcoma is seen permeating bone trabeculae. The microphotograph is taken under semipolarized light to highlight the lamellar nature of the preexisting bone trabeculae

Surgical Pathology: Grossly, the surrounding bone is thickened; the mass may have irregular borders. Extension into the medullary cavity or the periosteum should be minimal to qualify for the designation of intracortical.

Microscopically, these tumors are usually intensely osteoblastic. Small amounts of chondroblastic or fibroblastic areas are occasionally seen. The neoplastic cells in the osteoblastic areas are "normalized" and may appear bland. It is often possible, nevertheless, to identify entrapped bone, this constituting the most helpful microscopic sign to make a diagnosis of malignancy.

Differential Diagnosis: Osteoblastoma, though difficult to differentiate radiologically, is separable by virtue of its vascularized loose stroma and osteoblastic rimming. Entrapped lamellar bone and neoplastic cartilage is virtually never found in osteoblastoma.

Periosteal osteosarcoma may come into the differential. These are, however, by definition more superficially located. The majority of periosteal osteosarcomas microscopically are chondroblastic and differ from the intensely blastic intracortical osteosarcomas.

Management: The number of cases described is too few to draw conclusions regarding the optimal management of these lesions. Intuitively, wide local resection would be desirable, and the role of adjuvant or neoadjuvant chemotherapy needs to be established. Some of these cases have recurred and metastasized if the surgery has been marginal.

Periosteal Osteosarcoma

These lesions have formerly been called juxtacortical chondrosarcoma. They represent a subtype of surface osteosarcoma, characterized by a predilection for the diaphysis of long bones and showing prominent chondroblastic differentiation. The age range and clinical presentation are similar to that in conventional osteosarcoma.

Radiographically, the tumors are located on the external surface of the cortex, and extend into the surrounding soft tissues. The lesions are predominantly lucent, mineralization if any is confined to the base of the tumor adjacent to the cortex. There is a characteristic spiculated (radiating) pattern of calcification, which is oriented perpendicular to the cortex. Intramedullary, extension should be absent.

Surgical Pathology: Grossly, the tumors are sharply demarcated, lobulated, and cartilaginous. Microscopically, there are dominant chondrosarcomatous areas (Grade 2–3) with at least focal osteoid formation. Usually, the osteoid is present in the centers of the lobules. In some cases, the cartilage forms islands separated by anaplastic spindle cells. The malignant osteoid is often thin and lacy, surrounding these spindle cells. There are often broad spicules near the underlying cortex. Fibroblastic foci may be present in a minor component.

Differential Diagnosis: True "peripheral chondrosarcomas" are generally metaphyseal, rather than diaphyseal, large and lack the radiating spicules of bone seen in the periosteal osteosarcomas. Histologically, they tend to have a lower-grade chondroblastic differentiation. High-grade surface osteosarcomas can be distinguished by their predominantly osteoblastic, anaplastic microscopic appearance. Parosteal osteosarcomas rarely enter the differential, since they are entirely different by radiological and microscopical grounds. Whereas periosteal osteosarcomas are lytic, the parosteal osteosarocamas are sclerotic, often intensely so. Again the metaphyseal location and the fibroblastic/osteoblastic appearance of the parosteal osteosarcomas should be easily recognized.

Management: The outcome of periosteal osteosarcoma is similar to that of intramedullary conventional osteosarcoma (13). The surgical management is wide local resection. Chemotherapy is more controversial. The current practice is to usually give both neoadjuvant and adjuvant chemotherapy similar to that in conventional osteosarcoma.

High-Grade Surface Osteosarcoma

A rare variant of an osteosarcoma arises from the outer cortex of the bone and has a microscopic appearance similar to that of the conventional high-grade osteosarcoma. Intramedullary extension is, however, absent or minimal. The lesions are often diaphyseal, the presentation and the location otherwise are similar to those of high-grade, conventional intramedullary osteosarcoma.

Radiographs show a mineralized mass, attached to the outer cortical surface with minimal underlying cortical erosion. The amount and quality of mineralization of the matrix is, however, variable but is often maximal near the base. Periosteal reaction may be absent or marked, sometimes with well-formed Codman's angles.

Surgical Pathology: Grossly, the tumors are bulky, multilobulated masses with a variegated appearance. The dense sclerosis of the parosteal and the chondroid appearance of the periosteal variants are absent. Microscopically, they resemble the conventional osteosarcoma.

Differential Diagnosis: A low-grade fibro-osseous area should be sought, to exclude a dedifferentiated parosteal osteosarcoma. This has an uncertain prognostic significance but probably no therapeutic consequence.

Management: The biologic behavior of these lesions parallels the conventional high-grade intramedullary variants and currently has a fairly good outcome (14). They should be treated on similar lines surgically, and by similar chemotherapeutic protocols.

Parosteal Osteosarcoma

A parosteal osteosarcoma is a well-differentiated, low-grade, fibro-osseous variant of an osteosarcoma that arises on the surface of bone. This is considered to be a special variant of osteosarcoma, since the prognosis is often much better, as compared to the conventional type.

The presentation is often a painless mass most commonly situated in the posterior lower thigh, the site of over two-thirds of these tumors. Other common sites include the tibia and the humerus. The patients tend to be symptomatic for longer periods than the conventional osteosarcoma and show a slight female predilection. Most studies have shown a tendency to involve slightly older age groups as compared to the conventional osteosarcoma.

Radiographically, these lesions are characterized by a dense mass of bone attached to the outer metaphyseal cortex by a broad base (Fig. 15a, b). Plain X-ray has occasionally underdiagnosed these lesions as osteochondromas. There is dense mineralization, which is often less prominent peripherally. The tumor tends to encircle the parent bone, a feature demonstrable by CT scanning. On plain films, a lucent line between the mass and the bone can be suggestive of this nature to wrap around the bone. Periosteal new bone is usually absent. Intralesional lucencies are uncommon. If seen, they should raise the possibility of *dedifferentiation* within the tumor. This is especially *true of deep-seated lucencies*. CT scans in dedifferentiated tumors may demonstrate satellite lesions and intramedullary extension.

The radiological differential diagnosis of parosteal osteosarcomas includes florid reactive periostitis or a bizarre parosteal osteochondromatous proliferation (Nora's lesion).

Surgical Pathology: Grossly, a large ossified exophytic mass with a broad base or, less often, demonstrating encirclement is identified.

The gross semblance to an osteochondroma may be considerable, including the presence of a cartilaginous cap. The lesions are heavily ossified, and may be lobulated. Less ossified areas may represent cartilage, fibrous tissue, fat or more importantly, areas of dedifferentiation. Areas of intramedullary spread should be documented.

On microscopy, parosteal osteosarcomas show long narrow bone trabeculae arranged in a parallel fashion or ill-defined areas of osteoid and woven bone with osteoblastic rimming separated by a fibrous stroma (Fig. 15). The trabeculae may show maturation (normalization), which may result in lamellar bone. The spaces between the trabeculae are often filled with spindled fibroblastic tissue showing *only minimal cytologic atypia*. Most lesions are Grade 1 histologically (Fig. 16).

About half the lesions, in some series have shown the presence of cartilage. In about a third, this was present peripherally, simulating the cap of an osteochondroma. In others, it was admixed with the tumor. The islands of cartilage or the cartilage cap are low grade, and would at the most meet the criteria for Grade 2 chondrosarcoma. The columnar (physis like) arrangement of the cartilage cap that is seen in osteochondromas is not usually seen in parosteal osteosarcoma. High-grade areas resembling conventional osteosarcomas should be interpreted as evidence of dedifferentiation.

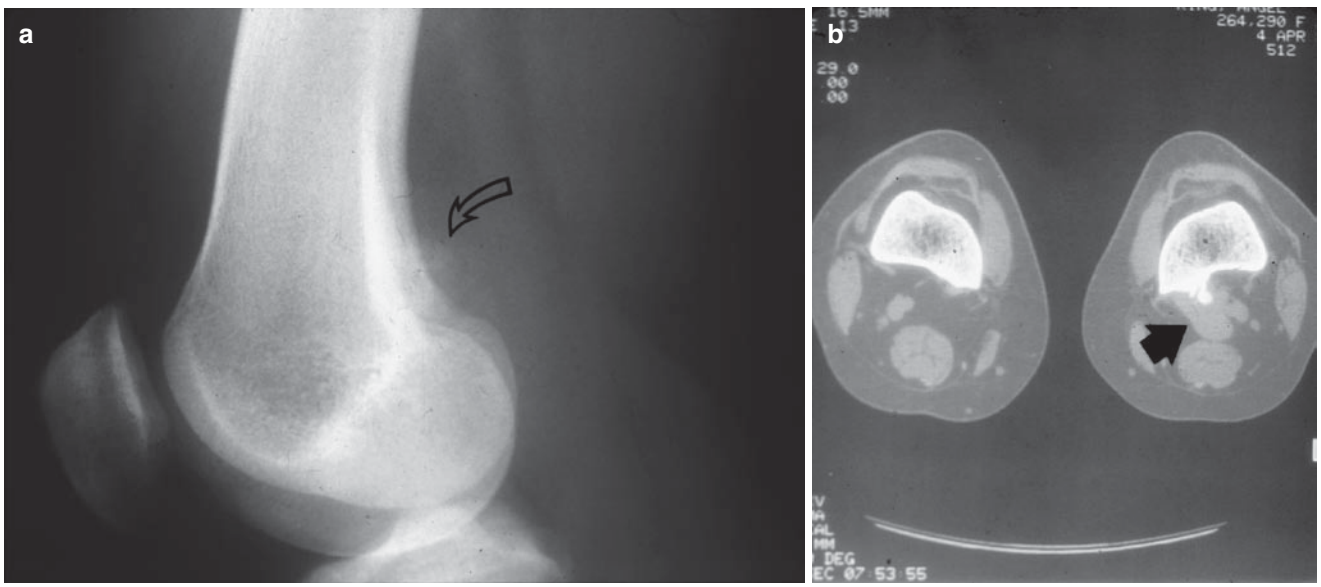

Fig. 15 Parosteal osteosarcoma (plain film **a** and CT scan **b**). The posterior aspect of the femur is a favored site of parosteal osteosarcoma. The tumor in this case was exophytic, and showed no medullary extension

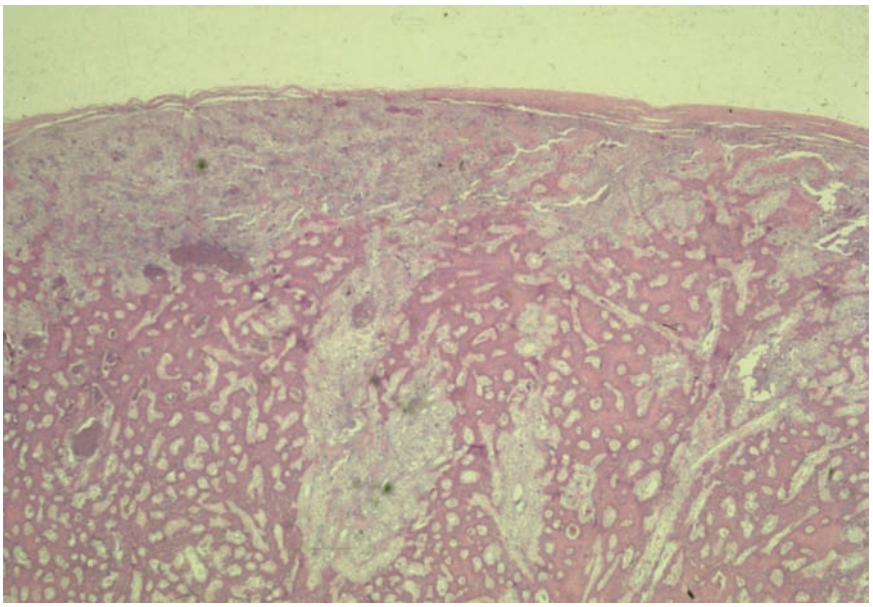

Fig. 16 Parosteal osteosarcoma. The histologic appearance of this particular case was of a low-grade, osteoblastic type of an osteosarcoma. Some examples can have a large cartilaginous cap, and simulate an osteochondroma

The clinical and epidemiological profiles of patients with dedifferentiated parosteal osteosarcoma are similar to those of parosteal osteosarcoma. It is therefore critical to sample the lesions thoroughly to exclude this possibility.

Parosteal osteosarcoma differentiates from conventional type by having one or supernumerary ring chromosome with or without other added genetic abnormalities. Most common abnormalities are gain of 12q13-15 and abnormal long arm of chromosome 12 (12q), associated with low-grade osteosarcomas.

Differential Diagnosis: The lesions should be differentiated from high-grade surface osteosarcomas and conventional osteosarcomas with a prominent extraosseous component. The difference from periosteal osteosarcomas is straightforward, and has been described earlier. Osteochondromas need to be separated, and the extension of the medullary cavity into the extracortical mass should be demonstrated to diagnose the lesion as an osteochondroma. Again, in contrast to the parosteal osteosarcoma, the osteochondromas are lucent toward the center (representing the marrow). Microscopically, the osteochondromas lack an atypical fibrous stroma/osteoid and are composed of bone marrow and bone; their chondrocytes have a columnar arrangement. Bone marrow is usually (but not always) absent in parosteal osteosarcoms.

Reactive soft tissue and periosteal processes may be difficult to differentiate on radiological grounds. Such conditions include myositis ossificans and reactive periostitis. Evidence of zonation is helpful in diagnosing these conditions as benign and this feature is not seen in parosteal osteosarcoma. Finally, there is a cortical irregularity seen in the posterior femur in about 10% of boys (less in girls), which should not be overdiagnosed. Microscopically, this lesion resembles an NOF and disappears with time. Its characteristic location is at the attachment of the adductor magnus muscle to the medial supracondylar ridge.

Management: The tumor is generally managed with wide local excision without adjuvant chemotherapy, since the incidence of systemic metastases is thought to be low. However, inadequately resected tumors recur, and these recurrences are frequently of a higher grade. Parosteal osteosarcomas with intramedullary extension tend also to be of higher grade, and certainly, dedifferentiated forms should be managed with aggressive surgery and chemotherapy depending on the specific situation and stage of the lesion.

Cartilage Lesions

- Osteochondroma
- Subungual exostosis
- Nora's lesion
- Benign chondroma
- Chondroblastoma
- Chondromyxoid fibroma
- Chondrosarcoma and related variants

Osteochondroma

An osteochondroma (or osteocartilaginous exostosis) is an outgrowth of bone, containing the combination of medullary and cortical bone. It projects from the cortical surface and is

covered with a cartilage cap. The direction of growth is away from the closest joint and at an angle with the cortex of the parent bone. The term *exostosis* is used to refer to any outgrowth of a bone (bony spur) from the cortical surface and is a more general term than the specific entity of osteochondroma, or osteocartilaginous exostosis.

The origin of the osteochondroma was earlier thought to be from a displaced epihyseal cartilage, which herniates through a periosteal defect. Support for this came from the finding that osteochondromas are entirely covered by periosteum, and the marrow cavity of the parent bone continues into the osteochondroma. Currently, the idea that these are true neoplasms has come from the finding of consistent clonal genetic alterations in these lesions. Genes belonging to the EXT family have been identified recently, and are possibly linked to the development of benign multiple osteochondromas. These genes are thought to be tumor suppressor genes, and their loss is thought to be responsible for the tumor formation. EXT1 is thought to be present on chromosome 8, EXT2 on chromosome 11, and EXT3 on chromosome 19, respectively. There may be other genes of this family.

Osteochondromas are most often seen in the first two decades of life, with no sex predilection. They develop for the most part in long bones, formed of enchondral ossification. The growth of the lesion often parallels that of the patient, in the sense, that it is most rapid during the adolescent growth spurt and may become quiescent after epiphyseal closure. At times the osteochondroma may regress. There is an increased incidence of these neoplasms in bones, which have been irradiated.

Multiple osteochondromas can be seen in both familial and sporadic setting. The inheritance is autosomal dominant. Multiple osteochondromas are generally associated with a generalized osseous modeling defect. There may be an associated limb growth asymmetry. The familial forms are termed multiple hereditary exostoses or diaphyseal (or metaphyseal) aclasis. Another term, less often used is hereditary deforming chondrodysplasia. Some syndromes associated with multiple osteochondromas are Langier-Giedion (associated with facial dysmorphic features and mental retardation) and Defect-11 (Potocki-Schaeffer) syndrome. Secondary osteochondromas and osteosarcomas have also been reported in pediatric patients after associated autologous hematopoietic stem cell transplant (15). Because of the increased risk, these patients are recommended to have continuous skeletal surveys.

Most osteochondromas are solitary, asymptomatic, and incidental findings. Some, however, come to attention following impingement on nerves, mechanical blocking of joint motion, a fracture through the stalk, a cosmetic deformity, bursae and subsequent pain or inflammation forming on top of them, vascular complications such as a pseudoaneurysm secondary to frictional trauma.Long-standing osteochondromas rarely show a malignant change (mostly in the form of a secondary chondrosarcoma). The incidence of secondary chondrosarcoma arising on osteochondroma is unknown, owing to selection bias, varying forms of treatment, and follow-up. Some studies report it in the order of less than 1% for solitary osteochondromas and only a little more for multiple osteochondromas. The supervening malignancy is almost always a low-grade chondrosarcoma. Individuals with multiple osteochondromatosis have, however, a greater tendency to develop high-grade chondrosarcomas. Patients with multiple osteochondromas also seem to have a higher incidence of flat bone involvement.

Radiologically, osteochondromas appear in the metadiaphyseal region (Fig. 17). The MRI scan is useful for measuring the thickness of the cartilage cap and locating the presence of wide fibrous septae within the osteochondroma. The MR or the CT scan can be utilized for establishing the continuation of the native medullary cavity into the marrow cavity of the osteochondroma. This is an important feature and helps establish the diagnosis. Sometimes osteochondromas are covered by a bursa, which may contain osteocartilaginous loose bodies detectable on ultrasound or CT examination.

Surgical Pathology: Specimens, which have been entirely (extraperiosteally) resected, are covered by a layer of periosteum. There is a well-defined bony stalk, capped by cartilage (Fig. 18). The stalk may be narrow and pedunculated or broad. The multiple forms tend to have broader stalks. The thickness of the cartilage cap varies with age, being greater in younger patients. In adults, the cartilage may be entirely eburnated leaving behind only residual bone. The finding of a cartilage cap of over 2 cm in an adult is suspicious of a chondrosarcoma developing on an osteochondroma. If a bursa is resected with the osteochondroma, this may contain within it deposits of fibrin (rice bodies) or calcified cartilaginous bodies. Cut section of an osteochondroma may be remarkable for foci of calcified mosaics of cartilage, osteoid, or amorphous debris. These variegated areas should be sampled, but are not necessarily worrisome. Unlike polypoid carcinoma, secondary chondrosarcomas rarely if ever invade into the stalk of the osteochondroma. Regions of the cap showing cystic change should also be sampled.

Microscopically, the presence of a periosteum over the cartilage cap can be seen. The chondrocytes of the superficial portion of the cap contain occur in clusters and in lacunae. Those toward the base, line up simulating a growth plate. Below this, enchondral ossification is often seen (Fig. 19). In actively growing osteochondromas, occasional binucleate chondrocytes may be seen within the cartilage cap. The stalk shows a medullary cavity containing fatty or hematopoietic marrow.

An important feature to remember is that large disorganized masses of cartilage, bone, and amorphous calcified debris may be present within the stalk. Focally, the cartilage may be necrotic. These features should not be taken as evidence of stalk invasion by a chondrosarcoma.

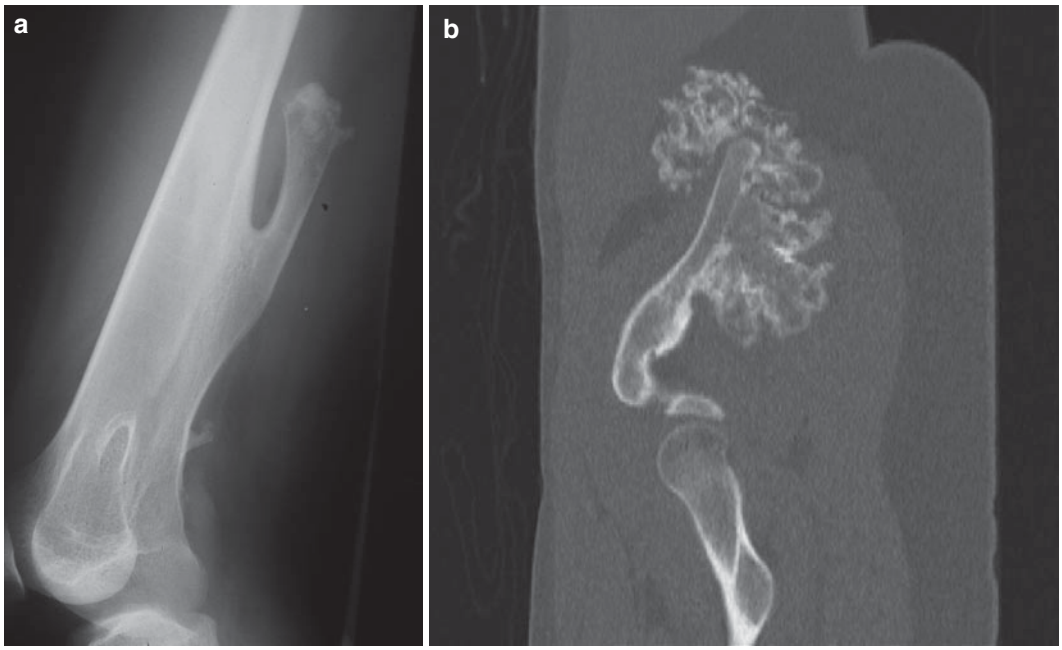

Fig. 17 **a** Plain film of an osteochondroma is seen at the distal end of the femur, characteristically growing away from the knee. Continuity between the cortex of the osteochondroma and the underlying bone is obvious. **b** CT scan of a large osteochondroma of the iliac wing with extension into the pelvis. The medullary cavity of the ilium extends into the osteochondroma

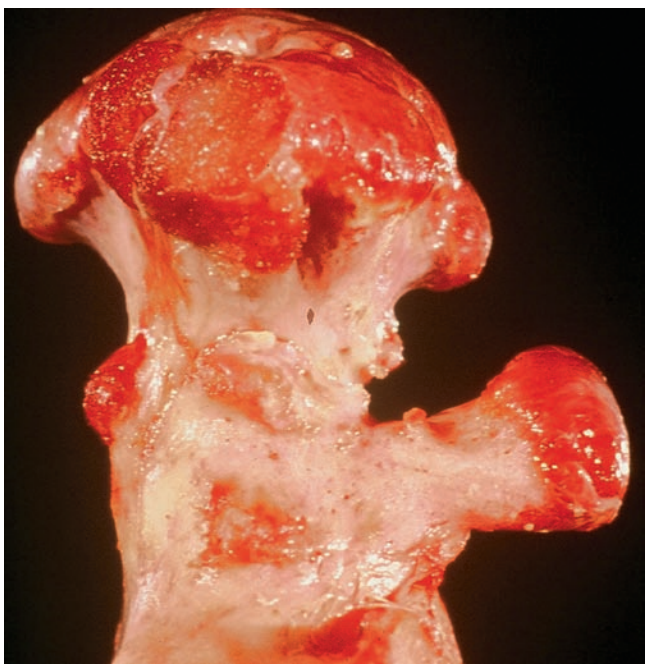

Fig. 18 Outer aspect of an osteochondroma arising on the upper fibula demonstrating the continuity of the cortex of the lesion and the underlying bone

It is important to exclude malignant change in an osteochondroma, most often this is a supervening chondrosarcoma. Chondrosarcomatous cartilage is cellular, often shows prominent myxoid change, and may have wide fibrous bands which accentuate its lobular character. These bands at times may be quite cellular. A search should be made for evidence of underlying bone destruction or extension of the cartilage into the soft tissues beyond the confines of the periosteum. Unequivocal chondrosarcomas show evidence of permeation and bone entrapment (Figs. 20a, b and 21a, b).

A spindle cell proliferation occurring within an osteochondroma may be the result of a repair reaction from trauma. It is important to pay attention to the cytologic features of this proliferation and exclude a parosteal osteosarcoma. High-grade sarcomatous change is uncommon both in secondary chondrosarcomas and in parosteal osteosarcomas. High-grade sarcomatous change indicates dedifferentiation.

Differential Diagnosis: The main diagnostic dilemma when faced with a specimen of an osteochondromatous growth is whether there is a malignant change supervening on it. The clues to its occurrence have already been discussed above. Specimen X-rays to demonstrate "lucencies" and a fuzzy border between the cartilage and the bone can be utilized to help in choosing areas to sample. The distinction of an osteochondroma from a parosteal osteosarcoma has been discussed earlier. The distinction from other exostoses can be done by the demonstration of a continuation of a medullary cavity into the outgrowth. This feature can be demonstrated either grossly on cut section of the osteochondroma or preoperatively on the imaging studies.

Management: Symptomatic or cosmetically distressing osteochondromas are often excised. Recurrence has been

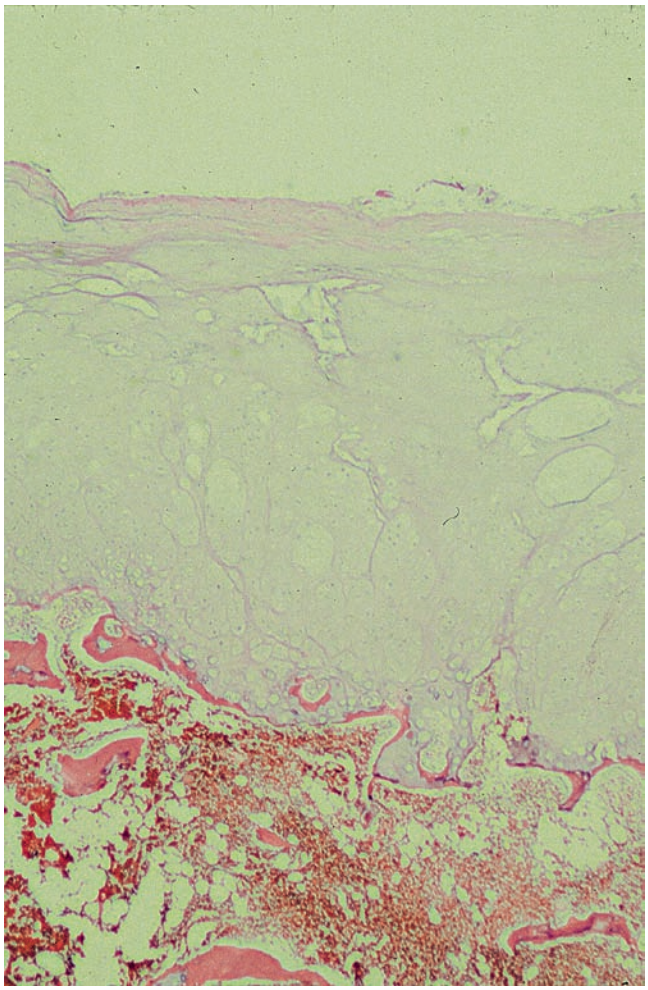

Fig. 19 An osteochondroma showing a thin cartilage cap lined by perichondrium on the surface. There is only slight myxoid change in the cartilage. There is endochondral ossification occurring at the junction with the underlying bone and marrow

associated with the failure to remove the cartilaginous cap or its covering periosteum (called a subperiosteal resection). Chondrosarcomas supervening on an osteochondroma require a wide excision.

Subungual Exostoses

The term subungual exostoses refers to bony protuberances that develop in the distal phalanges of the bones of the hands and feet on the dorsal aspect (subungual). Patients with these lesions often give a history of prior trauma.

Radiologically, the lesions do not show a continuity of the cortex with the protubrance, and this feature helps differentiate the entity from an osteochondroma.

Surgical Pathology: The specimens show proliferating fibrocartilaginous tissue resembling callus. There is a tendency to show mature bone formation in an orderly pattern, which allows the diagnosis to make and prevent misdiagnosis of this lesion as a sarcoma. Skin included in the biopsy or excision specimen should be assessed for excluding the rare entity of a melanoma producing an osteoblastic reaction.

Bizarre Parosteal Osteochondromatous Proliferation (Nora's Lesion)

This is an exophytic outgrowth from the cortex, consisting of a mixture of cartilage, fibrous tissue, and bone. The lesion is clinically benign but microscopically disturbing. The lesions have a predilection for the bones of the hands and feet; long bone involvement is less common but recognized.

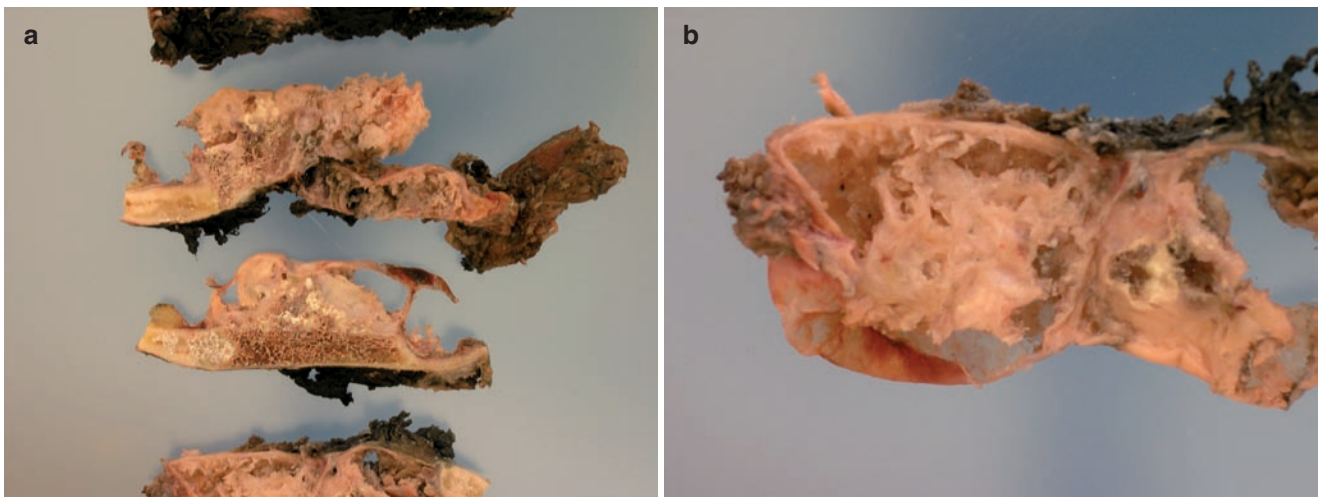

Fig. 20 **a** Secondary chondrosarcoma arising on an osteochondroma of the rib. The lesion was large (5 cm) and extended into the soft tissues of the chest. **b** Prominent cystification is seen as a result of myxoid change

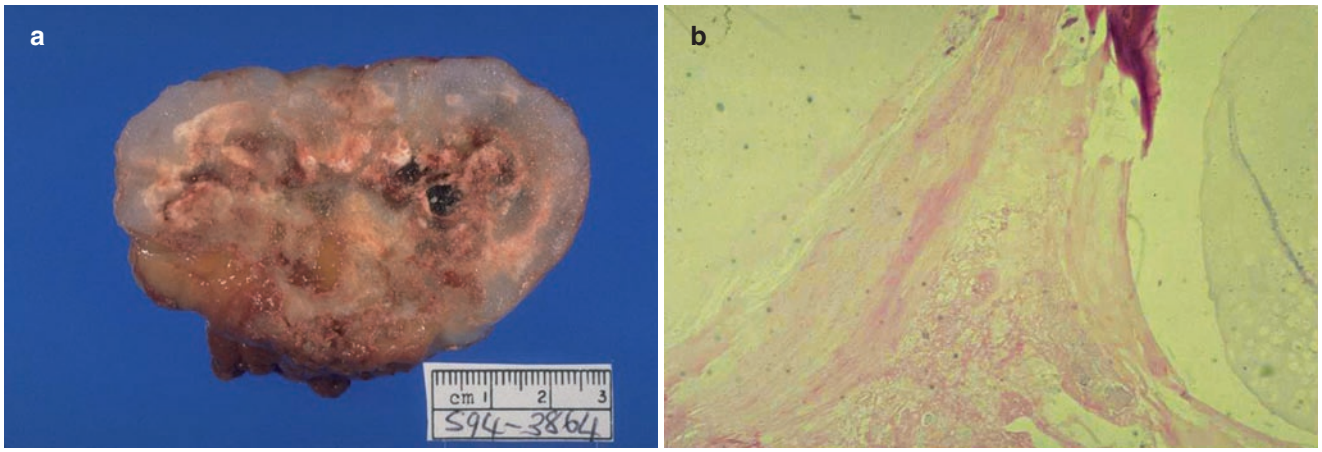

Fig. 21 **a** Chondrosarcoma arising in an osteochondroma. The patient had hereditary multiple exostoses. This particular lesion became painful and started growing after 15 years of surveillance. The thickness of the cartilage cap at excision was 2.0 cm. **b** The photomicrograph shows broad fibrous bands within the lesion, which were visualized by MRI as well

There is a wide age range but most cases are in the third decade.

Radiologically, the outgrowth mimics an osteochondroma or a parosteal osteosarcoma, in that it arises directly from the cortex, and has an identifiable pedicle. The lesions range from about 0.5 to 3.0 cm. The location of the lesion, when present in the hands or feet, is away from the nail bed. This helps to distinguish it from a subungual exostosis. The lack of continuity with the cortex helps distinguish it from an osteochondroma.

Surgical Pathology: Grossly, the lesions have a stalk and may have a well-defined cartilage cap. The mass may sometimes show lobulations. Microscopically, there is a mixture of cartilage, bone, and a spindle cell element. The cartilage may form a cap and is often very cellular, with enlarged, bizarre nuclei. The chondrocytes often show bi- or multinucleation. The interface with the underlying bone is irregular and there are admixtures of bone and cartilage prominent at this junction. At times, there is no cap, and the cartilage is admixed with bone and the spindle cells. The bone may show considerable osteoblastic prominence, and is more irregular than what is typically seen in osteochondromas. A helpful feature, in the diagnosis, is the blue tinctorial quality of the bone in routine sections. Fibrous tissue and osteoclast type giant cells may be intermixed.

Differential Diagnosis: Osteochondroma enters the differential but is differentiated by the presence of a medullary cavity within the stalk, which continues into and communicates with the medullary cavity of the underlying bone. Further, the degree of cellularity and atypia seen in Nora's lesion is far greater than that expected in an osteochondroma.

Myositis ossificans and fracture callus are other entities that enter the differential but unlike Nora's lesion these show a well-defined pattern of zonation.

Parosteal osteosarcoma is an important differential to exclude. Osteosarcomas are infrequent in the bones of the hands and feet. More importantly, they show a spindle cell atypia which is not seen in Nora's lesion.

Management: Marginal excision suffices in most cases. Recurrences should be treated with wide excision.

Benign Chondroma

Benign chondromas are benign cartilaginous neoplasms and can be thought of as occuring in either a *central* location within the bone (enchondroma) or on the *surface* (periosteal chondroma). There are perhaps some overlaps (enchondroma protruberans). In flat bones, the distinction between these types can be unclear. Chondromas are often situated in the metaphysis or diaphysis; multiple chondromas can occur as a skeletal dysplasia. Multiple enchondromas sometimes tend toward unilaterality (Ollier disease). Multiple enchondromas can also rarely be associated with angiomas of the soft tissues (Maffucci syndrome).

The most frequent locations of enchondromas are the bones of the hands and feet (half of all enchondromas occur in this location). Periosteal chondromas are more frequent in the appendicular skeleton. Flat bones are less often the site of benign chondromas.

Multiple enchondromatosis is a nonhereditary disorder, characterized by multiple enchondromas. The extent of the disease may be variable. Sometimes, limbs in one-half of the body are involved. The affected limb is often shortened and deformed. Any site (diaphysis, metaphysis or epiphysis) may be involved. The lesions do not progress beyond puberty. ubsequent growth should be suspicious for a supervening chondrosarcoma. This occurrence is said to be in the order of upto 30% in some series.

Maffucci syndrome is a rare, nonhereditary congenital disorder consisting of enchondromatosis with hemangiomas

(usually of the cavernous type). The latter can be located in various parts of the skin and soft tissue and show frequent phlebolith formation. Patients with this disorder are prone to the development of second malignancies including those of the bones and joints.

Clinically, enchondromas are often asymptomatic and often discovered incidentally. Pain and pathological factors may occur in enchondromas of the phalanges; however, the presence of pain or fracture in long tubular bones is unusual (these features are more common in low-grade chondrosarcomas which can also occur in these locations).

Radiologically, chondromas (both en- and periosteal-) are small lesions, often showing well-defined or sclerotic margins, sometimes with lobulated edges. Mineralization within the lesion takes place in the form of semicircles and circles (Cs and Os).

Periosteal chondromas appear as eccentric longitudinally oriented periosteal masses. They often erode the cortex and produce a concave, sclerotic contour. Periosteal new bone is formed, which buttresses the lesion and gives a concave appearance.

Enchondromas are lucent, mostly central, and diaphyseal. Matrix calcification may occur, especially in the phanlanges. They frequently expand the parent bone. Chondromas are frequently "hot" on Technetium bone scans.

Surgical Pathology: Grossly, the tumors are well circumscribed, and mostly small (3–5 cm) lesions. Periosteal chondromas may be covered in a thin shell of periosteum, or reactive bone. On cut-sections, chondromas are composed of semitranslucent, hyaline cartilage. Cyst fromation is unusual, and raises the possibility of the lesion representing a chondrosarcoma.

Microscopically, the features of chondromas vary with the location. In most chondromas, irrespective of location, the cartilage has a lobular configuration that is characteristic. The lobules are separated by fibrous or lamellar bony septae. These may be rimmed by reactive woven bone or calcification (the basis for the C's and O's of the radiological picture). Ischemic necrosis of chondrocytes may occur in calcified areas.

Enchondromas, in the tubular long bones (excluding the hands and feet), show small chondrocytes, lying in lacunae (Fig. 22). They have round, regular nuclei, which are barely visible at low magnification. Binucleation of chondrocytes and necrotic foci are extremely rare. Binucleation of chondrocytes should, however, be distinguished from the presence of two or more chondrocytes lying in a single lacuna. Calcification may be seen and bone formation is often seen surrounding the lobules of cartilage.

Enhondromas of the hands and feet can be alarmingly cellular. Chondrocytes may be present in clusters, or even sheets. Nucleomegaly and binucleation, as well as slight myxoid change of cartilage are permissible. Permeation of the cortex or entrapment of bone however, is not permissible, and is a sign that the lesion is a chondrosarcoma. Similarly, extreme hypercellularity, nuclear pleomorphism, and extensive myxoid change are ominous features.

Periosteal chondromas also show cytologic atypia. However, they are well-demarcated lesions, and show no tendency to permeation. Myxoid change is unusual (Fig. 23).

Multiple enchondromas can also be quite cellular, with the chondrocytes tending to spindle. Atypia and myxoid change, however, should be taken seriously and a chondrosarcoma should be excluded.

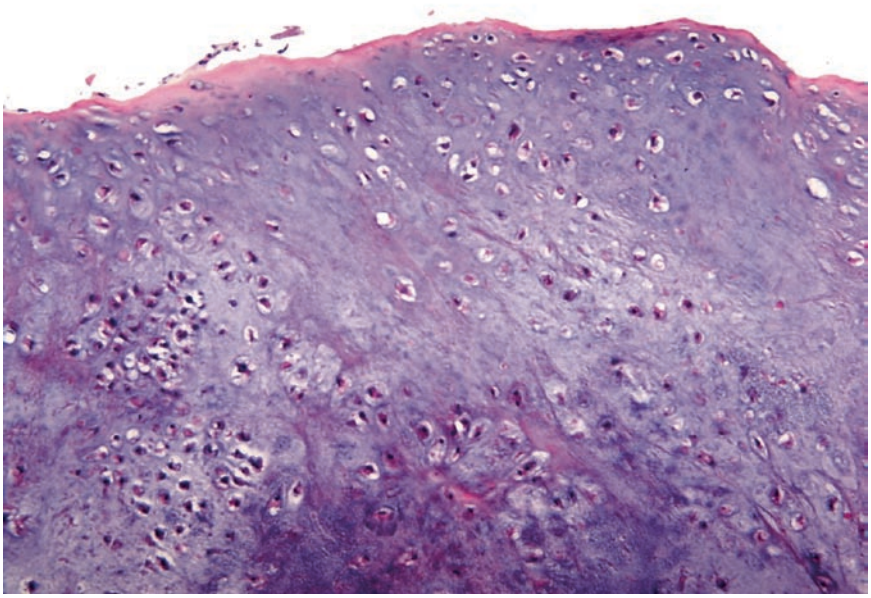

Fig. 22 Well-delineated lobule of cartilage from an enchondroma. The lesion is relatively hypocellular and composed of typical chondroblasts lacking atypia, mitoses, necrosis, and myxoid change

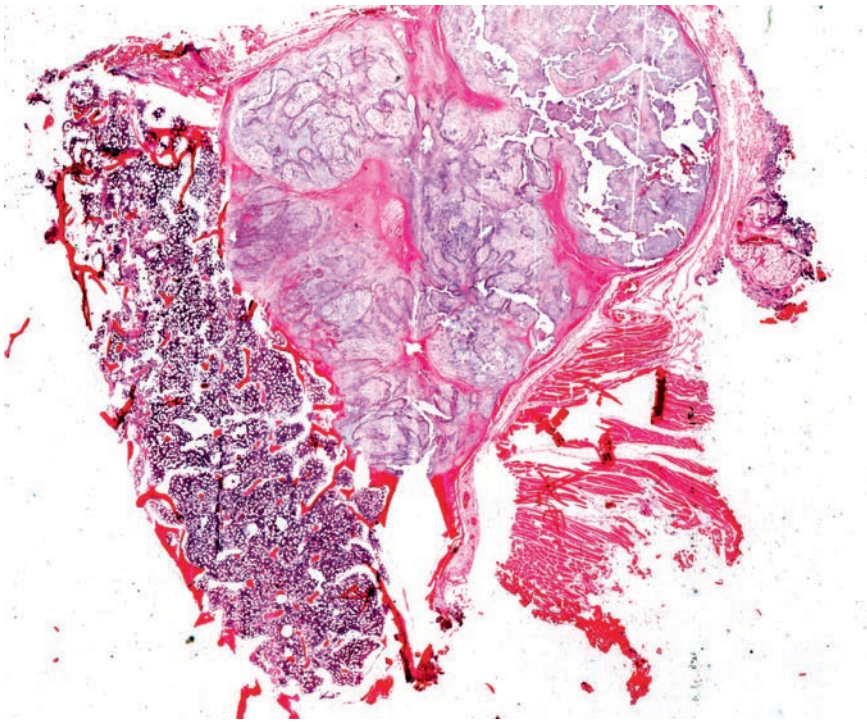

Fig. 23 Periosteal chondroma. This small lesion is arising on the surface of the underlying bone

Differential Diagnosis: Juxtacortical chondrosarcoma and periosteal osteosarcoma are the main neoplasms to exclude from periosteal chondromas. Invasion into the soft tissues, a more marked cytological atypia and radiological appearances should be used to help in this differentiation.

The main lesion to exclude is a low-grade chondrosarcoma. In some cases, this can be difficult. Size can be a clue, since chondrosarcomas tend to be large. There is an overlap in the amounts of cellularity, mitotic activity, and other cytological features of atypia. Thus, enchondromas of the phalanges may often exhibit considerable cellularity and myxoid change; however, in the flat bones of the sternum, pelvis, and shoulder girdle, these features should be taken seriously and indicate a chondrosarcoma. Clinical features (such as pain or pathological fracture) and radiological features (such as cortical scalloping and breakthrough) are suggestive of a low-grade chondrosarcoma. Features such as permeation of the cortical bone, entrapment of preexisting bone trabeculae, and cortical breakthrough with extension into the soft tissues in absence of a fracture are features of chondrosarcoma and should not be seen in enchondromas.

An additional problem is the occurrence of a chondrosarcoma on a preexisting long-standing enchondroma. This diagnosis is made when two clearly defined grades of cartilage can be seen coexisting. One is a benign, hypocellular component and the other is a clearly hypercellular, atypical component. Sometimes serial X-rays can be of help, in identifying these cases. In the majority of cases, one can never be absolutely certain about the presence of a preexisting benign enchondroma in a chondrosarcomatous lesion.

Ollier, Louis Xavier Edouard Leopold (1830–1900): Ollier was born in December 1830 at Vans, Ardeche. His father and grandfather had both been physicians. He studied natural science and then medicine at the University of Montpellier. He graduated in 1856, and wrote a thesis on the histologic studies of 400 neoplasms. He was appointed senior surgeon at Hotel-Dieu, Lyons. He was involved with care of the war wounded following the German invasion in 1870 and received international recognition for his work. He was invested Commander of the Legion d'Honneur by President Carnot in Paris in 1894. He died in 1900 and is considered the father of French orthopedic surgery. In 1897, he had presented a 6-year-old girl in whom deformities of the forearm and thigh were associated with swelling of the fingers. He later went on to demonstrate lucencies of the diaphysis of her long bones, and termed the condition dyschondroplasia. This condition is now eponymically named after him (multiple enchondromatosis). When associated with hemangiomas, the term Maffucci syndrome is used.

Multiple Enchondromatosis and Ollier Disease

Multiple enchondromas may occur, generally in a sporadic fashion (but occasional families are reported with the disease). The involvement is often unilateral. Growth of the lesions may occur in childhood, but continued or renewed

growth in adulthood is suspicious for secondary malignancy (secondary chondrosarcoma may occur in up to 20% of cases). Some studies have implicated a gene encoding for a receptor of parathyroid hormone (PTH) and PTH-related peptide (PTHR1 gene) (16).

Surgical Pathology of Enchondromas in Ollier Disease

In enchondromas of Ollier's disease, focal necrosis and/or myxoid change may occur. This change is seen not infrequently in the short tubular bones of the hands and feet. The enchondromas of Ollier's disease may be alarmingly cellular. These lesions may also show considerable atypia, rendering the differentiation from low-grade chondrosarcoma very difficult. Necrosis or myxoid change in this setting favors a chondrosarcoma.

Management: The management is usually that of marginal excision or curettage and bone graft or methyl methacrylate packing, if needed. Recurrences are managed by wide procedures. Spontaneous remission of some chondromas have been reported, albeit rarely.

Chondroblastoma

Chondroblastoma is a benign cartilaginous neoplasm, showing predilection for the epiphysis. Lesions also occur in secondary epiphyses, and apophyses such as the greater trochanter of the femur, or the tuburosity of the humerus. The majority of the neoplasms occur in patients under 25 years. Chondroblastomas in unusual locations, however, may occur in older age groups. About 20–30% of chondroblastomas may occur in flat bones or the short tubular bones. Most of the latter are in the talus or in the calcaneus. Occasional lesions occur in the craniofacial skeleton especially the temporal bone, which is formed partly by enchondral ossification. The patients often present with pain, sometimes long-standing.

Some chondroblastomas can metastasize, and in these cases, resection of the metastases usually produces good results (it is thus debated whether these lesions may be "passively" transported to the lung, rather than truly "metastasizing"). In rare cases, a protracted or aggressive course is seen; these lesions (often in hindsight) have been termed aggressive chondroblastomas.

Radiologically, chondroblastomas are lytic geographic lesions, with well-delineated or sclerotic margins (Fig. 24a, b). They are centered in the epiphysis, but they may grow into the metaphysis. There is no matrix production in the majority of cases. In about a third of cases, fine matrix calcifications or trabeculations may be seen. Penetration into the joint is unusual. A secondary ABC component is not infrequent. Chondroblastomas may rarely be large, aggressive and show cortical breakthrough.

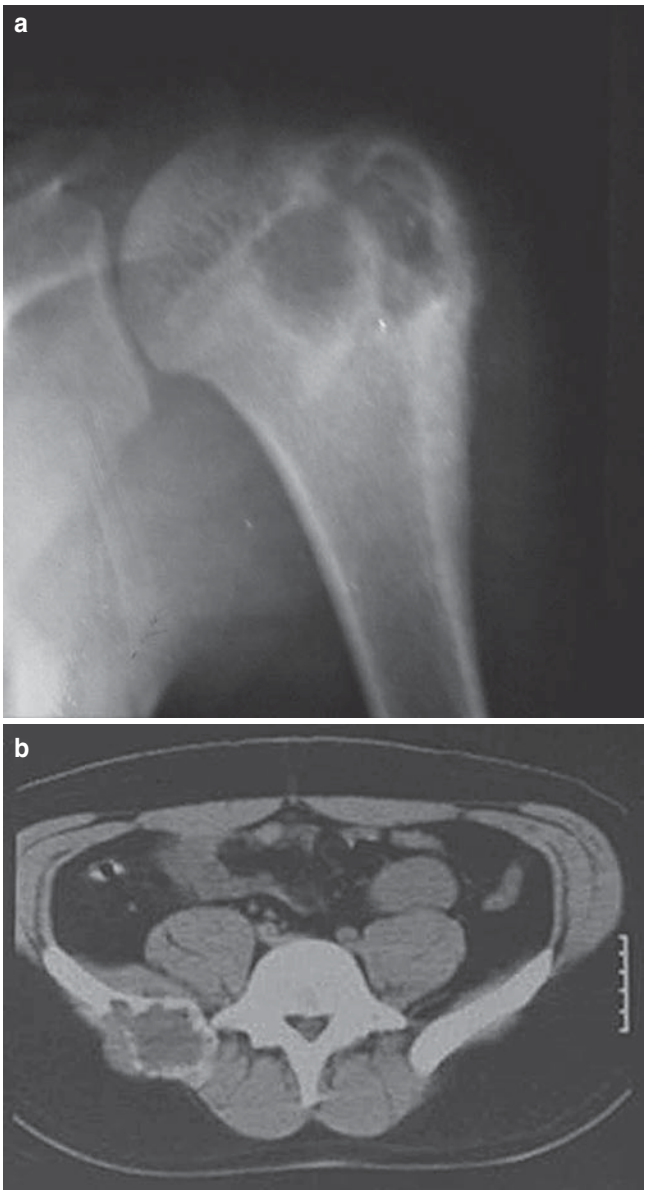

Fig. 24 **a** Chondroblastoma. This example occurred in the humerus. It is located in the epiphysis and is a well-demarcated, geographic lesion. **b** Another example of chondroblastoma occurring in the flat bones of the pelvis. There is considerable bony expansion caused by the lesion

Surgical Pathology: Grossly, they are circumscribed variegated lesions. A secondary ABC component may be seen. Blue gray areas may represent cartilage; yellow gritty areas may represent calcification or secondary woven bone.

Microscopically, the tumors show a spectrum of histologic appearances (Fig. 25a–c). This is due to the inconstant amounts of matrix, secondary changes (ABC like), and cytological variability.

The chondroblast is typically a polygonal to oval cell with a sharp cytoplasmic border, lightly staining or clear cytoplasm. Some chondroblastomas, however, lack this feature and may be referred to as the syncytial variant. The nucleus of the chondroblast is round to oval. Often there is

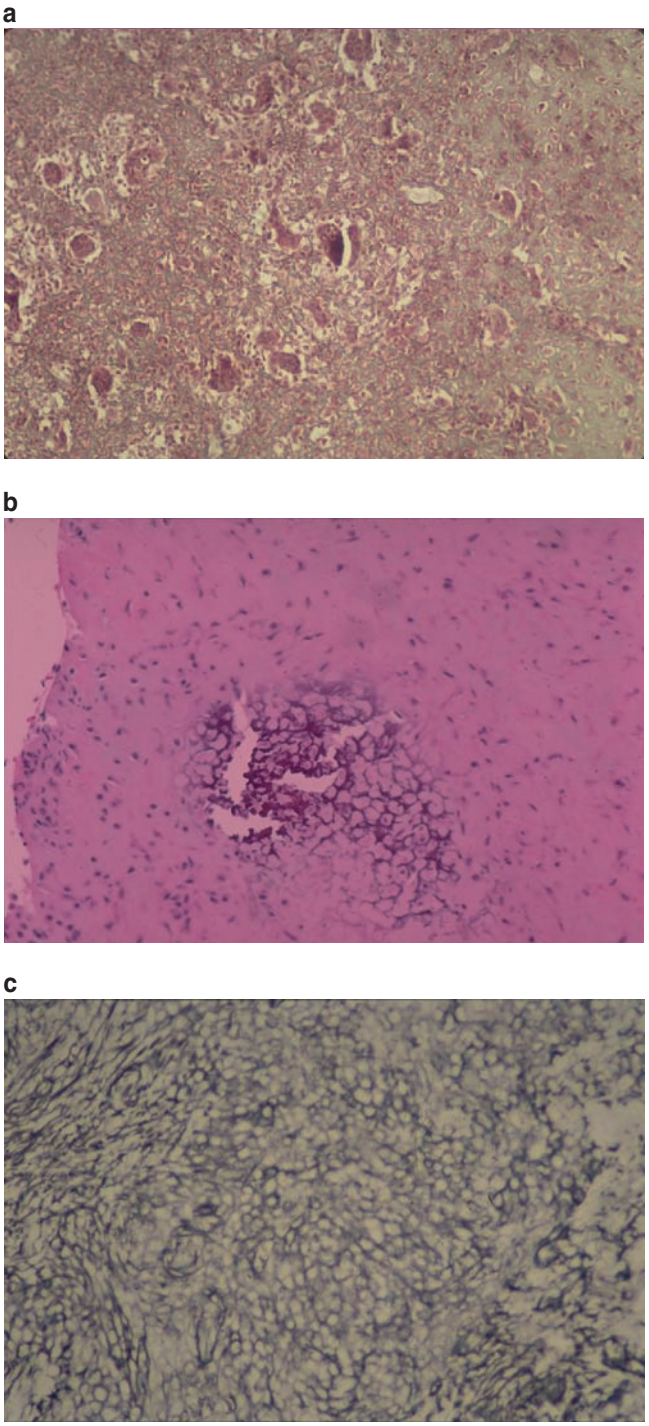

Fig. 25 **a** Chondroblastoma characterized by polygonal cells in a background matrix. There is a sprinkling of multinucleate giant cells. **b** Chicken-wire calcification in a chondroblastoma. **c** Chondroblastoma, reticulin stain outlines the lesional cells

prominent nuclear grooving (a feature, which can be utilized in fine needle aspiration). Mitotic figures may be seen but are not very frequent. Atypical mitoses are absent. Some chondroblastomas comprise of cells that have abundant pink cytoplasm. These have been referred to as epitheloid variants. In still other examples, a sprinkling or focal aggregates of spindle cells may be seen. Scattered osteoclast-type giant cells may be seen in many chondroblasomas. About a quarter of chondroblastomas show a small number of cells with enlarged, hyperchromatic nuclei. These are not related to an adverse outcome. Pigmented cells (hemosiderin-laden macrophages as well as pigmented chondroblasts) are sometimes prominent. Pigment is often prominent in lesions occurring in the craniofacial and skull bones.

The matrix often has an eosinophilic quality in most cases, which is a clue to the diagnosis of its chondroid nature. Calcification may be found focally, or more typically surrounding the chondroblast. The latter is especially true in foci of necrotic chondroblasts. The result is a characteristic "chicken wire" pattern of calcium deposition. This feature is present in almost two-thirds of the cases in most series.

The diagnosis of chondroblastoma is made by establishing a chondroid differentiation; however, very obvious chondroid differentiation may not be readily apparent. In other cases, chondroid matrix may dominate the picture. The matrix in chondroblastomas is often pink-staining rather than blue. Mature chondrocytes are unusual. In some cases, features suggestive of a chondromyxoid fibroma may be seen. Focal cellular atypia or necrosis could be seen in upto 10% of cases. Vascular invasion is rare but is sometimes seen especially in lesions of the skull bones.

Immunohistochemically, S-100 protein is frequently (but not invariably) demonstrable in the chondroblast. The tumor cells are also positive for neuron-specific enolase and vimentin. Some studies have reported positivity for epithelial markers such as cytokeratin and epithelial membrane antigen.

The genetic overview of these chondroblastomas and their aggressive/malignant counterpart is very limited since only a handful of cases have been studied. The most recurrent chromosomal abnormalities involve chromosomes 5 and 8 (17).

Differential Diagnosis: Radiologically, the differential diagnosis includes epiphyseal lesions such as giant cell tumor (GCT) and clear cell chondrosarcoma.

The majority of the chondroblastomas, however, occur in an age group when the epiphyses are open. GCT and clear cell chondrosarcomas are more typically neoplasms of an older age group. Histologic differentiation from the typical GCT requires attention to the chondroblast.

Clear cell chondrosarcomas are composed of broad sheets of cells with a voluminous clear cytoplasm. Although cells indistinguishable from chondroblasts may be found in clear cell chondrosarcoma, these are a very minor component. As predictable, S-100 stains cannot be employed in this situation, since both these tumors are of cartilage lineage. Some osteosarcomas can resemble chondroblastomas. These lesions often have a spindle cell stromal component with significant cellular atypia.

Management: The majority of these tumors are managed by marginal procedures such as curettage and bone graft or methyl methacrylate cement packing. Cryosurgical techniques may add a measure of safety. As with many other cartilage tumors, soft tissue implantations are associated with recurrence and care has to be taken at surgery to avoid spillage. Recurrences (which usually manifest themselves within the first 2 years) are managed by wide excisions. Recurrences may be more common in flat bones rather than long bones (18). About 1% of chondroblastomas may behave aggressively. Late metastases too have been reported, but these instances are extremely rare. Successful resections of pulmonary metastases have been reported with good results.

Chondromyxoid Fibroma

Chondromyxoid fibroma is a benign but locally aggressive cartilaginous tumor characterized by lobules of spindle-shaped or stellate cells in a myxoid (or chondroid) stroma. These tumors were first recognized and described by Jaffe and Lichtenstein in 1948. Chondromyxoid fibromas share some features with chondroblastomas. It is possible that some previously described examples of myxomas of the appendicular skeleton were in fact, chondromyxoid chondromas.

The majority of the patients are below the age of 30 years. The presentation is usually with mild, transient pain, often long-standing. Most cases occur in the long bones of the appendicular skeleton, especially the tibia, but at least a quarter of cases are seen in the flat bones especially the ilium. Involvement of the short tubular bones of the hands and feet is not infrequent.

Radiographically, the lesions are geographic, with well-defined usually sclerotic margins, often eccentric and centered about the metaphysis. Epiphyseal extension may be seen. Chondromyxoid fibromas of the hands and feet are often central and cause expansion of the short tubular bones. Those in the flat bones are often irregularly lobulated. Frequently, there is a radiographic impression of trabeculae seeming to traverse the lesion. Matrix calcification in any site is extremely unusual and should raise suspicion of a chondrosarcoma. A series of cases have been described, however, which were heavily mineralized. Several of these cases were surface lesions (19).

Surgical Pathology: Grossly, the lesions are small, circumscribed, and lobulated. Often, there is a semitranslucent quality to the sample.

Microscopically, the tumors are variable, and may show several different components in varying proportions. The overall pattern is that of lobules, that may be easily seen under low magnification, or may be small, and appreciated, only under intermediate power magnification. The lobules have a hypercellular periphery and septae surrounding hypocellular myxoid matrix (Fig. 26). The fibrous component is usually small and often confined to the septae separating the lobules. These septae on occasion contain blood vessels, osteoclast-type giant cells, and osteoid. The cells in the septae may be spindle or stellate. In some examples, the region between the lobules may resemble chondroblastomas. In curetted material, the septae may be difficult to visualize. The myxoid component is variably cellular. This is true

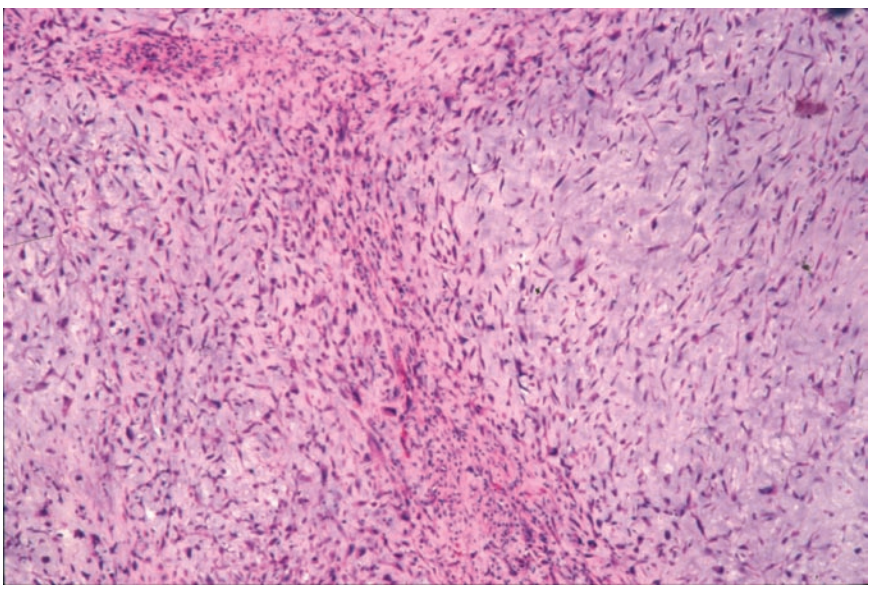

Fig. 26 Chondromyxoid fibroma. There is a lobulated lesion with cartilaginous differentiation. The center of the lobule is hypocellular. A condensed hypercellular periphery is characteristic of this lesion

within as well as between lobules. Pleomorphic cells are frequent, and should not be overinterpreted as malignant. Occasionally, the semblance to chondrosarcoma is seen. In chondromyxoid fibromas, however, there is an absence of cellularity in the center of the lobules and very few mitoses. In this instance, it is important to remember that upto 10% of chondromyxoid fibromas can have necrotic foci. Upto a third of lesions can have either chunky or fine, lace-like calcification.

Genetic studies are limited but have found clonal abnormalities of chromosome 6 (20).

Differential Diagnosis: Chondrosarcoma is the most frequent lesion to prove problematic. Both these tumors can have a lobular growth pattern, peripheral cellularity, atypical cells, and a myxoid stroma. Similarly, reactive osteoid can be seen along the edges of the lobules of both lesions. Permeative growth pattern and bone entrapment are seen only in chondrosarcoma.

Extragnathic Fibromyxoma: This is a controversial entity, which could enter the differential diagnosis of chondromyxoid fibroma. As the name implies, the predominant tissue is fibrous, with a myxoid stroma, but chondroid, osteoid, bone, and calcification can occur to variable degrees. The age range of these fibromyxomas is broader and the location predominantly metaphyseal. Lobulation and the alternating hyper- and hypocellular areas, both characteristic features of chondromyxoid fibromas are absent in extragnathic fibromyxomas.

Management: As with chondroblastomas, these lesions are managed by marginal procedures such as curettage and bone/cement packing. Again, in common to many other cartilage tumors, soft tissue implantations are frequent and associated with recurrence. Care has to be taken at surgery to avoid "spillage." Recurrences (which usually manifest themselves within the first 2 years) are managed by wide excisions.

Chondrosarcoma and Its variants

- Conventional chondrosarcoma
- Dedifferentiated chondrosarcoma
- Clear cell chondrosarcoma
- Mesenchymal chondrosarcoma
- Juxtacortical chondrosarcoma

Conventional Chondrosarcoma

A malignant tumor in which there is differentiation of the neoplastic cells to form chondroid but *not* osteoid. These tumors are referred to as *primary* when arising on a previously normal bone and *secondary* when arising on underlying benign, usually cartilaginous, neoplasms, such as osteochondromas.

Again, depending on their location within the bone they can be thought of as *central* or intramedullary, *peripheral* or having an epicenter in the cortex. Peripheral chondrosarcoms must be differentiated from periosteal osteosarcomas. Confusingly, in radiological literature the term peripheral chondrosarcoma is used to describe secondary chondrosarcomas arising on an osteochondroma. In addition to these, a minority of chondrosarcoms, arising juxtaposed with highly malignant tumors such as osteosarcomas, malignant fibrous histiocytomas, and fibrosarcomas. Such chondrosarcomas are called *dedifferentiated*.

Chondrosarcomas tend to occur in age groups somewhat older than the de novo osteosarcomas. Primary chondrosarcomas have a peak incidence in the fifth to seventh decades, and secondary osteosarcomas in the fourth and fifth decades. Less than 2% chondrosarcomas occur in patients less than 20 years of age.

Pain (with or without a mass) is the commonest presentation of patients with a central chondrosarcoma, whereas a mass (with and without pain) is the common presentation of peripheral chondrosarcomas.

Chondrosarcomas are often centered around the trunk and the proximal limbs. About two-thirds of chondrosarcomas occur in the limb girdles, femora, and humeri. Involvement of the craniofacial skeleton, spine, and the small bones of the hands and feet are rare. There is some controversy over chondrosarcoma of the base of the skull. It is possible that at least some of these cases might represent chondroid chordoma.

Chondrosarcomas have a slow biologic evolution, compared to osteosarcomas. Metastases are infrequent by comparison, and occur late in the course of disease. Recurrent chondrosarcomas have been found to behave with a greater degree of malignancy, and may more often dedifferentiate.

Radiologically, chondrosarcomas tend to be large lesions. Central chondrosarcomas arise in either the diaphysis or the metaphysis (Fig. 27a–e). Epiphyseal origin (and joint involvement) is rare, except in the clear cell variant of chondrosarcoma where an epiphyseal location is typical. Intramedullary spread is common and can be extensive. Peripheral chondrosarcomas appear as masses protruding from the bone. Matrix calcifications are common in both of these types of the conventional chondrosarcoma. They take the form of "C's and O's" as is common in tumors of cartilage origin. The margins of the lesion can vary from irregular geographic to permeative. Areas of increased lucency or inhomogeniety within the lesion should raise suspicion of dedifferentiation.

Surgical Pathology: High-grade chondrosarcomas are relatively straightforward to diagnose. They are composed of cellular cartilage showing extension into soft tissues and/or permeation of bone with entrapment of preexisting trabeculae. There may be widespread mitotic activity, multinucleation of chondrocytes, and necrosis. In fact, in such cases

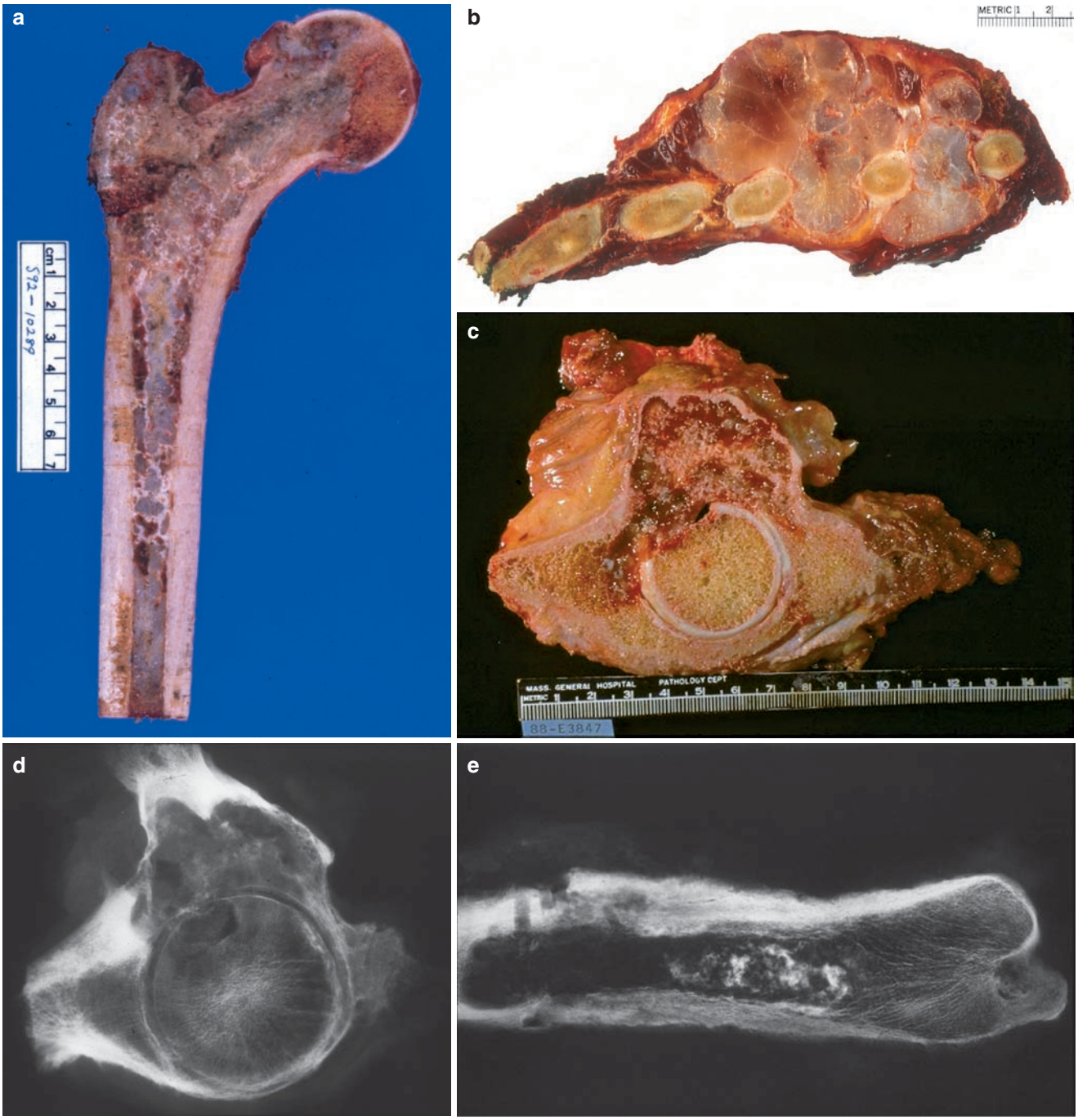

Fig. 27 Chondrosarcoma of the proximal femur **a**, sternum **b** and pelvis **c** & **d**. Picture e is from a different patient with a femoral chondrosarcoma. The patient in part **a** was initially thought to be a metastasis and treated by a screw and side plate, the tract of which is visible. Parts **d** and **e** are specimen radiographs showing cortical scalloping and the classic popcorn-like calcification seen in cartilage tumors. Pictures from the patient with the pelvic chondrosarcoma (**c** and **d**) are contributed by Dr Andrew Rosenberg, Massachusetts General Hospital

although malignancy is obvious, it may be necessary to exclude other malignancies that have considerable cartilage as a component, such as chondroblastic osteosarcoma.

Low-grade *c*hondrosarcomas, on the contrary, can be difficult to diagnose and differentiate from benign but cellular cartilage lesions such as chondromas. Experience and long follow-up studies have shown that different rules apply in different locations. For example, cartilage tumors of the sternum are almost always malignant regardless of the histologic appearance. On the contrary, chondromas of the hands and feet, perossteal chondromas, enchondromas of Ollier's disease and Maffucci syndrome, synovial chondromatosis, and

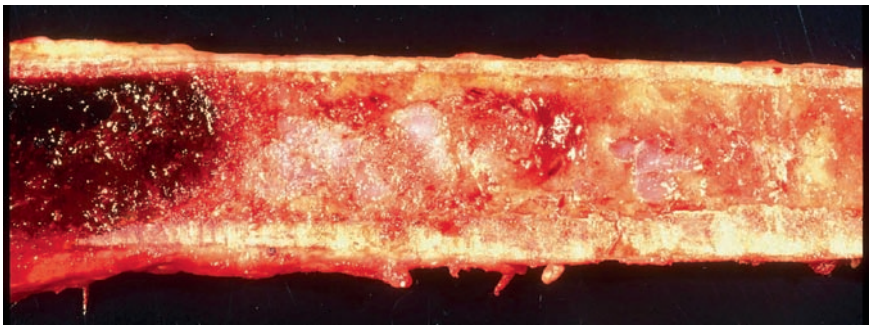

Fig. 28 Lobules of cartilage are seen within the diaphysis in this low-grade chondrosarcoma

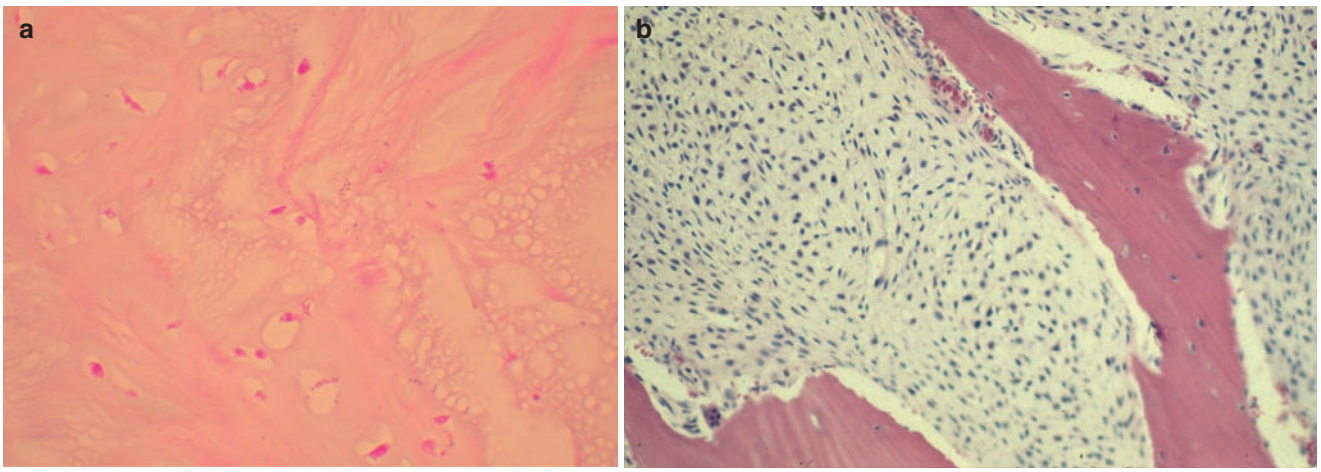

Fig. 29 **a** Early myxoid change in cartilage. **b** Grade 2 (of 3) chondrosarcoma infiltrating preexisting bony trabeculae

soft tissue chondromas of the hands and feet are most often benign, inspite of sometimes alarming cellularity.

Grossly, a lobular architecture, often with a hyaline quality is appreciated (Fig. 28). Foci of hemorrhage, necrosis, and cystic (liquifactive or myxoid) change may be present. The matrix of chondrosarcomas can vary in consistancy from firm hyaline cartilage to thin mucus-like. Mucus-like (myxoid) cartilage that runs is very suggestive of chondrosarcoma. Needless to say, that histologic sampling should be extensive, and include the various grossly different areas (especially those looking different from mature cartilage) to exclude high-grade tumor or foci of dedifferentiation.

Microscopically, chondrosarcomas are frequently lobular. Except at the very periphery, these lobules are completely coalescent. Necrotic foci can later calcify. Myxoid change is frequent. Myxoid change is a "bubbly" transformation of cartilage that can lead to cystification or liquefaction (Fig. 29a). A marked myxoid change or necrosis should be taken seriously and suggests malignancy in the proper setting.

A low power view suggestive of infiltration or entrapment of native bone is one of the most helpful clues and is diagnostic of chondrosarcoma (Fig. 29b). This bone can often be seen as "islands" of bone, usually necrotic bone. Chondrosarcomas also tend to be more cellular than chondromas. This is especially true in the larger bones. Enchondromas of small bones can be cellular but grow by pushing borders rather than infiltration. Thus, an infiltritative border is a very important criterion for ruling in malignancy. The creation of a soft tissue mass by the tumor growing out of bone (in the absence of fracture or previous surgery) is a definite sign of malignancy.

Peripheral/secondary chondrosarcomas, especially those arising on osteochondromas, often lack an infiltrative quality and frequently demonstrate a "pushing" border. Matrix deposition can vary from minimal to extensive. Qualitatively, it can be hyaline or myxoid. Wide fibrous septae are seen in some cases and these form a diagnostic clue in chondrosarcomas developing secondarily on osteochondromas (see section on osteochondroma). Calcification can be present. This is often around the lobules of cartilage. Reactive woven bone may be present; however, malignant osteoid would require the lesion to be reclassified as an osteosarcoma. When chondrosarcomas supervene on a previous osteochondroma, the thickness of the cartilage cap increases, and the normal columnar arrangement of chondrocyte columns is lost. Nodules of cartilage can sometimes be found lying in the adjacent soft tissues in such instances.

Grading of Chondrosarcomas: The cellularity of chondrosarcomas can be variable, some allowances have to be made for location. Chondrocyte atypia, mitoses, and multinucleation are features to be taken into account but no feature by itself is sufficient to be diagnostic. Chondrocyte nuclear enlargement (over 10 microns) should be noted. Nucleoli and "signet ring" chondrocytes are frequent in some lesions.

Grading of chondrosarcomas is imperfect. Since there is imperfect correlation between histologic appearance and biologic behavior, and since features such as size, location, and radiological appearances play a major role in determining the outcome of these lesions, the grading system has become of necessity somewhat subjective.

The group at MD Anderson has suggested that tumors composed of innocuous hyaline cartilage or sparse cellularity containing cells with dark, pyknotic nuclei no larger than a lymphocyte are referred to as Grade 1. Grade 2 is divided into two subtypes. Grade 2A lesions are more cellular, more than 20% of the cells have nuclei larger than the size of lymphocytes. Binucleation and nucleoli may be seen, but mitoses are not identified. Grade 2B lesions are cellular, have numerous binucleate cells, occasional bizarre nuclei, or spindling. The cellular areas correspond to the periphery of the lobules. Mitoses may be found but are less than 1 per 10 high-power fields. Grade 3 lesions contain 2 or more mitoses per 10 high-power fields. In the experience of the MD Anderson group, it is the Stage 2B and Stage 3 lesions alone that have the capacity for distant metastases (21).

At the Mayo Clinic, chondrosarcomas are graded on the basis of cellularity and atypia. Since mitotic activity is uncommon in chondrosarcomas, it is not used. Grade 1 chondrosarcomas are relatively hypercellular as compared to enchondromas and have moderate atypia. Grade 2 chondrosacomas are more cellular with more pronounced atypia. Grade 3 chondrosarcomas are extremely uncommon, and are characterized by extreme cellularity, large bizzarre nuclei, and small foci of spindling at the periphery of the lobules. This is the schema suggested by the WHO in their current fascicle, published in 2000. About two-thirds of the lesions seen there corresponded to Grade 1 in one study, about a third were Grade 2, and Grade 3 was only a very small fraction.

Techniques such as ploidy studies to differentiate between the various grades or between low-grade and benign cartilage have been less than successful. Genetic studies have been very limited in number and are not conclusive or clinically useful. Preliminary studies show that chondrosarcomas may show multiple chromosomal aberrations. The most frequent is characterized by periploidy affecting 9p12-22 region, found between NORI and EWS genes. A bad prognostic chromosal abnormality (loss of 13q) has been found associated with metastasis (22).

Differential Diagnosis: As mentioned above, the greatest difficulty is present in the distinction of benign, atypical cartilage (seen, for example, in enchondromas, chondromyxoid fibromas, osteochondromas, and Nora's lesion.), and low-grade chondrosarcomas. Radiological and growth characteristics are extremely important in making this distinction; histologic changes may not be useful by themselves in the vast majority of lesions. The histologic clues toward the aggressiveness of a cartilage lesion include an infiltrative margin, and entrapment of (necrotic) bone. Infiltration of the Haversian system is particularly important. A periosteal chondroma should be distinguished from a chondrosarcoma. Clues that can help this distinction include size (periosteal chondromas are most often less than 3 cm, the reverse is true of chondrosarcomas, which are mostly over 5 cm). An osteochondroma should also be distinguished from a secondary chondrosarcoma; this is best done by paying attention to the thickness of the cartilage cap. A cap wider than 1 cm should raise suspicion, and those over 3 cm are almost always chondrosarcomas. Other features used for the differentiation are given above.

A chondroblastic osteosarcoma may enter the differential with chondrosarcomas. Locating typical areas of malignant osteoid formation would be required for this distinction. In this, reference must be made to the occasional surrounding woven bone that often surrounds chondrosarcoma lobules. This should not be confused with malignant osteoid.

An entity that sometimes may be mistaken for chondrosarcoma is tophaceous pseudogout. This is generally separable by the finding of crystals, by polarized microscopy, and by the presence of a granulomatous response. It should be remembered that the tissue processing for regular histology may dissolve the crystals, making the diagnosis difficult (23).

Management: Wide excision (amputation or resection) is the preferred therapy. Marginal or intralesional procedures have a high rate of recurrences, although an extremely thorough curettage with cryotherapy in selected cases has given acceptable results. Low-grade chondrosarcomas tend to have a favorable outcome for the most part, and less mutilating procedures can be considered (24). Chemotherapy has not been effective in chondrosarcomas.

Dedifferentiated Chondrosarcoma

Dedifferentiated chondrosarcoma is a term that refers to lesions with a high-grade, *nonchondromatous* sarcoma (such as osteosarcoma, MFH, and rhabdomyosarcoma) associated with, and presumably arising from, a low-grade cartilaginous neoplasm. The origin, histiogenesis, and mechanism of evolution of dedifferentiation are controversial. The term *chondrosarcoma with additional mesenchymal component* has been used instead of dedifferentiated chondrosarcoma; this term is descriptive and accurate. The term should not be used to designate high-grade *chondrosarcoma* arising in a benign or low-grade cartilage neoplasm (such neoplasms are called secondary chondrosarcomas).

Most patients are over 50 years of age. Pain and pathologic fractures are the most common presenting features. The distribution of the lesions parallels the distribution of conventional chondrosarcomas.

Radiographically, dedifferentiated chondrosarcomas are often large lesions. They are often associated with soft tissue masses. The radiographic appearance is that of a bimorphic lesion, in many but not all cases (Fig. 30a). In the typical (bimorphic) cases, a lytic mass or a soft tissue mass is often seen in continuation with or adjacent to a lesion with features of a chondrosarcoma, the transition between the two components being characteristically abrupt. Cortical penetration is frequent, although this may be missed on conventional X-rays and may require CT or MR imaging to demonstrate. In the remainder of cases, the appearance is that of a chondrosarcoma.

Surgical Pathology: Grossly, the lesion reflects the radiological appearances. The two components are usually easily identified, the cartilage appearing translucent and lobular. The cartilage component is mostly centrally located, and may be extremely small and easily overlooked. The high-grade sarcoma is usually tan, hemorrhagic, and focally necrotic. The fleshy, anaplastic sarcomatous component frequently destroys the cartilaginous component. In a few cases, the reverse is true, with the anaplastic component being minor, and the majority of the lesion being that of a well-differentiated chondrosarcoma.

Microscopically, the lesion has two components – a chondrosarcoma and a high-grade sarcoma. The chondrosarcoma component is most frequently low grade (about three-fourths are Grade 1, the remainder Grade 2 chondrosarcoma). The junction between the two components is most often quite sharp (Fig. 30b). Fibrosarcoma and pleomorphic sarcoma (malignant fibrous histiocytoma) are the most frequent supervening sarcomas, but osteosarcoma, rhabdomyosarcoma, and angiosarcoma have also been described. Some lesions may cluster, suggesting a metastatic carcinoma. In this regard, it is important to remember that some lesions can be positive for cytokeratins, thus reinforcing the potential misdiagnosis of metastatic carcinoma. Attention paid to the radiographic appearance suggesting chondrosarcoma is extremely helpful in making the correct diagnosis.

Differential Diagnosis: Dedifferentiated chondrosarcoma may be confused with mesenchymal chondrosarcoma, and chondroblastic osteosarcoma.

In chondroblastic osteosarcoma, the cartilage component is most frequently of a high grade. Again the irregular mixing of the various components should be sought to arrive at a correct diagnosis.

Mesenchymal chondrosarcoma is a small cell neoplasm, with the admixture of low-grade cartilage and a spindle or round cell neoplasm, the latter frequently arranged in a hemangiopericytomatous pattern. The small cell component of a mesenchymal chondrosarcoma can easily be distinguished from the sarcomatous component of a dedifferentiated chondrosarcoma.

In addition, fibrosarcoma and MFH may enter the differential, but the absence of a neoplastic cartilage component in these should help delineate these two entities from a dedifferentiated chondrosarcoma.

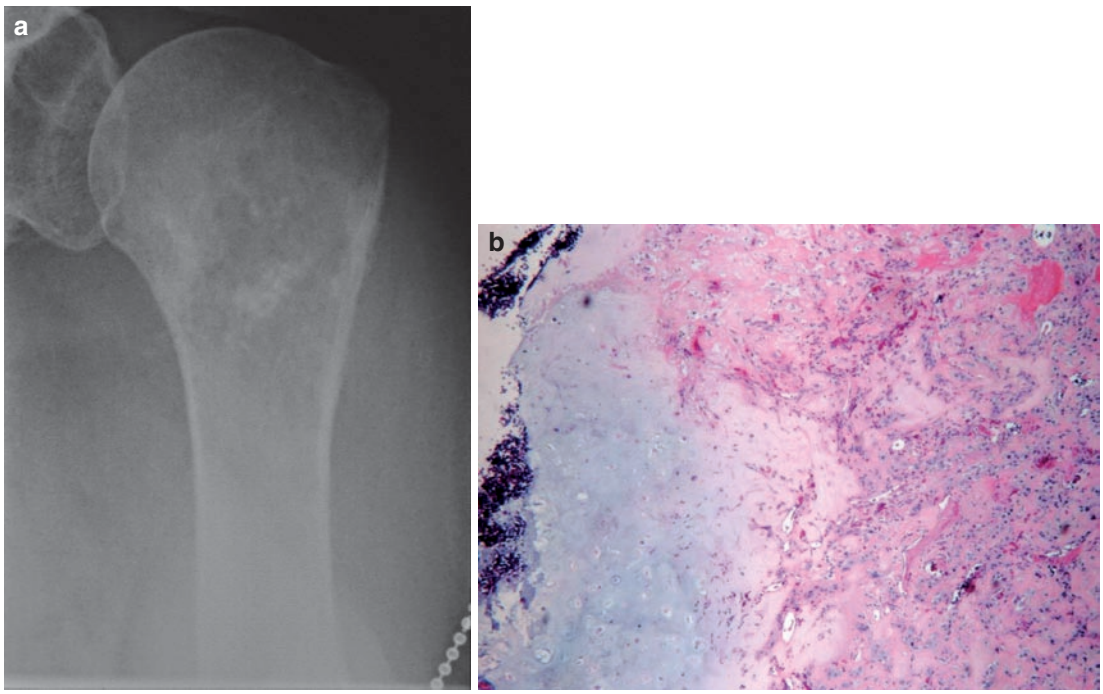

Fig. 30 **a** Plain radiogram of a patient with dedifferentiated chondrosarcoma. The lesion is large and involves the proximal third of the humerus, with aggressive margins distally; however, in the epicenter popcorn calcification typical of cartilage is seen and immediately adjacent to it the lesion has well-defined margins. **b** Low-grade cartilage and sarcoma are seen juxtaposed with a sharp delineation between them

Management: The management is that of high-grade sarcomas. The prognosis is generally dismal, widespread metastases being frequent. Chemotherapy has been used, and may be advantageous; however, the results of preoperative chemotherapy have not been very encouraging.

Clear Cell Chondrosarcoma

Clear cell chondrosarcomas are malignant, but slow-growing tumors, composed of neoplastic chondrocytes having abundant clear cytoplasm, with a sparse intercellular matrix. Foci of conventional chondrosarcoma may also be present. These tumors are often mistaken clinically as well as histologically for chondroblastomas and osteoblastomas.

Most patients are in the third or fourth decades, with a slight male predominance. The presentation is usually with pain and with joint symptoms. The joint symptoms reflect the preferred localization of these neoplasms to the epiphyseal regions of long tubular bones of the appendicular skeleton.

Radiologically, the epiphysis is the epicenter of these tumors, a location shared by chondroblastoma and giant cell tumor (GCT). They are usually geographic, lytic, expansile, and focally calcified neoplasms. The margins are well defined. Sclerosis around the edge may occur but is uncommon. Cortical destruction is rare, but a few cases have extended into soft tissues.

Surgical Pathology: Grossly, the appearance is tan, soft, and granular. Significant amounts of hyaline cartilage formation are unusual, but small foci may be found. Cystic change is often present.

Microscopically, unlike conventional chondrosarcomas, the clear cell variant can be quite rich in multinucleated giant cells. This explains, why, in the past, this tumor has been referred to as an atypical chondroblastoma. New bone formation may occur centrally within the tumor. The dominant cell is the "clear cell" chondrocyte, with a sharp cell border and a round, vesicular nucleus, with a prominent nucleolus (Fig. 31). Powdery cytoplasm may be aggregated near the cell border or the nuclear membrane. There may be cells with a powdery eosinophilic cytoplasm scattered throughout the lesion. These clear cells stain for S-100 protein – a feature they share with other chondroid cells. Mitotic figures are rare. Matrix is sparse and may be focally calcified. Foci of conventional (Grade 1) chondrosarcoma may be present, and is prominently seen in about half the cases. Foci of osteoid may be present. This osteoid is typically lined by chondroblasts and should not be interpreted as an osteosarcoma. Ultrastructurally, the cells exhibit features of chondrocytes including deeply indented nuclei, large dilated, rough endoplasmic reticulum, and substantial glycogen. The clearing of the cytoplasm, however, is not due to glycogen but instead represents a low-density granular material.

Differential Diagnosis: The characteristic location and radiological picture is helpful in making the diagnosis. The location of the lesion generates a differential diagnosis with chondroblastoma; however, chondroblastomas should not show clear cells. Metastatic clear cell carcinoma (such as renal cell carcinoma) may enter the differential diagnosis. Metastatic deposits are more frequently metaphyseal. Again, identifying areas of gland formation and the positivity of the carcinomas for epithelial markers would aid excluding them. In passing, it may be stated that S-100 positivity is not infrequent in renal

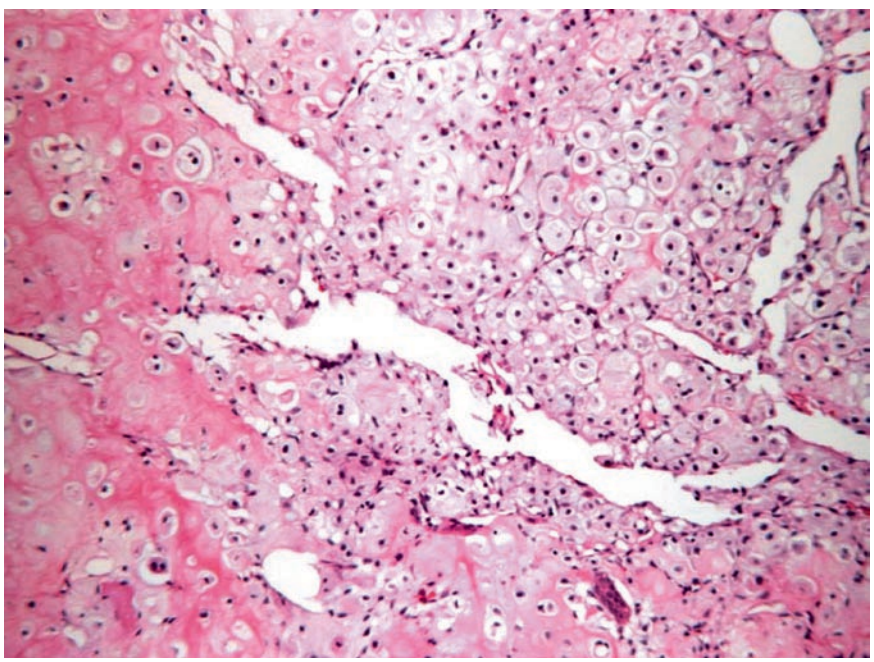

Fig. 31 Clear cell chondrosarcoma showing the characteristic clear chondrocytes

cell carcinomas, and some reports have suggested that there may be positivity for epithelial markers in clear cell chondrosarcomas. In practice, the lobulated appearance of a clear cell chondrosarcoma along with areas of bone formation is quite different from the appearance of a renal cell carcinoma, and the use of immunohistochemistry is generally not required.

Management: These neoplasms are usually managed by wide resectional procedures. There appear to be no histologic markers for prognosis or predicting lesions likely to metastasize. Late metastases have been reported – and can occur up to 15 years after initial surgery.

Mesenchymal Chondrosarcoma

Mesenchymal chondrosarrcomas are malignant cartilage-forming tumors that primarily are composed of small round to oval cells arranged in a hemangiopericytoma-like pattern along with low-grade cartilage. Small areas of osteoid may be present. There is often an abrupt transition to low-grade cartilage from these small round cell areas. Some of these cases have in the past been called polyhistioma or primitive multipotential primary sarcoma of bone. The tumor was first described by Lichtenstein and Bernstein in 1959.

The majority of the patients are below the age of 40 years. The favored sites are maxilla, mandible, ribs, vertebrae pelvis, and femur. Involvement of other long and short tubular bones, including multicentric lesions, has been reported. Some lesions occurring in the soft tissues and meninges have also been reported.

Radiologically, a lytic/destructive defect, with small foci of mineralized cartilage is frequently seen. The margins may be geographic, moth-eaten, or permeative. Occasional cases with sclerotic margins have been reported.

Surgical Pathology: Grossly, the sample may appear lobulated; cartilage is usually not identified grossly. The appearance may be soft, gray, or tan, and often well demarcated.

Microscopically, the tumor is composed of a combination of anaplastic small stromal cells and islands of benign-appearing chondroid. The stromal cells may vary from "small, round, blue" cells to spindle-shaped cells. The stromal cells are often arranged in a hemangiopericytoma, or less commonly, an alveolar or even a herring-bone fashion. Interspersed within these is low-grade cartilage, which may form only a small component of the neoplasm. The border between the two components is usually sharp. The cartilage component may sometimes be calcified, or even ossified (Fig. 32a, b).

Differential Diagnosis: Several tumors enter the differential diagnosis. Both mesenchymal chondrosarcoma and Ewings' tumor contain glycogen. In small biopsies, where the cartilage component is not present, this may prove a problem. Small cell osteosarcoma and other "small blue cell" tumors enter the differential in the same way. Small cell osteosarcoma is distinguished by the presence of lacy osteoid and by the absence of cartilage. Immunohistochemistry may be required to differentiate lymphomas and undifferentiated carcinomas in some selected cases.

Management: Wide resection followed by chemotherapy has been the mainstay. Radiation therapy has been successful in some cases. The outcome of this tumor is unpredictable, the number of cases studied have been small, and insufficient to give generalizations. Late metastases have been reported.

Juxtacortical (Periosteal/Parosteal) Chondrosarcoma

A malignant extramedullary, subperiosteal cartilaginous tumor that lacks osteoid production typically erodes the underlying cortical bone. The majority of the patients tend to be older than 20 years. The appendicular skeleton is the preferred site; both the metaphysis and the diaphysis can be the site of origin.

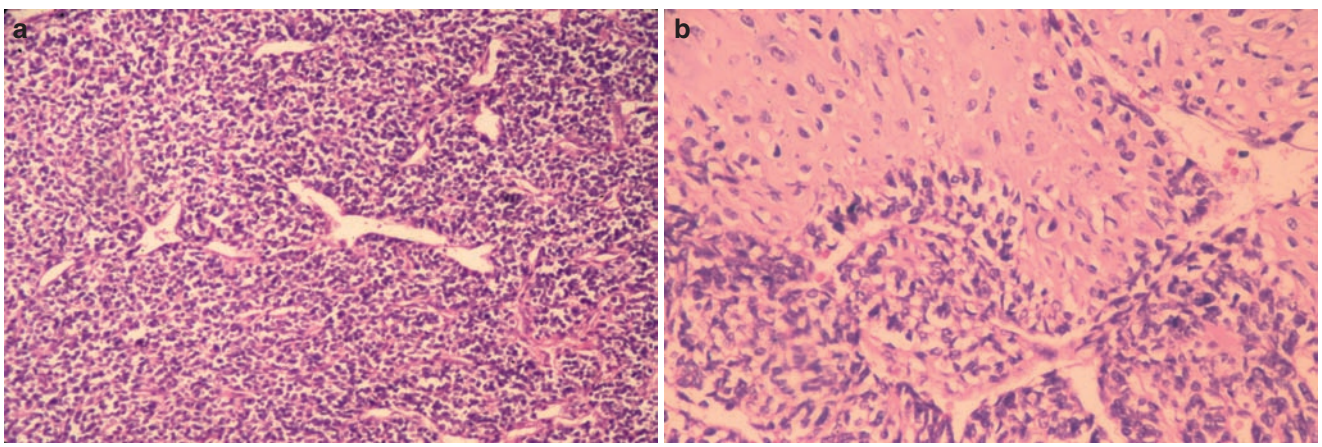

Fig. 32 Mesenchymal chondrosarcoma. The lesion shows a small cell malignancy arranged in a hemangiopericytomatous pattern **a** with abrupt transition to low-grade cartilage **b**

Radiologically, the lesions have a sharply defined border; a saucer-shaped defect is often seen in the underlying cortex. The lesions often grow to large sizes. The C's and O's of cartilage calcification are frequently seen.

Surgical Pathology: Grossly, the tumors are lobulated, cartilaginous, and sharply demarcated. The medulla is typically not involved. Microscopically, the lobules are made up of well-differentiated (Grade 1–2) hyaline-type cartilage. They are generally separated by fibrous bands but may be encased by metaplastic bone. The stroma may show focal myxoid change. Neoplastic bone formation by definition is absent.

Differential Diagnosis: The two common problem lesions to be excluded are the periosteal chondroma and the periosteal osteosarcoma. The former is occasionally difficult to exclude, and there may be some overlap both radiologically and microscopically. A width of over 5 cm or a width more than the length suggests malignancy. Periosteal osteosarcomas are an extremely chondroblastic variant of osteosarcoma. With differing criteria and recognition, there have frequently been misclassifications. Some authors have not recognized the entity of juxtacortical chondrosarcoma and included these cases as examples of periosteal osteosarcoma. Those that differentiate between these, use the criteria of neoplastic bone formation as diagnostic of osteosarcoma. The clue, of generally visualizing a higher grade of chondrosarcoma in periosteal osteosarcoma, is of advantage in making the distinction.

Management: Wide surgical procedures are the mainstay of treatment. Marginal or intralesional procedures are associated with poorer outcomes (25).

Vascular Lesions

- Lymphangioma and hemangioma
- Skeletal angiomatosis
- Gorham's disease
- Hemophilic pseoudotumor
- Vascular tumors in the immunocompromised
- Hemangioendothelioma
- Epitheloid hemangioendothelioma
- Angiosarcoma
- Hemangiopericytoma
- Glomus tumor

Solitary Lymphangioma and Hemangiomas

Lymphangioma and hemangiomas are a benign proliferation of lymphatic or vascular channels that occur in and replace bone. Some lesions occur in the setting of polyostotic angiomatosis, and are associated with soft tissue lesions.

The presentation is usually with pain, the spine (the commonest site for hemangioma is the vertebral body), calvarium, temporal bone (may present with facial palsy), pelvis, ribs, and the long bones of the appendicular skeleton are the most frequent sites. Many cases, especially in the vertebrae are asymptomatic but may be associated with muscle spasm or nerve root symptoms (10% of patients have had hemangioma in the vertebrae in certain autopsy series). Sacral hemangiomas are associated with multiple congenital anomalies (26).

Radiologically, lymphangiomas may occupy most of the medullary cavity or be seen as small intracortical lytic defects. With modern scanning techniques, the diagnosis can be made preoperatively in many cases.

On plain films, hemangiomas are generally lytic, intramedullary lesions with characteristic thickened vertical striations, the so-called corduroy cloth pattern. On CT scan, this is seen as a polka dot appearance. Vertebral hemangiomas mostly affect the body rather than the posterior elements. Spread into the laminae, pedicles, spinous, or transverse processes is less common. In the calvarium, the lesions are centered in the diploe, but there may be "bulges" of the outer and the inner tables. A periosteal reaction if present can be of the "sunburst" type. Radiologically, intracortical hemangiomas must be differentiated from osteoid osteomas.

Surgical Pathology: Grossly, the lesions are often cystic with either straw-colored fluid (lymphangioma) or blood (hemangioma), the trauma of surgery may lead to blood in the cystic spaces in lymphangioma, making the distinction difficult. Intact hemangiomas are red, soft masses with vertical striations of bone. Epitheloid hemangiomas are similar to their soft-tissue counterparts and can be myxoid grossly.

Microscopically, the lesions are composed of lymphatic or vascular channels, which can vary markedly in size. A loose fibrous stroma supports the vessels. Infrequently, thick-walled vessels of the arteriovenous malformation type are seen. There may be prominent aggregates of lymphocytes in lymphangiomas. The cystic spaces are mostly empty in lymphangiomas but occasionally contain an eosinophilic material. A small amount of blood may be present, even in lymphangiomas. Epitheloid hemangiomas have plump (epitheloid or hob-nail) endothelial cells. The vascular channels are often highlighted by vascular stains such as Factor VIII-related antigen, Ulex europaeus, CD 31, CD 34, and podoplanin (D-240).

Differential Diagnosis: The main differential diagnosis of lymphangioma is hemangioma. The latter sometimes is indistinguishable. Hemangiomas contain blood rather than eosinophilic proteinaceous material in the lumen and often lack the lymphocytes in the wall. Ultrastructurally, lymphatic channel endothelia are said to lack the Weibel-Palade body (that houses the Von-Willebrand factor). The distinction is rarely important. Other differentials include skeletal angiomatosis (a more extensive process), and higher grade vascular

lesions like hemangioendotheliomas and angiosarcomas. The latter two are differentiated on cytological appearances (see below). Some authors have suggested that epihteloid hemangiomas and epitheloid hemangioendotheliomas are within a spectrum of entities not easily separable on histological grounds. Others however recognize lesions that have well-formed vessels or sheets of epitheloid endothelial cells as epitheloid hemangioma while reserving the term epithelioid hemangioendothelioma for lesions that are myxoid and have cords of cells with intra-vascular lumina.

Management: Surgery, with intralesional or marginal procedures is the usual option. Although some hemangiomas "heal" with time, the majority of the symptomatic ones require either surgery or radiation for treatment.

Skeletal Angiomatosis

Angiomatosis is a multifocal or diffuse intraosseous proliferation of benign hemangiomatous or lymphangiomatous channels. There may be associated extraosseous vascular malformations or combined "skeletal-extraskeletal" angiomatosis in continuity (Fig. 33). The patients are often symptomatic with pain or extraskeletal manifestations such as chylous or hemorrhagic effusions or thrombocytopenia. Most patients are in the first two decades of life. The skull, vertebrae, long bones ribs, and pelvic bones are the most frequently involved. Gnathic involvement is rare (Fig. 34).

Radiologically, the lesions are lytic, and often have well-defined margins. There may be bony expansion; periosteal reactions are, however, unusual.

Surgical Pathology: Grossly, the entire marrow cavity is often involved. The lesions are often surrounded by sclerotic bone. Microscopically, the lesions are identical to solitary vascular lesions. The cortex of the bone is often involved.

Differential Diagnosis: The main differential is massive osteolysis (Gorham's disease) discussed below. The differentiation is mainly made on clinical grounds.

Management: Transformation to malignancy is rare, if ever. Lesions may progress, stay stationary, or regress. Radiation has been used on occasion, with mixed results.

Massive Osteolysis (Gorham's Disease, Vanishing, or Disappearing Bone Disease)

Resorption of most or almost all the bone is associated with a proliferation of benign vascular channels. The essential difference with skeletal angiomatosis (thought to be the same condition by some authors) is that of extent and aggressiveness. Additionally, Gorham's disease involves one or contiguous bones in contrast to the multifocal nature of skeletal angiomatosis. Extraskeletal manifestations are rare. Most cases occur below 35 years. Pain is a frequent presenting symptom. There is a predilection for mandible, rib, femur, scapula, humerus, and sternum. Radiologically, there is a lucent change in the medullary region, or alternatively, a concentric destruction of the cortex with tapering at ends ("sucked candy effect"). About three-quarters of the cases show involvement of contiguous bones.

Surgical Pathology: The gross and microscopic appearances are similar to those in skeletal angiomatosis (Fig. 36a, b).

Differential Diagnosis: This includes skeletal angiomatosis and Paget's disease (especially in a situation of pathologic fracture, when the lytic phase gets accelerated). Skeletal

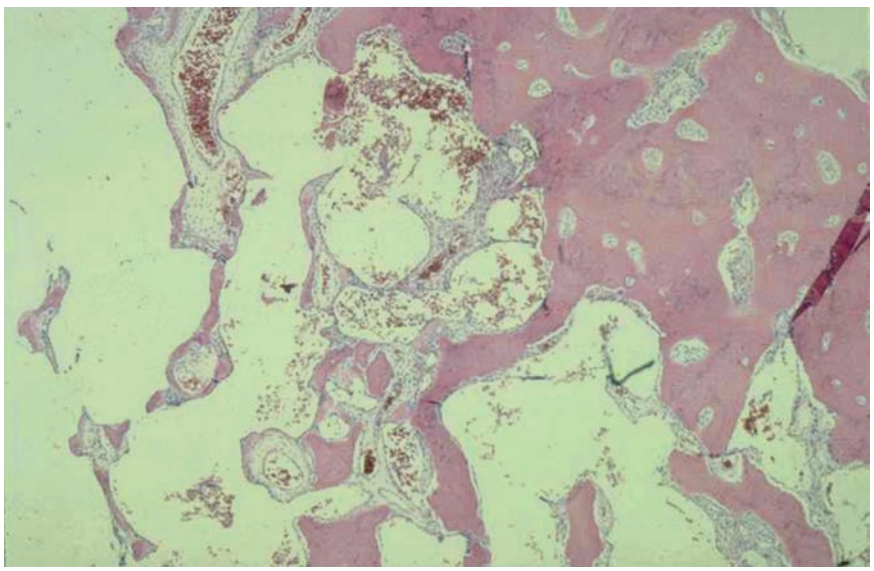

Fig. 33 Skeletal angiomatosis in a 30-year-old male. Multiple bones and soft tissue involvement by a capillary hemangioma-like proliferation

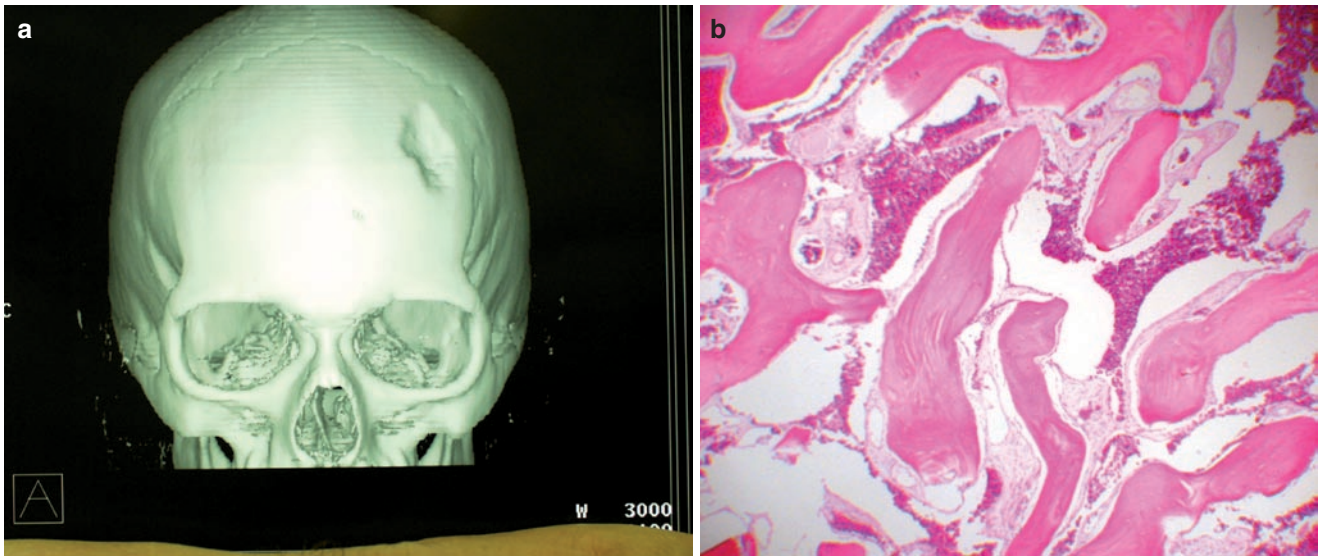

Fig. 34 **a** A teenager with Gorham's disease. It started with a small palpable skull defect that was felt by the patient but rapidly went on to destroy the bone. It was resected and the defect was repaired by a titanium plate. The photomicrographs **b** are from the lesional tissue which show a proliferation of cytologically bland vascular channels within bone. The disease recurred within 2 years and went on to destroy most of the front of the skull, with extension into the nasal region and cerebrospinal fluid (CSF) rhinorrhea. The disease has not responded to radiation therapy and the patient is alive with disease at 10-year follow-up. She risks meningitis and infection from the extensive bony loss

angiomatosis is differentiated on clinical grounds. Paget's disease tends to affect older individuals; the diagnosis is made by finding the typical lesion of Paget's such as mosaic bone elsewhere in the biopsy.

Management: Most cases have been treated by radiation. Embolization, bone grafting, and resection with reconstruction have had mixed results. There is no means of knowing when the disease will arrest. Most therapy is focused on the deformities that are present and defining for these affected patients.

Hemophilic Pseudotumor

Although not strictly a vascular proliferation, it is discussed here since it forms a tumor-like lesion and may mimic several aggressive bone neoplasms.

Pseudotumors can cause massive bone destruction. They arise secondary to the large amounts of hemorrhage that occurs in bleeding disorders. This hemorrhage is often intra-articular, and is associated with reactive synovitis and degenerative bone disease. Less often, the patients develop soft tissue or skeletal pseudotumors. When located subperiosteally, they can cause considerable periosteal lifting and demonstrate convincing Codman's triangles on X-rays.

The presentation is most often in males (owing to the X-linked nature of the disease) but can occur at any age. Painless, enlarging masses are the most common; however, pain and neural deficits are sometimes present. Any site can be involved, but the buttocks and lower extremities are the most commonly affected. Radiologically, large areas of the bone may be involved. Usually, there are geographic lytic lesions, sometimes with well-defined margins mimicking an ABC. Occasionally, more aggressive margins that mimic malignant bone tumors may be seen. Bony expansion can be seen in some lesions.

Surgical Pathology: Grossly, the masses may mimic thrombus or hematomas and are often confined by the periosteum. Microscopically, there is reactive woven bone, fibrous tissue, and repair reaction at the periphery of the lesion. More centrally, there is often blood in various stages of degeneration. A zonation phenomenon similar to myositis ossificans or fracture callus can often be seen.

Differential Diagnosis: Radiologically, the pseudotumor mimics an ABC or neoplasm such as a telangiectatic osteosarcoma. MR scans may detect blood, and this further suggests these possibilities. A correct history is invaluable in bringing to mind the possibility of pseudotumor. Microscopically, although the fibroblasts and focal osteoid may mimic osteosarcoma, the lack of atypia and absence of high-grade areas should help establish the diagnosis. As before, the appropriate history is invaluable.

Management: Attention is paid to the levels of clotting factors as well as to the joint integrity. Under proper control of clotting parameters, local therapy can be attempted in situations where nerve compression is detected. If joint destruction is advanced, then procedures such as compression arthrodesis are considered.

Vascular Tumors in the Immunocompromized

Both Kaposi's sarcoma and Bacillary angiomatosis have been described in bone. The features are similar to their better known soft tissue counterparts.

Hemangioendothelioma

Some authors use the terms, hemangioendothelioma and angiosarcoma interchangeably. In this case, usually a grade is attached. Others prefer to reserve the term angiosarcoma for the histologically higher-grade lesions. It is important for communication to clarify the usage, if in doubt. In the current discussion, angiosarcoma is used for high-grade lesions.

In a well-known grading system utilizing the interchangable terminology, Grade 1 hemangioendotheliomas are lesions having well-formed vascular channels, with little or no atypia. Grade 2 lesions are made of cuboidal cells with obvious atypia, but vascular channel formation is evident. Grade 3 lesions are made of atypical cells with less obvious vascular spaces. Grade 4 lesions correspond to poorly differentiated angiosarcomas (27).

Epitheloid (Histiocytoid) Hemangioendothelioma

This is considered to be a low-grade malignancy composed of *endothelial cells* having conspicuous cytoplasm. The tumors have a variable degree of vasoformative features. These vary from vacuolization of cells to well-formed vascular channels. Patients can often have concomitant cutaneous or soft tissue disease. It may be related to the lung lesion known as the intravascular bronchoalveolar cell tumor (IVBAT). This means that soft tissue or lung "metastases" should raise the question of possible multifocal primary tumors. Such multifocal disease is not uncommon.

There is a wide age range with a clustering of cases between 10 and 30 years. Patients often present with pain, and sometimes with a pathologic fracture. Skull, the axial skeleton, and the lower extremity are the most frequent sites.

The radiographic appearance is usually lytic, with sharp to blurred margins (Fig. 35a). A soap-bubble appearance or bone expansion may be seen. There may be extension into the soft tissues.

Surgical Pathology: Grossly, the tumors are soft and red. They may have poorly demarcated borders or soft tissue extension. Microscopically, it is seen as a proliferation of

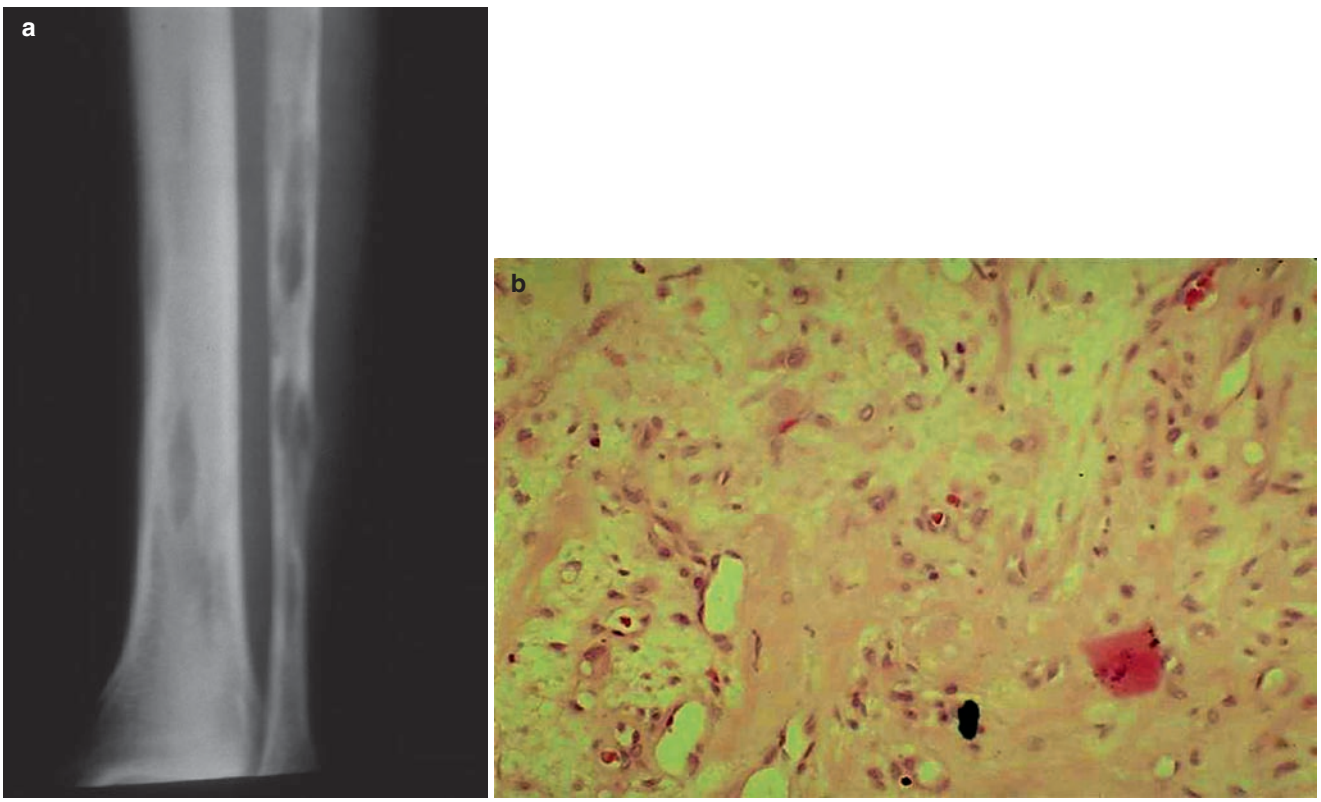

Fig. 35 **a** Epitheloid hemangioendothelioma in the tibia and fibula of a 35-year-old male patient. The lesion is composed of epitheloid cells in a myxoid background. **b** Intracellular lumina formation can be seen

cells having ample amphophilic or faintly eosinophilic cytoplasm. The cells may have intracytoplasmic vacuoles (which may on occasion have entrapped erythrocytes) (Fig. 35b). Larger lumens may be seen formed of the coalescence of the smaller lumina. In these, there may be residual thin strands of cytoplasm bridging across. Upto 1–2 mitotic figures per 10 high-power fields may be seen. An inflammatory infiltrate rich in eosinophils (but often containing lymphocytes and plasma cells) is usually present. Small foci of hemorrhage or necrosis may be present. The stroma is usually myxoid or fibrous but may on occasion resemble that of hyaline cartilage. There are four major patterns of tumor. In the first, the cells may be plump, polygonal, or somewhat elongated with large vacuoles resembling signet ring cells. In the second, these cells may aggregate into cords or clusters. In the third, there are well-formed lumina, some containing erythrocytes. And in the last, there is prominent spindling with intervening nests of epitheloid cells. The first three are usually associated with a myxoid or chondromyxoid stroma, leading to the designation by some as a myxoid angioblastoma. There is often reactive bone formation in the periphery of the tumor. This in some instances may mimic osteoblastoma, since it is well formed with plump osteoblasts. However, the presence of obvious vasoformative cells should help establish the correct diagnosis.

Immunohistochemically, the tumor cells stain for vascular markers, such as von Willibrand factor (VIII-related antigen), Ulex europaeus lectins, CD 31 and CD 34.

Differential Diagnosis: This includes metastatic adenocarcinoma, skeletal adamantinoma, and angiosarcoma. Immunohistochemical positivity of the epitheloid cells for endothelial markers such as von Willebrand factor (VIII-related antigen) or Ulex europaeus lectin is helpful in this differential. Renal cell carcinomas in particular can be very vascular and mimic vascular tumors. Adenocarcinomas are often associated with a desmoplastic reaction that is lacking in vascular tumors. Adenocarcinomas are positive for cytokeratins, and often for epithelial membrane antigen, Leu M1 (CD 15), B72.3, carcinoembryonic antigen, and so on. It must be remembered that both adamantinoma and epitheloid hemangioendotheliomas show positivity for cytokeratins. Both adenocarcinomas and adamintinomas lack the positivity for vascular markers such as Factor VIII-related antigen, CD 31 and CD 34.

The microscopic distinction from angiosarcoma is based on the greater amount of cytologic atypia, proliferative activity, and often wide architectural patterns seen in the latter. Since epitheloid angiosarcomas have been described, it is essential to take into account several of these features to make the diagnosis.

Management: Resection is the method of choice when possible. The clinical course tends to be indolent (but literature – especially older literature) is frequently contradictory. This may be because of the inclusion of entities such as angiosarcomas or hemangiomas in these series. The presence of multifocal disease does not confirm a poorer prognosis.

Angiosarcoma

This is a high-grade (sometimes surface) sarcoma of bone composed of atypical endothelial cells.

Premalignant conditions are thought to include radiation, long-standing chronic osteomyelitis, and possibly benign vascular lesions. However, secondary angiosarcomas are exceedingly rare.

There is a wide age range, but most patients are over the age of 30 years. Pain is the typical presenting complaint. The femur, tibia, and humerus are the most frequently involved. Vertebrae, ribs, and pelvic bones are not infrequent but virtually all bones can be involved.

Radiographically, these are lytic, destructive, permeated lesions. There is often soft tissue extension. Multifocality is not uncommon.

Surgical Pathology: Grossly, the lesions are soft, red, spongy and focally firm, gray, and solid. Microscopically, the diagnosis is usually not difficult. There are areas of well-formed anastomosing vascular channels lined by atypical endothelial cells, with large vesicular or hyperchromatic nuclei. There are often solid, poorly differentiated areas where the vasoformative nature may be undiagnosible.

Differential Diagnosis: The distinction from epitheloid hemangioendothelioma is essentially that of grading or degree of cytologic atypia, proliferative activity, and architectural diversity. Higher amounts of all these are seen in angiosarcomas as compared to hemangiendotheliomas. It is important to remember that these tumors have considerable architectural diversity. They may have extensive areas of poorly differentiated tumor, where the vasoformative nature and immunohistochemical stains for vascular differentiation may be absent.

Management: Wide resection is the treatment of choice. The role of chemotherapy in an adjuvant setting is under consideration. The outlook and prognosis for these tumors is poor.

Hemangiopericytoma/Solitary Fibrous Tumor

Hemangiopericytoma is a potentially low-grade malignant tumor consisting of pericyte-like cells and a prominent vascular pattern and shares similarity with its soft tissue counter part (soft tissue hemangiopericytoma/solitary fibrous tumor).

These are uncommon tumors, they have a wide age range and frequently present with pain. On occasion, a paraneoplastic syndrome of hypophosphatemic osteomalacia has been described (see section on oncogenic osteomalacia and metabolic bone disease).

Common sites of involvement are the pelvis, femur, vertebrae, and mandible. Less often, other bones such as clavicle, humerus, scapula, and fibula are seen.

Radiographically, a wide spectrum of patterns (reflecting the histologic grade) is seen. Most are predominantly lytic lesions but frequently have a trabecular, honeycomb, or reticulated pattern similar to the kind seen in hemangiomas. The margins of these lesions are very variable.

Surgical Pathology: Grossly, the lesions are nondescript and may be gray or tan and generally solid. Microscopically, they resemble the more common soft tissue counterparts. There are several thin-walled or sinusoidal vessels, with pericyte-like round, oval, or spindle cells in the background stroma. The vessels are usually branched in a "deer-antler"-like configuration, which can be highlighted by reticulin or von Willebrand antigen stains. Some tumors are more poorly differentiated and have areas of cells arranged in ill-defined bundles. The cells may be uniform, or show mild-to-marked degrees of cytologic atypia. Similarly, the mitotic rate can be very variable.

Differential Diagnosis: As in soft tissues, the diagnosis of hemangiopericytoma is one of exclusion. A variety of tumors can exhibit hemangiopericytoma-like areas. Some tumors regularly do so, notably synovial sarcomas, mesenchymal chondrosarcomas, malignant fibrous histiocytomas, and small cell osteosarcomas as well as a solitary fibrous tumor. Another tumor which has raised controversy is the meningeal tumor which may invade the skull and present as an osseous tumor. This tumor is regarded as a hemangiopericytoma rather than a meningioma.

Management: Wide local resection is the treatment of choice. The role of adjuvant chemotherapy or radiotherapy is uncertain at present. Late metastases can be seen in some cases.

Glomus Tumor

A benign, highly vascular tumor composed of small uniform specialized smooth muscle cells resembling those of the glomus body. Osseous glomus tumors are less frequent than their soft tissue counterparts. They are most frequent in the distal phalanx but may be seen in the ulna, coccyx, and rarely in other locations. There is a wide age range and a slight female predominance. The presentation is usually with extreme pain. True osseous glomus tumors should be distinguished from soft tissue tumors that erode into the bone from the outside. These tumors are usually lytic "punched out" lesions.

Surgical Pathology: Grossly, they are bloody and friable. Microscopically, they are frequently composed of sheets of relatively uniform cells. The vascular component may be composed of indistinct capillaries or of large blood vessels (glomangiomas).

Management: Intralesional and marginal procedures are usually adequate.

Giant Cell Lesions

- Giant cell tumor (GCT)
- Giant cell reparative granuloma

Giant Cell Tumor (Osteoclastoma)

GCT is a locally aggressive neoplasm characterized by large numbers of osteoclast-type giant cells, uniformly distributed in a population of plump epitheloid or spindle cells.

Several tumors can have giant cells as a component, including NOFs (non-ossifying fibroma, metaphyseal fibrous defect), chondroblastoma, chondromyxoid fibroma, unicameral and aneurysmal bone cyst (ABC), hyperparathyroidism, Paget's disease, and reparative giant cell granulomas/solid ABC. These entities should be excluded.

GCTs are more common in the skeletally mature adult population (peak third decade). In this age group, they occur in the region of the epiphysis. Only about 15% of the patients are less than 20 years, and less than 5% have open epiphyses at diagnosis. In this age group, there is a tendency for the tumors to occur in a metaphyseal or epimetaphyseal location.

Complaints are usually nonspecific; there may be pain or a mass. About 10% patients present with a pathologic fracture. Serum chemistries are generally normal. An elevated serum Ca^{2+} should raise the possibility of hyperparathyroidism, and an elevated serum alkaline phosphatase should raise the possibility of Paget's disease. About one half of all GCTs arise around the knee. Other common sites include the distal radius, proximal femur, proximal humerus, and distal tibia. The flat bones most commonly involved are those of the sacrum and pelvis. Craniofacial involvement is unusual except in the context of Paget's disease. Most giant cell lesions of the gnathic skeleton are thought to be giant cell reparative granulomas rather than true GCTs. The same may be true of GCTs of the hands and feet. Some studies, however, have suggested that GCTs of the hands and feet may be more aggressive, associated with a younger age and more prone to multicentricity (28). Although as a group, multicentric tumors are uncommon (once hyperparathyroidism excluded), these tumors do occur, and this is especially true in the peripheral appendicular skeleton. These multifocal tumors may pursue an aggressive course.

GCTs may rarely arise in the context of Paget's disease of bone. Rarely even histologically typical GCTs can metastasize, and in this situation they often behave indolently similar to the phenomenon seen in chondroblastomas ("benign" metastasizing tumors).

Radiographically, most lesions are epiphyseal (Fig. 36a), but they frequently extend to the metaphysic. They are lytic, and geographic, but rarely do they have sclerotic margins. Aggressive periosteal reactions and calcifications (sunburst, onion skinning or Codman's angles) are unusual, and should

make the diagnosis suspect. Lesions extending into the soft tissue often have a thin rim of bone (the "egg-shell"). There have been several attempts at predicting the aggressiveness of these tumors preoperatively (29). Ennekings system conceives of three kinds (or stages) of lesions. These are termed benign latent, benign active and aggressive GCTs. Differentiation is made subjectively on the basis of imaging data. The benign latent tumors are devoid of features of local aggressiveness. The benign active ones are symptomatic, and on imaging studies show bone expansion. The aggressive tumors correspond to the hypervascular lesions that erode into the soft tissues and may have an associated pathologic fracture.

Surgical Pathology: Grossly, the GCTs may be hemorrhagic, and have focal ABC-like areas. Some may be tan or fleshy. The tumor may abut the cartilage – extension through the cartilage into the joint, however, is rare. Tumor may, however, extend along the cruciates or other intra-articular ligaments, or alternatively extend into the joint from the lateral side. These features should be looked for and reported if found. Expansion of the bone is common, and extension through the periosteum into the soft tissues, however, is unusual, even with large lesions.

Microscopically, the diagnosis is made on the background population of stromal cells. These are round to oval, with nuclei resembling those of the giant cells (Fig. 36b). Occasionally, the stromal cells appear slightly spindled. Mitotic figures may be abundant with 2 to 3 per high-power field. A high mitotic rate does not correlate with biological behavior. Multinucleated osteoclast like giant cells are numerous and diffusely distributed. They contain a few to hundreds of nuclei, which resemble the nuclei of the stromal cells. Occasional cases may have broad bands collagen coursing through, especially in recurrent tumors. About half the GCTs contain reactive osteoid and woven bone, especially at the advancing edge of the lesion and in areas of soft tissue extension. Reactive woven bone and osteoid may also be seen in the "benign" metastases in the lung. They do not warrant a revision of the diagnosis to osteosarcoma, provided the stromal cells show no cytologic atypia. Cartilage is distinctly uncommon in unfractured GCTs. Areas of infarct-like necrosis and foam cells are common.

The stroma of GCTs is usually vascular, and contains numerous thin-walled capillaries, areas of hemorrhage, and foamy or hemosiderin-laden macrophages. Upto 40% GCTs are thought to have foci of intravascular invasion. This phenomenon may explain the "benign" metastases of a GCT. This phenomenon, however, has not been associated with a more aggressive behavior. GCT may be associated with a secondary ABC-like change.

Histologic grading of GCTs has not been found to correlate with metastasis, recurrence, or local aggressiveness.

The term "malignant" GCT has been used in various ways. It has been used to designate true bone sarcomas (such as osteosarcomas or malignant fibrous histiocytomas) which are rich in giant cells. The term has also been used to describe a "dedifferentiated" GCT (a typical GCT juxtaposed with a high-grade sarcoma). Another use has been to describe GCTs that have metastasized. In view of all these, the term is confusing and is best avoided. It is important, however, to exclude (on the basis of cytologic atypia of the stromal cells) the entity of giant cell-rich osteosarcoma.

About 1–2% of otherwise typical GCTs metastasize. These are generally identical, histologically to the primary tumor. Most are detected within a year of resection, but some occur upto a decade later. There are no microscopic features to predict this phenomenon. Such metastases are indolent

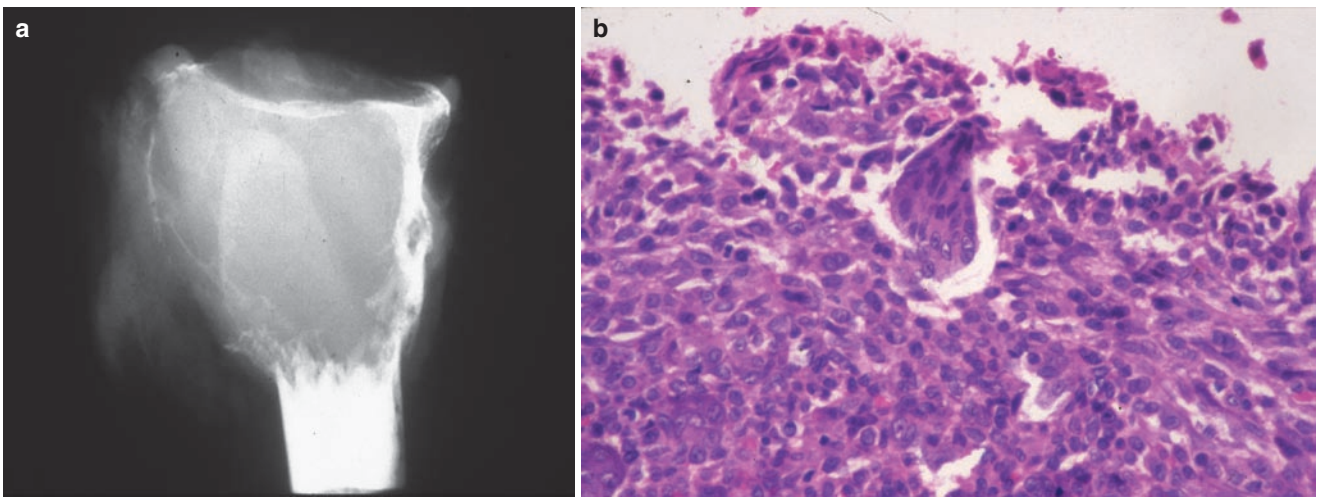

Fig. 36 Giant cell tumor. **a** The epiphyseal location of this example at the distal radius is characteristic. **b** Giant cell tumor showing multinucleate giant cells and stromal cells

and amenable to resection. A sarcomatous transformation should be excluded in these cases.

Differential Diagnosis: GCTs have to be differentiated from a variety of tumors containing giant cells. On the benign end, there are the giant cell reparative granulomas and the brown tumors of hyperparthyroidism. True GCTs usually have a more uniform distribution of giant cells, often with more nuclei. In the reparative granulomas, they tend to be aggregated, mostly around areas of hemorrhage. The stroma of GCTs contains less fibrosis and is composed of characteristic mononuclear cells. Stromal hemorrhage is focal, if present. In contrast, in the reparative granulomas, there is a fibrotic stroma, hemorrhage, and hemosiderin deposition. Foci of reactive bone are more common in reparative granulomas.

Other entities, which enter the differential diagnosis, include NOFs, benign fibrous histiocytomas, ABCs, osteosarcoma, and metastatic carcinoma.

GCTs may contain foci of spindled stromal cells as well as xanthomatous foamy macrophages. These are usually focal and the characteristic radiological picture of an NOF (metaphyseal, cortical lesion with sclerotic margins) should help in the differentiation.

ABC formation in a GCT is not unusual. True ABCs, however, are metaphyseal and do not contain the typical mononuclear stromal cells of GCT.

The GCTs must also be differentiated from osteosarcomas with prominent giant cells. This is a serious diagnostic problem. In such osteosarcomas, there may be sheets of giant cells, most of which are histologically bland. Osteoid production is present in giant cell rich osteosarcoma, though it may be minimal. It may be limited to thin strands encircling mononuclear pleomorphic stromal cells. The latter usually have hyperchromatic nuclei, often with numerous atypical mitoses. The radiographic pattern suggests a permeative growth, not extending into the epiphyses. An active growth plate should by itself lead to questioning the diagnosis of GCTs (although these certainly do occur in children). The anaplasia may be focal, and if the radiological picture is atypical for a GCT, the lesion should be extensively sampled.

Carcinomas that may have osteoclast-type giant cells include those of the breast, thyroid, and pancreas. Immunohistochemical staining for epithelial antigens should exclude this possibility in suspicious cases.

Management: Recurrence has been linked to the kinds of surgical procedure done (intralesional, marginal, or wide). Adequacy of excision and absence of residual tumor is clearly important. Earlier studies had remarked on the high rate of recurrence associated with curettage. With modern high-speed burrs, cryosurgical procedures, methylmethacrylate packing, and so on, this has proved less of a problem. The rates of recurrence have approached those achieved by wide resections. Late recurrence of GCTs (after 5 years) is suspicious for sarcoma transformation.

Radiotherapy given in the past for GCTs has had low cure rates with about a 5% rate of sarcomatous transformation.

Malignant GCTs

For a strict definition of malignant GCTs, the pathologist must demonstrate zones of typical GCT, adjacent to an unequivocal malignant tumor (collision tumor), or alternatively (and more commonly), show evidence of a previous sample of typical GCT in a malignant tumor. Malignant transformation of a GCT can take several years, and literature suggests that radiation therapy may have a facilitatory role.

Giant Cell Reparative Granuloma

A benign, intraosseous proliferation characterized by granuloma-like aggregates of giant cells in a fibrovascular stroma. The lesion is commonly seen in the gnathic skeleton. Cherubism of children may be related to this kind of reaction occurring bilaterally in the jaws. The reaction is thought to be related to, or identical to, a solid ABC. The recent finding of translocations involving the USP6 gene in a number of these lesions supports the interpretation that these lesions are part of the spectrum of aneurysmal bone cyst.

Reparative granulomas have a broad age range. The symptoms are nonspecific. Laboratory investigations should be reviewed to exclude hyperparathyroidism. In the long bones, the metaphysis is the most common site of involvement. In the bones of the hands and feet, it represents a distinct clinicopathologic entity. In this location, there is a predisposition to involvement in children and the involvement of distal bones (phalanges and metatarsals or metacarpals.

Radiologically, the lesions are lucent, expansile, and in the short tubular bones are diaphysiometaphyseal. Soft tissue extension is absent, and the margins are mostly well-defined but not scerotic.

Surgical Pathology: The gross findings are nondescript. Microscopically, there is a prominent fibroblastic stroma containing foci of giant cells (often centered around areas of hemorrhage). Some giant cells contain phagocytosed red cells and hemosiderin. Stromal mitoses occur (but are usually less than GCTs). Trabeculae of osteoid are frequent. These may contain reactive woven bone or "metaplastic"-type bone. Cartilaginous foci are absent unless there is a supervening fracture. Foci of secondary ABC are common. Lymphocytes and plasma cells may be frequently seen in the stroma. The stromal and multinucleate cells may express histiocytic markers.

Differential Diagnosis: Brown tumors of hyperparathyroidism have to be excluded before diagnosis of a reparative

granuloma. Laboratory investigations should be reviewed. GCTs enter the differential and are discussed above. Solid areas of an ABC, the "solid" ABC, and reparative giant cell granulomas are related if not identical lesions and cannot be distinguished histologically.

Management: Intralesional and marginal procedures are considered adequate therapy.

Fibrous Lesions

- Desmoplastic fibroma
- Fibrosarcoma

Desmoplastic Fibroma

A nonmetastasizing but locally aggressive lesion composed of cytolgically typical fibroblasts and in an abundantly collagenized stroma. This lesion is considered to be the bone counterpart of the soft tissue aggressive fibromatosis.

Patients range in age from 1 to 70 years but most cases occur by the age of 40 years. Presentation is by swelling, pain, or fracture; the patients have often been symptomatic for 2–3 years.

The lesions are most frequent in the metaphysis of the long bones. The mandible, pelvis, ribs, vertebrae, or the small tubular bones of the hands and feet are involved less frequently. Radiographically, the lesions are lucent, and may expand the bone. The lesions frequently have coarse trabeculations coursing the lytic areas (Fig. 37a). Periosteal reaction is usually absent. The margins are usually sharp but may occasionally be focally permeated. CT scans often demonstrate a soft tissue shadow.

Surgical Pathology: Grossly, the tumor is gray/fibrous and may be whorled, similar to that of the soft tissue desmoid.

Microscopically, the tumors are hypocellular. They demonstrate a proliferation of spindle cells separated by abundant collagen (Fig. 37b). Entrapped bone may be present. Soft tissue extension is commonly seen. Nucleoli and mitotic figures are inconspicuous to absent. There is often a prominent vascular component, similar to that of the soft tissue desmoid.

Genetic studies using fluorescence in situ hybridization have shown that trisomies of chromosomes 8 and 20 occur in a subset of these tumors, similar to those of the soft tissue desmoids (30).

Differential Diagnosis: The main consideration is the exclusion of fibrosarcoma. The latter is suggested when the nuclear atypia and cellularity is increased, or more than an occasional cell shows nucleoli. Mitotic figures are more readily seen in fibrosarcomas as compared with desmoplastic fibromas. The entrapped trabecular bone in the desmoplastic fibroma may on occasion have to be differentiated from a FD, but in desmoplastic fibroma, the bone is lamellar, and may show orientation.

Management: Wide procedures are preferred. Radiation and chemotherapy are not indicated.

Fibrosarcoma

Fibrosarcoma is a malignant spindle cell lesion that exclusively exhibits fibrous differentiation. Osteoid and chondroid matrices are absent.

The skeletal site distribution is similar to that of osteosarcoma, but the age is more evenly distributed from the second to the seventh decades.

The diagnosis of fibrosarcoma is made far less frequently nowadays, than it had been in the past since several entities such as rhabomyosarcoma and leiomyosarcoma have been recognized and described in the last few decades. These had previously been lumped with fibrosarcoma in the past. Thus, figures of age, sex, and site distributions taken from older literature may not be valid.

The presentation is usually with pain and swelling. About 25% of lesions may arise in the context of preexisting osseous

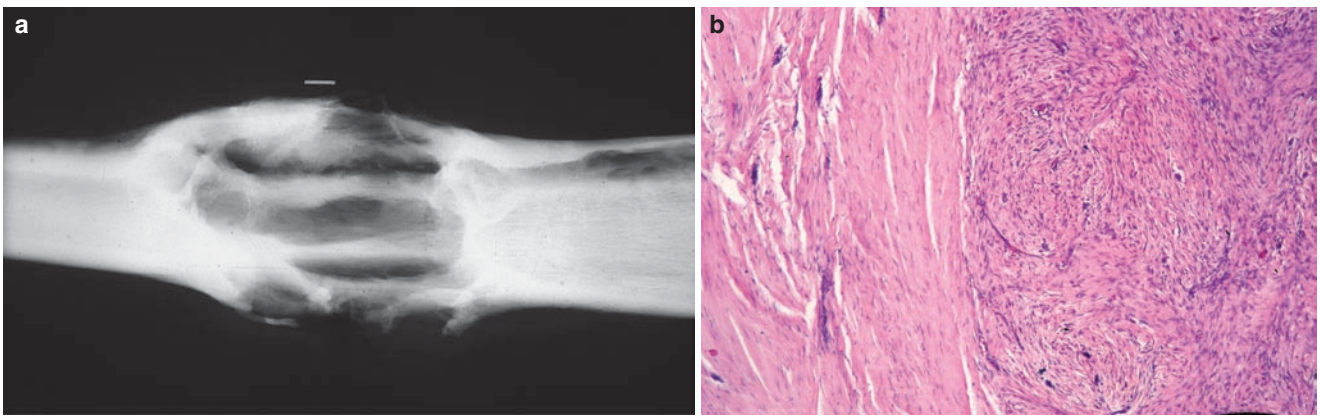

Fig. 37 Desmoplastic fibroma X-rays and microphotograph. **a** There is a trabeculated appearance on X-rays, a frequent finding. **b** The histology is that of a bland, relatively hypocellular proliferation of fibroblasts

lesions such as GCTs, Paget's disease, enchodroma, osteochondroma, chronic osteomyelitis, FD, and bone infarct. The lesions are mostly intramedullary and metaphyseal. Periosteal-based lesions may be examples of soft tissue fibrosarcomas with secondary bone extension.

Radiologically, the lesions most frequently show aggressive, permeative margins although geographic lesions are sometimes seen.

Surgical Pathology: Grossly, the tumors vary from gray, fibrous to soft fleshy tumors with infiltrative margins. Areas of hemorrhage or necrosis may be present in high-grade tumors. Microscopically, the spectrum ranges from tumors that are heavily collagenized, and difficult to separate from desmoplastic fibromas to others are more that cellular, with bizarre, mitotically active spindle cells with considerable cytologic atypia. The spindle cells are consistently arranged in a "herring-bone" fashion of interlacing fascicles. Some tumors may be myxoid. Most tumors show evidence of cortical breakthrough.

Differential Diagnosis: Desmoplastic fibroma enters the differential diagnosis, and is excluded mainly on the basis of the increased mitotic activity and greater cellular atypia seen in fibrosarcomas as compared with desmoplastic fibromas. The complete absence of malignant osteoid formation and of chondroid areas helps to exclude osteosarcomas and dedifferentiated chondrosarcomas, both of which may contain extensive areas of fibroblastic differentiation. Spindle cell melanomas should be excluded on the basis of S-100 stains; in selected cases electron microscopy may be used. Spindle cell carcinomas (such as renal cell carcinomas) can similarly be excluded on the basis of stains for low and high molecular weight cytokeratins and epithelial membrane antigen.

Management: The lesions are generally treated by wide local resection. Chemotherapy is often used, particularly for high-grade lesions showing cytologic atypia or increased mitotic activity.

Fibrohistiocytic Lesions

- Benign fibrous histiocytoma
- Malignant fibrous histiocytoma

Benign and Atypical Fibrous Histiocytoma/ Nonossifying Fibroma (NOF)

Several lesions show common histologic features such as a storiform pattern, histiocyte-like giant cells, foam cells, and a polymorphic infiltrate. Such lesions are often grouped under the general heading of benign fibrous histiocytomas (or NOF/metaphyseal fibrous defect/cortical fibrous defect), even though many such entities may be unrelated to each other or to histiocytes.

A metaphyseal fibrous defect is an intracortical proliferation of fibrous tissue and histiocytes. Larger lesions may involve the medullary cavity. There have been suggestions that metaphyseal defects can, with time, move from the metaphysis to the diaphysis (as the bone grows). A small percentage of lesions arise in patients with neurofibromatosis. Lesions arising in the context of cafe-au-lait spots have been called the Jaffe-Campanacci syndrome.

The incidence of these lesions may be age related. Up to 35% of all children (if screened) are said to have these lesions. They are most common between the ages of 4 and 8 years. The majority of the lesions in this group are less than 0.5 cm. The incidence falls below 2 and above 14 years of age. Since most lesions last about 2 years before disappearing by healing by sclerosis (the healing phase or the so-called ossifying NOFs), this pattern of prevalence may be expected. Symptomatic cases usually have larger lesions, and may present with pain or pathologic fracture. The distal femur, distal tibia proximal tibia, and fibula account for the vast majority of lesions. Occasional cases have been associated with hypophosphatemic (oncogenic) osteomalacia.

Radiographically, most lesions are geographic, lytic lesions with lobulated sclerotic margins. In the healing phase, there may be varying amounts of sclerosis within the lesion.

Surgical Pathology: Grossly, the lesions are gray/yellow and if resected (although excision/resection of these lesions is unusual), may be rimmed by sclerotic bone. Microscopically, the lesions are predominantly fibrous, often having a storiform arrangement. Foamy histiocytes (xanthoma cells), hemosiderin-laden macrophages, and multinucleated giant cells are present in varying proportions. In the presence of fracture or in the healing phase, there may be reactive woven bone present.

Differential Diagnosis: FD can enter the differential in some instances. The prominent osteoblastic rimming of reactive woven bone in NOFs should, however, help in the distinction. Also, in NOFs the fibrous component has a prominent storiform pattern, which would be absent in FD. Giant cells are often prominent in NOFs, which may lead to question the possibility of GCT. The latter, however, has a characteristic stroma which is absent in NOFs. The radiographic findings can be extremely useful in this distinction.

Management: Only symptomatic lesions (or if there is diagnostic uncertainty) are generally considered for treatment. Intralesional procedures are generally sufficient.

Malignant Fibrous Histiocytoma

A malignant neoplasm composed of cells resembling fibroblasts, myofibroblasts, and histiocytes by light microscopy. Malignant osteoid and low-grade areas are absent. Several

tumors including osteosarcomas may have MFH-like areas within them.

There is a wide age and sex distribution. The presentation is usually with pain or a mass. Premalignant conditions such as Paget's disease, FD, bone infarcts, or radiation occur in a small percentage of cases. Some lesions have arisen in the context of orthopedic implants. The metaphyseal regions of long bones are the most frequently involved. Involvement of the small bones of the hands and feet, as well as multicentric origin is rare but reported.

Radiographically, these are ill-defined lytic lesions (Fig. 38a). They may be associated with a pathologic fracture in up to 25% of cases. Cortical expansion and breakthrough with minimal periosteal reaction is frequently seen. The radiological differential is with other high-grade sarcomas, infections, and vascular lesions.

Surgical Pathology: Grossly, the tumor is similar to that of other high-grade sarcomas, often having a variegated appearance with hemorrhage and necrosis. The margins are frequently permeative. Microscopically, these lesions have a wide range of appearances. The lesions may be dominated by fibrous tissue, or like soft tissue MFH, exhibit a variety of patterns – such as inflammatory, myxoid, pleomorphic-storiform, hemangiopericytomatous, and epitheloid. Metastatic lesions often mimic the primary lesion morphologically. Nuclear atypia and mitotic rate can often be impressive (Fig. 38b). Multinucleated malignant giant cells are found in most examples. Histiocyte-like cells with grooved nuclei are also frequent. Fibrosis is often variable, and may be absent. Spindle cell areas with a storiform arrangement are common. Chronic inflammatory cells may be often seen.

Differential Diagnosis: This includes the other high-grade sarcomas such as fibrosarcomas and osteosarcomas. The fasicular arrangement of the former and the presence of areas of malignant osteoid formation of the latter should be helpful in distinguishing these entities. Metastatic spindle cell carcinoma and melanoma should be excluded in all cases. Immunohistochemical demonstration of cytokeratins and epithelial membrane antigen in the former and S-100 positivity with cytokeratin negativity in the latter would be helpful in this differential. Sometimes a variety of cytokeratins and melanoma markers may be required. In this regard, it is important to remember that scattered cytokeratin positivity is seen in some MFHs (31).

Management: Wide surgical resection with neoadjuvant and adjuvant chemotherapy forms the basis of management in most centers. Radiation therapy in selected cases and in some centers is also used.

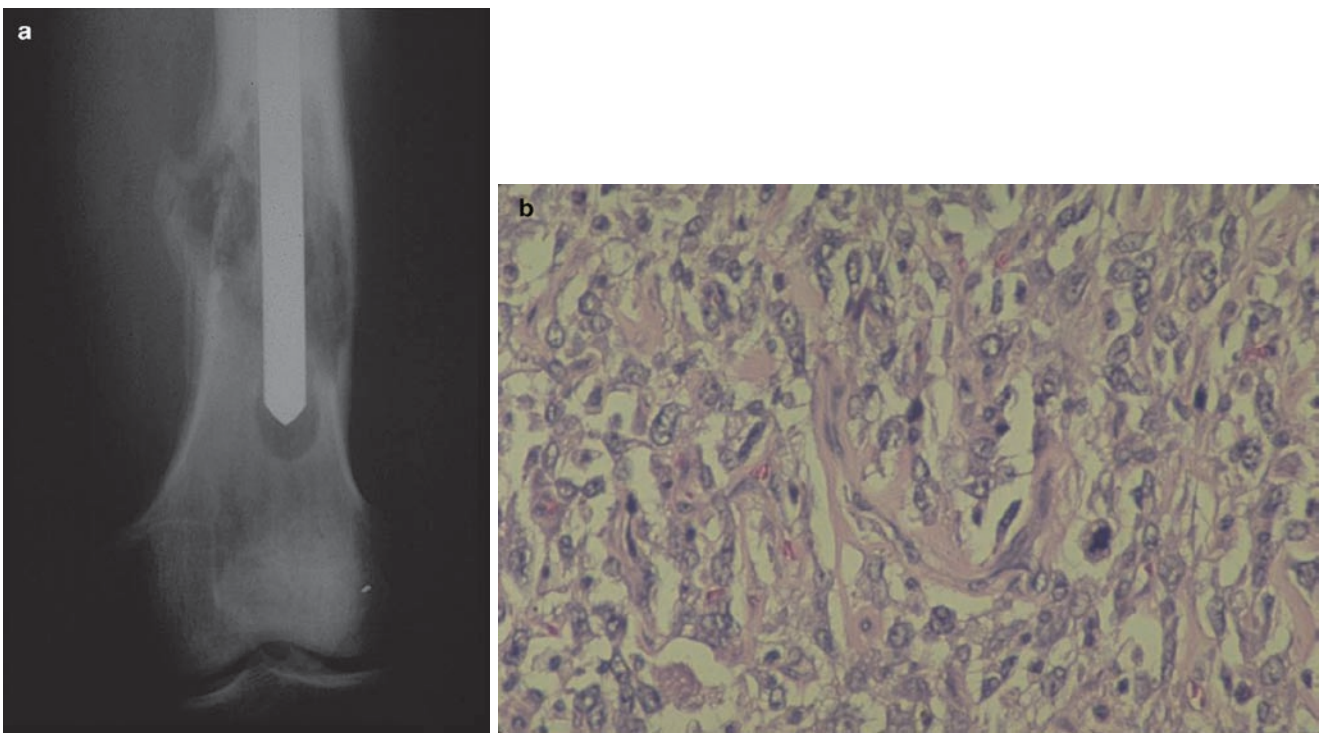

Fig. 38 **a** Malignant fibrous histiocytoma, arising at the site of a previous intramedullary nail (contributed by Dr Andrew Rosenberg, Massachusetts General Hospital). It is seen as a zone of lysis and destruction at the tip of the nail. **b** Malignant fibrous histiocytoma showing bizzare pleomorphic cells with no matrix production

Other Mesenchymal Lesions

- Fibrous dysplasia
- Campanacci's disease (osteofibrous dysplasia)
- Fibrocartilaginous mesenchymoma
- Adamantinoma
- Ewing sarcoma
- Intraosseous lipoma
- Intraosseous liposarcoma
- Leiomyosarcoma
- Intraosseous schwannoma
- Malignant mesenchymoma
- Conventional chordoma
- Chondroid chordoma

Fibrous Dysplasia (Jaffe-Lichtenstein Syndrome)

Fibrous dysplasia (FD) is a benign, mono-ostotic (80% of cases), or polyostotic (20% of cases) proliferation of fibrous tissue and bone. The osseous component is irregularly distributed and consists of woven bone with inconspicuous osteoblastic rimming. Cartilage formation (fibrocartililaginous dysplasia) is seen in less than 10% of cases.

Mono-ostotic FD may be seen at any age, although most cases occur below 30 years, polyostotic FD generally presents before the age of puberty. Presentation may be with pain, pathologic fracture, deformity (especially gnathic or upper femoral FD), or be asymptomatic. A reduction in activity with age is seen in many lesions, with a possible reactivation at the time of pregnancy. Polyostotic FD with macular skin lesions, precocious puberty, with or without fibromyxomatous soft tissue tumors is known eponymically as McCune Albright syndrome. The association of FD with a soft tissue or intramuscular myxoma is known as the Mazabraud syndrome. Very rarely, secondary sarcomas may develop on FD.

About one-third of mono-ostotic FD involves the cranifacial bones, another third the tibia/femur, and about 20% the ribs. In patients with polyostotic FD, the femur, tibia, and pelvis are commonly involved. In many of these cases, small bones of the hands and feet, the ribs, and the skull may also show lesions.

Pathogenesis of Fibrous Dysplasia

The pathogenesis and molecular basis of FD is poorly understood. The endocrinopathies associated with FD, in the McCune-Albright syndrome, are associated with normal or decreased levels of trophic hormones. This suggests an autonomic function of the endocrine glands.

In some cases, skin from patients with associated café-au-lait spots has been found to have somatic mutations in the signal-transducing guanine-binding proteins. This mutation is present in the lesional tissue only, and causes activation of the trimeric stimulatory guanine nucleotide-binding protein, G-protein (guanine nucleotide protein), which has three subunits (α, β, and γ).

This protein couples a receptor to an intracellular effector, in turn, causing a dissociation of the α-chain of the Gs trimer. The dissociation is associated with a substitution of a GTP for GDP bound to the α-chain. The α-chain activates adenylyl cyclase, causing an increase in cAMP in the cell. The α-chain has an inherent GTPase function, resulting in the GTP being converted back to GDP. This conversion causes the α-chain to reassociate with the rest of the Gs, resulting in inactivation of adenylyl cyclase.

The point mutation in McCune-Albright syndrome (mutation of the GNAS1 gene on chromosome 20q13) results in a single amino acid substitution that disrupts the GTPase function of the $\alpha\tilde{}$-chain. This results in the activation of Gs in the absence of receptor activation. Such activating Gs mutations cause increased adenylyl cyclase and hence increased cAMP. Hormones are inappropriately produced and there are presumed local proliferative advantages to the cells in endocrine tissues containg the mutation.

Mutations were not identified in bone lesions for several years after the description from soft tissue lesions, but recently evidence that they occur in bone lesions from both McCune-Albright and mono-ostotic FD have been found (32). Because the mutations are found only in lesional tissue, FD is not a germline disorder, and is not heritable.

It has been suggested that the mutation in McCune-Albright syndrome is present in a mosaic pattern, probably since it originated during fetal development in a variety of cells. In mono-ostotic disease, the mutation probably occurs later in life and results in a single tumor.

Activation of Gs has a different effect, depending on the cell in which it occurs. For instance, in the skin it causes hyperpigmentation. In the endocrine tissues, it causes hormonal secretion.

A number of growth factors are expressed in FD. The expression of these factors is probably caused by Gs activation, and is responsible for the phenotypic behavior of the cells – causing the bone resorption of normal bone, and the formation of dysplastic bone. Cytokines expressed in FD include – platelet-dervied growth factors (PDGFs) (mitogens), bone morphogenetic proteins (BMPs) (bone inductive), c-fos (a nuclear transcription regulator), and interleukins involved with bone resorption.

Chromosomal studies of FD have found that lesions contain chromosomal abnormalities but not a specific abnormality common to all cases. This finding suggests that FD is caused

by a single cell with a proliferative advantage, and supports the idea that it is a neoplasm.

In summary, FD is a proliferation of spindle cells due to a somatic mutational event, either occuring in a mosaic pattern, early in fetal life (McCune-Albright syndrome), or at an isolated site in bone, probably later in life, and resulting in mono-ostotic disease.

The radiological appearances can be variable. The majority of cases are intramedullary, geographic lesions with well-defined, often sclerotic margins and a "ground-glass" matrix. These are intensely hot on bone scans. A few lesions may be more sclerotic or show calcified cartilage. Bony expansion is marked in some examples, especially lesions involving the ribs. FD of the femoral neck (and sometimes other bones) is often accompanied by a pathologic fracture.

Surgical Pathology: Grossly, FD is firm, fibrous white or red with a variable amount of "grittiness." Secondary cyst formation is occasionally seen. Some lesions contain grossly visible cartilage.

Microscopically, there are trabeculae of woven bone in a background of moderately cellular fibrous tissue (Fig. 39). The trabeculae often obtain a variety of shapes (C's, circles, etc.) and are sometimes referred to as "Chinese-letters." Since the osteoid tends to merge into the background, it is often called "metaplastic," a rather meaningless term in this context. Osteoblasts are interspersed in the woven bone but are not conspicuous around the trabeculae. The latter feature, called rimming, is more commonly seen in other examples of woven bone formation such as fracture-callus and myositis ossificans. In some cases of FD, small foci of lamellar bone may also be seen. This fibro-osseous proliferation may show an infiltrative pattern at the junction with nonlesional bone. The junction is also remarkable for reactive woven bone, and may be confusing in small biopsies. The fibrous stroma is highly variable in microscopic appearance. It may be highly or sparsely cellular, myxomatous, or show considerable collagenization. The fibroblasts usually have plump ovoid nuclei but may show elongated narrow ones in some cases or in some areas. Multinucleate osteoclast-type giant cells may be present. Cartilage with peripheral enchondral ossification is sometimes present. The cartilage may be present in long islands, rounded nodules or simulate a growth plate. Collections of foam cells are common. They may be mistaken for metastatic clear cell carcinoma in small biopsy samples.

Differential Diagnosis: This includes osteofibrous dysplasia, reactive woven bone, well-differentiated intraosseous osteosarcoma, and desmoplastic fibroma. Osteofibrous dysplasia (although histologically similar) is a cortically based entity (as opposed to the intramedullary location of FD) which most often affects the tibia or fibula in children. Reactive woven bone may be seen around various benign and malignant lesions. It is characterized by organization (zonation) and bony trabeculae lined by osteoblasts. Well-differentiated intraosseous osteosarcoma has short curved bone trabeculae similar to that of FD but has cytologic atypia and permeative growth pattern. Desmoplastic fibroma is usually heavily collagenized, and though such areas can be present focally in FD, it is much more extensive and uniform in the desmoplastic fibroma.

Management: This is directed toward the treatment of its complications such as deformities, along with surgical extirpation of the disease. Usually wide procedures are adopted, since the recurrence rate of marginal methods is high. Reports of secondary neoplasia superimposed on FD are emerging. Some of these may have been examples of unrecognized well-differentiated intraosseous osteosarcoma in the past.

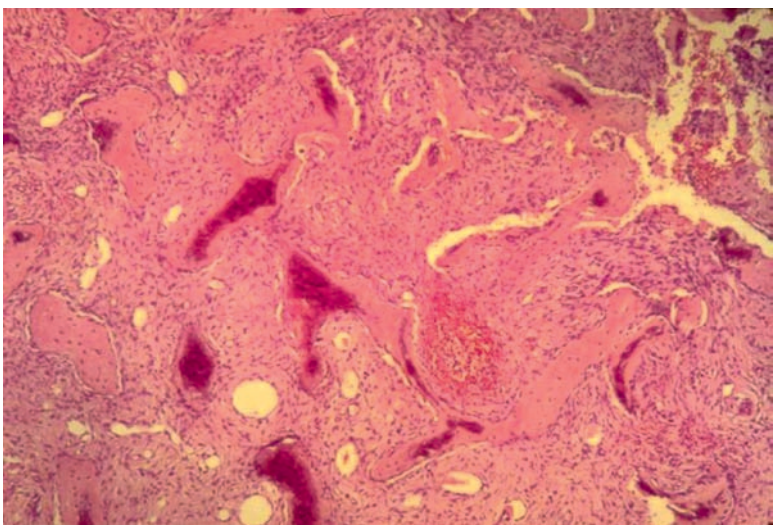

Fig. 39 Fibrous dysplasia. The lesion is characterized by emerging bone trabeculae in a fibrous background

Henry Jaffe (1896–1979) – Jaffe was born in New York in 1896. He qualified in medicine (University School of Medicine, NY) in 1920, and joined the Montefiore Hospital. At the age of 28, he was appointed pathologist and director of laboratories at the Hospital for Joint Diseases – a post he retained till his retirement. He published extensively and his two masterpieces "Tumors and Tumerous conditions of Bone and Joints" and "Metabolic, Degenerative and Inflammatory Diseases of Bone and Joints" remain relevant till today. His paper on FD included descriptions of the McCune-Albright syndrome and polyostotic FD. It was published in 1942 along with Lichtenstein as a coauthor.

Louis Lichtenstein (1906–1977) – Lichtenstein was born in New York in 1906. He qualified from Yale University Medical School in 1929, and trained in pathology at the Mt. Sinai Hospital. He spent 12 years at the Hospital for Joint Diseases before moving to several centers in Los Angeles and San Francisco. His early work was in renal and metabolic disorders but later concentrated on bone pathology. His books "Bone Tumors" and "Diseases of the Bones and Joints" ran to several editions and are widely used till today. His paper on FD was published in 1938, but subsequent to other papers by McCune and Bruch as well as Albright. Later, in 1942, he wrote on the same topic with his colleague Jaffe as a coauthor.

Campanacci's Disease (Osteofibrous Dysplasia)

Osteofibrous dysplasia is a cortically based fibro-osseous proliferation with a predilection for the tibia (and less frequently fibula) in children and infants.

It was initially described by Kempson in 1966 and termed ossifying fibroma. Kempson thought it to be an aggressive lesion. Later, Campanacci from Bologna, Italy, thought it to be benign, and preferred to call it osteofibrous dysplasia. It differs from the ossifying fibroma of jaw, and the term "ossifying fibroma" of long bone has potential for confusion, and is best avoided. The alternative term intracortical FD is sometimes used for Campanacci's disease to emphasize its cortical location. There may be a poorly understood relationship with adamantinoma of long bone (extragnathic type).

The condition is usually diagnosed in the first decade of life (often in the first 5 years). Some adult patients are on record, however. Presentation is usually with a bowing deformity, pathologic fracture, or pseudarthrosis. Usually, involvement is limited to a single bone (mostly the tibia), occasionally, the ipsilateral fibula or bilateral involvement may be encountered. The radiographic appearance is highly characteristic. There is a cortically based, diaphyseal, geographic lucency with sclerotic margins (Fig. 40). The anterior cortical surface is the one usually involved, the entire lesion may show a bubbly appearance with confluent lucencies.

Surgical Pathology: Grossly, the lesional tissue may be fibrous or gritty, in resected cases the lesion is contained by the periosteum. Microscopically, bony trabeculae showing prominent osteoblastic rimming and a fibrous background characterize the lesion. Like FD, the fibrous tissue is variably cellular and may show prominent collagenization. Campanacci and Laus have described a zonation phenomenon in larger lesions (33). This is reflected in the more fibrous center and the more osseous periphery seen in many of their cases. Focal collections of giant cells may be present in a pattern reminiscent of giant cell reparative granuloma. Some studies have demonstrated cytokeratin-positive cells in many of these cases (34). The latter finding has led to speculation on whether these cases might be examples of extragnathic adamantinoma with poorly developed epithelial islands.

Differential Diagnosis: FD and adamantinoma are the main lesions that may enter the differential. FD occurs in older individuals, shows no predilection for the tibia or fibula and is predominantly an intramedullary process. Microscopically, the osteoblastic rimming of bony trabeculae is less prominent in FD. Adamantinoma (like osteofibrous dysplasia) shows a predilection for the diaphysis of the tibia. Further, adamantinomas may contain extensive fibrous tissue simulating osteofibrous dysplasia. The epithelial component may be small and overlooked especially in small biopsies. Since adamantinoma is a lesion found in the adolescents, it is mandatory to carry out extensive sampling before labeling a lesion as osteofibrous dysplasia in this age group.

Management: Since the lesions can spontaneously regress, stay stationary, or slowly progress, a conservative approach is

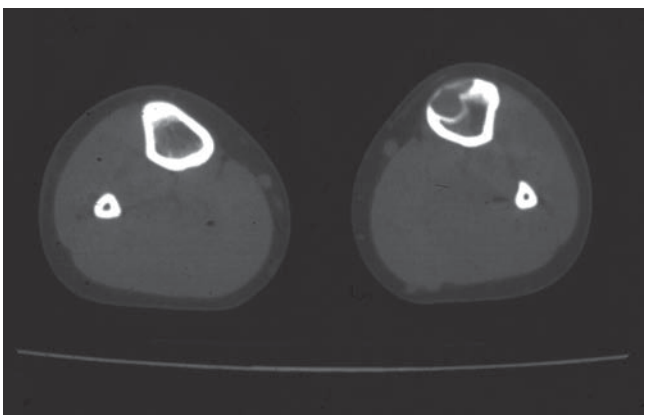

Fig. 40 Osteofibrous dysplasia occuring in the tibia of a child. The lesion is limited to the cortex of the bone.

not unreasonable. Lesions usually do not progress beyond skeletal maturity. Resections performed before the age of 15 years have a high rate of recurrences. Biopsies may not be required in typical cases, so the treatment is often directed toward the management of deformities and fractures. Deformities may require osteotomy, but a nonoperative approach is preferred for fractures.

Fibrocartilaginous Mesenchymoma

Fibrocartilaginous mesenchymoma was described by Dahlin and coworkers in 1984 (35). There is a tendency for this lesion to recur, but malignant behavior is not seen as was initially thought. The lesion occurs in young individuals and may have a predilection for the fibula. The number of cases described, however, is extremely small, and conclusions of its characteristics cannot be drawn.

Radiologically, the lesion is geographic, metaphyseal, and often abuts the growth plate. Cartilage matrix may be seen on X-rays.

Surgical Pathology: Microscopically, there is a combination of bone, spindle cells, and cartilage. The cartilage has a characteristic appearance of epiphyseal plate formation. A dense, spindle cell proliferation is seen between well-formed bony trabeculae, but there is no or little collagen.

Management: Wide local procedures. Adjuvant therapy is not indicated.

Adamantinoma

Adamantinoma is considered to be a low-grade malignant neoplasm, with epithelial differentiation, which shows a marked predilection for the tibia.

It has an uncertain and controversial relationship with Campanacci's disease or osteofibrous dysplasia (36). It arises in patients, somewhat older than those with osteofibrous dysplasia, but shares the same predilection for the tibia.

The tumor is an entirely different entity from the ameloblastoma seen in the jaw (although an alternative name of the jaw lesion is adamantinoma, particularly in older literature). The tibial (or extragnathic adamantinomas) are biphasic tumors having an epithelial and a mesenchymal element, and lack the differentiation toward odontogenic epithelium. Some extragnathic adamantinomas may have a pretibial origin and a possible relationship to cutaneous eccrine carcinomas.

The relationship with osteofibrous dysplasia has been raised in a number of cases of Campanacci's disease have progressed to adamantinoma. The problem is that a percentage of these cases may have been adamantinomas to begin with. Sampling error may have contributed to "missing" the epithelial component leading to these cases being misdiagnosed as Camapanacci's disease. An alternative possibility suggested that adamantinomas are the result of reparative processes and regression. This regression at the extreme could result in osteofibrous dysplasia (37).

Some authors recognize a classic (or aggressive form, with a tendency to occur in older age groups) and a well-differentiated form (or indolent, nonmetastasizing form occurring in younger age groups). This distinction needs to be confirmed on larger series before being adopted.

Patients display a wide age range, occurrence in infancy is unusual, most cases occur in the second and third decades. Presentation can be with pain, fracture or be discovered incidentally.

Radiologically, most lesions affect the tibial diaphysis. A very small number of cases have involved bones other than the tibia; these bones include the fibula, femur, other long bones, pelvis, and the short tubular bones. The lesions are often diaphyseal, eccentric, epicentered in the cortex, with a "soap-bubble" appearance. Primary intramedullary origin or cortical breakthrough is seen in a small number of cases. The lesions usually show a geographic margin, that is, only rarely sclerotic.

Surgical Pathology: Grossly, the tumor is well demarcated in resection specimens (Fig. 41a, b). A lobular growth pattern may be evident. Cystic spaces and hemorrhage are common. Microscopically, the tumor consists of epithelial islands in a fibrous stroma. The nuclei of adamantionoma are usually bland and the mitotic rate is usually low in most cases. A variety of growth patterns may be evident in the epithelial component. These include spindled, basaloid, tubular, and squamoid. The spindle pattern in particular can be difficult to recognize as epithelial in the absence of immunohistochemical stains. A clue, which the spindle cell proliferation is from an adamantinoma rather than fibrosarcoma, is the obvious lack of atypia. Anastamosing spaces, with the appearance of vascular channels, are seen in some cases.

Differential Diagnosis: Osteofibrous dysplasia enters the diagnosis. Stains for cytokeratin are helpful in making this distinction; however, a few scattered positive cells in otherwise typical osteofibrous dysplasia should not be interpreted as adamantinoma. Metastatic carcinoma enters the differential, but the distal appendicular skeleton (such as the tibia) is a relatively infrequent site for metastatic carcinoma. A bland cytologic appearance would better fit with adamantinoma rather than metastatic carcinoma. Vasoformative lesions such as epitheloid hemangioendothelioma may be misinterpreted as the tubular form of adamantinoma. Appropriate immunohistochemistry for von Willebrand antigen, CD 34, CD 31, and Ulex europaeus could confirm the vascular nature of these lesions. Synovial sarcoma is in the differential, and may extend into the bone. The epithelial component of the synovial sarcoma may be indistinguishable from that of adamantinoma. However, the mesenchymal component of a synovial sarcoma, however, tends to be far more cytologically atypical than the bland osteofibrous dysplasia-like stroma of an adamantinoma.

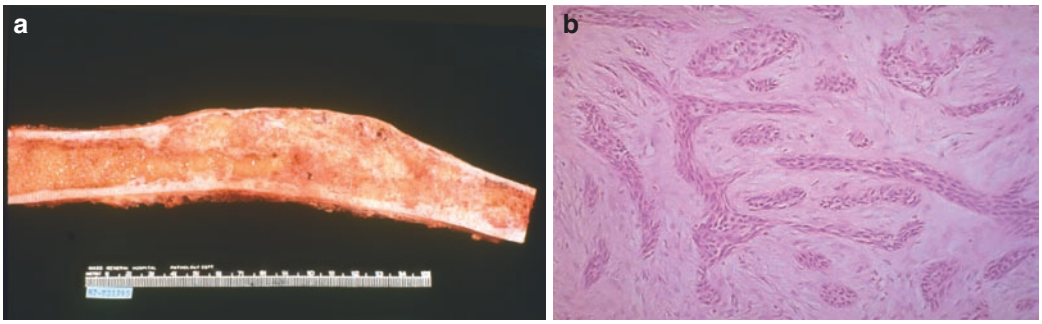

Fig. 41 Osteofibrous dysplasia. The CT scan shows the lesion occurring in the tibia of a 6-year-old. The process is limited to an intracortical location. **a** Adamantinoma – gross specimen (contributed by Dr Andrew Rosenberg, Massachusetts General Hospital). The lesion involves the cortex and part of the medulla of the tibia. **b** Histologically, it is composed of epithelial islands in a fibrous background

Management: Adamantinoma is a lesion prone to recurrences. Occasional cases metastasize to the lungs, lymph nodes, other bones, and so on. Wide surgical procedures are used. At present there seem to be no consistent histologic or clinical markers of predicting the lesions that would be more likely to show an aggressive biologic behavior.

Ewing Sarcoma

Ewing tumor (or Ewing sarcoma) is a primary osseous neoplasm composed of small round cells with no matrix production.

The neoplasm takes its name after James Ewing (1921) who considered it an endothelioma. After several years of controversial search for its histogenesis and its relationship with peripheral neuroectodermal tumors (PNETs), some facts about its molecular defects have emerged. It is now considered to be one of the less differentiated tumors from the group of neoplasms with neuroectodermal differentiation. Tissue culture studies in the presence of differentiation agents like cAMP have showed that the tumor develops neural features (38). The possibility that it arises as a result of adenovirus infection has been raised, but definitive proof is lacking.

Ewing sarcoma tends to afflict patients at young ages. The majority of patients are in the first two decades of life. Patients above the age of 30 are exceedingly rare. In children below 5 years of age, metastatic neuroblastoma should be conscientiously excluded. Localized pain and a mass are the most common presenting symptoms. There may be fever, leukocytosis, and a raised sedimentation rate. These bring up the clinical differential of acute osteomyelitis, an entity which can mimic Ewing tumor both clinically and radiologically. Upto 10% of patients may have skeletal metastases at the time of presentation.

The tumor involves the long tubular bones such as the femur as well as some flat bones like the pelvis and ribs in greater frequencies than the short tubular bones of the hands and feet or sites such as skull, vertebrae, or sternum; however, any bone may be affected. Although diaphyseal location is more common, tumors may also occur in the metaphysis. Epiphyseal location, even though reported, is rare.

Radiologically, the lesions are ill defined, lytic with permeative margins. A periosteal reaction if present is of the onion skin, sunburst, or other rapidly growing type. A soft tissue component is often present and is well detected by CT or MR scans (Fig. 42a). The extent of involvement by MR is frequently far greater than that demonstrated by plain X-rays. Rare cases of surface (periosteal) Ewing tumor, producing a saucerization effect, are on record.

Surgical Pathology: Grossly, the tumor may be firm or glistening, or more friable, mimicking pus. Hemorrhage and cystic change may be evident.

Microscopically, the classic form is very cellular and consists of sheets and large nests of uniform, small, round to polygonal cells with scanty cytoplasm (Fig. 42b). The chromatin is finely dispersed usually with no nucleoli and a variable number of mitotic figures. Perivascular cuffing may be evident in areas of necrosis. Rosettes are seen in a small minority of cases, and may cause a misdiagnosis of the lesion as a metastatic neuroblastoma.

Reticulin is scant in most cases of Ewing sarcoma. Cytoplasmic glycogen demonstrated by the periodic acid Schiff (PAS) stain is evident in many (but not all) cases; the demonstration is better and more consistent if the tumor is fixed in 80% alcohol (or other nonaqueous-based fixatives) rather than formalin.

An immunohistochemical stain, Mic 2 (CD 99) is available for use in formalin-fixed paraffin-embedded tissue (Fig. 42c). This stains the protein expression of a pseudoautosomal

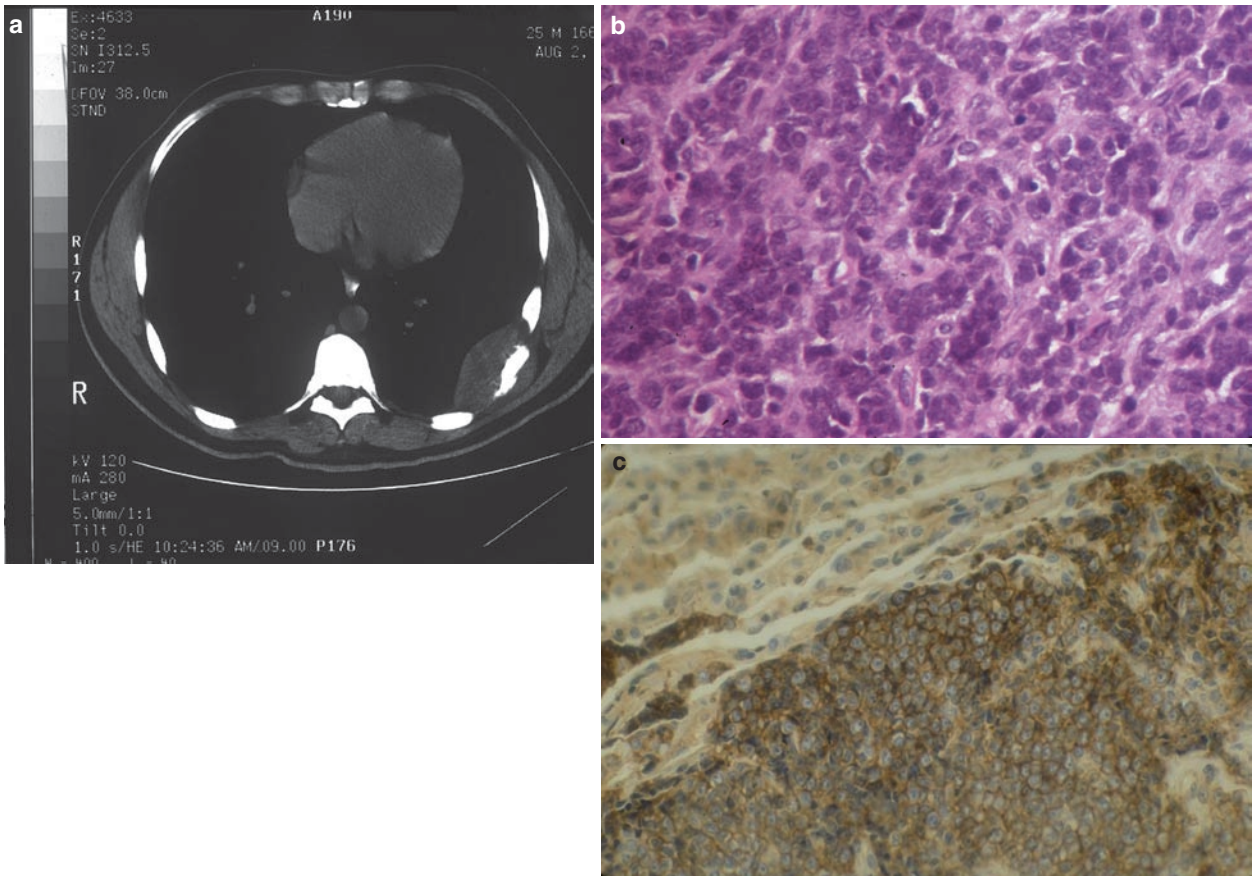

Fig. 42 Ewing's sarcoma involving the rib. **a** There is a prominent soft tissue shadow on the CT scan. **b** The lesion is composed of small blue round cells. **c** The cells stain with CD 99 (Mic-2) in a membranous pattern

gene located on the X- and the Y chromosomes. It shows membranous positivity in the large majority (if not all cases) of Ewing's sarcoma and PNETs. This immunomarker also stains rhabdomyosarcomas and cells from acute lymphoblastic leukemia; however, these tumors tend to show cytoplasmic rather than membranous staining.

Ewing sarcoma cells also usually express vimentin. Occasional cases may express weak-focal staining for cytokeratin, although an occasional case may express strong "adamantinoma-like" positivity (39). Neuron-specific enolase and other neural-specific markers may be positive. Leukocyte-common antigen, markers of muscle, and blood vessel differentiation should be absent.

Variants from this classic pattern include a large cell type and a filigree pattern. In the large cell type, the cells may be larger, and cytologically may show nucleoli. The filigree pattern refers to a bicellular architecture, separated bystroma (40). These tumors are generally positive for glycogen by PAS stain but may require electron microscopy to demonstrate this on occasion. Spindle cell cytology, differentiation into muscle or ganglion cells, or extracellular matrix is absent. Some authors recognize on morphologic basis, an "atypical" Ewing sarcoma characterized by one or more of the features – lack of glycogen, brisk (over 2 per high-power field) mitoses, neoplastic vascular formation, spindling at the periphery of the tumor, some amount of extracellular matrix, lobular architecture, or alveolar pattern.

Ultrastructurally, the features include a lack of visible differentiation along with varying amounts of glycogen. The latter is often present in the form of "lakes." Occasional intermediate filaments might be seen as may primitive cell junctions, but cell processes and dense core granules by definition should be absent.

Ewing tumors show a characteristic t(11;22) chromosomal translocation. By molecular methods, this chromosomal abnormality corresponds to the EWS/FL1 gene fusion. The EWS gene (located on chromosome 22 at q12) is translocated to the FL1 (a gene of the ETS family located on chromosome 11). This results in the formation of a chimerical protein product, and is seen in about 85% of patients. A second translocation has been identified in about 15% of patients. This is the t(21;22) translocation, which fuses the EWS gene with a different member of the ETS family, the ERG gene located on chromosome 21q22. This gives a hybrid EWS/ERG product. Whether these two kinds of Ewing sarcoma behave differently

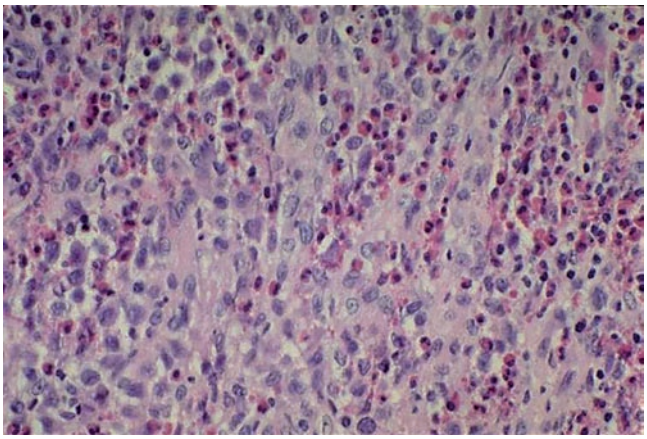

Fig. 43 Langerhans cell histiocytosis. The large grooved histiocytes are present in an inflammatory background rich in eosinophils

clinically is unknown. These two kinds cannot be distinguished at the light microscopic level. Diagnostically, this is a convenient method of confirming or establishing the diagnosis of Ewing tumor in selected cases.

Differential Diagnosis: Small cell osteosarcoma and mesenchymal chondrosarcoma are distinguished primarily on morphologic grounds, and their production of osteoid or cartilage matrices. Reactive bone around an otherwise typical Ewing tumor may, however, be found, and should not be misinterpreted as malignant osteoid.

Lymphoma is differentiated on the basis of the standard immunohistochemical markers for the various lymphoma entities and on the basis of CD 99 negativity in most lymphomas. Ewing sarcoma is negative for the leukocyte common antigen (CD 45). It should be remembered that CD 99 stains certain lymphocytes including cells from acute lymphoblastic leukemia.

Metastatic neuroblastoma occurs in greater frequency than Ewing's, in patients below the age of 5 years and should be excluded in this age group. Light microscopic clues, such as Homer-Wright pseudorosettes and a pink fibrillary background or ganglion cell differentiation, should be looked for. However, these may be present in peripheral neuroectodermal tumors (PNET), an entity related to Ewing sarcoma. Immunohistochemically, neural markers such as neuron-specific enolase may be present in both neuroblastoma and Ewing sarcoma and so are not helpful. Ultrastructurally, the neuroblastoma may show neuritic cell processes containing neurofilaments, neural tubules, and dense core granules. These, however, are found in PNETs. Biochemical demonstration of raised catecholamine metabolite levels or CT scan demonstration of an adrenal mass is contributory.

PNETs: This is an entity closely related to Ewing sarcoma; it is differentiated on morphologic grounds by having definite evidence of neuroectodermal differentiation (Homer-Wright rosettes and immunopositivity for synaptophysin, neurofilaments, and neuron-specefic enolase). However, whether this difference is biologically sound is still a question. Some studies, however, have suggested that PNETs may have a poorer prognosis, thus justifying their separation.

Management: The primary modality of treatment of Ewing sarcoma has shifted from radiation to surgery over the past two decades. Chemotherapy (with or without radiation) is used in a neoadjuvant and adjuvant setting. As life expectancy increases, the problem of second malignancies is also increasing. Some studies have correlated a lower age, smaller tumor burden, low levels of lactate dehydrogenase, and acute phase reactants in patients to an improved outcome. Tumors with the bicellular, filigree pattern have a poorer outcome. Other forms of "atypical" Ewing sarcoma and a lack of response to neoadjuvant chemotherapy have also been associated with a poorer survival. These parameters of prognosis, however, need additional studies and multivariate analysis.

James Ewing 1866–1943. James Ewing was born in Pittsburgh, the son of a judge and a school teacher. He had osteomyelitis, at the age of 14, which partially crippled him, but continued to be active in sports especially tennis and boxing. In 1891, he received his degree and interned at the Roosevelt hospital and Sloan Maternity Center in New York. In 1894, he went to Austria to study under Professor Kolisko, who was chair of pathology at Vienna and the successor of Professor Karl von Rokitansky. He returned to the United States and worked with Dr Prudden at the Columbia University's College of Physicians and Surgeons. Dr Ewing was a contract surgeon in the Spanish American war of 1898, during which time he took an interest in blood morphology and. In 1899, he became the first professor of pathology at the newly opened Cornell Medical School. After the death of his wife in 1903, Ewing devoted himself to his son James Jr and his work. He became interested in venereal lymphosarcoma of dogs and other cancers and directed the Memorial hospital medical board. In 1919, he wrote a book on neoplastic diseases. His name is eponymically associated with a tumor, which he called a diffuse endothelioma of bone, and first presented to the New York Pathological Society in 1920. He was averse to biopsies, especially through unbroken skin, a practice he felt would cause infections and advocated therapy (including amputations) based on clinical judgement alone. He was especially against the use of frozen sections. He did, however, allow needle biopsies, especially for breast tumors. He was a protagonist of radiotherapy, and developed a laboratory for this. He encouraged subspecialty surgery and attracted surgeons for this as director of the Memorial Hospital.

Intraosseous Lipoma

Intraosseous lipoma is a benign tumor showing differentiation to mature adipose tissue, arising from within the medullary cavity. There is a wide age range, the commonest presentation is with pain, but many lesions are asymptomatic and discovered incidentally on X-rays. The common sites include long tubular bones, ribs, calvarium, gnathic bones, sacrum, and calcaneum. Radiologically, the lesions are geographic, lytic, with sclerotic margins. CT scans can be very helpful, since the CT scan numbers are rarely so low in other lesions (Hounsfield numbers from within the lesion are often below −70). There may be focal matrix formation if the lesions undergo degenerations such as infarction or dystrophic calcification. In such cases, the CT scan values are less helpful. A "parosteal" variant of the intraosseous lipoma has been described.

Surgical Pathology: Grossly, the lesions are discrete, lobulated, and yellow. Areas of dystrophic calcification or fat necrosis with cyst formation may be visible. Microscopically, the lesions are composed of mature adipose tissue with scattered preexisting trabeculae coursing within this. Areas of dystrophic calcification and fat necrosis may occur.

Management: Intralesional or marginal procedures are usually sufficient. Some case reports of dedifferentiation, however, are on record.

Intraosseous Liposarcoma

Intraosseous liposarcoma is a malignant sarcoma with differentiation to adipose tissue, resembling its soft tissue counterpart. These are uncommon lesions and are represented by case reports. Pain is the common presentation. Long bones are the common sites of involvement. The radiographic appearances are those of aggressive lesions and resemble those of other sarcomas.

Surgical Pathology: Grossly, the tumors may be gray, white, or yellow and firm or gelatinous. Microscopically, the majority corresponds to the soft tissue "pleomorphic" type of liposarcoma. Lipoblasts are identifiable. Rare cases of myxoid liposarcomas have also been described in bone.

Differential Diagnosis: The lesion should be differentiated from other sarcomas, such as malignant fibrous histiocytoma and "de-differentiated" lesions. This is done on the basis of routine histomorphology supported by immunohistochemistry or other means in a fashion similar to those of the soft tissue lesions. Malignant "mesenchymoma" contain more than one kind of tissue. Metastatic liposarcoma should be excluded by imaging techniques. Adenocarcinoma with signet ring cells may have to be excluded in some cases. This is done by appropriate immunohistochemical stains for epithelial differentiation seen in carcinomas.

Management: Wide surgical procedures with adjuvant and neoadjuvant chemotherapy are the preferred approach.

Leiomyosarcoma

Intraosseous leiomyosarcoma is a malignant spindle cell neoplasm of intraosseous origin exhibiting smooth muscle differentiation. These are rare tumors and mostly described as case reports. There is a wide age range but is more common after the second decade. The distal femur and proximal tibia are the most common sites, but any bone can be involved. The radiological features are those of aggressive lesions and resemble other sarcomas.

Surgical Pathology: The gross and microscopic features are similar to those of the soft tissue counterpart. There are interweaving fascicles of spindle cells having a pink fibrillary cytoplasm. There may be focal storiform areas. Occasionally, the cells may be rounded with a pale clear cytoplasm. Osteoclast-type giant cells may be found focally or dispersed. Ultrastructurally, actin-sized filaments with dense bodies may be seen. Pinocytic vesicles are prominent. Immunohistochemical demonstration of muscle-specific actin and less commonly desmin is seen. Cytokeratin positivity may be present focally.

Differential Diagnosis: Metastatic leiomyosarcoma must be excluded. Other sarcomas may need to be excluded on the basis of histomorphology and immunohistochemistry or electron microscopy. Spindle cell carcinomas may enter the differential and appropriate immunohistochemical support may be helpful.

Management: Protocols and surgical procedures similar to other spindle cell sarcomas are employed.

Intraosseous Schwannoma

A benign neoplasm of Schwann cell differentiation characterized by a cellular (Antoni A) and a loose, hypocellular myxoid (Antoni B) areas. There is a wide age range, with most cases occurring in the fourth decade. Mandible, sacrum, and other vertebrae followed by other bones are the common sites of involvement. Vertebral lesions may result in nerve deficits, and sacrum lesions can often be extremely large. However, in these locations, the alternative possibility, that these represent nerve root or spinal tumors with bony extension needs to be considered. The association of these lesions with neurofibromatosis is unclear. Patients with neurofibromatosis often develop bone lesions – mainly of the NOF type. Some cases of pseudoarthrosis of tibia occur in neurofibromatosis. Review of such cases which in the past had been diagnosed "fibrous" tissue would be revealing. Skeletal psammomatous schwannomas have also been described in a subgroup of patients with cardiac myxomas and Cushings syndrome (41).

Radiologically, schwannomas are lytic, sharply demarcated defects that often expand the involved bone. Occasionally, sclerotic margins are the most frequent; however, cortical breakthrough may be seen.

Surgical Pathology: Grossly, the lesions are nonspecific gray, yellow, or hemorrhagic. Microscopically, the lesions show the characteristic features of schwannomas. Antoni A areas may be particularly prominent with verocay body formation. Secondary changes such as lipid or hemosiderin-laden macrophages may be prominent. Thick-walled blood vessels are frequently found. Scattered large, pleomorphic nuclei may be found. These should not be overinterpreted as suggestive of malignancy. Other features such as a high mitotic rate are more helpful in predicting an aggressive or malignant behavior. Immunohistochemical demonstration of S-100 and vimentin is possible in the vast majority of lesions. Other markers such as CD57 or glial fibrillary acid protein (GFAP) are more variable and may be absent. Melanotic schwannomas have pigmented spindle cells and psammomatous concretions, and show evidence of melanogenesis by electron microscopy. S-100 and HMB-45 stains are usually positive in these cases.

Differential Diagnosis: Schwannomas with large pleomorphic nuclei may be mistaken for sarcomas if their nerve sheath origin and benign radiographic nature is not recognized.

Benign fibrous histiocytoma and NOF are often in the differential, especially in cases where foam cells and spindle cells are prominent. The Antoni A and B areas, the thick-walled blood vessels are clues, and S-100 stains useful in this differential.

Desmoplastic fibroma is usually more collagenized and lacks the myxoid background of schwannomas. Again, immunohistochemical staining for S-100 protein is helpful in establishing the nature of the lesion.

Management: Intralesional and marginal procedures are usually sufficient.

Malignant Mesenchymoma

A sarcoma consisting of two or more differentiated mesenchymal elements other than fibrosarcoma or malignant fibrous histiocytoma. There is a wide age range, most lesions occurring in the long bones.

Surgical Pathology: Combinations formed from entities such as liposarcoma, osteosarcoma, rhabdomyosarcoma, angiosarcoma, and chondrosarcoma have been described.

Differential Diagnosis: Dedifferentiated sarcomas (especially chondrosarcoma) are often in the differential. The usual pattern of malignant fibrous histiocytoma and chondrosarcoma should not be termed a malignant mesenchymoma in such cases. True malignant mesenchymomas are said to have a high-grade chondrosarcomatous component intermixed with the other sarcoma components, and this is unusual in dedifferentiated tumors where a low-grade and high-grade component are seen and often lie separately or adjacent but not intermixed. High-grade osteosarcoma by definition can include chondroblastic and MFH-like areas and should not be called a malignant mesenchymoma.

Management: Similar to other sarcomas. This is said to have a poorer outcome than other spindle cell sarcomas; however, the paucity of well-documented cases has precluded a controlled study so far.

Conventional Chordoma

This is a low-grade malignant tumor occurring predominantly in the axial skeleton and in the region of the embryonic notochord. There is a particular predilection to the caudal and cranial extremes; the clivus and the sacrum are the commonest sites. They have a differentiation toward (but not identical to) fetal notochord. Vestigial rests of notochord-like tissue, located in the spheno-occipital region are sometimes found and termed ecchordosis physaliphora. A benign counterpart of the tumor, the giant notochordal rest has been described (42).

Symptoms are a reflection of the anatomic location of the tumor. Thus, those located at the spheno-occipital region result in headache, cranial nerve palsies, visual field disturbances, and endocrinopathies. Cervical tumors may result in spinal cord compression. Sacrococcygeal tumors may produce lower back pain, urinary bladder or bowel dysfunction, paraesthesias, or a pelvic or sacral mass.

Radiologically, chordomas are midline tumors that expand and destroy bone. About half the lesions in most series occur in the sacrum, the other half is localized to the clivus. Locations other than these are exceedingly rare. Matrix calcifications are sometimes present in the clivus region.

Surgical Pathology: Grossly, they are lobulated, soft, myxoid masses, and may mimic a chondrosarcoma.

Microscopically, the lesions are lobulated, and have a myxoid background. This material is sulfated mucopolysaccharide that is hyaluronidase resistant. The lobules are separated by fibrous septa. The tumor frequently extends beyond the grossly identified margins.

Within these lobules are cells arranged in cords, sheets or occasionally, haphazardly. At least some of these cells contain vacuolated cytoplasm (physaliphorous cells). Some cells may have abundant eosinophilic cytoplasm or may mimic signet ring cells. Nuclear pleomorphism is mild and mitotic activity low to absent. Some cases are seen with considerable "degenerative" atypia present in the tumor cells. Such lesion should not be considered as dedifferentiated.

Immunohistochemical positivity for epithelial markers is seen in the tumor cells, and corroborated by ultrastructural visualization of tonofilaments and desmosomes. These

immunostains and ultrastructural features suggest the relationship with neuroectoderm. A newly recognized marker brachyury may be helpful diagnostically (43). This takes advantage of the fact that the transcription factor brachyury is involved in notochord development. Early data suggests that it might be a good marker for chordomas.

Differential Diagnosis: Metastatic adenocarcinoma forms an important differential. True gland formation if seen is suggestive of an adenocarcinoma. Most metastatic carcinomas have a greater degree of cytologic atypia than chordomas, and lack the lobulated growth pattern. Mucin stains may be of value. Neutral mucins (PAS and mucicarmine positive) are suggestive of adenocarcinoma. Immunohistochemical studies have to be interpreted with caution, since chordomas express cytokeratins and epithelial membrane antigen.

Liposarcoma: The vacuolated cells of chordoma may be mistaken for a liposarcoma and vice versa. A lobular growth pattern favors a chordoma. Fat stains, mucin stains, and immunohistochemical stains for epithelial markers may help confirm the diagnosis. It is important to remember that S-100 positivity may be seen in both these entities.

Myxoid Chondrosarcoma: This tumor is less common in the axial skeleton, the reverse being true of chordomas. However, the lobular pattern, the cord-like arrangement of cells, and S-100 positivity is common to both. Physaliphorous cells are seen in chordomas, and immunostains for cytokeratins would help confirm the diagnosis. Myxoid chondrosarcoma (chordoid sarcoma) may express epithelial membrane antigen; cytokeratin positivity is, however, not seen in these variants.

Myxopapillary ependymoma enters the differential in the sacrum. Ependymomas stain with glial fibrillary acid protein, and this helps distinguish them from chordomas.

Chordoid meningioma is a rare type of meningioma that mimics chordoma. The location (well-circumscribed mass attached to dura) helps distinguish this lesion. Additionally, chordoid meningiomas often have more typical areas, and are rich in a lymphoplasmacytic infiltrate. They are generally negative for cytokeratin. Giant notochordal rests/benign notochordal tumors have been described by Yamaguchi and others. These are small, well circumscribed lesions that lack lobular growth pattern and do not generally have the myxoid matrix of true chordomas. They do however have physialiphorous cells.

Management: Wide excision is the optimal treatment. Owing to the anatomic site, however, this is not always possible in many cases. In these cases, debulking followed by radiation has been attempted. Some cases can undergo dedifferentiation to a malignant fibrous histiocytoma. This change is seen in a proportion of patients who have received radiation therapy, or have had multiple recurrences. Some chordomas, however, have dedifferentiated without either of these factors being applicable. The outcome of these patients is predictably poor.

Chondroid Chordoma

This is a variant of conventional chordoma, which has foci of cartilaginous differentiation. This tumor is said to have a predilection for the spheno-occipital region. The tumor is a controversial entity, as some authors equate it with a chondrosarcoma. The diagnosis is best reserved for cases with clear-cut admixture of the two components.

Management: The management is similar to that of the conventional chordoma. The chondroid variant of chordoma is said to be prognostically better than conventional chordomas.

Proliferations of the Hematopoietic Elements

- Plasma cell myeloma
- Leukemia deposits (granulocytic sarcoma)
- Non-Hodgkin lymphoma
- Hodgkin disease
- Langerhans cell histiocytosis
- Erdheim-Chester disease

These entities are more extensively discussed in texts specializing in hematology. These lesions frequently occur as a differential diagnosis in assessing bone neoplasms. Because they may be difficult to distinguish radiologically, some of these lesions will be mentioned briefly.

Plasma Cell Neoplasms (Plasma Cell Myeloma/ Plasmacytoma)

Plasma cell neoplasms constitute one of the most frequent neoplasms to affect bone, especially so in the older age groups. The condition results from the expansion of a single clone of immunoglobulin secreting plasma cells. Plasma cell myeloma is a bone marrow-based, multifocal plasma cell neoplasm characterized by a serum monoclonal protein and skeletal destruction with osteolytic lesions, pathologic fractures, bone pain, hypercalcemia, and anemia. Plasmacytomas are clonal proliferations of plasma cells that are cytologically and immunophenotypically identical to those of plasma cell myeloma, but manifest a localized osseous or extraosseous growth pattern. In the variant known as POEMS syndrome, there may be sclerotic bone lesions, along with *P*olyneuropathies, *O*rganomegaly, *E*ndocrine abnormalities, and *S*kin changes. Patients may present with anemia, pallor, back pain, repeated infections, pathologic fractures, hepatosplenomegaly, hypercalcemia, and renal insufficiency.

Radiologically, there are lytic bone lesions (punched out defects), which are not necessarily hot on bone scans and generalized osteoporosis. The most common bones affected include vertebral column, ribs, skull, and the pelvis. The lesions may be located in the diaphysis or metaphysis. The radiological differential diagnosis frequently includes metastatic carcinoma, lymphoma, and hyperparathyroidism.

Surgical Pathology: Grossly, the tissue is soft, pink, or gray. Microscopically, the lesions are composed of sheets or aggregates of mature to immature, pleomorphic, or anaplastic plasma cells. Less differentiated examples may show prominent nucleoli immature or "plasmablastic" morphology. Amyloid deposition may be seen in some cases. The plasma cells are usually positive for CD38, CD56, CD79a, CD138, and an immunoglobulin light chain (κ or λ). In the very poorly differentiated or anaplastic examples, there may be difficulty in distinguishing from lymphoma and other nonhematopoietic disorders (osteomyelitis) and immunohistochemical stains to establish clonality (κ and λ) may be required.

Management: This systemic disease is treated with chemotherapeutic agents including high-dose corticosteroid therapy, alkylating agents (bisphosphonates), antitopoisomerase II alpha agents, Velcade, thalidomide, monoclonal antibodies (Bortezomib), radiation therapy, and stem cell transplant. Impending fracture or pathologic fracture is managed by intermedullary stabilization or by a variety of osteosynthetic devices depending on the anatomical location. Polymethacrylate cement is often used to provide adequate stabilization and allow early return to function. Radiation may be required to manage intractable pain or nonresectable lesions.

Leukemia

Although the frequency of such lesions may be higher than thought, these rarely come to the surgical or musculoskeletal pathologist's attention since the diagnosis is usually based on clinical or pathologic grounds. Very occasionally, the initial presentation is with osseous lesions that may be mistaken for osteomyelitis radiologically. The lesions are usually permeative and metaphyseal-diaphyseal.

Surgical Pathology: The microscopic appearance of these tumors consists of a proliferation of blasts. Auer rods and/or azurophilic granules may be present in some myeoblasts. Immunophenotypic studies by flow cytometry or immunohistochemistry for myeloid and lymphoid markers and cytochemical stains (nonspecific esterase) are useful in the diagnosis. The differential diagnosis includes small round cell tumors: Ewing's sarcoma, metastatic neuroblastoma, small cell osteosarcoma, mesenchymal chondrosarcoma, rhabdomyosarcoma, and occasionally osteomyelitis. In problematic cases, DNA studies on snap frozen material could be helpful.

Non-Hodgkin Lymphoma

Bone lymphomas are very uncommon before the second decade. Osseous lymphoma lesions are more common as a *secondary* rather than a primary form of involvement.

Although rare, the majority of the *primary* osseous lymphomas would be considered of the diffuse large cell variety in the WHO classification. In the United States, the majority of these are B-cell lymphomas. In Japan, about 10% may be of T cell. Primary bone lymphomas tend to occur more frequently in the appendicular skeleton (reverse of secondary lymphomas which are more common in the axial skeleton). Involvement of the digits is unusual. Radiologically, the lesions are lytic, blastic, or mixed and often extensive. Lytic lesions are often moth-eaten or permeated.

Surgical Pathology: The microscopic appearance is that of a lymphoid proliferation. Lesions may show a diffuse or nodular involvement. There is often considerable variability of tumor cells, a feature that helps distinguishing lymphoma from Ewing sarcoma. Some of these lesions, however, may have a fibroblastic or spindled component. A very rare signet ring form of lymphoma has also been described. In both these instances, immunophenotypic studies by flow cytometry or immunohistochemical stains are useful in the diagnosis. A panel to both establish the diagnosis and classify it often includes CD45 (leukocyte-common antigen or LCA), B- and T-cell markers, and other markers to differentiate lymphoma from its mimics such as Ewing tumor (CD99 or Mic-2).

Hodgkin Lymphoma

Secondary involvement in patients with stage IIIB or IV Hodgkin disease is not uncommon. Presentation as bone involvement as the initial or only site is distinctly uncommon or rare. There is a slight predilection to axial skeletal involvement. The radiological features include lytic, blastic, or mixed lesions.

Surgical Pathology: Microscopically, nodular sclerosing or mixed cellularity-type subtypes are the most frequently seen in lymph nodes. Immunohistochemical studies for CD15, CD30, CD45 (LCA), and PAX-5 are the most helpful. The differential diagnosis includes LCH and other non-Hodgkin's lymphomas.

Other Lesions: Several other hematologic entities can involve the skeleton usually, secondarily. Entities such as systemic mastocytosis or sinus histiocytosis with massive

lymphadenopathy can occasionally show involvement of the bone as the first presentation. The features of most of these in bone are similar to the soft tissue counterparts.

Langerhans Cell Histiocytosis

LCH is a proliferation of cells showing differentiation toward activated Langerhans cells and are related to histiocytes. Terms such as Histiocytosis X, Eosinophilic granuloma, Letterer-Siewe, and Hand-Schuller-Christian disease have in the past been used for some of these proliferations depending on the clinical presentation and extent of involvment.

The cells bear ultrastructural resemblance to Langerhans cells of the skin, and have the characteristic "Birbeck" granules. Immunohistochemically, they express S-100 protein and CD1a. LCH is generally considered to be a neoplasm because it is clonal, although in prior years, it had been considered to be a reactive condition.

The disease can affect several organ systems in addition to bone, and a staging system for the entity has been developed by the several workers and the histiocytosis society (44).

The disease is more common in the first three decades of life, although no age is completely exempt. Pain and swelling are the most frequent presentations for patients with disease limited to osseous involvement. In systemic disease, a variety of symptoms can occur depending on the organ involved including diabetes insipidus, exophthalmos, skin lesions, and mastoiditis. However, solitary skeletal involvement outnumbers visceral involvement by a factor of at least 2 to 1, and is the most frequent site. Almost any bone and any location within the bone can be involved. Involvement of the small bones of the hands and feet, however, is less common. Radiologically, the lesions are lytic, geographic and may occasionally show bony expansion. The gross appearance is nonspecific. Microscopically, the lesions comprise of a proliferation of histiocytoid cells, with variable amounts of cytoplasm (Fig. 43). The cell borders may be well defined or syncitium-like. The nuclei have characteristic "grooves" and may be reniform or coffee bean-like. Multinucleated giant cells may be present. A variable number of mitotic figures may be seen. There is frequently an accompanying inflammatory response, often rich in eosionphils. Lipid-laden histiocytes are sometimes seen. The proliferative cells show immunohistochemical features of activated Langerhans cells as mentioned above.

Differential Diagnosis: This includes granulomatous inflammation, osteomyelitis, and Hodgkin's disease. Osteomyelitis in particular may be difficult to distinguish from LCH on X-rays as well, and the diagnosis may have to rest on immunohistochemical demonstration of cells positive for S-100 and CD1a in selected cases. Hodgkin's disease would depend on the demonstration of the diagnostic Reed-Sternberg cells and the appropriate immunohistochemical profile using a panel of CD-15, CD-30, epithelial membrane antigen, CD 45 markers.

Management: This depends on the stage. Localized disease in bone often requires local modalities only. Installation of steroids is widely practiced but of uncertain utility. Generalized disease is often treated with some form of chemotherapy. Vinblastine, VP-16 corticosteroids, and so on are often used. Radiotherapy is used in certain locations, such as in weight bearing bones.

Erdheim-Chester Disease

This is a condition of unknown cause but may be related to LCH. Most patients are male, and present either asymptomatically or with weight loss and bone pain.

Radiologically, the characteristic finding is of a bilateral, symmetric sclerosis of the metadiaphyseal regions of the long bones. In some patients, the disease progresses to systemic involvement of deep organs such as the lung or pituitary.

Surgical Pathology: Microscopic exam of the involved tissue showes an infiltration by foamy macrophages and lymphocytes. True Langerhans cells are not seen, but the involvement of bone and pituitary suggests the relationship.

Metastatic Bone Disease

Osseous metastases may occur with a variety of primary tumors, the frequency of each, depends on the age of the patient. For example, in young children, neuroblastoma would be common, whereas in older adults metastatic carcinoma would predominate. The majority of metastases present as multiple lesions and can be identified on X-rays, bone scans, or more sensitively by MR scans.

Tumors Metastasizing to Bone

The incidence of metastatic disease at autopsy is far higher than the clinical incidence. The former may be as high as 70% or even higher in patients dying of carcinoma. In adults, the primary lesions that are most frequently present with metastatic bone disease include breast, lung, prostate, kidney, and thyroid.

The hypothesized mechanism of spread in most malignancies is via the hematogenous route. This includes the arterial as well as the venous system, especially the vertebral venous plexus of Batson. In addition, the location and spread pattern of tumors is probably dependent on a variety of local factors such as adhesion molecules. These include members of the cadherin, immunoglobulin, integrin, selectin, hyluronate receptor, and sialomucin families. For example, certain prostate

carcinoma tumor lines have an affinity for type I collagen owing to this kind of adhesion molecule affinity.

Once the carcinoma has adhered to bone, there are a variety of bone-derived growth factors that may help in carcinoma cell growth. Mitogenic factors such as transforming growth factor-β (TGF-β), insulin-like growth factors I and II may be able to modulate the growth of colorectal, breast, and prostate tumors. Likewise, platelet derived growth factors (PDGFs) are mitogenic for a variety of tumor cell lines (45).

Blastic and Lytic Metastases

Radiologically, tumors may destroy bone (lytic) or cause sclerosis (blastic). Some tumors tend to be always lytic (renal cell carcinoma). In others, blastic or mixed patterns are seen (prostate and breast carcinoma). In yet others a change may be seen after therapy (breast carcinoma).

It is reasonable to hypothesize, that, carcinomas and other metastatic tumors stimulate or secrete a variety of cytokines when in contact with bone. These in turn influence the bone producing and resorbing cells locally. They are thus responsible for the various osteoblastic and osteoclastic effects seen histologically and also reflected on the blastic and lytic lesions seen radiologically as well as the cold and hot scans seen by radioisotope scans.

Such cytokines could include interleukins such as IL-1, IL-6, TGF-β, PDGF, plasminogen activator, and BMPs. Tumors therefore probably act *via stimulation of bone cells* to produce bone formation and resorption. It is unlikely that these effects are by the carcinoma cells primarily, although some such models have been hypothesized (45). In a study, it was found that tumors producing both blastic and lytic metastases produced BMPs; suggesting that other or additional mechanisms are in play (46).

Systemic Effects

Certain tumors can cause large amounts of osteolysis, and may result in generalized osteoporosis, or hypercalcemia. This is probably done by the secretion of humoral factors such as PTH, tumor necrosis factor alpha (TNF-α), vitamin D, cathepsin D, colony-stimulating factors, E-series prostaglandins, IL-1, IL-6.

Clinical Presentation

Adult patients commonly present with pain, swelling, tenderness, or pathologic fracture. The same can occur in children, but many cases are detected in this age group as part of a work-up for a known malignancy. Although any site can be involved, the bones of the axial skeleton and proximal appendicular skeleton are more frequently affected.

Radiologic findings vary. Blastic, lytic, or mixed lesions are possible. The majority of lesions are lytic, especially those from kidney, thyroid, and the gastrointestinal tract. Carcinoma prostate, carcinoid tumors, and medulloblastomas not infrequently produce blastic metastases. Some carcinomas, such as breast, may produce either blastic or lytic lesions. Periosteal reactions are infrequent, the lesions often being geographic and occasionally expansile.

Surgical Pathology: Grossly, it is often impossible to differentiate secondary tumors from primary ones. Some primary tumors tend to be more sharply demarcated (e.g., many lytic tumors), and some tend to be exquisitely vascular (kidney and thyroid tumors), but in many cases no general rules can be made. Carcinomas that are metastatic to bone can vary from hard, bony tumors to soft, fleshy, or friable.

Microscopically, well-differentiated metastatic tumors do not pose a problem. For example, renal cell or thyroid carcinomas can often be diagnosed, and the primary sites identified even without resorting to immunohistochemistry. In other cases, the single undifferentiated epithelial cells may be missed without special stains such as mucicarmine or immunostains for epithelial markers. Spindle cell carcinomas and undifferentiated neoplasms pose a special problem since they mimic sarcomas. Reactive bone formation in such cases may mimic osteosarcoma. It is important also to remember that some sarcomas can be positive for epithelial markers such as cytokeratin – leiomyosarcomas, MFH, epitheloid osteosarcomas, and epitheloid hemangioendotheliomas are some tumors of this type.

Differential Diagnosis: Blastic metastases may mimic osteosarcoma. Sarcomatoid (spindle cell) carcinomas are a particular problem. Immunohistochemistry may be of value in such cases. It should be recalled that renal cell carcinoma and melanoma can often be sarcomatoid and express vimentin. This antibody used alone without additional testing with cytokeratin, epithelial membrane antigen, and S-100 protein may therefore be misleading and suggest a mesenchymal tumor such as a malignant fibrous histiocytoma.

Management: The therapeutic strategy involves attempts to identify the primary site and give appropriate chemotherapy and in certain cases, endocrine therapy. This utilizes imaging methods and biopsies of the primary and metastatic sites. Pain management is important. This can be done via surgical (resection, stabilization, or other) means. Radiation therapy may occasionally be required for this. Pain may also be helped by drugs, patient-controlled analgesia, or percutaneous infusional continuous regional analgesia.

Impending pathologic fractures, especially in weight-bearing bones may need prophylactic stabilization. Local antitumor effects can be improved in certain cases by including antitumor drugs in the methylmethacrylate cement utilized for the surgical stabilization procedure.

Predicting the fracture risk, however, is difficult. Existing guidelines for diaphyseal lesions include a 2.5-cm lesion or over 50% cortical destruction. These guidelines, however, may not be accurate (47). Also, site-specific criteria are needed (e.g., in the spine as opposed to weight-bearing long bones). Current approaches to develop such criteria include computer modeling and the use of engineering principles such as the composite beam theory.

Additional modalities being assessed to decrease the amount of tumor lysis includes the use of bisphosphonates. These substances (especially the third-generation bisphosphonates such as alendronate and risedronate) may limit the amount of bone pain, hypercalcemia, and tendency toward pathologic fracture.

Future modalities may exploit tumor cell properties, ability to grow in bone environment, adhesion to bone matrix, and ability to cause osteolysis.

References

1. Vayego SA, De Conti OJ, Varella-Garcia M. Complex cytogenetic rearrangement in a case of unicameral bone cyst. Cancer Genet Cytogenet 1996; 86:46–49.
2. Struhl S, Edelson C, Pritzker H, et al. Solitary (unicameral) bone cyst. The fallen fragment sign revisited. Skeletal Radiol 1989; 18:261–5.
3. Malawer MM. The diagnosis, treatment and management of unicameral bone cysts by percutaneous aspiration, hemodynamic evaluation and intracavitary methylprednisolone acetate. Orth Surg Update Series Volume Four, Lesson 26, 1986 CPEC, New Jersey.
4 Panoutsakopoulos G, Pandis N, Kyriazoglou I, et al. Recurrent t(16;17)(q22;p13) in aneurysmal bone cysts. Genes Chromosomes Cancer 1999; 26:265–266.
5. Oliveira AM, Perez-Atayde AR, Inwards CY, et al. USP6 and CDH11 oncogenes identify the neoplastic cell in primary aneurysmal bone cysts and are absent in so-called secondary aneurysmal bone cysts. Am J Pathol 2004; 165:1773–1780.
6. Sanerkin NG, Mott MG, Roylance J. An unusual intraosseous lesion with fibroblastic, osteoclastic, osteoblastic, aneurysmal and fibromyxoid elements. “Solid” varient of aneurysmal bone cyst. Cancer 1983; 51:2278–2286.
7. Baruffi MR, Volpon JB, Neto JB, Casartelli C. Osteoid osteomas with chromosome alterations involving 22q. Cancer Genet Cytogenet 2001; 124:127–131.
8. Tuy BE, Obafemi AA, Beebe KS, Patterson FR. Case report: elevated serum Beta human chorionic gonadotropin in a woman with osteosarcoma. Clin Orthop Relat Res 2008 Apr; 466(4):997–1001.
9. Miretti S, Roato I, Taulli R, Ponzetto C, Cilli M, Olivero M, Di Renzo MF, Godio L, Albini A, Buracco P, Ferracini R. A mouse model of pulmonary metastasis from spontaneous osteosarcoma monitored in vivo by Luciferase imaging. PLoS ONE. 2008 Mar 19; 3(3):e1828.
10. Clark JC, Dass CR, Choong PF. A review of clinical and molecular prognostic factors in osteosarcoma. J Cancer Res Clin Oncol. 2008 Mar; 134(3):281–297.
11. Bacci G, Balladelli A, Forni C, Ferrari S, Longhi A, Benassi MS, Briccoli A, Serra M, Picci P. Adjuvant and neo-adjuvant chemotherapy for Ewing’s sarcoma family tumors and osteosarcoma of the extremity: further outcome for patients event-free survivors 5 years from the beginning of treatment. Ann Oncol. 2007 Dec; 18(12):2037–2040.
12. Ellis JH, Siegel CL, Martel W, Weatherbee L, Dorfman HD. Radiologic features of well-differentiated osteosarcoma, 1988. AJR Am J Roentgenol 1988; 151:739–742.
13. Rose PS, Dickey ID, Wenger DE, et al. Periosteal osteosarcoma: long-term outcome and risk of late recurrence. Clin Orthop Relat Res 2006 Dec; 453:314–317.
14. Staals EL, Bacchini P, Bertoni F. High-grade surface osteosarcoma: a review of 25 cases from the Rizzoli Institute. Cancer2008 Apr 1; 112(7):1592–1599.
15. Bordigoni P., Clement L., Turello R, et al. Osteochondroma after pediatric hematopoietic stem cell transplantation: report of eight cases. Bone Marrow Transplant 2002; 29:611–614.
16. Hopyan S, Gokgoz N, Poon R, et-al.. A mutant PTH/PTHrP type I receptor in enchondromatosis. Nat Genet 2002; 30:306–310.
17. Swarts SJ, Neff JR, Hohansson SL et al. Significance of abnormalities of chromosome 5 and 8 in chondroblastoma. Clin Orthop 1998; 189–193.
18. Turcotte RE, Kurt A, Sim FH, Unni KK, McLeod RA. Chondroblastoma. Hum Pathol 1993; 24:944–949.
19. Robinson LH, Unni KK, O’Laughlin S, Beabout JW, Siegal GP. Surface chondromyxoid fibroma of bone. Mod Pathol 1994; 7:10A.
20. Tallini G, Dorfman H, Brys P, et al. Correlation between clinicopathological features and karyotype in 100 cartiliginous and chordoid tumors. A report from the chromosome and morphology (CHAMP) collaborative and study group. J Pathol 2002; 196:194–203.
21. Ayala AG, Jae YR, Raymond AK. Bone tumors in Anderson’s pathology, 10th Edition. Ed. Damjanov I and Linder J. 1996. CV Mosby, St. Louis.
22. Naumann S, Krallman A, Unni K, et al. Translocation der(13;21)(q10;q10) in skeletal and extraskeletal mesenchymal chondrosarcoma. Mod Pathol 2002; 15(5):572–576.
23. Ishida T, Dorfman HD, Bullough PG. Tophaceous pseudogout (Tumoral calcium pyrophosphate dihydrate crystal deposition disease). Hum Pathol 1995; 26(6):587–593.
24. Leerapun T, Hugate RR, Inwards CY, Scully SP, Sim FH. Surgical management of conventional grade I chondrosarcoma of long bones. Clin Orthop Relat Res 2007 Oct; 463:166–172.
25. Papagelopoulos PJ, Galanis EC, Mavrogenis AF, et al. Survivorship analysis in patients with periosteal chondrosarcoma. Clin Orthop Relat Res 2006 Jul; 448:199–207.
26. Goldberg NS, Hebert AA, Esterly NB. Sacral hemangiomas and multiple congenital abnormalities. Arch Dermatol 1986; 122:684–687.
27. Unni KK. Hemangioendothelioma and Hemangiopericytoma *In* Dahlin’s Bone Tumors. Raven-Lippincott, Philadelphia 1996 .
28. Wold LE, Swee RG. Giant cell tumors of the hands and feet. Sem Diag Path 1984; 1:173–184.
29. Enneking WF. Musculoskeletal Tumor Surgery. Churchill Livingstone, New York: 1983, pp. 87–88.
30. Bridge JA, Swarts SJ, Buresh C, et al. Trisomies 8 and 20 characterize a subgroup of benign fibrous lesions arising in both soft-tissue and bone. Am J Pathol 1999; 154:729–733.
31. Rosenberg AE, O’Connell JX, Dickersin GR, Bhan A. Expression of epithelial markers in malignant fibrous histiocytoma of the musculoskeletal system: an immunohistochemical and electron microscopic study. Hum Pathol 1993; 24:284–293.
32. Alman BA. Greel DA. Wolfe HJ. Activating mutations of Gs protein in monostotic fibrous lesions of bone. J Orthop Res 1996 Mar; 14(2):311–315.
33. Campanacci M, Laus M. Osteofibrous dysplasia of the tibia and fibula J. Bone Jt. Surg 1981; 63A:367–275.
34. Sweet DE, Vinh TN, Devaney K. Cortical osteofibrous dysplasia of long bone and its relationship to adamantinoma. A clinicopathologic study of 30 cases. Am J Surg Pathol 1992; 16: 282–290.

35. Dahlin DC, Berton F, Beabot JW, Campanacci M. Fibrocartilaginous mesenchymoma with low-grade malignancy. Skeletal Radiol 1984; 12:263–269.
36. Unni KK. Adamantinoma of long bones: the mystery endures. Adv Anat Pathol 1996; 3(1):16–21.
37. Czerniak B, Rojas-Corona RR, Dorfman H. Morphologic diversity of long bone adamantinoma. The concept of differentiated (regressing) adamantinoma and its relationship to osteofibrous dysplasia. Cancer 1989; 64:2319–2334.
38. Cavazzana AO, Miser JS, Jefferson J, Triche TJ. Experimental evidence for a neural origin of Ewing's sarcoma of bone. Am J Pathol 1987; 127:507–518.
39. Bridge JA, Fidler ME, Neff, JR, et al. Adamantinoma-like Ewing's sarcoma: genomic confirmation, phenotypic drift. Am J Surg Pathol 1999 Feb; 23(2):159–165.
40. Nascimento AG, Unni KK, Pritchard DJ, Cooper KL, Dahlin DC. A clinico-pathologic study of 20 cases of large-cell (atypical) Ewing's sarcoma of bone. Am J Surg Path 1980; 4:29–36.
41. Carney JA. Psammomatous melanotic schwannoma. A distinctive, heritable tumor with special associations, including cardiac myxoma and the Cushing's syndrome. Am J Surg Pathol 1990; 14:206–22.
42. Yamaguchi T, Yamato M, Saotome K. First histologically confirmed case of a classic chordoma arising in a precursor benign notochordal lesion: differential diagnosis of benign and malignant notochordal lesions. Skeletal Radiol 2002; 31:413–418.
43. Vujovic S, Henderson S, Presneau N, Odell E, Jacques T, Tirabosco R, et al. Brachyury, a crucial regulator of notochordal development, is a novel biomarker for chordomas. J Pathol 2006.
44. Komp DM. Concepts in staging and clinical studies for treatment of Langerhans cell histiocytosis. Sem Oncol 1991; 18(1):18–23.
45. Orr FW, Sanchez-Sweatman OH, Kostenuik P, Singh G. Tumor-bone interaction in skeletal metastasis. Clin Orthop 1995; 312:19–33.
46. Khurana JS, Ogino S, Shen T, Parekh H, Scherbel U, Delong W, Feldman MD, Zhang PJ, Wolfe H, Alman BA. Bone Morphogenetic Proteins (BMPs) are expressed by both bone forming and non-bone forming lesions. Arch Pathol Lab Med 2004 Nov; 128(11):1267–1269.
47. Hipp JA, Springfield DS, Hayes WC. Predicting pathologic fracture risk in the management of metastatic bone disease. Clin Orthop 1995; 312:120–135.

Chapter 20
Tumors of Soft Tissue

Paul J. Zhang

Except for the skeleton, the rest of the human body is made of "soft" tissues. However, in a more restrictive way, the term of soft tissue is synonymous to soft connective tissue, most of which is mesenchymal origin. In addition to the skeletal system and the somatic compartments of the body, soft connective tissue also exists in all the visceral organs of the body. Therefore, soft-tissue tumors can also occur in all visceral organs. For practical purpose, the term of soft-tissue tumors is restricted to tumors primarily originating in the soft tissues of the somatic compartments. Because bone is also part of the connective tissue originating from mesenchyme, some tumors of bone and the soft tissues share a similar histology and biology. Thus, differentiating a bone from a soft-tissue origin in these tumors is difficult if not impossible on histologic ground alone because the same tumor can arise independently in either soft tissue or bone and subsequently involve the other. The distinction of primary site in these cases can only be resolved by clinical and radiologic correlation. Nevertheless, many tumors of mesenchymal origin are more prone to arise either in soft tissue or bone and histologic evaluation can help to determine the primary site and extent of the disease with appropriate clinical correlation. The knowledge of soft-tissue tumors can surely benefit the pathologists who frequently deal with bone tumors or tumor-like condition in bone. This chapter is primarily written with this purpose in mind to complement the rest of the contents of the book and not to replace any other major monographs of soft-tissue tumor pathology as bench references for surgical pathologists.

Incidence

As per the recent WHO Classification of Tumors of Soft Tissue, soft-tissue tumors are classified into benign, intermediate, and malignant categories according to their biologic behavior (1). The majority of soft-tissue tumors are benign. The annual incidence of new malignant soft-tissue tumors (sarcomas) is 30 per million which is about 1% of the benign soft-tissue tumors or all malignant tumors of human body (1). Except for those which commonly occur in childhood, the incidence of adult-type soft-tissue sarcomas increases with age. Extremities are the most common site for soft-tissue sarcomas followed by the trunk, retroperitoneum, and the head and neck region.

Prognostic Factors

The most important factors predictive of the biologic behavior of soft-tissue sarcomas are tumor site (location), anatomic extent of sarcoma (size and invasion), and histologic grade. In general, most benign or low-grade soft-tissue tumors are less than 5 cm in size, superficially located, and histologically well differentiated with little histologic deviation from their normal counterparts. Although generally speaking, benign soft-tissue tumors do not supposedly recur locally after excision, in some occasions, they may do so, especially after an incomplete excision (albeit in a significantly lower incidence than that of tumors in intermediate and malignant categories). In these cases, however, these recurrences are generally slow growing and nondestructive. They are amenable to repeat excision. In contrast, tumors of an intermediate category are locally aggressive either without or with rare incidence of metastasis. Compared to intermediate categories, malignant soft-tissue tumors (sarcomas) have significant risk of metastatic potential in addition to local destructive growth and higher risk of recurrence. Sarcomas tend to be larger than 5 cm and located in deep soft-tissue compartments. Sarcomas are graded to predict the probability of distant metastasis and overall survival. The most commonly used grading systems are the National Cancer Institute (NCI) system and the Fédération Nationale des Centres de Lutte Contre le Cancer (FNCLCC) system. Sarcomas are graded to low, intermediate, and high grade according to the semiquantitative assessment of mitotic count, tumor necrosis, and various histologic features (differentiation in FNCLCC or histologic type, cellularity, and pleomorphism in NCI system) (2, 3).

J.S. Khurana (ed.), *Bone Pathology*, DOI 10.1007/978-1-59745-347-9_20,

Soft-tissue sarcomas can be staged based on both histological and clinical information using the system developed by International Union Against Cancer (UICC) and the American Joint Committee on Cancer (AJCC) or by the Musculoskeletal Tumor Society (Enneking) system as described in the chapter on Bone tumors. The UICC/AJCC or TNM staging systems incorporate histological grade, tumor size, depth, regional lymph node status, and distant metastasis (4, 5).

Diagnosis

As for bone tumors, radiographic and imaging studies have played significant role in the diagnosis and staging of soft-tissue tumors. Magnetic resonance imaging (MRI) is superior to other choices of imaging studies in evaluating soft-tissue tumors due to its ability to distinguish tumor tissue details and its relationship to adjacent tissues and organs. In addition, it can be used to guide biopsy, plan surgery, monitor response to therapy, and tumor local recurrence. However, definitive diagnosis of soft-tissue sarcoma can only be achieved by histiologic evaluation of the tumor tissue which can be obtained by the fine needle aspiration (FNA), needle core biopsy, incisional biopsy, and excisional biopsy. In addition to histologic evaluation, biopsy procedures also provide tissue for other ancillary tests such as electron microscopy (EM), flowcytometry, cytogenetics, and variety of molecular tests in soft-tissue sarcomas. All these biopsy methods have their own advantages and disadvantages. While incisional biopsy has been remained as standard approach to obtain adequate tissue specimen in sarcoma for histologic diagnosis before more definitive therapeutic intervention, the minimally invasive procedures such as FNA and needle core biopsy have been increasingly used in the last two decades in diagnosis of soft-tissue tumors. These minimally invasive procedures are easily performed in the physician's office with quick turnaround time, and well tolerated and received by patients. These can be used as a part of initial work-up, or as a mean to obtain more definitive diagnosis for guiding further patient management. However, their utility has been hampered by the concern of sampling adequacy in a large soft-tissue tumor. In addition, the ability of pathologist to evaluate the pathology is heavily dependent upon the quality and adequacy of tissue samples which are more difficult to control in these minimally invasive procedures than those of incisional and excisional ones. Multiple passes of the needle in different areas of the tumor has been performed to improve tissue sampling in FNA and needle core biopsy. When they are well performed, the tissue specimen from these minimally invasive procedures can usually provide initial sufficient assessment of the tumor as if it is mesenchymal, hematopoietic, or epithelial in nature. However, pathologists and clinicians should be aware of the difficulty in clearly classifying and grading the tumor in these small specimens. The pathologic findings in these small specimens should only be accepted as a minimal pathologic condition and it should always be kept in mind that more severe condition cannot be ruled out.

Although an excisional biopsy may provide adequate tissue, it is not a recommended procedure. It is typically a one-step procedure for diagnostic as well as therapeutic purposes and yields almost the entire tumor for adequate tissue sampling. The downside of excisional biopsy is lack of any histologic assessment of the lesion before excision or resection of the tumor. Because of this, the tumor is often not excised widely enough or not properly handled surgically. Unnecessary manipulation of the tumor tissue in vivo could potentially contaminate the surgical field which makes further clean-up surgery more difficult and eventually failure of local control of the disease.

Compared to FNA and needle core biopsy, the incisional biopsy is more invasive, but provides a more generous sample for histiologic and other ancillary tests. The accuracy of diagnosis based on an incisional biopsy may still be affected by the sampling issue as discussed above, but it is a superior method to obtain adequate tissue for diagnosis before major surgery. Since a more definitive therapeutic procedure will follow, the small contaminated areas (such as the biopsy site and scar) are included in the surgical approach during the therapeutic excision.

The advantages, disadvantages, and limitations of these diagnostic procedures as they relate to soft-tissue sarcomas are found in Table 1. The choice of the biopsy procedure should be dependent upon the experience of the physician with these techniques, their availability, the purpose of the biopsy, and patient acceptance of the procedure (6).

Other Ancillary Tests and Special Procedures

In addition to conventional histologic evaluation, many ancillary studies using different technologies can be useful in the diagnosis and prognosis of sarcomas in the laboratory of surgical pathology.

Flow cytometry: A Technology Used to Evaluate Tumor Surface Marker Expression and DNA Ploidy

Flow cytometry requires fresh tissue specimen although paraffin embedded tissue can also be used as a less than optimal option. It has been widely used in the diagnosis and classification of hematopoietic neoplasms and in the prognosis of certain epithelial tumors. However, in soft-tissue sarcoma, flow cytometry has no role in diagnosis, so far, and, except for some pediatric sarcomas, little utility in the prognosis of sarcomas.

Table 1 Comparison of various methods of tissue sampling in diagnosis of soft tissue tumors

Method	FNA	Core-needle	Incisional	Excisional
Invasiveness	Minimal	Minimal	Small	Significant
Sampling	Worse	Worst	Good	Best
Evaluation format	Cytology	Histology	Histology	Histology
Accuracy for definitive Diagnosis	No Minimal condition	Yes for HG No for LG	Acceptable	Reliable
Biopsy site contamination	No	Minimal	Small (bx tract)	Significant
Main advantages	Minimally invasive, well tolerated, quick turnaround time, virtually no complication, good for initial screen evaluation	Minimally invasive method for histologic evaluation, neglectable side effect, good for initial screen evaluation	Recommended for pretreatment diagnosis followed by surgery	Superior tissue sampling for histologic evaluation and grading
Main disadvantages	Lack of histology evaluation and difficult to reach definitive diagnosis	Poor sampling in sizable mass precludes accurate grading	Small possibility of sampling error and tumor being undergraded	Adverse effect on achieving local controls, potential local extensive tumor spread
Tissue for other studies	Minimal	Minimal	Yes	Yes

Ultrastructural Analysis: Visualization of Various Cellular Elements Under Electron Microscope to Determine Tumor Cell Lineage

Fresh tissue fixed in 4% glutaraldehyde is required for electron microscopy in order to achieve optimal tissue preservation for ultrastructural analysis. EM is labor intensive and a costly test. The role of electron microscopy in classifying cell lineage in diagnosis of tumors has been largely replaced by the more easily accessible and cost-effective immunohistochemistry in the last two decades. Because of the high magnification used in EM there is a disadvantage in having limited tissue sampling. Thus, fewer electron microscopic examinations are now performed. Inevitably, the experience of many pathologists in ultrastructural analysis is limited nowadays and the report of the study tends to be nondefinitive and add little value in the diagnosis in many cases. However, in the diagnosis of sarcomas, electron microscopy still remains relatively effective in differentiating fibroblast from myofibroblast, sarcoma from a sarcomatoid carcinoma, and in identifying neural/nerve sheath cell in the hands of an experienced diagnostic electron microscopist. In fact, many believe that ultrastructural evaluation is the only reliable way to definitively distinguish a fibroblast from a myofibroblast.

Immunohistochemistry (IHC): Tissue Staining Process Utilizing Immunologic Principle to Visualize Cellular Protein or Peptide Product (Tumor Marker) on Tissue Section

IHC can be performed on routinely fixed, paraffin-embedded tissue section. Because of the use of various antigen retrieval techniques, more and more antigens or tumor markers become detectable by IHC on paraffin section. Technically, the procedure is relatively simple and can be performed in many surgical pathology laboratories. It has become the most commonly used ancillary test by surgical pathologist in their routine practice and plays a significant role in their diagnostic accuracy. However, it must be remembered that many of these immunomarkers or antibodies are only specific for the peptides related to cell lineage differentiation but not really specific for the tumors per se. Therefore, immunohistochemical study cannot replace the morphologic evaluation in tumor diagnosis. It should always be used to confirm or exclude a diagnosis which has been suspected on morphologic evaluation. A tumor diagnosis should never be made solely based on immunohistochemical findings without morphologic correlation. Immunohistochemical findings should always be interpreted with great caution when the results are pointing at the opposite direction of one's morphologic impression.

The main application in soft-tissue sarcoma pathology is to detect tumor markers specifically related to certain mesenchymal phenotypes which might not be otherwise obvious based on the histologic appearance of the tumor, therefore to improve the ability and consistency of the pathologist to classify sarcomas. In addition, IHC detection of various cell proliferation markers, oncoproteins, and tumor suppressive proteins are also commonly used in research and some of these markers have been shown to have potential grading and prognostic implication in sarcomas. Table 2 is a list of tumor markers commonly used for diagnostic and potentially prognostic purpose.

Cytogenetic and Molecular Diagnostic Tests

Please see chapter 5 where these are discussed in detail.

Table 2 Summary of immunostains according to histogenic lineage and their potential utility

Category	Tumor marker	Utility
Nonspecific mesenchymal	Vimentin	Limited
Epithelial	Cytokeratin, EMA	Synovial sarcoma, epithelioid sarcoma, sarcomatoid carcinoma
Mesothelial	Calretinin, D240, CK5, WT-1	Mesothelioma
Endothelial	CD31, CD34, Factor VIII, D240, WT-1, Fli-1	Angiosarcoma, hemangioma, lymphangioma, hemangioendothelioma
Myogenic	Muscle actin, desmin, myoglobin, myogenin, myoD	Leiomyosarcoma, rhabdomyosarcoma, rhabdoid tumor
Chondroid	S100, GFAP, D2-40	Chondrosarcoma, chondroma
Lipogenic	S100	Liposarcoma
GI stromal	CD34, c-kit	GIST
Osteogenic	Osteocalcin, osteonectin	Osteosarcoma
Neural and nerve sheath	S100, NF, NSE, GFAP synaptophysin, Mic2	Nerve sheath tumor, neuroendocrine tumor, PNET/EWS
Histiocytic	MITF, CD68, S100, CD1a	Giant cell tumor, Langerhan cell tumor, true histiocytic tumor
Dermal dendritic fibroblast	CD34, F13a, D2-40	Dermatofibroma, SFT, DFSP
Myofibroblast	Actin, calponin, Alk	Myofibroblastic tumor
Hematopoietic	LCA, myeperoxidase, CD20, CD3, other CDs	Lymphoma, leukemia
Reticulum dendritic cell	CD35, CD21, S100, CD68	Reticulum dendritic cell sarcoma
Melanocytic	S100, HMB45, Melan-A, MITF, MAGE-1	Melanoma, angiomyolipoma (PEComa)
Germ cell	c-kit, D240, PLAP, MAGE1	Germ cell tumor
Oncoprotein and tumor suppressor	P53, Ras, c-myc, BCL2, β-catenin, WT-1, NF1, RB, cyclin D1, IN1, Her2, Alk	Potential prognostic implication
Proliferation	PNCA, Ki67	Potential grading implication

Treatment

Except for certain pediatric sarcomas, surgery remains as the choice of therapy for majority of soft-tissue sarcomas. Similar to the treatment for bone sarcomas, amputation is now only used for a minority of advanced and mostly complicated tumors since the introduction of limb-sparing surgery in the late 1960s. Wide excision of tumor with 1–2 cm margin clearance is usually sufficient for low grade, smaller than 5 cm, superficial, and/or intramuscular sarcomas. The local control of the disease and disease-free survival heavily depend upon the width of margins of excision. The frequency of local recurrence is around 10% after amputation, 15–40% following wide excision and 65–70% after marginal or incomplete excision. For larger or deeper tumors excised with close margin of tumor clearance, postoperative adjuvant radiotherapy can be added to reduce local recurrence and prolong recurrence-free survival time. Preoperative neoadjuvant radiotherapy is used especially for large (usually >15 cm) and initially unresectable tumors which might become resectable after high dose of radiotherapy. Chemotherapy plays a major role in the treatment of pediatric round cell sarcomas; however, its role is still controversial in adult sarcomas and currently remains investigational.

Soft-Tissue Tumors with Histologic Features Similar to that of Tumors of Bone and Cartilage

This section discusses soft-tissue tumors that have a major histological similarity to osseous tumors. Very focal or minor component of reactive or metaplastic bone or cartilaginous differentiation can be seen in a variety of otherwise typical soft-tissue tumors. These minor components have no impact in the prognosis nor the diagnosis of the tumor. Hence, soft-tissue tumors with only a minor/metaplastic metaplastic osteogenic or chondroblastic differentiation are not included in this category of soft-tissue tumors.

Soft-Tissue Chondroma (Chondroma of Soft Part, Extraskeletal Chondroma)

Soft-tissue chondroma is a benign soft-tissue tumor with histologic differentiation toward adult-type hyaline cartilage similar to that of enchondroma in bone. The overwhelming majority of soft-tissue chondromas occur in the fingers, hands, and feet, most frequently in adults of 40s–60s years old (7). Rarely, tumors have been reported in other sites such

as head and neck, skin, and dura (8, 9). Most tumors present as a solitary lesion involving tendons of the intraarticular synovium or periosteum. Radiographically, they are well-demarcated, lobulated lesions with central and peripheral calcification (10).

Histopathology

Similar to enchondroma, soft-tissue chondromas are made of mature, lobulated hyaline cartilage with variable cellularity, mild nuclear atypia, binucleation, ossification, calcification, and occasionally some myxoid matrix (11). Immunohistochemically, the tumor cells are positive for S100 and GFAP.

Differential Diagnosis

The diagnosis of soft-tissue chondroma is usually not difficult with classic radiographic and histologic presentations. In some cases the lesion may need to be differentiated from calcifying aponeurotic fibroma, giant cell tumor of tendon sheath, subungual osteochondroma, periosteal chondroma, synovial chondromatosis, well-differentiated chondrosarcoma, chordoma, and extraskeletal chondrosarcoma.

Treatment and Prognosis

Conservative local excision is recommended to preserve the function of the digit, hand, or foot. Although 15–20% of lesions locally recur, re-excision is usually curative (7). Malignant transformation has not been described in soft-tissue chondroma.

Fibromatoses

Fibromatoses are conditions of uniform fibroblastic proliferations in soft tissue similar to those seen in desmoplastic fibroma of the bone. The lesions are divided into superficial and deep types and the clinical behavior of the lesion is dependent upon anatomic location.

Superficial Fibromatoses

This group of fibromatoses arises in superficial fascia or aponeuroses of the hand (palmar fibromatosis, Dupuytren disease) and foot (plantar fibromatosis, Ledderhose disease) and knuckle pads soft tissue. The lesions initially occur as painless firm nodule in palmar and plantar aspects of the hands and feet and later become cord-like indurations which can lead to flexion contractures in some cases. About 50% of cases are bilateral, and up to 20% of patients with palmar fibromatosis have concurrent plantar lesion (12, 13). Many patients have a significant family history of similar disease suggestive of a hereditary condition. Some patients also have concurrent epilepsy, diabetes, cirrhosis, or alcoholism (14).

Deep Fibromatoses (Desmoid Tumor, Intraabdominal and Extraabdominal Fibromatoses)

Deep fibromatoses may occur in intraabdominal sites (or abdominal wall) in middle-aged female patients (abdominal fibromatosis) and extraabdominal sites in younger age (extraabdominal fibromatosis). Shoulder is the most commonly extraabdominal site followed by chest wall and thigh. Mesenteric fibromatosis can be seen in patients with Gardner's syndrome (familial polyposis associated with mesenteric fibromatosis). In around 50% of intraabdominal fibromatoses, patients have history of recent pregnancy and prior abdominal surgery. Regardless of the site, deep fibromatoses are slow growing, poorly defined, firm masses which are initially asymptomatic and later present with signs symptoms due to involvement of adjacent anatomic structures and organs by the disease (15). Because of the deep location, and initial asymptomatic presentation, the lesions are usually larger than superficial fibromatoses at the time of surgery.

Histopathology

The histologic hallmark of fibromatoses is a proliferation of bland and uniform fibroblastic-type stromal cells. These cells are typically spindle or fusiform in shape with normochromatic nuclei, very small or no nucleoli and a poorly defined, fibrillary eosinophilic cytoplasm which merges with a very characteristic wavy collagenous stromal matrix (Fig. 1). The lesional cell nuclei and the fibrillary collagenous matrix are typically arranged in fascicles or bundles mimicking those seen in normal tendon, ligament, or fascia (Fig. 2). The cellularity and the amount of collagenous matrix varies from case to case. In a more proliferative or younger stage, some lesions can become alarming hypercellular with a few mitotic figures. There is less collagenous matrix which tends to be more myxoid. Older lesions are less cellular with more collagenous matrix and hyaline change (Fig. 3). More often, the growth phase of fibroblastic proliferation can vary from areas to areas in a given lesion. The lesional cells can also show a variable degree of myofibroblastic differentiation which is usually correlated to the

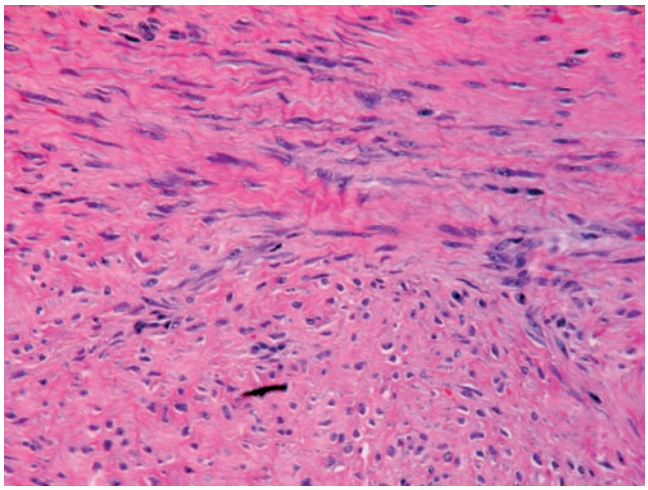

Fig. 1 Bland spindle fibroblastic-type cells with fibrillary eosinophilic cytoplasm which merges with a very characteristic wavy collagenous fibers in desmoid tumor

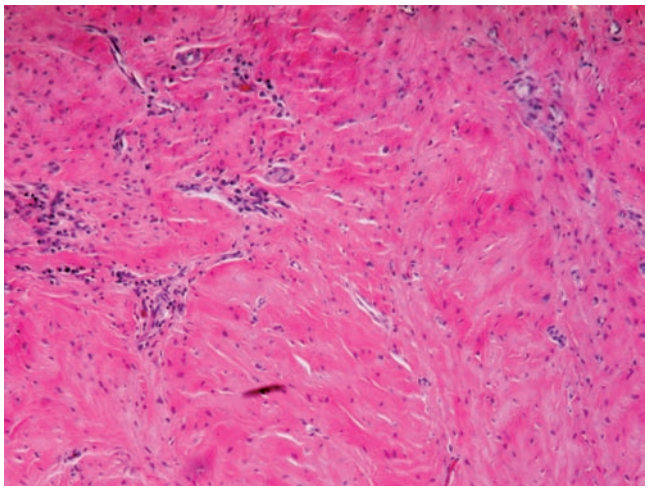

Fig. 2 Dense collagenous matrix in a case of desmoid tumor. The collagen is arranged in fascicles or bundles mimicking those seen in normal tendon, ligament, or fascia

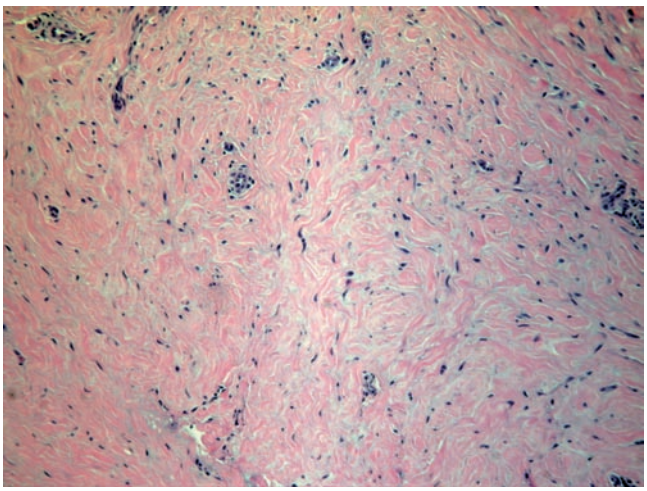

Fig. 3 A older lesion of desmoid tumor. It shows less cellular and more collagenous matrix and hyaline change

in a case of desmoid tumor. The collagen is amount of SMA immunostaining and rare desmin reactivity in some cases. In addition, abnormal nuclear accumulation of β-catenin can be detected immunohistochemically in the lesional cells of deep fibromatosis but not superficial fibromatoses due to either APC inactivating mutation or activating β-catenin mutations in these lesions (16).

The histologic differences between deep and superficial fibromatoses are only apparent under low power magnification. The deep fibromatoses are usually sizable, poorly circumscribed mass. Slender irregular projections of bland fibroblastic-type cells are frequently seen arising at the periphery of the lesion inserting into the adjacent normal tissue and organ. The degree of the infiltration into surrounding tissue is often underestimated surgically and grossly or even microscopically when the infiltrative portion of lesion is well organized and hypocellular and arranged along the preexisting fascia plan and tissue septae mimicking normal histologic landmarks or scar.

Superficial fibromatoses are usually smaller in size (<2.0 cm) and relatively less infiltrative and local destruction of adjacent neurovascular bundles and bony structures is minimal.

Differential Diagnoses

Differential diagnosis between deep and superficial fibromatoses is usually not difficult with proper clinical knowledge of the anatomic location of the lesion and adequate low power histologic evaluation. Fibromatoses need to be differentiated from various reactive fibroblastic/myofibroblastic lesions such as scar, fibrosis, and nodular fasciitis, and various low-grade spindle cell tumors such as cellular myxoma and neurofibroma and spindle cell sarcoma such as fibrosarcoma. It has been suggested that immunohistochemical detection of nuclear β-catenin expression can be used to differentiate desmoid tumor from superficial fibromatosis or reactive fibroblastic changes such as scar.

Treatment and Prognosis

Local excision is the treatment of choices. The status of the surgical margin is the key for adequate local control of the disease. Superficial fibromatoses are considered benign but have a risk of local recurrence after inadequate excision. However, the recurrence is usually small and easily re-excised with little local destruction (17). Because of the larger size and deep location, it is difficult to achieve complete excision with clear surgical margins in deep fibromatoses. The incidence of local recurrence in deep fibromatoses has ranged from 25% to 80% (18). Deep fibromatoses are

currently categorized in the intermediate group between benign tumor and sarcoma with no metastatic potential in the current issue of WHO Classification of Tumors of Soft Tissue and Bone (1). Radiation has been used in some recurrent cases in an attempt to improve local control but its effectiveness is still controversial.

Giant Cell Tumor of Soft Part

Giant cell tumors of soft parts is a rare primary soft-tissue tumors and frequently presents as painless masses in superficial soft tissue of the extremities in adult patients (19).

Histopathology

The histologic appearances and immunohistochemical characteristics of giant cell tumor of soft parts are similar to that of giant cell tumors of bone. Metaplastic ossification and blood-filled cystic spaces like those seen in aneurysmal bone cysts are commonly seen (Fig. 4) (19).

Differential Diagnosis

Differential diagnosis between giant cell tumor of soft part and giant cell tumors of bone is solely based on anatomic location of the tumors. In addition, giant cell tumors of soft part need to be differentiated from various osteoclast-like giant cell-rich tumors such as giant cell tumors of tendon sheath, giant cell fibroblastoma, and giant cell-rich malignant fibrous histiocytoma.

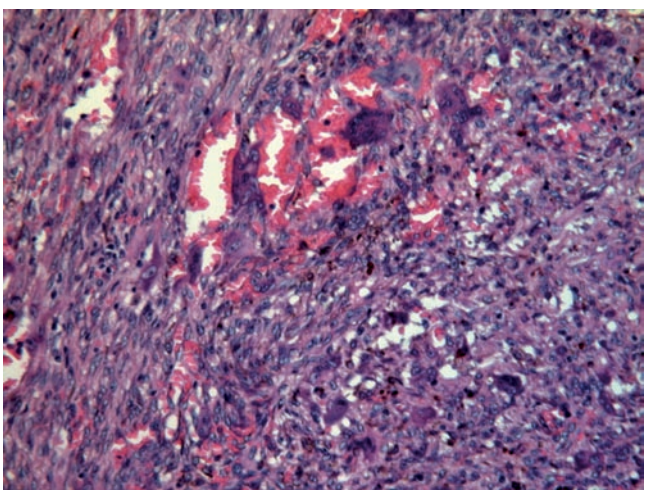

Fig. 4 Giant cell tumor of soft part with blood-filled microcytic areas.

Treatment and Prognosis

Surgical excision is treatment of choice. Local recurrence rate is around 10% frequently following incomplete surgical excision. The tumors are categorized in the intermediate group with rare incidence of metastasis in current WHO Classification of Tumors of Soft Tissue and Bone (1). Similar to giant cell tumors of bone, no clinicopathological factors can be used to predict the biologic behavior of the tumors (19).

Extraskeletal Osteosarcoma

Extraskeletal osteosarcoma is a rare soft-tissue sarcoma that is significantly less frequently seen than its osseous counterpart. Unlike osseous conventional osteosarcoma, it typically occurs in older patients in their fifth decade of life. The tumors frequently arise in the deep soft tissues. The most common site is the thigh, followed by buttock, shoulder, trunk, and retroperitoneum. Some cases have been associated with previous radiation, Thorotrast administration, and trauma. Typically, it presents as a deep-seated soft-tissue mass, painful in one-third of cases. CT and MRI usually reveal variable mineralization within the mass (20).

Histopathology

Various histologic subtypes of osteosarcoma described in bone can be seen in extraskeletal osteosarcoma. Osteoblastic variant is the most common type followed by fibroblastic, chondroid, telangiectatic, small cell, and well-differentiated variants. Neoplastic bone formation is most prominent in the center of the tumor with the peripheral areas being more cellular. Except osteoblastic, chondroblastic, and fibroblastic differentiations, no other lineages of histologic differentiation should be detectable in extraskeletal osteosarcomas.

Differential Diagnosis

Metaplastic ossification ranging from osteoid to woven bone formation can be seen in synovial sarcoma, epithelioid sarcoma, liposarcoma, and carcinosarcoma. Osteogenic differentiation can also be seen as a phenomenon of dedifferentiation in various soft-tissue sarcomas. In the above tumors, other histogenic lineages or histologic characteristics of original tumors are usually present.

Treatment and Prognosis

Extraskeletal osteosarcoma is a high-grade soft-tissue sarcoma. Up to 75% of patients die of disease within 5 years

despite radical surgery and adjuvant therapy. Factors associated with better prognosis are small size (<5 cm), fibroblastic, and chondroblastic subtype and low proliferation index (20, 21).

Extraskeletal Mesenchymal Chondrosarcoma

Although more often seen as a bone tumor, this high-grade sarcoma can occasionally occur in the soft tissues. There is bimodal age distribution associated with anatomic location. Patients around 25 years old tend to develop head and neck lesion while patients in their 40s tend to develop the tumor in the deep musculature of the body and extremities (21).

Histopathology

The histopathology of extraskeletal mesenchymal chondrosarcoma is virtually identical to those arising in bone. See Chapter *Bone Tumors*.

Extraskeletal Ewing's Sarcoma (EWS)/Primitive Neuroectodermal Tumors (PNET)

EWS and PNET are a group of round cell sarcomas sharing similar histologic features, immunohistochemical profiles, tissue culture properties, and chromosomal aberrations. Similar to their counterparts in bone, extraskeletal EWS/PNET primarily occur in adolescents and young adults. The tumor usually presents as painful and rapid growing mass in paravertebral regions, chest wall, retroperitoneum, and lower extremities (21).

Histopathology

Theoretically, EWS and PNET can be differentiated from each other by absence (EWS) or presence (PNET) of neuroectodermal differentiation at histological, immunohistochemical, and ultrastructural levels. The histologic appearance of the tumor is typical small round cell morphology similar to that of those arising in bone (Fig. 5). Rossette formation is seen in PNET as evidence of neuroectodermal differentiation. Immunohistochemically, the tumor is strongly positive for MIC2 (CD99) and Fli-1. Immunoreactivity with various neural markers such as NSE, synaptophysin, or S100 might be seen in some PNET cases. Strong MIC2 and Fli-1 immunoreactivity is characteristic but not specific for EWS/PNET.

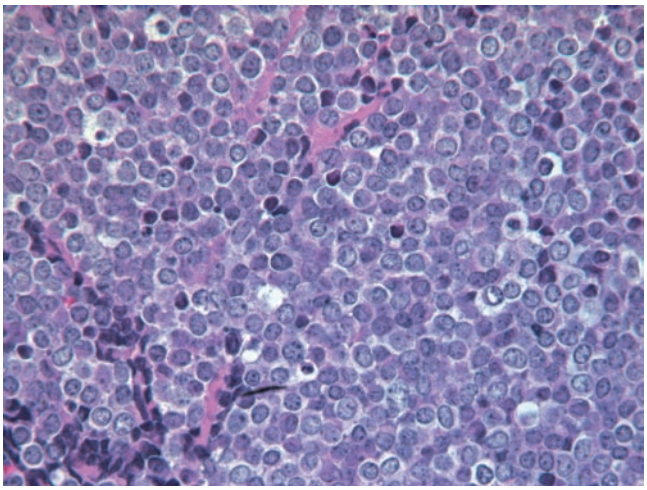

Fig. 5 Sheet of monotonous primitive round cells with fine nuclear chromatin and little cytoplasm in EWS

Differential Diagnosis

A long list of tumors with round cell features, many of which can exhibit MIC2 positivity, can be potentially confused with EWS/PNET. These include other sarcomas with round cell morphology such as rhabdomyosarcoma; desmoplastic small round cell tumor; round cell liposarcoma; mesenchymal chondrosarcoma; neuroblastoma; poorly differentiated synovial sarcoma; carcinoma with neuroendocrine differentiation such as small cell carcinoma, neuroendocrine carcinoma, and Merkel cell carcinoma; and hematopoietic neoplasms such as lymphoma and chloroma.

Treatment and Prognosis

Treatment and prognosis are similar to EWS of bone. Tumors commonly metastasize to lung and bone. Postchemotherapy tumor necrosis is an important prognostic factor.

Soft-Tissue Tumors with Chondro-Osseous Differentiation

This group of soft-tissue tumors shows a certain degree of chondro-osseous differentiation, but they do not mimic any bone tumors. Rarely focal chondroid or osseous differentiation can be seen in various otherwise typical benign and malignant soft-tissue tumors. When these features are present, histologic distinction between metaplastic (benign) and neoplastic (malignant) is important. When these components are identified as benign and metaplastic, they bear no diagnostic as well as prognostic significance and the tumors can

be diagnosed as chondroid or ossifying variants of the original tumors such as chondroid or ossifying lipoma. However, if chondroid and osseous elements are identified as neoplastic (either histologically low or high grade), they are considered as phenomenon of dedifferentiation, in many cases, a sign of tumor progression of the original soft-tissue tumor such as dedifferentiated liposarcoma.

Ossifying Fibromyxoid Tumor

Ossifying fibromyxoid tumor is a rare soft-tissue tumor of uncertain lineage (peripheral nerve origin has been suggested by some becaue of its S100 reactivity) (22). It affects adults in their 50s. Majority (70%) of the cases occur in the lower extremities followed by trunk (20%) and head and neck (10%). The tumors frequently attach to underlying tendons and deep fascia. An origin from a nerve has not been documented. It usually presents as slow-growing, painless subcutaneous mass. Calcifications within or around a well-circumscribed mass can be seen on Rontgenograms in some cases (22).

Histopathology

The tumor is multilobulated and well circumscribed (Fig. 6). Tumor cells are monotonously round or oval with scant eosinophilic cytoplasm. They form cords, nests, and trabeculae in a fibromyxoid matrix (Fig. 7). Characteristic ossification, usually in the form of lamellar bone, can be seen as a partial shell of the tumor or within the tumor in 70% of the cases. However, this histologic hallmark might not be present in some cases (nonossifying variant). The fibromyxoid stroma in both ossifying and nonossifying variants can be extremely myxoid or fibrous in different cases. Hypercellularity and increased mitotic count (>8/10 high power fields (hpf)) have been seen in cases described as "atypical" or "malignant." Immunohistochemically, many ossifying fibromyxoid tumors are positive for S100 and desmin (22).

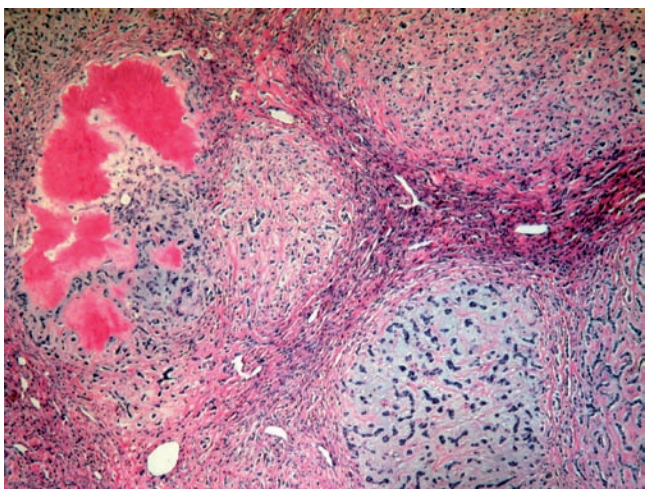

Fig. 6 The multilobulated and well-circumscribed growth pattern in ossifying fibromyxoid tumor with ossification

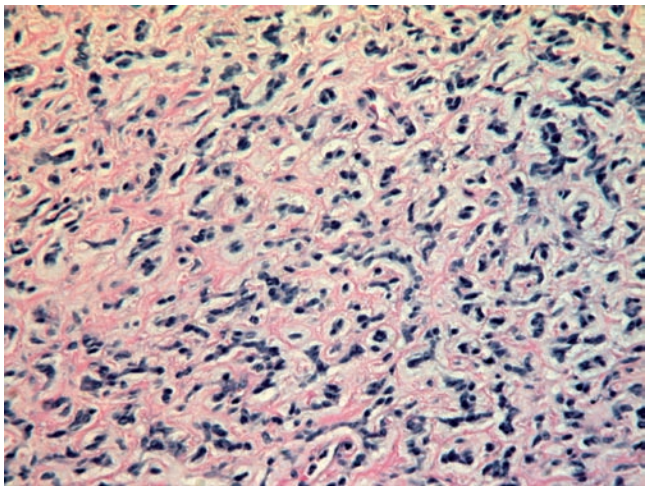

Fig. 7 Monotonous round and oval tumor cells with scant eosinophilic cytoplasm forming cords, nests, and trabeculae in fibromyxoid matrix in a case of ossifying fibromyxoid tumor.

Differential Diagnosis

Tumors with fibromyxoid features and S100 reactivity such as parachordoma, chordoma, chondroid or ossifying lipoma, myxoid liposarcoma, neurofibroma, and pleomorphic adenoma (mixed tumor) are on the list of differential diagnosis for ossifying fibromyxoid tumor.

Treatment and Prognosis

Surgical resection is the treatment of choice. The tumor is classified in the intermediate group of the recent WHO Classification of Soft Tissue Tumors. It has propensity (30%) for local recurrences but metastases are extremely rare. No histologic factors can predict the metastatic potential. "Atypical" or "malignant" histology have been seen in some tumors with recurrences (22).

Extraskeletal Myxoid Chondrosarcoma (Chordoid Sarcoma)

Typically a slow growing, deep-seated soft-tissue sarcoma occurs in musculature of adults in their 50s and 60s. Lower extremities and their limb girdles are involved in 70% of cases followed by the trunk and upper extremities and their girdles (23).

Histopathology

Extraskeletal myxoid chondrosarcoma is a well-defined, multilobulated, myxoid (gelatinous) mass divided by fibrous septa (Fig. 8). The tumor cells are polygonal and oval with eosinophilic cytoplasm, and form clusters, cords, irregular trabeculae, and cribiform nests in myxoid matrix (Fig. 9). Despite the name, there is no hyaline cartilage formation and as typically seen in chondrosarcoma of bone. Some tumors are hypercellular with very scant myxoid matrix. Mitotic activity is usually low in well-differentiated tumors and increased in cellular types as well as in the epithelioid/anaplastic variants. Focal S100, cytokeratin, EMA, synaptophysin, and NSE can be seen in some cases (23, 24).

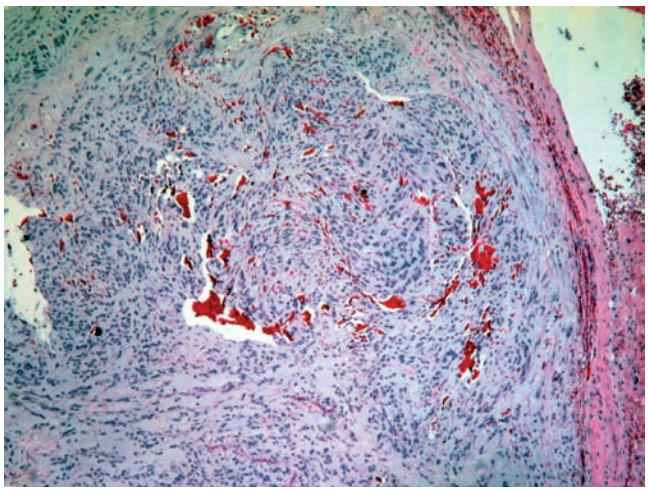

Fig. 8 The well-defined, multilobulated pattern of growth with myxoid (gelatinous) matrix divided by fibrous septa in extraskeletal myxoid chondrosarcoma

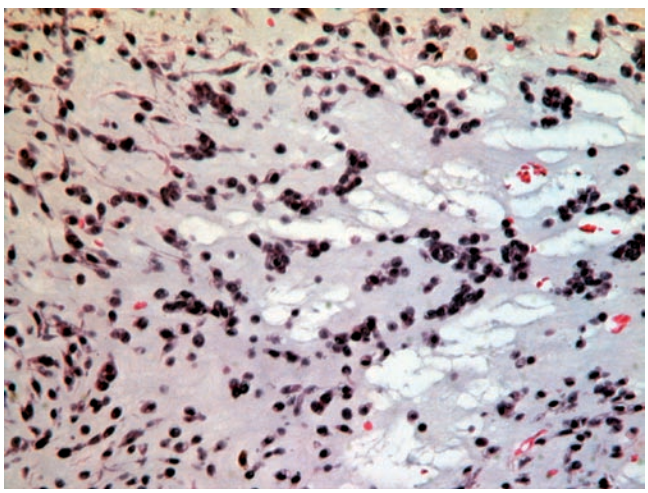

Fig. 9 The polygonal and oval tumor cells with eosinophilic cytoplasm in clusters, cords, irregular trabeculae, and cribiform nests in myxoid matrix in myxoid chondrosarcoma

Differential Diagnoses

Tumors with myxoid and/or chondroid features such as myxoma, parachordoma, chordoma, chondromyxoid fibroma, chondroid lipoma, myxoid liposarcoma, and pleomorphic adenoma (mixed tumor) need to be differentiated from extraskeletal myxoid chrondrosarcoma.

Treatment and Prognosis

Surgical resection is the treatment of choice. The patients have a high potential for local recurrence (50% at 10 years). Early metastasis is found at the time of diagnosis in 40% of cases. The most common site for metastasis is lung. However, patients can survive 5–15 years even after developed lung metastasis. Overall, 5-, 10-, and 15-year survivals are about 90, 70, and 60%, respectively (23). Tumor size greater than 10 cm, hypercellularity, high mitotic rate, and anaplastic features have been suggested to be adverse prognostic factors (24).

Tumors Derived from Cellular Elements Existing in Both Bone and Soft Tissue

Both intraosseous and extraosseous soft tissue contains vascular, adipose, smooth muscle, and peripheral nerve tissues. Tumors derived from these tissues can arise in either bone or soft tissue. However, except for vascular tumors, tumors of lipogenic tissue, peripheral nerve, and myogenic differentiation are comparatively rare in bones. Only vascular tumors will be discussed here and the other aforementioned tumors will be discussed in the section of tumors primarily arising in soft tissue.

Vascular Tumors

Vascular tumors are amongst the most common soft-tissue tumors. Majority of them are benign and occur in young patients. The tumors are thought to be derived from or differentiate towards, the endothelium lining the blood vessel or lymphatic vessel (lymphatic endothelium). Histologic distinction between blood vessel tumors and lymphatic vessel tumors can be speculated based on the histologic appearance of the vascular tumor when the lesion is well differentiated but it could be impossible in poorly differentiated tumors. The current availability of lymphatic endothelial-specific markers such as D2-40, podoplanin, and Lyv has enabled us to better recognize vascular tumors of lymphatic endothelial

origin. Because of these markers, some specific forms of vascular tumors such as Kaposi sarcoma, Kaposiform hemangioendothelioma, Hobnail hemangioma, and Dabska or retiform hemangioendothelioma are now known to be of lymphatic endothelial origin (25, 26).

Benign

Benign vascular tumors are more common in children and many of them are considered as malformation rather than true neoplastic conditions.

Capillary Hemangioma (Pyogenic Granuloma)

Capillary hemangioma is the most common type of hemangioma which commonly occurs in young patients (juvenile hemangioma). It characteristically involves the skin of the head and neck region and periparotid soft tissue, and usually appears shortly after birth. Histologically, similar lesions can occur in mucosa of the head and neck region and skin of other age groups associated with ulceration and granulation tissue-like growth. These lesions have been called pyogenic granuloma and granulation tissue-like hemangioma (27).

Histopathology

The lesion is composed of multilobulated proliferation of plump to flat endothelial cells forming capillary-size caliber vascular spaces. The lumina of the lesional vessels can be very small and inconspicuous. In some cases they are often associated with variable degree of pericyte proliferation (Fig. 10). In lesions with better-formed vascular lumina, arborizing channels can occasionally be traced up to a small feeding arteriole. The lobular architecture of arborizing vascular spaces lined by plump endothelial cells is very similar to those seen in granulation tissue particularly when the lesions are ulcerated (pyogenic granuloma) (Fig. 11a, b). Mitotic figures can be seen but nuclear pleomorphism and "dropping" type of infiltrative growth are absent. The endothelial cells are positive for endothelial markers such as CD34, CD31, and Factor VIII, and the pericytic cells are variably positive of smooth muscle actin immunohistochemically.

Differential Diagnosis

Capillary hemangioma should be differentiated from other benign vascular lesions such as cellular angiolipoma and should not be overdiagnosed as Kaposi sarcoma, Kaposiform hemangioendothelioma, and well-differentiated angiosarcoma.

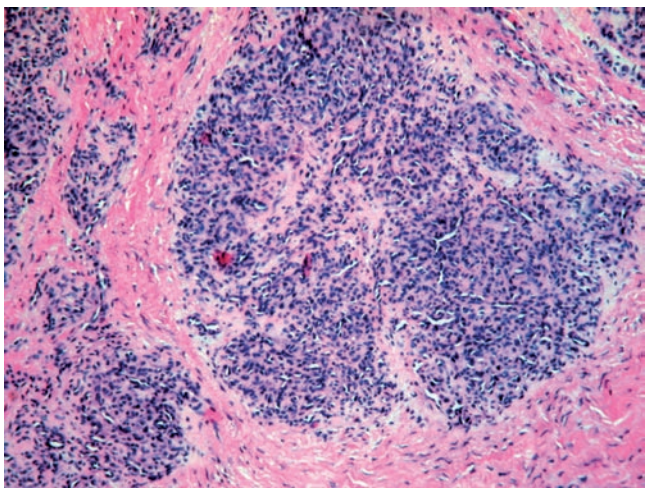

Fig. 10 Lobulated proliferation of plump to flat endothelial cells forming capillary-sized caliber vascular spaces with some degree of pericytic proliferation in capillary hemangioma

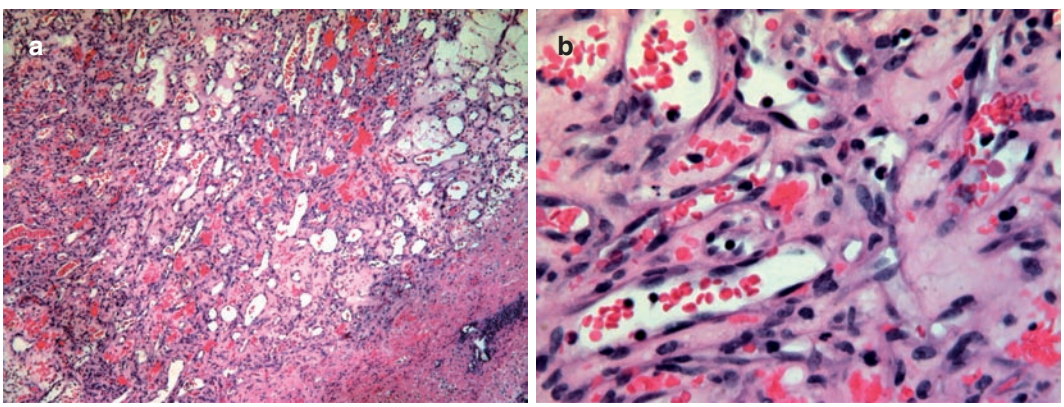

Fig. 11 **a** The lobular architecture of arborizing vascular spaces lined by plump endothelial cells similar to those seen in granulation tissue in capillary hemangioma (pyogenic granuloma). **b**. Bland endothelial cells in pyogenic granuloma

Treatment and Prognosis

Many of the juvenile lesions regress spontaneously. Large lesions affecting vital structures or causing severe cosmetic problems can be treated with corticosteroids and interferon (28). Lesions in older patients can be excised. Local recurrence is not infrequent after incomplete excision. There is thought to be no risk of malignant transformation.

Cavernous Hemangioma

Cavernous hemangioma is the second most common benign vascular lesion of childhood. It is usually located in the deep soft tissue of the upper body with a tendency to interfere the adjacent structures. Rarely the lesion can occur in superficial location (29).

Histopathology

The lesion is has a diffuse distribution or clusters of thin-walled, medium to large caliber vein-like, blood-filled vascular spaces lined by flat endothelium (Fig. 12). A small component of capillary hemangioma might be present in some cases.

Differential Diagnosis

Because of the diffuse distribution of the vascular spaces in some cases, the lesion should be differentiated from well-differentiated angiosarcoma, intramuscular hemangioma, arteriovenous hemangioma, and angiomatosis.

Treatment and Prognosis

Cavernous hemangioma can be cured by local excision. It can recur after incomplete excision. There is thought to be no risk of malignant transformation.

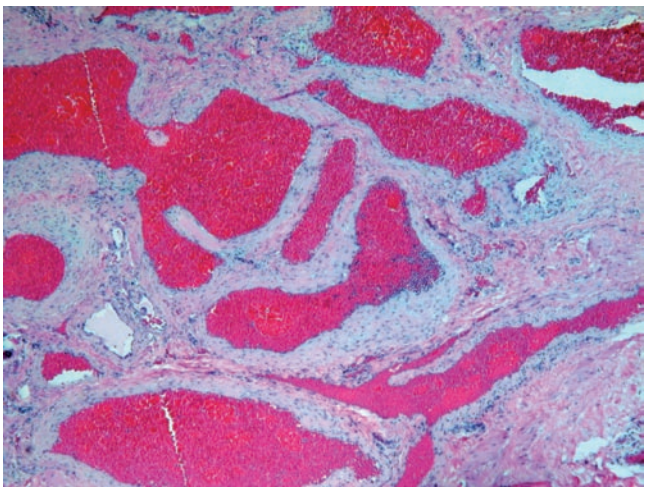

Fig. 12 Blood-filled cavernous vascular spaces lined by flat endothelial cells in cavernous hemangioma

Histocytic (Epithelioid) Hemangioma (Angiolymphoid Hyperplasia with Eosinophilia)

The lesion typically occurs in superficial location of the head and neck region and distal extremities as a slow growing, painless nodule (30).

Histopathology

Epithelioid hemangioma are composed of a well-defined proliferation of small-sized vessels lined by plump, polygonal endothelial cells with amphophilic or eosinophilic cytoplasm in a background of prominent lymphoid and eosinophilic inflammatory reaction (Figs. 13 and 14). The epithelioid endothelial cells can sometimes replace the luminal lining of a large vessel. The epithelioid endothelial cells react with endothelial markers (CD31, CD34, and Factor VIII) and sometimes with cytokeratin and EMA.

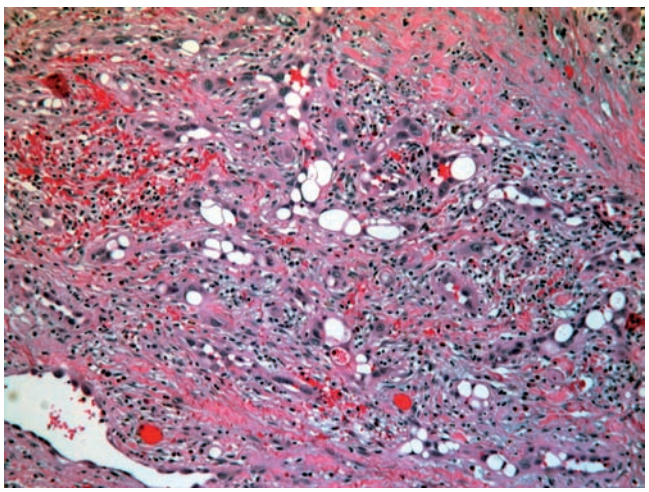

Fig. 13 Plump, polygonal endothelial cells in a background of prominent lymphoid and eosinophilic inflammatory reaction

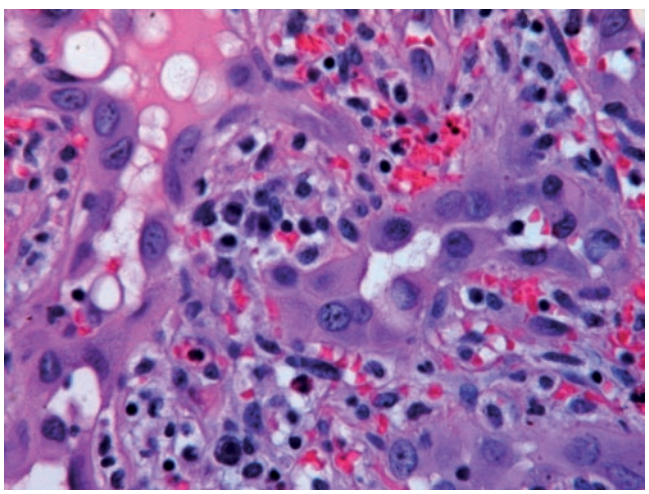

Fig. 14 Epithelioid endothelial cells in epithelioid hemangioma

Differential Diagnosis

Epithelioid hemangioma needs to be differentiated from epithelioid angiosarcoma, epithelioid sarcoma, carcinoma, and melanoma.

Treatment and Prognosis

Epithelioid hemangioma is a benign lesion which should be treated by complete excision with follow-up. About one-third of cases recur after surgery. No documented metastasis has been reported (30) but multifocal involvment can be seen.

Intramuscular Hemangioma (Intramuscular Angiolipoma)

This type of hemangioma usually occurs in young adults. The most common location is thigh, followed by head and neck, upper extremities, and trunk. It presents as a long-standing, painful, deep-seated mass which radiographically appears to be hypervascular (31).

Histopathology

The morphology of the intramuscular hemangioma can be capillary, cavernous, or mixed type. The vascular proliferation is typically poorly defined within skeletal musculature and associated with variable amount of mature adipose tissue. It lacks nuclear pleomorphism and mitotic figures are hard to find.

Differential Diagnosis

Because of the diffuse growth pattern, angiomatosis and angiosarcoma need to be differentiated from intramuscular hemangioma.

Treatment and Prognosis

Wide local excision is recommended for treatment. Although intramuscular hemangioma is a benign vascular lesion, local recurrence is high (15–30%) due to the difficulty in complete excision of the lesion (32).

Angiomatosis

Angiomatosis implies a benign vascular proliferation or malformation involving a large area of body such as limbs and visceral organs. It typically occurs in infants and children. The affected areas might become enlarged or hypertrophic, frequently with discoloration.

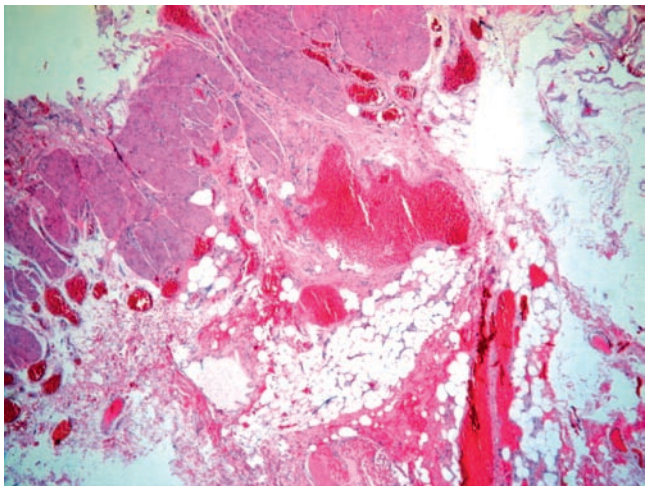

Fig. 15 Diffuse thin-walled, small-sized vascular proliferation in angiomatosis involving bowel wall

Histopathology

Angiomatosis is a diffuse proliferation of small to medium-sized, irregular thin-walled vessels in the dermis, subcutis, skeletal muscle, and/or visceral organs. The process might be associated with variable amount of mature adipose tissue and lymphoid aggregates (Fig. 15).

Differential Diagnosis

Angiomatosis needs to be differentiated from intramuscular hemangioma and arteriovenous hemangioma.

Treatment and Prognosis

Excision of the lesion is difficult and usually associated with high local recurrence (50%). The lesions might be fatal if vital organs or structures are involved. No metastasis and malignant transformation have been reported (33).

Arteriovenous Hemangioma (AV Malformation)

This form of vascular lesion can occur at deep or superficial location. It is usually associated with arteriovenous shunting. Radiographic correlation to identify the arterial and venous components is necessary to confirm the diagnosis. The lesion tends to occur deep in the head and neck region the lower extremities of young patients or in submucosa and subcutis of adult patients (34).

Histopathology

Twisted and tangled medium to large caliber arteries and abnormal veins with a thickened intima and media are the

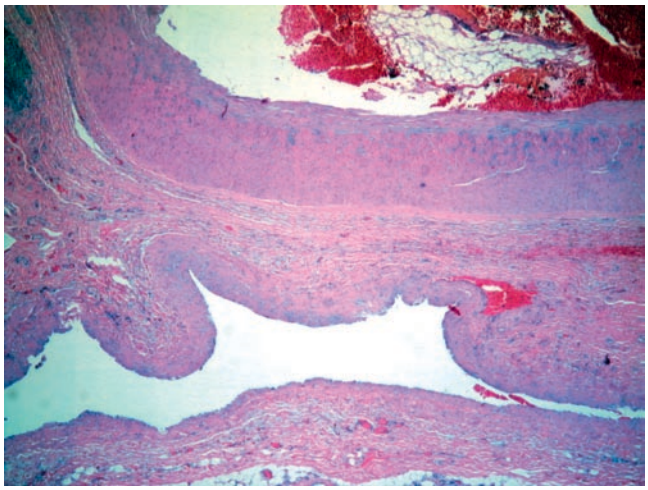

Fig. 16 Large caliber artery and abnormal vein with thicken intima and media in AVM

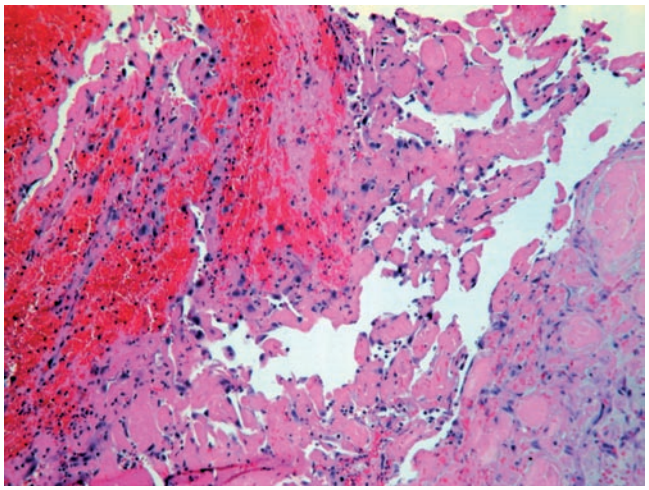

Fig. 17 Intravascular papillary projections with fibrinous stroma lined by flat to plump endothelial cells in papillary endothelial hyperplasia

main findings (Fig. 16). Capillary and cavernous hemangioma-like areas can also be seen.

Differential Diagnosis

Capillary and cavernous hemangioma and angiomatosis need to be differentiated from arteriovenous hemangioma.

Treatment and Prognosis

The success of the surgery is dependent upon the extent of involvement (which can often be assesed radiographic evaluation). Local recurrence is common after surgical excision due to the difficulty in complete excision.

Papillary Endothelial Hyperplasia (Intravascular Vegetant Hemangioendothelioma of Masson)

Although it was originally described by Masson as a form of hemangioendothelioma, it is now known as a form of an organizing thrombus within or around a vessel. The superficial veins of the head and neck, fingers, and trunk are commonly affected (35).

Histopathology

A well-defined vascular lesion composed of numerous interanastomosing channels and papilla lined by flat to plump endothelial cells some of which have enlarged and hyperchromatic nuclei. The stroma or the papillary cores can be fibrinous to hyalinized (Figs. 17 and 18). Occasional mitotic figures can be seen. The intravascular growth pattern can sometimes be appreciated at low magnification with or without reticulum and elastic stains.

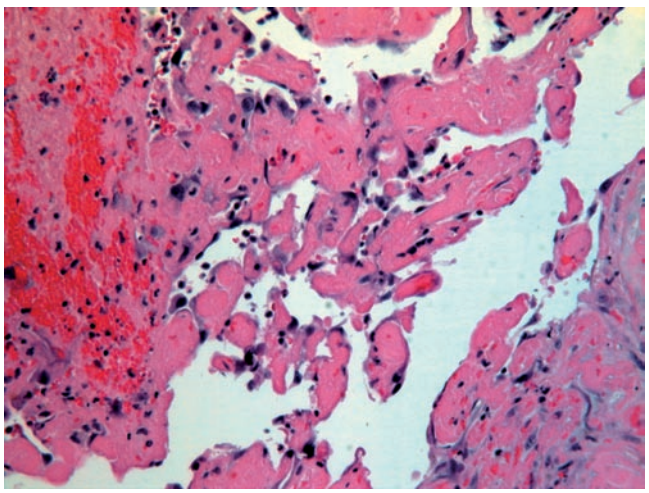

Fig. 18 Some endothelial cells in papillary endothelial hyperplasia have enlarged and hyperchromatic nuclei

Differential Diagnosis

Angiosarcoma and other types of hemangioma need to be differentiated from papillary endothelial hyperplasia.

Treatment and Prognosis

The lesion is benign but is it is usually excised because of the clinical concern for other types of soft tissue or vascular tumors. The lesion is curable by local excision.

Spindle Cell Hemangioma (Spindle cell Hemangioendothelioma)

This lesion was once considered as a form of borderline vascular tumors and therefore named as hemangioendothelioma. It typically occurs in the dermis and subcutis of the distal

extremities of young adults. Some cases have been associated with multiple enchondromas, possibly a variant of Muffucci's syndrome (36).

Histopathology

The lesion is characterized by a multinodular growth of bland spindle cells in between cavernous-like or irregular gaping vascular channels lined by epithelioid endothelial cells (Figs. 19 and 20).

Differential Diagnosis

Kaposi sarcoma and angiosarcoma are on the list of differential diagnosis with spindle cell hemangioma.

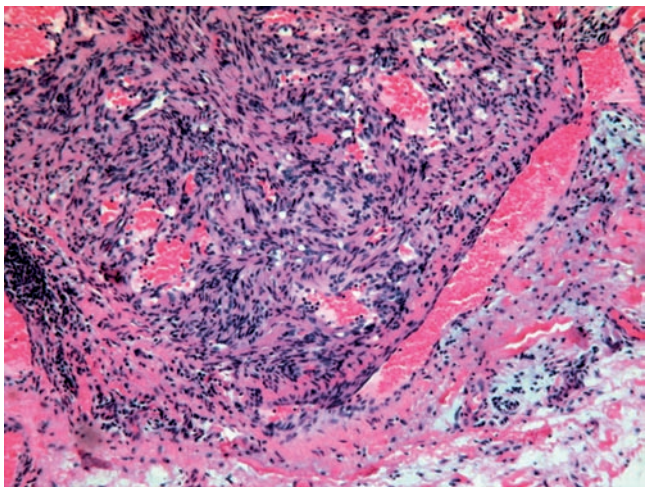

Fig. 19 Vague nodular growth of bland spindle cells in between irregular gaping vascular channels lined by epithelioid endothelial cells in spindle hemangioma

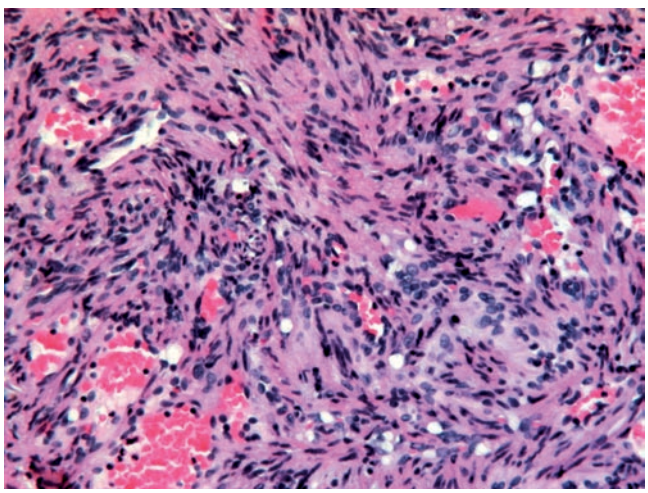

Fig. 20 High magnification of the spindle cell hemangioma in Fig. 19.

Treatment and Prognosis

Local excision is the treatment of choice. Local recurrences happen in two-third of cases.

Lymphangioma

Lymphangioma most frequently occurs in the neck followed by axilla, groin, oral cavity, and other sites. In many cases, the lesion presents at birth or shortly after birth. The cystic type of lymphangioma of the neck is usually associated with Turner syndrome (37). Clinically, it presents as slow-growing painless swelling or cystic mass containing watery and milky fluid.

Histopathology

The lesion is composed of variable-sized, thin-walled vessels lined by flat endothelial cells. The vascular spaces can be empty or contain proteinaceous fluid and some lymphocytes. Lymphoid aggregates can be seen in the interstitium (Fig. 21). In addition to CD31, CD34, and Factor VIII, the endothelium of the lymphanigoma is also positive for podoplanin or D2-40.

Differential Diagnosis

Cavernous hemangioma and AV hemangioma need to be differentiated from lymphangioma.

Treatment and Prognosis

Local excision is the treatment of choice. Local recurrences are due to incomplete excision. Malignant transformation has not been reported.

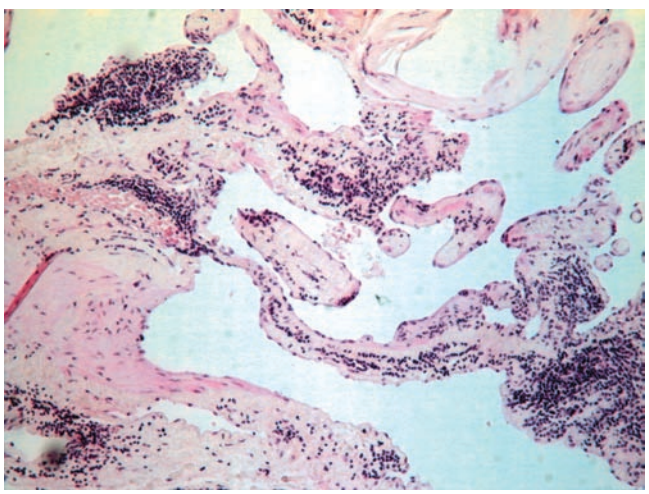

Fig. 21 Variable-sized, thin-walled empty vascular channels lined by flat endothelial cells with lymphocytes in stroma.

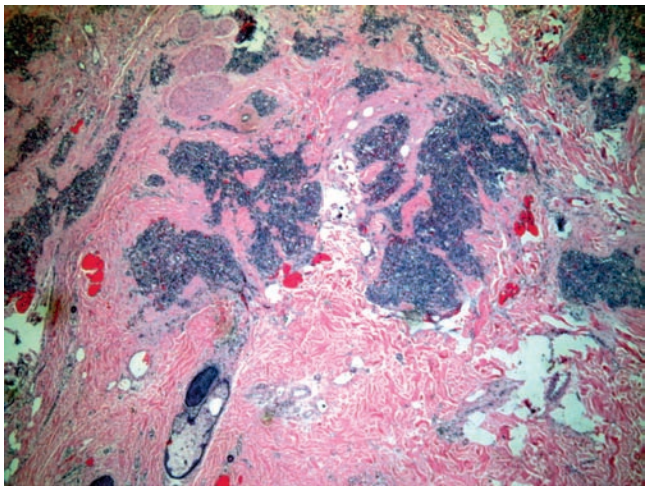

Fig. 22 Low magnification of Karposiform hemangioendothelioma shows irregularly lobular vascular structure

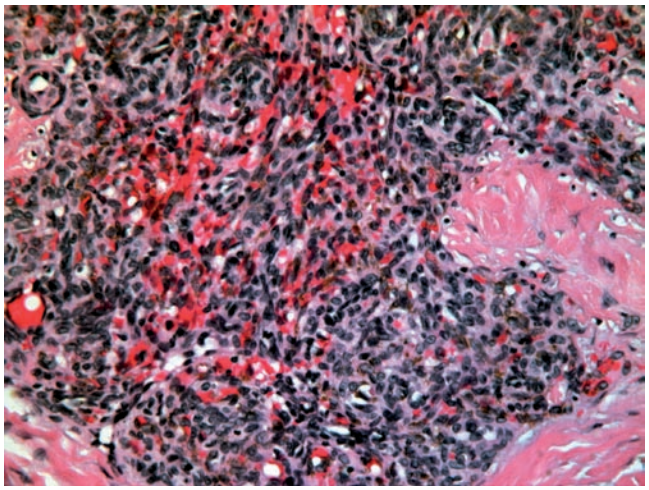

Fig. 23 High magnification shows the compact bland spindle cells in a vague nodule in a case of Kaposiform hemangioendothelioma

Borderline (Hemangioendothelioma)

Kaposiform Hemangioendothelioma and Tufted Angioma

Although originally described mainly as a pediatric lesion, increasing number of cases have been recognized in adult patients. The lesion most commonly occurs in retroperitoneum and skin followed by head and neck region, mediastinum, and deep soft tissue of trunk and extremities (38). Despite the Kaposi-like features, the lesion has no association with HIV infection or human herpes virus 8 (HHV-8). HHV8. Acquired tufted angioma is a histologically and clinically similar lesion restricted to skin of adult patients and is likely a dermal variant of Kaposiform hemangioendothelioma. Patients with large Kaposiform hemangioendothelioma or tufted angioma are at risk of developing consumption coagulopathy (Kasabach–Merritt syndrome).

Histopathology

The lesion is a poorly defined and infiltrative growth of vaguely lobular, capillary-sized vessels and bland spindle cells in between the vessels. The capillary-sized vessels are often lined by plump endothelium. The spindle cells can form compact fascicles or be loosely arranged. In some areas, the spindle cells might become round and whorled, the so-called "glomeruloid" nests (Figs. 22 and 23). Fragmented red blood cells and fibrin thrombi can be seen in the vascular spaces and the slit-like spaces between the spindle cells. Increased lymphatic channels are seen in the adjacent areas. Lymphatic endothelial markers such as D2-40 are found to be positive in endothelial as well as spindle cells of the lesion in the majority of the cases (39). In cases of tufted angioma, the lesion tends to show more capillary-hemangioma-like features and less of a spindle cell component. Unlike a true capillary hemangioma, the lobular structures of tufted hemangioma are described as "cannon ball" and show a "dropping" infiltrative growth pattern similar to that of Kaposiform hemangioendothelioma.

Differential Diagnosis

Kaposiform hemangioendothelioma needs to be differentiated from cellular capillary hemangioma, Kaposi sarcoma, and angiosarcoma.

Treatment and Prognosis

Kaposiform hemangioendothelioma is a locally aggressive lesion (40). The prognosis depends upon the location and size. Lesions in skin and somatic soft tissue are curable after complete excision. Large and intraabdominal tumors have poor outcome for local controls.

Epithelioid Hemangioendothelioma (Intravascular Bronchioalveolar Tumor)

Epithelioid hemangioendothelioma is the most common type of hemangioendothelioma. It occurs in all age groups and affects both sexes equally. The tumor usually presents as painful nodule in superficial or deep soft tissue of the extremities (41). There is a tendency towards multifocality, including visceral organs such as lung, liver, and bone. Pulmonary lesions have been called intravascular bronchioalveolar tumor, and are often seen in younger females. The tumor can also occur at mesothelium-lined cavities, lymph node, and atrium. In soft tissue, many lesions derive from a vessel, usually a vein.

Histopathology

The tumor is typically characterized by poorly defined, intravascular growth of short cords or nests of epithelioid cells in myxohyaline stroma with perivascular extension (Fig. 24). In some lesions, however, the originating vessel and the intravascular pattern might not be apparent. The epithelioid endothelial cells have eosinophilic granular to glassy cytoplasm which frequently has intracytoplasmic lumina containing red blood cells (Fig. 25). Variable degree of cytologic atypia and mitotic activity can be seen in some cases.

Differential Diagnosis

Epithelioid angiosarcoma, mesothelioma, signet ring cell adenocarcinoma, and epithelioid sarcoma enter to the list of tumors that need to be differentiated from epithelioid hemangioendothelioma.

Treatment and Prognosis

The biologic behavior of epithelioid hemangioendothelioma ranges from typical borderline tumor to full malignancy. In soft tissue, the overall local recurrence is around 15%, metastatic rate is up to 30%. The and mortality is around 15% in 5-year follow-up. Atypical cytology and increased mitotic rate are associated with high metastatic rate and mortality (41). Pleural lesions are the most aggressive ones which probably should be considered as a form of epithelioid angiosarcoma (42). The data should be interpreted with caution, since it is somewhat conjecture to differentiate a metastasis from a multifocal lesion.

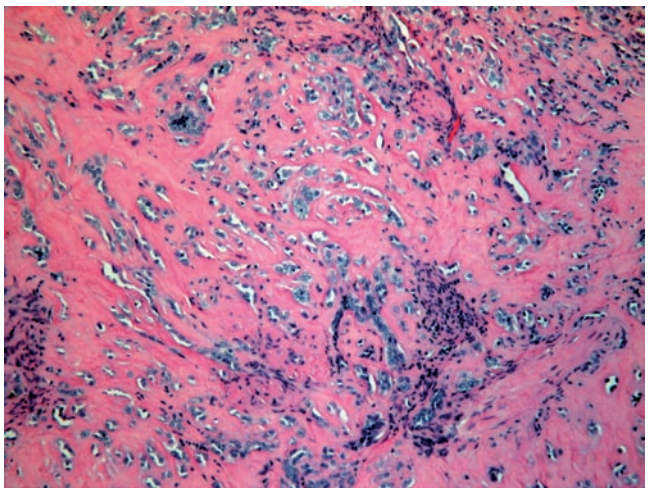

Fig. 24 Short cords and nests of epithelioid endothelial cells in myxohyaline stroma in epitheloid hemangioendothelioma

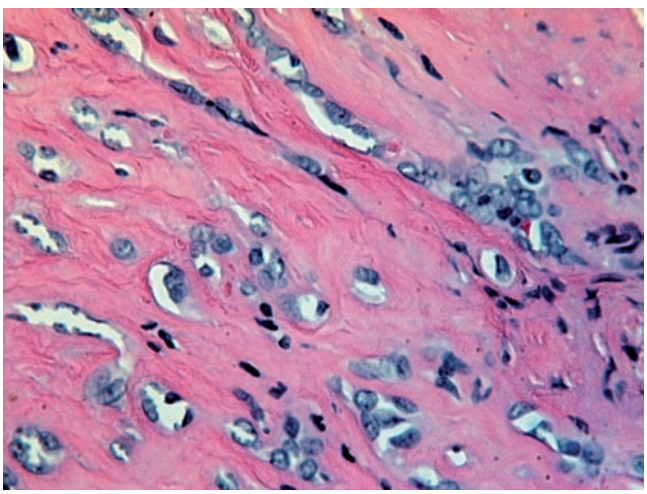

Fig. 25 The tumor cells in epitheloid hemangioendothelioma have eosinophilic granular to glassy cytoplasm and frequently have intracytoplasmic lumina containing red blood cells

Hobnail Hemangioendothelioma (Dabska Tumor, Papillary Intralymphatic Angioendothelioma)

Hobnail hemangioendothelioma is a very rare vascular tumor, more commonly seen in pediatric patients and only about 25% of the cases occur in adults (43). Limbs are most frequently site followed by trunk. It typically presents as slow-growing, painless, ill-defined, cutaneous plague or nodule.

Histopathology

The tumor is composed of cavernous thin-walled vascular spaces with prominent intraluminal papillary tufts with hyaline cores lined by hobnail endothelial cells. Some of the endothelial cells show intracytoplasmic lumina. A variable number of lymphocytes can be seen within and around the vascular spaces. The growth pattern is poorly defined and diffuse. In addition to nonspecific endothelial markers such as CD31, CD34, and Factor VIII, lymphatic-specific endothelial markers such as VEGFR-3 and D2-40 are positive in lesional cells.

Differential Diagnosis

Epithelioid hemangioendothelioma, hobnail hemangioma, epithelioid hemangioma, and angiosarcoma can sometimes be confused with hobnail hemangioendothelioma.

Treatment and Prognosis

Hobnail hemangioendothelioma is a locally aggressive lesion. Wide local excision is recommended for optimal local control. Metastasis has been reported but is rare (44). However, its metastatic potential still needs further investigation.

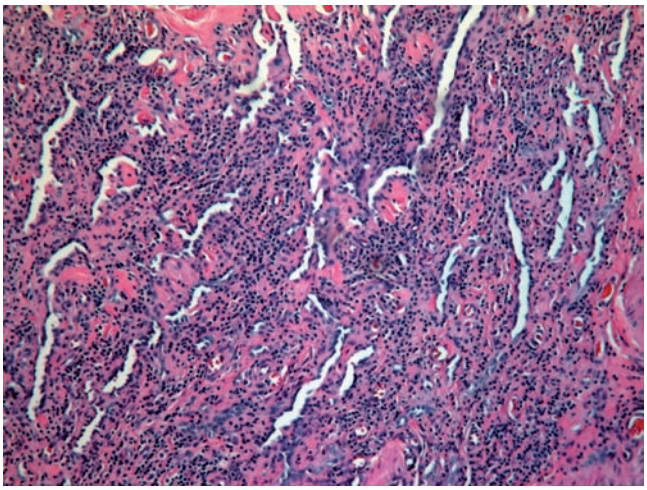

Fig. 26 Formation of elongated and arborizing vascular channels resembling rete testis in retiform hemangioendothelioma

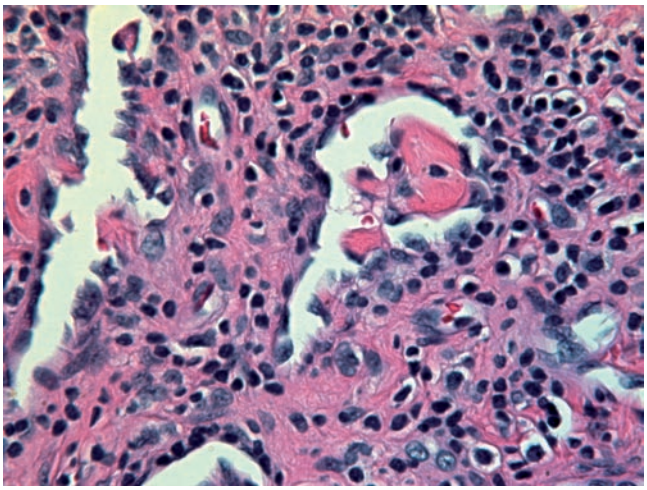

Fig. 27 Under high magnification, the vascular channels of a retiform hemangioendothelioma, are lined by plump or hobnail endothelial cells sometimes with intravascular papillary tufts.

Retiform Hemangioendothelioma

Retiform hemangioendothelioma is a very rare vascular tumor, likely a variant of hobnail hemangioendothelioma. It typically involves the skin and subcutis of the distal extremities of young adults and presents as a slow growing plague or nodule.

Histopathology

The lesion is poorly defined and characterized by formation of elongated and arborizing vascular channels lined by plump or hobnail endothelial cells resembling the rete testis (Fig. 26). Often, there are foci of solid vascular proliferation in the lesion. The hobnail cells have scant cytoplasm and hyperchromatic nuclei. No pleomorphism is seen and mitotic figures are hard to find. Lymphocytes are frequently present in vascular spaces and perivascular fibrous stroma. In some cases, there are intravascular papillary tufts similar to those seen in hobnail hemangioendothelioma (Fig. 27). The immunophenotype of the endothelial cells are similar to that of hobnail hemangioendothelioma and D2-40 has been shown to be positive in two cases the author has recently encountered.

Differential Diagnosis

Same as hobnail hemangioendothelioma.

Treatment and Prognosis

Wide local excision is recommended for optimal local control. Multiple local recurrences are common, often over period of many years. A single case of regional lymph node metastasis has been reported but so far no deaths related to this lesion have been reported (45).

Kaposi's Sarcoma

Kaposi's sarcomas (KS) occurs in the following four different clinical settings: classic indolent form in elderly men of Mediterranean or east European decent; endemic African form in middle-aged and children of Equatorial Africa; iatrogenic form in solid organ transplant patients or any patients received immunosuppressive agents for various diseases; and lastly the AIDS-associated form in HIV-1 infected individuals (46). All forms of KS are associated with HHV-8 infection (47). Skin is the most common site of involvement but mucosa, lymph node, and visceral organs might be affected as well. The lesions typically present as ill-defined purplish red macules, plaques, and nodules. Classic forms of the lesion tend to occur in the distal extremities and may be associated with lymphoedema. Iatrogenic forms usually occurs a few months to years after transplantation or immunosuppressive treatment. In addition to skin of the face, genitalia and extremities, AIDS-related KS also frequently involves the mucosa, lymph nodes, GI tract, and lung.

Histopathology

The histologic features of KS are the same in all four forms. In early stage (patch stage) of the skin disease, there is a subtle increase in slightly irregular vascular channels. The endothelial cells lining the vascular spaces are flat with little atypia. There are variable numbers of poorly formed vascular channels recognized as slit-like spaces lined by attenuated or spindle endothelial cells in a dissecting pat-

tern of growth in dermis (Fig. 28). Variable numbers of lymphocytes, plasma cells, and extravasated red blood cells are seen around the vascular or slit-like spaces. In the later plaque stage, the above histologic features of the patch stage become more exaggerated. The lesion is usually slightly raised and the slit-like spaces and the spindle cell component of the lesion become more obvious. There are more siderophages and hyaline globules likely resulted from the destroyed red blood cells. Finally, the lesion develops into nodular stage which is characterized by even more dominant slit-like spaces and spindle cell proliferation in intersecting fascicles. The lesional cells show mild nuclear pleomorphism and frequent mitotic figures (Figs. 29 and 30). The spindle cells and endothelial cells of the KS are positive for lymphatic endothelial markers such as D2-40 (podoplanin) in addition to CD34 and CD31 (26). The lesional cells are also positive for HHV-8.

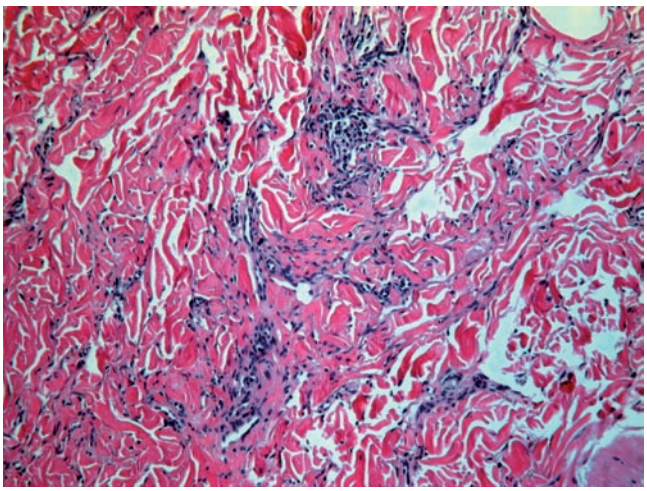

Fig. 28 Early Kaposi sarcomas (*KS*) lesions are characterized by poorly formed vascular channels recognized as slit-like spaces lined by attenuated or spindle endothelial cells in a dissecting pattern of growth in dermis

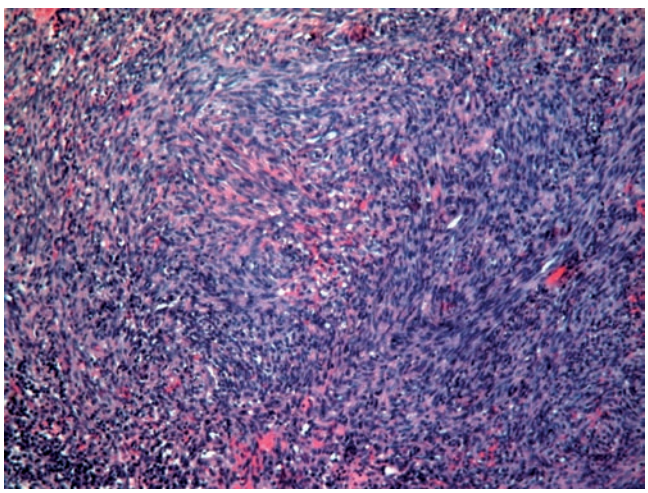

Fig. 29 Later stage of Kaposi sarcoma (*KS*) is composed of a highly cellular spindle cell proliferation with frequent extravasated red blood cells but little vascular formation

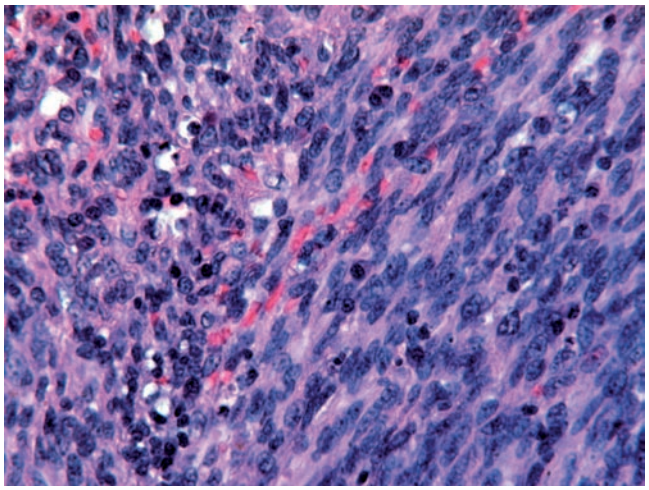

Fig. 30 High magnification reveals uniform neoplastic spindle cells with high N/C ratio, frequent mitotic figures, and extravasated red blood cells in Kaposi sarcomas (*KS*).

Differential Diagnosis

Dependent on the phase of the lesion, Kaposi sarcoma can be confused with cellular capillary hemangioma, pyogenic granuloma, spindle cell hemangioma, tufted angioma, Kaposiform hemangioendothelioma, bacillary angiomatosis, angiosarcoma, and various spindle cell sarcomas.

Treatment and Prognosis

Kaposi sarcoma has been treated with surgery, radiation, and chemotherapy. The prognosis of Kaposi sarcoma depends upon the clinical form of the disease. The classic form is indolent disease and has the best prognosis. It is same as the endemic form when the lesion is confined to skin. However, a variant of endemic form with lymphadenopathy in children is very aggressive and highly lethal. The course of iatrogenic KS is unpredictable, although some iatrogenic KS regressed completely after withdrawal of the immunosuppressive agents. The AIDS-related KS is the most aggressive form of the disease, particularly when the disease has spread to multiple visceral organs.

Malignant

Angiosarcoma

All malignant vascular tumors are named angiosarcoma without making distinction between blood vessel and lymphatic vessel origin. Angiosarcoma most frequently involves

skin of the head and neck in elderly patients without any predisposing factors. It also arises in various clinical settings associated with chronic lymphedema (post-mastectomy), radiation, synthetic vascular graft, and exposure to carcinogenic agents such as Thorotrast, arsenic compounds, or vinyl chloride (48). Only less than a quarter of cases arise in deep soft tissue of extremities, trunk, and head and neck in adult patients. Rarely angiosarcomas can involve breast, body cavities, and various visceral organs such as lung, liver, and spleen. The lesion presents as a poorly defined, usually multicentric, rapidly growing mass. Other syndromes such as coagulopathy, anemia, hemorrhage, and problems with increased AV shunting are seen in one-third of the patients.

Histopathology

It is typically composed of irregularly shaped anatomosing, sinusioidal vascular channels lined by bland or atypical endothelial cells in a dissecting growth pattern. The endothelial cells have tendency to form intraluminal tufts and papillary proliferations. Mitotic figures are present but not always numerous. In some very well-differentiated angiosarcomas, the histologic appearance might simulate that of hemangioma. In these cases, the histologic features distinguishing angiosarcoma and hemangioma are the disturbing pattern of infiltrative growth at low magnification, focal mild cytologic atypia, and tufting formation (Fig. 31a, b). When the lesion is less differentiated, the neoplastic endothelial cells becomes more epithelioid and/or more spindle appearance with less or no vascular channel formation. Nuclear pleomorphism and mitotic figures are more obviously apparent. When the lesion is poorly differentiated with little vascular channel formation, cells with intracytoplasmic lumina with red blood cells might be the only evidence suggestive of endothelial origin of the tumor (Fig. 32a, b). Endothelial markers such CD34, CD31, Factor VIII, and Fli-1 are positive in majority of the well-differentiated cases and only variably positive in poorly differentiated cases. About one-third of the angiosarcomas are also positive for D2-40 suggesting a lymphatic endothelial differentiation in these cases (26).

Differential Diagnosis

Well-differentiated angiosarcoma needs to be differentiated from hemangioma and angiomatosis. When poorly differentiated, the tumor needs to be differentiated from Kaposi sarcoma, other poorly differentiated sarcomas, metastatic

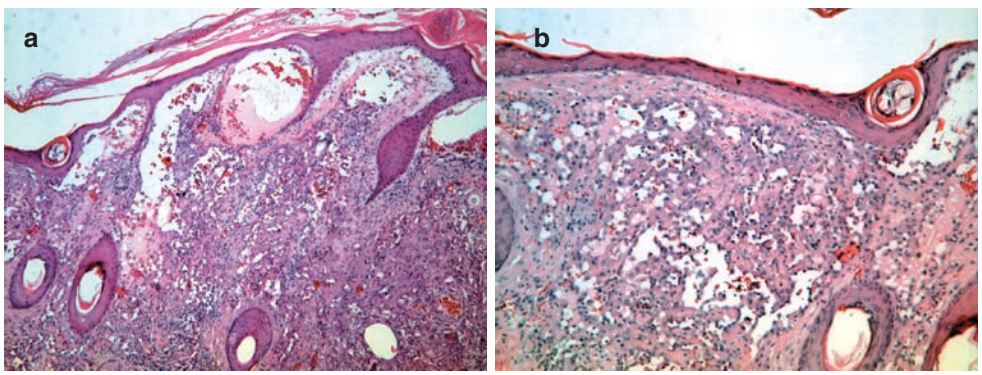

Fig. 31 **a** Complex anastamosing vascular channels exhibit infiltrative growth pattern at low magnification in well-differentiated angiosarcoma. **b** The neoplastic endothelial cells show cytologic atypia and tufting formation

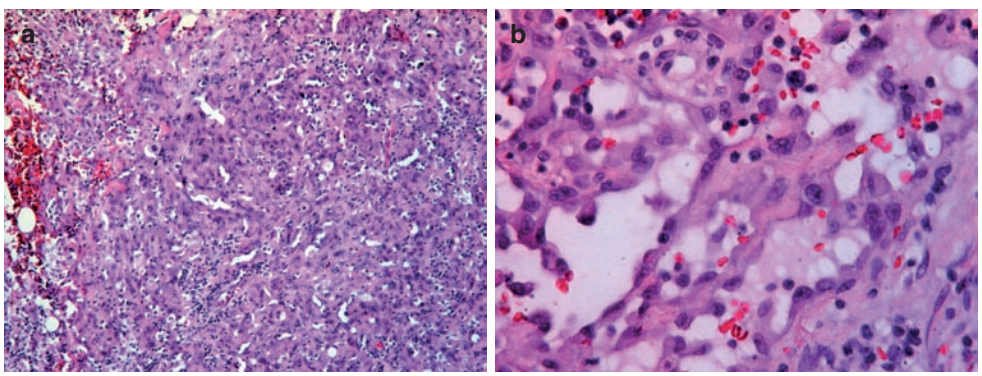

Fig. 32 **a** Solid growth pattern of epitheloid cells with little vascular channel formation in a poorly differentiated epithelioid angiosarcoma. **b** Poorly form vascular spaces lined by highly atypical endothelial cells, some with intracytoplasmic lumina

carcinoma, mesothelioma, melanoma, epithelioid hemangioendothelioma, and epithelioid sarcoma.

Treatment and Prognosis

Surgical excision is the treatment of choice but complete excision is usually difficult due to multicentric and infiltrative growth of the tumor. Prognosis, in general, is poor. Histologic grading seems to be associated with prognosis only in skin and breast angiosarcomas (49). Angiosarcomas in deep soft tissue, body cavities, and visceral organs are generally considered as high-grade tumor regardless their histologic differentiation. Common metastatic sites are regional lymph nodes, liver, lung, and spleen.

Tumors of Primarily Soft-Tissue Origin

Most of the tumors in this group show histologic differentiation toward certain mesenchymal elements commonly seen in soft connective tissue, such as adipocyte, fibroblast, or myocyte, while some show uncertain histologic differentiation.

Lipogenic Tumors

Tumors with lipogenic differentiation are amongst the most common soft-tissue tumors and majority of them are benign.

Benign

Lipoma

Lipoma is the most common soft-tissue tumor in humans. It frequently affects adults in their fifth and sixth decades of life and is rare in pediatric patients. Obese individuals have a higher incidence of lipoma (50). It can occur superficially in the subcutis as well as deeply in soft tissue. The superficial lipoma is usually solitary and more commonly seen in shoulder, back, neck, and abdomen. Multiple lipomas account for less than 5% of cases. Deep lipomas typically occur within or between skeletal muscle (intramuscular or intermuscular lipoma) and on the surfaces of bone (parosteal lipoma). Occasionally, deep lipoma can occur in tendon sheath (lipoma of tendon sheath) and around nerve (perineural lipoma) in younger patients. Superficial lipomas present as a slowly growing, painless mass. Deep lipomas tend to be less circumscribed and larger and can be painful in some cases if they compress a nerve.

Histopathology

Lipomas are typically composed of fully mature adipose tissue which has little difference at cytologic level from the normal mature adipose tissue. Lipomas however have a slight irregularity in the size and shape of adipocytes along with the a subtle loss of normal lobulation. Lipomas are characteristically encapsulated. Variable amounts of myxoid, chondroid, and fibrous tissue can be seen in some cases and these have been called myxoid lipoma, chondroid lipoma, and fibrolipoma, respectively (Fig. 33). By definition, lipoma should not show immature adipose tissue however, lipoblasts can be encountered in chondroid lipoma. These lipoblasts are vacuolated cells arranged in clusters in the myxoid stroma. No nuclear pleomorphism is evident. A few reactive lipoblasts might also be seen adjacent to fat necrosis which is not infrequently seen in all forms of lipoma. In addition, fat necrosis can induce accumulation of many histiocytes which contain foamy cytoplasm and larger nuclei and sometimes are mistaken for lipoblasts. The deep lipomas are poorly defined and often there is entrapment of the surrounding normal tissue in the periphery of the lesion giving an impression of infiltrative growth pattern. Frequently, the entrapped surrounding tissue shows atrophic change (Fig. 34).

Differential Diagnosis

Lipoma needs to be differentiated from spindle cell lipoma, angiolipoma, myxoma, lipomatosis, well-differentiated liposarcoma, and atypical lipomatous tumor.

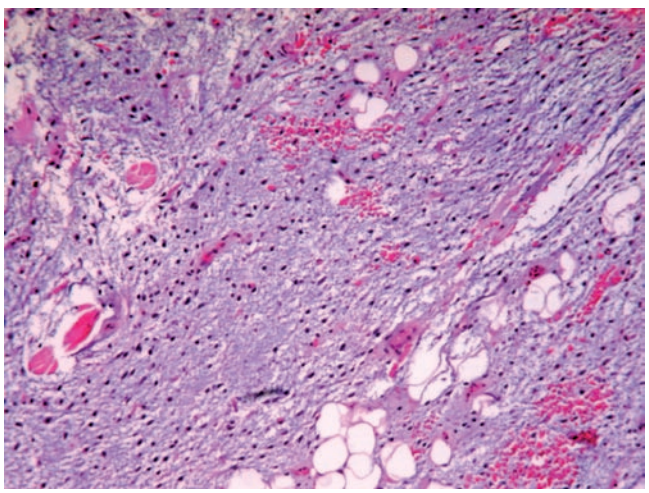

Fig. 33 Myxoid change in the matrix of a lipoma (myxoid lipoma). There is lack of nuclear atypia and rich vasculature in the lesion

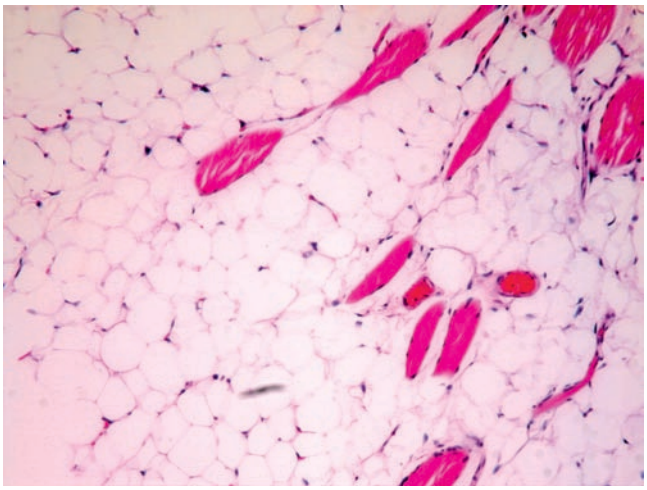

Fig. 34 Entrapped skeletal muscle fibers in an intramuscular lipoma

Treatment and Prognosis

Superficial lipomas are easily treated by simple local excision. Recurrence may occur if the lesion is not completely excised. Risk of local recurrence is significantly higher in deep lipomas. Complete local control of the disease might require total removal of the involved skeletal muscle or structure or compartmental resection (51).

Lipomatosis

Lipomatosis is a diffuse overgrowth of mature adipose tissue. It occurs in the following clinical settings: (1) idiopathic diffuse lipomatosis in early childhood involving large areas of the trunk and extremities; (2) idiopathic pelvic lipomatosis in young to middle-aged black male patients; (3) cervical symmetric lipomatosis in middle-aged men with history of liver disease or extensive alcohol consumption; (4) steroid lipomatosis in the face and mid-upper back of patients who are receiving steroid therapy or have increased endogenous production of adrenocortical steroids; (5) HIV lipodystrophy in visceral organs, breast, and cervical fat pads of AIDS patients treated with protease inhibitors or patients receiving other forms of antiretroviral therapy. Clinically, the patients have massive accumulation of the fat in the affected areas, which sometime can be symptomatic due to compression of the vital structures or organs in the regions (52).

Histopathology

Histologic features of all types of lipomatosis are identical and characterized by completely normal appearing mature adipose tissue replacing and entrapping the surrounding normal tissues, structures, or organs.

Differential Diagnosis

Histologic appearance of lipomatosis can be confused with intramuscular lipoma, angiomatosis with fat overgrowth, or well-differentiated liposarcoma.

Treatment and Prognosis

Surgical excision is palliative and local recurrence is very high after surgery. Cervical lipomatosis may compress the larynx and become fatal. Except for idiopathic form of lipomatosis, the course of the disease may remit with the correction of the patient's underlying conditions.

Angiolipoma

Angiolipoma typically presents as a painful subcutaneous nodule in the extremities and trunk of young adults. Multiple lesions are seen in two-third of the cases. Small numbers of patients (5%) have familial history (53).

Histopathology

The lesion is usually circumscribed and less than 2 cm in the subcutis. It is composed of mature adipose tissue and branching capillary-sized vessels frequently containing fibrin thrombi. The vascular component is more prominent in the periphery of the lesion. The proportion of the adipose tissue and vascular tissue can vary significantly from case to case and the histologic appearance of angiolipoma can mimic that of a lipoma with few vessels at one end of the spectrum to that of capillary hemangioma at the other (Figs. 35 and 36).

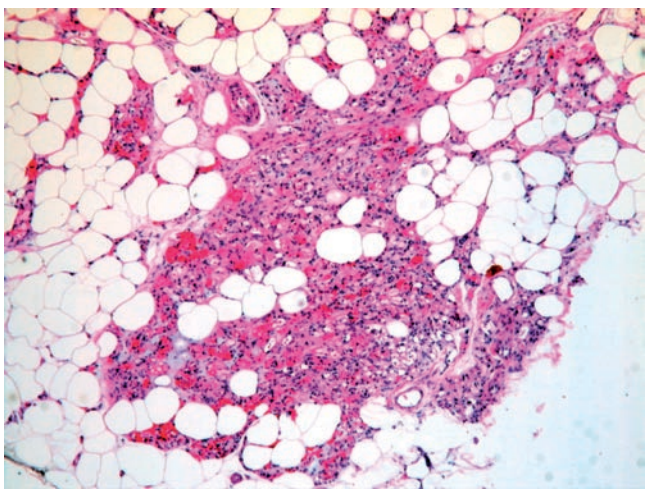

Fig. 35 Mature adipose tissue and clusters of short branching capillary-sized vessels in angiolipoma

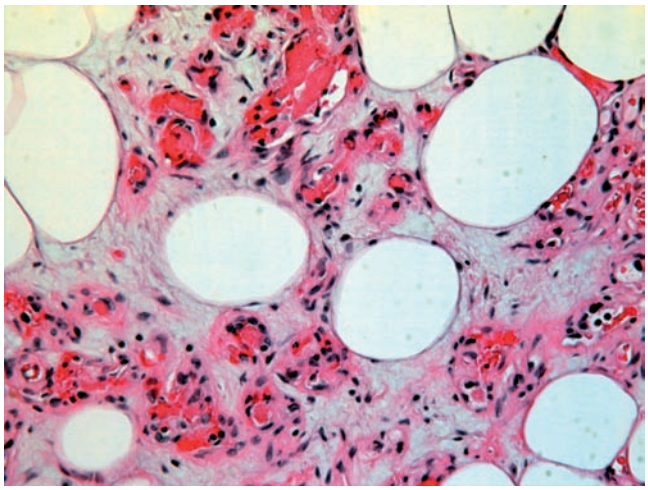

Fig. 36 The bland endothelial cells and frequent fibrin thrombi in the vessels of angiolipoma

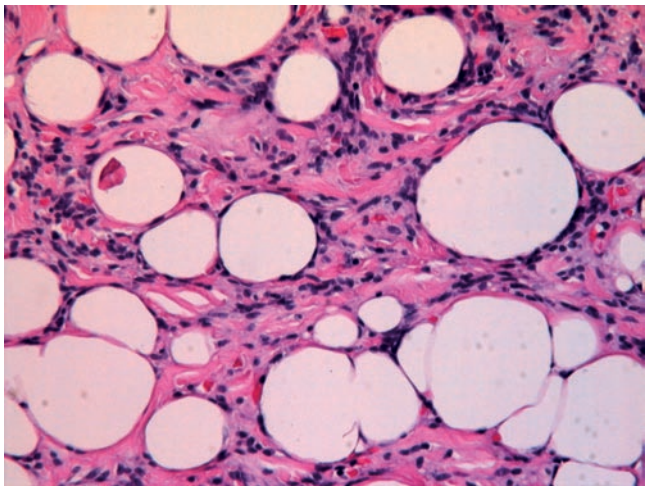

Fig. 37 Bland and uniform short spindle cells proliferation in a spindle cell lipoma

Differential Diagnosis

Lipoma, capillary hemangioma, and angiosarcoma might need to be differentiated from angiolipoma.

Treatment and Prognosis

Angiolipoma is treated with surgical excision with little risk of recurrence.

Spindle Cell Lipoma/Pleomorphic Lipoma

Spindle cell lipoma and pleomorphic lipoma represent two ends of the histologic spectrum of a distinct fatty tumor. Clinically, spindle cell lipoma/pleomorphic lipoma presents as a painless, slow-growing, well-defined subcutaneous nodule most commonly in the posterior neck or shoulder of men in the fourth decade of life. Rare cases with multiple lesions and familial history have been reported (54).

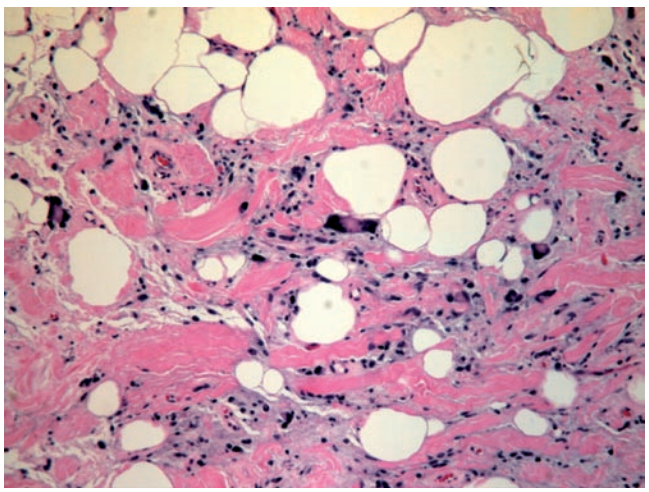

Fig. 38 Pleomorphic hyperchromatic floret-like multinucleated giant cells with thick ropey-like collagen fibers and variable myxoid stromal change in a pleomorphic lipoma

Histopathology

Both spindle cell lipoma and pleomorphic lipoma are well circumscribed with variable amount of mature adipose tissue. The histologic characteristics of spindle cell lipoma is the presence of bland and uniform short spindle cells associated with thick ropey-like collagen fibers with variable myxoid stromal change (Fig. 37). Variable mast cells, plasma cells, and lymphocytes are seen in some cases. At other end of the spectrum, pleomorphic lipoma is characterized by the presence of hyperchromatic floret-like multinucleated giant cells in addition to the short spindle cells (Fig. 38). Not infrequently, there are cases with histologic features in between these two ends of the histologic spectrum. Despite the variation in histologic appearance, the lesion is uniformly inactive in mitosis. Both lesions are immunohistochemically positive for CD34 (Fig. 39).

Differential Diagnosis

Angiolipoma, spindle cell liposarcoma, solitary fibrous tumor, and low-grade myxofibrosarcoma are on the list of differential diagnosis for spindle cell lipoma. Sclerosing-type well-differentiated liposarcoma, pleomorphic liposarcoma, and pleomorphic sarcoma are on the list of differential diagnosis for pleomorphic lipoma.

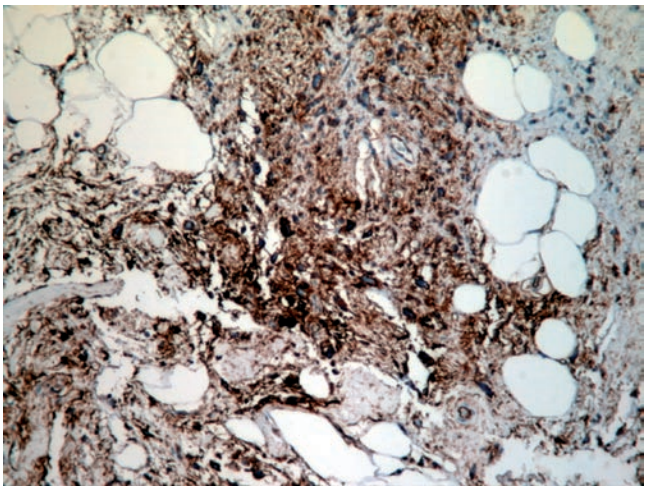

Fig. 39 Strong CD34 immunoreactivity in pleomorphic lipoma

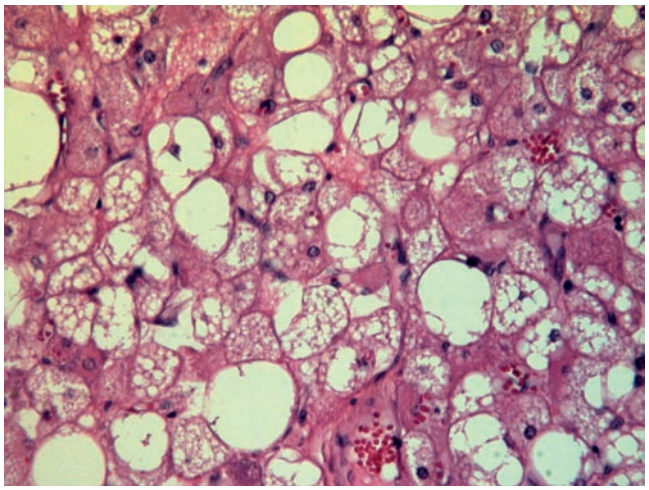

Fig. 40 Polygonal brown fat cells have abundant multivacuolated eosinophilic cytoplasm in a hibernoma

Treatment and Prognosis

Conservative surgical resection is considered sufficient for treatment because both spindle cell lipoma and pleomorphic lipoma rarely recur locally.

Hibernoma

Hibernoma commonly occurs in young patients as slow-growing, painless mass in subcutis. It usually affects thigh, scapular region, chest wall, and inguinal and axillary regions. Small number of cases present as intramuscular lesion.

Histopathology

The histologic hallmark of hibernoma is lobules of polygonal brown fat cells which have abundant multivacuolated eosinophilic cytoplasm with a small central nucleus (Fig. 40). Sometimes the remnants of brown fat can be admixed in otherwise normal, mature adipose tissue from the scapular and axillary regions of adults. Mitotic figures and nuclear atypia may be very rarely seen and should not be considered as sign of malignancy.

Differential Diagnosis

Focal brown fat change can be seen in some cases of liposarcoma. Hibernoma should be differentiated from liposarcoma with focal brown fat change. Granular cell tumor and adult-type rhabdomyoma are also on the list of differential diagnosis for hibernoma.

Treatment and Prognosis

Hibernoma is cured by complete excision. Local recurrence is very unusual (55).

Borderline

See well-differentiated liposarcoma/atypical lipomatous tumor.

Malignant

Liposarcoma

Liposarcoma is the most common type of soft-tissue sarcomas in adults and occurs primarily in the fifth through seventh decades of life. There are four types of liposarcomas as defined by their clinico-pathological features. These are well-differentiated liposarcoma/atypical lipomatous tumor, myxoid/round cell lipoma, pleomorphic liposarcoma, and dedifferentiated liposarcoma.

1. Well-Differentiated Liposarcoma and Atypical Lipomatous Tumor – Atypical lipomatous tumor, used to be called atypical lipoma, has been used preferentially to describe a group of superficially located, low-grade lipomatous tumors which have been called well-differentiated liposarcoma when present in deep location regardless of the identical histological, biological, and karyotypical characteristics. The use of different terminology for the diagnosis of identical tumors reflects the importance of anatomic site in tumor prognosis in soft-tissue tumors. When the tumor arises in a superficial location, it is usually smaller at the time of the diagnosis because of the early attention to the tumor growth by the patients. Complete excision of the tumor is easily achievable because of superficial location and earlier detection. In this case, it is reasonable to avoid the use of the word sarcoma to avoid unnecessary alarm and/or overtreatment (56). In contrast, deep-seated tumors tend to be ignored for longer time and grow larger with more extensive regional involvement before patients seek medical attention. Complete excision of the tumor is usually difficult at the time of surgery due to deep

location, larger size, and more extensive involvement of adjacent structures, which inevitably lead to poor local control of the disease and eventually the risk of patient demise even in the absence of metastasis and/or dedifferentiation. The use of the term "sarcoma" is therefore justified to reflect the difference in prognosis in deep-seated tumors.

Well-differentiated liposarcoma occurs most frequently in deep soft tissue of the extremities followed by retroperitoneum, paratesticular area, and mediastinum. It presents as painless mass which can slowly grow to very large size without causing any significant mass effect in deep location particularly in retroperitoneum, and in obese patients.

Histopathology

The tumors are slightly lobulated and fleshy yellow to white on cut surface in gross examination. There are four histologic types of well-differentiated liposarcoma: lipoma-like, sclerosing type, inflammatory type, and spindle cell type. The tumor usually preserves the lobulated architecture that is composed of relatively mature but more variable adipocytes. There are variable numbers of atypical adipocytes with enlarged, irregular, and hyperchromatic nuclei scattered within the mature adipocytes in lipoma-like liposarcoma (Fig. 41). In the sclerosing type, there are in addition, pleomorphic hyperchromatic stromal cells usually in multinucleated forms, seen more frequently in the lobular fibrous septa or in a hyaline fibrous stroma. The fibrous areas can sometimes dominate the tumor with little lipogenic areas (Fig. 42). The tumor also can also be dominated by chronic inflammatory infiltrates composed of lymphoplasmacytic cells (inflammatory type of well-differentiated liposarcoma) (Figs. 43 and 44). The spindle cell variant is least common type of well-differentiated liposarcoma and it is

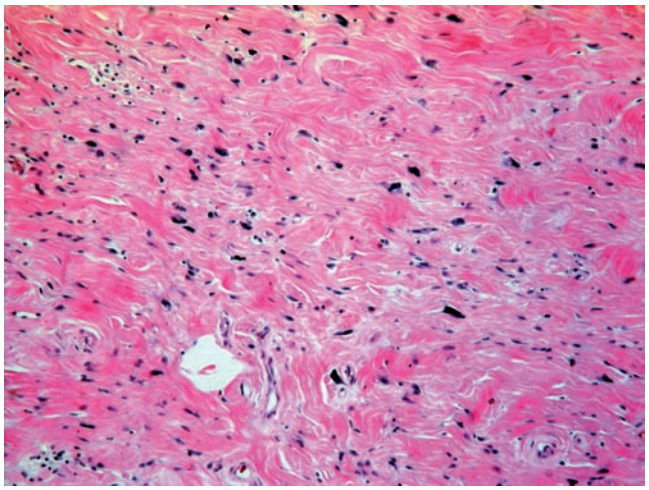

Fig. 42 Pleomorphic hyperchromatic stromal-type cells, some in multinucleated form in a hyaline fibrous stroma in a sclerosing liposarcoma

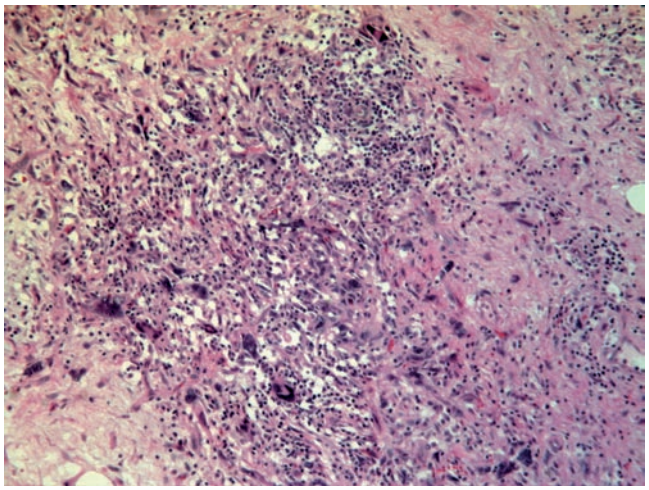

Fig. 43 Florid chronic inflammatory infiltrates in a pleomorphic liposarcoma

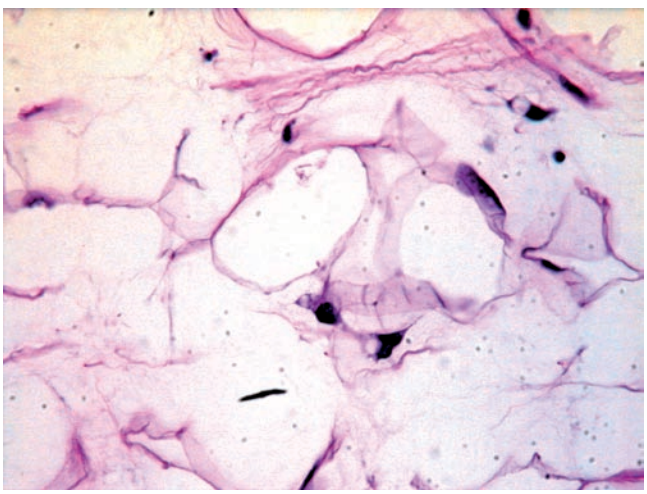

Fig. 41 Rare atypical adipocytes with enlarged, irregular, and hyperchromatic nuclei scattered within the mature adipocytes in a lipoma-like liposarcoma

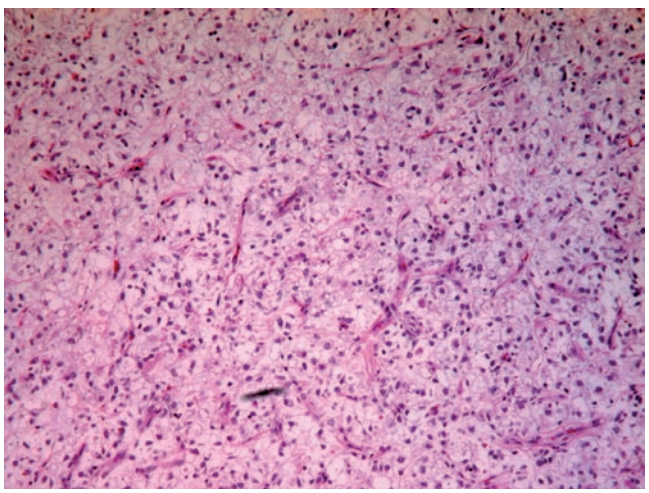

Fig. 44 Rich delicate arborising, short branching capillary vasculatures in the myxoid stroma in pattern referred as "chicken wire or chicken finger" under low magnification in a myxoid liposarcoma

characterized by the presence of bland spindle cells in myxoid fibrous background associated with lipoma-like liposarcoma. Tumors with mixed features of the above histologic variants are not infrequent. Although lipoblasts can be seen in all forms of well-differentiated liposarcoma, extensive search for lipoblasts is neither rewarding, nor necessary for the diagnosis. On the other hand, finding of lipoblasts is not pathognomic of the diagnosis of liposarcoma as lipoblasts can be seen in various benign fatty tumors or lesions.

Differential Diagnosis

The differential diagnosis for lipoma-like well-differentiated liposarcoma includes lipoma with fat necrosis, lipomatosis, and myxoid liposarcoma. Sclerosing and spindle cell liposarcomas need to be differentiated from spindle cell/pleomorphic lipoma, myxofibrosarcoma, pleomorphic sarcoma, and dedifferentiated liposarcoma. The inflammatory liposarcoma needs to be differentiated from infection, inflammatory fibrosarcoma, inflammatory myofibroblastic sarcoma, and various lymphoproliferative disorders.

Treatment and Prognosis

Atypical lipomatous tumor and well-differentiated liposarcoma can be cured by complete surgical excision. The most important prognostic factor is anatomic location. Atypical lipomatous tumors have excellent prognosis after complete excision with very low risk of recurrence because of the superficial location (620). Deep-seated tumors and tumors in the retroperitoneum and mediastinum, spermatic cord have high risk of local recurrence simply due to the difficulty in complete excision of the tumor at the time of surgery (57). Regardless of the location, the tumors have no potential to metastasize unless dedifferentiation takes place. The risk of dedifferentiation is also location dependent. Superficial tumors have very low risk of dedifferentiation while the retroperitoneal tumors have the highest risk (20%) of dedifferentiation (57). See discussion in dedifferentiated liposarcoma.

2. Myxoid/Round Cell Liposarcoma– Myxoid liposarcoma and round cell liposarcoma are now considered two opposite ends of histologic spectrum of a group of liposarcomas with an identical karyotype. It frequently involves the deep soft tissue of the extremities and very rarely occurs in retroperitoneum and superficial location. Patients tend to develop myxoid/round cell liposarcoma in the fourth to fifth decades of life, a decade younger than the other type of liposarcoma. It is also the most common type of liposarcoma in pediatric patients (58). It typically presents as painless swelling in the deep soft-tissue compartment of the involved limb.

Histopathology

On gross examination, the lesion is typically multinodular, tan, and gelatinous on cut surface in tumors with myxoid histologic features and white fleshy in tumors with round cell features. Histologically, the tumor is composed of variable numbers of monotonous round cells at different stage of differentiation ranging from primitive round cells to vacuolated lipoblasts.

The well-differentiated end of the histologic spectrum is represented by myxoid phenotype. The tumor cells are individually scattered in a myxoid stroma with a slightly increased cellularity in the periphery of the lobules. Mitotic figures are rare. There are rich delicate arborising, short branching capillary vasculatures in the myxoid stroma in pattern referred as "chicken wire" under low magnification (Figs. 45 and 46). Accumulation of amorphous

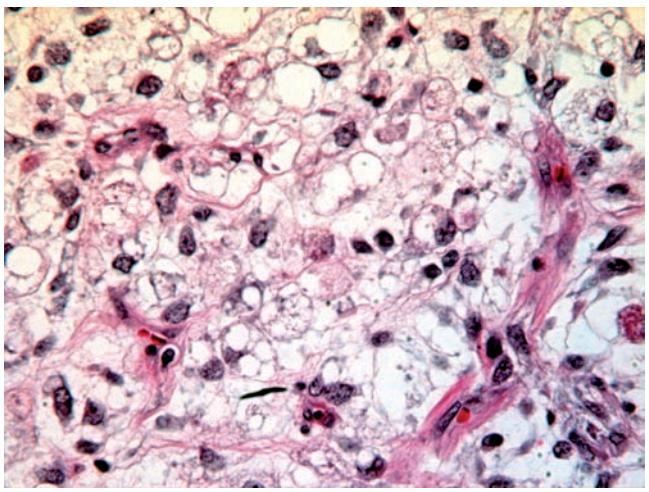

Fig. 45 The neoplastic cells are relatively monotonous and round with poorly defined cytoplasm well spaced away from each other in myxoid stroma in myxoid liposarcoma

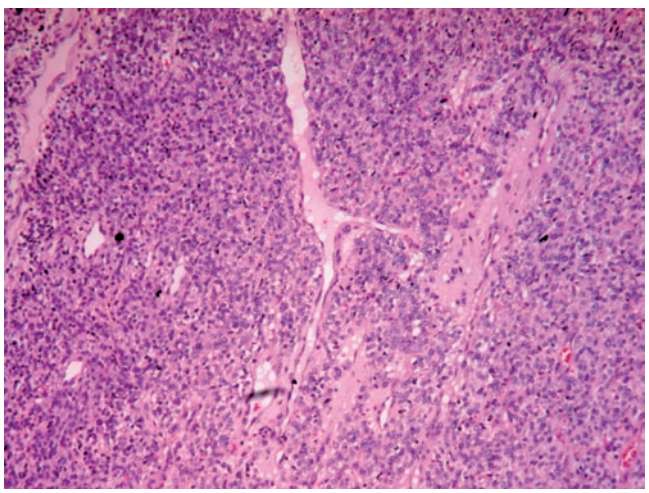

Fig. 46 Closely packed primitive round cells with high N/C ratio, active mitotic activity, and little myxoid stroma in round liposarcoma

mucin-like material in myxoid stroma forms variable-sized confluent pools or microcystic appearance.

On the other end of the spectrum, the poorly differentiated tumors are represented by round cell phenotype that is characterized by closely packed primitive round cells with higher nucleus to cytoplasm ratio and frequent mitoses (Figs. 47 and 48). There is little or no myxoid stroma in the round cell areas.

Several, tumors show both myxoid and round cell features. The cellularity and the amount of extracellular myxoid matrix in the areas between these two components are intermediate between typical myxoid and round cell morphologies. Because the transition areas are more hypercellular than pure myxoid areas, they are commonly confused with round cell component. However, compared to pure round cell component, there is still some myxoid stroma between tumor cells which tend to look like those in myxoid areas and are not so closely packed as seen in round cell areas.

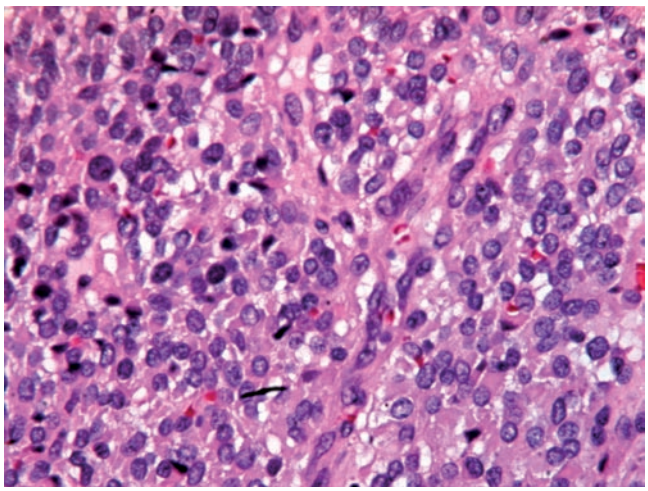

Fig. 47 High magnification of round cell liposarcoma shows overlapping of hyperchromatic nuclei and high mitotic activity. Some cells with vacuolated cytoplasm suggestive of lipogenic activity

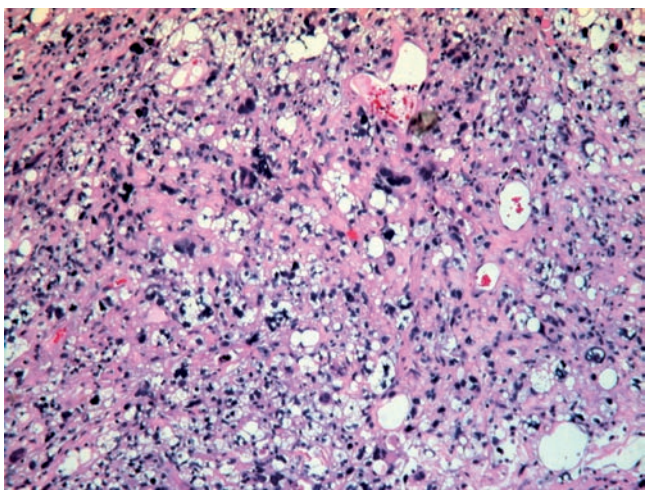

Fig. 48 Numerous pleomorphic cells, many of which can be recognized as lipoblasts by the presence of cytoplasmic multivacuolation in pleomorphic liposarcoma

Differential Diagnosis

Tumors with prominent myxoid features need to be differentiated from various myxoid tumors such as myxoid dermatofibrosarcoma protuberance, myxofibrosarcoma, myxoid lipoma, and other myxoid tumors. Tumor with prominent round cell features need to be differentiated from various round cell tumors such as Ewing's sarcoma, poorly differentiated synovial sarcoma, rhabdomyosarcoma, desmoplastic small round cell tumor, lymphoma, and small cell carcinoma.

Treatment and Prognosis

Wide local excision with clear surgical margins is the treatment of choice. Myxoid/round cell liposarcomas tend to recur locally. Up to one-third of patients may develop distant metastasis. Tumor behavior depends upon the histologic type or grade. Tumors with more than 75% round cell areas (pure round cell liposarcoma) are considered high grade and are aggressive. Tumors with no or <5% round cell component (pure myxoid liposarcoma) are considered low grade and have the best prognosis. The majority of the tumors have more than 5% but less than 75% round cell components and will have prognosis between the pure myxoid and pure round cell types. Synchronous and metaschronous multifocal soft-tissue metastases are not uncommon and usually carry a poor prognosis (59). The amount of transition area does not seem to have a significant impact in prognosis (60).

3. Pleomorphic Liposarcoma– This is the least common form of liposarcoma. It has a predilection for the deep soft tissue of the extremities and many of the patients are over 50 years old. Rarely the tumors arise superficially (61). Clinically, it presents as a rapid growing firm mass.

Histopathology

Pleomorphic liposarcoma is usually firm, multinodular, and white to yellow in gross appearance. Histologically, it is characterized by presence of numerous pleomorphic cells, many of which can be recognized as lipoblasts by the presence of cytoplasmic multivacuolation. There are many other less pleomorphic cells which are spindle to round in shape and have similar hyperchromatic nuclei in a fibrous background (Figure 49). Mitotic figures are frequent and tumor necrosis is common.

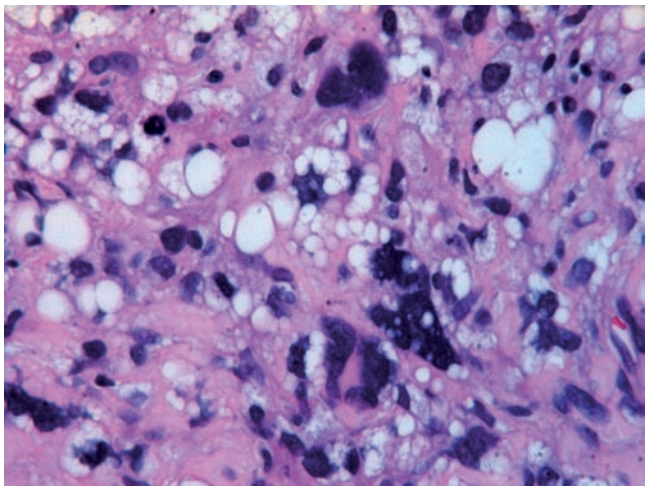

Fig. 49 Neoplastic lipoblasts and anaplastic pleomorphic cells in pleomorphic liposarcoma

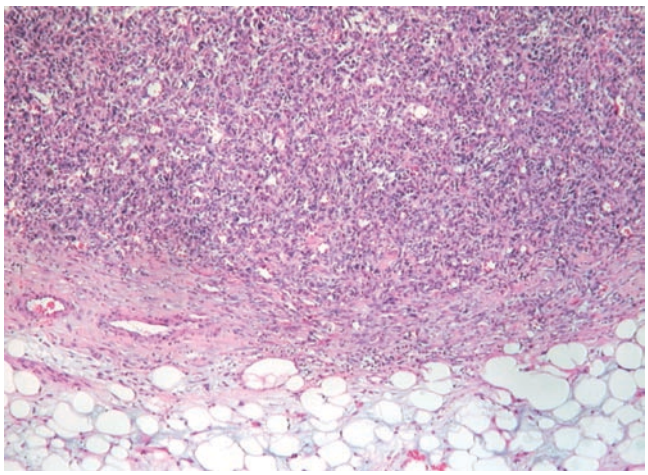

Fig. 50 Nonlipogenic neoplastic element represented by pleomorphic MFH-like area shows abrupt juxtaposition to the well-differentiated liposarcoma which is frequently underdiagnosed as normal fat by surgeons or pathologists

Differential Diagnosis

Pleomorphic liposarcoma should be differentiated from variety of pleomorphic sarcomas such as pleomorphic lipoma, sclerosing liposarcoma, pleomorphic fibrosarcoma, or pleomorphic poorly differentiated sarcomas.

Treatment and Prognosis

Wide excision with clear surgical margins is the treatment of choice. In general, pleomorphic liposarcoma are very aggressive tumors with 30–50% metastatic rate and 40–50% of mortality during short period of time. Lung is the most common site for metastasis (61).

4. Differentiated Liposarcoma– Presence of nonlipogenic neoplastic elements in primary or recurrent well-differentiated liposarcoma is considered dedifferentiation. The incidence of dedifferentiation is estimated to be 10%, It is more common in deep seated or retroperitoneal lesions (62). Any recent episodes of rapid growth of an otherwise long standing and stable soft-tissue mass are alarming signs and may portend dedifferentiation.

Histopathology

Gross examination reveals a heterogenous tumor with tan gray firm nodules or areas seen juxtaposed with soft fatty areas. The former representing a high-grade sarcoma and the latter a well-differentated liposarcoma. The histologic hallmark of dedifferentiation is the presence of nonlipogenic neoplastic elements which are usually abrupt juxtaposition to the well-differentiated liposarcoma in the background. The most commonly seen nonlipogenic element is fibrosarcomatous with variable myxoid and pleomorphic features (Fig. 51). However, chondroblastic, osteogenic, myogenic, angiomatous, and neural elements can be seen as well. The dedifferentiated elements can be histologically high or low grade. Not infrequently, the dedifferentiated component occupies the majority of the tumor mass and only very small portion of well-differentiated liposarcoma can be found in the periphery of the specimen. This well-differentiated area can be misinterpreted as normal fat. Careful search for atypical cells in the remnant of "normal appearing fat" adjacent to dedifferentiated area is the key for a proper diagnosis. Immunohistochemical study might be useful to confirm the presence of nonlipogenic elements in tumors.

Differential Diagnosis

When the separate areas of well-differentiated liposarcoma and high-grade sarcoma are seen juxtaposed, the diagnosis of dedifferentiated liposarcoma is straightforward. Otherwise, the tumors need to be differentiated from pleo-

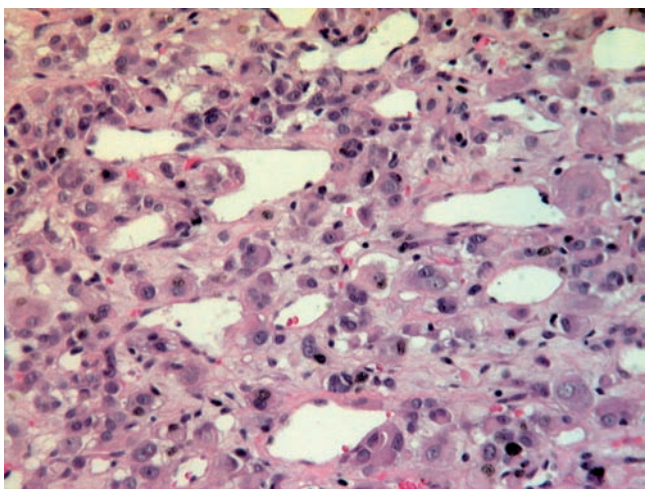

Fig. 51 Another dedifferentiated liposarcoma shows hemangiopericytoma-like vasculature and large globoid rhabdoid cell differentiation

morphic lipoma, spindle cell lipoma, sclerosing liposarcoma, well-differentiated liposarcoma, pleomorphic fibrosarcoma, myxofibrosarcoma, leiomyosarcoma, rhabdomyosarcoma, and extraskeletal osteosarcoma. Thorough sampling and examination of a large well-differentiated liposarcoma or a seemingly nonlipogenic sarcoma in areas where liposarcoma is common are crucial to establish the diagnosis.

Treatment and Prognosis

Surgical resection with wide clear margins is the treatment of choice. However, complete excision at the time of surgery is usually difficult due to the large size and deep location. Sometimes, only the dedifferentiated portion of the tumor is recognized as lesion and the peripheral well-differentiated areas are mistakenly considered to be normal fat and thus incompletely removed. Recurrence is very high after surgery and occurs in 40% of all cases and in almost all retroperitoneal cases in long-term follow-up. The distant metastasis occurs in 15–20% of the cases and the overall mortality is around around 30% in 5 years. The retroperitoneal lesions have the worse prognosis. The extent and grading of the dedifferentiation do not seem to have significant prognostic impact (63).

Tumors with Fibroblastic/Myofibroblastic/ "Fibrohistocytic" Differentiation

Benign

Elastofibroma

Elastofibroma is a rare tumor-like soft-tissue lesion. It almost exclusively occurs in the deep soft tissue between the lower scapula and the chest wall. It is usually ill-defined and adherent to the underlying periosteum. It affects elderly individuals, particularly those with long history of manual labor. There is a female predilection (64).

Histopathology

The lesion is an ill-defined, rubbery white lesion characterized microscopically by hyalinized collagenous stroma and abundant large coarse, intensively eosinophilic fibers which can be fragmented into variable lengths and globules (Fig. 52). Elastic stain highlights a dense core and irregular serrated margins in these fibers.

Differential Diagnosis

Elastofibroma needs to be differentiated from fibromatosis, keloid, nuchal fibroma, and fibrolipoma.

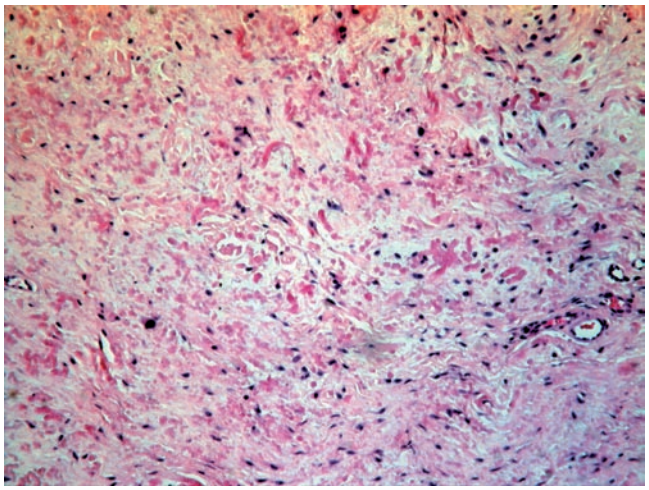

Fig. 52 Large coarse, intensively eosinophilic elastic fibers fragmented into variable lengths and globules in elastofibroma

Treatment and Prognosis

Local recurrence is very rare after simple excision of the lesion.

Myxoma (Intramuscular Myxoma, Juxta-Articular Myxoma, Cutaneous Myxoma)

In soft tissue, myxoma more frequently occurs intramuscularly, adjacent to large joints and in subcutaneous site. It is usually asymptomatic. Some cases of multiple intramuscular myxoma have been associated with fibrous dysplasia and Albright syndrome and given the term Mazabraud syndrome (65, 66).

Histopathology

Myxoma has gelatinous and slimy appearance grossly. Microscopically, it is composed of uniform bland spindle- and stellate-shaped cells with tapering, weak eosinophilic and fibrillary cytoplasm scattered in abundant myxoid matrix. Vacuolation and cystic changes are common and vasculature is very scant in the myxoid stroma. In the periphery, the lesion is poorly defined and a short distance of infiltration into the adjacent skeletal muscle or other tissues is commonly seen (Fig. 53). Areas of hemorrhage and hemosiderin deposition, and chronic inflammation might be present. Although myxoma is typically paucicellular, increased cellularity with some amount of fibrous or fibrovascular tissue can be seen focally or diffusely. Lesions with diffusely increased cellularity have been called cellular myxoma. Regardless of the hypercellularity, mitoses, nuclear atypism, or necrosis should not be present in cellular myxoma.

Differential Diagnosis

In its typical hypocellular form, myxoma needs to be differentiated from ganglion cyst, dermal mucinoses, myxoid

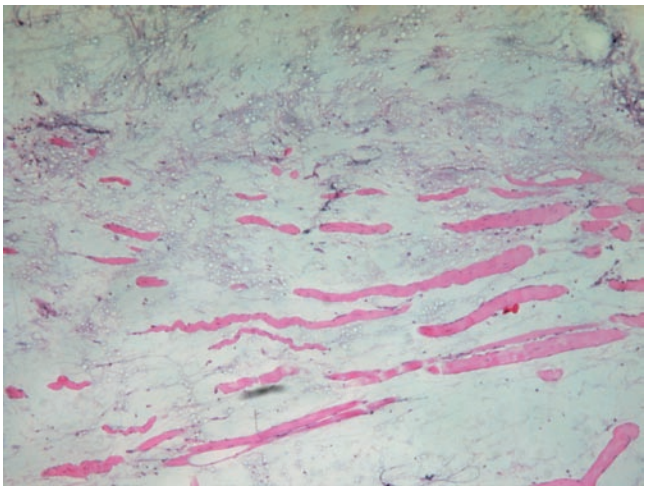

Fig. 53 Uniform bland spindle- and stellate-shaped cells scattered in abundant myxoid matrix with entrapped skeletal muscle in periphery of a myxoma

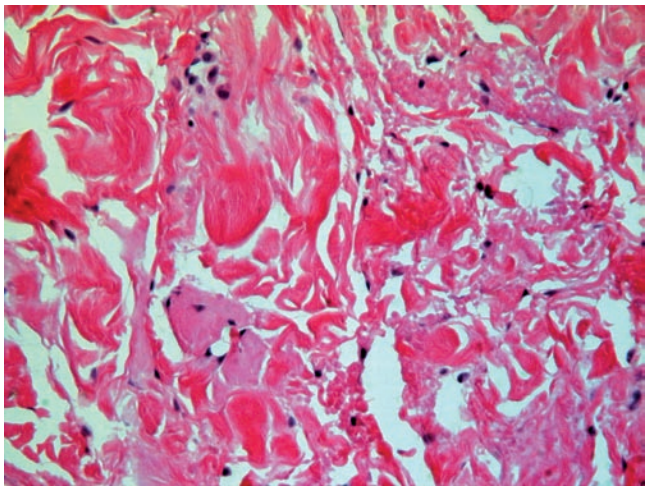

Fig. 54 Haphazardly arranged thick strands or bundles of hyaline amorphous collagenous tissue in nuchal fibroma

neurofibroma, myxoid neurothekeoma, and myxoid lipoma. Cellular myxoma needs to be differentiated from myxoid dermatofibrosarcoma protuberans, low-grade myxofibrosarcoma, myxoid liposarcoma, and botryoid rhabdomyosarcoma.

Treatment and Prognosis

Typical paucicellular intramuscular myxoma rarely recurs even after incomplete excision. Cellular myxoma has a slightly increased risk of local nondestructive recurrence. Local recurrence has been reported in one-third of juxta-articular myxoma (67).

Nuchal Fibroma

Nuchal fibroma has a predilection for the subcutis of interscapular and upper paraspinous regions of adults. It is more common in men. It is usually asymptomatic. Forty percent of patients have diabetes mellitus (68).

Histopathology

Nuchal fibroma is composed of paucicellular dense collagenous tissue in haphazardly arranged thick strands or bundles and hyaline amorphous sheets (Figs. 53 and 54). The lesion is poorly defined and frequently involves the subcutis with entrapment of the mature adipocytes.

Differential Diagnosis

Keloid, fibromatosis, and fibrolipoma need to be differentiated from nuchal fibroma.

Treatment and Prognosis

Nuchal fibroma is a benign disease and can be cured by local excision. Recurrence is not infrequent and requires re-excision.

Keloid

Keloid is benign cutaneous scar-like fibrous overgrowth. It has a predilection for blacks and may also be familial. It tends to affect the upper body and head and neck region frequently at the sites of recent trauma or surgery. It presents as raised nodular/multinodular firm cutaneous lumps.

Histopathology

Keloid is characterized microscopically by nodular dermal proliferation of glassy, hyalinized coarse bundles or strands of collagen tissue in haphazard arrangement. A few slender bland fibroblasts are scattered between the collagenous strands (Fig. 55).

Differential Diagnosis

The gross appearance of the lesion is very characteristic. Microscopically however, hyperplastic scar, fibromatosis, nuchal fibroma, and scleroderma are on the list of differential diagnosis for keloid.

Fibroma of Tendon Sheath

Fibroma of tendon sheath presents as a small firm painless nodule attached to the tendons of the hands and feet in adults.

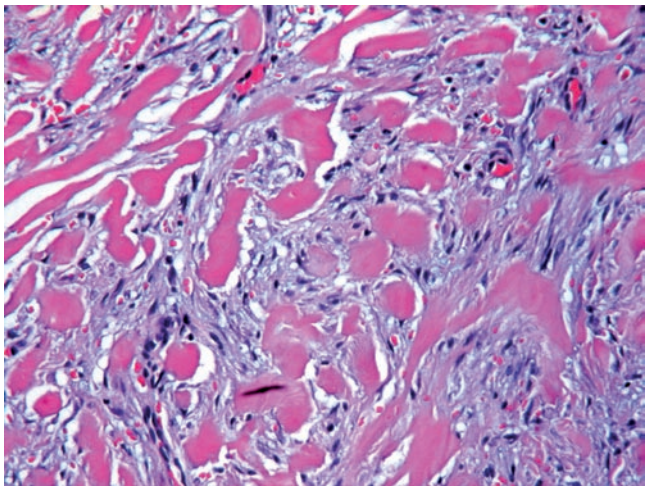

Fig. 55 The characteristic glassy, hyalinized coarse bundles or strands of collagen tissue in haphazard arrangement in keloid

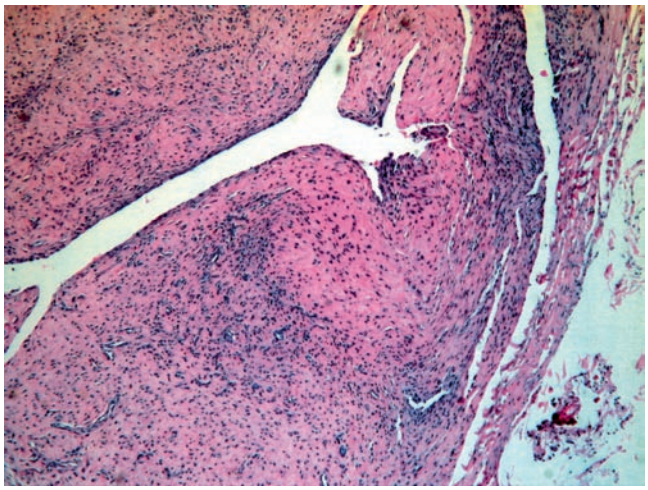

Fig. 56 Lobulated growth of dense collagenous matrix and bland spindle fibroblasts/myofibroblasts in variable cellularity with cleft spaces present between the lobules in fibroma of tendon sheath

Histopathology

The lesion is a well-demarcated, multilobular white mass. It is composed of dense collagenous matrix and scattered bland, variably cellular, spindled fibroblasts or myofibroblasts. Cleft spaces are present between the lobules within the lesion (Fig. 56). There is lack of giant cells. Association of the lesion with a tendon is usually evident on histologic examination.

Differential Diagnosis

The cellular variant of fibroma of tendon sheath needs to be differentiated from nodular fasciitis, giant cell tumor of tendon sheath, fibromatosis, and fibrosarcoma.

Treatment and Prognosis

Conservative surgical resection is recommended to preserve the anatomic integrity and the function of the hands or feet. Nondestructive recurrence is seen in around 25% of cases (69).

Desmoplastic Fibroblastoma

Desmoplastic fibroblastoma is a rare benign soft-tissue tumor commonly occurring in older individuals. It involves the various peripheral sites such as arm, shoulder, lower extremities, and back usually as a superficial painless nodule. Occasionally, the lesion can reach the fascia and even into the skeletal muscle.

Histopathology

Desmoplastic fibroma is a well-circumscribed, white, and firm nodule. Histologically, it is characterized by abundant delicate fibers of collagenous tissue in haphazard pattern, scattered slender or stellate-shaped fibroblasts and myofibroblasts, and inconspicuous vascularity.

Differential Diagnosis

Desmoplastic fibroblastoma might be confused with fibromatosis and nuchal fibroma

Treatment and Prognosis

Recurrences have not been reported after local excision (70).

Calcifying Aponeurotic Fibroma

A rare benign soft-tissue tumor occurs more commonly in younger individuals. It primarily involves the distal extremities and presents as poorly defined painless mass associated with aponeuroses and tendons.

Histopathology

The lesion is usually poorly defined and is hypercellular with central serpiginous zones of calcification with adjacent hyaline and chondroid changes on low magnification. The lesional cells are round to plump fibroblasts sometimes palisading around the calcified areas or arranged in cords. The plump fibroblasts in chondroid areas might be confused with chondroblasts. The stromal tissue between the calcified and cellular areas is usually hyalinized. Rare osteoclast-like multinuclear giant cells are present in some cases (71).

Differential Diagnosis

Chondroma of soft part, fibromatosis, epithelioid hemangioendothelioma, and epithelioid sarcoma need to be differentiated from calcifying aponeurotic fibroma.

Treatment and Prognosis

Local recurrences are common but are not destructive. Conservative surgery is recommended to conserve the functionality of the structure involved by tumor.

Intermediate

Solitary Fibrous Tumor (SFT)

Since it was first recognized as a distinct clinico-pathologic entity at a pleuropulmonary site, solitary fibrous tumor has been reported in a wide variety of extrapulmonary sites such as head and neck, chest wall, mediastinum, retroperitoneum, abdominal cavity, extremities, thyroid, meninges, liver, adrenal, urinary bladder, prostate, and testes (72). It usually presents as slow growing painless mass.

Histopathology

The tumor is usually a firm white nodule which is well demarcated. Histologically, it is identical to that of its pleuropulmonary counterpart. It is composed of patternless proliferation of fibroblast-type spindle cells in variable cellularity and collagenous fibrous matrix. There is an alternation of hyper and hypocellular areas. Open gorged and/or branching vein-like vasculatures similar to those seen hemangiopericytoma can be seen focally or predominantly (Fig. 57). Strongly eosinophilic collagenous fibers of variable sizes and usually do not form any particular pattern (Fig. 56). Entrapped mature adipocytes can be present (Fig. 58). There is lack of significant nuclear pleomorphism, necrosis, and active mitotic activity in majority of the cases. Malignant cases exhibit diffuse or focally increased cellularity, significant nuclear pleomorphism, tumor necrosis, and high mitotic activity (>2 mitotic figures/10 hpf). Many malignant SFT derive from high-grade transformation in typical SFT and others represent de novo tumors (Fig. 59). Rarely, dedifferentiation into other histologic lineages such as liposarcoma and rhabdomyosarcoma can be seen (Fig. 60) (73).

Differential Diagnosis

Tumors with low-grade histology need to be differentiated from hemangiopericytoma, spindle cell lipoma, and mammary-type myofibroblastoma. Malignant solitary fibrous tumor needs to be differentiated from fibrosarcoma, pleomorphic undifferentiated sarcoma, synovial sarcoma, and malignant peripheral nerve sheath tumor.

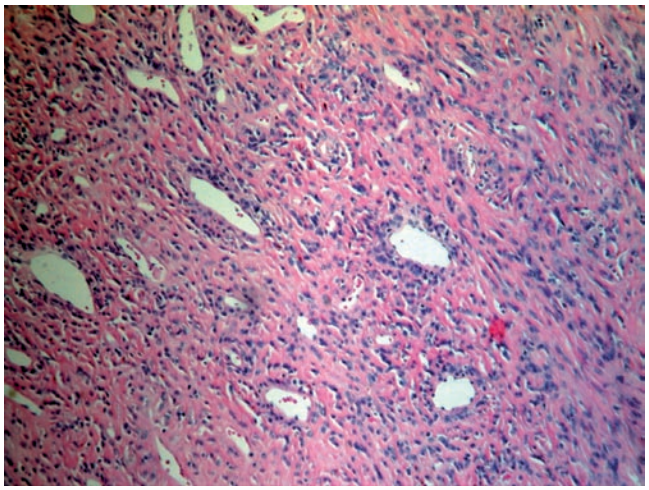

Fig. 57 Patternless proliferation of fibroblast-type spindle cells in variable cellularity and collagenous fibrous matrix with some open gorged, vein-like vasculature in a SFT

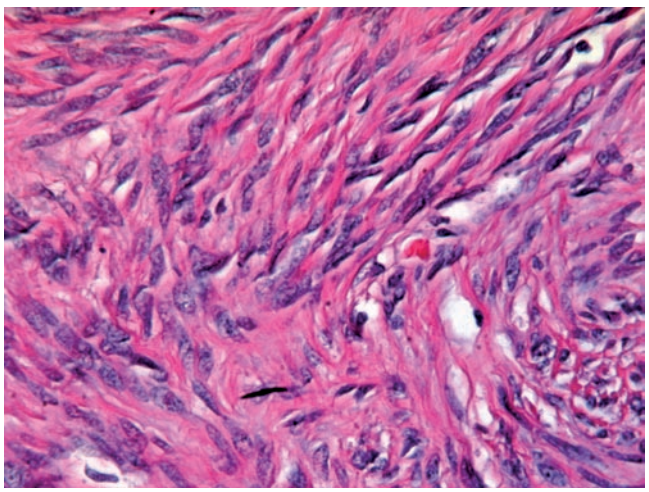

Fig. 58 The bland spindle cells and strongly and wavy eosinophilic collagenous fibers in SFT

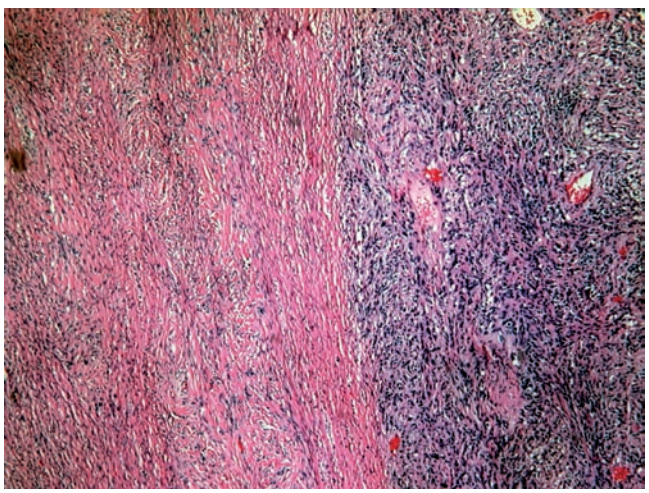

Fig. 59 High-grade transformation in SFT showing an abrupt juxtaposition of typical SFT (*left*) and high-grade fibrosarcoma-like area (*right*)

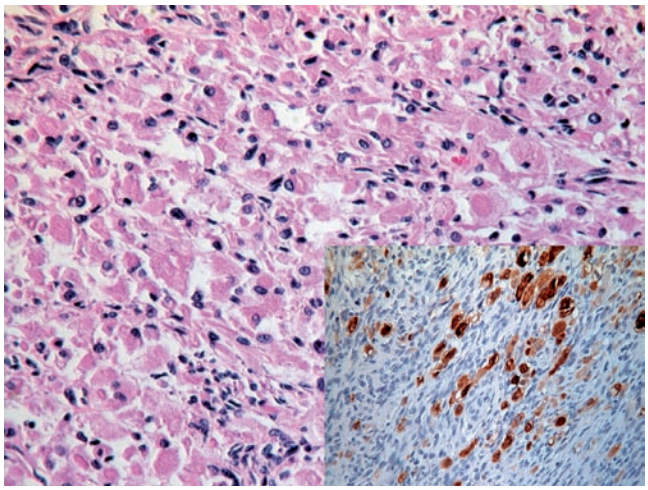

Fig. 60 Rhabdomyoblastic differentiation in a pleural SFT; insert shows myoglobin immunoreactivity

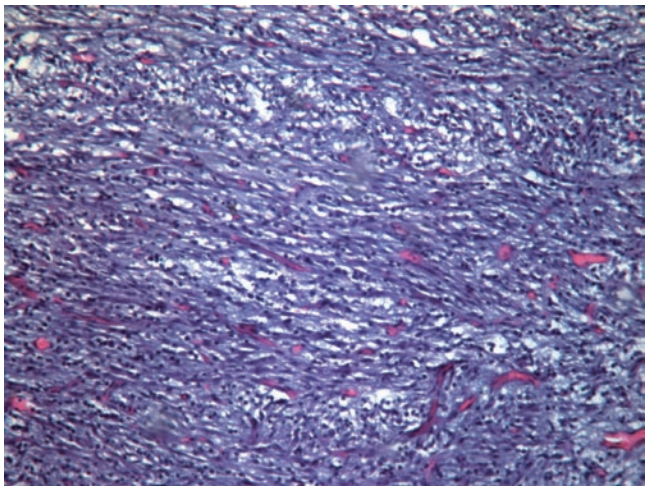

Fig. 61 Loosely arranged myofibroblastic-type of cells in the myxoid vascular stroma infiltrated by abundant plasma cells, lymphocytes, and eosinophils in an inflammatory myofibroblastic tumor

Treatment and Prognosis

Surgical excision with clear margins is the treatment of choice. Malignant solitary fibrous tumors behave aggressively with a high incidence of local recurrence and a full metastatic potential. Similar to their pleuropulmonary counterparts, majority of the tumors with typical low-grade histology behave in a benign fashion with low risk of local recurrence and no risk of metastasis. However, the histologic features cannot perfectly predict biological behavior in all cases and around 10–15% of the typical solitary fibrous tumors have been reported to develop metastasis with long-term follow-up (74).

Inflammatory Myofibroblastic Tumors (Inflammatory Pseudotumor, Plasma Cell Granuloma, Inflammatory Fibrosarcoma)

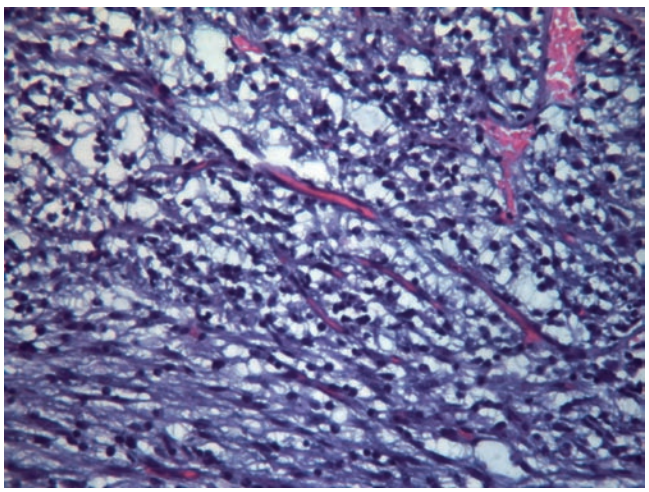

Fig. 62 High magnification of inflammatory myofibroblastic tumor, showing a bland cytology and inflammatory cells

Inflammatory myofibroblastic tumor occurs more frequently in children and young adults and can involve soft tissue and a variety of visceral organs. Lung, mesentery, and omentum are the most common visceral sites. Its clinical symptoms depend upon its anatomic location but it usually presents as mass with fever, weight loss, anemia, and pain.

Histopathology

Inflammatory myofibroblastic tumor is a well-circumscribed, multinodular firm white/tan mass with a whorled fleshy cut surface. Microscopically, it is composed of spindle to plump fibroblasts and myofibroblasts with weak eosinophilic or basophilic cytoplasm. Typically, the lesional cells are loosely arranged in the myxoid vascular stroma infiltrated by abundant plasma cells, lymphocytes, and eosinophils (Figs. 61 and 62). Sometimes the lesional cells are packed to form fascicules in a variable myxoid and collagenous stroma similar to those seen in smooth muscle tumor or fibromatosis. The tumor can also become very sclerotic and hypocellular with relatively sparse plasma cells and eosinophils. Calcification and osseous metaplasia can occasionally be seen in the sclerotic lesion. Increased cellularity, presence of atypical polygonal cells with large nuclei and prominent nucleoli, and increased mitoses are seen in tumors with malignant transformation (75). Large ganglion-like cells or Reed–Sternberg-like cells can be seen in some cases. The tumor cells are immunohistochemically positive for smooth muscle actin and desmin. Cytoplasmic ALK immunoreactivity is detected in around 50% of the cases (76). However, ALK reactivity has little impact in the diagnosis of inflammatory myofibroblastic tumor because of its low sensitivity and specificity.

Differential Diagnosis

Fibromatosis, fibrosarcoma, leiomyosarcoma, and Hodgkin lymphoma, granulation tissue, inflammatory reaction to various etiologies are on the list of differential diagnoses for inflammatory myofibroblastic tumor.

Treatment and Prognosis

Surgical resection is the treatment of choice. Rare cases regress spontaneously or after treatment with corticosteroids and nonsteroidal anti-inflammatory agents (75). Extrapulmonary tumors recur in 25% of the cases (77). Rare cases can metastasize with fatal outcome. Tumors with malignant histologic features or malignant transformation (inflammatory fibrosarcoma) are more aggressive.

Dermatofibrosarcoma Protuberans (DFSP)

DFSP is a low-grade sarcoma of the dermis and subcutis and affects the trunk and extremities of young to middle-aged adults. In its early stage, it presents as a plaque and small nodule which grows progressively to protuberant stage characterized by multinodular dermal and subcutaneous mass.

Histopathology

DFSP is grossly tan white and firm mass mainly centered in deep dermis and subcutaneous tissue with an infiltrative growth pattern. Histologically, the tumor is composed of monotonous fibroblast-like spindle cells arranged in uniform storiform pattern throughout the lesion with little intervening collagenous stroma throughout the lesion, a feature different from dermatofibroma and other fibrous tumors (Fig. 63). The tumor cells have slender nuclei with weak fibrillary eosinophilic cytoplasm. In the myxoid variant of DFSP, the characteristic storiform pattern is absent due to the increased intercellular myxoid stroma. One to five percent of the cases contain melanin pigment and these pigmented variants are called Bednar tumor (78). Nuclear hyperchromasia, pleomorphism, and tumor necrosis are absent and mitotic activity is scant in classic DFSP. In the periphery, tumor cells form arrays of long and narrow projections in lateral as well vertical directions to infiltrate the subcutis or other adjacent structures. High-grade transformation occurs in small number of the cases, particularly in recurrent cases. The histologic features of high-grade transformation are usually that of classic fibrosarcoma characterized by loss of storiform pattern and presence of fascicular pattern with larger tumor nuclei, hyperchromasia, and more active mitotic activity (79). High-grade transformation to pleomorphic undifferentiated sarcoma (MHF) can also occur. The immunoprofile of DFSP is CD34 positive, and Factor XIIIa and D2-40 negative, the opposite of dermatofibroma. In addition, DFSP is negative for smooth muscle actin and S100.

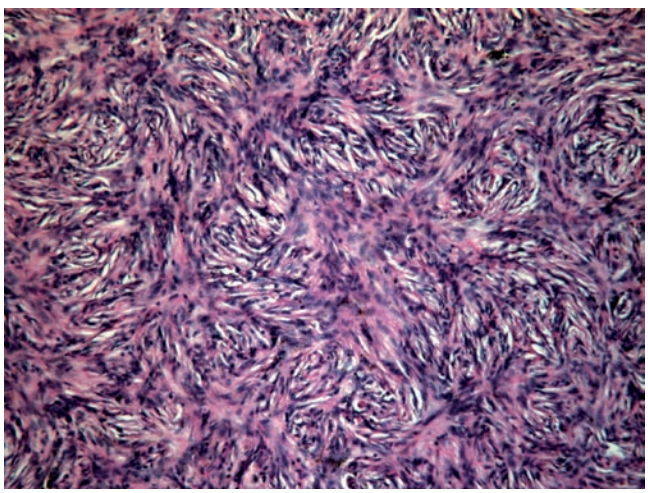

Fig. 63 Monotonous fibroblast-like spindle cells arranged in uniform storiform pattern with little intervening collagenous stroma in DFSP

Differential Diagnosis

Cellular dermatofibroma, benign fibrous histiocytoma, low-grade myxofibrosarcoma, myxoid liposarcoma, myxoid neurofibroma, and cellular myxoma are some of the lesions which can be confused with DFSP.

Treatment and Prognosis

Surgical excision with wide normal tissue margin is recommended because the slender infiltrating projections into the surrounding tissue are usually grossly underestimated during surgery. Local recurrence is common and occurs in 30–60% of cases. Metastases to lung or lymph nodes are extremely rare unless multiple recurrence and/or high-grade transformation have taken place (80).

Malignant

Myxofibrosarcoma (Myxoid Malignant Fibrous Histiocytoma)

Myxofibrosarcoma is considered to be one of the most common sarcomas in elderly patients. It affects the limbs most commonly. It is extremely rare in retroperitoneum or abdominal cavity. About two-thirds of cases develop in dermal/subcutaneous tissues and the remainder in deep fascia and deep soft tissue. It usually presents as a slow but persistent growing and painless mass (81).

Histopathology

Cutaneous lesions usually present as multiple poorly defined gelatinous nodules. Deep-seated tumors tend to form a single mass with an infiltrating margin. Under low magnification, the low-grade tumor shows multinodular growth pattern with incomplete fibrous septa, abundant myxoid stroma, and a very distinct curvilinear vasculature composed of elongated thin-wall, capillary-size blood vessels (Fig. 64). The tumor cells are spindle or stellate in shape. They are present either as individual cells within a myxoid matrix or as small fascicles in more cellular areas. Tumor cells tend to be condensed around the thin-wall vessels. Mild nuclear pleomorphism is seen (Fig. 65). In high-grade lesion, the tumor becomes hypercellular with less myxoid stroma, less vasculature, and more significant nuclear pleomorphism. Not infrequently, large tumor cells have vacuolated cytoplasm mimicking lipoblasts. In addition, bizarre multinucleated giant cells are sometimes seen. Increased mitotic activity and atypical mitotic figures are frequently seen with presence of tumor necrosis and hemorrhage. Immunohistochemically, there is no specific marker for myxofibrosarcoma.

Differential Diagnosis

Low-grade fibromyxoid sarcoma, cellular myxoma, myxoid liposarcoma, nodular fasciitis, and myxoid neurofibroma need to be differentiated from myxofibrosarcoma.

Treatment and Prognosis

Surgical resection with wide normal tissue margin is crucial to achieve good local control. Local recurrences are common and occur in 50–60% of cases. Low-grade lesions do not have metastatic potential unless high-grade transformation take place after multiple recurrences. Intermediate to high-grade lesions develop metastases to lung, bone, and lymph nodes in 20–35% of cases. Deep-seated high-grade tumors are more aggressive than cutaneous tumors with the same histologic grade. A local recurrence within 12 months increases tumor-associated mortality (81).

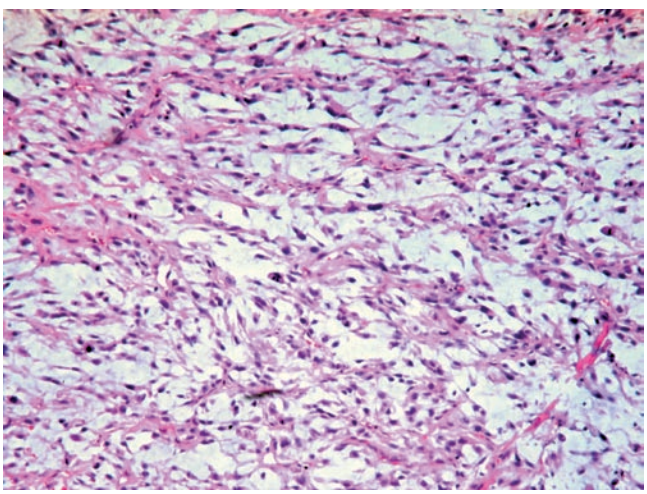

Fig. 64 Hypocellularity, abundant myxoid stroma, and a very distinct curvilinear vasculature composed of elongated thin-wall, capillary-size blood vessels in a low-grade myxofibrosarcoma

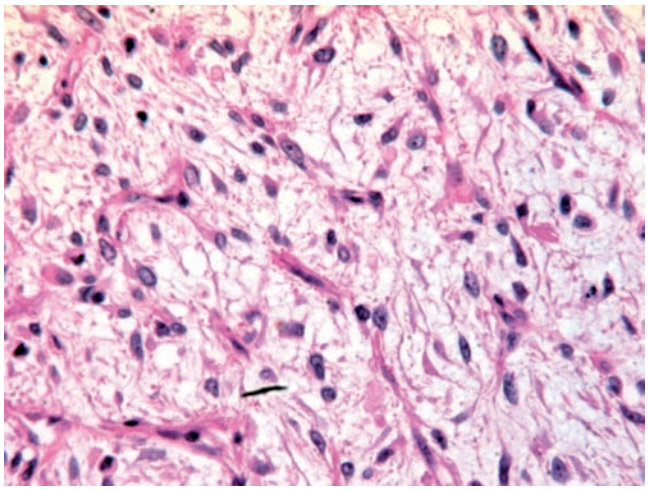

Fig. 65 More close-up examination reveals spindle and stellate tumor cells with eosinophilic fibrillary cytoplasm and atypical nuclear features in myxoid matrix

Low-Grade Fibromyxoid Sarcoma (Hyalinizing Spindle Cell Tumor with Giant Rosettes)

Low-grade fibromyxoid sarcoma is rare and typically occurs in young- to middle-aged adults. It has a predilection for the subfascial location of proximal extremities and trunk. It presents as a slow growing painless deep soft-tissue mass.

Histopathology

The tumor is composed of hypocellular population of uniformly bland, mitotically inactive fibroblast-type spindle cells in rich myxoid and fine collagenous fibrous stroma (Fig. 66a, b). The extent of cellularity, myxoid change, and fibrous stroma vary from areas to areas. The lesional cells show little striking pattern formation or short fascicular and whorling pattern in some cases. Some curvilinear small blood vessels or thick-walled arteriole-like vessels are seen but they are usually not numerous as seen in myxoid liposarcoma or myxofibrosarcoma. A subset of low-grade fibromyxoid sarcomas show giant rosettes characterized by hyalinized collagenous core rimmed by epithelioid fibroblasts (Fig. 67) (82). Areas of increased cellularity and nuclear pleomorphism are very unusual in primary tumors

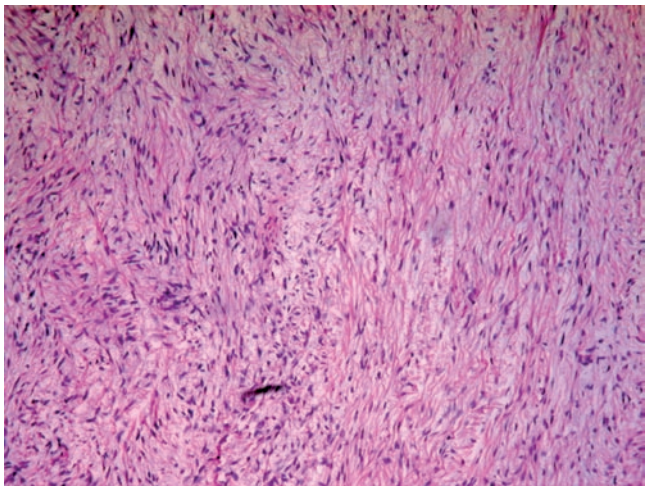

Fig. 66 Uniformly bland, mitotically inactive fibroblast-type spindle cells in rich myxoid and fine collagenous fibrous stroma in low-grade fibromyxoid sarcoma

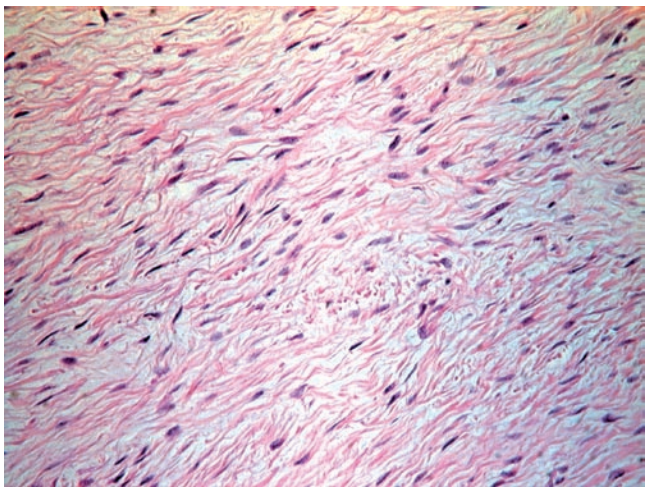

Fig. 67 High magnification shows bland cytology in the lesional stromal cells of a low-grade fibromyxoid sarcoma.

but can be seen in recurrent cases. Any significant increase in cellularity, nuclear atypism, pleomorphism, tumor vasculature, and/or mitotic activity could represent high-grade transformation or other sarcomas with fibromyxoid features. The immunophenotype of the low-grade fibromyxoid sarcoma is that of typical fibroblast and nonspecific.

Differential Diagnosis

Low-grade myxofibrosarcoma, cellular myxoma, myxoid neurofibroma, solitary fibrous tumor and fibromatosis need to be differentiated from low-grade fibromyxoid sarcoma.

Treatment and Prognosis

Surgical excision with clear normal tissue margin is the treatment of choice. Despite the bland histology, the tumors have a paradoxically aggressive behavior with relatively high incidence of local recurrence (68%) and metastasis (40%) in long-term follow-up (83). The most significant prognostic factor is probably the ability of the pathologist to correctly diagnose the tumor as a sarcoma with recurrent and metastatic potential and to treat it accordingly at first place.

Adult Fibrosarcoma

Although fibroblasts commonly exist in connective tissue and visceral organs, the incidence of fibrosarcomas accounts for only 1–3% of all adult sarcomas due to the very strict diagnostic criteria (84). It typically involves deep soft tissue of the extremities, trunk, and head and neck region of middle-aged and older adults. It can also derive from a preexisting low-grade fibroblastic tumor such as DFSP, SFT, and areas of scar, burn, or radiation therapy.

Histopathology

Fibrosarcoma is usually a solid white to tan firm mass. Histologically, it is composed of relatively uniform spindle cells characteristically arranged in fascicles running at different directions. At low magnification, a classic herringbone pattern is formed when the fascicles run in parallel but opposite direction (Fig. 67). Focal vague storiform growth pattern can also be seen. The tumor cells have fusiform and hyperchromatic nuclei with variable-sized nucleoli (Figs. 68 and 69). When the fascicles are sectioned transversely, the nuclei might look round instead of spindle on section. The tumor cell nuclei are closely packed with little intervening cytoplasm and extracellular stroma. Mitotic figures are always present but necrosis is not frequently seen. In some cases, less cellular areas with more collagenous stroma simulating fibromatosis

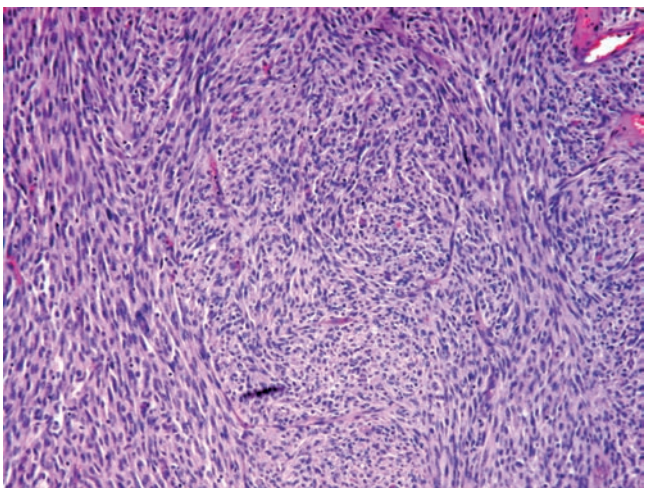

Fig. 68 Relatively uniform spindle cells characteristically arranged in fascicles and herringbone pattern in fibrosarcoma

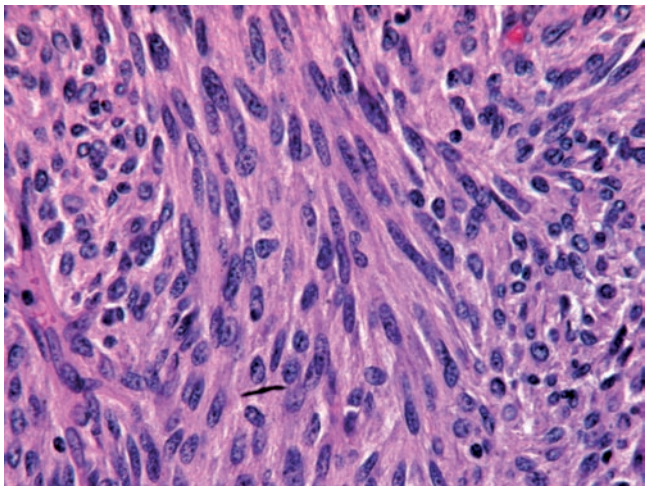

Fig. 69 High magnification shows fusiform and hyperchromatic nuclei with variable-sized nucleoli which are closely packed with little intervening cytoplasm and extracellular stroma in fibrosarcoma

can be seen focally. Although cytologic pleomorphism is allowed as one of the malignant features in a variety of other sarcomas, fibroblastic-type sarcomas with significant pleomorphism are currently classified as undifferentiated pleomorphic sarcomas or pleomorphic MFH instead of pleomorphic fibrosarcoma. Immunohistochemically, fibrosarcomas are typically positive for vimentin and variably positive for smooth muscle actin. Immunostains are performed primarily to exclude other spindle cell sarcomas in the differential diagnosis.

Differential Diagnosis

Because the fascicular pattern of growth is also commonly seen in a variety of spindle cell sarcomas and the lack of any specific fibroblastic markers, the diagnosis of fibrosarcoma is a diagnosis of exclusion. Differential diagnosis usually involves nodular fasciitis, fibromatosis, leiomyosarcoma, monophasic synovial sarcoma, pleomorphic undifferentiated sarcoma (MFH), malignant peripheral nerve sheath tumor, myofibroblastic sarcoma, and sarcomatoid carcinoma.

Treatment and Prognosis

Surgical excision with wide clear margin is the treatment of choice. In addition to a relatively high incidence of local recurrence, fibrosarcomas have full metastatic potential (85). Sites for metastasis are lung, bone, and rarely lymph nodes. Tumors with high cellularity, minimal collagen matrix, high mitotic rate (>20/10 hpf), and necrosis are more aggressive.

Malignant Fibrohistiocytoma (MFH) and Pleomorphic Undifferentiated Sarcoma

MFH used to be the most common diagnosis in adult soft-tissue sarcomas (86). Because of the availability of modern ancillary tests, reclassification of tumor entity, and our current concept of fibrohistiocytic differentiation, many tumors might have, in the past, been diagnosed as MFH have now been reclassified along other histological lineages (87). The remaining tumors with MFH morphology are now diagnosed as either myxofibrosarcomas (discussed above) or, if they have significant pleomorphism, as pleomorphic undifferentiated sarcoma (88). Pleomorphic undifferentiated sarcomas occur in older adults and affect the deep soft tissue of the limbs, trunk, and rarely retroperitoneum.

Histopathology

The tumors tend to be large and heterogenous on cut surface with necrosis and hemorrhage. Histologically, it is characterized by proliferation of significantly pleomorphic neoplastic cells. The morphology of tumor cells ranges from spindle, polygonal to bizarre giant mononuclear or multinucleated cells (Fig. 70a, b). Areas with more spindle cell features can show storiform pattern. The polygonal cells usually have abundant weakly eosinophilic or basophilic cytoplasm rendering a histiocytoid appearance. Variable poorly organized collagenous tissue and myxoid change are seen. Many tumors also contain numerous osteoclast-like multinucleated giant cells (giant cell MFH) and some are overwhelmed by exten-

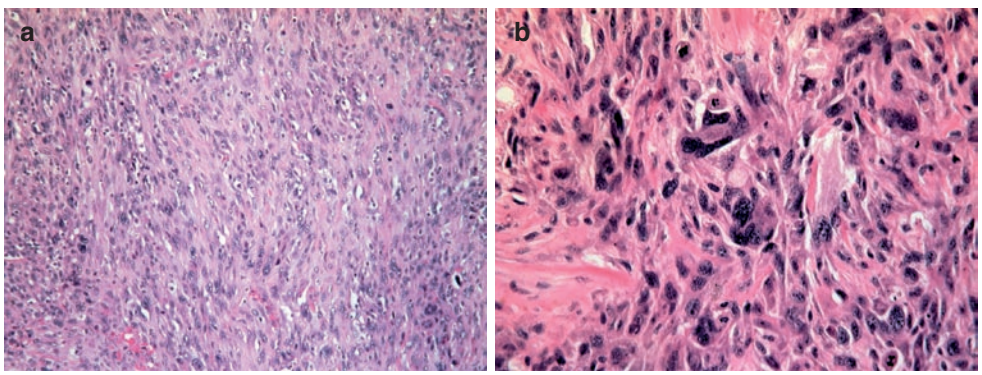

Fig. 70 **a** Pleomorphism in an undifferentiated spindle cell sarcoma. **b** Anaplastic bizarre giant mononuclear or multinucleated cells in pleomorphic undifferentiated sarcoma (MFH)

sive inflammatory infiltrates composed of histiocytes, neutrophils, eosinophils, lymphocytes, and plasma cells (inflammatory MFH). The tumor cells usually are positive for vimentin and variably for CD68, neither of which is specific for pleomorphic undifferentiated sarcoma. Instead, the use of immunohistochemical staining is mainly to exclude tumors in the differential diagnosis.

Differential Diagnosis

Because so many poorly differentiated tumors can exhibit pleomorphism and lack of specific morphologic and immunophenotypic features, the diagnosis of pleomorphic undifferentiated sarcoma is established by exclusion of (1) pleormophic sarcomas of other histologic lineages such as pleomorphic liposarcoma, pleomorhpic leiomyosarcoma, and pleomorphic rhabdomyosarcoma; (2) giant cell-rich tumors such as giant cell tumor of soft part, extraskeletal osteosarcoma, and giant cell-rich carcinomas; and (3) other tumors with extensively inflammatory reactions such as inflammatory myofibroblastic tumor and Hodgkin's lymphoma.

Treatment and Prognosis

Surgical excision with wide clear normal tissue margin is treatment of choice. Because of the deep location and large size, complete excision is usually difficult in many cases. Local recurrence for tumors diagnosed as pleomorphic MFH ranges from 40 to 60% and metastasis to lung, lymph nodes, liver, and bone occurs in 25–50% of the cases (89).

Tumors with Myogenic Differentiation

Benign

Leiomyoma

Leiomyoma can occur in superficial and deep soft-tissue locations, abdominal/pelvic cavity, and various visceral organs such as genital–urinary tracts and upper GI tract. Leiomyomas of the visceral organs are not discussed in this chapter. Most of soft-tissue leiomyomas occur in the superficial or cutaneous location and less frequently in deep location of extremities, retroperitoneum, abdominal, and pelvic cavity. They likely arise from the pilar arrector muscle or smooth muscle of vascular wall in these locations. Leiomyomas mainly affect young to middle-aged adults. Retroperitoneal, abdominal, and pelvic tumors have predilection for female sex.

Histopathology

Leiomyoma is well-circumscribed, gray-white, firm mass. The size of the tumors tends to be smaller in superficial tumors than those of deep tumors. Histologically, the tumors are composed of spindle cells of smooth muscle type with cigar-shaped nuclei and eosinophilic fine fibrillary cytoplasm with variable cytoplasmic vacuoles (Figs. 71 and 72). The tumor cells form well-organized intersecting fascicles. Epithelioid cellular morphology can be seen in some cases. There should not be nuclear atypia. Mitotic figures are hard to find with mitotic rate of <1/50 hpf in most of cases and <5/50 hpf in retroperitoneal and pelvic peritoneal lesions in females. No tumor necrosis is present. Areas of degenerative and reactive changes such as fibrosis, hyalinization, myxoid change, and calcification can be found in larger tumors.

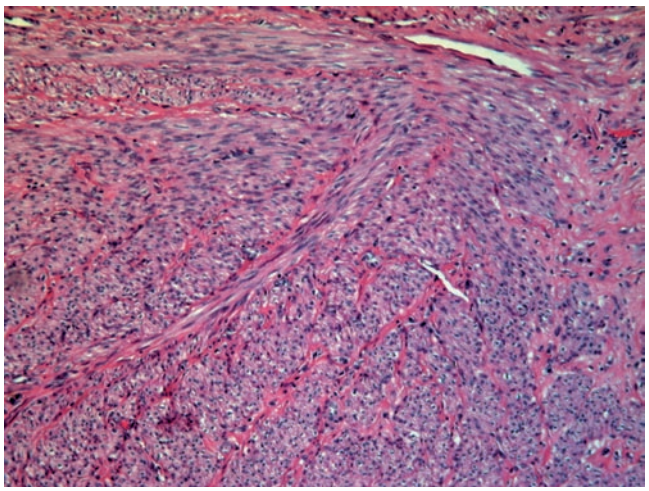

Fig. 71 Smooth muscle-type spindle cells form well-organized fascicles in leiomyoma

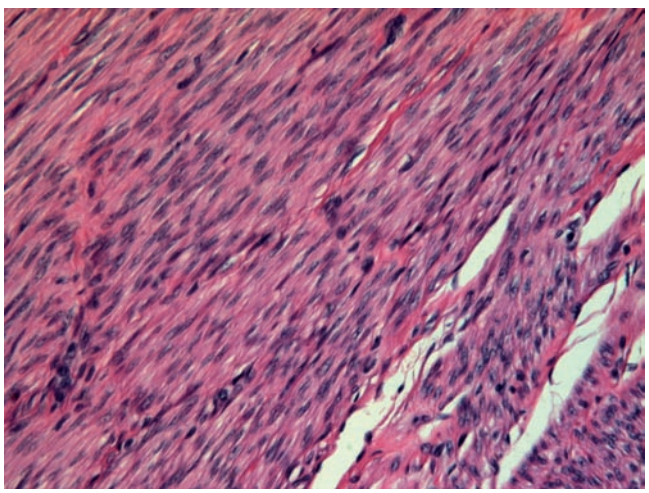

Fig. 72 Rather uniform and bland spindle cells of smooth muscle type with cigar-shaped nuclei and eosinophilic fine fibrillary cytoplasm with variable cytoplasmic vacuoles in leiomyoma

Differential Diagnosis

Extreme caution should be taken in dealing with smooth muscle tumors from deep locations. Any nuclear atypia should always prompt vigorous search for mitotic figures and additional sampling of the tumor to rule out well-differentiated leiomyosarcoma. Soft-tissue leiomyoma should also be differentiated gastrointestinal stromal tumor (GIST) and various benign or low-grade fibrous and myofibroblastic tumors.

Treatment and Prognosis

Leiomyoma can be cured by complete excision. Nondestructive recurrences occur occasionally in deep soft-tissue lesions (90). The prognosis is excellent for cutaneous leiomyoma after local excision. In cases of deep smooth muscle tumor where benignity cannot be 100% certain, complete excision with close follow-up is recommended.

Rhabdomyoma

Rhabdomyomas are rare benign tumors of skeletal muscle lineage. There are adult, fetal, and genital types of rhabdomyomas. Adult soft-tissue rhabdomyomas commonly occur in the head and neck of young to middle-aged adults with a 3:1 male predilection. They typically present with airway obstruction however, many present as asymptomatic mucosal and soft-tissue masses (91). Genital rhabdomyomas are very rare and present as a polypoid mass in the vagina, vulva, or cervix of young females (92). Fetal rhabdomyomas commonly occur at a younger age (median age 4 years) with similar male predilection as adult rhabdomyomas and also affect the soft tissue and mucosal sites of the head and neck region. Some cases are congenital and some are seen in patients with nevoid basal cell syndrome (93). Unlike cardiac rhabdomyomas, there does not seem to be an association with tuberous sclerosis in soft-tissue rhabdomyoma.

Histopathology

Rhabdomyomas are usually small (median size 3.0 cm), well-circumscribed, tan to brown solid mass. Histologically, adult rhabdomyoma is composed of closely packed uniform large polygonal rhabdoid cells with single round nucleus, abundant eosinophilic, granular cytoplasm, and distinct cytoplasmic membrane (Fig. 73a, b). The cytoplasm of some cells is variably vacuolated giving a "spider" appearance to the remaining cytoplasm. Cytoplasmic eosinophilic crystalline and cross-striation are seen focally.

Genital-type rhabdomyomas are usually polypoid masses that are composed of round or strap-like well-matured rhabdomyoblasts with more abundant intercellular fibrous stroma and dilated vein-like vascular spaces.

Fetal rhabdomyomas are composed of bland fetal-type rhabdomyoblasts which are either primitive spindle cells with little cytoplasm or long strap cells with more eosinophilic cytoplasm. The fetal-type rhabdomyoblasts are arranged haphazardly and loosely in abundant myxoid stroma. The rhabdomyoblasts in some fetal type cases show more advanced cytoplasmic differentiation toward adult-type rhabdomyomas (intermediate, juvenile, or cellular type).

In all variants of rhabdomyomas, there is lack of tumor necrosis and mitotic activity. Although prominent nucleoli can be seen in some rhabdoid or ganglion-like rhabdomyoblasts, significant nuclear atypia or pleomorphism is absent.

PAS stain can highlight intracellular glycogen in adult and genital rhabdomyomas. Rhabdomyomas are also positive for myoglobulin, desmin, and common muscle actin.

Differential Diagnosis

Rhabdomyosarcoma (treated or untreated), leiomyosarcoma, granular cell tumor, hibernoma, treated immature teratoma, and paraganglioma need to be differentiated from rhabdomyomas.

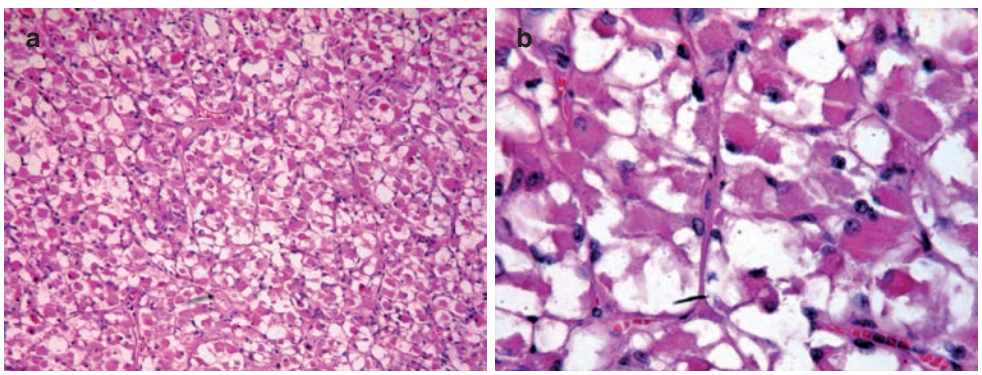

Fig. 73 **a** Closely packed uniform large polygonal rhabdoid cells with single round nucleus, abundant eosinophilic, granular cytoplasm, and distinct cytoplasmic membrane in rhabdomyoma. **b** The cytoplasm of some cells is variably vacuolated giving a "spider" appearance to the remaining cytoplasm in rhabdomyoma

Treatment and Prognosis

Local excision is the treatment of choice. Local recurrence is low and mainly due to incomplete excision in adult and fetal rhabdomyomas (91, 93). Malignant transformation and metastasis have not been reported.

Malignant

Leiomyosarcoma

Soft-tissue leiomyosarcoma usually occurs in older adults and also rarely in children with HIV infection. There are three types of leiomyosarcomas according to anatomic locations: retroperitoneum/intraabdominal type, cutaneous/subcutaneous type, and major vessel type. Leiomyosarcomas of the retroperitoneum and inferior vena cava have a female predilection. Its clinical presentations are determined by its size and location. Cutaneous/subcutaneous leiomyosarcomas present as palpable masses and deep lesions might become symptomatic due to mass effect on adjacent structures such as genital urinary tracts, gastrointestinal tract, and major blood vessels (94).

Histopathology

Leiomyosarcoma appears to be tan to gray in color frequently with a heterogeneous cut surface. Histologically, it is composed of a proliferation of spindle cells with cigar-shaped nuclei and fibrillary eosinophilic cytoplasm. Intracytoplasmic vacuoles at one end of the nucleus are characteristic but not pathognomonic of smooth muscle differentiation. The tumor cells can form whorling fascicles, a storiform pattern, and/or palisading pattern (Figs. 74 and 75). The tumor cigar-shaped nuclei frequently show transverse nuclear indentation and inward nuclear envelope folding. Nuclei are usually hyperchromatic or vesicular with variable pleomorphism. Mitotic activity is easily identified and atypical mitotic figures are frequent. Tumor necrosis, variable fibrous and myxoid stroma, and focal hemangiopericytoma-like vasculature can also be seen. In addition to typical spindle cell morphology, some leiomyosarcomas can exhibit epithelioid or significant pleomorphic cytologic features focally or diffusely. Immunohistochemically, leiomyosarcomas are positive for SMA, desmin, and other smooth muscle markers. Focal cytokeratin, EMA, CD34, and S100 may also be detected in some cases.

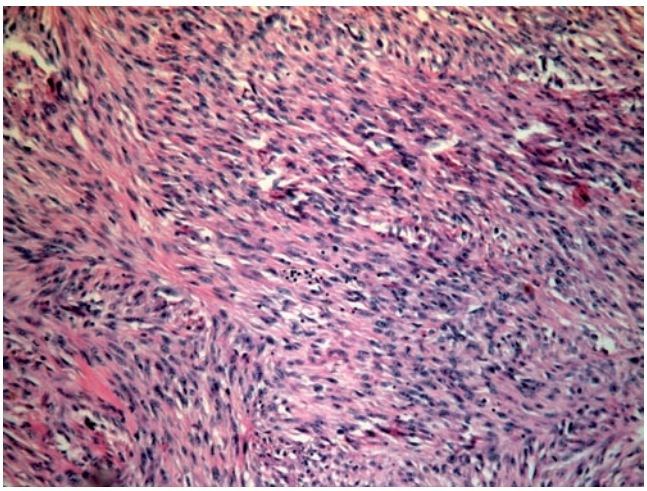

Fig. 74 Spindle cells in leiomyosarcoma form variable whorling fascicles and nuclear atypia

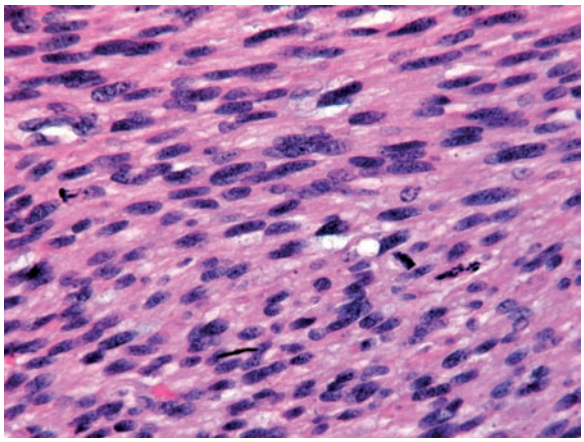

Fig. 75 Tumor cells of leiomyosarcoma have cigar-shaped nuclei and fibrillary eosinophilic cytoplasm with intracytoplasmic vacuole at one end of the nucleus characteristic but not pathognomonic for smooth muscle differentiation

Differential Diagnosis

Typical leiomyosarcoma needs to be differentiated from a variety of spindle cell tumors such as leiomyoma, myofibroblastic sarcoma, intimal sarcoma, monophasic synovial sarcoma, fibrosarcoma, gastrointestinal stromal tumor, spindle cell rhabdomyosarcoma, angiomyolipoma, malignant hemangiopericytoma, and malignant peripheral nerve sheath tumor. Pleomorphic leiomyosarcoma needs to be differentiated from other pleomorphic sarcomas such as pleomorphic rhabdomyosarcoma, pleomorphic undifferentiated sarcoma (MFH), and pleomorphic liposarcoma. Epithelioid leiomyosarcoma needs to be differentiated from round cell liposarcoma, carcinoma, and melanoma.

Treatment and Prognosis

Surgical excision with wide clear margin is the treatment of choice. Prognosis is heavily dependent upon tumor location and size, both of which are usually closely related. Other prognostic factors are histologic grade, and bone and vascu-

lar involvement. Leiomyosarcomas of retroperitoneum and large vessels have the worse prognosis with high incidences of local recurrence and distant metastasis. The outcomes of cutaneous and subcutaneous leiomyosarcomas are better than that of other nonretroperitoneal leiomyosarcoma regardless of the histologic grade (95). Lung is the most common site for metastasis. Other sites for metastasis are skin, soft tissue, and bone.

Rhabdomyosarcoma

Rhabdomyosarcomas are a group of sarcomas with differentiation towards either striated muscle or rhabdomyoblasts. They are subclassified to embryonal, alveolar, and pleomorphic types. Rhabdomyosarcoma is the most common sarcoma of pediatric population.

Embryonal rhabdomyosarcoma accounts for three fourths of all rhabdomyosarcomas and primarily occurs in children younger than 15 years old (96). It typically affects the head and neck region, paratesticular area, urinary tract, and biliary tract. There are two variants of embryonal rhabdomyosarcomas: botryoid and spindle cell variants. Botryoid type occurs in mucosa of the head and neck, biliary tract, and urinary tract of young children. Spindle cell rhabdomyosarcoma is very rare and typically occurs in the scrotal soft tissue and head and neck site. Alveolar rhabdomyosarcoma most commonly occurs in deep soft tissue of limbs, and less commonly in paranasal sinuses, paraspinal and perineal regions. It can occur at all ages but more often in older children or young adults (97). Pleomorphic rhabdomyosarcoma is extremely rare and occurs almost always in adults older than 45 years old. It usually affects the deep soft tissue of the lower extremities.

In addition to a rapid growing mass, the clinical presentation of a rhabdomyosarocoma is usually related to the mass effects to adjacent organs and structures.

Histopathology

Rhabdomyosarcomas are poorly circumscribed, fleshy, and tan mass. Embryonal rhabdomyosarcomas show a diverse histologic appearance. The tumor cells can be round, spindle, and/or strap shape with hyperchromatic and vesicular nuclei (Fig. 76). The cytoplasm of the tumor cells can be scant and amphophilic to abundant fibrillary eosinophilic dependent upon the degree of myoid differentiation (Fig. 77). Many pretreated embryonal rhabdomyosarcomas are dominated by primitive undifferentiated round rhabdomyoblasts with rare strap cells or cells with cross-striation (Fig. 78). Tumor cells tend to show more myoid differentiation or maturation after chemotherapy. Tumor cells are usually arranged haphazardly with alternating hypercellular and myxoid hypocellular zones. Multinucleated giant tumor cells are rare.

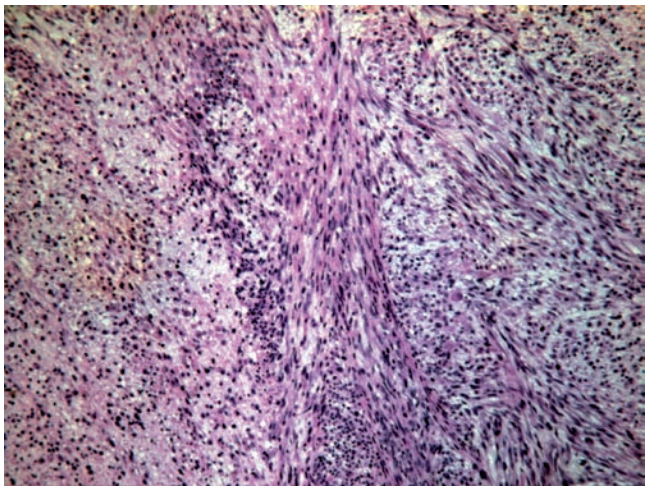

Fig. 76 Spindle and round cells with hyperchromatic and vesicular nuclei in myxoid stroma in embryonal rhabdomyosarcoma

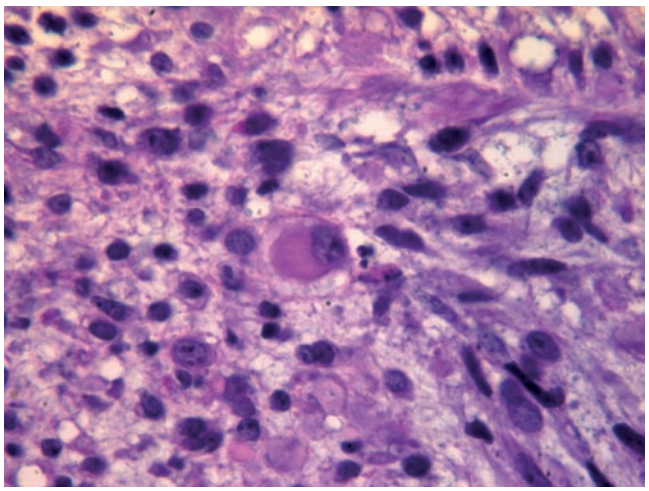

Fig. 77 The cytoplasm of the rhabdomyosarcoma tumor cells can be scant and amphophilic to abundant fibrillary eosinophilic dependent upon the degree of myoid differentiation

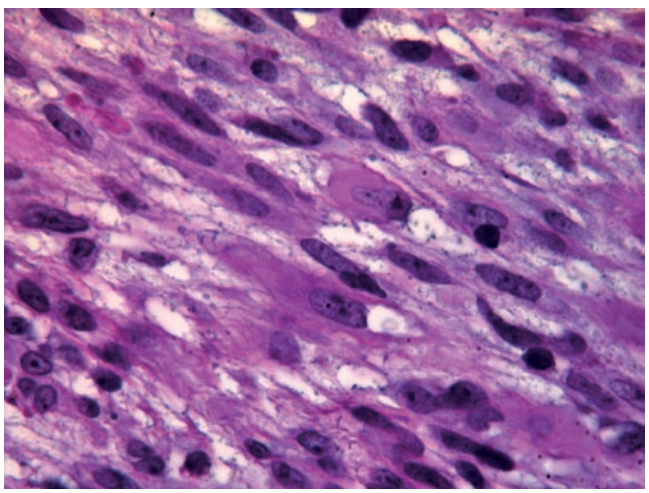

Fig. 78 Rare strap cells in a rhabdomyosarcoma

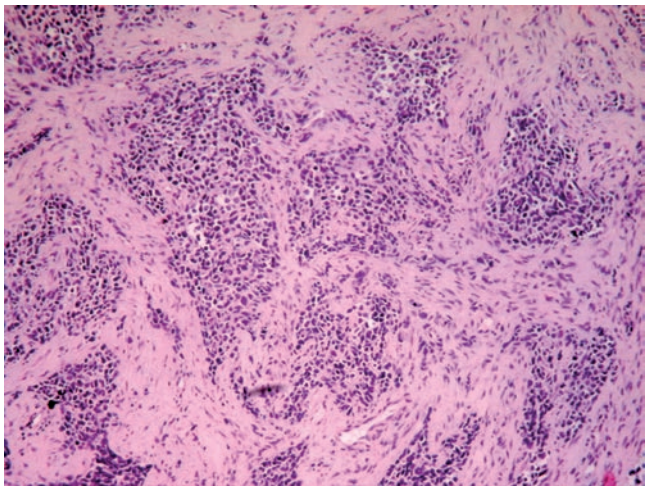

Fig. 79 Nests of atypical round cells with alveolar growth pattern and fibrovascular septae around the nests in alveolar rhabdomyosarcoma

Botryoid rhabdomyosarcoma presents as a polyploid mass on the mucosal surface. Histologically, it is composed of round to spindle rhabdomyoblasts with a myxoid background. The submucosa shows a zone of increased cellularity (Cambium layer). Spindle cell variants are composed of monotonous spindle rhabdomyoblasts arranged in whorls or fascicles. The spindle rhabdomyoblasts are typically fusiform with moderate amount of bright eosinophilic cytoplasm sometimes with cross-striation.

Alveolar rhabdomyosarcoma is typically a round cell sarcoma characterized by an alveolar growth pattern. The alveolar pattern is the result of loss or lack of extracellular matrix in a nest of round rhabdomyoblasts and presence of fibrovascular septae around the nest (Fig. 79). Sometimes this characteristic alveolar pattern is not apparent in some tumors which show solid sheets or nests of tumor cells and are referred to solid variant of alveolar rhabdomyosarcoma (98). In rare cases, mixed typical alveolar pattern and embryonal features are seen.

Pleomorphic rhabdomyosarcoma is characterized by numerous large and pleomorphic rhabdomyoblasts which can be globoid, spindle, and tadpole in shape with hyperchromatic nuclei and abundant eosinophilic cytoplasm (Fig. 80a, b). Although the tumor cells have a rhabdoid appearance in general, cross-striation is extremely hard to find and identification of striated muscle differentiation usually requires either ultrastructural examination or immunohistochemical evaluation (99).

Immunohistochemically, rhabdomyoblastic cells are positive for nonspecific myogenic markers such as desmin, common muscle actin, and more specific myogenic markers such as myoD, myogenin, and myoglobin. Myogenin staining pattern is usually diffuse in alveolar rhabdomyosarcoma and spotty in embryonal rhabdomyosarcomas. Chapter 5 has additional details on the molecular diagnosis of rhabdomyosarcoma.

Differential Diagnosis

Because of the wide spectrum of histologic appearance of rhabdomyosarcomas, the list of differential diagnosis is long and includes various round cell tumors such as EWS/PNET, poorly differentiated synovial sarcoma, lymphoma, melanoma, olfactory neuroblastoma, and round cell liposarcoma; spindle cell sarcomas with smooth muscle differentiation such as leiomyosarcoma; and various pleomorphic poorly differentiated sarcomas and carcinomas with rhabdomyoblastic differentiation such as Wilm tumor, Triton tumor, immature teratoma, malignant mixed mellerium tumor, and dedifferentiated sarcomas. The treated rhabdomyosarcoma should also be differentiated from their benign counterpart rhabdomyoma.

Treatment and Prognosis

Chemotherapy is the treatment of choice for rhabdomyosarcoma although its effectiveness in adult patients is still

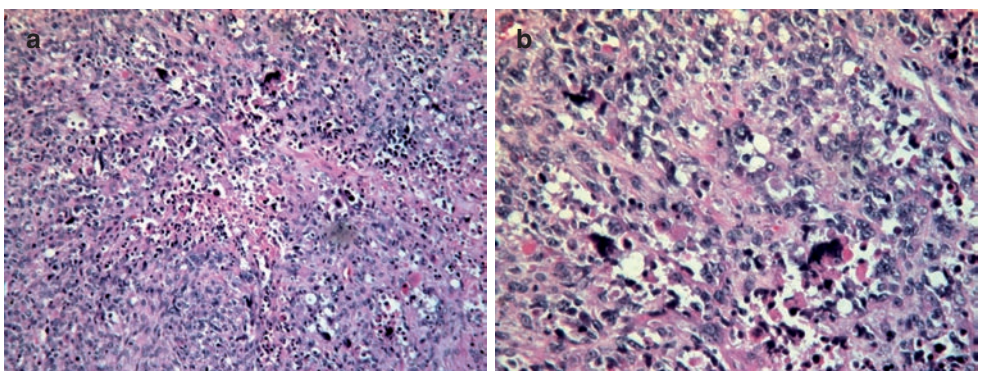

Fig. 80 **a** Large and pleomorphic rhabdomyoblasts in globoid, spindle or tadpole shape with hyperchromatic nuclei and abundant eosinophilic cytoplasm in pleomorphic rhabdomyosarcoma. **b** Despite the rhabdoid appearance in general, cross-striation is extremely hard to find in pleomorphic rhabdomyosarcoma

unclear. Prognosis depends upon stage, histologic type, age, and tumor site. Older age, alveolar type, anaplastic feature, and parameningeal and extremity tumors have worse prognosis (100). Young age, botryoid and spindle variant of embryonal rhabdomyosarcoma, paratesticular and orbital tumors tend to have better prognosis. Chemotherapy is less effective for pleomorphic rhabdomyosarcoma and the prognosis for pleomorphic rhabdomyosarcoma is generally poor (99).

Tumors with Neuroectodermal Differentiation

Benign

Traumatic Neuroma

Traumatic neuroma is a benign disorganized proliferation of traumatized nerve. It usually presents as a painful nodule arising from the proximal stump of the severed nerve.

Histopathology

Traumatic neuroma is a circumscribed gray-white nodule usually associated with nerve fibers. Histologically, there is a disorganized proliferation of nerve bundles or fascicles composed of axons, Schwann cells, and perineurial cells in a fibrocollagenous stroma with variable myxoid change (Fig. 81).

Differential Diagnosis

Traumatic neuroma needs to be differentiated from neurofibroma, other forms of neuromas, and scar.

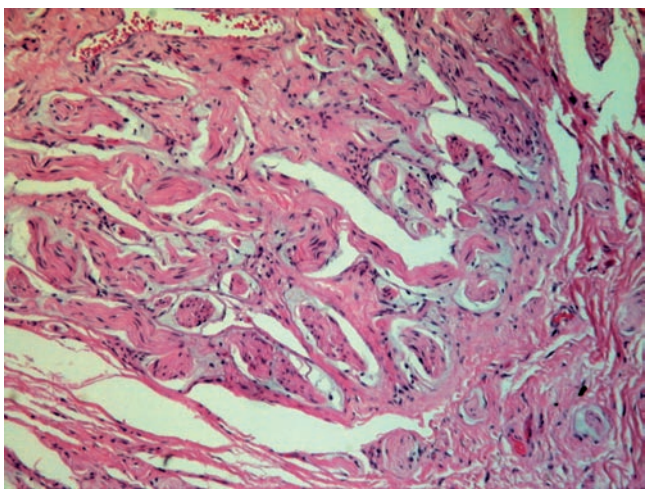

Fig. 81 Disorganization of nerve bundles or fascicles with proliferation of schwann cells and perineurial cells in fibrocollagenous stroma with mild myxoid change in a traumatic neuroma

Treatment and Prognosis

The treatment is simple excision with proper placement of the proximal stump of the nerve into normal soft tissue.

Schwannoma (Neurilemoma)

Schwannoma is a benign peripheral nerve sheath tumor with exclusively schwannion differentiation. It occurs more commonly in adult life. It can arise almost everywhere in the body but is usually associated with peripheral nerve of the head and neck, extremities, mediastinum, and paraspinal region. It presents as a slow-growing mass with symptoms associated with pressure on adjacent structures.

Histopathology

Schwannoma is usually an encapsulated mass eccentrically associated with a nerve. Histologically, it is composed of nodular or multinodular growth of spindle cells exhibiting Schwann cell differentiation. The spindle cells have angulated, comma-shaped, or bullet-shaped nuclei with fine chromatin, and ill-defined eosinophilic fibrillary cytoplasm (Fig. 84). The cellularity alternates from areas to areas with variable myxoid to hyaline stromal changes. In the cellular areas (Antoni A areas), the cells are arranged in short fascicles, swirls and/or palisading pattern (Verocay bodies) (Fig. 82). The hypocellular areas (Antoni B areas) are characterized by myxoid and variable fibro/hyaline stroma (Fig. 83). Various degenerative/reactive changes such as hemorrhage, hemosiderin deposition, organizing thrombi, inflammatory infiltrate, xanthomatous infiltrate, pseudocyst formation, calcification, necrosis, hyalinized thick-walled vessels, and presence of pleomorphic and hyperchromatic nuclei are commonly seen.

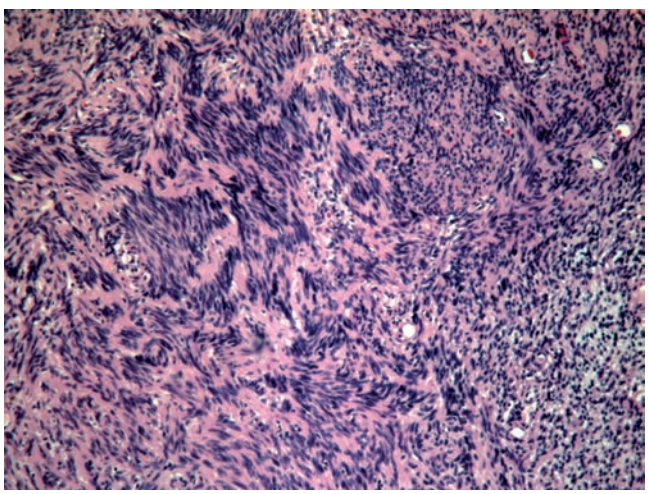

Fig. 82 Cellular areas (Antoni A areas) of schwannoma characterized by short fascicles, swirls, and/or palisading pattern (Verocay bodies)

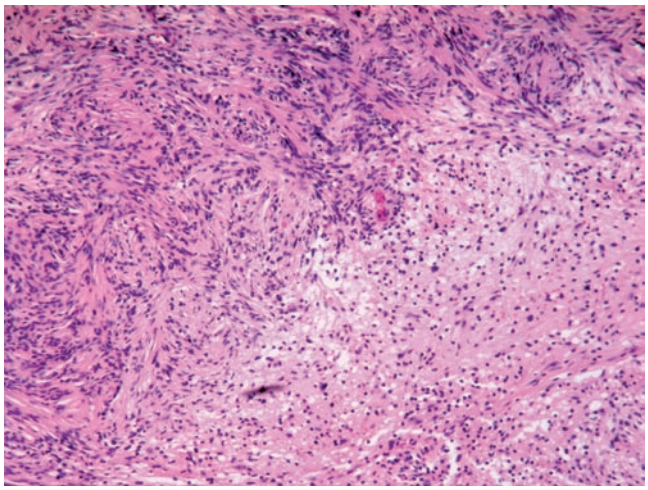

Fig. 83 Hypocellular areas (Antoni B areas) alternating with cellular areas and characterized by myxoid and variable fibro/hyaline stroma in Schwannoma

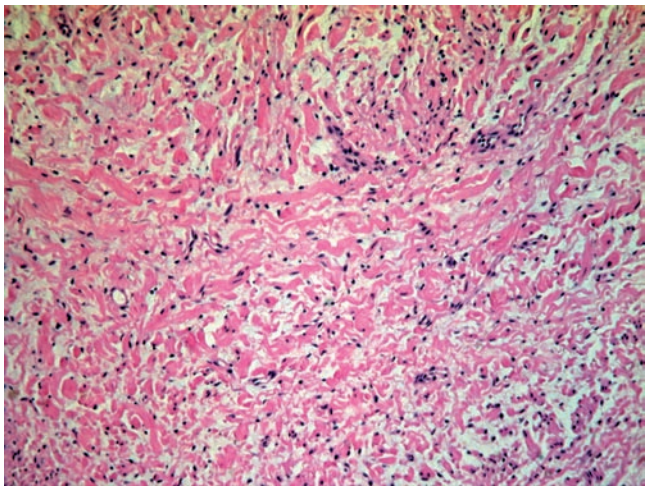

Fig. 84 Comma-shaped schwann cells admixed with numerous fibroblast-like spindle cells in abundant delicate fibrocollagenous fibers in a case of Schwannoma.

Lesions with uniformly hypercellular areas without Antoni B areas are called cellular schwannoma. They have a tendency to arise in the paraspinal region. Although mitotic activity is very scant in conventional schwannoma, increased mitotic activity is common in cellular schwannoma (101). However, there are no atypical mitotic figures or significant nuclear atypia. Immunohistochemically, schwannoma is strongly positive for S100, D2-40, and NSE but negative for neurofilament.

Differential Diagnosis

Neurofibroma, leiomyoma, inflammatory reaction, gastrointestinal stromal tumor, fibrosarcoma, leiomyosarcoma, spindle cell melanoma, and malignant peripheral nerve sheath tumor sometimes need to be differentiated from schwannoma. In addition to the above malignant tumors, cellular schwannoma also needs to be differentiated from malignant peripheral nerve sheath tumor.

Treatment and Prognosis

Conservative local excision is adequate for cure with preservation of the functional nerve. Recurrence is rare even after incomplete excision in conventional schwannoma but high in cellular schwannomas which cannot be completely excised. Malignant transformation is extremities rare.

Neurofibroma

Neurofibroma is another benign peripheral nerve sheath tumor. In addition to Schwann cells, the tumor also contains variable numbers of fibroblasts, and axonal processes of neurons. Multiple neurofibromas are usually associated with von Recklinghausen's disease (NF-1). Majority of localized neurofibromas are usually sporadic and tend to occur in early adulthood. Sporadic localized neurofibroma presents as a painless, slow-growing mass usually in the superficial location closely associated with nerve trunk. In NF-1 patients, neurofibromas are larger, more diffuse, and multiple in deep and superficial locations, frequently with plexiform growth pattern involving the nerve trunk (plexiform neurofibroma).

Histopathology

Neurofibroma can be an encapsulated fusiform mass (localized neurofibroma) or a plexiform mass (plexiform neurofibroma) derived from a nerve. It can also show diffuse growth without capsule (diffuse neurofibroma). Histologically, it is proliferation of Schwann cells, fibroblasts, and perineurial cells in fascicular, whorling, storiform, and/or haphazard pattern. Concentric structures resembling pacinian bodies are seen in some cases (pacinian neurofibroma). The Schwann cells are cytologically similar to those seen in schwannoma but have little schwanian organization as seen in schwannoma. The Schwann cells are admixed with numerous fibroblast-like spindle cells in abundant fibrocollagenous stroma with variable myxoid, inflammatory, or xanthomatous change (Fig. 84). Variable numbers of neuronal axons are entrapped in the lesion. In plexiform neurofibroma, the nerve sheath proliferation is primarily confined within the perineurium of numerous disorganized nerve fascicles in a plexiform growth pattern (Fig. 85). Scattered hyperchromatic pleomorphic cells and increased cellularity (cellular neurofibroma) are seen in some cases (Fig. 86). However, in these cases, mitoses are very rare. Inflammatory cells and fibroblasts may account for some of the perceived cellularity. Immunohistochemically, the Schwann cells in neurofibroma are positive for S100. The

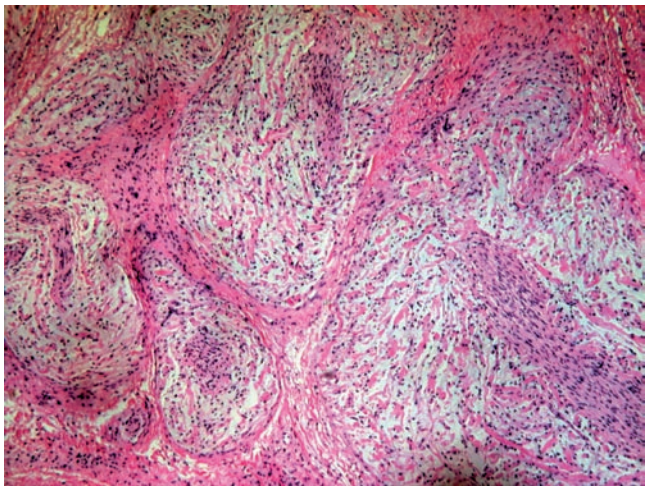

Fig 85 Nerve sheath proliferation confined within the perineurium of numerous disorganized nerve fascicles in a plexiform neurofibroma

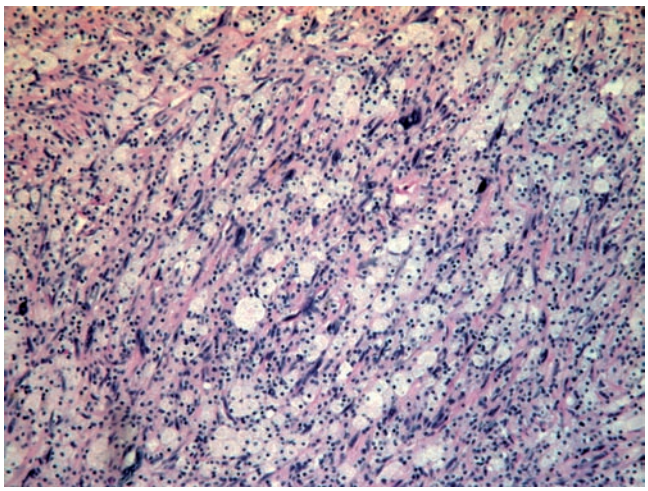

Fig. 86 Scattered hyperchromatic pleomorphic cells and florid foamy xanthomatous inflammation in a neurofibroma

entrapped axons are positive for neurofilament. As opposed to schwannoma, schwannoma, D2-40 (podoplanin) is usually negative in neurofibroma.

Differential Diagnosis

Neurofibroma needs to be differentiated from schwannoma, low-grade myxofibrosarcoma, myxoma, blue nevus, myxoid DFSP, desmoplastic melanoma, and malignant peripheral nerve sheath tumor.

Treatment and Prognosis

Localized and diffuse cutaneous neurofibromas rarely undergo malignant transformation and can be treated with local excision. However, resection of localized intraneural neurofibroma requires sacrifice of the parent nerve. Because of the low risk of malignant transformation, excision of major functional nerves might not be warranted. The same is true in case of plexiform neurofibroma which has the highest risk of malignant transformation (5%) (102). However, excision of the tumor and the parent nerves might be inevitable in cases with pain and rapid increase in size which may herald malignant transformation (103).

Granular Cell Tumor (Granular Cell Schwannoma, Granular Cell Myoblastoma)

Granular cell tumors were earlier thought to be myogenic origin. Currently however, they are thought to have a neural differentiation (104). It tends to occur as a superficial mass in the tongue, chest wall, and arms of adults. Rarely, granular cell tumor involves visceral organs.

Histopathology

Granular cell tumor is typically a poorly defined submucosal or dermal lesion. Histologically, it is characterized by proliferation of round or polygonal cells with uniform central nuclei and abundant, coarse granular eosinophilic cytoplasm (Fig. 87). The tumor cells are arranged in nests, strands, cords, and sheets in an alarming infiltrative growth pattern in some cases. Nerves are frequently seen adjacent to or entrapped within hyperplasia. The overwhelming majority of cases show no significant nuclei pleomorphism or mitotic activity. Malignant cases are rare and can be diagnosed by the presence of three of the following features: marked cellularity, pleomorphism, high nucleus to cytoplasmic ratio, nucleolar prominence, increased mitoses, prominent spindling of the cells, and frequent necrosis (105). The immunophenotype of granular cell tumors are that of peripheral nerve

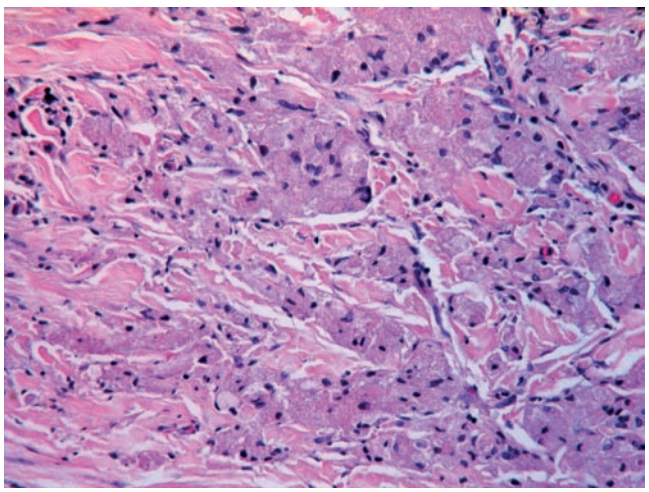

Fig. 87 Round or polygonal cells with uniform small nuclei and abundant, coarse granular eosinophilic cytoplasm in granular cell tumor

sheath which is positive for S100 but negative for melanocytic, myoid, and epithelial markers.

Differential Diagnosis

Granular cell tumor should be differentiated from adult rhabdomyoma, hibernoma, paraganglioma, alveolar soft part sarcoma, squamous cell carcinoma, and secondary granular cell change in reactive conditions or variety of sarcomas and carcinomas.

Treatment and Prognosis

Local excision is the treatment of choice. Local recurrence is rare. Histologically malignant cases have metastatic potential. However, complete benign histologic appearance cannot guarantee a benign clinical behavior in large deep-seated tumors with recurrence.

Malignant

Malignant Peripheral Nerve Sheath Tumor (MPNST, Malignant Schwannoma, Neurofibrosarcoma)

MPNST comprises around 5% of soft-tissue sarcomas. It usually occurs in young adults. Many are derived from neurofibromas in NF-1 patients in a period of 10–20 years and some arise de novo in normal peripheral nerves. It affects large- and medium-sized nerves in the proximal limbs and trunk more frequently than small nerves. The sciatic nerve is most frequently affected. Symptoms of nerve compression are common. Pain or rapid enlargement of a neurofibroma in NF-1 patients may herald malignant transformation (103). Historically, only sarcomas occuring in a nerve trunk, neurofibroma, or in NF-1 patients qualified for the diagnosis of MPNST. Currently however, all sarcomas that show nerve sheath differentiation on morphological grounds are included provided this is supported on either immunohistochemical or ultrastructural studies morphologically identical to those that do with immunohistochemical and/or ultrastructural evidence of nerve sheath differentiation.

Histopathology

MPNST is usually a circumscribed nodular/multinodular mass with a pseudocapsule. The cut surface is gray-tan with variable amounts of necrosis and hemorrhage. Association of neurofibroma or nerve trunk is often evident. Histologically, high-grade MPNST exhibits various morphologies but little peripheral nerve sheath differentiation while low grade can show features bordering with cellular schwannoma and cellular neurofibroma but with more significant cellular clowding, larger nuclei, and hyperchromatia (105). More typically, it is composed of a proliferation of oval to spindle cells with nuclei that are wavy or angulated and have tapered ends and coarse chromatin. The cells have scant to moderate amount of weakly eosinophilic, poorly defined cytoplasm and grow in fascicles, whorls, rarely rosettes, and palisading pattern (Figs. 88 and 89). The cellularity varies sharply from areas to areas. Mitotic activity is high with atypical mitotic figures. Geographic necrosis is common with perivascular tumor preservation in high-grade lesions. A hemangiopericytoma-like vascular pattern can be seen focally. Pleomorphism usually is not a common feature but can be seen focally. The background stroma can be fibrocollagenous or myxoid. Various divergent differentiations such as osteogenic, chondroblastic, rhabdomyoblastic, vascular, and epithelial differentiations can be seen in some tumors. MPNST with rhabdomyosarcomatous differentiation is called malignant

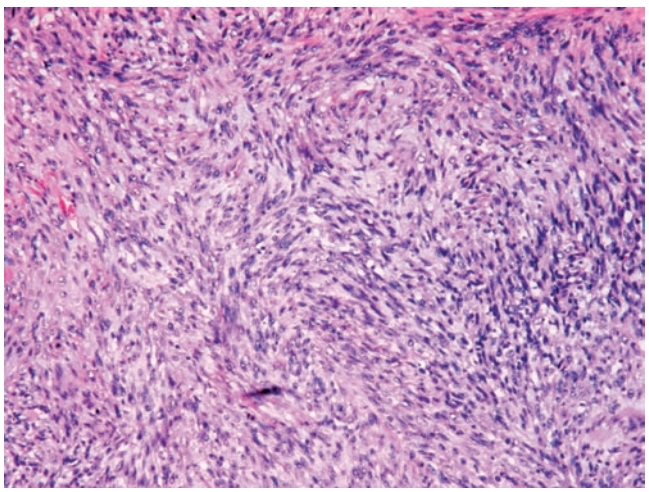

Fig. 88 The spindle tumor cells in MPNST have scant to moderate amount of weakly eosinophilic, poorly defined cytoplasm and grow in fascicles and whorls pattern

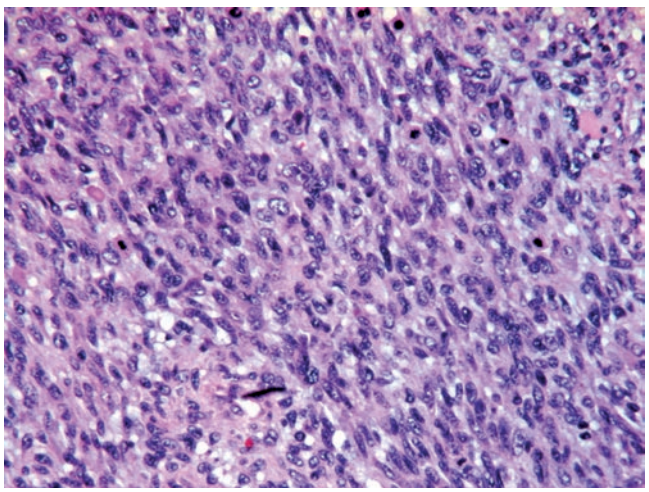

Fig. 89 Large vesicular hyperchromatic nuclei, sometimes with prominent nucleoli seen in high magnification

Triton tumor. The tumor cells can also become epithelioid focally or diffusely (epithelioid MPNST). As opposed to benign nerve sheath tumors, the MPNSTs are either negative or only focally positive for S100. The tumor can also react with various markers related to its divergent differentiation. Epithelioid variants can show focal to diffuse cytokeratin reactivity. Melanocytic markers such as HMB45 and melan-A are usually negative.

Differential Diagnosis

The differential diagnosis for MPNST is broad, particularly for those unrelated to nerves, neurofibromas, and NF-1 patients. Before the diagnosis can be made, one should exclude various spindle cell sarcomas such as monophasic synovial sarcoma, fibrosarcoma, leiomyosarcoma, malignant gastrointestinal stromal tumor, dedifferentiated liposarcoma, clear cell sarcoma, cellular schwannoma, cellular neurofibroma, hemangiopericytoma, and malignant solitary fibrous tumor; and tumors with epithelioid cell morphology such as melanoma and carcinoma. When divergent differentiations are present, the tumor should also be differentiated from rhabdomyosarcoma and extraskeletal osteosarcoma, and biphasic synovial sarcoma.

Treatment and Prognosis

Wide en bloc resection of the tumor is the treatment of choice. Postoperative radiation is recommended to improve local control. Local recurrence is high (40–68%) in cases treated with surgery alone. Approximately 30–65% of cases developed metastasis. There is no significant difference in prognosis between typical MPSNT and those with divergent differentiation, and between patients with and without NF-1. However, tumor location, size, grade, and completeness of resection are prognostically importance (105).

Clear Cell Sarcoma of Soft Tissue (Malignant Melanoma of Soft Parts)

Clear cell sarcoma usually occurs in young adults and affects most commonly the extremities. It typically attaches to aponeuroses and tendons. It presents as a slowly growing mass frequently with pain and tenderness.

Histopathology

Clear cell sarcoma is a gray-white lobulated mass in deep soft tissue. Histologically, the tumor is composed of polygonal or spindle cells with eosinophilic or clear cytoplasm and vesicular nuclei with prominent nucleoli. The tumor cells grow in a nested or fascicular pattern separated by delicate fibrous septa giving a multilobulated appearance in low magnification (Figs. 90 and 91). Wreath-like multinucleated giant cells and melanin are seen in some cases. Immunohistochemically, the tumor is positive for a wide range of melanocytic markers such as S100, HMB45, melan-A, MITF, and MAGE, and some neural markers such as NSE, synaptophysin, and CD57.

Differential Diagnosis

The challenge to diagnose clear cell sarcoma is to differentiate it from malignant melanoma and epithelioid malignant peripheral sheath tumor, both can exhibit similar morphologic as well as immunophenotypic features. In many cases, the differentiation can only be made according to molecular findings and/or clinical presentation (please see Chapter 5 for molecular diagnosis).

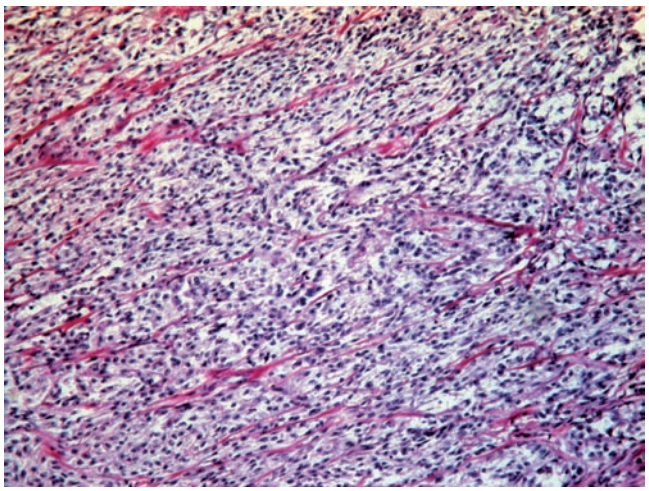

Fig. 90 Spindle cells with clear cytoplasm and vesicular nuclei in a nested or fascicular pattern separated by delicate fibrous septa in a clear cell sarcoma of soft parts

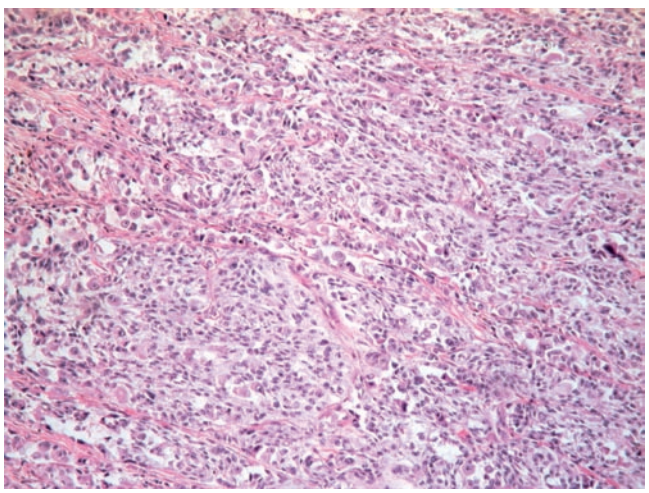

Fig. 91 The tumor cells become more polygonal with eosinophilic cytoplasm with prominent nucleoli in another clear cell sarcoma of soft part

Treatment and Prognosis

Like many other sarcomas, clear cell sarcoma is primarily treated with wide local excision. Local recurrence and metastasis to lung, lymph nodes, and bone are common. Recurrences and metastasis are common, even more than 10 years after the surgery. The 5-, 10-, and 20-year survival was 67%, 33%, and 10% (106). Tumor size greater than 5.0 cm, tumor necrosis, vascular invasion, and local recurrence are adverse prognostic factors (106).

Tumors with Pericytic Features

Glomus Tumor

Glomus tumor is a rare benign soft-tissue tumor. Glomus bodies are normally situated in the dermis of distal extremities and subungual region of the digits and in the precoccygeal soft tissue (glomus coccygeum). It is an innervated arteriovenous anastomosis invested by specialized perivascular muscle cells known as glomus cells. These cells regulate arterial flow and temperature under physiologic circumstances. The glomus tumor characteristically occurs in dermis or subungual region of distal extremities and presents with pain that may be exacerbated by temperature change. Glomus tumors are usually small and solitary. Rare cases present with multiple lesions have been called glomangiomatosis which have been associated with autosomally dominant inheritance.

Histopathology

Glomus tumors are typically composed of glomus-like cells and vessels. The glomus-like cells are uniform round to ovoid epithelioid cells which are thought to be modified smooth muscle cells. The tumor nuclei have bland chromatin pattern with absent or inconspicuous nucleoli (Fig. 92). Mitotic figures are very hard to find. The glomus-like cells form nests and trabeculae cuffing around thin-walled, capillary-sized vessels. According to the proportion of these two components, glomus tumors can be subcategorized as solid glomus tumor and glomangioma. In some cases, cells with more smooth muscle differentiation are present and are referred to glomangiomyoma. Tumors with large size (>2 cm), deep location, moderate to high nuclear grade, increased mitotic rate (>5/10 hpf) and presence of atypical mitotic figure are considered malignant. Tumors with only one of the above malignant features other than nuclear pleomorphism are considered as glomus tumors of uncertain malignant potential (107). Immunohistochemically, the tumor is only positive actin and vimentin.

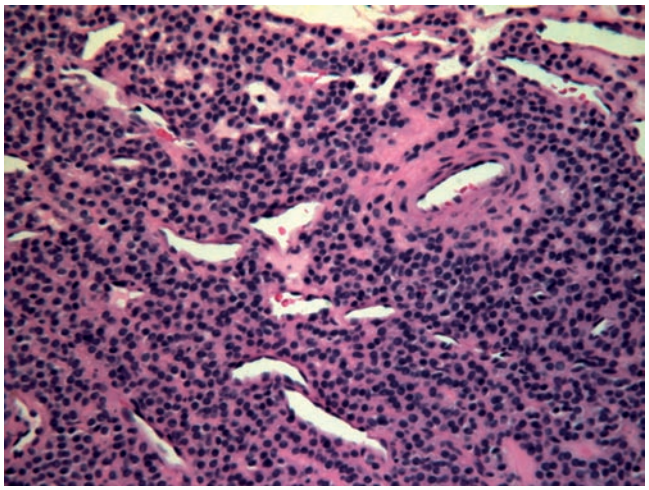

Fig. 92 Uniform round to ovoid glomoid cells arranged in nests and trabeculae cuffing around thin-walled, capillary-sized in glomus tumor

Differential Diagnosis

Hemangioma, arterio-venous malformation, hemangiopericytoma, myopericytoma, epithelioid leiomyoma, nevus and epithelioid sarcoma need to be differentiated from glomus tumor. One should also avoid overdiagnosing glomus tumor on normal glomus bodies incidentally found in tissue from distal extremities and precoccygeal region.

Treatment and Prognosis

Complete excision is the treatment of choice. However, conservative local excision to preserve the normal function of the digit is acceptable, but runs the risk of local recurrence. Tumors with malignant histologic features (1%) are more aggressive and metastasize in 40% of the cases (107).

Hemanigopericytoma

Whether or not hemangiopericytoma (HPC) is a distinct entity is debatable. It is a known fact that characteristic HPC features can be seen in several different soft-tissue tumors. These were likely diagnosed as HPC before these entities were well recognized, such as SFT, gastrointestinal stromal tumor, monophasic synovial sarcoma, and myopericytoma. However, after careful exclusion of other entities with HPC features, there is still small number of tumors with dominant HPC features that fit well into what has long been described as soft-tissue hemangiopericytoma. HPC typically occurs in adults and involves deep soft tissue of the thigh, pelvis, and retroperitoneum. HPC diagnosed in dura and head and neck region share certain histologic features with soft-tissue HPC but are considered different entities which will not be discussed here.

Histopathology

The tumor is usually well-circumscribed and vaguely lobulated. The histologic hallmark of HPC is the presence of thin-wall ramifying and gaping vessels in a so-called stag-horn-like pattern and perivascular proliferation of monotonous round to oval mesenchymal cells (pericytes) (Figs. 93 and 94). Fascicular, storiform, or palisading pattern might be present focally but should not be prominent. Similarly, variable fibrosing and hyalinized matrix might be seen but should not be prominent. Immunohistochemically, pure HPC can be focally and weakly positive for SMA and CD34 but either these markers should not be strongly or diffusely positive.

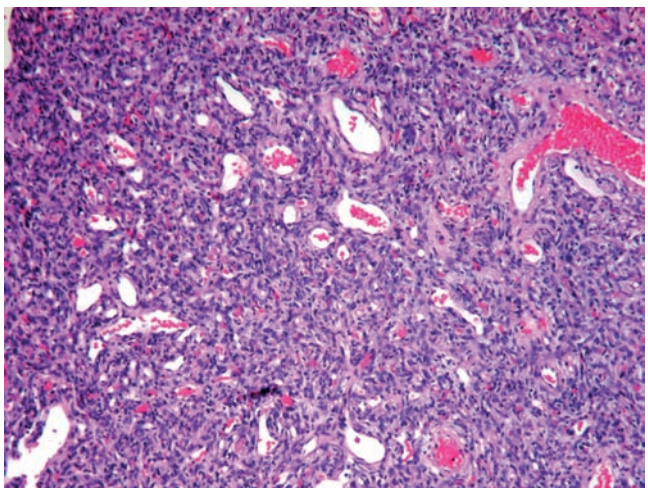

Fig. 93 Thin-wall ramifying and gaping vessels in a so-called stag-horn-like pattern and perivascular proliferation of round to oval mesenchymal cells in HPC

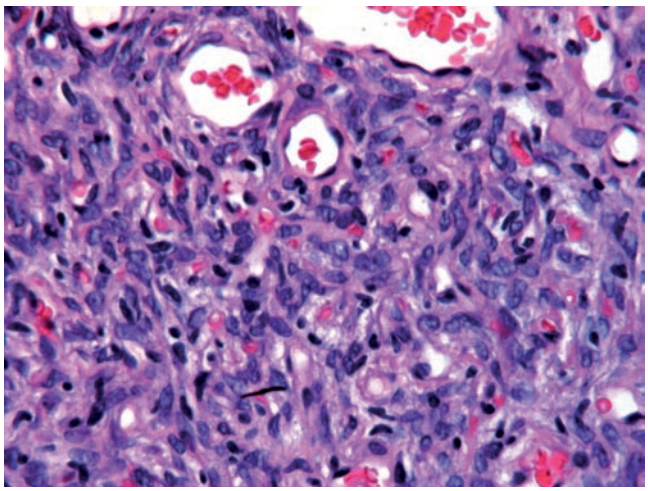

Fig. 94 Perivascular proliferation of shortly spindle mesenchymal cells (pericytes) in high magnification in HPC

Differential Diagnosis

Regardless of its characteristic histologic features, HPC is a diagnosis of exclusion. HPC should be differentiated from glomus tumor, myopericytoma, solitary fibrous tumor, monophasic synovial sarcoma, mesenchymal chondrosarcoma, nerve sheath tumor, gastrointestinal stromal tumor, angiosarcoma, and dedifferentiated liposarcoma.

Treatment and Prognosis

Surgical excision is the treatment of choice. Although some HPC are likely low grade or benign, tumors with greater than four mitotic figures per 10 hpf, nuclear atypia, hypercellularity, necrosis, hemorrhage, multiple local recurrences, and/or large size of deeply located tumor (>5 cm) are likely malignant (108). Metastatic rates range from 10% to 60%, and lung and bone are the most frequent metastatic sites.

Myopericytoma

Myopericytoma is a recently described benign entity with differentiation toward perivascular myoid cells. It is usually a slow growing cutaneous and subcutaneous nodule occurring most commonly in middle-aged adults.

Histopathology

Myopericytoma is a relatively well-circumscribed nodule. It is composed of monotonous oval-spindle cells with myoid-like eosinophilic cytoplasm arranged concentrically around variably sized, short-branching, gaping, thin-wall vessels (Figs. 95–97). However, the histologic spectrum of myopericytoma can span

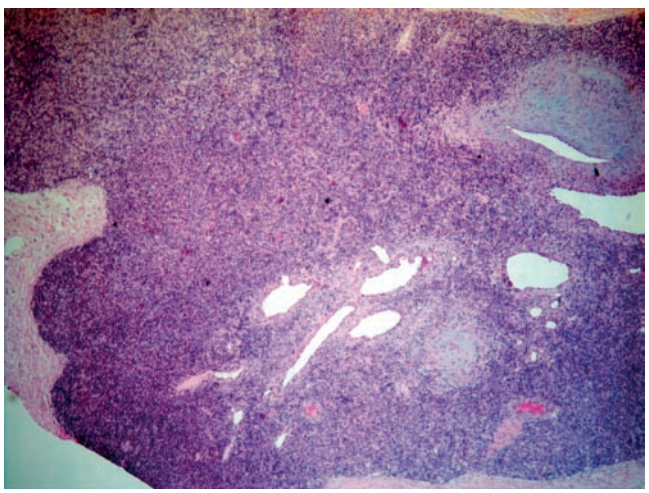

Fig. 95 The well-circumscribed nodule in dermis in a myopericytoma

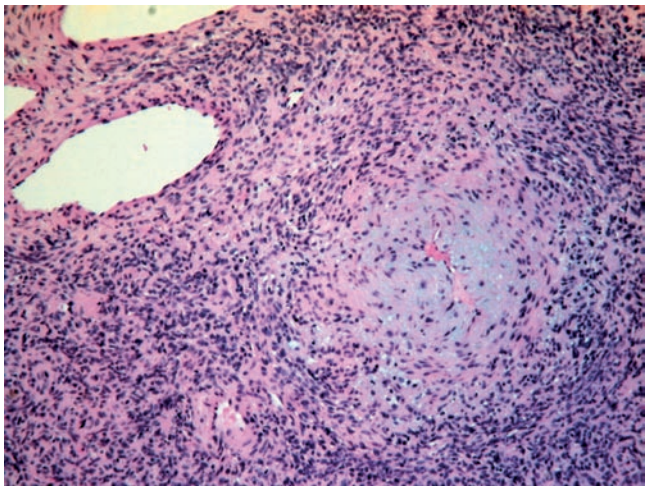

Fig. 96 Myopericytoma is composed of monotonous oval-spindle cells with myoid-like eosinophilic cytoplasm arranged concentrically around variably sized, short branching, gaping, thin-wall vessels

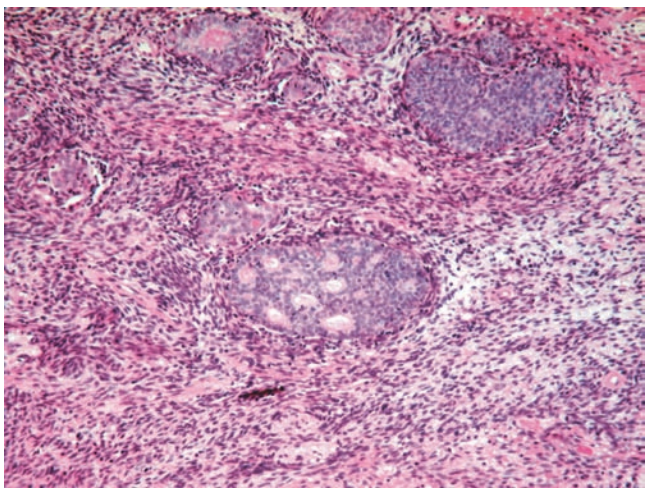

Fig. 97 The typical biphasic appearance of synovial sarcoma characterized by proliferation of neoplastic epithelial and spindle cells

among myofibroma, angioleiomyoma, infantile hemangiopericytoma, and glomus tumor (109). Immunohistochemically, myopericytoma is usually diffusely and strongly positive for SMA and focally for desmin and CD34 in some cases.

Differential Diagnosis

Because of the wide range of morphologic spectrum, myopericytoma should be differentiated from hemangiopericytoma, angioleiomyoma, and glomus tumor.

Treatment and Prognosis

Myopericytoma is a benign lesion which can be cured by simple surgical excision. Recurrence can occur but not common. Rare cases of malignant myopericytoma have been reported (110).

Tumors with Divergent or Ambiguous Differentiation

Synovial Sarcoma

Synovial sarcoma is an uncommon soft-tissue sarcoma accounted for 5–10% of all soft-tissue sarcoma (111). Despite the name, there is no evidence to suggest that synovial sarcomas arise from or differentiate toward synovium. It frequently arises in the deep soft tissue adjacent to joints or tendons of extremities and less commonly the head and neck region. It is a slow-growing mass often associated with pain. Other symptoms related to mass effect might occur. Bone involvement and calcification are present in less than one-third of cases.

Histopathology

Synovial sarcoma is typically circumscribed multinodular mass with a tan or gray cut surface. According to the histologic features, synovial sarcomas are classified as either biphasic or monophasic. The typical biphasic variant is characterized by proliferation of neoplastic cells exhibiting both epithelial and spindle cell phenotypes. The epithelial cells form glandular structures or solid nests and have abundant cytoplasm and oval nuclei. Between the epithelial elements, there is a proliferation of spindle cells that have scant cytoplasm and indistinct cell borders (Figs. 97 and 98). In rare cases, the epithelial component can be very overwhelming with very little spindle cell component. The monophasic variant is composed of only short spindle cells which are monotonous and form vague fascicular, whirling, and rarely palisading patterns (Fig. 99). Extracellular matrix is usually scant except for variable myxoid matrix in the less cellular areas alternating with hypercellular areas. Calcification is present in some cases. Presence of hemangiopericytoma-like vascular pattern is common but usually focal. When the tumor is poorly differentiated, it is heavily populated by primitive small round cells with hyperchromatic nuclei and active mitotic activity (112). Immunohistochemically, both epithelial and spindle cells are positive for cytokeratin and EMA. In addition, synovial sarcoma is frequently positive for CD99 and BCL2. Focal S100 reactivity is present in one-third of cases.

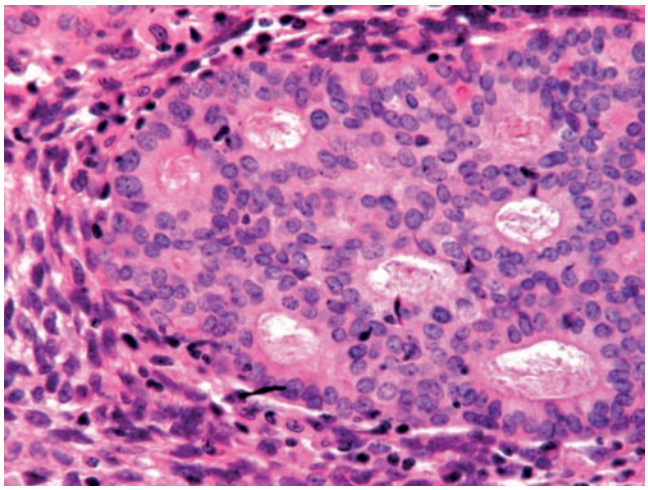

Fig. 98 The epithelial cells have columnar features and form glandular structure in contrast to the surrounding spindle cells with scant cytoplasm and indistinct cell borders

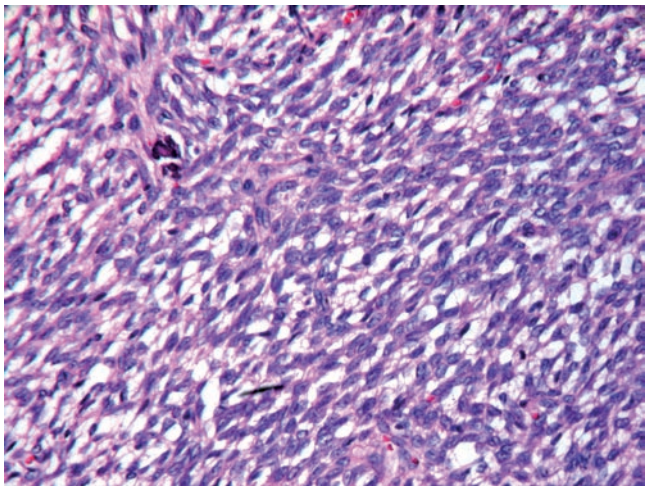

Fig. 99 Monotonous short spindle cells arranged in vague fascicular pattern in a typical monophasic synovial sarcoma

Differential Diagnosis

Synovial sarcoma should be differentiated from adenocarcinoma, mesothelioma, carcinosarcoma, fibrosarcoma, malignant peripheral nerve sheath tumor, hemangiopericytoma, malignant solitary fibrous tumor, EWS/PNET, round cell liposarcoma, and rhabdomyosarcoma.

Treatment and Prognosis

Wide excision with clear margin is the treatment of choice. Postoperative radiation has been used in some cases to improve local control. About 50% of the tumors recur and 40% metastasize to lungs, regional lymph nodes, and bone. Five-year survival is 36–76% and 10-year survival is 20–63% (113). Young age, small tumor size, low mitotic rate, and calcification are associated with favorable prognosis and poorly differentiated morphology is associated with poor prognosis (114). The histologic types (biphasic vs. monophasic) do not have impact in prognosis. The prognostic significance of different fusion gene (SYT/SSX1 vs. SYT/SSX2) is further discussed in chapter 5.

Alveolar Soft Part Sarcoma

Alveolar soft part sarcoma is very rare and mainly occurs in youth or young adults with female predilection. It usually arises in lower extremities and the head and neck region. It presents as slow growing, painless mass. One-third of patients present with metastatic lesion in lung, brain, or bone even before the primary lesion is evident.

Histopathology

Alveolar soft part sarcoma is usually a poorly defined, pale, yellow, soft mass often containing areas of hemorrhage and necrosis. Histologically, it is characterized by organoid growth of relatively uniform and large polygonal cells with abundant granular, eosinophilic cytoplasm in nests and islands. The nests or islands are separated by delicate fibrovascular tissue and exhibit a paraganglioma-like pattern or pseudoalveolar appearance attributed to loss of cellular adherence in tumor cells (Figs. 100 and 101). Sheet-like growth pattern can be seen in some pediatric cases. PAS positive intracytoplasmic crystals are seen in some but not all cases. Vascular invasion is a common finding. There is

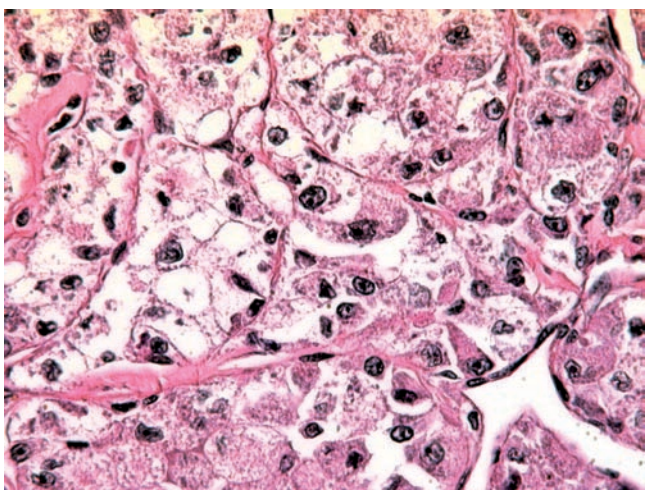

Fig. 100 Epithelioid nests and islands separated by delicate fibrovascular tissue rendering a paraganglioma-like pattern or pseudoalveolar appearance in alveolar soft part sarcoma

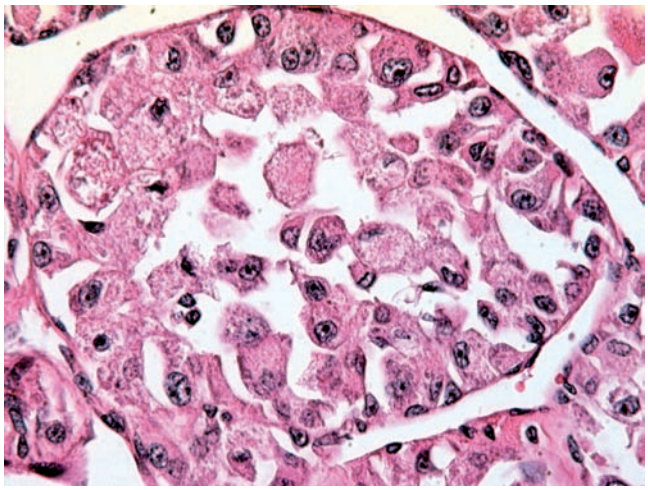

Fig. 101 The alveolar growth of large polygonal cells with abundant, granular, eosinophilic cytoplasm and hyperchromatic nuclei with prominent nucleoli

increased TEF-3 immunoreactivity in alveolar soft part sarcoma (115), the tumor shows inconsistent desmin, S100, and NSE reactivity. Please see chapter 5 for details on the molecular diagnosis of this tumor.

Differential Diagnosis

Alveolar soft part sarcoma can mimic paraganglioma, renal cell carcinoma, melanoma, granular cell tumor, and rhabdoid tumor.

Treatment and Prognosis

Although tumor can be controlled locally by surgical excision with clear margins, alveolar soft part sarcoma is very prone to producing metastases. Metastasis can develop early even before the detection of the primary lesion or years later after complete excision of the primary lesion. The survival rate is around 60% at 5 years, 38% at 10 years, and 15% at 20 years. Older age and larger size are adverse prognostic factors for metastasis. Common sites for metastasis are lung, bone, and brain (116).

Desmoplastic Small Round Cell Tumor (DSRCT)

DSRCT is an aggressive tumor of uncertain histogenesis. It primarily affects children and young adults with strong male predilection. The overwhelming majority of the tumors arise in the abdominal cavity and are closely related to the peritoneal surface. Patients usually present with a rapid development of abdominal distention, acute abdomen, and ascites (117).

Histopathology

The tumor is typically multinodular on the peritoneal surface with multiple satellite lesions which are firm and gray-white on cut surface. Histologically, there is a proliferation of nesting uniform small round cells with high nuclear/cytoplasmic ratio and hyperchromatic nuclei in a striking desmoplastic stroma (Figs. 102 and 103). Pleomorphism, rhabdoid, and epithelial differentiation as well as rosettes can be seen in some cases. Mitotic figures and tumor necrosis are common. Immunohistochemically, tumor cells are positive for cytokeratin, EMA, vimentin, desmin, WT-1, and NSE. Please see chapter 5 for molecular diagnogis.

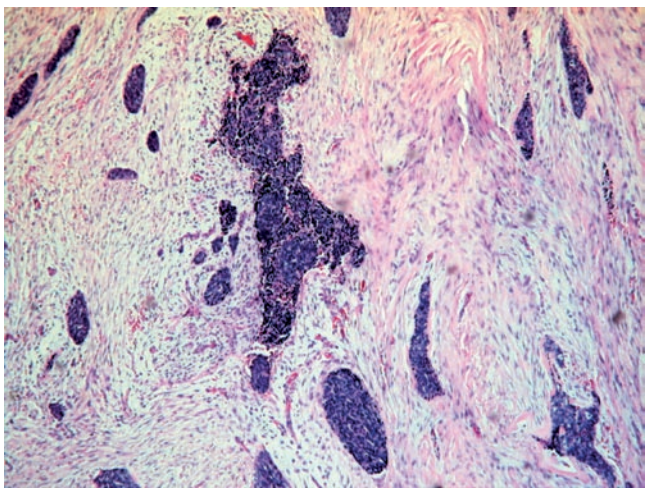

Fig. 102 Nests of blue round cells in striking desmoplastic stroma in desmoplastic small round cell tumor (*DSRCT*)

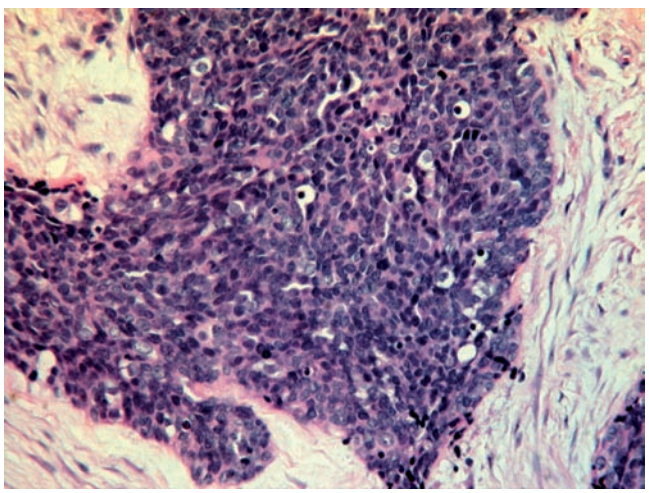

Fig. 103 Small round cells with high nuclear/cytoplasmic ratio and hyperchromatic nuclei under high magnification

Differential Diagnosis

DSRCT should be differentiated from small cell carcinoma, EWS/PNET, rhabdomyosarcoma, Wilm tumor, round cell liposarcoma, and carcinoids.

Treatment and Prognosis

Many tumors are not resectable at the time of diagnosis due to the wide spread of the disease in peritoneum. In addition to surgical debulking, various aggressive neoadjuvant therapy have been used to treat the disease. Prognosis remains very poor despite and multimodal therapy (118).

Epithelioid Sarcoma

Epithelioid sarcoma typically arises in the distal extremities of young adults. It presents as a painless and slow growing solitary or multiple nodules in the skin, subcutis, fascia, or tendons (119). The lesion typically grows or recurs along the fascia, tendons, or nerve sheath toward the proximal extremities. Ulceration is commonly seen in cutaneous lesions.

Histopathology

Epithelioid sarcoma is characterized by coalescing nodular or multinodular growth of polygonal to short spindle neoplastic cells arranged around an amorphous hyaline or necrotic area simulating granuloma. The tumor cells usually exhibit little pleomorphism and have strong eosinophilic to somewhat clear cytoplasm. Variable fibrosis or hyalinization is present (Figs. 104 and 105). In addition, epithelioid sarcoma can simulate squamous carcinoma in low magnification when the lesion is dominated by eosinophilic epithelioid cells, or fibroma when dominated by spindle cells and hyaline stroma. Immunohistochemically, epithelioid sarcoma is positive for cytokeratin, EMA, and vimentin but negative for In1-1 (120).

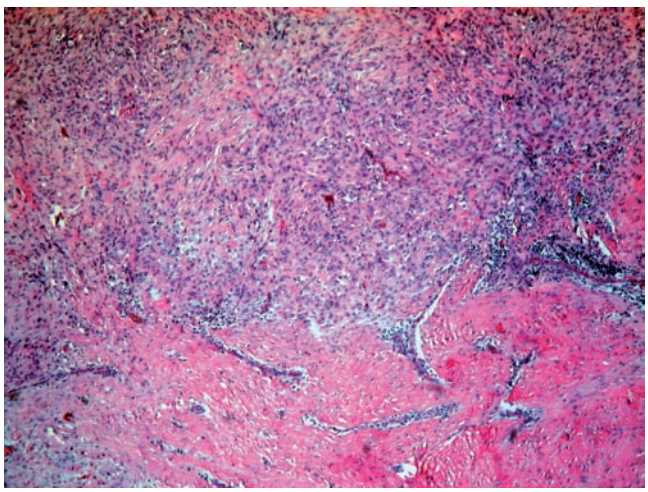

Fig. 104 Coalescing nodular growth of polygonal to short spindle neoplastic cells in epithelioid sarcoma

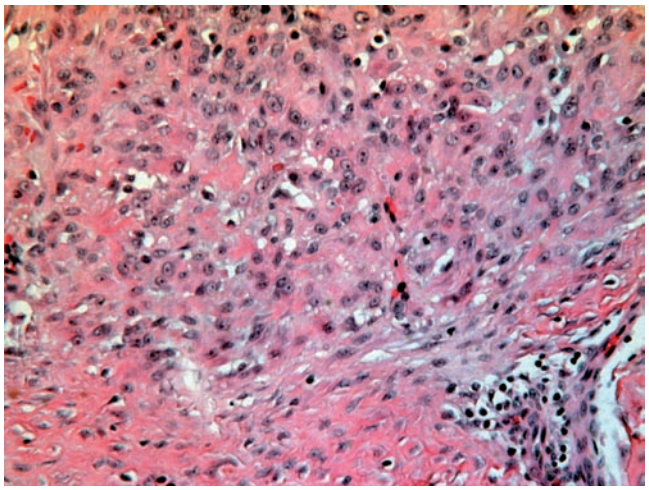

Fig. 105 The polygonal tumor cells have strong eosinophilic cytoplasm and large nuclei with prominent nucleoli in epithelioid sarcoma

Differential Diagnosis

Epithelioid sarcoma needs to be differentiated from granulomatous lesions, fibroma, squamous cell carcinoma, synovial sarcoma, epithelioid hemangioendothelioma, and melanoma.

Treatment and Prognosis

Surgical excision is the treatment of choice. Because of relatively small size and slow growing nature, its aggressiveness is usually underestimated. Recurrence occurs in 30–70% of the cases due to incomplete local excision particularly in multifocal lesions. Metastasis occurs in around 50% of cases, usually after multiple recurrences. Male gender, older age, >5 cm tumor size, deep location, nuclear pleomorphism, frequent mitotic activity, vascular and neural invasion, and recurrence are adverse prognostic factors. The common sites for metastasis are, in descending order, lung, regional lymph nodes, skin, soft tissue, and brain. Five- and ten-year survival rates range from 50% to 80% (119, 121).

Angiomatoid Fibrous Histiocytoma

Angiomatoid fibrous histiocytoma frequently affects the subcutis and deep dermis of the upper extremities of young

adults. It presents as a slow-growing mass occasionally associated with systemic symptoms such as fever, anemia, and weight loss.

Histopathology

Angiomatoid fibrous histiocytoma is well circumscribed in the deep dermis and subcutis. It is characterized by multinodular proliferation of relatively uniform histiocytoid/myoid cells with vesicular nuclei and eosinophilic cytoplasm. Pseudoangiomatoid or cystic hemorrhagic areas without endothelial lining are seen in the center of the lesion. In the periphery, there is cuff of dense lymphocytes and plasma cells sometimes with germinal center formation (Fig. 106). Immunohistochemically, the tumor cells can show demin, CD68, and EMA reactivity.

Differential Diagnosis

Angiomatoid fibrous histiocytoma should be differentiated from MFH, reactive hemorrhagic change in lymph node, metastatic melanoma, or other neoplasms.

Treatment and Prognosis

Angiomatoid fibrous histiocytoma is an indolent tumor which can be cured by complete local excision. Low incidence (2–11%) of local recurrence is seen after incomplete excision. Risk of metastasis to regional lymph nodes is less than 1% (122).

Non-Neoplastic Conditions Frequently Misdiagnosed as Sarcoma (Pseudosarcoma)

Nodular Fasciitis

Nodular fasciitis is a relative fibro/myofibroblastic proliferation which frequently involves extremities, trunk, and head and neck region of young adults. In infants, the lesion tends to involve the scalp (cranial fasciitis). It usually presents as rapid growing subcutaneous or less frequently intramuscular mass, sometimes with tenderness. The size of the lesion is usually around 2 cm and no larger than 5 cm. However, some cranial lesions might grow larger than those in the soft tissue and erode the skull (123).

Histopathology

Nodular fasciitis might appear to be circumscribed grossly with gray-white firm mass, sometimes with fleshy or central cystic change on cut surface. Histologically, it is a nonencapsulated nodular or stellate lesions usually associated with fascia underneath the subcutis or intramuscularly. It is characterized by a proliferation of fusiform- or stellate-shaped stromal cells with plump spindle nuclei. The lesional cells are arranged loosely in a haphazard, vaguely whorled, or storiform pattern in a variably myxoid matrix with "feathery" appearance. The loosely arranged stellate-shaped stromal cells with the myxoid matrix simulate fibroblasts in cell culture (Figs. 107 and 108). Cellularity is variable. Some lesions might become very hypercellular with increased mitotic activity. As a rule, however, there is lack of nuclear hyperchromasia/atypia and atypical mitotic figures. Extravasated

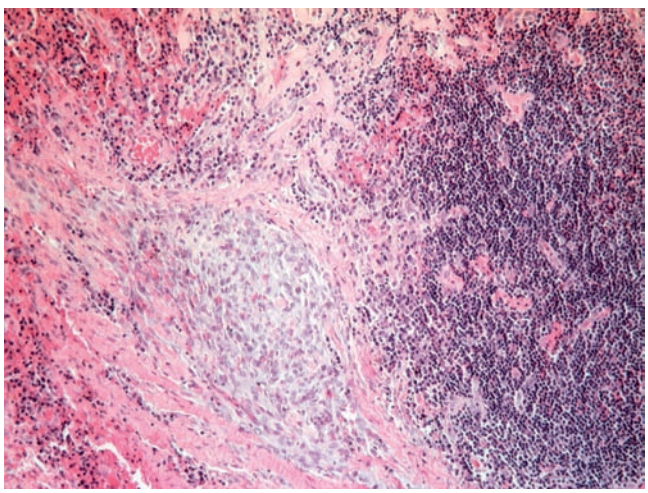

Fig. 106 Nodular proliferation of relatively uniform histiocytoid/myoid cells with vesicular nuclei and weak eosinophilic cytoplasm and the adjacent cuff of dense lymphocytes in angiomatoid fibrous histiocytoma.

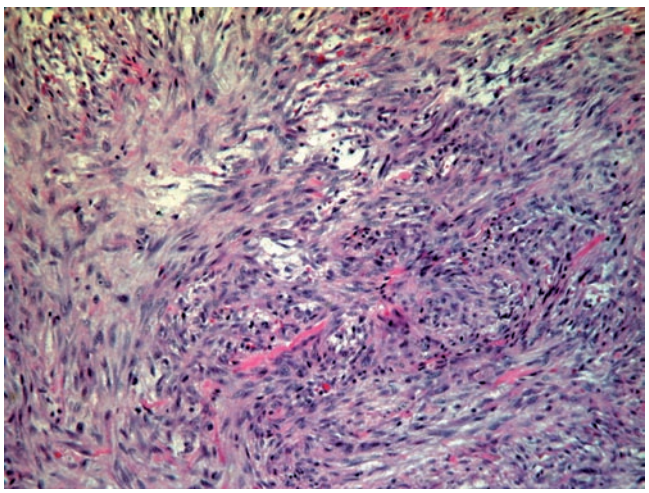

Fig. 107 Stellate myofibroblastic cells loosely arranged in a haphazard, vaguely whorled pattern in myxoid and microcystic background with "feathery" appearance in nodular fasciitis

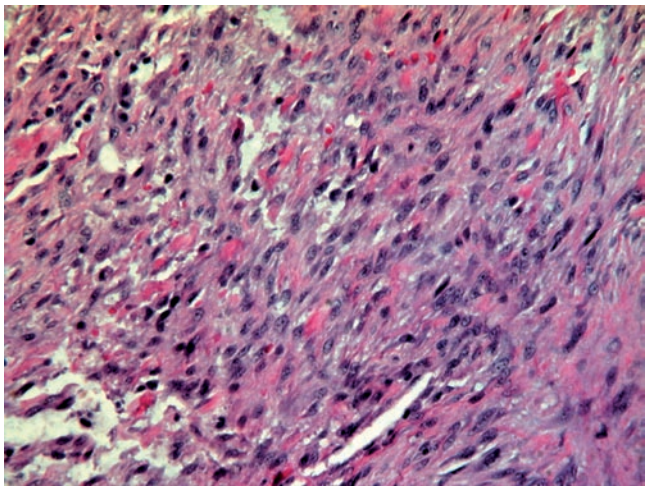

Fig. 108 The fusiform- or stellate-shaped myofibroblastic cells with plump spindle nuclei and extravasated red blood cells in nodular fasciitis

red cells, chronic inflammatory cells, and osteoclast-like giant cells are frequently seen. Proliferation of small vessels can be prominent in some lesions. Although the matrix is mainly myxoid, hyaline, or keloid-like collagen deposition can be seen focally in some or even prominent in rare cases. In children and young adults, the process tends to involve small- to medium-sized vessels with intravascular component (intravascular fasciitis). Immunohistochemically, nodular fasciitis is positive for vimentin and also shows SMA and MSA reactivity consistent with myofibroblastic differentiation.

Differential Diagnosis

Hypercellularity, presence of frequent mitotic figures, and the infiltrative growth pattern are the features frequently misinterpreted as sarcomatous changes. Nodular fasciitis should be differentiated from myxofibrosarcoma, MFH, fibrosarcoma, fibromatosis, DFSP, leiomyosarcoma, and Kaposi's sarcoma.

Treatment and Prognosis

Simple local excision is adequate for treatment. Recurrence is rare even after incomplete excision. There is no risk of metastasis.

Proliferative Fasciitis/Myositis

Proliferative fasciitis/myositis is a benign fibroblastic/myofibroblastic entity similar to nodular fasciitis. It occurs much less than nodular fasciitis and involves deep fascia and subcutis (proliferative fasciitis) or skeletal muscle (proliferative myositis (124, 125)). Its clinical presentation is similar to that of nodular fasciitis.

Histopathology

The hallmark of proliferative fasciitis and proliferative myositis is the presence of large ganglion cell-like fibroblasts in addition to other features seen in nodular fasciitis. Atrophic multinucleated skeletal muscle cells are frequently seen in proliferative myositis (Figs. 109 and 110). The lesion also tends to be less demarcated and more cellular than nodular fasciitis.

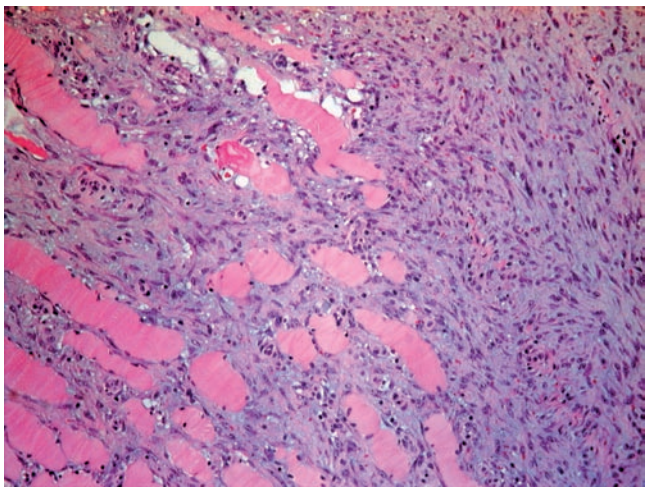

Fig. 109 Cellular spindle cell proliferation entrapping skeletal muscle fibers in proliferative myositis

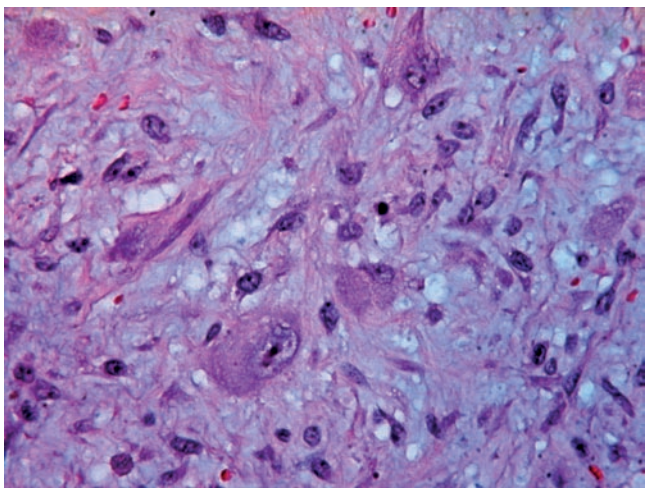

Fig. 110 Large ganglion cell-like fibroblasts in addition to the myofibroblast-type cells seen in nodular fasciitis

Differential Diagnosis

Not infrequently, proliferative fasciitis/myositis is misdiagnosed as MFH, rhabdomyosarcoma, ganglioneuroblastoma, metastatic melanoma, and rhabdoid tumor.

Treatment and Prognosis:

Similar to nodular fasciitis.

References

1. WHO Classification of Tumors Pathology and Genetics. Tumor of Soft Tissue and Bone. Lyon: IARC Press, 2002.
2. Costa J, Wesley RA, Glatsteim E, Rosemberg SA. The grading of soft tissue sarcomas. Results of a clinico-histopathologic correlation in a series of 163 cases. Cancer 1984; 53:530–541.
3. Coindre JM, Terrier P, Bui NB, Bonichon F, Collin F, Le DV, Mandard AM, Vilain MO, Jacquemier J, Duplay H, Sastre X, et al.. Prognostic factors in adult patients with locally controlled soft tissue sarcoma. A study of 546 patients from the French Federation of Cancer Centers Sarcom Group. J Clin Oncol 1996; 14:869–877.
4. Sobin LH, Wittekind CH, Eds. International Union Against Cancer (UICC). TNM Classification of Malignant Tumors. 5th ed. New York: John Wiley & Sons, Inc., 1997.
5. Fleming ID, Cooper JS, Henson DE, Hutter RVP, Kennedy BJ, Murphy GP, et al., Eds. American Joint Committee on Cancer Staging Manual. 5th edition. Philadelphia: J.B. Lippincott, 1997.
6. Zhang PJ, Brooks JJ. Modern pathological evaluation of soft tissue sarcoma specimens and its potential role in soft tissue sarcoma research. Curr Treat Options Oncol 2004; 5:441–450.
7 Chung EB, Enzinger FM. Chondroma of soft parts. Cancer 1978; 41:1945–1954.
8. Ando K, Goto Y, Hirabayashi N, Matsumoto Y, Ohashi M. Cutaneous cartilaginous tumor. Dermatol Surg 1995; 21:339–341.
9. Brownlee RD, Sevick RJ, Rewcastle NB, Tranmer BI. Intracranial chondroma. AJNR Am J Neuroradiol 1996; 18:889–893.
10. Bansal M, Goldman AB, DiCarlo EF, McCormack R. Soft tissue chondromas: diagnosis and differential diagnosis. Skel Radiol 1993; 22:309–315.
11. Nayler S, Heim S. Soft tissue chondroma. In: WHO Classification of Tumors Pathology and Genetics, Tumor of Soft Tissue and Bone. Lyon: IARC Press, 2002:180–182.
12. Mikkelsen QA. Dupuytren's disease – initial symptoms, age of onset and spontaneous course. Hand 1977; 9:11–15.
13. Allen RA, Woolner LB, Ghormlely RK. Soft tissue tumors of the sole: with special reference to plantar fibromatosis. J One Joint Surg Am 1955; 37:14.
14. Ling RSM. The genetic factor I Dupuytren's disease. J Bone Joint Surg Br 1963; 45:709.
15. Hayry P, Reitamo JJ, Totteman S, Hopfner-Hallikainen D, Sivula A. The desmoid tumor. II. Analysis of factors possibly contributing the etiology and growth behavior. Am J Clin Pathol 1982; 77:674–680.
16. Miyoshi Y, Iwao K, Nawa G, Yoshikawa H, Ochi T, Nakamura Y. Frequent mutations in the beta-catenin gene in desmoid tumors from patients without familial adenomatous polyposis. Oncol Res 1998; 10:591–594.
17. Aluisio FV, Mair SD, Hall RL. Plantar fibromatosis: treatment of primary and recurrent lesions and factors associated with recurrence. Foot Ankle Int 1996; 17:672–678.
18. Merchant NB, Lewis JJ, Woodruff JM, Leung DH, Brennan MF. Extremity and trunk desmoid tumors: a multifactorial analysis of outcome. Cancer 1999; 88:2045–2052.
19. Folpe AL, Morris RJ, Weiss SW. Soft tissue giant cell tumor of low malignant potential: a proposal for the reclassification of malignant giant cell tumor of soft parts. Mod Pathol 1999; 12:894–902.
20. Chung EB, Enzinger FM. Extraskeletal osteosarcoma. Cancer 1987; 60:1132–1142.
21. Meis-Kindblom JM, Enzinger FM. Extraskeletal Ewing's sarcoma. In: Color Atlas of Soft Tissue Tumors. Mosby-Wolfe, 1996:294–295.
22. Enzinger FM, Weiss SW, Liang CY. Ossifying fibromyxoid tumor of soft parts. A clinicopathological analysis of 59 cases. Am J Surg Pathol 1989; 13:817–827.
23. Meis-Kindblom JM, Bergh P, Gunterber B, Kindblom LG. Extraskeletal myxoid chondrosarcoma: a reappraisal of its morphologic spectrum and prognostic factors based on 117 cases. Am J Surg Pathol 1999; 23:636–650.
24. Oliverra AM, Sebo TJ, McGrory JE, Gaffey TA, Rock MG, Nascimenta AG. Extraskeletal myxoid chondrosarcoma: a clinicopathologic, immunohistochemical and ploidy analysis of 23 cases. Mod Pathol 2000; 13:900–908.
25. Debelenko LV, Perez-Atayde AR, Mulliken JB, Liang MG, Archibald TH, Kozakewich HP. D2-40 immunohistochemical analysis of pediatric vascular tumors reveals positivity in kaposiform hemangioendothelioma. Mod Pathol 2005; 18:1454–1460.
26. Kahn HJ, Bailey D, Marks A. Monoclonal antibody D2-40, a new marker of lymphatic endothelium, reacts with Kaposi's sarcoma and a subset of angiosarcomas. Mod Pathol 2002; 15:434–440.
27. Weiss WS, Goldblum JR. Granular tissue-type (pyogenic granuloma) hemangioma. In: Enzinger and Weiss's Soft Tissue Tumors. 4th ed. Mosby-Harcourt: Philadelphia, 2001: 864–865.
28. Meis-Kindblom JM, Enzinger FM. Capillary hemangioma. In: Color Atlas of Soft Tissue Tumors. Mosby-Wolfe, 1996:138–145.
29. Meis-Kindblom JM, Enzinger FM. Cavernous hemangioma. In: Color Atlas of Soft Tissue Tumors. Mosby-Wolfe, 1996:138–149.
30. Olsen TG, Helwig EB. Angiolymphoid hyperplasia with eosinophilia. A clinicopathologic study of 116 cases. J Am Acad Dermatol 1985; 12:781–796.
31. Beham A, Fletcher CD. Intramuscular angioma: a clinicopathologic analysis of 74 cases. Histopathology 1991; 18:53–59.
32. Caloje E. Intramuscular angioma. In: WHO Classification of Tumors Pathology and Genetics, Tumor of Soft Tissue and Bone. Lyon: IARC Press, 2002:156–157.
33. Rao VK, Weiss SW. Angiomatosis of soft tissue. An analysis of the histologic and clinical outcome in 51 cases. Am J Surg Pathol 1992; 16:764–771.
34. Rusin LJ, Harrel ER. Ateriovenous fistula. Cutaneous manifestations. Arch Dermatol 1976; 112:1125–1128.
35. Meis-Kindblom JM, Enzinger FM. Papillary endothelial hyperplasia (intravascular vegetant hemangioendothelioma of Masson). In: Color Atlas of Soft Tissue Tumors. Mosby-Wolfe, 1996:150–151.
36. Meis-Kindblom JM, Enzinger FM. Spindle cell hemangioendothelioma. In: Color Atlas of Soft Tissue Tumors. Mosby-Wolfe, 1996:159–160.
37. Chervenak FA, Isaacson G, Blakemore KJ, Breg WR, Hobbins JC, Berkowitz RL, Tortora M, Mayden K, Mahoney MJ. Fetal cystic hygroma. Cause and natural history. N Engl J Med 1983; 309:822–825.
38. Zuberberg LR, Nickoloff BJ, Weiss SW. Kaposiform hemangioendothelioma of infancy and childhood. An aggressive neoplasm associated with Kasabach-Merritt syndrome and lymphangiomatosis. Am J Surg Pathol 1993; 17:321–328.
39. Debelenko LV, Perez-Atayde AR, Mulliken JB, Liang MG, Archibald TH, Kozakewich HP. D2-40 immunohistochemical analysis of pediatric vascular tumors reveals positivity in kaposiform hemangioendothelioma. D2-40 immunohistochemical analysis of pediatric vascular tumors reveals positivity in kaposiform hemangioendothelioma. Mod Pathol 2005; 18:1454–1460.

40. Mac-Moune LF, To KF, Choi PC, Leung PC, Kumta SM, Yuen PP, Lam WY, Cheung AN, Allen PW. Kaposiform hemangioendothelioma: five patients with cutaneous lesion and long follow-up. Mod Pathol 2001; 14:1087–1092.
41. Mentzel T, Beham A, Calonje E, Katernkamp D, Fletcher CD. Epithelioid hemangioendothelioma of skin and soft tissues: clinicopathologic and immunohistochemical study of 30 cases. Am J Surg Pathol 1997; 21:363–374.
42. Zhang PJ, Livolsi VA, Brooks JJ. Malignant epithelioid vascular tumors of the pleura: report of a series and literature review. Hum Pathol 2000; 31:29–34.
43. Fanburg-Smith JC, Michal M, Partanen TA, Alitalo K, Miettinen M. Papillary intralymphatic angioendothelioma (PILA): a report of twelve cases of a distinctive vascular tumor with phenotypic features of lymphatic vessels. Am J Surg Pathol 1999; 23:1004–1010.
44. Dabska M. Malignant endovascular papillary angioendothelioma of the skin in childhood. Clinicopathologic study of 6 cases. Cancer1969; 24:502–510.
45. Mentzel T, Stengel B, Katenkamp D. Retiform hemangioendothelioma. Clinico-pathologic case report and discussion of the group of low malignancy vascular tumors. Pathologe 1997; 18:390–394.
46. Lamovec J, Knuutila S. Kaposi sarcoma. In. WHO Classification of Tumors Pathology and Genetics, Tumor of Soft Tissue and Bone. Lyon: IARC Press, 2002:170–172.
47. Chang Y, Cesarman E, Pessin MS, Lee F, Culpepper J, Knowles DM, Moore PS. Identification of herpesvirus-like DNA sequences in AIDS-associated Kaposi's sarcoma. Science 1994; 266:1865–1869.
48. Meis-Kindblom JM, Enzinger FM. Angiosarcoma. In: Color Atlas of Soft Tissue Tumors. Mosby-Wolfe, 1996:164–167.
49. Molitor JL, Llombart A, Guinebretiere JM, Zemoura L, Spielmann M, Contesso G, de Vathaire F, Zelek L, Kaylitalire L, Le Chevalier T, Genin J. Angiosarcoma of the breast. Apropos of 8 cases and review of the literature. Bull Cancer 1997; 84:206–211.
50. Mantse L. Liposuction under local anesthesia: a retrospective analysis of 100 patients. J Dermatol Surg Oncol 1987; 13:1333–1338.
51. Bjerregaard P, Hagen K, Daugaard S, Kofoed H. Intramuscular lipoma of the lower limb. Long-term follow-up after local resection. J Bone Joint Surg Br 1989; 71:812–815.
52. Nielsen GP, Rosenberg AE. Lipomatosis. In. WHO Classification of Tumors Pathology and Genetics, Tumor of Soft Tissue and Bone. Lyon: IARC Press, 2002:23–24.
53. Kanter WR, Wolfort FG. Multiple familial angiolipomatosis: treatment of liposuction. Ann Plast Surg 1988; 20:277–279.
54. Fanburg-Smith JC, Devaney KO, Miettinen M, Weiss SW. Multiple spindle cell lipomas: a report of 7 familial and 11 nonfamilial cases. Am J Surg Pathol 1998; 22:40–48.
55. Furlong MA, Fanburg-Smith JC, Miettinen M. The morphologic spectrum of hibernoma: a clinicopathologic study of 170 cases. Am J Surg Pathol 2001; 25:809–814.
56. Dei Tos AP. Liposarcoma: new entities and evolving concepts. Ann Diagn Pathol 2000; 4:252–266.
57. Weiss SW, Rao VK. Well-differentiated liposarcoma (atypical lipoma) of deep soft tissue of the extremities, retroperitoneum, and miscellaneous sites. A follow-up study of 92 cases with analysis of the incidence of "dedifferentiation". Am J Surg Pathol 1992; 16:1051–1058.
58. Antonescu C, Ladanyi M. Myxoid liposarcoma. In. WHO Classification of Tumors Pathology and Genetics, Tumor of Soft Tissue and Bone. Lyon: IARC Press, 2002:40–43.
59. Antonescu CR, Tschernyansky SJ, Decuseara R, Leung DH, Woodruff JM, Brennan MF, Bridge JA, Neff JR, Goldblum JR, Ladanyi M. Prognostic impact of p53 status, TLS-CHOP fusion transcript structure, and histological grade in myxoid liposarcoma: a molecular and cliniopatholgic study of 82 cases. Clin Cancer Res 2001; 7:3977–3987.
60. Smith TA, Easley KA, Goldblum JR. Myxoid/round cell liposarcoma of the extremities. A clinicopathologic study of 29 cases with particular attention to extent of round cell liposarcoma. Am J Surg Pathol 1996; 20:171–180.
61. Downes KA, Goldblum JR, Montgomery EA, Fisher C. Pleomorphic liposarcoma: a clinicopathologic analysis of 19 cases. Mod Pathol 2001; 14:179–184.
62. Weiss WS, Goldblum JR. In: Enzinger and Weiss's Soft Tissue Tumors. 4th ed. Philadelphia: Mosby-Harcourt, 2001:539–569.
63. Henrichks WH, Chu YC, Goldblum JR, Weiss SW. Dedifferentiated liposarcoma: a clinicopathological analysis of 155 cases with a proposal for an expanded definition of dedifferentiation. Am J Surg Pathol 1997; 21:271–281.
64. Nagamine N, Nohara Y, Ito E. Elastofibroma in Okinawa. A clinicopathologic study of 170 cases. Cancer 1982; 50:1794–1805.
65. Schwindinger WF, Francomano CA, Levine MA. Identification of a mutation in the gene encoding the alpha-subunit of the stimulatory G protein of adenylyl cyclase in McCuen-Albright syndrome. Proc Natl Acad Sci USA 1992; 89:5152–5156.
66. Shenker A, Chanson P, Weinstein LS, Chi P, Spiegel AM, Lomri A, Marie PJ. Osteoblastic cells derived from isolated lesions of fibrous dysplasia contain activating somatic mutations of the Gs alpha gene. Hum Mol Genet 1995; 4:1675–1676.
67. van Roggen JF, McMenamin ME, Fletcher CD. Cellular myxoma of soft tissue: a clinicopathological study of 38 cases confirming indolent clinical behavior. Histopathology 2001; 39:287–297.
68. Michal M, Fetsch JF, Hes O, Miettinen M. Nuchal-type fibroma: a clinicopathologic study of 52 cases. Cancer 1999; 85:156–163.
69. Chung EB, Enzinger FM. Fibroma of tendon sheath. Cancer 1979; 48:1945–1954.
70. Miettinen M, Fetsch JF. Collagenous fibroma (desmoplastic fibroblastoma): a clinicopathologic analysis of 63 cases of a distinctive soft tissue lesion with stellate-shaped fibroblasts. Hum Pathol 1998; 29:676–682.
71. Allen PW, Enzinger FM. Juvenile aponeurotic fibroma. Cancer 1970; 26:857–867.
72. Guillou L, Fletcher JA, Fletcher CDM, Mandahl N. Extrapleural solitary fibrous tumour and haemangiopericytoma. In. WHO Classification of Tumors Pathology and Genetics, Tumor of Soft Tissue and Bone. Lyon: IARC Press, 2002:86–90.
73. Zhang PJ, Brooks JJ. Malignant solitary fibrous tumor: a transformation and dedifferentiation phenomenon in some cases. Mod Pathol 2004; 17, Supplement 1:21A.
74. Hasegawa T, Matsuno Y, Shimoda T, Hasegawa F, Sano T, Hirohashi S. Extrathoracic solitary fibrous tumors: their histological variability and potentially aggressive behavior. Hum Pathol 1999; 30:1464–1473.
75. Coffin CM, Humphrey PA, Dehner LP. Extrapulmonary inflammatory myofibroblastic tumor: a clinical and pathological survey. Semin Diagn Pathol 1998; 15:85–101.
76. Li XQ, Hisaoka M, Shi DR, Zhu XZ, Hashimoto H. Expression of anaplastic lymphoma kinase in soft tissue tumors: an immunohistochemical and molecular study of 249 cases. Hum Pathol 2004; 35:711–721.
77. Coffine CM, Watterson J, Priest JR, Dehner LP. Extrapulmonary inflammatory myofibroblastic tumor (inflammatory pseudotumor). A clinicopathologic and immunohistochemical study of 84 cases. Am J Surg Pathol 1995; 19:859–872.
78. Dupree WB, Langloss JM, Weiss SW. Pigmented dermatofibrosarcoma protuberans (Bednar tumor). A pathologic, ultrastructural, and immunohistochemical study. Am J Surg Pathol 1985; 9:630.
79. Connelly JH, Evans HL. Dermatofibrosarcoma protuberans. A clinicopathologic review with emphasis on fibrosarcomatous areas. Am J Surg Pathol 1992; 16:921–925.
80. Bowne WB, Antonescu CR, Leung DH, Katz SC, Hawkins WG, Woodruff JM, Brennan MF, Lewis JJ. Dermatofibrosarcoma protuberans: a clinicopathologic analysis of patients treated and followed at a single institution. Cancer 2000; 88:2711–2720.
81. Merck C, Angervall L, Kindblom LG, Oden A. Myxofibrosarcoma. A malignant soft tissue tumor of fibroblastic histiocytic origin. A clinicopathologic and prognostic study of 110 cases using

multivariate analysis. Acta Pathol Microbiol Immunol Scand Suppl 1983; 228:1–40.
82. Lane KL, Shannon RJ, Weiss SW. Hyalinizing spindle cell tumor with giant rosettes: a distinctive tumor closely resembling low-grade fibromyxoid sarcoma. Am J Surg Pathol 1997; 21:1481–1488.
83. Evens HL. Low-grade fibromyxoid sarcoma. A report of 12 cases. Am J Surg Pathol 1993; 17:595–600.
84. Fisher C. The value of electron microscopy and immunohistochemistry in the diagnosis of soft tissue sarcomas: a study of 200 cases. Histopathology 1990; 16:441–454.
85. Pritchard DJ, Soule EH, Taylor WF, Ivins JC. Fibrosarcoma – a clinicopathologic and statistical study of 199 tumors of the soft tissues of the extremities and trunk. Cancer 1974; 33:888–897.
86. Weiss SW, Enzinger FM. Malignant fibrous histiocytoma: an analysis of 200 cases. Cancer 1978; 41:2250.
87. Fletcher CDM. Pleomorphic malignant fibrous histiocytoma: fact or fiction? A critical reappraisal based on 159 tumors diagnosed as pleomorphic sarcoma. Am J Surg Pathol 1992; 16:213–228.
88. Fletcher CDM, van den Berg E, Molenaar WM. Pleomorphic malignant fibrous histiocytoma/undifferentiated high grade pleomorphic sarcoma. In: WHO Classification of Tumors Pathology and Genetics, Tumor of Soft Tissue and Bone. Lyon: IARC Press, 2002:120–122.
89. Weiss SW. Malignant fibrous histiocytoma. A reaffirmation. Am J Surg Pathol 1982; 6:773–784.
90. Paal E, Miettinen M. Retroperitoneal leiomyomas: a clinicopathologic and immunohistochemical study of 56 cases with a comparison to retroperitoneal leiomyosarcomas. Am J Surg Pathol 2001; 25:1355–1363.
91. Kapadia SB, Meis JM, Frisman DM, Ellis GL, Heffner DK, Hyams VJ. Adult rhabdomyoma of the head and neck: a clinicopathologic and immunophenotypic study. Hum Pathol 1993; 24:608–617.
92. Kapadia SB, Norris HJ. Rhabdomyoma of the vagina. Mod Pathol 1993; 6:75A.
93. Kapadia SB, Meis JM, Frisman DM, Ellis GL, Heffner DK. Fetal rhabdomyoma of the head and neck: a clinicopathologic and immunophenotypic study of 24 cases. Hum Pathol 1993; 24:754–765.
94. Evans HL, Shipley J. Leiomyosarcoma. In: WHO Classification of Tumors Pathology and Genetics, Tumor of Soft Tissue and Bone. Lyon: IARC Press, 2002:131–134.
95. Hashimoto H, Daimaru Y, Tsuneyoshi M, Enjoji M. Leiomyosarcoma of the external soft tissues. A clinicopathologic immunohistochemical, and electron microscopic study. Cancer 1986; 57:2077–2088.
96. Gurney JG, Davis S, Severson RK, Fang JY, Ross JA, Robison LL. Trends in cancer incidence among children in the U.S. Cancer 1996; 78:532–541.
97. Newton WA, Jr., Soule EH, Hamoudi AB, Reiman HM, Shimada H, Beltangady M, Maurer H. Histopathology of childhood sarcomas, intergroup rhabdomyosarcoma studies I and II: clinicopathologic correlation. J Clin Oncol 1988; 6:67–75.
98. Tsokos M, Webber BL, Parham DM, Wesley RA, Miser A, Miser JS, Etcubanas E, Kindella T, Grayson J, Glatstein E. Rhabdomyosarcoma. A new classification scheme related to prognosis. Arch Pathol Lab Med 1992; 116:847–855.
99. Furlong MA, Mentzel T, Fanburg-Smith JC. Pleomorphic rhabdomyosarcoma in adults: a clinicopathologic study of 38 cases with emphasis on morphologic variants and recent skeletal muscle-specific markers. Mod Pathol 2001; 14:595–603.
100. Raney RB, Anderson JR, Barr FG, Donaldson SS, Pappo AS, Qualman SJ, Wiener ES, Maurer HM, Christ WM. Rhabdomyosarcoma and undifferentiated sarcoma in the first two decades of life: a selective review of intergroup rhabdomyosarcoma study group experience and rationale for intergroup rhabdomyosarcoma study V. Am J Pediatr Hematol Oncol 2001; 23:215–220.
101. Woodruff JM, Susin M, Godwin TA, Martini N, Erlandson RA. Cellular schwannoma. A variety of schwannoma sometimes mistaken for a malignant tumor. Am J Surg Pathol 1981; 5:733–744.
102. Ducatman BS, Scheithauer BW, Piepgras DF. Malignant peripheral nerve sheath tumors. A clinicopathologic study of 120 cases. Cancer 1985; 57:2006–2021.
103. Sorensen SA, Mulvihill JJ, Nielsen A. Long-term follow-up of von Rechlinghausen neurofibromatosis: survival and malignant neoplasms. N Engl J Med 1986; 314:1010–1015.
104. Fisher ER, Wechsler H. Granular cell myoblastoma – a misnomer. Electron microscopic and histochemical evidence concerning its Schwann cell derivation and nature (granular cell schwannoma). Cancer 1962; 15:936–954.
105. Fanburg-Smith JC, Meis-Kindblom JM, Fante R, Kindblom LG. Malignant granular cell tumor of soft tissue: diagnostic criteria and clinicopathologic correlation. Am J Surg Pathol 1998; 22:779–794; Scheithauer BW, Woodruff JM, Erlandson RA. Primary malignant tumors of peripheral nerve. In: Tumors of the Peripheral Nervous System, Atlas of Tumor Pathology Third Series, AFIP, 1999:303–356.
106. Lucas DR, Nascimento AG, Sim FH. Clear cell sarcoma of soft tissues. Mayo Clinic experience with 35 cases. Am J Surg Pathol 1992; 16:1197–1204.
107. Folpe AL, Fanburg-Smith JC, Miettinen M, Weiss SW. Atypical and malignant glomus tumors: analysis of 52 cases with a proposal for the reclassification of glomus tumors. Am J Surg Pathol 2001; 25:1–12.
108. Enzinger FM, Smith BH. Hemangiopericytoma. An analysis of 106 cases. Hum Pathol 1976; 7:61–82.
109. Granter SR, Badizadegan K, Fletcher CD. Myofibromatosis in adults, glomangiopericytoma, and myopericytoma: a spectrum of tumors showing perivascular myoid differentiation. Am J Surg Pathol 1998; 22:513–525.
110. McMenamin ME, Fletcher CDM. Malignant myopericytoma: expanding the spectrum of tumors with myopericytic differentiation. Histopathology 2002; 41:450–460.
111. Kransdorf MJ. Malignant soft tissue tumors in a large referral population: distribution of diagnoses by age, sex, and location. AJR Am J Roentgenol 1995; 164:129–134.
112. van de Rijin M, Barr FG, Xiong QB, Hedges M, Shipley J, Fisher C. Poorly differentiated synovial sarcoma: an analysis of clinical pathologic and molecular genetic features. Am J Surg Pathol 1999; 23:106–112.
113. Weiss WS, Goldblum JR. Synovial sarcoma. In: Enzinger and Weiss's Soft Tissue Tumors. 4th ed. Philadelphia: Mosby-Harcourt, 2001:1483–1509.
114. Willen H, Akerman M, Dal Cin P, De Wever I, Fletcher CD, Mandahl N, Mertens F, Mitelman F, Rosai J, Rydholm A, Sciot R, Tallini G, van den Berghe H, Vanni R. Comparison of chromosomal patterns with clinical features in 165 lipomas: a report of the CHAMP study group. Cancer Genet Cytogenet 1998; 102:46–49.
115. Ladanyi M, Argani P, Hutchinson B, Reuter VE. Prominent nuclear immunoreactivity for TFE3 as a specific marker for alveolar soft part sarcoma and pediatric renal tumors containing TFE3 gene fusions. Mod Pathol 2002; 15:312A.
116. Lieberman PHI, Brennan MF, Kimmel M, Erlandson RA, Garin-Chesa P, Flehinger BY. Alveolar soft part sarcoma. A clinicopathologic study of half a century. Cancer1989; 63:1–613.
117. Gerald WL, Miller HK, Battifora H, Miettinen M, Sliva EG, Rosai J. Intraabdominal desmoplastic small round cell tumor. Report of 19 cases of a distinctive type of high-grade polyphenotypic malig-

nancy affecting young individuals. Am J Surg Pathol 1991; 15:499–513.
118. Kushner BH, LaQuaglia MP, Wollner N, Meyers PA, Lindsley KL, Ghavimi F, et al. Desmoplastic small round-cell tumor: prolonged progression-free survival with aggressive multimodality therapy. J Clin Oncol 1996; 14:1526–1531.
119. Chae DR, Enzinger FM. Epithelioid sarcoma. Diagnosis, prognostic indicators and treatment. Am J Surg Pathol 1985; 9:214–263.
120. Zhang PJ, Pasha TL, Goldblum JR. Expression of tumor suppressor gene Ini1 is down-regulated in epithelioid sarcoma (ES), biologic and diagnostic implications. Mod Pathol 2005; 18, Supplement:23A.
121. Bos GD, Pritchard DJ, Reiman HM, Dobyns JH, Iistrup DM, Landon GC. Epithelioid sarcoma. An analysis of fifty-one cases. J Bone Joint Surg Am 1988; 70:863–870.
122. Fanburg-Smith JC, Miettinen M. Angiomatoid "malignant" fibrous histiocytoma: a clinicopathologic study of 158 cases and further exploration of the myoid phenotype. Hum Pathol 1999; 30:1336–1343.
123. Lauer DH, Enzinger FM. Cranial fasciitis of childhood. Cancer 1980; 45:401–406.
124. Chung EB, Enzinger FM. Proliferative fasciitis. Cancer 1975; 36:1450–1348.
125. Enzinger FM, Dulcey F. Proliferative myositis. Report of thirty-three cases. Cancer 1967; 20:2213–2223.

Index

A
ABC. *See* cyst, aneurysmal
Acetabular loosening lesions, 212
Acetabular reconstructions
  formal reconstruction, 261
  hip arthroplasty, 262–263
Achondrogenesis, 241
Achondroplasia, 242–243
Activin receptor IA/activin-like kinase-2, 240
Adamantinoma, 334–335
Adipocytic tumors
  benign
    hibernoma, 106
    lipoblastoma, 106–108
    lipoma, 108
  malignant
    myxoid and pleomorphic liposarcoma, 109
    well-differentiated and dedifferentiated liposarcoma, 108–109
AER. *See* Apical epidermal ridge
Aggressive fibromatosis/desmoid tumor, 113
Albers-Schonberg marble bone disease, 233–234
Alveolar soft part sarcoma (ASPS), 110
Amyloidosis/amyloid tumor, 233
Anatomical zones, neoplasms
  distal femur and proximal tibia
    hinge knee prosthesis and stem design, 256
    patellar tendon reattachment and soft tissue coverage, 258
    primary and metastatic tumors, 254
  femoral replacement prostheses, 259
  proximal femur, 254
Aneurysmal bone cyst (ABC), 98–99
Angiography, 144
Apical epidermal ridge (AER), 18, 19, 40
Arthritis, septic, 25, 88, 193, 201–202
Arthrodesis, 262
Arthropathies
  animal models, 187–188
  definition, 187
  destructive arthritidies
    ankylosing spondylitis, 204–205
    juvenile rheumatoid arthritis (JRA), 199–201
    pigmented villonodular synovitis (PVNS), 205
    psoriatic arthritis, 204
    rheumatoid arthritis (RA), 197–199
    septic arthritis, 201–202
  joint-related conditions, 206
  nondestructive and nonproductive arthropathies, 206
  productive arthritidies
    hemochromatosis, 196
    hemophilia, 195–196
    neuropathic arthropathy, 193
    ochronosis, 196
    osteoarthritis, 191–192
    osteochondral loose bodies, 192–193
  radiological aspects
    arthritis, 188–189
    bone alignment, 189
    cartilage space, 189
    definitive diagnosis, 191
    disease distribution, 189, 191
    osteopenia/sclerosis, 189
    soft tissues, 191
Articular cartilage
  fibrous type, 58–59
  hyaline, 58
  superficial tangential zone (STZ), chondrocytes, 57–58
  vascularization and innervation, 59
Aseptic loosening lesions
  causes, 211–212
  clinical features and basic aspects, 212
ASPS. *See* Alveolar soft part sarcoma
Aubin, J.E., 11
Avascular necrosis. *See* Osteonecrosis

B
Barr, F.G., 104
Basic multicellular units (BMUs), 129–130
Benign bone tumors
  aneurysmal bone cyst (ABC), 98
  dysplasia, 99
  epithelial and osteofibrous dysplasia components, 98
  non-ossifying fibroma, 99
  osteoblastoma, 100
  osteoid osteoma, 99–100
  osteomodulin (OMS), 98–99
  perivascular epithelioid cells (PECs), 99
Biliary rickets, 223
Biomaterials, 209
Biomechanics
  bone composition, 70
  bone design
    anisotropy, 71
    calcaneus, 72
    diseases and bone fractures, 73
    engineering analysis, 71
    periosteal bone formation, 72
    skeletal system, 71
    trabecular bone loss, 73
  bone mineral density (BMD), 69
  bone properties and fracture mechanics, 70
  joint
    definition, 61–62
    hip and knee joint, range of motion, 62
  osteoporosis, 69
  tissue, 62

Biopsy
open and needle techniques, 249
standard rules, 249–250
BMD. *See* Bone mineral density
Bone
biopsy, 130–131, 222
densitometry
dual energy X-ray absorptiometry (DEXA), 145
quantitative CT (QCT) and MRI, 146
focal osseous lesions, pathology
bone reaction, 149–150
cortical destruction, 149
diagnostic approach, 146
location and radiographic anatomy, 147
ossified matrix, 150
pathologic margin, 147
size and shape, 150
morphogenetic protein-4 (BMP-4), 240
quality, 220
Bone biology
blood supply
arterial supply, long bones, 6
nerve supply, 7
bone and cartilage regulation
androgens, 36, 38, 41
calcitonin, 36–37
calcitriol and osteogenesis, 37–38
endocrine, 36
estrogens, 36, 38, 41
growth hormone, 38
paracrine/autocrine, 40
parathyroid hormone, 37
proteolipids, 33
retinoic acid and osteogenesis, 38
vitamin A, 38
vitamin D, 37
bone cells
bone-lining, 8, 9
osteoblasts, 8–18
osteoclasts, 12–16
osteocytes, 11–12
osteoprogenitor, 7
bone matrix, 6
bone remodeling
apposition and resorption, 35
fibrovascular tissue, 35
collagen
adhesion proteins, 26–27
classification, 23
cross-linking, 24–25
cytokines and growth factors, 27–28
mineralization proteins, 26
non-collagenous matrix proteins, 25
osteoactivin (OA), identification and characterization, 31
enzymes
alkaline phosphatase, 31–32
hydrated (muco) polysaccharide gels, 32
growth factors
bone morphogenetic proteins, 39–40
insulin-like growth factors (IGF), 40
mechanosensory systems and stretch studies, 41–42
platelets-derived growth factors (PDGFs), 41
prostaglandins and interleukins, 41
transforming growth factor-beta (TGF-β), 35–36, 38–41
mineralization process
calcium hydroxyapatite, 33
hypothesized mechanisms, 33–35
matrix vesicles, 34
mineral deposition, 34–35
osteoid calcification, 32
surgical pathology, 34
morphology
bone, composite tissue, 2
compact bone, 4–6
connective tissue system, 4
cortical bone, 3
formation and resorption, 1
hydroxyapatite crystals, 1
immature and mature bone, 3
long bone, 2
microscopic features, 4
spongy bone, 4, 6
tibia, 2
skeleton, 1, 3
Bone cells
bone-lining, 8
osteoblasts
bone-lining cells, 8
differentiation, 10–11
granulocyte-macrophage colony stimulating factor (GM-CSF), 8
molecular regulation, 9–11
osteoid synthesis, 8
trabecular bone surface, 8
osteoclasts
differentiation regulation, 13–14
molecular mechanism, mediated bone resorption, 13
primary bone-resorbing cells, 12
RANK signaling pathway, 14
tartrate-resistant alkaline phosphatase (TRAP), 13
osteocytes, 11–12
osteoprogenitor, 7
Bone development
endochondral bone formation
fibroblast growth factor (FGF), 18
hypertrophic chondrocytes, 17
mesenchymal stem cells, 16
molecular regulation, 18
ossification, 16
SOX9 gene mutation, 17
membranous (intramembranous) bone formation, 16
skeletal muscle
contractile filaments characteristics, 20
contraction mechanism, 20–21
maturation development, 22–23
neuromuscular spindle, 21
organization, light and electron microscope level, 19–20
origin, 21–22
type(s), 19
Bone grossing
common specimens
DJD and osteonecrosis, 127
gangrene, ulcer, and trauma amputations, 126
pathological fracture, 127
resections, bone tumors, 127–128
resections, soft-tissue tumors, 127
decalcification, 125–126
general guidelines, 125
MSTS (Enneking) staging system, 128
Bone histomorphometry
basic multicellular units (BMUs), 129
bone biopsy, 130–131
bone formation
bone lamination, 136

intermittent apposition, 137
label escape and recognition error, 136–137
labeling agent, 137
mineral apposition rate (MAR), 135
mineralization front identification, 135
skewed sampling error, 136
bone labels
labeling schedules, 132
tetracycline labeling, 132
undecalcified section preparation, 132–133
bone resorption, 134
chemical component measurements and indices, 130
trabecular bone separation, 137–138
undecalcified bone histology evaluation
bone balance, 135
bone formation and resorption, 134
metabolic bone disease, 134
surface measurements, 134
undecalcified histological bone section, 129
Bone mineral density (BMD), 39, 69, 220
Bone morphogenetic proteins (BMPs), 171
Bone specimens, 125
Bone tumors and tumor-like lesions
bone-forming lesions
enostosis (Bone Island), 289
osteoblastomas, 292–293
osteoid osteoma,290–292
osteoma, 289–290
osteosarcoma and its variants, 293–303
cartilage lesions
benign chondromas, 307–309
bizarre parosteal osteochondromatous proliferation, 306–307
chondroblastoma, 310–312
chondromyxoid fibroma, 312–313
enchondromatosis and Ollier's disease, 309–310
osteochondroma, 303–306
subungual exostoses, 306
cystic lesions
aneurysmal bone cyst, 287–289
intraosseous ganglion, 287
simple (unicameral) bone cyst, 285–286
subchondral (synovial) cyst, 286
fibrohistiocytic lesions
benign and atypical fibrous histiocytoma, 329
malignant fibrous histiocytoma, 329–330
fibrous lesions
desmoplastic fibroma, 328
fibrosarcoma, 328–329
giant cell lesions
giant cell reparative granuloma, 327–328
giant cell tumor, 325–327
hematopoietic lesions
Hodgkin and non-Hodgkin lymphoma, 341–342
Langerhans cell histiocytosis, 342
plasma cell myeloma, 340–341
mesenchymal lesions
adamantinoma, 334–335
Campanacci's disease, 333–334
chondroid chordoma, 340
conventional chordoma, 339–340
Ewing's sarcoma, 335–337
fibrous dysplasia, 331–333
intraosseous lipoma, 338
intraosseous liposarcoma, 338
intraosseous schwannoma, 338–339
leiomyosarcoma, 338
malignant mesenchymoma, 339
vascular lesions
angiosarcoma and glomus tumor, 320
epitheloid hemangioendothelioma, 324
hemangiopericytoma, 324–325
hemophilic pseudotumor, 322
lymphangioma and hemangiomas, 320–321
massive osteolysis, 321–322, 326
skeletal angiomatosis, 321
vascular tumors, 323
Brachytherapy, 277
Bridge, J.A., 93, 104
Brittle bone disease. *See* Osteogenesis imperfecta (OI)

C
Calcitonin, 219–220
Calcium, 218
Campanacci's disease, 331, 334–335
Capillary hemorrhages, 229
Carcinogenicity, 209, 211
Cartilaginous tumors
benign type
chondromyxoid fibroma, 100
enchondroma, 101
hyaline cartilage, 100
parathyroid hormone-related peptide receptor gene (PTHrP), 100
synovial chondromatosis, 100–102
malignant type
adipose tissue, 107–108
dedifferentiated chondrosarcoma, 103
extraskeletal myxoid chondrosarcoma, 102
skeletal myxoid chondrosarcoma, 102
CCS/MSP. *See* Clear cell sarcoma/malignant melanoma of soft parts
centigray (cGy), definition, 277
CGH. *See* Comparative genomic hybridization
Charcot's joints. *See* Neuropathic arthropathy
Chemical examination, 87–88
Chondrodysplasia punctata, 243
Chondrodystrophy
achondrogenesis, 241–244
achondroplasia, 241–244
chondrodysplasia punctata, 241–243
diastrophic dwarfism, 243
fibrochondrogenesis, 241
hypochondroplasia, 243
kniest syndrome, 244
metaphyseal chondrodysplasias, 243–244
metatropic dwarfism, 242
multiple epiphyseal dysplasia, 244
spondyloepiphyseal dysplasias, 244
thanotropic dwarfism (TD), 241
Chondroid sarcoma, 350
Chondromalacia patella, 207
Chondrosarcomas
clear cell chondrosarcoma
management and differential diagnosis, 318–319
surgical pathology, 318
conventional chondrosarcoma
differential diagnosis, 311–312
grading process, 316
management, 316
surgical pathology, 313–315
dedifferentiated chondrosarcoma
differential diagnosis and management, 317–318
surgical pathology, 317
juxtacortical chondrosarcoma, 320
mesenchymal chondrosarrcoma

Chondrosarcomas (*cont.*)
management, 319
surgical pathology and differential diagnosis, 319
Christopherson, W.M., 110
Chronic anticonvulsant therapy, 227
Chronic multifocal recurrent osteomyelitis, 183
Cisplatin
organ-specific chemotherapy, 274
osteosarcoma chemotherapy, 273
Clear cell sarcoma/malignant melanama of soft parts (CCS/MSP), 109–110
Codman's triangle, 150
Collagen
adhesion proteins, 26–27
classification, 23
cross-linking
collagen synthesis, 24
osteogenesis, 25
tropocollagen, 24
cytokines and growth factors
connective tissue growth factor (CTGF), 28–30
plasminogen activators, 28
mineralization proteins, 26
non-collagenous matrix proteins, 25–26
osteoactivin (OA), identification and characterization, 31–32
Common specimens
DJD and osteonecrosis, 127
gangrene, ulcer, and trauma amputations, 126
pathological fracture, 127
resections, bone tumors, 127–128
resections, soft-tissue tumors, 127
Comparative genomic hybridization (CGH), 96
Complex regional pain syndrome (CRPS). *See* Reflex sympathetic dystrophy
Congenital fibrosarcoma, 111–112
Congenital syphilis, 184
Connective tissue growth factor (CTGF), 28–30
Conventional tomography, 144
Courtney, A.C., 75
CTGF. *See* Connective tissue growth factor
Cysts
aneurysmal, 98, 99, 102, 126, 149, 151, 285, 286–289, 325, 327
ganglion, 153, 287, 375
unicameral, 147, 285–287, 325
Cytogenetics applications
electron microscopy, 84–85
immunohistochemistry
antibodies usage, musculoskeletal pathology, 84
bone tumors analysis, 83–84
diagnostic tool, 84
osteoblastic and muscle differentiation, 84
retinoblastoma gene (Rb), 83
Cytokines, 56

D
Deep venous thrombosis (DVT), 168
Degioanni, J.J.C., 74
Dermatofibrosarcoma protuberans (DFSP), 110–111
Destructive arthritidies
ankylosing spondylitis, 205
gout, 203–204
juvenile rheumatoid arthritis (JRA), 200–201
pigmented villonodular synovitis (PVNS), 151, 156
psoriatic arthritis, 204
rheumatoid arthritis (RA), 197–199
septic arthritis, 200–203
DEXA. *See* Dual energy X-ray absorptiometry
DFSP. *See* Dermatofibrosarcoma protuberans
Diastrophic dwarfism, 243
Dual energy X-ray absorptiometry (DEXA), 73, 145–146
Duyck, J., 76
Dysostoses. *See* Metaphyseal chondrodysplasias
Dysplasia epiphysealis multiplex. *See* Multiple epiphyseal dysplasia

E
Engelman disease, 245
Enteric rickets, 223
Enzymes
alkaline phosphatase, 26, 30–32, 35
hydrated (muco) polysaccharide gels, 32
Epitheloid hemangioendothelioma, 324
Ewing's sarcoma
and osteosarcoma
adjuvant and neoadjuvant chemotherapy, 269–270
histologic assessment of tumor response, 270
primary tumor treatment, 270
radiation therapy
second malignant neoplasm (SMN), 280
XRT, 281–283
External beam radiation therapy. *See* Teletherapy
Extremity sarcoma resection
allograft reconstructions, 254
turndown and turnup procedures, 252

F
Fanconi syndrome, 226
Femoral replacement prostheses, 259
Fibroblast growth factor (FGF), 219
Fibrocartilaginous mesenchymoma, 331, 334
Fibrochondrogenesis, 241
Fibrodysplasia ossificans progressiva (FOP), 239–240
Fibromatosis, 156
Fibrous dysplasia, 226, 331–333
Flourodeoxyglucose (FDG), 145
Flowcytometry, 348
Fluorescence in situ hybridization (FISH), 105, 107
Fluorosis, 227–228
Focal osseous lesions
bone reaction, 149–150
cortical destruction, 149
diagnostic approach, 146
location and radiographic anatomy, 147
ossified matrix, 149–150
pathologic margin, 147–148
size and shape, 150
Fracture prediction
bone mineral density measurement, 73–74
exercise role, strengthening bones, 74–76
calcium and hydroxyproline excretion, 74
fracture fixation device design, 75–76
osteogenic potential, 75
physiologic effect, musculoskeletal unloading, 74
Wolff law, 74–75
fracture prevention, 74
Fungal osteomyelitis, 185

G
Gadolinium-enhanced images, 142, 155
Ganglion, 153, 157
Gastric rickets, 223

Gaucher's disease, 236
Gerald, W.L., 104
Goode, A.W., 74
Gorham's disease, 320–322
Gorlick, R., 95
Granulocyte-macrophage colony stimulating factor (GM-CSF), 8
Gray (Gy), definition, 277
Greenspan, S.L., 75

H
Hallor, K.H., 110
Hartmann, C., 54
Haversian system, 70
Healing
  bone healing
    traumatic bone disruption, 159
    types of fractures, 159–160
  musculoskeletal tissue healing, 159
  tendons and ligaments healing, 169–170
Hemangioma, 155
Hematomas, 156–157
Heterotopic ossification (HO), 173–174
High-turnover renal osteodystrophy, 229–230
Histochemical staining, 213
Hodgkin lymphoma, 341–342
Hooke's law, 62
Huang, H.Y., 96
Hydroxyproline
  FISH and interphase cytogenetics, 81–82
  musculoskeletal tumors, 82
  pyridinoline and deoxypyridinoline, 81
Hypochondroplasia, 243
Hypophosphatasia, 247

I
Iliac bone–tetracycline system, 132
Iliac reconstructions, 261
Immunohistochemistry (IHC), 343
Implant failure, 210
Insulin-like growth factors (IGF), 40
Intraosseous lipoma, 338
Intraosseous liposarcoma, 338
Intraosseous schwannoma, 338–339

J
Joint functions
  classification, 51–52
  embryology
    intervertebral discs, 54–55
    joint ossification, 55
    synovial, 54
  joint types, movements
    arthrokinematics, 53–54
    osteokinematics, 53
Joint pathology, radiological diagnosis, 59
Joint types, movements
  arthrokinematics
    condyloid knee joint, 53–54
    pivot joint, 53
    plane and ball-and-socket joint, 53
    saddle-shaped (sellar) joint, grid representation, 54
  osteokinematics, 53
Juvenile rheumatoid arthritis (JRA), 200–203

K
Kaposiform hemangioendothelioma/tufted angioma, 362
Kaposi's sarcomas (KS), 364–365
Kniest syndrome, 242
Kotz, R., 254
Kurmasheva, R.T., 104

L
Ladanyi, M., 95, 106, 110
Langerhans cell histiocytosis (LCH)
  differential diagnosis and management, 342
  Erdheim-Chester disease, 342
  metastatic bone disease, 342–343
Langer-Saldino type achondrogenesis, 241
Leach, C.S., 74
Legg-Calve-Perthes disease, 176–177
Leukemia, 341
Limb development
  apical epidermal ridge (AER), 18
  molecular biology, limb formation, 19
  Wnt signaling, 19
Limb-sparing surgery (LSS)
  current indications and management, 251
  description, 249
Lipogenic soft tumors
  angiolipoma, 368–369
  hibernoma, 370
  lipoma, 367–368
  lipomatosis, 368
  liposarcoma, 370–375
  spindle cell lipoma, 369–370
Lipoma, 152
Liposarcoma
  dedifferentiated liposarcoma, 374–375
  myxoid/round cell lipoma, 372–373
  pleomorphic liposarcoma, 373–374
  well-differentiated liposarcoma/atypical lipomatous tumor, 370–372
Local tumor control
  surgical intentions, 251
  surgical procedures, 250–251
  wound margins, 250
Low-turnover renal osteodystrophy, 230
Lysosomal storage diseases, 236

M
Magnetic resonance imaging (MRI)
  disc disease, 140
  hemangioma, 152–154
  inflammatory arthridities and soft-tissue tumors, 142
  lipoma, 152
  soft-tissue lesions and cysts, 150–155
  spin-echo imaging, 141
Malignant peripheral nerve sheath tumor (MPNST), 392–393
May, W.A., 98
Mechanical properties
  bone
    human femoral cortical bone, 63
    segmental tibia fracture, 66
    stress pattern, 64
    subtrochanteric femur and transverse patella fracture, 65
    Wolff's law, 64
  cartilage, 67
  intervertebral disk
    anisotropic and viscoelastic, 66

Mechanical properties (*cont.*)
tensile properties, 67
Young's modulus, 66–67
tendon and ligament, 66
Medical management, skeletal metastases, 274–275
Melorheostosis, 244–245
Metabolic bone diseases
Albers-Schonberg marble bone disease, 233–234
amyloidosis/amyloid tumor, 233
Gaucher's disease, 236
lysosomal storage diseases, 236
osteogenesis imperfecta (OI), 245–246
osteoporosis, 219–222
Paget's disease, 232–233
primary hyperparathyroidism, 230–231
pycnodysostosis, 234
renal osteodystrophy, 229
rickets and osteomalacia, 222–228
Metaphyseal chondrodysplasias, 243–244
Metaphyseal hemorrhage, 229
Metastatic lesions management, neoplasms
pathologic fractures, 265–266
principles, 263–264
surgical intervention, 263
surgical management, 264
Metatropic dwarfism, 242
Methyl methacrylate (MMA)
bone formation, 134
histomorphometry, 133
Mirra's criteria, 202
Mucopolysaccharidosis. *See* Lysosomal storage diseases
Multiple epiphyseal dysplasia, 244
Musculoskeletal allografts, 214
Musculoskeletal neoplasms
anatomical zones
distal femur and proximal tibia, 254–259
femoral replacement prostheses, 259
proximal femur, 254
biopsy
open and needle techniques, 249
standard rules, 249–250
metastatic lesions management
pathologic fractures, 265–266
principles, 263–264
surgical intervention, 263
surgical management, 263–264
pelvic resections classification
reconstruction after resection, 260–263
terminology, 260
Musculoskeletal system radiology
bone densitometry
dual energy X-ray absorptiometry (DEXA), 145–146
quantitative CT (QCT) and MRI, 146
bone pathology, 146–151
description, 139
imaging modalities
angiography, 144
conventional tomography, 144
CT scan, 140
magnetic resonance imaging (MRI), 140–144
radiography, 139
radionuclide imaging, 144–145
Myositis ossificans (MO), 157, 174–175
Myositis ossificans progressiva. *See* Fibrodysplasia ossificans progressiva (FOP)

N
Nerve sheath tumors, 157
Nishimori, S., 39
Nogueira, E., 96
Non-Hodgkin's lymphoma, 341
Nonrhabdo soft tissue sarcomas (NRSTS)
prognostic variables, 273
radiation therapy, 282–283
spectrum of disease, 273
treatment principles, 272

O
OA. *See* Osteoactivin
OMS. *See* Osteomodulin
Orthopedic devices complications
aseptic loosening (osteolysis)
causes, 211–212
clinical features and basic aspects, 212–213
infections, 210–211
systemic reaction, 211
toxicity and tumorigenicity, 211
Orthopedic practice laboratory
acid phosphatase, 81
bone metabolism assays, 79
calcitonin, 80
chemical examination, 87–88
clinical chemistry
bone formation, markers, 79
bone turnover, markers, 80
crystals examinations, 86–87
cytogenetics applications
electron microscopy, 84–85
immunohistochemistry, 83–84
Ewing's sarcoma, chromosomal translocation, 82
hydroxyproline
FISH and interphase cytogenetics, 81–82
musculoskeletal tumors, 82
pyridinoline and deoxypyridinoline, 81
immunological examinations, 88
microscopic examination, 86
parathyroid hormone assay, 80
serum alkaline phosphatase, 81
skeletal muscle tumors, 83
synovial
fluid analysis, 85–86
fluid interpretation, 88–89
sarcomas, 82–83
tissue banking, 79
vitamin D assay, 80
Ossified matrix, 150
Ossifying fibromyxoid tumor, 355
Osteitis deformans. *See* Paget's disease
Osteitis sclerosis, 182–183
Osteoactivin, 31
Osteochondritides, 177
Osteochondritis dissicans, 206
Osteochondrodysplasias. *See* Chondrodystrophy
Osteofibrous dysplasia, 333–334
Osteogenesis imperfecta (OI)
clinical and genetic features, 246
surgical pathology and histology, 234–235
types, 234
Osteogenic sarcoma, 303. *See also* Osteosarcoma
Osteolysis. *See* Aseptic loosening lesions

Osteomalacia
causes
chronic anticonvulsant therapy, 227
fibrous dysplasia, 226
fluorosis, 227–228
gastrointestinal causes, 223–224
genetic-based disorders, 224–226
oncogenic osteomalacia, 226–227
renal tubular acidosis, 226
vitamin D deficiency, 223
disease characterization, 222
oncogenesis, 226–227
pathology and management, 228
Osteomodulin (OMS), 99
Osteomyelitis sclerosis, 182
Osteonecrosis, 175–177
Osteopetrosis, 246–247
Osteopoikilosis, 245
Osteoporosis
bone biopsy, 222
diagnostic approaches and management, 220
disease characterization, 219
mechanism and pathogenesis, 220–221
risk factors, 220
Osteosarcoma
conventional osteosarcoma, 293–297
and Ewing's sarcoma
adjuvant and neoadjuvant chemotherapy, 269–270
histologic assessment of tumor response, 270
primary tumor treatment, 270
high-grade surface osteosarcoma, 301
intraosseous well-differentiated osteosarcoma, 299–300
multifocal osteosarcoma, 297–298
parosteal osteosarcoma, 302–303
periosteal osteosarcoma, 301
small cell osteosarcoma, 298–299
subtypes of, 293
telangiectatic osteosarcoma, 299

P
Page, M., 172
Paget's disease, 232–233
Parasitic osteomyelitis, 185–186
Parathyroid hormone (PTH), 80, 217–218
Parathyroid hormone-related protein (PTHrP), 219
Parenti-Fraccaro type achondrogenesis, 241
Parrot's pseudoparalysis. *See* Congenital syphilis
Patellar tendon reattachment, 258–259
PDGF. *See* Platelets-derived growth factors
PEC. *See* Perivascular epithelioid cell
Pediatric fracture
buckle/torus fracture, 163
complete fracture, 163
epiphyseal fracture, 163–164
fracture remodeling, 160–161
greenstick fracture, 163
overgrowth phenomenon, 161, 162
progressive deformity and rapid healing, 161–162
Pelvic resections classification
reconstruction after resection
acetabular reconstructions, 261–263
iliac reconstructions, 261
pelvic sarcomas, 260–261
terminology, 260
Peripheral primitive neuroectodermal tumors (pPNETs), 95–96
Perivascular epithelioid cells (PECs), 99
Perthes disease. *See* Legg-calve-perthes disease
Phosphorus, 218–219
Pigmented villonodular synovitis (PVNS), 156
Plasma cell neoplasms, 340–341
Platelets-derived growth factors (PDGFs), 41
Positron emission tomography (PET), 145
Preimplant analysis, 209
Primary bone tumors
osteosarcoma
cytogenetic analysis, 91–93
fusion genes, sarcomas, 92
oncogenes, 95
pathogenic mechanisms, telomerase and ALT, 95
tumor suppressor genes, 93–95
tumors ewing family
genomic imbalances, comparative genomic hybridization (CGH), 96
molecular genetics, 96–98
peripheral primitive neuroectodermal tumors (pPNETs), 95
Primary hyperparathyroidism, 230–231
Primitive neuroectodermal tumors (PNET), 354
Productive arthritidies
calcium pyrophosphate dihydrate (CPPD) crystal deposition disease, 193–195
hemochromatosis, 196
hemophilia, 195–196
neuropathic arthropathy, 193
ochronosis, 196–197
osteoarthritis, 191–192
osteochondral loose bodies, 192–193
Progressive diaphyseal hyperostosis. *See* Engelman's disease
Progressive osseous heteroplasia (POH), 240–241
Prosthetic devices. *See* Orthopedic devices complications
Prosthetic materials, surgical pathology, 209–215
Proximal femur, 254
PTHrP. *See* Parathyroid hormone-related protein
Pycnodysostosis, 234, 245
Pyogenic osteomyelitis
acute infections, 179–180
chronic infections, 180–182

R
Radiation therapy
biologic principles of, 278–279
clinical issues
intensity-modulated radiation therapy (IMRT), 279–280
three dimensional conformal radiation therapy (3D-CRT), 279
for Ewing's sarcoma
second malignant neoplasm (SMN), 280
XRT, 280–281
nonrhabdomyosarcomatous soft tissue sarcoma, 282–283
physical aspects of
brachytherapy, 277
X-ray and electron beams, 277–278
rhabdomyosarcomas, 281–282
Radiography, 139
Radionuclide bone scan, 268
Radionuclide imaging technique, 144–145
Rambaut, P.C., 74
Reflex sympathetic dystrophy, 175
Renal osteodystrophies, 229

Renal tubular acidosis. *See* Fanconi syndrome
Rhabdomyosarcomas
  radiation therapy, 281–282
  risk classification
    clinical group and invasiveness, 271
    histology, site and age, 270–271
  soft-tissue tumors, myogenic differentiation, 385–386
  treatment principles
    chemotherapy, 272
    specimen analysis, 272
Rheumatoid arthritis
  chronic synovitis, 199–200
  clinical features, 197
  etiology, 197
  radiological features, 197–198
  surgical pathology, 198–199
Rheumatoid arthritis/osteoarthritis, 59
Rickets
  biliary, 223
  gastric, 223
  glomerular, 227
  tubular, 224

S
Sandberg, A.A., 93
Sarcoma
  acute effects of chemotherapy, 273–274
  clinical evaluation
    biopsy, 268
    diagnostic imaging, 268
  late effects of chemotherapy
    organ-specific chemotherapy, 274
    second malignancies and growth disturbances, 274
  nonrhabdo soft tissue sarcomas (NRSTS)
    prognostic variables, 273
    spectrum of disease, 273
    treatment principles, 273
  osteosarcoma, 252
  osteosarcoma and Ewing's sarcoma
    adjuvant and neoadjuvant chemotherapy, 269-270
    histologic assessment of tumor response, 270
    primary tumor treatment, 270
  pelvic sarcoma, 260–261
  rhabdomyosarcomas
    risk classification, 270–272
    treatment principles, 272
Sarmiento, A., 172
Sawyer, J.R., 104
Schneider, V.S., 74
Scurvy, 228–229
Short-trunk dwarfism. *See* Kniest syndrome
Singh, A.P., 213
Skeletal dysplasias
  chondrodystrophy
    achondrogenesis, 241
    achondroplasia, 242–243
    chondrodysplasia punctata, 243
    diastrophic dwarfism, 243
    fibrochondrogenesis, 241
    hypochondroplasia, 243
    kniest syndrome, 242
    metatropic dwarfism, 242
    multiple epiphyseal dysplasia, 244
    spondyloepiphyseal dysplasias, 244
    thanotropic dwarfism (TD), 241
  congenital deficiencies, 247
  description, 239
  osteogenesis imperfecta, 245–246
Skeletal metastases, medical management of, 274–275
Skeletal trauma
  biologic enhancement
    osteoconductive methods, 171
    osteogenic methods, 171
    osteoinductive methods, 171–172
  bone healing, fractures
    traumatic bone disruption, 159
    types of fractures, 159–160
  complications, 168–169
  distraction osteogenesis, 169
  mechanical and biophysical enhancement
    electrical stimulation, 172–173
    mechanical stimulation, 172
    ultrasound stimulation, 173
  musculoskeletal tissue healing, 159
  orthopedic surgery problems
    heterotopic ossification (HO), 173–174
    legg-calve-perthes disease, 176–177
    myositis ossificans, 174–175
    osteonecrosis, 175–176
    other osteochondritides, 177
    reflex sympathetic dystrophy, 175
  pediatric fracture
    buckle/torus fracture, 163
    complete fracture, 163
    epiphyseal fracture, 163–164
    fracture remodeling, 160–161
    greenstick fracture, 163
    overgrowth phenomenon, 161
    progressive deformity and rapid healing, 161–162
  rigid condition biology, 166–168
  semi-rigid condition biology, 165–166
  tendon and ligament healing, 169–170
  types of fixation, 164–165
Skytting, B., 106
Snow, C.M., 75
Soft tissue coverage, 258–259
Soft-tissue lesions, 150–151
Soft tissue sarcomas, genetic abnormalities
  basic-helix loop-helix regulatory motif (bHLH), 104
  cytogenetic analysis, 103
  desmoplastic small round cell tumor, 104–106
  fluorescence in situ hybridization (FISH), 104
  fusion genes, 104
  myogenic transcription factors, 104
  rhabdomyosarcoma (RMS), 103
  synovial sarcoma
    RT-PCR analysis, 105
    SYT and SSX proteins, 106
    SYT-SSX1/SYT-SSX2 fusion, 106
  translocation juxtaposes, 103
Soft-tissue tumors
  ancillary test and special procedures
    flowcytometry, 348–349
    immunohistochemistry (IHC), 349
    ultrastructural analysis, 349
  with chondro-osseous differentiation
    extraskeletal myxoid chondrosarcoma, 355–356
    ossifying fibromyxoid tumor, 355
  diagnosis, 348

with divergent/ambiguous differentiation
alveolar soft part sarcoma, 397–398
angiomatoid fibrous histiocytoma, 399–400
desmoplastic small round cell tumor (DSRCT), 398–399
epithelioid sarcoma, 399
synovial sarcoma, 396–397
fibrohistocytic differentiation
adult fibrosarcoma, 382–383
calcifying aponeurotic fibroma, 377–378
dermatofibrosarcoma protuberans, 380
desmoplastic fibroblastoma, 377
elastofibroma, 375
fibroma of tendon sheath, 376–377
inflammatory myofibroblastic tumor, 379–380
low-grade fibromyxoid sarcoma, 381–382
malignant fibrohistiocytoma (MFH), 383–384
myxofibrosarcoma, 380–381
myxoma, 375–376
nuchal fibroma and keloid, 376
solitary fibrous tumor (SFT), 378–379
histologic features
extraskeletal Ewing's sarcoma (EWS), 354
extraskeletal mesenchymal chondrosarcoma, 354
extraskeletal osteosarcoma, 353–354
fibromatoses, 351–353
giant cell tumors, 353
soft-tissue chondroma, 350–351
incidence, 347
lipogenic tumors
angiolipoma, 368–369
hibernoma, 370
lipoma, 367–368
lipomatosis, 368
liposarcoma, 370–375
spindle cell lipoma, 369–370
with myogenic differentiation
leiomyoma, 384–385
leiomyosarcoma, 386–387
rhabdomyomas, 385–386
rhabdomyosarcomas, 387–389
with neuroectodermal differentiation
clear cell sarcoma, 393–394
granular cell tumor, 391–392
malignant peripheral nerve sheath tumor (MPNST), 392–393
neurofibroma, 390–391
schwannoma, 389–390
traumatic neuroma, 389
non-neoplastic conditions
nodular fasciitis, 400–401
proliferative fasciitis/myositis, 401–402
with pericytic features
glomus tumor, 394
hemanigopericytoma, 394–395
myopericytoma, 395–396
prognostic factors, 347–348
treatment, 350
vascular tumors
angiomatosis, 359
arteriovenous hemangioma, 359–360
capillary hemangioma, 357–358
cavernous hemangioma, 358
epithelioid hemangioendothelioma, 362–363
histocytic (epithelioid) hemangioma, 358–359
hobnail hemangioendothelioma, 363
intramuscular hemangioma, 359
Kaposiform hemangioendothelioma/tufted angioma, 362
Kaposi's sarcomas (KS), 364–365
lymphangioma, 361
malignant type, 365–367
papillary endothelial hyperplasia, 360
retiform hemangioendothelioma, 364
spindle cell hemangioma, 360–361
Solitary fibrous tumor (SFT), 378–379
Spondyloepiphyseal dysplasias (SED), 244
Stress-strain curve, 62–63
Subperiosteal hemorrhage, 229
Superficial tangential zone (STZ), 57–58
Surgical pathology, bone infections
AIDS, 186
chronic multifocal recurrent osteomyelitis, 183
congenital syphilis, 184–185
osteomyelitis and osteitis sclerosis, 182–183
parasitic and fungal osteomyelitis, 185–186
pyogenic osteomyelitis
acute infections, 179–180
chronic infections, 180–182
syphilitic osteomyelitis, 184
tubercular osteomyelitis, 183–184
Synovial chondromatosis, 206–207
Synovial fluid analysis, 85–89
Synovial joints
anatomy and histology
capsule vasculature and innervation, 55–56
mechanical stress effects, 57
synovial fluid, 57
synovial membranes, 56
synoviocytes, 56–57
embryology
chondrification, 55
chondrogenic region, 54
dynamic axial loading, 55
embryonic development, 54
ossification, 55
sclerotomal segment proliferation, 54
vascular endothelial growth factor (VEGF), 55
vertebra and intervertebral discs, 54–55
Synovial sarcomas, 157
Syphilitic osteomyelitis, 184

T
Tabin, C.J., 54
Takahira, T., 110
Tarkkanen, M., 93
Tartrate-resistant alkaline phosphatase (TRAP), 13
Teletherapy, 277
TGF-β. *See* Transforming growth factor-beta
Thanotropic dwarfism (TD), 241
Thomas, T., 75
Tilton, F.E., 74
Tissue replacement
ceramics and glasses, implants, 68
engineered tissue, 68
metals and polymers, orthopedics, 67
ultra-high molecular weight polyethylene (UHMWPE), 67
Transforming growth factor-beta (TGF-β), 38–39
TRAP. *See* Tartrate-resistant alkaline phosphatase
Triffit, J.T., 11
Tubercular osteomyelitis, 183–184
Tufted angioma, 362

U
Ulaner, G.A., 95
Ultra-high molecular weight polyethylene (UHMWPE), 67, 212
Ultrasound, 146, 151
Urist, M.R., 39

V
Vascular endothelial growth factor (VEGF), 55
Vascular soft tumors
  angiomatosis, 359
  arteriovenous hemangioma, 359–360
  capillary hemangioma, 357–358
  cavernous hemangioma, 358
  epithelioid hemangioendothelioma, 362–363
  histocytic (epithelioid) hemangioma, 358–359
  hobnail hemangioendothelioma, 363
  intramuscular hemangioma, 359
  Kaposiform hemangioendothelioma/tufted angioma, 362
  Kaposi's sarcomas (KS), 364–365
  lymphangioma, 361
  malignant type, 365–367
  papillary endothelial hyperplasia, 360
  retiform hemangioendothelioma, 364
  spindle cell hemangioma, 360–361
VEGF. *See* Vascular endothelial growth factor
Vitamin D, 218
Vitamin D-dependent rickets, 225–226

W
Wang, J., 111
Waters, B.L., 110
Wear debris, 212
Whedon, G.D., 74, 75
Witzke, K.A., 75
Wolff, J., 70
Wolff's law, 64, 74, 75

X
Xiao, Z., 34
X-linked hypophasphatemic rickets, 224–225